PROCEEDINGS

VETERINARY PATHOLOGY SERVICE
WEDNESDAY SLIDE CONFERENCE
2016-2017

JOINT PATHOLOGY CENTER
SILVER SPRING, MD 20910
2016-2017

JOINT PATHOLOGY CENTER
VETERINARY PATHOLOGY SERVICE

The 2016-2017 Wednesday Slide Conference is dedicated to our friend and mentor, Dr. Robert Moses McCully (1928-2017). Dedicated veterinarian, pathologist, father, and soldier - there were none finer.

A man of exceptionally sharp mind, incisive wit, boundless energy, and pride in your two professions, sir, you have inspired us all.

Case	JPC No.	Slide ID No.	Species	Lesion / condition	Tissue	Page
Conference 1	**24-Aug-16**					
1	4006379	27-Jul-32	Ferret	Chordoma	Cervical vertebra	1-6
2	3156017	07/428	Cat	Lymphoma	Liver	6-9
3	4035590	M	Mink	Canine distemper virus	Lung	9-14
4	3164901	09-1045	Dog	*Lycoperdon spp*. fungal pneumonia	Lung	14-18
Conference 2	**31-Aug-16**					
1	4085101	Case #1	Rabbit	Liver torsion	Liver	19-24
2	4083953	D16-01	Cat	Granulomatous lymphadenitis/*Histoplasma capsulatum*	Lymph node	24-29
3	4085318	G11362-A661	Horse	Suppurative embolic neprhitis/*Actinobacillus equuli*	Kidney	29-32
4	4083344	6M22955	Calf	Bovine Respiratory Disease Complex/*Mannheimia haemolytica*	Lung	32-36
Conference 3	**7-Sep-16**					
1	4084953	CHIN1	Chinchilla	*Listeria monocytogenes*	Liver	38-42
2	4003035	11-106289	Ox	Bovine respiratory syncytial virus	Lung	42-46
3	4066311	13A888	Rhesus macaque	Polyarteritis nodosa-like syndrome/SIV	Kidney	46-51
4	4083871	15-0048	Marmoset	Pseudomembranous colitis/*Clostridium difficile*	Colon	51-56
Conference 4	**14-Sep-16**					
1	4083954	D16-02	Sheep	Johne's disease/*Mycobacterium avium ss paratuberculosis*	Ileum	57-62
2	4085381	RUSVM Case #2	Dog	Metastatic rhabdomyosarcoma	Lung	62-67
3	4082892	26-Jul-41	Cat	Fungal dermatitis/*Lagenidium sp.*	Haired skin	67-72
4	4003084	S1103067	Alpaca	Pyogranulomatous meningoencephalitis/*Coccidioides immitis*	Cerebrum	72-78
Conference 5	**28-Sep-16**					
1	4084648	Case 1	African hedgehog	Osteosarcoma	Skull	79-84
2	4003264	V254/10	Dog	Osteomyelitis/*Nocardia sp.*	Rib	84-89

3	4085013	HB6474	Dog	Rectal polyp	Colon	89-92
4	4066248	D15-000804	Calf	Bovine pestivirus (BVDV)	Colon	93-97
Conference 6	**5-Oct-16**					
1	4084736	2016A	Duck	Granulomatous pericarditis/*Riemerella anatipestifer*	Heart	98-102
2	4084567	5-Oct-35	Cat	Meningoencephalitis/*Cryptococcus neoformans*	Cerebrum	102-108
3	4003103	10471-11	Cat	Pyogranulomatous splenitis/*Francisella tularensis*	Spleen	109-113
4	4003102	TAMU 2011-2	Coyote	*Sarcoptes scabiei*	Haired skin	113-117
Conference 7	**19-Oct-16**					
1	4084136	16-23	Rat	Acinar atrophy/Rat polyomavirus	Harderian gland	118-124
2	4066315	13A815	Rhesus macaque	Diaphragmatic endometriosis	Diaphragm	124-128
3	4083858	16-3320D	Sheep	Necrosupporative placentitis/*Campylobacter jejuni*	Placenta	128-133
4	4002842	20109-13350	Dog	Ovarian mixed germ cell tumor	Ovary	133-138
Conference 8	**26-Oct-16**					
1	4083864	16-Dec-77	Horse	Nasal rhinosporidiosis/*Rhinosporidium seeberi*	Nasal mass	139-144
2	4086389	O398/15	Pig	Myocarditis and endocarditis/PCV-2	Heart	144-150
3	4085382	S16-0248	Guinea pig	Bronchitis and bronchiolitis/Guinea pig adenovirus	Lung	150-155
4	4084218	17-Jun-41	African green monkey	Necrotizing pneumonia/*Yersinia enterocolitica*	Lung	155-160
Conference 9	**2-Nov-16**					
1	4066544	14L-2800B	Rabbit	Vulvar myxomatosis/Myxomatosis virus (Leporipoxvirus)	Vulva	161-165
2	4084542	DX16-0081	Mouse	Systemic candidiasis/*Candida albicans*	Kidney	165-170
3	4084692	Case#1	Rat	Mast cell tumor	Thymus	170-175
4	4087116	MS15-05586	Mouse	Hepatic necrosis/Azoxymethane toxicity	Liver	175-178

Conference 10	**9-Nov-16**					
1	4019839	AzVDL 02-3362	Cat	Urinary capillariasis/*Capillaria feliscati*	Urine	179-184
2	4084209	15N0368	Horse	Haemochromatosis	Liver	184-189
3	4086860	B110209	Dog	Fanconi-like syndrome	Kidney	189-194
4	4084201	16-2046	Dog	Transmissible venereal tumor	Dermal cytology	194-198
Conference 11	**16-Nov-16**					
1	4088440	Case1	Rat	Retinal dysplasia	Eye	201-205
2	4084739	E3133/15	Rabbit	Granular cell tumor	Testis	205-211
3	4066368	1408 1229	Rabbit	Liver cocciciosis/*Eimeria stiedae*	Liver	211-214
4	4050931	T4422/12 or 13	Mole	Necrotizing hepatitis/ *Toxoplasma gondii* and *Cyclospora talpae*	Liver	214-219
Conference 12	**14-Dec-16**					
1	4048850	14-309/6 or 7	Dog	Cerebellar abiotrophy	Cerebellum	220-224
2	4084300	N14-281	Horse	Spinal cord necrosis	Spinal cord	224-227
3	4006284	W1111-03	Ox	Central chromatolysis/*Aspergillus clavatus*	Spinal cord	227-231
4	4083741	A16-6925-12	Ox	Thrombotic meningoencephalitis/*Histophilus somni*		231-236
Conference 13	**4-Jan-17**					
1	4084214	F1475435	Dog	Prostatitis/*Brucella canis*	Prostate and testis	238-242
2	4066261	D15-008849	Dog	Oligodendroglioma	Cerebrum	242-247
3	4085316	05-7078-B	Calf	Congenital hypotrichosis and Poxvirus	Haired skin	247-253
4	4084539	N9882548	Cat	Necrotizing and hemorrhagic splenitis/*Pneumocystis carinii*	Spleen	253-257
Conference 14	**11-Jan-17**					
1	4075851	HSRL-425	Dog	Neuroendocrine carcinoma	Spleen	258-262
2	4083862	7-Mar-88	Horse	Equine multinodular pulmonary fibrosis/Equine herpesvirus-5	Lung	262-268
3	4084949	CAN2	Dog	Extramedullary plasmacytoma	Colon	268-272

4	4088269	E-522/16	Rabbit	Nephroblastoma	Kidney	272-275
Conference 15	**18-Jan-17**					
1	4066310	WSC#2	Alligator	Pneumonia/*Beauveria bassiana*	Lung	276-280
2	4066860	15-5172	Boa constrictor	Stomatitis/Boid inclusion body disease	Skull cross-section	280-285
3	4085109	G9428	Nilgiri langur	Cysticercosis/*Cysticercus longicollis*	Skeletal muscle	285-290
4	4083952	28-Jan-56	Cynomolgus macaque	Histiocytic alveolitis with intracytoplasmic crystalline protein	Lung	290-294
Conference 16	**25-Jan-17**					
1	4066394	AR-14-1021	Sheep	Bronchopneumonia/*Trueperella pyogenes*	Lung	295-299
2	4085015	Case 2	Cat	Meningoencephalitis/Mutated feline enteric coronavirus (FIP)	Cerebrum	300-304
3	4090482	15-008432	Dog	Pneumonia/*Acanthamoeba* spp	Lung	304-310
4	4084207	16-9986	Horse	Choriomeningoencephalitis/*Borrelia burgdorferi*	Cerebrum	310-316
Conference 17	**1-Feb-17**					
1	4017925	12A208	Pigtail macaque	Necrotizing periorchitis/Rhesus cytomegalovirus	Testis	317-322
2	4085507	T1339/16	Guinea pig	Amelanotic melanoma	Haired skin	322-326
3	4019364	11A228	Rhesus macaque	Granulomatous lymphadenitis/Mycobacterium tuberculosis	Lymph node	326-332
4	4089353	12-May-27	Rat	Mesothelioma and interstitial cell tumor	Testis and epididymis	333-338
Conference 18	**8-Feb-17**					
1	4083683	NF-15-1564	Goat	Caruncular amyloidosis	Placenta	339-343
2	4084216	2-Oct-60	Goose	Enteritis and necrotizing placentitis/West Nile virus	Small intestine and pancreas	343-349
3	4085377	15N499	Ox	Intraerythrocytic protozoan trophozoites/*Babesia bovis*	Cerebrum	349-356
4	4087119	14-9	Cat	Bronchointerstitial pneumonia/Influenza virus	Lung	356-362
Conference 19	**15-Feb-17**					
1	4067574	15-0609	Squirrel	Encephalitis/*Baylisascaris procyonis*	Cerebrum	363-366

2	4084212	WHL16188	Elk	Necrotizing vasculitis/Odocoileus adenovirus	Rumen	367-372
3	4085402	X-25548-15	Veiled chameleon	Pneumonia/*Mycobacterium chelonae*	Lung	373-377
4	4085315	G13060-A786	California sea lion	Metastatic carcinoma	Urinary bladder	377-383
Conference 20	**22-Mar-17**					
1	4068726	W255-15	Horse	Encephalitis/*Halicephalobus gingivalis*	Cerebellum	384-389
2	4086885	15842#185	Dog	Meningioma, transitional	Cerebrum	389-393
3	4085376	16N74	Bovine calf	Necrotizing meningoencephalitis/Bovine herpesvirus 1 or 5	Cerebrum	394-400
4	4066658	A00629	Dog	Astroglial dystrophy with Rosenthal fibers	Cerebrum	400-403
Conference 21	**31-Mar-17**					
1	4050655	12B2212	Dog	Synovial myxoma	Stifle joint	404-409
2	4069828	JPC WSC-2	Ox	Physeal dysplasia/Lead toxicity	Rib	410-414
3	4084206	16N0558	Horse	Equine bone fragility syndrome	Bone	414-420
4	4084557	P3554.15	Cat	Feline gastrointestinal eosinophilic sclerosing fibroplasia	Lymph node	421-425
Conference 22	**5 APR 17**					
1	4081675	2671-16	Cynomolgus macaque	Hepatoblastoma	Liver	425-430
2	4087117	MS1602402	Mouse	Placentitis/*Pasteurella pneumotropica*	Placenta	430-434
3	4035521	EX54BF-1 or 2	Mouse	Myoepithelioma	Salivary gland	434-437
4	4069981	AFIP 2013	Rhesus macaque	Bronchitis/*Pneumonyssus simicola*	Lung	437-441
Conference 23	**19-Apr-17**					
1	4033348	TAMU-02 2013	Sheep	Skeletal muscle degeneration and necrosis/ionophore toxicosis	Skeletal muscle	442-447
2	4068000	13A456	Rhesus macaque	Bismuth intranuclear inclusions	Kidney	447-453
3	4084474	27-Feb-04	Rat	Histiocytic sarcoma	Lung	453-457
4	4089360	20-Dec-47	Mouse	Hepatocholangiocarcinoma	Liver	457-460
Conference 24	**26-Apr-17**					

1	4002948	S354/10 or S370/10	Psittacine bird	Protozoan megaloschizonts/*Haemoproteus* spp	Skeletal muscle or proventriculus	461-465
2	4081674	3019-15	Dog	Esophagitis and arteritis/*Spirocerca lupi*	Esophagus and aorta	466-470
3	4084011	14-6189	African penguin	Interstitial pneumonia/*Sarcocystis falcatula*	Lung	470-476
4	4084734	E2889/15	Dog	Granulomatous scleritis/*Onchocerca lupi*	Globe	476-480
Conference 25	**16-May-17**					
1	4065818	WSC 1617	Zebrafish	Myocyte degeneration and necrosis with intrasarcoplasmic meronts/*Pleistophora hyphessobryconis*	Skeletal muscle	481-486
2	4084010	15-3213	Puffer fish	Proliferative branchitis/*Amyloodinium ocellatum*	Gill	486-492
3	4084652	A15-25281	Seahorse	Necrogranulomatous nephritis/*Nocardia asteroides*	Kidney	492-496
4	4085971	R1 or R2	Salmon	Pancreatic loss, epicarditis, red and white skeletal muscle necrosis/Salmonid alphavirus	Pancreas, pyloric cecae, skeletal muscle, heart	496-504

Joint Pathology Center
Veterinary Pathology Services

WEDNESDAY SLIDE CONFERENCE 2016-2017

C o n f e r e n c e 1

24 August 2016

CASE I: 48422 (JPC 4006379).

Signalment: 4-year-old male castrated sable ferret (*Mustela putorius furo*).

History: The ferret presented with a one-week history of ataxia. The owner noted a mass on the left neck. The ferret was eating but otherwise lethargic. Owners elected euthanasia due to worsening of clinical signs and the inoperable nature of the mass.

Gross Pathology: Within the subcutis and skeletal muscle of the neck just caudal to the skull, there is a large, firm, multinodular, smooth, white to tan, 5 x 3.5 x 1.5 cm mass extending to the left lateral and ventral aspect of the neck. The mass is adhered to the first cervical vertebra, extending caudally to the mid-cervical region and ventrally to the level of the trachea, but is not adhered to the trachea or esophagus. The central region of the mass is attenuated. After removal of the skull, evaluation of C1 reveals that the mass infiltrates into and effaces the left cranial articular fovea (articular facet of the atlas). After decalcification, further sectioning of the mass reveals that it extends into the vertebral canal and compresses the cervical spinal cord.

Cervical vertebrae, ferret. A large mass is present over the cranial cervical vertebrae. (Photo courtesy of: Animal Medical Center, 510 East 62nd St. New York, NY 10065 http://www.amcny.org/)

In the caudal aspect of the left cranial lung lobe, a 0.5 cm diameter firm, smooth, white nodule is observed. The spleen is diffusely congested and enlarged, and contained a 2 x 2 x 1.2 cm soft, smooth, red nodule. Two renal cortical cysts are observed in the right kidney, measuring approximately 0.4 cm each.

Laboratory results: N/A

Histopathologic Description: A de-calcified transverse section through the cervical vertebra, cervical spinal cord and

surrounding skeletal muscle is examined. Infiltrating into the epaxial musculature, cervical vertebral pedicle, articular processes and extending into the vertebral canal with compression of the adjacent cervical spinal cord is a multilobular, infiltrative, poorly demarcated neoplasm. Neoplastic lobules are separated by eosinophilic fibrovascular connective tissue. Lobules are comprised of large polygonal cells with distinct cell borders and abundant, amphophilic to clear, vacuolated cytoplasm (physaliferous cells) surrounded by variable amounts of amphophilic, mucinous stroma. Nuclei are round to oval and often peripheralized, with finely stippled chromatin and multiple nucleoli. There are zero mitotic figures in 10 high power (400x) fields. Multifocally in the center and at the periphery of lobules, scattered aggregates of cartilage and woven bone are interspersed within the physaliferous cells. Bony trabeculae contain osteocytes and are lined by osteoblasts. Chondrocytes lie within a lightly eosinophilic to amphophilic matrix or are occasionally entrapped within bone. Rare binucleate cells are found. Small aggregates of lymphocytes, plasma cells and macrophages are present at the periphery of the mass.

Cervical vertebra, ferret. This fixed specimen (likely proximal C-3 with dorsal spinous process at 10 o'clock) is unilaterally effaced by a multilobular mass which also compresses the spinal cord. (Photo courtesy of: Animal Medical Center, 510 East 62nd St. New York, NY 10065 http://www.amcny.org/)

Cervical vertebra (presumptive axis), ferret. The cervical vertebra is partially effaced by the chordoma, which compresses the spinal cord. (HE, 5X)

Vertebral bone has scalloped borders, with osteoclasts in Howship's lacunae. Fragmented woven bone (reactive bone) is interspersed with numerous plump osteoblasts and fibroblasts. Neoplastic compression of the cervical spinal cord results in shifting of the ventral medial fissure away from the mass. The white matter of the spinal cord exhibits mild, multifocal vacuolation in the dorsal, lateral and ventral funiculi, within which are few Gitter cells containing myelin degradation products. Scattered, multifocal swollen axons (spherocytes) are present in the ventral and lateral funiculi. Variation in neuronal cytoplasmic staining is present with no loss of Nissl substance (decalcification artifact, presumptive). Surrounding epaxial skeletal muscles, and more prominently, muscle adjacent to the dorsal spinous process undergoes degeneration and regeneration, manifesting as myocyte size variation, sarcoplasmic hypereosinophila and vacuolation, loss of striation, satellitosis, central nuclei, and nuclear rowing.

Contributor's Morphologic Diagnoses: 1. Cervical spine: Chordoma, with local

infiltration of skeletal muscle, vertebral bone and vertebral canal.
2. Cervical spinal cord: Focal compression with midline shift, mild, moderate Wallerian degeneration and spheroid formation.
3. Cervical skeletal muscles: Multifocal myodegeneration and regeneration.
4. Lung (caudal aspect left cranial lung lobe, not submitted): Multifocal chordoma metastasis.

Contributor's Comment: Chordomas are the 5th most common tumor in domestic ferrets, and the most common musculoskeletal tumor.[1,11] Chordomas are slow growing, locally aggressive neoplasms derived from remnant fetal notochord [1,4,6-12,14] believed to originate from the primitive mesoderm.[1,2] The notochord persists between the vertebrae and expands to form the nucleus pulposus of intervertebral disks in some animals (visible in the section).[1,5,8,9] Cell rests of residual notochord remain outside of the intervertebral disks in an estimated 2% of humans, and chordomas are thought to arise from these cell rests.[1,4,8,9] Histologically, ferret chordomas are characterized by lobules of physaliferous cells surrounding cartilage with a central core of bone and cartilage. [1,4,6-12,14] Notochord-induced differentiation of bone and cartilage within the neoplasm is one hypothesis for the bone and cartilage formation within these neoplasms.[4]

Chordomas can occur anywhere along the axial skeleton. In the ferret, common sites include the tail tip (most common site), cervical vertebral column (second most common site**),** thoracic vertebral column, and the coccygeal region.[1,4,6-12,14] The sacrococcygeal and spheno-occipital regions are the most common sites of chordoma occurrence in humans, with the remainder

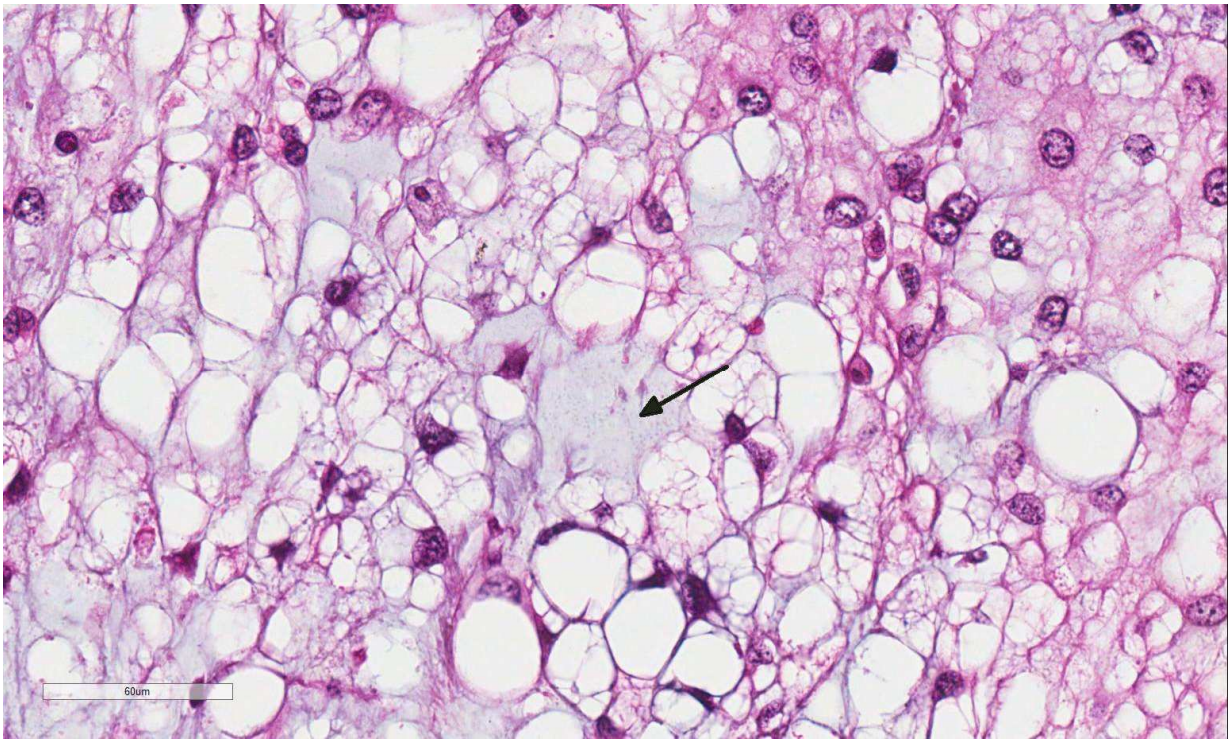

Cervical vertebra (presumptive axis), ferret. The neoplasm is composed of polygonal cells with large clear vacuoles which often peripheralize the nucleus (physaliferous cells) separated by moderate amounts of blue mucinous matrix (arrow). (HE, 400X)

found in the vertebral axis.[4,14] Up to 30% of human chordomas are reported to metastasize, typically during the phase of recurrent disease, with common sites of metastasis reported to be bone, lung, lymph node, skin and liver.[1,4,14] Rare cases of local and distant skin metastases have been reported in the ferret.[1,4,14] Vascular invasion was equivocal in the submitted section, however, was observed rarely in other sections of the mass and pulmonary metastases were present. One study evaluated cell proliferation indices in 5 ferret chordomas, and found that they were not predictive of metastatic potential.[8]

In humans, there are 3 recognized subtypes of chordoma: classic chordoma, chondroid chordoma, and chordoma with malignant spindle cell component (dedifferentiated). It has been suggested that ferret chordomas may act as an animal model for the chondroid subtype of human chordoma.[4,14] Differentiation between classic and chondroid subtypes in humans is significant, as chondroid chordomas are associated with a survival rate 3 times greater than that of classic chordomas.[1,8] Although the chondroid component was not prominent in the submitted section, it was more frequently observed in other sections of the mass.

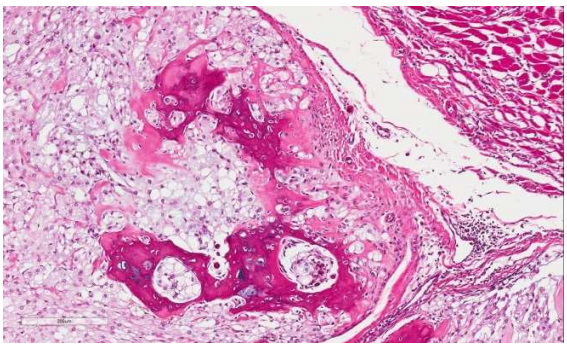

Cervical vertebra (presumptive axis), ferret. Multifocally, several lobules of the neoplasm contain foci of mineralizing woven bone. (HE, 200X)

Immunohistochemical analysis of chordomas in the ferret typically show dual expression of cytokeratin and vimentin, with variable expression of S-100 protein and neuron specific enolase (NSE).[1,4,6-12,14] In one study of chordomas in 20 ferrets, 75% were positive for S-100 and 85% were positive for NSE.[4] The S-100 positivity is thought to be due to glycosaminoglycan content within the stroma, and NSE is expressed in cells with high metabolic activity.[1,4]

JPC Diagnosis: Cervical vertebra (axis): Chordoma.

Conference Comment: This case nicely characterizes an example of a common neoplasm in the axial skeleton of a ferret. The contributor provides an excellent histologic description, including the ancillary findings of degeneration of the spinal cord, peripheral nerves, and adjacent skeletal muscle as a result of compression from this infiltrative neoplasm.

Aside from humans and ferrets, chordomas have been rarely reported in the axial skeleton of Fischer 344 rats[11], mice[13], dogs[6,9], and cats[2]. In addition, 24 cases of spontaneous primary intestinal chordomas as well as nine spontaneous vertebral chordomas, were recently reported in the aged laboratory zebrafish[3]. In dogs, chordomas have been reported in the brain, spinal cord, and skin[6]. Of the three reported cases of feline chordoma, one was initially diagnosed as chronic granulomatous inflammation due to the interpretation of the characteristic physaliferous cells as atypical, foamy macrophages; it was subsequently dis-covered to be an example of a classic chordoma-like subtype, which then metastasized to multiple lymph nodes[2].

In all species, chordomas tend to be slow growing and locally invasive.[1-14] Typically, distant metastasis is associated with the classic chordoma and dedifferentiated spindle cell subtypes in humans, rather than the chondroid type which forms islands of cartilage and bone most commonly in the ferret and mink.[1,4,8,10,14] In a large study of Fischer 344 rats there was an exceptionally high 75% incidence of pulmonary metastasis in animals diagnosed with chordomas.[11] The histomorphology of chordomas in the Fischer rat is similar to the classic type in humans, which may explain the more aggressive biologic behavior in these rodents as compared to other animals.[11] Prior to this case, visceral metastasis had not yet been reported in the ferret. However, the contributor recently published this case report, to include pulmonary metastasis via hematogenous spread; this is the first known case of visceral metastasis in the ferret[5]. The authors hypothesized that the metastatic potential in ferrets may increase over time, highlighting the importance of prompt surgical excision. Most cases of ferret chordomas occur at the tail tip making complete surgical excision relatively simple.[1,4,5,14] Chordomas in other locations, such as this case, are substantially more difficult to excise.[5]

Chordomas in ferrets may histologically resemble chondrosarcomas due to the cartilaginous component. Conference participants briefly discussed immunohistochemistry as a method by which to differentiate chordoma from chondrosarcoma. As mentioned by the contributor, chordomas consistently demonstrate dual immunopositivity for vimentin and cytokeratin, while chon-drosarcomas are immunonegative for cytokeratin. Chordomas are also typically positive for S-100 and neuron-specific enolase (NSE); the S-100 and NSE positivity does not suggest neural crest origin, however.[10,12] Other neoplasms of interest that typically express both vimentin and cytokeratin include: mesothelioma, synovial sarcoma, meningioma, renal cell carcinoma, adrenal carcinoma, and endometrial sarcoma.[12]

Contributing Institution: The Animal Medical Center
Department of Pathology
510 East 62nd St. New York, NY 10065
http://www.amcny.org/

References:

1. Camus MS Rech RR, Choy FS, Fiorello CV, Howerth EW. Pathology in practice, chordoma on the tip of the tail of a ferret. *J Am Vet Med Assoc*. 2003;235(8):949-51.
2. Carpenter JL, Stein BS, King NW Jr, Dayal YD, Moore FM. Chordoma in a cat. *J Am Vet Med Assoc.* 1990;197:240-242.
3. Cooper T, Murray K, et al. Primary intestinal and vertebral chordomas in laboratory zebrafish (*Danio rerio*). *Vet Pathol*. 2015;52(2):388-392.
4. Dunn DG, Harris RK, Meis JM, Sweet DE. A histomorphologic and immune-ohistochemical study of chordoma in twenty ferrets (*Mustela putorius furo*). *Vet Pathol*. 1991;28:467-473.
5. Frohlich J, Donovan T. Cervical chordomas in a domestic ferret (Mustela putorius furo) with pulmonary metastasis. *J Vet Diagn Invest*. 2015;27(5)656-659.
6. Gruber A, Kneissi S, Vidoni B, Url A. Cervical spinal chordoma with chondromatous component in an dog. *Vet Pathol.* 2008;45(5):650653.
7. Koestner A, Bilzer T, Fatzer R, Schulman FY, Summers BA, Van Winkle TJ. Chordoma. In: *Histological Classification of Tumors of the Nervous System of Domestic Animals*, 2nd series, vol. V, pp. 36. Armed Forces Institute of Pathology, Washington, D.C., 1999.

8. Munday JS Brown CA, Richey LJ. Suspected metastatic coccygeal chordoma in a ferret (*Mustela putorius furo*). *J Vet Diagn Invest.* 2004;16(5):454-458.
9. Munday JS, Brown CA, Weiss R. Coccygeal chordoma in a dog. *J Vet Diagn Invest.* 2003;15(3):285-288.
10. Pye GW, Bennett RA, Roberts GD, Terrell SP. Thoracic vertebral chordoma in a domestic ferret (*Mustela putorius furo*). *J Zoo Wildl Med* 2000;31(1):107-111.
11. Stefanski SA, Elwell MR, Mitsumori K, Yoshitomi K, Dittrich K, Giles HD. Chordomas in Fischer 344 rats. *Vet Pathol.* 1988;25(1):42-47.
12. Takeshi Y, Tetsuo O, et al. Histochemical and immunohistochemical characterization of chordoma in ferrets. *J Vet Med Sci*. 2015;77(4):467-473.
13. Taylor, K, Garner M, et al. Chordomas at high prevalence in the captive population of the endangered Perdido Key Beach mouse (*Peromyscus polinotus trissyllepsis*). *Vet Pathol*. 2016;53(1):163-169.
14. Williams BH, Eighmy JJ, Berbert MH, Dunn DG. Cervical chordoma in two ferrets (*Mustela putorius furo*). *Vet Pathol*. 1993;30:204-206.

CASE II: 48422 (JPC 4006379).

Signalment: 16 year old, female, domestic shorthair, *Felis catus*.

History: The cat had decreased appetite and weight loss. It was icteric with a temperature of 38°C. The heart rate was 220 beats/min and the respiration rate was 92 breaths/min. Lymph nodes were unremarkable by palpation. Ultrasound of the abdomen showed moderate amounts of fluid, and a liver with rounded edges and a marbled parenchyma with reduced number of visible hepatic- and portal veins. Lymph nodes in the cranial abdomen, near the spleen and pancreas were enlarged and hypoechoic.

Gross Pathology: The cat was thin and icteric. The abdominal cavity contained 50 ml clear yellow fluid with a few floccules. The liver was slightly enlarged with rounded edges and lighter in color than normal with a lobular pattern and a decreased texture. Multifocally scattered, light gray, soft nodules, 0.5-5.0 mm in diameter were present in the hepatic parenchyma. The mesenteric lymph node was enlarged, light yellow-gray, moderately firm, and measured 4.0x1.5x1.5 cm. The pancreas was macroscopically normal.

Laboratory results: Clinical pathology: AST: 193 U/L (ref: 0-60), ALT: 258 U/L (ref: 0-75), AP: 339 U/L (ref: 0-40), amylase: 880 U/L (ref: 0-800), total protein: 56 g/L (ref: 60-82), albumin: 21 g/L (ref: 25-39), bile acids: 392 µmol/L (ref: 0-5), total bilirubin: 215 µmol/L (ref: 0-4), WBC: 4.2 x 10e9/L (ref: 5.5-17), lymphocytes: 0.6 x 10e9/L (ref: 1.5-7.0), platelets: 30 x 10e9/L (ref: 180-400).

Immunohistochemical staining of mesenteric lymph node and liver showed immunoreactivity with rabbit anti-human CD3 (DakoCytomation, A 0452) and confirmed that the infiltrating cells were T lymphocytes.

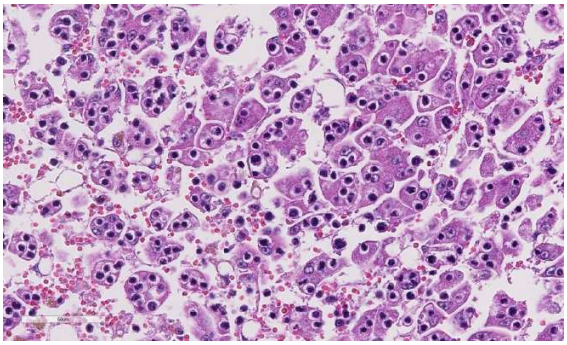

Liver, cat. Hepatic cords are diffusely dissociated and hepatocytes contain multiple lymphocytes within their cytoplasm. Intrahepatocytic lymphocytes are surrounded by a clear vacuole. (HE, 400X)

Histopathologic Description: In the liver, there are multifocal to confluent, randomly spaced areas with numerous infiltrating small lymphoid cells. The cells are located both in the sinusoids and appear to be located within the cytoplasm of hepatocytes. Some of the cells are also located close to or in invaginations of the hepatocellular membrane. The cells are small, with a narrow rim of eosinophilic cytoplasm. They have a small, densely stained round to irregular nucleus with indistinct nucleolus. There is little degree of anisocytosis and anisokaryosis. There is <1 mitotic figure per 10 HPF. The lymphoid cells present within the hepatocellular cytoplasm are surrounded by a clear halo. There is severe dissociation of hepatocytes, seen as single rounded large hepatocytes with up to 8 lymphoid cells within the cytoplasm. In areas with few lymphoid cells, there are moderate vacuolation of hepatocytes with variably sized clear vacuoles.

Contributor's Morphologic Diagnoses: Liver: malignant lymphoma with emperipolesis of lymphocytes and severe dissociation of hepatocytes

Contributor's Comment: Feline lymphoma commonly occurs as thymic, alimentary multicentric and cutaneous syndromes.[8] This cat had involvement of the mesenteric lymph node and liver. It is indicated that Feline leukemia virus (FeLV) positive cats are associated with the mediastinal and multicentric form of lymphoma and that the thymic and alimentary forms predominate in FeLV negative cats.[2,8] The FeLV status of this cat was not known.

Hepatic lesions morphologically identical to those in this cat, has been reported earlier in two cats diagnosed with lymphoblastic lymphosarcoma.[3]Although emperipolesis is the phenomenon of viable cells entering the cytoplasm of other cells without damage to either host cell or the engulfed cells,[3] the clinical pathology of this cat, similar to the cats presented by Ossent et al,[5] indicates severe hepatic failure. In addition, histology of the liver shows extensive hepatocellular dissociation.

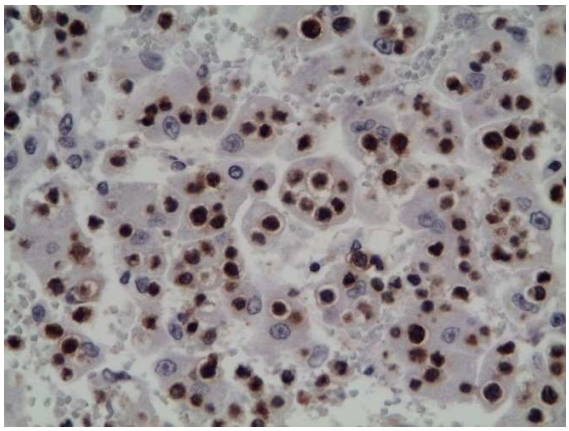

Liver, cat. Intrahepatocytic lymphocytes stain strongly positive with anti-CD-3 immunohistochemical stain. (anti-CD3, 400X) (Photo courtesy of: Norwegian School of Veterinary Science, Institute of Basic Sciences and Aquatic Medicine, PO box 8146 Dep, 0033 Oslo Norway. http://www.veths.no/Venstremeny/English/)

JPC Diagnosis: 1. Liver: T-cell lymphoma, hepatocytotropic.
2. Liver: Regeneration, micronodular, multifocal, mild.

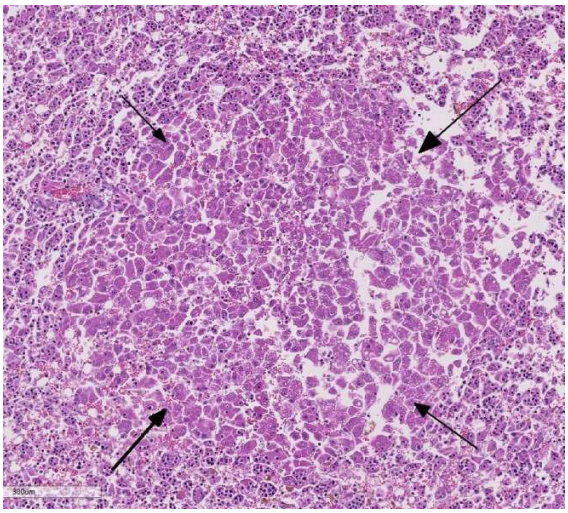

Liver, cat. Scattered throughout the section are rare nodules of proliferating hepatocytes which contain few intrahepatocytic lymphocytes (arrows). The mild lipidosis seen diffusely through the section is best demonstrated here. (HE, 400X)

Conference Comment: This case generated discussion amongst the conference participants regarding the use of the term emperipolesis. As mentioned by the contributor, emperipolesis is an uncommon biological process, in which a cell penetrates the cytoplasm of another living cell. [1,4,6,7] Unlike phagocytosis where the engulfed cell is killed by lysosomal enzymes of the macrophage, the engulfed cell exists as a viable cell within another.[7] The pathogenesis and significance of this phenomenon is currently unknown.[1] Emperipolesis has been rarely reported in the human literature associated with autoimmune hemolytic anemia, multiple myeloma, leukemia, and malignant lymphoma.[1] In this case, there is clear evidence of hepatocellular injury and cholestasis supported by the animal's clinical icterus along with severe serum biochemistry abnormalities. Clinicopathologic serum elevations in AST and ALT, as well as hypoalbuminemia and hypoproteinemia support hepatocellular injury in addition to hepatocellular swelling, lipofuscin deposition, and hepatic lipidosis. Cholestasis is confirmed by severe elevations in bile acids, total bilirubin, and elevated ALP.

Given the degree of hepatocellular injury and cholestasis, conference participants unanimously preferred the term hepatocytotropism over emperipolesis as a more representative term for the infiltrating T-cell lymphocytes in this case. This terminology was recently proposed as an alternative to emperipolesis in similar cases malignant lymphoma in the dog with distinct tropism for hepatocytes.[4] Transmission electron microscopy in the dog as well as the previously reported cases in cats, showed lymphocytes within invaginations of the hepatocyte cell membrane rather than within the cytoplasm, as required for emperipolesis.[4,6,7] In addition, hepatocytotropism is more analogous to the epitheliotropism present in cutaneous and intestinal T-cell lymphoma in the dog and cat.[4]

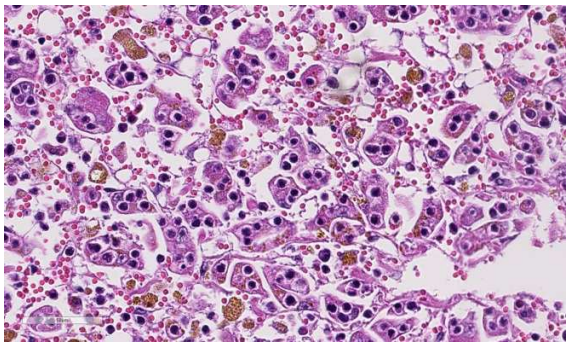

Liver, cat. In areas of marked hepatic cord dissociation, Kupffer cells contain abundant granular brown pigment, which likely represents a combination of iron (confirmed with Perl's stain), bile pigment, and lipofuscin from hepatocellular damage. (HE, 400X)

Several conference participants also commented on the degree of hepatic cord discohesion with dislocation of hepatic plates and diffuse loss of normal architecture in this case. Some speculated this to be partially due to moderate autolysis of the tissue. There was further discussion and

some speculation that hepatic discohesion could be due to a defect in β-catenin through the Wnt signaling pathway, common in hepatic neoplasms.[9] This pathway has a major role in cell adhesion to the basement membrane and cell polarity in the liver and gastrointestinal tract. In addition, β-catenin binding to E-cadherin is responsible for maintaining intercellular adhesion.[5] Normally, after acute hepatocellular insult, the liver is stimulated to regenerate via the Wnt pathway. The Wnt receptor signals through cell surface receptor, frizzled (FRZ), to deactivate the destruction complex, APC. The tumor suppressor APC normally binds to and destroys β-catenin.[5] With the APC deactivated, β-catenin signaling drives the expression of target genes that are critical for cell cycle progression and contribute to initiation of the regeneration process.[5,9] Even in the multifocal microregenerative nodules without hepatocytotropic lymphocytes, there is hepatic cord discohesion. Regardless of the pathogenesis, the disassociation of the hepatic cords likely disrupts bile canalicular transport and secretion of bilirubin leading to severe hepatic cholestasis and icterus in this case.[6]

Contributing Institution: Norwegian School of Veterinary Science
Institute of Basic Sciences and Aquatic Medicine
Oslo, Norway
http://www.veths.no/Venstremeny/English/

References:

1. Amita K, Shankar S, et al. Emeripolesis in a case of adult T cell lymphoblastic lymphoma (mediastinal type)-detected at FNAC and imprint cytology. *Online J Health Allied Scs.* 2011;10:11.
2. Fry, M, McGavin M. Bone marrow, blood cells, and the lymphatic system. In: Zachary JF, McGavin MD, eds. *Pathologic Basis of Veterinary Disease.* 5th ed. St. Louis, MO: Elsevier; 2012:698-705.
3. Humble JG, Jayne WHW, Pulvertaft RJV: Biological interaction between lymphocytes and other cells. *Br J Heamatol* 1956;2:283-294.
4. Keller S, Vernau W, et al. Hepatosplenic and hepatocytotropic T-cell lymphoma: two distinct types of lymphoma in dogs. *Vet Pathol*. 2012;50:281-290.
5. Kumar V, Abbas A, Aster J. Neoplasia. In: Kumar V, Abbas A, Aster J, eds. *Robbins and Cotran Pathologic Basis of Disease*. 9th ed. Philadelphia, PA; Saunders Elsevier; 2015: 296-297.
6. Ossent P, Stöckli RM, Pospischil A: Emperipolesis of lymphoid cells in feline hepatocytes. *Vet Pathol*. 1989;26:279-280.
7. Suzuki M, Kanae Y, et al. Emperipolesis-like invasion of neoplastic lymphocytes into hepatocytes in feline T-cell lymphoma. *J Comp Path*. 2011;144:312-316.
8. Valli V, Kiupel M, Bienzle D. Hematopoietic system. In: *Jubb, Kennedy, and Palmer's Pathology of Domestic Animals*, ed. Maxie MG, 4th ed., Vol. 3. Saunders Elsevier, Philadelphia, PA, 2016:103-104.
9. Wang E, Yeh S. et al. Depletion of β-catenin from mature hepatocytes of mice promotes expansion of hepatic progenitor cells and tumor development. *PNAS*. 2011;108:18384-18389.

CASE III: M (JPC 4035590).

Signalment: 16-week-old female and male mink kits, *Mustela vison*

History: Kits were vaccinated subcutaneously at 6 weeks of age with 3 portions of the 4-way combination vaccine including inactivated mink enteritis virus, *Clostridium botulinum* Type C bacterin-toxoid and inactivated *Pseudomonas*

aeruginosa bacterin. Kits were vaccinated at approximately 10-12 weeks of age with the modified- live canine distemper virus portion of the 4-way combination vaccine via aerosol spray.

Lung, mink. At subgross magnification, the section of lung is markedly congested. (HE, 5X)

Approximately 10 days later, mortality started with 5- 10 dead kits per day. Mortality was concentrated in 2 of 8 barns and the mahogany mink were primarily affected. Affected mink kits had "wet heads" and were screaming, seizuring before dying. This producer mixes his own feed on farm and in the last week, had a feed change to fish, chicken and processed meats. Only the chicken is fresh daily, the other protein sources are frozen. As of a week ago, antibiotics (CSP 250) were mixed in the feed. The older mink are fine.

Gross Pathology: Four mink kits were submitted for postmortem examination. They were in good body condition with ample internal and external fat stores. They were mildly to moderately dehydrated. The lungs were diffusely mottled purple/red and were edematous. The tracheal lumina did not contain fluid or exudate. Stomachs were generally either empty or contained brown flecked mucus or brown fluid. The small intestines were generally empty and only a small amount of gold brown mucoid to pasty material was in the rectum. Livers were red tinged with yellow. The spleens were small.

Laboratory results: Negative for Aleutian disease by CIE testing. Multiple tissues including lung, spleen, liver, adrenal gland and brain had positive immunohistochemical (IHC) staining for canine distemper virus (CDV).

Histopathologic Description: The lung is markedly congested with alveoli containing eosinophilic edema fluid, small amounts of fibrin and red blood cells. Multifocally, small to moderate numbers of macrophages with abundant often foamy cytoplasm, less frequently multinucleated cells and infrequent neutrophils are also collecting in alveolar spaces. Bronchial lumina contain eosinophilic edema fluid, small numbers of red blood cells, macrophages, multinucleate cells, neutrophils and degenerate cells. Many of the bronchi and nearby vessels are rimmed by one to two cell thick lymphohistiocytic cuffs. Numerous large eosinophilic spherical to rectangular inclusions morphologically compatible with viral inclusions are present within the cytoplasm of normal and proliferative bronchial and bronchiolar epithelium and occasionally within macrophages or multinucleated cells. Strong positive staining for CDV is present within bronchiolar epithelium and alveolar macrophages on immunohistochemistry.

Contributor's Morphologic Diagnoses: 1. Marked pulmonary congestion and moderate pulmonary edema.
2. Proliferative bronchitis, bronchiolitis and multifocal histiocytic pneumonia with eosinophilic intracytoplasmic inclusions.
3. Very mild acute suppurative bronchitis, bronchiolitis and pneumonia

Contributor's Comment: The host range of canine morbillivirus (canine distemper virus,

CDV) is broad and species in all families in the order Carnivora, including *Canidae*, *Mustelidae*, *Procyonidae*, *Hyaenidae*, *Ursidae* , *Viverridae* and *Felidae* are considered susceptible.[9] Canine distemper virus causes multisystemic disease in farmed mink[4] with juvenile mink being most susceptible with a mortality rate of 90% as compared to a more variable rate of 20-90% in adult mink.[9] Outbreaks of CDV infection on commercial mink farms have been associated with infected raccoons (*Procyon lotor*) and striped skunks (*Mephitis mephitis*) found on the farm premises[4]. The transmission of the virus is mainly by aerosol or through direct contact with oral, nasal or conjunctival fluid as the canine distemper virus does not survive long in the environment and it can be rapidly in-activated by ultraviolet light, drying, heat and common disinfectants. However, it is possible for the gloves used for handling infected mink to act as fomites and transmit sufficient virus to infect susceptible mink for a short period of time.[2]

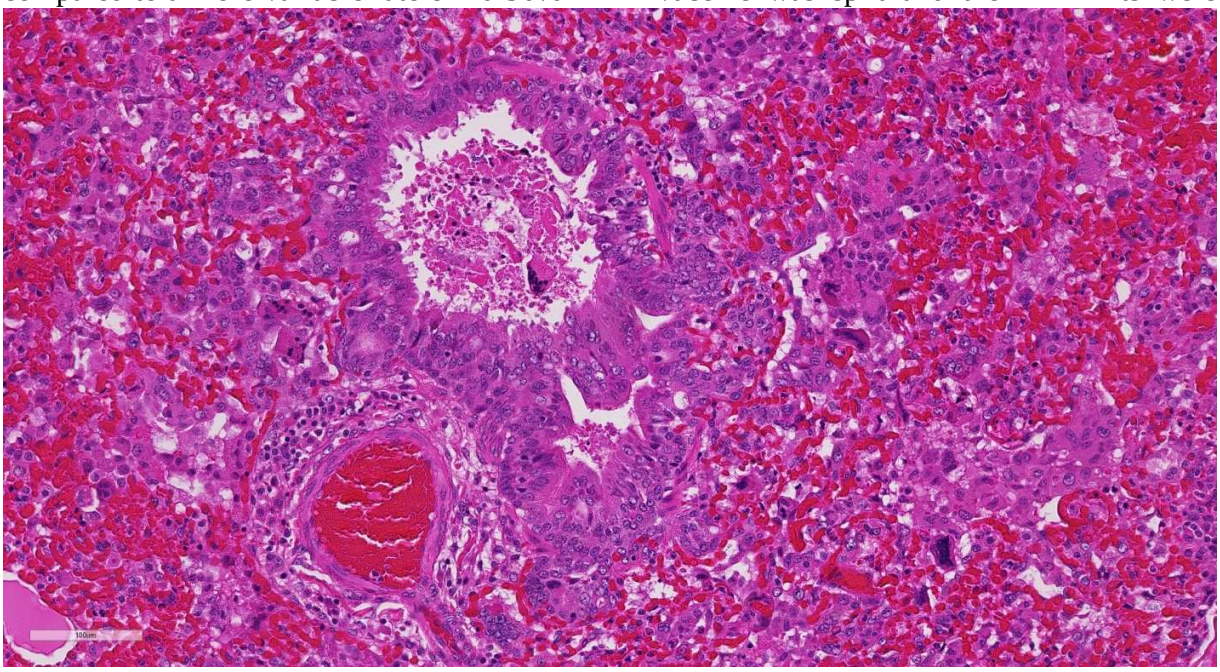

Lung, mink. There is marked hyperplasia of bronchiolar epithelium which extends into the surrounding alveoli. Viral syncytia may be seen in lumen of the affected airway as well as within macrophages in surrounding alveoli. (HE, 5X)

Routine vaccination of kits via subcutaneous injection using a multivalent vaccine including canine distemper virus is typically carried out after weaning.[4] Some producers will also revaccinate the mature females and males being retained for breeding at this time (J Mitchell, personal communication). On this farm, the 4-way combination vaccine was split and the mink kits were immunized by subcutaneous injection for mink enteritis virus, *Clostridium botulinum* Type C and *Pseudomonas aeruginosa* at 6 weeks of age. Four to six weeks later, the kits were given the canine distemper virus portion of the vaccine by aerosol spray, however, as the vaccine is meant to be given by subcutaneous injection it is likely the mink kits were not sufficiently immunized against canine distemper virus and subsequently developed clinical disease.

At necropsy, the most consistent lesions were identified in the lungs with pro-liferative bronchitis and bronchiolitis and variable numbers of large rectangular

eosinophilic intracytoplasmic inclusions identified in bronchial and bronchiolar epithelium. Low numbers of multinucleated cells in alveoli occasionally also contain intracytoplasmic inclusions. Small accumulations of neutrophils were aggregating in small airways and secondary bacterial bronchopneumonia is reported to commonly occur.[4] The diagnosis of CDV in these individuals was confirmed with IHC.

In experimental infections with the virus given by injection, young mink are reported to develop reddening of the skin progressing to dermatitis, conjunctivitis and nasal discharge, but dyspnea is uncommon.[4] However, histologically, pulmonary lesions are common and the intracytoplasmic and intranuclear viral inclusions are most often present in the respiratory or bladder epithelium.[4] Viral inclusions are not identified in the transitional epithelium of the bladder in this case, despite the tremendous numbers visible in the lung tissues.

JPC Diagnosis: Lung: Bronchiolar epithelial hyperplasia, marked, with mild histiocytic bronchiolitis, and epithelial and histiocytic intracytoplasmic viral inclusion bodies.

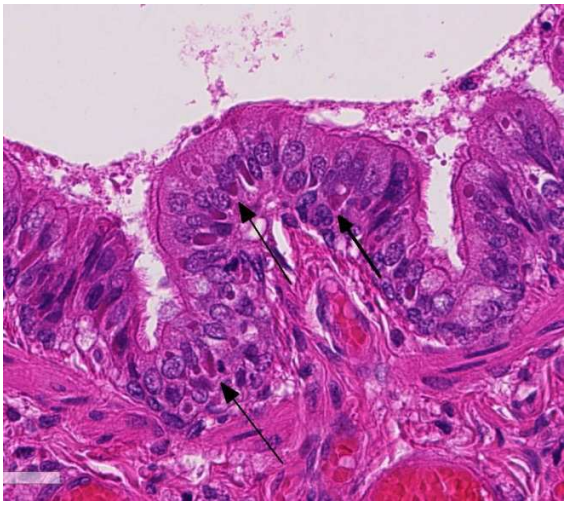

Lung, mink. Bronchiolar epithelium contains one or multiple 2-4um irregularly round intracytoplasmic viral inclusions. (HE, 320X)

Conference Comment: Canine distemper virus (CDV) is an enveloped, single stranded RNA (ssRNA) virus of the genus *Morbillivirus* in the *Paramyxoviridae* family[1-8]. *Morbilliviruses* are highly contagious pathogens that are responsible for some of the most devastating diseases that affect mammals worldwide. Other members of this genus include measles virus, peste des petits ruminants virus, rinderpest virus, phocine distemper virus, and dolphin morbillivirus.[6] CDV is one of the most important and ubiquitous infectious diseases of wild and domestic predators with high morbidity and mortality in imm-unologically naïve populations.[5] As men-tioned by the contributor, mustelids (i.e. ferrets, minks, and badgers) are particularly sensitive to the virus with mortality up to 100% in non-vaccinated ferrets.[5]

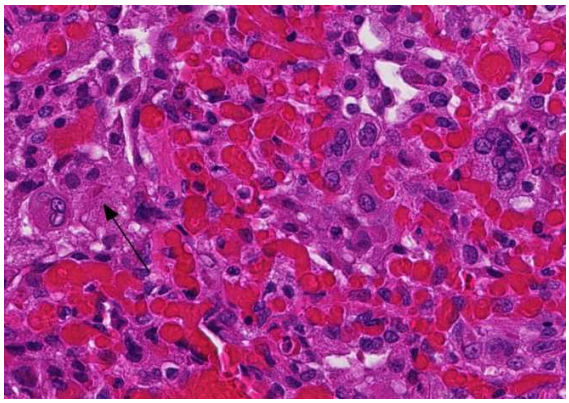

Lung, mink. Alveoli contain numerous macrophages which occasionally contain intracytoplasmic viral inclusions (arrow). A multinucleated viral syncytium is present at right. (HE, 400X)

Like all paramyxoviruses, CDV contains six structural proteins: nucleocapsid (N), phospho (P), large (L), matrix (M), hemagglutinin (H), and fusion (F) protein. The viral envelope contains *H*, used for attachment to the host cell receptor, and *F*, required for entry and syncytia formation. In

this case, syncytial cells are occasionally present within bronchioles and alveoli.[1,6]

CDV is typically transmitted via inhalation of infected aerosols.[3,4] The virus enters macrophages, lymphocytes, and dendritic cells via the signaling lymphocyte activation molecule (SLAM) receptor binding to H viral protein within the first day of infection.[1,6] The virus spreads to local lymph nodes and other lymphoid organs within two to five days post infection. Primary viral replication in the lymphoid tissues leads to severe immunosuppression and viremia. About eight to ten days post-infection, CDV disseminates to several epithelial tissues (respiratory, intestinal, and urinary) and the central nervous system. The virus uses epithelial cell receptor nectin-4 to gain entry into epithelial cells.[1,4,6]

Unfortunately, in this case, the conference participants had difficulty assessing the alveolar septal changes due to poor insufflation of the lung. However, conference participants easily identified numerous intracytoplasmic viral inclusions within histiocytes and the markedly hyperplastic bronchiolar epithelium. In addition, some recognized rare intranuclear inclusions. CDV is unique because it causes both intranuclear and intracytoplasmic inclusions.[3,7,8] Given that CDV is an ssRNA virus that requires RNA-dependent RNA polymerase complex present only in the cytosol to replicate, the presence of intranuclear inclusions is initially confounding.[7] However, CDV infection induces the cellular stress response which causes elevated expression of heat shock proteins. These proteins translocate viral nucleocapsid (N) proteins from the cytoplasm into the nucleus as part of the normal host cell response to cellular stress. Under normal circumstances, the N protein would be too large to pass through nuclear pores.[7] N proteins form the basis for nuclear body formation, and propagation of viral nucleocapsids. These particles eventually partially, or completely fill the nucleus resulting the in the formation of the intranuclear inclusion body visible by light microscopy.[7,8]

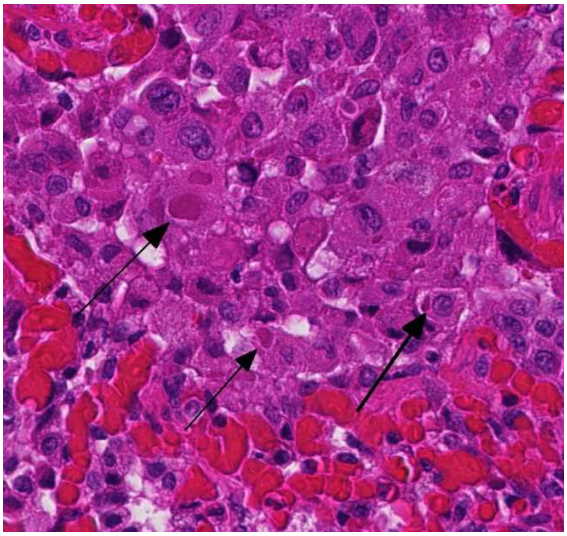

Lung, mink. In this field, numerous alveolar macrophages contain variably-sized viral inclusions (arrows). (HE, 400X)

The contributor mentions the wide range of species now infected by CDV and related viruses. Additionally, lethal outbreaks in rhesus and cynomolgus macaques originating in China have been documented within the last decade.

Contributing Institution: Animal Health Laboratory
University of Guelph, Guelph, Ontario, Canada
http://ahl.uoguelph.ca

References:

1. Beineke A, Baumgartner W, Wohlsein P. Cross species transmission of canine

distemper virus-an update. One Health. 2015; 1:49-59.
2. Budd J. Distemper. In: Infectious diseases of wild mammals. 1st ed. Ames, IA: Iowa State Press; 1970:36-49.
3. Caswell J, Williams K. Respiratory system. In: Maxie MG, ed. Jubb, Kennedy, and Palmer's Pathology of Domestic Animals. Vol 2. 6th ed. Philadelphia, PA: Elsevier Saunders; 2016: 574-575.
4. Hunter DB. Respiratory System of Mink. In: Hunter B, Lemieux N, eds. Mink: Biology, Health and Disease. Guelph, Ontario: Graphic and Print Services, University of Guelph; 1996:13-1 – 13-15.
5. Kuipel M, Perpinan D. Viral Diseases in Ferrets. In: Biology and Diseases of the Ferret. 3rd ed. Ames, IA: Wiley Blackwell; 2014:439-450.
6. Noyce R, Depeut S, Richardson C. Dog nectin-4 is an epithelial cell recepotor for canine distemper virus that facilitates virus entry and syncytia formation. Virology. 2013;436:210-220.
7. Oglesbee M. Intranuclear inclusions in paramyxovirus-induced encephalitis: evidence for altered nuclear body differentiation. Acta Neuropathol. 1992;84:407-415.
8. Oglesbee M, Krakowa S. Cellular stress response induces selective intranuclear trafficking and accumulation of morbillivirus major core protein. Lab Invest. 1993; 68:109-107.9. Williams ES. Canine Distemper. In: Williams ES, Barker IK, eds. Infectious diseases of wild mammals. 3rd ed. Ames, IA: Iowa State Press; 2001:50-59.
10. Qiu W[1], Zheng Y, Zhang S, Fan Q, Liu H, Zhang F, Wang W, Liao G, Hu R. Canine distemper outbreak in rhesus monkeys, China. Emerg Infect Dis. 2011 Aug;17(8):1541-3.
11. Sakai K[1], Nagata N, Ami Y, Seki F, Suzaki Y, Lethal canine distemper virus outbreak in cynomolgus monkeys in Japan in 2008. J Virol. 2013 Jan;87(2):1105-14.

CASE IV: 09-1045 (JPC 3164901).

Signalment: 5 year old, ovariohysterectomized female Cavalier King Charles spaniel, *Canis familiaris*.

History: An adult spayed female Cavalier King Charles Spaniel reported to be 5 years old from a the household with multiple dogs exhibiting increased respiratory rate and cough. During thoracic radiographs the patient became agonal and arrested despite attempted cardiopulmonary resuscitation. Radiographs revealed pneumonia. The patient was presented for necropsy 1.5 hours following death

Gross Pathology: The trachea is diffusely mildly compressed dorsoventrally. Excluding a limited regional portion of the cranial aspect of the left cranial lung lobe, the lungs are diffusely dark red, heavy, and sink in formalin. The heart is mildly

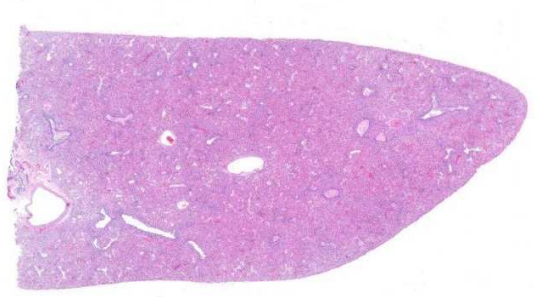

Lung: At subgross magnification, the lung is markedly congested, diffusely hypercellular, and there are blood vessels are surrounded by perivascular cuffs. (Photo courtesy of: University of Tennessee College of Veterinary Medicine, Department of Pathobiology, 2407 River Drive, Room A201, Knoxville, TN 37996 http://www.vet.utk.edu/)

enlarged with mild nodular thickening of the mitral valve. A small portion of the cerebellar vermis protrudes through a mildly narrowed and irregular foramen magnum.

Laboratory results:

Microbiology
Sample: Lung
Test: Aerobic Culture
Result: No growth seen in 3 days

PCR/DNA sequencing
99 % nucleotide identity with *Lycoperdon pyriforme* (AY854075.1, strain AFTOL-ID-48) over 682 bp.

Histopathologic Description: Lung: Alveoli and bronchioles frequently are filled with macrophages, neutrophils, cellular debris, erythrocytes, multinucleate giant cells and edema. The macrophages are frequently vesciulate, occasionally glassy eosinophilic material (hyalin membranes). Alveolar epithelial cells are multifocally cuboidal (type II pneumocyte hyperplasia) with rare binucleate and multinucleate cells. There is multifocal loss of the bronchiolar epithelium, with infrequent epithelial dysplasia. A few peribronchiolar macrophages contain black granular pigment (anthracosis). Moderate numbers of plasma cells with fewer lymphocytes surround pulmonary vessels. Vascular endothelial cells are frequently hypertrophic. Pleural mesothelial cells are hypertrophic.

Contributor's Morphologic Diagnosis: Marked, diffuse, histiocytic interstitial pneumonia with fungal spores.

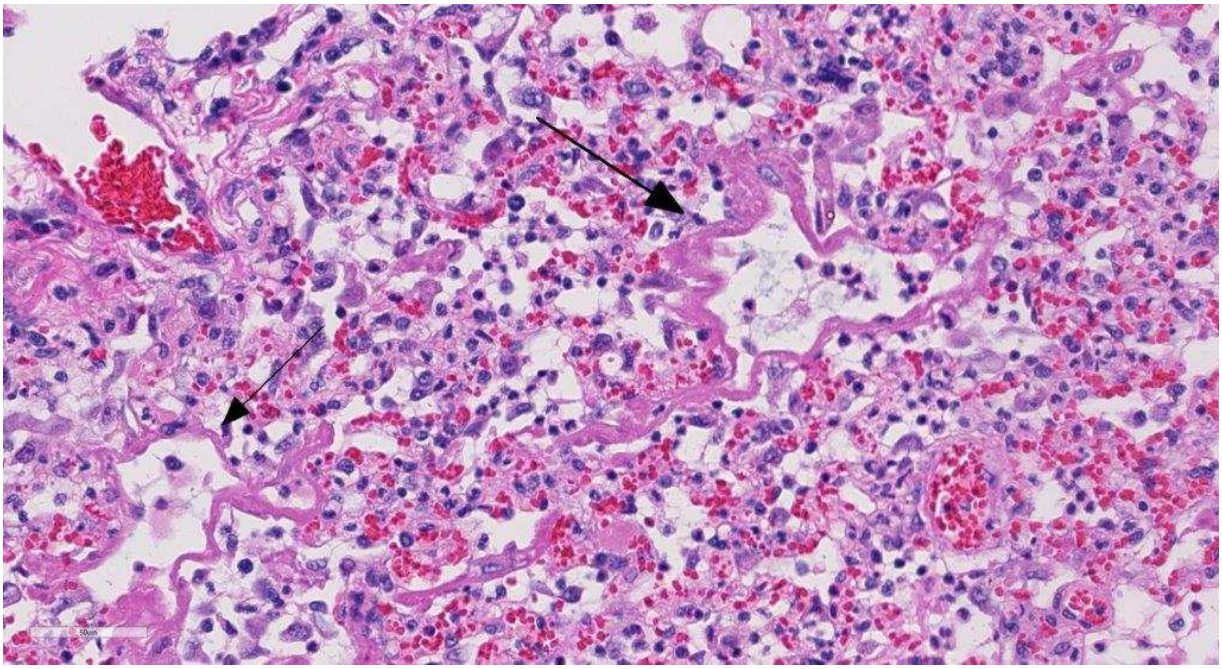

Lung, dog. Alveoli and distal airways are often lined by thick mats of fibrin (hyaline membranes). Alveoli contain moderate numbers of neutrophils and macrophages as well as fibrin. Septa are expanded by edema, fibrin, as well as increased numbers of circulating neutrophils. (HE, 260X)

containing cellular and karyorrhectic debris. Random, individual to multiple, golden-brown, 3-5µm diameter fungal spores are present both within macrophages and free within the alveolar lumens. Alveolar septa are occasionally lined by finely fibrillar to

Contributor's Comment: The intra-histiocytic and free fungal spores within the lung were identified as spores of "puffball" mushrooms by PCR and DNA sequencing. Eleven species of puffball mushrooms

(*Lycoperdon sp*.) are indigenous to the area from which this case originated (greater Smoky Mountains). Inhalation of spores has been reported infrequently in association with pneumonia (pulmonary lycoperdonosis) in dogs[1,8] and humans[7,9].

JPC Diagnosis: Lung: Pneumonia, interstitial, necrotizing, fibrinosuppurative, and histiocytic, diffuse, chronic, severe with hyaline membrane formation and rare intrahistiocytic fungal spores.

Conference Comment: Pulmonary lesions caused by the inhalation of *Lycoperdon sp.* spores are theorized to result from the host hypersensitivity response to fungal spores acting as foreign bodies rather than an infectious process.[2,7] The failure to culture *Lycoperdon* from a reported case and inability of this saprophytic fungus to germinate under normal physiologic body temperatures supports this theory.[7] Hypersensitivity pneumonitis (HP), also known as extrinsic allergic alveolitis, is caused by

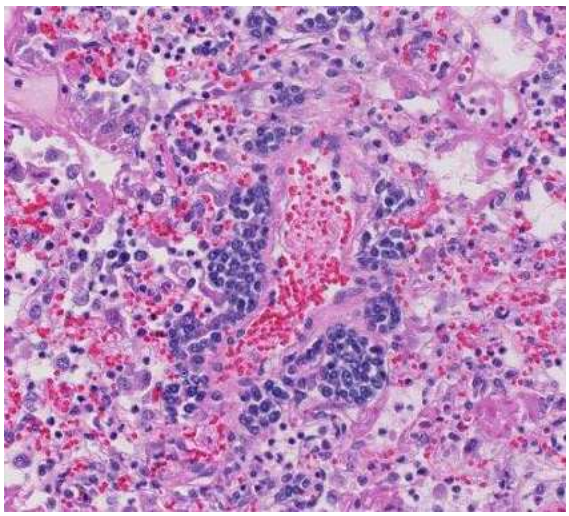

Lung, dog. Vessels throughout the sections are cuffed y 3-5 layers of lymphocytes and fewer plasma cells. (HE, 280X)

intense and often prolonged exposure to inhaled organic antigens such as fungal spores, but can also include bacterial products and animal proteins. This disease is commonly diagnosed in dairy cows and horses housed indoors and usually affect multiple animals within a group. It results from chronic inhalation of spores of thermophilic actinomycetes (*Saccharopolyspora rectivirgula*) found in moldy hay.[5,6] This is followed by an antibody response to inhaled antigen and local deposition of antigen-antibody complexes (Arthus reaction) as well as the formation of multifocal granulomas suggesting a T-cell-mediated response. This type of reaction suggests both type III and type IV hypersensitivity response [2,5,7] (See WSC 2012-2013, conference 22, case 4 for a review of hypersensitivity reactions).

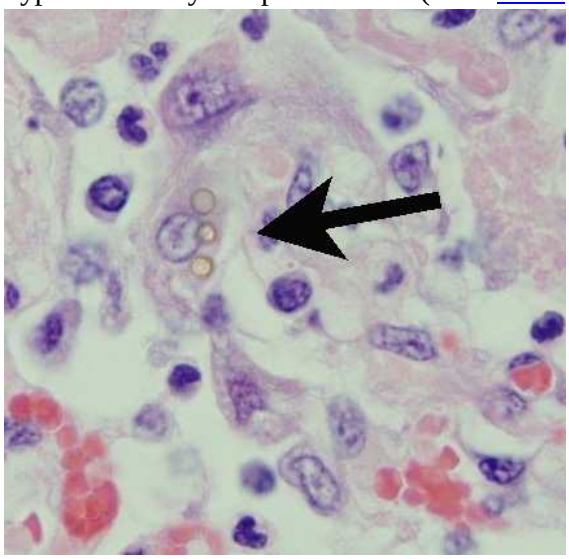

Lung: Rare macrophages contain single or multiple 4-6um golden-brown fungal spores. (HE, 400X)(Photo courtesy of: University of Tennessee College of Veterinary Medicine, Department of Pathobiology, 2407 River Drive, Room A201, Knoxville, TN 37996 http://www.vet.utk.edu/)

Characteristic lesions in animal and human HP include proliferation of type II pneumocytes and fibrosis of alveolar septa and peribronchiolar tissue. In severe cases, hyaline membranes composed of fibrin, serum proteins, and cell debris line the alveolar septa.[5] This hyaline membrane

causes alveolar occlusion resulting in severe hypoxia and death.

Conference participants noted the severe necrotizing and inflammatory changes to the lung interstitium, but had difficult time finding the rare fungal spores present in the tissue. Interestingly, clinical disease of lycoperdonosis in humans and dogs only occurs following a massive inhalation dose of puffball conidia[7]; however in this section there is a paucity of spores present. As a result, there was discussion of differentials

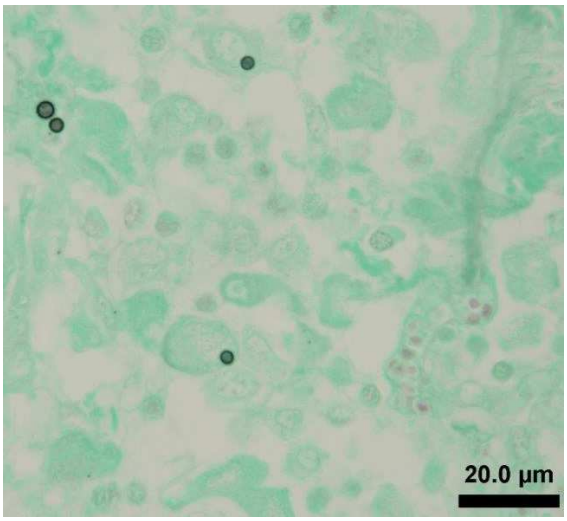

Lung: Fungal spores are argyrophilic on a Gomori methenamine silver stain. (GMS, 400X) (Photo courtesy of: University of Tennessee College of Veterinary Medicine, Department of Pathobiology, 2407 River Drive, Room A201, Knoxville, TN 37996 http://www.vet.utk.edu/)

for hyaline membrane formation, which is the most striking histologic feature in this case. Acute respiratory distress syndrome (ARDS) in the dog was discussed as having a similar histopathologic appearance to this case. In addition to hyaline membranes, type II pneumocyte hyperplasia, and bronchiolar epithelial necrosis is a consistent feature of ARDS. Inciting causes include: trauma, shock, disseminated intravascular coagulation, septicemia, smoke inhalation, oxygen toxicity, viral infection, and strangulation among others.[4]

This case was additionally studied in consultation with the Department of Pulmonary and Mediastinal Pathology at the Joint Pathology Center, who disagreed with the purported mechanisms discussed above, based on the morphologic changes noted in this section. Their interpretation is that this section of lung is diagnostic for diffuse alveolar damage (DAD) due to a toxic reaction to *Lycoperdon* spores rather than HP, published in a case report from this animal.[2] DAD is the most commonly identified form of interstitial lung disease and is the histologic correlate to the clinical condition of ARDS, discussed by conference participants.[4] The pulmonary pathologists describe an intra-alveolar inflammatory infiltrate composed predominantly of neutrophils and macrophages. This is admixed with focal plasma cells and lymphocytes, hyaline membranes, and acute inflammation of bronchiolar epithelium, along with multifocal fungal spores. They see no histologic evidence to support the diagnosis of HP. They also note the importance of recognizing this entity as DAD, and not HP, due to the high mortality rate for DAD, even with intensive supportive treatment.

Contributing Institution: University of Tennessee
College of Veterinary Medicine
Department of Pathobiology
www.vet.utk.edu/departments/path

References:

1. Aleghat T, Kellett-Gregory L, Van Winkle T: Lycoperdonosis in a dog, *Vet Pathol*. 2009;46:1046.
2. Alenghat T, Pillitteri C et al. Lycoperdonosis in two dogs. *J Vet Diagn Invest*. 2010;22:1002-1005.

3. Buckeridge D, Torrance A, Daly M. Puffball mushroom toxicosis (lycoperdonosis) in a two-year-old dachshund. *Vet Rec.* 2011;168:304.
4. Caswell J, Williams K. Respiratory system. In: Maxie MG, ed. *Jubb, Kennedy, and Palmer's Pathology of Domestic Animals*. Vol 2. 6th ed. Philadelphia, PA: Elsevier Saunders; 2016: 514.
5. Husain AN. The Lung. In: Kumar V, Abbas AK, Aster JC, eds. *Pathologic Basis of Disease.* 9th ed. Philadelphia, PA: Elsevier Saunders; 2015:694-695.
6. Lopez A. Respiratory system, mediastinum, and pleurae. In: Zachary JF, McGavin MD, eds. *Pathologic Basis of Veterinary Disease.* 5th ed. St. Louis, MO: Elsevier; 2012:513.
7. Munson E, Panko D, Fink, J. Lycoperdonosis: Report of Two Cases and Discussion of the Disease: *Clin Microbiol Newsl*. 1997;19(3):17-20.
8. Rubensohn M: Inhalation pneumonitis in a dog from spores of puffball mushrooms. *Can Vet Journal*. 2009;50(1):93.
9. Taft T, Cardillo R et al. Respiratory illness associated with inhalation of mushroom spores-Wisconsin, 1994. *MMWR Morb Mortal Wkly Rep*. 1994;43(29):525-526.

Self-Assessment - WSC 2016-2017 Conference 1

1. The cellular origin of chordoma is:
    a. Neural crest
    b. Notochord
    c. Somatic myotomes
    d. Bone marrow pluripotent cells

2. The process in which intact cells traverse hepatocytes or bone marrow cells without causing damage to either cell is called:
    a. Polesis
    b. Benign phagocytosis
    c. Intracellular trafficking:
    d. Emperipolesis

3. Disassociation of hepatic plates in certain infectious and neoplastic disease is the result of defect in:
    a. Acyl-glycerol in the Kreb's cycle
    b. B-catenin in the Wnt pathway
    c. E-cadherin in the EMT pathway
    d. Cathepsin B in the caspase cascade

4. Canine distemper virus is which type of virus:
    a. Single-stranded RNA virus
    b. Single-stranded DNA virus
    c. Double-stranded RNA virus
    d. Double-stranded DNA virus

5. The pathogenesis of pulmonary disease ascribed to lycoperdonosis is which of the following:
    a. Toxic damage to Type 1 pneumocytes
    b. Endotoxin release and damage to septal capillaries
    c. Hypersensitivity
    d. Generation of weak acids by degenerating spores within alveoli

Joint Pathology Center
Veterinary Pathology Services

WEDNESDAY SLIDE CONFERENCE 2016-2017

C o n f e r e n c e 2

31 August 2016

CASE I: Case #1(JPC 4085101).

Signalment: Adult female zika hybrid rabbit (*Oryctolagus cuniculus*).

History: This rabbit was part of an experimental vaccine development study. It was vaccinated twice against rabbit hemorrhagic disease virus followed by a challenge infection with rabbit hemorrhagic disease virus type 2. There were no obvious clinical findings in this rabbit following the challenge infection, and it was euthanized two weeks after the challenge infection according to the experimental plan.

Gross Pathology: The caudate lobe is mildly and diffusely shrunken with slightly rounded angles, a diffuse tan surface, and a sharp hilar demarcation line separating it from the inconspicuous remaining liver lobes. A cross section shows a markedly thickened, tan capsule; a chocolate-brown parenchyma with a pronounced tan periportal lobular pattern; and a firm texture.

Laboratory results: None

Histopathologic Description: Liver (two sections): There is diffuse disruption and collapse of the hepatic architecture with loss (atrophy) and replacement of > 95% of centrilobular and midzonal to panlobular hepatocytes by a moderately cellular, loose, reticular meshwork of pleomorphic spindloid cells (fibroblasts) and capillary sprouts. Centrilobularly-oriented parts of

Liver rabbit. Torsion of the lobus caudatus (flipped to the left side to expose the hilar demarcation line and the undivided right hepatic lobe).(Photo courtesy of: Friedrich-Loeffler-Institut, Federal Research Institute for Animal Health, Department of Experimental Animal Facilities and Biorisk Management, Südufer 10, 17493 Greifswald – Insel Riems, Germany. https://www.fli.de)

the remaining periportal hepatocytes display cellular swelling due to cytoplasmic feathery vacuolation (hydropic degeneration). There is a moderate amount of binucleated hepatocytes (regeneration).

There is mild, multifocal, centrilobular sinusoidal dilatation by erythrocytes (congestive hyperemia), as well as mild multifocal accumulations of extravascular erythrocytes (hemorrhages) and a moderate, diffuse infiltration by macrophages, mostly stuffed with multiple, cytoplasmic, brown granules (hemosiderosis), and lesser and variable concentrations and combinations of lymphocytes, plasma cells, and heterophils.

There is a moderately increased amount of periportal bridging bundles of collagen fiber-rich tissue (fibrosis), a severely increased number of portal bile ducts (biliary hyperplasia), moderately dilated lymphatic vessels, and severe thickening of the hepatic capsule (fibrosis).

There is a centrally located, 500 µm in diameter, relatively thin-walled blood vessel (vein) which is completely occluded by a variable amount of a densely packed, hypereosinophilic, fibrillary to beaded mass (fibrin-rich thrombus), which is partially and/or completely (depending on the slide) replaced by fibroblasts and numerous small caliber blood vessels with hypertrophic endothelium (granulation tissue), mildly infiltrated by hemosiderin laden macrophages (hemosiderosis).

Liver, rabbit. Cross section of the torsioned lobus caudatus showing a pronounced lobular pattern and thickenend capsule due to fibrosis..(Photo courtesy of: Friedrich-Loeffler-Institut, Federal Research Institute for Animal Health, Department of Experimental Animal Facilities and Biorisk Management, Südufer 10, 17493 Greifswald – Insel Riems, Germany. https://www.fli.de)

The other section of liver is unremarkable.

Contributor's Morphologic Diagnosis: Liver. Hepatocellular degeneration and loss (atrophy), diffuse, chronic, severe with reticular replacement, periportal bridging and capsular fibrosis, bile duct hyperplasia, venous thrombosis, congestive hyperemia, hemorrhage, and hemosiderosis.

Contributor's Comment: **Etiology:** The slide shows two sections from two strikingly different liver lobes from the same animal. The morphological changes in the section originating from the caudate lobe are consistent with subclinical, chronic, liver lobe torsion, whereas the architecture in the other section is unchanged. The etiology of liver lobe torsion remains enigmatic; however, a species-specific anatomical configuration with deep hepatic sulci, surgical or external trauma, congenital absence of hepatic ligaments, mass lesions within the affected lobe, and dilatation of abdominal organs are known to represent predisposing factors.[2,7] According to a recent review, the caudate lobe is affected in 62% of cases in rabbits, whereas the left lateral lobe is most prone to torsion in most other species.[4] The anatomic nomenclature of the liver of rabbits is controversial;[1] it generally consists of a left liver lobe, a quadrate lobe, a right liver lobe surrounding the gall bladder, a caudate lobe, and a processus papillosus. Some authors

subdivide the left and right lobe into medial and lateral parts;[1]however, there is no distinct subdivision in the present case.

Epidemiology: Liver lobe torsion occurs rarely in many species including rabbits, dogs, cats, pigs, horses, otters, rats, mice and human beings.[4]

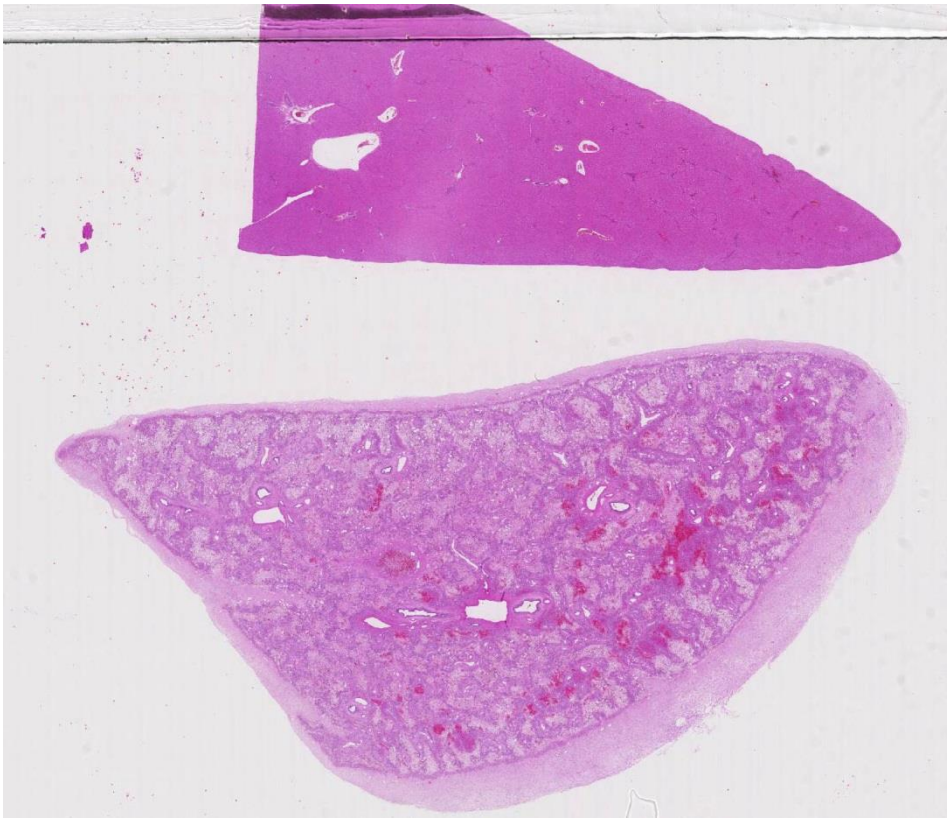

Liver, rabbit. Subgross magnification of a normal section of liver (top) and a section from the torsed lobe (bottom). The capsule is markedly thickened with a retiform pallor representing hepatocellular loss. There is multifocal hemorrhage throughout the section. (HE, 4X)

Clinical course: Clinical sequelae of liver lobe torsion range from subclinical, to an acute crisis with lethargy, abdominal pain, jaundice, anorexia, vomiting, collapse and sudden death.[7,8] Immediate partial hepatectomy is suggested to be the treatment of choice in symptomatic rabbits.[6]

Pathogenesis: Liver lobe torsion results in constriction of venous return leading to venous and/or arterial thrombosis, marked venous congestion, infarction, and ischemic necrosis of the affected lobe.[2] Affected rabbits may develop shock, abdominal hemorrhage, and/or septic peritonitis leading to acute cardiovascular failure and death. Liver lobe torsion may be diagnosed incidentally in surviving animals. These animals will have lobular hepatocellular atrophy, fibrosis, and chronic inflammation.[8]

JPC Diagnosis: Liver: Hepatocellular loss, centrilobular and midzonal, diffuse, severe, with marked portal bridging fibrosis, biliary hyperplasia, edema, and capsular fibrosis.

Conference Comment: The contributor provides a concise summary of hepatic torsion in the rabbit. This challenging case serves as a characteristic example of the liver's response to chronic severe hepatocellular injury secondary to congestion and ischemia caused by venous occlusion. In general, the liver responds to injury in three primary manifestations: regeneration, ductular reaction, and fibrosis.[2,5]

When hepatic injury is limited and the reticulin meshwork is intact, regeneration of mature hepatocytes is stimulated by hepatocyte growth factor (HGF), epidermal growth factor (EGF), transforming growth factor-α (TGF-α), and insulin-like growth factor (IGF).[2] Interleukin-6 (IL-6) secreted

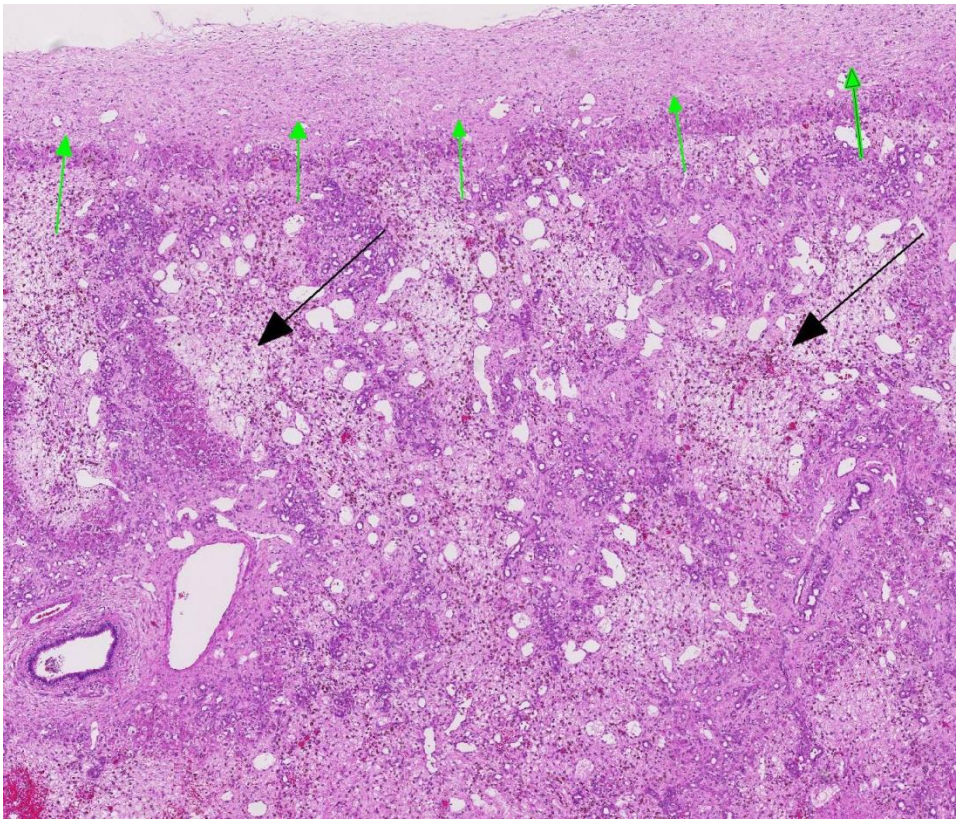

Liver, rabbit. Higher magnification of previous image which the capsule is markedly expanded by fibrous connective tissue (green arrows). The pale areas represent loss of centrilobular and midzonal hepatocellular loss. Marked biliary reduplication is evident at this magnification. There is diffuse dilation of both veins and lymphatics in this section. (HE, 60X)

by TGF-α activated Kupffer cells also stimulates hepatocellular regeneration.[2] Once hepatic mass has been replaced, transforming growth factor-β (TGF-β) inhibits ongoing proliferation of hepatocytes. In this case, there are occasional periportal multinucleated and vacuolated hepatocytes, suggesting attempted regeneration and degeneration.[2]

Ductular reaction is a similarly complex process. In severe liver injury with extensive loss of mature hepatocytes, there is stimulation of bipotential progenitor cells (oval cells in rodents), which normally reside in the periportal canals of Hering.[2,3,5] The canals conduct bile from bile canaliculi to bile ducts and are partially lined by hepatocytes and biliary epithelium.[2,5] Differentiation of bipotential progenitor cells, as well as de-differentiation and biliary metaplasia of mature hepatocytes, in response to severe liver damage is the basis for biliary ductular reaction patterns.[2,5]

Conference participants briefly disussed the types of ductular reactions and a relatively new classification pattern proposed by Desmet.[3] Ductular reactions are classified into type 1, in which mature bile ducts proliferate secondary to cholestasis; type 2 which is hepatocyte ductular metaplasia induced by inflammation, intoxication, or hypoxia; and type 3, which is the activation and proliferation of liver bipotential progenitor cells in response to massive hepatic parenchymal loss.[2,3] In this case, the ductular reaction likely started as type 2 and likely progressed to type 3 in response to chronic venous occlusion, hypoxia, fibrosis, and diffuse severe hepatocellular loss secondary to hepatic torsion.[2,3,5]

Finally, hepatic fibrosis also begins at the molecular level. Hypoxic hepatocytes induce hypoxia-inducible factor 1- α (HIF-1 α) and platelet derived growth factor (PDGF) to activate hepatic stellate cells within the space of Disse.[2] These cells then transform into myofibroblasts resulting in progressive diffuse hepatic fibrosis.[2] This stimulates centrilobular and periportal

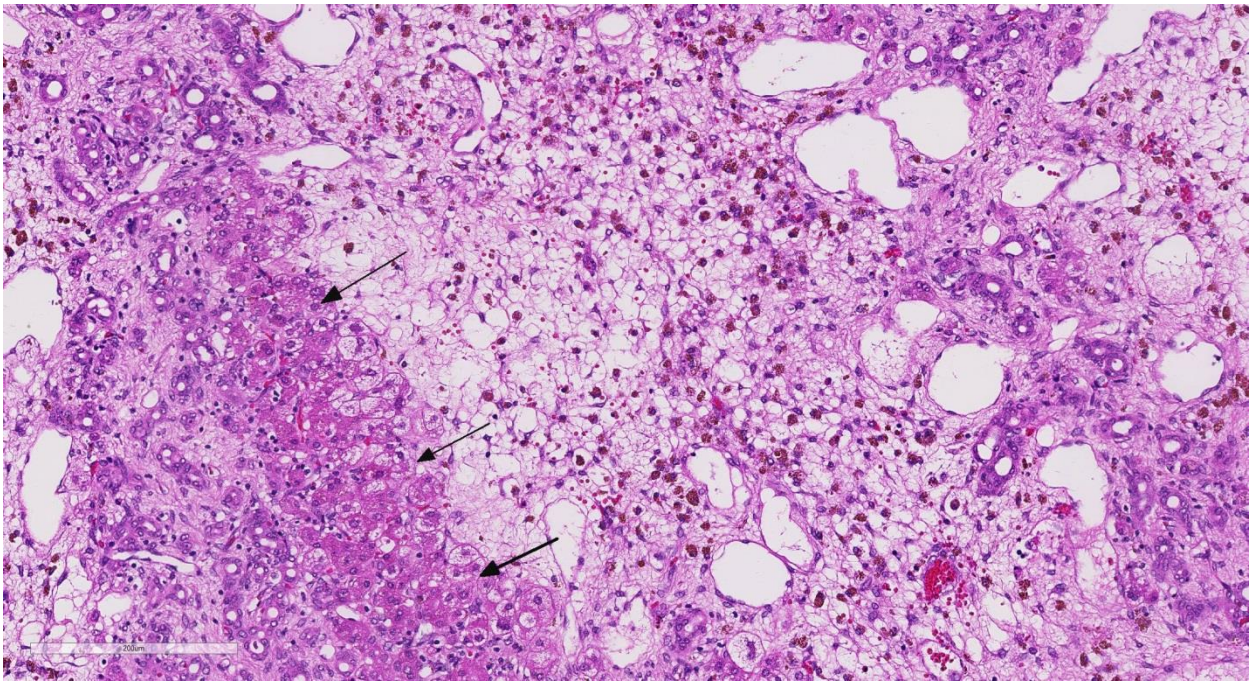

Liver, rabbit. There is diffuse loss of centrilobular and midzonal hepatocytes, with occasional sparing of periportal hepatocytes (arrows). The centrilobular and mizonal parts of the lobule are expanded by edema and contain large numbers of hemosiderin-laden macrophages. At left are large numbers of proliferating bile ductules and dilated lyphoatics. Remaining hepatocytes are often swollen with abundant fat and glycogen. (HE, 260X)

hepatocytes to dedifferentiate and eventually assume a biliary ductular phenotype.[3] On-going hypoxia and fibrosis then results in massive parenchymal loss. Remaining bi-potential progenitor cells in the canals of Hering then differentiate toward the biliary duct phenotype rather than differentiating to mature hepatocytes.[3] Persistence of ductular reaction further contributes to portal and periportal fibrosis through secretion of previously mentioned profibrogenic growth factors.[2]

Contributing Institution: Friedrich-Loeffler-Institut
Federal Research Institute for Animal Health
Department of Experimental Animal Facilities and Biorisk Management
Greifswald, Germany
https://www.fli.de

References:

1. Angeli C. Sonographische Untersuchung der abdominalen Organe beim Kaninchen. Vet Med Dissertation (Thesis). Ludwig-Maximilians-Universität, Munich, Germany; 2008. *https://edoc.ub.uni-muenchen.de/8735/1/Angeli_Carmen.pdf*
2. Cullen JM, Stalker MJ. Liver and Biliary System. In: Maxie MG, ed. *Jubb, Kennedy, and Palmer's Pathology of Domestic Animals*. Vol 2. 6th ed. Philadelphia, PA: Elsevier Saunders; 2016: 258-353.
3. Desmet VJ. Ductal plates in hepatic ductular reactions. Hypothesis and implications. I. Types of ductular reaction reconsidered. *Virchows Arch* 2011; 458:251-259.
4. Graham J, Basseches J. Liver Lobe Torsion in Pet Rabbits. Clinical Consequences, Diagnosis and

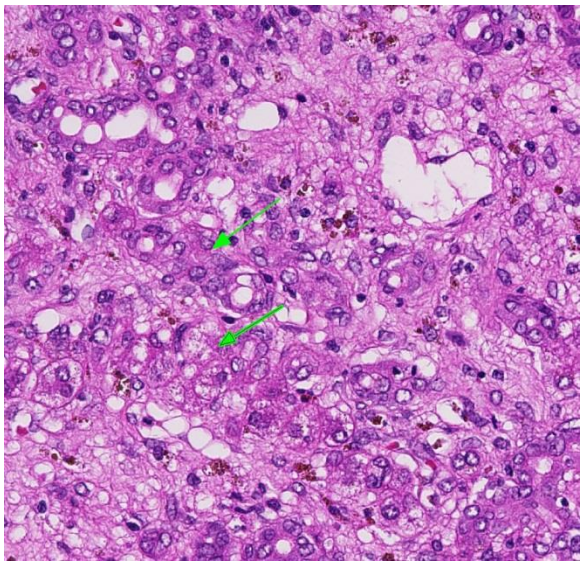

Liver, rabbit. Hepatocytes are regenerating within areas of proliferating bile ducts (Desmet Type 2 reaction). (HE, 400X)

Treatment. *Vet Clin Exot Anim.* 2014; 17:195-202.

5. Rothuizen J, Bunch SE, Charles JA, et al. Morphological classification of parenchymal disorders of the canine and feline liver: 1. Normal histology,

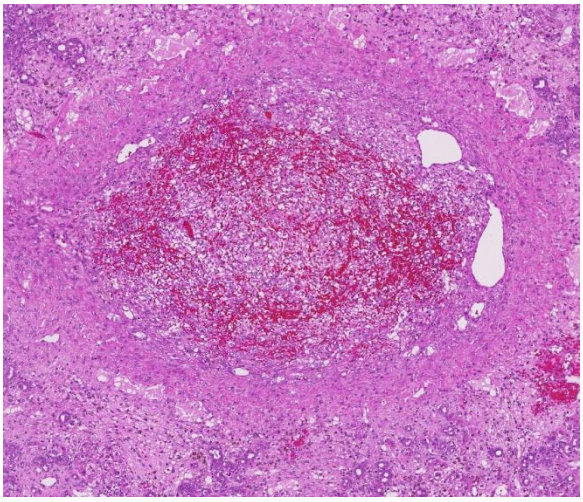

Liver, rabbit. A large branch of the portal vein is occluded by a large fibrinocellular thrombus. (HE, 40X)

reversible hepatocytic injury and hepatic amyloidosis; and 2. Hepatocellular death, hepatitis and cirrhosis. In: *WSAVA Standards for clinical and histological diagnosis of canine and feline liver disease*. St. Louis, MO: Elsevier; 2006:78-79, 85-88.

6. Stanke NJ, Graham JE, Orcutt CJ, Reese CJ, Bretz BK, Ewing PJ,

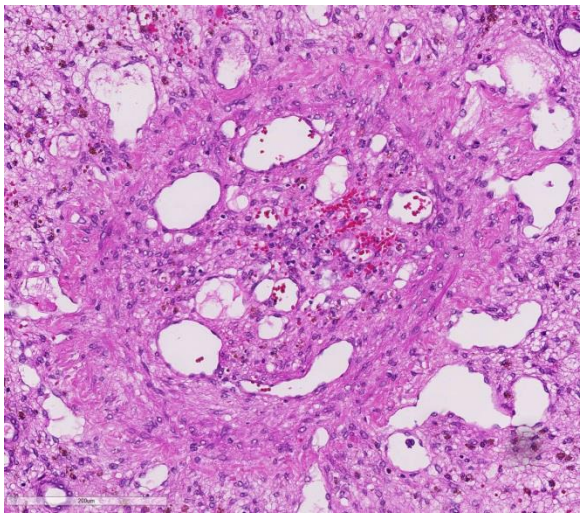

Liver, rabbit. The dilated lymphatics surrounding a sublobular vein impart the appearance of a "rose window" and attest to the severe edema in this section. (HE, 320X)

Basseches J. Successful outcome of hepatectomy as treatment for liver lobe torsion in four domestic rabbits. *JAVMA.* 2011; 238:1176-1183.

7. Wenger S, Barrett EL, Pearson GR, Sayers I, Blaey C, Redrobe S. Liver lobe torsion in three adult rabbits. *J Small Animal Practice.* 2009; 50:301-305.
8. Weisbroth SH. Torsion of the Caudate Lobe of the Liver in the Domestic Rabbit (Oryctolagus). *Vet Pathol.* 1975; 12:13-15.

CASE II: D16-01 (JPC 4083953).

Signalment: 1-year-old castrated male domestic shorthair (*Felis catus*).

History: The cat initially was presented to the referring veterinarian for anorexia and weight loss; upon examination, the cat had a fever, sneezing, and ocular and nasal discharge. The referring veterinarian prescribed prednisolone and doxycycline. Two weeks later, the cat was presented to the Kansas State University Veterinary Health Center. The cat was thin, and had fever, increased respiratory effort, peripheral lymphadenopathy, and ocular discharge. FIV-/FeLV and FCoV testing was negative. The cat was treated with blood transfusions, antibiotics, steroids, and oxygen supplementation, but worsened over the next two days. The cat was subsequently euthanized and sent to necropsy.

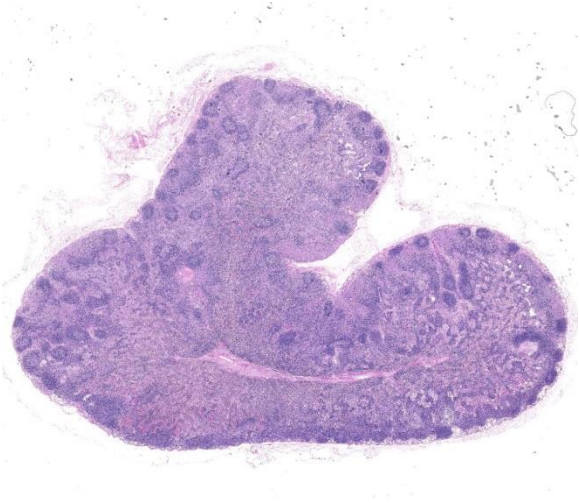

Lymph node, cat. Sinuses throughout the node are expanded by a prominent cellular infiltrate which separates and occasionally effaces lymphoid follicles (HE, 5X)

Gross Pathology: The cat was emaciated with diffuse pallor of the mucous membranes. The frontal sinuses were filled with thick yellow mucus. The submandibular, tracheobronchial, and mesenteric lymph nodes were diffusely enlarged, and the tracheobronchial lymph nodes were mottled dark-red and white. The lungs were diffusely orange-red and meaty with white miliary nodules. All lung sections sank in formalin.

Laboratory results: CBC revealed minimally regenerative anemia, leukopenia consisting of neutropenia with toxic changes and increased bands, and thrombocytopenia. Serum chemistry revealed hyperglycemia, hypoalbuminemia, decreased anion gap, decreased ALT and ALP, and increased bilirubin.

A bone marrow aspirate showed high nucleated cellularity with rare precursor cells and abundant macrophages containing numerous round to oval yeast bodies (~2-4 microns in diameter) that have a thin outer halo with an eccentrically placed, crescent shaped, basophilic nucleus. The findings were consistent with histoplasmosis.

Histopathologic Description: Lymph node: The subcapsular and medullary sinuses of the lymph node are diffusely expanded by proteinaceous fluid and large numbers of macrophages. In the medullary sinuses, macrophages contain abundant hemosiderin, and there is frequent erythrophagocytosis. Occasional multinucleated giant cells are present, bearing up to 5 nuclei. Macrophages frequently contain intracytoplasmic 2-4 um diameter yeasts consisting of a 1-2 um diameter basophilic nucleus and a 1-2 um clear halo (capsule). The cortex of the lymph node contains numerous active germinal centers.

Large numbers of macrophages with intracytoplasmic yeasts are also present in the lungs (alveolar interstitium and lumina), spleen (red pulp), liver (portal tracts and sinusoids), kidney (perivascular interstitium), intestine (lamina propria and Peyer's patches), and bone marrow (diffuse), as well as circulating macrophages in the brain and heart vasculature.

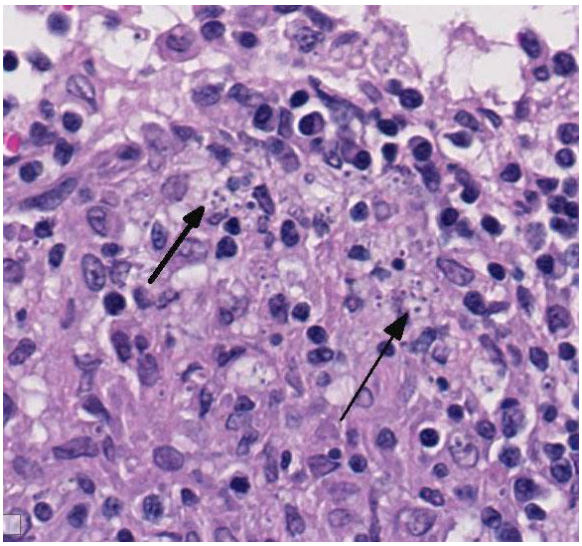

Lymph node, cat. The paracortex is expanded by large numbers of epithelioid macrophages which contain numerous 2-4um intracytoplasmic yeasts (arrows) (HE, 360X)

A GMS stain revealed abundant intracytoplasmic 2-4 µm diameter yeasts.

Contributor's Morphologic Diagnosis Lymph node; Granulomatous lymphadenitis, diffuse, severe, with numerous intrahistiocytic yeasts consistent with *Histoplasma capsulatum var capsulatum*

Contributor's Comment: *Histoplasma capsulatum* is a dimorphic fungus that exists in a parasitic yeast form called "*Histoplasma capsulatum*", and an environmental mycelial form called "*Ajellomyces capsulata*".[7] The organism is endemic in the St. Lawrence, Ohio, and Mississippi River valleys.[6] It is soil-borne and prefers nitrogen-rich organic matter such as bird and bat excrement.[3] The disease is non-contagious and affects humans as well as a wide variety of animals.[7] Infection is usually subclinical without signs or lesions, and can result in a latent state.[3]; however, clinically evident disseminated infection can occur with immunosuppression and/or heavy infectious dose, and usually results in death.[3] In this case, the cat was treated with steroids, which most likely predisposed it to the severe disseminated form of the disease.

Infection begins with ingestion or inhalation of soil contaminated with *Histoplasma* microconidia.[4] Pulmonary or gut-associated macrophages phagocytose the microconidia, which germinate into the yeast form and replicate within phagosomes.[7] In immunocompetent animals, Th1 cell-mediated immune responses eliminate the infection; in immunosuppressed states, the yeast-laden macrophages disseminate widely via the lymphatics and blood vessels to lymph nodes, liver, bone marrow, spleen, adrenal glands, etc.[7]

Histoplasma capsulatum evades the host's extracellular immune defenses by residing intracellularly within macrophages, and by concealing immunostimulatory beta-glucan cell wall components with non-immunostimulatory alpha-glucans.[5,7] The yeast is internalized via macrophage complement receptors such as CR3 and CR4 while avoiding activation of pro-inflammatory

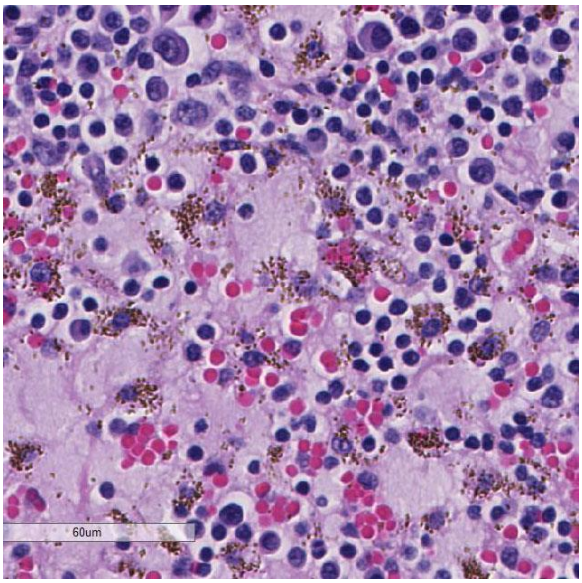

Lymph node, cat. Medullary sinuses are expanded by edema, hemorrhage, and erythrophagocytic and hemosiderin-laden macrophages. Medullary cords contain large numbers of plasma cells, indicating reactive hyperplasia. (HE, 400X)

receptors such as TLR2 and TLR4.[5] Once inside the phagosome, the fungus produces antioxidant enzymes including superoxide dismutase Sod3 and catalases CatB and CatP.[5,7] It also prevents acidification of the phagosome and fusion of lysosomes by as yet unknown mechanisms.[5] Other described virulence factors are involved with nutrient acquisition and production, including iron-scavenging hydroxamate siderophores, calcium-binding protein Cbp1, and various nucleic acid- and vitamin-synthesizing enzymes.[5,7]

Clinical signs include fever, malaise, emaciation, diarrhea, nonregenerative anemia, and respiratory distress.[2-4] Gross lesions include enlargement or thickening of affected organs – including lymph-adenopathy, splenomegaly, hepatomegaly, thickened bowel walls, and interstitial pneumonia.[2-4] Histologically, organ involvement is characterized by granulomatous infiltration with large numbers of mononuclear phagocytes bearing characteristic intracellular yeasts, as well as variable numbers of lymphocytes, plasma cells, and multinucleated giant cells.[3,4] Histochemical stains such as silver stains, periodic acid-Schiff, or Giemsa stains can highlight yeast organisms. For antemortem diagnosis, cytology from rectal scrapings or fine needle aspirates from lymph nodes and internal organs can also demonstrate intrahistiocytic yeasts.[3,4,6] Fungal culture is hazardous, however, due to infectivity of microconidia produced in the mycelial phase. Ketoconazole, itraconazole, and fluconazole alone or in combination with amphotericin B has been used to successfully treat dogs and cats.[2-4] Itraconazole is the recommended treatment of choice.[3,4]

JPC Diagnoses: 1**.** Lymph node: Lymphadenitis, granulomatous, multifocal to coalescing, marked, with mild reactive lymphoid hyperplasia and sinus edema.
2. Lymph node: Draining hemorrhage with hemosiderosis.

Conference Comment: The contributor provides an excellent summary of the virulence factors produced by *Histoplasma capsulatum* to evade the host immune response and produce severe disease. Post-exposure, the infected host requires both innate and adaptive immunity to neutralize the pathogen and overcome the virulence factors mentioned above.[5] Macrophages rapidly phagocytose inhaled conidia and subsequently stimulate pro-inflammatory cytokines such as IFN- γ, TNF-α, and IL-12 associated with a Th1 cell mediated response.[5,7] Macrophages also produce superoxide radicals, nitric oxide and other lysosomal enzymes to destroy the phagocytosed pathogen.[1] However, as mentioned by the contributor, *Histoplasma capsulatum* evades destruction within the phagolysosome and can survive, replicate, and disseminate to multiple tissues within macrophages.[5] In this case, conference participants noted several instances of characteristic narrow-based budding of the organism within macrophages.

Conference participants also discussed dendritic cells as an important component of the innate immune response to this organism. Dendritic cells typically phagocytose and destroy the organism with higher efficacy than macrophages. In addition, they present antigens to naïve CD4+ and CD8+ lymphocytes via MHC-1 to generate a T cell mediated immune response and destroy infected cells.[1] Cell-mediated immunity (CMI) is crucial for the host to clear the organism and T cells, as the central effectors CMI, are necessary to degrade the pathogen.[1,5,7] Severe disease occurs in immunosuppressed animals as

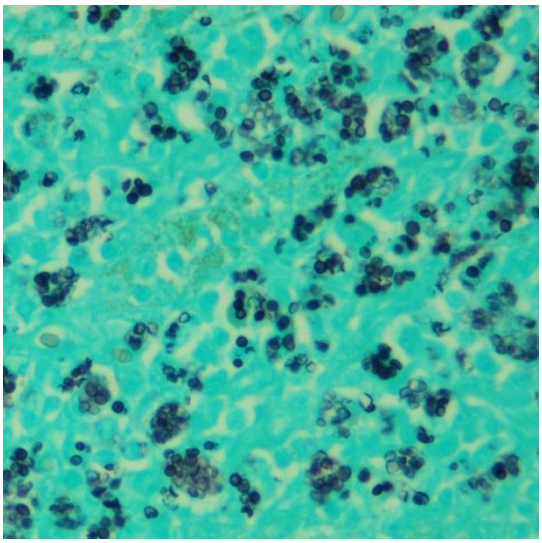

Liver, cat. A silver stain demonstrates the large numbers of intracytoplasmic yeasts within the cytoplasm of numerous macrophages (GMS, 400X) (Photo courtesy of:

well as hosts with a bias toward a Th2 humoral response. Humoral immune responses generally have a limited role in the clearance of intracellular pathogens.[5,7]

The nature of the inflammation within the lymph node generated spirited discussion during the conference, as it has so many times before over the many years of the Wednesday Slide Conference. Some conference participants preferred histiocytic, rather than granulomatous lymphadenitis. Those favoring the term "histiocytic" noted the paucity of multinucleated giant cells and lack of activated fibroblasts surrounding aggregates of infected macrophages, histologic features often associated with the more typical granulomatous response. Due to variation in sections, others noted more numerous multinucleated giant cell macrophages surrounding accumulated epithelioid macrophages and preferred granulomatous lymphadenitis. Conference participants also posited that the subcapsular location of many of the aggregating macrophages may be secondary to antigen presentation within pre-existent lymphoid follicles. This would stimulate follicular lymphoid hyperplasia and medullary plasmacytosis with Russell body-laden Mott cells, as seen in this case.

Contributing Institution: Kansas State Veterinary Diagnostic Laboratory
1800 Denison Avenue
Manhattan, KS 66506
http://www.ksvdl.org

References:

1. Ackerman M. Inflammation and healing. In: McGavin MD, Zachary JF, eds. *Pathologic Basis of Veterinary Disease*. 5th ed. St. Louis, MO:Mosby Elsevier; 2012: 89-146.
2. Aulaka HK, Aulakh 2. KS, Troy GC. Feline histoplasmosis: a retrospective study of 22 cases (1986-2009). *J Am Anim Hosp Assoc.* 2012; 48(3):182-187.
3. Brömel C, Greene CE: Histoplasmosis. In: Greene CE, ed. *Infectious Diseases of the Dog and Cat.* 4th ed. St Louis, MO: Elsevier Saunders; 2012:614-621.
4. Brömel C, Sykes JE. Histoplasmosis in dogs and cats. *Clin Tech Small Anim Pract.* 2005; 20(4):227-32.
5. Garfoot AL, Rappleye CA. Histoplasma capsulatum surmounts obstacles to intracellular pathogenesis. *FEBS Journal* 2015; 283:619-633
6. Kerl ME: Update on canine and feline fungal diseases. *Vet Clin North Am Small Anim Pract* 2003; 33:721-747.
7. Woods, JP. Revisiting old friends: Developments in understanding *Histoplasma capsulatum* pathogenesis. *J Microbiol* 2016; 54:265-276.

CASE III: G11362-A661 (JPC 4085318).

Signalment: 2-month-old female Belgian warmblood foal (*Equus ferus caballus*).

History: The foal had a sudden onset of diarrhea and fever (40°C). Blood examination revealed elevated liver values and abdominal ultrasound showed edema of the colon wall. Despite treatment the foal died quickly.

Gross Pathology: The foal was admitted for necropsy and postmortem examination revealed a good nutritional condition, and moderate dehydration. Petechial bleedings were noticed on the pleura, the pericardium, the thymus, the splenic capsule and on the serosa of the intestine. The kidneys showed numerous cortical white to gray foci and congestion of the medulla. The intestines were dilated with an edematous wall and a mucoid gray content.

Kidney, foal: Grossly, the kidney surface is studded by the projections of embolic microabscesses. (Photo courtesy of:

Laboratory results: Bacteriology of the kidney: positive for *Actinobacillus equuli subsp. Haemolyticus*

Parasitology of the feces: positive for strongyles.

Histopathologic Description: Kidney: Randomly scattered within the cortex and occasionally extending into the medulla, there are numerous embolic microabscesses (0.3-0.40 mm in diameter) that regularly center on and efface glomeruli. These abscesses are composed of abundant necrotic debris (karyorrhexis, karyolysis, and pyknotic nuclei), admixed with many degenerate and non-degenerate neutrophils, fewer macrophages, lymphocytes and plasma cells. Multifocally within these microabscesses, there are large colonies of basophilic coccobacilli (1x2 µm). Abscesses occasionally extend into adjacent interstitium and tubules, with degeneration and necrosis of tubular epithelium. There are multifocal areas of congestion, hemorrhage, and fibrin thrombi within vessels.

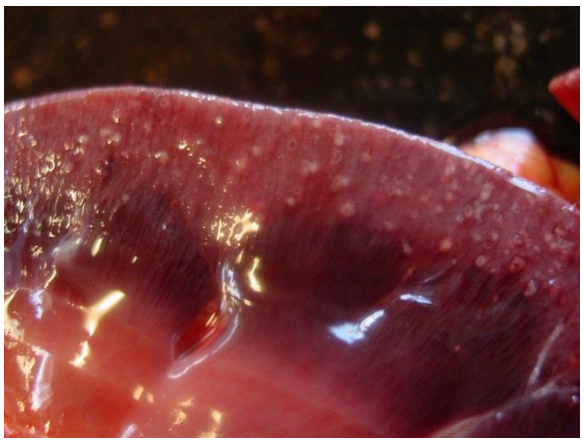

Kidney, foal: On cut section, microabscesses are present throughout the cortex, largely outlining glomeruli. (Photo courtesy of:

Contributor's Morphologic Diagnosis Kidney: Acute, severe, suppurative, embolic nephritis with intralesional coccobacilli.

Contributor's Comment: Actinobacillosis, also known as sleepy foal disease, is caused by *Actinobacillus equuli.* This is a small, nonmotile, gram-negative, pleomorphic coccobacillus. Certain strains of *A. equuli*

form part of the normal flora of the gastrointestinal and respiratory tracts of horses.[3-5] There is a high degree of strain variability within horse populations and within individual horses over time. It is currently unknown whether there are specific strains of *A. equuli* with greater virulence for foals and/or adult horses or whether such strains are common in-habitants of the equine gastrointestinal and respiratory tracts.[5]

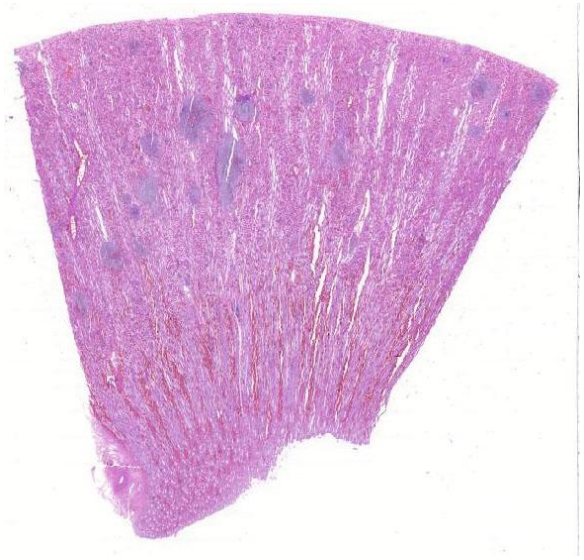

Kidney, foal: On subgross examination, areas of inflammation are scattered through randomly thoughout the cortex, and extend linearly along vessels into the outer medulla. (HE, 6X)

Two subspecies of *Actinobacillus equuli* have been identified: *A. equuli subsp. equuli*, and *A. equuli subsp. haemolyticus*.[1] The former appears to be pathogenic, while the latter's pathogenicity appears to be associated with its expression of a repeats-in-structural-toxin (RTX) called Aqx, which is cytotoxic for equine leukocytes.[1]

Typically actinobacillosis is a disease of newborn foals and the pathogenesis of the infection remains speculative. Infection is probably acquired in utero, during parturition, or shortly after birth as an umbilical infection.[1] Death may occur due to fulminating septicemia. In foals that survive for several days, microabscesses are seen in the kidney and other organs and a polyarthritis can be present. These microabscesses have an embolic origin and are characterized by the presence of numerous, 1-3 mm, white pinpoint foci on the cut surface throughout the renal cortex. Microscopically, glomerular capillaries contain numerous bacterial colonies intermixed with necrotic debris and extensive infiltrates of neutrophils that often obliterate the glomerulus.[4]

The lesions in our case are classic for *Actinobacillus equuli*, and the foal was also positive for strongyles. It has been postulated that migrating strongyle larvae from the intestinal tract may play a role in infection.

JPC Diagnosis: Kidney, cortex and medulla: Nephritis, embolic, suppurative,

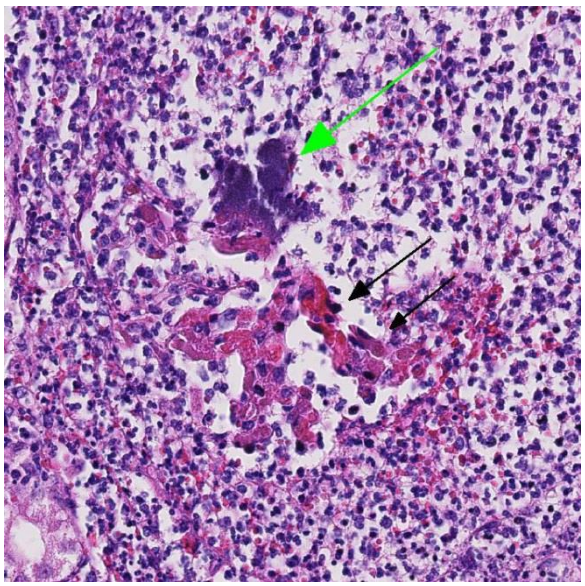

Kidney, foal: Glomeruli are often effaced by large numbers of degenerate neutrophils admixed with cellular debris. Here, the remnant of a glomerulus contains a large bacterial colony (green arrow) within the fragmented tuft. (black arrow) (HE, 400X)

acute, severe, with large colonies of coccobacilli.

Conference Comment: Despite some slide variability, the histopathologic appearance of this lesion is a classic for suppurative and embolic nephritis caused by *Actinobacillus equuli*. This entity is the most common cause of suppurative and embolic nephritis in young horses.[1] In pigs, embolic nephritis is most commonly caused by *Erysipelothrix rhusiopathiae*. In cattle, *Trueperella pyogenes* from valvular endocarditis causes numerous septic emboli, which shower the renal cortex causing randomly distributed microabscesses and infarcts. *Corynebacterium pseudotuberculosis* is most com-mon in sheep and goats, *Pasteurella multocida* in rabbits, and *Streptococcus moniliformis* in mice.[1,4] In dogs, *Prototheca zopfii* organisms have been identified as a common cause of embolic nephritis secondary to systemic protothecosis.[1] Endotoxin expressed by gram-negative bacteria and *Streptococcus* sp. causes endothelial damage, vasculitis, and bacterial emboli.[1,4] Most conference participants noted ectatic tubules containing necrotic and sloughed tubular epithelial cells, fibrin, hemorrhage, and proteinaceous fluid. Participants also noted occasional fibrin thrombi with colonies of coccobacilli within glomerular tufts, as well as parietal cell hyperplasia secondary to the effects of endotoxin.

This case illustrates the characteristic appearance of the large colony-forming coccobacilli, *Actinobacillus equuli*, in tissue section. In addition to discussing causes of embolic nephritis in other species, conference participants also reviewed other bacteria that form large colonies in tissue. These bacteria are difficult to distinguish from one another other on hematoxylin and eosin stain (H&E), and require special stains or bacterial culture.[1] Gram-positive large colony forming bacteria include: *Staphylococcus*, *Streptococcus*, *Actinomyces*, and *Corynebacterium* spp.; while gram-negative large colony forming bacteria include *Yersinia* and *Actinobacillu*s spp.[1,4] Several conference members men-tioned the acronym, YAACSS, as a helpful mnemonic device to remember which bacteria form large colonies in tissue section.

Contributing Institution: Department of Pathology, Bacteriology and Poultry Diseases
Faculty of Veterinary Medicine
Ghent University
Merelbeke, Belgium
http://www.vetpbp.ugent.be

References:

1. Cianciolo RE, Mohr FC, Urinary system, In: Maxie MG, ed. *Jubb, Kennedy, and Palmer's Pathology of Domestic Animals*. Vol 2. 6th ed. Philadelphia, PA: Elsevier Saunders; 2016: 432-433.
2. Frey J. The role of RTX toxins in host specificity of animal pathogenic Pasteurellaceae. *Vet Microbiol*. 2011; 153:51-58. WSC 2012-2013.
3. Matthews S, Dart AJ, Dowling BA, et al. Peritonitis associated with Actinobacillus equuli in horses: 51 cases. *Aus Vet J*. 2001; 79:536-539.
4. Newman SJ: Urinary System. In: eds. McGavin MD, Zachary JF: *Pathologic Basis of Veterinary Disease*. 5th ed. St. Louis, MO: Mosby Elsevier; 2012:649.
5. Patterson-Kane JC, Donahue JM, Harrison LR. Septicemia and peritonitis due to Actinobacillus equuli infection in an adult horse. *Vet Pathol*. 2001; 38:230-232.

CASE IV: 6M22955A (JPC 4083344).

Signalment: 2-month-old male crossbreed calf (*Bos taurus*).

History: Respiratory issues in multiple 2-month old calves.

Gross Pathology: Cranioventral lung lobes were consolidated and covered in areas with fibrin.

Laboratory results: Lung: *Mannheimia haemolytica*

Immunohistochemistry: Bovine viral diarrhea virus (BVD)

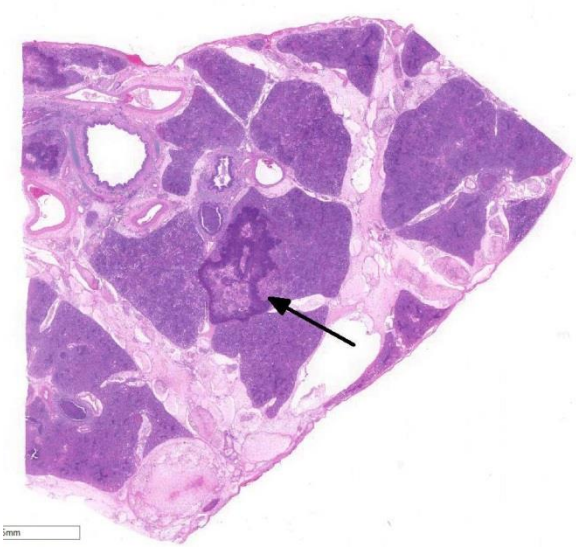

Lung, calf: Subgross examination demonstrates diffuse filling of airways and alveoli with a cellular exudate and a focal area of infarction outlined by a dense band of cellular debris (arrow). The interlobular septa are expanded by edema and fibrin thrombi within lymphatics. (HE, 5X)

Animal ID	Specimen	Result	Comment
A	Assorted	Positive	marked immunolabeling

PCR - Bovine Respiratory Bacterial Panel

Animal ID	Specimen	Target Agents	Ct / Result
A, Tube #1	Lung	*Pasteurella multocida*	>40 / Negative
		Mycoplasma bovis	>40 / Negative
		Mannheimia haemolytica	19.7 / Positive
		Histophilus somni	16.9 / Positive

PCR - Bovine Respiratory Viral Panel

Animal ID	Specimen	Target Agents	Ct / Result
A, Tube #1	Lung	IBR	/ Negative
		BCV	/ Negative
		BRSV	/ Negative
		BPI3	/ Negative

Histopathologic Description: Lung: There are marked multifocal and extensive areas of necrosis demarcated by dense zones of neutrophils which form a subgross mosaic pattern. The necrotic regions contain large amounts of seroproteinaceous fluid, red blood cells, neutrophils and cell debris; some cells are degenerate with elongate nuclei (streaming leukocytes/oat cells). In remaining tissue, multifocal bronchi and bronchioles are dilated and contain large numbers of neutrophils and cell debris. There is diffuse thickening of the inter-lobular septa by edema and infiltrates of neutrophils. In one lobular area there is moderate thickening of alveolar septa by mild to moderate type II cell hyperplasia and occasional infiltrates of lymphocytes and macrophages. The pleura is thickened by edema and covered in some areas by a thick mat of fibrin and cell debris.

Contributor's Morphologic Diagnoses Marked multifocal and extensive acute necrotizing and fibrinosuppurative pneumonia/bronchopneumonia with fibrinous pleuritis.

Contributor's Comment: Bovine respiratory disease (BRD) complex is multifactorial and susceptibility is related to stress, environmental and housing

conditions, management, hydration and immune status, and exposure/levels of microbial pathogens.[5] Feedlot density has increased progressively in the United States and global demand for beef is trending upward; therefore, the incidence of BRD may continue to increase over time.[5] Viral infections with agents such as bovine respiratory syncytial virus (BRSV), bovine parainfluenza virus 3 (BPIV-3), bovine viral diarrhea virus (BVDV), bovine coronavirus (BCV), and bovine herpesvirus (BHV-1) can damage mucosal epithelia, decrease mucin production, as well as hinder innate and adaptive immune responses. This predisposes calves to secondary infections with bacteria, such as *Mannheimia haemolytica* and *Histophilus somni*, as in this case, as well as *Pasteurella multocida*, and *Mycoplasma bovis*.[1]

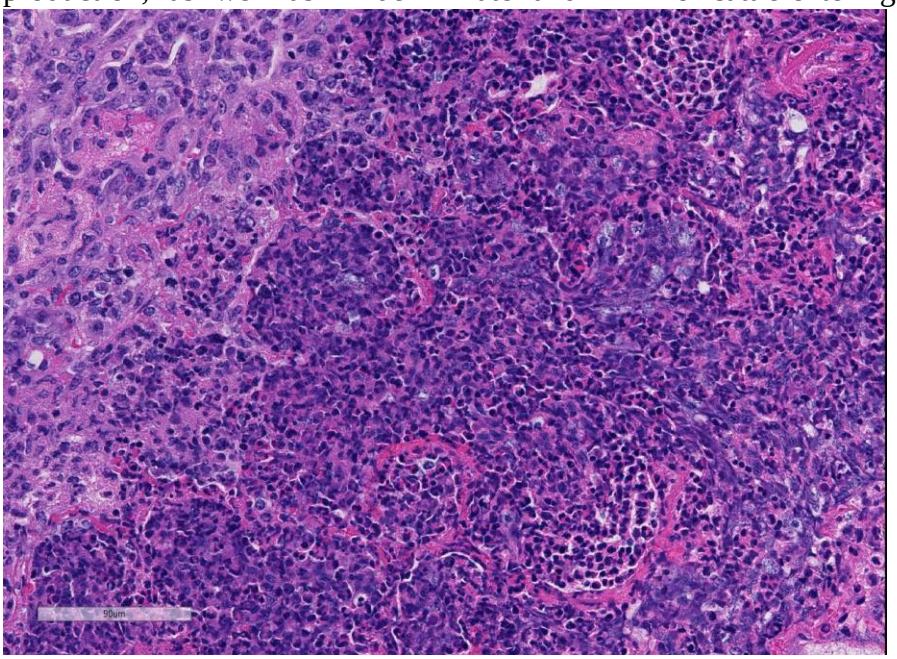

Lung, calf: Alveoli are filled with degenerate neutrophils with streaming nuclei (oat cells) admixed with abundant cellular debris. (HE, 300X)

In a 2005 study, the prevalence of BVDV was determined in 2000 cattle arriving to a feedlot. The prevalence of persistently infected (PI) cattle was only 0.3%, but 2.6% of chronically ill cattle, and 2.5% of dead cattle were BPIV-3 positive. Cattle exposed to a PI animal had an increased risk for treatment of BRD by 43%. In total, 15.9% of initial respiratory tract disease conditions were associated with exposure to a PI animal. Thus, very few cattle arrive to feedlot PI; however, those cattle are much more likely to require treatment and at place other cattle at-risk for incidence of respiratory disease.[4,6] Of the subtypes of BVDV, BVDV1b subtype is more commonly identified than BVDV1a and BVDV2a based on a survey of BVD isolates of cattle entering feedlots.[3] Experimentally, it has also been shown that exposure of steers to steers PI with BVDV enhances *M. haemolytica* disease severity.[1]

In this case, the animal had significant BVDV antigen detected by immunohistochemistry, which could alter lung and mucosal (e.g. tonsil) immunity, thus pre-disposing to enhanced bacterial rep-lication/colonization. Other factors such as stress and other viruses (e.g., BRSV, BPIV-3, coronavirus, BHV-1), could have contributed to this predisposition along with the BVD, although lesions of RSV, BPIV-3, and BHV-1 were not seen and BHV (IBR), BCV, BRSV, and BPIV-3 were not detected by PCR.

JPC Diagnosis: Lung: Bronchopneumonia, fibrinosuppurative and necrotizing, diffuse, severe, with numerous necrotic leukocytes (oat cells)

Conference Comment: This case is an excellent example of a classic presentation of the bovine respiratory disease complex (BRD). *Mannheimia haemolytica* is a gram-negative coccobacillus of the *Pasteurellaceae* family. It is typically is a commensal bacterium in the nasopharynx and tonsillar crypts of immunocompetent ruminants.[2] Many members of this family of bacteria can produce respiratory disease and septicemia in naïve and immunosuppressed domestic animals.[2,4,5] Other common pathogenic members of this family include: *Pasteurella multocida* of rabbits, swine, ruminants, and cats; *Bibersteinia trehalosi* and *Histophilus somni* in ruminants; *Actinobacillus pleuropneumoniae*, *A. suis*, *and Haemophilus parasuis* in swine; and *A. equuli* in horses.[2]

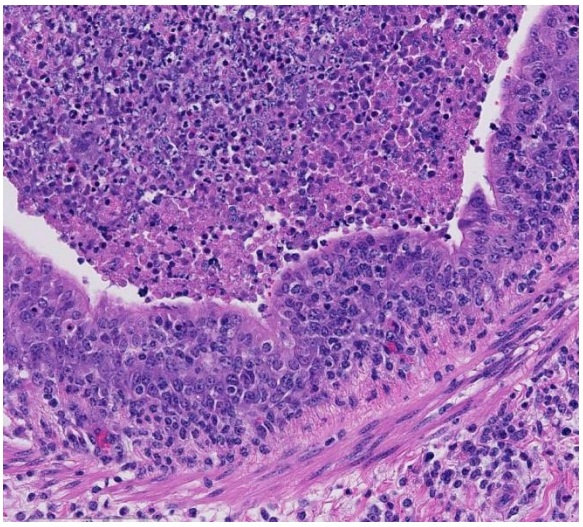

Lung, calf: Bronchioles are lined by moderately hyperplastic epithelium which is infiltrated by low numbers of neutrophils and cellular debris. The lumen contains abundant refluxed exudate from the surrounding alveoli. (HE, 300X)

There are twelve serotypes of *M. haemolytica* based on their capsular polysaccharide antigens.[2,5] Serotypes 1 and 2 are typically isolated from the upper respiratory tract of cattle as part of the normal commensal flora;[2] however, in a naïve or stressed animal, serotype 1 is often isolated from pneumonic lungs. As mentioned by the contributor, stress and cold weather causes the proliferation of commensal bacteria in the upper respiratory tract, overwhelming pulmonary defenses. In addition, co-infection with the respiratory viruses mentioned above can reduce mucociliary escalator clearance and impair the function of alveolar macrophages.[2]

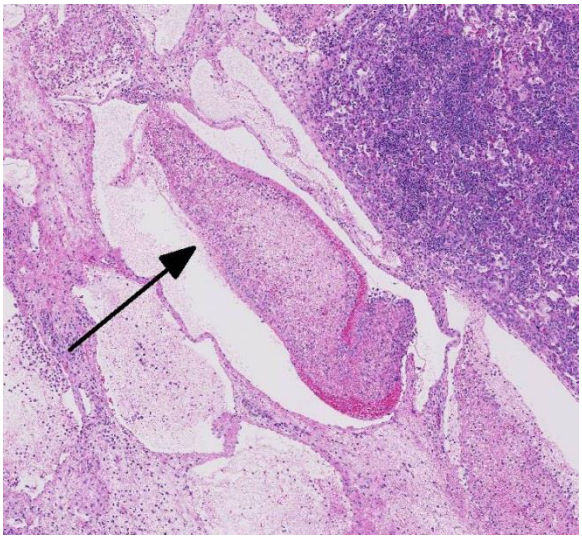

Lung, calf: Interlobular septa are expanded by abundant fibrin, edema, and moderate numbers of infiltrating neutrophils. Interlobular septa often contain fibrinocellular thrombi. (ARROW) (HE, 60X)

Conference participants briefly discussed the various virulence factors for *M. haemolytica* and how they contribute to the classic histopathologic appearance of this case. Virulence factors include: leukotoxin, lipopolysaccharide, capsular polysaccharide, transferring-binding proteins A and B, O-sialogylcoprotease, neuraminidase, IgG1-specific protease, outer membrane proteins, adhesins and fimbriae.[2] These virulence factors allow *M. haemolytica* to resist host clearance, avoid host defenses, and impair leukocyte function. The result is massive recruitment of neutrophils into alveoli, as seen in this case.[2,5] Neutrophils are ineffective at killing bacteria and cause damage to capillary endothelial cells,

resulting in hemorrhage, fibrin and edema in alveolar, interstitial, and interlobular spaces.[2]

Leukotoxin, a type of repeats in toxin (RTX), is an important exotoxin produced by *M. haemolytica*. It induces leukocyte recruitment at low concentrations and lysis of leukocytes and platelets in high concentrations.[2] Leukotoxin binds to CD18 on the leukocyte surface, forming a pore in the cell membrane. Interestingly, BoHV-1 causes the up-regulation of CD18 on the surface of neutrophils which makes these cells more susceptible to leukotoxin.[2] Lytic and necrotic leukocytes exhibit a streaming pattern of basophilic chromatin and are commonly referred to as "oat cells." [1,2,5,6]

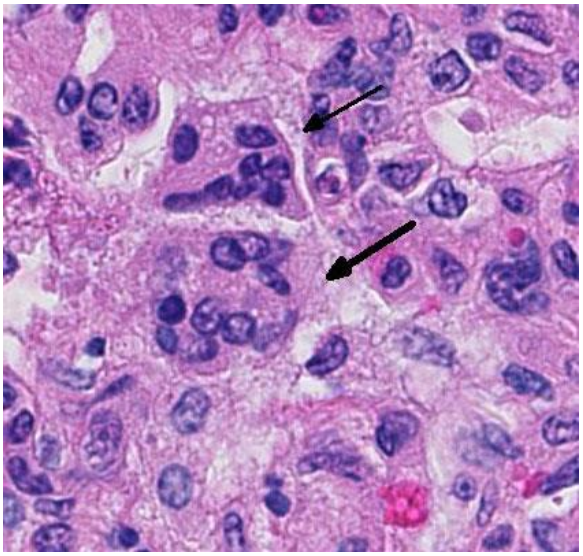

Lung, calf: Rare multinucleate viral syncytia (arrows) are present within some sections. (HE, 400X)

Most conference participants noted multi-focal fibrin thrombi present throughout pulmonary parenchyma. Additionally, in many slides, there was a sharply demarcated area of tinctorial change with loss of differential staining surrounded by a band of degenerate neutrophils- interpreted as an infarct. Focal areas of coagulation necrosis and infarction are characteristic for *M. haemolytica*.[2] These are secondary to thrombosis as well as direct damage to the lung by leukocyte secretion of pro-inflammatory IL-8, oxygen radicals, and nitric oxide synthetase. Activated alveolar macrophages also express tissue factor, which promotes the formation of fibrin thrombi.[2]

Contributing Institution: College of Veterinary Medicine
Iowa State University
Ames, IA
https://www.vetmed.iastate.edu/vpath

References:

1. Burciaga-Robles L, Step D, Krehbiel C, et al. Effects of exposure to calves persistently infected with bovine viral diarrhea virus type 1b and subsequent infection with *Mannheima haemolytica* on clinical signs and immune variables: Model for bovine respiratory disease via viral and bacterial interaction. *J An Sci*. 2010; 88:2166-2178.
2. Caswell J, Williams K. Respiratory system, In: Maxie MG, ed. *Jubb, Kennedy, and Palmer's Pathology of Domestic Animals*. Vol 1. 6th ed. Philadelphia, PA: Elsevier Saunders; 2016: 537-546.
3. Fulton W, Ridpath J, Ore S, et al. Bovine viral diarrhea virus (BVDV) subgenotypes in diagnostic laboratory accessions: Distribution of BVDV 1a, 1b and 2a subgenotypes. *Vet Microbiol*. 2005; 111:35-40.
4. Loneragan G, Thomson D, Montgomery D, et al. Prevalence, outcome, and health consequences associated with persistent infection with bovine viral diarrhea virus in feedlot cattle. *J Am Vet Med Assoc*. 2005; 226:595-601.

5. Mosier D. Review of BRD pathogenesis: The old and the new. *Anim Health Res Rev*. 2014; 15:166-168.
6. O'Conner A, Sorden S, Apley M. Association between the existence of calves persistently infected with bovine virus diarrhea virus and commingling on pen morbidity in feedlot cattle. *Am J Vet Res*. 2005; 66:2130-2134.

Self-Assessment - WSC 2016-2017 Conference 2

1. Which of the following is not true concerning liver lobe torsion?
    a. The caudate lobe is affected in 62% of cases in rabbits, whereas the left lateral lobe is most prone to torsion in most other species.
    b. When hepatic injury is limited and the reticulin meshwork is intact, regeneration of mature hepatocytes is stimulated by hep-atocyte growth factor (HGF), epidermal growth factor (EGF), transforming growth factor-α (TGF-α), and insulin-like growth factor (IGF).
    c. Once hepatic mass has been replaced, tran-sforming growth factor-β (TGF-β) inhibits ongoing proliferation of hepatocytes.
    d. Hypoxic hepatocytes transform into myofibroblasts resulting in progressive diffuse hepatic fibrosis.

2. Which of the following is true about *Histoplasma capsulatum*?
    a. It survives within macrophages.
    b. It is the only dimorphic fungus that does not have a mycelial phase in the environment.
    c. It is endemic to the San Joaquin Valley.
    d. Clearance of the organism is largely the result of an effective humoral response.

3. Which of the following does not produce large colonies in tissue?
    a. Yersina enterocolitica
    b. Actinobacillus equuli
    c. Klebsiella pneumonia
    d. Corynebacterium kutscheri

4. The severity of Bovine Respiratory Disease (BRD) is worsened by concurrent infection with bovine pestivirus.

    a. True
    b. False

5. Which of the following viruses is not considered part of the syndrome of Bovine Respiratory Disease?
    a. Bovine herpesvirus-1
    b. Bovine coronavirus
    c. Bovine retrovirus
    d. Bovine
    e. parainfluenza virus-3

Self-Assessment - WSC 2016-2017 Conference 2

1. Which of the following inhibits hepatocellular proliferation?
    a. TGF-α
    b. TGF-β
    c. Hypoxia-inducible factor 1-α
    d. Platelet derived growth factor

2. Which of the following is a common cause of embolic nephritis in the dog?
    a. *Prototheca zopfii*
    b. *Streptococcus moniliformis*
    c. *Actinobacillus equuli*
    d. *Erysipelothrix rhusiopathiae*

3. True or False: Co-infection of *Mannhemia hemolytica*-infected cattle with BVDV lessens the severity of the effects of *M. hemolytica.*
    a. True
    b. False

4. Which of the following is not true concerning *Mannheimia hemolytica?*
    a. *Mannheimia haemolytica* is a gram-negative coccobacillus of the *Pasteurellaceae* family.
    b. Leukotoxin, a type of repeats in toxin (RTX), is an important exotoxin produced by *M. haemolytica*.
    c. Serotypes 1 and 2 are typically isolated from the upper respiratory tract of cattle as part of the normal commensal flora, while serotype 2 is most commonly isolated from pneumonic animals.
    d. There are twelve serotypes of *Mannheimia hemolytica.*

5. Which of the following does not produce large colonies in tissue?
    a. Yersinia enterocolitica
    b. Actinobacillus equuli
    c. Klebsiella pneumoniae
    d. Corynebacterium kutscheri

Joint Pathology Center
Veterinary Pathology Services

WEDNESDAY SLIDE CONFERENCE 2016-2017

C o n f e r e n c e 3

7 September 2016

CASE I: CHIN1 (JPC 4084953).

Signalment: One-year-old female chinchilla (*Chinchilla lanigera*).

History: The owner had three chinchillas. Through the summertime, they were held in a fenced part of the garden. Animals were fed with guinea pig chow, apples, and raisins. Four days before death, they refused food, and one animal circled. All animals died and one was submitted for necropsy.

Gross Pathology: The liver was slightly enlarged with numerous pinpoint necrotic foci. Multifocal randomly distributed white foci were also visible throughout the small and large intestine, and few foci were in the myocardium.

Laboratory results: *Listeria monocytogenes* was isolated on bacterial culture of the liver.
Tissue gram stain: in necrotic foci, there are numerous intra- and extracellular road-shaped bacteria consistent with *Listeria monocytogenes*.

Histopathologic Description: Liver: There are multifocal, randomly distributed foci measuring 100-200 µm characterized by hepatocyte loss which are replaced with necrotic cellular debris and moderate numbers of degenerate neutrophils (lytic necrosis) and few macrophages. Often, necrotic foci contain variable numbers of intracellular and extracellular rod-shaped bacteria. Multifocally, randomly distributed smaller foci of hepatocytes are characterized by swollen, hypereosinophilic cytoplasm and loss of nuclei (coagulative necrosis). Throughout the liver are moderate numbers of hepatocytes that contain distinct cytoplasmic vacuoles consistent with lipid. Multifocally, mainly in periportal areas, there are scant infiltrates of lymphocytes and plasma cells.

Contributor's Morphologic Diagnosis: Liver: Moderate to severe, multifocal and random necrotizing and suppurative hepatitis with rod-shaped bacteria consistent with *Listeria monocytogenes*.

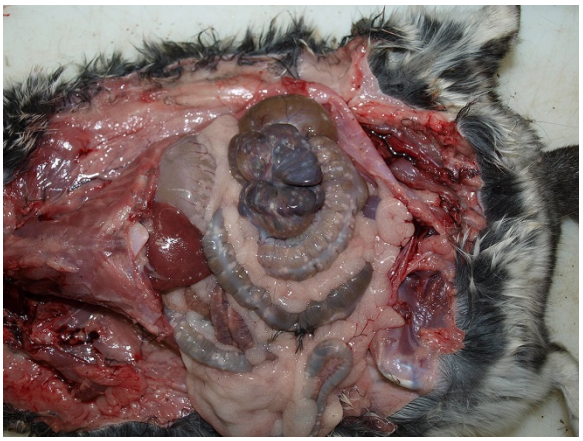

Abdominal viscera in situ, chinchilla: Numerous pinpoint foci are present within the liver and throughout the small and large intestine. (Photo courtesy of: Department of Veterinary Pathology, Faculty of Veterinary Medicine University of Zagreb, Heinzelova 55, 10000 Zagreb, Croatia. http://www.vef.unizg.hr/)

Contributor's Comment: Listeriosis is caused by *Listeria monocytogenes*, a gram-positive, facultatively anaerobic bacillus that is ubiquitous in the environment. The organism is commonly isolated from tissues of normal animals, including tonsils, other gut-associated lymphoid tissue, and feces of ruminants. The bacterium has also been isolated from soil, animal feed, water, and improperly stored silage.[1, 9] *Listeria monocytogenes* has more than 11 serotypes; almost all animal infections are caused by serotypes 1/2a, 1/2b, and 4b.[1]

Listeria monocytogenes is a facultative intracellular pathogen that invades host macrophages, neutrophils, and epithelial cells. Important virulence factors include the surface protein internalin, which interacts with host cell E-cadherin on the host cells, allowing the bacterium to cross the intestine, placenta, and blood-brain barrier. Once inside the cell, the organism also utilizes cholesterol-binding hemolysin to lyse phagolysosomes and escape into the cytoplasm. The organism proliferates in the host cell cytoplasm and migrates against the cell membrane to form protrusions that can then be taken up by adjacent cells.[1]

Listeria monocytogenes behaves as three separate rarely overlapping diseases or syndromes: infection of the gravid uterus with abortion; septicemia with miliary visceral abscesses or necrosis; and encephalitis.[1] Septicemic (systemic) listeriosis occurs in aborted fetuses and neonatal lambs, calves, foals up to one week of age, and young rabbits; it is characterized by multisystemic bacterial colonization and multifocal multisystemic areas of coagulative necrosis or microabscesses formation.[1, 7] Necrotic foci are numerous in the liver, but much less numerous in the heart and other viscera. Neonates generally become infected in utero.[1]

Liver, chinchilla. Closer view of the liver, with multiple foci of pinpoint necrosis scattered throughout all lobes. (Photo courtesy of: Department of Veterinary Pathology, Faculty of Veterinary Medicine University of Zagreb, Heinzelova 55, 10000 Zagreb, Croatia. http://www.vef.unizg.hr/)

Chinchillas are particularly susceptible to infection with *Listeria monocytogenes* and most reports mention massive outbreaks involving a significant number of animals on chinchilla farms.[3, 8] A single case report of listeriosis in a chinchilla caused by *Listeria*

ivanovii has been described, and lesions were also characterized with necrotic and suppurative hepatitis.[2] Currently, chinchillas are becoming more common as pets, and less are kept for fur production. In the presented case, the source of infection remains unknown, but it may be speculated that infection occurred due to contamination of water or food during the time when animals were kept in the garden.

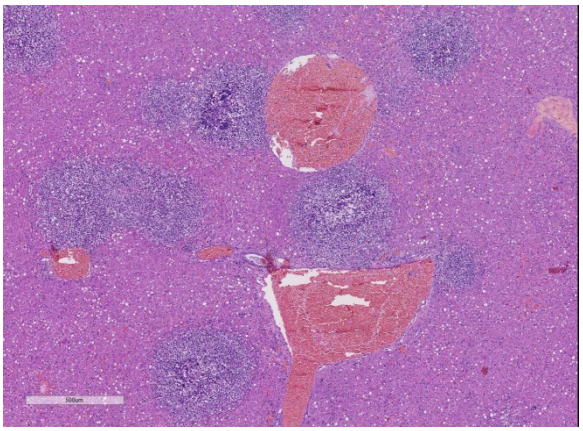

Liver, chinchilla: Areas of lytic necrosis are scattered randomly throughout the hepatic parenchyma. (HE, 40X)

JPC Diagnosis: Liver: Hepatitis, necrotizing, multifocal, random, marked, with intrahistiocytic and extracellular bacilli, chinchilla (*Chinchilla lanigera*).

Conference Comment: The contributor provides a thorough overview of the clinical manifestations, epidemiology, and pathogenesis of *Listeria monocytogenes* in the highly susceptible chinchilla. Most cases of listeriosis in humans and animals are secondary to ingestion of contaminated food and water, and the disease is particularly common in ruminants fed improperly fermented and stored silage.[1,2,6,8] Chinchillas, like rabbits and guinea pigs, are monogastric hind-gut fermenters and are more susceptible to the septicemic form of this disease rather than the encephalitic form, the typical manifestation in adult ruminants.[5,6]

After ingestion of the bacteria and translocation from the intestinal tract, the main target organ is the liver.[1,4,6] The organism has a tropism for hepatocytes and has the ability to penetrate the host cell using the surface protein internalin, mentioned by the contributor.[1] The bacterium then replicates within the host cell cytoplasm. *Listeria monocytogenes* also has the ability to co-opt the host cell actin filaments using the bacterial actin assembly-inducing protein (ActA) to migrate to the host cell membrane and induce pseudopod-like protrusions that can be transferred to another host cell.[4] Subsequent recruitment of neutrophils leads to lysis of hepatocytes, release of the organism, and ensuing

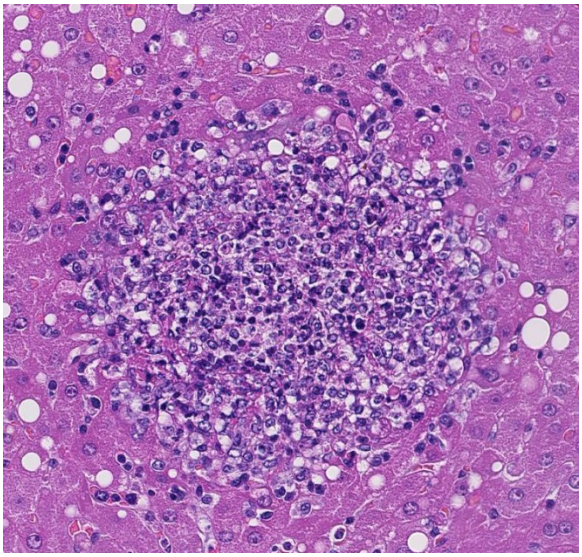

Liver, chinchilla: Necrotic foci are composed of moderate numbers of viable and degenerate neutrophils admixed with moderate numbers of infiltrating macrophages and cellular debris. (HE, 175X)

bacteremia.[6] Dissemination of the organism to multiple tissues such as the heart, brain, spleen, lymph nodes, and intestinal tract causes the classic lesion of multiple random miliary white foci of necrosis in the chinchilla.[6] Conference participants discussed

the differential diagnosis for the macroscopic finding of miliary white foci in the liver of rodents, which includes: *Yersinia pseudotuberculosis*, *Yersinia pestis*, *Francisella tularensis*, *Escherichia coli*, and group b *Streptococcus spp*, among others.

Conference participants also noted multifocal moderate macrovesicles within hepatocytes that often peripheralize the nuclei, interpreted as lipid vacuolar degeneration. This animal had a reported clinical history of inappetence for four days prior to death. Gross photographs document abundant mesenteric and subcutaneous fat

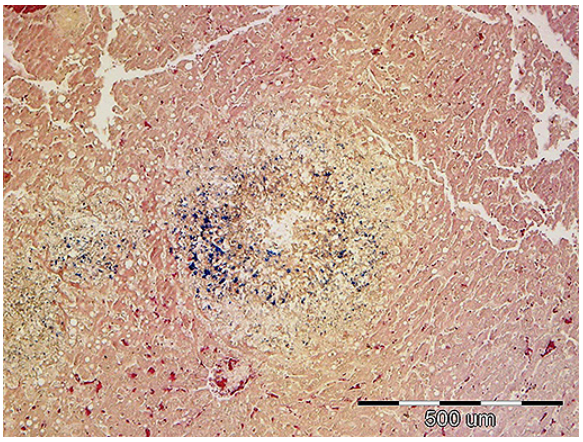

Liver, chinchilla: A tissue Gram stain demonstrates the presence of numerous gram-positive bacilli within necrotic foci. (Gram, 100X) (Photo courtesy of: Department of Veterinary Pathology, Faculty of Veterinary Medicine University of Zagreb, Heinzelova 55, 10000 Zagreb, Croatia. http://www.vef.unizg.hr/)

stores. Anorexia in this animal likely caused excessive delivery of free fatty acids from abundant adipose tissue. Excessive delivery of fatty acids, in conjunction with hepatocyte damage from the bacterial infection, likely impaired synthesis and secretion of lipoproteins leading to excessive accumulation of triglycerides in hepatocytes.[9]

Listeria monocytogenes was first described in 1926 by microbiologist Dr. Everitt G. Murray based on six cases of sudden death in young rabbits. He described it as a disease that causes an infiltration of large mononuclear leukocytes and named it *Bacterium monocytogenes*.[5] The bacterium was renamed in 1940 to *Listeria monocytogenes* in honor of famed surgeon and pioneer of antiseptic technique, Dr. Joseph Lister. Interestingly, *Listeria monocytogenes* was not identified as a foodborne pathogen until 1981.[4]

Contributing Institution: Department of Veterinary Pathology
Faculty of Veterinary Medicine University of Zagreb
Zagreb, Croatia.
http://www.vef.unizg.hr/

References:

1. Cantile C, Youssef S. Nervous system. In: Maxie MG, ed. *Jubb, Kennedy, and Palmer's Pathology of Domestic Animals*. 6th ed. Vol 1. St. Louis, MO: Elsevier; 2016: 362.
2. Kimpe A, Decostere A, Hermans K, Baele M, Haesebrouck F. *Isolation of Listeria ivanovii from a septicaemic chinchilla (Chinchilla lanigera)*. Veterinary Record. 2004; 154: 791-792.
3. KirinusI JK, KrewerI C, ZeniI D, MonegoI F, da SilvaII MC, KommersII GD, de VargasI AC. *Outbreak of systemic listeriosis in chinchillas*. Ciência Rural, Santa Maria 2010; (40): 686-689.
4. McAdam A, Milner D, Sharpe A. Infectious Diseases. In: Kumar V, Abbas A, Aster J, eds. *Robbins and Cotran Pathologic Basis of Disease*. 9th ed. Philadelphia, PA; Saunders Elsevier; 2015: 366.
5. Murray E, Webb R, Swann M. A disease of rabbits characterized by a large mononuclear leucocytosis,

caused by a hitherto undescribed bacillus Bacterium monocytogenes. *J Pathol Bacteriol*. 1926; 29:407–439.
6. Norton J, Reynolds R. Diseases and Veterinary Care. In: *The Laboratory Rabbit, Guinea Pig, Hamster, and other Rodents*. Oxford, UK: St. Louis, MO: Elsevier, 2012: 995.
7. Percy DH, Barthold SW. Guinea Pig. In: Percy DH, Barthold SW, eds. *Pathology of Laboratory Rodents and Rabbits*. 4th ed. Ames, IA: Blackwell; 2016: 226-227.
8. Wilkerson MJ, Melendy A, Stauber E. *An outbreak of listeriosis in a breeding colony of chinchillas*. J Vet Diagn Invest. 1997; (9): 320-323.
9. Zachary JF. Mechanisms of Microbial Infections. In: Zachary JF, McGavin MD, eds. *Pathologic Basis of Veterinary Disease*. 5th ed. St. Louis, MO: Elsevier Mosby; 2012: 192-195

CASE II: 11-106289 (JPC 4003035).

Signalment: One-month-old female Holstein calf (*Bos taurus*).

History: This animal had diarrhea complicated with pneumonia.

Gross Pathology: Presented was a severely thin animal with no body fat. A catheter tube was inserted on the left dorsal-lateral back, tunneled through subcutaneous, and ended at the left side of stomach. The spleen was markedly enlarged with prominent white pulp. All peripheral lymph nodes were four to six times enlarged. This animal had mild to moderate thymic and muscular atrophy.

Laboratory results:

Lung PCR positive for bovine respiratory syncytial virus
Lung PCR positive for *Mycoplasma bovis*
Lung IHC positive for bovine respiratory syncytial virus
Aerobic culture of lung – no respiratory pathogens isolated

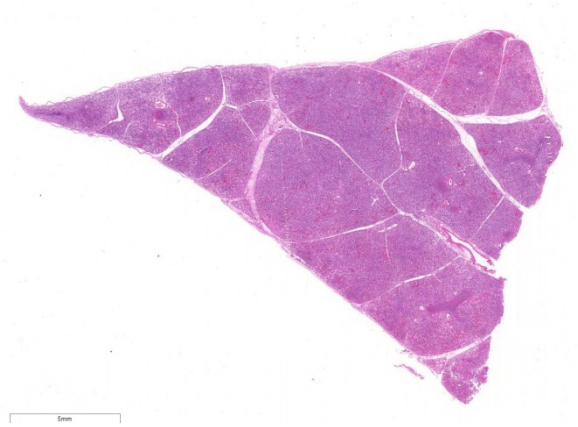

Lung, calf: At subgross magnification, the lung is diffusely consolidates, airways are full of a cellular exudate, and intralobular septa are diffusely expanded by edema and clear space. (HE, 4X)

Histopathologic Description: Diffusely, alveoli contain moderate numbers of neutrophils and macrophages, along with sloughed type II pneumocytes and occasional syncytial cells, and variable fibrin and erythrocytes. Bacteria are present in alveoli in some sections. Alveolar septal walls are variably lined by type II pneumocytes. Bronchi contain large numbers of neutrophils, sloughed cells, and syncytial cells. Bronchiolar epithelium varies from columnar to cuboidal or occasionally flattened, and intracytoplasmic eosinophilic inclusions are sometimes present in bronchiolar epithelial cells and syncytial cells. Occasional syncytial cells are present in the bronchiolar epithelium. Scattered larger bronchioles and bronchi often are filled with necrotic cells and debris and degenerating neutrophils. Interlobular septae are distended by edema fluid.

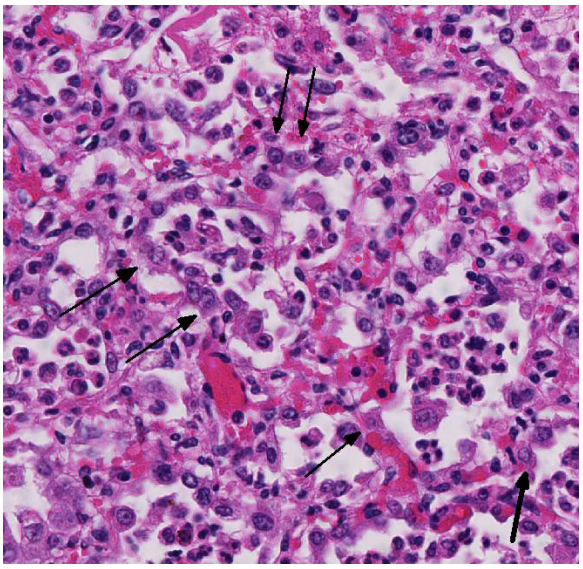

Lung, calf: Diffusely alveolar spaces are filled with low to moderate numbers of neutrophils and fewer macrophages, and alveolar septa are lined by patchy Type II pneumocyte hyperplasia (arrows). (HE, 400X)

Contributor's Morphologic Diagnoses 1. Lung: Pneumonia, interstitial, proliferative, with syncytial cells and neutrophilic and histiocytic alveolitis, and intracytoplasmic viral inclusions
2. Lung, bronchi and bronchioles: Intraluminal necrotic exudate

Contributor's Comment: The proliferative interstitial pneumonia in this case is attributed to infection with bovine respiratory syncytial virus (BRSV). The necrotic exudate that is present in the bronchi and to a lesser extent in the bronchioles is likely associated with co-infection with *Mycoplasma bovis*.

BRSV is a cause of "enzootic pneumonia" in 2-week to 5-month-old calves with a peak incidence at 1-3 months of age. BRSV can also cause fatal bronchointerstitial pneumonia in feedlot cattle but a role of BRSV in acute interstitial pneumonia in the late feeding period is questionable.[1]

BRSV is a member of the *Pneumovirus* genus in the family *Paramyxoviridae*. Experimental infections result in less severe clinical disease than natural cases, attributed to a reduction in virulence as a result of in vitro passage of the virus. In natural infections, viral antigen can be located in bronchiolar epithelium, type II pneumocytes, and macrophages, and less frequently in the nasal, tracheal, and bronchial epithelium.[1]

Gross lesions of natural BRSV infection differ in cranioventral and caudodorsal areas of the lung. The cranioventral lung is atelectatic, collapsed, deep red or mottled, and rubbery. In contrast, the caudodorsal areas fail to collapse and are edematous, heavy and firmer than normal. Variations of the gross lesions do occur, such that some cases may have a generalized rubbery texture with no difference between cranial and caudal lung, and in some cases there may be formation of bullae.[1]

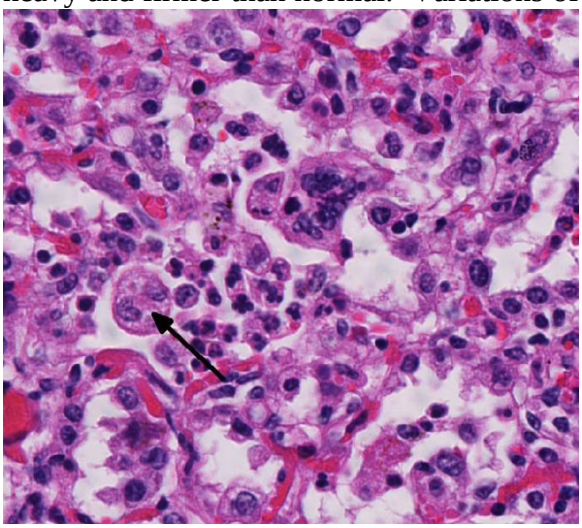

Lung, calf: Alveoli contain multinucleated viral syncytia which often contain intracytoplasmic viral inclusions (arrow). (HE, 400X)

Microscopic lesions of BRSV pneumonia include bronchointerstitial pneumonia with necrotizing bronchiolitis, formation of bronchiolar epithelial syncytia, and exudative or proliferative alveolitis. In acute lesions, bronchioles are lined by flattened

epithelium, bronchiolar lumens contain necrotic epithelial cells and neutrophils. Alveoli contain neutrophils and macro-phages; hyaline membranes are in-frequent. Syncytia may be difficult to distinguish from the multinucleate macro-phages that clear fibrin from alveoli in cases of fibrinous pneumonia, however, the presence of bronchiolar syncytia is a more reliable indicator of viral infection. Intracytoplasmic eosinophilic inclusion bodies are occasionally present in syncytial cells and uncommonly in bronchiolar and alveolar epithelium.[1]

BRSV infections in calves have many similarities to human RSV infections. Children vaccinated with formalin-killed RSV vaccine reportedly had more severe respiratory disease than those who were not vaccinated.[3] Similarly, there are reports of exacerbated disease after vaccination of cattle with formalin-killed vaccine. Kalina et al[5] showed that vaccination with formalin killed vaccine can enhance the disease, and attributed this to a shift to a Th2 immune response. Experimental infection of calves with BRSV, followed by infection with *Histophilus somni* resulted in an infection that was more severe than *Histophilus* alone; this was attributed to a shift to IgE production by the BRSV infection.[4] Current trends are to develop vaccines for BRSV that shift the immune response to a Th1 response that will favor virus-killing mechanisms.

The calf in this study was co-infected with *Mycoplasma bovis*, and the necrotic cells and necrotic debris in the airways are attributed to *M. bovis* infection. The mycoplasmal infection in this calf probably is in early stages of development, since the necrotic lesions have not progressed beyond the airways. The early lesions of experimental *M. bovis* infection consist of

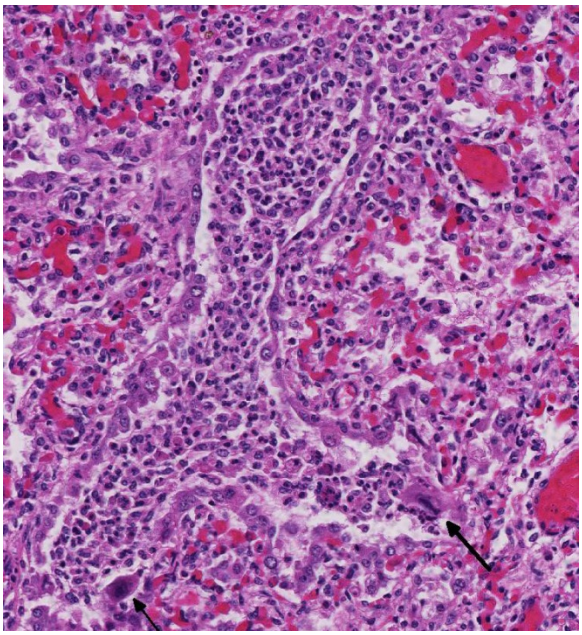

Lung, calf: The lumina of bronchioles are filled with large numbers of viable and degenerate neutrophils; bronchiolar epithelium is multifocally necrotic, segmentally attenuated or hypertrophic, and there are several viral syncytia within the population (arrows). (HE, 400X)

suppurative exudates within small bronchioles, in which the leukocytes are stated to have a characteristic appearance-they are necrotic but retain their cellular outlines, and have hypereosinophilic cytoplasm, and unapparent or fragmented nuclei.[1]

JPC Diagnosis: Lung: Pneumonia, bron-chointerstitial, necrotizing and histiocytic, subacute, diffuse, severe, with type II pneumocyte hyperplasia, syncytial cells, and epithelial intracytoplasmic viral inclusion bodies, Holstein, *Bos taurus*.

Conference Comment: This case generated intense discussion among conference participants regarding the pattern of inflammation present within the section of lung. The morphologic patterns of pneumonia can be classified based on the initial site of involvement and the spread of the lesion. In general, there are four

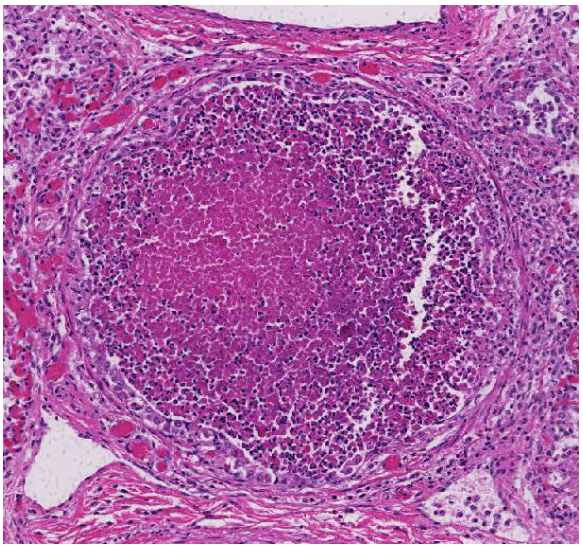

Lung, calf: The exudate of several bronchioles contains an exudate undergoing lytic necrosis, suggestive of mycoplasmal infection. (HE, 400X)

morphologic patterns of lung disease: airway disease involves inflammation and necrosis targeting bronchi and bronchioles; bronchopneumonia involves inflammation and necrosis of alveoli and bronchioles due to due to aerogenous bacteria less than 5 μm in diameter; interstitial pneumonia arises from disease of the non-airway tissues, such as alveolar and interlobular septa; and bronchointerstitial pneumonia is a combination of airway and interstitial lung disease.[1] As mentioned by the contributor, typically bovine respiratory syncytial virus (BRSV) causes bronchointerstitial pneumonia with necrotizing bronchiolitis, type II pneumocyte hyperplasia, exudative or proliferative alveolitis, and syncytial cell formation.[1,5] In this case, there is severe necrosis of the bronchiolar epithelium. This is in contrast with bronchopneumonia, where bronchioles and alveoli are filled with leukocytes as a result of bacterial infection of the airways, but necrosis of the epithelium is usually not present.

Like the contributor, some conference participants favored breaking the pattern of inflammation into two distinct processes. Participants argued that BRSV causes a fibrinous and proliferative interstitial pneumonia with a secondary suppurative and necrotizing bronchopneumonia caused by early co-infection with *Mycoplasma bovis*, detected by PCR in this case. Participants favoring the pattern of bronchointerstitial pneumonia countered that the virus causes the necrotizing lesions in the bronchi, bronchiolar epithelium, and type I pneumocytes, as well as thickening of the alveolar septae by infiltrates of leukocytes, and type II pneumocyte hyperplasia. They also point out that there is little evidence for typical *M. bovis* lesions in this case. *M. bovis* classically causes a bronchopneumonia with distention of bronchioles and alveoli by a caseonecrotic exudate with an eosinophilic core, and are rimmed by "ghost-like" leukocytes remnants.[1] Most conference participants agreed that those lesions associated with *M. bovis* are not a prominent feature of this case. Ultimately, participants agreed that the lesions in this case are characteristic for BRSV, which causes bronchointerstitial pneumonia in the cranio-ventral lung lobes.[1,2,5]

Conference participants also discussed additional causes of syncytial cells in the bovine lung, other than BRSV. Bovine parainfluenza virus 3 (BPIV-3), a member of the genus *Respirovirus* in the *Paramyxoviridae* family, can also induce the formation of syncytia with intracytoplasmic inclusion bodies.[1] Similar to BRSV, another *Paramyxoviridae* family virus, BIPV-3 induces syncytial cell formation via a fusion (F) transmembrane glycoprotein.[1,5] BIPV-3 usually causes mild bronchitis and bronchiolitis in cattle. Multinucleated alveolar macrophages can also resemble syncytial cells in cattle with fibrinous or granulomatous pneumonia. However, in BRSV, there would likely be both alveolar and bronchiolar syncytial cells.[1]

Contributing Institution:
Kansas State University
Dept. Diagnostic Medicine/Pathobiology
1800 Denison, Mosier Hall
Manhattan, KS 66506
http://www.vet.k-state.edu/depts/dmp/index.htm

References:

1. Caswell JL, Williams KJ. Respiratory system. In Maxie MG, ed. *Jubb, Kennedy and Palmer's Pathology of Domestic Animals*. 6th ed., Vol 2. Philadelphia, PA:Saunders Elsevier; 2016:539-554.
2. Gershwin LJ. Bovine respiratory syncytial virus infection: immunopathogenic mechanisms. *Anim Health Res Rev*. 2007; 8:207-213.
3. Gershwin LJ, Berghaus LJ, Arnold K, Anderson ML, Corbeil LB. Immune mechanisms of pathogenetic synergy in concurrent bovine pulmonary infection with Haemophilus somnus and bovine respiratory syncytial virus. *Vet Immunol Immunopathol*. 2005; 107:119-130.
4. Kalina WV, Woolums AR, Berghaus RD, Gershwin LJ. Formalin-inactivated bovine RSV vaccine enhances a Th2 mediated immune response in infected cattle. *Vaccine*. 2004; 29:1465-1474.
5. Sacco R, McGill L, Pillatzki A, Palmer M, Ackermann M. Respiratory syncytial virus infection in cattle. *Vet Pathol*. 2014; 51:427-436.

CASE III: 13A888 (JPC 4066311).

Signalment: Five-year-old male rhesus macaque (*Macaca mulatta*).

History: This animal was assigned to the research project of alcohol, HIV infection & host defense. Ethanol was administered via the gastric catheter with 30% ethanol in water (w/v) as a 0.5-hour prime, followed immediately by a 4.5-hour maintenance infusion. The concentration of ethanol in blood was 50 to 60 mM. The animals received ethanol four consecutive days per week for the duration of the study. Three months after ethanol administration, this animal was intravenously inoculated with simian immunodeficiency virus (SIV) 251 about one year before sacrifice. *Streptococcus pneumoniae* was inoculated in right lung seven months before sacrifice.

Six months after SIV inoculation, this animal began to show chronic, mild leukocytosis, mild neutrophilia, and moderate thrombocytopenia. The animal developed weight loss, loss of muscle mass, enlargement and restriction of stifles, enlarged lymphoid tissue, and mild splenomegaly and hepatomegaly.

Gross Pathology: Presented was a severely thin animal with no body fat. A catheter tube was inserted on the left dorsal-lateral back, tunneled through subcutaneous, and ended at the left side of stomach. The spleen was markedly enlarged with prominent white pulp. All peripheral lymph nodes were four to six times enlarged. This animal had mild to moderate thymic and muscular atrophy.

Laboratory results: N/A

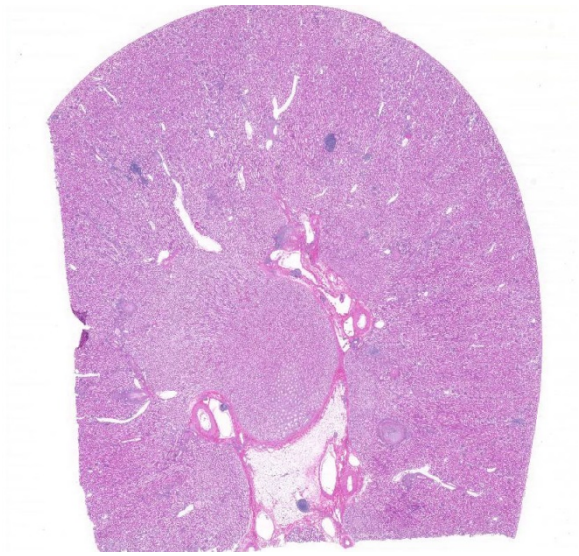

Kidney, macaque. At subgross magnification, there are lymphoid nodules scattered throughout the section, and several vessels, predominantly arcuate arteries at the corticomedullary junction, are expanded and surrounded by a cellular infiltrate. (HE, 5X)

Histopathologic Description: Kidney: Multifocally the small and medium-sized arteries are expanded and variably disrupted by proliferation of the tunica intima, smooth muscular hyperplasia, and infiltration of inflammatory cells. The lumina of affected arteries are partially to completely occluded and lined by hypertrophic endothelial cells. Usually, the tunica media are segmentally to circumferentially thickened by smooth muscle hyperplasia, fragmented collagen bundles, and reactive fibroblasts. The tunica adventitia is markedly expanded by numerous neutrophils, lymphocytes, plasma cells, and fewer macrophages and eosinophils. Some subendothelial tunica intima and tunica media are disrupted and markedly expanded by thick bands of deeply eosinophilic hyaline to fibrinoid material admixed with cellular and karyorrhectic debris and many erythrocytes (necrosis and hemorrhage). Multifocally the renal tubules are ectatic, lined by attenuated epithelial cells, and contain hypereosinophilic homogenous material (protein casts) and cellular debris. Multifocally the interstitium is infiltrated by many lymphocytes and plasma cells. Occasionally the interstitium is expanded by lymphoid aggregates (lymphoid hyperplasia and dysplasia). Some glomerular tufts are senescent and shrunken with ectatic Bowman's spaces.

Contributor's Morphologic Diagnoses: 1. Kidney, medium and small arteries: Arteritis, proliferative and necrotizing, multifocal.
2. Kidney, lymphoplasmacytic interstitial nephritis, multifocal, mild.
3. Kidney, interstitial lymphoid hyperplasia and dysplasia.

Contributor's Comment: Arteriopathy is also noted in the small to medium arteries of the mesentery, testis, liver, gall bladder, pancreas, urinary bladder, and bone marrow. The systemic vascular lesions in this monkey resemble those found in polyarteritis nodosa (PAN)-like syndrome in HIV patients. PAN-like syndrome has been described in HIV patients in the literature.[6,7] While target organs are usually muscles, nerves, skin and gastrointestinal tract, renal polyarteritis nodosa in HIV patients has also been reported.[2] PAN-like syndrome occurs in fewer than 1% of HIV patients. The underlying mechanism is thought to involve cell or immune-complex-mediated inflammation, like classic PAN in other species. Although the histopathological changes are similar between two entities, there are several important differences between PAN in HIV patients and so-called classic or idiopathic PAN. First, the waxing and waning clinical course of classic PAN is not seen in patients with HIV infection. Second, classic PAN can be associated with hepatitis B virus infections, but in HIV patients, the serology for HBV is always negative. Third, the affected arteries in HIV-associated PAN tend to be smaller than that seen in classic PAN.[4]

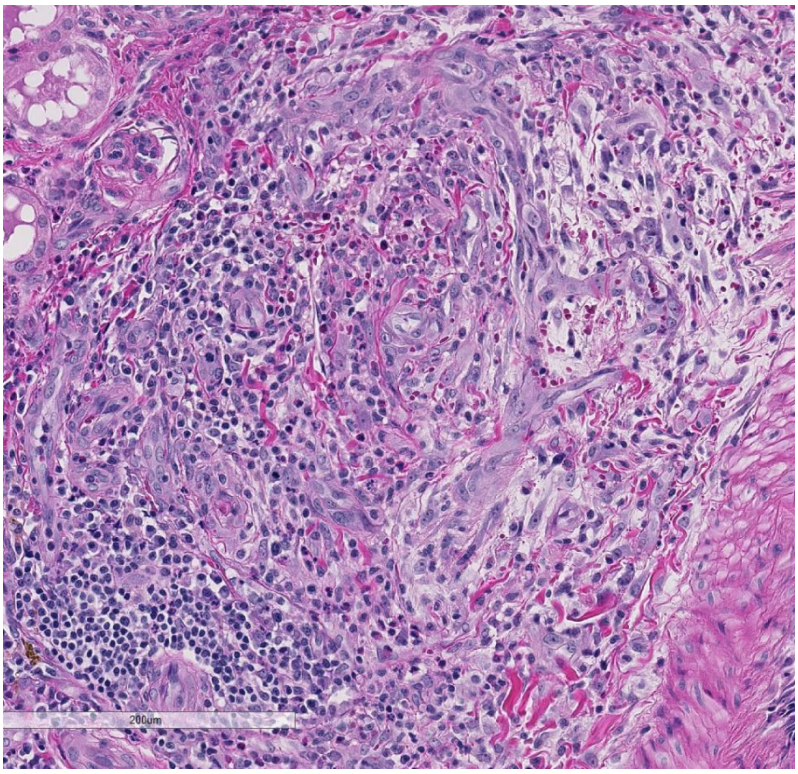

Kidney, macaque. Arcuate arteries and branches are often replaced by a large mass of tortuous vessels with prominent endothelium. The adventitia is expanded by low to moderate numbers of lymphocytes and plasma cells, and fewer macrophages. (HE, 320X)

Pulmonary arteriopathy is the most common vasculopathy in macaques infected with SIV. Nineteen of 85 animals infected with SIV developed pulmonary arteriopathy characterized by intimal thickening, luminal occlusion, and internal elastic laminae fragmentation and interruption.[3] Pulmonary artery hyperplasia and/or plexiform arteriopathy were present in eight of 13 (62%) SHIV-infected macaques.[5] However, the pulmonary arteries were histopathologically normal in the current case. This observation is consistent with the two published cases, in which, arteriopathy was mild or absent in the lungs.[11] These observations suggested a different pathogenesis between pulmonary arteriopathy and PAN-like syndrome in SIV infected monkeys.

PAN-like syndrome has been reported in two SIV-infected rhesus macaques.[11] Vasculopathy is prominent in kidney, intestine, pancreas, liver, heart, lymph nodes, spleen, and testis. Histologically, disseminated arteriopathy is characterized by intimal thickening and fibrosis with varying degrees of vasculitis. Intranuclear inclusion bodies were CMV positive by immunohistochemistry in multiple organs in these two monkeys. Intranuclear inclusion bodies were not observed in the current case but immunohistochemistry for CMV or other viral agents was not performed in the current case.

Based on extensive experience on this model, it is unlikely that ethanol administration was associated with PAN-like syndrome in this monkey. There is no documentation of alcohol and arteriopathy in the literature. Although this animal was inoculated with Streptococcus pnenumonae, grossly and microscopically there was no current evidence of Streptococcus infection. Renal interstitial lymphoid hyperplasia and dysplasia are not uncommon findings in SIV-infected monkeys.

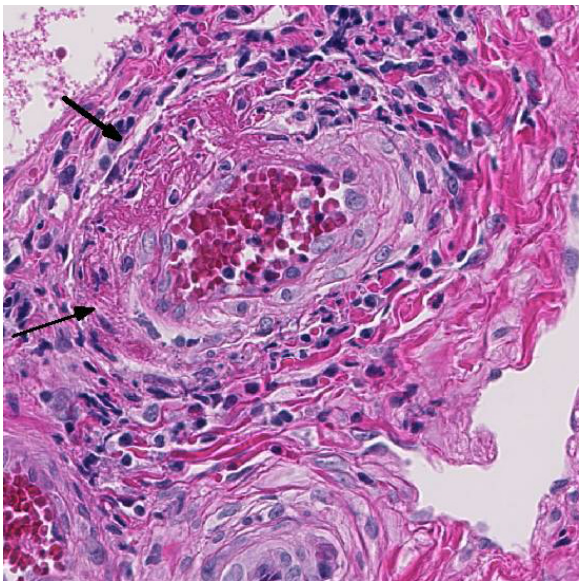

Kidney, macaque. There is transmural hyaline change within the wall of smaller arterioles as a result of extrusion of protein from the lumen. (arrows) (HE, 320X)

JPC Diagnosis: 1. Kidney, small arteries and arterioles: Arteriopathy, proliferative and necrotizing, multifocal, mild to marked, with adventitial inflammation, rhesus macaque (*Macaca mulatta*).
2. Kidney: Interstitial nephritis, lympho-plasmacytic, multifocal, mild.

Conference Comment: Although the specific etiology and pathogenesis of this lesion are unclear, the contributor provides an excellent example of a polyarteritis nodosa (PAN)-like syndrome in a non-human primate. PAN-like syndromes are thought to be a type III hypersensitivity reaction secondary to antigen:antibody complex deposition in medium to small caliber arteries.[1] Immune complex deposition results in complement activation leading to segmental, circumferential, and proliferative arteritis. This syndrome has been well described in the aged Sprague-Dawley rat and beagles.[9,10] In rats, lesions most often occur in the muscular medium-sized arteries of the mesentery, pancreas, testis, hepatic, coronary, uterine, cerebral, adrenal, and renal arteries.[10] This condition in beagles is associated with beagle pain syndrome. In these cases, the coronary and meningeal arteries are most affected, and clinically dogs are febrile, lose weight, and have cervical pain.[9] Typically in domestic species, PAN-like syndrome spares the pulmonary circulation, large arteries and glomeruli.[11] The association of SIV as part of the pathogenesis of the arteriole lesions, in this case, remains unclear.

The JPC strives to avoid using the suffix "-opathy" in a morphologic diagnosis due to its non-specific nature; however, in rare instances, this terminology may be appropriate, especially in cases where the primary process underlying the lesion is difficult to ascertain. While the SIV-positive status of this particular animal suggests a causal relationship, PAN has also been seen as a spontaneous finding in macaques, as well as a toxic lesion association with administration of cyclosporine and tacrolimus (WSC 2003-2004, Conference 20, Case 1). The term arteriopathy can be modified by other descriptors such as proliferative and necrotizing to further define the underlying process. Much of the literature on this disease uses the term arteriopathy to describe this finding in arteries and arterioles in SIV-infected rhesus macaques.

During a discussion of the vessel wall changes in this case, some conference participants preferred the term hyaline change to describe the circumferential homogenous, eosinophilic, proteinaceous material deposited within the external elastic membrane of arterioles rather than the well-ensconced term fibrinoid necrosis. Fibrinoid necrosis has been classically used by both human and veterinary pathologists to describe the brightly eosinophilic changes in the injured vessel associated with immune complex, plasma protein, and complement

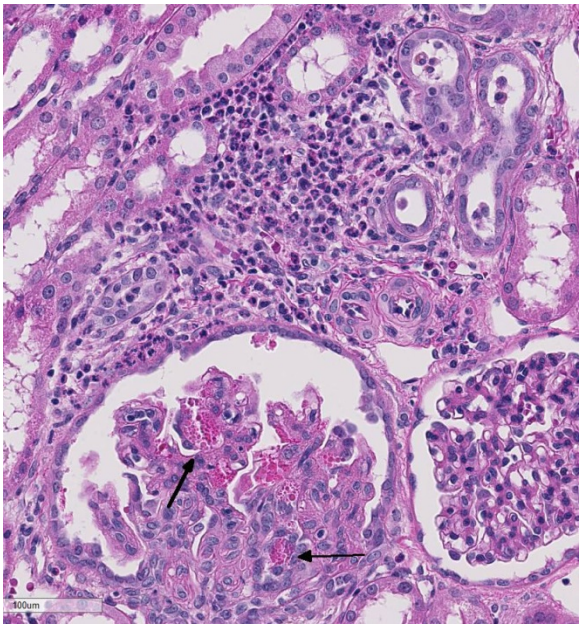

Kidney, macaque. There are multiple foci of eosinophilic inflammation scattered throughout the interstitium; tubules within these areas are mildly atrophic. Within the adjacent glomerular tuft, there is extrusion of protein into the mesangium (arrows)

protein deposition within vessels.[1] Fibrinoid necrosis implies a pathogenesis that may or may not be present. The brightly eosinophilic homogenous protein accumulation obscures the structural detail of the blood vessel, thus making it difficult or impossible to determine if there is fibrin or necrosis present within the arteriole wall. Hyalinosis describes the accumulation of leaked eosinophilic proteinaceous material secondary to endothelial damage and increased vascular permeability without making assumptions about the pathogenesis.

Finally, several participants found multinucleated giant cells within the tubular epithelium and lumina of collecting ducts within their sections. Multinucleated giant cells have been described as a common incidental finding in macaques[8]; however, a number of participants ascribed them as a potential corroborating sign of lentivirus infection in this macaque.

Contributing Institution:
The Division of Comparative Pathology
Tulane National Primate Research Center
18703 Three Rivers Rd.
Covington, LA 70433.
http://tulane.edu/tnprc

References:

1. Alpers C, Chang A. The kidney. In: Kumar V, Abbas AK, Fausto N, Aster JC, eds. *Robbins and Cotran Pathologic Basis of Disease*. 9th ed. Philadelphia, PA:Saunders Elsevier; 2015:903.
2. Angulo JC, Lopez JI, Garcia ME, Peiro J, Flores N: HIV infection presenting as renal polyarteritis nodosa. *Int Urol Nephrol*. 1994; 26(6):637-641.
3. Chalifoux LV, Simon MA, Pauley DR, MacKey JJ, Wyand MS, Ringler DJ: Arteriopathy in macaques infected with simian immunodeficiency virus. *Lab Invest*. 1992:67(3):338-349.
4. Chetty R: Vasculitides associated with HIV infection. *J Clin Pathol*. 2001; 54(4):275-278.
5. George MP, Brower A, Kling H, Shipley T, Kristoff J, Reinhart TA, et al.: Pulmonary vascular lesions are common in SIV- and SHIV-env-infected macaques. *AIDS Res Hum Retroviruses*. 2011; 27(2):103-111.
6. Gisselbrecht M, Cohen P, Lortholary O, Jarrousse B, Gayraud M, Lecompte I, et al.: Human immunodeficiency virus-related vasculitis. Clinical presentation of and therapeutic approach to eight cases. *Ann Med Interne*. 1998; 149(7):398-405.
7. Libman BS, Quismorio FP, Jr., Stimmler MM: Polyarteritis nodosa-like vasculitis in human immuno-

deficiency virus infection. *J Rheumatol*. 1995; 22(2):351-355.
8. Lowentine, L.J. A primer of primate pathology lesions and nonlesions. *Tox Pathol* 2003; 31:91-102.
9. Miller L, Van Vleet J, Gal A. Cardiovascular system and lymphatic vessels. In: McGavin MD, Zachary JF, eds. *Pathologic Basis of Veterinary Disease*. 5th ed. St. Louis, MO:Mosby Elsevier; 2012:587.
10. Percy DH, Barthold SW. Rat. In: *Pathology of Laboratory Rodents and Rabbits*, 4th ed., Ames, IA: Blackwell Publishing; 2016:156.
11. Robinson W, Robinson N. Cardio-vascular system. In: Maxie MG, ed. *Jubb, Kennedy, and Palmer's Pathology of Domestic Animals*. Vol 3. 6th ed. Philadelphia, PA:Elsevier; 2016:71.
12. Yanai T, Lackner AA, Sakai H, Masegi T, Simon MA: Systemic arteriopathy in SIV-infected rhesus macaques (Macaca mulatta). *J Med Primatol*. 2006; 35(2):106-112.

CASE IV: CHIN1 (JPC 4084953).

Signalment: Adult female common marmoset (*Callithrix jacchus*).

History: This marmoset was one of a cohort in quarantine that had a history of intermittent diarrhea of undetermined origin. There had been a brief response to Baytril therapy. Several animals had then been used for terminal experimental manipulation subsequent to their rapid clinical deterioration.

Gross Pathology: The entire large bowel, cecum through rectum, was dilated and had a swollen, edematous appearance from the serosal surface. On opening, the bowel lumen was filled with large amounts of clear, thick gelatinous material. Underlying this content, there was an irregular pattern of coalescing cream-colored nodularity. This superficial mucoid material was adhered to remaining underlying mucosa, although it

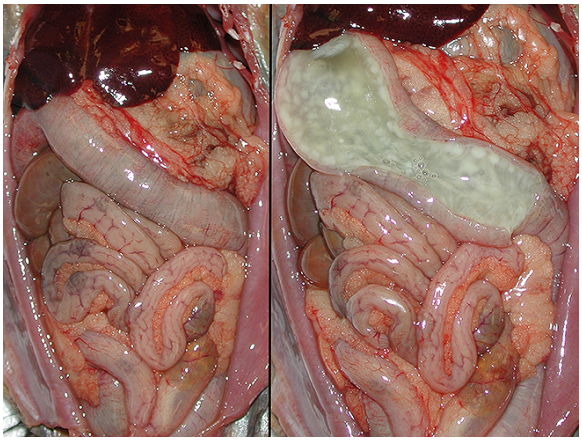

Colon, marmoset: The colon is markedly distended and filled with a clear gelatinous material. Nodular whitish areas of necrosis are present within the underlyingmucosa. (Photo courtesy of: University of Pittsburgh, Division of Laboratory Animal Resources, http://www.dlar.pitt.edu/)

was possible through blunt dissection, to "peel" this off as a layer. Minimal fecal content was present within the large intestine. Stomach and small intestine were also largely empty with the exception of a very small amount of semi-solid ingesta in the distal ileum.

Laboratory results: N/A

Histopathologic Description: Full-thickness pieces were evaluated from different segments of the colon. All were similar in appearance. Diffuse necrosis of the superficial mucosa was present with an associated thick exudative layer of fibrin, mucin, leukocytes (primarily neutrophils) and nuclear debris. Patchy basophilic aggregates of bacterial colonies including numerous large rod-shaped organisms were

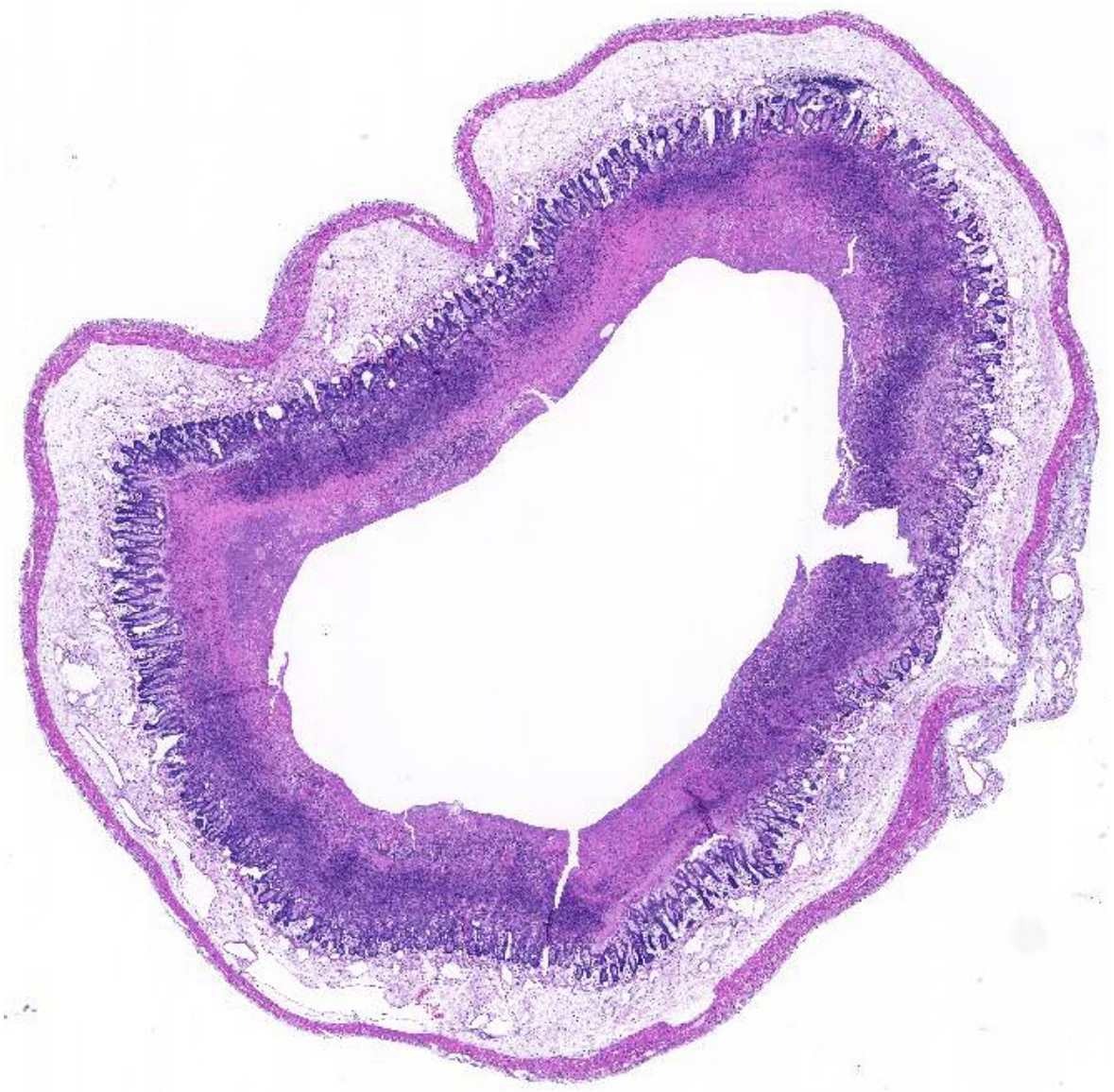

Colon, marmoset. The mucosa is covered with a fibrinonecrotic membrane which is border on its deepest aspect by a dense band of basophilic cellular debris. There is marked edema of the submucosa, as well as edema in the lamina propria and serosa. (HE, 5X)

scattered throughout the overlying necrotic membrane. In many areas, a characteristic striated pattern formed by columns of PMN cells and mucin was present. Inflammatory infiltrates extended into deeper intact mucosal crypt structures, which also often contained abundant mucinous debris. The submucosa (and to a much lesser extent, muscularis) was markedly expanded by edema & mild scattered inflammatory infiltrates and had prominently dilated vascular and lymphatic vessels.

Contributor's Morphologic Diagnosis: Colitis, fibrinonecrotizing and pseudo-membranous, diffuse, severe, with extension of inflammation into crypts and marked submucosal edema.

Contributor's Comment: The gross and microscopic findings in this case are consistent with *Clostridium difficile* colitis, also referred to as *C. difficile*-associated disease (CDAD). Fecal content submitted from this and other animals in the cohort

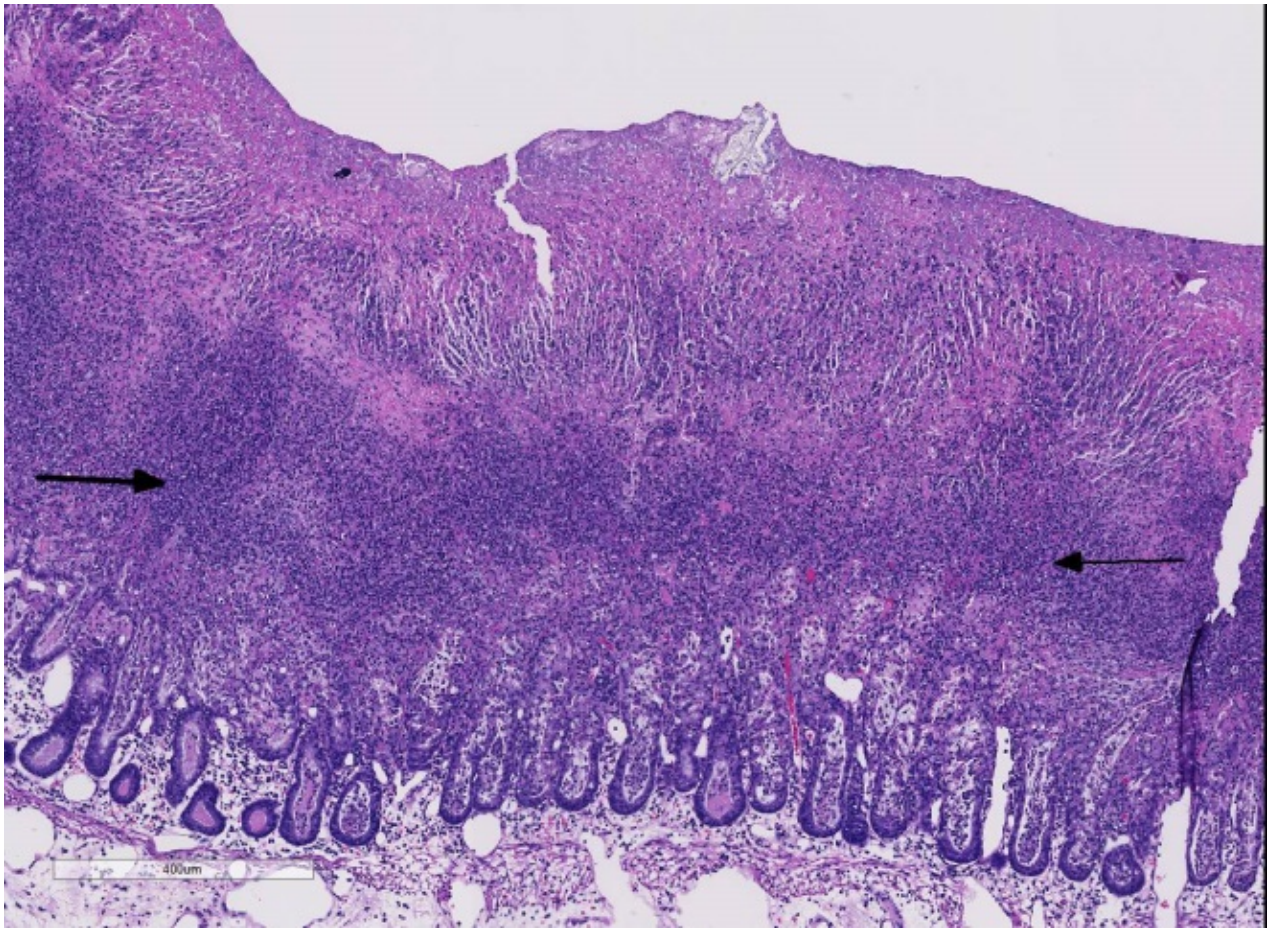

Colon, marmoset. A dense band of cellular debris is present in the middle of the mucosa as delimiting the leading edge of the diffusing exotoxin of C. difficile (arrows), and resulting mucosal necrosis. Subjacent colonic glands are distended and filled with cellular debris. (HE, 45X)

was PCR-positive for *C. difficile* Toxin B gene.

C. difficile is a confirmed pathogen in humans and a wide variety of mammals. Infection is a well-recognized clinical entity in horses, pigs, hamsters and rabbits.[6] Disease in horses occurs in both adults and foals, with both antibiotic treatment and hospitalization being clear risk factors. Gross and microscopic lesions may not be sufficient to distinguish CDAD from other causes of acute equine enteric disease, including those associated with other clostridial pathogens.[3] Conversely, primarily neonatal pigs appear susceptible to infection – usually around 5 days of age.[14] Hamsters are the most susceptible animals to natural infection, with as little as 1 colony forming unit leading to disease in antibiotic pretreated animals.[7] Although *C. spiriforme* is a more common pathogen, *C. difficile* does cause peracute death without clinical signs in rabbits.[2]

Reports of natural or experimental infection exist in many other species including guinea pigs, mice, rats, domestic cats and dogs, calves, ostriches, prairie dogs and non-human primates.[6,12] This is to the contributor's awareness, the first documented cases of the entity in this primate species (marmoset).

Although the cecum and colon are the sites most often affected in the majority of

species, the nature of lesions present, their location/distribution, and age of host susceptibility all vary significantly. Specifically, foals and rabbits consistently develop severe lesions in the small intestine.[6]

C. difficile is recognized as one of the most important nosocomial pathogens in humans, causing illness ranging from mild diarrhea to fulminant colitis. Antibiotic use and hospitalization are significant risk factors, with recurrence being common (15-20% of cases). The disease has been well characterized histologically, occurring in three stages: 1) focal epithelial necrosis along with fibrin-rich exudates, 2) marked exudation protruding through an area of mucosal ulceration (characterized as classical "volcano" lesions), and 3) diffuse, more severe mucosal ulceration with necrosis and associated pseudomembrane composed of fibrin, leukocytes and cellular debris. In cases where disease has progressed to pseudomembrane formation, endoscopy can be diagnostic, and although a rapid means of testing, it is invasive and expensive.[10]

C. difficile infection occurs when the natural flora in the gut is disrupted.[9] Although this is often associated with antibiotic administration, in some species, stress, change of diet, transportation, starvation, and medical or surgical treatment can initiate disease.[3] After oral ingestion, spores, which are resistant to the acidity of the stomach, germinate into the vegetative form in the small intestine, leading to toxin production resulting in colitis.[4] Other factors such as host susceptibility or virulence factors of the infecting strain may also be integral in determining the clinical outcome of infection. Both toxins, TcdA and TcdB, are cytotoxic, causing disruption of the actin cytoskeleton and tight junctions, resulting in decreased transepithelial resistance, fluid accumulation and destruction of the intestinal epithelium. These substances also cause the release of various inflammatory mediators from enterocytes, mast cells and macrophages.[9] In humans, host response appears critical and protective in the clinical outcome, with patients having elevated levels of IgG and IgA against toxin A.[13]

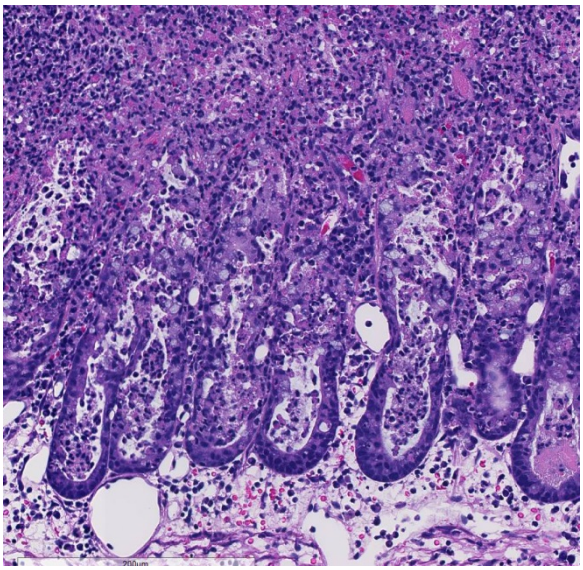

Colon, marmoset. Higher magnification of the affected colon glands, which are ectatic and filled with variable amounts of necrotic enterocytes, cellular debris, and degenerate neutrophils (crypt abscesses) (HE, 140X)

The detection of *C. difficile* by culture is rarely performed for diagnostic purposes because of the slow turnaround time.[5] Rather, identification of *C. difficile* toxins in the stool using ELISA methods are commonly used. These have excellent specificity, but variable sensitivity (75-85%). PCR methods to detect the toxin A and B genes responsible for the production of virulence factors are available (Cleveland Clinic paper synopsis).

Although infection and disease in man and animals has long been considered nosocomial and/or antibiotic related, recent

studies have explored whether zoonotic and foodborne transmissions occur. Certainly significant percentages of both companion and food animals are known to carry *C. difficile*. Although there are no scientific reports explicitly confirming that *C. difficile* can be acquired via foods or contact with animals, there is sufficient laboratory and epidemiological data to suggest that this may occur and that interventions to prevent transmission should be adopted.[5,11]

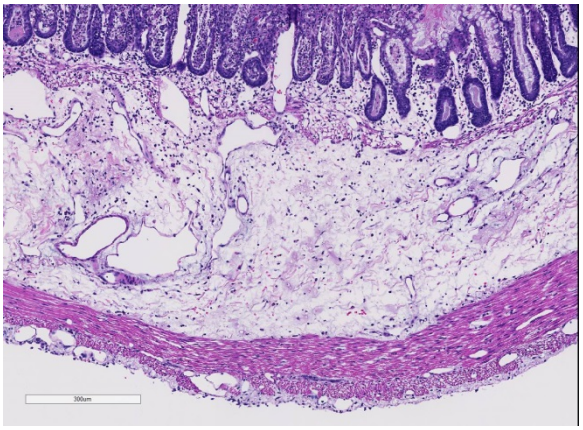

Colon, marmoset. There is marked edema and lymphatic dilation within the submucosa, which is less severe than that seen in the lamina propria and serosa. (HE, 60X)

The specific source of the infection in these marmosets was not determined, nor was the role of the fluoroquinolone treatment used in their initial empirical therapy (though this class of antimicrobials may pose a greater risk for development of disease than others).[4] This case does underscore the importance of awareness by both clinicians and pathologists of the potential for antibiotic-associated diarrheal diseases to occur in multiple species.

JPC Diagnosis: Colon: Colitis, necrotizing, circumferential, diffuse, severe, with fibrinocellular pseudomembrane and marked submucosal edema.

Conference Comment: The contributor provides an outstanding review of general information, diagnosis, pathogenesis, gross and microscopic lesions, and epidemiology of pseudomembranous colitis caused by *Clostridium difficile* across many species.

Conference participants noted the presence of a prominent circumferential fibrino-necrotic membrane replacing the apical mucosal epithelium, with a sharp line of demarcation separating necrotic tissue from relatively unaffected crypt epithelium. Also, within ulcerated areas this case nicely demonstrates the classic "volcano" lesions of florid fibrinosuppurative exudation through intestinal crypts.[3] As mentioned by the contributor, *C. difficile* elaborates A and B toxins which diffuse into the tissue from the lumen and destroy the apical mucosal epithelium, in addition to causing the marked submucosal edema demonstrated in this case. Necrosis of the deeper mucosal surface and the colonic tunica muscularis has been reported in chronic cases.[3]

In addition to *C. difficile*, conference participants discussed measles virus as a unique differential for enteritis in common marmosets, and other new world monkeys. This highly contagious, aerosolized virus belongs to the genus *Morbillivirus*, in the *Paramyxoviridae* family.[1,8] Marmosets are highly susceptible to measles infection and clinical disease is characterized by severe gastritis and colitis.[1] High mortality has been reported in marmosets infected with natural virus from human contact.[1] Histologic lesions of measles in marmosets include: epithelial necrosis in the stomach, cecum, and colon, with syncytia, and intracytoplasmic viral inclusion bodies in the mucosal epithelium and the gut-associated lymphoid tissue (GALT).[8] Modified live human vaccines against measles have produced active disease in marmosets and are not recommended as a preventative.[1,8]

Contributing Institution: University of Pittsburgh
Division of Laboratory Animal Resources
Pittsburgh, PA
http://www.dlar.pitt.edu/

References:

1. Albrecht P, Lorenz D, et al. Fatal measles infection in marmosets pathogenesis and prophylaxis. *Infect Immun*. 1980; 27:969-978.
2. Carman RJ, Evans RH. Experimental and spontaneous clostridial enteropathies of laboratory and free living lagomorphs. *Lab Anim Sci*. 1984; 34: 443-452.
3. Diab SS, Rodriguez-Bertos A, Uzal FA. Pathology and diagnostic criteria of *Clostridium difficile* enteric infection in horses. *Vet Pathol*. 2013; 50(6):1028-1036.
4. Gould CV, McDonald LC. Bench-bedside review: *Clostridium difficile* colitis. *Crit Care*. 2008; 12:203.
5. Gould LH, Limbago B. *Clostridium difficile* in food and domestic animals: a new foodborne pathogen. *Clin Infect Dis*. 2010; 51(5):577-582.
6. Keel, MK, Songer JG: The comparative pathology of *Clostridium difficile*-associated disease. *Vet Pathol*. 2006; 43: 225-240.
7. Larson HE, Borriello SP. Quantitative study of antibiotic-induced susceptibility to *Clostridium difficile* enterocecitis in hamsters. *Antimicrob Agents and Chemother*. 1990; 34(7): 1348-1353.
8. Lowenstine LJ. Measles virus infection, nonhuman primates. In: Jones TC, Mohr U, Hunt RD, eds., *Monographs On Pathology of Laboratory Animals, Nonhuman Primates*. Vol 1. Washington, DC:Springer-Verlag, International Life Sciences Institute; 1993:33.
9. Maja R, Wilcox MH, Gerding DN. *Clostridium difficile* infection: new developments in epidemiology and pathogenesis. *Nat Rev Microbiol*. 2009; 7:526-536.
10. Price AB, Davies DR: Pseudo-membranous colitis. *J Clinc Pathology*. 1977; 30:1-12.
11. Rodriguez-Palacios A, Borgmann S, Kline TR, LeJeune JT. *Clostridium difficile* in foods and animals: history and measures to reduce exposure. *Anim Health Res Rev*. 2013; 14:11-29.
12. Rolland RM, Chalifoux LV, Snook SS, Ausman LM, Johnson LD. Five spontaneous deaths associated with *Clostridium difficile* in a colony of cotton top tamarins (*Sanguinus oedipus*). *Lab Anim Sci*. 1997; 47(5):472-6.
13. Warny M, Vaerman JP, Avesani V, Delmee M. Human antibody response to *Clostridium difficile* toxin A in relation to clinical course of infection. *Infect Immun*. 1999; 62(2):384–389.
14. Waters EH, Orr JP, Clark EG, Schaufele CM: Typhlocolitis caused by *Clostridium difficile* in suckling piglets. *J Vet Diagn Invest*. 1998; 20: 104-108.

Self-Assessment - WSC 2016-2017 Conference 3

1. Which of the following is not a characteristic syndrome associated with *Listeria monocytogenes* infection?
    a. Abortion
    b. Encephalitis
    c. Septicemia
    d. Uveitis

2. Which of the following listerial virulence factors allows the bacteria to cross the intestine, blood-brain and placental barriers?
    a. E-cadherin
    b. Internalin
    c. Hemolysis
    d. Actin-assembly-inducing protein

3. True or False: Inclusion bodies arecommonly seen in bronchiolar and alveolar epithelium in calves infected with BRSV.
    a. True
    b. False

4. Which of the following is not true concerning periarteritis-nodosa (PAN) in patients infected with HIV*?*
    a. PAN-like syndrome occurs in approximately 10% of patients.
    b. Affected arteries in HIV-associated PAN tend to be smaller than that seen in classic PAN.
    c. Classic PAN can be associated with hepatitis B virus infections, but in HIV patients, the serology for HBV is always negative.
    d. The waxing and waning clinical course of classic PAN is not seen in patients with HIV infection.

5. Which of the following species most often develops severe lesions in the small intestine as a result of overgrowth of *Clostridium difficile*?
    a. Man
    b. Rabbits
    c. Cattle
    d. Pigs

Joint Pathology Center
Veterinary Pathology Services

WEDNESDAY SLIDE CONFERENCE 2016-2017

C o n f e r e n c e 4

14 September 2016

CASE I: D16-02 (JPC 4083954).

Signalment: One-year-old, female, Hampshire sheep (*Ovis aries*).

History: A one-year-old, female, Hampshire sheep was received for necropsy to the Kansas State Veterinary Diagnostic Laboratory at Kansas State University (KSU). She was presented earlier to the KSU teaching hospital with a clinical history of being down and unable to get up. She was being treated with Baytril® for two days, but her condition worsened over time. She was eventually euthanized. The sheep belonged to a herd with a history of chronic malnutrition. The owner has lost a steady number of sheep over the years. The flock was being treated for coccidiosis at the time of submission.

Gross Pathology: The sheep was thin with prominent ribs and scant amounts of body fat. There were no significant gross lesions in any organ, including the gastrointestinal tract.

Laboratory results: Real-time PCR from paraffin block shavings was strongly positive for *Mycobacterium avium paratuberculosis* (MAP).

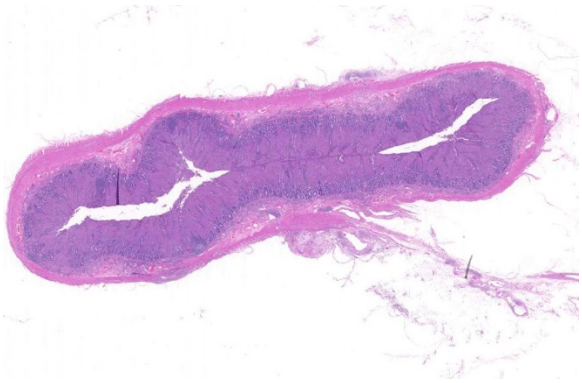

Intestine, sheep. The intestinal mucosa is moderately thickened by an eosinophilic cellular infiltrates that separates and replaces crypts. Villi are markedly blunted. (HE, 4X)

Histopathologic Description: Small intestine (ileum): There is diffuse blunting, shortening and fusion of the intestinal villi. The lamina propria is markedly expanded and crypts at the base of mucosa are widely separated by a diffuse sheet of epithelioid macrophages admixed with rare multi-nucleated giant cells, and small numbers of lymphocytes and plasma cells. These macro-phages have abundant, finely-granular to foamy, eosinophilic cytoplasm. The sub-mucosa is diffusely expanded by infiltrating

macrophages admixed with small to moderate numbers of lymphocytes, plasma cells, and increased clear space and ectatic lymphatics (edema). The serosa is diffusely expanded by mild edema, dilated lymphatics that contain intraluminal plugs of macrophages, and small to moderate numbers of macrophages, lymphocytes and plasma cells that predominantly surround the lymphatics. There are rare intraepithelial coccidian parasites within the crypts. The macrophages in the lamina propria of the intestine contain numerous intracytoplasmic acid-fast bacilli.

Contributor's Morphologic Diagnosis: Small intestine (ileum): Granulomatous enteritis with villus atrophy, lymphangitis, diffuse, severe, chronic with numerous intrahistiocytic acid-fast bacilli.

Contributor's Comment: The microscopic findings are diagnostic for ovine paratuberculosis. Paratuberculosis, or Johne's disease, is an infectious and chronically progressive granulomatous disease which affects domestic and wild ruminants worldwide. The causative agent, *Mycobacterium avium paratuberculosis* (MAP), is a slow growing mycobactin-dependent acid-fast bacillus that has been linked to Crohn's disease in humans. The bacteria may persist in the environment for extended periods of time, a continuing concern while implementing control programs.[7]

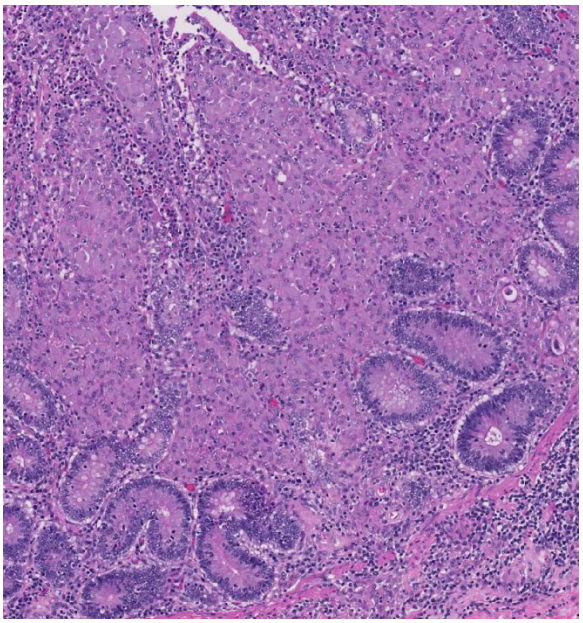

Intestine, sheep. Higher magnification of the infiltrate of macrophage with fewer lymphocytes and neutrophils which markedly expands the lamina propria and effaces intestinal crypts. (HE, 63X)

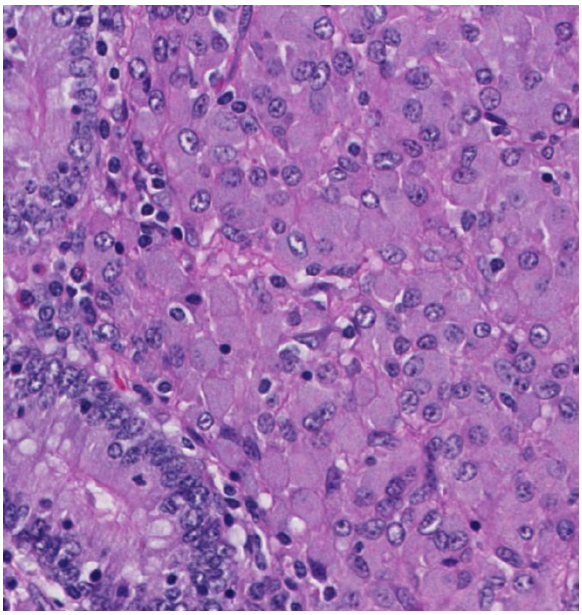

Intestine, sheep. Still higher magnification of the mucosal infiltrate, demonstrating large plump macrophages with gray, granular cytoplasm (which corresponds to the large number of intracytoplasmic bacilli.) (HE, 300X)

Sheep are usually infected early in life via the fecal-oral route, although infection can also be acquired through consumption of contaminated colostrum or *in utero* during advanced stages of the disease. A recent study characterized the pathology following experimental infection of MAP in adult sheep and found focal lesions restricted to the intestinal lymphoid tissue.[2] The M cells, specialized non-villous epithelial cells located in the Peyer's patches of small intestine, act as a main portal of entry and facilitate translocation of MAP across the intestinal epithelium where they are

phagocytized by macrophages. Macrophage recognition of MAP is mediated by host pathogen recognition receptors (PRRs), including Toll-like receptors (TLRs) and intracellular NOD-like receptors (NLRs). The MAP bacterium has a unique ability to replicate within macrophages by blocking or modulating antimicrobial activities that allow long-term survival.[5]

Broadly, two distinct phenotypes have been recognized based on the histologic features and the pathogen load: the lepromatous (organism-rich or multibacillary) form and the tuberculoid (paucibacillary) form. It is generally accepted that animals with paucibacillary lesions have a dominant Th1 type (IFN-γ) immune response, while animals with multibacillary lesions tend to have predominant Th2 type (antibody) response.[8] The progression in the severity of disease and degree of intestinal bacterial load parallels a switch from Th1 to a Th2 response.[3] In the present case, the ileum showed diffuse multibacillary feature (Type 3b) according to well-established histo-logical criteria for classifying lesions associated with natural paratuberculosis in sheep.[6]

Although the pathogenesis of Johne's disease in small ruminants is generally accepted to be similar to that in cattle, the clinical manifestations and gross pathology tend to be more insidious. Affected sheep show poor quality fleece, chronic wasting, and submandibular edema secondary to hypoalbuminemia, but overt diarrhea is not a common feature unlike in cattle. Enteric gross lesions are mild with little obvious thickening and no transverse ridges. Mineralized tubercle-like lesions in the mucosa, submucosa, serosa, and lymphatics of the intestine or lymph nodes have also been reported in goats and occasionally in sheep.[9]

The diagnosis of Johne's disease is difficult because of the organism's fastidious growth requirement and the lack of a specific diagnostic test that is sensitive enough to detect subclinical animals. Traditionally, fecal culture for MAP is considered the gold standard for diagnosis but is time-consuming and has poor reliability. As the humoral immune response is elicited late during infection, serological tests such as enzyme-linked immunosorbent assay (ELISA) are even less sensitive than fecal culture. The use of PCR for detection of MAP by amplifying the IS900 gene

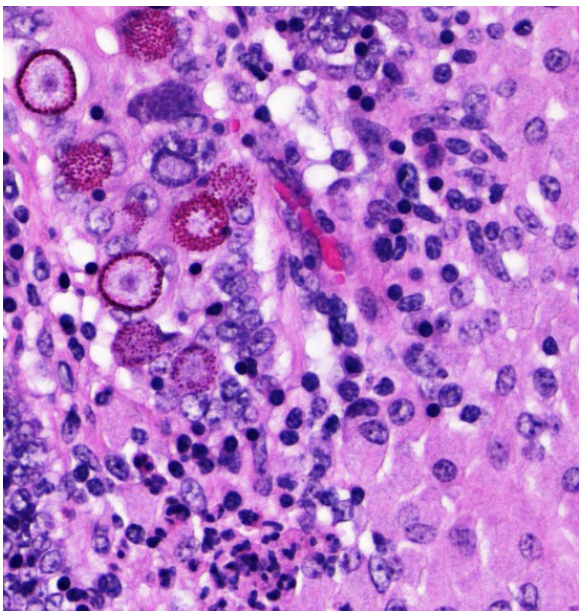

Intestine, sheep. Some sections contained coccidial gametocytes within the intestinal epithelium. (HE, 400X) (Photo courtesy of: Department of Diagnostic Medicine and Pathobiology, Kansas State Veterinary College of Veterinary Medicine, 1800 Denison Avenue, Manhattan, KS 66506, http://www.vet.k-state.edu/depts/dmp/index.htm

sequence in fecal samples has vastly improved the detection of low shedders.[10] Vaccination can be useful, but current vaccines have significant drawbacks that prevent their widespread use.

JPC Diagnosis: 1. Ileum: Enteritis, granulomatous, diffuse, severe, with villar

blunting, crypt loss, moderate serosal granulomatous lymphangitis and numerous acid-fast intrahistiocytic bacilli, Hampshire sheep, *Ovis aries*.
2. Ileum, crypts: Rare coccidian gamonts, schizonts, and oocysts.

Conference Comment: The contributor provides an excellent example, description, and thorough characterization of *Mycobacterium avium* subsp *paratuberculosis* (MAP) infection in sheep. Conference participants discussed different types of lesions associated with MAP infection, as well as virulence factors that allow the organism to evade immune destruction. The type of lesion produced is associated with the stage of disease. The major lesions of MAP are typically confined to the ileum, large intestine, and draining lymph nodes.[9] Occasionally, aortic and endocardial subintimal fibrosis and metastatic mineralization occurs due to overproduction of a vitamin D analog produced by macrophages during the granulomatous inflammatory disease.[1,9]

The **focal** form of MAP infection is typified by small, well-demarcated, granulomas in the lymphatic tissue of the intestine and lymph nodes; these are characteristic for the initial and latent stages of infection in adult animals. **Multifocal** forms are present in subclinical infections, and animals manifest with small granulomas in lymphoid tissue and in the lamina propria of the intestine; however, the normal histological architecture of the intestine is not drastically changed. This multifocal form is often subclinical and affected animals can still shed the organism and be infectious to herd mates resulting in the "iceberg effect," because in an infected herd, only a small percentage of the animals demonstrate clinical signs. Sheep and goats are generally thought to be more susceptible to clinical disease and have a shorter incubation period.[2,3,4,9,11]

Diffuse lesions are characterized by generalized granulomatous enteritis that affects both lymphoid tissue and the lamina propria of the intestine. This form, unlike the multifocal form, causes characteristic widespread cerebriform thickening of the intestinal wall. The diffuse form is divided into two categories based on the cell types and numbers of acid-fast bacteria (AFB) present: 1) the multibacillary/histiocytic form is composed of sheets of epithelioid macrophages with large numbers of intracytoplasmic AFB; and 2) the paucibacillary/lymphocytic form is typified by numerous lymphocytes within the lamina propria surrounding scattered granulomas with macrophages containing few or no AFB.

The focal, multifocal, or diffuse paucibacillary lesions are associated with the tuberculoid form mentioned by the contributor, and are a consequence of host bias toward a cell-mediated immunity response, with predominance of M1 or classically activated macrophages. Classically activated macrophages are more effective at killing intracellular bacteria. The diffuse multibacillary lepromatous form, present in this case, is associated with the less effective humoral response and M2, or alternatively activated, macrophages.[4,9,11]

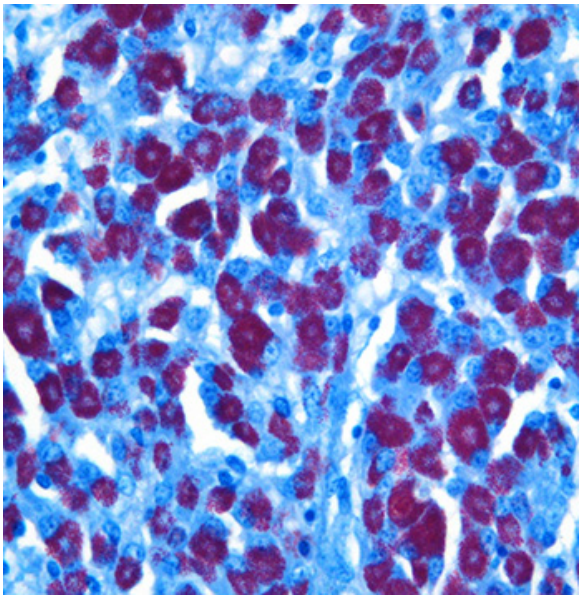

Intestine, sheep. An acid-fast stain on the mucosal infiltrate demonstrates large numbers of intracytoplasmic acid-fast bacilli. (AF, 400X) (Photo courtesy of: Department of Diagnostic Medicine and Pathobiology, Kansas State Veterinary College of Veterinary Medicine, 1800 Denison Avenue, Manhattan, KS 66506, http://www.vet.k-state.edu/depts/dmp/index.htm)

The virulence factors expressed by mycobacterial agents play a major role in the lesion type and pathogenicity of the organism. A recent study identified the macrophage subsets within granulomatous lesions in bovine paratuberculosis,[4] and as mentioned by the contributor, the pathogenesis in sheep is likely similar to that of cattle. The MAP organism, like other mycobacterial agents, does not secrete toxins; instead, its virulence is based on properties of its cell wall. Mannose and CD14 receptors expressed on macrophages stimulate phagocytosis of the organism. After phagocytosis, the mycobacterial cell wall receptor lipoarabinomannan (LAM) inhibits macrophage phagosome maturation by inducing expression of cytokines IL-10 and TGF-β through activation of TLR2 in the phagosome.[4,9,11] The bacterium can also inhibit acidification of the phagosome and phagosome-lysosome fusion. The cytokine IL-10 suppresses M1 macrophage activation, and thus the cell- mediated response, and enhances the Th2 humoral response. Further recruitment of alternatively activated M2 macrophages leads to widespread infection and progressive inflammation.[4,9,11] As the severity of the inflammation increases, MAP secretes exochelins, iron reductases, and siderophores to acquire iron from ferritin stored in macrophages, and inhibits iron-dependent conversion of H_2O_2 into hydroxyl radicals via the Fenton reaction.[11]

Several conference participants also noted rare intraepithelial coccidian microgamonts, macrogamonts, schizonts, and oocysts within the intestinal crypts. In sheep, the likely causes of coccidioisis in the small intestine are *Eimeria christenseni*, *E. ahsata*, *E. brakuensis*, and *E. crandallis*. In the cecum and colon of sheep, the most likely cause is *E. ovinoidalis*.[9]

Contributing Institution:

Department of Diagnostic Medicine and Pathobiology
Kansas State Veterinary College of Veterinary Medicine
1800 Denison Avenue
Manhattan, KS 66506
http://www.vet.k-state.edu/depts/dmp/index.htm

References:

1. Alshahrani F, Ajiohani N. Vitamin d: deficiency, sufficiency, and toxicity. *Nutrients*. 2013; 5(9):3605-3616.
2. Delgado L, Marin JF, Munoz M, et al. Pathological findings in young and adult sheep following experimental infection with 2 different doses of *Mycobacterium avium subspecies paratuberculosis*. *Vet Pathol*. 2013;50(5):857-866.

3. Dennis MM, Reddacliff LA, Whittington RJ. Longitudinal study of clinicopathological features of Johne's disease in sheep naturally exposed to *Mycobacterium avium subspecies paratuberculosis*. *Vet Pathol*. 2011;48(3):565-575.
4. Fernandez M, Benavides J, et al. Macrophage subsets within granulomatous intestinal lesions in Bovine paratuberculosis. *Vet Pathol*. 2016; Jun 17: pii: 0300985816653794. [Epub ahead of print].
5. Koets AP, Eda S, Sreevatsan S. The within host dynamics of *Mycobacterium avium ssp. Paratuberculosis* infection in cattle: where time and place matter. *Vet Res*. 2015;46(1):1-17.
6. Perez V, Marin JG, Badiola J. Description and classification of different types of lesion associated with natural paratuberculosis infection in sheep. *J Comp Pathol*. 1996;114(2):107-122.
7. Robbe-Austerman S. Control of paratuberculosis in small ruminants. *Veterinary Clinics of North America: Food Animal Practice*. 2011;27(3):609-620.
8. Sweeney RW. Pathogenesis of paratuberculosis. *Veterinary Clinics of North America: Food Animal Practice*. 2011;27(3):537-546.
9. Uzal F, Plattner B, Hostetter J. Alimentary system. In: *Jubb, Kennedy, and Palmer's Pathology of Domestic Animals*. Vol 2. 6th ed. Philadelphia, PA: Elsevier Limited; 2016: 194-197.
10. Windsor P. Paratuberculosis in sheep and goats. *Vet Microbiol*. 2015;181(1):161-169.
11. Zachary JF. Mechanisms of microbial infections. In: McGavin MD, Zachary JF, ed. *Pathologic Basis of Veterinary Disease*. 5th ed. St. Louis, MO: Elsevier; 2012:172-173.

CASE II: RUSVM Case 2 (JPC 4085381).

Signalment: Ten-year-old female mixed breed dog (*Canis familiaris*).

History: This dog presented to the RUSVM Spay Clinic for preoperative evaluation for elective ovariohysterectomy. The owner reported no significant medical history. Physical exam abnormalities included severe tick infestation; mildly but uniformly enlarged peripheral lymph nodes, and multiple mammary masses ranging in size from 1cm to 1.5cm diameter. Masses were present throughout the mammary chain but were concentrated in the caudal glands. Hematologic and chemistry findings included a moderate thrombocytopenia (65 x 109/l, range 200-500); severe lymphocytosis (16.2 x 109/l, range 1-4.8); and significantly elevated plasma protein (10.1 g/dl, range 6-7.5). The patient was prescribed doxycycline 100mg (8.5mg/kg) q24h for 21 days on the presumptive diagnosis of rickettsial disease. Further diagnostics were strongly recommended but declined. Surgical sterilization was postponed until further workup could be pursued.

Nine months later the patient represented to the RUSVM Emergency Service in respiratory distress. The owner indicated the patient's condition had been deteriorating and elected euthanasia, which was performed with 3ml of pentobarbital (200mg/ml).

Gross Pathology: At necropsy, a 12 x 9 x 8 cm, spheroid, hard mass was within the

Presentation, dog. The patient presented at autopsy with multiple mammary masses. (Photo courtesy of: Ross University School of Veterinary Medicine, 485 US Highway 1, South Building B, 4th floor, Iselin, NJ 08830 http://www.rossu.edu/veterinary-school/)

subcutis of the ventrocaudal abdomen, apparently replacing the left inguinal mammary gland. On cut surface, the mass was mottled pale pink and grey, gritty, and had a peripheral 3 cm cavitated area containing soft gelatinous opaque material. Six smaller firm nodular masses were present in other mammary glands, ranging in size from 0.5 to 2 cm. Similar 0.5-1.5 cm discrete, grey-white, nodular to sessile masses were heavily disseminated throughout the lungs, replacing nearly 90% of the parenchyma. The kidneys, spleen, and liver had a few similar masses, and a similar solitary 0.7cm mass spanned the epicardium and superficial myocardium of the right ventricular free wall.

Laboratory results: N/A

Histopathologic Description: Histologically, the large mammary mass and the kidney, spleen, liver, and lung masses consisted of embryonal rhabdomyosarcoma. A section of lung with multiple metastases is submitted for examination. The tumors were composed of large elongate tube-like to fusiform cells admixed with fewer round myoblastic cells and organized into interwoven bundles and streams of within myxomatous stroma. The elongate cells resembled myotubes, often having multiple tandemly aligned oval nuclei and poorly discernable sarcoplasmic cross striations ("strap cells"). Sarcoplasmic cross-striations were accentuated with phosphotungstic acid hematoxylin (PTAH) stain and enhanced by polarized light on preparations stained with Picrosirius red stain.

Tumor cells express moderate to marked and diffuse vimentin protein, moderate to marked and segmental desmin protein, but were negative for myoglobin, and smooth muscle actin.

When evaluated with electron microscopy, tumor cells varied from round, immature myoblast cells with variable amounts of cytoplasm to multinucleated myotubular developing skeletal muscle cells. The cytoplasm contained moderate amounts of mitochondria, glycogen, and ribosomes. Immature myoblast cells have eccentrically located nuclei with heterochromatin and one or two large nucleoli. The multinuclear tumor cells had indented nuclei with heterochromatin and abundant mitochondria and glycogen. Tumor cells contained myofilaments with Z-band like structures.

Lung, dog. Much of the pulmonary parenchyma was replaced by numerous 0.5-1.5cm whitish nodules. (Photo courtesy of: Ross University School of Veterinary Medicine, 485 US Highway 1, South Building B, 4th floor, Iselin, NJ 08830 http://www.rossu.edu/veterinary-school/)

Unequivocal cell junctions were present in the tumor cells.

Contributor's Morphologic Diagnosis: Lung: Metastatic rhabdomyosarcoma, embryonal

Contributor's Comment: Canine rhabdomyosarcomas are histologically classified as embryonal, botryoid, alveolar, and pleomorphic.[1] The mixture of round immature myoblastic cells and multi-nucleated myotubular cells resembling developing skeletal muscle are consistent with the embryonal subtype of rhabdomyosarcoma. In this case, the predominance of the myotubular cells is further indicative of the myotubular variant of embryonal rhabdomyosarcoma.

In humans, embryonal rhabdomyosarcoma is the most common type, and predominantly affects children.[7] Similarly, embryonal rhabdomyosarcoma is the most common type diagnosed in dogs, and usually involves dogs under two years of age. However, when excluding the botryoid type of embryonal rhabdomyosarcoma of the urinary bladder, approximately half of the reported cases of canine embryonal rhabdomyosarcoma occur in adult dogs, as observed in this case.[1] In humans, embryonal rhabdomyosarcoma is considered an intermediately aggressive variant of rhabdomyosarcoma. Canine rhabdomyosarcoma, in general, is considered an aggressive malignancy having a metastatic rate which appears to approximate that of grade three soft tissue sarcomas. However, there is too little data to make conclusions regarding the prognostic significance of histological subtypes in dogs. The present case would appear to comprise the first report of histologically-confirmed metastasis of embryonal rhabdomyosarcoma in an adult dog (>2 years), but appears to be of intermediate malignancy since the dog survived over nine months following clinical diagnosis of the mammary mass.

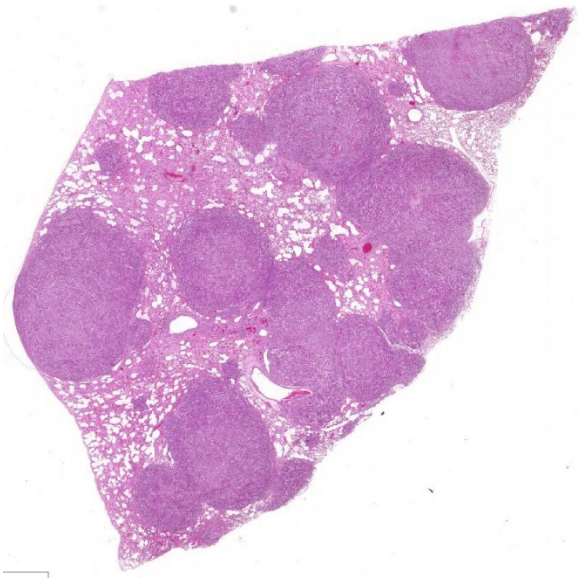

Lung, dog. Subgross examination of the submitted section reveals that neoplastic nodules replace approximately 80% of the tissue. (HE, 4X)

Rhabdomyosarcoma has occasionally been reported in dogs to emerge from organs lacking striated muscle, including skull,[4] meninges,[6] greater omentum,[8] gingiva,[9] spleen, perirenal, and mammary gland.[2] In such instances, the neoplasm is thought to arise from stem cells capable of myogenic differentiation. In the present case, the large mammary mass is presumed to be the primary tumor because it was the largest of all masses and was first recognized clinically. Mammary rhabdomyosarcoma is very rare in humans and usually affects adolescent girls, is metastatic rather than primary breast tumor, and is alveolar subtype.[5] Similar to the present case, the other reported case of canine mammary rhabdomyosarcoma involved an adult female, and was also of the embryonal subtype.[2]

JPC Diagnosis: Lung: Rhabdomyosarcoma, metastatic, mixed breed dog, *Canis familiaris*.

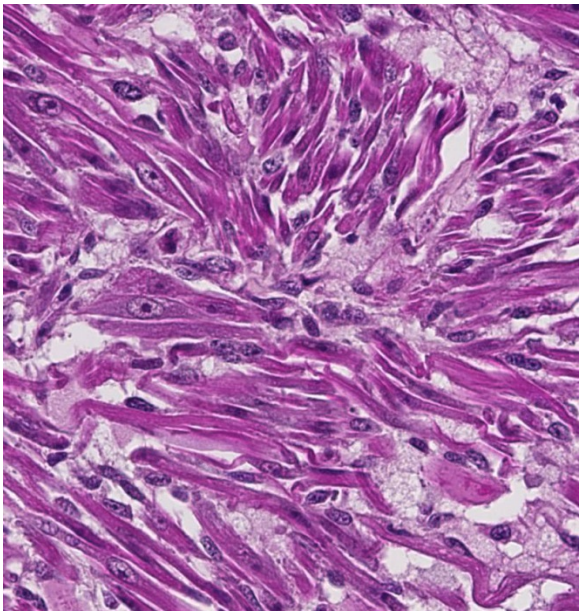

Lung, dog. Higher magnification reveals that neoplastic cells are spindled to strap-like with abundant cytoplasm, and one or more nuclei which line up in the center of the cell. (HE, 400X)

Conference Comment: The contributor provides an excellent example of a metastatic rhabdomyosarcoma (RMS) in the dog. RMS is a rare, malignant, neoplasm arising from pluripotent mesenchymal stem cells that differentiate toward skeletal muscle.[1,3] As a result of their pluripotent origin, RMS has a highly variable age of onset, location, gross, and histological appearance.[3]

As mentioned by the contributor, skeletal muscle neoplasms often arise in areas where skeletal muscle is not normally present. Common locations in the canine are the larynx and urinary bladder.[3] Laryngeal rhabdomyomas are formally known as laryngeal oncocytomas due to their characteristic eosinophilic, granular, PAS-positive cytoplasm. The name was changed to rhabdomyoma due to the presence of myofilaments with Z-bands on transmission electron microscopy (TEM), and positive immune-reactivity for muscle markers.[3] In the urinary bladder, RMS is also known as botryoid rhabdomyosarcoma. This most commonly occurs in young (<2 years), large breed bitches, with Saint Bernard dogs over-represented. Grossly, these botryoid neoplasms occur at the trigone and cause urinary obstruction.[3] Interestingly, they have also been associated with hypertrophic osteopathy in dogs.[3] In pigs, cardiac rhabdomyomas are benign incidental findings and are thought to be Purkinje cell origin due to expression of protein gene product (PGP) 9.5, a Purkinje fiber marker.[3]

Almost all RMSs are typically aggressive with local infiltration and distant metastasis to other muscles, liver, spleen, and the lung.[3] In this case, in addition to the lung and adjacent mammary tissue, there is metastasis to the kidneys, spleen, liver, epicardium, and myocardium.

RMS in humans and veterinary species has been classified into different categories

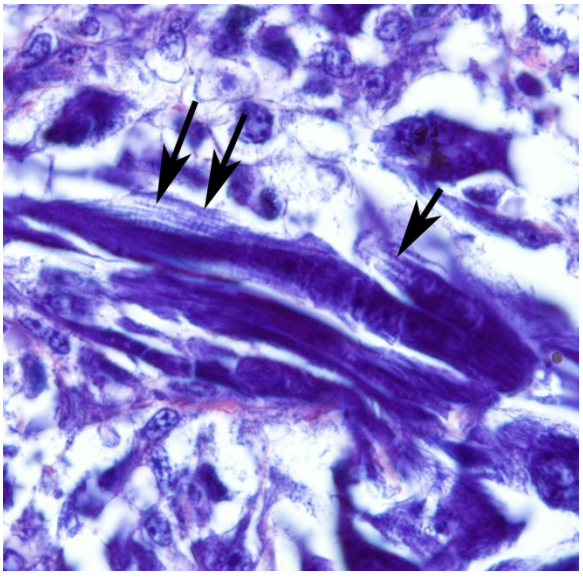

Lung, dog. Cross-striations are demonstrable on a phosphotungstic acid-hematoxylin stain (arrows). (PTAH, 400X) (Photo courtesy of: Ross University School of Veterinary Medicine, 485 US Highway 1, South Building B, 4th floor, Iselin, NJ 08830 http:/www.rossu.edu/veterinary-school/)

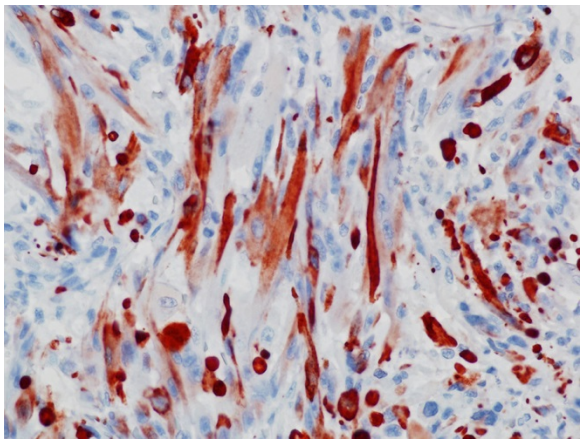

Lung, dog. Neoplastic cells exhibit strong cytoplasmic immunopositivity for desmin. (anti-desmin, 400X) (Photo courtesy of: Ross University School of Veterinary Medicine, 485 US Highway 1, South Building B, 4th floor, Iselin, NJ 08830 http://www.rossu.edu/veterinary-school/)

depending on the degree of differentiation towards skeletal muscle:

- **Embryonal:** Divided based on cell morphology: myotubular, myoblastic, spindle cell, and botryoid. Embryonal RMS is typically encountered in animals <2 years old, and occur on the face, skull, masticatory muscle, oropharynx, trachea, axilla, scapula, perirenal, tongue, flank, leg, mammary gland, and hard palate. Botryoid RMS occurs in the urinary bladder and uterus. [1,2,3] The mammary gland is theorized to be the primary tumor location in this case.
    - Myotubular: Multinucleated strap cells and racquet cells with cross-striations.
    - Myoblastic: Most common form, and is composed of small round cells with abundant eosinophilic cytoplasm.
    - Spindle cell: Low cellularity and arranged in a storiform pattern.
    - Botryoid: Submucosal location with mixed round and myotubular cells. The term botryoid is due to grape-like appearance grossly.[1,3]
- **Alveolar**: Sheets of small, undifferentiated round cells on a fibrous framework arranged in "alveolar-like" structures due to lack of cohesiveness in the center of neoplastic nests. These are usually found in the hip, maxilla, omentum, and uterus.[1,3]
- **Pleomorphic**: Extremely rare and only reserved for RMS that do not display any features of embryonal or alveolar RMS. They are characterized by haphazardly arranged plump spindle cells with marked anisocytosis and aniso-karyosis and bizarre mitotic figures. This type is more common in

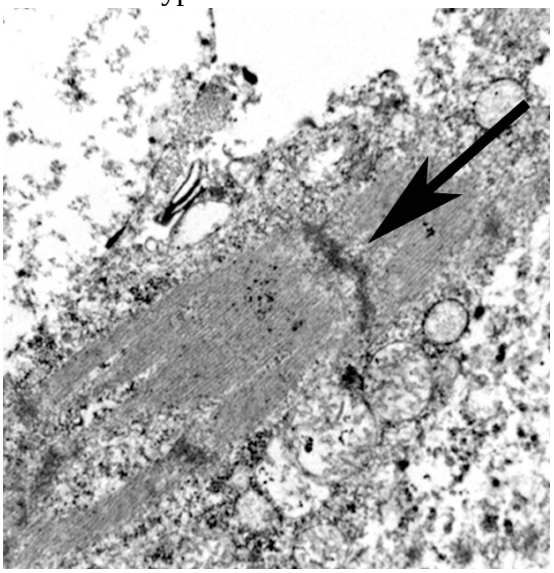

Lung, dog. Ultrastructurally, neoplastic cells demonstrate well-formed myofibrils and Z-bands (arrow). (Photo courtesy of: Ross University School of Veterinary Medicine), 485 US Highway 1, South Building B, 4th floor, Iselin, NJ 08830 http://www.ross.edu/veterinary-school/)

adults.[1,3]

The use of immunohistochemistry (IHC) to identify vimentin, desmin, α-actins, myoglobin, myogenin, and MyoD1 in conjunction with TEM to identify of sarcomeric structures, Z-bands, and large mitochondria, can also be useful in the diagnosis RMS.[1,2,3]

Contributing Institution:
Ross University School of Veterinary Medicine
485 US Highway 1
South Building 1, 4th Floor
Iselin, NJ 08830
http://www.rossu.edu/veterinary-school/

References:

1 Caserto BG: A comparative review of canine and human rhabdomyosarcoma with emphasis on classification and pathogenesis. *Vet Pathol*. 2013; 50(5):806-826.

2 Cooper BJ, Valentine BA: Tumors of muscle. In: Meuten DJ, ed. *Tumors in Domestic Animals. Fourth Edition* ed. Ames, Iowa: Iowa State Press; 2002:319-364.

3 Cooper BJ, Valentine BA. Muscle and tendon. In: *Jubb, Kennedy, and Palmer's Pathology of Domestic Animals*, ed. Maxie MG, 6th ed., Vol. 1. Saunders Elsevier, Philadelphia, PA, 2016:241-243.

4 Da Roza MR, De Amorim RF, Carneiro FP, Benatto N, Barriviera M, Miguel MC: Aggressive spindle cell rhabdomyosarcoma in an 11-month-old boxer dog. *J Vet Med Sci*. 2010; 72(10):1363-1366.

5 Hays DM, Donaldson SS, Shimada H, Crist WM, Newton WA, Jr., Andrassy RJ, et al.: Primary and metastatic rhabdomyosarcoma in the breast: neoplasms of adolescent females, a report from the Intergroup Rhabdomyosarcoma Study. *Med Pediatr Oncol*. 1997; 29(3):181-189.

6 Illanes OG: Juvenile parameningeal rhabdomyosarcoma in a dog causing unilateral denervation atrophy of masticatory muscles. *J Comp Pathol*. 2002; 126(4):303-307.

7 Newton WA, Gehan EA, Webber BL, Marsden HB, van Unnik AJM, Hamoudi AB, et al.: Classification of rhabdomyosarcomas and related sarcomas. Pathologic aspects and proposal for a new classification-an intergroup rhabdomyosarcoma study. *Cancer*. 1995; 76(6):1073-1085.

8 Sarnelli R, Grassi F, Romagnoli S: Alveolar rhabdomyosarcoma of the greater omentum in a dog. *Vet Pathol*. 1994; 31(4):473-475.

9 Snyder LA, Michael H: Alveolar rhabdomyosarcoma in a juvenile labrador retriever: case report and literature review. *J Am Anim Hosp Assoc*. 2011; 47(6):443-446.

CASE III: 15183 (JPC 4082892).

Signalment: Three-year-old ovario-hysterectomized female domestic shorthair cat (*Felis catus*).

History: This cat had a history of tail chewing, hair loss and recurring dermatitis over the tail and caudodorsum, occurring

Haired skin, cat. The skin of the caudodorsum had a large area of ulceration and crusting in proximity to a previous caudectomy site. (Photo courtesy of: University of Minnesota, Veterinary Diagnostic Laboratory, http://www.vdl.umn.edu)

since this cat was acquired as a kitten from Florida. Affected areas of skin were alopecic with erythema, crusted papules, plaques, and nodules. There was limited to no clinical response to treatment with fluoxetine, topical antibiotics and regular flea prevention and the cat deteriorated following injections of depomedrol and cefovecin. Following biopsy and initial diagnosis, the cat underwent tail amputation; however, the cat had recurring dermatitis over the caudodorsum 3 weeks postoperatively and was euthanized and submitted for necropsy.

Gross Pathology: At necropsy, there were two reddened, ulcerated areas over the caudodorsum with variable brown crusts and dried red-brown exudate. The caudal, larger area of ulceration and crusting was overlying a healing scar within the skin (interpreted as part of the surgical site from the previous tail amputation). The cranial, smaller area of ulceration was not associated with the previous surgical wound. On cut section, these areas extended into and expanded the subcutis, with poorly demarcated, tan to pink, firm, multifocal to coalescing nodules. There was no gross involvement of the underlying vertebrae and no gross evidence of spread to lymph nodes or visceral organs.

Laboratory results: Previous biopsy and culture of the affected areas yielded scant mold; further identified as *Lagenidium* sp. by 18S/ITS (internal transcribed spacer) nucleic acid amplification and sequence analysis. Culture of necropsy samples was unable to repeat isolation of *Lagenidium* spp.

Histopathologic Description: The section examined was taken from the cranial, smaller area of skin ulceration not associated with the previous surgical wound. Underlying a locally extensive area of ulcerated epidermis and expanding the dermis and subcutis, there is a poorly demarcated, non-encapsulated infiltration of large numbers of eosinophils, moderate lymphoplasmacytic and histiocytic infiltrates and fewer neutrophils, with extensive, multifocal areas of eosinophilic necrotic and karyorrhectic cellular debris. Within areas of necrosis, there are small to moderate numbers of predominantly negatively stained, extracellular, 10-15 µm diameter hyphae with variably prominent round or bulbous dilatations and intermittent right angle branching. Areas of necrotic cellular debris and inflammatory cellular infiltrate surround

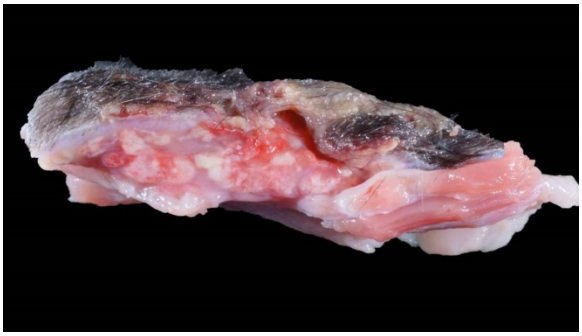

Haired skin, cat. On cut section, the dermis is expanded by numerous white-tan nodules. (Photo courtesy of: University of Minnesota, Veterinary Diagnostic Laboratory, http://www.vdl.umn.edu)

and isolate small aggregates of irregular, eosinophilic collagen fibers (collagenolysis).

Special Stains: Staining with Grocott's methenamine silver (GMS) yielded moderate numbers of broad, thick-walled hyphae of varying diameters that are occasionally septate. Staining with Periodic-Acid-Schiff (PAS) highlights hyphae with similar morphology, albeit less prominently.

Contributor's Morphologic Diagnosis:
1. Skin, caudodorsum: Dermatitis, panniculitis, steatitis and myositis, eosinophilic and histiocytic, with lympho-plasmacytic infiltrates, marked, locally extensive, chronic with multifocal necrosis and hyphae
2. Skin, caudodorsum: Ulceration, multi-focal, moderate to marked, chronic

Contributor's Comment: The fungal hyphae present in this case are consistent with a recurrence of dermatitis associated with *Lagenidium* sp., previously confirmed in this cat by 18S/ITS nucleic acid amplification and sequence analysis. Members of the genus *Lagenidium* sp. are a group of the *Oomycetes*, closely related to *Pythium* sp. and often referred to as 'water molds'. *Oomycetes* are frequently pathogens of plants, nematodes, and insect larvae;

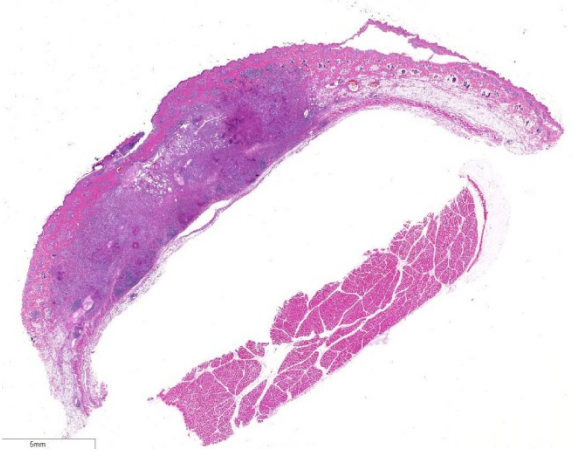

Haired skin, cat. Subgross examination reveals diffuse cellular infiltration by a profound cellular infiltrate with multifocal areas of necrosis. (HE, 5X)

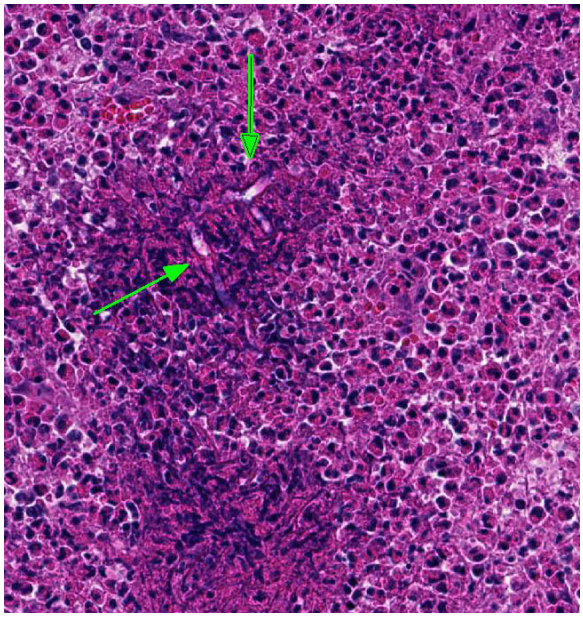

Haired skin, cat. Large sheets of eosinophils surround areas of necrosis, which contain outlines of fungal hyphae. (HE, 400X)

however, they are occasionally associated with disease in mammals.[2] The most widely known *Lagenidium* species is *Lagenidium giganteum*, a pathogen of mosquito larvae that has previously been implemented as a biologic control agent.[2] Although stages of oomycetes may be morphologically similar to fungal hyphae, oomycetes are phylogenetically distinct from fungi.[7,8] In contrast to fungi, the cell wall of oomycetes contains cellulose and β-glucan rather than chitin[8], and the cell membranes lack ergosterol.[7] Oomycetes also differ from fungi with respect to life stages produced, including the production of sporangia and biflagellate zoospores.[7]

Most case reports of lagenidiosis involve dogs; however, there have been several recent reports in cats.[7] Infection with *Lagenidium* sp. in dogs typically occurs in young to middle-aged dogs and most frequently occurs in southeastern United States.[2,3,7] Exposure to water bodies such as lakes and ponds is frequently, but not always, reported.[3] Recent molecular work has led to the description of two closely

related pathogens in dogs; *Lagenidium giganteum* forma *caninum* and *Paralagenidium karlingii*.[5] *Lagenidium giganteum* forma *caninum* causes cutaneous or subcutaneous disease with frequent widespread dissemination, involving visceral organs, lymph nodes and/or great vessels.[3] *Paralagenidium karlingii* infection in dogs results in chronic ulcerative and/or nodular dermatitis that does not typically disseminate.[5] Recommended treatment for lagenidiosis is wide surgical resection where possible.[1,3,7] Prognosis is poor for disseminated disease, with lagenidiosis poorly responsive to medical therapy.[2,9]

Differential diagnoses for lagenidiosis on clinical presentation and histopathology may include pythiosis, resulting from infection with the oomycete, *Pythium insidiosum*; and zygomycosis, involving infection with fungal organisms such as *Basidiobolus ranarum* and *Conidiobolus* spp..[1,2,5] All may result in granulomatous and/or eosinophilic inflammation and morphologically appear as broad, irregular branching hyphae that are rarely to occasionally septate.[1] Differentiation is clinically important due to differing treatment and prognosis[7,8].

Diagnosis of lagenidiosis can be challenging. Cytology and histopathology yield hyphae with similar morphology to pythiosis and zygomycosis.[4] Although there may be subtle differences in size and/or morphology of hyphae, histopathology cannot be used for definitive differentiation.[3] Fungal culture is possible but can be difficult due to the fastidious nature of *Lagenidium* sp. (particularly the sexual stages). Definitive diagnosis requires confirmation through molecular assays on tissue or cultured isolates.[3,7,9] *Lagenidium* sp. should be considered a differential in cats with granulomatous to eosinophilic, nodular to ulcerative dermatitis.

JPC Diagnosis: Haired skin and subcutis: Dermatitis, panniculitis and myositis, eosinophilic and gran-ulomatous, and eosinophilic, focally extensive, marked, with multifocal necrosis, ulceration, and fungal hyphae, domestic shorthair, *Felis catus*.

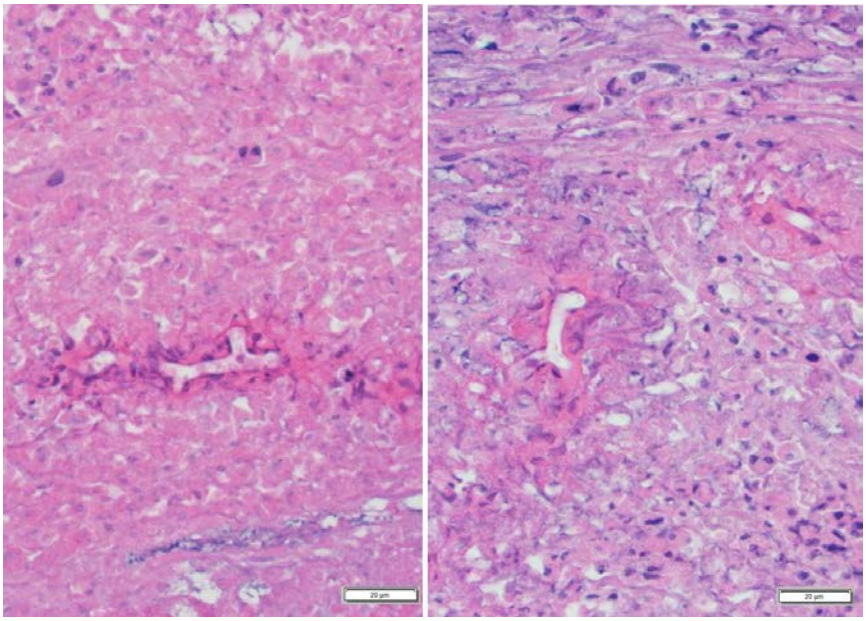

Haired skin, cat. Fungal hyphae measure 10-15 um with right angle branching. (Periodic acid-Schiff, 600X)(Photo courtesy of: University of Minnesota, Veterinary Diagnostic Laboratory, http://www.vdl.umn.edu)

Conference Comment: The contributor provides an excellent example and overview of the pathogenic Oomycete water mold, *Lagenidium sp*. As mentioned above, *Lagenidium* sp. is strikingly similar in geographic distribution, clinical, and histologic appearance to the more commonly diagnosed Oomycete, *Pythium insidiosum*.[6] As a result, the

majority of conference participants had pythiosis as their top differential for this lesion.

Infection with both *Pythium insidiosum* and *Lagenidium* spp. typically, but not always, occurs when the host has prolonged contact with standing or stagnant water containing the motile aquatic flagellate zoo-spores.[2,3,6] This infectious form of the organism is attracted by animal fur, damaged skin, and intestinal mucosa. As a result of contact with standing water, infections in domestic animals are most commonly reported in the limbs, ventral thorax, and abdomen. When a mammalian host with a skin injury enters a contaminated pond, the oomycete zoospores of will encyst upon contact with the injured skin and mechanically penetrate the tissue, causing clinical disease.[6]

Like pythiosis, this disease is typically highly aggressive and lesions in the great

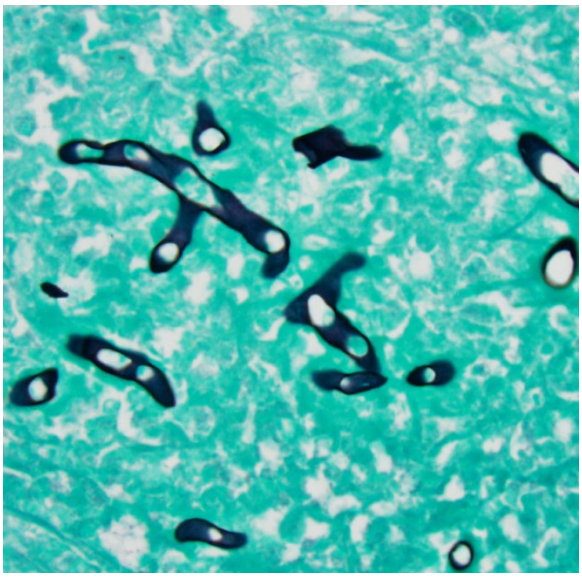

Haired skin, cat. Fungal hyphae are thick-walled with non-parallel walls and occasional septa. (Gomori methenamine silver, 600X)(Photo courtesy of: University of Minnesota, Veterinary Diagnostic Laboratory, http://www.vdl.umn.edu)

vessels, mediastinum, lungs, and esophagus have been reported in dogs. However, unlike pythiosis, gastrointestinal disease has not been reported in *Lagenidium* spp.[6] Both entities are associated with a poor to grave prognosis even with wide surgical excision of cutaneous masses because the majority of animals infected with this pathogen have occult, non-resectable, disease in regional lymph nodes or distant sites when initially diagnosed.[2,3] In dogs infected with the less aggressive species, *Paralagenidium karlingii* mentioned by the contributor, surgery that achieves three cm margins is often curative.[7] Medical therapy for lagenidiosis is typically ineffective because ergosterol, the target for most antifungal drugs, is lacking in the Oomycete cell membrane.[6,7]

Conference participants discussed this lesion as a great example of chronic-active inflammation. Chronic-active inflammation occurs when the inciting inflammatory stimulus has not been removed from the chronic inflammatory process and continues to elicit an acute inflammatory response.[1] In this case, surrounding fungal hyphae are numerous eosinophils, neutrophils, and fibrin admixed with brightly eosinophilic plasma protein that is reminiscent of Splendore-Hoeppli material.

Contributing Institution:
University of Minnesota
Veterinary Diagnostic Laboratory
1333 Gortner Ave.
St. Paul, MN 55108
http://www.vdl.umn.edu

References:

1. Ackermann M. Inflammation and healing. In: McGavin MD, Zachary JF, eds. *Pathologic Basis of Veterinary Disease*. 4th ed. St. Louis, MO:Mosby Elsevier; 2012:127.

2. Grooters AM. Pythiosis, lagenidiosis and zygomycosis. *Vet Clin Small Anim*. 2003; 33:695-720.
3. Grooters AM, Hodgin EC, Bauer RW, Detrisac CJ, Znajda NR, Thomas RC. Clinicopathologic findings associated with *Lagenidium* spp. infection in 6 dogs: Initial description of an emerging oomycosis. *J Vet Intern Med*. 2003;17:637-646.
4. Grooters AM, Foil CS. Miscellaneous fungal infections. In: Greene CE, ed. *Infectious Diseases of the Dog and Cat*. 4th ed. Philadelphia, PA: WB Saunders; 2012:681-683.
5. Hartfield JN, Grooters AM, Waite KJ. Development and evaluation of an ELISA for the quantification of anti-*Lagenidium giganteum forma caninum* antibodies in dogs. *J Vet Intern Med*. 2014; 28:1479-1484.
6. Mauldin E, Peters-Kennedy J. Integumentary system. In: Maxie MG, ed. *Jubb, Kennedy, and Palmer's Pathology of Domestic Animals*. Vol 1. 6th ed. Philadelphia, PA:Elsevier; 2016:657-660.
7. Mendoza L, Vilela R. The Mammalian pathogenic oomycetes. *Curr Fungal Infec Rep*. 2013; 7:198-208.
8. Raffaele S, Kamoun S. Genome evolution in filamentous plant pathogens: why bigger can be better. *Nature Reviews Microbiology*. 2012; 10:417-430.
9. Znajda NR, Grooters AM, Marsella R. PCR-based detection of *Pythium* and *Lagenidium* DNA in frozen and ethanol-fixed animal tissues. *Vet Dermatology*. 2002; 13:187-194.

CASE IV: S1103067 (JPC 4003084).

Signalment: Adult female alpaca (*Vicugna pacos*).

History: The animal had a five-week duration of illness that consisted of progressive severe weight loss, and a subacute onset of unilateral blindness on the left, with right head tilt and circling to the right. There were palpably soft areas of the skull that were originally diagnosed as skull fractures. Radiographs were not taken. Treatments included antibiotics, steroids, non-steroidal anti-inflammatory drugs, and supportive therapy. In the absence of response to treatment, a brain tumor was suspected and the owner elected euthanasia.

Gross Pathology: The referring veterinarian removed the head and disposed of the remainder of the carcass. The calvarium was deformed with pronounced nodular doming and multifocal marked thinning and translucency over the caudodorsal aspect of the left and, to a lesser extent, the right cerebral hemispheres. The calvarium and intact brain were fixed in formalin and submitted to the CAHFS- San Bernardino laboratory for histologic examination.

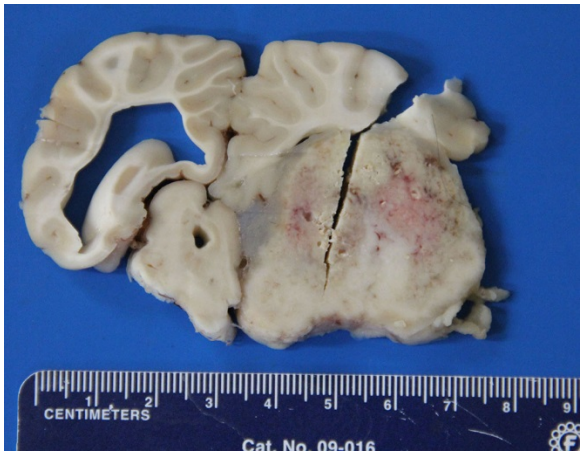

Cerebrum, alpaca: The right cerebrum is 50% effaced by a large granuloma which effaces the lateral ventricle, crosses the midline and has resulted in expansion of the left lateral ventricle and 3rd ventricle. (Photo courtesy of California Animal Health and Food Safety Laboratory – San Bernardino Branch, University of California Davis, 105 W. Central Avenue, San Bernardino, CA 92408 http://cahfs.ucdavis.edu/)

On removal of the calvarium, a large, firm mass with several, irregular, soft areas were identified in the right cerebral hemisphere. The caudal half of the right hemisphere was moderately enlarged, misshapen and firm, with focal nodularity of the meningeal surface of the caudolateral aspect of the hemisphere. Transverse sectioning of the rostral half of both cerebral hemispheres revealed bilateral, moderate hydrocephalus (dilated lateral ventricles / reduced thickness of the cerebral grey and white matter). Extending caudally from the optic chiasm to the posterior extremity of the right cerebral hemisphere, was an irregular, nodular, roughly egg-shaped mass with approximate dimensions of 5.5 cm [length] x 3-4 cm [width] x 3.5-4 cm [height]. The mass markedly expanded and distorted the right lateral ventricle, and deformed/ partially replaced the right thalamus. Further caudally, there was partial replacement of the right diencephalon / mesencephalon by the mass. The left thalamus / mesencephalon was laterally displaced and the left ventricle was dilated (hydrocephalus) from the rostral

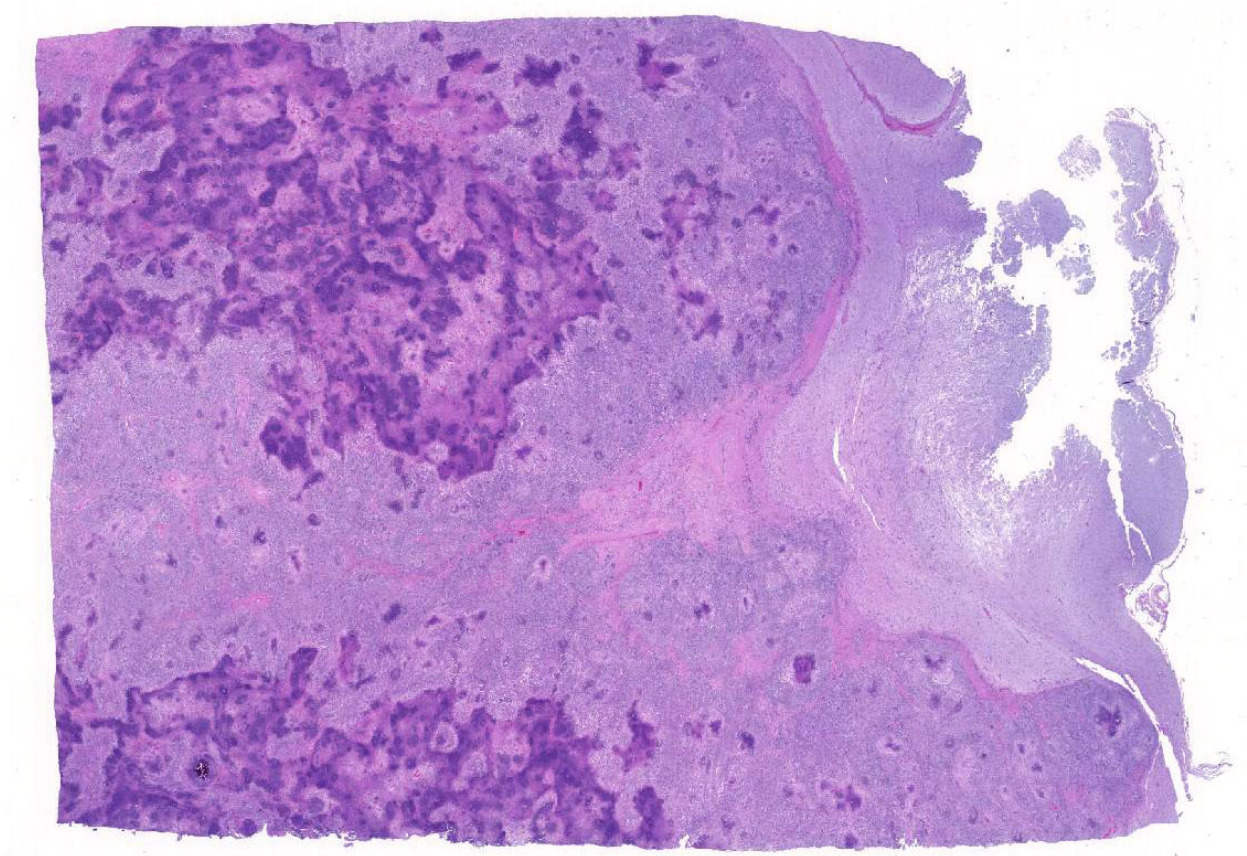

Cerebrum, alpaca: The section is 90% effaced by granulomatous inflammation containing geographic outlines of lytic necrosis. The cerebrum at right contains a large area of cavitary necrosis. (HE, 4X)

to the caudal extremities.
On cross section, the mass was firm, slightly gritty, and mottled, tank/pink/cream with scattered yellow foci of approximately 0.2 cm in diameter.

Laboratory results: N/A

Histopathologic Description: Brain, cerebral cortex: Affecting approximately 90% of the white matter and disrupting the normal architecture is a well-demarcated, non-encapsulated inflammatory focus. The focus consists of multiple, discrete to coalescent, variably-sized cores of necrosis, viable and degenerate neutrophils, extravasated red cells and /or mineral, interspersed with expanses of granulomatous to mixed inflammation and plump reactive astrocytes. Large numbers of fungal spherules of varying sizes and stages of development and occasional clusters of endospores are scatted throughout the necrotic cores, in few multinucleate giant cells, or free amongst the mixed inflammatory infiltrate. Spherules are round, range in size from 20-60 um in diameter, and are surrounded by a 3–5 um thick, double contour, hyaline wall. Spherules are empty, or contain either granular to flocculent, basophilic material or 4–5 um oval endospores. In some sections, the inflammatory focus regionally extends to involve the meninges, while in others the border is irregular with peripheral, discrete pyogranulomas. Neuropil bordering the inflammatory focus is either rarified (malacic) with proteinaceous effusion (edema), gitter cell infiltration and astrocyte proliferation, or is irregularly infiltrated by aggregates of lymphoplasmacytic cells.

In other sections (slides not submitted), there is marked dilation of the lateral ventricle accompanied by multifocal, mild to moderate cuffing of subependymal blood vessels by plasma cells. One section of the lateral ventricle contains clumps of cellular debris, purulent exudate, and several small spherules. A moderate lymphoplasmacytic infiltrate is present in the choroid plexus.

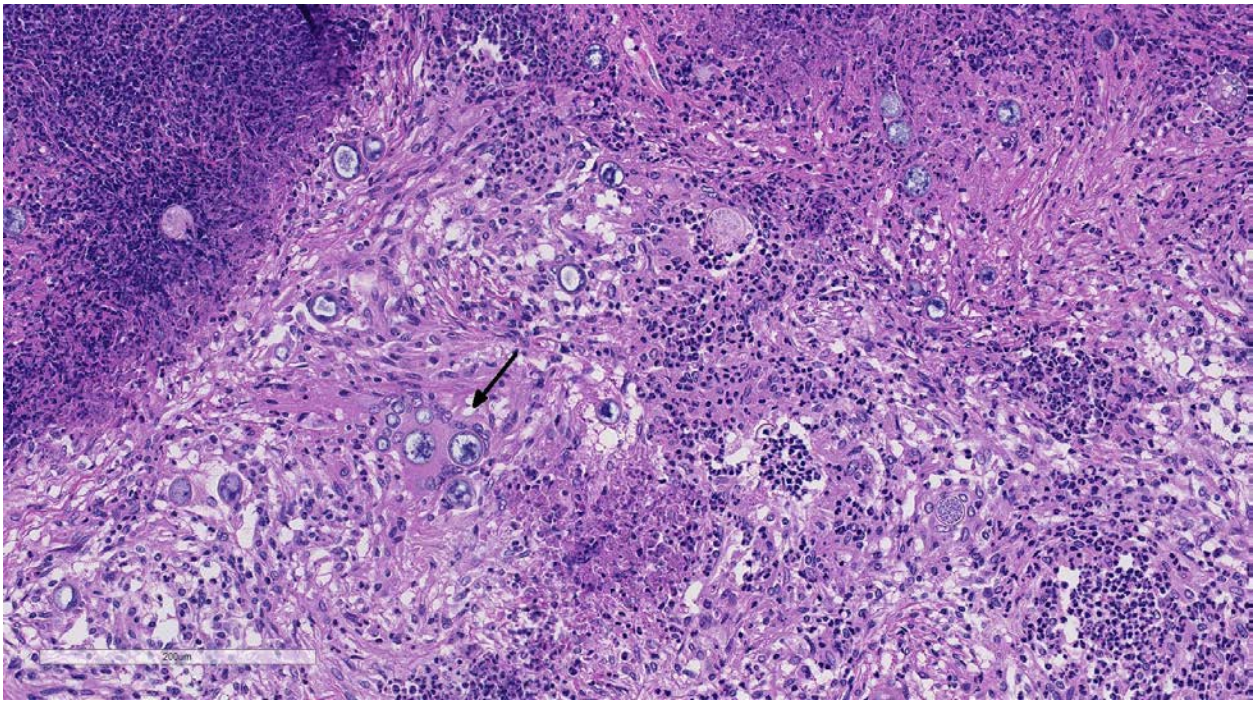

Cerebrum, alpaca: Enmeshed in a bid of spindling epithelioid macrophages, astrocytic processes, and fibroblasts within loosely arranged collagen, and spherules of Coccidioides immitis are present within foreign body-type multinucleated macrophages (arrow), surrounded by aggregates of neutrophils, and scattered throughout areas of lytic necrosis. (HE, 400X)

Contributor's Morphologic Diagnosis:
Brain, right cerebral cortex including the lateral ventricles and meninges:
1. Meningoencephalitis, necrotizing and pyogranulomatous, focally extensive, chronic, severe, with numerous intralesional fungal spherules and endospores, etiology consistent with *Coccidioides* spp.
2. Hydrocephalus, bilateral, moderate.

Contributor's Comment: The dimorphic soil fungi, *Coccidioides immitis* and *C. posadassi*, are the causative agents of coccidioidomycosis, a systemic fungal disease in man and animals.[8] The disease is endemic in arid regions of southwestern USA, Mexico, Central and South America[9], and is commonly known as desert fever, valley fever, or San Joaquin Valley fever.[8] Coccidioidomycosis has been reported in a large variety of domestic animals including dogs[2], cats[17], horses[10], llamas[4], and wild animals including chimpanzee[11], bottlenose dolphin[13], free- living California sea lions[7], Przewalski's horses[16], and mountain lion.[1]

Fungal mycelia survive well in dry, hot conditions; grow after intense rainfall and release arthroconidia which are disseminated by the wind.[3,9] Inhalation of airborne arthroconidia is the most common route of infection, although local traumatic inoculation has been associated with cutaneous and subcutaneous lesions.[3] The arthroconidia migrate to bronchi and alveoli and transform to yeast forms (immature spherules) of 10-20 um in diameter. As spherules mature they enlarge up to 100 um in diameter and are surrounded by a double contour, 4-5 um hyaline wall. Spherules undergo endosporulation forming numerous uninucleated endospores 2-5 um in diameter. Mature spherules rupture to release endospores that form new spherules in tissue or mycelia if released to the environment.[3,14] Dissemination to other organs is through

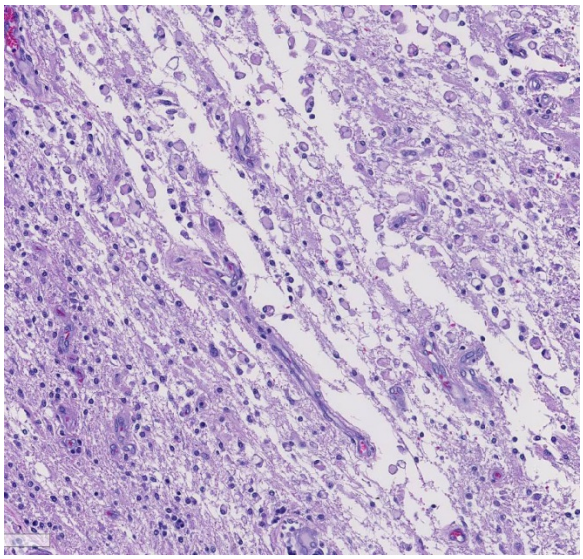

Cerebrum, alpaca: A large focus of cavity necrosis (right) is present adjacent to the granuloma, suggesting an infarct as a result of vascular interruption. Cellular debris, presumably the majority of which is myelin, is being phagocytized by numerous Gitter cells. (HE, 400X)

blood or lymphatics, and fungi are believed to reach the central nervous system through leukocytic trafficking and hematogenous spread from primary sites of infection.[3,12]

Three main virulence mechanisms by which *Coccidiodes* spp. survive in host environment have been described.[12] These include:

1. Production of dominant spherule outer wall glycoprotein (SOWgp) which modulates the host immune response resulting in compromised cell-mediated immunity
2. Depletion of SOWgp presentation on endospore surface preventing host recognition of the pathogen
3. Induction of host arginase 1 (decreased nitric oxide production) and coccidial urease which contribute to tissue damage at sites of infection.

Successful host immunological response to *Coccidioides* spp. is dominated by cell-mediated immunity[9,12, 15], particularly Th1, and in general is related to the phase of the

organism involved.[11] Due to the marked increase in size as the spherules mature, phagocytosis is restricted to initial yeast cells from germinated arthroconidia, and endospores released from ruptured spherules.[12] Inhaled arthroconidia elicit an initial response composed primarily of neutrophils with fewer macrophages and lymphocytes; in later stages, a granulomatous response predominates.[1,2]

Although the spherule form shed from lesions is not readily infectious, arthroconidia from mature cultures are easily aerosolized and are highly infectious.[14] As such, *Coccidioides immitis* is designated as Biosafety Level 3, and is classed as a select agent of bioterrorism in the United States due to its high virulence and infectious nature.[6]

JPC Diagnosis: 1. Cerebrum and meninges: Meningoencephalitis, pyogranulomatous and necrotizing, focally extensive severe with intra- and extracellular endosporulating yeasts, alpaca (*Vicugna pacos*).
2. Cerebrum, grey matter: Necrosis, focal, moderate.

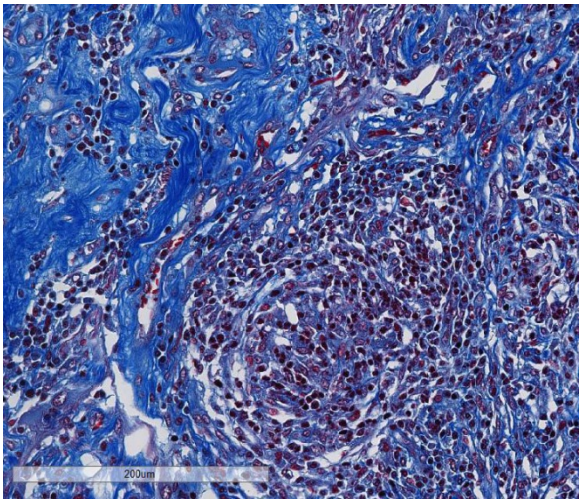

Cerebrum, alpaca. A Masson's trichrome stains reveals abundant collagen within the granuloma, which is unusual, as fibrocytes are not a normal parenchymal component in the brain. It is likely that fibrocytes penetrated into the granuloma from the adjacent meninges. (Masson's trichrome, 320X)

Conference Comment: The contributor provides a striking example and a concise review of the epidemiology, pathogenesis, and virulence factors of these dimorphic, endosporulating fungi. South American camelids, such as llamas and alpacas, are exquisitely susceptible to coccidioidal infection and clinical cases usually present with severe respiratory and/or disseminated infection.[9] In any species, disseminated disease can occur either early, or several months after initial infection.[3,9] In dogs, up to 22% can have disseminated systemic infection without a history of respiratory disease. However, cases of systemic lesions without pulmonary involvement are theorized to reflect clinical resolution of the lung, rather than extra-pulmonary infection.[3,9]

The most common presentation of disseminated disease is lameness due to osteomyelitis.[9,10] This typically occurs late in the disease and is characterized by osteolytic granulomas surrounded by proliferative new bone growth. Painful draining tracts in the overlying skin, palpable bone swelling, and enlarged and reactive regional lymph nodes are additional signs of disseminated disease.[3] However, generalized lymphadenopathy is uncommon in this disease.[3,9] Other clinical signs of disseminated disease are variable and are usually dependent on the organ infected. Animals with central nervous system (CNS) disease, such as this case, typically have seizures, progressive ataxia, and are comatose in severe cases. Other organs affected include: eyes, liver, spleen, kidney, and testes.[3,9] Abortion has also been reported in both horses and an alpaca in Southern California.[5]

This case generated enthusiastic debate among conference participants regarding

whether the profound pyogranulomatous inflammation effacing 90% of the histologic section originated from the cerebrum or the meninges. Participants favoring cerebral origin argued that the cerebrum is lost and replaced by an astrocytic scar with spindled and palisading epithelioid macrophages. Participants favoring meningeal origin noted that the spindled cells are birefringent and likely represent collagen and fibrous connective tissue deposition secondary to chronic pyogranulomatous inflammation. A Masson's trichrome stain revealed abundant blue staining collagen within the granuloma. Given that fibrocytes are not a normal component of the neuropil, it is likely that fibrocytes penetrated into the granuloma from the adjacent meninges. The granuloma was also diffusely immune-negative for glial fibrillary acidic protein (GFAP), supporting a meningeal origin of the granuloma rather than an astrocytic scar in the cerebrum.

Several conference participants also noted a focal area of cavitary necrosis within the cerebrum adjacent to the pyogranuloma. This is likely due to thrombosis of a vessel adjacent to the large granulomatous nodule, creating an infarct in the section of the cerebrum. Unfortunately, none of the conference participants noted vascular thrombi within their tissue sections. The vascular thrombi may be out of the plane of section.

Contributing Institution:

California Animal Health and Food Safety Laboratory
San Bernardino Branch
University of California Davis
105 W. Central Avenue,
San Bernardino, CA 92408
http://cahfs.ucdavis.edu

References:

1. Adaska JM. Peritoneal coccidioidomycosis in a mountain lion in California. *J Wildl Dis*. 1999; 35:75-77.
2. Ajithdoss DK, Trainor KE, Snyder KD, Bridges CH, Langohr IM, Kiupel M, Porter BE. Coccidioidomycosis presenting as a heart base mass in two dogs. *J Comp Pathol*. 2010; 145:132-137.
3. Caswell JL, Williams KJ: Respiratory system. In: Maxie MG, ed. *Jubb, Kennedy, and Palmer's Pathology of Domestic Animals*. 6th ed. Vol 2. St. Louis, MO: Elsevier; 2016: 583-584.
4. Coster ME, Ramos-Vara J, Vemulapalli R, Stiles J, Krohne SG. *Coccidioides posadasii* keratouveitis in a llama (*llama glama*). *Vet Ophthalmol*. 2010; 13:53-57.
5. Diab S, Johnson S, et al. Case report: abortion and disseminated infection by *Coccidioides posadasii* in an alpaca (*Vicugna pacos*) fetus in Southern California. *Med Mycol Case Rep*. 2013; 2:159-162.
6. Dixon DM. *Coccidioides immitis* as a select agent of bioterrorism. *J Appl Microbiol*. 2001; 91:602-605.
7. Fauquier DA, Gulland FMD, Trupkiewicz JG, Spraker TR, Lowenstine LJ. Coccidioidomycosis in free-living California sea lions (*Zalophus californianus*) in Central California. *J Wildl Dis*. 1996; 32:707-710.
8. Fisher MC, Koening GL, White TJ, Taylor JW. Molecular and phenotypic description of

Coccidioides posadasii sp. previously recognized as the non-Californian population of *Coccidioides immitis*. *Mycologia*. 2002; 94:73-84.

9. Graupmann-Kuzma A, Valentine BA, Shubitz LF, Dial SM, Watrous B, Tornquist SJ. Coccidioidomycosis in dogs and cats: a review. *J Am Anim Hosp Assoc*. 2008; 44:226-235.
10. Higgins JC, Leith GS, Pappagianis D, Pusterla N. Treatment of *Coccidioides immitis* pneumonia in two horses with fluconazole. *Vet Record*. 2006; 159:349-351.
11. Hoffman K, Videan EN, Fritz J, Murphy J. Diagnosis and treatment of ocular coccidioidomycosis in a female captive chimpanzee (*Pan troglodytes*) a case study. *Ann NY Acad Sci*. 2007; 1111:404-410.
12. Hung C-Y, Xue J, Cole GT. Virulence mechanisms of *Coccidioides*. *Ann NY Acad Sci*. 2007; 1111:225-235.
13. Reidarson TH, Griner LA, PappagianisD, McBain J. Coccidioidomycosis in a bottlenose dolphin. *J Wildl Dis*. 1998; 34:629-63, 1998.
14. Shubitz LF, Dial SM. Coccidioidomycosis: a diagnostic challenge. *Clin Tech Small Anim Pract*. 2005; 220:226.
15. Shubitz LF, Dial SM, Galgiani JN. T-lymphocyte predominance in lesions of canine coccidioidomycosis. *Vet Pathol*. 2010; 45:1008-1011.
16. Terio KA, Stalis IH, Allen JL et al. Coccidioidomycosis in Przewalski's horses (*Equus przewalskii*). *J Zoo Wildl Med*. 2003; 34:339-345.
17. Tofflemire K, Betbeze C. Three cases of feline ocular coccidioidomycosis: presentation, clinical features, diagnosis and treatment. *Vet Ophthalmol*. 2010; 13:166-172.

Self-Assessment - WSC 2016-2017 Conference 4

1. Which of the following is not a characteristic symptom or finding associated with Johne's disease in small ruminants?
    a. Overt diarrhea
    b. Mild enteric lesions with minimal gut thickening
    c. Chronic wasting
    d. Mineralized tubercle-like lesions in the mucosa

2. Which of the following toxins is secreted by *M. avium* var paratuberculosis*?*
    a. Lipopolysaccharide
    b. RTX-1
    c. Lipoarabinomannan
    d. None of the above.

3. In which species are cardiac rhabdomyomas thought to be of Purkinje fiber origin?
    a. Swine
    b. Dogs
    c. Mice
    d. Cattle

4. Which of the following is not true concerning lagenidiosis?
    a. Most cases have been reported in dogs.
    b. Exposure to water is often reported in affected animals.
    c. Histopathology cannot be used for the differentiation of *Lagenidium* from *Zygomyces* or *Pythium*.
    d. Gastrointestinal disease is commonly associated with skin disease in *Lagenidium* infection.

5. Which of the following is not a mechanism which allows *Coccidioides sp.* to survive in the host environment
    a. Production of wall glycoproteins which compromises host cell-mediated immunity
    b. Induction of decreased host nitric oxide production
    c. Depletion of glycoproteins on endospores, preventing host recognition
    d. Switching from a Th1 to a Th2 response as parasite load increases

Joint Pathology Center
Veterinary Pathology Services

WEDNESDAY SLIDE CONFERENCE 2016-2017

C o n f e r e n c e 5

28 September 2016

Conference Moderator:
Julie B. Engiles VMD, DACVP
Assoc. Professor of Pathology
New Bolton Center
Department of Pathobiology
University of Pennsylvania
382 West Street Road
Kennett Square, PA 19348

CASE I: Case 1 (JPC 4084648).

Signalment: Three-year-old, female, African hedgehog (*Atelerix albiventris*).

History: The animal presented for bloody vulvar discharge, right-sided facial paralysis, and multiple skin masses. Elective ovario-hysterectomy was performed and multiple skin masses were removed. A firm multi-nodular mass was observed arising from the internal ear canal. Due to the worsening of clinical signs, the animal was humanely euthanized and submitted for postmortem examination.

Gross Pathology: On necropsy, the animal was in good body condition. Gross examination revealed a multilobulated, white and tan mass measuring 2.5 cm arising from the right parietal bone and extending toward the right occipital lobe, surrounding the external auditory meatus and protruding through the internal ear canal, as well as rostrally to the right frontal lobe involving the right turbinates. The cut surface was yellow, white, and tan, with few white areas of mineralization. In transverse sections, the mass focally compressed the cerebral hemi-spheres, cranial nerves and partially

Cranium, hedgehog. A 2.5cm white-tan multilobular mass arises from the right parietal bone and extends to the right occipital bone, surrounding the external auditory meatus. (Photo courtesy of: Departamento de Patología (Pathology Department). Facultad de Medicina Veterinaria y Zootecnia, Universidad Nacional Autónoma de México. Mexico city, Mexico.Web site: http://fmvz.unam.mx/fmvz/departamentos/patologia/acerca.html

obliterating the ear meatus. Both lateral ventricles were moderately dilated.

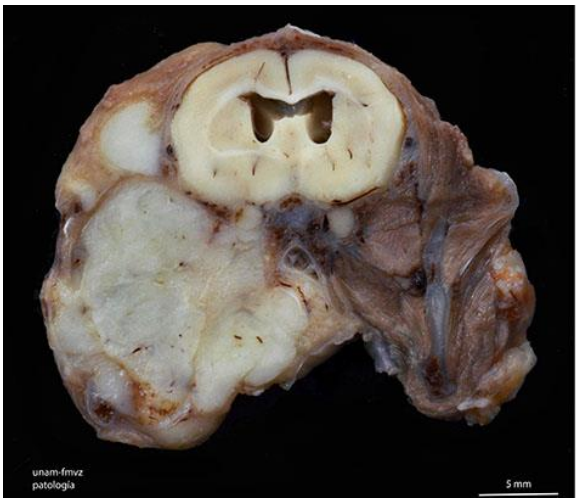

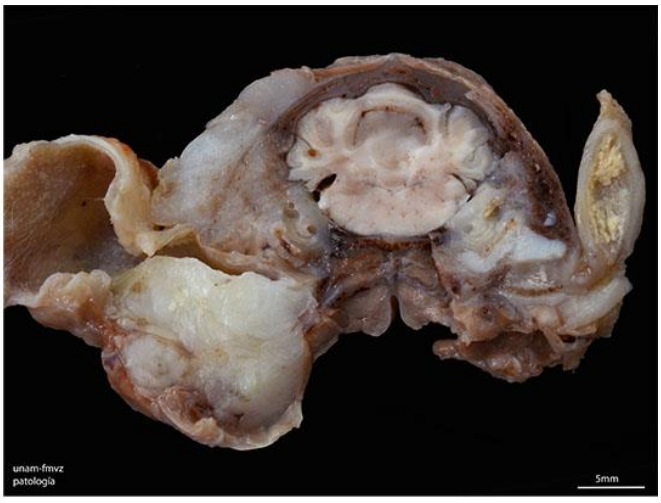

Transverse sections at the level of midbrain and hindbrain, hedgehog: In transverse sections, the mass compresses the cerebral hemispheres, cranial nerves and partially obliterates the ear meatus. Lateral ventricles were moderately dilated. (Photo courtesy of: Departamento de Patología (Pathology Department). Facultad de Medicina Veterinaria y Zootecnia, Universidad Nacional Autónoma de México. Mexico city, Mexico.Web site: http://fmvz.unam.mx/fmvz/departamentos/patologia/acerca.html)

Laboratory results: N/A

Histopathologic Description: Microscopic examination revealed that this mass arises from the skull, protrudes both internally and externally, and compresses the brain. The mass is composed of multiple well-demarcated nodules, rimmed by a thick layer of fibrous connective tissue arranged in sheets of polyhedral to spindle-shaped cells with large interspersed areas of coagulative necrosis. Numerous islands and lakes of osteoid are present throughout the tumor. The neoplastic cells have abundant eosinophilic cytoplasm and large, round to ovoid nuclei with finely stippled chromatin and often prominent nucleoli. There is marked anisocytosis and anisokaryosis. The mitotic rate is low, averaging two per ten 400x high powered fields. In some sections, cranial nerves are markedly compressed by the neoplasm, with multifocal axonal swelling and spheroid formation (Wallerian degeneration). Neurons at this level are shrunken and hypereosinophilic (necrosis).

Contributor's Morphologic Diagnosis: Skull: Osteoblastic osteosarcoma, with cranial nerve compression, Wallerian degeneration, and neuronal necrosis.

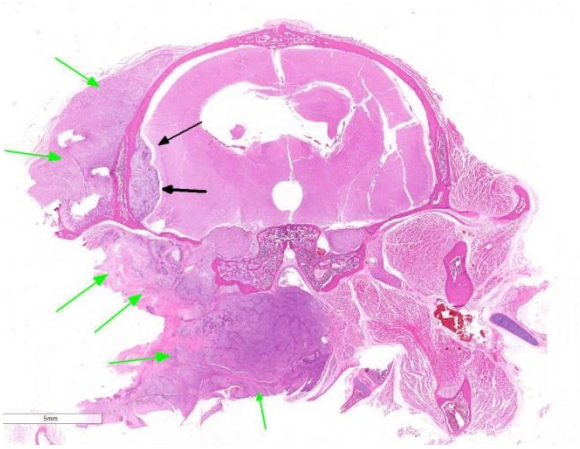

Transverse section of head at the level of hippocampus. The neoplasm is present external to the cranium (green arrows) as well as traversing the cranium and compressing the lateral cerebral hemisphere (black arrow). (HE, 5X)

Contributor's Comment: Neoplasms in African hedgehogs are common and represent one of the main causes of disease in this species. In retrospective studies, the prevalence of neoplasia has ranged from 29% to 51%. Of these, 85% are malignant, portending an overall poor prognosis.[3] Osteosarcomas in this species have been reported in skeletal and extraskeletal locations. Skeletal locations include: mandible,[3] ribs,[1,6] and vertebra.[8] Reported extraskeletal sites include the subcutis over the scapula[2] and flank.[7] One documented case of osteosarcoma is theorized to be associated with retroviral infection.[6] Multiple concurrent neoplasms are present in a small percentage of hedgehogs with neoplasia.[3] In this case, multiple trichoepitheliomas and an endometrial stromal sarcoma were also present.

Although osteosarcoma accounts for up to 85% of malignant bone tumors in dogs and 70% in cats,[2] the occurrence in African hedgehogs is unusual. In dogs, osteosarcomas can be subclassified according to the predominant histologic pattern into six different categories: poorly differentiated, osteoblastic, chondroblastic, fibroblastic, teleangiectatic and giant-cell rich osteosarcoma. This classification scheme is an adaptation of a system developed for use in human medicine. Osteoblastic osteosarcoma is the most common subtype, and it can be further sub-classified into non-productive and productive, based on the tumor bone produced. According to this classification, this osteosarcoma would be classified as a productive osteoblastic osteosarcoma.[2]

Additionally, intracranial, extracranial, and skull base neoplasms often compress the facial nerve and may result in facial paralysis.[5] In this case, cranial nerve involvement can be seen in some slides. Nerves are clearly compressed and surrounded by the neoplastic tissue, leading to Wallerian degeneration. Wallerian degeneration is a process that occurs when a nerve fiber is cut or crushed, leading to axonal separation from the neuronal cell body which degenerates distal to the injury.[9]

JPC Diagnosis: Bone, cranium: Osteosarcoma, African hedgehog, *Atelerix albiventris*.

Conference Comment: Transverse histologic sections of the cranium from this case spanned from the level of the rostral diencephalon to the caudal metencephalon. As a result, conference participants noted marked slide variation based on the anatomic location of this neoplasm and its effects on the adjacent tissue. Due to extensive variation in tissue sections submitted, histologic lesions noted by participants that may not be present on every slide include: Wallerian degeneration of the cerebrum and peripheral nerves; compression of the cerebrum and peripheral nerves with adjacent neuronal necrosis; hydrocephalus of the lateral, third, and fourth ventricles; osteosarcoma (OSA)

tumor emboli within adjacent vessels; skeletal muscle degeneration, regeneration, and necrosis; and hyperkeratosis of the external ear canal.

As mentioned by the contributor, neoplasia is an extremely common antemortem and postmortem finding in the African hedgehog. However, mesenchymal neoplasms, such as in this case, are relatively uncommon with an incidence of only about 4% at necropsy.[1,3,8] Epithelial neoplasms of the integument are the most common type, followed by round cell tumors.

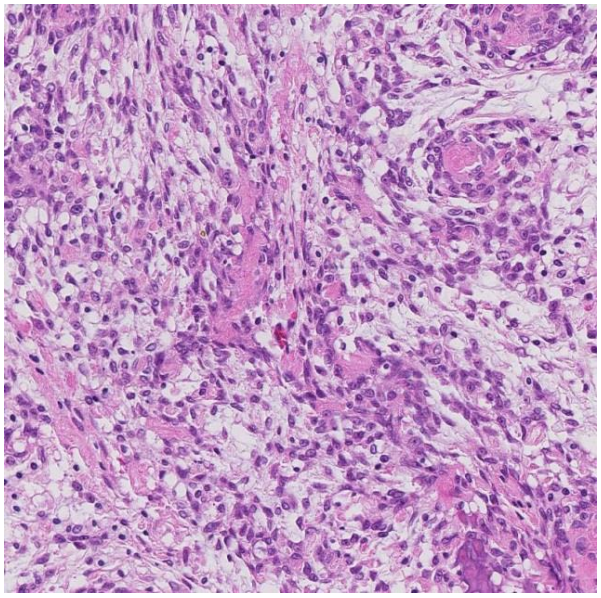

Cranium, hedgehog. The neoplasm is composed of short streams of spindled cells which produce moderate amounts of osteoid. (144X)

Osteosarcoma is the most common mesenchymal neoplasm reported in African hedgehogs.[3]

In dogs and cats, osteosarcoma is characterized by rapid progression and early metastasis to the lungs, resulting in short survival times and high mortality rate.[2] This aggressive biologic behavior is similar in reported cases of osteosarcoma in African hedgehogs.[1,3,8] The contributor describes six different categories of osteosarcoma in dogs based on the predominant histologic pattern. These include:

1. **Poorly differentiated**:
    - Variation in cell size from small primitive mesenchymal to large and pleomorphic undifferentiated cells
    - Identification depends on presence of unequivocal tumor osteoid
    - Highly aggressive and associated with pathological fractures.
2. **Osteoblastic**:
    - Anaplastic osteoblasts; variable amounts of basophilic cytoplasm, and hyperchromatic, eccentric nuclei
    - Further subclassified as nonproductive or productive based on presence or absence of tumor bone production
    - Productive osteoblastic OSA is the most common subtype in dogs
3. **Chondroblastic**:
    - Neoplastic cells produce both chondroid and osteoid matrices
4. **Fibroblastic**:
    - Interlacing bundles of spindle cells resembling fibrosarcoma that produce osteoid or bone
5. **Telangiectatic**:
    - Solid areas and large blood-filled spaces lined by malignant osteoblasts that occasionally form spicules of osteoid
    - Resembles hemangiosarcoma, but is

immunonegative for factor VIII and CD31
    - Most malignant classification with least favorable prognosis.
6. **Giant cell-rich**:
    - Tumor giant cells predominate with nuclear atypia and a high mitotic rate
    - Must be differentiated from the benign giant cell tumor of bone[2]

The conference moderator cautioned participants that histologic classification of osteosarcoma is often complicated by their heterogeneous nature, as several microscopic patterns are often evident within a single neoplasm. Regardless of classification, the prognosis for all subtypes of canine central osteosarcoma is considered poor.[2] The conference moderator also mentioned different grading systems for osteosarcoma based on nuclear pleomorphism, mitotic index, necrosis, multinucleated cells, the amount of tumor matrix, and vascular invasion. Unfortunately, no histologic grading system has gained widespread acceptance by veterinary pathologists due to marked variation in histomorphology of the neoplastic cells within different regions of the same tumor.[2]

Contributing Institution:

Department of Pathology
Faculty of Veterinary Medicine and Animal Husbandry
Universidad Nacional Autónoma de México
Mexico city, Mexico.
http://fmvz.unam.mx/fmvz/departamentos/patologia/acerca.html

References:

1. Benoit-Biancamano M, d'Anjou M, Girard C, Langlois I. Rib Osteoblastic Osteosarcoma in an African Hedgehog (*Atelerix Albiventris*). J Vet Diagn Invest. 2006; 18:415–418.
2. Craig LE, Dittmer KE, Thompson KG. Bones and joints. In: Maxie MG ed. *Jubb, Kennedy, and Palmer's Pathology of Domestic Animals*. Vol 1. 6th ed. St. Louis, MO: Elsevier; 2016:110-116.
3. Heatley J, Mauldin G, Cho D. A Review of Neoplasia in the Captive African Hedgehog (*Atelerix albiventris*). Semin Avian Exot Pet. 2005; 14:182–192.
4. London C, Dubilzeig R, Vail D, Ogilvie G, Hahn K, Brewer W, DVM; Hammer A, O'Keefe D, Chun R, McEntee M, McCaw D, Fox L, Norris A, Klausner J. Evaluation of dogs and cats with tumors of the ear canal: 145 cases (1978-1992). J Am Vet Med Assoc. 1996; 208: 1413-18.
5. Marzo S, Leonetti J, Petruzzelli G. Facial paralysis caused by malignant skull base neoplasms. Neurosurg Focus. 2002; 12 (5): 1-4.
6. Peauroi J, Lowenstine L, Mun R, D. Wilson. Multicentric Skeletal Sarcomas Associated with Probable Retrovirus Particles in Two African Hedgehogs (Atelerix albiventris). Vet Pathol. 1994; 31:481-484.
7. Phair K, Carpenter J, Marrow J, Andrew, G, Bawa. Management of an Extraskeletal Osteosarcoma in an African Hedgehog (*Atelerix albiventris*). Journal of Exotic Pet Medicine. 2011; 20 (2): 151–15.
8. Rhody J, Schiller C. Spinal Osteosarcoma in a Hedgehog with Pedal Self-Mutilation. Vet Clin Exot Anim. 2006; 9: 625–631.
9. Zachary JF. Nervous System. In: Zachary JF, McGavin MD, eds. *Pathologic Basis of Veterinary*

Disease. 5th ed. p.p. 959 St. Louis, MO: Elsevier; 2012.

CASE II: V254/10 (JPC 4003264).

Signalment: Four-year-old, castrated male, Labrador retriever (*Canis familiaris*).

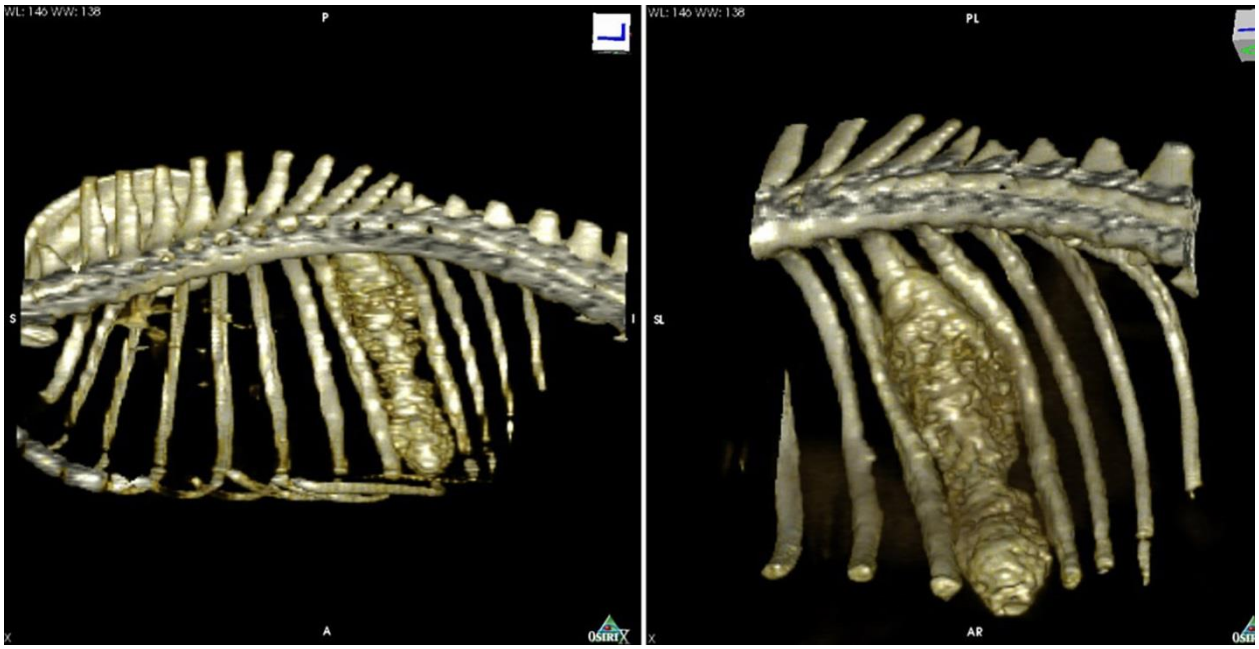

Rib, dog. Three-dimensional CT reconstruction of a rib mass. (Photo courtesy of: Dep. Vet Resources, Weizmann Institute, Rehovot 76100, Israel http://www.weizmann.ac.il/vet/)

History: This sample is from a rib mass. The animal had an initial history of moderate thrombocytopenia, mild leukopenia and mild anemia detected during a routine CBC. Ehrlichiosis was suspected and the dog was started on a course of doxycycline. CBC values did not normalize in response to the antibiotics and the dog was referred to a specialty practice, where pronounced thrombocytopenia (40,000/microL), mild anemia and mild leucopenia were documented. PCR for *Ehrlichia canis* could not be performed while the dog was on antibiotic therapy; however, the main differential diagnosis remained chronic ehrlichiosis. Cytology of the marrow showed general hypocellularity and a mild increase in plasma cells. The dog was clinically healthy and no other abnormalities were noted. As marrow destruction in ehrlichiosis has been shown to be immune-mediated, a course of prednisone in an immunosuppressive dose was added to the doxycycline. Subsequent CBC showed improvement in all 3 blood cell lines but whenever steroids were tapered, the dog relapsed. Treatment was therefore continued and eventually the dog became cushinoid. Another immunosuppressive drug (mycophenolate) was added to the regimen. CBC improved but the dog developed ulcerated subcutaneous abscesses on the limbs. These were treated conservatively and resolved but additional abscesses developed and there were several episodes of fever. Culture of one abscess yielded *Nocardia* spp. The culture results of the remaining abscesses are unknown.

Immunosuppressant therapy was discontinued, but later resumed because of severe thrombocytopenia. A few weeks later, the dog presented with a 15cm diameter swelling on the side of the chest. The swelling appeared to be due to a subcutaneous abscess. The abscess was drained but recurred, at which point surgical debridement was performed. During this procedure, a connection to the rib was identified. The mass was evaluated by CT and resected. Material was submitted for bacterial culture and *Corynebacterium* spp and *Nocardia farcinica* were isolated.
Eventually, the dog recovered, his CBC normalized, and he is now reportedly in good health.

Gross Pathology: There is a 15 cm diameter firm mass attached to a rib.

Laboratory results: N/A

Histopathologic Description: Mass on rib: There are multiple large bacterial colonies surrounded by abundant accumulation of cellular debris, neutrophils, histiocytes and rare multinucleated cells. In the surrounding tissue, there is widespread fibrosis and proliferation of woven bone. The fibrous tissue is of variable maturity and within it there is multifocal hemorrhage and severe multifocal to coalescing infiltration of neutrophils, histiocytes with lesser plasma cells and lymphocytes. The woven bone is arranged in a lattice. Bone trabeculae are commonly invested with a single layer of active osteoblasts and fibrovascular tissue of low cellularity occupies the intertrabecular spaces (reactive bone). The bacterial colonies (sulfur granules) are amphophilic to basophilic, have irregular circular, undulant and vermiform shapes and are composed of dense mats of rods and filamentous bacteria. The outer perimeter of the colonies is covered by a thin eosinophilic rim.

On special stains, the bacteria are gram positive and strongly stain with a modified acid fast stain, Fite-Faraco, and inconsistently with Ziehl Neelsen (ZN). In the modified ZN stain, long filamentous and beaded organisms are easily seen.

Contributor's Morphologic Diagnosis: Rib: Severe pyogranulomatous osteomyelitis with bacterial colonies consistent with *Nocardia* spp.

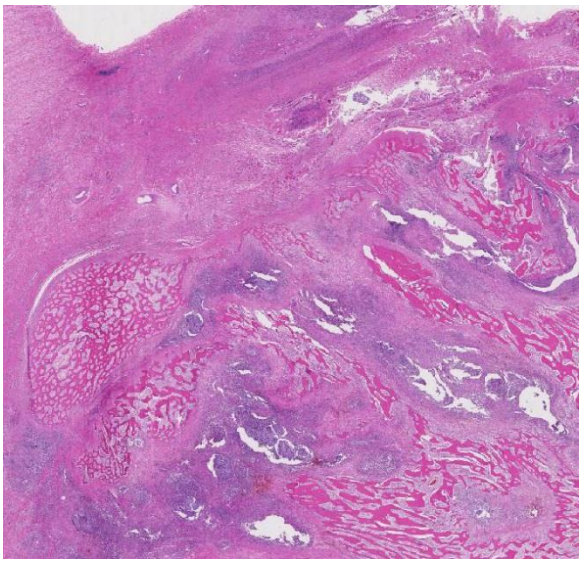

Rib, dog. There is loss of cortical architecture, and a dense inflammatory infiltrate traverses among trabeculae of proliferating woven bone. (HE, 5X)

Contributor's Comment: The morphologic features and staining characteristics of the bacterial colonies are consistent with *Nocardia* spp. which was supported by culture. In dogs, distemper and other causes of immunosupression may predispose to nocardiosis.[3] There are two recent reports of nocardial infection in dogs treated with immunosuppressive agents.[6] In the current case, immunosuppressive treatment was used because the clinicians thought the pancytopenia with preferential involvement of the platelets was due to subacute to chronic ehrlichiosis. In their experience,

dogs often recover from acute and subclinical ehrlichiosis but go on to develop subclinical and progressive bone marrow suppression, which is typically detected too late in the course of the disease. In this case, the ongoing myelosuppression was detected fortuitously but long-term immuno-suppression (to which putative *E. canis*-induced myelosuppression may have been a contributing factor) led to opportunistic bacterial infection.

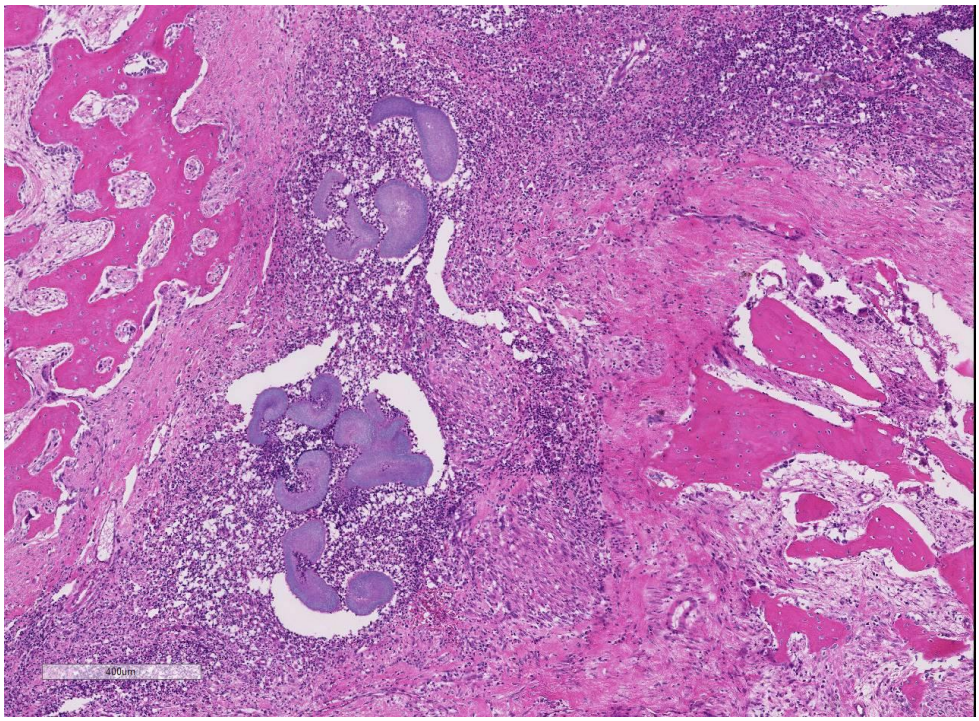

Rib, dog. The suppurative and histiocytic infiltrate is centered on large colonies of filamentous bacilli enmeshed in a pink matrix of Splendore-Hoeppli material. (HE, 47X)

Actinobacteria are gram-positive, terrestrial, or aquatic bacteria which constitute one of the dominant bacterial phyla. Most *Actino-bacteria* of medical significance belong to the order *Actinomycetales*. Due to their filamentous appearance, these organisms were thought to be fungi for many years but were later shown to be higher bacteria.[3,7] *Actinomyces* and *Nocardia* are the most common *Actinomycetes* which cause disease.[7] Organisms in the genus *Nocardia* are aerobic, gram-positive and partially acid fast saprophytes with a worldwide distribution. They commonly occur in soil and decaying organic matter and may cause opportunistic infection. *N. asteroides* is the species most commonly implicated in disease and has been recovered from lesions in humans, dogs, cats, cattle, goats, horses, pigs, marine mammals and fish.[6] Cattle and dogs are the most commonly affected animals, but these infections are sporadic.[3] Infection is not contagious and affected animals do not constitute a public health hazard.[7] Failure to distinguish properly between *Nocardia* and *Actinomyces* in earlier reports has caused confusion in the literature regarding nocardiosis in animals.[3]

Typically, nocardial infection originates from organisms introduced into skin wounds or aspirated into the respiratory tract, leading to superficial skin lesions, and necrotizing pneumonia, respectively.[3,7] Infections may remain localized at the site of introduction but there is a tendency for the organisms to spread either by direct extension or vascular invasion and hematogenous dissemination.[4,7] There is evidence that strains within the same species vary markedly in their virulence.[4] Cell-mediated immunity and neutrophils appear to be of critical importance in defense against these bacteria.[6,7] In dogs, infections are more

common in the young (<1-year-old), which may be due to increased exposure or to reduced resistance.[7]

The typical gross cutaneous lesions caused by infection with filamentous bacteria (*Actinomyces* and *Nocardia*) consist of abscesses, cellulitis, draining fistulous tracts, and dense fibrous masses.[7] Lesions progress slowly by local extension. The exudate is variable and can contain white, yellow, tan or gray "sulfur granules."[4,7] Histologically, pyogranulomatous inflammation is commonly seen.[4,7] The sulfur granules consist of masses of organisms, which may be bordered by clubbed corona of brightly eosinophilic Splendore-Hoeppli material.[4,7] It has been reported that the shape of this material is characteristic for the agent involved.[1] *Nocardia* spp. have a limited tendency to clump together, thus they typically do not form granules.[4,7] However, in some cases, nocardial lesions are morphologically indistinguishable from those induced by *Actinomyces*[7], as appears to be the case here. In gram-stained sections, the bacteria are seen as branched and beaded filaments up to 1µm wide. Fragmentation of the filaments produces coccobacillary forms. The beaded appearance is due to alternating gram-positive and gram-negative regions in the filament and is more evident in *Nocardia* spp. *Actinomyces* are acid-fast negative with most acid-fast stains. Many, but not all, *Nocardia* spp. stains strongly with modified Ziehl-Neelsen. Some acid-fast negative *Nocardia spp.* cannot be differentiated from *Actinomyces* in sections, and culture is required.[7]

The cutaneous and subcutaneous nodules are progressive and may extend to involve underlying bone, as appears to have occurred in this case. The lesion is similar to "lumpy jaw" in cattle, a classic example of actinomycotic mycetoma. In this condition, traumatic implantation of *Actinomyces bovis* in the mandibular mucosa progresses to involve the mandibular bone.[7] In cattle, *N. asteroides* can also cause granulomatous mastitis when contaminated drugs for the treatment or prevention of mastitis are introduced through the teat canal. This condition may also occur in outbreaks.[2] As noted above, a second relatively common site of infection with filamentous bacteria (*Nocardia*, *Actinomyces* and *Bacteroides*) in dogs and cats is the thoracic cavity, causing pyogranulomatous pleuritis with intra-thoracic accumulation of blood-stained pus and reactive mesothelial cells, so-called "tomato soup." This is no longer considered pathognomonic of nocardial infection.

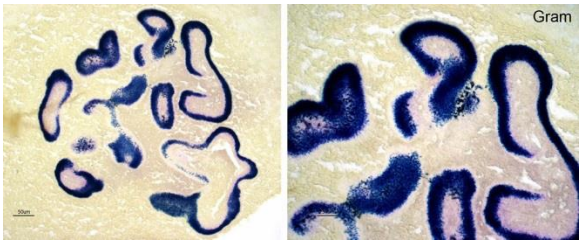

Rib, dog. A tissue Gram stain demonstrates that the bacilli are gram-positive. (Gram, 200X) (Photo courtesy of: Dep. Vet Resources, Weizmann Institute, Rehovot 76100, Israel http://www.weizmann.ac.il/vet/)

JPC Diagnosis: Bone: Osteomyelitis, pyogranulomatous and sclerosing, with new bone formation and colonies of filamentous bacteria, Labrador retriever, *Canis familiaris*.

Conference Comment: This case nicely demonstrates the histopathologic appearance of sulfur granules in tissue section. Sulfur granules, which are usually located within neutrophil abscesses or pyogranulomas, are distinct masses of bacteria bordered by eosinophilic radiating projections of Splendore-Hoeppli material characteristic for actinomycetes bacteria.[2,7] Although, formation of granules is a more common feature of actinomycosis, *Nocardia* spp may

form sulfur granules which are indistinguishable from *Actinomyces* spp. These structures can be seen grossly as small yellow granular material present within the exudate.[2,7]

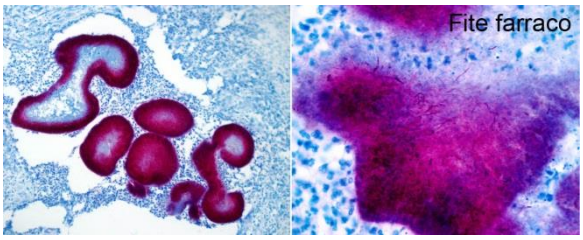

Rib, dog. The filamentous bacilli are also acid-fast. (Fite-Furaco, 200X) (Photo courtesy of: Dep. Vet Resources, Weizmann Institute, Rehovot 76100, Israel http://www.weizmann.ac.il/vet/)

Conference participants briefly discussed the pathogenesis of the Splendore-Hoeppli phenomenon. As mentioned above, Splendore-Hoeppli reaction is typically the brightly eosinophilic, radiating, club-shaped, material around bacterial colonies in histologic sections.[2,5,7] This material is composed of antigen-antibody complexes, tissue debris, and fibrin. Although the exact nature of this reaction is unknown, it is thought to be a localized immune response to an antigen-antibody deposition related to fungi, parasites, bacteria or inert materials. The characteristic formation of the Splendore-Hoeppli reaction around infectious agents or biologically inert materials is likely the body's attempt to contain the injurious agent on the part of the host. However, it also likely prevents phagocytosis and intracellular killing of the agent leading to prolonged damage or infection.[5]

Identification of the tissue as costal bone in this section was difficult for all conference participants. As a result, participants discussed effective strategies for differentiating reactive new bone formation from neoplastic bone disease, given the lack of normal tissue architecture. The conference moderator instructed that first one must look for evidence of the parent bone structural elements such as osteons within complex mature lamellar bone to differentiate new bone formation from osseous metaplasia. Next, to differentiate reactive bone from neoplastic bone, one must look at the characteristics and orientation of the osteoblasts. Given that osteoblasts are terminally differentiated products of mesenchymal stem cells, there should be no mitotic activity within this cell population.[8] Additionally, in reactive bone formation, osteoblasts form highly organized groups connected by gap junctions allowing the cells to function in a well-regulated manner. In tumor bone, neoplastic mesenchymal cells are haphazardly arranged and produce an osteoid matrix without the regularity and regimentation present in reactive bone osteoblasts.

Contributing Institution:
Department of Veterinary Resources
Weizmann Institute
Rehovot, Israel
http://www.weizmann.ac.il/vet/

References:

1. Bestetti G. Morphology of the "sulphur granules" (Drusen) in some actinomycotic infections. A light and electron microscopic study. *Vet Pathol*. 1978; 15:506-18.
2. Foster RA. Female Reproductive System. In: McGavin MD, Zachary JF, ed. *Pathologic Basis of Veterinary Disease*. 5th ed. St. Louis, MO: Elsevier; 2012:1124-1125.
3. Gyles CL. Nocardia, Actinomyces, and Dermatophilus. In: Carlton L, Thoen CO, ed. *Pathogenesis of*

bacterial infections in Animals. 2nd ed. Ames, IA: Iowa State University Press, 1993:124-6.
4. Hargis, Ann M, Ginn, Pamela E: The Integument. In: McGavin MD, Zachary JF, ed. *Pathologic Basis of Veterinary Disease*. 5th ed. St. Louis, MO: Elsevier; 2012:1034.
5. Hussein MR. Mucocutaneous Splendore-Hoeppli phenomenon. *J Cutan Pathol*. 2008; 35(11):979-988.
6. MacNeill AL, Steeil JC, Dossin O, Hoien-Dalen PS, Maddox CW. Disseminated nocardiosis caused by *Nocardia abscessus* in a dog. *Vet Clin Pathol*. 2010; 39:381-5.
7. Mauldin E, Peters-Kennedy J. Integumentary system. In: Maxie MG, ed. *Jubb, Kennedy, and Palmer's Pathology of Domestic Animals*. Vol 1. 6th ed. Philadelphia, PA:Elsevier; 2016:637-638.
8. Pittenger MF, Mackay AM, Beck SC, Jaiswal RK, Douglas R, Mosca JD, Moorman MA, Simonetti DW, Craig S, Marshak DR. Multilineage potential of adult human mesenchymal stem cells. *Science*. 1999; 284:143-7.

CASE III: HV6474 (JPC 4085013).

Signalment: Ten-year-old, ovario-hysterectomized female, miniature dachshund (*Canis familiaris*).

History: The animal had a one-month history of hematochezia. A rectal mass was found and surgical excision of the mass was performed by the rectal pull-through technique.

Gross Pathology: There was a polypoid mass (5×3×1 cm) on the rectal mucosa.

Laboratory results: N/A

Histopathologic Description: The large polyp showed severe cellular infiltration, granulation tissue, epithelial cell proliferation, interstitial mucus accumulation, hemorrhage, and osteoid formation. At the base of the polyp, goblet cells proliferated without cellular atypia and crypts were dilated due to abundant mucinous material accumulation. Mucous inflammation consisted of predominant neutrophil infiltration and less frequent macrophage, plasma cell, and lymphocyte infiltration. There are similar small lesions in the adjacent polyps.

Rectum, dog. A polypoid mass measuring 5×3×1 cm arises from the rectal mucosa (Photo courtesy of: Laboratory of Comparative Pathology, Department of Veterinary Clinical Sciences, Graduate School of Veterinary Medicine, Hokkaido University.)

Contributor's Morphologic Diagnosis: Rectum: Polyp, with severe inflammation, epithelial cell proliferation, mucus accumulation in crypts (Inflammatory polyps of miniature dachshunds).

Contributor's Comment: Colorectal polyps are relatively common in dogs. These polyps include non-neoplastic (hyperplastic or inflammatory) polyps and neoplastic polyps such as adenoma and adenocarcinoma. In Japan, Miniature Dachshunds show a significantly higher tendency to develop multiple polyps than other breeds.[5] Recently, it was proposed to refer to these polyps as inflammatory polyps of miniature dachshunds.[7] These polyps are non-neoplastic single or multiple polypoid lesions arising from the rectum and distal colon, and are characterized by mucosal proliferation without cellular atypia and significant inflammatory cell infiltration.[5] Microscopically, the inflammatory polyps show inflammatory cell infiltration, hyperplastic goblet cells with dilated crypts, mucus accumulation in crypts, granulation tissue, and occasional osteoid formation.[1,8]

In comparisons based on epithelial composition, the polyps displayed a thickened mucosa containing increased goblet cells, dilated crypts filled with a large amount of mucus, and mild inflammatory infiltration (mainly lymphocytes and macrophages) in the early stage.[8] In later stages, leukocyte infiltration was more severe and consisted of mostly neutrophils and macrophages. Additionally, interstitial mucus accumulation, granulation tissue, and occasional osteoid formation were seen.[8] In this case, predominant neutrophil infiltration, interstitial mucus accumulation, granulation tissue and osteoid formation were observed in the polyp; therefore, the lesion is comparable to that in late stage.

Although the pathogenesis remains unclear, some studies suggested that the arachidonic acid cascade, increased IL-8 production in macrophages, dysregulation of toll-like receptors and proinflammatory cytokines, and IL-17A upregulation in T cells are associated with the lesion formation.[2,6,7] Additionally, 80% of cases responded to immunosuppressive therapy with prednisolone and cyclosporine.[5] These findings indicate that inflammatory polyp of miniature dachshunds is an immune-

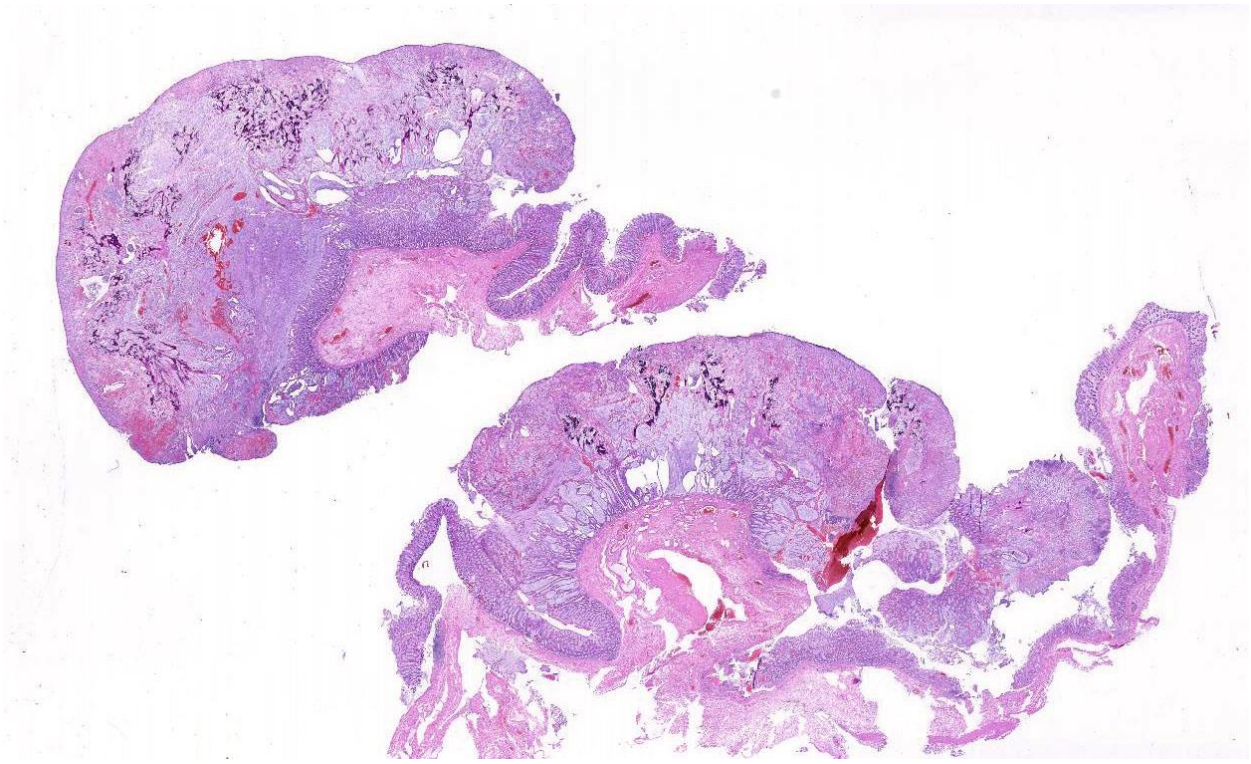

Rectum, dog. The submitted material contains two sections of a dome-shaped polyp arising from the rectal mucosa. (HE, 5X)

mediated disease. However, Igarashi et al reported that two cases developed adenomas secondary to inflammatory colorectal polyps during long-term medical therapy.[4] Further investigations are required to elucidate the pathogenesis, oncogenesis, and prognosis in inflammatory polyps of miniature dachshunds.

JPC Diagnosis: Rectum: Inflammatory polyp, miniature dachshund, *Canis familiaris*.

Conference Comment: The contributor provides a compelling example and concise summary of colorectal inflammatory polyps of miniature dachshunds (IPMD). It is unknown why inflammatory polyps occur much more commonly in miniature dachshunds than any other breed of dog in Japan.[8] Colorectal polyps are commonly present as single or multiple friable, lobulated, sessile, or pedunculated lesions on the mucosa.[1-8] Among the polypoid masses present in the intestinal tract of dogs, the major histopathologic subtypes include nonneoplastic and hyperplastic polyps, papillary adenomas, and papillary adenocarcinomas.[8] Most conference participants agreed that the late-stage inflammatory polyp, in this case, was difficult to differentiate from a neoplastic papillary adenoma or mucinous papillary adenocarcinoma.

In a recent study by Uchida et al. published in *Veterinary Pathology*, they classify IPMD into early (stage 1) and late (stages 2 and 3) lesions based on the histopathology of the mucosal epithelial components and inflammatory cells present.[8] In addition, they use immunohistochemistry to distinguish inflammatory polyps from neoplastic cells of adenomas and adenocarcinomas using cytokeratin 20 (CK20) and beta-catenin. Normally, intestinal goblet cells and enterocytes are strongly immunopositive for CK20. The markedly hyperplastic goblet cells, which is a key histologic feature of IPMD, are also strongly immunopositive for CK20, while neoplastic cells of adenomas and adenocarcinomas were immunonegative. This indicates that inflammatory polyps are a proliferation of well-differentiated epithelial tissue and non-neoplastic. The authors also demonstrate that IPMD expressed only intracytoplasmic beta-catenin, while neoplastic cells of adenomas and adenocarcinomas expressed both intracytoplasmic and intranuclear beta-catenin.[8]

There have been reports of dogs with later stage (stage 3) IPMD developing rectal adenomas secondary to neoplastic transformation.[5] Chronic inflammation and the production of pro-inflammatory cyto-kines can induce mutations in oncogene and tumor suppressor genes. In humans, the connection between chronic inflammatory

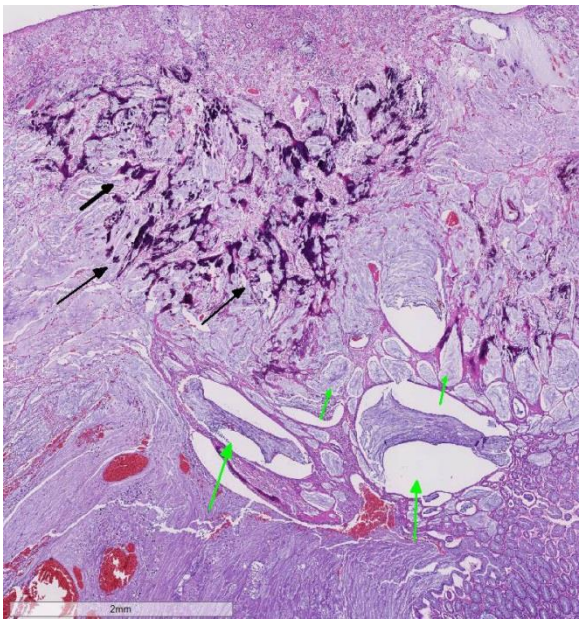

Rectum, dog. The polyp contains numerous dilated glandular structures filled with mucin at the interpace with the mucosa (green arrows), and numerous trabeculae of mineralized woven bone (black arrows). (HE, 5X)

bowel disease and development of both inflammatory polyps and colorectal carcinoma is well established.[5] Aberrant activation of the Wnt/beta-catenin pathway occurs in the vast majority of colorectal cancers in humans and dogs and likely plays a role in neoplastic transformation of late stage IPMD.[5,8]

Inflammatory colorectal polyps are typically treated with immunosuppressive therapy and endoscope guided polypectomy.[1,5,8] Unfortunately, recurrence after polypectomy is common. Recent research suggests that dysbiosis of the gastrointestinal tract is

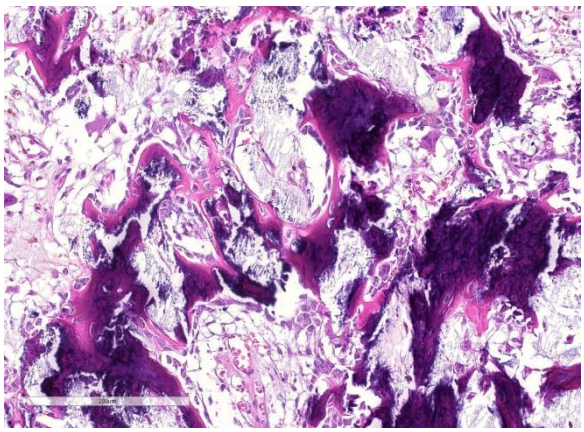

Rectum, dog. Higher magnification of the traveculae of woven bone. Bony spicules are lined by osteoblasts and rare osteoclasts, and interstices contain fat and mucin. (HE, 144X)

associated with IPMD and may be a potential future therapeutic target.[3]

Contributing Institution:
Laboratory of Comparative Pathology
Department of Veterinary Clinical Sciences
Graduate School of Veterinary Medicine
Hokkaido University
http://www.vetmed.hokudai.ac.jp/en/department/

References:

1. Fukushima K, Eguchi N, Ohno K, et al. Efficacy of leflunomide for treatment of refractory inflammatory colorectal polyps in 15 miniature dachshunds. *J Vet Med Sci*. 2016; 78(2):265-9.
2. Igarashi H, Ohno K, Maeda S, et al. Expression profiling of pattern recognition receptors and selected cytokines in miniature dachshunds with inflammatory colorectal polyps. *Vet Immunol Immunopathol*. 2014; 159(1-2):1-10.
3. Igarashi H, Ohno K, Horigome A. Fecal dysbiosis in miniature dachshunds with inflammatory colorectal polyps. *Res Vet Sci*. 2016; 105:41-46.
4. Igarashi H, Ohno K, Ohmi A, et al. Polypoid adenomas secondary to inflammatory colorectal polyps in 2 miniature dachshunds. *J Vet Med Sci*. 2013; 75(4):535-538.
5. Ohmi A, Tsukamoto A, Ohno K, et al. A retrospective study of inflammatory colorectal polyps in miniature dachshunds. *J Vet Med Sci*. 2012; 74(1):59-64.
6. Ohta H, Takada K, Torisu S, et al. Expression of CD4+ T cell cytokine genes in the colorectal mucosa of inflammatory colorectal polyps in miniature dachshunds. *Vet Immunol Immunopathol*. 2013; 155(4):259-263.
7. Tamura Y, Ohta H, Torisu S, et al. Markedly increased expression of interleukin-8 in the colorectal mucosa of inflammatory colorectal polyps in miniature dachshunds. *Vet Immunol Immunopathol*. 2013;156(1-2):32-42.
8. Uchida E, Chambers JK, Nakashima K, et al. Pathologic features of colorectal inflammatory polyps in miniature dachshunds. *Vet Pathol*. 2016; 53(4):833-839.

CASE IV: D15-000804 (JPC 4066248).

Signalment: Six-month-old female mixed breed calf (*Bos taurus*).

History: This heifer was running a fever of 103.6 F and was suspected of a respiratory disease. She was treated with Baytril® and oxytetracycline, but died a week later. The animal was submitted for necropsy to the Kansas State Veterinary Diagnostic Laboratory.

Gross Pathology: The mucosa of the distal part of the small intestine was diffusely dark red and the lumen contained dark brown, mucoid, sludgy material. The wall of spiral colon and cecum was thick, edematous and the lumen contained thick clots of blood. The colonic and cecal mucosae were diffusely dark red.

Laboratory results: Immunohistochemistry (IHC) revealed strong positive immuno-reactivity for bovine viral diarrhea virus (BVDV) in the crypt epithelial cells. IHC was negative for bovine corona virus.

Histopathologic Description: Diffusely, there is marked necrosis of the epithelial cells lining the crypts. Multifocally, the crypts are markedly ectatic and filled with abundant mucus admixed with karyorrhectic cellular debris and low to moderate numbers of degenerate leukocytes. Remaining crypts are lined with attenuated epithelium that is occasionally hyperplastic. The crypts contain moderate numbers of degenerate neutrophils, admixed with necrotic debris (crypt abscesses). The adjacent lamina propria is moderately expanded by large aggregates of lymphocytes, plasma cells, fewer neutrophils, and moderate amounts of fibrin.

The overlying mucosa is diffusely eroded

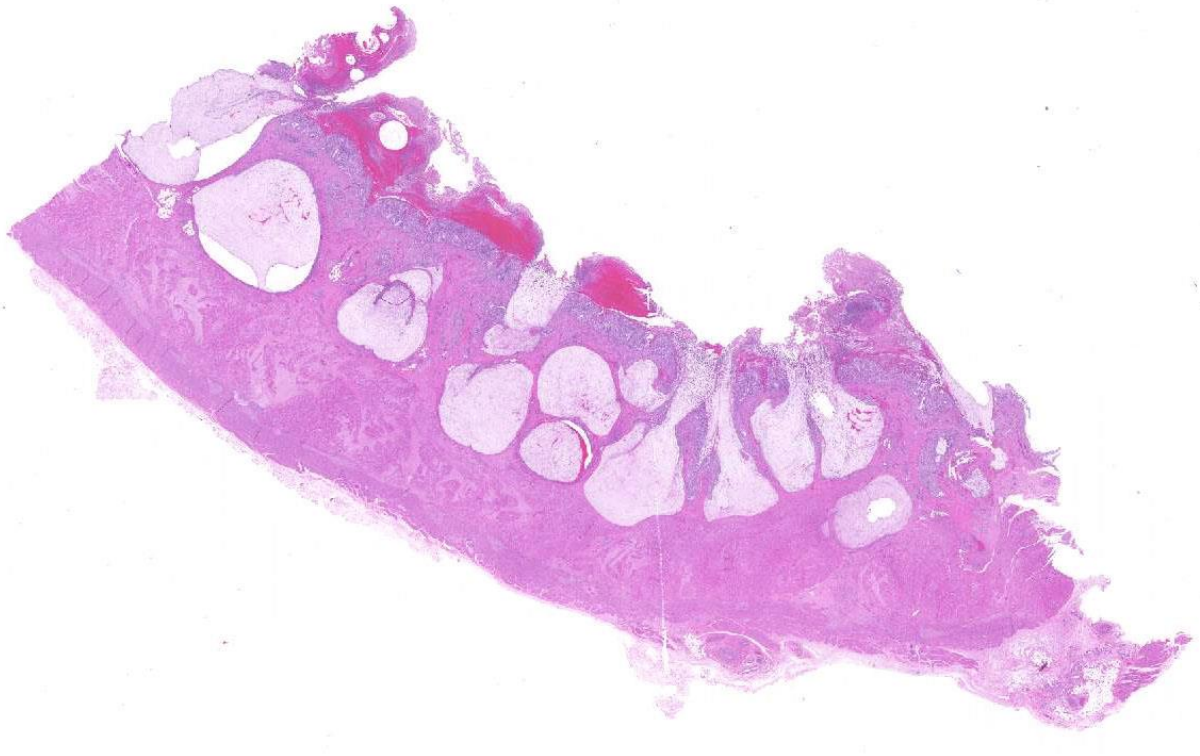

Colon, ox: At low magnification, colonic crypts are markedly ectatic and invade into the underlying muscular tunics. The mucosa is decreased in thickness and covered by a layer of hemorrhage and necrotic debris. (HE, 4X)

and covered by a thick layer of necrotic cellular debris admixed with numerous degenerate neutrophils, abundant fibrin, large numbers of extravasated erythrocytes, and rare bacterial colonies. The tunica muscularis is expanded by moderate amounts of edema and fibrin.

Contributor's Morphologic Diagnosis: Colon: Colitis, necrotizing, diffuse, severe, with multifocal crypt abscessation.

Contributor's Comment: The clinical history, gross and microscopic findings are consistent with mucosal disease caused by persistent infection with bovine viral diarrhea virus. Bovine viral diarrhea is an economically important disease of cattle and other even-toed ungulates that are caused by bovine viral diarrhea virus (BVDV). BVDV belongs to the *Pestivirus* genus of the family *Flaviviridae*. It has two recognized genotypes, (BVDV-1 and BVDV-2) based on antigenic and genetic differences. These genotypes are further classified into cytopathic (cp) and non-cytopathic (ncp) biotypes based on *in vitro* cell culture characteristics. Ncp BVDV strains do not induce apoptosis in cultured cells, are ubiquitous in nature and frequently isolated from bovine tissues while cp BVDV strains are infrequently isolated unless accompanied by ncp BVDV and induce apoptosis in susceptible cell lines. The molecular basis for cytopathogenicity was reported to involve mutations that lead to increased expression of NS3 protease in cp strains versus little to no expression in ncp strains.[5] However, it is important to note that *in vitro* cytopathogenicity does not correlate with virulence or the clinical severity of the disease.

The pathogenesis and the clinical manifestations of BVDV infection in cattle are dependent on the age, immune status as well as the biological properties of the infecting strain.[3] Previously described cp and ncp biotypes are closely associated with two fundamentally different forms of infection in cattle; either transient or persistent. In areas where BVDV infection is endemic, acute infection with ncp BVDV results in transient viremia with mild clinical signs that include low-grade fever, diarrhea and coughing. The infection is cleared within a few days and the seropositive animals are protected from re-infection for life. In contrast, fetal infection within second to fourth months of gestation results in immunotolerance and lifelong persistent infection. Persistently infected (PI) calves develop severe clinical disease referred to as mucosal disease that is characterized by widespread necrosis of the alimentary mucosa and lymphoid tissues. Mucosal disease only develops in PI cattle and is the result of persistent infection with a ncp strain followed by a subsequent post-natal infection with a cp strain that arise from mutation/s in already persisting ncp strain. The ability of the ncp strain to inhibit the induction of type-I interferon (IFN) in the fetus is generally believed to enable the virus to establish persistent infection. Research in last decade has identified two

Colon, ox: In the submitted section, the necrotic mucosa is interrupted by markedly dilated crypts which infiltrate down into the underlying muscularis. Such crypts often invade underlying Peyer's patches, but there is an almost total loss of lymphoid tissue in this section. (HE, 25X)

candidate genes that interfere with host cell's IFN induction namely E^{rns}, a structural glycoprotein with RNase activity and N^{pro}, an N-terminal autoprotease.[2]

The PI calves are a major concern because they shed large amounts of virus and are an important source of infection for the uninfected animals in the herd. Control programs are specifically designed to detect and eliminate PI animals. There are a wide range of diagnostic tools available to detect virus and virus-specific immune response.[4] Multiple ELISA kits are commercially available for detection of BVDV-specific antibodies in various biological samples including serum and milk. These kits are cost effective and generally used for screening large herds or conducting seroprevalence studies. It is important to

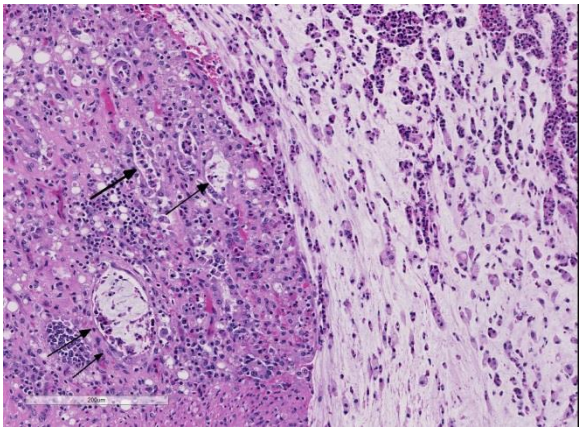

Colon, ox: Higher magnification of the colonic mucosa at the edge of the necrotic crypt. Glands are dilated and contain a combination of sloughed epithelial cells as well as neutrophils and are only segmentally lined by attenuated regenerating epithelium (crypt abscesses) (arrows). The massively dilated crypt contains aggregates of neutrophils, individualized muciphages, and abundant mucin. (HE, 100X)

note that PI infected animals are seronegative. RT-PCR is now widely accepted as a standard for BVDV diagnosis while immunohistochemistry remains one of the popular methods for antigen detection from the ear notch tissue samples.

JPC Diagnosis: Colon: Colitis, necrotizing diffuse, severe with pseudomembrane formation, marked crypt abscessation, crypt herniation, and lymphoid depletion, mixed breed calf, *Bos taurus*.

Conference Comment: The contributor provides an excellent summary of the epidemiology, pathogenesis, and diagnostic testing for persistent infection and mucosal disease in animals infected with bovine pestivirus. Other members of the *Pestivirus* genus of veterinary importance are classical swine fever virus and border disease virus.[6] Emerging pestiviruses include: Bungowannah virus, isolated from swine in an Australian piggery; atypical (HoBi-like) pestiviruses identified in Europe, Asia, and

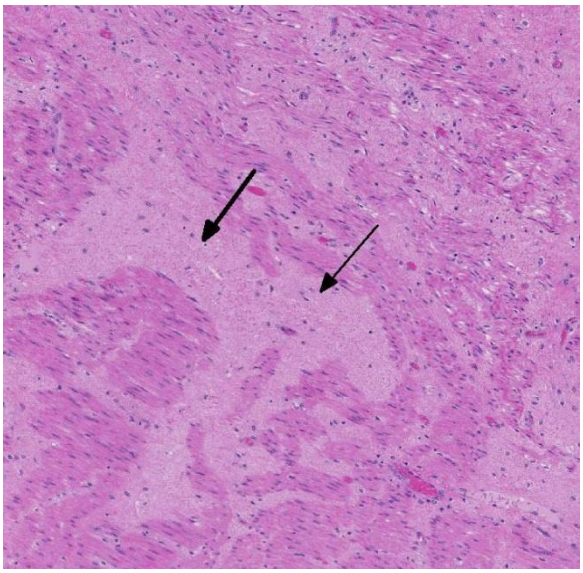

Colon, ox: Smooth muscle of the muscular tunics contains large lakes of edema fluid (arrows) (HE, 48X)

South America, discussed below; the pronghorn antelope pestivirus strains; and the giraffe strain of pestivirus (PG2).[5]

There are basically two forms of clinically severe BVDV in cattle. The first is mucosal disease in persistently infected cattle

described by the contributor. The second is the more recently recognized severe acute BVD caused by highly virulent strains of bovine pestivirus. Viruses from both BVDV-1 and BVDV-2 species can induce severe acute BVD, however, this form is usually caused by BVDV-2.[2, 6] Severe acute BVD is characterized by high morbidity and high mortality in all age groups of susceptible animals and has a peracute to acute course, with fever, sudden death, diarrhea, or pneumonia. It can also be associated with thrombocytopenic syndrome

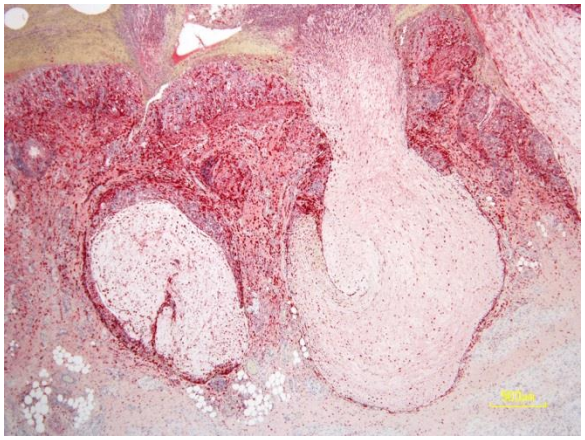

Colon, ox. Immunohistochemistry reveals strong positive immunoreactivity for bovine viral diarrhea virus throughout the mucosa, and submucosa. (Photo courtesy of: Department of Diagnostic Medicine and Pathobiology, Kansas State Veterinary College of Veterinary Medicine, 1800 Denison Avenue, Manhattan, KS 66506, http://www.vet.k-state.edu/depts/dmp/index.htm) (anti-BVDV, 100X)

characterized by severe epistaxis, hyphema, mucosal hemorrhage, and bloody diarrhea. This syndrome is typically associated with infection by non-cytopathic high-virulence BVDV-2 species.[2,6] Severe acute disease resembles both mucosal disease, malignant catarrhal fever, and rinderpest virus infection grossly. Histologically, rinderpest (*Paramyxoviridae*, morbillivirus) is distinguished from BVDV by the presence of intranuclear and intracytoplasmic inclusion bodies as well as syncytial cells. Malignant catarrhal fever (*Herpesviridae*, gammaherpesvirus) can be distinguished from BVDV by the appearance of the lymphoid organs; involution of lymphoid tissue occurs in BVD and lymphoproliferation occurs in MCF.[6] Regardless, antigenic or molecular characterization of the virus is required for definitive diagnosis. In this case, the contributor used immunohistochemistry, which is a highly specific modality to test for BVDV antigen in affected tissue.

In addition to persistent infection, early embryonic death, and abortion, in utero infection with bovine pestivirus can induce teratogenic lesions if a fetus is infected between 90-120 days of gestation. These lesions include: microcephaly, cerebellar

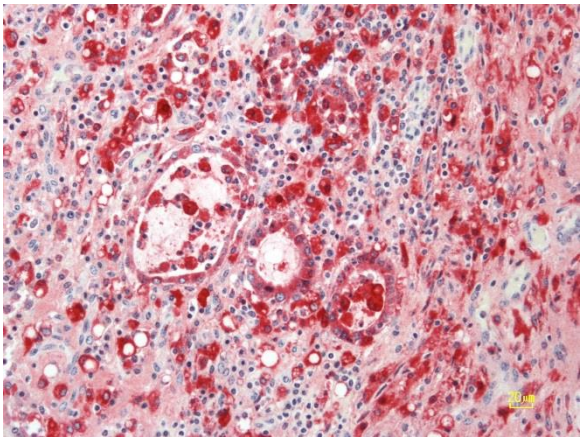

Colon, ox. Immunohistochemistry reveals strong positive immunoreactivity for bovine viral diarrhea virus within crypt epithelium. (Photo courtesy of: Department of Diagnostic Medicine and Pathobiology, Kansas State Veterinary College of Veterinary Medicine, 1800 Denison Avenue, Manhattan, KS 66506, http://www.vet.k-state.edu/depts/dmp/index.htm) (anti-BVDV, 400X)

hypoplasia and dysgenesis, hydranencephaly, hydrocephalus, and defective myelination of the spinal cord, microphthalmia. Other reported lesions include congenital cataracts, retinal degeneration, and optic neuritis. By day 135, the fetus is immunocompetent and will produce antibodies against the virus.[6]

Conference participants briefly discussed the emerging atypical pestivirus known as BVDV-3 or HoBi-like virus. This strain was recently recognized in Europe in fetal bovine serum imported from Brazil, where the disease is likely endemic. The clinical disease caused by this virus closely resembles BVDV infection, including growth retardation, reduced milk production, respiratory disease, reduced reproductive performance, and increased mortality among young animals.[1,6] In addition, commercially available BVDV diagnostic tests may not be able to detect HoBi-like viruses or to differentiate between BVDV and HoBi-like viruses. Current vaccines against BDVD have very little cross-protection against HoBi-like viruses.[1,6] Emergence of this pathogen could have negative implications for control and eradication programs for BVDV worldwide.

Contributing Institution:

Department of Diagnostic Medicine and Pathobiology
Kansas State Veterinary College of Veterinary Medicine
1800 Denison Avenue
Manhattan, KS 66506
http://www.vet.k-state.edu/depts/dmp/index.htm

References:

1. Bauermann FV, Ridpath JF, Weiblen R, Flores EF. HoBi-like viruses: An emerging group of pestiviruses. *J Vet Diagn Invest*. 2013; 25(1):6-15.
2. Brodersen BW. Bovine viral diarrhea virus infections: Manifestation of infection and recent advances in understanding pathogenesis and control. *Vet Pathol*. 2014; 51**:**453-464.
3. Brown CC, Baker DC and Barker IK. The alimentary system. In: Maxie MG, ed. *Pathology of Domestic Animals*. Vol 2. 5th ed. St. Louis, MO: Saunders Elsevier; 2007:140-147.
4. Lanyon SR, Hill FI, Reichel MP, Brownlie J. Bovine viral diarrhoea: Pathogenesis and diagnosis. *The Veterinary Journal*. 2014; 199: 201-209.
5. Schweizer M, Peterhans E1. Pestiviruses. *Annu Rev Anim Biosci*. 2014; 2:141–63.
6. Uzal FA, Plattner BL, Hostetter JM, Alimentary system. In: Maxie MG, ed. *Pathology of Domestic Animals*. Vol 2. 6th ed. St. Louis, MO; Saunders Elsevier; 2016:122-127.

Self-Assessment - WSC 2016-2017 Conference 5

1. Which of the following is true about neoplasia in hedgehogs?
    a. Neoplasia is extremely uncommon in the hedgehog.
    b. Osteosarcomas are the most common tumor in the hedgehog.
    c. 85% of tumors in hedgehogs are malignant.
    d. Herpesvirus has been reported in association with osteosarcoma in the hedgehog.

2. Splendore-Hoeppli material is composed of which of the following?
    a. Degranulated mast cell material
    b. Antigen-antibody complexes
    c. Major basic protein
    d. Degenerate chromatin from lysed lymphocytes

3. Which of the following is not true about colorectal inflammatory polyps of miniature dachshunds?
    a. They are classified into three stages based on the histology of the mucosal epithelial components and the inflammatory cells present.
    b. Hyperplastic goblet cells in these polyps are strongly positive for CK20, while those of adenomas and adenocarcinomas are immunonegative.
    c. Although they are presumed to be inflammatory in nature, immunosuppressive therapy, including prednisolone and cyclosporine, have not proven to yield a response.
    d. Studies suggest that increased IL-8 production in macrophages may be involved in the formation of inflammatory polyps.

4. True or false? The ability of the ncp strain to inhibit the induction of IL-1 in the fetus is generally believed to allow the BVDV virus to establish persistent infection.
    a. True
    b. False

5. At which date is a fetus considered immunocompetent and can produce antibodies against the BVDV virus?
    a. 45 days
    b. 120 days
    c. 135 days
    d. 160 days

Joint Pathology Center

Veterinary Pathology Services

WEDNESDAY SLIDE CONFERENCE 2016-2017

C o n f e r e n c e 6

5 October 2016

CASE I: 2016A (JPC 4084736).

Signalment: 20-day-old domestic duck (*Anas platyrhynchos*).

History: The outbreak site was a duck farm with 4000 ducks in Japan. In January 2014, an increased mortality in the 14- to 21-day-old duck flock was reported to veterinary officials by the owner. The mortality rate was 16%, i.e. 316 out of 2020 birds. Clinical signs of some ducks included reduced movement, ataxia, and dorsal recumbency with leg paddling.

Gross Pathology: The surface of the heart and liver was covered by white fibrinous exudate.

Laboratory results: Bacteria were isolated from the brain, heart, liver, and spleen. Total DNA was extracted from the bacterial colonies, and PCR was performed for bacterial 16S ribosomal RNA. The genetic sequence of the PCR product revealed that isolates were 99.9% identical to *Riemerella anatipestifer* (RA) type strain.

Histopathologic Description: The epicardium is thickened due to the edema, hemorrhage, and abundant fibrinous exudate surrounded by heterophils, macrophages, and multinucleated giant cells. Heterophilic and fibrinous serositis are also observed in the liver, air sac, and intestine. Gram-negative stained bacterial colonies are rarely found in the fibrinous exudates in the body cavity.

Contributor's Morphologic Diagnosis: Heterophilic, granulomatous and fibrinous pericarditis with rare gram-negative bacterial rods**.**

Contributor's Comment: *Riemerella anatipestifer* (RA) is a non-spore forming, non-motile, gram-negative rod.[14] *Riemerella anatipestifer* infection is a bacterial disease that primarily affects domestic ducks.[10] Young ducklings are more susceptible to the disease than adults.[10,14] *Riemerella anatipestifer* infection occurs as an acute or chronic form, characterized by fibrinous pericarditis, perihepatitis, air sacculitis, and meningitis.[10,14] *Riemerella anatipestifer* transmission can occur horizontally via the

Pericardium, duck. The pericardium is diffusely covered with a whitish fibrinous exudate. (Photo courtesy of: National Institute of Animal Health, National Institute of Animal Health, National Agriculture and Food Research Organization (NARO), 3-1-5Kannondai, Tsukuba, Ibaraki 3050856, Japan, (WSC ID95), http://www.naro.affrc.go.jp/english/niah/index.html)

respiratory tract and skin wounds,[10] whereas vertical transmission of RA via eggs is controversial. [7,8,11] Interestingly, some studies document that RA can be a part of the normal flora in the throat of some domestic and wild duck species.[3,15] At least 21 serotypes have been reported for RA, although there is some confusion regarding its classification.[12,13,14] Serotyping RA can be useful for epidemiological analyses and a vaccination strategy.[12,13]

Characteristic pathological findings, such as pericarditis and perihepatitis observed in the present case, are highly suggestive of RA infection. However, a definitive diagnosis of RA infection requires isolation and identification of RA from ducks suspected to be infected.[9,10,14] There are difficulties associated with the identification of RA.[9,10] *Riemerella anatipestifer* is characterized by the absence of species-specific biochemical properties.[5] Genetic sequencing of bacterial 16S ribosomal RNA and matrix-assisted laser desorption/ionization-time-of-flight (MALDI-TOF) mass spectrometry are currently considered useful for the identification of RA.[4,8,13,16]

Other bacterial infections such as colibacillosis may cause gross lesions similar to those seen in RA-infected ducks.[6] The differential diagnosis also include salmonellosis, pasteurellosis, strept-ococcosis, and *Coenonia anatina* infection.[14]

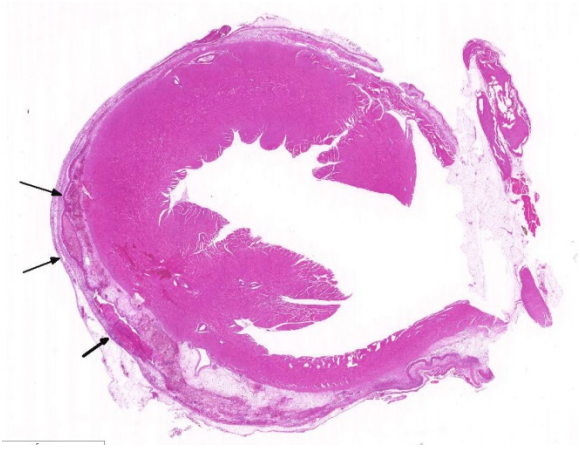

Heart, duck. The epicardium is diffuse, expanded by linear granulomas (arrows), hemorrhage, fibrin and edema. (HE, 10X)

JPC Diagnosis: Heart: Epicarditis, heterophilic and granulomatous, diffuse, severe with mild multifocal subepicardial necrotizing myocarditis, domestic duck, *Anas platyrhynchos*.

Conference Comment: *Riemerlla anatipestifer* (RA), also known as new duck disease or duck septicemia, is the causative agent of epizootic infectious polyserositis, a major problem of domestic ducks worldwide. It is also reported to be pathogenic for turkeys, chickens, pheasants, geese, and other waterfowl.[11] In geese, RA has been called goose influenza or septicemia anserum exsudativa.[5] This agent causes major economic loss in the duck industry due to high mortality rates of up to 75%, weight loss, and condemnations in ducklings under eight weeks old. Stress from adverse environmental conditions is the main predisposing factor for this disease.[4,10]

As mentioned by the contributor, fibrinous pericarditis and epicarditis are the most characteristic lesions of RA. This case represents the chronic form of the disease, with progression from fibrinous to granulomatous epicarditis with abundant granulation tissue on the epicardial surface. The pericardium was likely removed prior to tissue processing and is not present in the microscopic sections submitted for evaluation.

Many conference participants had little experience with this entity histologically, which led to a discussion of the differential diagnosis for epicarditis and polyserositis in avian species. While not a typical presentation for *Pasteurella multocida*, fowl cholera can cause similar lesions in poultry, chickens, and waterfowl.[4] *Salmonella pullorum* causes peritonitis and death in hatchling chicks; and peritonitis, arthritis,

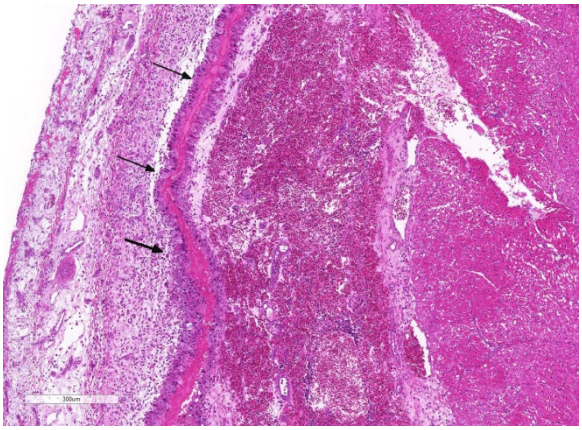

Heart, duck. Higher magnification of the epicardium with a linear granuloma surrounding brightly eosinophilic material. There is extensive edema, heterophilic inflammation, and hemorrhage of the epicardium. (HE, 40X)

and pericarditis in adults, and is often characterized by large hetrophilic granulomas in the myocardium. *Escherichia coli* and other coliform infections also can lead to fibrinous and heterophilic rmyocarditis, and should be considered as a differential in most avian species.[4] *Coenonia anatine*, described by the contributor and briefly discussed during conference, also causes exudative serositis in ducks and geese.[12] *Riemerella columbina* causes similar disease as RA in pigeons.[12] While not mentioned during conference, West Nile Virus, an arbovirus of the family *Flaviviridae*, should also be considered as a

differential for necrotizing myocarditis of many avian species, with young chickens and geese being most likely to develop clinical disease and mortality.[1]

Participants also discussed the three main rule-outs for polyserositis, pneumonia, and polyarthritis in pigs; among these include *Haemophilus parasuis*, *Mycoplasma hyorhinis*, and *Streptococcus suis*.[5] In horses, the most likely etiologies for polyserositis are *Streptococcus equi* and *Streptococcus zooepidemicus*.[2]

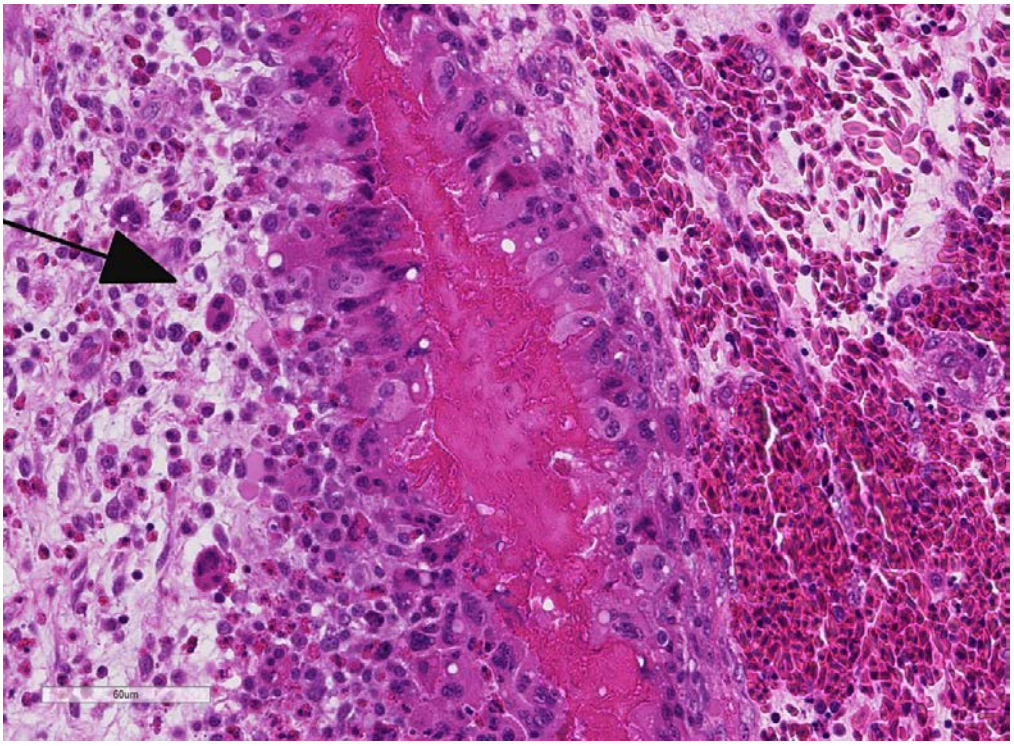

Heart, duck. Higher magnification of the linear granuloma (arrow) with epithelioid and foreign body macrophages centered on a dense eosinophilic aggregate of fibrin and heterophilic debris. Numerous macrophages and heterophils are present in the surrounding tissue. (HE, 232X)

Contributing Institution:

National Institute of Animal Health
National Agriculture and Food Research Organization (NARO)
Kannondai, Tsukuba, Ibaraki 3050856, Japan
http://www.naro.affrc.go.jp/english/niah/index.html

References:

1. Capua I. Arthropod-borne viruses. In: Pattison M, McMullin PF, Bradbury JM, Alexander DJ, eds. *Poultry Diseases*. 6th ed. Philadelphia, PA: Saunders Elseveier; 2008:421-422.
2. Caswell JL, Williams KJ. Respiratory System. In: Maxie MG, ed. *Jubb Kennedy and Palmer's Pathology of Domestic Animals*. Vol 2. 6th ed. Philadelphia, PA: Elsevier Saunders; 2016:578.
3. Cha SY, Seo HS, Wei B, Kang M, Roh JH, Yoon RH, Kim JH, Jang HK. Surveillance and characterization of *Riemerella anatipestifer* from wild birds in South Korea. *J Wildl Dis*. 2015; 51:341-347.
4. Christensen H, Bisgaard M. Phylogenetic relationships of Riemerella anatipestifer serovars and related taxa and an evaluation of specific PCR tests reported for R. anatipestifer. *J Appl Microbiol*. 2010; 108:1612-1619.
5. Christensen JP, Bojesen AM, Bisgaard M. Fowl Cholera. In:

Pattison M, McMullin PF, Bradbury JM, Alexander DJ, eds. *Poultry Diseases*. 6th ed. Philadelphia, PA: Saunders Elsevier; 2008:149-154.
6. Craig LE, Dittner KE, Thompson KG. Bones and Joints. In: Maxie MG, ed. *Jubb Kennedy and Palmer's Pathology of Domestic Animals*. Vol 1. 6th ed. Philadelphia, PA: Elsevier Saunders; 2016:151-152.
7. Glünder G, Hinz KH. Isolation of *Moraxella anatipestifer* from embryonated goose eggs. *Avian Pathol*. 1989; 18:351-355.
8. Hess C, Enichlmayr H, Jandreski-Cvetkovic D, Liebhart D, Bilic I, Hess M. *Riemerella anatipestifer* outbreaks in commercial goose flocks and identification of isolates by MALDI-TOF mass spectrometry. *Avian Pathol*. 2013; 42:151-156.
9. Hinz KH, Ryll M, Kohler B, Glunder G. Phenotypic characteristics of *Riemerella anatipestifer* and similar micro-organisms from various hosts. *Avian Pathol*. 1989; 27:33-42.
10. Leibovitz L. A survey of the so-called "anatipestifer syndrome". *Avian Dis*. 1972; 16:836-851.
11. Mavromatis K, Lu M, Misra M, Lapidus A, et al. Complete genome sequence of *Riemerella anatipestifer* type strain (ATCC 11845). *Stand Genomic Sci*. 2011; 4:144-153.
12. Pathanasophon P, Phuektes P, Tanticharoenyos T, Narongsak W, Sawada T. A potential new serotype of *Riemerella anatipestifer* isolated from ducks in Thailand. *Avian Pathol*. 2002 31:267-270.
13. Rubbenstroth D, Ryll M, Knobloch JK, Köhler B, Rautenschlein S. Evaluation of different diagnostic tools for the detection and identification of *Riemerella anatipestifer*. *Avian Pathol*. 2013; 42:17-26.
14. Ruiz JA, Sandhu T. *Riemerella anatipestifer* infection. In: Swayne DE, ed. *Disease of poultry*, 13th ed. Ames, IA; Wiley Blackwell publishing, 2013:823-828.
15. Ryll M, Christensen H, Bisgaard M, Christensen JP, Hinz KH, Köhler B. Studies on the prevalence of *Riemerella anatipestifer* in the upper respiratory tract of clinically healthy ducklings and characterization of untypable strains. *J Vet Med B Infect Dis Vet Public Health*. 2001; 48:537-546.
16. Tsai HJ, Liu YT, Tseng CS, Pan MJ. Genetic variation of the ompA and 16S rRNA genes of *Riemerella anatipestifer*. *Avian Pathol*. 2005; 34: 55-64.

CASE II: 49587 (JPC 4084567).

Signalment: 8-year-old ovario-hysterectomized Siamese mix cat (*Felis catus*).

History: Two-week history of cluster seizures. No other previous medical history. Upon presentation, the patient was hypo-thermic (96 F), with a pulse of 120. She was exhibiting open-mouthed breathing with a respiratory rate of 45. Due to the anticipated duration of intensive care, euthanasia was elected. A postmortem MRI was performed, which revealed a focal lesion in the left caudate nucleus. Differential diagnoses included infectious causes, a vascular event, and neoplasia.

Gross Pathology: Central Nervous System: The distal aspect of the cerebellar vermis

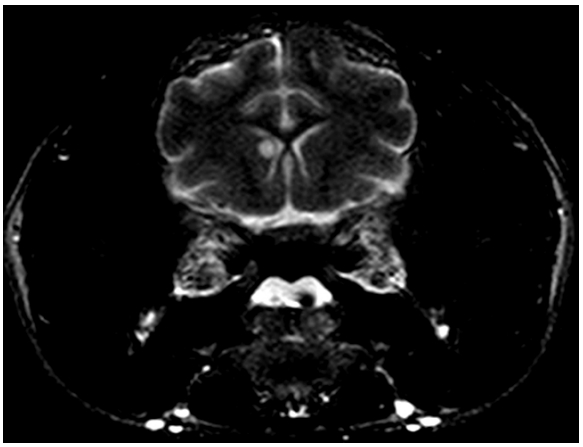

Cerebrum, cat. Results of a postmortem MRI. There is a focal lesion in the left caudate nucleus. (Photo courtesy of the Animal Medical Center, 510 East 62nd St. New York, NY 10065 www.amcny.org)

can be observed from the foramen magnum. Upon removal of the brain, the vermis is flattened over the brainstem (cerebellar coning). The brain is fixed whole and sectioned, which reveals diffuse, mild expansion of the leptomeninges and widening of sulci by yellow to brown, gelatinous material and a focal, 0.5 cm diameter, gelatinous mass at the left caudate nucleus.

Pulmonary: The lungs are mottled tan to medium red. Multiple nodules are present, and the tracheobronchial lymph nodes are markedly enlarged. The right cranial lung lobe has a large, firm to soft, smooth, tan to white mass that measures 2.5 x 2.5 x 1 cm. Within the left cranial lung lobe, at the junction between the cranial and caudal subsets, there is a focal, firm, 2 x 2 x 1 cm nodule. Smaller nodules are present at the distal aspect of the left cranial lung lobe that measure up to 1 cm in diameter. A large nodule is present with the accessory lobe that measures 2.5 x 1.3 by 1 cm.

Hemolymphatic: The mediastinal and tracheobronchial lymph nodes are markedly enlarged. All are soft to firm and pale tan to white. The largest of the mediastinal lymph nodes measures 1.7 x 2 x 1 cm and the tracheobronchial lymph nodes measure up to 1.5 x 1.0 x 1.0 cm.

Internal: In the omentum adjacent to the pancreas, there is a soft, smooth, tan to white mass that measures 1.6 x 1.6 x 1.3 cm. The regional omentum is hyperemic and thickened.

Laboratory results: Postmortem cytology of lung nodules, lymph nodes, omental nodule: Impression smears are similar and consist of mixed inflammatory cell populations including foamy macrophages, lymphocytes, and plasma cells. Inflammatory cells are intermixed with numerous yeast organisms which are

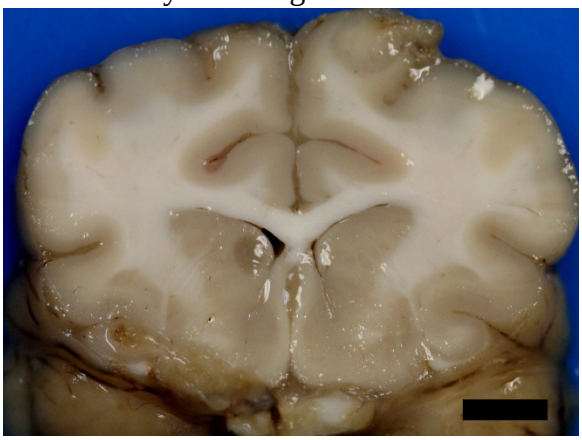

Cerebrum, cat. A well-demarcated lesion is present in the caudate nucleus, and the leptomeninges are multifocally expanded by a gelatinous brown material. (Photo courtesy of the Animal Medical Center, 510 East 62nd St. New York, NY 10065 www.amcny.org)

surrounded by a large, clear capsule, and occasionally exhibit narrow based budding (*Cryptococcus* spp).

Histopathologic Description: A section of the cerebral cortex at the level of the caudate nucleus or thalamus is examined. Diffusely, the leptomeninges are expanded by coalescing sheets of yeasts, interspersed by multifocal inflammatory populations. Sulcal widening is prominent. Yeasts are round to oval, approximately 5-10 um in diameter, with a thin, 1 um wall and are surrounded by

a large, 10-20 um diameter clear capsule. Occasional narrow-based budding is observed. Inflammatory populations interspersed by the yeasts are comprised predominantly of lymphocytes, plasma cells, and macrophages. The yeasts multifocally extend into the regional cerebral cortical parenchyma which exhibits white matter vacuolation and gliosis. In some of the sections, there is a focal nodule comprised of yeasts at the level of the caudate nucleus. Multifocally, scattered lymphocytes and plasma cells are present within and surrounding the nodule, both within Virchow-Robin spaces and less frequently, the regional parenchyma with mild accompanying gliosis. Occasional yeasts are observed within the lateral ventricles or Virchow Robin spaces in some slides. Throughout the cerebral cortex, there are increased numbers of branched, small caliber arterioles (edema) with increased numbers of glial cells, as well as mild vacuolation and gliosis of the centrum semiovale. Small numbers of vessels throughout the sections contain perivascular

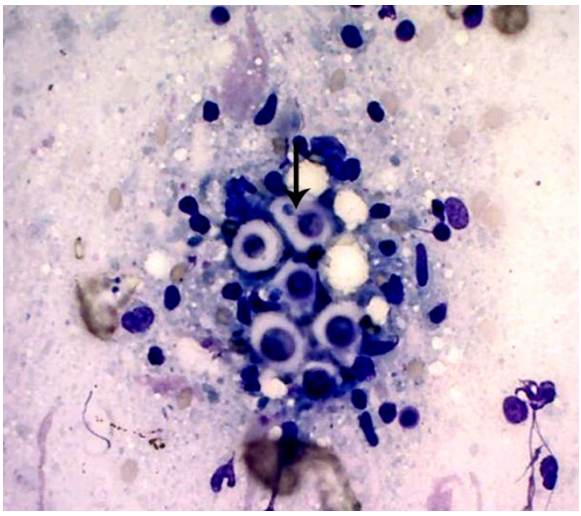

Impression smear, cat. Impression smears of nodules from the lung, lymph nodes, and omentum revealed numerous yeasts with a clear capsule and narrow-based budding (arrow), admixed with macrophages, neutrophils, and cellular debris. (Photo courtesy of the Animal Medical Center, 510 East 62nd St. New York, NY 10065 www.amcny.org)

aggregates of Gitter cells with intracytoplasmic brown pigment (lipofuscin). Neurons throughout the sample also contain intracytoplasmic brown pigment (lipofuscin).

Special stains: Gomori methenamine silver (GMS) and mucicarmine reveal positive staining of yeasts and highlights narrow based budding. The capsule is light pink with the mucicarmine stain.

Contributor's Morphologic Diagnosis: Brain: Meningoencephalitis, lymphoplasmacytic, histiocytic, multifocal to coalescing, severe with myriad encapsulated yeasts (etiology consistent with *Cryptococcus* spp), rare parenchymal in-filtration with regional spongiosis and gliosis; cerebral edema, diffuse, mild.

Contributor's Comment: The gross, cytologic and histologic findings are consistent with disseminated *Cryptococcus* spp. infection of the respiratory tract and central nervous system (CNS). Cryptococcosis is the most common systemic mycosis of cats,[3,5] infection of which is thought to be acquired from the environment.[5] Infection is not contagious or zoonotic, as is typical for the systemic mycoses.[3] Cryptococcosis in dogs and cats is primarily caused by two encapsulated, dimorphic, basidiomycetous fungi, *Cryptococcus neoformans* and *Cryptococcus gattii*.[5,7] The yeast phase is found under routine laboratory conditions and within mammalian host tissues.[5] Infection can occur from inhalation of the basidiospore stage or desiccated yeasts from the environment.[1] The infectious form can be found in soil, pigeon or other avian guano, and decaying organic matter.[3,5] The initial site of infection is hypothesized to be the nasal cavity, lungs, and/or gastrointestinal tract.[4,7] The skin, lymph nodes, CNS, and eyes are frequently affected.[7] Additional

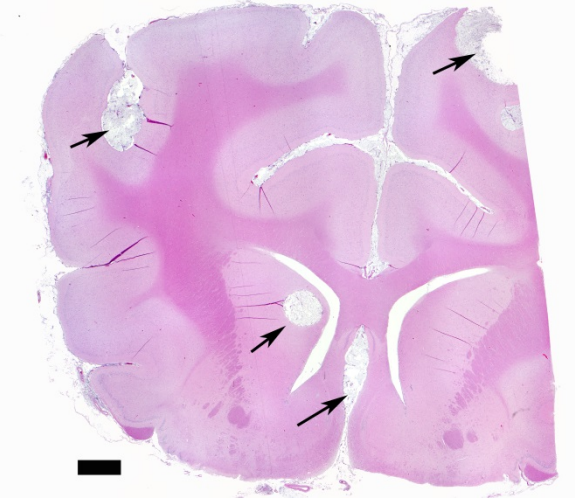

Cerebrum, cat. The meninges are multifocally expanded by aggregates of yeasts (arrows) and fewer inflammatory cells. There is also a focal circular lesion in the left caudate nucleus. (Photo courtesy of the Animal Medical Center, 510 East 62nd St. New York, NY 10065 www.amcny.org) (HE, 4X)

testing for species identification was not performed in this case.

Pathogenesis is dependent upon the amount of organism present upon exposure, virulence of the strain and immune status of the host. *Cryptococcus* has been called "a sugar-coated killer with designer genes",[5] due to its virulence factors.[5] The four main virulence factors include the ability to grow at 37 degrees C, its polysaccharide capsule, melanin production and secretion of degradative enzymes.[2,5] The polysaccharide capsule provides protection from the environment and host,[5] is comprised of negatively charged glucuronoxylomannan and enlarges after infection of the host.[5] The capsule is chemotactic for neutrophils, however, inhibits phagocytosis via its negative charge and blocks the antibody Fc receptor from communicating with host phagocytes. It interferes with leukocyte migration, can deplete complement and inhibits T cell responses. Resolution of infection in immunocompetent animals requires a T-helper cell 1 (Th1) pattern of cytokine and lymphocyte-mediated adaptive immune response.[2,4] Tumor necrosis factor, IL-12, IL-18, GM-CSF and IF-γ among others play a role in host defense.[2] Humoral factors are thought to aid in clearance via antibodies and complement.[2] Melanin or a melanin-like compounds are produced from diphenolic compounds via the enzyme laccase (phenoloxidase)[2,5] which help protect the organism from oxidative damage[7] and may modulate the host immunoinflammatory response.[3] Interestingly, rare *Cryptococcus* spp without a capsule can be easily phagocytized and incite a strong granulomatous response.[3]

Yeasts were more prominent than inflammation in the majority of the sample. *Cryptococcus* infection in cats has been shown to have relatively less inflammation than infections in dogs, which may reflect differences in infecting strains and/or underlying unrecognized defects in the immune or inflammatory response.[6-8] The cat, in this case, had no significant previous medical history, however, FIV/FeLv status was unknown. In one Australian study, Siamese, Birman and Ragdoll cats were found to be predisposed to *Cryptococcus* infection.[5] This cat was described as a Siamese mix.

After infection of the respiratory tract, fungal organisms are thought to spread hematogenously via macrophages, frequently to the CNS.[5] Extension of nasal cavity infection across the cribriform plate, frontal sinus or along cranial nerves into the brain may also occur.[5,7,8] Histologic evaluation of samples from the nasal cavity did not reveal any fungal organisms, and the frontal sinus was grossly normal. Ocular abnormalities can occur in up to one-third of affected cats,[5] however, no histologic evidence of infection of the eye or optic nerves was present in this case. Neurologic signs vary depending upon the location of

the lesions. Obtundation, behavioral changes, hyperesthesia, tremors, seizures, circling, head pressing, ataxia, paresis, head tilt, vestibular signs, and blindness are common clinical signs.[5] The cat, in this case, exhibited obtundation and cluster seizures. Meningeal involvement is common, as in this case, and is considered a predilection site.[6] Grossly, the leptomeninges may be unremarkable, or cloudy to thickened, with gelatinous mucoid material and sulcal widening.

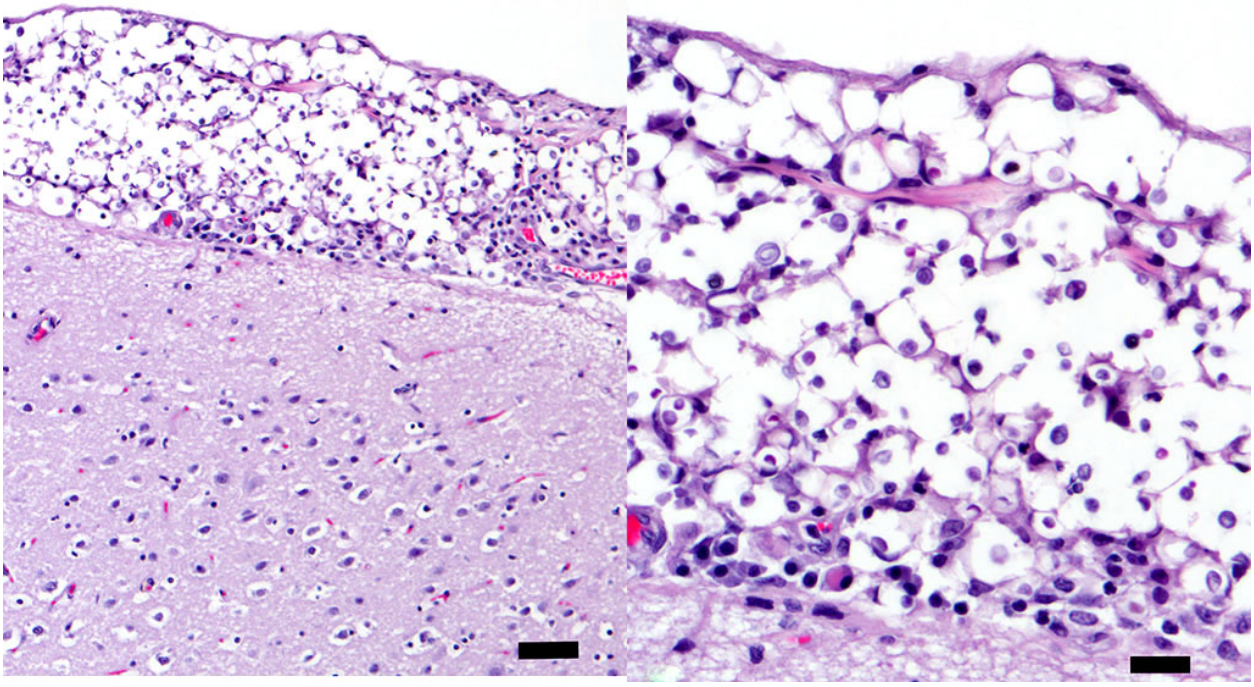

Cerebrum, cat. There is marked expansion of the leptomeninges with numerous 3-6um budding yeasts with a prominent clear capsule. In the 400X image at left, there low numbers of plasma cells at the periphery, attesting to the chronicity of the lesion. (Photo courtesy of the Animal Medical Center, 510 East 62nd St. New York, NY 10065 www.amcny.org) (HE, 10X and 40X)

Histologically, tightly packed yeasts give a "soap bubble" appearance.[3,6] The leukocytic response can consist of neutrophils, macrophages, multinucleate giant cells, lymphocytes, plasma cells and eosinophils, which is dependent upon host immune status.[8] In humans, CNS involvement manifests as meningitis, meningo-encephalitis, or Cryptococcomas, which are tumor-like intraparenchymal masses containing yeasts and inflammatory cells,[7] similar to the focal nodule observed with imaging and evaluation of the gross specimen in this case. Gelatinous pseudo-cysts are cystic extensions of Virchow-Robin spaces with collections of yeasts, and can also be detected with imaging modalities.[7] One study of cats and dogs with CNS *Cryptococcus* infection identified three histopathologic patterns: 1) Pseudocyst formation with expansion of cryptococcal organisms along Virchow-Robin spaces with multifocal intraparenchymal pseudocysts, 2) Diffuse meningitis only without pseudocysts or parenchymal involvement and 3) meningoencephalitis without pseudocyst formation.[7] These patterns were not found to correlate with the type of *Cryptococcus* sp. or treatment.[7]

JPC Diagnosis: Brain, cerebrum: Meningitis, lymphoplasmacytic and histiocytic, diffuse, moderate, with numerous narrow based budding and encapsulated yeasts, etiology consistent with

Cryptococcus sp., Siamese cat mix, *Felis catus*.

Conference Comment: The contributor provides an outstanding summary of the epidemiology, pathogenesis, clinical signs, gross and histologic patterns associated with disseminated cryptococcosis in dogs and cats. Cryptococcosis is a fungal disease with worldwide distribution and is the most common systemic mycotic disease in cats.

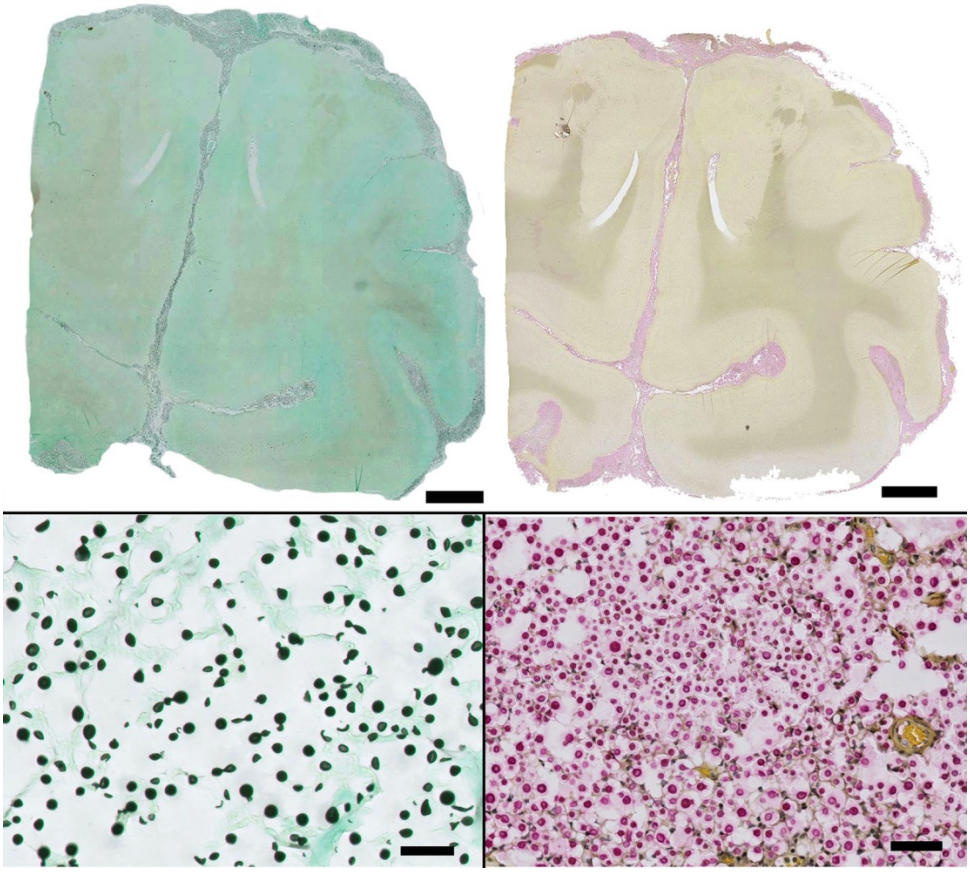

Cerebrum, cat. Gomori methenamine silver (GMS) and Mucicarmine reveal positive staining of yeasts and highlights narrow based budding. The capsule is light pink with the Mucicarmine stain (Photo courtesy of the Animal Medical Center, 510 East 62nd St. New York, NY 10065 www.amcny.org) (HE, 4X)

Dogs, horses, cattle, and humans are also affected by this dimorphic, basidiomycete, yeast-like fungi.[1,3,8,9] The diagnosis is typically based on identifying the organism and its characteristic thick capsule on histologic sections or cytologic preparations. *Cryptococcus* sp. is the only pathogenic mycotic organism with a thick capsule making the histopathologic diagnosis relatively straightforward; especially when there is a myriad of organisms, as in this case.[2] The thick polysaccharide capsule gives lesions a gelatinous appearance seen in the gross photograph and noted by the contributor. Distention of the leptomeninges by the organism is commonly observed in cats and occurs through a repetitive process of macrophage phagocytosis, cell lysis, and subsequent chemotaxis of additional macrophages allowing an expansive accumulation of the polysaccharide capsule.[3,8] Participants also identified multifocal narrow based budding in their sections further differentiating this fungus from *Blastomyces* sp, which have characteristic broad-based budding.[3]

The contributor noted that the distal aspect of the cerebellar vermis could be observed from the foramen magnum and upon removal of the brain, the vermis was flattened over the brainstem interpreted as cerebellar coning indicating cerebellar herniation. In humans, prognostic indicators for cryptococcosis include abnormal mental status, history of seizures, high antigen titers within serum and cerebral spinal fluid (CSF), poor host inflammatory response,

and high CSF pressure.[7] This animal likely had increased intracranial pressure secondary to infection leading to herniation of the cerebellum, altered mental state, and seizure activity. Increased intracranial pressure secondary to *Cryptococcus* sp. infection of the central nervous system is a negative prognostic indicator in humans and animals.[3,7]

Conference participants discussed different histochemical stains to highlight the thick capsule of this organism. The capsule can by highlighted by mucicarmine and in wet mounts, it stains with India ink. In addition to the periodic acid-Schiff and Grocott's methenamine silver stain run by the contributor, the yeasts also stain with Fontana-Masson stains due to their production of melanin via a virulence factor, laccase. A positive culture is required for definitive diagnosis.[3] Participants also noted the relative lack of inflammation within the neuropil of this animal. As mentioned by the contributor, in contrast to other mycotic infections, such as *Blastomyces* sp, *Coccidioides* sp, and *Histoplasma* sp, the host inflammatory reaction is often quite minimal, likely due the polysaccharide capsular component glucuronoxylomannan, preventing yeast recognition by phagocytes, induction of IL-10, and disruption of dendritic cell activation and maturation.[2,5]

Contributing Institution:
Animal Medical Center
510 East 62nd St.
New York, NY 10065
www.amcny.org

References:

1. Burns RE and Mohr, CF. Pathology in Practice. *J Am Vet Med Assoc*. 2010; 236:1069-1070.
2. Carroll SF, Guillot L, Qureshi ST. Mammalian model hosts of cryptococcal infection. *Comp Med*. 2007; 57(1):9-17.
3. Caswell JL, Williams KJ. Respiratory system. In: Maxie MG, ed. *Jubb, Kennedy, and Palmer's Pathology of Domestic Animals*. Vol 2. 6th ed. Philadelphia, PA: Elsevier; 2016:582-583.
4. Lorente-Méndez C, Martínez CM, Corpa JM. Pathology in practice. *J Am Vet Med Assoc*. 2009; 235:1407-1409.
5. Malik R, Krockenberger M, O'Brien CR, Martin P, Wigney D, Medleau L. Cryptococcosis. In: Greene CE, ed. *Infectious Diseases of the Dog and Cat*. 3rd ed. St. Louis, MO: Elsevier Inc; 2006:584-598.
6. Summers BA: Inflammatory diseases of the central nervous system. In: Cummings JF, de Lahunta A, eds. *Veterinary Neuropathology*. St. Louis, MO: Mosby-Year Book, Inc.; 1995:151-155.
7. Sykes JE, Sturges BK, Cannon MS, et al. Clinical signs, imaging features, neuropathology, and outcome in cats and dogs with central nervous system cryptococcosis from California. *J Vet Intern Med*. 2010; 24:1427–1438.
8. Zachary JF: Nervous system. In: McGavin MD, Zachary JF, eds. *Pathologic Basis of Veterinary Disease*. 5th ed. St. Louis, MO: Mosby, Inc.; 2012:891-893.
9. Uchiumi K, Stowe DM, DeVanna JC, Wilcox JL, Neel JA. Pathology in practice. *Cryptococcus* sp in a dog. *J Am Vet Med Assoc*. 2014; 245:893-895.

CASE III: 10471-11 (JPC 4003103).

Signalment: 8-month-old female domestic shorthair cat (*Felis catus*).

History: Patient presented for lethargy, depression, and inappetence. Rectal temperature was 105.1F. Initial treatment consisted of antibiotics, anti-inflammatory drugs, and subcutaneous fluids. Five days later, icterus with hypoglycemia, hypo-albuminemia, and leucopenia were noted. Rectal temperature was 103F. The patient died the following day.

Gross Pathology: The spleen was enlarged with a roughened serosal surface. Multiple white pinpoint foci were observed on the serosal surface. The cut surface bulged and had a granular appearance. No other gross lesions were indicated by the submitting veterinarian.

Laboratory results: *Francisella tularensis* was isolated from the spleen and from a lymph node sample.

Histopathologic Description: In sections of spleen, there is disseminated and coalescing necrosis of germinal centers which extends into adjacent red pulp. Foci of necrosis are accompanied by an inflammatory response comprised of neutrophils and macrophages.

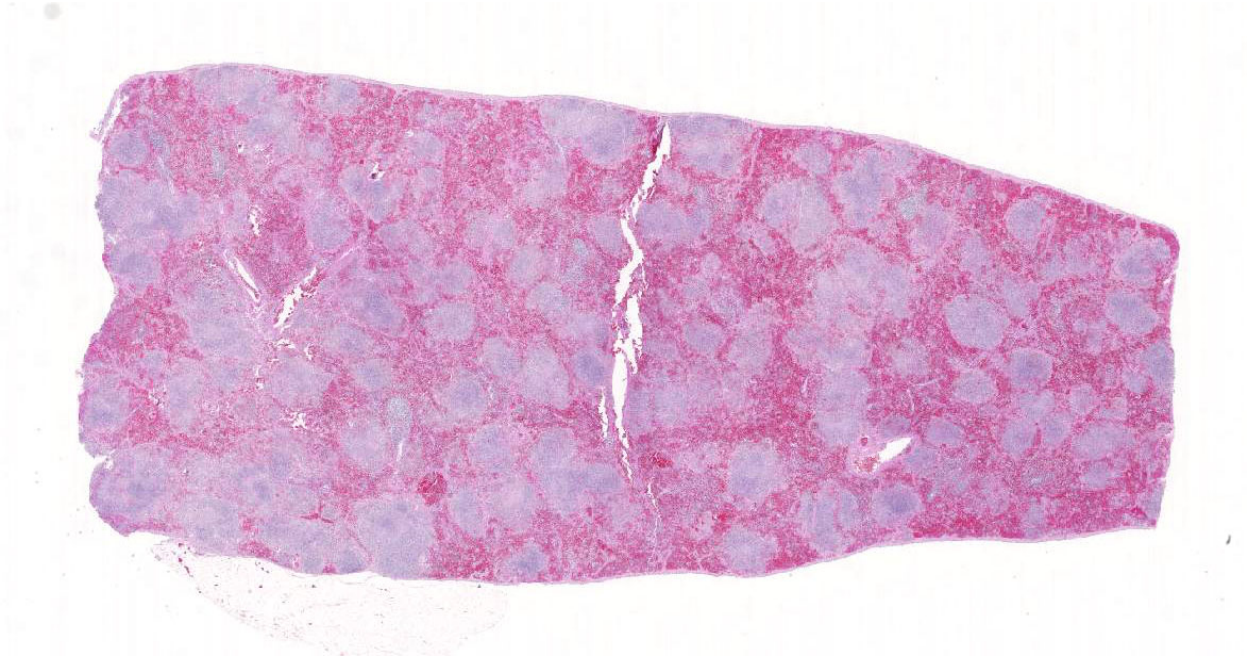

Spleen, cat. At subgross magnification, white pulp is largely necrotic and areas of lytic necrosis coalesce throughout the slide. A few depleted lymphoid follicles retain their architecture. (HE, 5X)

By use of special technique, numerous small gram-negative coccobacilli are seen within necrotic foci and the cytoplasm of individual inflammatory cells.

Contributor's Morphologic Diagnosis: Severe, subacute, multifocal, coalescing, necrotic, and pyogranulomatous splenitis

Contributor's Comment: *Francisella tularensis* is a gram-negative, facultative intracellular pathogen.[5] *F. tularensis* is subdivided into two subtypes. Type A is *F. tularensis subsp. tularensis* and has and infectious dose in humans of <10 CFU's, whereas type B is *F. tularensis subsp. holarctica* which as an infectious dose of <103 CFU and a milder form of tularemia in humans.[5] The organism is abundant in nature and infects many mammalian and arthropod species.[7] *F. tularensis* type A has been isolated from cats on numerous occasions and can be transmitted from cats and other animals (deer, personal experience) to humans.[1,3,7]

Diagnosis, in some cases, may be difficult, but culture appears to be more sensitive than immunohistochemistry.[7] Gross lesions consist of multiple pinpoint white foci on the spleen, liver, and lymph nodes. As a facultative intracellular parasite, it may persist for years as a latent infection.[7] The genes for several virulence factors have been identified and shown to share some features with the intracellular parasite, *Listeria monocytogenes*.[4] Tularemia in other mammalian species such as horses and sheep are often associated with heavy infestation by ticks such as *Dermacentor andersoni* and *Amblyomma americanum*.[7] One serologic survey indicated 12 – 24 percent of cats had antibodies to *F. tularensis* due to natural exposure.[6] Those serologically positive animals were negative for *F. tularensis* DNA, indicating infection may be may have been cleared naturally. Tularemia should be considered in a differential diagnosis of unexplained febrile illness in cats.

JPC Diagnosis: Spleen: Splenitis, necrotizing, multifocal to coalescing, severe, with mild lymphoid depletion and fibrin deposition, domestic shorthair cat, *Felis catus*.

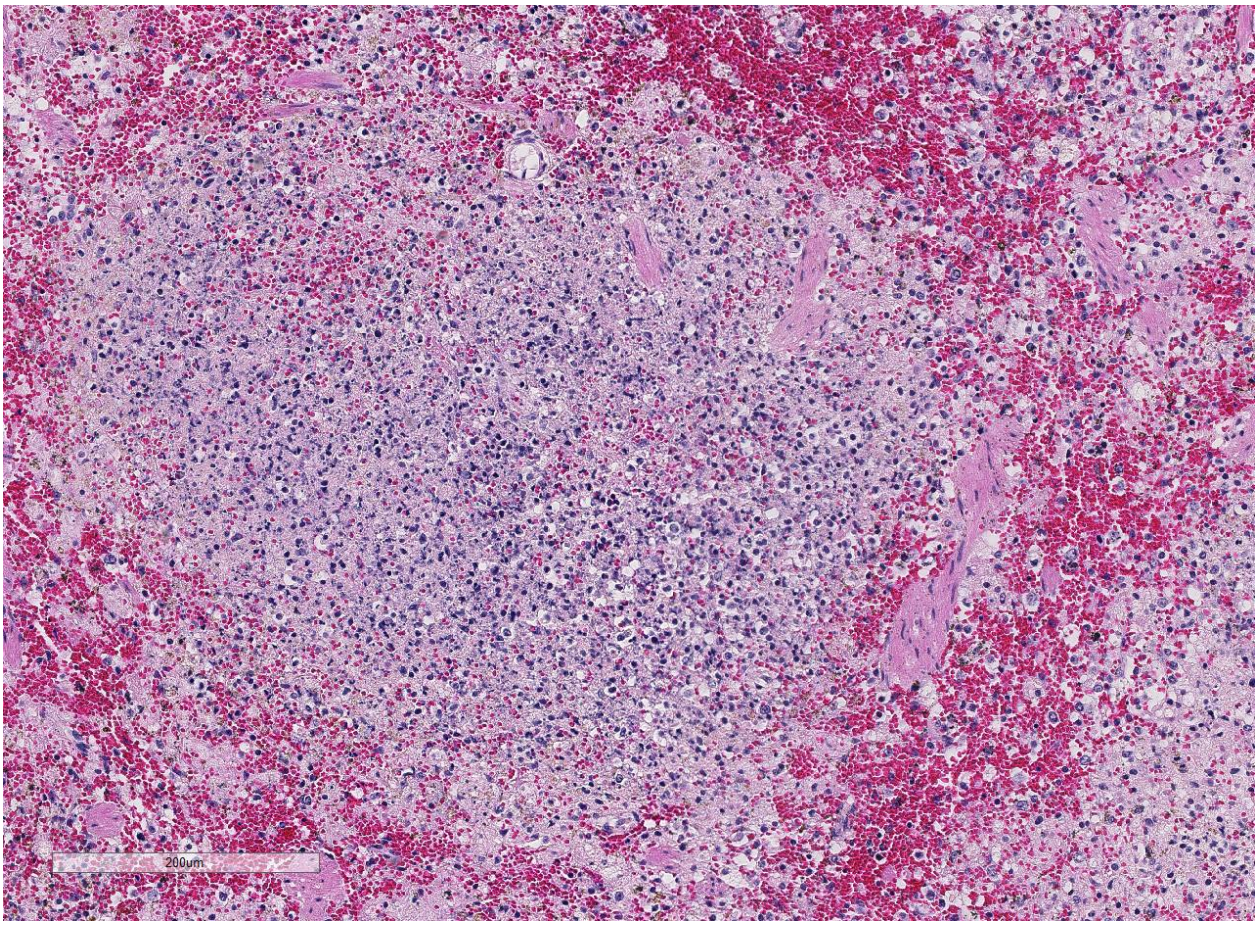

Spleen, cat. Higher magnification of a necrotic lymphoid follicle. The lytic necrosis extends into the surrounding tissue and there is hemorrhage within the marginal zone.

Conference Comment: The contributor provides a great example of typical lesions of *Francisella tularensis*. In cats, there often is severe systemic disease and pathological manifestations are dependent on the dissemination of the pathogen.[1,8,9] As mentioned by the contributor, classic gross lesions for tularemia are miliary white foci 2mm or more in diameter in the liver, spleen, and lymph nodes. Histologically, the lesions are characterized by focal areas of severe necrosis, as seen in this case.[8] This gram-negative, intracellular bacillus can infect humans, wild rabbits, rodents, and over 100 species of wild and domestic mammals, birds, fish, and reptiles.[3,9] In the North America, the wild rabbit is the reservoir for the *biovar tularensis* (type A). *Biovar holarctica* (type B) is more common in aquatic species such as beavers and muskrats. *F. tularensis biovar mediasiatica* and *F. novicida* are restricted to central Asia.[7,8] Sporadic outbreaks of tularemia are known to occur in sheep and foals in association with heavy infestation with *Dermacentor andersoni* and *Amblyomma americanum* ticks. Typically, enlargement of the liver, spleen, and kidneys with miliary foci of necrosis are seen on post-mortem examination.[8] Dogs are generally highly resistant to natural infection, but there have been rare reports of mild disease in canines.[8]

The most common route of infection for humans originates from cleaning and skinning infected rabbits as well as arthropod bites. Humans can also be infected via contaminated water supplies and consumption of undercooked meat.[6] In addition to natural infection, *F. tularensis* is considered to be a serious potential bioterrorism agent, because it is one of the most infectious pathogenic bacteria known. As mentioned by the contributor, inhalation of as few as 10 organisms can cause severe pneumonic tularemia disease leading to serious illness and death.[1,6]

Experimentally-induced lesions from inhalation in African green monkeys included necrotizing pyogranulomatous lesions which targeted the lung and lymphoid tissue in addition to disseminated miliary necrotic foci on multiple organs and moderate to marked lymphoid depletion of the splenic white pulp and mediastinal lymph nodes.[6] Conference participants agreed that in this case, both red and white pulp of the spleen are affected by necrosis; however, lesions generally centered on the white pulp and extended into the red pulp in conjunction with severe lymphoid depletion and lymphocytolysis. There are currently no vaccines available to prevent disease.[6] As a result, conference participants discussed that extreme care needs to be taken when dealing with and shipping suspect tularemia cases.

These facultative intracellular organisms are most commonly located within macrophages, but may also be present extracellularly in exudates and necrotic debris. The organisms can also infect and survive in dendritic cells, neutrophils, hepatocytes, and lung epithelial cells. The ability of *F. tularensis* to infect macrophages, evade the immune system by preventing phagolysosome fusion, rapidly replicate within macrophages, and disseminate widely throughout the body is the key to its pathogenesis.[1,7,8]

Contributing Institution:

School of Veterinary Medicine & Biomedical Sciences
Veterinary Diagnostic Center
Fair Street and East Campus Loop
University of Nebraska-Lincoln
Lincoln, NE 68583-0907
http://www.nvdls.unl.edu

References:

1. Brotcke A, Weiss DS, Kim CC, et al. Identification of Mg1A-regulated genes reveals novel virulence factors in *Francisella tularensis*. *Infect immune*. 2006; 74:6642-6655.
2. Gyuranecz M, Szeredi L, Makrai L et al. Tularemia of European Brown Hare (*Lepus europaeus*): A pathological, histopathological, and immunohistochemical study. *Vet Pathol*. 2010; 47(5):958-63.
3. Inzana TJ, Glindemann GE, Snider G, et al. Characterization of a wild-type strain of *Francisella tularensis* isolated from a cat. *J Vet Diagn Invest*. 2004; 16:374-381.
4. Magnarelli L, Levy S, Koski R. Detection of antibodies to *Francisella tularensis* in cats. *Res Vet Sci*. 2007; 82:22-26.
5. Pechous RD, MCCarthy TR, Zahrt TC. Working toward the future: Insights into *Francisella tularensis* pathogenesis and vaccine

development. *Microbiol Mol Biol Rev*. 2009; 73:684-711.
6. Twenhafel NA, Alves DA, Purcell BK. Pathology of inhalational *Francisella tularensis* spp. tularensis SCHU S4 infection in African green monkeys (*Chlorocebus aethiops*). *Vet Pathol*. 2009; 46:698-706.
7. Valentine BA, DeBey BM, Sonn RJ, Stauffer LR, Pielstick LG. Localized cutaneous infection with *Francisella tularensis* resembling ulcero-glandular tularemia in a cat. *J Vet Diagn Invest*. 2004; 16:83-85.
8. Valli VEO. Hematopoietic system. In: Maxie MG, ed. *Jubb, Kennedy, and Palmer's Pathology of Domestic Animals*. Vol 3. 6th ed. Philadelphia, PA:Elsevier; 2016:184-186.
9. Weinberg AN, Branda JA. Case 31-2010: A 29-year-old woman with fever after a cat bite. *N Engl J Med*. 2010; 363:1560-1568.

CASE IV: TAMU-02 2011 (JPC 4003102).

Signalment: Adult male coyote (*Canis latrans*).

History: This animal was found in a storeroom at a racetrack. Police were called because the animal was acting aggressively. The animal was shot twice with a shotgun, and presented for necropsy of suspected "chupacabra."

Gross Pathology: Over a dozen punctures in the right thoracic wall were associated with five fractured ribs and hemothorax with over seven pleural punctures (euthanasia procedure). An emaciated canid with severe alopecia and thickening of the skin sparing only sparse tan hairs on the dorsal midline and distal extremities was necropsied. Bilaterally, the pinnae had up to 3mm thick tan crusts (hyperkeratosis) with thick, white to tan exudate extending into the ear canals. Milder white to tan flaking and crusts extended along the dorsal midline.

Laboratory results: Rabies negative; Genetic testing: Coyote (*Canis latrans*)

Histopathologic Description: Ear pinna: Diffusely the epidermis has parakeratotic hyperkeratosis and thick serocellular crusting composed of keratin, eosinophilic karyorrhectic debris, erythrocytes, degenerate and nondegenerate neutrophils, large colonies of bacterial cocci and numerous embedded mites and their eggs. Mites have ~200 x 400um, characterized by jointed appendages, 3um chitinous exoskeleton, dorsal spines, striated muscle, intestinal and reproductive structures and a body cavity. Eggs are oval and thin-shelled, measuring ~30-60um. Diffusely, the epidermis is hyperplastic with prominent rete pegs, festooning, spongiosis, and multifocal areas of ulceration. Within the dermis is an inflammatory infiltrate composed of eosinophils, neutrophils, and plasma cells with fewer macrophages and

Presentation, coyote. The presented carcass exhibited severe emaciation and diffuse alopecia, with evidence of a shotgun blast on the right thorax and shoulder. (Photo courtesy of: Dept of Veterinary Pathobiology, College of Veterinary Medicine and Biomedical Sciences, Texas A&M University http://vetmed.tamu.edu/vtpb)

lymphocytes. Multifocally, superficial and deep dermal vessels are congested and there is lymphangiectasia. Follicles are atrophic.

Contributor's Morphologic Diagnosis: Severe, seroexudative, hyperkeratotic, hyperplastic, and eosinophilic dermatitis with mites and bacteria.

Contributor's Comment: A story from the "south of the border down Mexico way." The media and locals really wanted this animal not to be a recognized species (see chupacabra website[1]). However, genetic testing identified it as a "plain, old-fashioned" coyote.

Sarcoptes scabiei has been reported to have occurred in 10 orders, 27 families, and 104 species.[2,8,9] Mites are highly contagious, but varieties may show high host specificity. Gross findings range from mild scaling and alopecia on the limbs and ventrum to near complete alopecia with hyperpigmentation, lichenification and severe crusting. Histologic changes include pronounced hyperkeratosis with extensive serocellular crusting, pronounced acanthosis, hyperplasia of the stratum spinosum, infiltration of neutrophils, lymphocytes, and plasma cells, and varying degrees of superficial dermatitis, vasodilation, and dermal edema.[9] It is surprising how thick macroscopic lesions may be characterized as epidermitis. The inflammatory reaction varies between species and individuals, and in the absence of mite detection, no one change is pathognomonic of sarcoptic mange.

Epizootics of sarcoptic mange caused by

Ear pinna, coyote. The pinna were covered by dense plaque-like hyperkeratotic crusts with white exudate within the ear canal. (Photo courtesy of : Dept of Veterinary Pathobiology, College of Veterinary Medicine and Biomedical Sciences, Texas A&M University http://vetmed.tamu.edu/vtpb)

Sarcoptes scabiei in coyotes have been reported in Montana, Alberta, Wisconsin, Pennsylvania, New York, Kansas, Texas, Louisiana and South Dakota. Reports of mangy coyotes in south Texas go back to the 1920's. Adult males and particularly transient coyotes are significantly more likely to be infected. Severely affected animals have significantly less body fat. Infected individuals may be listless, show less fear of humans and are significantly more likely to seek shelter or food near human settlements. Mortality rates are higher in infected individuals; however, in southern climates, mange has not been shown to directly cause death.[2,8,9]

The myth of "El Chupacabra" appears to have arisen in Puerto Rico in the early 1990's and spread from there to South America, Mexico and the southern United States. Originally described as being ~3 feet tall with dorsal spines, leathery skin, a kangaroo-like posture, fangs and a forked

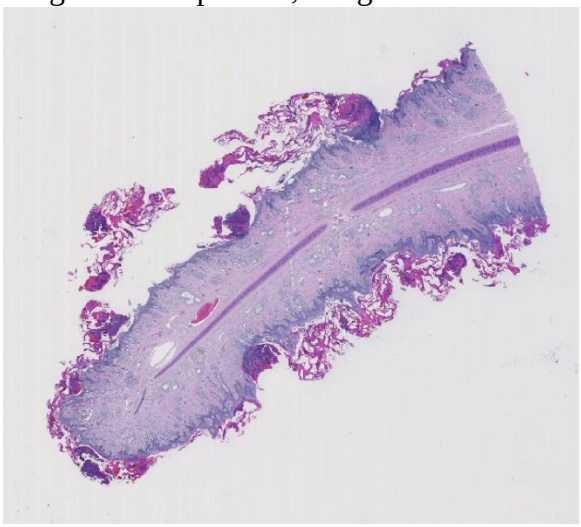

Ear pinna, coyote. The submitted section of ear pinna is covered by a thick hyperkeratotic crust with scattered basophilic pustules (arrows.) (HE, 4X)

tongue, the legend has morphed to include creatures resembling leathery dogs with pronounced spinal ridges and eye sockets. Be it the work of vampires, sadists, Santaría cultists or drug lords, chupacabra has provided a mythical explanation for unusual deaths of animals and humans.

The altered appearance and increased human contact of affected coyotes (the only animals identified as chupacabras and examined thus far in a scientific fashion) with sarcoptic mange provides a diagnosis, albeit banal, for the "chupacabra" phenomenon. Deflating the myth, it is hard to tell your kids that, "a mangy coyote will come after you if you don't do your homework or eat your supper."

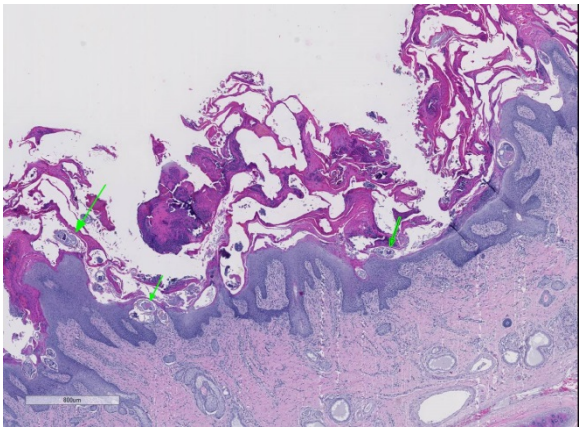

Ear pinna, coyote. Higher magnification of the pinna demonstrating marked epidermal hyperplasia, superficial dermal inflammation, and numerous cross- and tangential sections of adult mites embedded within the hyperkeratotic crust. (HE, 10X)

JPC Diagnosis: 1. Haired skin, pinna: Epidermal hyperplasia and hyperkeratosis, diffuse, severe, with mild eosinophilic dermatitis and numerous intracorneal mites, coyote, *Canis latrans*.
2. Lymph node, paracortex: Plasmacytosis, marked.

Conference Comment: The contributor provides a concise and insightful summary of the epidemiology, gross, and histologic lesions associated with *Sarcoptes scabiei* in a coyote. In this section of pinna, the mites are numerous and have a thin cuticle which is thickened by striated muscular attachments. The most striking and

diagnostic features are the numerous cuticular spines present on the chitinous exoskeleton of the adult female mites in this section. Male mites are approximately two-thirds the size of the females and do not have prominent cuticular spines.[2,4,6] *S. scabiei* mites are relatively host specific and different varieties are morphologically indistinguishable.[2,6] The mite is common in humans, pigs, dogs, and goats and uncommon to rare in cattle, sheep, horses, and cats. It is the most important ecto-parasite in swine causing maculopapular eruptions on the rump, flank, and abdomen of young growing pigs (hypersensitivity form) and thick crusts on the pinnae, head, neck, and legs of older multiparous sows (hyperkeratotic chronic form).[6]

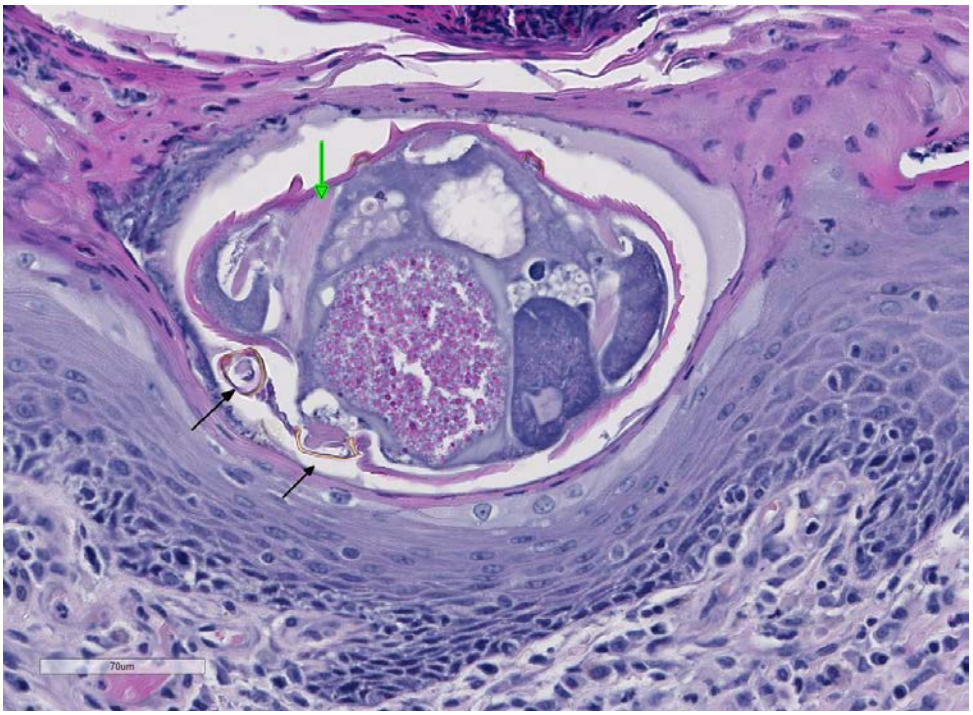

Ear pinna, coyote. Cross section of S. scabiei within the stratum corneum. Diagnostic features include a spiked chitinous exoskeleton, striated muscle (green arrow), and jointed appendages (black arrows). HE, 400X)

Recently, there has been a suspected increase in host range of this ectoparasite with subsequent global diversification.[3,7] As a result, *S. scabiei* has been introduced to novel species, likely due to increased human interaction.[7] Most severely affected are the wild canids such as coyotes, red foxes, and grey wolves in North America; the southern hairy-nosed wombat in Australia; and the chamois, red deer, roe deer, and ibex in Europe. The introduction of this pathogen into new locations and hosts has been shown to produce high morbidity and mortality in these species.[3,6,7]

The pathogenesis involves direct damage due to the burrowing mite, irritation from mite excretions, and hypersensitivity to mite antigens in the cuticle, saliva, and feces. This leads to both an immediate (type I) and delayed (type IV) hypersensitivity reaction causing an intense pruritus and alopecia.[2,4,5,6] Pruritus causes decreased food intake (or ability to catch prey), dehydration, and severe weight loss along with secondary bacterial or fungal dermatitis. Eventually, animals succumb to the emaciation and dehydration if not properly treated. Poorly nourished or immunosuppressed animals develop massive mite burdens known as "Norwegian type scabies."[4,5,6]

Conference participants noted several examples of female mites burrowing into and under the stratum corneum forming "molting pockets" in the skin where the female will mate and lay eggs.[4]

Interestingly, many had difficulty finding eggs within their sections despite the presence of numerous molting pockets. Conference participants also discussed other types of burrowing mites that affect veterinary species such as *Notoedres* sp. and *Knemidocoptes* sp.[6] Additionally, participants noted mild reactive lymphoid hyperplasia with paracortical plasmacytosis in the adjacent lymph node. This reaction is relatively mild and likely related to chronic inflammation.

Contributing Institution:

Dept. of Veterinary Pathobiology
College of Veterinary Medicine and Biomedical Sciences
Texas A&M University
College Station, TX 77843-4467
http://vetmed.tamu.edu/vtpb

References:

1. http://www.monstropedia.org/index.php?title=Chupacabra.
2. Bornstein S, Morner T, Samuel WM. *Sarcoptes scabiei* and sarcoptic mange. In: Samuel WM, Pybus MJ, Kocan AA eds. *Parasitic Disease of Wild Mammals*. 2nd ed, Ames, IA: Iowa State University Press; 2001:107-119.
3. Fraser T, Charleston M, Martin A, et al. The emergence of sarcoptic mange in Australian wildlife: An unresolved debate. *Parasit Vectors*. 2016; 9:316.
4. Gross TL, Ihrke PJ, Walder EJ, Affolter VK. *Skin Diseases of the Dog and Cat Clinical and Histopathologic Diagnosis.* 2nd ed. Ames, IA: Blackwell Publishing Professional; 2005:216-219.
5. Hargis AM, Ginn PE. Integument. In: McGavin MD, ed. *Pathologic Basis of Veterinary Disease*. 5th ed. St. Louis, MO:Elsevier; 2012:1042-1045.
6. Mauldin E, Peters-Kennedy J. Integumentary system. In: Maxie MG, ed. *Jubb, Kennedy, and Palmer's Pathology of Domestic Animals*. Vol 1. 6th ed. Philadelphia, PA:Elsevier; 2016:673-680.
7. Murray M, Edwards M, Abercrombie B, St. Clair C. Poor health is associated with use of anthropogenic resources in an urban carnivore. *Proc Biol Sci*. 2015; 282(1806):20150009.
8. Pence DB, Ueckerman E. Sarcoptic mange in wildlife. *Rev Sci Tech*. 2002; 21:385-398.
9. Pence DB, Windberg LA, Pence BC, Sprowls R. The epizootiology and pathology of sarcoptic mange in coyotes, *Canis latrans*, from South Texas. *J Parasitol*. 1983; 69:1100-15.
10. Pence DB, Windberg LA: Impact of a sarcoptic mange epizootic on a coyote population. *J Wildlife Mgmt*. 1994; 58:624-633.

Self-Assessment - WSC 2016-2017 Conference 6

1. Which of the following is not true about *Riemerella anatipestifer*
    a. The classic lesions are fibrinous pericarditis, perihepatitis, and meningitis.
    b. *R. anatipestifer* is a gram-negative, non-motile rod.
    c. *R. anatipestifer* can infect other species of birds, including poultry.
    d. The disease has a higher mortality in adult ducks than in ducklings.

2. Which of the following is not a virulence factor of *Cryptococcus* sp.?
    a. Polysaccharide capsule
    b. Production of nitric oxide
    c. Secretion of degradative enzymes
    d. Melanin production

3. Which of the following is not true about Cryptococcus infection in cats?
    a. Cryptococcus is the most common systemic mycosis of cats.
    b. Cryptococcus infection in casts has been shown to have relatively less inflammation than infections in dogs..
    c. CNS infections may arise either hematogenously via infected macrophages or via extension across the cribriform plate.
    d. The broad-based budding of Cryptococcus helps to differentiate it from other dimorphic fungi in tissue section.

4. In North America, wild rabbits are the reservoir for which of the following?
    a. Francisella tularensis biovar mediasiatica
    b. Francisella tularensis biovar holoarctica
    c. Francisella tularensis biovar tularensis
    d. Francisella tularensis biovar novicida

5. Which of the following is not a component of the chupacabra of legend?
    a. Leathery skin
    b. Forked tail
    c. Fangs
    d. A kangaroo-like posture

Joint Pathology Center

Veterinary Pathology Services

WEDNESDAY SLIDE CONFERENCE 2016-2017

C o n f e r e n c e 7

19 October 2016

Conference Moderator:
Timothy K Cooper DVM, PhD, DACVP
Associate Professor
Department of Pathology
Penn State College of Medicine
500 University Drive, M.C. H054
Hershey, PA 17033

CASE I: 16-23 (JPC 4084136).

Signalment: Four-month-old, male, X-SCID rat (*Rattus norvegicus*).

History: Rats within this colony were under clinical and pathologic investigation after a positive serology result for *Pneumocystis carinii* during routine quarterly sentinel surveillance. Few rats displayed evidence of mild to moderate respiratory distress and were sacrificed for follow-up *P. carinii* PCR and lung histopathologic evaluation. Lesions in the lungs suggested another viral etiologic agent in addition *to P. carinii*, and a full pathology evaluation was performed on two more rats.

Gross Pathology: Characteristic gross findings expected for the X-SCID strain (1) were present in all rats examined and consisted of severe thymic hypoplasia, unidentifiable lymph nodes, and hypoplastic spleens. All adult rats had mild crusting of the rostral nasal turbinates and multifocal, 1-2 millimeter diameter, white-tan foci on the pleural surface and fewer within the parenchyma on cut section. Few similarly-sized red foci were also present on the pleural surface and throughout the parenchyma.

Laboratory results: Rats within this colony tested positive for *Pneumocystis carinii* via serology and PCR of nasal swabs.

After histopathology was performed, additional PCR tests were submitted for rat cytomegalovirus and mouse adenoviruses 1 & 2. An additional PCR for polyomavirus was performed with primers designed using

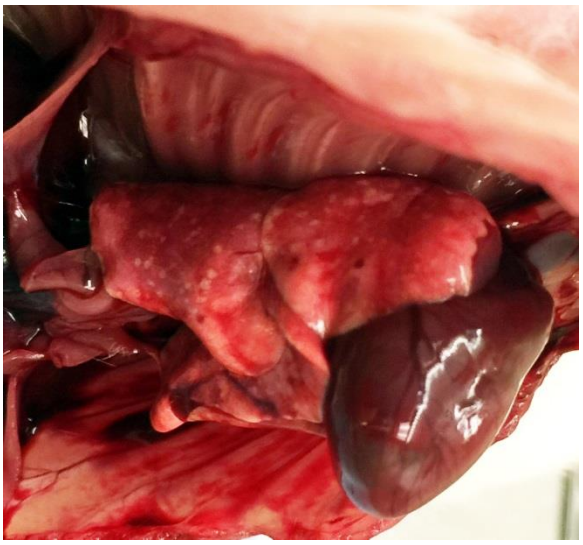

Lung, X-SCID rat. Adult rats in this group had severe thymic hyperplasia, and multifocal 1-2mm white-tan as well as red foci are scattered through the parenchyma. The white-tan foci are consistent with Pneumocystis carinii. (Photo courtesy of: Division of Laboratory Animal Resources, University of Pittsburgh, http://www.dlar.pitt.edu/)

a target a region of the VP1 gene that is partially conserved among polyomaviruses, including those found in mice and hamsters; all follow-up PCR tests were negative.

Histopathologic Description: Harderian gland: There is severe atrophy and loss of the glandular acini with replacement by fibrous connective tissue. The epithelium of remaining glands is often necrotic or attenuated and infiltrated by mixed inflammatory cells composed of lympho-cytes, plasma cells, macrophages, and fewer neutrophils and mast cells. These inflammatory cells are present surrounding glands, ducts, and extend into fibrous connective tissue. There are increased numbers of intralobular and interlobular ducts which are dilated and lined by hyperplastic or attenuated epithelium and multifocally contain sloughed cells and cellular debris. Occasionally, ductal and acinar epithelial cells contain eosinophilic to amphophilic intranuclear inclusion that are up to 35µm in diameter and are sometimes surrounded by a clear halo.

Contributor's Morphologic Diagnosis: Harderian gland: Acinar atrophy, diffuse, severe, with fibrosis, lymphoplasmacytic inflammation, ductal hyperplasia, and epithelial intranuclear inclusion bodies.

Contributor's Comment: Additional histopathologic lesions, including epithelial necrosis, hyperplasia, dysplasia, and intranuclear inclusion bodies, were present in the nasal cavity, lung, salivary gland (parotid and submandibular), prostate gland, and uterus.

Immunohistochemistry of the organs listed above showed strong staining with the pan-polyomavirus marker, PPIT.[6] The virus was

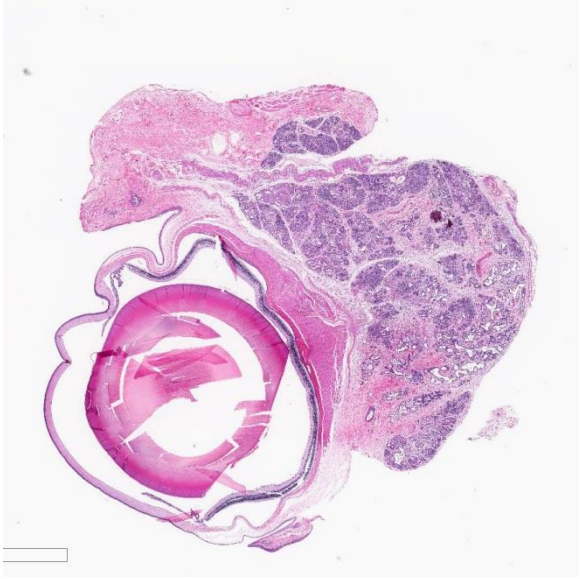

Eye, with Harderian gland, X-SCID rat. At subgross magnification there is marked basophilia of the Harderian gland with dilation of numerous glands and expansion of the interstitial connective tissue. (HE, 4X)

subsequently isolated from the salivary and Harderian glands of rats within this colony and sequenced. This is a novel polyomavirus phylogenetically distinct from the rat polyomavirus isolated and sequenced from feral Norway rats in 2015.[2]

Polyomaviruses (PyVs) are a family of DNA tumor viruses that are known to infect a variety of mammals, birds, and fish.[1] Most mammalian polyomaviruses cause subclinical infections with life-long persistence in their natural immune competent hosts. However, when the host immunity is compromised, the virus can reactivate and cause disease.[5] Until this discovery, five distinct PyVs have been identified in rodent hosts: murine PyV, mouse pneumotropic virus, hamster PyV, Mastomys PyV, and Rat PyV, whose full genomes are available in the GenBank database.[2]

The first polyomavirus in rats was described as a wasting disease in athymic nude rats by Ward, et al, in 1984.[7] Inclusion bodies were described in the salivary glands, Harderian glands, lungs, and nasal glands, similar to those present in this colony.[7] Also, similar to the previously described report is the fact that X-SCID rats are severely immune suppressed.[3] This strain has severely hypo-plastic lymphoid organs and markedly decreased T cells, B cells, and NK cells, making them an excellent model for xenotransplantation studies.[3] This severe immune suppression makes them particularly susceptible to viral infections like PyV. It is not yet clear where these rats were infected with the virus or whether immune competent rats can be infected, show clinical symptoms, or have histologic

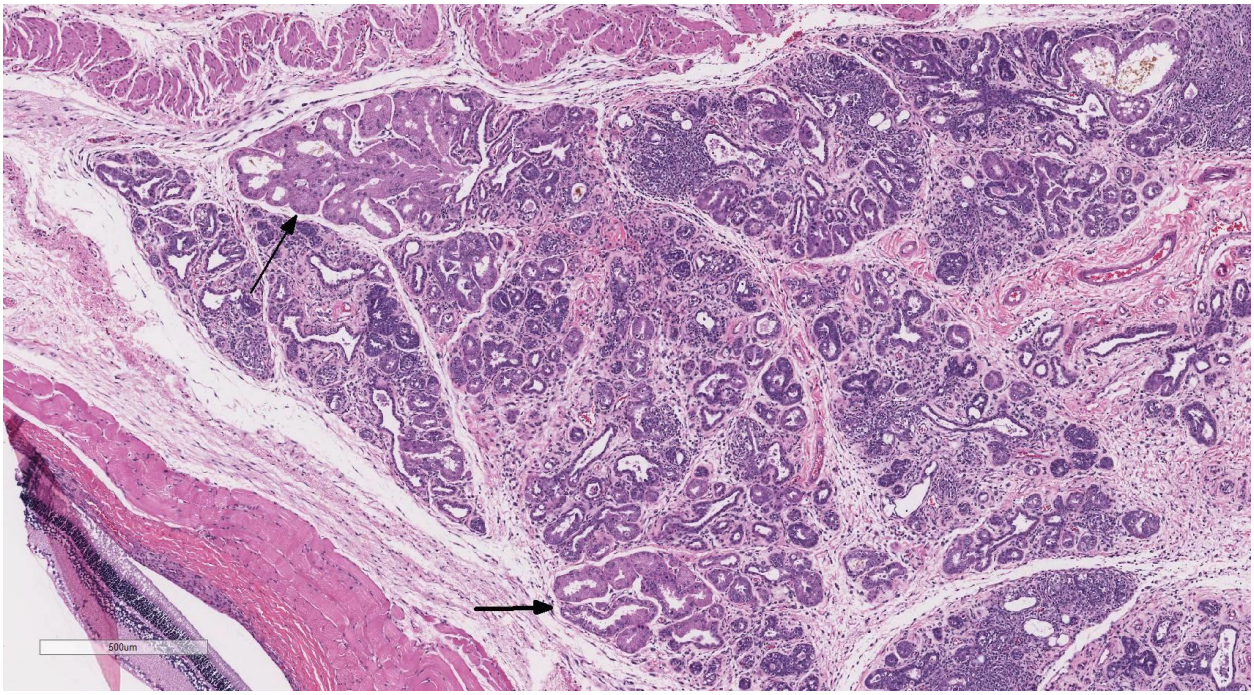

Harderian gland, X-SCID rat. There are diffuse changes within the Harderian gland. Few normal acini remain (black arrows). Other acini exhibit necrosis, atrophy, and regeneration, as well as moderate lymphocytic inflammation. (HE, 46X)

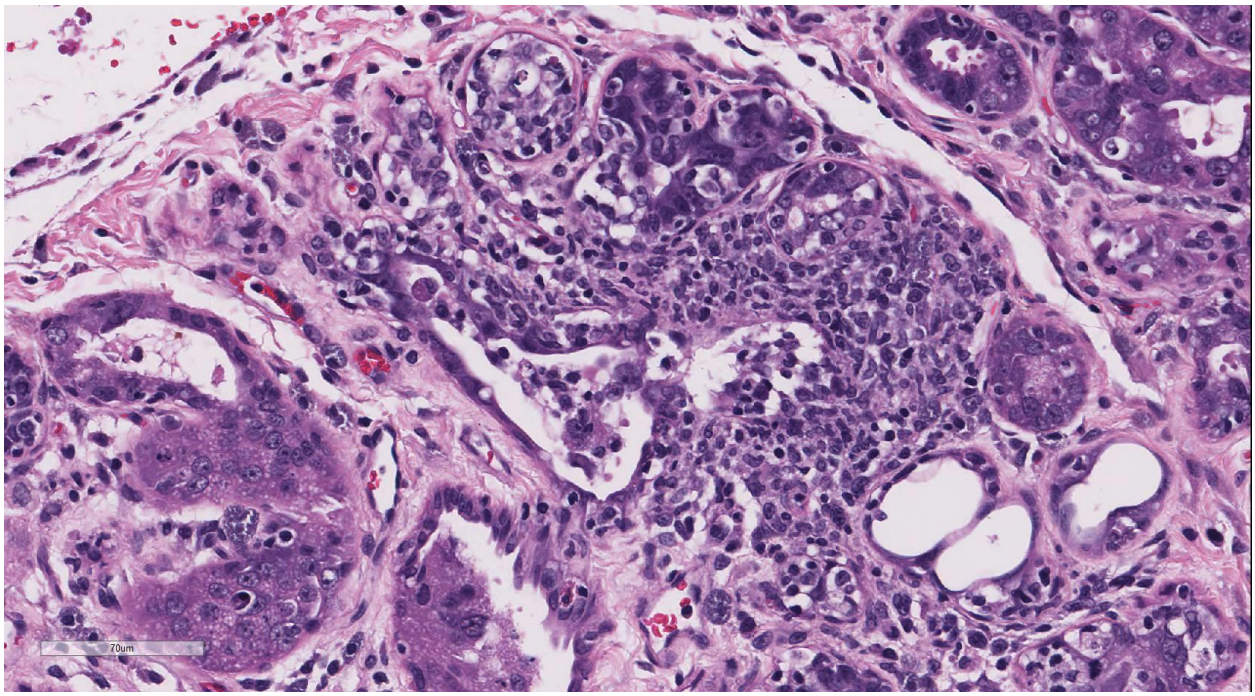

Harderian gland, X-SCID rat. Affected glands display a range of features including necrosis, attenuation of lining epithelium, and regenerative changes including piling up and mild dysplasia. Affected acini are surrounded and infiltrated by moderate numbers of lymphocytes, macrophages, and fewer neutrophils. (HE, 400X)

lesions when infected with this novel Rat PyV. A full description of pathology findings and genomic sequencing information for this novel virus is pending publication (Rigatti and Toptan, et al).

JPC Diagnosis: Harderian gland: Dacryoadenitis, necrotizing and histiocytic, chronic, diffuse, moderate to severe, with edema and occasional epithelial intranuclear inclusion bodies, X-SCID rat, *Rattus norvegicus*.

Conference Comment: The contributor provides an outstanding description and synopsis of the lesions of a novel polyomavirus (PyV) infection in an X-SCID rat. Particularly striking are the characteristic large, prominent epithelial intranuclear viral inclusions that marginate the chromatin and often enlarge the nucleus; there is variation among the slides in the number of intranuclear inclusions present.

As mentioned by the contributor, the majority of mammalian PyVs cause subclinical infections with life-long persistence in immune competent natural hosts, much like herpesviruses.[4] However, when the host immunity is compromised, such as in this particular strain of rat, the virus can cause disease. Polyomaviruses are of particular research interest, and murine PyVs are used as models of persistent virus infection in human disease.[1,2,3,6] The most well-known human PyVs, BK virus and JC virus, are associated with severe disease in immunosuppressed human patients; and Merkel cell PyV is associated with Merkel cell carcinoma, a rare and highly aggressive neoplasm of neuroendocrine cells of the skin.[2] The virus has long been established as potentially carcinogenic, causing many different types of tumors in experimental systems, hence the name poly(many)-oma(tumor)-virus.

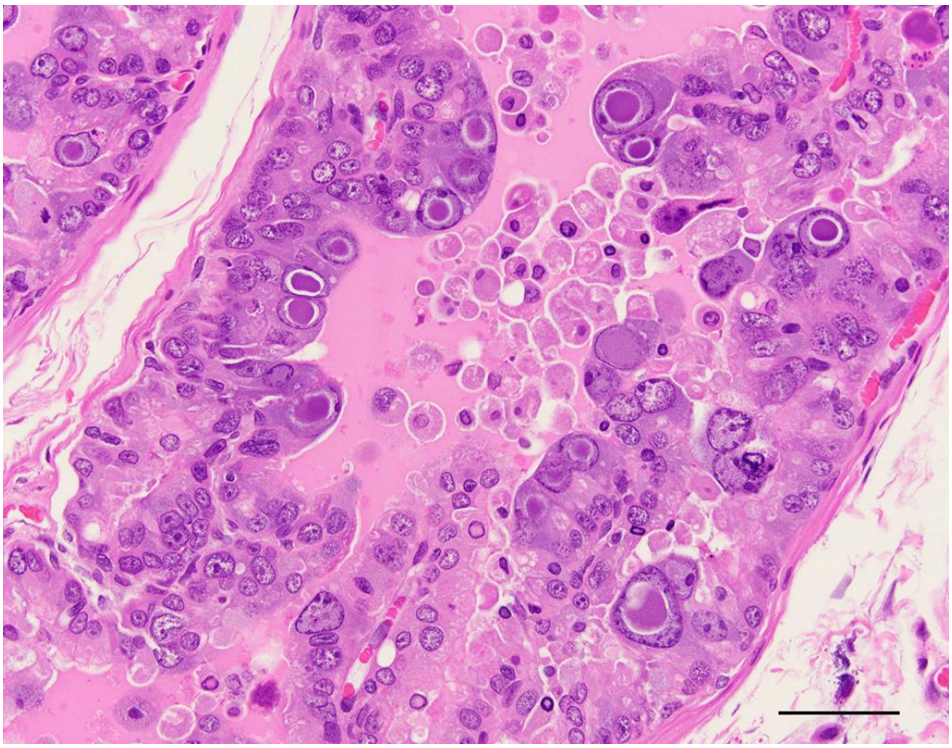

Harderian gland, X-SCID rat. Occasionally, ductal and acinar epithelial cells are karyomegalic and contain eosinophilic to amphophilic intranuclear inclusions that are up to 35µm in diameter and are sometimes surrounded by a clear halo (HE, 400X) (Photo courtesy of: Division of Laboratory Animal Resources, University of Pittsburgh, http://www.dlar.pitt.edu/)

Conference participants noted that this case nicely demonstrates cytomegaly, karyomegaly, and glassy intranuclear inclusions characteristic of PyV infection in the Harderian gland. Many participants noted that rat cytomegalovirus infection can cause similar inclusions in the Harderian gland of rats, with large eosinophilic "owl-eye" inclusions that marginate the chromatin.[4] However, PyV inclusions in tissue have a homogenous basophilic or amphophilic appearance, which is distinct from cytomegalovirus and adenoviral inclusions.[4] Participants also discussed that sialodacryoadenitis virus, a highly contagious betacoronavirus, which can cause similar lesions in the Harderian gland of rats; however, that virus does not result in the formation of intranuclear inclusions.[4]

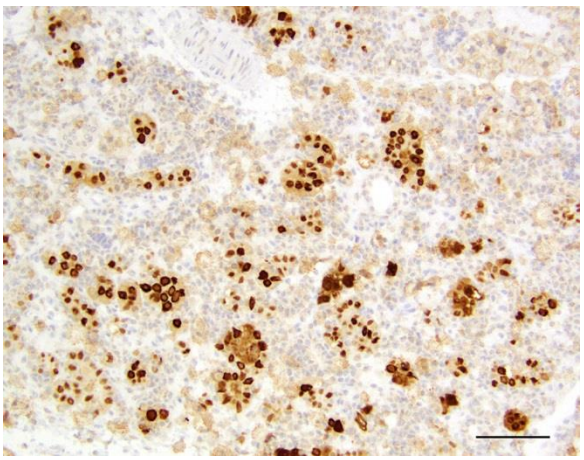

Harderian gland, X-SCID rat . **Acinar epithelial cells exhibit strong intracytoplasmic positivity for pan-polyomavirus marker(anti-PPIT(2), 100X)** ***(Photo courtesy of: Division of Laboratory Animal Resources, University of Pittsburgh, http://www.dlar.pitt.edu/)***

Attendees discussed some other significant PyVs of veterinary importance, including simian virus 40 (SV40) which caused progressive multifocal leukoencephalopathy in immunosuppressed rhesus macaques; the *Mesocricetus auratus* PyV1 which induces trichoepithelioma and lymphoma in hamsters; the K virus and murine pneumotropic virus in mice; *Procyon lotor* PyV1 which causes high-grade neuroglial olfactory tumors in raccoons; Aves PyV1 that results in budgerigar fledgling disease in psittacine birds; and goose hemorrhagic PyV1, the cause of hemorrhagic nephritis and enteritis in anseriform birds.[1-7]

The conference moderator cautioned participants that, while inclusions present in the intra-orbital Harderian gland are due to viral infection, pseudoinclusions and syncytial cells in the exorbital lacrimal gland are part of its normal anatomy and should not be confused for viral cytopathic effect. In addition, participants noted numerous mast cells within the interlobular connective tissue, which is also a normal finding in rats. The moderator further observed that within the adjacent eye the retinal epithelium lacks pigment, indicating that this rat is an albino. As a result of the lack of pigmentation, albino rats are much more susceptible to retinal degeneration and cataract formation induced by ultraviolet light as compared to normally pigmented animals. Degenerative changes may also occur in the Harderian glands of rats exposed to high-intensity lights.[4]

Contributing Institution:

Division of Laboratory Animal Resources
University of Pittsburgh
S1040 Thomas E. Starzl Biomedical Science Tower
200 Lothrop Street
Pittsburgh, PA 15261
http://www.dlar.pitt.edu/
http://pitt.edu/

References:

1. Buck CB, Van Doorslaer K, Peretti A, Geoghegan EM, Tisza MJ, An P, Katz JP, Pipas JM, McBride AA, Camus AC, McDermott AJ, Dill JA, Delwart E, Ng TF, Farkas K, Austin C, Kraberger S, Davison W, Pastrana DV, Varsani A. The ancient evolutionary history of polyomaviruses. *PLos pathogens*. 2016; 19:12(4):e1005574.

2. Ehlers B, Richter D, Matuschka FR, Ulrichd RG. Genome sequences of a rat polyomavirus related to murine polyomavirus, *rattus norvegicus* polyomavirus 1. *Genome Announc*. 2015; 3(5):e00997-15.
3. Mashimo T, Takizawa A, Voigt B, Yoshimi K, Hiai H, Kuramoto T, Serikawa T. Generation of knockout rats with x-linked severe combined immunodeficiency (X-SCID) using zinc-finger nucleases. *PLoS one*. 2010; 5(1):8870.
4. Percy DH, Barthold SW. Rabbit. In: *Pathology of Laboratory Rodents and Rabbits*, 4th ed., Ames, IA: Blackwell Publishing; 2016:122,161.
5. Stevens H, Bertelsen MF, Sijmons S, Van Ranst M, MaesP. Characterization of a Novel Polyomavirus Isolated from a Fibroma on the Trunk of an African Elephant (*Loxodonta africana*). *PLoS one*. 2013; 8(10):1-9.
6. Toptan T, Yousem SA, Ho J, Matsushima Y, Stabile LP, Fernández-Figueras MT, Bhargava R, Ryo A, Moore PS, Chang Y. Survey for human polyomaviruses in cancer. *JCI Insight*. 2016; 1(2):85562.
7. Ward JM, Lock A, Collins Jr MJ, Gonda MA, Reynolds CW. Papovaviral sialoadenitis in athymic nude rats. *Lab Animals*. 1984; 18:84-89.

CASE II: 13A815 (JPC 4066315).

Signalment: 20-year-old female Indian rhesus macaque (*Macaca mulatta*).

History: This animal had 2 months of lethargy, large clitoris, pain/discomfort vaginal bleeding. The body weight lost 3 kg in 2 months. A large firm mass was palpable in the lower abdomen, mainly on left side. The mass was round, measuring 7 x7 cm. Ultrasound revealed large mass with multiple round cavities inside. The animal developed a moderate regenerative anemia. Although extensive care and treatment were given, euthanasia was elected due to the grave prognosis.

Gross Pathology: Presented was a thin, dehydrated aging animal. A large, firm mass was palpated at the lower abdomen. The subcutaneous tissue over the abdominal mass was dark-red and edematous. Extending from the uterus to the abdominal wall and incorporating with ovaries, ovary ducts, and serosa of the colon was a 15 -20 cm in diameter, dark-red cystic masses, which contained a large amount of dark-red fluid on the cut section. Multifocal variable-sized, dark-red cystic masses are also noted on the diaphragm, liver, and mesentery. The central tendon of the diaphragm was fragile and easily pierced by force. Other findings included severe thymic atrophy and mild, bilateral hydronephrosis.

Laboratory results: N/A

Histopathologic Description: Expanding and disrupting the diaphragm are multiple, unencapsulated masses composed of variable tortuous endometrial glands surrounded by abundant, densely cellular endometrial stroma. The endometrial glands are generally lined by simple columnar, ciliated epithelial cells. Some parts of glands are lined by flattened to pseudostratified cells. Occasionally the epithelial cells form islands or papillary projections in the lumen. The epithelial cells have indistinct cell borders, a moderate amount of eosinophilic cytoplasm, and prominent basilar nuclei. Nuclei are round to oval with finely stippled

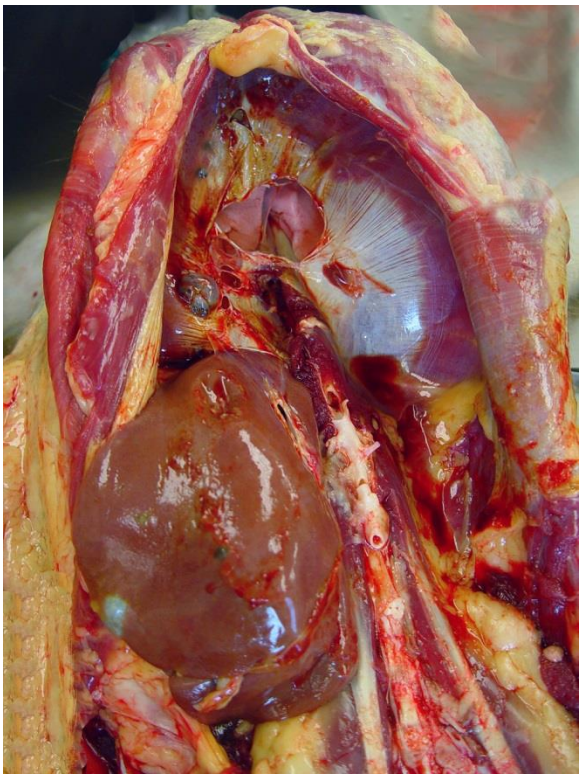

Diaphragm, rhesus macaque. Multifocal variably-sized, dark-red cystic masses are present on the diaphragm, liver and mesentery. A large defect is present in the tendinous portion of the diaphragm caused by digital pressure. (Photo courtesy of: Division of Comparative Pathology, Tulane National Primate Research Center, 18703 Three Rivers Rd., Covington, LA 70433. http://tulane.edu/tnprc/)

chromatin and 1-2 prominent nucleoli. There are large amounts of amorphous, eosinophilic material and admixed with numerous erythrocytes. The endometrial stroma is composed of spindle cells with indistinct cell borders, scant eosinophilic, fibrillar cytoplasm and an oval to elongate nucleus with finely stippled chromatin. The mitotic figures are 1-2/HPF in both glandular epithelium and stroma. Diffusely the serosa is markedly expanded by reactive fibroblasts, edema, hemorrhage, and many lymphocytes, plasma cells, and macrophages. Some macrophages contain abundant cytoplasmic brown pigment (hemosiderosis). Multifocally the muscle adjacent to the masses showed variable degeneration and necrosis.

Contributor's Morphologic Diagnosis: Diaphragm, Endometriosis.

Contributor's Comment: Endometriosis usually occurs in the pelvis and the most commonly involved organs are ovaries, uterosacral and broad ligaments, and parietal pelvic peritoneum. Diaphragmatic endometriosis is rare, often asymptomatic, and always associated with severe pelvic involvement.[4,7] Ectopic endometriosis has also been reported in umbilicus, skin, vagina, vulva, cervix, inguinal canal, upper abdominal peritoneum, liver, spleen, gastrointestinal tract, urinary system, breasts, pleural cavity, brain, eye, lymph nodes, lung and pericardium in human.[4] Pleural and lung endometriosis have been reported in an aged rhesus macaque1 and sooty mangabey (2009 conference 19, case 01), respectively.

Diaphragmatic endometriosis, like in this case, can involve entire thickness of the muscle. It is common to extend into pleural space in human, but not presented in this

Diaphragm, rhesus macaque. The diaphragm is expanded by several cellular masses which contain cystic, blood-filled centers. (HE, 5X).

case.[4] The pathogenesis of endometriosis has been well discussed in the previous conferences (2011 conference 11, case 01 and 2009 conference 19, case 01). The primary theory of Sampson's three-fold transplantation likely applies to this case. The retrograde "regurgitation" of endometrial cells passes through the oviducts into the peritoneal cavity and proliferates in ectopic sites.[8]

JPC Diagnosis: Diaphragm: Endometriosis, rhesus macaque, *Macaca mulatta*.

Conference Comment: Endometriosis is characterized by the presence of well-differentiated, viable, and hormone responsive endometrial glands and stroma outside the uterus.[1,4,5,7] This is one of the most common gynecologic diseases encountered in female humans as well as Old World primates.[1] There have been rare reports of endometriosis in the elephant shrew, long-tongued bat, and one case report of an endometrioma in a dog.[3,7] The most widely studied animal model for endometriosis in humans is the baboon. The prevalence of endometriosis in captive female baboons is as high as 20%. It is thought that baboons in captivity develop endometriosis at a higher rate than wild baboons because of regular menstrual cycles without intervening pregnancy in this population of animals.[7] The vast majority of endometriosis cases in Old World primates occurs within the abdominal cavity and is grossly identifiable as blood-filled "chocolate" cysts which can progress to fibrotic scars in chronic cases. Typically, endometriosis demonstrates positive immunoreactivity for pancytokeratin, vimentin, estrogen receptor, and progesterone receptor.[1]

In this case, several conference participants noted that the endometrial glands are filled with abundant hemorrhage, consistent with active menses in this animal. The endometrial tissue in endometriosis is responsive to cycling estrogen and progesterone, and therefore will undergo cycles of proliferation and degradation in response to the normal menstrual cycle.[1,7,8] Hemorrhage associated with endometriosis can be severe enough to cause anemia and can rarely rupture causing hemorrhagic

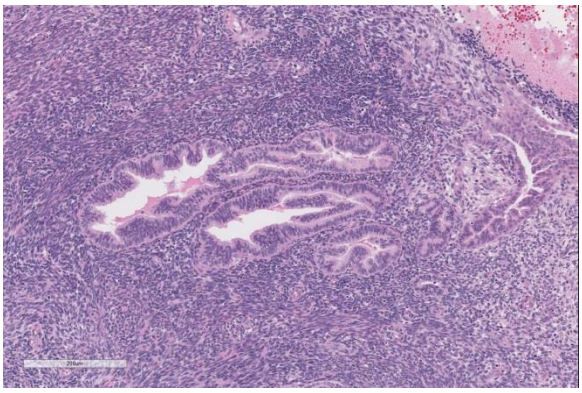

Diaphragm, rhesus macaque. The masses are composed of well-differentiated endometrial glands surrounded by dense interlacing bands of endometrial stroma. (HE, 320X)

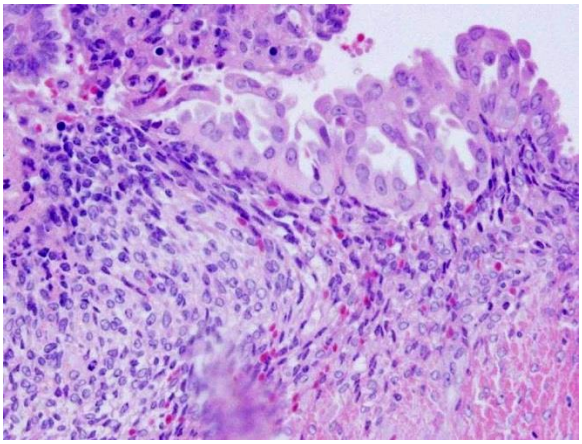

Diaphragm, rhesus macaque. There is multifocal epithelial plaque formation and decidualization of underlying stroma (Arias-Stella reaction)(Photo courtesy of: Dr. Tim Cooper)(HE, 400X).

ascites.[1,2,7,8] Conference participants discussed various risk factors for the development of endometriosis in non-human primates. These include chronic uninterrupted estrus cycles throughout life, resulting in increased endometrial turnover compared to multiparous primates. Females older than ten years with an affected first-degree relative are also predisposed. Non-laparoscopic abdominal surgical procedures, including hysterectomy and cesarean section, are also implicated, in addition to estradiol implants.[1,5] The moderator also discussed that aged non-human primates are much more likely to develop endometriosis compared to older women due to lack of menopause in these species.[5] Unfortunately, the reproductive history of this animal was not provided.

The conference moderator also discussed the importance of distinguishing well-differentiated endometrial tissue in endometriosis from endometrioid carcinoma. In endometrioid carcinoma, glands will be irregular with little to no intervening stroma and demonstrate significant nuclear atypia. Endometrioid carcinoma has been rarely reported to develop from endometriosis.[1,4] In addition, multifocally within this section there are large areas where the endometrial epithelial cell nuclei are rounded and vesicular with abundant pale vacuolated cytoplasm, consistent with stromal decidualization and epithelial plaque reaction. Decidualization of the endometrial glands occurs under the influence of progesterone and is a response to blastocyst implantation or other trauma to the endometrial stroma. This is required for maintenance of normal pregnancy in humans and non-human primates.[2] In endometriosis, it is thought that this reaction develops secondary to elevated progesterone. Endometrial decidualization is non-neoplastic, but grossly and histologically mimics malignant neoplastic lesions such as mesothelioma and carcinomatosis. In a recent article in *Veterinary Pathology*, Atkins et al. demonstrates that the decidualized stroma stained positive for vimentin, CD10, progesterone, and estrogen consistent with reported deciduosis in humans.[2]

Contributing Institution:

Tulane National Primate Research Center
18703 Three Rivers RD.
Covington, LA 70433
http://tulane.edu/tnprc/

References:

1. Assaf BT, Miller AD. Pleural endometriosis in an aged rhesus macaque (*Macaca mulatta*): A histopathologic and immunohistochemical study. *Vet Pathol*. 2012; 49(4):636-641.
2. Atkins HM, Lombardini ED, Caudell DL, et al. Decidualization of endometriosis in macaques. *Vet Pathol*. 2016; 53:1252-1258.
3. Paiva BH, Silva JF, Ocarino NM, et al. A rare case of endometrioma in a bitch. *Acta Vet Scand*. 2015; 57:31.

4. Ceccaroni M, Roviglione G, Rosenberg P, Pesci A, Clarizia R, Bruni F, et al. Pericardial, pleural and diaphragmatic endometriosis in association with pelvic peritoneal and bowel endometriosis: A case report and review of the literature. *Wideochir Inne Tech Maloinwazyjne*. 2012; 7(2):122-131.
5. Fazleabas AT, Brudney A, Gurates B, Chai D, Bulun S. A modified baboon model for endometriosis. *Ann N Y Acad Sci*. 2002; 955:308-17.
6. Hastings JM, Fazleabas AT. A baboon model for endometriosis: Implications for fertility. *Reprod Biol Endocrinol*. 2006; 4:1-7.
7. Nezhat C, King LP, Paka C, Odegaard J, Beygui R. Bilateral thoracic endometriosis affecting the lung and diaphragm. *JSLS*. 2012; 16(1):140-142.
8. Van der Linden PJ. Theories on the pathogenesis of endometriosis. *Hum Reprod*. 1996; 11(3):53-65.

CASE III: 16-3320D (JPC 4083858).

Signalment: Age unspecified female Columbia X Rambouillet ewe (*Ovis aries*).

History: A flock of 7500 ewes were

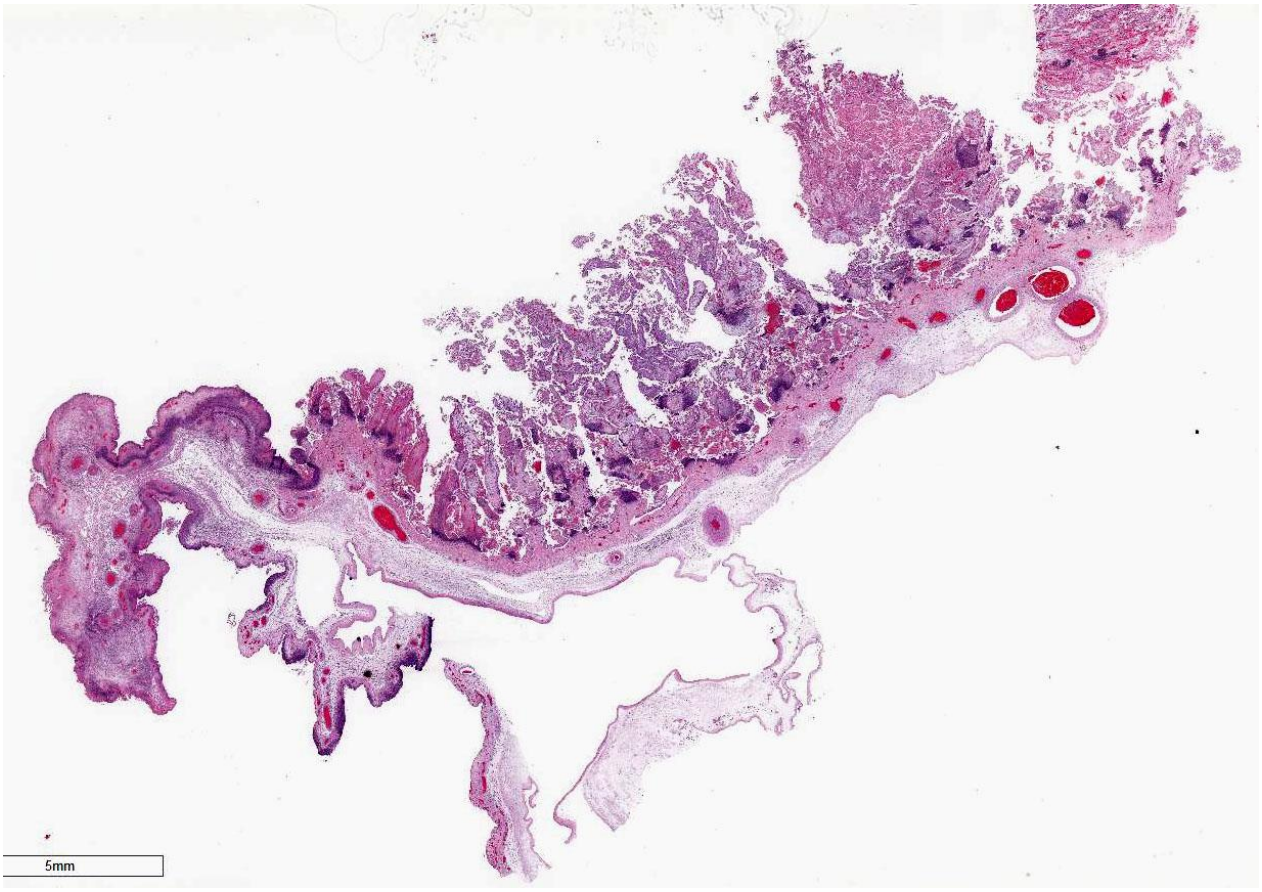

Placenta, sheep. There is multifocal to coalescing necrosis of cotyledonary, intercotyledonary, and allantoic epithelium, often outlined by a dense band of cellular infiltrate. (HE, 4X)

grouped in mobs of 1500. Over the course of the 2016 lambing season, 1200 ewes, ranging in age from 2 – 8 years aborted. Abortions continued even after feeding tetracycline pellets. At the end of the lambing season, older aborted ewes were culled and younger recovered ewes were mixed with ewe lambs as a vaccination strategy.

Gross Pathology: Three fetuses and placentas were markedly autolyzed and had no significant gross lesions. A fourth placenta was in good to fair post-mortem condition. That placenta had inter-cotyledonary edema and multifocal tan-grey discoloration of cotyledons.

Laboratory results: Numerous *Campylobacter jejuni* were isolated from one of four placentas. Other tests performed with negative results included FA for *Leptospira interogans*, ELISA for *Chlamydophila* sp. and PCR for pestivirus. Selenium level in one of three livers was marginal. Immunohistochemistry for *Coxiella burnetii* on fixed placenta was negative.

In two previous submissions from the same farm, *C. jejuni* was isolated from fetal tissue pools, stomach contents or placentas from four additional aborted fetuses.

Histopathologic Description: Both cotyledonary and intercotyledonary areas were characterized by necrosis of tropho-blastic and intercoteledonary epithelium,

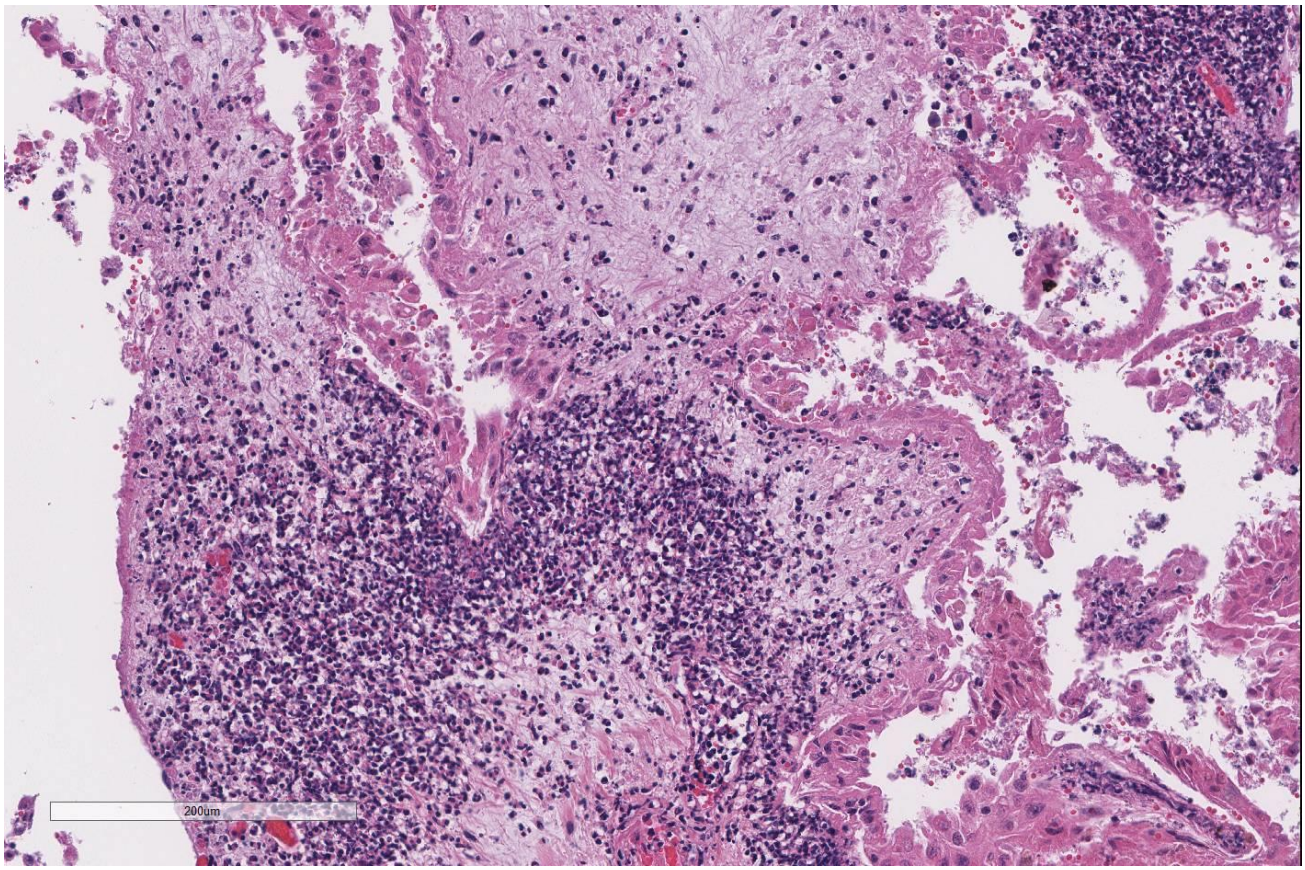

Placenta, sheep. Necrotic cotyledonary vill exhibit diffuse loss of cytoplasmic staining; a dense band of degenerate neutrophils is present the necrotic villus. (HE, 4X)

with hypereosinophilic shrunken cytoplasm and karyorrhectic or karyolytic nuclei. Foci of necrosis were expanded by necrotic cellular debris and large numbers of degenerate neutrophils within the immediate underlying chorioallantoic connective tissue. Several areas of necrosis are associated with many clustered bacilli. Adjacent trophoblasts often contain small intracytoplasmic bacilli. Rare trophoblasts contain, intracytoplasmic, 2 µm diameter, basophilic material. Scattered throughout the chorioallantois, many blood vessels are surrounded by neutrophils and a few vessels are partially occluded by large aggregates of fibrin and neutrophils. Rare small vessels are lined by necrotic endothelial cells with separation of the wall by neutrophils and fibrin (fibrinoid necrosis). Diffusely the chorioallantoic connective tissue is expanded by edema and all vessels are markedly congested.

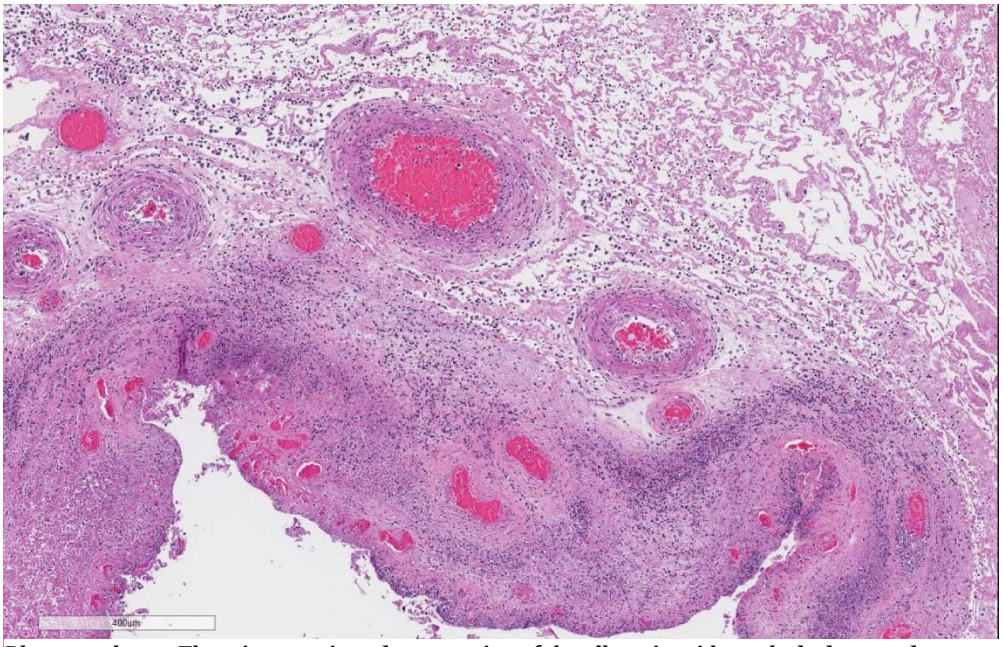

Placenta, sheep. There is necrosis and suppuration of the allantois, with marked edema and moderate necrotizing arteritis of the allantochorion. (HE, 100X)

Similar lesions were seen in placentas from the other fetuses submitted. No significant lesions were identified in any of the fetal tissues.

Contributor's Morphologic Diagnosis: Placentitis, necrosuppurative, cotyledonary and intercotyledonary, diffuse, severe, with necrotizing vasculitis and bacteria.

Contributor's Comment: *Campylobacter jejuni* is one of three species in the genus causing reproductive and enteric disease in a variety of animal species and in humans.[8] *C. fetus subsp. venerealis* primarily causes infertility and abortion in cattle, whereas *C. fetus subsp fetus* and *C. jejuni* are important causes of abortion in small ruminants and occasionally cattle. *C. jejuni* is an important cause of food-borne illness in people and has become an increasingly important cause of late term abortions in small ruminants.[4] Abortions have also been documented in humans and in dogs.[6] In sheep, infection by either *C. fetus f*etus or *C. jejuni* causes late term abortion, still birth or weak lambs. Transmission is by the oral route. Placentas are not retained and often have gross lesions of intercoteledonary edema and cotyledonary necrosis. Aborted fetuses may have characteristic gross lesions of necrotizing hepatitis and histologic lesions of suppurative bronchopneumonia (neither present in this case). Occasionally ewes become ill and die due to endometritis.[8]

Campylobacter is reportedly the most common cause of abortion in sheep and *C. jejuni* is now the most common species to cause abortion in sheep flocks.[4] Recently, a single clone of *C. jejuni* (SA) has been shown experimentally to cause abortion in sheep[9] and it is genetically similar to clones causing gastroenteritis in people.[5] In addition, most isolates of *C. jejuni* from sheep abortions in the United State (including the one in this case) are highly resistant to tetra-cyclines, the only approved drug for treating infection in sheep.[4] In contrast, isolates from the United Kingdom are susceptible to tetracyclines[9], suggesting common treatment of sheep abortions with teracyclines in this country may have led to the emergence of the resistant clone. Drug resistance and links to human enteric disease indicate that owners, veterinarians, and laboratory personnel should be cautioned about zoonotic potential when handling suspect fetal tissues.

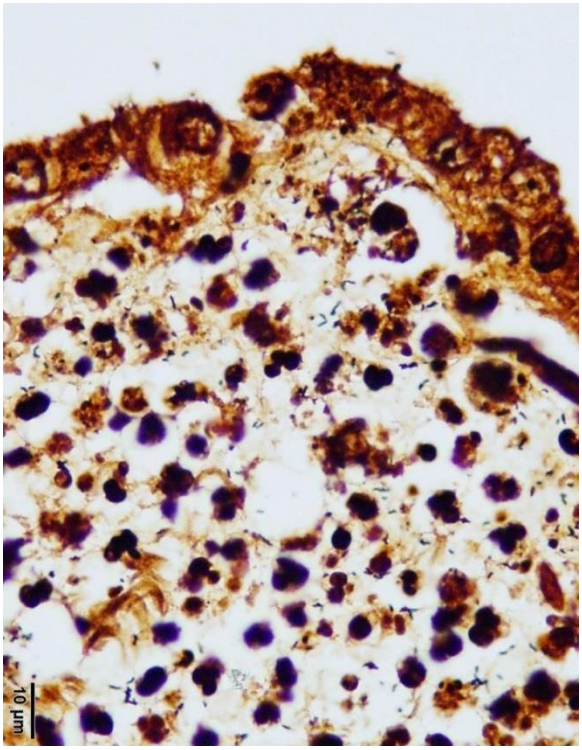

Placenta, sheep. Villar stroma contains numerous short often branching bacilli consistent with Campylobacter. (Warthin Starry 4.0, 400X). (Photo courtesy of: Dr. Tim Cooper).

Other important differential diagnoses for placentitis in sheep and goats include *Brucella ovis*, *Brucella mellitensis*, *Toxoplasma gondii*, *Chlamydophila abortus* and *Coxiella burnetii*.[8] The most common manifestation of ovine brucellosis in the US is epididymitis in rams; abortion with placentitis is less common. *Toxoplasma gondii* should have characteristic gross and histologic lesions, with the presence of organisms within the placental lesions, but can also be ruled out by PCR. The three main differentials, in this case, are *C. jejuni*, *C. abortus* and *C. burnetii* due to the presence of intracellular bacteria on H&E. The bacteria were not positive with the Gimenez stain, making diagnosis of the two latter organisms less likely. *C. abortus* was eliminated by Ag ELISA on the placenta and *C. burnetii* by immunohistochemistry. Because of the high likelihood of encountering zoonotic agents associated with small ruminant abortions, examination of all sheep and goat abortuses, especially if accompanied by fetal membranes, should be performed in a biosafety cabinet.

JPC Diagnosis: Placenta, cotyledonary and intercodyledonary: Placentitis, necrosuppurative, diffuse, severe with necrotizing vasculitis.

Conference Comment: The contributor provides a concise summary of abortion in small ruminants caused by a *Campylobacter* spp as well as other important differential diagnoses for abortion in these animals. Despite some minor slide variability, conference participants unanimously noted the outstanding preservation and high quality of the section of placenta in this case.

Prior to discussing the case, the conference moderator spent some time reviewing placentation in ruminants. The different components of the placenta were discussed and participants identified individual layers and their orientation within the tissue section. All ruminants have cotyledonary villous epitheliochorial nondeciduate placentation. The placenta is comprised of the maternal endometrium and the fetus derived fused chorioallantoic membranes (CAM). Because ruminant placentas are nondeciduate, the maternal endometrium and fetal CAM are in contact but they do not fuse. In addition, in cotyledonary placentation, there are multiple areas where the CAM villi insert into pockets or crypts in the area of the endometrium known as the placentome, which is a combination of the fetal cotyledon and maternal caruncle. Specific to small ruminants, the caruncles have lost their epithelium, leaving five tissue layers which separate maternal and fetal blood: endothelium, connective tissue, epithelium of the CAM, and endothelium and connective tissue of the endometrium.[1]

Conference participants noted that, in this case, there are multifocal brown globular pigment present in the maternal side of the placenta in the subchorial area where hematoma and hemophagocytosis are often most prominent and a normal finding. Additionally, thrombosis within the chorionic plate, present in some slides in this case, is also a normal finding in the post-partum placenta. However, if there is similar brown staining material on the CAM, it could be indicative of meconium deposition, which is a result of pre-parturient fetal stress. Meconium staining was not seen by conference participants in this case.

Transmission of *Campylobacter* spp. often occurs via fecal-oral route most commonly through contamination of water supplies.[8] The organism is a common commensal bacterium in the intestinal tract of cattle, sheep, and swine as well as dogs, cats, and rodents. When taken in orally in susceptible animals, there is a transient bacteremia. The bacteria are then localized to the gut and bile. In pregnant ewes, the bacteria localize to the uterus via the Surface (S)-layer protein, which is thought to allow the bacteria to colonize and translocate from the uterus to the placenta and subsequent abortion in about 25% of cases.[8]

Characteristic findings of campylo-bacteriosis are edematous intercotyledonary areas and friable yellow cotyledons with necrotizing and suppurative placentitis and vasculitis most severe in chorionic villi. There will often be large dense Gram-negative bacterial emboli within chorionic capillaries, although that was not a prominent feature in this case.[8] However, numerous *Campylobacter* spiral organisms are present throughout the tissue and easily visualized on the Warthin-Starry silver stain. Many conference participants noted intra-cellular bacilli within trophoblasts on the H&E. In the fetus, there will typically be yellow hepatic foci with targetoid depressed red centers (necrotizing hepatitis) and fibrinous peritonitis.[8]

Contributing Institution:

Department of Veterinary Microbiology and Pathology
College of Veterinary Medicine
Washington State University
Pullman, WA
http://vmp.vetmed.wsu.edu/about-vmp

References:

1. Bacha WJ, Bacha LM. *Color Atlas of Veterinary Histology*. 3rd ed. Baltimore, MD: Lippincott Williams & Wilkins; 2012:243-260.
2. Headstrom OR, Sonn RJ, Lassen ED, et al. Pathology of *Campylobacter*

jejuni abortion is sheep. *Vet Pathol*. 1987; 24:419-426.
3. Hazlett MJ, McDowall R, DeLay J, et al. A prospective study of sheep and goat abortion using real-time polymerase chain reaction and cut point estimation shows *Coxiella burnetii* and *Chlamydophila abortus* infection concurrently with other major pathogens. *J Vet Diagn Invest.* 2013; 25(3):359-368.
4. Sahin O, Plummer PJ, Jordan DM, et al. Emergence of a tetracycline-resistant *Campylobacter jejuni* clone associated with outbreaks of ovine abortion in the United States. *J Clin Micro*. 2008; 46:1663-1671.
5. Sahin O, Fitzgerald F, Stroika S, et al. Molecular evidence for zoonotic transmission of an emergent, highly pathogenic *Campylobacter jejuni* clone in the United States. *J Clin Micro*. 2012; 50:680-687.
6. Sahin O, Burrough ER, Pavlovic N, et al. *Campylobacter jejuni* as a cause of canine abortions in the United States. *J Vet Diag Invest*. 2014; 26:699-704.
7. Sanad YM, Jung K, Kashoma I, et al. Insights into potential pathogenesis mechanisms associated with *Campylobacter jejuni*-induced abortions in ewes. *BMC Vet Res*. 2014; 10:274-287.
8. Schlafer DH and Foster RA. Diseases of the gravid uterus, placenta and fetus In: Maxie MG, ed. *Jubb Kennedy and Palmer's Pathology of Domestic Animals*. Vol 3. 6th ed. Philadelphia, PA: Elsevier Saunders; 2016:407-408.
9. Wu Z, Sippy R, Sahin O, et al. Genetic diversity and antimicrobial susceptibility of *Campylobacter jejuni* isolates associated with sheep abortion in the United States and Great Britain. *J Clin Micro*. 2014; 52:1853-1861.

CASE IV: 20109-13350 (JPC 4002842).

Signalment: Nine-year-old, female, Papillon (*Canis familiaris*).

History: The dog presented for the mammary masses near the right third nipple and under the left forth nipple. As a result of the physical examination, the ovarian mass was also found. The ovaries and uterus were surgically resected with the mammary masses. The left ovarian mass, left uterus, and mammary masses were sent to our laboratory for pathological examination.

Gross Pathology: The left ovarian mass after fixed in neutral-buffered formalin was 5.2 x 4.5 x3.2 cm and was soft with milky white smooth to nodular surface. The cut surface showed white to light yellow solid area with necrosis.

Laboratory results: N/A

Histopathologic Description: The left ovarian mass consists of multiple lobules surrounded by a thin connective tissue stroma with very few interstitial glands of original ovarian structures. There are occasional multifocal to coalescing areas of necrosis in the mass. Lymphocytes and plasma cells slightly infiltrated in stroma around tumor cells. Each lobule mainly composed of solid and irregular nests of round tumor cells. Ductal structures and keratinizing epithelial cell nests were often mingled. Neoplastic round tumor cells showed a high N/C ratio and resembled to germ cells of seminoma/dysgerminoma. The

tumor cells have large round nuclei with scattered chromatin and one or a few large nucleoli. The cytoplasm is abundant with weak-eosinophilic or clear, and infrequently vacuolated. Mitotic figures are frequently seen. The nuclear figure of epithelial tumor cells are similar to that of round tumor cells.

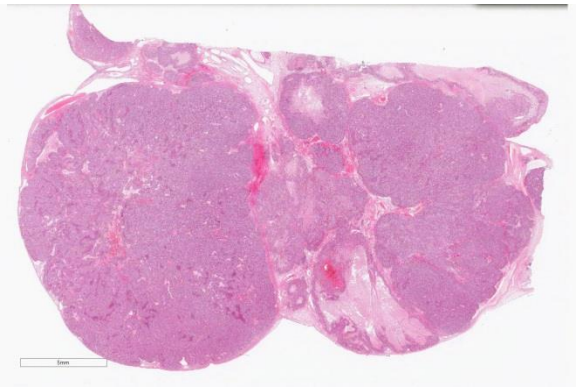

Ovary, dog. The ovary is totally effaced by an expansile multinodular neoplasm with large areas of necrosis. (HE, 4X)

Immunohistochemically, both round and epithelial tumor cells are cytoplasmic weakly positive for alpha-fetoprotein and cytoplasmic granular positive for CD30. Each tumor cell types also are positive for octamer 4 (OCT4). Cytokeratin AE1/AE3 and CAM5.2 is strongly-expressed in the cytoplasm of epithelial tumor cells and weakly positive in less than 50% of round tumor cells. However, cytokeratin 7 and 20 are negative in both tumor cells. Vimentin expression is seen in some part of round tumor cells, but is not observed in epithelial tumor cells.

Contributor's Morphologic Diagnosis: Mixed germ cell tumor in canine ovary (dysgerminoma with embryonal carcinoma).

Contributor's Comment: Canine ovarian tumors are divided into sex cord-stromal (gonadostromal) tumors, germ cell tumors, epithelial tumors, and mesenchymal tumors. Epithelial tumors and sex cord-stromal (gonadostromal) tumors are the most common (80-90%). Germ cell tumors are less common, and account for 6% to 12% of canine ovarian tumors. Germ cell tumors are further classified to dysgerminoma, teratoma and embryonal carcinoma according to the WHO classification.[1,2,6,9,] In addition, yolk sac tumor and polyembryoma, chorio-carcinoma, and mixed germ cell tumor are included among ovarian germ cell tumors of human WHO classification. In canine ovarian germ cell tumors, dysgerminoma is most common and followed by teratoma.[2,9]

The present tumor is mostly composed of round tumor cells, which resemble seminoma/dysgerminoma. Positive immuno-

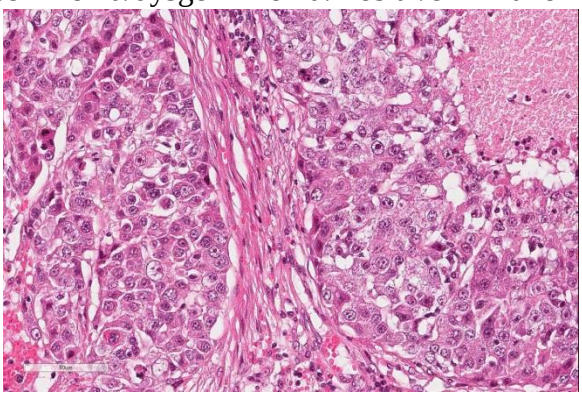

Ovary, dog. The neoplasm is largely composed by sheets of mildly anisokaryotic polygonal germ cells. (HE, 196X)

reactivitiy for OCT-4 of round tumor cells was also consistent with that of dysgerminoma, because OCT-4 is sensitive and specific immunohistochemical marker for dysgerminoma,[3] However, ductal structures and keratinizing epithelial cell nests were often mingled, and these tumor cells including round tumor cell showed positive for embryonal carcinoma markers (AFP and CD30). Embryonal carcinoma composed of undifferentiated cells of epithelial appearance with solidly cellular areas, glands, and papillary projections.[8,13,14] Areas of solid growth in embryonal carcinomas histologically resemble dysgerminomas.[8] In humans, embryonal carcinoma is a rare germ cell tumor and

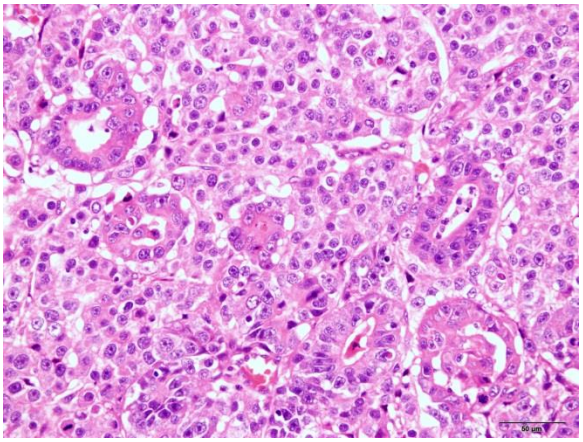

Ovary, dog. Neoplastic cells arranged in ducts are scattered throughout the neoplasm. (HE, 4X) (Photo courtesy of: Department of Pathology, Faculty of Pharmaceutical Science, Setsunan University,45-1 Nagaotohge-cho, Hirakata, Osaka 573-0101, JAPAN)

occurs as a component of mixed germ cell tumors more than pure embryonal carcinoma.[14] In animals, no pure embryonal carcinomas have been reported, but a combination (mixed) germ cell tumor with embryonal carcinoma has been reported in only two rats and a cynomolgus monkey.[11,15]

Embryonal carcinomas are immuno-histochemically distinguishable from dysgerminoma based on testing for AFP, CD30, cytokeratin AE1/AE3, CAM5.2 and cytokeratin 7, which are positive in embryonal carcinoma.[3,6,7] Thus, in the present case, immunoreactivity of tumor cells did not perfectly satisfy the diagnostic criterion for both dysgerminoma and embryonal carcinoma. In addition, round tumor cells, which resemble dysgeminoma, are only partially positive for vimentin. In contrast, epithelial tumor cells forming ducts and nests were mostly negative for vimentin. Vimentin is immunopositive in dysgerminoma, and the reactivity is higher than embryonal carcinoma.[4,8,13] We considered that the present tumor was partially differentiated from dysgerminoma, and have the characteristics of both dysgerminoma and embryonal carcinoma. Thus, the present tumor was diagnosed as dysgerminoma with embryonic differentiation (mixed germ cell tumor composed of dysgerminoma and embryonal carcinoma) rather than pure embryonal carcinoma.

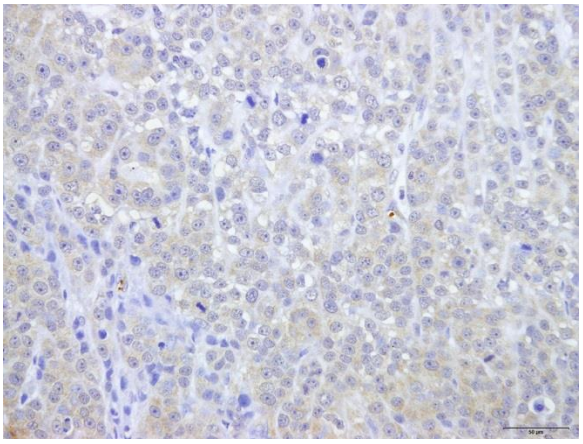

Ovary, dog. Neoplastic germ cells demonstrate weak cytoplasmic immunoreactivity for alpha-fetoprotein. (anti-alphafetoprotein, 200X) (Photo courtesy of: Department of Pathology, Faculty of Pharmaceutical Science, Setsunan University,45-1 Nagaotohge-cho, Hirakata, Osaka 573-0101, JAPAN)

JPC Diagnosis: Ovary: Mixed germ cell tumor, papillon, *Canis familiaris*.

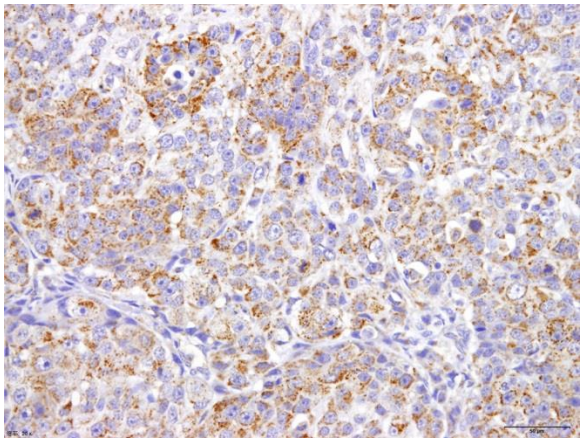

Ovary, dog. Neoplastic germ cells demonstrate moderate cytoplasmic immunoreactivity for octamer 4. (anti-octamer 4, 200X) (Photo courtesy of: Department of Pathology, Faculty of Pharmaceutical Science, Setsunan University,45-1 Nagaotohge-cho, Hirakata, Osaka 573-0101, JAPAN)

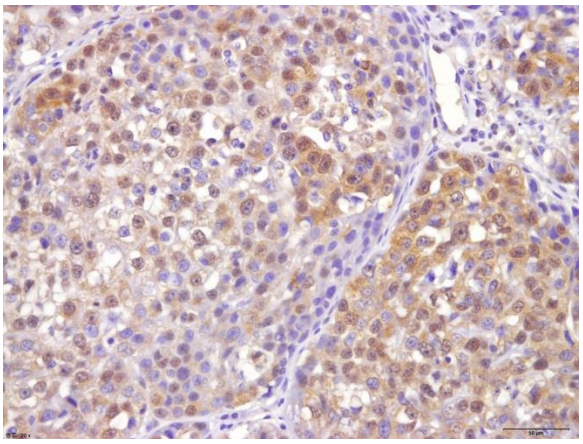

Ovary, dog. Neoplastic germ cells demonstrate moderate cytoplasmic immunoreactivity for CD30. (anti-CD30, 200X) (Photo courtesy of: Department of Pathology, Faculty of Pharmaceutical Science, Setsunan University,45-1 Nagaotohge-cho, Hirakata, Osaka 573-0101, JAPAN)

Conference Comment: The contributor provides a challenging diagnostic case of a rare ovarian neoplasm in a dog. Due to near effacement of the normal structures of the ovary by the neoplasm, some conference participants had trouble identifying the tissue as ovary. However, at the periphery of the neoplasm in all examined sections, there is a small amount of subsurface epithelial structures and granulosa cell islands characteristic of canine ovary.

As mentioned by the contributor, tumors of the ovary are uncommon and have been described in many species. They typically originate from three distinct embryologic cell types: epithelial tumors of Mullerian origin (adenoma or carcinoma), sex cord stromal tumors (granulosa cell tumor and thecoma), and germ cell tumors (dysgerminoma, teratoma, yolk sac tumors). Mixed germ cell tumors are a combination of germ cells and sex cord stromal cells. In male dogs, mixed germ cell tumors are the fourth most common primary testicular neoplasm and are typically characterized by a combination of seminoma and Sertoli cell tumor, with the tubular structures of Sertoli cell tumors containing neoplastic germ cells.[5,10,12] They are extremely rare in the ovary with reported cases in a Labrador retriever and a cynomolgus monkey.[10,11,15] Among canine ovarian tumors, granulosa cell tumors and epithelial tumors are by far the most common.[12] In this case, the contributors posit that this is a dysgerminoma mixed with an embryonal carcinoma, favoring the diagnosis of a mixed germ cell tumor.

This interesting case stimulated discussion among conference participants. Some favored the diagnosis of mixed germ cell tumor and others favored a sex cord stromal tumor, dysgerminoma, or a collision tumor. We reviewed this case in consultation with physician genitourinary pathologists at the Joint Pathology Center, who agreed with the contributor and the majority of conference participants, that there are foci suggesting a yolk sac tumor (5%), embyronal carcinoma (~25%) and predominantly dysgerminoma (70%), thus favoring the diagnosis of a mixed germ cell tumor. This case was also studied in consultation with Dr. Robert Foster, a board certified veterinary pathologist and

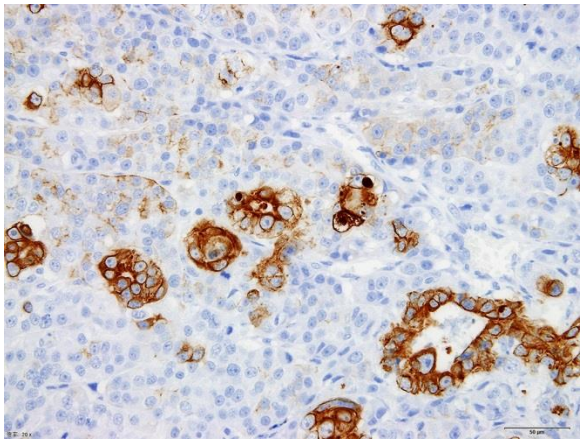

Ovary, dog. Neoplastic cells which form ductal structures exhibit strong cytoplasmic immunoreactivity for AE1/AE3 cytokeratins. (anti-cytokeratin, 200X) (Photo courtesy of: Department of Pathology, Faculty of Pharmaceutical Science, Setsunan University,45-1 Nagaotohge-cho, Hirakata, Osaka 573-0101, JAPAN)

recognized expert with extensive experience in the area of veterinary reproductive pathology. He offers a dissenting view that the highly anaplastic cells may not be germ cells and instead favors the diagnosis of a poorly differentiated ovarian sex cord stromal tumor. He also notes that immunohistochemistry in ovarian tumors can be problematic in domestic species.

Contributing Institution:

Department of Pathology,
Faculty of Pharmaceutical Science,
Setsunan University,
45-1 Nagaotohge-cho, Hirakata
Osaka 573-0101, JAPAN
mailto:ozaki@pharm.setsunan.ac.jp

References:

1. Akihara Y, Shimoyama Y, Kawasako K, et al. Immuno-histochemical evaluation of canine ovarian tumors. *J Vet Med Sci.* 2007; 69:703-708.
2. Bertazzolo W, Dell'Orco M, Bonfanti U, et al. Cytological features of canine ovarian tumours: a retrospective study of 19 cases. *J Small Anim Pract.* 2004; 45:539-545.
3. Liang Cheng, Shaobo Zhang, Aleksander Talerman,et al. Nuclear or cytoplasmic localization of Bag-1 distinctly correlates with pathologic behavior and outcome of gastric carcinomas. *Hum Pathol*. 2010; 41:716-723.
4. Cossu-Rocca P, Jones TD, Roth LM, et al. Cytokeratin and CD30 expression in dysgerminoma. *Hum Pathol***.** 2006; 37:1015-1021.
5. Foster RA. Male genital system Wilcock BP, Njaa BL. Special senses. In: Maxie MG, ed. *Jubb, Kennedy and Palmer´s. Pathology of Domestic Animals*. 6th ed Vol. 3. St Louis, MO: Elsevier Saunders; 2016:496.
6. Kennedy PC CJ, Edwards JF, et al. Histological classification of tumor of genital system of domestic animals. *In*: *World Health Organization International histological classification of tumors of domestic animals.* Wasington, DC.1998.
7. Leroy X, Augusto D, Leteurtre E, et al. CD30 and CD117 (c-kit) used in combination are useful for distinguishing embryonal carcinoma from seminoma. *J Histochem Cytochem.* 2002; 50:283-285.
8. Lifschitz-Mercer B, Walt H, Kushnir I, et.al. Differentiation potential of ovarian dysgerminoma: an immuno-histochemical study of 15 cases. *Hum Pathol***.** 1995; 26**:**62-66.
9. Patnaik AK, Greenlee PG: Canine ovarian neoplasms: a clinicopathologic study of 71 cases, including histology of 12 granulosa cell tumors. *Vet Pathol.*1987; 24:509-514.
10. Robinson NA, Manivel JC, Olson EJ. Ovarian mixed germ cell tumor with yolk sac and teratomatous components in a dog. *J Vet Diagn Invest*. 2013; 25:447-452.
11. Sawaki M, Shinoda K, Hoshuyama S, et al. Combination of a teratoma and embryonal carcinoma of the testis in SD IGS rats: a report of two cases. *Toxicol Pathol*. 2000; 28**:**832-835.
12. Schlafer DH, Foster RA. Female genital system. In: Maxie MG, ed. *Jubb, Kennedy and Palmer´s. Pathology of Domestic Animals*. 6th ed Vol. 3. St Louis, MO: Elsevier Saunders; 2016:377-378.
13. Suster S, Moran CA, Dominguez-Malagon H, et al. Germ cell tumors

of the mediastinum and testis: a comparative immunohistochemical study of 120 cases. *Hum Pathol.* 1998;29:737-742.
14. Ulbright TM: Germ cell tumors of the gonads: a selective review emphasizing problems in differential diagnosis, newly appreciated, and controversial issues. *Mod Pathol*. 2005.18(Suppl 2): 61-79.
15. Yokouchi Y, Imaoka M, Sayama A, et al. Mixed germ cell tumor with embryonal carcinoma, chorio-carcinoma, and epithelioid trophoblastic tumor in the ovary of a cynomolgus monkey. *Toxicol Pathol***.** 2011; 39:553-558.

Self-Assessment - WSC 2016-2017 Conference 7

1. Which of the following is not a distinct form of polyomavirus in in rodents?
    a. Mouse pneumotropic virus
    b. Rat respiratory virus
    c. Mastomysys polyomavirus
    d. Hamster polyomavirus

2. Which is the following is not true regarding endometriosis ?
    a. New World monkeys are not affected by this condition.
    b. The abdominal cavity is the most common site for endometriosis.
    c. Rhesus macaques are the most commonly used animal model for human endometriosis.
    d. Both endometrial glands and stroma are seen in endometriosis.

3. Typically, endometriosis does not demonstrate immunopositivity for which of the following markers?
    a. Pancytokerating
    b. Chromagranin A
    c. Estrogen receptors
    d. Progesterone receptors
    e.
4. Which of the following is not true concerning *Camplyobacter jejuni*?
    a. It is an important cause of food-borne illness in humans.
    b. In sheep, *C. jejuni* results in late-term abortion
    c. *C. jejuni*-related abortions have also been documented in humans.
    d. Aborted fetuses rarely if ever show lesions.

5. Mixed germ cell tumors of the gonads are a combination of:
    a. Germ cells and sex cord stromal cells
    b. Germ cells and endothelial cells
    c. Sex cord stromal cells and sustentacular cells
    d. Germ cells and epithelial cells of the rete

Joint Pathology Center

Veterinary Pathology Services

WEDNESDAY SLIDE CONFERENCE 2016-2017

Conference 8

26 October 2016

CASE I: 1525970 (JPC 4083864).

Signalment: 18-year-old, thoroughbred mare (*Equus caballus*).

History: The mare had a several year history of a polyp in the nasal cavity. The mass was surgically removed and submitted as an excisional biopsy.

Gross Pathology: The biopsy sample comprised a 2 x 1.5 x 1 cm smooth, pink-tan, spongy mass with multifocal ulcers and a narrow stalk at one edge.

Laboratory results: N/A

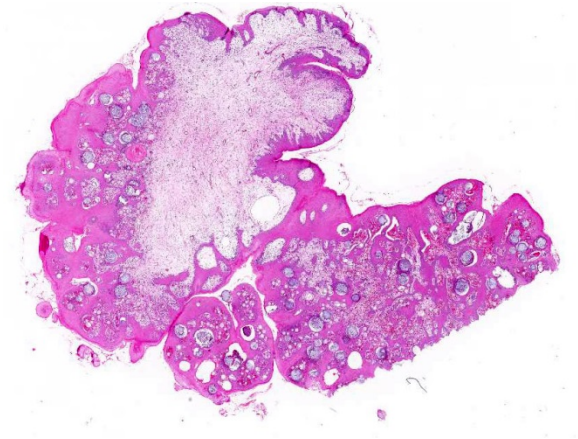

Nasal mucosa, horse. A polypoid proliferation of the nasal mucosa is submitted for examination. Large numbers of juvenile and mature sporangia are present within the submucosa, and few mature sporangia are present within the overlying epithelium. (HE, 4X)

Histopathologic Description: Representative sections of the tissue comprise a polypoid proliferation of loose fibrovascular tissue covered by a hyperplastic, acanthotic stratified squamous epithelium with multifocal erosions and an eosinophilic exudate of mucin admixed with necrotic neutrophils, debris and erythrocytes. Numerous protistan organisms at varying stages of development are embedded within the surface exudate, epithelium, and submucosa, which is infiltrated by moderate numbers of lymphocytes, plasma cells, macrophages, fewer neutrophils, and variable amounts of hemorrhage and edema. Immature sporangia (trophocytes) are round and 10-100 µm diameter, with a 2 µm thick eosinophilic wall, lacy amphophilic cytoplasm, and a single, central, round karyosome (nucleus). Intermediate sporangia lack a nucleus and contain innumerable immature sporangiospores (endospores). Immature endospores are 1-4 µm diameter, with a thin wall, scant to moderate amounts of lightly basophilic cytoplasm, and irregularly round, para-central eosinophilic structures. Mature

sporangia located throughout the epithelium are spherical and 100-400 µm diameter, with a 2-5 µm thick, bilamellar, outer eosinophilic and inner amphophilic wall. The mature sporangia contain mature endospores or a mixture of mature and immature endospores. Mature endospores are 5-8 µm diameter spherical structures with a thin unilamellar wall, scant clear cytoplasm, and multiple, central, round eosinophilic bodies. Within mature sporangia, immature endospores are often located peripherally or emerge unilaterally from the wall of the sporangium. Mature sporangia are multifocally ruptured, releasing mature endospores through an apical pore in the epithelium or into the adjacent stroma, and surrounded by dense aggregates of neutrophils with fewer lymphocytes, plasma cells, and macrophages.

Contributor's Morphologic Diagnosis: Horse, nasal mass: Chronic polypoid and suppurative rhinosinusitis with protistan sporangia and endospores (consistent with *Rhinosporidium seeberi*)

Contributor's Comment: *Rhinsporiduim seeberi* is an uncommon cause of rhinitis and nasal polyps in humans, dogs, cats, horses, cattle and waterfowl.[3, 4, 7, 9, 10, 11, 12] The organism was originally identified in tissue extracted from nasal polyps of people in Argentina, and has since most commonly been diagnosed in tropical climates such as India and Sri Lanka.[3] It has been reported sporadically in horses from the Americas and Europe. [2, 9, 10, 11,]

Patients with nasal rhinosporidiosis may be asymptomatic, or present with clinical signs that include respiratory noise, sneezing, nasal discharge, and epistaxis.[2, 3, 4] If masses become large, obstruction of the nasal passage can occur.[1, 3] Examination of the nasal cavity reveals a unilateral polypoid mass protruding from the nasal mucosa,

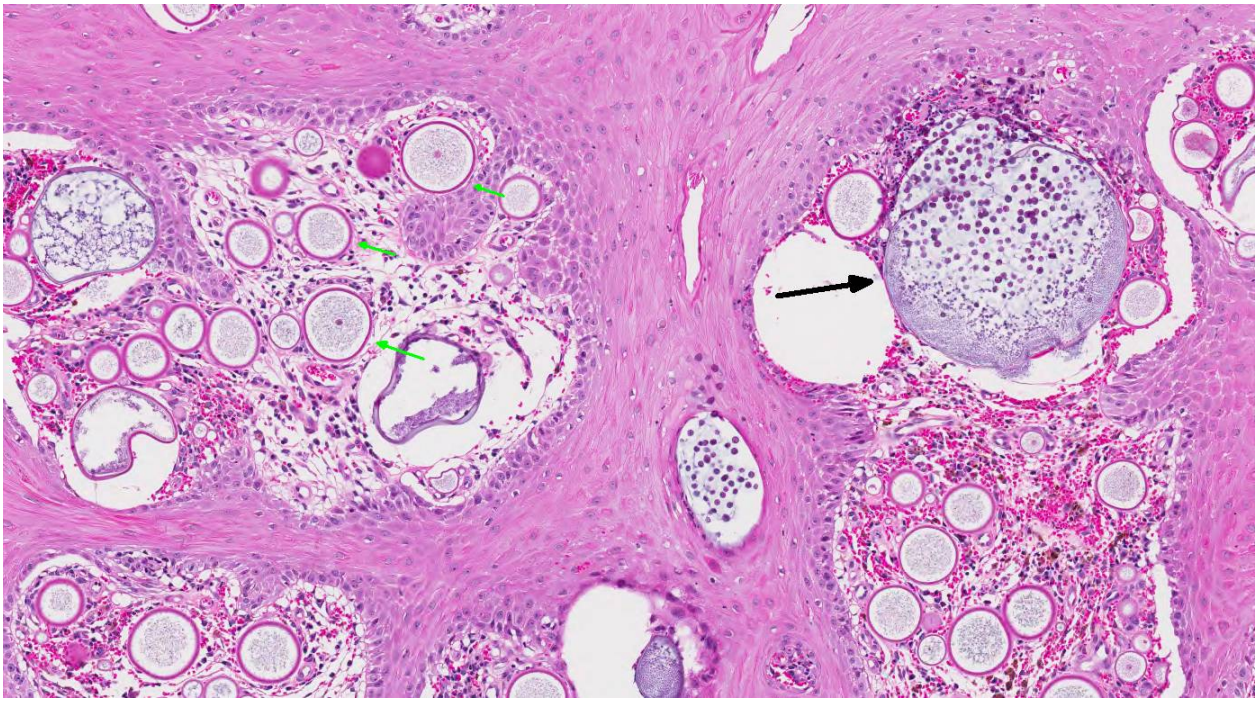

Nasal mucosa, horse. Numerous immature (green arrows) sporangia and few mature (black arrow) sporangia are scattered throughout the submucosa. (HE, 10X)

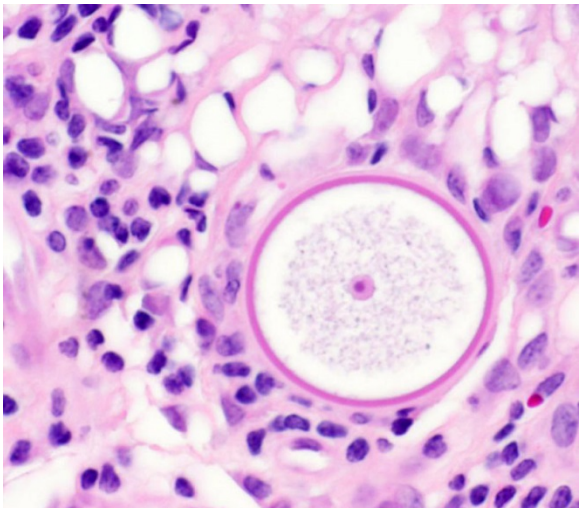

Nasal mucosa, horse. Immature sporangia have a 2 um thick eosinophilic wall, lacy amphophilic cytoplasm, and a single, central, round karyosome. (H&E, 40X) (Photo courtesy of: University of Pennsylvania, School of Veterinary Medicine, Department of Pathobiology http://www.vet.upenn.edu/research/academic-departments/)

though laryngeal masses in association with *R. seeberi* have been reported in horses.[2, 11] Close inspection of the surface of the mass may reveal small, white foci. In humans, there are reports of nasal, ocular, laryngeal and genital rhinosporidiosis.[3]

Histologic examination reveals a fibrovascular polyp covered by stratified squamous to pseudostratified ciliated columnar epithelium. Sporangia in varying stages of development are observed throughout the fibrovascular and epithelial components of the polyp. Identification of sporangia with endospores in a polypoid nasal mass is diagnostic for *R. seeberi*.[7] Organisms are readily observed in H&E-stained sections; however, histochemical stains, such as GMS and PAS, can be used to highlight the walls of the sporangia.[5] Polymerase chain reaction (PCR) and DNA sequence analysis of tissue samples can be used to confirm the etiologic agent.[2]

The classification of *R. seeberi* has long been controversial. The organism was once considered to be protozoan, fungus, or a cyanobacterium. More recently, phylogenetic analysis categorized *R. seeberi* as a eukaryote within the class *Mesomycetozoa*, a group of aquatic protistan parasites.[5, 6]

The pathogenesis of rhinosporidiosis is poorly understood, though stagnant water appears to be the reservoir for *R. seeberi*. The proposed mechanism of infection involves pre-existing defects in the epithelial barrier of the nasal passage, allowing mature endospores to enter the nasal mucosa from contaminated water.[3] Once within host tissues, endospores localize to the sub-epithelial connective tissues and mature into immature sporangia (trophocytes). Immature sporangia have thick, unilamellar eosinophilic walls, a central nucleus, and fine cytoplasm. As immature sporangia become intermediate sporangia, a bilamellar wall develops, the nucleus is lost, and the

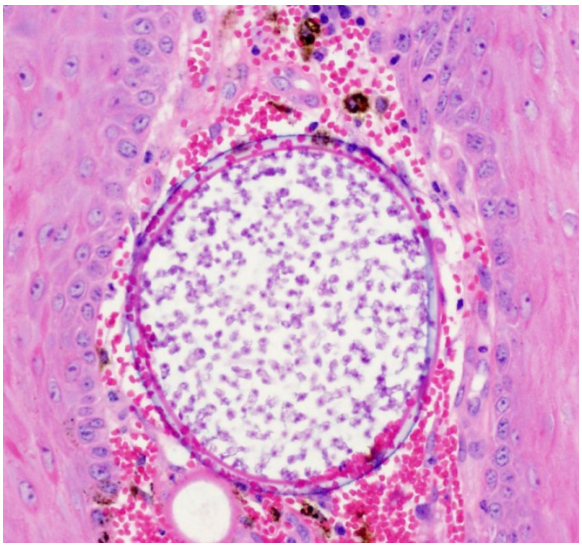

Nasal mucosa, horse. Intermediate sporangia lack a nucleus and contain innumerable immature sporangiospores (endospores). Immature endospores are 1-4 um diameter, with a thin wall, scant to moderate amounts of lightly basophilic cytoplasm, and irregularly round, paracentral eosinophilic structures. (H&E, 20X) (Photo courtesy of: University of Pennsylvania, School of Veterinary Medicine, Department of Pathobiology http://www.vet.upenn.edu/research/academic-departments/)

cytoplasm condenses to form immature sporangiospores (endospores). Intermediate sporangia eventually become larger, contain both immature and mature endospores, and are localized within the superficial epithelium. At this stage, the sporangia are considered mature and will continue to house developing endospores until release. Mature endospores contain multiple, central eosinophilic bodies, and are released from sporangia through apical pores in the epithelium into the nasal passage. Infective, mature endospores released into the nasal passage are then excreted into the environment along with nasal secretions.[7]

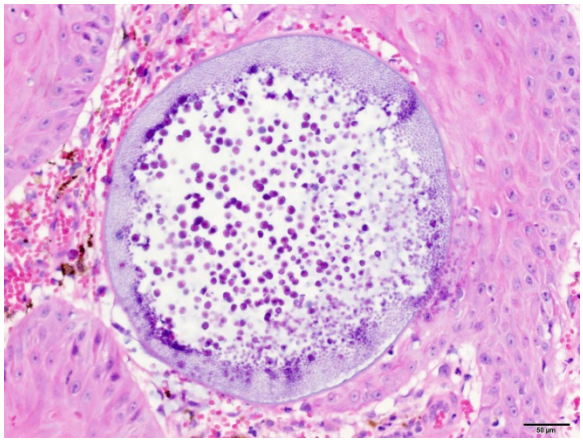

Nasal mucosa, horse. Mature sporangia are round, 100-400 um diameter, and have a 2-5 um thick, bilamellar wall (outer eosinophilic and inner amphophilic). The mature sporangia contain mature endospores, or a mixture of mature and immature endospores Within mature sporangia, immature endospores are often located peripherally, or emerge unilaterally from the wall of the sporangium. (H&E, 20X) (Photo courtesy of: University of Pennsylvania, School of Veterinary Medicine, Department of Pathobiology http://www.vet.upenn.edu/research/academic-departments/)

Surgical removal of any visible polyps is the treatment of choice for nasal rhino-sporidiosis. Excision is typically curative; however, recurrence is reported.[2, 3, 7] A diagnosis of concurrent nasal adeno-carcinoma and rhinosporidiosis was reported in a cat housed on a horse farm.[1]

In this horse, infectious organisms were embedded within a polypoid proliferation, grossly and histologically resembling a nasal polyp. Because rhinosporidiosis in humans is associated with polypoid proliferations, the authors speculate the proliferative (polypoid) response in this horse may be secondary to chronic infection and

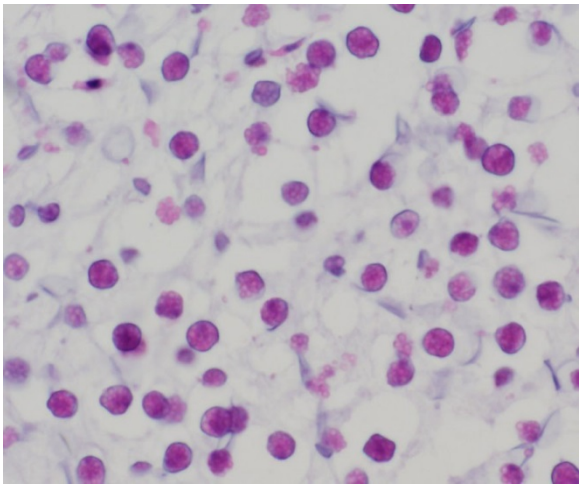

Nasal mucosa, horse. Mature endospores are spherical, 5-8 um diameter, with a thin unilamellar wall, scant clear cytoplasm and multiple, central, round eosinophilic bodies. (H&E, 40X) (Photo courtesy of: University of Pennsylvania, School of Veterinary Medicine, Department of Pathobiology http://www.vet.upenn.edu/research/academic-departments/)

inflammation, rather than represent a primary nasal polyp. Free endospores within the submucosa often elicit a pyo-granulomatous to granulomatous response; however, in this case, the predominant inflammatory infiltrates were neutrophils admixed with lymphocytes, plasma cells, and macrophages.

For this horse, travel history, clinical signs, laboratory findings and post-operative follow-up were not provided by the submitting veterinarians.

JPC Diagnosis: Nasal mass: Rhinitis, polypoid, chronic-active, diffuse, severe, with numerous protistan sprorangia and endospores, thoroughbred, *Equus caballus*

Conference Comment: The contributor provides an exceptional review of the epidemiology, clinical presentation, gross lesions, histopathologic findings, and differential diagnosis for *Rhinosporidium seeberi* in horses. Conference participants were impressed by the tremendous numbers of protistan endospores and striking variation in the size of the sporangia in the section. Despite slight slide variability, conference participants noted chronic mixed inflammation with hemorrhage, edema, and granulation tissue in the subepithelial connective tissue and stalk of the nasal polyp.

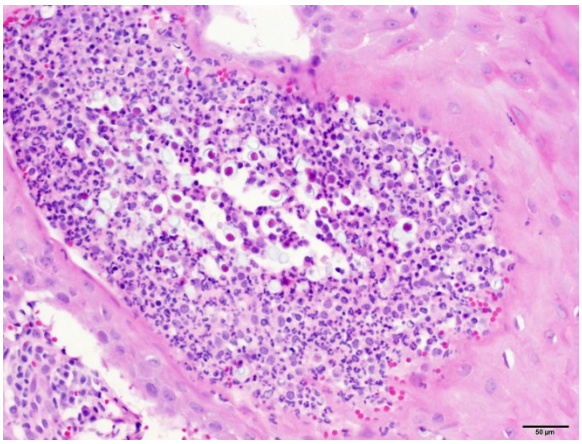

Nasal mucosa, horse. Mature sporangia are often ruptured, releasing mature endospores through an apical pore in the epithelium, or into the adjacent stroma. Numerous neutrophils infiltrate the connective tissue surrounding ruptured sporangia, admixed with lesser lymphocytes, plasma cells, and hemosiderin-laden macrophages. (H&E, 20X) (Photo courtesy of: University of Pennsylvania, School of Veterinary Medicine, Department of Pathobiology http://www.vet.upenn.edu/research/academic-departments/)

Rhinosporidium seeberi is one of the few pathogens which reproduce by endosporulation.[3] The endospore is implanted in tissues and grows into much larger and variably sized sporangia. As sporangia grow and mature, endospores are produced and released into the surrounding tissue generating marked pyogranulomatous inflammation and effectively reinitiating the pathogen's lifecycle.[3] Conference participants discussed other endosporulators of veterinary significance including: *Prototheca wickerhamii*, *Chlorella* sp., *Coccidioides* sp., and *Batrachochytrium dendrobatidis*. Based on the size of the sporangia and observation of endosporulation, the differential diagnosis in this case includes *Coccidioides* sp. (see 2016-2017 WSC 4 Case 4). The endospores of *Rhinosporidium seeberi* contain inner granules, while *Coccidioides* sp. endospores do not. Also, *R. seeberi* endospores completely stain with Periodic acid-Schiff (PAS), while only the walls of the endospores stain in *Coccidioides* sp.[8] However, finding large sporangia in a polypoid nasal mass of a horse is typically considered diagnostic for rhinosporidiosis.[1,3]

Contributing Institution:
University of Pennsylvania
School of Veterinary Medicine
Department of Pathobiology
http://www.vet.upenn.edu/research/academic-departments/

References:

1. Brenske BM, Saunders GK. Concurrent nasal adenocarcinoma and rhinosporidiosis in a cat. *J Vet Diagn Invest*. 2010; 22:155-157.
2. Burgess HJ, Lockerbie BP, Czerwinski S, Scott M. Equine laryngeal rhinosporidiosis in western Canada. *J Vet Diagn Invest*. 2012; 24(4):777-780.
3. Caswell J, Williams K. Respiratory system, In: Maxie MG, ed. *Jubb,*

Kennedy, and Palmer's Pathology of Domestic Animals. Vol 1. 6th ed. Philadelphia, PA: Elsevier Saunders; 2016: 579-586.
4. Das S, Kashyap B, Barua M, Gupta N, Saha R, Vaid L, Banka A. Nasal rhinosporidiosis in humans: New interpretations and a review of the literature of this enigmatic disease. *Med Mycol*. 2011; 49:311-315.
5. Easley JR, Meuten DJ, Levy MG, Dykstra MJ, Breitschwerdt EB, Holzinger EA, Cattley RC. Nasal rhinosporidiosis in the dog. *Vet Pathol*. 1986; 23:50–56.
6. Fredricks DN, Jolley JA, Lepp PW, Kosek JC, Relman DA. *Rhinosporidium seeberi*: A human pathogen from a novel group of aquatic protistan parasites. *Emerg Infect Dis*. 2000; 6(3):273-282.
7. Herr RA, Ajello L, Taylor JW, Arseculeratne SN, Mendoza L. Phylogenetic analysis of *Rhinosporidium seeberi*'s 18S small-subunit ribosomal DNA groups this pathogen among members of the protoctistan Mesomycetozoa clade. *J Clin Microbiol*. 1999; 37:2750–2754.
8. Jones TC, Hunt RD, King NW. Diseases caused by fungi. In: *Veterinary Pathology*. 6th ed. Baltimore, MD: Williams and Wilkins; 1997: 527.
9. Kennedy FA, Buggage RR, Ajello L. Rhinosporidosis: A description of an unprecedented outbreak in captive swans (*Cygnus* spp.) and a proposal for revision of the ontogenic nomenclature of *Rhinosporidium seeberi*. *J Med Vet Mycol*. 1995; 33:157-165.
10. Leeming G, Hetzel U, Campbell T, Kipar A. Equine rhinosporidiosis: An exotic disease in the UK. *Vet Rec*. 2007; 160:552-554.
11. Moisan PG, Baker SV. Rhinosporidiosis in a cat. *J Vet Diagn Invest*. 2001; 13:352-354.
12. Myers DD, Simon J, Case MT. Rhinosporidiosis in a horse. *J Am Vet Med Assoc*. 1964; 145:345-347.
13. Nollet H, Vercauteren G, Martens A, Vanschandevijl K, Schauvliege S, Gasthuys F, Ducatelle R, Deprez P. Laryngeal rhinosporidiosis in a Belgian warmblood horse. *Zoonoses Public Health*. 2008; 55:274-278.

Ramachandra Rao PV, Jain SN, Hanumantha Rao TV. Animal rhinosporidiosis in India with case reports. *Ann Soc Belge Med Trop*. 1975; 55(2);119-124

CASE II: 0398/15 (JPC 4086389).

Signalment: Young male York-shire/Hampshire cross pig (*Sus domestica*).

History: Two piglets (about three-weeks-old) had been growing slowly and showed respiratory symptoms with rapid breathing. They were both treated with antibiotics (penicillin) but died suddenly. The piglets were sent to necropsy. A few weeks later a small number of fattening pigs had reduced growth rate and were in poor body condition, the pigs were euthanized and sent to necropsy. All pigs were from the same specific pathogen-free farm (SPF). The submitted slide is from one of the fattening pigs.

Once a year tests are taken to show freedom from: swine influenza virus, *Actinobacillus pleuropneumoniae* (APP), *Mycoplasma hyopneumoniae* (SEP), *Sarcoptes scabiei*, Swine dysentery (*Brachyspira hyo-*

dysenteriae), Intestinal spirochetosis (*Brachyspira pilosicoli)*, other Brachyspira-subspecies, toxin-producing *Pasteurella multocida*, *Salmonella* and *Lawsonia intracellularis*. The farm was not vaccinated against PCV-2.

Gross Pathology: At necropsy, the fattening pig was in poor body condition and presented with a mottled myocardium, enlarged lymph nodes, multiple white foci scattered throughout the kidneys, firm cranioventral lung, and mild ascites. The two piglets were in poor body condition, the hearts had marked dilatation of left and right ventricle and atrium (dilated cardio-myopathy) and the piglets presented signs of cardiac failure with acute stasis in liver, ascites, and pulmonary edema.

Heart, piglet. The heart of the submitted piglet had marked dilation of the right and left atria and ventricles.

Laboratory results: Immunohistochemistry heart: positive for PCV-2 (piglet)

PCR lymph node: Positive for PCV 2 (fattening pig).

Histopathologic Description: Heart: Multifocal to coalescing chronic severe granulomatous interstitial inflammation with loss of myocytes is present. The inflammatory cells are dominated by lymphocytes, plasma cells, and macrophages with fewer neutrophils and eosinophils. Few multinucleated giant cells are also seen. Multifocally, the myocytes are degenerated or necrotic with loss of striations and eosinophilic swollen cytoplasm, loss of nuclei, and occasionally pyknotic nuclei, scattered degenerated Purkinje fibers are also seen. Multifocally, there are small foci of basophilic homogenous material (mineralization). The outer walls of medium and large sized vessels are infiltrated by varies amount of mononucleated inflammatory cells and the vessels have marked thickened tunica adventitia due to inflammation and edema, multifocal small sized vessels have degenerated walls with infiltration of mixed inflammatory cells (vasculitis). The endocardium is moderately thickened with abundant mixed inflammatory cells, reactive fibroblasts and angiogenesis (granulation tissue).

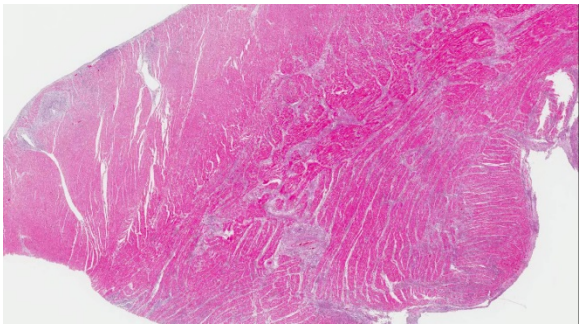

Heart, piglet. Subgross magnification of the submitted section of left ventricle reveals a significant inflammatory infiltrate throughout the myocardium, epicardium, and endocardium, which replaces myofibers. (HE, 4X)

On the Masson trichrome stain, there is a moderate amount of extracellular collagen present in areas with myocyte loss and with reactive fibroblasts.

Contributor's Morphologic Diagnosis: Heart: Myocarditis and endocarditis, multifocal to coalescing, interstitial, severe, chronic, lymphoplasmacytic and histiocytic with multinucleated giant cells (granulomatous) and vasculitis.

Contributor's Comment: Porcine circovirus (genus *Circovirus*, family *Circoviridae*) is a small (17nm diameter), non-enveloped virus that contains circular single-stranded DNA.[3,8] The virus was initially discovered in 1998 and was first isolated from pigs with *post weaning multisystemic wasting syndrome* (PMWS). The virus is highly prevalent in the domestic pig population all over the world and PCV-2 infection is common in herds as a subclinical disease. PCV-2 infection has been associated with several disease complexes including PMWS, enteric disease, respiratory disease, porcine dermatitis and nephropathy syndrome and reproductive disorders.[3,8,10] Vaccine against PCV-2 has been used since 2006, which have been effective controlling and preventing PCV-2 associated diseases. Although the majority of the conventional pigs entering the market are now vaccinated, PCV-2 still remains an important differential diagnosis for various disease manifestations in pigs.[8] In PMWS, pigs exhibit a systemic

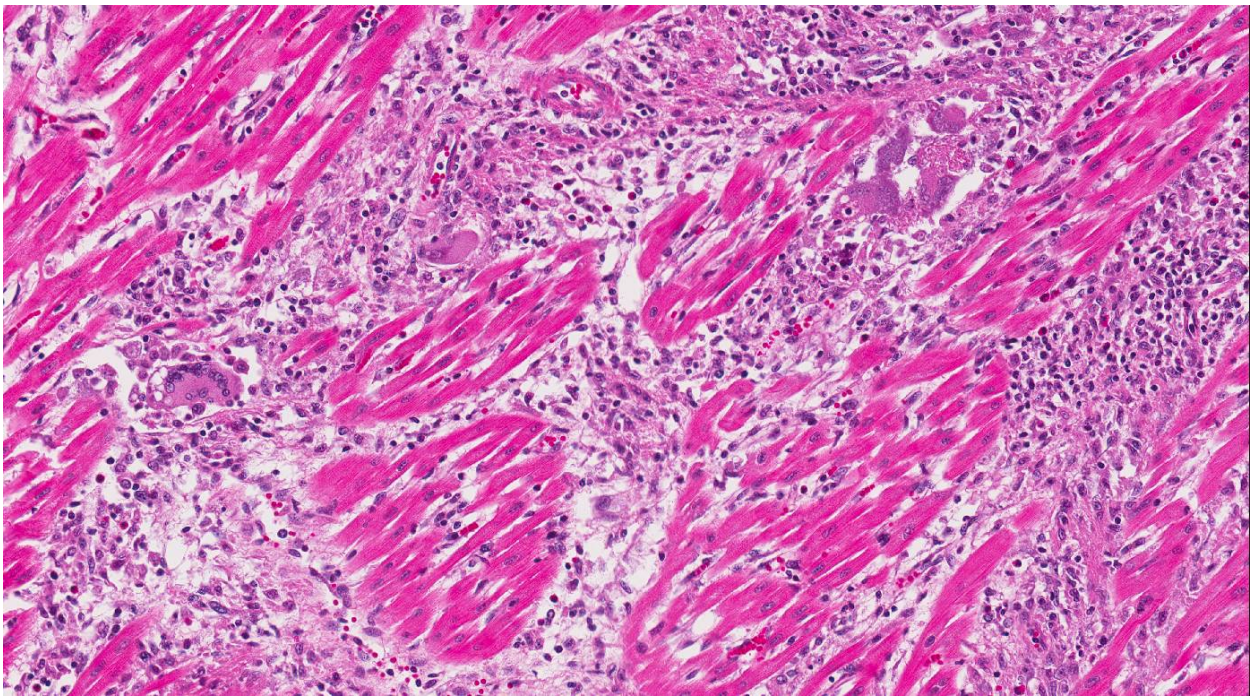

Heart, piglet. A granulomatous infiltrate separates, infiltrates, and replaces myofibers, which contains small amount of wispy collagen. Multinucleated giat cells are scattered throughout the infiltrate. (HE, 200X)

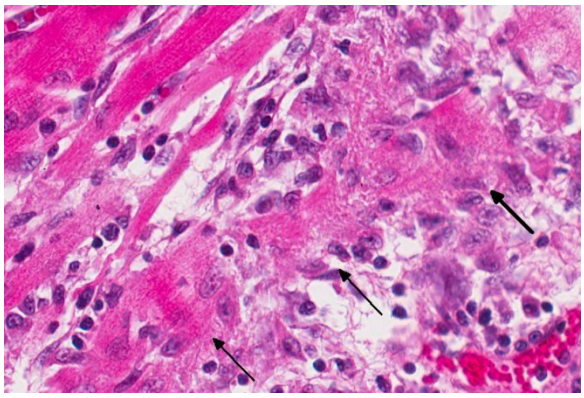

Heart, piglet. In areas of inflammation, degenerate myofibers (black arrows) exhibit loss of cross striations and fragmentation. (HE, 400X)

infection involving several organ systems and the disease is characterized by loss of weight or wasting in combination with various other clinical signs such as dyspnea, diarrhea, pallor, and jaundice. Other clinical signs include coughing, fever, central nervous signs, or sudden death.[3,8] On gross necropsy, lymphadenopathy is the most consistent feature of PMWS, but the gross lesions and severity are highly variable.[8] Diagnosis is mainly based on clinical findings and typical gross and histological lesions, and is supported by demonstration of active PCV2 infection by immuno-histochemistry or PCR.[3]

Porcine circoviral antigen and nucleic acid are most consistently present in the cytoplasm of monocytes, macrophages and dendritic cells throughout the body. Vascular smooth muscle and endothelial cells occasionally express circoviral antigen.[3] PCV2 induces characteristic lesions in the lymphoid system which includes lymphoid depletion and granulo-matous inflammation with multi-nucleated giant cells, lesions are commonly observed in the tonsils, spleen, Peyer´s patches, and lymph nodes. In the respiratory system, bronchinterstitial pneumonia may be a feature and the virus can cause meningoencephalitis and vasculitis in CNS. In the digestive system, the most frequent lesion is granulomatous enteritis characterized by increased number of macrophages and scattered multinucleated giant cells in the mucosa and submucosa of the ileum and occasionally the colon and cecum. In the kidney, lesions are characterized by lymphoplasmacytic or granulomatous interstitial nephritis. In the vascular system, PCV2 antigen has been demonstrated in endothelial cells and in inflammatory cells in the arterial walls and chronic lymphoplasmacytic vascular lesions has been described among pigs infected with PCV2.[8,10] In foetuses, lesions are most prominent in the cardiovascular system, especially in the heart where cardio-myocytes are degenerated, or lost and replaced by fibrous connective tissue. In addition, there is non-suppurative myo-carditis and occasionally multinucleated giant cells.[2,6, 8,11] Heart failure and dilated cardiomyopathy is described as a feature among aborted foetuses and very young animals secondary to myocarditis.[2,6,8,11]

The presented case from the pig-farm showed typical gross and histological lesions of PCV2 infection that are compatible with the described cases in the literature. The fattening pig had lymphoid depletion and granulomatous inflammation in lymph node and granulomatous inflammation with vasculitis in kidney and heart. A purulent bronchopneumonia was seen in the lungs; however, the material was not cultured but secondary bacterial infection is most likely. The two young piglets with dilated cardiomyopathy had chronic granulomatous myocarditis at on histopathology. The diagnosis was supported by demonstrating active PCV2 infection with PCR and immuno-histochemistry.

JPC Diagnosis: Heart: Pancarditis, transmural, lymphohistiocytic, multifocal to coalescing, marked, with vasculitis, myocardial loss, and fibrosis, Yorkshire/Hampshire cross pig, *Sus domestica*.

Conference Comment: The contributor provides an excellent summary of porcine circovirus-2 (PCV-2) infection in swine. There are two separate genotypes of PCV have been implicated in this species. PCV type 1 (PCV-1) is generally thought to be nonpathogenic and does not cause disease in pigs, although it has been implicated as a potential cause of congenital tremors in newborn piglets.[3] PCV-2 is pathogenic in pigs and causes post weaning multisystemic wasting syndrome (PMWS) discussed by the contributor above. PMWS is a multifactorial systemic disease and clinically manifests at 25-150 days of age with most cases occurring between 7 and 15 weeks.[3-6,9] The six fundamental clinical signs include wasting, dyspnea, lymphadenopathy, diarrhea, pallor, and jaundice. Coughing, fever, gastric ulceration, and meningitis have also been reported. Serum antibodies to PCV-2 are very common in swine herds around the world, and positive antibody titer does not necessarily equate to clinical PMWS.[3] However, co-infection of PCV-2 with porcine reproductive and respiratory syndrome virus (PRRSV), and/or porcine parvovirus (PPV), produces more severe clinical disease; although, PCV-2 has been shown to be sufficient to produce disease in susceptible animals without co-infection.[3,4,6,9,10]

Conference participants discussed that lymphoplasmacytic and histiocytic myocarditis with varied numbers of multinucleated giant cells and myocardial degeneration, loss, and replacement by fibrosis are typical histologic changes associated with infection by PCV-2.[3,4] In addition, necrotizing vasculitis, a key histologic feature in this case, has been implicated as a hallmark lesion in PCV-2 infection, as well as the severe form of systemic porcine circovirus-associated disease (PCVAD), discussed below.[1-3,9] Participants also noted the lack of unique and characteristic intracytoplasmic basophilic botryoid viral inclusion bodies, typically associated with PCV-2 infection. Inclusion bodies may be present within macrophages; however, they are not always identified. Definitive diagnosis of PMWS is based on a combination of typical clinical signs of disease, typical histologic lesions, and detection of PCV-2 in affected tissues via immunohistochemistry, as demonstrated by the contributor in this case. [3]

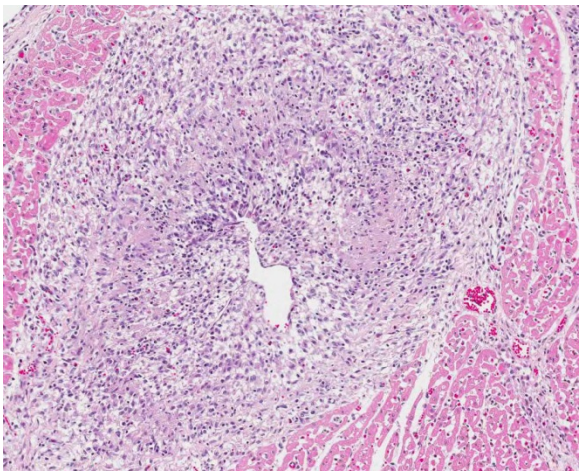

Heart, piglet. The walls of coronary vessels are effaced by granulomatous inflammation which extends into and replaces surrounding myofibers. (HE, 200X)

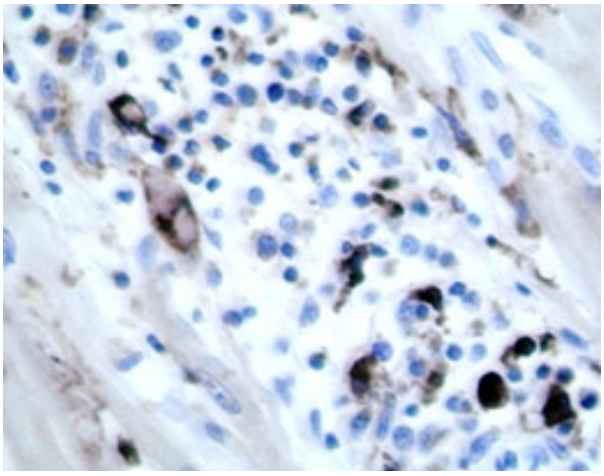

Heart piglet. Macrophages within the interstitial infiltrate exhibit strong cytoplasmic immunopositivity for porcine circovirus-2 viral antigen. (anti-PCV-2, 400X)

As mentioned above, infection with PCV-2 alone can cause disease in pigs; however, it is more commonly identified in a complex of multiple pathogen infection, known as PCVAD. This syndrome results from co-infection of PCV-2 with PPV, PRRSV, encephalomyocarditis virus (EMCV), swine influenza virus, or *Mycoplasma hyo-pneumonia*, or a combination of these agents.[1,3,4,10] It can also occur from PCV-2 infection in association with recent vaccination.[3,4] Despite the economic losses caused by PCV-2, PMWS, and PCVAD, the pathogeneses underlying the clinical findings remain largely unclear; however, they are likely related to macrophage activation prior to infection and subsequent endothelial cell modulation.[7] Conference participants discussed that antigens for PCV-2 can be found in macrophages, monocytes, and dendritic cells, as well as endothelial cells and vascular smooth muscle.

Contributing Institution:
Swedish University of Agricultural Sciences
Department of Biomedical Services and Veterinary Public Health
Pathology Section
Uppsala, Sweden
http://www.slu.se/en

References:

1. Allan GM, Ellis JA. Porcine circoviruses: A review. J Vet Diagn Invest. 2000; 12:3-14.
2. Brunborg IM, Jonassen CM, Mildal T, et al. Association of myocarditis with viral load of porcine circovirus type 2 in several tissues in cases of foetal death and high mortality in piglets. A case study. *J Vet Diagn Invest* 2007; 19:368-375
3. Caswell JL and Williams KJ. Respiratory system. In: Maxie MG, ed. *Jubb, Kennedy and Palmer´s. Pathology of Domestic Animals* 6th ed Vol. 2. St Louis, MO: Elsevier Saunders; 2016:527-529.
4. Cushing TL, Steffen D, Duhamel GE. Pathology in practice: Myocarditis attributable to PCV-2 infection in a pig fetus. J Am Vet Med Assoc. 2013; 242:317-319.
5. Harding JC. The clinical expression and emergence of porcine circovirus 2. *Vet Microbiol*. 2004; 98:131-135.
6. Madson DM, Patterson AR, Ramamoorthy S, et al. Effect of Porcine Circovirus Type 2 (PCV2) vaccination of the dam on PCV2 Replication in utero. *Clinical and vaccine immunology*. 2009; 830-834.
7. Marks FS, Almeida LL, et al. Porcine circovirus 2 (PCV2) increases the expression of endothelial adhesion/junctional molecules. *Braz J Microbiol*. 2016; 47:870-875.
8. Opressnig T, Janke BH and Halbur PG. Cardiovascular lesions in pigs naturally or experimentally Infected with porcine circovirus type 2. *J Comp. Path.* 2006; 134:104-110.
9. Opriessnig T, Langohr I. Current state of knowledge on porcine

circovirus type 2-associated lesions. *Vet Pathol*. 2012; 50(1):23-33.
10. Segalés J. Porcine circovirus type 2 (PCV2) infections: Clinical signs, pathology and laboratory signs. *Virus Res*. 2012; 164:10-19.
11. West KH, Bystrom JM, Wojnarowicz C, Shantz N, et al. Myocarditis and abortion associated with intrauterine infection of sows with porcine circovirus 2. *J Vet Diagn Invest*. 1999; 11:530-532.

CASE III: S16-0248 (JPC 4085382).

Signalment: Adult male and female Guinea pigs (*Cavia porcellus*).

History: In a collection of guinea pigs, three adult animals died within two weeks. All of them showed signs of dyspnea and two of them had been treated with antibiotics. Two animals were dissected.

Gross Pathology: The thoracic cavity of both animals contained approximately 2 ml of a red and turbid fluid. The cranial lung lobes and the accessory lobe of both animals were diffusely red and heavy. In parts of the caudal lobes, there are multifocal firm areas.

Laboratory results: Bacteriological examination of lung tissue (cultivation): No bacteriological or mycological agent was detectable.

Histopathologic Description: Depending on the cut-section, up to 100% of the lung tissue is affected. Diffusely within the bronchi and bronchioles are abundant degenerate and non-degenerate neutrophils, sloughed hypereosinophilic necrotic epithelial cells, admixed with fewer macrophages and lymphocytes. Epithelial cells of the bronchi and bronchioles are usually detached and necrotic, exhibiting a hypereosinophilic cytoplasm and pyknotic nucleus. Epithelial cells often contain a 7-10 μm, amphophilic, round to oval, intranuclear inclusion body which peripheralizes the chromatin. Depending on the cut-section, around the bronchi and bronchioles, as well

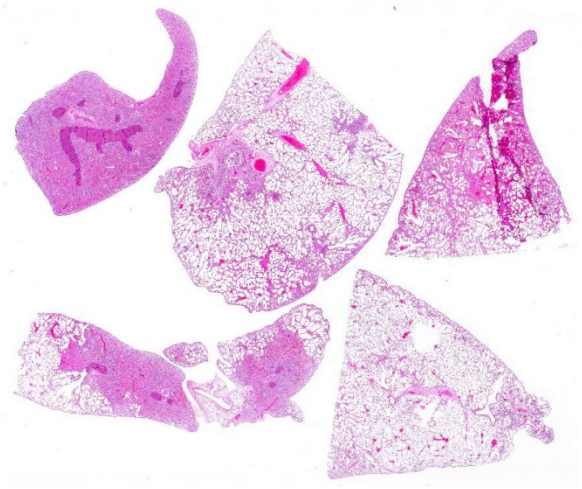

Lung, guinea pig. Multiple sections of lung exhibit variable degrees of consolidation. Airways are multifocally filled with a dense brightly eosinophilic exudate. (HE, 4x)

as perivascular, there is a cuff of a variable number of inflammatory infiltrates mainly composed of lymphocytes and fewer plasma cells. In some alveolar lumina, a small number of macrophages and lesser neutrophils are recognized. The interstitium is multifocal markedly thickened by inflammatory cells, mainly consisting of neutrophils and fewer lymphocytes. In addition, there is multifocal activation and hyperplasia of pneumocytes type 2. In some areas, the alveolar lumina are filled with eosinophilic, beaded fibrillar material (fibrin) admixed with a moderate amount of neutrophils. Adjacent to these areas, multiple vessels are filled with eosinophilic, amorphous material (thrombi). Multifocal the alveolar lumina are filled with homogeneous, eosinophilic, proteinaceous material (alveolar edema) and the lumina of

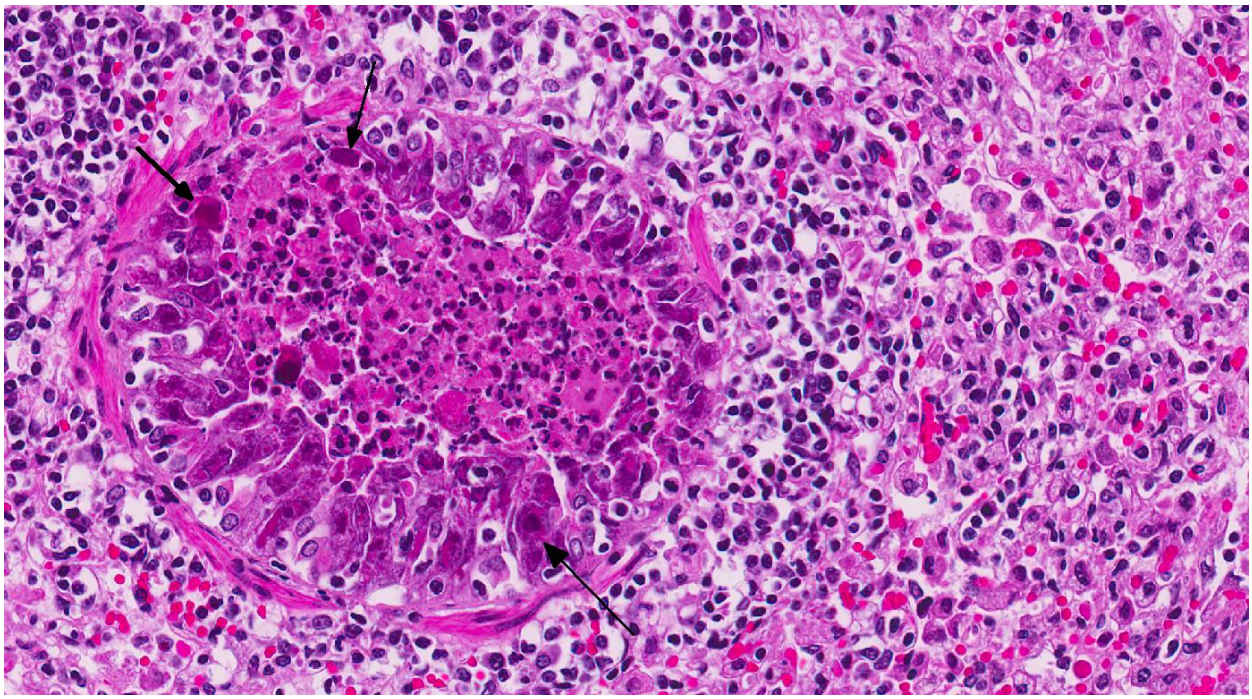

Lung, guinea pig. There is diffuse necrosis of airway epithelium. Necrotic epithelial cells are hypertrophic and nuclei are expanded by a deeply basophilic viral inclusion. (HE, 400X)

the vessels are distended and filled with numerous free erythrocytes (hyperemia). Multiple alveoli are collapsed (atelectasis).

The inclusions are typical for adenoviruses and the diagnosis was confirmed by subsequent transmission electron microscopy.

Contributor's Morphologic Diagnosis: Bronchitis and Bronchiolitis, diffuse, subacute, necro-suppurative, severe with epithelial amphophilic intranuclear inclusion bodies and mild acute bronchointerstitial pneumonia

Contributor's Comment: More than 100 antigenic types of adenoviruses have been identified that infect mammals and birds. In addition, there are 47 human adenovirus types are classified and five more candidate types are presently being studied.[2] The family of *Adenoviridae* is divided into four serological genera: *Mastadenovirus,* viruses that infect only mammalian species (e.g. human adenovirus 2); *Aviadenovirus*, viruses that infect only birds (e.g. fowl adenovirus 1); *Atadenovirus* that includes viruses with a wider host range, including snakes, lizards, ducks, goose, chickens, possums, and ruminants; *Siadenovirus*, which includes frog adenovirus 1 and turkey adenovirus 3, as well as several others of raptors, budgerigars, and tortoises.[3]

Adenovirus virions are non-enveloped, hexagonal, and have an icosahedral symmetry, 70-90 nm in diameter, with one (genus *Mastadenovirus*) or two (genus *Aviadenovirus*) fiber projections from each vertex of the capsid.[2,3]

The genome consists of a single linear molecule of double-stranded DNA, 26 to 45 kbp in size with inverted terminal repeats. Infection may be productive, abortive, or latent. In productive infections, the viral genome is transcribed in the nucleus, mRNA

is translated in the cytoplasm, and virions self-assemble in the nucleus. In latent infections and in transformed and tumor cells, viral DNA is integrated into the host genome.[2,3] Intranuclear inclusion bodies are formed, which contain numerous virions in paracrystalline arrays.[2,4]

Adenoviruses have a narrow host range and many adenoviruses cause persistent infections. Reactivation of a latent infection can take place by immunosuppression, e.g. Equine adenovirus causes severe disease in immunocompromised hosts.[3]

In dogs two types of canine adenoviruses are well known, type 1 and 2. Type 1 (CAdV-1) causes infectious canine hepatitis, a potentially fatal disease involving vasculitis and hepatitis. Type 1 infection can also cause respiratory and eye infections. Canine adenovirus 2 (CAdV-2) is one of the potential causes of kennel cough. Core vaccines for dogs include attenuated live CAdV-2, which produces immunity to CAdV-1 and CAdV-2. CAdV-1 was initially used in a vaccine for dogs, but corneal edema was a common complication.[3]

In horses, adenoviral infections are usually asymptomatic or cause a mild upper respiratory disease. In Arabian foals with a primary severe combined immunodeficiency disease, equine adenovirus 1 can cause bronchopneumonia and generalized disease, involving pneumonia and destruction of pancreatic and salivary gland tissue.[3]

In ruminants, bovine adenovirus-3 causes mild respiratory disease. Occasionally calves suffer from a severe respiratory or enteric disease.[3]

In sheep, adenoviral infections occasionally cause cytomegalic bronchiolar and alveolar epithelial cells similar to cytomegalovirus. Lambs can suffer from a severe respiratory or enteric disease.[3]

In non-human primates (NHPs) it can cause mild to moderately severe respiratory and enteric disease and keratitis/conjunctivitis.[3]

The avian adenoviral infections are divided into groups. Group I causes inclusion body hepatitis, respiratory and enteric infections in chickens, turkeys, and geese. Group II causes turkey hemorrhagic enteritis, marble spleen disease. And group III causes egg drop syndrome in chickens and ducks.[3]

In humans, an adenoviral infection causes a respiratory disease, pharyngitis, and follicular conjunctivitis.[3]

Some adenoviruses have shown to be oncogenic in laboratory animals. Cells from a number of rodent species and humans can be transformed in culture by adenoviruses. The frequency of malignant transformation is extremely low. Some adenoviruses, such as Ad2 and Ad5, have not been shown to be oncogenic in animals. Tumorigenic potential has been attributed to the capacity of some adenoviruses to turn off the expression of

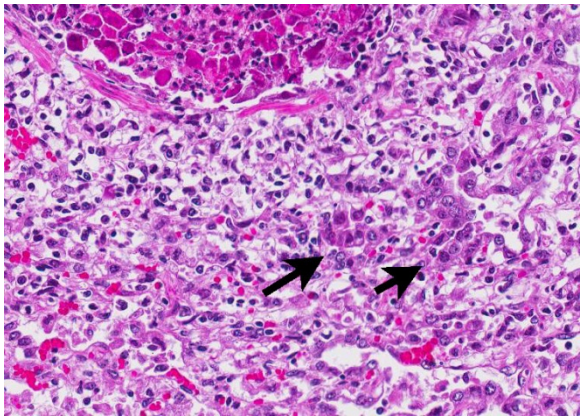

Lung, guinea pig. Alveolar septa in the adjacent parenchyma are expanded by fibrin and edema and often lined by type II epithelium. Alveolar spaces contain increased numbers of macrophages, as well as fibrin and edema.

genes of the major histocompatibility complex and thus to allow the transformed cells to overcome host defenses and grow into solid tumors. [2,5]

Viral pneumonia caused by adenovirus is one of the most common infections in breeding colonies and collections of guinea pigs. Guinea pigs are susceptible to a respiratory adenovirus that causes pulmonary disease and inclusions in respiratory epithelium. Guinea pig adenovirus (GPAdV-1) has been reported in Europe, North America, and Australia. The infection is characterized by a low morbidity, but drastically high (up to 100%) mortality rate.[1] Incubation time varies between 5 to 10 days. The animals die within 24 to 48 hours after showing the first clinical signs.[3] Clinical disease most often appears in young animals. Affected animals may show no clinical signs or can be severely dyspneic. The characteristic macroscopic lesions involve a consolidation of the cranial lobes of the lungs and hilus.[1,4]

A diagnosis may be confirmed by immunocytochemistry, serology, PCR, or the presence of adenoviral particles in affected cells by electron microscopy. Recently, a homotypic antigen has been developed using the GPAdV hexon gene incorporated into replication-defective adenovirus vector. This assay has proven to be more sensitive than the mouse adenovirus (MAV), which was used in the past for serological testing of GPAdV.[1]

JPC Diagnosis: Lung: Pneumonia, bronchointerstitial, necrosuppurative, multifocal, acute, severe with necrotizing bronchitis, type II pneumocyte hyperplasia and epithelial intranuclear inclusion bodies, Guinea pig, *Cavia porcellus*.

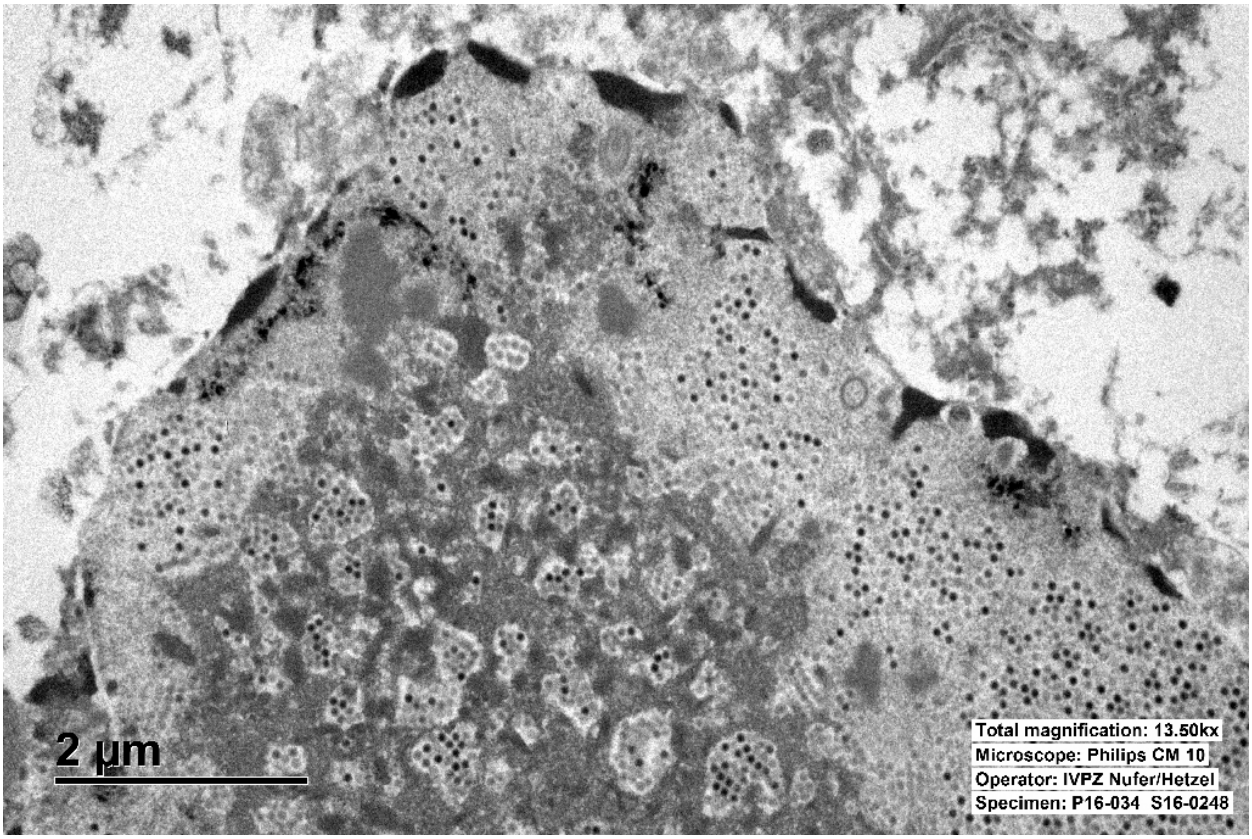

Lung, guinea pig. Electron micrograph of a bronchiolar epithelial cell nucleus showing crystalline arrays of hexagonal adenovirus virions. (Mag=13,500) (Photo courtesy of: Institute of Veterinary Pathology, Vetsuisse-Faculty (University of Zurich), Winterthurerstrasse 268, CH-8057 Zurich)

Conference Comment: The contributor provides a good summary of different adenoviruses in various affected species. As mentioned above, the most common adenoviral diseases of veterinary importance are the equine adenovirus-1 (inclusions within intestinal epithelial cells of SCID foals), canine adenovirus-1 (inclusions in hepatocytes and endothelial cells of puppies), canine adenovirus-2 (inclusions in alveolar macrophages of dogs with kennel cough), and adenoviral infection of rhesus macaques (inclusions in pancreatic acinar cells of non-human primates).[3] A novel adenovirus in domestic pigeons has recently been identified (pigeon adenovirus 2), however, it has not yet been implicated in causing clinical disease in this species.[6]

In this case, conference participants readily identified the prominent and highly characteristic intranuclear amphophilic inclusions within the exfoliating bronchial and bronchiolar epithelial cells, along with moderate to severe peribronchial leukocyte infiltration. Typically, adenoviruses are associated with prior immune suppression.[2,3] In Guinea pig adenoviral infection (GPAdV-1), the mortality rate in clinically affected animals is nearly 100%, with young and immunosuppressed animals being the most affected. Typical lesions have been observed in the airways of clinically normal animals, emphasizing the importance of immune suppression in this disease entity. Some participants posited that there may be a secondary bacterial infection that contributed to the pulmonary changes in this Guinea pig.[5] Viruses are known to damage the respiratory epithelium, which plays a role in the pathogenesis of bacterial pneumonia by inhibiting bacterial clearance and facilitating adhesion.[2,3,5] In this case, there is clear epithelial targeting of the bronchial and bronchiolar epithelium with

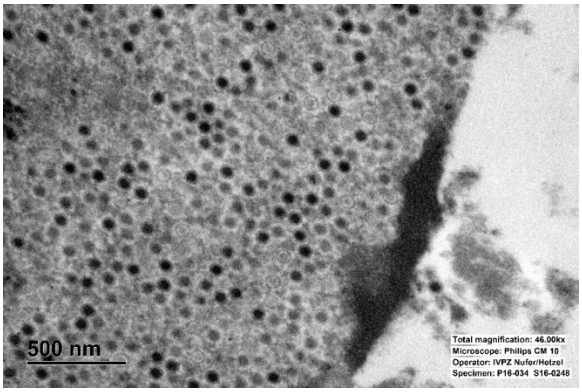

Lung, guinea pig. Hexagonal viral particles in lattice arrays are found in the nucleus and cytoplasm of bronchiolar epithelial cells. (Mag=46,000) (Photo courtesy of: Institute of Veterinary Pathology, Vetsuisse-Faculty (University of Zurich), Winterthurerstrasse 268, CH-8057 Zurich)

suppurative exudate filling airways and extending into the surrounding interstitium. However, no additional agents were detected by the contributor. Conference participants discussed the differentials for severe respiratory disease in Guinea pigs, including: parainfluenza virus, Guinea pig cytomegalovirus, and bacterial pneumonia of the lower respiratory tract, such as *Bordetella bronchiseptica*.[5] Definitive diagnosis is made by immunohisto-chemistry, PCR, or the demonstration of the adenovirus particles in affected cells by transmission electron microscopy (TEM).[5]

Ultrastructurally, adenoviral inclusions are composed of prominent intranuclear paracrystalline arrays of virions and unassembled viral capsid proteins, demonstrated nicely by the TEM image provided by the contributor. Adenovirus is not the only virus that will form hexagonal paracrystalline arrays in affected tissue. Conference participants discussed other viruses that form ultrastructural para-crystalline arrays. These include poly-omavirus, papillomavirus, picornavirus, iridovirus, and circovirus.[3]

Contributing Institution:
Institute of Veterinary Pathology
Vetsuisse Fakultät
Universität Zürich
Winterthurerstrasse 268
CH-8057 Zürich
http://www.vet.uzh.ch/en.html

References:

1. Butz N, Ossent P, Homberger FR. Pathogenesis of Guinea pig adenovirus infection. *Lab Anim Sci*. 1999; 49(6):600-604.
2. Doerfler W. Adenoviruses. In: Baron S, ed. *Medical Microbiology*. 4th ed. Galveston (TX): University of Texas Medical Branch at Galveston; 1996. Chapter 67.
3. Fenner FJ, Gibbs E, Paul J, Murphy FA. et al. In: *Veterinary Virology*. 2nd ed. Academic Press, Inc.; 1993:203-212.
4. Naumann, S., Kunstyr, I., Langer, I., Maess, J., Horning, R. Lethal pneumonia in Guinea pigs associated with a virus. *Lab Anim*. 1981; 15:235- 242.
5. Percy DH, Barthold SW. Guinea pig. In: *Pathology of Laboratory Rodents and Rabbits*, 4th ed., Ames, IA: Blackwell Publishing; 2016:218-219.
6. Teske L, Rubbenstroth D, et al. Identification of a novel aviadenovirus, designated pigeon adenovirus 2 in domestic pigeons (*Columba livia*). *Virus Res*. 2016; 227:15-22, [Epub ahead of print].
7. Yabe Y, Samper L., Bryan E., Taylor G., Trentin J. Oncogenic Effect of Human Adenovirus Type 12, in Mice. *Science*. 2003;03:46-47.

CASE IV: 15144 (JPC 4084218).

Signalment: Two-month-old male African green monkey (*Chlorocebus aethiops sabaeus*).

History: This animal was found dead in the enclosure on the morning of the day of necropsy.

Gross Pathology: Approximately 75% of the left and 50% of the right lung lobes were replaced by randomly scattered, multifocal to coalescing, umbilicated, 3x3x3 mm to 1.5x3x2cm, firm, off-white to tan nodules, surrounded by 1-5 mm wide dark red zones. The remainder of the left lung was dark red, heavy and wet, and the lateral aspect was adhered to the adjacent costal pleura. Neither side collapsed upon opening the thoracic cavity, and the left lung sank in formalin.

Laboratory results: Aerobic bacterial culture positive for *Yersinia enterocolitica.*

Histopathologic Description: Most of the architecture is effaced and replaced by fragmented eosinophilic cellular and karyorrhectic to streaming nuclear debris (necrosis), innumerable neutrophils, many degenerate, and large foamy macrophages. Colonies of small bacterial rods are prominent in areas of necrosis. The wall of the left bronchus is transmurally effaced by similar necrotic inflammatory exudate which extends into the lumen and also lies within

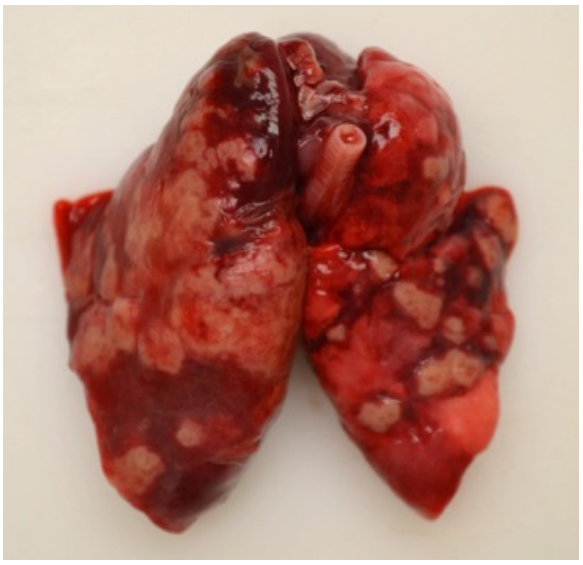

Lung, African green monkey. The pulmonary parenchyma is replaced by multifocal to coalescing, umbilicated, tan nodules. (Photo courtesy of: Wake Forest School of Medicine, Section on Comparative Medicine, Medical Center Boulevard \ Winston-Salem, NC 27157 www.wakehealth.edu)

adjacent bronchioles. The remaining alveolar spaces are filled with homogeneous proteinaceous material (edema fluid), frequent neutrophils and foamy alveolar macrophages. Connective tissue fibers surrounding the pulmonary vasculature are separated by clear space (edema).

Contributor's Morphologic Diagnosis: Pneumonia, multifocal, chronic, severe, necrotizing with bacilli (consistent with *Yersinia enterocolitica*).

Contributor's Comment: *Yersinia enterocolitica* is a short gram-negative bacillus within the family *Entero-bacteriaceae*. It is an important food-borne pathogen that is commonly found in the gastrointestinal tract of humans and other species. Pigs and rodents are sources of human infection, and transmission occurs through contaminated food and water. This pathogen most often produces necrotizing gastrointestinal lesions with large colonies of bacteria in humans and animals, but can also affect the urinary, respiratory, musculo-skeletal, integumentary and cardiovascular systems in humans.[1,7]

Yersinia enterocolitica is classified into 6 biotypes and 57O group strains. Among the 6 biotypes, all except the 1A biotype (1B and 2-5) are pathogenic. 1B/O:8, 2/O:5, 2/O:9, 3/O:3 and 4/O:3 are most commonly isolated from humans. 1B/O:8 is considered the "new world" strain and is highly pathogenic to humans and predominantly present in the United States, while 4/O:3 and 2/O:9 are found in the Europe and Asia. Strain 4/O:3 has frequently been isolated from pigs and 1B/O:8 has been isolated from rodents. [1,3,7]

Pathogenic strains of *Y. enterocolitica*

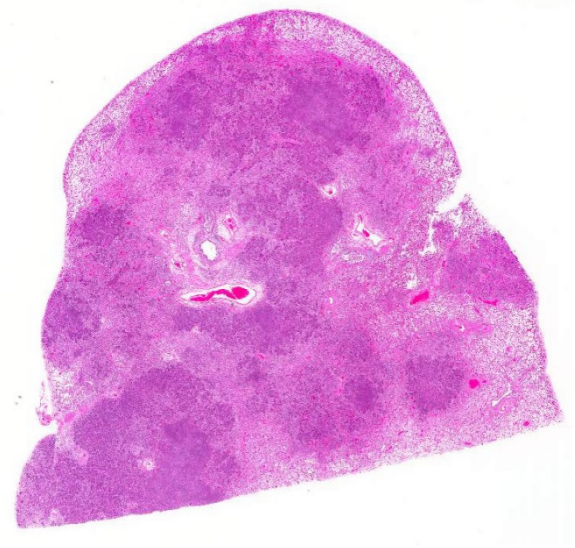

Lung, African green monkey. Approximately 80% of the pulmonary parenchyma is effaced by coalescing areas of lytic necrosis. (HE, 4X)

contain the virulence plasmid pYV/pCD which encodes *Yersinia* adhesin A (yadA), Ysc-Yop type III secretion system (TTSS), chromosomally encoded virulence genes ail, myfA, ystA, ysa, and the high pathogenicity island (HPI-) that aids in iron acquisition. The expression of virulence genes depends on temperature and calcium availability *in-vivo*. Virulence proteins produced by PYV plasmid resist phagocytic killing and complement mediated lysis of the bacteria by the host.

Successful infection begins with colonization of the distal small intestinal mucosa. Attachment and entry into the intestinal epithelial cells are facilitated by yadA and *INV*, respectively. Upon entering the epithelial cells the bacteria preferentially enter M cells in the Peyer's patches where macrophages internalize them and transport them to the mesenteric lymph nodes (MLN).

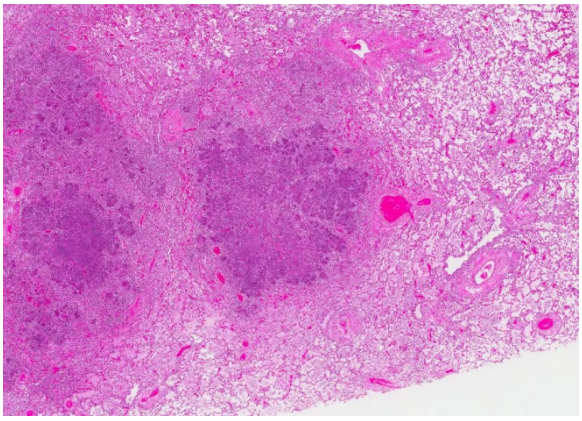

Lung. African green monkey. Higher magnification of areas of lytic necrosis and surrounding parenchyma.

Yersinia bacteria multiply within the macrophages and also extracellularly in the lymphoid organs leading to abscess formation, often bacteremia and frequently, hepatitis. [1,3,7]

This case was the first in an outbreak involving more than 20 *Y. enterocolitica* fatalities in 2015 – 2016, and was unique in that the pneumonia occurred in the absence of intestinal and MLN lesions. The finding of necrotizing tracheitis and large airway orientation in the lung suggests a respiratory route of infection. Some reports in humans have also suggested primary infection by inhalation, without gastrointestinal involvement. [2,9]

JPC Diagnosis: Lung: Pneumonia, necrosuppurative, multifocal to coalescing, subacute, severe, with fibrin thrombi, hemorrhage, edema, and numerous colonies of coccobacilli, African green monkey, *Chlorocebus aethiops sabaeus*.

Conference Comment: The contributor provides a rare case of pneumonia caused by *Yersinia enterocolitica* in an African green monkey, as well as an excellent discussion of the virulence factors and pathogenesis of the bacterium. Despite the highly usual presentation, this case illustrates the characteristic appearance of the gram-negative coccobacilli forming multifocal to coalescing bacterial microcolonies surrounded by intense infiltrates of viable and degenerate neutrophils and necrotic cellular debris filling and replacing pulmonary architecture. *Yersinia* sp. Micro-colonies are readily distinguishable from other large colony-forming bacteria such as *Actinomyces, Actinobacillus, Coryne-*

bacterium, *Staphylococcus* and *Streptococcus* spp.[9] Other species of *Yersinia (pseudotuberculosis* and *pestis*) have the same histologic appearance in tissue section as is present in this case.

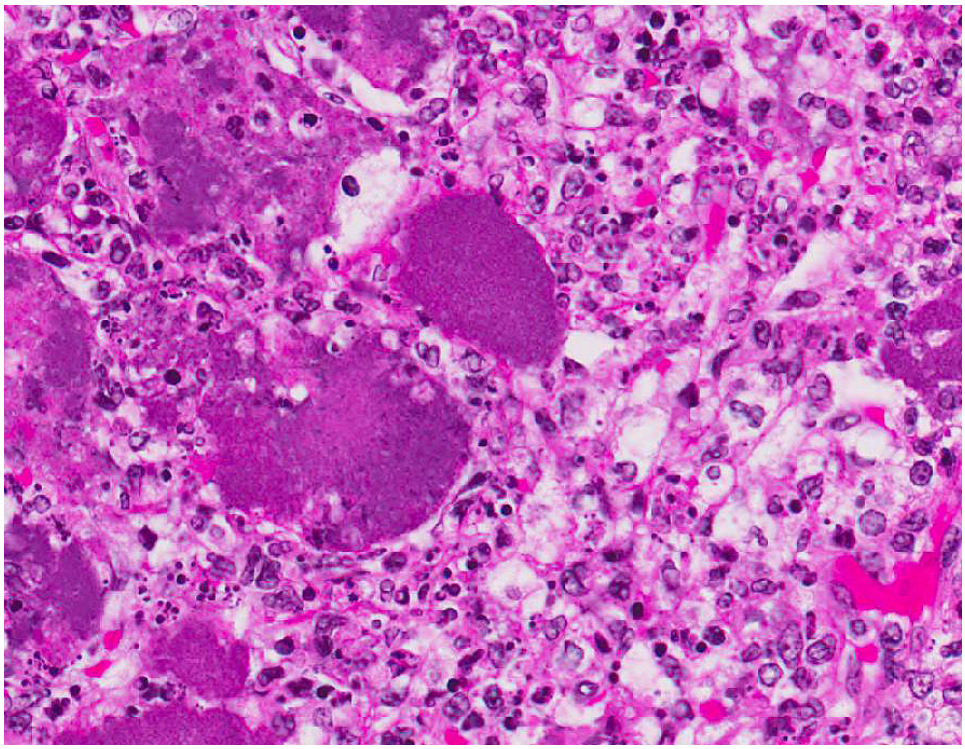

Lung, African green monkey. Areas of lytic necrosis contain large colonies of coccobacilli admixed with numerous degenerate neutrophils admixed with abundant cellular debris. (HE, 400X)

Speciation of the bacteria requires culture or bacterial isolation.[1,9]

Yersinia enterocolitica has a worldwide distribution and affects a many different animal species and humans.[1,2,7,9] As mentioned by the contributor, the most common mode of transmission is caused by foodborne outbreaks in humans. In nonhuman primates, infections are typically acquired by the fecal-oral route.[8,9] The organism can be shed in the feces by asymptomatic animals in the collection, as well as by rodents and birds in the environment where it can survive and grow at low temperatures. Disease is often secondary to stress, poor nutrition, environmental flooding, and cold weather.[9] The contributor suggests that the route of infection for this animal is via inhalation of the organism, perhaps via aerosolized feces, causing the development of necrotizing tracheitis and pneumonia without gastrointestinal lesions.

Many conference participants noted the presence of numerous large fibrin thrombi within peribronchial veins and lymphatic vessels. Gram-negative bacteria, such as *Yersinia* spp, commonly cause sepsis and its associated coagulopathy. During gram-negative septic shock, lipopolysaccharide (LPS, endotoxin) induces increased tissue factor (TF) and factor XII expression.[4,5,6] TF (factor III) then forms a complex with plasma factor VII as part of the extrinsic coagulation pathway. This complex activates factor X of the common pathway and factor IX of the intrinsic pathway, leading to the formation of thrombin (factor II) which generates fibrin from fibrinogen (factor I). Fibrin is cross-linked and polymerized via factor XIII

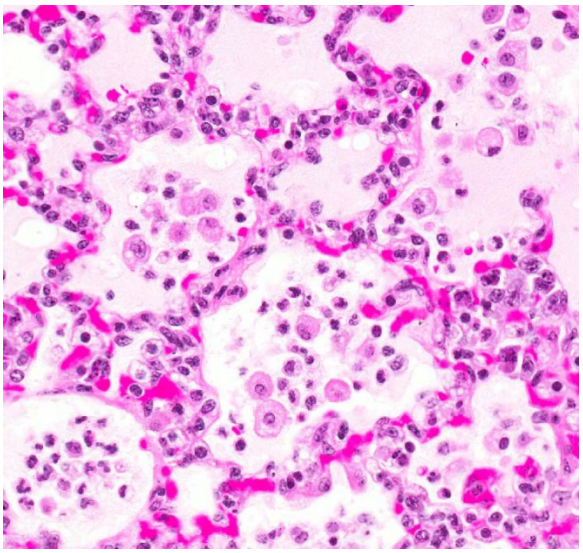

Lung, African green monkey. Alveoli within the remaining lung contains abundant edema and moderate numbers of macrophages and neutrophils. Alveolar septa are expanded by edema, and circulating neutrophils and macrophages. (HE, 400X)

and deposited as a fibrin clot. During sepsis, procoagulant activity predominates over anticoagulation and fibrinolysis due to inhibition of tissue factor pathway inhibitor (TFPI), thrombomodulin, and protein C as well as activation of plasminogen activator inhibitor (PAI-1), and previously mentioned TF.[5,6] This leads to disseminated intravascular coagulation (DIC) and exuberant fibrin deposition. DIC eventually consumes critical blood-clotting factors leading to hemorrhage and shock.[5,6] However, a recent study in mice has shown that fibrin can also perform critical protective functions during infection with *Yersinia enterocolitica*. These studies suggest that fibrin may be an attempt by the host to physically trap bacteria limiting dissemination, in addition to facilitating the recruitment and activation of neutrophils and macrophages within infected tissues via interleukin 6 (IL-6) and monocyte chemotactic protein-1 (MCP-1).[5] In fact, mice treated with the anticoagulant warfarin prior to inoculation with *Yersinia enterocolitica* had a markedly higher systemic bacterial burden and shortened survival time compared to untreated mice.[5]

Contributing Institution:

Wake Forest School of Medicine Department of Pathology, Section on Comparative Medicine, Medical Center Boulevard, Winston-Salem, NC 27157 www.wakehealth.edu

References:

1 Galindo CL, Rosenzweig JA, Kirtley ML, Chopra AK. Pathogenesis of *Y. enterocolitica* and *Y. pseudo-tuberculosis* in human yersiniosis. *J Pathog* 2011; 2011:182051.

2 Hosaka S, Uchiyama M, Ishikawa M, Akahoshi T, Kondo H, Shimauchi C, et al. *Yersinia entero-colitica* serotype O:8 septicemia in an otherwise healthy adult: analysis of chromosome DNA pattern by pulsed-field gel electrophoresis. *J Clin Microbiol* 1997; 35(12):3346-3347.

3 Kay BA, Wachsmuth K, Gemski P, Feeley JC, Quan TJ, Brenner DJ. Virulence and phenotypic characterization of *Yersinia enterocolitica* isolated from humans in the United States. *J Clin Microbiol* 1983; 17(1):128-138.

4 Kumar V, Abbas AK, Fausto N. Hemodynamic Disorders, Thromboembolic Disease, and Shock. In: *Robbins and Cotran Pathologic Basis of Disease*. 9th ed.

Philadelphia, PA:Elsevier Saunders; 2015:117-134.
5 Luo D, Szaba FM, Kummer LW, et al. Protective roles for fibrin, tissue factor, plasminogen activator inhibitor-1, and thrombin activatable fibrinolysis inhibitor, but not factor XI, during defense against the gram-negative bacterium *Yersinia enterocolitica*. *J Immunol*. 2011; 187(4):1866-1876.
6 Mosier DA. Vascular disorders and thrombosis. In: McGavin, MD, ed. *Pathologic Basis of Veterinary Disease*. 6th ed. St. Louis, MO:Elsevier; 2017:51-72.
7 Sabina Y, Rahman A, Ray RC, Montet D: *Yersinia enterocolitica*: Mode of transmission, molecular insights of virulence, and pathogenesis of infection. *J Pathol*. 2011; 2011:429069.
8 Simmons J, Gibson S. Bacterial and mycotic disease of nonhuman primates. In: Abee CR, Mansfield K, Tardif S, Morris T eds. *Nonhuman Primates in Biomedical Research: Diseases*. Vol 2. 2nd ed. Philadelphia, PA: Elsevier; 2012:138-140.
9 Wong KK, Fistek M, Watkins RR. Community-acquired pneumonia caused by *Yersinia enterocolitica* in an immunocompetent patient. *J Med Microbiol* 2013; 62(4):650-651.
10 Uzal FA, Plattner BL, Hostetter JM. Alimentary system In: Maxie MG, ed. *Jubb, Kennedy, and Palmer's Pathology of Domestic Animals*. Vol 2. 6th ed. Philadelphia, PA: Elsevier; 2016:176-177.

Self-Assessment - WSC 2016-2017 Conference 8

1. *Rhinosporidium seeberi* is currently classified as a:
    a. Fungus
    b. Mesomycetozoan
    c. Cyanobacterium
    d. Protozoan

2. Porcine circovirus-2 has NOT been associated with which of the following disease complexes?
    a. Post-weaning multisystemic wasting syndrome
    b. Exudative diasthesis
    c. Porcine dermatitis and nephropathy syndrome
    d. PCV-2 associated enteritis

3. Which of the following is true about guinea pig adenovirual pneumonia?
    a. It is most often seen in older animals
    b. It causes inclusions in endothelial cells and profound hemorrhage into alveoli
    c. The characteristic macroscopic lesion involve consolidation of the cranial lobes of the lungs and hilus.
    d. The disease is characterized by a high morbidity and low mortality.
    e.
4. Which of the following is not true concerning *Yersinia enterocolitica*?
    a. It is a short gram-negative rod within the family *Enterobacteriaceae.*
    b. Rodents and small ruminants are sources of human infection.
    c. Expression of virulence proteins depends on temperature and calcium availability in vivo.
    d. Virulence proteins produced by the PYV plasmid resist phagocytic killing and complement-mediated lysis of the bacteria.

5. Which of the following is not true concerning yersinial infections?
    a. Infection is usually fecal-oral.
    b. *Yersinia* can survive and grow at extremely high temperatures.
    c. The organism is often shed by asymptomatic hosts.
    d. The presence of extensive fibrin in yersinial infection may be protective for the host.

Joint Pathology Center

Veterinary Pathology Services

WEDNESDAY SLIDE CONFERENCE 2016-2017

C o n f e r e n c e 9

2 November 2016

Victoria Hoffmann, VMD, DACVP
Division of Veterinary Resources
National Institutes of Health
Bethesda, MD

CASE I: 14L-2800B (JPC 4066544).

Signalment: Adult, female, European rabbit (*Oryctolagus cuniculus*).

History: A member of the public found the collapsed rabbit in a field close to their home and presented it to the local veterinary practice where the rabbit was euthanized on humane grounds.

Gross Pathology: The eyelids were bilaterally severely swollen with an exudate lightly adhered to the surface. The nostrils had a bilateral discharge. The vulva was severely swollen.

Laboratory results: N/A

Histopathologic Description: The slide consists of a section of haired skin and vulva including mucocutaneous junction. There is diffuse moderate to severe hyperplasia of the mucosal epithelium. Multifocally epithelial cells throughout all the layers of the epithelium are enlarged, often degenerate, with clear intracytoplasmic spaces (intracellular edema). Often,

epidermal cells contain large, approximately 15 to 20 µm diameter, round to oval, homogenous, brightly eosinophilic cytoplasmic inclusions. The same inclusions may also be observed in sloughed epithelial cells and within the thickened stratum corneum showing moderate orthokeratotic hyperkeratosis. Randomly scattered throughout the epidermis there are

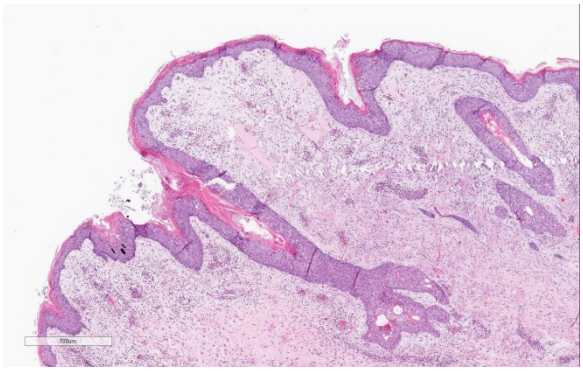

Vulva, mucocutaneous junction, rabbit. The epidermis is markedly and diffusely hyperplastic and there is overlying moderate orthokeratotic hyperkeratosis. The dermis is expanded by edema and is hypercellular. (HE, 4X)

occasional keratinocytes with hyper-eosinophilic cytoplasm and karyorrhectic nuclei (single cell necrosis). There are diffusely scattered basophilic granules within keratinocytes (keratohyaline granules) of the stratum granulosum and rarely deep within the stratum basale (dyskeratosis). Multifocally, the epithelial cells of the vaginal mucosa are expanded by a single large clear vacuole (intracellular edema / ballooning degeneration).

Diffusely the lamina propria is characterized by a loosely arranged slightly basophilic myxoid matrix admixed with edematous areas. Multifocally in the dermis there are plump elongated to polygonal fibroblasts with stellate processes. These cells have finely granular basophilic cytoplasm, a single distinct, round to elongate and centrally placed large nucleus with finely stippled chromatin and a single evident nucleolus. Anisocytosis and anisokaryosis are moderate and mitotic figures are rare.

Within the superficial dermis and surrounding the blood vessels in the deeper dermis there are moderate, multifocal to coalescing aggregates of lymphocytes, plasma cells, heterophils, and macrophages. Occasionally, in the superficial dermis, the inflammatory process is predominately heterophilic.

Contributor's Morphologic Diagnosis: 1. Vulva, mucocutaneous junction: Diffuse, subacute, moderate to severe epidermal hyperplasia with intracellular edema and intracytoplasmic viral inclusions.

2. Vulva, mucocutaneous junction: Multifocal to coalescing, subacute, moderate lymphoplasmacytic and heterophilic proliferative dermatitis and sub-mucosal proliferation with diffuse myxoid changes and edema.

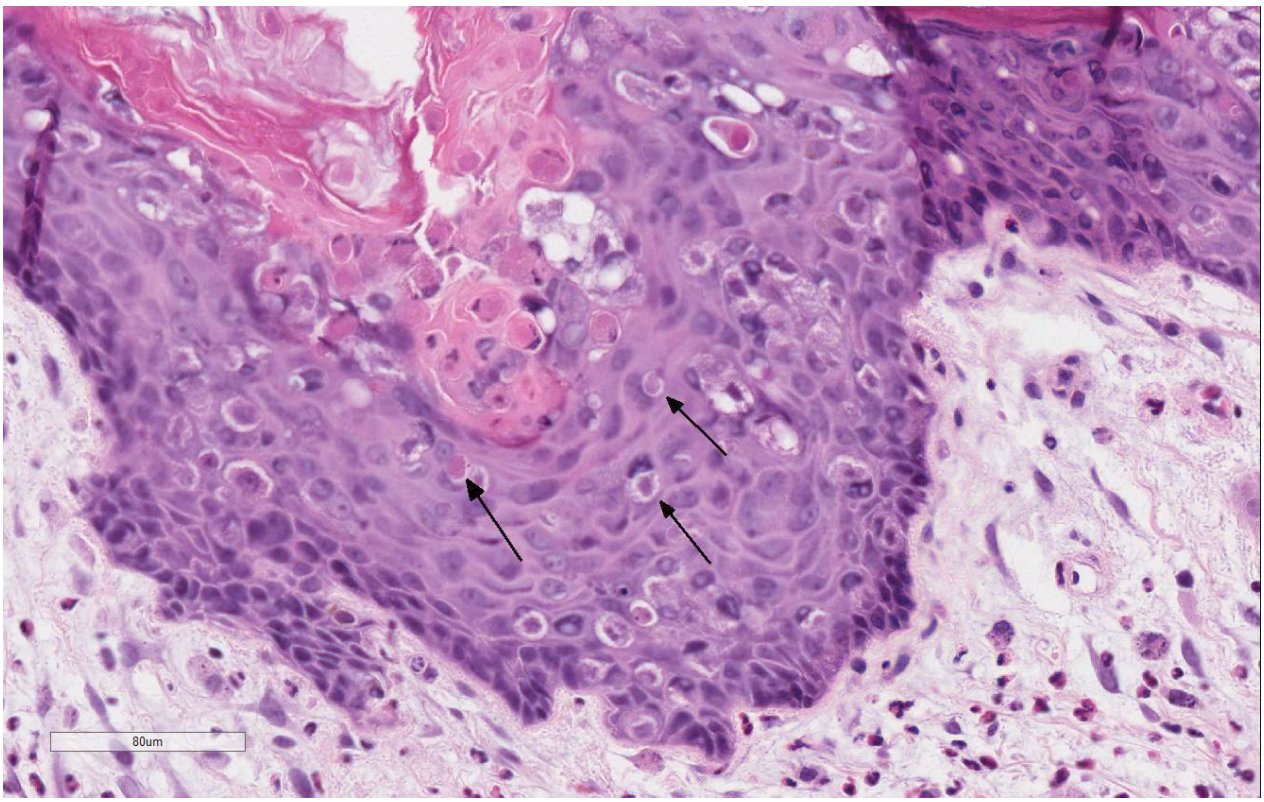

Vulva, rabbit. Scattered keratinocytes at all level of the epidermis contain 2-4um round eosinophilic viral inclusions (arrows), and multifocally, variable degrees of intracytoplasmic edema (ballooning degeneration) or apotptosis. (HE, 296X)

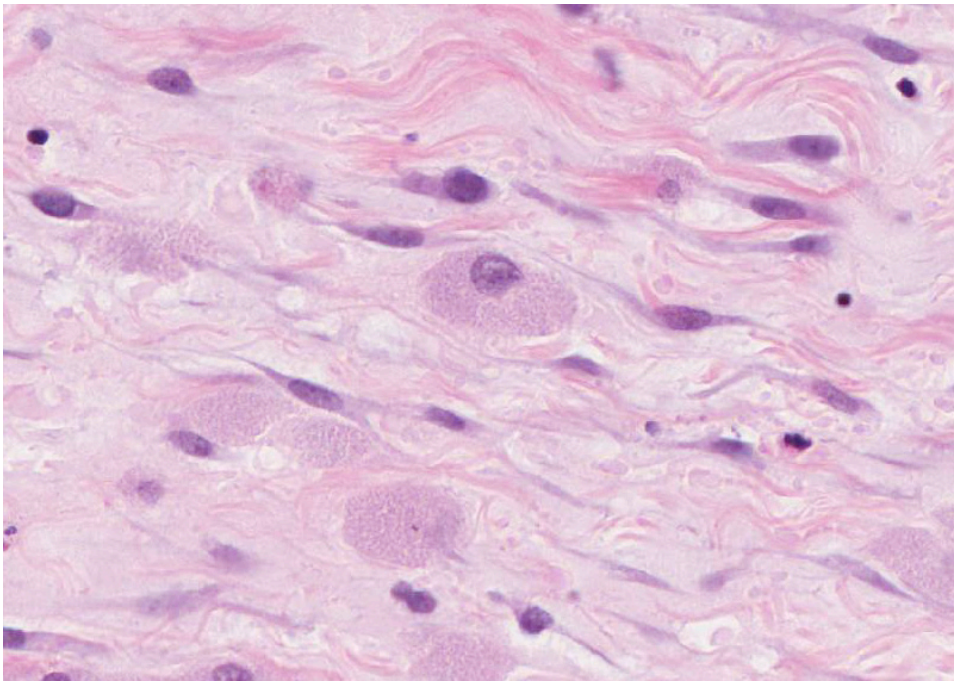

Vulva, rabbit. The dermis is markedly edematous and contains numerous polygonal "myxoma" cells with abundant granular amphophilic cytoplasm and anisokaryotic nuclei. (HE, 332X)

Contributor's Comment: Myxomatosis is a common, worldwide distribution disease of rabbits and is now endemic in the wild rabbit population in Europe. Hares may be carriers of the infection but very rarely exhibit clinical signs.[2] Originally myxomatosis was introduced in Europe to control the wild rabbit population.[9] Initially the disease had a very high mortality rate, but due to natural selection the wild rabbit population began to develop immunity to the disease and mortality rate is now approximately 25% in the European rabbits.[9]

Myxomatosis is caused by the Myxoma virus, a leporipoxvirus from the family of poxviruses.[6] Transmission of the virus requires a mosquito or flea vector, but it is possible for the virus to spread by direct contact. Due to transmission routes, domestic rabbits, especially the ones kept outdoors are at risk of contracting the virus from the wild rabbit population and therefore a vaccine has been developed.

There are two recognized forms of the disease: the classical, nodular form (as in this case); and the respiratory, amyxomatous form of the disease. The nodular form is often transmitted by vector route and causes the classical swelling of the eyelids, nodules over the skin, and edema of the genitalia. Usually, there is ocular and nasal discharge associated with the disease. The infection causes a severe depression of the host's immune system causing secondary infections to take hold and often the secondary infections are the ultimate cause of death. The amyxomatous form is usually due to a mild or attenuated strain of the virus;[6] this causes respiratory signs and rarely nodular lesions.

Other skin disease that may be confused for myxomatosis is Shope fibroma caused by the rabbit Shope fibroma virus (SFV, Leporipoxvirus). Shope fibroma virus induces discrete fibromas usually restricted to the distal limbs but occasionally may be found in the head.

JPC Diagnosis: Mucocutaneous junction, vulva: Atypical mesenchymal proliferation, diffuse, moderate, with epithelial and epidermal hyperplasia, ballooning degeneration, lymphoplasmacytic and heterophilic dermatitis, and epithelial intracytoplasmic eosinophilic inclusions, European rabbit, *Oryctolagus cuniculus*.

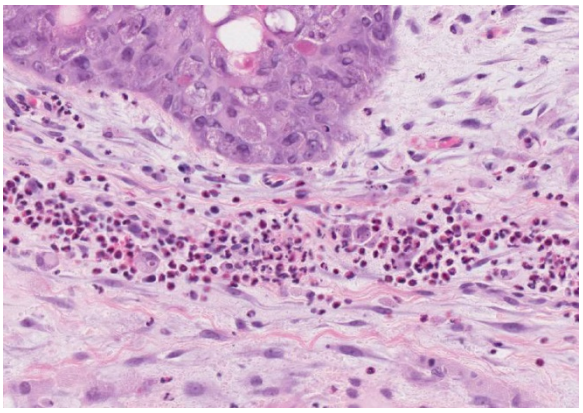

Vulva, rabbit. Superficial dermal vessels are surrounded by large numbers of heterophils which occasionally form dermal aggregates beneath the hyperplastic epidermis. (HE, 176X)

Conference Comment: Poxviruses are a large family of epitheliotropic double-stranded DNA viruses that cause several important cutaneous and systemic lesions in wild and domestic mammals, birds, and humans.[8] Most poxviruses cause a mild localized cutaneous lesion, but some can cause generalized systemic and fatal disease. An example of the latter is the rabbit myxoma virus, a member of the genus *Leporipoxvirus*, which can cause up to 90% mortality in naïve susceptible strains of wild rabbits.[2,8,9] However, through natural selection, genetically resistant strains of wild rabbits now have only about 25% mortality when infected with virulent strains of the virus in endemic areas.[9] Readers are encouraged to review 2012 Wednesday Slide Conference #2 Case 2 for a brief review of the fascinating history of this virus, and its use during attempted European rabbit (*Oryctolagus cuniculus*) eradication programs in Australia and France in the early 1950's.

Following inoculation, typically by an arthropod vector, susceptible rabbits develop localized skin tumors resembling fibromas caused by the rabbit (Shope) fibroma virus discussed above by the contributor.[3,9] Other characteristic gross lesions are pronounced gelatinous subcutaneous edema surrounding mucocutaneous junctions. In this case, the contributor noted severe swelling around the eyelids and vulva with nasal discharge grossly.[9]

While the microscopic staining of the tissue section of vulva is somewhat pale, this case nicely illustrates the classic histologic poxviral epithelial intracytoplasmic inclusions and ballooning degeneration.[8] In addition, there is a subepithelial proliferation of large stellate mesenchymal cells within a homogenous mucinous matrix. Conference participants also noted a moderate lymphoplasmacytic inflammatory infiltrate admixed with the atypical mesenchymal cells. In addition to being epitheliotropic, the myxoma virus is T-lymphocytotrophic and systemic spread occurs via lymphocytes and monocytes to draining lymph nodes.[9] Myxoma stellate cells are typically present in lymph nodes, bone marrow, spleen, and centrilobular areas of the liver. Degenerative and necrotizing lesions are usually confined to the lymphoid tissue in lymph nodes, lungs, and spleen with lymphoid depletion, particularly in the T-cell zones.[9]

Recently, there has been a great deal of interest in the rabbit myxoma virus as one of the promising new oncolytic viruses used in virotherapy for human cancer. Oncolytic viruses are engineered to preferentially infect and kill cancer cells while sparing normal host cells.[4,7] Several other oncolytic viruses originated from human pathogens (herpes simplex-1, measles, etc) and still retain some ability to replicate in normal host tissue. Myxoma virus is attractive to researchers because its pathogenicity is restricted to lagomorphs and thus it will not replicate or kill normal human host cells; but the virus does have significant oncolytic potential for a large variety of neoplasms in several animal species and humans.[4,7]

Contributing Institution:

University of Liverpool
Department of Veterinary Pathology, Leahurst Campus,
Chester High Road
Neston, England, United Kingdom
https://www.liv.ac.uk/vetpathology/

References:

1. Bangari DS, Miller MA, Stevenson GW, et. al. Cutaneous and systemic poxviral disease in red (*Tamiasciurus hudsonicus*) and gray (*Sciurus carolinensis*) squirrels. *Vet* Patho.l 2009; 46:667-672.
2. Barlow A., et al. Confirmation of myxomatosis in a European brown hare in Great Britain. *Vet Rec*. 2014; 175(3):75-6.
3. Berto-Moran A, Pacios I, Serrano E, Moreno S, Rouco C. Coccidian and nematode infections influence prevalence of antibody to myxoma and rabbit hemorrhagic disease viruses in European rabbits. *J Wildl Dis*. 2013; 49(1):10-17.
4. Chan WM, McFadden G. Oncolytic poxviruses. *Annu Rev Virol*. 2014; 1:119-141.
5. DiGiacomo RF, Mare CJ. Viral diseases. In: Manning PJ, Ringler DH, Newcomer CE, eds. *The Biology of the Laboratory Rabbit.* 2nd ed. San Diego, CA: Academic Press; 1994:178-180.
6. Kerr, P.J., et al., Myxoma virus and the Leporipoxviruses: An evolutionary paradigm. *Viruses*. 2015; **7**(3):1020-61.
7. Kinn VG, Hilgenberg VA, MacNeill AL. Myxoma virus therapy for human embryonal rhabdo-myosarcoma in a nude mouse model. *Oncolytic Virother*. 2016; 5:59-71.
8. Mauldin E, Peters-Kennedy J. Integumentary system. In: Maxie MG, ed. *Jubb, Kennedy, and Palmer's Pathology of Domestic Animals*. Vol 1. 6th ed. Philadelphia, PA:Elsevier; 2016:616-625.
9. Percy DH, Barthold SW. *Pathology of Laboratory Rodents and Rabbits*. rd ed. Ames, IA: Blackwell Publishing; 2016:261-263.

CASE II: DX16-0081 (JPC 4084542).

Signalment: Four-month-old female NOD.*Cg-Prkdc*^{scid}*Il2rg*^{tm1Wjl}/SzJ mouse, (*Mus musculus*).

History: Animal presented moribund after receiving a xenotransplant.

Gross Pathology: Discolored nodules were visible on the kidney. Secondary lymphoid tissues were markedly reduced in size consistent with the phenotype of the strain.

Laboratory results: Microbiology, Aerobic bacterial culture of both tympanic bullae:

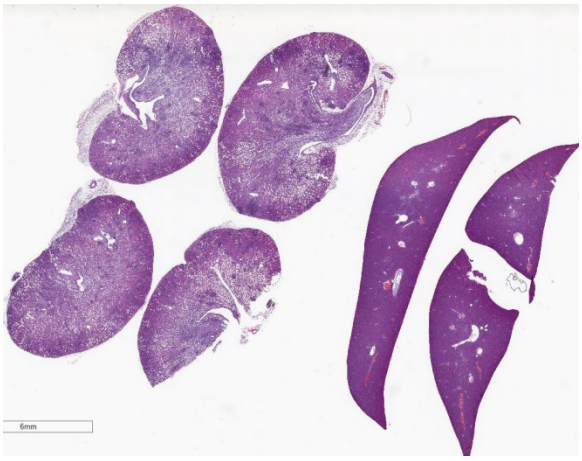

Kidney and liver, NOD mouse. The bisected kidneys show randomly scattered foci of cellular inflammation within the cortex and medulla. (HE, 5X)

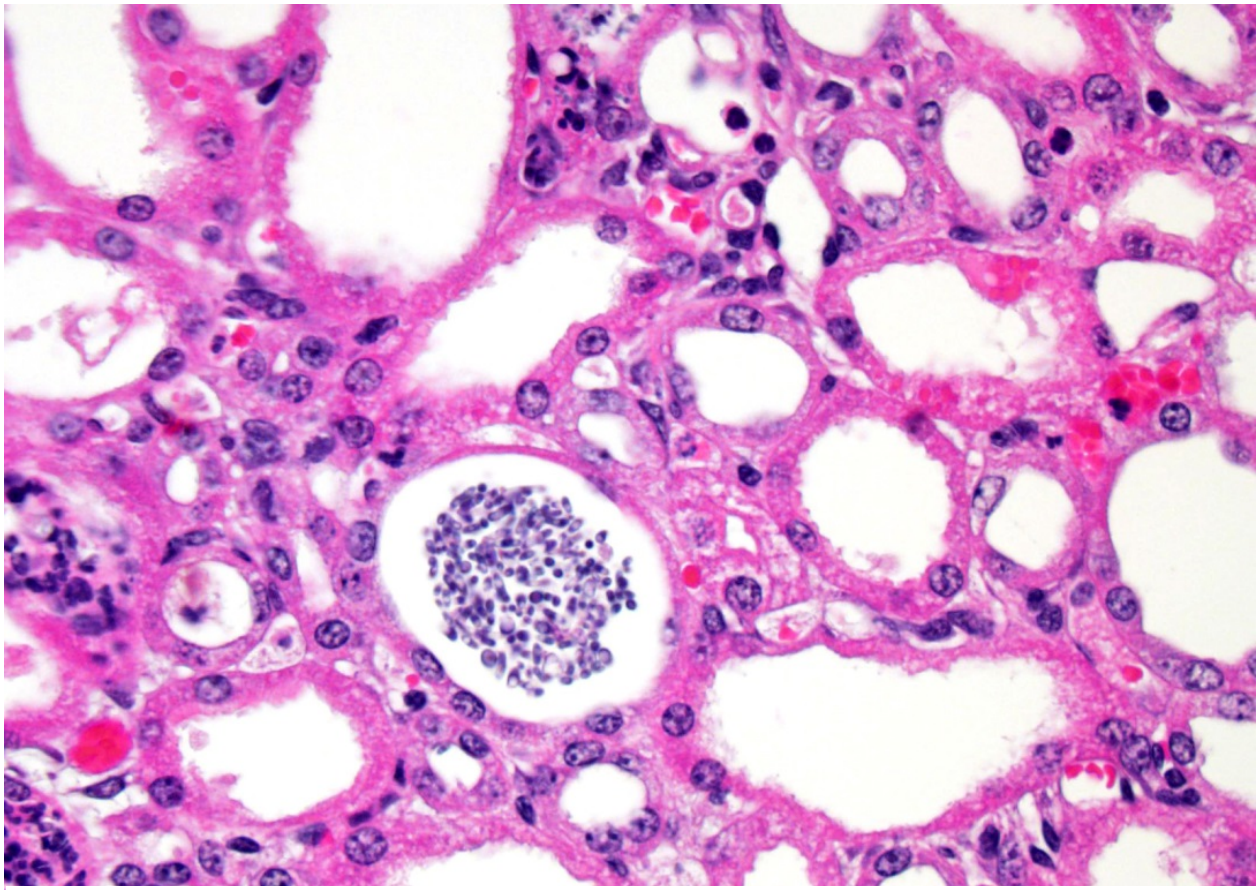

Kidney, NOD mouse. Numerous tubules contain large numbers of 3-6um thin-walled yeasts (blastospores). (HE, 400X)

Klebsiella pneumonia.

Microbiology, Aerobic bacterial culture of blood: *Staphylococcus xylosus*.

Histopathologic Description: There is marked, multifocal to coalescing neutrophilic inflammation and necrosis arranged in an embolic pattern and which distorts the overall structure of the kidneys as viewed subgrossly. Inflammation is centered on 0.5um wide X 8.0-10.0uM long fungal organisms that form non-branching hyphae and pseudohyphae. Organisms and the accompanying inflammatory response involve predominately vascular and perivascular, interstitial spaces and the tubules with limited extension into the kidney parenchyma. Affected renal tubules are variably ectatic and contain combinations of serocellular debris and acellular eosinophilic material. The renal interstitium is variably expanded by inflammation and reactive fibroblasts, especially where inflammation is present. The adjacent sections of liver are unremarkable.

Yeast forms are also observed in the following locations: Both ears, heart, and the stomach.

Contributor's Morphologic Diagnosis: Kidney: Tubulointerstitial nephritis, suppurative, bilateral, acute, severe with intratubular fungal organisms most consistent morphologically with *Candida albicans*.

Contributor's Comment: Non-obese diabetic (NOD)/severe combined immune

deficiency (SCID)/IL2rγnull (NSG) mice represent a severely immunocompromised mouse strain that is an important tool for xenotransplantation studies using patient-derived tissues. This strain is deficient in mature B cells, mature T cells, and natural killer (NK) cells. Additionally, macrophages and dendritic cells are defective regarding their functions.[5] While the severe immunodeficiency trait of the strain is useful for avoiding immune-mediated host rejection of foreign cells, this compromised status leaves NSG mice susceptible to a number of opportunistic pathogens. Three commonly encountered opportunistic pathogens of immuno-compromised laboratory mice are either observed in tissue lesions or are isolated from body fluids of this NSG mouse including *Candida albicans, K. pneumoniae* and *S. xylosus*.

Candida albicans, the organism observed in the renal lesions, is a common microbial component of the gastrointestinal tracts of mice and other species that is held in check by aspects of both the innate and adaptive immune responses.[3] The ability of different laboratory mouse strains and man to contain any disease that may be induced by *C. albicans* is often related to having the appropriate T-cell-directed phagocytic responses.[1] Interestingly the depletion of T lymphocytes in the human and mouse generally results only in a severe mucosal overgrowth of this yeast. Furthermore,

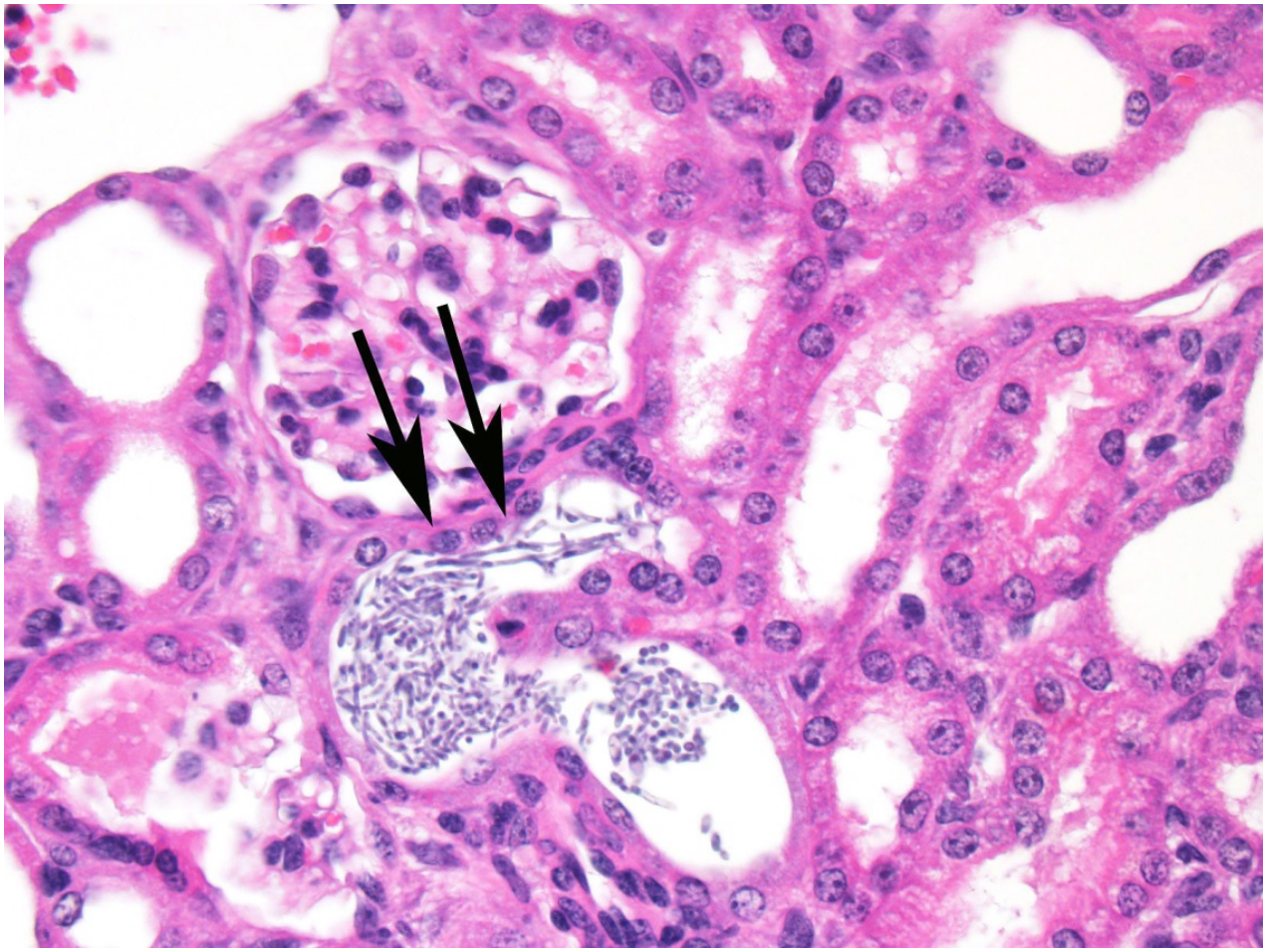

Kidney, NOD mouse. Within some tubules, yeasts have matured into pseudohyphae (arrows). (HE, 400X)

neither nude nor NOD-SCID mice have shown increased susceptibilities to developing systemic candidiasis, which indicate that the innate immune system offers protection, as well.[1] However, impaired NK cell function appears to be essential for immune-mediated signaling that shields against developing systemic candidiasis. Therefore, severely immuno-suppressed hosts, such as the NSG mouse, are uniquely susceptible to systemic disease induced by *C. albicans* infection.[4]

JPC Diagnosis: 1. Kidney: Pyelonephritis, suppurative, acute, multifocal, marked with pseudohyphae and yeast, NOD.*Cg-Prkdc*^{scid}*Il2rg*^{tm1Wjl}/SzJ mouse, *Mus musculus*.
2. Liver: No significant lesions

Conference Comment: In addition to being globally immuno-deficient and uniquely susceptible to a variety of opportunistic infections, non-obese diabetic (NOD)/ severe combined immune deficiency (SCID; NSG) mice are selectively bred as an animal model for type I diabetes mellitus (DM) in humans.[3] In NOD mice, DM develops as a result of spontaneously developing autoimmune insulitis in the pancreatic islets cells. The onset of DM is associated with a moderate glycosuria and a non-fasting hyperglycemia, which may be important for the proposed pathogenesis of this lesion discussed below.[3] As mentioned by the contributor, NOD-SCID mice have functional defects in macrophages, dendritic cells, natural killer (NK) cells, NKT cells, regulatory CD4+CD25+ cells, and are C5a deficient. The susceptibility of these mice to develop DM is much higher in a sterile environment.[3]

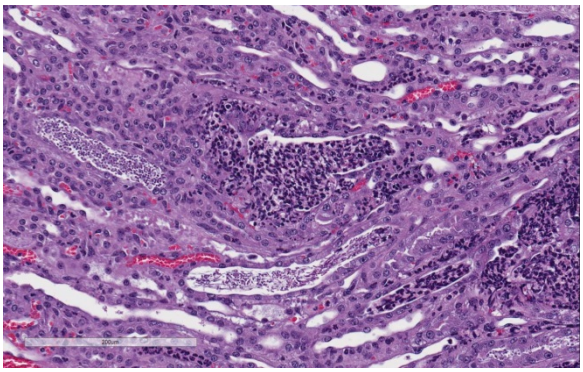

Kidney, NOD mouse. Adjacent tubules are filled with a mixture of yeast and large numbers of degenerate neutrophils. (HE, 200X)

Virulence of *C. albicans* is dependent on adherence of the organism to mucosal epithelial cells mediated by its virulence factor, adhesin. The important components of adhesins are agglutinin-like sequence (ALS) proteins and hypha-associated GPI-linked protein (Hwp1).[6,7] Superficial (localized) candidiasis produces relatively mild lesions in skin and mucous membranes while systemic (disseminated) candidiasis may involve any organ with the kidneys, heart valves, CNS and lungs most commonly affected. Immunosuppression, cytotoxic chemotherapy, diabetes mellitus, long-term glucocorticoid therapy, prolonged use of broad-spectrum antibiotics, or disruption of mucosal barriers predispose to infection. In addition, *C. albicans* can exist as yeast, pseudohyphae, or true hyphae depending on environmental conditions and temperature. This polymorphism enables *C. albicans* to infect a variety of tissues throughout the body.[6,7] The yeast form has been implicated in disseminated systemic infection while hyphae and pseudohyphae have stronger adherence and invasiveness due to the expression of ALS adhesins, catalases, and protein hydrolases, such as secreted aspartyl proteinases (SAP), which also supply the pathogen nutrients through protein degradation.[6,7]

Conference participants noted large numbers of *Candida* sp. pseudohyphae and yeast admixed with and surrounded by suppurative inflammation in the renal pelvis as well as filling and expanding renal

tubules in both the cortex and medulla. Occasionally tubules rupture and the inflammation extends into the adjacent renal interstitium. Participants agreed that this pattern of inflammation is consistent with pyelonephritis and retrograde extension of exudate into the renal tubules and renal parenchyma. The most common cause of pyelonephritis is via ascending infection from the lower urinary tract.[2] Opportunistic pathogens, such as *Candida albicans*, can commonly ascend into the kidney from the lower urinary tract, especially if there is glycosuria in a severely immuno-compromised and diabeteic animal. Females are predisposed to ascending urinary tract infections and pyelonephritis due to their relatively shortened urethra compared to males.[2] Alternatively, hematogenous suppurative and embolic nephritis usually results in multiple microabscesses within the glomeruli, multifocal vascultitis, and

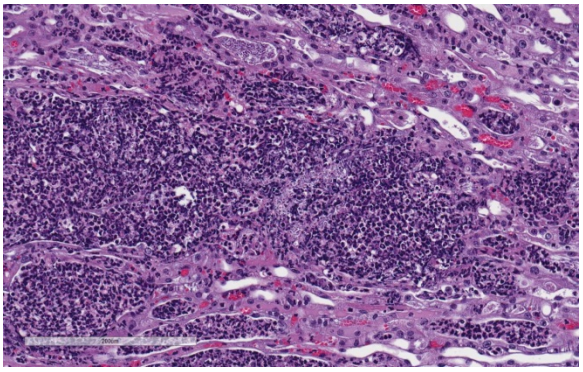

Kidney, NOD mouse. There is multifocal rupture of yeast- and neutrophil-laden tubules with extension of the inflammation into the adjacent interstitium. (HE, 200X)

hemorrhage within the medulla. In this case, conference participants noted perivascular in-flammation, but not significant vasculitis or glomerular lesions.[2]

Contributing Institution:
Veterinary Pathology Core Laboratory
St. Jude Children's Research Hospital
262 Danny Thomas Place
Memphis, TN, 38105-3678
https://www.stjude.org/research/departments-divisions/pathology

References:

1. Ashman, R, Farah, C, Wanasaengsakul, S, Hu, Y, Pang, G, Clancy, R. Innate versus adaptive immunity in *Candida albicans* infection. *Immunol Cell Biol*. 2004; 82(2):196-204.
2. Percy DH, Barthold SW. *Pathology of Laboratory Rodents and Rabbits*, 4th ed. Ames, IA: Blackwell Publishing; 2016:4,79.
3. Quintin J, Voigt J, Van der Voort R, et al. Differential role of NK cells against *Candida albicans* infection in immunocompetent or immunocompromised mice. *Eur J Immunol*. 2014; 44(8):2405-14.
4. Shultz L, Yoriko S, Najima Y, et al. Generation of functional human T-cell subsets with HLA-restricted immune responses in HLA class I expressing NOD/SCID/IL2rγ^{null} humanized mice. *Proc Natl Acad Sci USA*. 2010; 107:13022-13027.
5. Uzal FA, Plattner BL, Hostetter JM. Alimentary system. In: Maxie MG, ed. *Jubb, Kennedy, and Palmer's Pathology of Domestic Animals*. Vol 2. 6th ed. Philadelphia, PA:Elsevier; 2016:202.
6. Voon KC, Lee TY, Rusliza B, Chong PP. Dissecting *Candida albicans* infection from the perspective of *C. albicans* virulence and omics approaches on host-pathogen interaction: A review. *Int J Mol Sci*. 2016; 17:1643.

CASE III: Case #1 (JPC 4084692).

Signalment: Three-year-old, male, RCS rat (*Rattus norvegicus*).

History: The rat was kept as a non-treated animal in a long-term rat study. No clinical signs except coarse hair were found until the scheduled sacrifice at 152 weeks old.

Gross Pathology: A mass measured 40 x 30 x 15 mm, was observed in the anterior mediastinum, and adhered to the pleura of the lung. Small masses had found around main mass, and adhered to the lung and esophagus. The mass was soft, and the cut surface was milky white to yellow and grey-white.

Laboratory results: N/A

Histopathologic Description: Affecting approximately 80% of this section of thymus is an unencapsulated, poorly circumscribed, moderately cellular neoplasm composed of round to spindle-shaped cells arranged in sheets on a pre-existent fibrovascular stroma. Neoplastic cells have variably distinct cell borders, an abundant amount of lightly eosinophilic to amphophilic cytoplasm that is often obscured by fine eosinophilic granules. The nuclei of the tumor cells are generally centrally placed, round to elongate, with finely stippled chromatin, and 1-2 variably distinct nucleoli. Mitotic count averages about 1 per HPF. Almost all tumor cells have metachromatic granules when stained with toluidine blue stain. Immuno-histochemically, tumor cells are positive for c-kit, strongly positive for rat mast cell protease, and mostly negative for histamine as mast cell tumor markers. All tumor cells

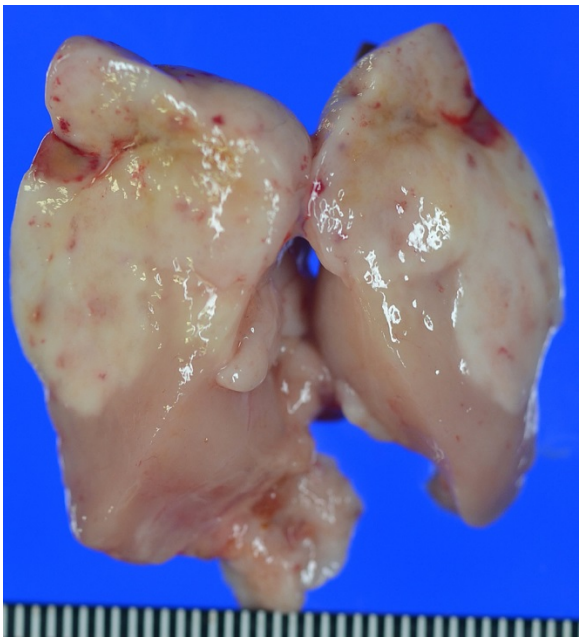

Anterior mediastinum, rat. A mass measured 40 x 30 x 15 mm, was observed in the anterior mediastinum, and adhered to the pleura of the lung. The mass was soft, and the cut surface was milky white to yellow and gray white in color (Photo courtesy of: Laboratory of Pathology, Faculty of Pharmaceutical Sciences, Setsunan University, 45-1 Nagaotohge-cho, Hirakata, Osaka 573-0101, Japan http://www.setsunan.ac.jp/~p-byori/)

are negative for cytokeratin AE1/AE3, and positive for vimentin. Ultrastructurally, the various sized granules contained homogeneous electron-dense material consistent with mast cell granules. The tumor metastasized and disseminated to the pleura of the lung and esophagus, and adventitia of the left ventricles and aorta.

The basophilic area at the periphery of the mass consists of a large number of lymphocytes and thymic epithelial cells similar to normal thymic tissue. Lympho-cytes in high cell density areas of epithelial cells are mostly a small cell type with coarse chromatin and fewer large lymphocytes. On the other hand, lymphocytes in low cell density areas of epithelial cells are nearly uniform medium-sized cell with fine stippled chromatin. Immunohistochemically, the thymic epithelial cells in high-cell-

Thymus, rat. 85% of the thymus (normal at left edge) is effaced by a neoplasm. (HE, 5X).

density areas exhibit positive cytokeratin 8 staining, which is expressed in thymic cortical epithelial cells. Thymic epithelial cells in low-cell-density areas are positive for cytokeratin 14 which is expressed in thymic medullary epithelial cells.

Contributor's Morphologic Diagnosis: Thymus: Malignant mast cell tumor with thymic epithelial hyperplasia

Contributor's Comment: This malignant tumor of thymic origin was located in the anterior mediastinum, invaded the adjacent thymus, and metastasized to the thoracic cavity. The tumor is characterized by a dense round cell proliferation, and has the features of a malignant round cell tumor. Neoplastic cells have intracytoplasmic metachromatic granules with toluidine blue stain and are strongly immunopositive for mast cell markers. Therefore, the tumor is diagnosed as a malignant mast cell tumor.

Mast cell tumor is a very common neoplasm of the skin in the dog and cat[5,6], and is composed of round cells with basophilic granules which are metachromatic when stained with toluidine blue. With regard to rodents, chemical and radiation-induced and spontaneous mast cell tumor have been reported in mice.[3,8] However, to our knowledge, mast cell tumors are extremely rare in rats. Rat mast cell tumors have only been reported in two case reports; and there are 12 cases/entries in the National Toxicology Program (NTP) pathology database.[2,3] Histopathologically, the mast cell tumors described in the two case reports originated in the thymus and in the eyelid, and they were characterized by a sheet-like proliferation of round cells with fine cytoplasmic eosinophilic granules. However, infiltration of eosinophils and an increase in collagen fibers are not observed, unlike in cases of these tumors in dogs and cats.[1,2,3,4] Because our case has similar morphologic features to previously reported cases, mast cell tumor in the rat may be characterized by eosinophilic granules in the cytoplasm. However, since this case has variable cell morphology and evidence of metastasis, the mast cell tumor in this case may have more malignant potential compared with previous reports.

This case is characterized by sheet-like proliferation of spindle to round cells with eosinophilic granules of various sizes. Differential diagnoses for the present tumor included thymoma, granular cell tumor, and globule leukocyte tumor. Thymoma, an epithelial tumor, is easily distinguishable from a round cell tumor; however, the patterns of cellular proliferation observed in the present case resemble that seen in tumors of epithelial origin, making the rat

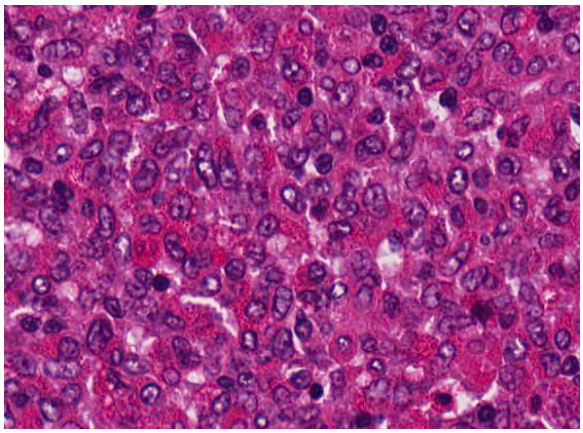

Thymus, rat. The neoplasm is composed of sheets of round cells with brightly eosinophilic granules and irregularly indented nuclei. (HE, 400X).

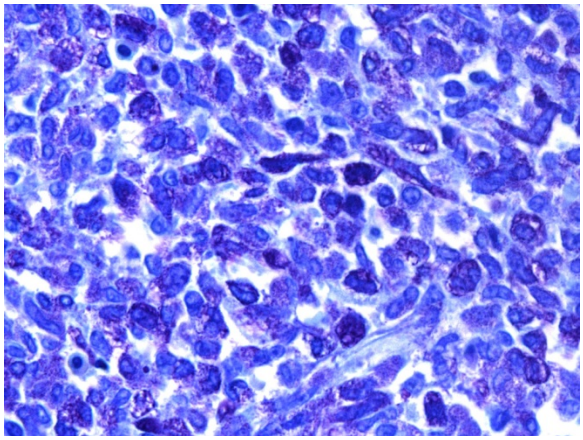

Thymus, rat. Neoplastic cells contain numerous metachromatic granules within their cytoplasm. (Toluidine blue, 400X). (Photo courtesy of: Laboratory of Pathology, Faculty of Pharmaceutical Sciences , Setsunan University, 45-1 Nagaotohge-cho, Hirakata, Osaka 573-0101, Japan http://www.setsunan.ac.jp/~p-byori/)

tumor difficult to differentiate from thymoma. Negative immunohistochemical staining for cytokeratin AE1/AE3 helps to rule out a thymoma in this rat. Granular cell tumors and globule leukocyte tumors are characterized as round cell tumors with eosinophilic granules, similar to those observed in the current case. Accordingly, metachromasia, using toluidine blue, was required to confirm the diagnosis.[2,7,9,12]

The thymic region of the tumor described here is composed of two areas with different densities, as well as different epithelial cell and lymphocyte morphologies, suggesting that cortical and medullary thymic components may have been maintained in the tumor. In humans, cortical and medullary thymic epithelial cells yield different expression patterns of cytokeratin. Medullary thymic epithelial cells express cytokeratin 5 and cytokeratin 14, whereas cortical thymic epithelial cells express cytokeratin 8 and cytokeratin 18.[5,11] Accordingly, immunohistochemical staining for different cytokeratins distinguishes between the cortex and the medulla of the thymus.

In this study, the expression patterns of cytokeratins 8 and 14 were analyzed in thymic epithelial cells of a normal RCS rat and shown to be similar to those observed in humans. Cytokeratins 8 and 14 were thus considered suitable markers for distinguishing between the cortex and medulla in RCS rats. In the RCS rat described here, the distribution of cytokeratins 8 and 14 corresponded to the areas with high and low epithelial cell densities, respectively. It was clear that the thymic area possessed both cortical and medullary components but that the epithelial cell density differed from that of the normal thymus. However, growth of solid tubules and epithelial cords, which represent a characteristic feature of benign thymoma, is not observed in our case. The area exhibiting high epithelial cell density represented the cortical component of the tumor with thymic epithelial hyperplasia; accordingly, this region was diagnosed as thymic epithelial hyperplasia. In our laboratory, we previously detected only one benign thymoma in about 20 RCS rats of over 120 weeks of age; however, almost all thymus showed severe involution. Therefore, this

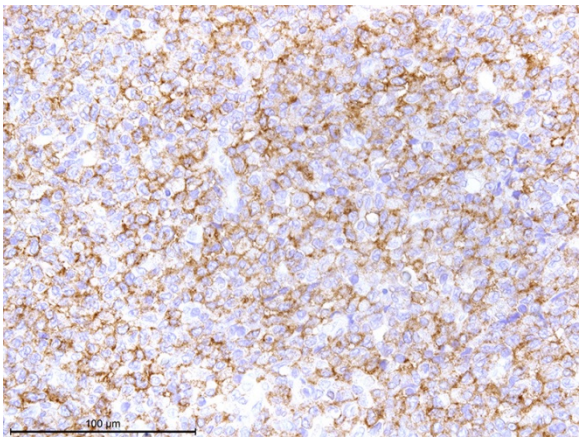

Thymus, rat. Neoplastic cells exhibit strong membranous positivtity for c-kit. (anti-c-kit, 400X). (Photo courtesy of: Laboratory of Pathology, Faculty of Pharmaceutical Sciences, Setsunan University, 45-1 Nagaotohge-cho, Hirakata, Osaka 573-0101, Japan http://www.setsunan.ac.jp/~p-byori/)

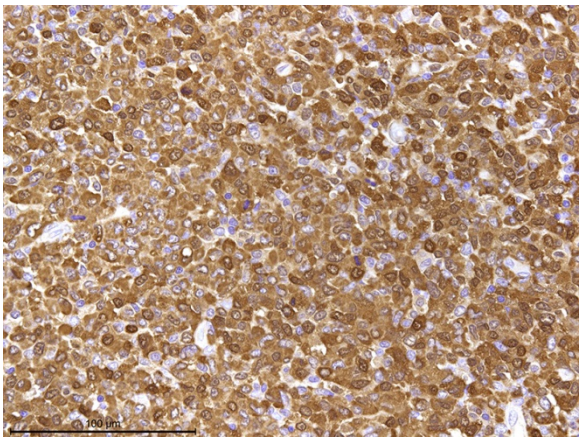

Thymus, rat. Neoplastic cells exhibit strong cytoplasmic positivity for rat mast cell protease. (anti-MCP, 400X). (Photo courtesy of: Laboratory of Pathology, Faculty of Pharmaceutical Sciences, Setsunan University, 45-1 Nagaotohge-cho, Hirakata, Osaka 573-0101, Japan http://www.setsunan.ac.jp/~p-byori/)

strain may not be prone to the development of thymic epithelial hyperplasia and thymoma.

JPC Diagnosis: Thymus: Mast cell tumor, RCS rat, *Rattus norvegicus*.

Conference Comment: Conference participants had great difficulty with the diagnosis and tissue identification in this case. While most attendees agreed that this case represented a malignant round cell neoplasm, none had mast cell tumor as a differential or thymus as the affected tissue. The neoplasm effaces the majority of the tissue; however, normal thymic parenchyma is present at the periphery of all examined tissue sections. As a result, the conference moderator led a discussion of the anatomical features of the rodent thymus.

The thymus is located in the mediastinum, cranial and ventral to the base of the heart and aortic arch with extension into the cervical region in the rat. It consists of two bilateral lobes joined by a connective tissue isthmus. Within the lobe, a thin capsule surrounds each lobule and gives rise to septae; however, septation is not apparent in this section.[10,11]

The thymus is unique among the lymphoid organs because it is supported by an epithelial framework, highlighted by the contributor's cytokeratin immuno-histochemical stains. It is divided into a cortex and medulla separated by a vascular corticomedullary zone. Histologically, the darkly staining cortex contains densely packed, small, immature T-lymphocytes, which obscure the epithelial cell population.[10,11] The medulla is less densely cellular than the cortex, and contains more mature T-cells, prominent epithelial cells, macrophages, dendritic cells, and B

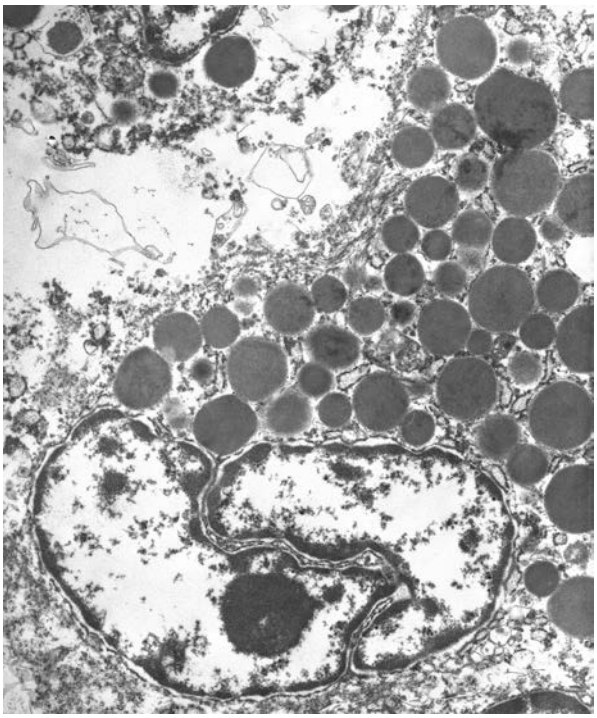

Thymus, rat. Neoplastic mast cells exhibit an indented nucleus, moderate amounts of round endoplasmic reticulum, and numerous variably-sized membrane-bound granules with granular contents. (Photo courtesy of: Laboratory of Pathology, Faculty of Pharmaceutical Sciences, Setsunan University, 45-1 Nagaotohge-cho, Hirakata, Osaka 573-0101, Japan http://www.setsunan.ac.jp/~p-byori/)

lymphocytes. Hassall's corpuscles are rare in rodents when compared with many other species, contributing to the difficulty participants had in tissue identification. In addition, given the age of this rat, the tissue is likely in an advanced stage of involution, further obscuring the normal architecture.[10,11]

Neoplastic cells in this section have numerous prominent pale eosinophilic cytoplasmic granules which are inconsistent with the deeply basophilic granules seen in well-granulated mast cell tumors in dogs and cats, as well as in normal rat mast cells. Conference participants considered other differentials including undifferentiated malignant round cell neoplasm, granular cell tumor, oncocytoma, balloon cell melanoma, and large granular lymphoma. In addition to the histochemical and immunohistochemical stains mentioned by the contributor that support the diagnosis of mast cell tumor, the provided transmission electron microscopy (TEM) image nicely demonstrates numerous intracytoplasmic homogenous electron dense granules consistent with mast cell granules.

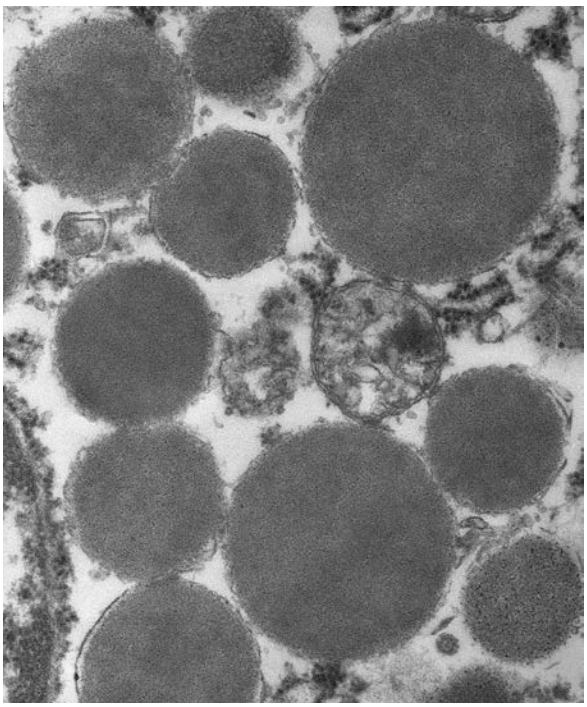

Thymus, rat. Higher magnification of the membrane-bound granules demonstrates that their contents are densely granular. A single mitochondria is present among them. (Photo courtesy of: Laboratory of Pathology, Faculty of Pharmaceutical Sciences, Setsunan University, 45-1 Nagaotohge-cho, Hirakata, Osaka 573-0101, Japan http://www.setsunan.ac.jp/~p-byori/)

Contributing Institution:
Laboratory of Pathology
Faculty of Pharmaceutical Science
Setsunan University,
Hirakata, Osaka, Japan
http://www.setsunan.ac.jp/~p-byori/

References:

1. Amihai D, Trachtenburg S, et al. The structure of mast cell secretory granules in the blind mole rat (*Spalax ehrenbergi*). *J Struct Biol*. 2001; 136:96-100.
2. Baselmans AH, Kuijpers MH, van Dijk JE. Brief communication: Histopathology of a spontaneously developing mast cell sarcoma in a Wistar rat. *Toxicol Pathol*. 1996; 24: 365-369.
3. Haseman JK, Hailey JR, Morris RW. Spontaneous neoplasm incidences in Fischer 344 rats and B6C3F1 mice in two-year carcinogenicity studies: A National Toxicology Program update. *Toxicol Pathol*. 1998; 26: 428-441.
4. Hosseini E, Pedram B, Bahrami AM, Moghaddam MH, Javanbakht J, Ghomi FE, Moghaddam NJ, Koohestani M, Shafiee R. Cutaneous mast cell tumor (mastocytoma): Cyto- histopathological and haematological investigations. *Diagn Pathol*. 2014; 9:9.
5. Lee EN, Park JK, Lee JR, Oh SO, Baek SY, Kim BS, Yoon S.

Characterization of the expression of cytokeratins 5, 8, and 14 in mouse thymic epithelial cells during thymus regeneration following acute thymic involution. *Anat Cell Biol*. 2011; 44:14-24.
6. Misdorp W. Mast cells and canine mast cell tumors: A review. *Vet Q*. 2004; 26:156-169.
7. Miyajima R, Hosoi M, Yamamoto S, Mikami S, Yamakawa S, Iwata H, Enomoto M. Eosinophilic granulated cells comprising a tumor in a Fischer rat. *Toxicol Pathol*. 1999; 27:233-236.
8. Miyakawa Y, Sato SI, Kakimoto K, Takahashi M, Hayashi Y. Induction of cutaneous mast cell tumors by N-methyl-N'-nitro-N-nitrosoguanidine followed by TPA in female mice of 4 out of 5 strains tested. *Cancer Lett*. 1990; 49:19-24.
9. Nagatani M, Nakamura A, Yamaguchi Y, Aikawa T, Tamura K. Spontaneous eosinophilic granulated round cell tumors in rats. *Vet Pathol*. 2001; 38:317-324.
10. Pearse G. Normal structure, function, and histology of the thymus. *Toxicol Pathol*. 2006; 34:504-514.
11. Sun L, Li H, Luo H, Zhao Y. Thymic epithelial cell development and its dysfunction in human diseases. *Biomed Res Int*. 2014; 206929.
12. Yamagishi Y, Katsuta O, Tsuchitani M. Mastocytoma in a Fischer 344 rat. *J Vet Med* Sci. 1992; 54:783-785.

CASE IV: MS15-5586 (JPC 4087116).

Signalment: One-month-old female Taconic line 8440 mouse (*Mus musculus*).

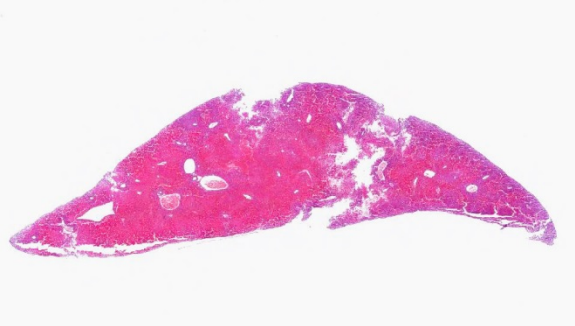

Liver, mouse. A single cross-section of the liver is presented for examination. (HE, 4X)

History: Four mice were presented dead. Three were found dead and one was euthanized prior to submission. According to the history, they were treated with azoxymethane.

Gross Pathology: All mice have congested livers with light brown apical margins.
Heart and kidneys are pale. The mice that were euthanized had blood tinged intestinal contents.

Laboratory results: Bacteriology*:* Small Intestine: *Enterococcus faecalis*, *Staphylococcus sciuri*, and *E. coli*; Negative for strict anaerobes.

Histopathologic Description: The liver has severe congestion of hepatic lobules with attenuation and loss of centrilobular hepatocytes. Portal zone hepatocytes are spared but have variably vacuolated cytoplasm.

Other histology findings include lymphocytolysis of the thymus. The mouse with intestinal hemorrhage has gastric ulcers. One mouse has necrosis of the adrenal cortex.

Contributor's Morphologic Diagnosis: Liver: Centrilobular to mid-zonal necrosis, and hemorrhage, severe, acute; micro-vesicular lipidosis mild to moderate

Contributor's Comment: Azoxymethane (AOM) is derived from the cycad palm nut of Guam. Ingestion has been associated with acute liver failure in cattle.[1]

In mice and rats, it is used as a mutagen in the study of colon carcinogenesis and liver failure. It is an alkylating agent that forms 06-methylguanine (0^6meG) adducts in DNA. 0^6meG formation has been found in human colon cancers. In the liver, AOM is oxidized to methylazoxymethanol by cytochrome P450 2E1 and transported to the colon where it methylates DNA which can cause G:C to A:T transition mutations.[2,3] Methylazoxymethanol is also associated with acute and chronic liver toxicity.[4]
At reported doses of 100 ug/g in mice AOM causes acute liver injury. It is characterized by hepatic necrosis and microvesicular lipidosis. The mechanism of action may be interference with beta-oxidation of fatty acids in the mitochondria[1] Hemorrhage is an indication of damage to sinusoidal endothelial cells.[4] Hepatic necrosis then progresses to liver failure and hepatic encephalopathy.

Acute liver failure is thought to lead to death via neurologic effects and hypotensive shock with multi-organ failure. Neurologic effects were thought to be a result of ammonia and other metabolites directly causing hepatic encephalopathy. More recent work has shown that inflammation-associated cytokine release contributes to brain edema and other clinical signs. Acute liver failure can result in cytokine storms with increased TNF-α, IL-1b, Il-6, and Il-12, There is also evidence of impaired neutrophil phagocytic activity and increased the risk of sepsis. Portal hypertension may cause increased bacterial translocation[5] cross the gut.[5, 6, 7]

JPC Diagnosis: Liver: Necrosis and hemorrhage, centrilobular to midzonal, acute, diffuse, severe with microvesicular

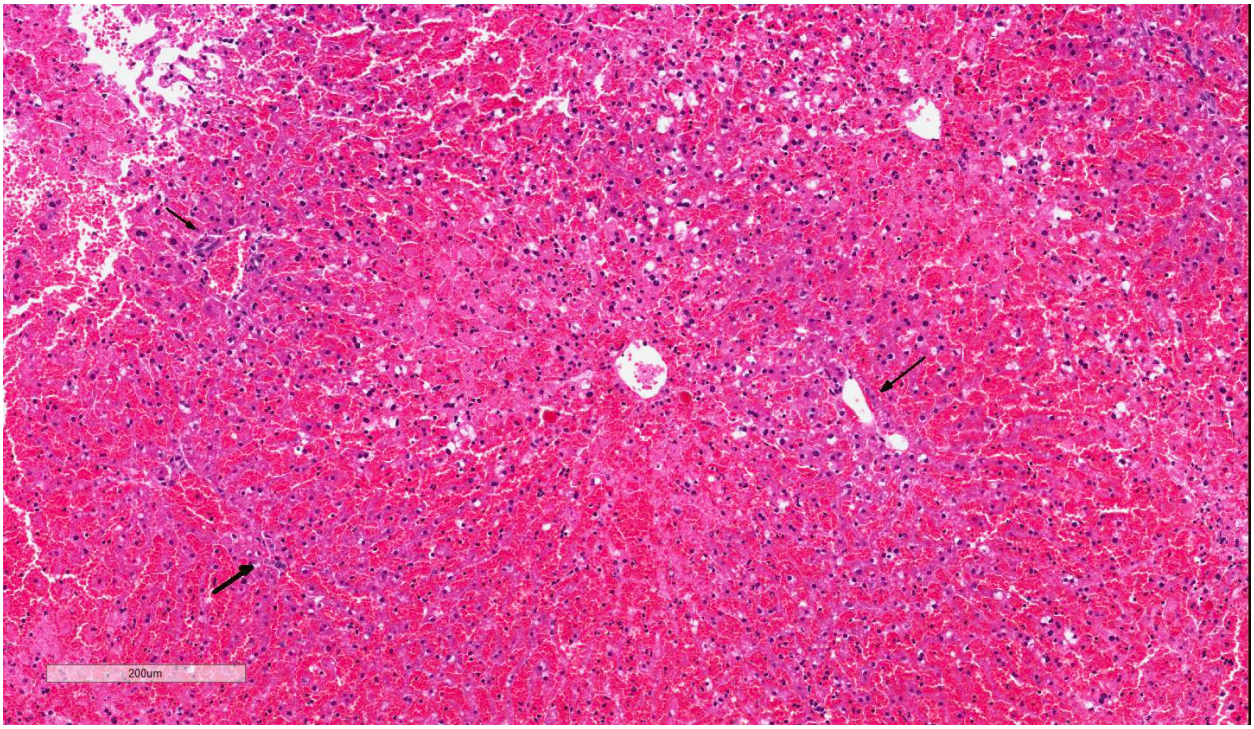

Liver, mouse. Hepatocellular architecture is diffusely lost, and there is diffuse hemorrhage within the centrilobular and midzonal areas. Portal areas are delimited by arrows. (HE, 63X)

lipidosis, Taconic line 8440 mouse, *Mus musculus*

Conference Comment: Despite some minor slide variability, the contributor provides a good example of the relatively stereotypical histologic changes associated with acute toxic hepatic injury. The liver is particularly susceptible to toxic injury due to constant exposure to ingested chemicals through the portal blood.[4] Additionally, hepatocytes are responsible for the metabolism of most endogenous and exogenous substances, by a process called biotransformation. This process is broken down into three phases based on the hepatic enzymes involved. Phase I reactions involve oxidation, reduction, hydrolysis, cyclization, and decyclization of the compound via cytochrome P450 monooxygenases (CYP) utilizing NADPH and oxygen in the smooth endoplasmic reticulum of hepatocytes. Phase II involves conjugation of the metabolite produced in phase I via glucuronidation, sulphation, acetylation, or methylation, ultimately resulting in a water soluble metabolite that is then excreted through urine or bile. Phase III reactions involve transporting the conjugated substances through the hepatocyte and into the bile canaliculus.[4,5,7]

Conference participants discussed the various mechanisms of hepatotoxic liver injury, which are divided into six categories based on the mechanism of action and cellular targets of the toxin.[4] The most common mechanism involves biotransformation of indirect-acting toxins by the CYP system, whichresults in bioactivated toxic metabolites that disrupt intracellular enzymatic pathways. CYP is abundant in the microsomes of the smooth endoplasmic reticulum in centrilobular zones which explains the prevalence of centrilobular to midzonal necrosis in some

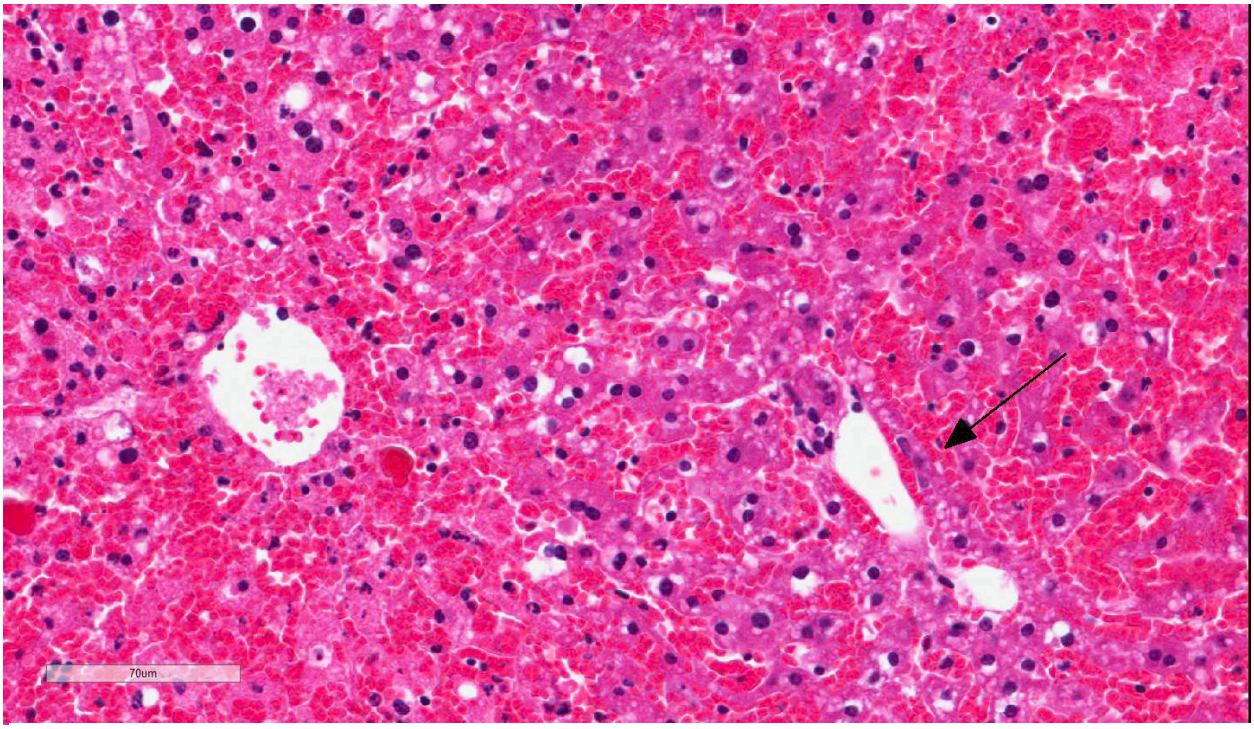

Liver, mouse. Hepatocytes within the centrilobular and midzonal areas of the lobule are shrunken and fragmented, with pyknotic or rrhectic nuclei, and there is marked hemorrhage in this area. A thin rim of viable hepatocytes, compressed by the marked congestion is present in portal areas. (HE, 224X)

toxic hepatopathies, including this case of azoxymethane toxicosis.[1,4,6] There is also inhibition of hepatic mitochondrial function, thus limiting beta-oxidation of fat and ATP generation via oxidative phosphorylation. This inhibition eventually leads to necrosis (due to production of damaging reactive oxygen species and lactic acid), as well as hepatocellular microvesicular lipid accumulation, as seen adjacent to areas of necrosis in this case.[4] Readers are encouraged to review 2012 WSC Conference 18 Case 2 for further discussion of other mechanisms of hepatotoxic liver injury.

In addition to hepatic necrosis, acute and fatal hepatotoxicity causes destruction of the endothelium of the sinusoidal lining cells, resulting in zonal areas of hemorrhage. Widespread hemorrhage is often associated with acute hepatocellular toxicity due to consumption of platelets and decreased production of clotting factors by the liver.[4] Centrilobular necrosis is the most common form of zonal hepatocellular necrosis observed in animals and may be caused by a variety of infectious, inflammatory, metabolic, and toxic insults. Although conference participants could not identify azoxymethane as the cause of the lesions in this mouse, most suspected a toxic etiology based upon the presence of centrilobular necrosis and hemorrhage combined with the lack of evidence of an infectious etiology.

Contributing Institution:
National Institutes of Health
Diagnostic and Research Services Branch
Division of Veterinary Resources
Bethesda, MD, 2892
https://www.nih.gov/

References:

1. Belanger M, et al. Neurobiological characterization of an azoxymethane mouse model of acute liver failure. *Neurochem Int.* 2006; (48):434-440.
2. Nyskolus LS, et al. Repair and removal of azoxymethane-induced 0^6-methyguanine in rat colon by0^6-methyguanine DNA methyltransferase and apoptosis. *Mutat Res*. 2013; 758: 80-86.
3. Sohn OS, et al. Metabolism of azoxymethane, methylazoxymethanol and N-nitrosodimethylamine by cytochrome p450IIE1. *Carcinogenesis*. 1991; 12 (1):127-131.
4. Stalker MJ, Cullen JM. Liver and biliary system, In: Maxie MG, ed. *Jubb, Kennedy and Palmer´s. Pathology of Domestic Animals.* Vol 2. 6th ed. St Louis, MO: Elsevier Saunders; 2016:325-330.
5. Tranah TH, et al. Systemic inflammation and ammonia in hepatic encephalopathy. *Metab Brain Dis*. 2013; 28:1-5.
6. Bemeur C, Desjardins P, Butterworth RF. Antioxidant and anti-inflammatory effects of mild hypothermia in the attenuation of liver injury due to azoxymethane toxicity in the mouse. *Metab Brain Dis*. 2010; 25:23-29.
7. Chastre A, et al. Inflammatory cascade driven by tumor necrosis factor-alpha play a major role in the progression of acute liver failure and its neurologic complications. *PLoS One*. 2012; 7(11):e49670.

Self-Assessment - WSC 2016-2017 Conference 8

1. Which of the following is not true concerning myxomatosis?
    a. Hares are carriers of the infection but very rarely exhibit clinical signs.
    b. Initial lesions are gelatinous edema surrounding mucocutaneous edema and a local nodule at an arthropod bite.
    c. The classic histologic lesion is epithelial ballooning degeneration and intracytoplasmic inclusions.
    d. Today, mortality in European rabbits has reached over 99%.

2. Which of the following describes a classic "myxoma cell?"
    a. A large epithelial syncytial cell with over 4 intracytoplasmic inclusions
    b. A lymphocyte within a node with up to 30 nuclei.
    c. A nuron with a large glassy amphophilic intranucler inclusion
    d. A large mesenchymal cell with granular cytoplasm and anisokaryotic nuclei.

3. Which of the following is not true about NOD/SCID mice?
    a. They are used as an animal model for type II diabetes mellitus.
    b. They are deficient in mature B-, T- and NK cells.
    c. They have innate deficiencies in macrophage and dendritic cell function.
    d. Diabetic animals manifest a moderate glycosuria and a non-fastinc hyperglycemia.

4. Ingestion of cycad palm nuts results in which of the following in cattle?
    a. Retinal degeneration
    b. Acute liver failure
    c. Laminitis and hood deformity
    d. Thyroid neoplasia

5. True or false: In humans, cortical and thymic epithelial cells express different patterns of cytokeratin?
    a. True
    b. False

Joint Pathology Center
Veterinary Pathology Services

WEDNESDAY SLIDE CONFERENCE 2016-2017

C o n f e r e n c e 10

9 November 2016

CASE I: AzVDL 02-3362 (JPC 4019839).

Signalment: Nine-year-old, female, Siamese cross, (*Felis catus*).

History: The cat presented for chronic cystitis unresponsive to antibiotic therapy and dietary changes. Pneumocystogram revealed a thickened uneven bladder wall with a small lumen. The cat was referred to an internal medicine service with the primary differential diagnosis of neoplasia. Ultrasound showed an irregular mass in the bladder wall at the trigone. A "traumatic catheterization" of the bladder was performed and cytologic preparations were submitted for evaluation.

Gross Pathology: None.

Laboratory results: The CBC at presentation to the specialty service was within reference interval. The only abnormality in the chemistry profile was hyperglycemia. The abnormalities in the urinalysis included glucosuria, mild pyuria and large numbers of variably sized transitional epithelial cells.

Cytologic Description: The preparation has large areas of dense cellularity. There are numerous linear structures (nematode uterus) containing oval bioperculated ova are present within the dense areas. Well-preserved and degenerate parasite ova are also scattered throughout the background. The ova are approximately 60 microns in length with a granular interior and a thick refractile shell. In the thinner areas of large cellular densities, the nucleated cells are present in organized sheets with well-defined cytoplasmic borders. The cells have round nuclei with mild anisokaryosis and a scant to small amount of basophilic cytoplasm. The background has a large number of lysed and degenerate cells with fewer small clusters of intact epithelial cells showing the same morphology as those within the dense clusters. There are areas of monolayer adjacent to the dense clusters with a moderate number of neutrophils and eosinophils. Eosinophils, neutrophils, and small lymphocytes are found throughout the background. Occasional small lymphocytes contain a few eosinophilic to azurophilic granules.

Table 1: Capillarid Species

Name	**Location**	**Host**
Eucoleus bouhmi	frontal sinus	fox, dog
Eucoleus aerophilus	bronchi	dog, cat, fox
Aonchotheca putorii	stomach, intestine	bear, hedgehog, raccoon, swine, bobcats, mustelids, cat
Aonchotheca spp	intestine	ruminants
Calodium hepaticum	liver	rodents, many occasional hosts including humans.
Pearsonema plica	urinary bladder	dog, fox, wolf
Pearsonema feliscati	urinary bladder	cat

Contributor's Cytologic Diagnosis: Transitionalcell hyperplasia with mild suppurative and eosinophilic inflammation and fragmented *Pearsonema (Capillaria) feliscati* nematode and numerous bio-perculated eggs.

Contributor's Comment: Urinary nematodiasis is caused by several genera and affects numerous species of domestic and wild animals (Table 1).[2, 5,10] The nematode species found in the kidney, ureters or renal vasculature are associated with clinical disease. The most spectacular of which is the giant kidney worm of dogs, *Dioctophyme renale*, that eventually destroys and replaces the renal parenchyma. Nematodes of the genera *Pearsonema* (*Capillaria*), on the other hand, are found within the urinary bladder and are often an incidental finding with minimal clinical disease evident.[2,10] The capillarid nematodes have been placed in several new genera based on location within the host, the most accepted of which are *Eucoleus* (nasal sinus and bronchi), *Aonchotheca* (intestine) and *Pearsonema* (urinary bladder) (Table 2)[2]. *Pearsonema plica* and *P. feliscati*, infect the domestic dog, fox, wolf, and cat. In most cases, the nematode is loosely attached to the urinary bladder mucosa and, less often, ureteral mucosa with mild inflammation and edema evident on histologic examination of the affected tissue.[7,8] Clinical disease is uncommon but has been reported in the dog and fox and rarely in the cat.[7,8] The prevalence of these parasites in the dog and cat is not known. However, a prevalence of 76% and 59% has been reported in two dog breeding kennels in the United States.[7] In this heavily parasitized population, hematuria, dysuria and pollakiuria were common findings in the dogs with confirmed infection.

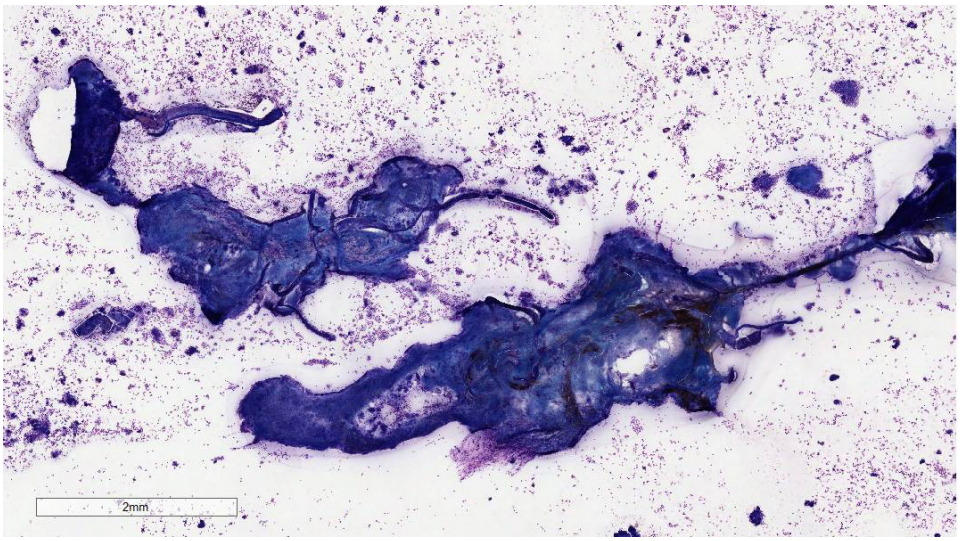

Urinary bladder, cat. Several large aggregates of protein encase tangential sections of adult nematodes. (green arrows.) (Wrights, 16X)

In the cat, the disease is rarely reported in the United States;[6] however, in Australia, an incidence of greater than 30% was found in one survey study.[8] No evidence of clinical cystitis was seen in the infected cats. On histological examination of the urinary bladder in the infected cats, the nematodes were superficially embedded in the mucosa with no breaching of the basal layer or basement membrane. A moderate inflammatory infiltrate that included eosinophils was seen in association with the embedded parasite. The lifecycle for *P. feliscati* is not determined.[2,6] It is assumed to be similar to *P. plica* which is thought to be through the earthworm as an intermediate host or a transport host such as a bird. Adult worms are 2.5 to 5 cm in length. The ova are elongate and approximately 60 microns in length and 27 microns in width. They have bipolar plugs (bioperculate), a thick shell with "globular" ridges enclosing a single cell.[10] The literature does not provide morphologic or biological characteristics other than the host to distinguish *P. plica* and *P. feliscati*. The cat is included in host species for both *P. feliscati and P. plica* in *Georgis' Parasitology for Veterinarians* with no mention of differential characteristics.[2] The capillarid in this case is given as *P. feliscati* based on host.

JPC Cytologic Interpretation: Presence of *Peasonema* spp nematode fragments and ova, mild transitional cell dysplasia, and low grade eosinophilic and neutrophilic inflammation, Siamese cross, *Felis catus*.

Conference Comment: The contributor provides a compelling cytologic specimen and outstanding review of capillarid

Table 2: Urinary Nematodes

Name	**Host**
Dioctophyme renale	dog, mink
Pearsonema plica, P. feliscati	dog, fox, wolf, cat
Stephanurus dentatus	swine
Trichosomoides crassicauda	rats
Crassicauda boopis	whales

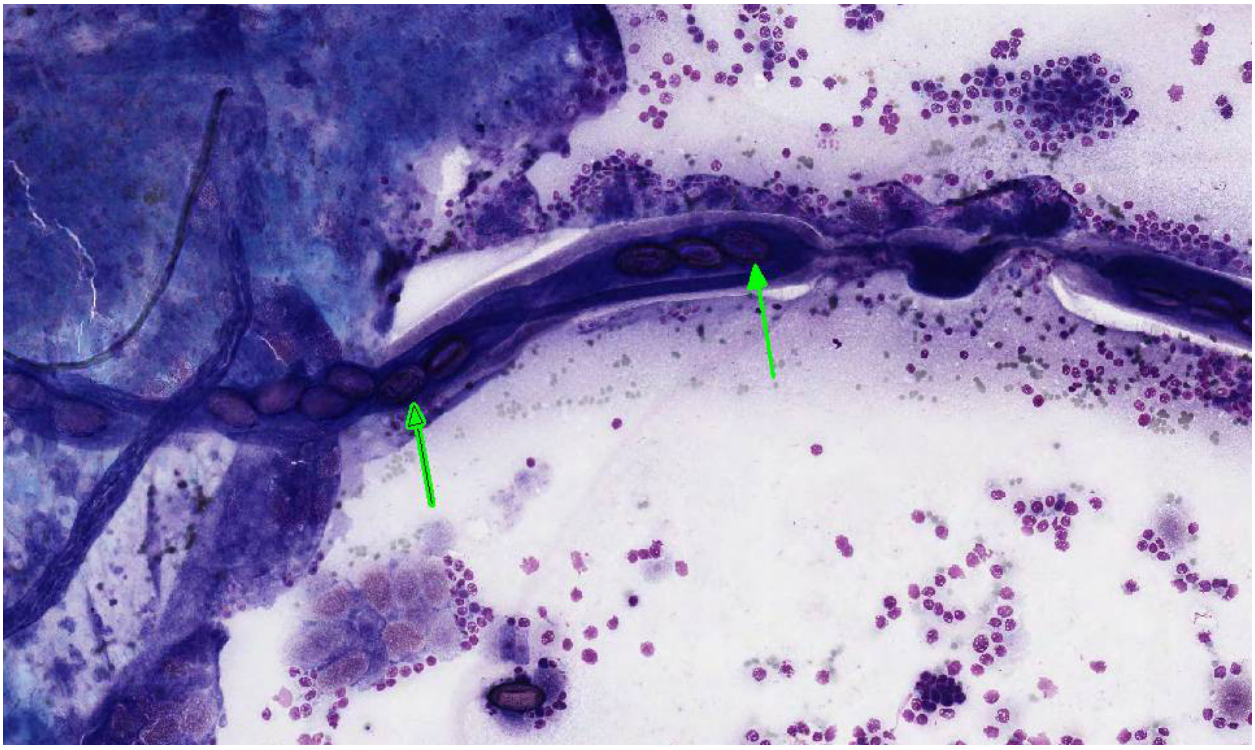

Urinary bladder, cat. Tangential sections of the adult female parasites contina numerous 25x50um eggs within the uterus. (Wrights, 124X).

nematodes affecting a wide variety of veterinary species. As mentioned by the contributor, the *Capillaria* genera have been reclassified based on the location of the adult parasite in the host; however, the genus name *Capillaria* is still widely used in the veterinary literature.

Typically, infection with *Pearsonema feliscati* is of little pathologic significance to the cat and is usually considered an incidental finding. Most studies show no relationship between the presence of adult capillarids in the bladder and significant cystitis.[8,9] Histologically, *Pearsonema feliscati* resides in the superficial epithelium of the urinary bladder and does not penetrate the basement membrane.[5] However, if the ureters become occluded with adult nematodes, cats may display the clinical signs of post-renal obstruction. The highest reported number of adult worms present from a single urinary bladder was 25 and large numbers of eggs were found in all bladders containing five or more adults.[9] In this case, the mild to moderate eosinophilic and neutrophilic inflammation may be secondary to a high parasite burden.

In both dogs and cats, *Peasonema plica* has been reported in the urinary bladder and ureter submucosa and is typically associated with mild subclinical inflammation and edema.[1,7] There is a higher prevalence of the parasite in wild red foxes (*Vulpes vulpes*) in many European countries and it is associated with an increased pathogenicity. This can result in severe cystitis, pollakiuria, dysuria and hematuria in this species.[1,3] In this case, both *Pearsonema plica* and *Pearsonema feliscati* have been implicated in urinary bladder infection in cats, conference participants could not distinguish between two cytologically.

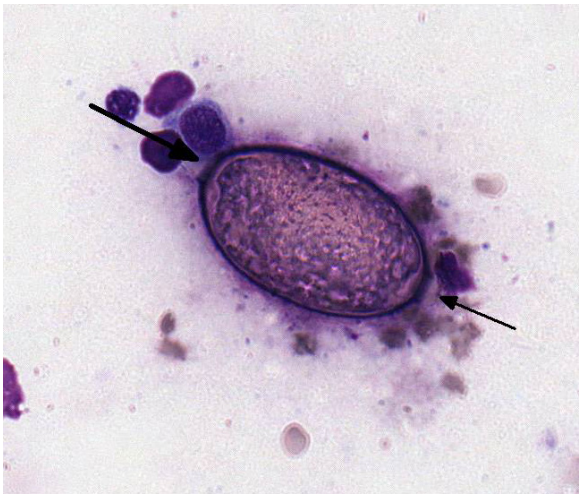

Urinary bladder, cat. Eggs are 25x50um, brown, with a bioperculated (arrows) brown refractile shell and granular contents. (Wrights, 830X)

Conference participants readily identified numerous bioperculate eggs free within the sample and inside the reproductive tract of adult nematode fragments. *Pearsonema* spp are a subclassification of aphasmid nematodes of the family *Trichuridae*. Histologically, aphasmid nematodes are characterized by thin eosinophilic cuticle, reduced polymyarian-coelomyarian musculature, two hypodermal bacillary bands, a stichosome esophagus, a spiny sheath and oval bioperculate eggs.[4] Cytologically, specific features of the adult nematode can be more difficult to appreciate than on histologic tissue section. However, the presence of the highly characteristic ova confirms the presence of a urinary capillarid nematode.

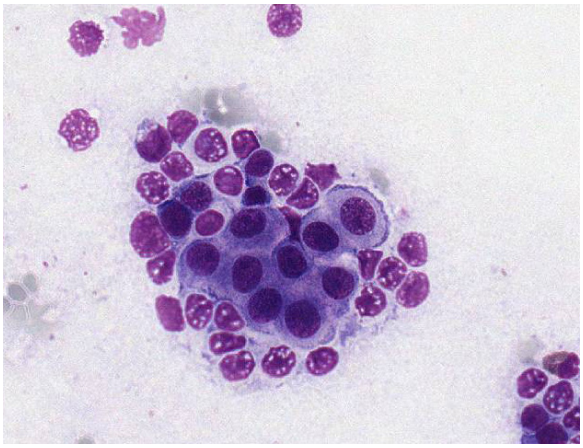

Urinary bladder, cat. There are numerous clusters of transitional epithelial cells with \in the specimen. (Wrights, 523X)

Participants also noted vacuolation, binucleation, anisokaryosis, and prominent nucleoli within the reactive sloughed urothelium. Transitional epithelial cells are among the most pleomorphic cells in the body and can demonstrate marked reactive change in response to a variety of insults. For this reason, the conference moderator reminded participants that care must be taken prior to over-interpreting reactive urothelium as malignancy.

Contributing Institution:
Arizona Veterinary Diagnostic Laboratory
2831 N. Freeway
Tucson, AZ 85705
http://cals.arizona.edu/vdl/

References:

1. Basso W, Spanhauer Z, Arnold D, Deplazes P. *Capillaria plica* (syn. *Pearsonema plica*) infection in a dog with chronic pollakiuria: Challenges in the diagnosis and treatment. *Parasitol Int*. 2014; 63:140142.
2. Bowen DD. *Georgis' Parasitology for Veterinarians*. 2008. (Kindle Locations 9850-9856). Elsevier Health. Kindle Edition.
3. Fernandez-Aguilar X, et al. Pearsonema (syn Capillaria) plica associated cystitis in a Fennoscandian artic fox (*Vulpes lagopus*): A case report. *Acta Vet Scand*. 2010; 52:39.
4. Gardiner CH, Poynton SL. Aphasmids. In: Gardiner CH, Poynton SL, eds. *An Atlas of Metazoan Parasites in Animal Tissues*. Washington, DC: Armed

Forces Institute of Pathology; 1999:40-43.
5. Lambertsen RH. Diseases of the common fin whale (*Balaenoptera physalus*): Crassicaudiosis of the urinary system. *Journal of Mammology*. 1986; 67(2):353-366.
6. Lautenslager JP. Internal helminthes of cats. *Vet Clin North Amer*. 1976; 6(3):353365
7. Senior DF, Solomon GB, Goldschmidt MH, et al. *Capillaria plica* infection in dogs. *J Am Vet Med Assoc*. 1980;176(9):901-905.
8. Waddell AH. Further observations of *Capillaria feliscati* in the cat. *Aust Vet J*. 1968;44(1):33-34.
9. Wilson-Hanson S, Prescott CW. *Capillaria* in the bladder of the domestic cat. *Aust Vet J*. 1982; 59:190-191.
10. Zajac, Anne M.; Conboy, Gary A. Veterinary Clinical Parasitology. 2011. (Kindle Locations 3752-3763). John Wiley and Sons. Kindle Edition.

CASE II: 15N0368 (JPC 4084209).

Signalment: Ten-year-old, mare, quarterhorse, (*Equus ferus caballus*).

History: This animal presented to the teaching hospital in November of 2014 for weight loss. At that time, blood work revealed hyperproteinemia and elevated blood ammonia (see laboratory results below). Ultrasound of the liver revealed rounded margins. A liver biopsy was performed and revealed nodular regeneration, bridging fibrosis, and arteriolar and bile duct proliferation. The clinical suspicion at that time was chronic pyrrolizidine alkaloid toxicity despite an absence of hepatocellular cytomegaly or karyomegaly.

The patient re-presented in January of 2015 for increasing lethargy, dull mentation and waxing and waning appetite. The horse was treated with minocycline, metronidazole, pentoxifylline, lactulose, vitamin E, and prednisolone.

The patient presented again in February of 2015 due to progression of clinical signs and failure to respond to treatment. Euthanasia was elected.

Gross Pathology: At necropsy, the liver was markedly reduced in size weighing 3.1 kg (0.7% of body weight) and had thick rounded margins. Some of the lobes appeared multinodular and there were multifocal areas of capsular fibrosis

Laboratory results:
February 2015: (reference ranges)
GGT 294 IU/L (8-22)
SDH 16 IU/L (0-8)
Resting bile acids 36 uMOL/L (4-11.5)
Plasma ammonia 242 UG/DL (5-59)

Postmortem liver heavy metal screen
Iron 5100 ppm (100-300)

Histopathologic Description: Liver: Within all sections, the hepatic capsule is variably thickened, and the lobular architecture is pronounced due to marked portal to portal bridging fibrosis. Dissecting bands of fibrosis variably infiltrate the surrounding parenchyma causing isolation of hepatic lobules and smaller clusters of hepatocytes. Rare isolated hepatocytes appear hyper-eosinophilic with pyknotic to karyolytic nuclei (individual cell apoptosis). Diffusely, hepatocytes contain variable amounts of coarse, dark brown, granular pigment (hemosiderin). Kupffer cells and

The liver was markedly reduced in size weighing 3.1 kg (0.7% of body weight) and had thick rounded margins. Some of the lobes appeared multinodular and there were multifocal areas of capsular fibrosis (Photo courtesy of: VMTH Anatomic Pathology, 1 Garrod Drive, University of California, Davis, CA 95616 http://www.vetmed.ucdavis.edu/vmth/lab_services/anatomic_pathology/index.cfm)

macrophages, which course throughout areas of fibrosis, contain similar, but more variably sized, dark brown cytoplasmic granules (hemosiderophages). Areas of fibrosis also contain small to moderate numbers of lymphocytes and plasma cells, with rare neutrophils, and abundant variably sized bile ducts and small-caliber blood vessels. Occasional small aggregates of lymphocytes and plasma cells are observed throughout the parenchyma. In some areas, the hepatic parenchyma has been completely replaced by mature fibrous tissue and proliferating bile ducts. In addition, mature fibrous tissue occasionally appears to occlude central and portal veins with rare evidence of recanalization (venoocclusive disease). Within one section there are large, multifocal areas of acute hemorrhage and edema that cause separation and dis-organization of the hepatic cords. Occasional individual collagen bundles are segmentally darkly amphophilic (sidero-calcinosis). Within the most severely affected sections, there are frequent, irregular, refractile crystals associated with small numbers of multinucleated giant cells and epithelioid macrophages (foreign body response).

Contributor's Morphologic Diagnosis: Liver: Severe, chronic, bridging portal and capsular fibrosis with lobular collapse, veno-occlusion, biliary hyperplasia and marked hepatocellular hemosiderosis.

Contributor's Comment: The abundant hepatocellular and Kupffer cell pigment was confirmed as iron using Perls' iron stain. Heavy metal analysis of the liver revealed an iron concentration of 5100 ppm, far exceeding the normal upper limit of 300 ppm. Perl's staining also revealed iron deposits within smooth muscle trabeculae of the spleen, and within renal tubular epithelium at the corticomedullary junction. Iron within splenic trabeculae and within fibrous tissue in the liver is occasionally

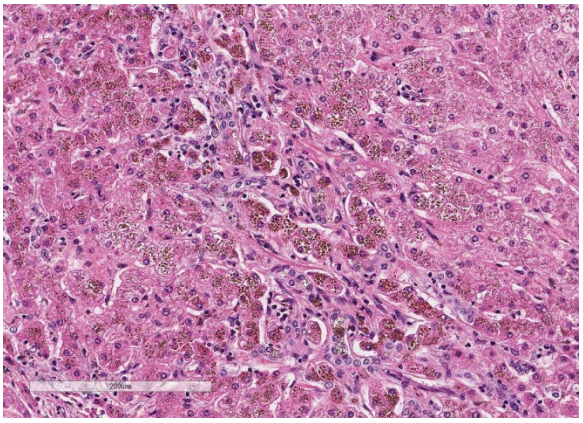

Liver, horse. There is moderate bridging portal fibrosis which breaches the limiting plate and entraps hepatocytes (center). Hepatocytes, especially in portal areas, contain abundant intracytoplasmic iron. (HE, 168X)

deposited in conjunction with calcium salts (siderocalcinosis). In addition, the most severely affected sections shows deposition of refractile clear crystals that are associated with a granulomatous foreign body response. These crystals are not birefringent under polarized light.

With the exception of certain avian species, including mynahs and toucans, hemochromatosis is a rare condition in domestic species. A hereditary form of hemochromatosis has been reported in Salers and Salers-cross cattle,[8] and there have been individual case reports in horses.[6] Cases of dietary iron overload have also been reported in sheep and cattle. Iron storage disease is classically divided into two entities: hemosiderosis (iron overload in the absence of clinical signs) and hemochromatosis (iron overload leading to hepatic damage including fibrosis, inflammation, and liver failure). In human medicine, iron storage disease is additionally subdivided into primary and secondary categories. Primary iron storage disease involves an inherent abnormality in iron metabolism. In humans, this is most commonly the result of one of two missense mutations in the HFE gene which encodes a protein involved in the interaction between transferrin and the transferrin receptor.[9] Secondary hemochromatosis occurs from excessive intestinal absorption of iron either due to iron excess within the diet, or as a response to increased demand for erythropoiesis. Secondary hemochromatosis can occur with any condition leading to chronic hemolysis. Although a very small amount of iron is eliminated through the bile, the body has no natural way of responding to excess iron and therefore iron accumulates over time, primarily in the liver. Iron accumulation results in hepatocellular toxicity through production of free radicals and organelle dysfunction, including lysosomal injury.[8] This can lead to hepatocellular necrosis that progresses to bridging fibrosis, bile duct hyperplasia, and venoocclusive disease, as observed in this case. In humans, hemochromatosis can also increase the risk of hepatocellular neoplasia[9] and in birds, has been shown to predispose to certain bacterial infections such as *Yersinia pseudotuberculosis*.[4]

Distinguishing between primary and secondary iron storage disease can be especially difficult in chronic cases. In

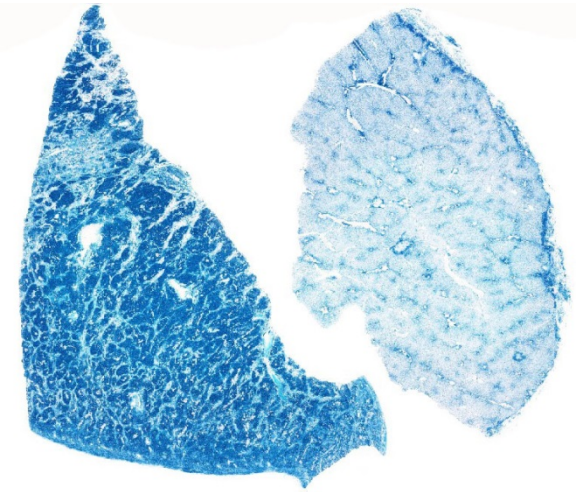

Liver, horse. The liver stains deep blue with a Perl's iron stain. (Perl's iron, 5X) (Photo courtesy of: VMTH Anatomic Pathology, 1 Garrod Drive, University of California, Davis, CA 95616 http://www.vetmed.ucdavis.edu/vmth/lab_services/anatomic_pathology/index.cfm)

humans, the pattern of hemosiderin deposition can be helpful.[6] In primary iron storage disease, hemosiderin accumulates first in hepatocytes while in secondary hemosiderosis, iron accumulates first within Kupffer cells and macrophages (reticulo-endothelial system). However, this requires that the liver is examined early in disease progression. In this case, a primary abnormality in iron metabolism is suspected based on the lack of clinical or histologic evidence of a second underlying disease process leading to chronic hemolysis, and feeding of a standard equine diet.

JPC Morphologic Diagnosis: Liver: Fibrosis, portal and bridging, diffuse, marked with hepatocellular degeneration and loss and intra-hepatocellular hemosiderosis, Quarterhorse, *Equus ferus caballus*.

Conference Comment: The contributor provides an outstanding example and thorough review of hemochromatosis in humans and veterinary species. Free iron is highly toxic to tissues due to its ability to participate in the generation of hydroxyl radical formation via the Fenton or Haber-Weiss reaction with hydrogen peroxide (H_2O_2) leading to lipid peroxidation and DNA damage.[5] As a result, iron is typically bound to transferrin while in circulation and either ferritin or hemosiderin when stored and sequestered in tissue. When iron is bound to these proteins, it cannot participate in these injurious reactions. Ferritin concentration is highest in the liver, spleen, and bone marrow and is stored in hepatocytes and/or macrophages.[1,3,5,7]

In hepatocytes, iron is derived from plasma transferrin, while iron stored within macrophages is a result of erythrocyte breakdown. Normally, to offset the attritional loss of daily iron, duodenal enterocytes absorb approximately 1 to 2 mg of iron per day from the diet via divalent metal transporter-1 (DMT-1) and a heme carrier protein-1 (HCP-1) on the luminal surface of the enterocytes.[5,9] Iron is transported from the cytoplasm of the enterocyte to the circulation by ferroportin.[1,7] Absorbed iron circulates bound to transferrin and is used primarily by erythroid precursors in the synthesis of heme. Macrophages in the spleen clear dead and dying erythrocytes and release the iron from heme to export it to the circulation or store it in ferritin. In iron-overload, transferrin is quickly saturated and iron is stored in the liver and various other tissues due to the lack of a regulated pathway for effective iron excretion.[3]

As mentioned above, hepatocytes are a major site of iron storage as ferritin and are also responsible for the production of type II acute phase protein, hepcidin, in response to inflammatory cytokine, interleukin-6.[1,3,5,7] Hepcidin is transported in by blood by alpha-2-macroglubulin and blocks the release of iron from enterocytes and

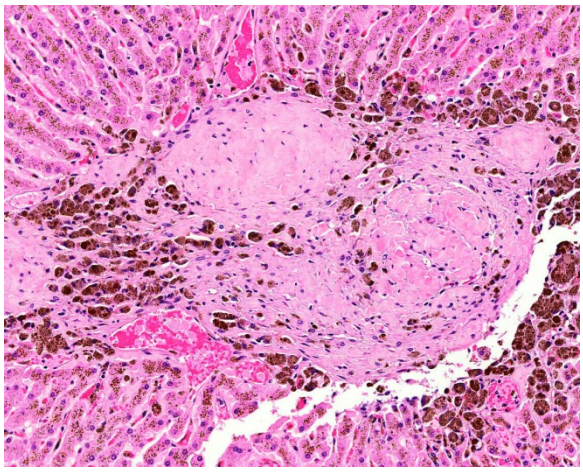

Liver, horse. Occasionally, fibrosis of portal areas obliterates portal veins (veno-occlusive disease). (HE, 100X) (Photo courtesy of: VMTH Anatomic Pathology, 1 Garrod Drive, University of California, Davis, CA 95616 http://www.vetmed.ucdavis.edu/vmth/lab_services/anatomic_pathology/index.cfm)

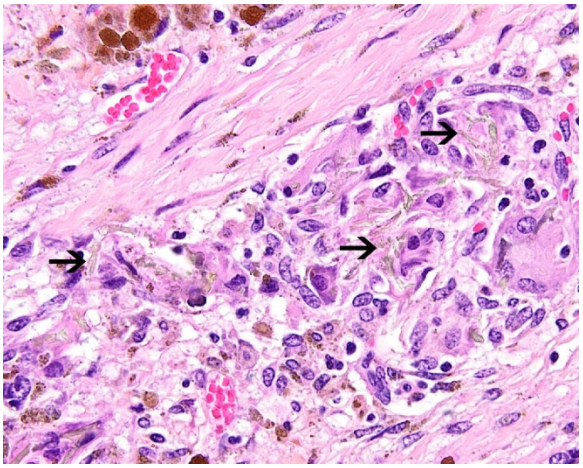

Liver, horse: Multifocally, non-refractile crystals are present within aggregates of epithelioid macrophages and multinucleated giant cells. (HE, 400X) (Photo courtesy of: VMTH Anatomic Pathology, 1 Garrod Drive, University of California, Davis, CA 95616 http://www.vetmed.ucdavis.edu/vmth/lab_services/anatomic_pathology/index.cfm)

macrophages by degrading the iron exporter, ferroportin. In humans, decreased hepcidin synthesis caused by mutations in the hepcidin gene, *HAMP*, causes severe hemochromatosis in juveniles.[1,5]

Within the cytoplasm, iron is stored as ferritin, which is reconverted into iron as needed by the body. If tissue ferritin levels are high, ferritin aggregates into hemosiderin globules, which is much more difficult to revert back to free iron. In hepatocytes overwhelmed with iron, most iron is stored as hemosiderin. Ferritin and hemosiderin readily stain with Pearls Prussian blue, demonstrated nicely in this case.[1,5]

Iron is a direct hepatotoxin and iron overload often results in the formation periportal bridging fibrosis with little inflammation.[1,5] In addition to the markedly elevated postmortem liver heavy metal screen (Iron: 5100 ppm [100-300]), clinical pathology data from the provided serum biochemistry supports the histologic findings in this case. Elevated sorbital dehydrogenase (SHD: 16 IU/L [0-8]) and elevated plasma ammonia (242 UG/dL [5-59]) indicate hepatocellular injury and decreased hepatic function respectively. In addition, elevated gamma-glutamyl transpeptidase (GGT: 294 IU/L [8-22]) and elevated resting bile acids (36 uMOL/L [0-20]) indicate cholestasis and biliary hyperplasia with decreased hepatobiliary function.[1,2,5,8]

Contributing Institution:
University of California Davis
VMTH Anatomic Pathology
1 Garrod Dr.
Davis, CA 95616
http://www.vetmed.ucdavis.edu/vmth/lab_services/anatomic_pathology/index.cfm

Clin Path Data:
See charts appended at end of document.

References:

1. Bain PJ. Liver. In: Latimer KS ed. *Duncan and Prasse's Veterinary Laboratory Medicine Clinical Pathology*. 5th ed. Ames, IA:Wiley-Blackwell; 2011:213-224.
2. Brockus CW. Erythrocytes. In: Latimer KS ed. *Duncan and Prasse's Veterinary Laboratory Medicine Clinical Pathology*. 5th ed. Ames, IA:Wiley-Blackwell; 2011:4
3. Cullen JM, Stalker MJ. Liver and biliary system. In: Maxie MG, ed. *Jubb, Kennedy, and Palmer's Pathology of Domestic Animals*. Vol 2. 6th ed. Philadelphia, PA:Elsevier; 2016:272.
4. Galosi L, Farneti S, Rossi G, et al. *Yersinia pseudotuberculosis*, serogroup O:1A, infection in two amazon parrots (*Amazona aestiva* and *Amazona oratrix*) with hepatic

hemosiderosis. *J Zoo Wildl Med*. 2015; 46(3):588-591.
5. Kumar V, Abbas AK, Fausto N. Red blood cell and bleeding disorders. In: *Robbins and Cotran Pathologic Basis of Disease*. 9th ed. Philadelphia, PA:Elsevier Saunders; 2015:650-651.
6. Lavoie JP, Tuescher JP. Massive iron overload and liver fibrosis resembling haemochromatosis in a racing pony. *Equine vet J*. 1993;25(6):552-554
7. Mazzaro LM, Johnson SP, Fair PA, Bossart G, Carlin KP, Jensen ED, Smith CR, Andrews GA, Chavey PS, Venn-Watson S. Iron indices in bottlenose dolphins (Tursiops truncatus). *Comp Med*. 2012; 62:508-515.
8. O'Toole D, Kelly EJ, McAllister MM, et al. Hepatic failure and hemochromatosis of Salers and Salers-cross cattle. *Vet Pathol*. 2001; 38(4):372-389.
9. Pietrangelo A. Hereditary hemochromatosis—A new look at an old disease. *N Engl J Med*. 2004; 350(23):2383-2397.
10. Weiss DJ. Iron and copper deficiencies and disorders of iron metabolism. In: Weiss DJ, Wardrop KJ, eds. *Schalm's Veterinary Hematology*. 6th ed. Ames, IA:Wiley-Blackwell; 2010:170.

CASE III: B110209 (JPC 4086860).

Signalment: Eight-year-old, female, Labrador retriever, (*Canis familiaris*).

History: The dog had a history of polyuria and polydipsia with several urinary accidents. Otherwise, she was clinically healthy. Initial blood work showed azotemia (BUN: 26 mg/dL [reference range: 5-20]; serum creatinine: 2.0 mg/dL [reference range: 0.6-1.6]) and glucosuria (4+) with normal blood glucose. There was also increased ALT (458 IU/L [reference range: 10-55]). Her urine was isosthenuric and contained fine granular casts. Her blood pressure was normal (systemic blood pressure: 140 mmHg). There was no history of exposure to toxins. Subsequent blood work one month later showed increased azotemia (BUN: 23 mg/dL; serum creatinine: 3.0 mg/dL), ALT (707 IU/L), and mild proteinuria (UPC: 1.3 [normal <0.5]).

Gross Pathology: A wedge biopsy of the renal cortex was submitted for evaluation. Wedge biopsies of liver were also harvested and submitted to a different diagnostic laboratory. No gross abnormalities were observed at surgery.

Laboratory results:
The unfixed renal tissue that had been submitted for IF evaluation, and a portion of the liver sample were submitted to Colorado State Diagnostic Laboratory to measure copper. There was evidence of copper hepatopathy (copper 2,690 ppm [>1,500 ppm in the liver is considered toxic]) and copper in the kidney 243.00 ppm (relevant reference range >100 ppm in non-hepatic tissue being indicative of toxicity). Urine was also submitted approximately 10 days after the biopsy. SDS-PAGE analysis of urine demonstrated proteinuria due to the presence of low molecular weight proteins, consistent with tubular damage and absence of glomerular injury. An aliquot of this urine sample was submitted to PennGen which documented generalized amino-aciduria and glucosuria without ketonuria or cystinuria warranting a diagnosis of acquired Fanconi syndrome.

glomeruli have minimal to mild mesangial

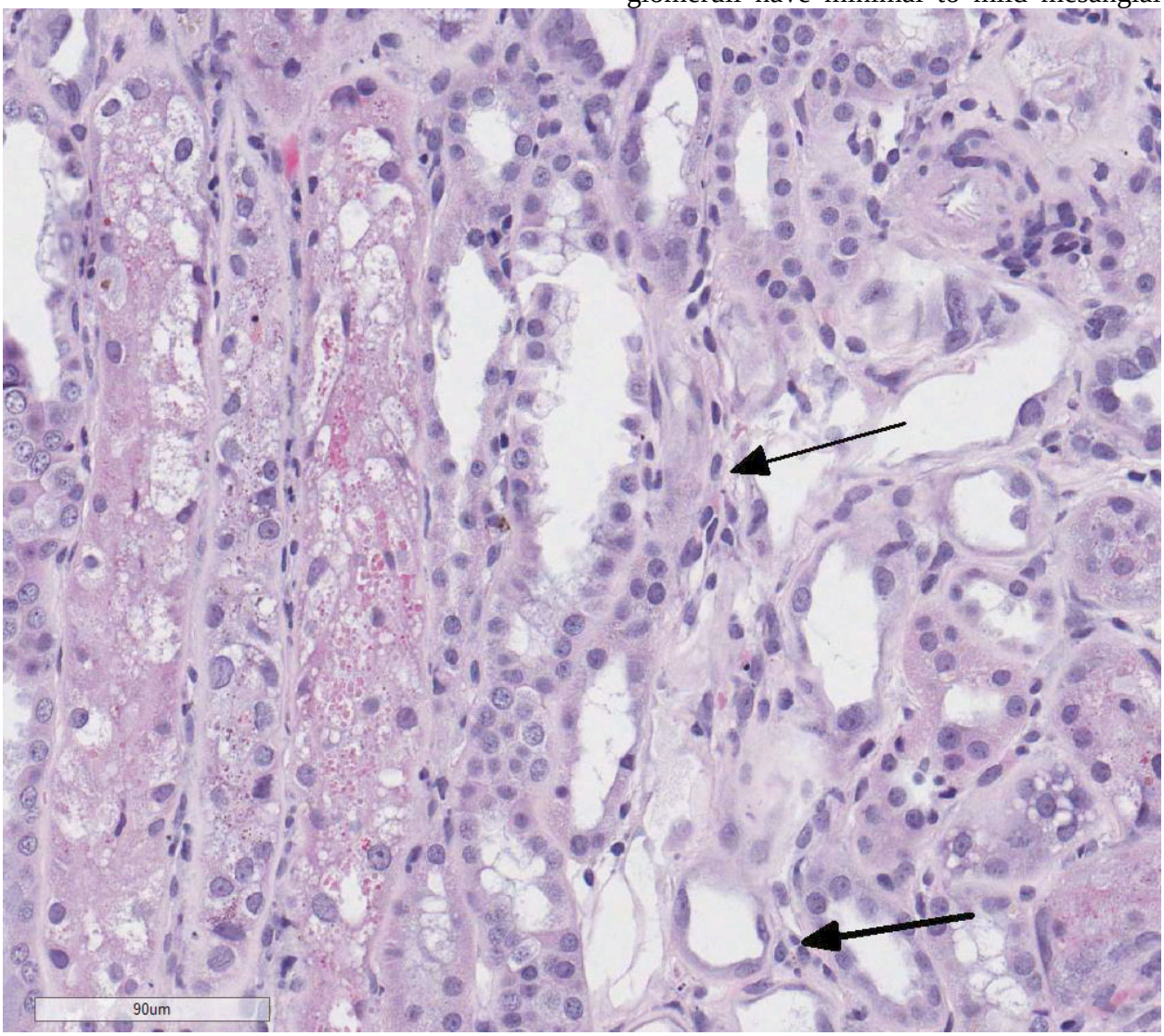

Kidney, dog. At left, tubular epithelium is swollen by clear vacuoles (hydropic degeneration) and numerous brown to pink intracytoplasmic granules. There are few necrotic and sloughed cells within the obliterated lumen. At right, atrophic and ectatic tubules are surrounded by collagen (arrows) which is infiltrated by low numbers of lymphocytes and neutrophils. (HE, 224X)

Histopathologic Description: (H&E): There is loss of the apical brush border of the proximal tubules. Scattered tubules are necrotic with cellular casts within lumens and attenuated or absent epithelial lining. Tubules are dilated and undergoing degeneration with single cell necrosis and apoptosis. The tubular epithelial cells contain variably sized cytoplasmic vacuoles with abundant granular pigment. There is marked epithelial cell karyomegaly. A few expansion and the interstitium is mildly expanded by fibroplasia with scattered aggregates of lymphocytes and macrophages.

Special stains: Rhodanine stain: Scattered tubular epithelial cells contain small and large red-brown granules, consistent with copper. PAS demonstrates multifocal marked loss of the apical brush borders. The trichrome stain demonstrates a few

large regions of mild to moderate interstitial fibrosis.

Contributor's Morphologic Diagnosis: Moderate to severe tubular degeneration with necrosis, regeneration, atrophy, epithelial cell karyomegaly and scattered intracytoplasmic copper within tubular epithelial cells. Mild multifocal interstitial fibrosis.

Contributor's Comment: The lesions presented in this case are indicative of renal proximal tubular injury, which was clinically supported by the urinalysis results. These acquired lesions have been associated with copper storage hepatopathy as a part of Wilson's disease in humans and dogs. Acquired Fanconi syndrome is characterized by impaired reabsorptive function of the proximal renal tubules. Clinical features include excessive loss of water, glucose, amino acids, uric acid in the urine, and electrolyte abnormalities. The inherited form of Fanconi-like syndrome is well described in Basenji dog and is thought to be due to increased amounts of cholesterol in the

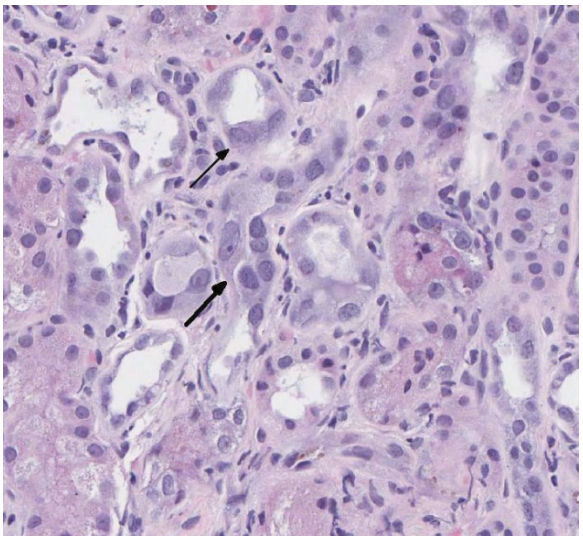

Kidney, dog: Tubules are occasionally lined by regenerating epithelium with large nuclei and basophilic cytoplasm. (HE, 256X)

tubular epithelial brush border compared to

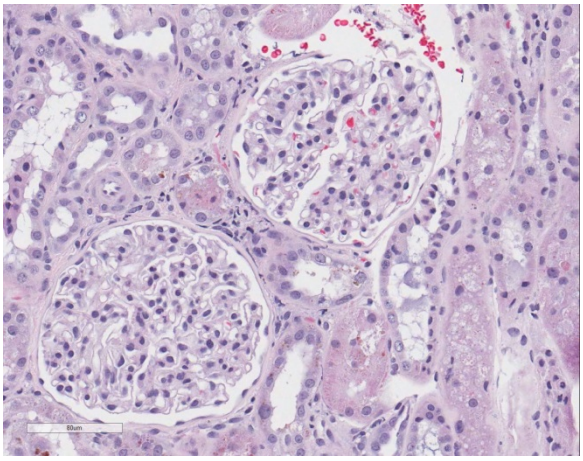

Kidney, dog. Glomeruli are mildly enlarged, hypercellular and have increased basement membrane material. Bowman's capsule is also expanded. (HE, 256X)

normal dogs. In contrast, acquired proximal renal tubulopathies have been loosely characterized in the literature and is attributed to many causes including copper hepatopathy, leptospirosis, hypo-parathyroidism, ethylene glycol toxicity, antibiotic, and chicken jerky treats.

In humans, Wilson's disease is an autosomal recessive disorder of copper metabolism caused by mutations in the *ATP7B* gene. Decreased expression of this gene leads to decreased biliary excretion of copper resulting in hepatic copper accumulation. Patients with Wilson's disease also accumulate copper in various tissues including the brain, eye, and kidney. Copper storage diseases have been reported in several canine breeds including Bedlington terrier, Labrador retriever, Doberman pinscher, Dalmatian, Skye terrier and West Highland white terrier. The inherited form of copper storage disease has been well documented in Bedlington terrier in which the copper metabolism domain containing 1 (*COMMD1*) gene is affected. The COMMD1 protein is important for copper excretion into bile during states of elevated intracellular copper. Hepatic histopathology of copper associated hepatopathies generally

present with mixed inflammation (neutrophilic, lymphoplasmacytic, histiocytic) and is usually localized to the centrilobular regions. Centrilobular necrosis, bridging fibrosis, and cirrhosis have also been described in copper-associated hepatitis. Of note, chronic liver injury will lead to increased amounts of copper in the hepatocytes, sometimes making it difficult to discern whether intracellular copper is the cause or the effect of the liver injury.

A few case series/reports have documented acquired proximal renal tubulopathies associated with copper storage hepatopathy in dogs. Breeds included are: Clumber spaniel, West Highland white terrier, Cardigan Welsh corgi, and Labrador retriever. The renal histologic findings in previous reported cases were consistent with the case presented here. Histologic evaluation of the renal tissues showed proximal tubular epithelial degeneration, necrosis, and regeneration. The tubular epithelial cells were plump with variably sized vacuoles. Using rhodanine stain, one case reported copper deposition was mainly localized to the corticomedullary junction and medullary areas; however copper staining can be variable. Therefore, mild tubular epithelial cell degeneration and loss of the apical brush border in the setting of clinical symptoms of Fanconi syndrome should alert the pathologist to possible copper-mediated damage to the renal proximal tubules. Assay of copper levels in the liver or kidney samples supports this pathogenesis.

In previous case reports of copper hepatopathy induced proximal renal tubular disease, there was improvement and resolution of clinical signs with copper chelation therapy, specifically using d-penicillamine. Additional therapies including supportive care, antioxidants, and low copper diet can also contribute to improvement of clinical signs.

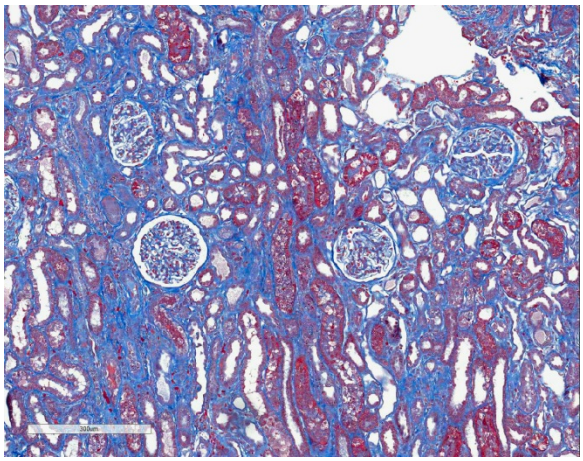

Kidney, dog. A Masson's trichrome demonstrates the large amount of fibrous connective within the interstitium, which is difficult to visualize on the HE-stained section. (Masson's trichrome, 88X)

JPC Morphologic Diagnosis: Kidney, tubules: Epithelial degeneration, regeneration, and necrosis, diffuse, marked, with karyomegaly, few tubular casts, intracytoplasmic pigment and interstitial fibrosis, Labrador retriever, *Canis familiaris*.

Conference Comment: The contributor provides an excellent example and thorough review of copper-associated acquired Fanconi-like syndrome. This syndrome is characterized by polyuria, polydipsia, hyposthenuria, glucosuria with normoglycemia, hyperphosphaturia, proteinuria, and amino aciduria due to impaired renal tubular absorption of glucose, phosphates, sodium, potassium, uric acid, and amino acids.[1,2,4,7] In this case, this animal had glucosuria with normoglycemia and amino-aciduria indicating poor proximal convoluted tubular functioning. Glucose is normally resorbed in the renal proximal tubules via the sodium-glucose co-transport system.[1,7,9] The concentration gradient established by this system also promotes sodium resorption from the tubular fluid. In

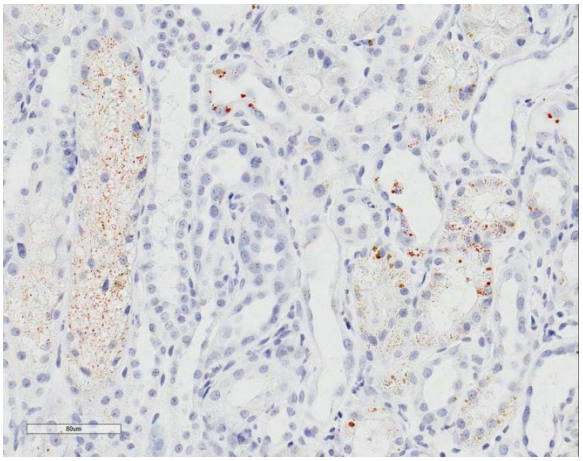

Kidney, dog: A rhodanine stain demonstrates abundant copper within degenerate/necrotic tubules. (Rhodanine, 252X)

congenital or acquired tubular defects of Fanconi-like syndrome, glucose is not resorbed and will cause an osmotic diuresis. This diuresis causes a marked decrease in kidney's ability to concentrate urine and will increase urine volume; indicated by polyuria and isosthenuria reported in this case.[1,7,9] The polydipsia is likely secondary to compensation from increased fluid loss in the urine.

Conference participants discussed the significance of the reported presence of low molecular weight proteins in the urine using sodium dodecyl sulfate polyacrylamide gel electrophoresis (SDS-PAGE). In general, there are four main types of proteinuria: pre-renal, glomerular, tubular, and hemorrhagic/inflammatory. In pre-renal proteinuria, small proteins such as hemoglobin dimers, myoglobin, and light chains are present in the plasma at increased concentrations and pass through the glomerulus and are incompletely resorbed by fully functioning tubules.[8] Glomerular proteinuria is characterized by damage to the glomerulus, thus enabling high molecular weight and negatively charged proteins to leak into the filtrate and pass into the urine due to loss of selective permeability.[8] In tubular proteinuria, proximal renal tubules are damaged or defective so low molecular weight proteins, like smaller globulins and some albumen, do not get resorbed from the ultra-filtrate and are excreted in the urine. Hemorrhagic/inflammatory proteinuria occurs due to hemorrhage or inflammation within the renal tubules, renal pelvis, or lower urinary tract. In this case, SDS-PAGE detected low molecular weight proteins within the urine and suggests that the primary lesion is in the proximal tubules rather than the glomeruli.[8] This finding is confirmed by the histopathology of the kidney in this case. The characterization of proteinuria by SDS-PAGE is a useful antemortem clinical tool to identify the main pathophysiologic mechanism involved.

Although not reported in this case, this animal was likely in a secretory metabolic acidosis due to renal tubular acidosis and loss of bicarbonate through the urine. In cases of Fanconi-like syndrome, the renal proximal tubules fail to resorb filtered bicarbonate.[3] Other causes of secretory metabolic acidosis include vomiting of intestinal contents rich in bicarbonate, diarrhea, and an inability to swallow saliva rich in bicarbonate in ruminants during dysphagia.[3] The hallmark of this type of acidosis is concurrent hyperchloremia as the body attempts to maintain electroneutrality. In addition, the anion gap will typically be normal because unmeasured anions are not increased.[3]

Contributing Institution:
Department of Biosciences
The Ohio State University
Columbus OH
https://vet.osu.edu/

Clin Path Data:
See chart appended at end of document.

References:

1. Appleman EH, Cianciolo R, Mosenco AS, Bounds ME, et al. Transient Acquired Fanconi Syndrome Associated with Copper Storage Hepatopathy in 3 Dogs. *J Vet Intern Med.* 2008; 22:1038-1042.
2. Coronado VA, O'Neill B,Nanji M, Cox DW. Polymorphisms in canine ATP7B: candidate modifier of copper toxicosis in the Bedlington terrier. *Vet J*. 2008; 2:293-96.
3. George JW, Zabolotsky SM. Water, electrolytes, and acid base. In: Latimer KS, ed. *Duncan and Prasse's Veterinary Laboratory Medicine Clinical Pathology*. 5th ed. Ames, IA: Iowa State University Press; 2011:163-166.
4. Hill TL, Breitschwerdt EB, Cecere T, Vaden S. Concurrent Hepatic Copper Toxicosis and Fanconi's Syndrome in a Dog. *J Vet Intern Med.* 2008; 22:219–22.
5. Hoffman G. Copper-Associated Liver Diseases. *Vet Clin Small Anim.* 2009; 39:489–511.
6. Hooper AN, Roberts BK. Fanconi syndrome in four non-basenji dogs exposed to chicken jerky treats. *J Am Anim Hosp Assoc*. 2011; 47:e178-87.
7. Langlois DK, Smedley RC, Schall WD, Kruger JM. Acquired proximal renal tubular dysfunction in 9 Labrador retrievers with copper-associated hepatitis (2006-2012). *J Vet Intern Med*. 2013; 27:491-9.
8. Stockham SL, Scott MA. Urinary system. In: Fundamentals of Veterinary Clinical Pathology. 2nd ed. Ames, IA: Blackwell Publishing; 2008:458-460.
9. Thompson MF, Fleeman LM, Kessell AE, Steenhard LA, Foster SF. Acquired proximal renal tubulopathy in dogs exposed to a common dried chicken treat: retrospective study of 108 cases (2007-2009). 2013. *Aust Vet J*. 9;368-73.

CASE IV: 16-2046 (JPC 4084201).

Signalment: Three-year-old, male, English setter mix, (*Canis familiaris*).

History: The three-year-old intact male English setter mix was picked up by county animal control when it was found roaming freely in a small rural community in Southern Arizona. Aspirate cytology from the preputial mass and several cutaneous masses were submitted.

Gross Pathology: The dog had a large ulcerated circumferential mass effacing the preputial mucosa and numerous variably sized cutaneous masses throughout the caudal dorsum, right and left flank, and inguinal regions. The superficial cervical lymph nodes were enlarged.

Laboratory results:
The dog was positive for *Ehrlichia canis* using in-house ELISA testing.

Preputial mass, dog. The prepuce is markedly expanded by a large ulcerated neoplasm, in addition to other masses on the caudal dorsum, flank, and inguinal regions. (Photo courtesy of: Arizona Veterinary Diagnostic Laboratory, University of Arizona, http://azvdl.arizona.edu/

Cytologic Description: The aspirate preparations from the dermal masses all revealed the same process. The preparations have high cellularity with large numbers of intact cells for evaluation. There is minimal hemodilution. The nucleated cell population consists of round cells with moderate anisokaryosis and anisocytosis. The nuclei are round with coarse "ropey" chromatin and often have a single large pale lightly basophilic nucleolus. The cytoplasm is lightly basophilic and contains small to moderate numbers of discrete round vacuoles. Mitotic figures are common and atypical mitoses are seen. There are occasional neutrophils and small lympho-cyte seen intermixed with the neoplastic round cells.

The cytology preparations from the prepuce showed the same cytological findings.

Contributor's Cytologic Diagnosis: Transmissible venereal tumor (TVT) metastatic to skin.

Contributor's Comment: Transmissible venereal tumor is a transplantable neoplasm that affects members of the canid family (domestic dogs, coyotes, foxes, and wolves).[3] The tumor has a global distribution and highest prevalence in regions with limited canine population control. The tumor spreads by sexual contact and is usually localized to the mucosal surface of the external genitalia of both male and female dogs. However, masses have been reported in the mucosal surfaces of the nasal passage, oral mucosa, anus, and conjunctival surfaces of the eye.[3,7] Metastatic disease is not common but has been documented. In most cases, metastasis is to the regional lymph nodes, but extension of the neoplasm to skin, kidney, brain, bone, peritoneum, and other tissues has been reported.[1,3] The tumor cells are aneuploid and have a unique long interspersed nuclear element (LINE-1) that may be useful to confirm TVT origin in cases involving tumors in unusual sites.[10,12]

While TVT is a relatively uncommon tumor in most of the United States, rural areas that have higher numbers of intact dogs, such as many parts of Southern Arizona, cases are seen on a regular basis. The histological and cytological characteristics of the neoplastic cells along with the location of the mass in

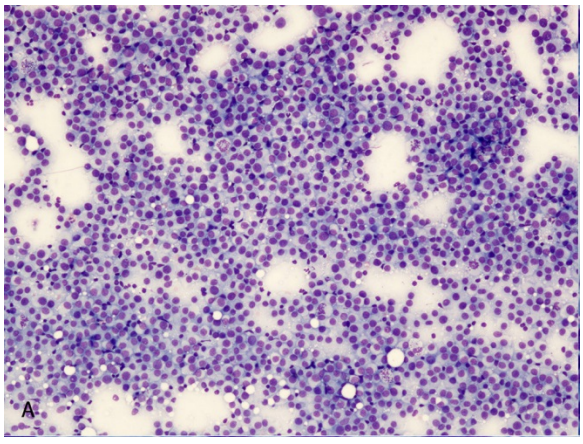

Preputial mass, dog. The cytologic preparation is densely cellular on a background of light blue protein. (Wright-Giemsa, 100X)

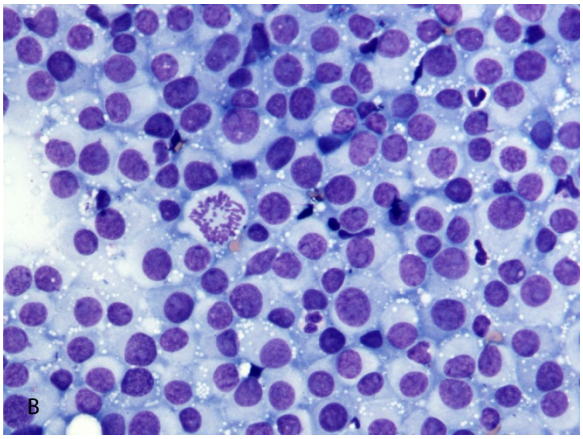

Preputial mass, dog. Neoplastic cells are monomorphic with mild anisokaryosis and a few lymphocytes and neutrophils in the background. (Wright-Giemsa, 200X)

association with the external genitalia make the diagnosis of this tumor relatively straight forward. In this case, the cytological and histological findings from the skin lesions and the preputial lesion were identical supporting metastatic disease. There is one report of a prepubertal female dog without any genital involvement.[4] It is proposed that the tumor cells were transplanted from the dam by cohabitation and grooming/social behaviors. While multicentric disease cannot be ruled out, it is unlikely that multiple sites of transplantation through intact haired skin would explain the presence of the skin lesions in this adult male dog with a concurrent preputial mass.

JPC Cytologic Diagnosis: Fine needle aspirate, cutaneous mass: Transmissible venereal tumor, English setter mix, *Canis familiaris*.

Conference Comment: Canine transmissible venereal tumor (TVT), also known as Sticker tumor or venereal granuloma, is an extremely old and remarkably stable transmissible cancer that first arose in canids approximately 11,000 years ago.[2,5] Based on genetic studies, the founder breed is thought to be closely related to wolves or ancient Eastern Asian dog breeds.[1] TVT dispersed across several continents about 500 years ago and is currently found on every continent in the world other than Antarctica.[5,12] It is the oldest known continuously passaged somatic cell lineage.[5] As mentioned by the contributor, TVT is mainly transmitted during coitus, but can also be transmitted by licking, biting, or rubbing behaviors.[2,8] The infecting cells are physically transplanted and grow as a xenograft in host tissue. Neoplastic cells are thought to be of histiocytic origin and are immune-positive for vimentin, lysozyme, alpha-1-antitypsin, glial fibrillary acidic protein, and are immune-negative for cytokeratin, S100, and muscle markers.[1,2,9]

Typical gross findings of TVT include solitary or multiple papillary, nodular, ulcerated, and inflamed masses on the mucous membranes of the penis, prepuce, vulva, and vagina, and/or skin and subcutis of the head, neck, limbs, trunk, scrotum, and perineum. There is occasional extension to the uterus and cervix.[2,9] A recent study demonstrated ocular lesions as the single manifestation of TVT with extension to the adjacent conjunctiva and nictitating membrane, presumably by extra-genital

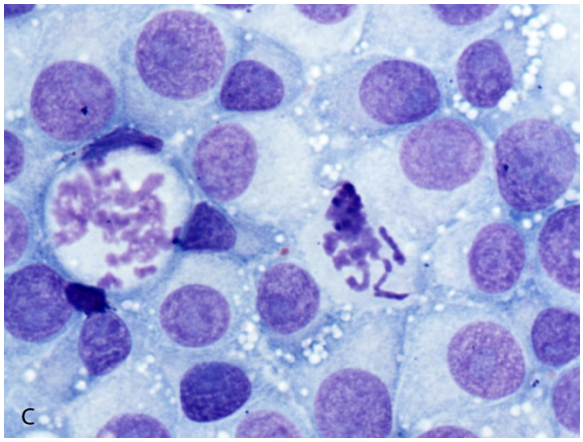

Preputial mass, dog. Neoplastic mast cells have moderate amounts of light blue cytoplasm and discrete vacuoles. There are two mitotic figures in this field. (Wright-Giemsa, 600X)

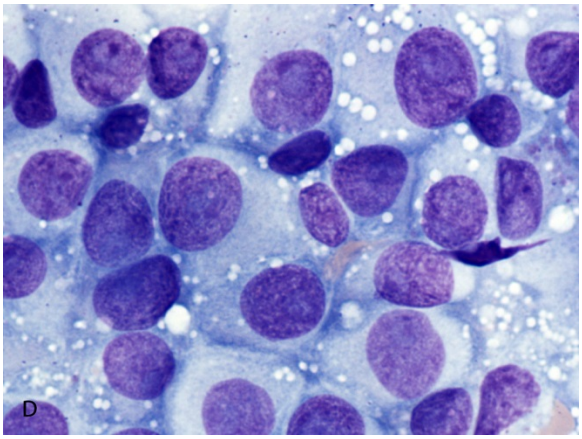

Preputial mass, dog. Nuclei are mildly anisokaryotic with prominent nucleoli. Few lymphocytes are present in between neoplastic cells. (Wright-Giemsa, 600X)

inoculation.[3] As mentioned by the contributor, metastasis uncommonly occurs in the draining lymph node.[9]

After transmission, tumorous lesions typically appear within two months. Conference participants discussed the pathogenesis of the tumor growth, stabilization, and regression phases. The initial growth stage is called the progressive phase (P). During the P phase, almost all TVT cells lack expression of major histocompatibility complex (MHC) I and II due to production of inhibitory cytokine transforming growth factor-beta (TGF-beta). This allows the TVT cells to grow and evade immune destruction by cytotoxic T-lymphocytes. After three to nine months, the tumor stabilizes and begins to spontaneously regress. During the regression (R) phase, interleukin-6 (IL-6) from infiltrating lymphocytes is thought to work in conjunction with interferon-gamma (IFN-gamma) to antagonize TGF-beta and increase MHC I and II expression on TVT cells.[1,8-10]

In addition to TVT, conference participants also discussed the devil facial tumor disease (DFTD), which is an emerging rapidly fatal transmissible tumor that is decimating the wild Tasmanian devil population.[8,11] This tumor is of Schwann cell origin and is spread through biting. Tumors occur primarily in the mouth, head, and neck. DFTD cells evade immune destruction via production of TGF-beta and down regulation of MHC-I and II expression, similar to TVT. However, unlike TVT, spontaneous regression has not been reported in DFTD, and mortality occurs in all affected animals via starvation and frequent metastasis.[8] Other transmissible tumors include clam leukemia of soft shell clams and the contagious reticulum cell sarcoma of Syrian hamsters first described in the 1960's.[6,8,11]

Contributing Institution:

Arizona Veterinary Diagnostic Laboratory
University of Arizona
2831 N. Freeway
Tucson, AZ 85705
http://azvdl.arizona.edu/

References:

1. Ganguly B, Das U, Das AK. Canine transmissible venereal tumor: A review. *Comp Oncol*. 2016; 14(1):1-12.
2. Gross TL, Ihrke PJ, Walder EJ, Affolter VK. *Skin Diseases of the Dog and Cat*. 2nd ed. Oxford, UK: Blackwell Publishing; 2005:800-803.
3. Komnenou AT, Thomas AL, Kyriazis AP, et al. Ocular manifestations of canine transmissible venereal tumor: A retrospective study of 25 cases in Greece. *Vet Rec*. 2015; 176(20):523-527.
4. Marcos R, Santos M, Marrinhas C, et al. Cutaneous transmissible venereal tumor without genital involvement in a prepubertal female dog. *Vet Clin Pathol*. 2006; 35:106–109.
5. Murchison EP, Wedge DC, et al. Transmissible dog cancer genome reveals the origin and history of an

ancient cell lineage. *Science*. 2014; 343:437-440.
6. Ostrander EA, Davis BW, Ostrander GK. Transmissible tumors: Breaking the cancer paradigm. *Trends Genet*. 2016; 32:1-15.
7. Park MS, Kim Y, Kang MS, et al., Disseminated transmissible venereal tumor in a dog. *J Vet Diagn Invest*. 2006; 18(1):130-133.
8. Pye RJ, Woods GM, Kreiss A. Devil facial tumor disease. *Vet Pathol*. 2016; 53(4):726-736.
9. Schlafer DH, Foster RA. Female genital system. In: Maxie MG, ed. *Jubb, Kennedy, and Palmer's Pathology of Domestic Animals*. Vol 3. 6th ed. St. Louis, MO: Elsevier; 2016:448-449.
10. Setthawongsin C, Techangamsuwan S, Tangkawattana S, et al. Cell-based polymerase chain reaction for canine transmissible venereal tumor (CTVT) diagnosis. *J Vet Med Sci*. 2016; 78(7):1167-1173.
11. Siddle HV, Kaufman J. A tale of two tumours: Comparison of the immune escape strategies of contagious cancers. *Mol Immunol*. 2013; 55:190-193.
12. VonHoldt BM, Ostrander EA. The singular history of a canine transmissible tumor. *Cell*. 2006; 126(3):445-447.

Case 2 - Clinicopathologic Data

Chemistry 15C02406 Final Report

Patient#:
Name:
Breed: EQ-QH
Sex: F
Color: Red Dun
Birth: 2005

Provisional Diagnosis/History: Chronic Liver Failure

Equine Foal Reference Intervals

LisAccn	Procs	SpecimenType	Vessel	Method	Collected	DrawnBy	Comment
15C02406	7794	Whole Blood	RTT	VEN	03Feb15 at 3:00pm.	azr	

Procedures Requested: 7794 Liver Panel-Large Animal

Liver Panel-Large Animal	Result	Horse Ref	Units	Comments
TOTAL PROTEIN	7.1	5.8-7.7	G/DL	
ALBUMIN	3.2	2.7-4.2	G/DL	
GLOBULIN	3.9	1.6-5.0	G/DL	
AST	315	168-494	IU/L	
ALKALINE PHOSPHATASE	212	86-285	IU/L	
GGT	294	8-22	IU/L	
SDH-37	16	0-8	IU/L	
BILIRUBIN TOTAL	1.5	0.5-2.3	MG/DL	
BILIRUBIN DIRECT	0.2	0.2-0.6	MG/DL	
BILIRUBIN INDIRECT	1.3	0.3-1.7	MG/DL	
HEMOLYSIS INDEX	11	0-14		
ICTERIC INDEX	3	0-4		
LIPEMIC INDEX	5	0-<1		

Comments: HEMOLYSIS INDEX: A hemolysis index value between 0 and 14 will not affect test results. ICTERUS INDEX: An icterus index value between 0 and 4 will not affect test results. LIPEMIA INDEX: A lipemic index value between 1 and 149 will effect the following test:TRIG.

Ammonia	Result	Horse Ref	Units	Comments
AMMONIA, PLASMA	242	5-59	UG/DL	

Bile Acid	Result	Horse Ref	Units	Comments
BILE ACIDS PRE/RESTING	36		uMOL/L	

Reference 0-20 umol/L

Case 3 - Clinicopathologic Data

Initial blood work:
BUN: 26 mg/dL [reference range: 5-20]
Creatinine: 2.0 mg/dL [reference range: 0.6-1.6]
Blood glucose: WNL
ALT (458 IU/L [reference range: 10-55]).

Urinalysis:
Glucosuria (4+)
Her urine was isosthenuric and contained fine granular casts.

Subsequent blood work one month later:
BUN: 23 mg/dL;
Serum creatinine: 3.0 mg/dL
ALT (707 IU/L)

Urinalysis:
Mild proteinuria (UPC: 1.3 [normal <0.5])
SDS-PAGE analysis demonstrated proteinuria due to the presence of low molecular weight protein.
An aliquiot from the urine sample documented generalized amino aciduria and glucosuria without ketonuria.

Self-Assessment - WSC 2016-2017 Conference 10

1. Which of the following is not true about *Pearsonema feliscati?*
    a. There are no significant differential characteristics between it and *P. plica*, a related species, other than host.
    b. Clinical disease is rare in the cat.
    c. Characteristic unioperculate eggs are readily identified in urinary sentiment.
    d. Pearonema is a subclassifiatio of aphasmid nematodes of the family *Trichuridae*

2. An inherent abnormality in iron metabolism is a form of which of the following?
    a. Hemosiderosis
    b. Hemochromatosis
    c. Primarily iron storage disease
    d. Secondary iron storage disease

3. Which of the folllowing enzymes is transported in the blood and results in the blockage of release of iron from enterocytes and macrophages
    a. Hepcidin
    b. Transferrin
    c. Alpha-2-macroglobulin
    d. Sorbitol dehydrogenase

4. What is the proposed cellular lineage of transmissible venereal tumor?
    a. B-cells
    b. Histiocytes
    c. Urothelium
    d. NK cells

5. Which of the following is a proximate cause of acquired Fanconi-like syndrome In the Basenjji dog?
    a. Increased expression of the COMMD1 gene.
    b. Increased cholesterol
    c. Mutations in the ATP7B gene
    d. Copper-associated hepatitis

Joint Pathology Center

Veterinary Pathology Services

WEDNESDAY SLIDE CONFERENCE 2016-2017

C o n f e r e n c e 11

16 November 2016

Andrew W. Suttie, BVSc, PhD, Diplomate ACVP
Covance Laboratories Inc.
14500 Avion Parkway
Chantilly, VA 20151-1130

CASE I: Case1 (JPC 4088440).

Signalment: Eight-week-old, female, Wistar-Han rat, (*Rattus norvegicus*).

History: Control rat from a 7-day exploratory toxicity study.

Gross Pathology: In the right and left eyes, diffusely opaque lens noted at necropsy.

Laboratory results: None.

Histopathologic Description: Eye, lens: Multifocally, there is disruption and dissolution of the lenticular fibers often replaced by variably sized, irregular vacuoles which contain spherical to irregularly-shaped globular eosinophilic aggregates (Morgagnian globules). Lens epithelial cells are multifocally swollen with abundant eosinophilic microvacuolated cytoplasm (bladder cells). At one pole, lens epithelial cells become spindyloid and are separated by fine collagen fibers (fibrous metaplasia). The iris is attached to the anterior lens capsule (posterior synechia).

Eye, retina: Diffusely, the retina is disorganized. The outer nuclear layer forms numerous rosettes which surround a central space that contain eosinophilic fibrils (rods and cones). There is thinning of the outer plexiform layer and multifocal blending of the inner and outer nuclear layers. Retinal pigment epithelium is frequently vacuolated admixed with occasional nuclear cell debris and infiltration of macrophages. There is minimal hemorrhage admixed with scattered macrophages, lymphocytes, and neutrophils within the vitreous space.

Contributor's Morphologic Diagnosis: 1. Eye, lens: Cataract, diffuse, moderate to severe, with epithelial hyperplasia, posterior synechiae, and fibrous metaplasia.
2. Eye, retina: Dysplasia.
3. Eye, retina: Degeneration, multifocal, mild.

Globe, rat. At subgross, the iris leaflet at right is moderately thickened and adherent to the anterior face of the lens (posterior synechia), and the retina is moderately atrophic. (HE, 5X).

Contributor's Comment: Cataracts are the most common lenticular disease in aged Sprague-Dawley and Wistar rats. Cataracts are subclassified by the location in the lens: nuclear cataract involving the central area of the lens; cortical cataract involving the lenticular surface; and posterior capsular cataract involving the posterior surface of the lens and often arising under the capsule.[6] The case present herein is an example of the latter classification. Posterior capsular cataracts were described in 32% of aged Wistar rats and overrepresented in females.[10] The pathogenesis of cataract formation involves initial lens swelling due to loss of Na-K-dependent ATPase osmotic pumps resulting in potassium loss and sodium and calcium entry into the lens causing vacuolation and protein aggregation of the lens epithelium (bladder cell formation) with subsequent denaturation and hydrolysis of lens fibers (Morgagnian globules).[6] Cataract is considered a major cause of visual impairment in diabetic patients. The initiating mechanism in diabetic cataract formation is the generation of polyols from glucose by the aldose reductase pathway, resulting in a similar increased osmotic stress as described in spontaneous cataract formation leading to lens fiber swelling and rupture.[6]

Retinal dysplasia is the disorderly proliferation and differentiation of the retina and is characterized by blending and folding of the retinal layers, rosette formation, most commonly the inner and outer nuclear layers, and occasionally degeneration. Retinal dysplasia is an incidental developmental anomaly. These retinal folds and blending of the layers have been described in Wistar rats occasionally showing microphthalmia and cataracts.[6] Retinal dysplasia is spontaneous or inherited and is rarely progressive.[9] A linear form of retinal dysplasia has been reported in Sprague-Dawley rats at 7-10 weeks of age consisting of loss of the outer layers of the retina resulting in confluency of the inner nuclear layer with the choroid.[9] The findings

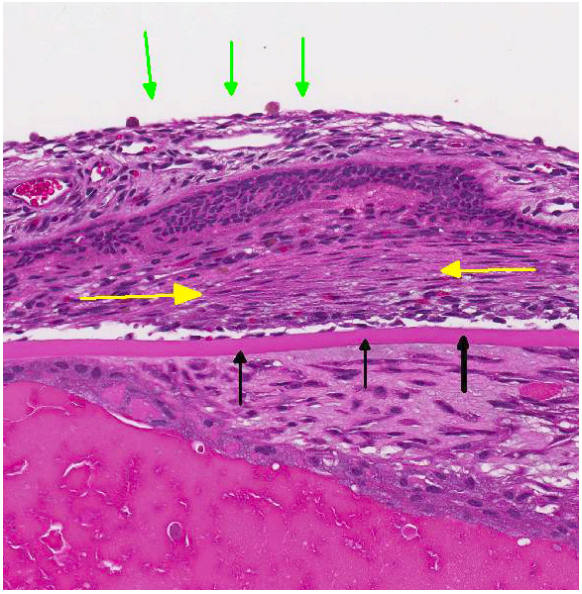

Globe, rat. The iris is covered by a pre- (green arrows) and post-iridal fibrovascular membrane (yellow arrows). The anterior lens capsule is delimited by black arrows. (HE, 80X)

described in this vehicle-treated animal were considered incidental.

JPC Diagnosis: 1. Eye, lens: Cataractous change, subcapsular, diffuse, characterized by Morgagnian globules, bladder cells, and fibrous metaplasia, with posterior synechia, Wistar-Han rat, *Rattus norvegicus*.
2. Eye, retina: Dysplasia.

Conference Comment: The contributor provides a superb example of the histologic changes associated with the formation of cataracts and retinal dysplasia in the rat. Cataracts result from exposure of the lens to a large variety of insults, including ultraviolet light, physical and chemical damage, increased intraocular pressure, numerous toxins, direct trauma, nutrient imbalance, and inflammation.[10] Spontaneous cataracts have also been reported to occur in up to 9.8% of Sprague-Dawley rats and 32% of aged (>2 years) Wistar rats.[2,10] Despite the wide variety of possible causes, the histologic lesions associated with cataractous change are relatively stereotypic across species. The lenticular lesions present in this case include Morgagnian globules, composed of bright eosinophilic globules of denatured lens protein; bladder cells, which are large foamy nucleated cells that may represent abortive epithelial attempts at new lens fiber formation; lens epithelial hyperplasia; and posterior migration of lens epithelium followed by fibroblastic metaplasia. The latter two changes are associated with chronic cataract formation.[10] Conference participants also noted the large size of the lens resulting in narrowing of the anterior chamber, which is a normal finding in the rat.[3]

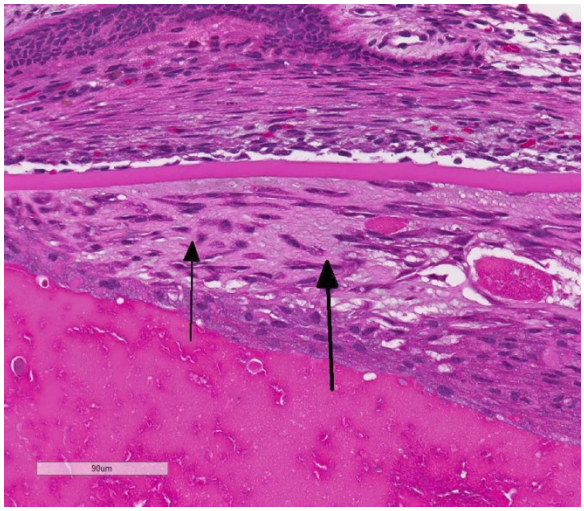

Globe, rat. There is multifocal fibrous metaplasia of subcapsular lenticular epithelium (black arrows). (HE, 228X)

This case also generated some spirited discussion among conference participants regarding whether the retinal changes represent a dysplastic or degenerative process. The albino Wistar rat is currently one of the most popular rats used for laboratory research and is exquisitely sensitive to phototoxicity due to the lack of melanin pigment.[3,7] Given the history of bilateral lesions, strain of the rat in this case, and relatively young age of the animal, the conference moderator posited that the cataractous change and retinal lesions could be secondary to phototoxicity. Rats housed in areas of greater light intensity, such as the outer columns and top racks, are more susceptible to developing phototoxic lesions.[7] Additionally, light-induced retinal degenerative changes typically manifest as disorganization and loss of photoreceptor cells in the outer retina, vacuolation of pigmented retinal epithelium, and accumulation of intracytoplasmic lipofuscin pigment, all of which are present in this case.[1]

Conference participants also discussed the possibility that the lesions in this case represent spontaneous and dysplastic change. Albino rodents are well known to have several kinds of spontaneous ocular lesions, including corneal dystrophy (calcium deposition), cataract, and retinal

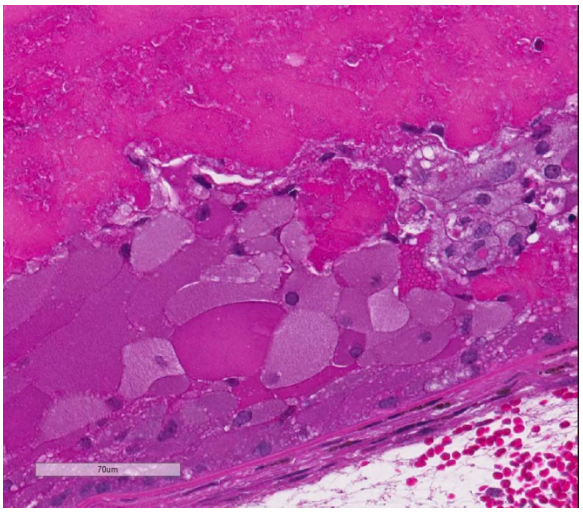

Globe, rat. At the periphery, lens fibers are swollen by large numbers of small vacuoles and often fragmented with liberation of globules of pink protein (Morgagnian cataract). (HE, 324X).

fold/dysplasia.[3] To help elucidate the possible underlying cause(s) of the retinal changes, this case was studied in consultation with the Dr. Leandro Teixeira, a board certified veterinary pathologist and recognized expert with extensive experience in the area of veterinary ocular pathology. Dr. Teixeira agrees with the contributor that the retinal rosettes, retinal folds, retinal atrophy, and blending of the inner and outer layers of the retina are common dysplastic changes in the rat, and are a result of faulty retinal development rather than a degenerative change. Similar dysplastic lesions can be induced by the administration of various toxins and carcinogens, such as cytosine arabinose, cycasin, N-methyl-N-nitrosurea, and trimethylin; however, this animal is reported to be a control rat and exposure to the aforementioned compounds is unlikely. Dysplastic lesions can be unilateral or bilateral, as in this case.[9] The lesions in the retinal pigmented epithelium, such as hypertrophy and vacuolation of pigmented epithelium and accumulation of lipofuscin, are also common mild cellular degenerative changes secondary to retinal dysplasia in the rat.

Contributing Institution:
Pfizer
Eastern Point Road
B274 MC1210
Groton, CT 06340
http://www.pfizer.com/

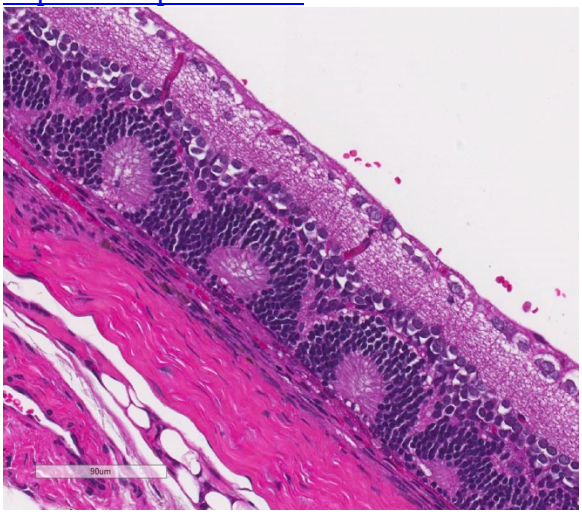

Globe, rat. There are numerous rosettes within the inner nuclear layer, the outer nuclear layer is mildly depleted. (HE, 228)

References:

1. Dubielzig RR, Ketring KL, McLellan GL, Albert DM. The retina. In: *Veterinary Ocular Pathology: A comparative review*. St. Louis, MO: Elsevier Saunders; 2010:360-366.
2. Durand G, Hubert MF, et al. Spontaneous polar anterior subcapsular lenticular opacity in Sprague-Dawley rats. *Comp Med*. 2001; 51:176-179.
3. Kazumoto S, Tomohiro M, et al. Characteristics of structures and lesions of the eye in laboratory animals used in toxicity studies. *J Toxicol Pathol*. 2015; 28(4):181-188.
4. Maggs D, Miller P, Ron O. *Slatter's Fundamentals of Veterinary*

Ophthalmology. 5th ed. St. Louis, MO: Elsevier Saunders; 2013:452.
5. Mellersh CS. The genetics of eye disorders in the dog. *Canine Genetics and Epidemiology*. 2014:1:3.
6. Pollreisz A and Schmidt-Erfurth U. Diabetic Cataract—Pathogenesis, Epidemiology and Treatment. *J Ophthalmol.* 2010; 1-8.
7. Percy DH, Barthold SW. Rat. In: *Pathology of Laboratory Rodents and Rabbits*. 4th ed. Ames, IA: Blackwell Publishing; 2016:161.
8. Poulsom R and Hayes B. Congenital retinal folds in Sheffield-Wistar rats. *Graefes Arch Clin Exp Ophthalmol* 1988; 226(1):31-3.
9. Schafer KA and Render JA. Comparative Ocular Anatomy in Commonly Used Laboratory Animals. Eds Weir AB and Collins W; Springer In: *Assessing Ocular Toxicology in Laboratory Animals*. 2012:229.
10. Wegener A, Kaegler M, Stinn W. Frequency and nature of spontaneous age-related eye lesions observed in a 2-year inhalation toxicity study in rats. *Ophthalmic Res*. 2002; 34(5): 281-7.
11. Wilcock BP, Njaa BL. Special senses. In: Maxie MG, ed. *Jubb, Kennedy and Palmer´s. Pathology of Domestic Animals*. 6th ed Vol. 1. St Louis, MO: Elsevier Saunders; 2016:436-474.

CASE II: E3133/15 (JPC 4084739).

Signalment: Twelve-year-old, male, dwarf rabbit, (*Oryctolagus cuniculus*).

History: Both testicles were submitted for histological examination because of increasing testicular size over time.

Gross Pathology: The formalin-fixed testicles measured 9 x 7 x 4 cm and 5 x 3 x 3 cm, respectively. The testicular parenchyma was almost completely replaced bilaterally by multilobulated, solid masses with a greyish cut surface. The mass was located on both sides within the testis and did not extend beyond the tunica albuginea.

Laboratory Results: Immuno-histochemistry was applied using commercially available antibodies. Tumor cells showed a diffuse immunolabelling for Melan-A and a multifocal expression of neuron-specific enolase in about 40-50% of the tumor cells. About 20-30% of the tumor cells displayed an immunolabelling for S-100 protein and single tumor cells expressed vimentin.

Neoplastic cells were negative for cytokeratin, α-smooth muscle actin, glial fibrillary acidic protein, and myelin basic protein.

Testes, rabbit. The formalin-fixed testicles measured 9 x 7 x 4 cm and 5 x 3 x 3 cm, respectively. The testicular parenchyma was almost completely replaced bilaterally by a multilobulated, solid mass with a greyish cut surface. The mass was located on both sides within the testis and did not extend beyond the tunica albuginea. (Photo courtesy of: Department of Pathology, University of Veterinary Medicine Hannover, Buenteweg 17, D-30559 Hannover, Germany, http://www.tiho-hannover.de/kliniken-institute/institute/institut-fuer-pathologie/

Samples for transmission electron microscopy were processed by direct pop-off technique from the HE- stained slide. The cytoplasm of the tumor cells was filled with numerous round, membrane-bound structures measuring about 500 to 1000 nm in diameter. These structures contained several membrane-bound, moderately electron-dense, round structures, measuring about 50 to 150 nm in diameter.

Histopathologic Description: The slide contains parts of the testicle, epididymis and tunica vaginalis. The majority of original testicular tissue is replaced by a multilobular, well demarcated, non-encapsulated, expansive, moderately cell-dense mass extending to the cut border on one side. Neoplastic cells are proliferated in solid fields supported by a small to moderate amount of fibrovascular stroma. The cells measure up to 70 µm in diameter and display a round to polygonal shape with an eccentrically located, 10 µm in diameter large, round to oval nucleus with finely stippled heterochromatin and one distinct, small, basophilic nucleolus. The abundant, eosinophilic, finely granular cytoplasm is surrounded by indistinct cell borders. Tumor cells show mild anisocytosis and anisokaryosis with a mitotic rate of 0-1 per high power field. In the cytoplasm of the tumor cells, a high number of PAS and PAS-diastase-resistant positive granules are present. These granules were also shown by Luxol Fast Blue staining. Remaining seminiferous tubules are compressed and lined by single Sertoli cells.
Multifocally within the tunica vaginalis there are few inflammatory cells, mainly consisting of plasma cells, lymphocytes, and fewer macrophages. In some slides eosinophilic, homogeneous, acellular material is present within the tunica vaginalis (edema). The epithelium of epididymal tubules is flattened and the diameter of the tubules is severely increased (dilatation). Within the epididymal tubules, no spermatozoa are present.

Contributor's Morphologic Diagnosis: Testicle: Granular cell tumor with severe testicular atrophy, dilatation of epididymal tubules and mild, chronic, multifocal, lymphohistiocytic and plasmacellular infiltration of the tunica vaginalis with

Testis, rabbit. A section of testis is submitted with epididymis at bottom. The testis (top) is replaced by a multilobular neoplasm. (HE, 5X)

edema.

Contributor's Comment: Testicular tumors in rabbits represent a rarely described entity. Mainly adult individuals are affected and interstitial cell tumors are most commonly reported.[6,7,19]

Granular cell tumors occur rarely in domestic and pet animals and have been reported in different species including horses, dogs, cats, guinea pigs, and rats.[2,6] In horses, granular cell tumors represent the most common primary neoplasm of the lung.[2,9] In dogs and rarely in cats, they occur in the oral cavity.[2,11] In rats, a meningeal localization has been described.[18] A variant of meningiomas, termed granular cell meningioma, has been reported in dogs located at the cerebral convexity, neurohypophysis, and spinal nerve roots.[1]

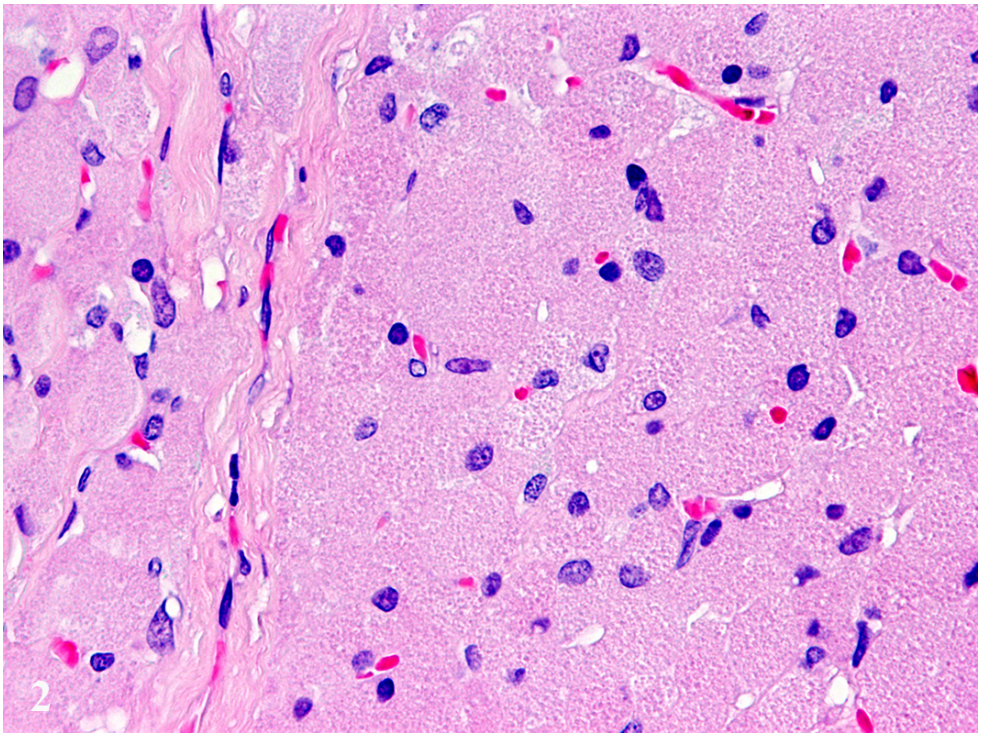

Testis, rabbit. Neoplastic cells range up to 40um in diameter, have, indistinct cell borders, and abundant pink granular cytoplasm. There is mild anisokaryosis. (HE, 400X)

Genital involvement of granular cell tumors has been reported in cats affecting the vulva.[5,6] Within the right atrium of a dog a granular cell tumor, also termed myoblastoma, has been described exhibiting typical cytoplasmic granules.[13] In guinea pigs, cutaneous granular cell tumors have been reported.[17]

The histogenetic origin of granular cell tumors remains unknown, but they are thought to derive from Schwann cells or related cells due to their histological, immunohistological and electron microscopic characteristics.[7,11] The immunoreactivity of granular cells to antibodies specific for S-100 protein, Melan-A, and neuron-specific enolase supports the potential neuroectodermal origin.[6,7]

Furthermore, ultrastructurally numerous round cytoplasmic structures are found surrounded by a membrane with a diameter of about 500 to 1000 nm containing round electron-dense structures, measuring about 50 to 150 nm in diameter. These findings are similar to reports about the ultrastructure of equine pulmonary granular cell tumors.[12,15] The membrane-bound structures tend to contain fragments of mitochondria or other organelles and are interpreted as secondary lysosomes.

The majority of granular cell tumors are reported to be benign, except one case in a cat, showing recurrence after excision and a high degree of pleomorphism with a high mitotic rate.[11] Granular cell tumors in cats generally tend to be more anaplastic.[11]

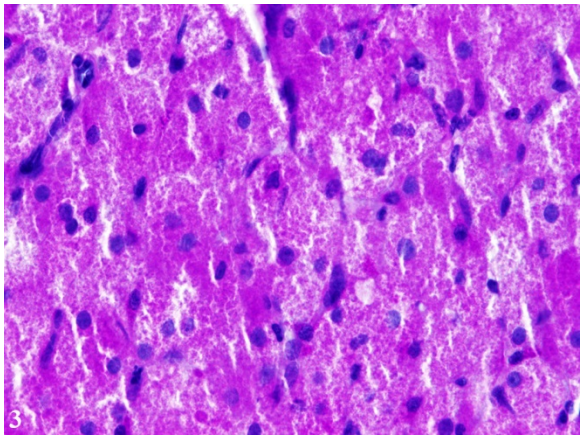

Testis, rabbit. Intracytoplasmic granules of neoplastic cells are strongly positive with a periodic acid-Schiff stain. (PAS, 400X)

As a differential diagnosis interstitial cell or Leydig cell tumor has to be considered because it shares histologic features with the granular cell tumor, e. g. eosinophilic granules within the cytoplasm.[6] In hematoxylin-eosin stained slides they are almost indistinguishable. However, testicular interstitial cell tumors lack PAS-positive and diastase-resistant cytoplasmic granules as well as Luxol Fast Blue stainable granules that are indicative for a granular cell tumor.[7,11] Furthermore, granular cell tumors express neuron-specific enolase, S-100 protein, and vimentin to a variable extent[6,7,19] as was shown in the present case. Additionally, transmission electron microscopy is a suitable tool to demonstrate the typical membrane-bound granules reported for granular cell tumors, leading to their name.[6,12]

JPC Diagnosis: Testis: Granular cell tumor, dwarf rabbit, (*Oryctolagus cuniculus*).

Conference Comment: The contributor provides an excellent summary of the major features of granular cell tumors (GCT). GCTs are histologically characterized by proliferating uniform polygonal neoplastic cells that contain abundant eosinophilic granules in their cytoplasm and a round eccentrically placed nucleus.[2] Conference participants discussed differential diagnoses for neoplasms with abundant granular eosinophilic cytoplasm to include rhabdomyomas, oncocytomas, balloon cell melanoma, and interstitial cell tumors. In addition to the histochemical and immunohistochemical stains mentioned by the contributor, transmission electron microscopy remains the best way to differentiate these histologically similar neoplasms. Ultrastructurally, oncocytomas and rhabdomyomas both contain large numbers of mitochondria which explain the abundant acidophilic granular appearance histologically.[2,3,6] In balloon cell melanoma, electron microscopically reveals numerous heterogeneous melanosomes within the cytoplasm. Interstitial cell tumors (also known as Leydig cell tumors) have an abundance of smooth endoplasmic reticulum and well-developed mitochondria with tubular and vesicular cristae. In GCT, the

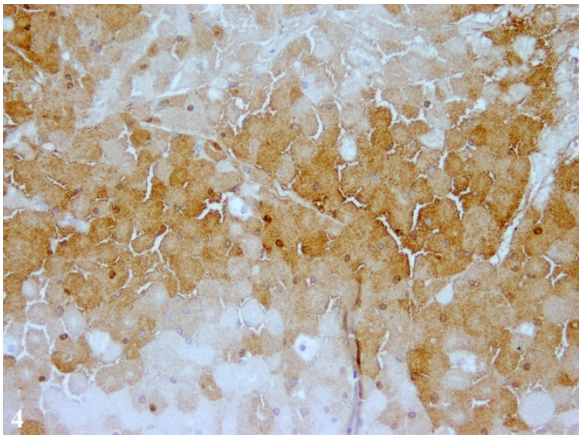

Testis, rabbit. Neoplastic cells show diffuse intracytoplasmic positivity fopr Melan A. (anti-Melan A, 400X)

granules are thought to be composed of numerous membrane-bound secondary lysosomes.[2,3,6]

In a 2015 *Veterinary Pathology* article, Suzuki et al. demonstrates that in canine lingual GCT, the cytoplasmic granules are positive for LC3, p62, NBR1, and ubiquitin. LC3 is localized on the membranes of autophagosomes and is a potent marker of autophagy. In addition, LC3, p62, and NBR1 are all required for production of the autophagosome.[14] This suggests that the cytoplasmic granules found in canine lingual GCT cells are autophagolysosomes which are a subset of secondary lysosomes that result from the fusion of a primary lysosome with a phagosome containing cytoplasmic

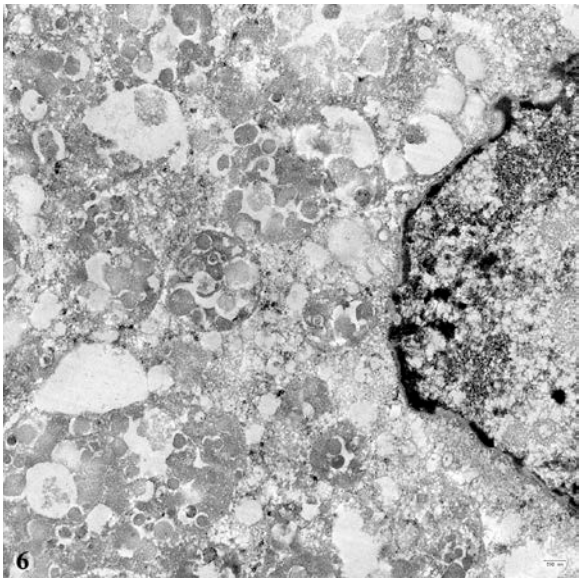

Testis, rabbit. The cytoplasm of neoplastic cells (nucleus at right is) filled with membrane-bound secondary lysosomes, which are characteristic of some types of granular cell tumors.

cellular constituents that are to be digested.[14] Recently, it has been suggested that autophagy might play a suppressive role in the initiation stages of a neoplasm by maintaining genomic stability and inducing cell senescence and autophagic death; but conversely plays a maintaining role in tumor growth in the later stages of tumorigenesis by supplying metabolic substrate, limiting oxidative stress, and maintaining cancer stem cell population.[8]

Due to near diffuse effacement and compression of the normal testicular architecture and distortion from diffuse ductular ectasia in the adjacent epididymis, conference participants had some trouble identifying the tissue of origin in this section. The key to identification of the tissue is dependent on a close investigation of the epididymis. The epididymis is a tightly coiled mass of thin tubules that carries sperm from the testes to the ductus deferens in the male reproductive system. In this case, the epididymal tubules are markedly dilated, lined by a single layer of attenuated cuboidal epithelium and contain an abundant amount of amphophilic inspissated proteinaceous material. Some participants noted that scattered throughout the lumen are very small numbers of degenerate spermatozoa thus identifying the tissue as epididymis with adjacent testis and tunica vaginalis.

Contributing Institution:

Department of Pathology
University of Veterinary Medicine Hannover
Buenteweg 17
D-30559 Hannover
Germany
http://www.tiho-hannover.de/kliniken-institute/institute/institut-fuer-pathologie/

References:

1. Cantile C, Youssef S. Nervous system. In: Maxie MG, ed. *Jubb, Kennedy, and Palmer's Pathology of Domestic Animals*. 6th ed. Vol. 1. St. Louis, Missouri: Elsevier; 2016:396–397.
2. Caswell JL, Williams KJ. Respiratory System. In: Maxie MG,

ed. *Jubb, Kennedy, and Palmer's Pathology of Domestic Animals.* 6th ed. Vol. 2. St. Louis, Missouri: Elsevier; 2016:482,498.
3. Goldblatt PJ, Gunning WT. Ultrastructure of the interstitial cells of Leydig, stimulated and unstimulated. *Ann Clin Lab Sci*. 1985; 15(6):441-450.
4. Goldschmidt MH, Dunstan RW, Stannard AA, Tscharner CV, et al. *Histological classification of epithelial and melanocytic tumors of the skin of domestic animals.* Vol III. 2nd series. Washington D.C.: Armed Forces Institute of Pathology. 1998:38-39.
5. Han X, Yu L, Yang S, Zheng J. Primary neuroendocrine tumor of the testis: a study of clinicopathological features. *Int J Clin Exp Pathol*. 2014; 7(4):1771–1776.
6. Irizarry-Rovira AR, Lennox AM, Ramos-Vara JA. Granular cell tumor in the testis of a rabbit: cytologic, histologic, immunohistochemical, and electron microscopic characterization. *Vet Pathol*. 2008; 45(1):73–77.
7. Kelley LC, Hill JE, Hafner S, Wortham KJ. Spontaneous equine pulmonary granular cell tumors: morphologic, histochemical, and immunohistochemical characterization. *Vet Pathol*. 1995 ;32(2):101–106.
8. Lu SZ, Harrison-Findik DD. Autophagy and cancer. *World J Biol Chem*. 2013; 4)3):64-70.
9. Maratea KA, Ramos-Vara JA, Corriveau LA, Miller MA. Testicular interstitial cell tumor and gynecomastia in a rabbit. *Vet Pathol*. 2007;44(4):513–517.
10. Ohnesorge B, Gehlen H, Wohlsein P. Transendoscopic electrosurgery of an equine pulmonary granular cell tumor. *Vet Surg*. 2002; 31(4):375–378.
11. Patnaik AK. Histologic and immunohistochemical studies of granular cell tumors in seven dogs, three cats, one horse, and one bird. *Vet Pathol*. 1993; 30(2):176–185.
12. Parker GA, Novilla MN, Brown AC,Flor WJ, Stedham MA. Granular cell tumor (myoblastoma) in the lung of a horse. *J Comp Pathol*. 1979;8 9(3):421–430.
13. Robinson WF, Robinson NA. Cardiovascular System. In: Maxie MG, ed. *Jubb, Kennedy, and Palmer's Pathology of Domestic Animals.* 6th ed. Vol. 3. St. Louis, Missouri: Elsevier; 2016:52–53.
14. Suzuki S, Uchida K, et al. The origin and role of autophagy in formation of cytoplasmic granules in canine lingual granular cell tumors. *Vet Pathol*. 2015; 52(3):456-464.
15. Turk MAM, Breeze RG. Histochemical and ultrastructural features of an equine pulmonary granular cell tumor (myoblastoma). *J Comp Pathol*. 1981; 91(4):478–481.
16. Wilkerson MJ, Dolce K, DeBey BM, Heeb H, et al. Metastatic Balloon Cell Melanoma in a dog. *Vet Clin Pathol*. 2003; 32(1):31-6.
17. Willmes A, de Leuw N, Wohlsein P. Fallbericht: *Kutaner Granular-zelltumor bei einem Meerschweinchen. Prakt Tierarzt*. 2013; 94:198–205.
18. Wright JA, Goonetilleke UR, Waghe M, Stewart M, Carlile A. Comparison of a human granular cell tumour (myoblastoma) with granular cell tumours (meningiomas) of the rat meninges--an immunohistological and ultrastructural study. *J Comp Pathol*. 1990;103(2):191–198.

19. Zwicker GM, Killinger JM. Interstitial cell tumors in a young adult New Zealand white rabbit. *Toxicol Pathol*. 1985; 13(3):232–235.

CASE III: E3133/15 (I have this as 1408 1229 and NOT E3133/15) (JPC 4084739).

Signalment: Twelve-week-old, female, rabbit, (*Oryctolagus cuniculus*).

History: Per contributor: "Rabbits have been dying around 12 weeks of age. No previous clinical signs. Another rabbit had liver abscesses as well. Rule out Pasteurella, Staph, tularemia? Yellow and white abscesses."

Gross Pathology: Tissue (liver) is submitted fixed in neutral buffered formalin. The liver parenchyma contains numerous, variably-sized, 0.1-0.2cm in diameter, firm, tan, elliptical nodules.

Laboratory results: N/A

Histopathologic Description: Significant microscopic lesions are focused on portal regions. Bile ducts are markedly dilated, tortuous and encased in abundant fibrous connective tissue. The biliary epithelium is markedly hyperplastic, usually lining papillary-type projections that fill the lumen of the dilated ducts. The hyperplastic biliary epithelium contains conspicuous sexual stages of protozoal micro- and macrogametes with less conspicuous asexual developmental stages. The bile duct lumens contain myriad oocysts. The fibrous connective tissue supporting the papillary projections and surrounding the dilated bile ducts contains infiltrates by primarily lymphocytes and plasma cells. Elsewhere in the sections, the hepatocytes exhibit mild, zonal (centrilobular) atrophy.

Contributor's Morphologic Diagnosis: Liver: Marked to severe, chronic, proliferative cholangitis, lymphoplasmacytic with portal and bridging portal fibrosis and myriad, intralesional protozoa consistent with *Eimeria stiedae*.

Contributor's Comment: Hepatic coccidiosis (*Eimeria steidae*) can occur in either wild or domestic rabbits and represents an important cause of mortality in commercial rabbitries.[4] Although infections can be subclinical or even incidental findings at necropsy, significant infections result in clinical signs of anorexia, lethargy, diarrhea, distended abdomen and poor weight gain. In this case, the young rabbits were dying around 12-weeks of age without premonitory clinical signs. Because of the acute mortality and gross lesions, the attending veterinarian was concerned about

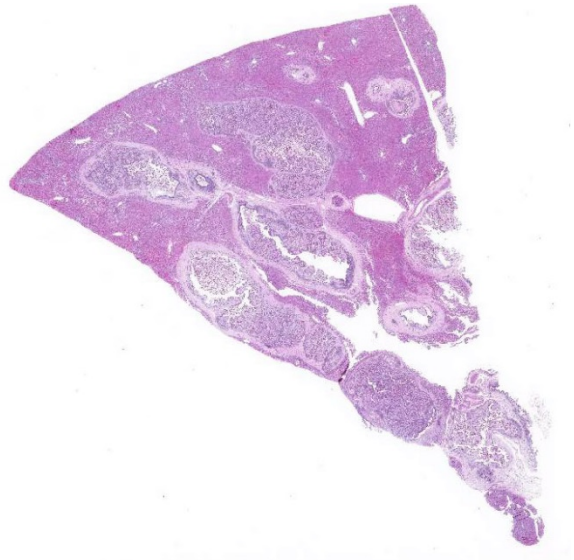

Liver, rabbit. Bile ducts are tortuous, markedly ectatic up to 4mm in diameter, and lined by markedly hyperplastic biliary epithelium. (HE, 4X)

Nonpathogenic	Slightly Pathogenic	Pathogenic	Highly Pathogenic
E. coecicola (appendix, sacculus rotundus, Peyers patches)	*E. perforans* (entire small intestine)	*E. media* (duodenum to jejunum)	*E. intestinalis* (lower jejunum and ileum)
	E. exingua (emall intestine	*E. magna* (jejunum and ileum)	*E. flavescens* (small intestine and cecum)
	E. vejdovskyi (ileum)	*E. piriformis* (colon)	
		E. irresidua (jejunum and ileum	

a differential diagnosis of tularemia in this case. There is some overlap of hepatic gross lesions and tularemia is not uncommon in this geographic region (Oklahoma). Concurrent infection by tularemia and hepatic coccidiosis has been previously described[2]; therefore, these gross liver lesions should always be microscopically investigated for possible tularemia, especially in wild rabbits.

After ingestion of sporulated oocysts, sporozoites penetrate the duodenal mucosa and eventually spread to the liver by lymphatic and hematogenous routes.[4] Upon reaching the liver, the sporozoites invade the biliary epithelium and enter the typical coccidian life cycle of schizogony, then gametogony with production of oocysts that are released into the bile ducts and passed into the intestine.[4] The prepatent period is approximately 15-18 days.[4]

The severity of disease appears to be related to the initial dose level of the oocyst inoculum.[3] Antemortem diagnosis is typically made by clinical signs and demonstration of oocysts in the feces. Post-mortem findings of the proliferative biliary lesions and histological identification of the organisms are pathognomonic for the disease.[4] Control of hepatic coccidiosis can be achieved with improvement of hygienic conditions, particularly removal of fecal material containing oocysts before they finish sporulation.[3] As it is probably impossible to remove all oocysts, control is augmented by prophylaxis with different anticoccidian drugs.[1,3] It should be noted that some are better than others and drugs that are effective in controlling chicken coccidiosis are not always efficacious in rabbits.

JPC Diagnosis: Liver: Cholangitis, proliferative, lymphoplasmacytic, chronic, diffuse, marked, with portal and bridging fibrosis and numerous intraepithelial coccidial schizonts, gamonts, and oocysts rabbit, *Oryctolagus cuniculus*.

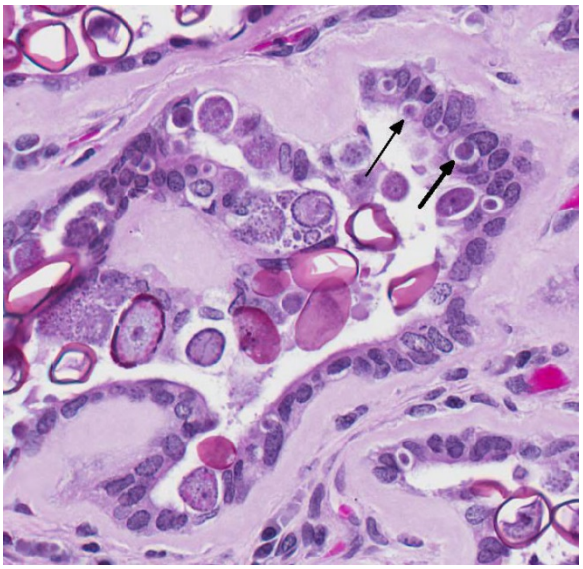

Liver, rabbit. Biliary epithelium contains developing schizonts (black arrows), gametocytes, and the lujmen is filled with shelled oocysts. (HE, 400X)

Conference Comment: The contributor provides a concise review of epidemiology, life cycle, and lesions associated with hepatic coccidiosis in rabbits. Conference participants readily identified the numerous coccidian schizonts containing merozoites, micro- and macrogametocytes, and micro- and macrogametes in the biliary epithelium and oocytes in the lumen of the markedly proliferative bile ducts. *Eimeria* sp. and *Isospora* sp. are relatively host specific coccidian parasites of the phylum Apicomplexa that typically affect the mucosal and ductular epithelial cells of the gastrointestinal tract mucosa in many different animal species.[3,4] Readers are encouraged to review WSC 2008 Conference 4 Case 3 for a list of important coccidian parasites of veterinary importance.

Eimeria sp. typically cause subclinical disease but can cause serious illness in young and immunosuppressed lagomorphs. Over 11 species of coccidian parasites have been described in rabbits and *E. stiedae* is the only coccidian parasite found in the liver and biliary epithelium.[3,4] As mentioned by the contributor, the rabbit is infected by ingestion of sporulated oocysts in the feces with sporozoites invading the duodenal mucosa. Sporozoites have been documented in the regional lymph nodes within 12 hours, in bone marrow within 24 hours, and in the liver within 48 hours via hematogenous spread by infecting mononuclear cells.[4] Rabbits with hepatic coccidiosis are often co-infected with intestinal *Eimeria* sp. Intestinal *Eimeria* sp. target specific segments of the intestinal tract in rabbits and are divided into four groups based on pathogenicity in the following table:

Table adapted from Pakandl M[3] and Percy DH and Barthold SW[4]

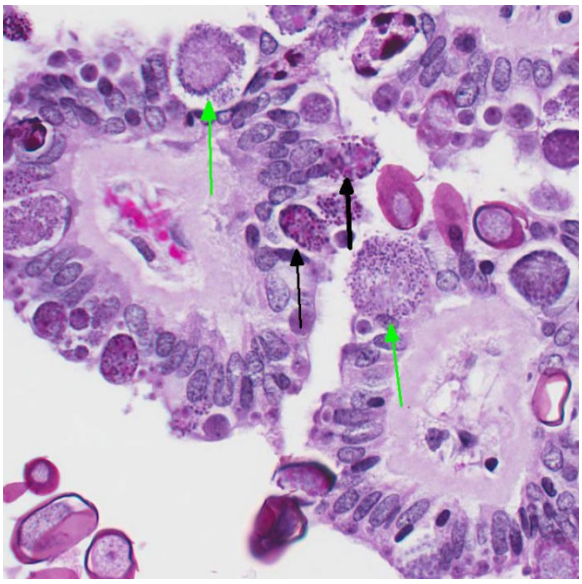

Liver, rabbit. Epithelial cells contain numerous microgametocytes (green arrows) and macrogameocytes (black arrows). (HE, 400X)

The marked proliferation of the biliary epithelium, seen in this case, is secondary to destruction and regeneration of the bile duct epithelium with extensive hyperplasia of the ductular epithelium. In addition, biliary outflow may be obstructed by numerous oocysts within the lumen of the bile duct

resulting in cholestasis and further distention of the bile duct.[4]

Conference participants discussed whether this case represents cholangiohepatitis with inflammation extending into the hepatic parenchyma or simply cholangitis with secondary mild centrilobular atrophy of hepatocytes and replacement by bridging fibrous connective tissue. Conference participants overwhelmingly agreed with the contributor that while the markedly dilated bile ducts compress the adjacent hepatic parenchyma, there is no disruption of the hepatic limiting plate; thus favoring the morphologic diagnosis of lympho-plasmacytic cholangitis.

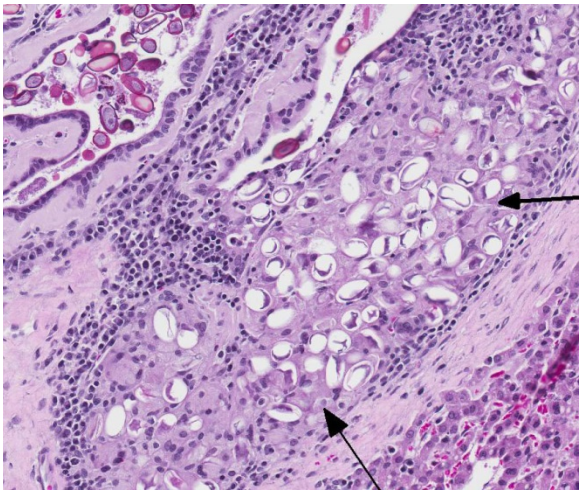

Liver, rabbit. Multifocally, aggregates of oocysts are phagocytized within epithelioid macrophages in subepithelial locations within expanded bile ducts. (HE, 400X)

Contributing Institution:
Department of Veterinary Pathobiology
Oklahoma Animal Disease Diagnostic Laboratory
Center for Veterinary Health Sciences
Oklahoma State University
http://www.cvhs.okstate.edu/

References:

1. Cam Y, Atasever A, Eraslan G, Kibar M Atalay O, Beyaz L, Inci A, Liman BC. *Eimeria stiedae*: experimental infection in rabbits and the effect of treatment with toltrazuril and ivermectin. *Exp Parasitol*. 2008; 119:164-172.
2. Kim DY, Reilly TJ, Schommer SK, Spagnoli ST. Rabbit tularemia and hepatic coccidiosis in a wild rabbit. *Emerg Inf Dis*. 2010; 16:2016-2017.
3. Pakandl M. Coccidia of rabbit: a review. *Folia Parasitol*. 2009; 56:153-166.
4. Percy DH, Barthold SW. Rabbit. In: *Pathology of Laboratory Rodents and Rabbits*. 4th ed. Ames, IA: Blackwell Publishing; 2016:297-300.

CASE IV: T4422/12 or 13 (JPC 4080931).

Signalment: Adult mole (*Talpa europaea*).

History: In the summer of 2012, a veterinarian found a dead mole in his garden in the west of the state of North-Rhine Westfalia, Germany. The animal was seen alive the day before. The vet opened and inspected the fresh carcass. He noticed lesions within lung and liver and numerous nematode larvae within the intestine. Sections of formalin-fixed liver, spleen, lung, kidney and heart were submitted for histopathological investigation.

Gross Pathology: The liver showed multiple miliary white and red foci disseminated within the parenchyma. The spleen was mildly enlarged. The lung was firm and had failed to collapse. Heart and kidneys were without any visible lesions.

Laboratory results: Histopathology of the lung revealed acute congestion, alveolar edema, and moderate suppurative broncho-

pneumonia. Nematodes are not detectable. The spleen has marked extramedullary hematopoiesis and multiple protozoal cysts within macrophages. Additionally, a chronic pericarditis and acute congestion of the kidneys is present.

Immunohistochemically, antigen of *Toxoplasma gondii* is detectable within liver and spleen using a polyclonal antiserum and the PAP method. Immunohistochemistry to detect antigen of *Neospora caninum* is negative in all tissues.

An attempt to amplify specific genomic sequences of *Toxoplasma gondii* as well as *Neospora caninum* using formalin fixed, paraffin embedded material of liver is unsuccessful (may be due to the long fixation time of the tissue samples in unbuffered formalin).

Histopathologic Description: Liver: Affecting 60% of the section, there are randomly distributed multifocal to coalescing areas of coagulative necrosis and hemorrhage, characterized by free erythrocytes in areas with hypereosinophilic hepatocytes with loss of cellular detail, pyknotic of absent nuclei but maintenance of the cell borders. Leukocytes with fragmented nuclei surround and infiltrate the necrotic regions.

Within necrotic foci and within the cytoplasm of adjacent hepatocytes are numerous protozoal cysts measuring 15 x 20 µm with a thin capsule and containing numerous 1-2 µm elongated zoites. Free within the necrotic areas are 1-2 µm elongated tachyzoites.

Portal areas are infiltrated by moderate numbers of lymphocytes, plasma cells, and eosinophils, often aggregated around bile ducts. There is a moderate increase of the number of bile ducts (hyperplasia). Within the bile duct epithelial cells, moderate

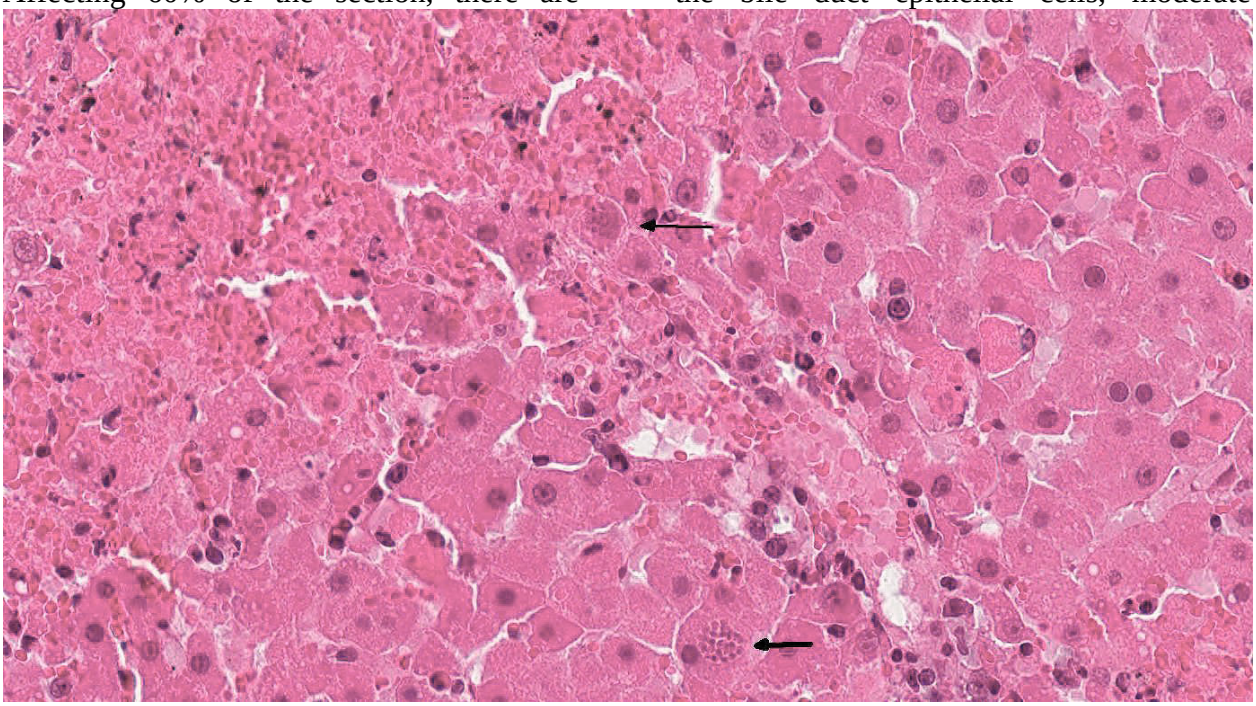

Liver, mole. Adjacent to areas of necrosis, hepatocytes contain intrcytoplasmic schizonts (black arrows) consistent with Toxoplasma gondii. (HE, 400X)

numbers of large, round to oval coccidial oocysts, about 20-40 µm in diameter, with a 1-2 µm thick eosinophilic wall, lightly basophilic granular cytoplasm, and one nucleus are visible.

Contributor's Morphologic Diagnosis: 1. Liver: Hepatitis, necrotizing, multifocal to coalescing, acute, severe, with protozoal cysts; etiology consistent with *Toxoplasma gondii*
2. Liver: Cholangitis, lymphoplasmacytic and eosinophilic, multifocal, moderate, subacute, with bile duct hyperplasia and intraepithelial coccidial oocysts: etiology consistent with *Cyclospora talpae*

Contributor's Comment: In Europe, only one member of the mole family *Talpidae* exists: a stable population of *Talpa europaea* is distributed from Spain to Russia and from Scandinavia to Greece. Moles can be found regularly in the wild (http://www.iucnredlist.org). Such small mammals are not routinely monitored regarding their health status and only rarely investigated in diagnostic laboratories; however, they are often reservoirs for disease. For example, bicolored white-toothed shrews are a proved reservoir for Borna disease virus[3] and moles may be a reservoir of hantavirus. In 60 % of captured moles in France, nova hantavirus was detected using RT-PCR.[10]

Only a few parasites have been described in moles and other insectivores.[5,11] However, it is known that *Cyclospora talpae* can be found in the epithelium of bile ducts in the liver and share similarities with *Eimeria stiedae* in rabbits. Toxoplasmosis has also been described in moles. In 1995, a similar case of combined toxoplasmosis and cyclosporiasis was documented in Bavaria.[9]

Due to their behavior, moles are a fossorial species that have extensive contact with soil and they can serve as intermediate hosts for *Toxoplasma gondii*. Moles also eat earthworms, which are identified as paratenic or transport hosts for these protozoans.[2,13] Seroprevalence for *Toxoplasma gondii* is about 40 % in wild moles in France.[1]

Toxoplasma gondii is a zoonotic protozoan which infects most mammalian and avian species. It is one of the most ubiquitous parasites and almost all homoeothermic species can be infected experimentally.[6] In domestic animals, overt disease is rare with the exception of abortion in sheep and goats. While felids are the definitive hosts (cats) and shed infective oocysts, the intermediate hosts (including cats) harbor parasitic stages in different tissue.[8,14] Predisposing factors for systemic toxoplasmosis are insufficiencies of the immune system (e.g. low levels of gamma-interferon) or concomitant infections. Recent observations regarding the pathogenesis of *Toxoplasma gondii* show that different TLRs are involved in the recognition of the parasite and there are also obvious differences between man and animal models in the effector mechanisms of toxoplasmosis.[15]

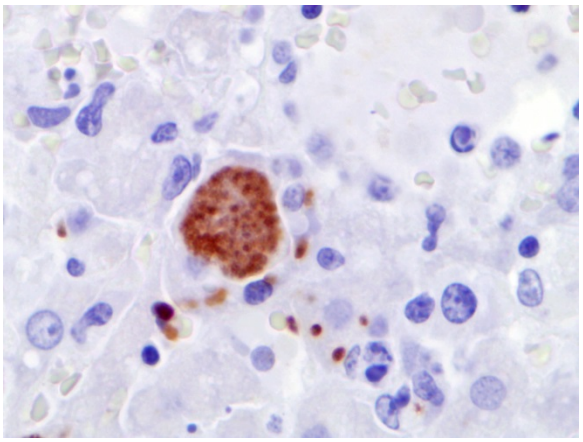

Liver, mole. Intrahepatocytic schizonts stain positively for T. gondii. (anti-T. gondii, 400X)

Macroscopic lesions in intermediate hosts infected by *Toxoplasma gondii* are variable and include splenomegaly and disseminated white foci of necrosis in liver and lung. Additional lesions may be found in myocardium and lymph nodes. In the liver toxoplasmosis is characterized histologically by foci of coagulative necrosis with less inflammatory infiltration.[8,14] Tachyzoites of *Toxoplasma gondii* may be present in hepatocytes and Kupffer cells. Special stains (Giemsa, Ziehl-Neelsen, PAS) can be applied but immunohistochemistry has been proven to detect the parasites easily within the tissue.[14] Differential diagnoses for toxoplasmosis are neosporosis and sarcosporidiosis, but the lesions, the tissue distribution as well as the affected species, are quite different.[14]

In humans, *Toxoplasma gondii* can cause abortion and stillbirth or severe neurologic and/or ocular disease in the fetus during pregnancy. The main routes of infection in man are ingestion of oocyst-contaminated soil and water or eating undercooked meat containing cysts. Other modes of transmission are less common. Most people infected after birth are asymptomatic, some may develop fever, malaise and lymphadenopathy. In immunocompromised individuals, overt disease may develop due to T cell deficiencies.[6,15] Interestingly, in human medicine, a coincidence between cerebral toxoplasmosis and mood disorders, schizophrenia, psychoses, depression or suicide and many other diseases and syndromes have been discussed.[7]

JPC Diagnosis: 1. Liver: Hepatitis, necrotizing, random, acute, marked, with protozoal cysts, mole, *Talpa europaea*.
2. Liver: Cholangitis, lymphoplasmacytic, multifocal, moderate, subacute, with biliary hyperplasia and intraepithelial coccidian oocysts.

Conference Comment: The contributor provides an excellent review of the epidemiology, gross, and histologic lesions associated with *Toxoplasma gondii*. This obligate intracellular apicomplexan protozoan parasite is typically associated with abortion and sporadic neurologic disease in domestic animals and humans. This case is indicative of the ubiquitous nature of this parasite and its incredibly wide range of susceptible hosts. Almost all "warm-blooded" homeothermic animals are susceptible to infection with a wide variety of organ systems affected.[12] The clinical signs of toxoplasmosis are variable and depend on the organ(s) involved. Tissue cysts containing bradyzoites will not usually be associated with inflammation until the cyst ruptures inciting severe local inflammation.[12]

In addition to the differential diagnoses of neosporosis and sarcosporidiosis mentioned by the contributor, another apicomplexan protozoan parasite of European moles that should be considered is *Elleipsisoma thomsoni*. This intraerythrocytic protozoan commonly encysts in the lungs and heart, but occasionally affects the liver, spleen, and kidneys.[11] However, demonstration of protozoal tachyzoites and cysts associated with coagulative necrosis in the liver is highly suggestive of *T. gondii* infection in any homeothermic species.[12] In this case, the contributor also demonstrated *T. gondii* antigen within hepatocytes via immunohistochemistry.

T. gondii is capable of infecting numerous cell types and its intracellular growth and replication causes eventual cell death. Attachment of the parasite to the cell occurs via the parasite major surface proteins

(SAG-1, P30) which are expressed in abundance on tachyzoites. The protozoan also binds extracellular laminin to its surface and then attaches to laminin receptors on host cells. The specialized apicomplexan club-shaped secretory rhoptry organelle then secretes lytic enzyme to facilitate cell penetration.[4,16]

The key feature of the pathogenesis of *T. gondii* is its ability to cross multiple types of barrier systems such as the intestinal mucosa, blood-brain barrier, blood-retinal barrier, and placenta by infecting endothelial cells causing vasculitis and ischemic necrosis. In addition, *T. gondii* avoids detection by the immune system by forming a parasitophorous vacuole within the host cell. The parasitophorous vacuole allows the parasite to develop while protected from the phagolysosomes of the host cell. Immuno-suppression of latently infected hosts allows cysts to rupture with reactivation of acute disease.[14,16]

Conference participants also identified coccidian oocysts within the biliary epithelium as a separate etiology from *T. gondii*. *Cyclospora talpae* is a very common extra-intestinal coccidian apicomplexan found within the biliary epithelium in wild European moles.[5] Participants noted moderate numbers of male microgamonts and female macrogamonts in the bile duct epithelium. As mentioned by the contributor, this coccidian parasite shares many similarities to *Eimeria stiedae* in rabbits.[8] Readers are encouraged to review Case 3 from this conference for a review of the epidemiology and pathogenesis of *E. stiedae* in a young immunosuppressed rabbit.

Contributing Institution:
Institut fuer Veterinaer-Pathologie
Justus-Liebig-Universitaet Giessen
Frankfurter Str. 96, 35392
Giessen, Germany
http://www.uni-giessen.de/cms/fbz/fb10/institute_klinikum/institute/pathologie

References:

1. Afonso E, Poulle ML, Lemoine M, Villena I, Aubert D, Gilot-Fromont E. Prevalence of *Toxoplasma gondii* in small mammals from the Ardennes region, France. *Folia Parasitol*. 2007; 54:313-314.
2. Bettiol SS, Obendorf DL, Nowarkowski M, Milstein T, Goldsmid JM. Earthworms as paratenic hosts of toxoplasmosis in eastern barred bandicoots in Tasmania. *J Wildl Dis*. 2000; 36:145-148.
3. Bourg M, Herzog S, Encarnação JA, Nobach D, Lange-Herbst H, Eickmann M, Herden C. Bicolored white-toothed shrews as reservoir for borna disease virus, Bavaria, Germany. *Emerg Infect Dis*. 2013; 19:2064-2066.
4. Dubey JP, Lindsay DS, Speer CA. Structures of *Toxoplasma gondii* tachyzoites, bradyzoites, and sporozoites and biology and development of tissue cysts. *Clin Microbiol Rev*. 1998; 11(2):267-299.
5. Duszynski DW, Wattam AR. Coccidian parasites (Apicomplexa: *Eimeriidae*) from insectivores. IV. Four new species in *Talpa europaea* from England. *J Protozool*. 1988; 35:58-62.
6. Elmore SA, Jones JL, Conrad PA, Patton S, Lindsay DS, Dubey JP. *Toxoplasma gondii*: epidemiology, feline clinical aspects, and prevention. *Trends Parasitol*. 2010; 26:190-196.

7. Flegr J, Prandota J, Sovičková M, Israili ZH. Toxoplasmosis--a global threat. Correlation of latent toxoplasmosis with specific disease burden in a set of 88 countries. *PLoS One*. 2014; 9:e90203.
8. Gardiner CH, Fayer R, Dubey JP. *An Atlas of protozoan parasites in animal tissue*. 2nd ed., Armed Force Institute of Pathology, American Registry of Pathology, Washington, DC, 1998.
9. Geisel O, Breuer W, Minkus G, Hermanns W. Toxoplasmosis causing death in a mole (*Talpa europaea*). *Berl Munch Tierarztl Wochenschr*. 1995; 108:241-243.
10. Gu SH, Dormion J, Hugot JP, Yanagihara R. High prevalence of Nova hantavirus infection in the European mole (*Talpa europaea*) in France. *Epidemiol Infect*. 2014; 142:1167-1171.
11. Mohamed HA, Molyneux DH. Developmental stages of *Cyclospora talpae* in the liver and bile duct of the mole (*Talpa europaea*). *Parasitology*. 1990; 101:345-350.
12. Mohamed HA, Molyneux DH, Walbanks KR. A coccidian in haemogamsid mites; possible vectors of *Elleipsisoma thomsoni* Franca, 1912. *Ann Parasitol Hum Comp*. 1987; 62:107-116.
13. Ruiz A, Frenkel JK. Intermediate and transport hosts of *Toxoplasma gondii* in Costa Rica. *Am J Trop Med Hyg*. 1980; 29:1161-1166.
14. Uzal FA, Plattner BL, Hostetter JM. Alimentary system. In: Maxie MG, ed. *Jubb, Kennedy and Palmer´s. Pathology of Domestic Animals.* Vol 2. 6th ed. St. Louis, MO: Elsevier Saunders; 2016:236-238.
15. Yarovinsky F. Innate immunity to *Toxoplasma gondii* infection. *Nat Rev Immunol*. 2014; 14:109-121.
16. Zachary JF. Mechanisms of microbial infections. In: Zachary JF, McGavin MD, eds. *Pathologic Basis of Veterinary Disease.* 5th ed. St. Louis, MO: Elsevier; 2012:239

Self-Assessment - WSC 2016-2017 Conference 11

1. Which of the following is not true concern cataract formation in rats?
    a. Cataracts are the most common lenticular disease in aged Sprague Dawley and Wistare rats.
    b. Cataract formation involves damage to NA-K-dependent ATPas osmotic pumps which result in potassium entry into the lens.
    c. Cataract is considered a major cause of visual impairment in diabetic patients.
    d. Spontaneous cataracts have been reported in up to 9.8% of Sprague-Dawley rats.

2. Which of the following is an incorrect association regarding granular cell tumors>
    a. Equine - lung
    b. Rat - meninges
    c. Dog and cat – oral cavity
    d. Guinea pigs - heart

3. Gross lesions of hepatic coccidiosis should always be microscopically investigated for which of the following diseases, which may grossly mimic it?
    a. Tularemia
    b. Plague
    c. Myxomatosis
    d. Viral hemorrhagic disease

4. Which of the following coccidian is considered non-pathogenic in rabbits?
    a. Eimeria flavescens
    b. Eimeria steidae
    c. Eimeria magna
    d. Eimeria coecicola

5. Which of the following proteins is not associated with the binding of *Toxoplasma gondii* to the cellular surface
    a. Laminin
    b. Lytic enzyme
    c. P30
    d. SAG-1

Joint Pathology Center

Veterinary Pathology Services

WEDNESDAY SLIDE CONFERENCE 2016-2017

C o n f e r e n c e 12

14 December 2016

Mark T. Butt, DVM, DACVP
President, Tox Specialists (TPS), LLC
8420 Gas House Pike, Suite G
Frederick, MD

CASE I: 14-309/6 or 7 (JPC 4048850).

Signalment: Five-month-old, female, Coton de Tulear, dog (*Canis familiaris*).

History: The dog presented with ataxia evolving since the age of four months, with a rapid onset of clinical signs. Neurological examination oriented towards a cerebellar origin of the ataxia. Magnetic Resonance Imaging revealed a decreased size of the cerebellum, without signs of inflammation. The dog was euthanized after ataxia had worsened.

Gross Pathology: The only significant gross lesion at necropsy was a reduction in size of the cerebellum, with slight asymmetry between the two hemispheres. The gyri were diffusely sharply delineated and shrunken.

Laboratory results: N/A

Cerebellum, dog. The cerebellum was shrunken with slight symmetry between the two hemispheres. The folia appear diminished in size. (Photo courtesy of: Anatomie pathologique, Vetagro Sup, Campus vétérinaire, 1, avenue Bourgelat, 69280 Marcy l'etoile, FRANCE)

Histopathologic Description: Diffusely, the cerebellar folia are slightly flattened. Severe loss of cells within the granular layer is present, multifocally leading to complete absence of this layer. Rarely, granular cells are swollen and vacuolated (degeneration), multifocally associated with empty baskets. Diffusely replacing this layer are glial cells

(mainly astrocytes). A discrete population of microglial cells is also present. The molecular layer is mostly normal in thickness, or more rarely thinner. Purkinje cells do not show remarkable degenerative changes.

Contributor's Morphologic Diagnosis: Cerebellum, Granular cell degeneration and loss, diffuse, severe, Coton de Tulear, canine.

Contributor's Comment: Cerebellar cortical abiotrophy is a spontaneous, premature and progressive degeneration and death of neurons without an intrinsically identifiable defect; it is well characterized in the dog and is described in several breeds. This condition is characterized by ongoing Purkinje neuronal cell degeneration and loss with reactive gliosis. Mostly, affected animals are healthy at the time of birth and develop clinical signs at several months of age, which worsen with time. In some breeds, a possible inherited genetic defect in the metabolism of the neurotransmitter glutamic acid has been proposed (or established).[2,11]

This case is an unusual form of a cerebellar degeneration in the Coton de Tuléar breed, characterized by a severe depletion in the granular cell layer, hence the name "cerebellar granuloprival degeneration" for this condition.[9] Rare cases of this condition in this breed have been published to date.[9] Similar to this case, all differ from the Purkinje cell atrophy reported in many canine breeds.

Some similarity between this Coton de Tuléar and cerebellar granuloprival hypo-plasia in cats caused by intrauterine parvovirus infection has been proposed. However, in Coton de Tuléars, there is no disorganization of the cerebellar cortex and

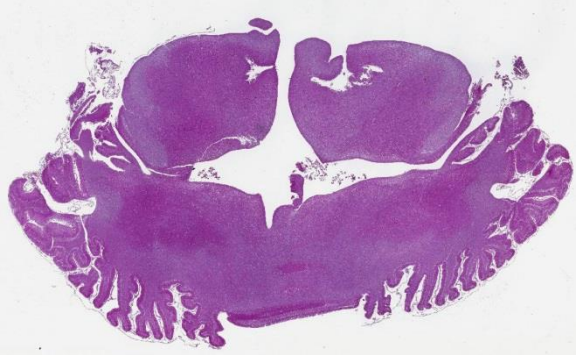

Cerebellum, dog. A section of cerebellum and brainstem is submitted. The paired caudal colliculi are at top, and cerebellar folia at left and right at the bottom. At subross magnification, the folia appear markedly thinned and hypocellular. (HE, 4X)

no lesions in the Purkinje cell layer. Parvovirus infection in dogs is not known to induce cerebellar changes.[9,12]

Contrary to what has been published, in this case there is no significant inflammatory change in the cerebellum.[9] The restriction of the disease specifically to Coton de Tuléar breed is favors a genetic basis for the lesions, but this hypothesis needs further analysis.

JPC Diagnosis: Cerebellum: Granular cell degeneration and loss, diffuse, severe, with spongiosis, and minimal multifocal Purkinje cell loss, Coton de Tulear, canine.

Conference Comment: The contributor provides a compelling example of an atypical form of cerebellar abiotrophy in the canine. Cerebellar abiotrophy, also known as cerebellar cortical degeneration, has been described as a hereditary defect in several breeds of dogs,[1,3,9] Arabian horses,[8] rabbits,[7] an alpaca,[6] and recently in goats.[5] Histologically, the characteristic distribution of lesions includes the marked loss and degeneration of the Purkinje cell neurons, often with retrograde degeneration in granular cells due to failure of synaptogenesis between parallel nerve fibers

of the granular cell layer and Purkinje cells.[1,3,5] In this Coton de Tuléar dog, there is diffuse and severe degeneration and loss of the granular cell layer, with only scattered loss of Purkinje cells. This histomorphology has been rarely reported in the veterinary literature as cerebellar granuloprival degeneration in a number of different canine breeds, including the Coton de Tuléar, as discussed by the contributor.[3,4,9] Neonatal cerebellar ataxia in Coton de Tuléar dogs has also been reported as Bandera's syndrome, suggesting a breed-related hereditary disease.[3]

Abiotrophy is a spontaneous cerebellar degenerative disease process characterized by premature loss of neurons in the cerebellum.[2] Conference participants discussed how this differs from cerebellar hypoplasia, a condition in which the cerebellum does not completely form during embryogenesis due to in-utero viral infections from parvoviruses or pestiviruses. Examples include feline parvovirus (panleukopenia), bovine pestivirus (bovine viral diarrhea virus), classical swine fever (hog cholera/pestivirus), sheep and goat pestivirus (Border disease), and rat parvovirus (Kilham rat virus).[2] Additionally, certain toxicities, such as organophosphates, and malnutrition can also cause cerebellar hypoplasia.[3] In contrast to animals born with cerebellar hypoplasia, those affected with abiotrophy are neurologically normal at birth and develop early-onset progressive cerebellar proprioceptive deficits during the post-natal period, in the case of this dog at four to five months.[1,3,5] Typical neurologic deficits include ataxia, head tremor, intention tremors, symmetrical hypermetria, broad-based stance, and loss of balance.[2]

In addition to the diffuse and severe

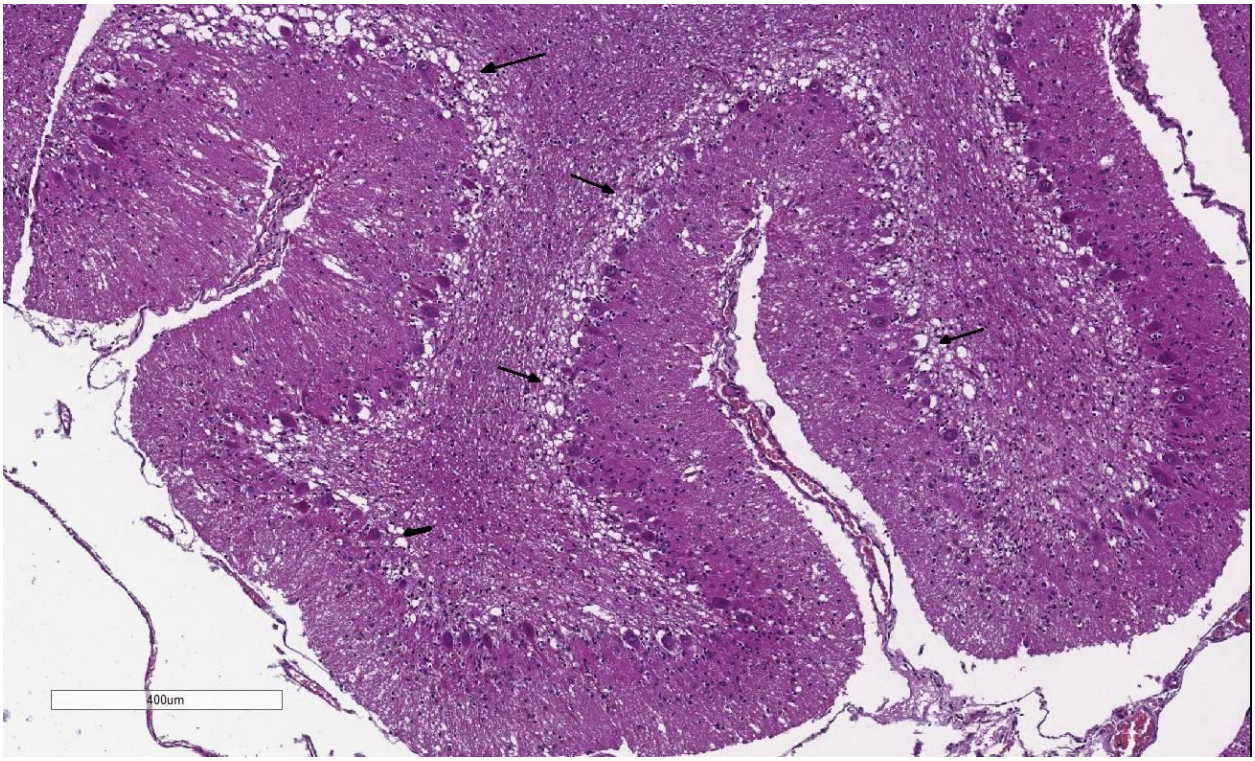

Cerebellum, dog. There is an almost total loss of the granular cell layer, and spongiosis at its normal location (arrows) The Purkinje cell layer is considered within normal limits. (HE, 46X)

degeneration and loss of the cerebellar molecular cell layer, the conference moderator noted an increase in the number of hypertrophic astrocytes with large vesicular nuclei within the Purkinje cell layer, interpreted as Bergmann gliosis. This astrocytic reaction occurs predominantly in areas where Purkinje cells are lost, described by several conference participants as empty baskets.[4] Bergmann glial cells are astrocytes with cell bodies located in the Purkinje cell layer with long radial processes that surround the synapses on Purkinje cell dendrites and extend to the molecular layer, terminating on the pial surface of the cerebellum;[10] they are essential for the normal differentiation, migration and maturation of Purkinje cell and granular cell neurons. The immunohistochemical stain, glial fibrillary acidic protein (GFAP), is useful in demonstrating the empty baskets surrounded by Bergmann gliosis in cases of cerebellar abiotrophy.[10]

The confounding aspect of this case is the severe selective depletion of granular cells with only scattered loss of Purkinje cells. The pathogenesis of cerebellar granuloprival degeneration in this breed has not yet been elucidated; it is hypothesized to be the result of an inherited disorder of granular cell development, but most Purkinje cells survive since their main excitatory input is from the olivary nucleus.[4] However, some authors suggest that Purkinje cells can be lost as result of granular cell depletion in chronically affected dogs.[4]

Contributing Institution:
Anatomie pathologique,
Vetagro Sup, Campus vétérinaire
1, avenue Bourgelat,
69280 Marcy l'etoile, France
http://www.vetagro-sup.fr/en/

References:

1. Berry ML, Machado UB. Cerebellar abiotrophy in a miniature schnauzer. *Can Vet J*. 2003; 44:657-659.
2. Cantile C, Youssef S. Nervous system. Maxie MG ed. In: *Jubb Kennedy and Palmer's Pathology of Domestic Animals*. Vol 1. 6th ed. Philadelphia, PA: Elsevier Saunders; 2016:275-276.
3. Coates JR, O'Brien DP, Kline KL, et al. Neonatal cerebellar ataxia in Coton de Tulear dogs. *J Vet Intern Med*. 2002; 680-689.
4. Huska J, Gaitero L, Heindrich SN, et al. Cerebellar granuloprival degeneration in an Australian kelpie and a Labrador retriever dog. *Can Vet J*. 2013; 54:55-60.
5. Koehler JW, Newcomer BW, Holland M, Caldwell JM. A novel inherited cerebellar abiotrophy in a cohort of goats. *J Comp Path*. 153:135-139.
6. Mouser P, Levy M, Sojka JE, Ramos-Vara JA. Cerebellar abiotrophy in an alpaca (*Lama pacos*). *Vet Pathol*. 2009; 46:1133-1137.
7. Sato J, Yamada N, Kobayashi R, et al. Morphometric analysis of progressive changes in hereditary cerebellar cortical degenerative disease (abiotrophy) in rabbits caused by abnormal synap-togenesis. *J Toxicol Pathol*. 2015; 28:73-78.
8. Scott EY, Penedo MC, Murray JD, Finno CJ. Defining trends in global gene expression in Arabian horses with cerebellar abiotrophy. *Cerebellum*. 2016; Oct 5. [Epub ahead of print].
9. Tipold A, Fatzer R, Jaggy A, Moore P, Vanevelde M.

Presumed immune-mediated cerebellar granuloprival degeneration in the Coton de Tuléar breed. *J neuroimmunol*. 2010; 110:130-133.
10. Yamada K, Watanabe M. Cyto-differentiation of Bergmann glia and its relationship with Purkinje cells. *Anat Sci Int.* 2002; 77:94-108.
11. Zachary JF, McGavin DM. Nervous system. In: *Pathologic Basis of Veterinary Disease*. 5th ed. St. Louis, MO: Mosby; 2012:816, 856-857.
12. Zachary JF, McGavin DM: Mechanisms of microbial infections. In: *Pathologic Basis of Veterinary Disease*. 5th ed. St. Louis, MO: Mosby; 2012:229.

CASE II: N14-281 (JPC 4084300).

Signalment: 17-year-old, neutered male, quarterhorse, (*Equus caballus*).

History: Horse developed severe atrophy of facial muscles on the left side of the face 2 months prior to presentation to the teaching hospital. The weekend prior to submission the patient developed rear limb ataxia. Probing palpation of the cervical region revealed hyperesthesia and hyper-responsiveness. Probing around the mid cervical region did not elicit a response. Treatment with dexamethasone yielded some improvement in clinical signs. The horse was euthanized at the owner elected request**.**

Gross Pathology: The muscles on the left side of the face were diffusely atrophied and hemorrhage was present in the anterior compartment of the right eye. There was narrowing of the spinal canal between C2 and C3. The dura mater at the C2-C3 articulation was focally reddened. The third cervical vertebral body (C3) contained a 2.5 x 1.5 cm region of red and depressed tissue (bony sequestration) rimmed by thick white tissue (fibrosis) at its ventral border. The dorsal vertebral body of C2 also had a 1.5 cm linear band of firm white tissue (fibrosis) that traversed the bone in a dorsal-ventral direction.

Laboratory results: N/A

Histopathologic Description: Extending from just caudal of C1 to C5, there is a locally extensive area of rarefaction and multifocal to coalescing accumulations of glial cells and gitter cells, unilaterally involving the dorsal funiculus at the level of the gracile and cuneate fasciculi. Spinal cord inflammation is most concentrated at C3 and includes significant perivascular cuffing, few to moderate lymphocytes and plasma cells and scattered eosinophils. The associated spinal gray column is unilaterally affected with similar inflammation in these sections. Numerous swollen axons

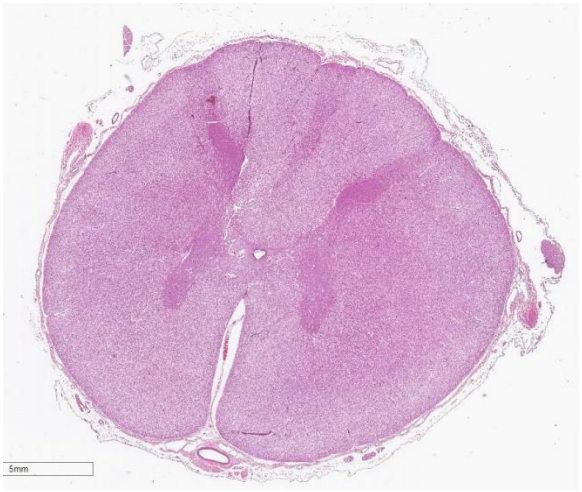

Cervical spinal cord, horse. There is no visible lesion in the cord at subgross. This cross section is identifiable as cervical spinal cord due to the small ventral horns and the large dorsal funiculus (composed of ascending sensorimotor axons). (HE, 4X)

(spheroids) are present at C2 and C3 spinal cord sections. At the level of C2, there are occasional glial nodules in the contralateral dorsal funiculus as well. Small numbers of lymphocytes and plasma cells are diffusely present in the meninges and are more concentrated over the dorsolateral funiculus. The dorsal spinal nerve root ganglia are infiltrated with small numbers of lymphocytes and plasma cells at the level of C2 and C3.

Contributor's Morphologic Diagnosis: Cervical spinal cord (C1-C5): Meningomyelitis, nonsuppurative and eosinophilic, unilateral, focally extensive, severe with spheroid formation, cervical spinal cord, dorsal funiculus

Contributor's Comment: The gross and histopathologic findings in this case are highly suggestive of cervical stenotic myelopathy. The unilateral distribution of the lesions coincides with the focus of stenosis observed in the spinal canal. Microscopic changes in the spinal cord include rarefaction, accumulations of glial and gitter cells, and lymphocytes, plasma cells, and scattered eosinophils. The horse, in this case, was 17 years old, considerably older than the typical case of cervical vertebral stenotic myelopathy (8-18 months and 1-4 years of age). However, several retrospective studies have documented this condition in horses up to 22 years of age.[3,4]

Cervical vertebral stenotic myelopathy, commonly referred to as "Wobbler's syndrome", is characterized by lesions in the spinal cord caused by narrowing of the spinal canal or compression by the vertebral articular processes.[6,7] There are two pathological syndromes: cervical vertebral instability (CVI) and cervical static stenosis (CSS). Clinical signs for both pathological syndromes include ataxia with the hindlimbs more commonly and more severely affected than the forelimbs.[7] Cervical vertebral instability is characterized by the narrowing of the spinal cord when the neck is ventroflexed. The cranial articular process of the vertebral bodies project in a ventromedial direction and impinge on the spinal cord. C-3 to C-5 of the spinal cord is the most affected area.[6] Young, rapidly growing horses between the ages of 8-18 months are predisposed to this condition. Breed dispositions include Thoroughbreds and Quarter horses, and males are affected more often than females. Contributing factors may be *ad libitum* feeding of high-energy and high-protein diet as well as copper deficiency.[6,7]

Cervical static stenosis is the less common syndrome. It is characterized by the compression of the spinal cord at the level of C-5 to C-7 due to the thickening of the ligamentum flavum and the dorsal laminae of the vertebral arches.[6] Predispositions are similar to those seen in CVI except horses aged one to four years are commonly affected.[3] The position of the neck does not determine whether or not the chord is compressed.

JPC Diagnosis: Spinal cord, dorsal medial fasciculi: Necrosis, focally extensive, asymmetric with lymphohistiocytic and eosinophilic perivasculitis and leptomeningitis, quarterhorse, *Equus caballus*.

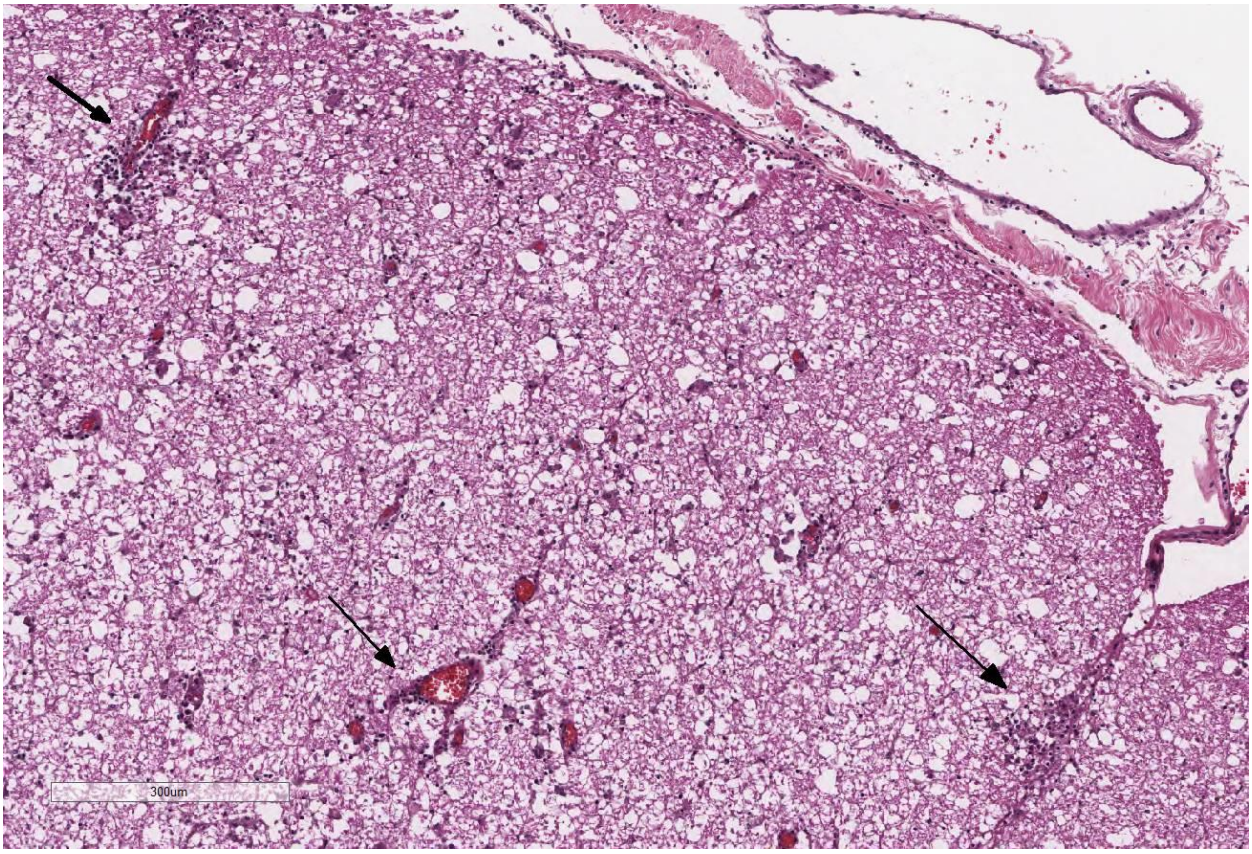

Cervical spinal cord, horse. The dorsal funiculus contains moderate numbers of dilated myelin sheaths and a lymphoplasmacytic and eosinophilic perivascular infiltrate. (HE, 84X)

Conference Comment: This interesting case generated spirited discussion amongst conference participants. While attendees essentially agreed with the contributor's histopathologic description and morphologic diagnosis, there was no consensus for the histogenesis of the necrotizing lesion in the spinal cord of this horse. The conference moderator offered an alternative interpretation of an infectious cause, with *Sarcocystis neurona* causing acute onset weakness, ataxia, and a focally extensive area of necrosis in the dorsal medial spinal cord with corresponding lymphohistiocytic and eosinophilic leptomeningitis. The conspicuous eosinophilic component of the perivasculitis and leptomeningitis in this case, may suggest a parasitic etiology. *S. neurona* is an apicomplexan protozoan parasite which causes equine protozoal myeloencephalitis (EPM), a relatively common and severe neurologic disease in horses. Opossums are the definitive host for the parasite and spread the disease by fecal shedding of sporocysts into the environment.[1] Unfortunately, no apicomplexan schizonts or merozoites were observed in any examined tissue sections. Other potential etiologies offered by conference participants included acute intervertebral disc rupture and fibrocartilaginous embolism, although disk material was not visualized within the section.

As noted by the contributor, the age of the horse (17-years-old) is a highly atypical presentation for both cervical stenotic myelopathy and cervical static stenosis.[2,3,5] While most cases of cervical stenotic

myelopathy involve ventral compression of the spinal cord and spinal nerves with Wallerian-type degeneration of the white matter of the dorsal and ventrolateral spinal cord affecting the descending spino-cerebellar tracts of both the pelvic and thoracic limbs,[2,5] in this section, the ventral and lateral spinal cord is relatively unaffected. The lesions seen in the submitted section of spinal cord are primarily located in the dorsomedial spinal cord at the level of the fasciculus gracilus and fasciculus cuneatus.

Some conference participants noted occasional scattered 2x5 um filamentous bacilli multifocally throughout the neuro-parenchyma. The brain and spinal cord are exquisitely susceptible to post-mortem autolysis and putrefaction. As a result, the conference moderator cautioned attendees against overinterpreting artifactual bacterial overgrowth within post-mortem tissue samples of the central nervous system, especially when they are not associated with inflammation, as in this case.

Contributing Institution:
College of Veterinary Medicine
1200 West Montgomery Road
Tuskegee University
Tuskegee Institute, Alabama 36088
http://www.tuskegee.edu/academics/colleges/cvmnah/school of veterinary medicine.aspx

References:

1. Bowman DD. Protozoans. In: *Georgis Parasitology for Veterinarians*. 9th ed. St. Louis, MO: Saunders Elsevier; 2009:104-105.
2. Janes JG, Garrett KS, McQuerry KJ, et al. Cervical vertebral lesions in equine stenotic myelopathy. *Vet Pathol*. 2015; 52:919-927.
3. Levine JM, Adam E, MacKay RJ, et al. Confirmed and presumptive cervical compression myelopathy in older horses: A retrospective study (1992-2004). *J Vet Intern Med*. 2007; 21:812-819.
4. Levine JM, Scrivani PV, Divers TJ, et al. Multicenter case-control study of signalment, diagnostic features, and outcome associated with cervical vertebral malformation-malarticulation in horses. *J Am Vet Med Assoc*. 2010; 237(7):812-822.
5. Reed SM. Cervical vertebral stenotic myelopathy: Pathogenesis. *Proceedings of the International Equine Neurology conference*. College of Veterinary Medicine, Cornell University, New York. 1997:45-49.
6. Thompson K. Bones and joints. In: *Pathology of Domestic Animals*, 5th Edition. Edinburgh : Saunders; 2007: 44-46.
7. Zachary JF, McGavin DM. Nervous system. In: *Pathologic Basis of Veterinary Disease*. 5th ed. St. Louis, MO: Mosby; 2012:816, 833-835.

CASE III: W1111-03 or W1112-03 (JPC 4006284).

Signalment: Six-month-old, male castrated, cross breed ox, (*Bos taurus*).

History: An outbreak of neurological disease occurred in a herd of 99, 6 to 12-month-old, mixed breed, beef cattle. The herd was grazing pasture with a daily supplementary ration of 2 kg/head of sprouted barley. Fifty-seven animals were affected and eighteen animals were euthanized after becoming recumbent and

unable to rise. The cattle had been fed hydroponically sprouted barley for seven months before the outbreak. Over the last few weeks of feeding, a green-blue downy mold had grown on the barley, its development had coincided with some unseasonably warm and humid spring weather. The mold did not have any effect on the appetite of the cattle which were being fed approximately 2 kg/head daily when adverse signs were first noticed. The first indication of toxicity was noticed by the owners when a 12-month-old cross-bred heifer showed signs of what was thought to be colic, based on her hunched posture and reluctance to walk. The next day another two cattle were noticed sick and three more the following day. At this stage the feeding of the sprouted barley was discontinued and the cattle were moved to another paddock. New cases continued to develop over the next 18 days. By six weeks, only a few of the affected cattle had not recovered, though all had lost considerable weight. A range of clinical signs was observed. Mildly sick cattle were instantly recognizable by the arching of their backs. Unless disturbed, most appeared to graze normally. Ataxia, knuckling of the hind fetlocks and hypermetria of hind limbs were also obvious in affected cattle. Some cattle developed progressively worsening ataxia with generalized muscle tremors. The cattle that were euthanized had progressed to posterior paralysis, recumbency and were often polypneic. One sternally recumbent animal appeared to be blind. Another was found in lateral recumbency displaying opisthotonos.

Spinal cord, ox. There is no visible lesion at subgross magnification. The prominent ventral horns and ventral emergence of the spinal nerves suggests that this is lumbar cord. (HE, 4X)

The mold on the barley sprouts was identified as *Aspergillus clavatus* (Agrifood Technology, Princes Hwy Werribee, Victoria 3030). *A. clavatus* is identifiable by its long, smooth conidiophore and huge club-shaped vesicle to which are attached uniseriate phialides.[3] The mould was confirmed as *A. clavatus* and a specimen is held at the DPI, Plant Diseases Herbarium, Knoxfield Victoria.

Gross Pathology: There were no remarkable gross changes seen in the internal organs of the necropsied animals.

Laboratory results: Biochemical analysis of sera from the two recently recumbent cattle found mild to moderate elevations in GLDH (428 and 30 U/L; reference range < 20 U/L) and LDH (2318 and 2395 U/L; reference range 50-400 U/L). CK was mildly elevated in one animal, as was AST in the other.

Histopathologic Description: Significant histological abnormalities are limited to the central nervous system. Neuronal changes are apparent in the brain and spinal cord (spinal cord sections submitted for WSC). Affected neurons are swollen and rounded, completely chromatolytic with pale or acidophilic cytoplasm, and the few nuclei captured in section are peripheral, shrunken and often pressed against the cell membrane. Many nuclei are affected, especially the red nuclei, dorsal motor nucleus of the vagus, reticular nucleus of the medulla and alpha motor neurons among the lateral and medial

motor neurons of the cervical and lumbar intumescences. Small gamma efferent neurons are not involved. There is no apparent cell loss or glial reaction. Within the brain and spinal cord, there is minor axonal swelling and myelin vacuolation with astrocytic swelling. Otherwise, the integrity of myelin and axons is preserved. The peripheral nervous system, including autonomic ganglia, peripheral nerves, and craniospinal nerve roots, shows no abnormality.

Contributor's Morphologic Diagnosis: Brain and spinal cord: chromatolytic neuronal degeneration, severe multifocal acute, with mild edema of myelin.

Contributor's Comment: The epidemiology, clinical signs, histological findings in the brain and spinal cord and mycological examination in this case[3] are consistent with those previously described and caused by *Aspergillus clavatus* tremorgenic neurotoxicosis.[5,6]

A clavatus is present in soil and commonly isolated from cereal grains and their germinated seeds and other feedstuffs. It also occurs commonly in pigeon droppings.[6] Tremorgenic syndromes have been experimentally reproduced in ruminants by feeding *A clavatus* pure cultures and *A clavatus* contaminated grains. A number of toxins have been isolated from A clavatus including cytochalasin E, tryptoquivaline, tryptoquivalone, patulin, but none have been tested in ruminants to determine responsibility for the tremorgenic syndrome. Toxic extracts from sorghum beer residue capable of reproducing the tremogenic syndrome in sheep dosed orally did not

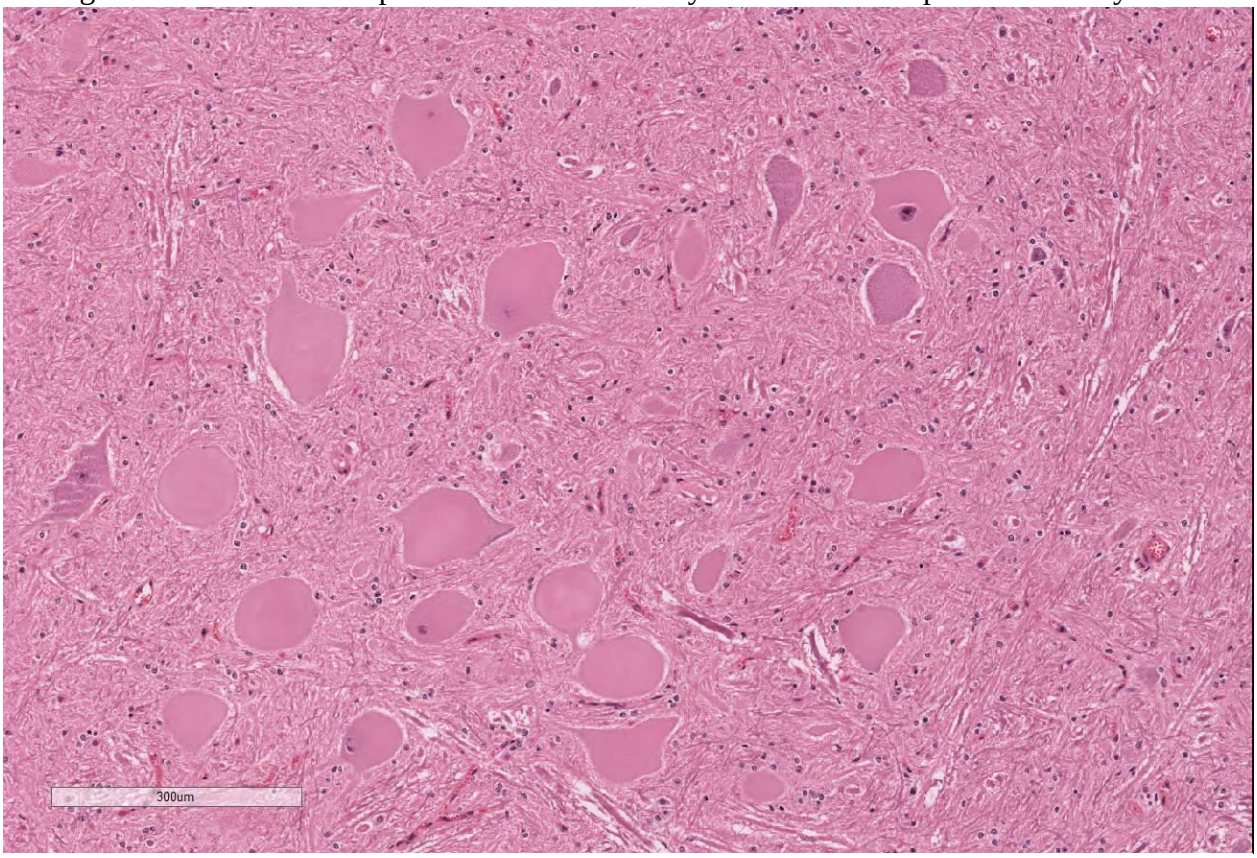

Spinal cord, ox. Neuronal cell bodies of the ventral horn are diffusely and markedly swollen with dispersal of Nissl substance (central chromatolysis). The cytoplasm is illed with numerous and distinct vacuoles , and nuclei are often peripheralized and occasionally hyperchromatic. (HE, 88X)

contain patulin, trypotquivalone or nortryptoquivalone so the identity of the toxin(s) remains undetermined.[6]

The case is submitted to the WSC with the kind permission of the surviving author, Dr C El-Hage, University of Melbourne.

JPC Diagnosis: Spinal cord, grey matter: Neuronal degeneration, multifocal, severe, with chromatolysis and vacuolar degeneration, cross breed ox, *Bos taurus*.

Conference Comment: The contributor provides a striking example of severe toxin-induced swelling and central chromatolysis of neuronal cell bodies (soma). In this case, the pathogenic process is most severe in the grey matter of the ventral horns. The ventral horn of the spinal cord contains nuclei for lower motor neurons that supply motor input to somatic muscle via axons in the white matter of the ventral funiculus. Typically, lesions in lower motor neurons produce flaccid paralysis, rather than the muscular tremors and hyperesthesia present in this case; however, as mentioned by the contributor, the pathogenic mechanisms of neuromycotoxicosis in *Aspergillus clavatus* have not yet been determined.

Some authors consider the mycotoxin patulin, produced by *Aspergillus* sp. and *Penicillium* sp, to be the major contributor to the neurotoxicity induced by *A. clavatus*.[1,4] Patulin has been implicated in previously reported cases of neurotoxicity in animals. In the brain and spinal cord, patulin inhibits acetylcholinesterase and the Na+/K+-ATPase resulting in a buildup of the stimulatory neurotransmitter acetylcholine.[1,4] Decreased breakdown of acetylcholine at the neuromuscular junction results in convulsions, tremors, stiffness, impaired locomotion, and hyperesthesia, seen clinically in this case.[4] Additionally, inhibition of the Na+/K+-ATPase may have devastating effects on the cell, including ionic depolarization of the cell membrane resulting in neuronal signal transduction deficiencies and disruption of the cell's concentration gradient causing increased osmolarity and cellular swelling.[4]

Conference participants discussed the degenerative changes associated with chromatolysis in the central nervous system. Chromatolysis represents a change in the histomorphologic appearance of the soma due to the central or peripheral dispersal pattern of the Nissl substance.[2] The chromatolyic pattern in this case is consistent with central chromatolysis. Central chromatolysis occurs in the large neurons of the brainstem, spinal motor neurons, and peripheral ganglia and is characterized by central clearance of Nissl granules and marked cellular swelling with pale, eosinophilic, homogenous, ground-glass appearance to the cytoplasm.[2] Soma nuclei are often peripheralized and possess prominent nucleoli. Typically, central chromatolysis occurs secondary to axonal injury and represents a reparative response in the soma, incorporating increased free ribosomes for protein synthesis, lysosomes, and mitochondria. This anabolic response required for axon regeneration is referred to as the axon reaction.[2] Central chromatolysis occurs in a number of neurodegenerative diseases, including copper deficiency in sheep and goats, grass sickness in horses, avian encephalomyelitis virus in chickens, and feline dysautonomia, known as Key-Gaskell syndrome, in cats. Peripheral chromatolysis is generally associated with cell body shrinkage rather than swelling. It is characterized by Nissl granules surrounding the nucleus and is a relatively nonspecific degenerative lesion.[2]

Contributing Institution:

University of Melbourne
Faculty of Veterinary Science
250 Princes Hwy
Victoria Australia, 3030
http://www.vet.unimelb.edu.au/

References:

1. Brotha CJ, Legg MJ, Truter M, Sulyok M. Multitoxin analysis of *Aspergillus clavatus*-infected feed samples implicated in two outbreaks of neuromycotoxicosis in South Africa. *Ondersepoort J Vet Res*. 2014; 12: doi:10.4102/ojvr.v81i1.848.
2. Cantile C, Youssef S. Nervous system. In: In: Maxie MG, ed. *Jubb Kennedy and Palmer's Pathology of Domestic Animals*. Vol 1. 6th ed. Philadelphia, PA: Elsevier Saunders; 2016:252-255,327.
3. Hage C M; Lancaster M J: Mycotoxic nervous disease in cattle fed sprouted barley contaminated with *Aspergillus clavatus*. *Aus Vet J*. 2004; 82:639-641.
4. Loretti AP, Colodel EM, Driemeier D, et al. Neurological disorder in dairy cattle associated with consumption of beer residues contaminated with *Aspergillus clavatus*. *J Vet Diagn Invest*. 2003; 15:123-132.
5. Maxie MG, Youssef S. Nervous system. In: *Jubb, Kennedy and Palmer's Pathology of Domestic Animals*. Maxie MG, ed. 5th ed, Edinburgh UK: Elsevier Saunders; 2007:369.
6. McKenzie RA, Kelly MA, Shivas RG, et al. *Aspergillus clavatus* tremorgenic neurotoxicosis in cattle fed sprouted grains. *Aus Vet J*. 2004; 82:635-638.

CASE IV: A16-6925-12 (JPC 4083741).

Signalment: 7-month-old male Angus ox (*Bos taurus*)

History: A previously healthy bull calf was presented to the Veterinary Teaching Hospital the day it was found down and unresponsive.

Gross Pathology: The brain is wet and soft with mildly dilated ventricles and excessive transparent watery cerebrospinal fluid. A 1 cm x 1.5 cm dark pink, softened and cavitated focus is in the left cerebral hemisphere, adjacent to the caudate nucleus and rostral to the optic chiasm. Less distinct foci of reddening and softening are found elsewhere in the meninges and parenchyma of the brain and spinal cord.

Mandibular, parotid, and cervical lymph nodes are enlarged to 2 cm in diameter. Petechiae and ecchymoses are scattered

Cerebrum, ox. Approximately 20% of the section is composed of a large area of hemorrhage and infarction. (HE, 5X)

through many skeletal muscles, esophageal adventitia, pulmonic trunk adventitia, visceral and parietal pleura, small intestinal serosa, and urinary bladder. The lungs are reddened. One liter of transparent yellow watery fluid is in the abdominal cavity. The small intestine, spiral colon, and descending colon have multifocal mucosal red foci. Several cestodes, up to 70 cm long, are in the jejunal lumen. Blood-tinged mucus is in the lumen of the descending colon.

Gross lesions are not observed in the pituitary gland, trigeminal nerves and ganglia, oral cavity, larynx, trachea, heart, thyroid gland, aorta, stomach, spleen, liver, gallbladder, pancreas, common bile duct, forestomachs, abomasum, adrenal glands, kidneys, testes, joints, or bone marrow.

Laboratory results: Aerobic culture of brain: *Histophilus somni*

Bovine herpesvirus fluorescent antibody test: Negative
Negative virus isolation
Fluorescent antibody test for rabies (Indiana State Department of Health): Negative
Fecal flotation: Numerous trichostrongyle-type eggs as well as eggs/ova of *Moniezia benedeni*, *Nematodirus* spp., *Eimeria* spp.

Histopathologic Description: In sections of cerebrum (submitted slide), brain stem, and spinal cord, many vessels (mainly veins and venules) have poorly organized thrombi rich in neutrophils. A few venules contain bacteria. The endothelium in affected vessels is disrupted with transmural extension of neutrophils and fibrinoid material or frank hemorrhage into Virchow-Robin space and beyond. Thrombi and hemorrhage are also in the leptomeninges. Surrounding neuroparenchyma is rarefied with hemorrhage, necrosis, and infiltration by neutrophils with fewer lymphocytes or macrophages. Thrombi are also in inflamed vessels of the ventricular myocardium and skeletal muscles. Neutrophils with fewer lymphocytes and macrophages infiltrate adjacent musculature. Myocytes are necrotic with hypereosinophilic sarcoplasm and pyknosis or karyorrhexis. Multifocal hemorrhage, necrosis, and aggregates of

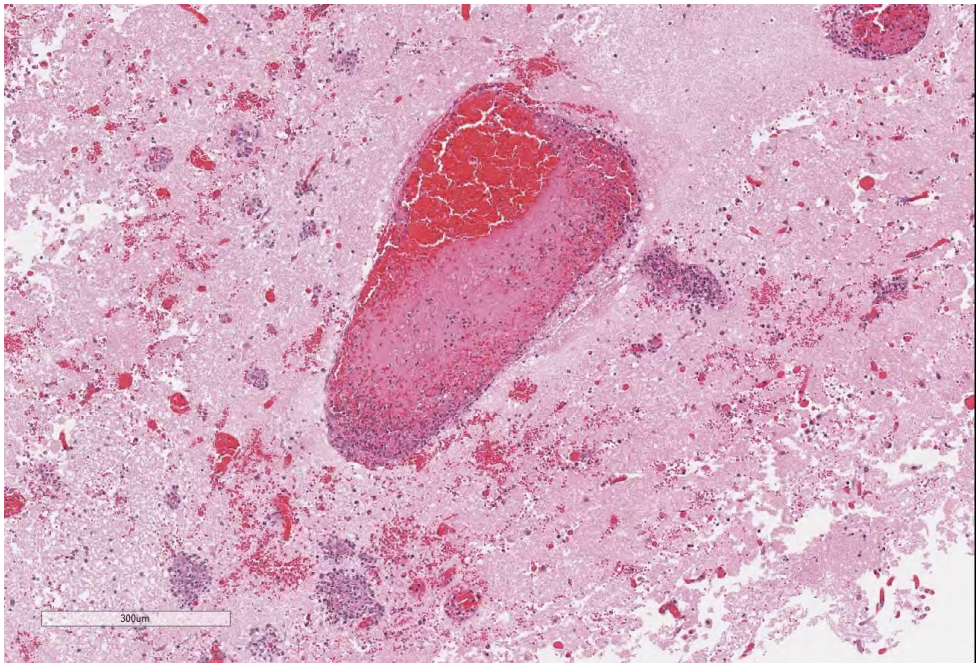

Cerebrum, ox. Vessels within the area of hemorrhage are partially to totally occluded by fibrincellular thrombi, and there is infiltration of inflammatory cells and hemorrhage within the walls and into the surrounding perivascular space (vasculitis). (HE, 84X)

neutrophils are in the tunica media of the pulmonic trunk.

Transmural hemorrhages in the small intestine are associated with submucosal fibrin thrombi, pleocellular leukocytic infiltration, and segmental necrosis of intestinal mucosa. The lung is congested with edematous interlobular septa. Alveolar spaces contain increased number of macrophages. A few poorly organized thrombi are in small pulmonary vessels.
Evaluated sections of lymph node, spleen, liver, kidney, adrenal gland, rumen (several ciliated protozoa), colon, trigeminal nerve and pituitary gland are within normal limits.

Contributor's Morphologic Diagnosis: Thrombotic meningoencephalitis with neutrophilic vasculitis.

Contributor's Comment: Rabies had been included in the clinical differential diagnosis, but the differential diagnosis at autopsy, based on the presence of multiple malacic hemorrhages in the brain and spinal cord, included thrombotic meningo-encephalitis and herpesviral

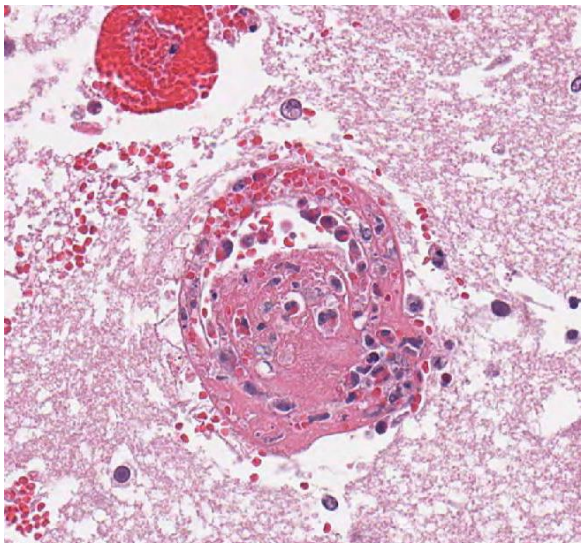

Cerebrum, ox. Multifocally, vessels are occluded and the wall is expanded by polymerized fibrin, hemorrhage, degenerate neutrophils, and cellular debris (fibrinoid necrosis). (HE, 360X)

encephalomyelitis. Histologically, the prominent and neutrophilic phlebitis with bacteria in the lumen of venules, plus the absence of trigeminal ganglionitis (and a negative FA test for rabies virus), prompted submission of brain for culture for *Histophilus somni*, which was isolated. Lesions of vasculitis, thrombosis, and inflammation were also detected histologically in the myocardium, pulmonic trunk, and skeletal muscles, but lung lesions were minimal in this case.

Histophilus somni is the cause of bovine thrombotic meningoencephalitis (TME), formerly known as thromboembolic meningoencephalitis (TEME). Currently, vasculitis (mainly phlebitis) is considered a primary lesion with thrombosis secondary to the local vasculitis, rather than the result of embolization from a distant site.[2] In fact, the tendency to induce thrombosis is a key feature of *H. somni*, and entails interactions of the bacterium with endothelial cells, leukocytes, and platelets.[1] The disease is reportedly more common in older calves and yearlings, and in late fall and early winter;[6] this 7-month-old calf died on the 23rd of November.

Lipooligosaccharide (LOS) is considered the major virulence factor of *H. somni*.[1,2] Its diverse activities contribute to the pathogenicity of *H. somn*i. Caspase-mediated apoptosis of endothelial cells (and of other host cells)[1] triggered by LOS (probably by its lipid A component), is thought to initiate the vasculitis of TME.[4] LOS is also thought to play a role in antigenic mimicry, inflammation (via Toll-like Receptor-4), resistance to phagocytosis and killing by leukocytes, and evasion of the immune response.[3]

Although most vaccine studies have been focused on the bovine respiratory disease

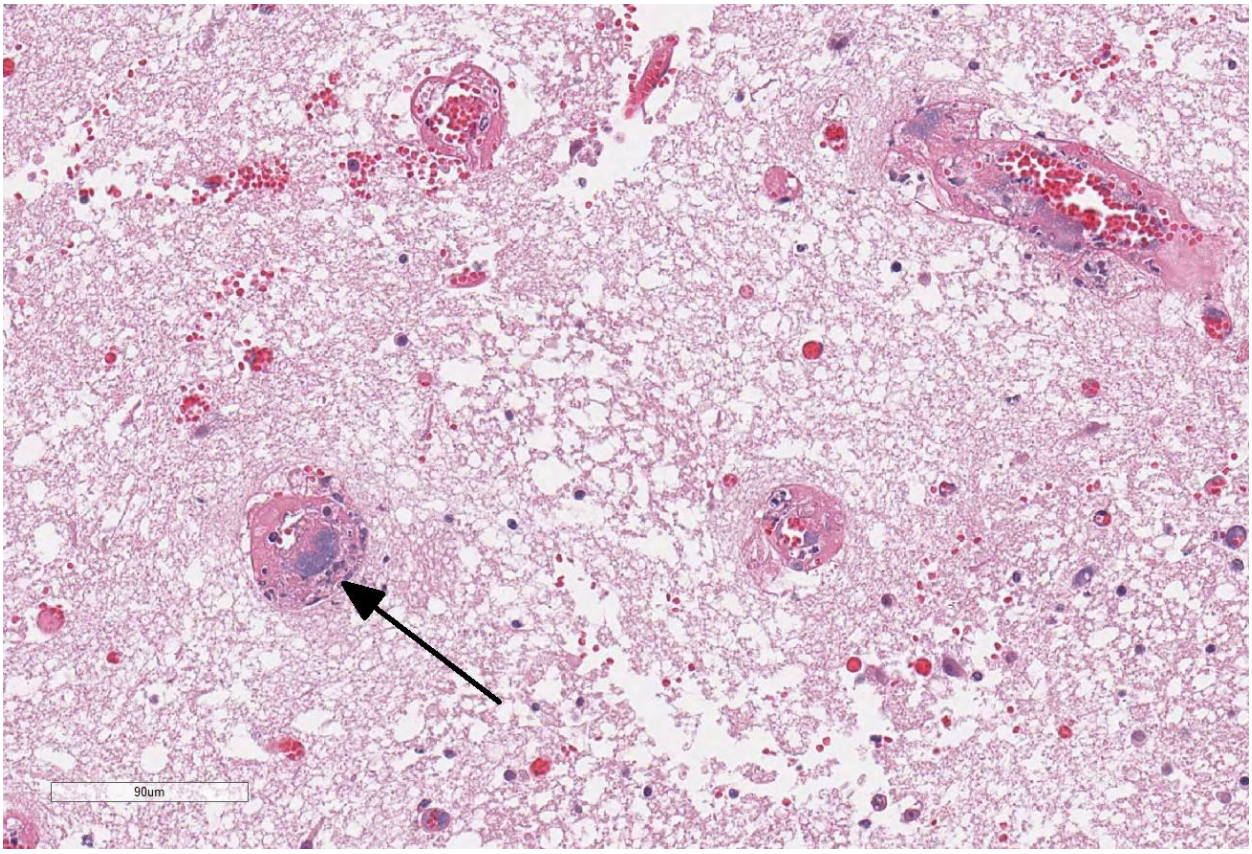

Cerebrum, ox. Thrombosed vessels often contain large colonies of coccobacilli (arrow). (HE, 348X)

complex, results suggest a role for humoral immunity. Macrophages that ingest *H. somni* are soon killed by the bacteria, so are unlikely to play a long-term role in dissemination of infection. This may also suggest that Th1 immunity is less important in disease control than humoral immunity.[3]

JPC Diagnosis: Brain: Vasculitis, fibrinous and necrotizing, multifocal, severe, with thrombosis, infarction, and numerous colonies of coccobacilli, Angus, *Bos taurus*.

Conference Comment: The contributor provides an outstanding example of the hallmark lesions of *Histophilus somni* in the brain of a feedlot calf. Conference participants localized the examined tissue section to the corpus striatum of the cerebrum due to the heterogeneous mix of white and grey matter tracts. *H. somni* is a facultative anaerobic gram-negative coccobacillus that is a normal commensal bacterium of the bovine genital tract and nasal cavity.[2] In 6 to 12-month-old calves, infection usually occurs following a stressor, such as transportation, inclement weather, crowding, or changes in diet.[2,3,6] Virulent strains of *H. somni* often cause septicemia resulting in a wide variety of lesions secondary to vasculitis and thrombosis caused by virulence factor, lipooligo-saccharide (LOS), discussed by the contributor above. Typical lesions associated with *H. somni* include thrombotic meningoencephalitis, myocarditis, mastitis, metritis, orchitis, conjunctivitis, necrotizing laryngotracheitis, and polyarthritis. *H. somni* also causes fibrinopurulent broncho-pneumonia as part of the bovine respiratory disease complex.[2,3,6] Readers are encouraged to read 2016 Wednesday Slide Conference

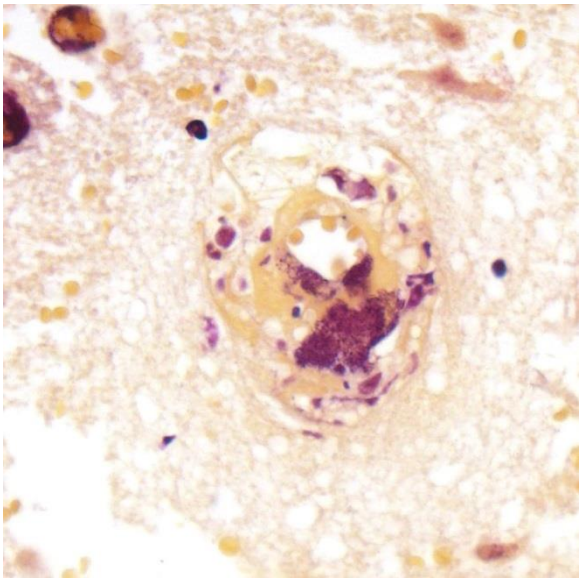

Cerebrum, ox. Bacterial colonies are better visualized with a Brown-Hopps tissue Gram stain. (BH, 400X)

#2 Case 4 for a review of the bovine respiratory disease complex. Small ruminants, bighorn sheep (*Ovis canadensis*), and North American bison (*Bison bison*) can also be affected; although the clinical manifestations are often not as severe likely due to less intensive management practices in these species.[6]

While the histologic lesions of *H.somi* are widespread, the bacteria has a tropism for the small venules of the cerebral vascular tissue and the most severe changes often occur within the brain, as in this case.[2] Affected calves often acutely die without treatment. In this case, there is severe fibrino-necrotic vasculitis and thrombi containing numerous coccobacilli resulting in a focally extensive infarct of the neuroparenchyma. Numerous colonies of bacteria are also present in the neuropil. Most conference participants agreed that the hemorrhage and infarction of the brain is a result of fibrinonecrotic vasculitis rather than a primary necrosuppurative meningoencephalitis.

As mentioned by the contributor, *H. somi* secretes an endotoxin (LOS) causing caspase 3-mediated apoptosis of endothelial cells leading to vasculitis and thrombus formation.[2] Recent studies indicate that *H. somni* can also stimulate endothelial cell tissue-factor (factor 3) activity and disrupt intercellular junctions enhancing pro-coagulant activity on the endothelial surface.[1] *H. somni* and LOS also activate bovine platelets, which further enhances tissue factor activity on the endothelial surface, upregulates leukocyte adhesion molecules (P-selectin, E-selectin, and ICAM-1), and initiates endothelial cell apoptosis via the FasL (caspases 8 and 9).[2,5] They also induce endothelial cell cytokine and reactive oxygen species production.[3,4,5] The mechanisms of *H. somni* induced vasculitis and thrombus formation are complex and research is ongoing to fully elucidate the pathogenesis.

Contributing Institution:
Purdue University
Indiana Animal Disease Diagnostic Lab
Purdue University Dept. Comparative

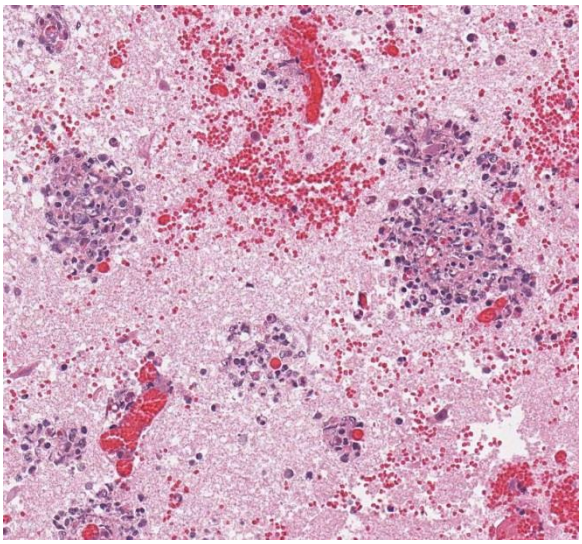

Cerebrum, ox. Numerous vessels are effaced by degenerate neutrophils and macrophages. (HE, 280X)

Pathobiology
406 S. University St.
West Lafayette, IN 47907
Animal Disease Diagnostic Laboratory: http://www.addl.purdue.edu/
Department of Comparative Pathobiology: http://www.vet.purdue.edu/cpb/

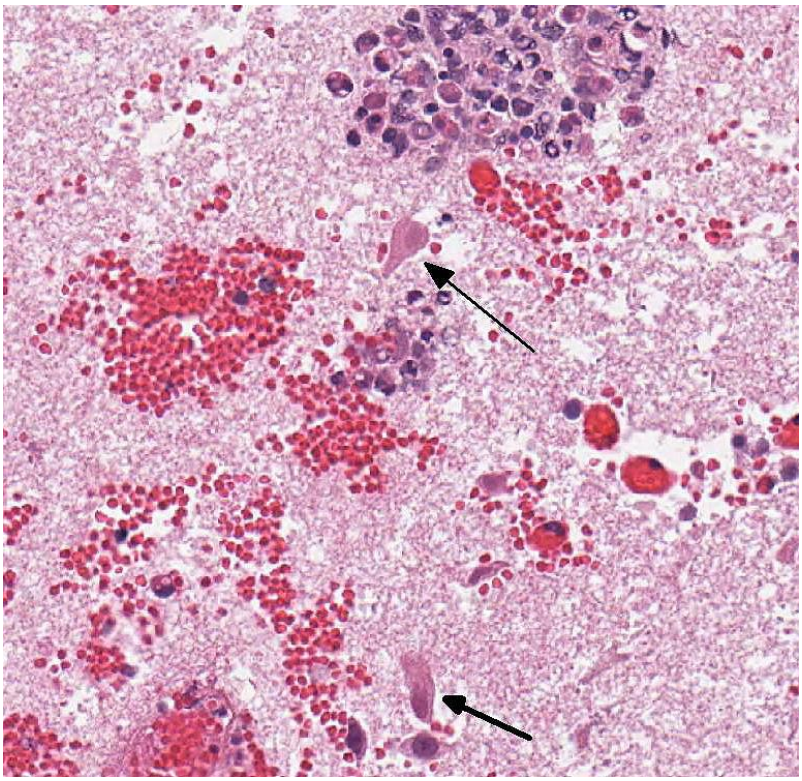

Cerebrum, ox. There are numerous necrotic neurons within the areas of infarction. (HE, 320X).

References:

1. Behling-Kelly E, Rivera-Rivas J, Czuprynski CJ. Interactions of *Histophilus somni* with host cells. *Curr Top Microbiol Immunol*. 2016; 396:71-87.
2. Cantile C, Youssef S. Nervous system. Maxie MG ed. In: *Jubb Kennedy and Palmer's Pathology of Domestic Animals*. Vol 1. 6th ed. Philadelphia, PA: Elsevier Saunders; 2016:364-365.
3. Corbeil LB. Host immune response to *Histophilus somni*. *Curr Top Microbiol Immunol*. 2016; 396:109-129.
4. Inzana TJ. The many facets of lipooligosaccharide as a virulence factor for *Histophilus somni*. *Curr Top Microbiol Immunol*. 2016; 396:131-148.
5. Kuckleburg CJ, McClenahan DJ, Czuprynski CJ. Platelet activation by *Histophilus somni* and its LOS induces endothelial cell pro-inflammatory responses and platelet internalization. *Shock*. 2008; 29:189-196.
6. O'Toole D, Sondgeroth KS. Histophilosis as a natural disease. *Curr Top Microbiol Immunol*. 2016;396:15-48.

Self-Assessment - WSC 2016-2017 Conference 12

1. Which of the following is the primary condition in cerebellar granuloprival degeneration?
    a. Purkinje cell granulation
    b. Depletion of the molecular layer
    c. Depletion of the granular layer
    d. White matter cavitation within the cerebellar folia

2. Which of the following is not true concerning cervical vertebral instability in the horse?
    a. Thoroughbreds and Quarter horses are primarily involved.
    b. One- to four-year-old horses are primarily affected.
    c. C3-C5 is the most affected area.
    d. *Ad libitum* feeding of high-energy and high-protein diets may be contributory.

3. Which of the following disease is not associated with central chromatolysis?
    a. Feline dysautonomia
    b. Aspergillus clavatus toxicosis
    c. Feline ischemic encephalopathy
    d. Avian encephalomyelitis

4. Which is the following is the key virulence factor of *H. somni*?
    a. Lipooligosaccharide
    b. Perforin
    c. YadA
    d. Edema factor

5. Which of the following mediates *H. somnus*-induced endothelial cell apoptosis?
    a. P-selectin
    b. E-selectin
    c. ICAM-1
    d. Caspase-3

Joint Pathology Center

Veterinary Pathology Services

WEDNESDAY SLIDE CONFERENCE 2016-2017

C o n f e r e n c e 13

4 January 2017

Cynthia M. Bell, MS, DVM, Diplomate ACVP
Director - Center for Comparative Oral and Maxillofacial Pathology
School of Veterinary Medicine, UW-Madison
Madison, WI 53706

CASE I: F1475435 (JPC 4084214).

Signalment: Ten-month-old, male, Labrador retriever, (*Canis familiaris*).

History: A 10-month-old, intact male, Labrador retriever presented to the referring veterinarian with a one-month history of pain when rising after sleeping. Physical exam revealed pain (2/10) on palpation of the lumbar spine. Radiographs showed collapse disk space at L1-L2 and end plate lysis of L1-L2 and L4-L5. Blood culture was positive for *Brucella canis.* The dog was referred to the Veterinary Teaching Hospital at Colorado State University for castration where the owner was counseled about the human health risk of *B. canis* and that the dog could continue to shed the bacteria even after castration and antibiotic treatment. The owner elected euthanasia because of the zoonotic risk. The body was submitted for necropsy.

Gross Pathology: None. The vertebrae were not evaluated for intervertebral disk disease or vertebral disease due to the public health concern.

Laboratory results: Blood culture: Positive for *Brucella canis*.

Histopathologic Description: Prostate gland: Multifocal and coalescing infiltrates of lymphocytes, plasma cells, and macrophages obliterate normal architecture, expand the interstitium, and spill into remaining glandular lumina. Low numbers of neutrophils are present. There are multifocal sites of coagulative necrosis. Redundant fibrous connective tissue expands the interstitium, in some fields, up to 2-3x normal. Gram staining is negative

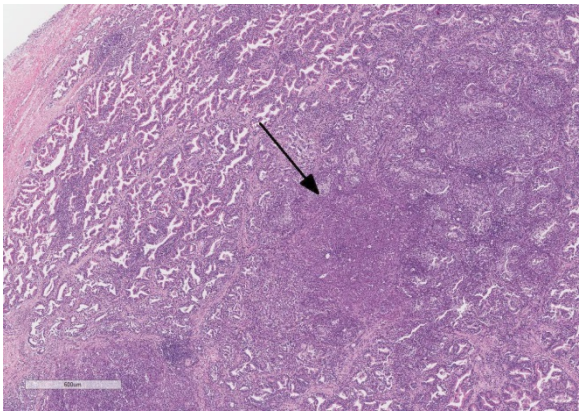

Testis, dog. There is diffuse glandular hypertrophy of the prostate. Aggregates of lymphocytes expand the interstitium, and multifocal areas of glandular tissue are effaced by an inflammatory infiltrate (arrow). (HE, 37X)

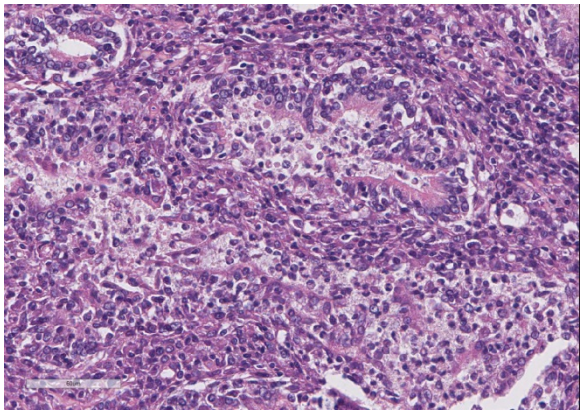

Testis, dog. Within inflamed areas, there is destruction of glands, necrosis of glandular epithelium, and infiltration by moderate numbers of neutrophils and macrophages. (HE, 360X)

for organisms.

Testis and epididymis: There is multifocal infiltration of the epididymal connective tissue stroma by small clusters of lympho-cytes, plasma cells, and few macro-phages with a perivascular to random distribution. The ducts contain a moderate amount of sperm. In the testis, there is a moderate to severe decrease in complete spermiogenesis, with many tubules lacking luminal spermatozoa. Gram staining is negative for organisms.

Contributor's Morphologic Diagnosis: 1. Prostate gland: Prostatitis, lympho-plasmacytic, multifocal to coalescing, chronic, severe, with parenchymal loss and fibrosis, Labrador retriever, *Canis familiaris.*
2. Epididymis: Epididymitis, lympho-plasmacytic, multifocal, chronic, moderate.

Contributor's Comment: *Brucella canis* is a gram-negative, rough or mucoid, facultative intracellular coccobacillus. Canids can be infected with four of the *Brucella* species (*B. canis*, *B. abortus*, *B. melitensis*, and *B. suis*) and serve as the reservoir species for *B. canis.* The bacteria was first isolated in 1966 in a colony of beagles and is now reported worldwide (the Americas, Europe, Asia, and South Africa).[12] The disease is especially prevalent in the southeastern United States.[5,6]

Infection occurs via bacterial penetration of mucus membranes, especially oral, conjunctival, and genital. Semen and vaginal fluids of infected canines have very high bacterial loads and exposure to these fluids is the most common route of mucosal transmission, with exposure to infected aborted fetuses, placental tissues, lochia, and urine (especially from male dogs) also serving as sources of infection.[4,12] In addition, *B. canis* has also been isolated from saliva, nasal and ocular secretions, milk, and feces, but the importance of these as sources of infection is unknown.[12]

Upon penetration of mucus membranes, the bacteria are taken up by phagocytes and trafficked to lymphatic organs and the genital tract. *Brucella canis* can persist intracellularly by evading phagosome-lysosome fusion and replicate within an endoplasmic reticulum-derived vacuole.[2,11] Bacteremia develops 1 to 4 weeks post infection and can persist, intermittently, for several years.[4,11]

Infected canids often show vague or non-specific clinical signs, including poor hair coat, lethargy, weight loss, back pain, lymphadenomegaly, and reproductive failure.[5] In bitches, there may be infertility, early embryonic death, fetal resorption, and late term abortion (45 to 60 days).[4,6] Aborted fetuses are born dead and partially autolyzed with subcutaneous congestion and edema.[12] Pups can be born alive but usually die shortly after birth. Brown to green vaginal discharge can occur for one to six weeks post abortion. In males, *Brucella* sp. can cause infertility, epididymitis, prostatitis, scrotal dermatitis (secondary to licking

trauma), testicular swelling or atrophy, and loss of libido.[4] Sterility can occur secondary to testicular damage that may result in autoimmune anti-sperm antibodies.[4,12] Less commonly, in both sexes infection can result in uveitis, diskospondylosis of the thoracic and lumbar spine, glomerulonephritis, and very rarely meningoencephalitis.

Gross lesions of brucellosis may be lacking or vague, often limited to splenomegaly, lymphadenomegaly, and in males, an enlarged epididymis. In the uterus, *Brucella* species cause chronic to subacute endometritis with glandular hyperplasia and reticular cell nodules.[4] In males, classic histologic findings are similar to what is presented in this case: lymphoplasmacytic interstitial epididymitis and prostatitis. Other findings can include focal hepatic necrosis, myocarditis, meningoencephalitis, hyaline thickening of the basement membrane of glomeruli, and granulomatous uveitis with retinitis.[4]

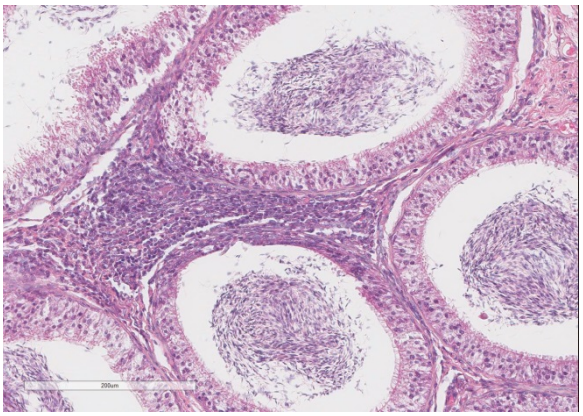

Epididymis, dog: The intertubular interstitium is expanded by moderate numbers of lymphocytes and fewer plasma cells. (HE, 196X)

The diagnosis of brucellosis can be made based on a history of reproductive failure and supportive serology with positive blood culture.[6] There is no effective treatment for *B. canis*. Treatment can eliminate active bacteremia but cannot eliminate bacteria residing in tissues; thus, infected tissues serve as sources for recurrent bacteremia.[12] Spaying and neutering infected dogs can help decrease shedding of the bacteria but does not eliminate infection.

Brucella canis is a zoonotic agent, but its significance as a human pathogen is poorly understood. Confirmed transmission to humans is not common, although it is likely that the disease is under-diagnosed.[4,6] Veterinarians, kennel workers, and people living with a *B. canis*-positive dog are at greatest risk of infection. In humans, *Brucella* causes vague clinical signs of fever, weakness, headache, joint pain, and enlarged lymph nodes;[12] it has also been associated with ocular lesions and endocarditis.[4,6] It is of greatest risk to immunosuppressed individuals, children, and pregnant women. In all cases, counseling about the potential health risks of living with a *B. canis*-positive dog should be provided.

JPC Diagnosis: 1. Prostate gland: Prostatitis, lymphocytic, multifocal to coalescing, chronic, severe.
2. Prostate gland: Hyperplasia, cystic, glandular, diffuse, moderate.
3. Epididymis: Epididymitis, lymphocytic, multifocal, mild.

Conference Comment: The contributor offers an excellent example of the typical lesions associated with *Brucella canis* in a male dog and a thorough summary of the epidemiology, clinical signs, pathogenesis, diagnosis, and public health implications associated with this pathogen.

Bacteria of the genus *Brucella* are most often associated with reproductive failure and abortion in a variety of mammals. *Brucella* consists of six classically recognized species based on the pre-

dominant host species and characteristic of the bacteria.[9] These include: *B. abortus* primarily affecting cattle; *B. melitensis* affecting sheep and goats; *B. suis* affecting pigs; *B. ovis* affecting sheep; *B. canis* affecting dogs; and *B. neotomae* affecting rodent species.[7] Two novel species of *Brucella*, *B. ceti* and *B. pinnipedialis*, have been isolated from marine mammals. *Brucella ceti* has been associated with abortion in cetaceans, while *B. pinnipedialis*, isolated from Northeastern Atlantic hooded seals, has a reduced pathogenicity due to its decreased ability to survive and multiply within macrophages. *Brucella microti* has recently been isolated from common voles and red foxes.[1,6,8,9]

Brucella species consist of both smooth and rough strains, with rough strains lacking the expression of the virulence factor O-side chain on the lipopolysaccharide (LPS) present on smooth strains.[8] The smooth strain LPS is non-endotoxic and allows entry into host cells via cholesterol-rich lipid rafts in the plasma membrane. In addition, the O-side chain prevents complement-mediated bacterial lysis and inhibits apoptosis of the infected cell. Both smooth and rough strains are adept at survival within macrophages due to expression of the VirB operon encoded type IV secretion system, which is induced by acidification of the phagosome during the respiratory burst. The VirB system neutralizes the pH of the phagosome and allows *Brucella* species to undergo intracellular replication and survival. Virulent strains also employ other methods to detoxify free radicals within the phagosome, including expression of superoxide dismutates. Intracellular survival and replication is the key to its virulence, and once infection is established, it tends to persist.[2,3,9,13]

Rough strain *Brucella* species are phagocytosed following recognition by toll-like receptor-4 (TLR-4) and are less virulent due to their lack of LPS O-side chain; however, as mentioned above, both have the ability to survive within phagocytes via the VirB operon.[3,9] *Brucella ovis* and *B. canis* are rough strain groups, while *B. abortus*, *B. melitensis*, and *B. suis* are more virulent and categorized under smooth strains.[3,7,9]

Conference participants discussed the emergence of zoonotic *B. canis* in underserved communities worldwide due to human interaction with populations of free-roaming canines. While *B. canis* is classified as a rough strain, and thus has a lower virulence, there have been sporadic reports of human infection. The incidence is likely under-reported due to its non-specific symptoms of low grade fever, joint pain, headache, and fatigue.[1,7]

Contributing Institution:

Colorado State University
College of Veterinary Medicine and Biomedical Sciences
Department of Microbiology Immunology and Pathology
http://csucvmbs.colostate.edu/academics/mip/

References:

1. Centers for Disease Control and Prevention [CDC]. Brucellosis (*Brucella melitensis, abortus, suis*, and *canis*). CDC; 2012 Nov. Available at: https://www.cdc.gov/brucellosis/index.html. Accessed 6 January 2017.
2. De Figueiredo P, Ficht TA, Rice-Ficht A, Rossetti CA, Adams LG: Pathogenesis and immunobiology of brucellosis: review of *Brucella*-host interactions. *Am J Pathol*. 2015; 185(6)**:**1505-17.

3. De la Cuesta-Zuluaga JJ, et al. Identification of the virB operon genese encoding the type IV secretion system, in Columbian *Brucella canis* isolates. *Vet Microbiol*. 2013. 163:196-199.
4. Greene CE, Carmichael LE: Canine Brucellosis. In: Green CE, ed. *Infectious diseases of the dog and cat*. 4th ed. St. Louis, Mo.: Elsevier/Saunders; 2012:398-411.
5. Hollett RB: Brucellosis. In: Ettinger SJ, Feldman EC, eds. *Textbook of veterinary internal medicine : diseases of the dog and the cat*. 7th ed. St. Louis, Mo.: Elsevier Saunders; 2010: 882-6.
6. Hollett RB: Canine brucellosis: outbreaks and compliance. *Theriogenology*. 2006;66(3)**:**575-87.
7. Kazmierczak J. Public health implication of Brucella cais infection in humans. Summary findings of Brucella canis Workgroup. March 2012. Available at: http://www.nasphv.org/Documents/BrucellaCanisInHumans.pdf. Accessed 6 January 2017.
8. Larsen AK, Nymo IH, Boysen P. et al. Entry and elimination of marine mammal *Brucella* spp. by hooded seal (*Cystophora cristata*) alveolar macrophages in vitro. *PLoS One*. 2013; 8: e70186. doi: 10.1371.
9. Olsen SC, Palmer MV. Advancement of knowledge of Brucella over the past 50 years. *Vet Pathol*. 2014; 51(6):1076-1089.
10. Schlafer DH, Foster RA. Female genital system. In: Maxie MG ed. In: *Jubb Kennedy and Palmer's Pathology of Domestic Animals*. Vol 3. 6th ed. Philadelphia, PA: Elsevier Saunders; 2016:402-406.
11. Von Bargen K, Gorvel JP, Salcedo SP: Internal affairs: investigating the Brucella intracellular lifestyle. *FEMS Microbiol Rev*. 2012;36(3)**:**533-62.
12. Wanke MM: Canine brucellosis. *Anim Reprod Sci*. 2004;82-83**:**195-207.
13. Zachary JF. Mechanisms of microbial infection. In: McGavin MD, Zachary JF, eds. *Pathologic Basis of Veterinary Disease*. 5th ed. St. Louis, MO: Mosby Elsevier; 2012:189-90, 197-8.

CASE II: D15-008849 (JPC 4066261).

Signalment: Six-year-old, castrated male, boxer, (*Canis familiaris*).

History: The dog presented with a 20-day history of seizure-like activity (lateral recumbency, drooling, and paddling) with increasing frequency. Phenobarbital administration controlled the symptoms for several weeks, but the dog gradually became lethargic and inappetant with head twitching behavior. The owners elected euthanasia due

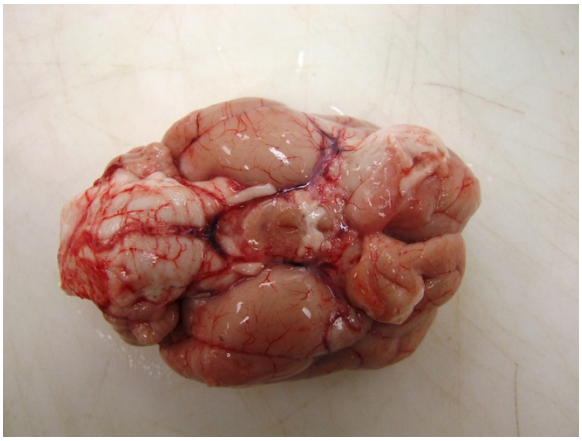

Cerebrum, dog . Note the asymmetric enlargement of the right rostral cerebrum. (Photo courtesy of: Department of Diagnostic Medicine and Pathobiology, Kansas State Veterinary College of Veterinary Medicine, 1800 Denison Avenue, Manhattan, KS 66506, http://www.vet.k-state.edu/depts/dmp/index.htm)

to concern about the dog's quality of life.

Gross Pathology: The rostral aspect of the right frontal lobe of the brain was enlarged, with shallow sulci and flattened gyri, and was deviated left of the midline. The brain was fixed in formalin and sectioned for examination. The cranioventral portion of the right cerebral hemisphere contained a gray, translucent, gelatinous, 2cm x 2cm x 4cm mass, extending from the frontal lobe of the cerebrum into the mesencephalon.

Laboratory results: Bloodwork was unremarkable.

Histopathologic Description: Within the white matter of the cerebral cortex, there is a poorly demarcated, unencapsulated, infiltrative neoplastic mass. The neoplasm is composed of round to polygonal cells arranged as a loose meshwork or occasionally as closely packed sheets with a honeycomb appearance and scant fibrovascular stroma. Neoplastic cells are 10-14 microns in diameter and have distinct cell borders; scant to moderate amounts of eosinophilic, fibrillar cytoplasm; a prominent perinuclear clear zone (perinuclear halo); and small, irregularly round, hyperchromatic nuclei with indistinct nucleoli. The mitotic rate is less than one per ten 400x high power fields. Capillary blood vessels within the mass are prominent with marked endothelial hypertrophy. Other variable features that are present in some slides: scattered foci of hemorrhage, glomeruloid microvascular proliferation, and pseudocystic cavities containing homogeneous, lightly basophilic (mucinous) material.

Neoplastic cells were negative for GFAP on immunohistochemical staining.

Cerebrum, dog. In the cranioventral portion of the right cerebral hemisphere, there is a gray, translucent, gelatinous mass causing deviation of midline. (Photo courtesy of: Department of Diagnostic Medicine and Pathobiology, Kansas State Veterinary College of Veterinary Medicine, 1800 Denison Avenue, Manhattan, KS 66506, http://www.vet.k-state.edu/depts/dmp/index.htm)

Contributor's Morphologic Diagnosis: Brain (cerebrum): Oligodendroglioma.

Contributor's Comment: This case had a classic signalment and presentation for canine oligodendrogliomas. Oligodendrogliomas occur most commonly in dogs, particularly in older animals and brachycephalic breeds (boxers, Boston terriers, and bulldogs), and rarely in other species including humans, cats, cattle, and horses.[1,2,9] In a study involving 173 dogs, it was found that dogs with oligodendrogliomas are 3.6 times more likely to have seizures compared with dogs with other types of primary brain tumors.[9] Other common presenting clinical complaints include mentation change, vision loss, neck pain, and vestibular syndrome.[9] Bloodwork is usually unremarkable, as it was in this case.

The most frequent location for oligodendrogliomas is the white or gray matter of the cerebral hemispheres, particularly the olfactory area and rostral lobes, but can

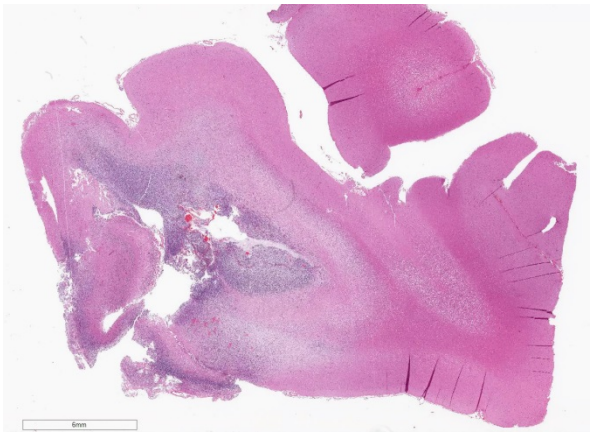

Cerebrum, dog. An infiltrative neoplastic mass is present within the white matter of the cerebral cortex, arranged as a loose meshwork or occasionally as closely packed sheets with prominent capillary blood vessels. This section shows a central pseudocystic cavity. (HE, 4X)

occur caudally or in the spinal cord.[5,9] Grossly, they appear as large, soft, gelatinous or mucoid, well-demarcated masses with grayish-blue matrix and gray to pink stroma on cut section.[1,2,5] Histologically, oligodendrogliomas are moderately to highly cellular, and characterized by dense sheets of uniform cells. [1,5] Delayed fixation causes an artifactual "honeycomb" cell pattern with a perinuclear halo effect. [1,2,5] Prominent microvascular proliferation is common, often with formation of a delicate "chicken-wire" pattern or vascular loops with glomerular-like tufts, as seen in this case. [1,2,5] Foci of hemorrhage, mineralization, or microcystic areas containing blue-staining mucinous material may also be present.[1,2,5] Tumors can extend along or through the leptomeninges or ependymal surfaces; intraventricular growth may be associated with widespread intraventricular metastases.[5]

Anaplastic oligodendrogliomas are characterized by focal or diffuse anaplasia with prominent proliferation of glomeruloid vessels at the tumor margins, nuclear polymorphism, and increased mitotic index (1-2 per HPF), necrosis, and/or meningeal infiltration.[1] Intermingled astrocytes are common, and in some tumors polymorphic multinucleated giant cells may be numerous.[1] Often, areas of necrosis with peripheral glial cell palisading can be found.[5] Due to the lack of malignant features, in this case, the tumor was diagnosed as a benign oligodendroglioma.

Oligoastrocytomas are rare mixed glial tumors composed of neoplastic astrocytes and oligodendroglia, in which the two cell populations may be diffusely intermingled or in geographically distinct clusters. [1,2,5] Canine oligoastrocytomas are predominantly composed of oligodendroglial cells with at least 25-30% neoplastic astrocytes; lower percentages of astrocytic elements are interpreted as reactive proliferating cells within oligodendrogliomas.[1,5] Anaplastic (malignant) oligoastrocytomas are characterized by increased cellularity, nuclear atypia, high mitotic activity, vascular proliferation, and necrosis, and may be difficult to differentiate from high-grade astrocytomas.[1]

Ultrastructurally, oligodendrogliomas have no obvious distinguishing features, appearing as cells with sparse microtubules and few organelles in the cytoplasm and frequent desmosomal junctions between cells.[5]

Historically, diagnosis of oligodendrogliomas has relied on gross and microscopic tumor morphology and negative GFAP staining of cells, due to lack of specific markers.[2,4,5] In recent years, several markers have been investigated, including doublecortin, olig2, and CNPase.[3,4] Doublecortin is a cytoplasmic neuronal precursor marker which is frequently expressed in oligodendrogliomas and

embryonal neoplasms such as neuroblastomas and PNETs, but infrequently expressed in astrocytomas.[3] Olig2 is a nuclear transcription factor that is required for oligodendrocyte differentiation but not astrocyte development, and has been shown to stain all oligodendrogliomas in one study.[4] Non-neoplastic astrocytes do not stain with Olig2; however, astrocytomas can have positive nuclear staining.[4] CNPase is a cytoplasmic phosphodiesterase that is expressed early in myelination.[4] It stains normal and neoplastic oligodendrocytes, but weak cytoplasmic staining of canine astrocytomas can also occur.[4] A combination of negative GFAP staining and positive Olig2 staining may be most helpful in identification of oligodendrogliomas. Positive staining for factor VIII-like antigen and smooth muscle actin highlights the neoplasm's characteristic microvascular proliferations.[5] In our case, the neoplasm stained negatively for GFAP. No staining for the other potential oligodendroglioma markers was attempted.

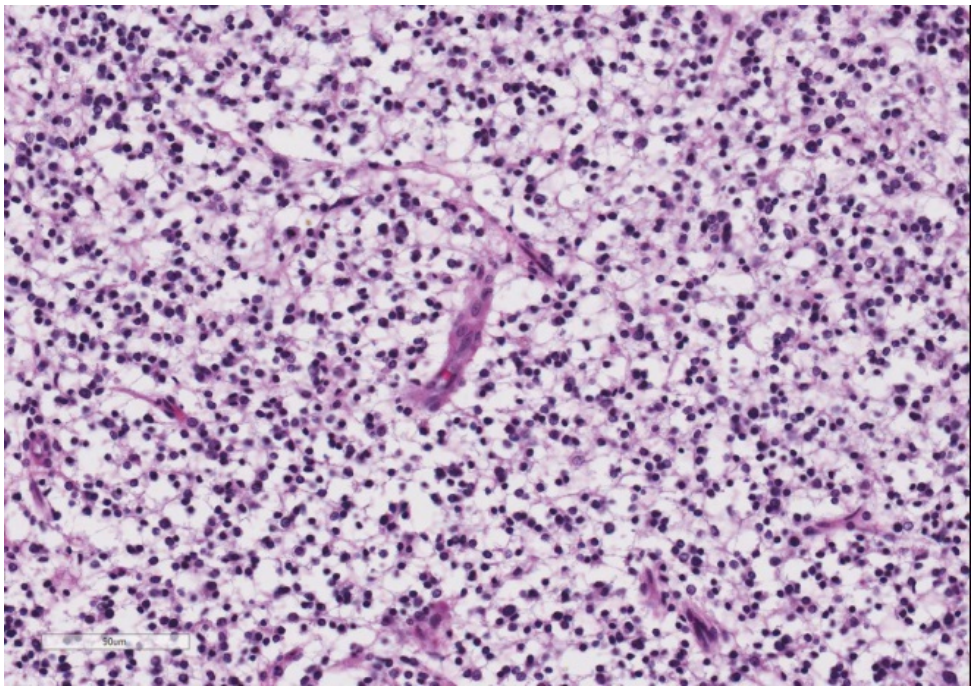

Cerebrum, dog. In many areas, the neoplastic cells are arranged as a loose meshwork with a characteristic "honeycomb" appearance. (HE, 224X)

JPC Diagnosis: Brain, cerebrum: Oligodendroglioma, boxer, *Canis familiaris*.

Conference Comment: Despite some moderate slide variability, the contributor provides a great example and com-prehensive review of oligodendrogliomas in the canine central nervous system (CNS). Oligodendrogliomas are the third most common primary neoplasm in the dog brain, after meningiomas and astrocytomas.[6] These soft gelatinous neoplasms typically arise in the telencephalic or diencephalic cerebral white matter, but can uncommonly occur in the brainstem, spinal cord, or within the ventricular system as a single tumor or as multiple concurrent oligodendrogliomas as a result of metastasis through the cerebrospinal fluid.[2,6,8]

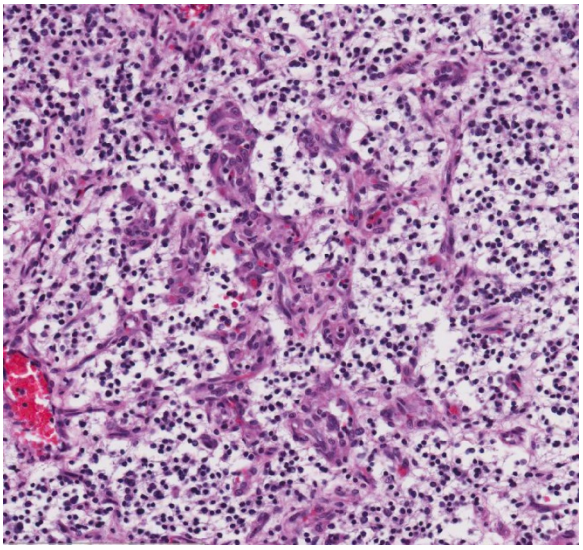

Cerebrum, dog. Multifocally, prominent capillary blood vessels have endothelial hypertrophy and a proliferative "glomeruloid" pattern. (HE, 168X)

Oligodendrogliomas originate from oligodendrocytes, which normally function to provide support and myelination to axons within the white matter tracts of the CNS.[7] Each oligodendrocyte can envelop up to 50 axons based on the thickness of the myelin sheath needed. Oligodendrocytes also serve a role in the production of neurotropic factors important for the remyelination of demyelinated axons in the CNS.[7] Schwann cells provide an equivalent function in the peripheral nervous system (PNS); however, unlike oligodendrocytes, Schwann cells can only envelope one part of a single axon. Schwann cells are also extremely important in axonal regeneration in the PNS.[10]

As mentioned by the contributor, positive immunohistochemical staining for oligodendrocyte transcription factor-2 (Olig2) in combination with negative glial fibrillary acidic protein (GFAP) has been shown to be an extremely useful tool in the diagnosis of oligodendrogliomas. The proportion of Olig2-positive cells has been shown to be significantly higher in oligodendrogliomas when compared with other glial tumors such as astrocytoma and oligoastrocytoma, mentioned above.[4,6] Prior to the conference, an Olig2 and GFAP stains were performed by the Joint Pathology center. In this case, neoplastic cells showed strong and diffuse intranuclear immunoreactivity to Olig2. Expression of intranuclear Olig2 immunoreactivity is restricted to the neoplasm and resident oligodendrocytes within the unaffected section of cerebrum. Additionally, neoplastic cells are diffusely immunonegative for GFAP. The GFAP-positive cells noted by conference participants at the periphery and within the neoplasm are interpreted as reactive astrocytes, which can occur due to tumor-induced activation of the residential astroglial network. This staining pattern is consistent with the contributor's diagnosis of an oligodendroglioma, in this case.[2,4,6,8]

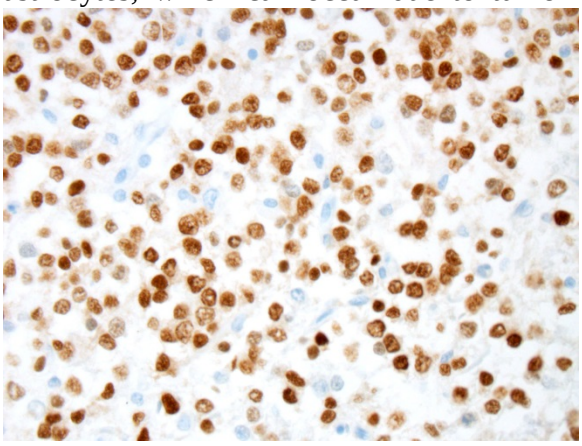

Cerebrum, dog. Neoplastic cells exhibit diffuse, strong intranuclear staining for olig-2. (anti-olig-2, 400X)

Contributing Institution:

Department of Diagnostic Medicine and Pathobiology
Kansas State Veterinary College of Veterinary Medicine
1800 Denison Avenue
Manhattan, KS 66506
http://www.vet.k-state.edu/depts/dmp/index.htm

References:

1. Burger PC, Scheithauer BW: Tumors of neuroglia and choroid plexus. In: *AFIP Atlas of Tumor Pathology, Series 4, Tumors of the Central Nervous System*. ed. Silverberg SG. Washington DC: ARP Press; 2007:225-233.
2. Cantile C, Youssef S. Nervous system. Maxie MG ed. In: *Jubb Kennedy and Palmer's Pathology of Domestic Animals*. Vol 1. 6th ed. Philadelphia, PA: Elsevier Saunders; 2016:400.
3. Ide, Uchida K, Kikuta F, Suzuki K, Nakayama H. Immunohistochemical characterization of canine neuro-epithelial tumors. *Vet Pathol*. 2010; 47(4)741-750.
4. Johnson GC, Coates JR, Wininger F. Diagnostic immunohistochemistry of canine and feline intracalvarial tumors in the age of brain biopsies. *Vet Pathol*. 2014; 51(1)146-160.
5. Koestner A, Higgins RJ. Tumors of the nervous system. In: *Tumors in Domestic Animals*. ed. Meuten DJ. 4th ed. Ames, IA: Iowa State Press; 2002:703-706.
6. Kovi RC, Wünschmann A, Armién AG, Hall K, Carlson T, Shivers J, Oglesbee MJ. Spinal meningeal oligo-dendrogliomatosis in two boxer dogs. *Vet Pathol*. 2013; 50(5):761-764.
7. Kremer D, Gottle P. et al. Pushing forward: Remylination as the new frontier in CNS disease. *Trends Neurosci*. 2016; 39(4):246-263.
8. Rissi DR, Levine JM, et al. Cerebral oligodendroglioma mimicking intra-ventricular neoplasia in three dogs. *J Vet Diagn Invest*. 2015; 27(3):396-400.
9. Snyder JM, Shofer FS, Van Winkle TJ, Massicotte C: Canine intracranial primary neoplasia: 173 cases (1986-2003). *J Vet Intern Med*. 2006; 20:669-675.
10. Toy D, Namgung U. Role of glial cells in axonal regeneration. *Exp neurobiol*. 2013; 22:68-76.

CASE III: 05-7078-B (JPC 4085316).

Signalment: Three-month-old, Pinzgauer-cross, steer, (*Bos taurus*).

History: Since birth, the calf failed to grow hair and maintained a thickened crusty skin. Shortly before death, the calf became anorexic and lethargic. The calf had developed disseminated pocks, sub-cutaneous nodules, and interdigital ulcers. This calf was the first on this farm with this presentation.

Gross Pathology: This three-month-old Pinzgauer-cross steer calf presented with severe generalized hypotrichosis with the exception of the preputial skin. Large areas of the skin, especially the trunk, were

Haired skin, calf. Large areas of the skin, especially the trunk, were covered with thick layers of keratin resulting in a fish scale or elephant skin appearance. (Photo courtesy of Oregon State University Diagnostic Laboratory http://vetmed.oregonstate.edu/diagnostic)

covered with thick layers of keratin resulting in a fish scale or elephant skin appearance. The thickened keratin layer had criss-crossed, deep fissures that extended into the dermis. There were scattered dermal, up to 7mm in diameter nodules over the trunk, thigh, and shoulder. Over the carpal and tarsal joints, the skin was smooth. The interdigital skin had multiple small (up to 5 mm) areas of ulceration. All subcutaneous and internal lymph nodes were moderately to severely enlarged (e.g., right prescapular lymph node measured 7 x 3 x 2). The oral mucosa had extensive erosions and the tongue had a focal area of hyperkeratosis over the fossa linguae. There were a few small areas of epithelial hyperplasia and hyperkeratosis in the esophagus and forestomachs. No significant gross lesions were present in other organs and tissues including bone marrow, eye, and liver.

Laboratory results: Electron microscopic examination of the skin identified poxviral particles in areas of ballooning degeneration. Immunohistochemistry on a section the skin did not identify bovine viral diarrhea virus.

Histopathologic Description: The section contains skin lesions of increasing severity along the length of tissue with one end much

Forestomachs, calf. There were a few small areas of epithelial hyperplasia and hyperkeratosis in the esophagus and forestomachs. (Photo courtesy of Oregon State University Diagnostic Laboratory http://vetmed.oregonstate.edu/diagnostic)

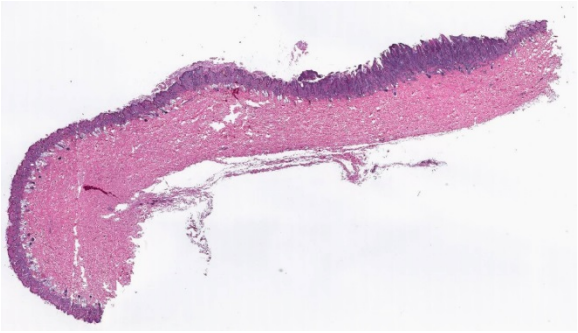

Haired skin. A section of haired skin demonstrates a diffuse hypercellularity of the epidermis and papillary dermis. 50% of the epidermis (at right), displays an increased level of hyperplasia. (HE, 4X).

more affected and distorted than the other. In the section of skin, there is mild to moderate epidermal hyperplasia with mild to severe compact orthokeratotic hyperkeratosis and segmental parakeratosis. In severely affected areas, hair follicles are rare and small for the follicles that are present. Some affected follicles contain clumps of keratin with no discrete hair shafts whereas other contains hair shafts that are angled, thin, and fragmented. Multifocally, the epidermis has severe ballooning degeneration with cytoplasmic eosinophilic inclusions in degenerate keratinocytes. This is associated with suppurative folliculitis and pustular epidermitis. Areas of hyperkeratosis are colonized by small numbers of *Malassezia* sp.

Contributor's Morphologic Diagnosis:
Severe epidermal compact hyperkeratosis
Severe follicular dysplasia and hyper-keratosis
Severe chronic ulcerative and pustular dermatitis with epithelial ballooning degeneration and intracytoplasmic viral inclusion bodies

Contributor's Comment: This Pinzgauer-cross calf suffered from a combination of ichthyosis and follicular dysplasia, which was complicated by surface *Malassezia* sp.

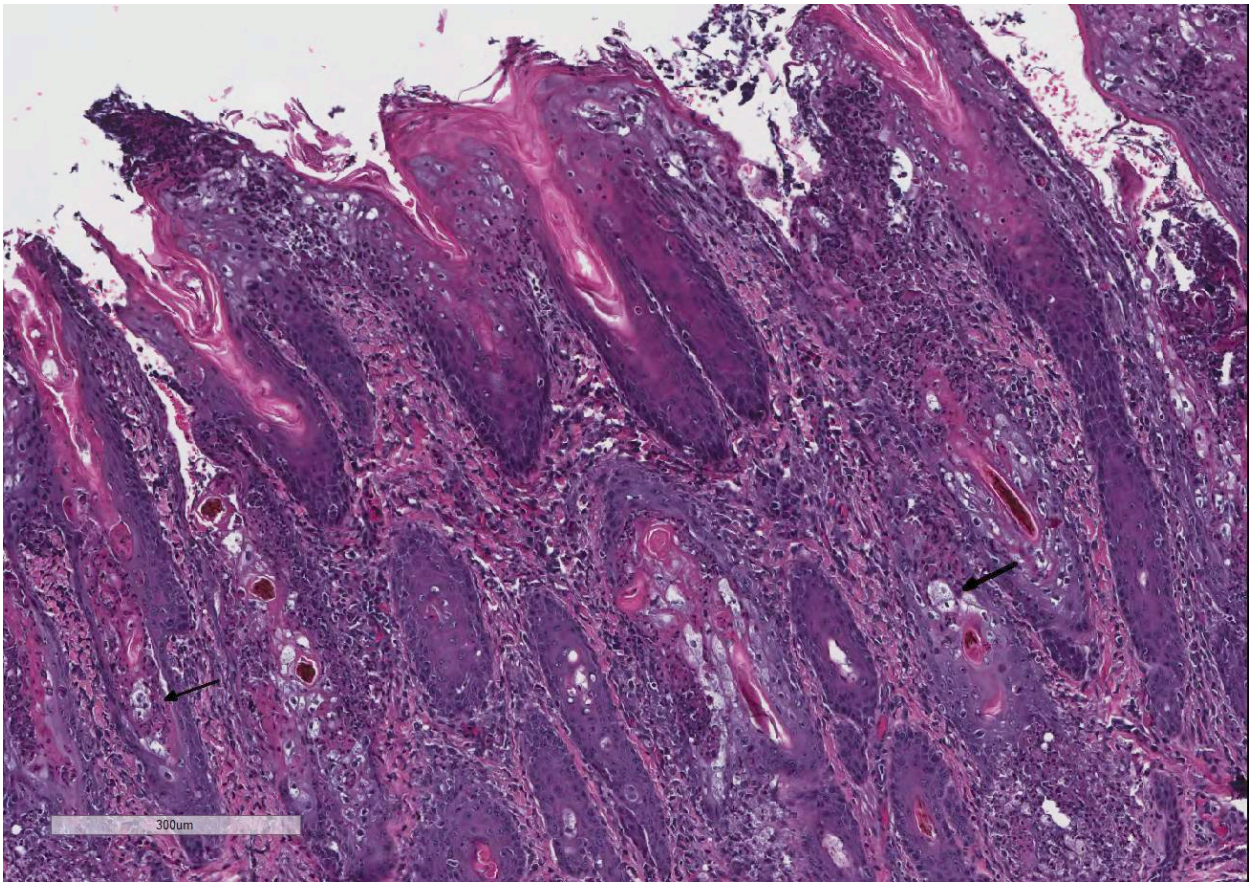

Haired skin, calf. A thick plaque of keratin scale spans several hair follicles, extending deeply within them. There is marked hyperplasia of the stratum basale and spongiosum, and small groups of cells which exhibit hydropic degeneration (arrows). There is multifocal pustule formation in the epidermis, as well as suppurative folliculitis. (HE, 288X).

infection, suppurative folliculitis, and changes compatible with a poxviral dermatitis. This constellation of maladies has not, to the best of the authors' knowledge, yet been described. Autosomal recessive ichthyosis with hypotrichosis syndrome has been described in humans, but not well established in the veterinary literature. The skin of this calf tested negative for bovine viral diarrhea virus by immunohistochemistry and an underlying virus induced immune deficiency was excluded in this case.

There are at least 36 types of ichthyosis described in humans.[14] Ichthyosis in animals has not been well correlated with human forms. However, there are five human ichthyosis correlates described in animals, which include ichthyosis vulgaris, x-linked ichthyosis, epidermolytic hyperkeratosis, lamellar ichthyosis and harlequin ichthyosis.[9]

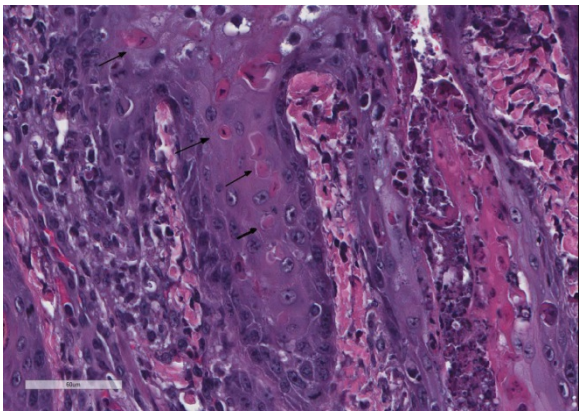

Haired skin, calf. There are numerous apoptotic cells scattered throughout the epidermis and follicular epithelium (arrows)

Ichthyosis is a rare skin condition that has been shown to affect cattle, dogs, pigs, chickens, mice and llamas[9], among others. Two inherited forms of ichthyosis, both through autosomal recessive genes, have been reported in cattle: ichthyosis fetalis and ichthyosis congenita. Ichthyosis fetalis is generally fatal and affected animals usually survive for only a few days after birth. This disease has been described in Norwegian red poll, Friesian, and brown Swiss calves, and this entity most closely resembles human harlequin ichthyosis.[2] Hairless skin is associated with ichthyosis fetalis and is characterized by large, horny, plates separated by deep clefts. Microtia, cataracts, thyroid hypoplasia, and eversion of mucocutaneous junctions are common features of this type of ichthyosis. These manifestations were not apparent in this case.

Ichthyosis congenita, a milder variant of ichthyosis, has been reported in Jerseys, Pinzgauer, Chianina, and Holstein-Friesian breeds.[9] The lesions of ichthyosis congenita are similar to those of ichthyosis fetalis, but less severe and often localized to the skin over the abdomen, inguinal region, joints and the muzzle. Ichthyosis congenita most closely resembles human lamellar ichthyosis. Due to the older age of this calf and clinical presentation, ichthyosis congenita is suspected in this case.

Eight genes have been linked to congenital ichthyosis: TGM1 (in people and Jack Russell terriers, but shown to not be the case in cattle[3]), ABCA12 [1], ABHD5(CG158)[7], 2 lipoxygenases (ALOXE3 and ALOX12B[5]), NIPAL4 (ICTHYIN, Golden retrievers[10]), LIPN[4], CYP4F22[13], and PNPLA-1(American bulldogs[16]). The listed mutations result in disruption of the normal protective barrier that the skin provides while ichthyosis represents the local response to restore that barrier[4]. For example, TGM deficiency results in the abnormal cross-linking of the cornified envelope. Lipoxygenase deficiency in ALOXE3 and ALOX12B mutations are directly associated with abnormal lipid metabolism, impairing the structural integrity of the lipid bilayers. GJB2 mutations affect gap-junction integrity. Accumulation of large amounts of keratin and impairment of the permeability barrier promote the colonization and subsequent infection of skin. The surface *Malassezia* sp. infection, suppurative folliculitis, and poxviral dermatosis likely represent secondary lesions to the ichthyosis.

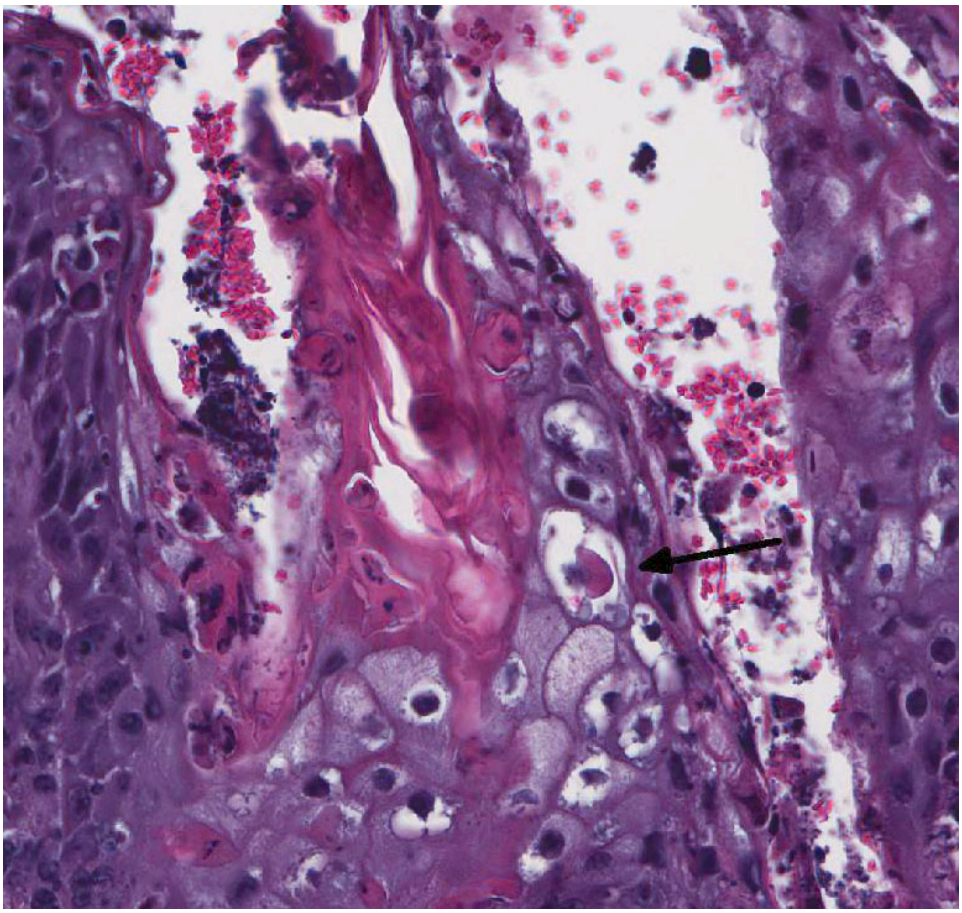

Haired skin, calf. Scattered throughout the proliferative epidermis, there are nests of cells which exhibit ballooning degeneration with large eosinophilic viral inclusions (arrow). (HE, 400X)

Follicular dysplasia or hypotrichosis is not an initial feature of ichthyosis congenita. However, hairlessness was present at birth in this calf, which suggests a primary rather than secondary process. Histologically, the follicular morphology is most consistent with follicular dysplasia. Based on genetic studies, an autosomal recessive component for follicular dysplasia has been described in cattle, such as for Herefords, Polled Herefords, Ayrshires, Guernseys, Jerseys, Holsteins and Black Angus.[8,12,15]

JPC Diagnosis: 1. Haired skin: Epidermal dysplasia, diffuse, severe, with focally extensive epidermal and follicular compact othokeratotic hyperkeratosis, suppurative epidermitis and folliculitis, and marked follicular dysplasia, Pinzgauer-cross, steer, *Bos taurus*. 2. Haired skin: Dermatitis, pustular, proliferative and ulcerative, focally extensive, severe with ballooning degeneration and intracytoplasmic viral inclusion bodies.

Conference Comment: Conference participants unanimously agreed that this is a fascinating case and both a diagnostic and descriptive challenge. The superimposition of the multiple processes in this case made it difficult to identify the etiology of the inflammatory process. In fact, given the degree of inflammation within the proliferative area, most participants did not initially identify poxviral intracytoplasmic inclusion bodies within areas of epidermal ballooning degeneration, confirmed by the contributor's provided transmission electron microscopy image. Readers are encouraged to review 2013 Wednesday Slide Conference 25 Case 3 for a review of poxviruses in various veterinary species.

Participants were struck by the diffusely malformed hair follicles numerous containing shrunken, twisted, coiled, fragmented and densely packed hair shafts consistent with follicular dysplasia.

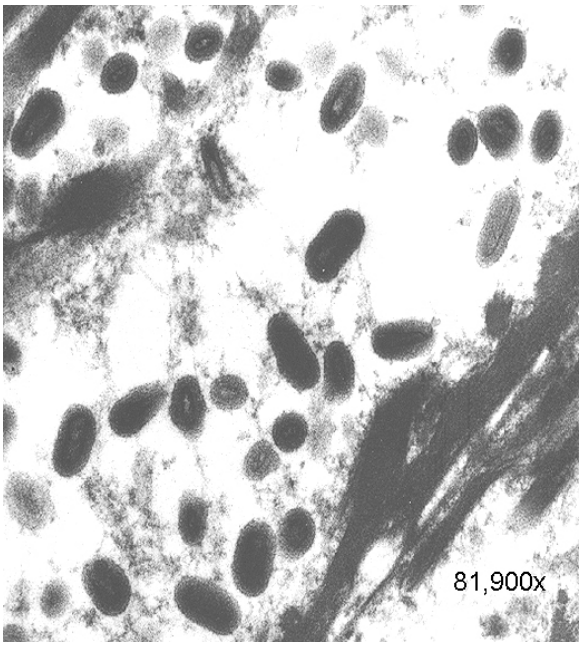

Haired skin, calf. Numerous poxviral particles were identified in the cytoplasm of cells exhibiting ballooning degeneration.

Follicular dysplasia is the congenital abnormality of the morphogenesis of hair follicles leading to changes in the quality and/or quantity of the hair shaft and resulting in hypotrichosis.[8,9,11] Congenital hypotrichosis has been widely reported in all domestic veterinary species, but is most common in calves. Various reported cases of congenital hypotrichosis in cattle have either been associated with an X-chromosome linked ectodermal dysplasia, autosomal dominant, or autosomal recessive hereditary conditions.[9,11] Cattle affected by X-linked ectodermal dysplasia also have concurrent dental disease characterized by incomplete dentition and lack of secondary tooth development and is known as hypotrichosis and anodontia (HAD). In Holsteins, this has been associated with an inherited defect in the ectodysplasin-1 (ED1) gene.[9,11]

Both lethal and viable variants of autosomal recessive and dominant forms of congenital hypotrichosis have been reported with generalized alopecia associated with excessive scaling, infundibular hyper-keratosis, easily broken and misshapen hair shafts, keratinocyte degeneration, and dilated apocrine glands. Other reported findings include subcapsular hepatic fibrosis, anemia, and neurologic deficits.[8,11] Non-genetic causes of hypotrichosis in calves include iodine deficiency, adeno-hypophyseal hypoplasia, maternal ingestion of the toxic plant *Veratrum album*, and intrauterine infection with bovine pestivirus.[9]

Contributing Institution:

Veterinary Diagnostic Laboratory
Oregon State University
134 Magruder Hall
Corvallis, OR 97331
http://vetmed.oregonstate.edu/diagnostic

References:

1. Charlier C, Coppieters W, Rollin F, et al. Highly effective SNP-based association mapping and management of recessive defects in livestock. *Nat Genet*. 2008;40(4):449-454.
2. Chittick EJ, Olivry T, Dalldorf F, Wright J, Dale B a, Wolfe B a. Harlequin ichthyosis in two greater kudu (Tragelaphus strepsiceros). *Vet Pathol*. 2002;39:751-756.
3. Dardano S, Gandolfi B, Parma P, et al. Characterization of bovine TGM1 and exclusion as candidate gene for ichthyosis in Chianina. *J Hered*. 2008;99(1):81-83.
4. Elias PM, Williams ML, Holleran WM, Jiang YJ, Schmuth M. Pathogenesis of permeability barrier abnormalities in the ichthyoses: inherited disorders of lipid metabolism. *J Lipid Res*. 2008;49(4):697-714.
5. Jobard F, Lefèvre C. Lipoxygenase-3 (ALOXE3) and 12 (R)-lipoxygenase (ALOX12B) are mutated in non-

bullous congenital ichthyosiform erythroderma (NCIE) linked to chromosome. *Hum Mol Genet*. 2002;11(1):107-113.
6. Jubb, Kennedy & Palmer's Pathology of Domestic Animals 5th edition
7. Lefèvre C, Jobard F, Caux F, et al. Mutations in CGI-58, the gene encoding a new protein of the esterase/lipase/thioesterase subfamily, in Chanarin-Dorfman syndrome. *Am J Hum Genet*. 2001;69(5):1002-1012.
8. Mansell JL. Follicular dysplasia in two cows. *Vet Dermatol*. 1999;10(2):143-147.
9. Mauldin EA, Peters-Kennedy J. Integumentary system. In: Maxie MG ed. In: *Jubb Kennedy and Palmer's Pathology of Domestic Animals*. Vol 1. 6th ed. Philadelphia, PA: Elsevier Saunders; 2016:530-532, 538-540.
10. Mauldin EA, Wang P, Evans E, et al. Autosomal Recessive Congenital Ichthyosis in American Bulldogs Is Associated With NIPAL4 (ICHTHYIN) Deficiency. *Vet Pathol*. 2015;52(4):654-662.
11. Mecklenburg L. An overview on congenital alopecia in domestic animals. *Vet Dermatol*. 2006;17(6):393-410.
12. Miller WH, Scott DW. Black-hair follicular dysplasia in a Holstein cow. *Cornell Vet*. 1990;80(3):273-277.
13. Ohno Y, Nakamichi S, Ohkuni A, et al. Essential role of the cytochrome P450 CYP4F22 in the production of acylceramide, the key lipid for skin permeability barrier formation. *Proc Natl Acad Sci U S A*. 2015;112(25):7707-7712.
14. Oji V, Tadini G, Akiyama M, et al. Revised nomenclature and classification of inherited ichthyoses: Results of the First Ichthyosis Consensus Conference in Sorèze 2009. *J Am Acad Dermatol*. 2010;63(4):607-641.
15. Scott DW. *Color Atlas of Farm Animal Dermatology*. 1st ed.; 2008.
16. Tamamoto-Mochizuki C, Banovic F, Bizikova P, Laprais A, Linder KE, Olivry T. Autosomal recessive congenital ichthyosis due to PNPLA1 mutation in a golden retriever-poodle cross-bred dog and the effect of topical therapy. *Vet Dermatol*. May 2016.

CASE IV: N9882548 (JPC 4084539).

Signalment: Three-year-old castrated male domestic shorthair cat (*Felis catus*).

History: History of inflammatory bowel disease treated with prednisolone. Presented with lethargy, anorexia, and a change in behavior (less social).

Gross Pathology: Hemoabdomen with multiple splenic masses on abdominal ultrasound and exploratory laparotomy with subsequent splenectomy.

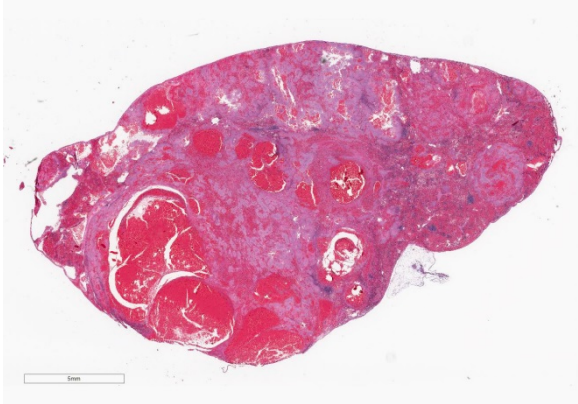

Spleen, cat: The normal splenic architecture is effaced by coalescing nodules of inflammation which alter splenic hemodynamics, often resulted in markedly dilated sinusoids and vessels. (HE, 5X)

On gross evaluation of the spleen, the spleen was enlarged with diffuse nodularity and rounded edges. Expanding the right ventral aspect, there was an approximately 7 x 3.5 x 2.5 cm mass-like swelling. On cut section, the parenchyma was dark red-purple with foci of hemorrhage.

Laboratory results: Moderate regenerative anemia (Hct 18.7%, reticulocyte count 171,000/uL), WBC within reference (8,900/uL), and moderate thrombocytopenia (90,000/uL).

Histopathologic Description: Multifocally throughout the splenic parenchyma, there are large areas of congestion, hemorrhage, necrosis, fibrin deposition and extensive accumulation of extracellular pale basophilic to amphophilic foamy to stippled material composed of 2-4 um diameter round structures each with a thin wall and a central basophilic granular core, consistent with cyst and trophozoite structures. There is a mild to moderate infiltrate composed of macrophages with fewer neutrophils and occasional macrophages contain similar round structures in the cytoplasm. In the intervening congested red pulp, there are numerous hematopoietic precursors including predominantly erythroid and megakaryocytic cells.

Special stain: The cell wall of the round structures is multifocally faintly positive for GMS (Gomori methenamine silver) stain and acid-fast negative.

Contributor's Morphologic Diagnosis: Spleen: Severe multifocal to coalescing congestion, hemorrhage, and necrosis with myriad extracellular and intrahistiocytic cysts and trophozoites, consistent with *Pneumocystis* spp.
Pneumocystis spp. confirmed with immuno-histochemistry, electron microscopy, and PCR testing. Sequencing suggests a novel species/strain.

Contributor's Comment: Given the lack of clinical signs referable to the respiratory tract and the extensive splenic involvement by the infection, the findings are consistent with extrapulmonary pneumocystosis in this case. A small splenic choristoma in the pancreas was also affected and a minor intravascular population of these organisms was identified in the liver at the time of biopsy.

Pneumocystis is a saprophytic organism that has somewhat uncertain taxonomy.

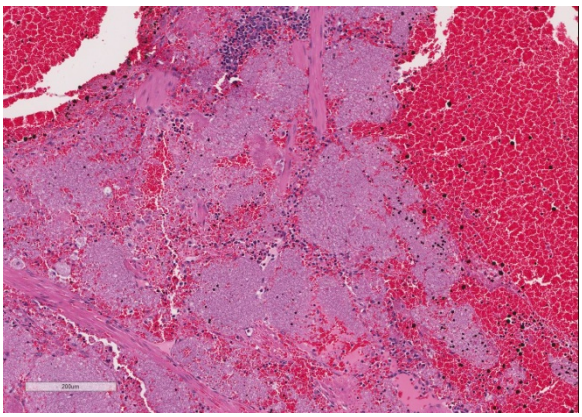

Spleen, cat. The splenic red pulp is markedly expanded by vague nodules of foamy exudate. (HE, 48X)

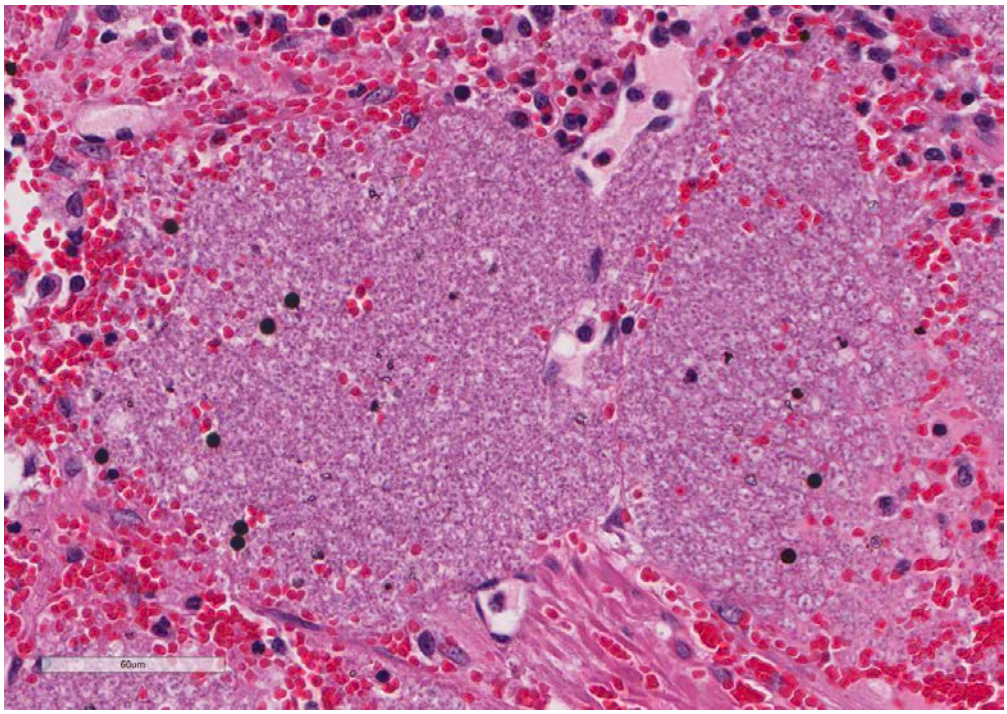

Spleen, cat. The foamy exudate is composed of numerous trophozoites with a central nucleus, consistent Pneumocystis carinii. (HE, 360)

Pneumocystis has been classified as a unicellular protozoan of the phylum *Sarcomastigophora*, subphylum Sarcodina. The reproductive behavior is similar to the ascospore formation of yeast cells and the staining properties resemble that of pathogenic fungi. Based on 16S-like rRNA, *Pneumocystis* is phylogenetically most closely related to the fungi of the class *Ascomycetes*. Multiple species have been designated, although there is some controversy in this area and several strains likely exist. The most widely referenced species are *Pneumocystis carinii* in dogs and *P. jiroveci* in humans, with several species indicated in the laboratory animal literature. The life cycle of *Pneumocystis* involves a tropho-zoite and a cyst form, both of which occur in the infected tissue.[5]

Pneumocystis is best known as an opportunistic organism that most commonly causes pneumonia, in particular in immuno-compromised people and animals. Clinical pneumonia occurs in many cases, but subclinical or latent infections are also common in many animal species, including cats. Clinical disease may occur via new infection or reactivation of a latent infection under conditions of stress, immuno-suppressive therapy, or with other underlying infection, such as canine distemper virus in dogs.[5] In dogs, most reported cases of pneumocystic pneumonia occur in animals with underlying immuno-deficiency, such as miniature Dachshund, Pomeranian and Cavalier King Charles spaniel dogs with combined immunodeficiency syndrome.[2,4] In cats, subclinical or latent infections are most common, and although *Pneumocystis* has been identified in the lungs in the cat, natural cases of clinical disease have not been reported.[5] Under experimental conditions, immunosuppression with glucocorticoid administration has led to pneumocystic pneumonia in cats.[5]

Extrapulmonary infection with *Pneumo-cystis* has been reported in humans, particularly with HIV/AIDS, and involves the spleen in some cases.[1,3] A case of extrapulmonary pneumocystosis has also been reported in a dog.[5] In humans with extrapulmonary infections, some cases have concurrent pneumocystic pneumonia, while

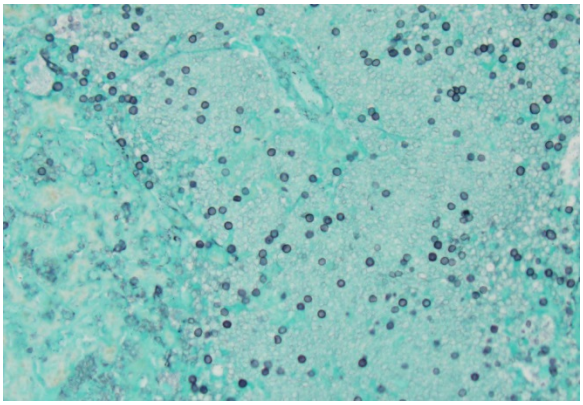

Spleen, cat. The exudate contains numerous argyrophilic viable P. carinii trophozoites. (GMS, 200X)

others do not, and those that do not are thought to either acquire a primary extra-pulmonary infection or have reactivation of a latent infection at extrapulmonary sites.[1] Other than spleen, reported sites for extrapulmonary involvement in humans include lymph node, liver, bone marrow, adrenal gland, gastro-intestinal tract, kidney, thyroid gland, heart, pancreas, central nervous system, bone, eyes or ears.[1,3] In a minority of cases, intravascular organisms are identified in the tissues,[1] which was present in the liver biopsy from this patient.

In pneumocystic pneumonia, the classic histologic appearance is of intra-alveolar aggregates of foamy eosinophilic material with only a minor infiltrate of macrophages and without significant neutrophilic inflammation. GMS staining highlights the 4-7um diameter cyst wall and more easily demonstrates the ovoid, irregular or crescent shape of the cysts. At extrapulmonary sites, *Pneumocystis* has similar tissue destruction with necrosis and a similar appearance of foamy eosinophilic material.[1,3] Methods of confirmation of *Pneumocystis* include cytologic or histologic morphologic appearance and GMS staining characteristics, PCR evaluation, immuno-histochemistry or immunofluorescence.[3,5]

JPC Diagnosis: Spleen: Splenitis, necrotizing and hemorrhagic, diffuse, severe with numerous extracellular and intra-histiocytic trophozoites, domestic shorthair, *Felis catus*.

Conference Comment: We thank the contributor for providing a thorough review of the epidemiology, pathogenesis, and comparative pathology of *Pneumocystis* spp. in humans and veterinary species. This outstanding case provided conference participants the opportunity to describe and identify a relatively common opportunistic pathogen in an extremely rare extra-pulmonary location and an uncommonly affected species. Despite the lack of case reports of feline splenic pneumocystosis in the veterinary literature, many conference participants included *Pneumocystis* sp. on their list of differential diagnoses due to the classic histomorphology, characterized by the presence of abundant extracelluar and intrahistiocytic foamy lightly eosinophilic material and absence of overwhelming inflammation. Although definitive vasculitis and thrombosis are not seen, conference participants also readily identified the

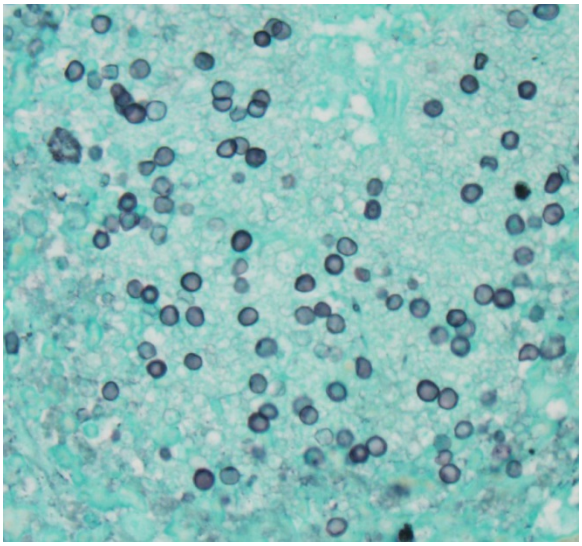

Spleen, cat. Higher magnification of Pneumocystis trophozoites. (GMS, 400X)

numerous brilliant hemodynamic changes present in the tissue section, indicated by severe congestion, marked dilation of sinusoids, and hemorrhage. Multifocal areas of extramedullary hematopoiesis are also identified, although its association with the infectious etiology is unclear.

As mentioned above, extrapulmonary pneumocystosis is rare but has been reported in a dog and immunocompromised people, typically affected with HIV/AIDS.[3,5,6] Postmortem analysis from previously reported human cases indicates that *Pneumocystis* sp. can disseminate throughout the body via hematogenous and/or lymphatic routes. It is thought that the vast majority of cases of extrapulmonary pneumocystosis result from hematogenous or lymphatic spread from the lung. However, in cases where the lungs are unaffected, such as in this cat, there may be reactivation of latent infection in extra-pulmonary organs due to severe immunosuppression.[6]

Contributing Institution:
Animal Medical Center
New York, NY
http://www.amcny.org/

References:

1. Cohen OJ and Stoeckle MY. Extrapulmonary *Pneumocystis carinii* infections in the acquired immunodeficiency syndrome. *Arch Intern Med*. 1991; 151:1205-1214.
2. Kanemoto H, Morikawa R, Chambers JK, et al. Common variable immune deficiency in a Pomeranian with *Pneumocystis carinii* pneumonia. *J Vet Med Sci*. 2015; 77(6):715-719.
3. Karam MB and Mosadegh L. Extra-pulmonary *Pneumocystis jiroveci* infection: A case report. *Braz J Infect Dis*. 2014; 18(6):681-685.
4. Lobetti R. Common variable immunodeficiency in miniature dachshunds affected with *Pneumocystis carinii* pneumonia. *J Vet Diagn Invest*. 2000; 12:39-45.
5. Lobetti R. Pneumocystosis. In: Greene CE, ed. *Infectious Diseases of the Dog and Cat*. 4th ed. St. Louis, MO: Elsevier Inc; 2012:689-695.
6. O'Neal CB, Ball SC. Splenic pneumocystosis: An atypical presentation of extrapulmonary *Pneumocystis* infection. *AIDS Reader*. 2008; 8:503-508.

Self-Assessment - WSC 2016-2017 Conference 13

1. Which of the following *Brucella* species is not infective for the dog?
    a. B. canis
    b. B. melitensis
    c. B. abortus
    d. B. suis

2. Which of the following is not true concerning *Brucella* species?
    a. Rough strains lack O-side chains on lipopolysaccharide.
    b. Both rough and smooth strains express the VirB opeon encoded type IV secretion system.
    c. The VirB operon encoded type IV secretion system allow brucellae to survive within phagosomes by acidification of the phagosome.
    d. Smooth strain LPS is non-endotoxic and allows entry into host cells via cholesterol-rich lipid rafts in the plasma membrane.

3. Which of the following markers would be expected to be negative in a canine oligodendroglioma?
    a. Olig2
    b. GFAP
    c. Doublecortin
    d. CNPase

4. X-linked ectodermal dysplasia in cattle is a combination of hypotrichosis and defects in?
    a. Corneas
    b. Hooves
    c. Horns
    d. Teeth

5. Pneumocystis sp. are most closely related to?
    a. Fungi
    b. Protozoa
    c. Bacteria
    d. Prions

Joint Pathology Center

Veterinary Pathology Services

WEDNESDAY SLIDE CONFERENCE 2016-2017

C o n f e r e n c e 14

11 January 2017

CASE I: HSRL-425 (JPC 4075851).

Signalment: 11-year-old, castrated male, Labrador retriever, (*Canis familiaris*).

History: The patient presented six months prior to euthanasia for evaluation of a cardiac arrhythmia and a several month history of intermittent coughing which had become more severe in the two days before initial presentation. An intermittent split P wave was noted on the ECG. Thoracic radiographs revealed a markedly enlarged heart, right atrial enlargement, enlarged pulmonary vessels, and a diffuse broncho-alveolar pattern. Echocardiography showed a space-occupying mass in the left atrium with mitral and tricuspid valve regurgitation. The patient was discharged with furosemide and returned six months later with exercise intolerance and respiratory distress. At that time due to the patient's declining condition the owner elected euthanasia.

Gross Pathology: A 5 x 6 x 8 cm, firm, multinodular mass is present on the proximocaudal aspect of the heart base, resting on the left atrium. On cross section, the mass is highly vascular and has a mottled red-to-brown mosaic pattern. The mass surrounds the pulmonary arteries, compressing the left pulmonary artery, but it is still patent. The mass is proximal to the pulmonary veins that are not compressed. Tumor invasion into the left atrial lumen is characterized by numerous nodular small projections, up to 0.5 cm, covered by intact endocardium. Left atrial luminal size is decreased due to compression by the mass. Mild endocardiosis of the mitral and tricuspid valves is evident. The right ventricle is distended and dilated in addition to an overall enlarged heart.

The abdomen contains 4 liters of sero-sanguinous clear fluid, with another 2 liters of clear creamy yellowish fluid in the

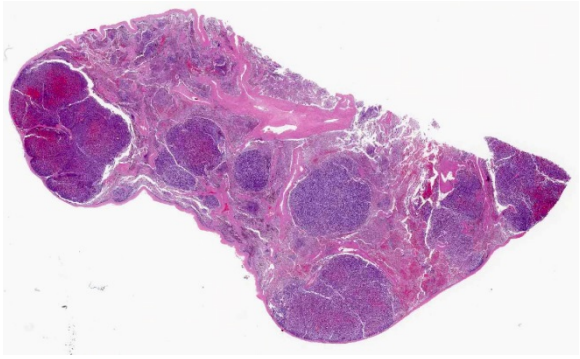

Spleen, dog. The spleen contains numerous well-demarcated neoplastic nodules. (HE, 5X).

thoracic cavity. The spleen has multiple firm white and hemorrhagic masses ranging from 1 mm to 3 cm in size. The consistencies of the splenic masses are similar to the heart mass. The left anterior lung is very pale, soft, and slightly decreased in size due to compression by the left atrial mass. Mediastinal lymph nodes are enlarged with effacement of normal architecture.

Laboratory results: Upon initial presentation, NOVA results are as follows:

- Glucose: 118 mg/dL (60-115)
- Ca++: 1.35 mmol/L (2.2-3.0)
- Mg++: 0.49 mmol/L (1.5-2.5)
- PCO2: 26.1 mmHg (34-40)
- PO2: 49.1 mmHg (85-100)
- SO2: 85.4 % (>90)
- BEecf: -7.3 mmol/L ([0]-[+6])
- nCa: 1.37 mmol/L (1.13-1.33)
- nMg: 0.50 mmol/L (0.26-0.41)

Histopathologic Description: Spleen: There are multiple variably-sized solid nodules effacing and replacing the splenic parenchyma. The neoplastic nodules are well demarcated and expansile. They are composed of large islands of polygonal cells separated by large connective tissue branches and supported by fine fibro-vascular stroma that subdivide the cells in small ribbons. The tumor cells are cuboidal to polyhedral in shape with a round nucleus and a moderate amount of granular lightly amphophilic cytoplasm. The cells are aligned along the small capillaries forming small packets where the cells show polarity with the cytoplasm towards the vessels. Mitotic activity is 11 mitotic figures in 10 hpf. There are areas of marked aniso-karyosis and occasional megalokaryosis (polymorphism) with prominent nucleoli. The large cells show a round eosinophilic prominent nucleolus.

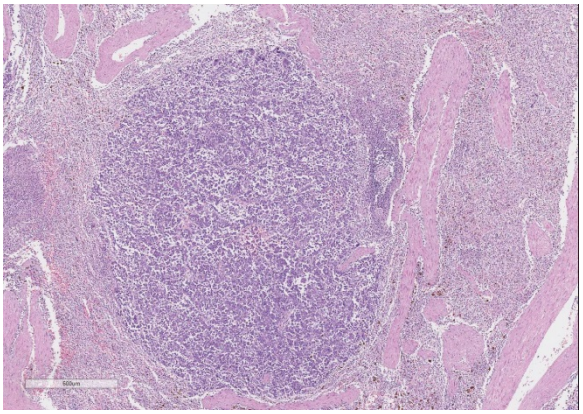

Spleen, dog. Neoplastic nodules are unencapsulated, mildly infiltrative, and neoplastic cells are arranged in nests and packets. (HE, 35X).

The adjacent splenic parenchyma is compressed and attenuated. There are small multiple aggregates of macrophages filled with large granulated golden pigment (hemosiderin- previous hemorrhages). The smooth muscle trabeculae are closer than expected due to collapse of the parenchyma with very few follicles.

Contributor's Morphologic Diagnoses:

1. Heart: Chemodectoma
2. Heart: Mild diffuse mitral and tricuspid valve myxomatous degeneration
3. Spleen: Chemodectoma, metastasis
4. Liver: Chronic severe congestive hepatopathy
5. Lymph Nodes: Chemodectoma, metastasis

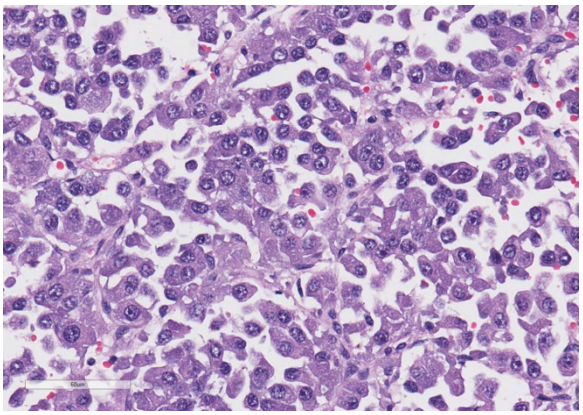

Spleen, dog. Neoplastic cells have granular basophilic cytoplasm with mild variation in nuclear size. (HE, 360X)

Contributor's Comment: Spleen is the only tissue submitted. Chemodectomas are primary neuroendocrine tumors arising most commonly from the chemoreceptor organs of the aortic and carotid bodies.[1,2,4,12] Other chemoreceptors that rarely develop neoplasia include the nodose ganglion of the vagus nerve, ciliary ganglion in the orbit, the pancreas, and the glomus jugulare along the recurrent branch of the glossopharyngeal nerve.[11] They are synonymous with heart base tumors or non-chromaffin, extra-adrenal, paragangliomas in veterinary medicine.[3,4]

Chemodectomas are uncommon neoplasms most often described in canines where they have an incidence of 0.19%.[14] Chemo-dectomas are the second most common cardiac tumor, behind hemangiosarcomas, representing 8% of cardiac tumors.[14] Contrary to humans, aortic body tumors are the more common form of chemodectoma in animals with carotid body tumors being less common and more malignant.[4] In dogs, aortic body tumors are encountered up to four times more frequently than carotid body tumors.[12] The aortic body is located adjacent to the adventitia of the aortic arch at the bifurcation of the subclavian artery while the carotid body is located at the bifurcation of the common carotid artery.[1,4,14] Paren-chymal cells of neuroectodermal origin and sustentacular or stellate cells are the primary cell types that make up the chemoreceptor organs.[4,11] The function of the aortic and carotid bodies is to sense fluctuations in the carbon dioxide, pH, and oxygen tension in blood, which helps to regulate respiration and circulation.[4,7] The aortic and carotid bodies can increase heart rate and elevate arterial blood pressure through the sympathetic nervous system and alter the depth, minute volume, and rate of respiration through the parasympathetic nervous system.[4] The chemoreceptor system is considered part of the parasympathetic nervous system, as it does not secrete catecholamines; however, the presence of secretory granules in the cytoplasm of the glomus cells, the functional cells of chemoreceptors, is inconsistent with this finding.[1,11,12]

Due to the lack of catecholamine production, the tumor's clinical manifestations are the result of being a space-occupying lesion. Smaller adenomas may go undetected, as they can be too small to cause clinical signs, while larger adenomas may press on the atria or displace the trachea and partially surround the major vessels at the base of the heart. Aortic body tumors can also be locally invasive and invade the lumen of the surrounding great vessels or heart chambers hindering blood flow.[4] Common clinical manifestation of aortic body tumors include ascites, pulmonary edema, nutmeg liver, hemothorax, hemopericardium, anasarca, dyspnea, cyanosis, splenomegaly, and arrhythmias.[6,10,12,15] Many of these clinical manifestations are consistent with right-sided congestive heart failure brought on by the tumor acting as a space occupying lesion or by local invasion of vessels resulting in the obstruction of blood flow.[15] Another way aortic body tumors cause lesions is

through metastasis to other parts of the body. It is rare for an aortic body tumor to metastasize, with the most common locations being the lungs and liver.[4] However, other locations have been identified including lymph nodes, myocardium, kidney, adrenal gland, bladder, spleen, and even bone.[4,5,7,12,14] Immunohistochemistry has been valuable to definitively confirm the diagnosis of chemodectomas.[8,12,15]

JPC Diagnosis: Spleen: Neuroendocrine carcinoma, metastatic, Labrador retriever, *Canis familiaris*.

Conference Comment: The contributor provides an excellent summary of the key features of chemodectomas in dogs. As is the tradition at the Joint Pathology Center, conference participants are not provided the full signalment, history, gross necropsy findings, or results of additional histochemical and immunohistochemical stains prior to the conference. Conference participants described nests and packets of neoplastic polygonal cells with small, round, hypochromatic nuclei separated and supported by a delicate fibrovascular stroma, and aptly determined the neoplasm to be of neuroendocrine origin; however, without the additional clinicopathologic information, the site of origin could not be definitively determined from histopathologic evaluation alone. As a result, participants discussed the most likely sites of origin for neuroendocrine chemoreceptor paragangliomas (also known as chemodectomas and glomus tumors) in animals.

Chemoreceptor organs are present in several sites of the body, such as the cartotid body, aortic body, nodose ganglion of the vagus nerve, ciliary ganglion of the orbit, pancreas, jugular vein, middle ear, and glomus jugulare near the glossopharyngeal nerve.[13]

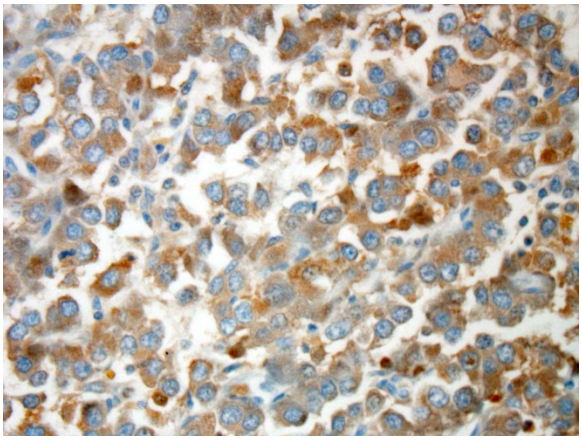

Spleen dog. Neoplastic cells exhibit moderate cytoplasmic immunopositivity for synaptophysin. (anti-synaptophysin, 400X)

As mentioned by the contributor, they are all highly sensitive to changes in blood pH, oxygen tension, and temperature, and can rapidly change respiratory and heart rate via the autonomic nervous system.[13] Metastasis occurs in about 1/3rd of cases of chemodectomas arising from the carotid body, and multicentric neoplastic transformation has been frequently reported in brachiocephalic dogs, possibly because of breed-associated anatomic malformations in the upper respiratory tract resulting in chronic hypoxia.[13]

Neoplastic cells in neuroendocrine tumors contain variable numbers of cytoplasmic secretory granules, best visualized by electron microscopy. Additionally, the number of granules is used to distinguish adenomas, which contain more numerous granules, from carcinomas. In addition, neoplastic cells typically will be immunopositive for chromogranin-A, neuron-specific enolase (NSE), synaptophysin, and S100 protein. Prior to the conference, the JPC performed tissue immunohistochemistry for chromogranin-A, NSE, and synaptophysin. Unfortunately neoplastic cells were immunonegative for all three stains; however, participants speculated the results may be due to suboptimal tissue fixation.[13]

Contributing Institution:
Western University of Health Sciences
College of Veterinary Medicine
Pomona, California 91766
http://www.westernu.edu/veterinary/

References:

1. Aupperle H, März I, Ellenberger C, Buschatz S, et al. Primary and secondary heart tumours in dogs and cats. *J Comp Pathol.* 2007; 136:18-26.
2. Brown PJ, Rema A, Gartner F. Immunohistochemical characteristics of canine aortic and carotid body tumours. *J Vet Med A Physiol Pathol Clin Med*. 2003;50:140-144.
3. Balaguer L, Romano J, Neito JM, Vidal S, Alverez C. Incidental finding of a chemodectoma in a dog: Differential diagnosis. *J Vet Diagn* Invest. 1990; 2:339-341.
4. Capen CC: Endocrine glands. *In*: Maxie MG, ed. *Jubb, Kennedy, and Palmer's Pathology of Domestic Animals*. 5th ed. Vol 3. St. Louis, MO: Elsevier; 2007:425-428.
5. Eriksson, Malin. "Aortic Body Tumors in Dogs." (2011). http://stud.epsilon.slu.se/2545/1/Eriksson_m_110502.pdf
6. Ehrhart N, Ehrhart, EJ, Willis J, Sisson D, Constable P, Greenfield C, Manfra-Maretta S, Hintermeister J. Analysis of factors affecting survival in dogs with aortic body tumors. *Vet Surg*. 2007; 31(1):44-48.
7. Johnson KH. Aortic body tumors in dogs. *J Am Vet Med Assoc*. 1968; 152(2):154.
8. Khodakaram-Tafti A, Shirian S, Shekarforoush SS, Fariman H, Daneshbod Y. Aortic body chemodectoma in a cow: Clinical, morphopathological, and immunohistochemical study. *Comp Clin Pathol*. 2011;20(6):677-679.
9. McManus BM, Allard MF, Yanagawa R. Hemodynamic disorders. In: *Rubin's Pathology: Clinicopathologic Foundations of Medicine*. ed. Rubin R, Strayer DS. 5th ed. Philadelphia, PA: Wolters-Kluwer; 2008:231-232.
10. Noszczyk-Nowak, Agnieszka, Nowak M, Paslawska U, Atamaniuk W, Nicpon J. Cases with manifestation of chemodectoma diagnosed in dogs in Department of Internal diseases with Horses, Dogs and Cats Clinic, veterinary medicine faculty, University of Environmental and Life Sciences, Wroclaw, Poland." *Acta Veterinaria Scandinavica*. 2010; 52:35.
11. Owen TJ, Bruyette DS, Layton CE. Chemodectoma in dogs. *Comp Cont Educ Pract*. 1996;18:253–265.
12. Paltrinieri S, Riccaboni P, Rondena M, Giudice C. Pathologic and immunohistochemical findings in a feline aortic body tumor. *Vet* Pathol. 2004; 41:195-198.
13. Rosol TJ, Grone A. Endocrine glands. In: Maxie MG, ed. *Jubb, Kennedy, and Palmer's Pathology of Domestic Animals*. 6th ed. Vol 3. St. Louis, MO: Elsevier; 2016:354-357.
14. Ware WA, Hopper DL. Cardiac tumors in dogs: 1982–1995. *J Vet Intern* Med. 1995; 13: 95-103.
15. Willis R, Williams AE, Schwarz T, Paterson C, Wotton PR. Aortic body chemodectoma causing pulmonary oedema in a cat. J *Small Anim Pract*. 2001; 42:20-23.

CASE II: 1529704 (JPC 4083862).

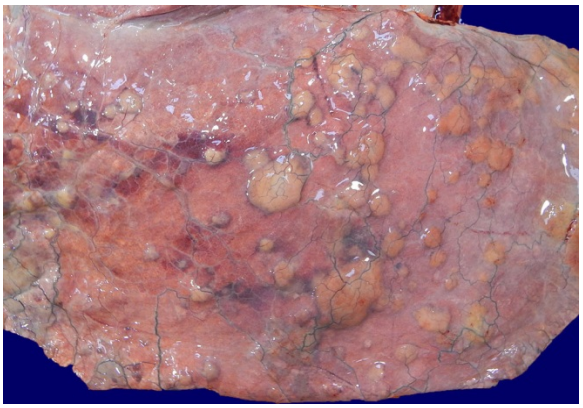

Lung, horse. Numerous 0.5-5cm tan nodules elevate the pleura in all lung fields. (Photo courtesy of: University of Pennsylvania School of Veterinary Medicine, Department of Pathobiology, 4005 MJR-VHUP, 3900 Delancey Street, Philadelphia, PA 19104 http://www.vet.upenn.edu/research/academic-departments/pathobiology)

Signalment: 14-year-old, thoroughbred, gelding, horse, (*Equus caballus*).

History: The patient was admitted for evaluation of chronic colic, and had a distended abdomen on arrival. The horse was diagnosed with uroperitoneum and was euthanized after a tear in the ventral portion of the urinary bladder was confirmed on abdominal ultrasound and cystoscopy. Clinical signs of disease involving other organ systems (*e.g*. respiratory tract) were not reported.

Gross Pathology: The patient was in satisfactory nutritional and good postmortem condition. The peritoneum contained abundant turbid, light-yellow fluid with a distinct ammonia odor *(i.e*. urine), and was hyperemic with adherent plaques of fibrin. The urinary bladder was distended and a 7 x 5 cm thin, gray-green and friable (necrotic) focus within the ventral wall was confirmed. However, examination of the lungs revealed multifocal to coalescing 0.5- 5 cm diameter firm tan nodules that extended into all fields, replacing the pulmonary parenchyma and elevating the visceral pleura (figure 1). Intervening pulmonary parenchyma was pale pink to dark red and mildly firm cranioventrally. The brain, spinal cord, and remainder of the thoracic and abdominal viscera were grossly unremarkable.

Laboratory results: None

Histopathologic Description: Approximately 80% of the pulmonary parenchyma was effaced by multifocal to coalescing nodules composed of proliferating spindle cells (fibroblasts) embedded within a fibrillar eosinophilic (collagenous) stroma, and infiltrated by large numbers of lymphocytes and histiocytes, with fewer neutrophils. Occasionally, alveolar macrophages contained 3-4µm diameter eosinophilic intranuclear inclusion bodies that peripheralized the chromatin (Cowdry Type A inclusions; figure 2 (arrow)). Within affected regions, the majority of alveoli were lined by plump cuboidal epithelial cells (bronchiolization). Affected alveoli, and occasional bronchi and bronchioles, were filled with numerous foamy macrophages, neutrophils, and cell debris. Within

Lung, horse. The submitted section contains several well demarcated nodules which efface the pulmonary parenchyma. (HE, 5X)

unaffected regions of lung, alveoli were often ectatic (hyperinflated), and there was mild multifocal alveolar hemorrhage.

Contributor's Morphologic Diagnoses: Lung: severe chronic multifocal–coalescing sclerosing lymphohistiocytic and neutrophilic bronchointerstitial pneumonia with intrahistiocytic intranuclear inclusion bodies (consistent with equine multinodular pulmonary fibrosis).

Contributor's Comment: Equine multinodular pulmonary fibrosis (EMPF), one of the relatively few differentials for interstitial lung disease in the horse, results in a unique gross and histologic appearance dominated by a nodular pattern of marked interstitial fibrosis.[10] Clinical signs of affected horses may include tachypnea, dyspnea, nasal discharge, coughing, lethargy, inappetence, and poor body condition. Affected horses may have increased bronchovesicular sounds, fever, and/or hypoxemia on clinical exam.[14] Hematology typically reveals a neutrophilia (in some cases with increased bands), lymphopenia or lymphocytosis, and monocytosis.[7,14] A nodular interstitial pattern is often identified on thoracic radiographs and ultrasound, resulting in differential diagnoses of EMPF, fungal pneumonia and pulmonary neoplasia.

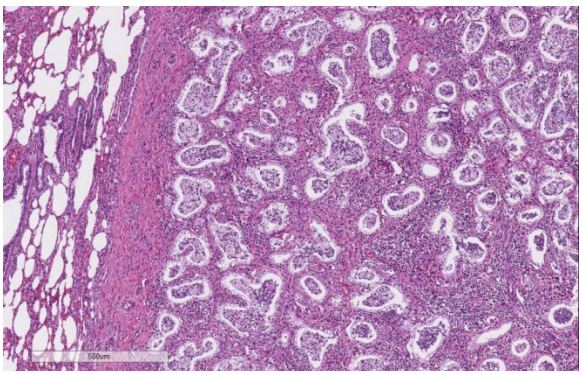

Lung, horse. The nodules are composed of alveolar spaces which are scatted through dense areas of fibrosis and a cellular infiltrate. Each nodule is surrounded by a thick fibrous capsule and compresses the adjacent parenchyma. (HE, 49X)

Concurrent with the interstitial pulmonary disease, thoracic ultrasonography may also reveal pulmonary artery dilation, consistent with pulmonary hypertension. Transtracheal wash fluid is predominantly neutrophilic (degenerate or non-degenerate), with fewer macrophages.[14] No breed or sex predilection has been established, and although affected horses are typically middle-aged or geriatric, cases have been reported in horses as young as four years-old.[12]

Two gross patterns of EMPF have been described, both of which are characterized by multifocal moderately firm, tan, bulging nodules throughout the pulmonary parenchyma. In the more common of the two gross forms (the form exhibited by this horse), these nodules are numerous but small (up to 5 cm in diameter), and coalesce, often resulting in scant intervening parenchyma. In the second gross pattern, the nodules are less frequent, larger (up to 10 cm in diameter), and discrete, with the intervening pulmonary parenchyma largely unaffected.[12] Histologically, both gross forms are characterized by extensive interstitial deposition of mature collagen, accompanied by moderate mixed inflammatory infiltrates, consisting predominantly of lymphocytes, macrophages and neutrophils. Alveoli in affected regions are typically lined by plump, cuboidal epithelium, and airways contain abundant neutrophils and macrophages. Alveolar macrophages occasionally contain amphophilic to eosinophilic intranuclear inclusion bodies. Less frequently, the nodules consist of dense sheets of disorganized collagen that completely efface the normal alveolar pattern.[12]

Equine herpesvirus-5 (EHV-5) is a gamma herpesvirus strongly associated with EMPF, and can be identified by polymerase chain reaction (PCR), immunohistochemistry

(IHC), in situ hybridization, virus isolation, and transmission electron microscopy (TEM).[2,7,12-14] Although causality has not been proven by meeting all of Koch's postulates, the main histologic and immunohistochemical features have been recapitulated in horses inoculated with EHV-5 isolated from EMPF-affected horses.[13] However, because inoculated horses lacked clinical signs associated with EMPF, were PCR-negative for the inoculated EHV-5 viruses (within the lungs), and the virus was unable to be re-isolated, the authors suggest that the immuno-histochemical detection of virus in the inoculated horses having deposition of fibrous connective tissue likely represented a pre-clinical, yet latent, phase of viral infection.[13] Further supporting EHV-5 as an important etiologic factor in the development of EMPF, quantitative real-time PCR performed in an affected horse revealed higher viral load within the lungs than in other tissues, with the highest load within the most severely affected/fibrotic regions of lung.[4] In addition, gamma herpesviruses have been associated with fibrotic lung diseases in other species, including a variably fibrotic broncho-interstitial pneumonia with syncytial cell formation in donkeys associated with asinine herpesvirus-4 and 5 (AHV-4 and 5),[3] and human idiopathic pulmonary fibrosis associated with human herpesvirus-8 (HHV-8) and Epstein-Barr virus.[10,11] Moreover, mice that are knockouts for the IFNγ cytokine receptor (an important mediator of the Th1 antiviral response), develop progressive pulmonary interstitial fibrosis after chronic infection with murine gamma herpesvirus-68.[5,11] Although the precise mechanisms of gamma herpesvirus-induced fibrosis and immune system evasion in most species are unknown, they are likely related to the specific viral-induced cytokine, chemokine, and/or receptor profile within

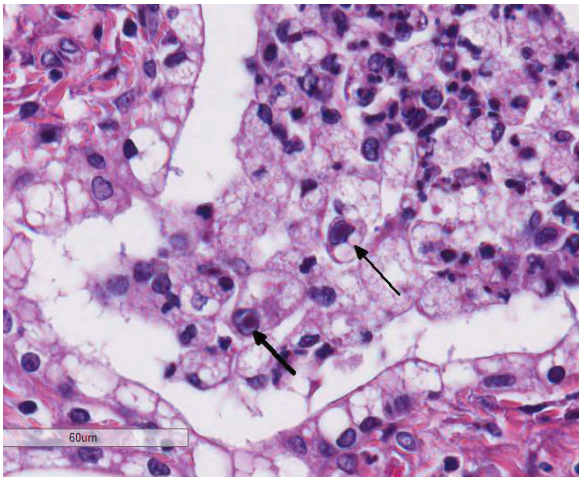

Lung, horse. Remaining alveolar spaces are lined by cuboidal Type II pneumocytes with vacuolated cytoplasm and contain a mixed histiocytic and neutrophilic exudate. Alveolar macrophages occasionally contain a 3-6um eosinophilic intranuclear viral inclusion surrounded by a clear halo. (HE, 400X)

the host, which either directs the immune system toward a Th2 response (thereby inhibiting a Th1 response and facilitating fibrosis), or at least prevents an effective Th1 antiviral response.[6,11] Such mechanisms have already been established in the study of human gamma herpesviruses, including viral CCL-1 (vCCL-1), vCCL-2, and vCCL-3 encoded by HHV-8 that activate Th2 cell chemokine receptors (CCR8, CCR3 and CCR8, and CCR4, respectively), and a viral IL-10 homologue produced by human Epstein-Barr virus that results in inhibition of the Th1 antiviral response.[6,11] In spite of supporting evidence of EHV-5 infection inciting EMPF, EHV-5 may not be the sole cause. As with many infectious diseases, concurrent viral infections (such as EHV-2 and AHV-4 or 5), and the host's immune status, may also be important contributors to the pathogenesis of EMPF.[1,5,11,12]

Although successful treatment with corticosteroid and antiviral (acyclovir) therapy is reported, overall, response to

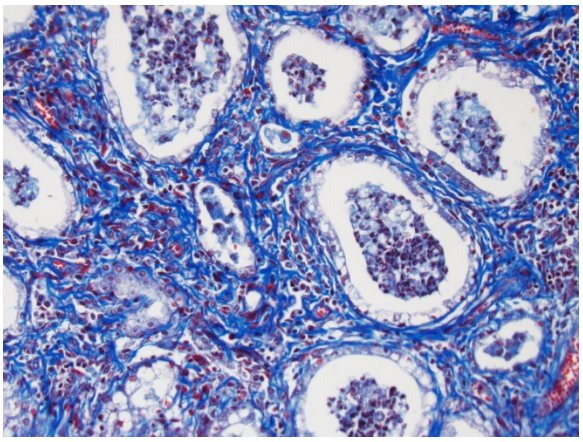

Lung, horse. A Masson's trichrome demonstrates the profound fibrosis which characterizes this lesion. (Masson's, 200X).

treatment is variable and the prognosis of this disease is generally considered poor.[14] This case was unusual in that there were no reported clinical signs that were clearly attributable to respiratory disease. However, a preclinical, latent phase of infection is considered unlikely given the presence of numerous inclusion bodies. Although the uroperitoneum accounted for the most recent episode of colic, it is possible that the pneumonia caused chronic lethargy and inappetence, vague signs that were interpreted as chronic colic. Regional transmural necrosis of the urinary bladder was confirmed histologically, and was attributed to pressure-induced ischemia secondary to distension. As there was no evidence of urethral obstruction, a neurogenic cause was suspected. However, no histologic lesions were identified within the spinal cord.

JPC Diagnosis: Lung: Fibrosis, interstitial, nodular, multifocal to coalescing, severe with lymphohistiocytic interstitial inflammation, alveolar neutrophilic and histiocytic exudate, type II pneumocyte hyperplasia and histiocytic intranuclear viral inclusion bodies, thoroughbred, *Equus caballus*.

Conference Comment: We thank the contributor for both an excellent example and thorough summary of equine multinodular pulmonary fibrosis (EMPF) in horses. This entity has also been extensively reviewed in previous Wednesday Slide Conferences (2011 Conference 1 Case 2, 2012 Conference 24 Case 3, 2013 Conference 18 Case 1), but it was chosen again because of its highly distinctive and unique histomorphology. Participants identified multifocal discrete lung nodules with abundant interstitial fibrosis, marked type II pneumocyte hyperplasia, and irregular alveolus-like spaces filled with an inflammatory exudate composed of neutrophils, fibrin, and alveolar macrophages which occasionally contain a 2-4 um magenta intranuclear inclusion body. Conference participants also noted especially prominent pleural arteries in areas adjacent to the nodules of fibrosis with hypertrophic smooth muscle in the tunica media indicative of pulmonary hypertension associated with pulmonary fibrosis.

As mentioned by the contributor, gamma herpesviruses have been associated with progressive pulmonary fibrotic disorders in humans, donkeys, horses, and rodents. In dogs, canine idiopathic pulmonary fibrosis is a progressive pulmonary fibrotic disorder predominantly in aged West Highland white terriers (WHWT).[9] Recently, investigators have tried to elucidate a relation between this disorder in WHWTs and gamma-herpesvirus infection; however, no evidence a connection was found. Given this condition's predilection for WHWT, it is thought that there is a genetic component to this disease in this breed of dog rather than an infectious etiology.[9]

In addition to pulmonary fibrosis, conference participants discussed the

association of a gamma herpesvirus with retroperitoneal fibromatosis (RF), an aggressive proliferation of highly vascular fibrous tissue subjacent to the peritoneum involving the ileocecal junction and mesenteric lymph nodes in rhesus macaques.[10] RF is associated with co-infection of simian retrovirus 2 (SIV) causing simian acquired immunodeficiency syndrome (SAIDS) and RF-associated herpesvirus (RFHV). This condition is closely related to Kaposi's sarcoma in humans, caused by co-infection of human herpesvirus 8 (HHV8) and human immuno-deficiency virus (HIV), and is one of the first illnesses associated with the development of AIDS.[10] Additionally, rhesus macaque rhadinovirus, another gammaherpesvirus, is also closely related to HHV8 and both have been associated with the development of B-cell lymphoma.[8]

Contributing Institution:

University of Pennsylvania School of Veterinary Medicine
Department of Pathobiology
Philadelphia, PA 19104
http://www.vet.upenn.edu/research/academic-departments/pathobiology

References:

1. Back H, Kendall A, Grandón R, et al. Equine multinodular pulmonary fibrosis in association with asinine herpesvirus type 5 and equine herpesvirus type 5: a case report. *Acta Vet Scand.* 2012;54(57):1-5.
2. Caswell JL, Williams KJ: Equine multinodular pulmonary fibrosis. In: Maxie MG ed. *Jubb, Kennedy, and Palmer's pathology of domestic animals.* Vol 2. 6th ed. St. Louis, Missouri: Elsevier; 2016:568-569.
3. Kleiboeker SB, Schommer SK, Johnson PJ, et al. Association of two newly recognized herpesviruses with interstitial pneumonia in donkeys (*Equus asinus)*. *J Vet Diagn Invest.* 2002;14:273-280.
4. Marenzoni ML, Passamonti F, Lepri E, et al. Quantification of *Equid herpesvirus 5* DNA in clinical and necropsy specimens collected from a horse with equine multinodular pulmonary fibrosis. *J Vet Diagn Invest.* 2011;23(4):802-806.
5. Mora AL, Woods CR, Garcia A, et al. Lung infection with γ-herpesvirus induces progressive pulmonary fibrosis in Th2-biased mice. *Am J Physiol Lung Cell Mol Physiol*. 2005;289:L711-L721.
6. Nicholas J. Human gamma-herpesvirus cytokines and chemokine receptors. *J Interf Cytok Res*. 2005;25:373-383.
7. Niedermaier G, Poth T, Gehlen H. Clinical aspects of multinodular pulmonary fibrosis in two warmblood horses. *Vet Rec.* 2010;166:426-430.
8. Orzechowska BU, Powers MF, et al. Rhesus macaque rhadinovirus-associated non-Hodgkin lymphoma: Animal model for KSHV associated malignancies. *Blood*. 2008; 112:4227-4234.
9. Roels E, Dourcy M, et al. No evidence of herpesvirus infection in West Highland white terriers with canine idiopathic pulmonary fibrosis. *Vet Pathol*. 2016; 53(6):1210-1212.
10. Rose TM, Strand KB, et al. Identification of two homologs of the Kaposi's sarcoma-associated herpesvirus (human herpesvirus 8) in retroperitoneal fibromatosis in different macaque species. *J Virol*. 1997; 71:4138-4144.
11. Tang Y, Johnson JE, Browning PJ, et al. Herpesvirus DNA is consistently detected in lungs of patients with

idiopathic pulmonary fibrosis. *J Clin Microbiol*. 2003;41(6):2633-2640.
12. Williams KJ. Gammaherpesviruses and pulmonary fibrosis: evidence from humans, horses and rodents. *Vet Pathol*. 2014;51(2):372-384.
13. Williams KJ, Maes R, Del Piero F, et al. Equine multinodular pulmonary fibrosis: a newly recognized herpesvirus-associated fibrotic lung disease. *Vet Pathol*. 2007;44:849-862.
14. Williams KJ, Robinson NE, Lim A, et al. Experimental induction of pulmonary fibrosis in horses with gammaherpesvirus Equine Herpesvirus 5. *PLoS ONE*. 2013;8(10):e77754, doi. 10.1371/journal.pone.0077754.
15. Wong DM, Belgrave RL, Williams KJ, et al. Multinodular pulmonary fibrosis in five horses. *J Am Vet Med Assoc*. 2008;232(6):898-905.

CASE III: CAN2 (JPC 4084949).

Signalment: Nine-year-old, female, golden retriever, (*Canis familiaris*).

History: The dog was brought to the clinic with a history of intermittent rectal prolapse. Clinical examination revealed a rectal mass (5 cm cranial from the anus), and the dog was referred to the surgical excision of the mass.

Gross Pathology: Rectal mass: an oval 3x5 cm mass, on cross section light brown in color and firm consistency.

Laboratory results: Immunohisto-chemistry – antibodies against CD 3, CD79 and MUM1 were applied. The tumor was CD79 and MUM1 positive, and CD3 negative. Congo red stain revealed amyloid deposits at the periphery of the tumor.

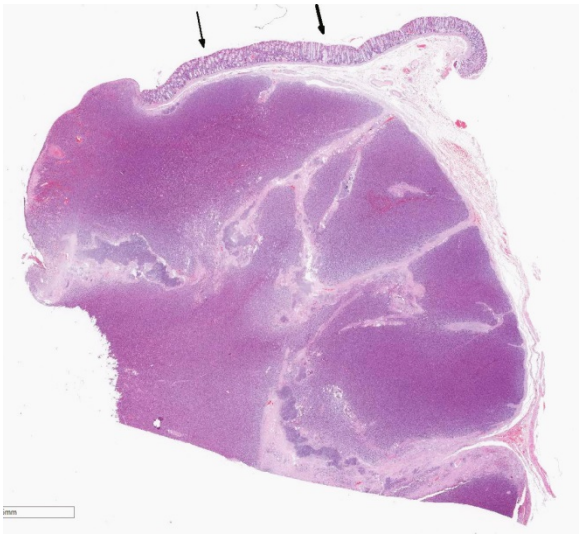

Rectum, dog. Within the wall of the rectum, there is a well-demarcated infiltrative mass that transmurally effaces the colonic wall. The overlying intact mucosa is delineated by arrows. (HE, 4X)

Histopathologic Description: Rectum: Expanding the submucosa and elevating the overlying ulcerated mucosa is a well circumscribed, partially encapsulated, densely cellular neoplasm composed of sheets and packets of round cells separated by a fine fibrous stroma. Neoplastic cells have variably distinct cell borders and moderate amounts of eosinophilic granular cytoplasm. Nuclei are round, rarely oval, usually eccentrically located with finely stippled to finely clumped chromatin and usually one indistinct nucleolus. There is moderate anisokaryosis, multifocal karyo-megaly and a moderate number of multinucleate cells. Mitotic figures average 10 per 10 HPF. Multifocally between neoplastic cells or at the periphery of the tumor are variably sized and shaped, extracellular deposits of amorphous, homogenous, eosinophilic material (amyloid) with multifocal islands of cartilage formation (cartilaginous metaplasia) that is occasionally mineralized.

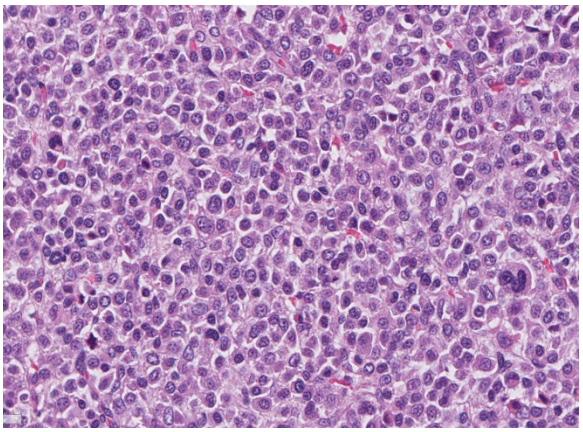

Rectum, dog. Neoplastic cells are round and arranged in poorly-defined nests and packets. Neoplastic cells have eccentric, occasionally helmet-shaped nuclei, are occasionally multinucleate, and exhibit moderate anisocytosis and anisokaryosis. (HE, 400X) (Photo courtesy of: Department of Veterinary Pathology, Faculty of Veterinary Medicine, University of Zagreb, Heinzelova 55, 10000 Zagreb, Croatia. http://www.vef.unizg.hr/)

Contributor's Morphologic Diagnoses: Rectum: Plasmacytoma (or Extramedullary Plasmacytoma), golden retriever, canine.

Contributor's Comment: Extramedullary plasmacytoma (EMP) is a relatively common tumor in older dogs and occur most frequently on the skin and mucous membranes, but has been reported in other areas such as the brainstem, spinal cord, lymph nodes, abdominal viscera, genitalia, and eyes.[2,9]

Plasmacytomas of the lower gastrointestinal tract are uncommon neoplasms in dogs, and rare in cats and other species. They are encountered most frequently in the submucosa of the distal colon and rectum of dogs, where they are associated with signs of large bowel diarrhea and bleeding[5]. Gastrointestinal EMP has also been reported in other sites, including the esophagus, stomach and small intestine.[10]

Histologically they resemble plasmacytomas of the skin, oral cavity or larynx. The tumor is formed by solid packets of pleomorphic round cells with various degrees of plasmacytoid maturation, especially at the periphery of the tumor. There is a frequent nuclear hyperchromasia and convolution. The cells are typically arranged in solid endocrine-like packets and there may be AL amyloid deposition among the tumor cells. The majority of the tumor growth is submucosal. A small proportion exhibit more aggressive behavior, including invasion of tunica muscularis, and some spread to regional lymph nodes and spleen.[9] Canine EMP histological typing system has been established and is helpful diagnostic tool, although the types cannot be used for a tumor grading system.[4]

An unusual finding in plasmacytomas is the presence of cartilage and bone in close association with amyloid deposits. Meta-plastic bone and cartilage have been described in two canine intestinal EMPs[5] and in human amyloidosis of tongue[11] and myelomas.[1] The exact pathogenesis of chondroid metaplasia in amyloidosis is not clearly described. Ramos Vara and colleagues hypothesized that in amyloidosis the inducing stimulus for bone formation is

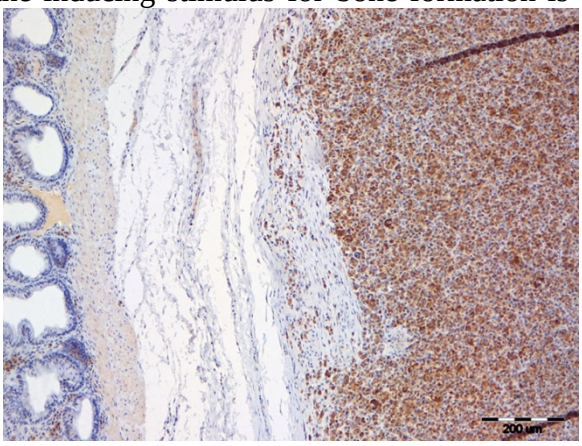

Rectum, dog. Neoplastic cells display strong membranous immunopositivity for CD-79. (anti-CD79, 100X)

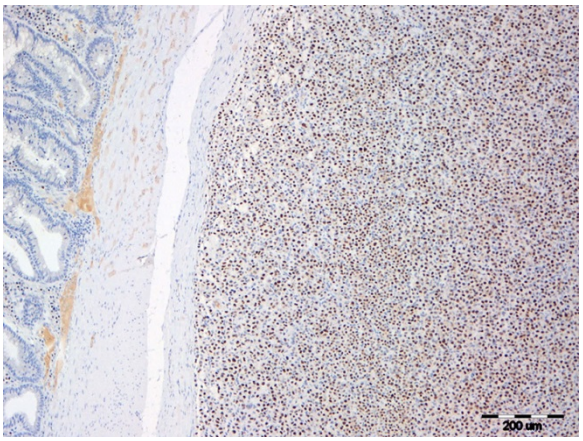

Rectum, dog. Neoplastic cells display strong nuclear immunopositivity for MUM-1. (anti-MUM1, 100X)

the amyloid deposits, with resultant stimulation of mesenchymal precursor cells to differentiate into cartilage- and bone-forming cells under the influence of soluble factors liberated by histiocytic and other cells.[5]

JPC Diagnosis: Colon: Plasmacytoma, extramedullary, golden retriever, *Canis familiaris*.

Conference Comment: The contributor provides a great example of a relatively common neoplasm in the skin or mucus membrane of dogs in an uncommon location within the abdominal viscera. Extra-medullary plasmacytomas of the lower gastrointestinal tract have been reported in dogs to occur most frequently in the submucosa of the distal colon and rectum, as in this case, and are considered a benign neoplastic proliferation of monoclonal B cells.[9] Rectal and colonic plasmacytomas represent only 4% of all extramedullary plasmacytomas in dogs.[6] Despite the uncommon location, conference participants identified solid packets of pleomorphic plasmacytoid round cells with a perinuclear clearing (Golgi complex) admixed with abundant homogenous smudgy material recognized as amyloid, commonly deposited in plasma cell tumors. The contributor confirmed the presence of amyloid via Congo-red staining and apple-green birefringence with polarized light. The conference moderator also pointed out the distinctive clumping pattern of the hetero-chromatin, giving the neoplastic cells the classic "clock face" histomorphology of plasma cells.[9]

The most striking feature of this case is the prominent streaks of amyloid within and surrounding the neoplasm, often admixed with foci of chondroid metaplasia. Amyloid is a proteinaceous substance composed of polypeptides arranged in beta-pleated sheets and is deposited in tissues in response to a number of pathogenic processes. Primary systemic or immunoglobulin associated amyloid (AL) is associated with light chains derived from plasma cells in monoclonal B cell proliferations of extramedullary plasmacytomas or multiple myelomas. The light chains are then converted to amyloid fibrils by proteolytic enzymes in macro-phages and deposited within tissues.[8] As mentioned by the contributor, chondroid metaplasia has been uncommonly reported to occur with amyloidosis secondary to a

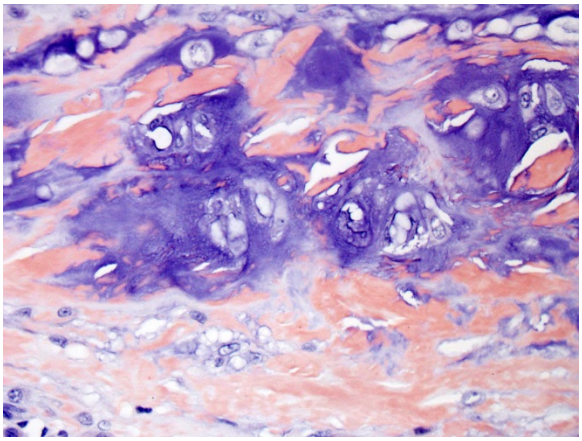

Rectum, dog. Scattered through the neoplasm are aggregates of congophilic amyloid protein which contain numerous well-differentiated chondrocytes encased in a bluish cartilaginous matrix. (Congo Red, 400X)

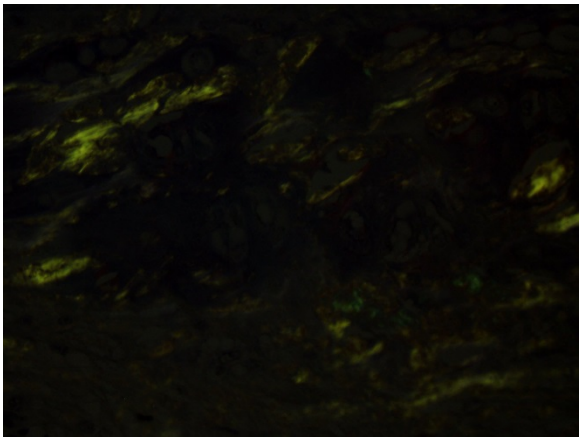

Rectum, dog. Lakes of amyloid exhibit distinct apple-green birefringence when illuminated with polarized light. (Congo Red, 400X).

variety of conditions, although the exact pathogenesis is currently unknown.[3,11]

Another type of amyloid is formed secondary to a variety of chronic inflammatory conditions inciting excessive release of serum amyloid associated (AA) acute phase protein, predominantly by the liver under the influence of interleukin-6 (IL-6) and IL-1. AA is then deposited in multiple organs including the spleen, pancreas, intestinal lamina propria, lymph nodes, kidneys and liver.[7,8,9] Amyloid-beta (AB) has been found in cerebral plaques of aging humans and rhesus macaques and is associated with Alzheimer's disease. Interestingly, neurofibrillary tangles, another feature of Alzheimer's disease in humans, have not been found in aging rhesus macaques.[7]

Contributing Institution:

Department of Veterinary Pathology
Faculty of Veterinary Medicine
University of Zagreb
10000 Zagreb
Croatia.
http://www.vef.unizg.hr/

References:

1. Karasick DV, Schweitzer ME, Miettinen M, O'Hara BJ. Osseous metaplasia associated with amyloid-producing plasmacytoma of bone: A report of two cases. Skeletal Radiol. 1996; 25:263–267.
2. Jacobs JM, Messick JB, Valli VE. Lymphoid Tumors. In: Meuten DJ, ed. *Tumors in Domestic Animals*. 4th ed. Iowa State Press; Blackwell Publishing; 2002: 163.
3. Gross TL, Ihrke PJ, Walder EJ, Affolter VK. *Skin Diseases of the Dog and Cat*. 2nd ed. Ames, IA: Blackwell; 2005: 870-871.
4. Platz SJ, Breuer W, Pfleghaar S, Minkus G, Hermanns W. Prognostic value of histopathological grading in canine extramedullary plasma-cytomas. *Vet Pathol*. 1999; 36: 23-27.
5. Ramos-Vara JA, Miller MA, Pace LW, Linke RP, Common RS, Watson GL. Intestinal multinodular AL deposition associated with extramedullary plasmacytoma in three dogs: Clinicopathological and immunohistochemical Studies. *J Comp Path.* 1998; 119: 239-249.
6. Rannou B, Helie P, Bedard C. Rectal plasmacytoma with intracellular hemosiderin in a dog. *Vet Pathol*. 2009; 46:1181-1184.
7. Simmons HA. Age-associated pathology in rhesus macaques (*Macaca mulatta*). *Vet Pathol*. 2016; 53(2):399-416.
8. Snyder PW. Diseases of immunity. In: McGavin MD, Zachary JF, ed. *Pathologic Basis of Veterinary Disease*, 6th ed. St Louis, MO: Elsevier Mosby; 2017:285.
9. Uzal FA, Plattner BL, Hostetter JM. Alimentary system. In: Maxie MG, ed. *Jubb, Kennedy, and Palmer's Pathology of Domestic Animals*. 6th

ed. Vol 2. St. Louis, MO: Elsevier; 2016:109.
10. Vail DM. Plasma Cell Neoplasms. In: Withrow SJ, Vail DM, eds. *Small Animal Clinical Oncology*. 4th ed. Philadelphia, PA: Elsevier Saunders; 2007: 769-784.
11. Vasudevan JA, Somanathan T, Patil SA, Kattoor J. Primary systemic amyloidosis of tongue with chondroid metaplasia. *J Oral Maxillofac Pathol*. 2013; 17(2): 266-268.

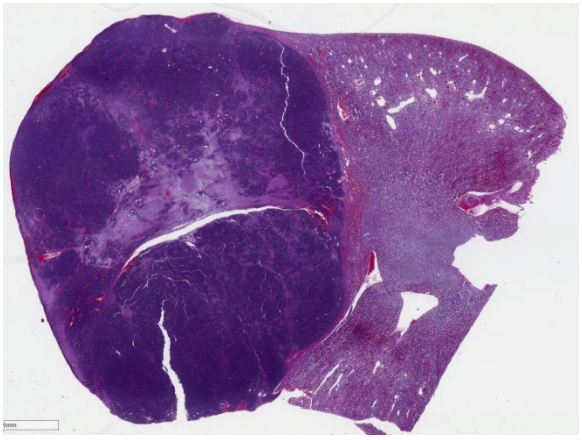

Kidney, rabbit. At one pole of the kidney, there is a densely cellular, nodular, expansile neoplasm. (HE, 5X)

CASE IV: E-522/16 (JPC 4088269).

Signalment: Three-year-old male rabbit (*Oryctolagus cuniculus*).

History: The animal presented two days of anorexia and lack of defecation. At physical examination, a single mass was detected by palpation at the right lumbar area. The presence of a round-shaped mass associated to the caudal pole of the right kidney was confirmed by ultrasonography. Clinicians suspected a neoplastic process, and a right nephrectomy was performed.

Gross Pathology: The complete right kidney was submitted for histopathologic evaluation. A well-circumscribed, oval white mass, 2x1.5 cm in diameter was observed at the caudal pole of the kidney. On section, its consistency was soft, and the cut surface was white and homogeneous.

Laboratory results: None

Histopathologic Description: Kidney: Replacing 50-75% of the renal tissue, there is a densely cellular, partially encapsulated but infiltrative nodular neoplasm which compresses adjacent parenchyma. The neoplasm is composed of a disorganized mixture of epithelial, mesenchymal, and blastemal components supported by an abundant fibrovascular stroma which, in some areas, is embedded in a loose, pale eosinophilic, collagenous matrix. The mesenchymal and blastemal components are predominant over the epithelial. Epithelial neoplastic cells are cuboidal to cylindrical and arranged in a tubular pattern. Occasionally, there are very scant tuft invaginations into the tubular lumen lined by flat epithelial cells (primitive glomerular structures). Those cells present well-defined cytoplasmic borders and moderate amount of bright eosinophilic cytoplasm. Nuclei are round, irregularly shaped, mostly basally located, with grossly stippled chromatin and less frequently, finely stippled chromatin with one basophilic nucleolus. There is low-grade anisokaryosis and anisocytosis, and low mitotic index (1/40X HPF). The mesenchymal component is arranged in a storiform pattern or disorganized bundles. Cells are fusiform, with an indistinct cytoplasmic border, scant eosinophilic cytoplasm, and fusiform centrally located nuclei with grossly stippled chromatin. There is a mild anisokaryosis and aniso-cytosis, and a low mitotic index (0-1/40X HPF). Some of these cells, organized in nest or ribbons, which are poorly differentiated

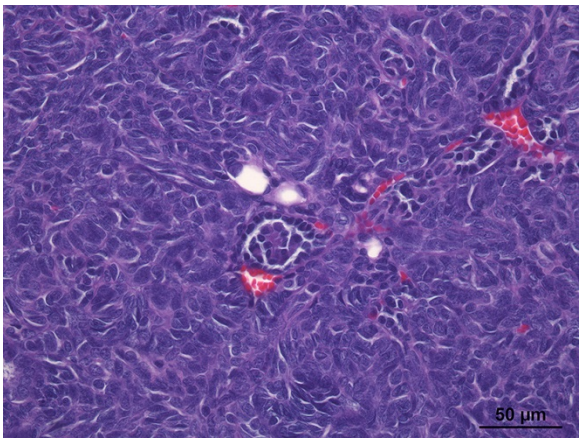

Kidney, rabbit. The neoplasm is composed of spindled to polygonal cells arranged in short streams which occasionally form tubules with papillary projections within, interpreted as "glomeruloid" structures. (HE, 400X) (Photo courtesy of: Servei de Diagnostic de Pathologia Veterinaria, Facultat de Veterinaria, Barcelona 08193, SPAIN)

are identified as possible blastemal cells. Multifocally, in the neoplastic mass there are areas of hypereosinophilia and loss of cytoplasmic and nuclear detail (coagulative necrosis) and mild lymphoplasmacytic inflammatory infiltrate is observed among the neoplasia. The adjacent renal parenchyma shows a moderate interstitial fibrosis, and intense congestion.

Contributor's Morphologic Diagnoses: Renal nephroblastoma.

Contributor's Comment: Nephroblastoma, or Wilms´ tumor, is the most common primary renal tumor of pigs and chickens, and occurs far less often in calves and dogs. It is frequently observed in young animals, although it may be seen in mature sows, and is more common in adult dogs than in pups. Clinically, it is usually an incidental finding except in dogs, in which some animals present with spinal dysfunction as result of compression of the spinal cord associated with neoplastic infiltration into the vertebral canal. Macroscopically, it is usually a solitary unilateral mass located at one pole of the kidney, but it can be multiple and/or bilateral. Nephroblastoma is a true

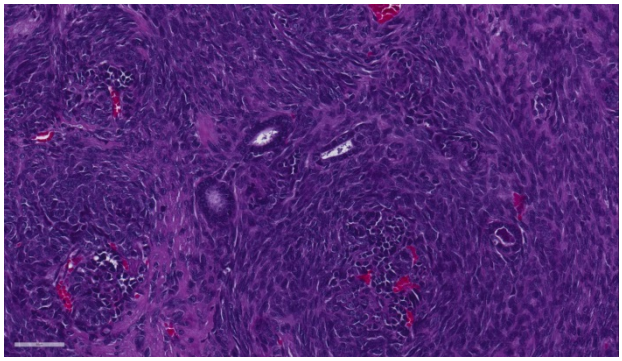

Kidney, rabbit. Neoplastic cells also often form well-differentiated tubules. (HE, 400X)

embryonal tumor that arises from primitive metanephric blastema and exhibits blastemal, epithelial, and stromal components in variable proportions. Histologically, it is characterized by the presence of primitive glomeruli, abortive tubules, and loose spindle-cell stroma that may differentiate into a variety of mesenchymal tissues.

Tubular and glomerular differentiation indicate a good prognosis, whereas anaplasia and sarcomatous stroma are associated with metastasis and a poor prognosis. In this case, the epithelial component is scant and poorly differentiated, and there is a clear predominance of undifferentiated mesenchymal cells. These features, in combination with the neoplasm's invasive growth pattern, suggest a poor prognosis.

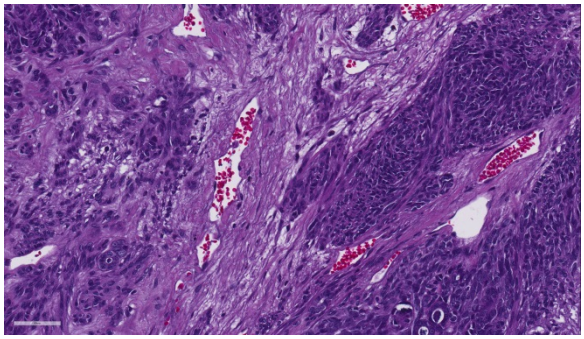

Kidney, rabbit. There are extensive areas of necrosis throughout the neoplasm. (HE, 400X)

The differential diagnosis for renal neoplasia in a rabbit includes renal carcinoma and renal lymphosarcoma. To confirm the diagnosis of nephroblastoma, immunohistochemistry was performed against Wilm's tumor suppressor gene1 (WT1), which has proven efficacious in dogs. This immunohistochemistry was kindly provided by Dr. Joan Carles Ferreres, head of the Pathology Department at the Parc Taulí Sabadell University Hospital. In this case, positive nuclear immunoreactivity was observed in the mesenchymal and blastemal components, as well as endothelial cells.

JPC Diagnosis: Kidney: Nephroblastoma, rabbit, *Oryctolagus cuniculus*.

Conference Comment: This case nicely demonstrates the blastemal, epithelial, and stromal components histologically characteristic for nephroblastomas. Conference participants readily identified the presence of scattered primitive glomeruli (formed by infolded papillary projections of polygonal cells within tubule lumina), as well as low numbers of tortuous, abortive tubules admixed with numerous blastemal cells and surrounded by an abundant loose spindle-cell stroma. Additionally, attendees noted several individualized well-differentiated renal tubules scattered throughout the neoplasm. Conference participants agreed that these likely represent entrapped non-neoplastic renal tubules within the neoplastic cell population rather than part of the epithelial component of the neoplasm. There is moderate slide variability, affecting the proportion of the three components present. When all three cell types are present in equivalent proportions, the neoplasm is referred to as triphasic or mixed;[7] however, in this case there appears to be a preponderance of spindle-cell stromal and blastemal components. Although not a prominent feature in this case, the spindle-cell stroma can occasionally differentiate into various types of mesenchymal tissue, such as striated muscle, collagen, adipose tissue, bone, or cartilage.[6,7]

Nephroblastoma rarely causes clinical signs, although polycythemia is an infrequently reported paraneoplastic syndrome in rabbits.[2] The vast majority of nephroblastomas are considered incidental findings and are noted during necropsy as a solitary (or occasionally bilateral) renal masses.[1] However, as mentioned by the contributor, when this neoplasm is characterized predominantly by a poorly differentiated sarcomatous stromal component, as in this case, it tends to metastasize to the lung and liver, portending an overall poor prognosis.[7]

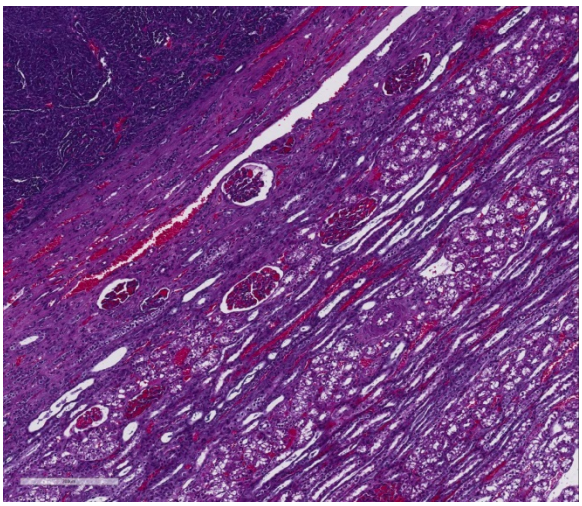

Kidney, rabbit. Growth of the neoplasm (upper left) has resulted in compression of the surrounding cortex and formation of a compression capsule.

While nephroblastomas are a relatively uncommon spontaneous neoplasm in pet rabbits, they can be rapidly induced at a high frequency in laboratory rabbits and rats after exposure to direct-acting alkylating carcinogens, such as dimethylnitrosamine.[6] Dimethylnitrosamine has also been reported to experimentally induce triphasic nephroblastomas in rainbow trout, similar to Wilm's tumor in humans.[3] Other than

lymphoma, nephroblastomas are the most common primary renal neoplasm in a variety of species of freshwater fish, with the Japanese eel over-represented. Research is ongoing to determine if potential carcinogens in the water may be inducing nephroblastomas in wild fish, with a particular focus on fish commonly consumed by people.[3]

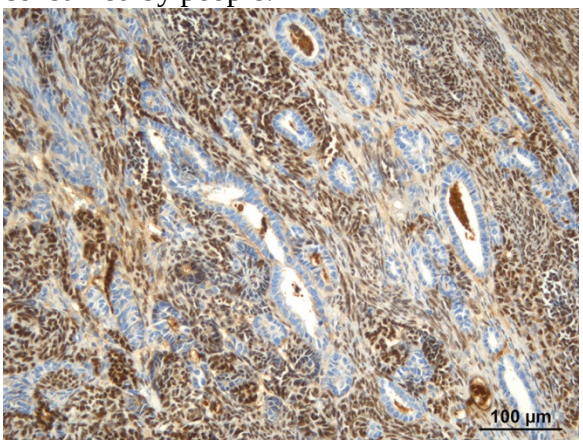

Kidney, rabbit. Neoplastic cells exhibit strong nuclear immunopositivity for Wilm's Tumor 1 (antigen). (anti-WT1, 400X)

Contributing Institution:
Universitat Autonoma de Barcelona
Servei de Diagnostic de Patologia Veterinaria
Barcelona, Spain
http://www.uab.cat/veterinaria/english

References:

1. Cianciolo RE, Mohr FC. The urinary system. In: Maxie MG ed. *Jubb Kennedy and Palmer's Pathology of Domestic Animals*. Vol 2. 6th ed. Philadelphia, PA: Elsevier Saunders; 2016:446-447.
2. Cooper TK, Griffith JW, et al. Spontaneous lung lesions in aging laboratory rabbits (*Oryctolagus cuniculus*). *Vet Pathol*. 2017; 54(1):178-187.
3. De Lorenzi D, Baroni M, Mandara MT. A true "triphasic" pattern: Thoracolumbar spinal tumor in a young dog. *Vet Clin Pathol*. 2007; 36:200-203.
4. Hassan J, Katic N, et al. Treatment of nephroblastoma with poly-cythemia by nephrectomy in a rabbit. *Vet Rec*. 2012; 170:465.
5. Lombardini ED, Hard GC, Hashbarger JC. Neoplasms in the urinary tract in fish. *Vet Pathol*. 2014; 51(5):1000-1012.
6. Meuten DJ. Tumours of the urinary system. In: Meuten DJ, ed. *Tumors in Domestic Animals*. Ames, IA: Iowa State Press; 2002:519-520.
7. Newman SJ. The urinary system. In: McGavin MD, Zachary JF, ed. *Pathologic Basis of Veterinary Disease*. 5th ed. St Louis, MO: Elsevier Mosby; 2012: 643.

Self-Assessment - WSC 2016-2017 Conference 14

1. Neuroendocrine carcinomas are typically immunopositive for each of the following except?
    a. Chromogranin A
    b. Neuron-specific enolase
    c. Cytokeratin
    d. Synaptophysin

2. Which of the following is the cause of equine multinodular pulmonary fibrosis ?
    a. Bovine papillomavirus-1
    b. Equine herpesvirus-5
    c. Equine herpesvirus-2
    d. Equine papillomavirus-1

3. Gamma herpesviruses have been identified in progressive pulmonary fibrotic disorders in each of the following species except
    a. Cats
    b. Humans
    c. Donkeys
    d. Rodents

4. Which of the following is commonly deposited in plasma cell tumors?
    a. Amyloid
    b. Chondroid matrix
    c. Melanin
    d. Bone

5. Which of the following has experimentally induced the formation of nephroblastomas in a variety of species?
    a. Aflatoxin
    b. Pyrollizidine alkalids
    c. Fumonisin B1
    d. Dimethylnitrosamine

Joint Pathology Center

Veterinary Pathology Services

WEDNESDAY SLIDE CONFERENCE 2016-2017

Conference 15

18 January 2017

CASE I: WSC#2 (JPC 4066310).

Signalment: 28-year-old, male, American alligator, (*Alligator mississippiensis*).

History: This alligator was housed with 10 others at a rescue facility in the northeastern United States. During the winter months, the animals were kept indoors in a house, living on wood floors, with access to an unspecified water source; there was reportedly visible mold in this environment. The alligators were not induced to hibernate during this time, and were housed at an ambient temperature of 74°F (23°C). This alligator was found dead with no premonitory signs.

Gross Pathology: An adult, 70.5 kg male American alligator was presented in good nutritional condition with abundant fat stores. There was an extensive adhesion of the right lung to the right dorsal body wall which enclosed approximately 75 mL of pale tan, thin liquid with grey to pale tan particulates. The pleural surfaces of both lungs had discrete to coalescing areas of firm, brown to pale tan discoloration which were more extensive in the right lung and extended into the parenchyma. On cut section there were extensive regions of parenchyma replaced by firm, white, crumbly material (caseous necrosis). Additionally, multiple subpleural cavitations and air spaces in the right lung were lined by white, slightly fuzzy, fungal mats. Numerous small, whitish foci up to 0.3 cm diameter were present in the liver, and similar individual foci were present in the heart, spleen, and kidney.

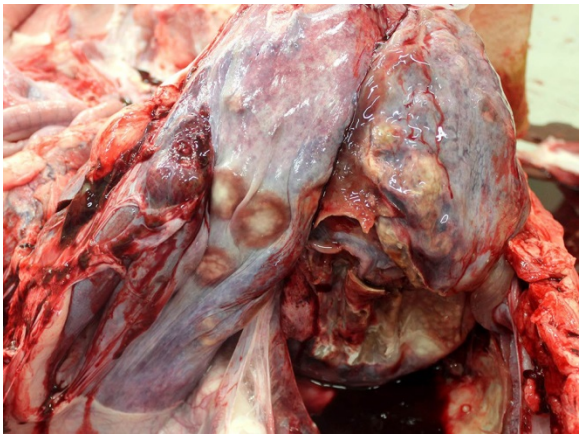

Lung and air sac, alligator. The pleural surfaces of both lungs had coalescing discrete areas of firm tan within the parenchyma. (Photo courtesy of Department of Pathobiology and Veterinary Science, Connecticut Veterinary Medical Diagnostic Laboratory, College of Agriculture, Health and Natural Resources, University of Connecticut, http://www.pathobiology.uconn.edu/)

Laboratory results: Fungal culture and identification: A swab from the lung was initially plated on potato dextrose agar (PDA) and inhibitory mold agar (IMA) with and without antibiotics and then incubated at 30°C for 14 days; this yielded heavy growth of white fungal colonies on both plate types. On PDA, the bottom of the colony had an orange to pink tinge, whereas on IMA the bottom of the colony was red. Cultures were submitted to the Fungus Testing Laboratory, University of Texas Health Science Center in San Antonio, Texas for identification. Combined phenotypic characterization and DNA sequencing of ITS and TEF targets identified the fungus as *Beauveria bassiana*.

Histopathologic Description: Up to 80% of the parenchyma is effaced by necrosis that extends to the pleural surface. Necrotic areas are characterized by variable loss of architectural detail with accumulation of fibrin, hypereosinophilic cellular debris, edema, hemorrhage, and inflammatory cells composed predominantly of heterophils and macrophages. Within the necrotic areas, there are numerous, lightly basophilic to transparent fungal hyphae that are 2-6 microns in diameter, septate, and parallel-walled with occasional right angle branching. At the air-tissue interface in a couple of large airways there are scattered hyphae that give rise to dense clusters of ampulliform conidiogenous cells measuring up to 3 microns in diameter, each with a single to several terminal round conidia measuring 1-3 microns in diameter. Large numbers of bacteria are also frequently admixed. Rarely, in areas of dense fungal growth, there are a few translucent, variably shaped, anisotropic crystals (oxalate crystals). Frequently, vessels are occluded by fibrin thrombi, and their walls contain necrotic debris, fibrin, moderate numbers of degenerate heterophils and occasional fungal hyphae (vasculitis). The parenchyma adjacent to necrotic areas is variably expanded by edema, mixed inflammatory cells, and reactive fibroblasts.

Lung and air sac, alligator. Multiple subpleural cavitations in the right lung were lined by white fuzzy fungal mats. (Photo courtesy of Department of Pathobiology and Veterinary Science, Connecticut Veterinary Medical Diagnostic Laboratory, College of Agriculture, Health and Natural Resources, University of Connecticut, http://www.pathobiology.uconn.edu/)

Contributor's Morphologic Diagnoses: Lung: severe, subacute, multifocal to coalescing, fibrinonecrotizing and heterophilic pneumonia and pleuritis with vasculitis, fibrin thrombi and intralesional bacteria and fungal hyphae and conidia, consistent with *Beauveria bassiana*.

Contributor's Comment: This is a case of mycotic pneumonia in an American alligator caused by *Beauveria bassiana*. Identification of this organism was based on the morphology of the fruiting bodies (conidiogenous cells and conidia) on H&E; its phenotypic characteristics in culture; and DNA sequence analysis, all of which differentiated it from other common agents of fungal pneumonia, particularly *Aspergillus* species. *Beauveria bassiana* is a ubiquitous soil saprophyte that is entomopathogenic, i.e. pathogenic to insects

due to an affinity for chitinous exoskeletons. As such, it has been widely used for more than 100 years as biocontrol of pest insects.[5] Though widespread in the environment, its upper temperature limit is around 30°C, and it is inactivated within hours or days when exposed to sunlight.[9] Due to the temperature limitations, *B. bassiana* rarely causes infections in mammals but is an opportunistic pathogen of reptiles, with previous reports in captive American alligators,[2] chelonians,[3,6] and in cold-

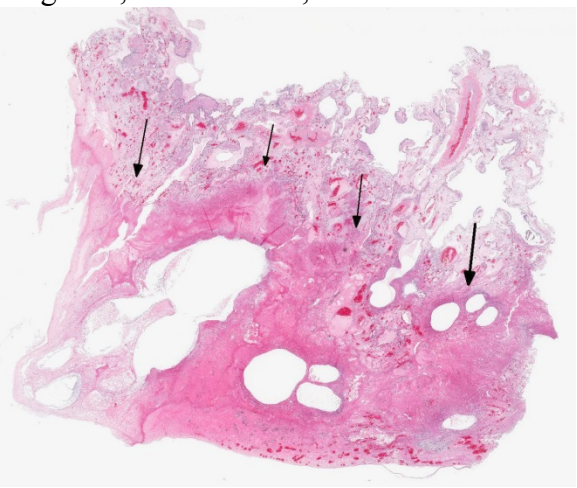

Lung, alligator. Approximately 75% of this section exhibits coagulative necrosis (arrows demonstrate line of demarcation from viable tissue.) (HE, 5X)

stunned Kemp's Ridley sea turtles.[6]

Exposure to low temperatures is often implicated as a contributing factor in these infections. Two previous cases in alligators occurred after a prolonged hibernation and brief heating system failure.[2] In the current case, the temperature of the indoor enclosure was reportedly kept at 23°C, well within the temperature range of *B. bassiana*. High levels of fungus in the environment and poor ventilation were also probably involved in this case, as mold was reportedly visible in the enclosure where this group of alligators was housed. Other predisposing factors for fungal pneumonia in captive reptiles include additional husbandry-related issues, such as humidity, hygiene, and nutrition, immunosuppression, overuse of antibiotics, and concurrent disease.[5] Shortly after diagnosis of this case, a second alligator from the same group died naturally, but a necropsy was not performed.

Transmission is thought to occur from inhalation or ingestion of fungal spores from the environment, and the lung appears to be the primary site of infection. Hematogenous dissemination of the infection from the lung to other tissues, such as liver and spleen, occurred in this case as in previous cases.[2,6] *Beauveria bassiana* produces several toxic compounds including oxalic acid, which promotes the formation of oxalate crystals within affected tissues;[9] only a few crystals were seen in this case.

JPC Diagnosis: Lung: Pneumonia, necrotizing, multifocal to coalescing, severe, with innumerable fungal hyphae and large colonies of mixed bacilli, American alligator, *Alligator mississippiensis*.

Conference Comment: This case provided conference participants the unique opportunity to describe lung pathology in an American alligator, an uncommonly seen species at the Joint Pathology Center. Prior

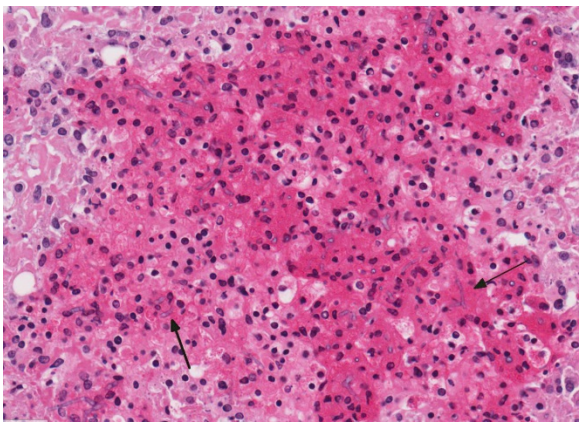

Lung, alligator. Heterophilic granulomas are scattered throughout the pulmonary parenchyma and contain numerous 2-4um diameter septate fungal hyphae (arrows). (HE, 360X)

to the discussion of this case, the conference moderator led a review of the normal functional anatomy and physiology of alligator lungs, which was poorly understood until relatively recently.[1,7] Research performed at the University of Utah indicates the external and internal morphology of alligator lungs is strikingly similar to the avian respiratory system, although in contrast to birds, alligators lack intra-abdominal air sacss.[1,7] Alligators have a highly efficient unidirectional style of breathing, originally thought to be unique to avian species as a consequence of the high oxygen demands of flight.[7] However, unlike birds, alligators use a diaphragm to pull air into the lungs. The air then travels one direction through bronchi which branch into numerous smaller parabronchi and continues further into alveolar-like spaces, called faveoli. Gas exchange then takes place within these faveoli, and the air then flows out of the lung via in a one-way loop and valve system.[7] Unidirectional breathing is much more efficient than the mammalian bellows-style breathing because there is no alveolar mixing of inspired and expired air. Research is ongoing to elucidate the exact mechanism of unidirectional air flow in alligators and other reptiles, as it was thought that air sacs were necessary for unidirectional air flow breathing.[1,7]

Reported cases of fungal pneumonia in reptiles caused by *Beauveria bassiana* are rare and typically involve extensive multifocal necrosis or granulomatous nodules with high numbers of fungal hyphae in the lungs with dissemination to the multiple abdominal organs, as present in this case.[2,3,6] Infection occurs after inhaling or ingesting fungal spores from the environment and development of disease in reptiles has been associated with low environmental temperatures and poor husbandry of captive reptiles. As mentioned

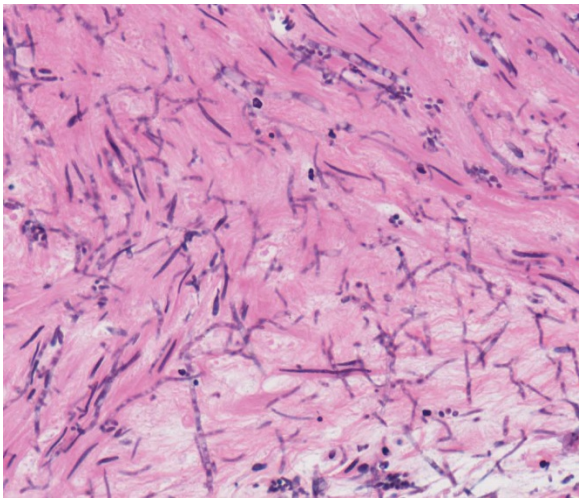

Lung, alligator. Necrotic tissue is replete with proliferating fungi which often form dense mats. (HE, 400X).

by the contributor, the fungus will not grow at mammalian physiologic temperatures (37°C)[2,3,6], although it has been very rarely reported to cause fungal keratitis in people associated with contact lens wear and prior treatment with corticosteroid eye drops.[4] The association of this fungus with low environmental temperatures and cold-shocked reptiles in previously reported cases prompted the conference moderator to discuss brumation in ectothermic animals.

Brumation is a time of dormancy in reptiles in response to colder winter weather (~21°C), and is similar, but not identical, to hibernation in mammals. During periods of brumation, reptiles have a markedly decreased metabolic rate, but do not fall into a deep sleep, and can regularly emerge to drink and bask during warm days. Additionally, reptiles typically do not eat during periods of brumation.[8]

Contributing Institution:
Department of Pathobiology and Veterinary Science
Connecticut Veterinary Medical Diagnostic Laboratory
College of Agriculture, Health, and Natural Resources

University of Connecticut
http://www.pathobiology.uconn.edu/

References:

1. Farmer CG. Similarity of Crocodilian and avian lungs indicates unidirectional flow is ancestral for Archosaurs. *Integr Comp Biol*. 2015; 55(6):962-971.
2. Fromtling RA, Jensen JM, Robinson BE, Bulmer GS. Fatal mycotic pulmonary disease of captive American alligators. *Vet Pathol*. 1979; 16:428-431.
3. Gonzalez Cabo JF, Espejo Serrano J, Barcena Asensio MC. Mycotic pulmonary disease by *Beauveria bassiana* in a captive tortoise. *Mycoses*. 1995; 38:167-169.
4. Lara Oya A, Medialdea ME, et al. Fungal keratitis due to *Beauveria bassiana* in contact lenses wearer and review of published reports. *Myco-pathologia*. 2016; 181:745-752.
5. Murray MJ. Pneumonia and normal respiratory function. IN Mader, DR, ed. *Reptile Medicine and Surgery*, St. Louis: W.B. Saunders Company; 1996: 402-403.
6. Pare JA, Jacobson ER. Mycotic diseases of reptiles. IN Jacobson ER, ed. *Infectious Diseases and Pathology of Reptiles*, Boca Raton: CRC Press; 2007: 538-539.
7. Sanders RK, Farmer CG. The pulmonary anatomy of *Alligator mississippiensis* and its similarity to the avian respiratory system. *Anat Rec*. 2013; 295(4):699-714.
8. Wilkinson A, Hloch A, et al. The effect of brumation on memory retention. *Sci Rep*. 2017; 7:40079.
9. Zimmermann G. Review on safety of the entomopathogenic fungi *Beauveria bassiana* and *Beauveria brongniartii*. *Biocontrol Sci Technol*. 2007; 17(6):553-596.

CASE II: 15-5172 (JPC 4066860).

Signalment: Four-year-old, male, red tail boa constrictor, (*Boa constrictor constrictor*).

History: The patient initially presented on 10/29/201 4 for a 4-5 month history of anorexia. At that time, there was atrophy of the epaxial muscles and a firm, but compressible swelling expanding the cranial cervical region. Ultrasound of this area revealed a soft-tissue mass, for which the tissue of origin was unclear. The mass did not appear to be associated with the trachea or within the esophageal lumen. The patient represented in January 2015 for continued anorexia, progressive lethargy, and recent regurgitation after forced feeding. The patient had lost a significant amount of weight and on examination, there was a large accumulation of necrotic material in the mouth. During this exam, a second mass was appreciated just caudal to the previously described cervical mass. At the owner's request, the patient was euthanized.

Gross Pathology: A 2 cm x 0.5 cm region of the hard palate is raised, irregularly surfaced, fleshy, and dark red. Extending from the esophageal wall and protruding into the lumen is a 2.5 cm x 1 cm x 1 cm, smooth, soft, pink and red mass, with a core of crumbly, brown-yellow material. Approximately 0.5 cm aboral to this mass is a 4.5 cm x 2.5 cm x 2.5 cm, smooth, firm, ovoid, pink and red mass that on section is composed of a central core of a crumbly, brown-yellow material (caseous necrosis) surrounded by a 0.7 cm wide rim of a fleshy, pink/red tissue. The corresponding eso-phageal serosa is firmly adhered to the local body wall. The esophageal mucosa, adjacent to the larger mass, has a 2 cm x 0.4 cm, poorly demarcated, mildly depressed, region composed of dozens of pinpoint red foci

(erosion). Within the lumen of the aboral esophagus, approximately 3.5 cm from the larger mass, are three rough, ovoid aggregates of a mottled brown, yellow, and green, crumbly material. This material is not adhered to the mucosa.

Oral cavity, boa constrictor: A 2x0.5 cm of the hard palate is raised, fleshy, and dark red. (Photo courtesy of Department of Biomedical Sciences, section of Anatomic Pathology, Cornell University, College of Veterinary Medicine.)

Laboratory results: N/A

Histopathologic Description: ORAL CAVITY: Severely expanding the sub-mucosa, confluent with a large region of epithelial ulceration, and obliterating the adjacent lamellar bone is a densely packed population of foamy macrophages with fewer granulocytes, lymphocytes, and plasma cells. Unilaterally the alveolar bone is disrupted and replaced by a similar inflammatory cell population and the islands of retained bone has irregular, scalloped edges and are lined by numerous osteoclasts within distinct Howship's lacunae. The superficial osteoid matrix commonly contains a thin, irregular, basophilic line (reversal line). Similar inflammatory cells efface the dentin and invade the pulp of a tooth. The surface epithelium is entirely replaced by a band of necrotic cellular debris and fibrin.

BRAIN, NOS: Occasional neurons contain discrete, intracytoplasmic, 1-10 um diameter, glassy, eosinophilic inclusions.

NASAL CARTILAGE: Commonly, the respiratory epithelial cells and submucosal gland epithelial cells contain discrete, intracytoplasmic, 1 -1 0 um diameter, glassy, eosinophilic inclusions. Scattered throughout the submucosa are scant numbers of lymphocytes and plasma cells.

ESOPHAGEAL MASSES (not submitted): Multifocally the esophageal wall is severely expanded by multiple unencapsulated, irregular masses composed of densely packed vacuolated macrophages mixed with

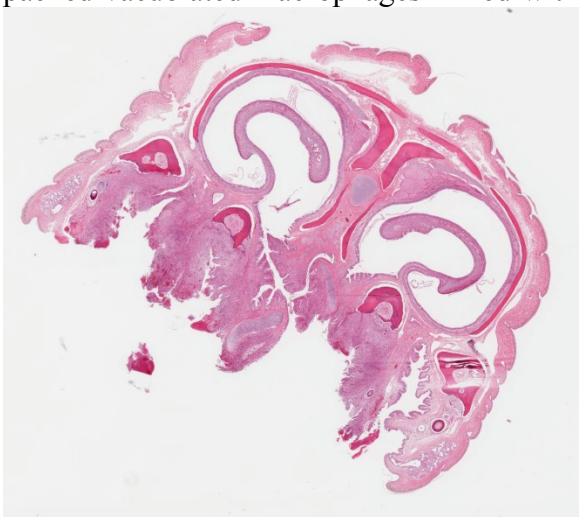

Oral cavity, boa constrictor: Large sections of the mucosa of the oral cavity is replaced by a densely cellular are of granulation tissue which extends through the submucosa and erodes underlying bone. (HE, 5X)

fewer small lymphocytes, plasma cells, granulocytes, and multinucleated nucleated giant cells. Lymphocytes are occasionally present in small, poorly defined islands and cells contain discrete, intracytoplasmic, 1-4 um diameter, glassy, eosinophilic inclusions. The overlying epithelial cells contain discrete, 2-6 um, glassy, eosinophilic, intra-cytoplasmic inclusions.

Additional findings include numerous discrete, 1-10um in diameter, glassy, eosinophilic, intracytoplasmic inclusions within multiple tissues including hepato-cytes, biliary epithelial cells, gastric mucosa, intestinal epithelium, tracheal epithelium, bronchiole epithelium, and the retinal ganglion cells. Concurrently within the liver, there were small numbers of randomly distributed macrophages, lymphocytes, and plasma cells.

Contributor's Morphologic Diagnoses: Oral cavity: Severe, diffuse, chronic, granulomatous and ulcerative stomatitis with numerous, eosinophilic, intracytoplasmic inclusion bodies

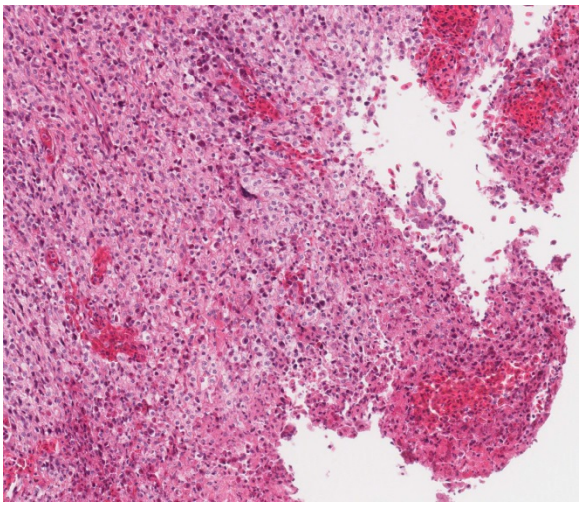

Oral cavity, boa constrictor: Higher magnification of the granulation tissue within the oral cavity populated by large numbers of macrophages and fewer heterophils with an ulcerated surface (lower right). (HE, 188X)

Esophageal mass (not submitted): Severe, multifocal, chronic, granulomatous and ulcerative esophagitis with numerous, eosinophilic, intracytoplasmic inclusion bodies

Stomach, intestine, trachea, lung, kidney, liver, nasal cavity, retina, and brain (not submitted): Severe, eosinophilic, intra-cytoplasmic inclusion bodies

Contributor's Comment: Inclusion body disease (IBD) is reported in multiple snake species, but most commonly within the family *Boidae* and *Pythonidae*. As the name implies, the characteristic finding in these cases are distinct, variably sized, eosinophilic, intracytoplasmic inclusions.[2] In one recent retrospective study, the prevalence of IBD in captive collections was approximately 19%. Although disease progression varies greatly between individuals and between species, the disease is classically associated with central nervous system signs, including head tremors, anisocoria, and opisthotonus.[9] Commonly the animal succumbs to complications secondary to immunosuppression.[15] In boas, the disease can have a more protracted progression of weeks to months[9] and typically patients have a previous history of regurgitation.[10] In addition, a proportion of boas can be subclinical carriers.[7-10] Meanwhile, pythons tend to display a more aggressive disease course of only a few weeks,[9] with a more profound inflammatory reaction.[10] Interestingly, regurgitation tends not to be a part of clinical disease in pythons.[10] Gold standard testing remains the histologic demonstration of intracytoplasmic inclusions in multiple organs, most notably the liver, stomach, and esophageal tonsils, however, their absence does not rule out the disease.[10] Although with further characterization of the underlying etiology,

molecular testing and immunohisto-chemistry[3] may be available in the future.

Although long considered to have an underlying infectious etiology, the cause of IBD has been elusive. Originally the disease was thought to be associated with a retrovirus, however, recently divergent arenaviruses have been implicated as the cause of IBD.[2-4,8-10] Of late, *in vitro* Koch's postulates have been met linking arenavirus to the development of IBD, however, in vivo studies have not be reported.[9] Arenaviridae are enveloped, negative sense, single stranded, bipartite RNA viruses.[2,8] Arenaviruses have previously been thought to only affect rodents, with infrequent but possible transmission to other mammal species (e.g. humans and bats).[2] The viral genome is composed of a small (S) segment and a large (L) segment. The S segment encodes the viral nucleocapsid protein (NP) and the glycoproteins (GP1 and GP2) while the L segment encodes the viral RNA-dependent RNA polymerase and a small ring domain containing protein[2,9] The distinction intracytoplasmic inclusions consist of a unique 68KDa protein, that has been named "inclusion body disease protein" (IBDP).[3,9,10] This protein has been demonstrated to be the arenaviral NP protein.[6] Boid-associated inclusion body arenaviruses tend to be highly divergent.[2,8,9]

Proposed theories as to the mode of transmission include direct contact, possible arachnid vectors (i.e. the snake mite, *Ophionyssus natricis*), mammalian vectors (i.e. live prey), and vertical transmission.[8-10] As several other arenaviruses are able to cross the species barrier, it remains possible that the highly divergent boid inclusion body disease associated arenaviruses (BIBDAV) may as well. A recent report showed that BIBDAV was infective to tick cells lines (mite cell cultures were not available) and

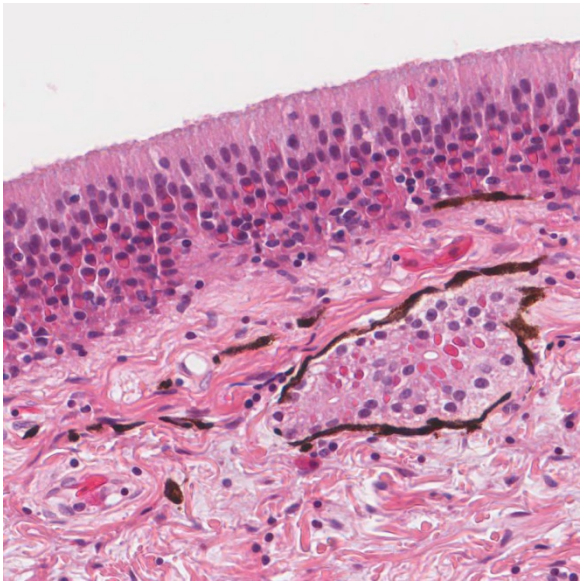

Nasal cavity, boa constrictor: Respiratory and submucosal gland epithelium contain numerous 2-4um round to oval intracytoplasmic viral protein inclusions. (HE, 400X)

this data may support the role of *Ophionyssus natricis* infestation in disease transmission.[8] Furthermore, maintenance of BIBDAV within mammalian (VERO E6) and boid cell lines appears to be temperature dependent, with strong growth at 30°C and inhibition of growth at 37°C. Thus, the authors purpose that transmission from a mammalian host is possibly hindered by the higher mammalian body temperature.[8]

Boid snakes have large well-developed esophageal tonsils, which can be enlarged and abscessed. In this case, the large esophageal masses may represent severely inflamed esophageal tonsils.

JPC Diagnosis: 1.Oral cavity: Stomatitis, ulcerative and histiocytic, chronic, multifocal to coalescing, severe, with granulation tissue and bone resorption, red tail boa constrictor, *Boa constrictor constrictor*.

2. Epithelial cells: epidermis, salivary gland, and nasal cavity: Intracytoplasmic protein inclusions of viral origin, numerous.

Conference Comment: Boid inclusion body disease (BIBD) is considered by many to be the most important viral infection of captive boas and pythons, often causing progressive and rapidly fatal multisystemic disease.[10] As mentioned by the contributor, the clinical presentation of BIBD is highly variable among individuals, especially in adult boas, where intracytoplasmic viral protein inclusions can be found in snakes without clinical signs.[2,6,10,13] However, the disease is still considered to be fatal due to severe impairment of immune function of leukocytes and myelopoietic cells, resulting in death due to opportunistic infections.[6,10] Interestingly, in this case, the conference moderator speculates that the extensive ulcerative stomatitis seen both grossly and histologically may be due to BIBD-induced starvation and regurgitation combined with the mechanical trauma from the reported forced feeding.

Typical gross findings associated with BIBD are usually limited to areas susceptible to secondary opportunistic infections, such as the oral cavity, gastrointestinal tract, lungs, liver, and kidney. Histologically, the hallmark of BIBD is the presence of numerous 1-4 um, pale, eosinophilic intra-cytoplasmic inclusion bodies in all major organs, especially the kidneys, liver, stomach, and brain. Inclusions are typically more prominent in the visceral organs of boas and central nervous system in pythons.[10] In this case, inclusions are widely distributed throughout.

Conference participants discussed the composition of the highly distinctive inclusion bodies associated with this disease. The inclusions, which ultrastructurally are cytoplasmic aggregates of electron-dense material, composed of an antigenically unique 68-kilodalton non-viral protein.[2,3,6,15] Recently, a novel group of arenaviruses were isolated from snakes with BIBD. In an in-vitro cell culture model, this arenavirus induces the pathognomonic inclusion bodies and was discovered to predominantly consist of arenaviral associated nuclear protein. This finding led to the suggestion of the formation of a novel genus called the *Reptarenavirus* and placing the remaining arenaviruses in the *Mammarenavirus* genus. There is still some controversy surrounding the formation of a new genus given the lack of *in vivo* confirmation.[3,9,11]

Conference participants discussed the importance of arenaviruses as zoonotic pathogens associated with rodent host species. In humans, arenaviruses, such as Lassa and Machupo (Bolivian hemorrhagic fever), cause outbreaks of rapidly fatal viral hemorrhagic fevers, not unlike the Ebolavirus.[1] Additionally, hamsters are the primary source of lymphocytic chorio-meningitis (LCM) virus causing meningo-encephalitis in humans and callitrichid hepatitis in New World primates.[13] Arenaviruses generally produce only mild or subclinical disease in their natural host species.

Contributing Institution:
Cornell University Department of Biomedical Sciences
Section of Anatomic Pathology
http://www.vet.cornell.edu/biosci/pathology/

References:

1. Bell TM, Bunton TE, Shaia CI, Raymond JW, Honnold SP, Donnelly GC, Shamblin JD, Wilkinson ER, Cashman KA. Pathogenesis of Bolivian

hemorrhagic fever in Guinea pigs. *Vet Pathol*. 2016; 53(1):190-199.
2. Bodewes, R, Kik, MJL, Raj S, et al. Detection of novel divergent arenaviruses in boid snakes with inclusion body disease in the Netherlands. *J Gen Virol*. 2013; 94:1206-1210.
3. Chang, L, Fu Am Wozniak, E, et al. lmmunohistochemical detection of a unique protein within cells of snakes having inclusion body disease, a world-wide disease seen in members of the families boidae and pythonidea. *PLoS One*. 2013. 8(12):1-16.
4. Charrel RN, de Lamballerie X. Zoonotic aspects of arenavirus infections. *Vet Microbiol*. 2010; 140:21320.
5. Drake, S, Marschang RE, Hetzel U, et al. Experimental infection of boa constrictor with an orthoreovirus isolated from a snake with inclusion body disease. *J Zoo Wildl Med*. 2014; 45(2):433-436.
6. Fowler ME, Miller RE. *Fowler's Zoo and Wild Animal Medicine*. Miller RE, Fowler ME eds. Vol 8. Philadelphia, PA; Saunders; 2014:70.
7. Hellebuyck, T, Pasmans F, Ducatelle, R, et al. Detection of arenavirus in a peripheral ondotogenic fibromyxoma in a red tail boa (*Boa constrictor constrictor*) with inclusion body disease. *J Vet Diagn Invest*. 2015; 27(2):245-248.
8. Hepojoki J, Kipar, A, Korzyukov, et al. Replication of boid inclusion body disease-associated arenaviruses is temperature sensitive in both boid and mammalian cells. *J Virol*. 2015; 89(2):1119-1128.
9. Hetzel U, Sironen T, Laurinmaki, P, et al. Isolation, identification, and characterization of novel arenaviruses the etiological agents of boid inclusion body disease. *J Virol*. 2013; 87(20):10918-10935.
10. Jacobson ER. *Infectious Diseases and Pathology of Reptiles, Color Atlas and Text*. Jacobson ER ed.1st ed. CRC Press, Boca Raton, 2007:185, 410-412.
11. Keller S, Hetzel U, et al. Co-infecting reptarenaviruses can be vertically transmitted in boa constrictor. *PLoS Pathog*. 2017; 13(1):e1006197.
12. Pees M, Schmidt V, Marschang RE, et al. Prevalence of viral infections in captive collection of boid snakes in Germany. *Vet Rec*. 2010; 166:422-425.
13. Montali RJ, Connolly BM, Armstrong DL, Scanga CA, Holmes KV: Pathology and immunology of callitrichid hepatitis, an emerging disease of captive new world primates caused by lymphocytic choriomeningitis virus. *Am J Path*. 1995; 148(5):144-149.
14. Schillinger L, Selleri P, Frye FL. Lymphoblastic lymphoma and leukemia blood profile in a red-tail boa (*Boa constrictor constrictor*) with concurrent inclusion body disease. J *Vet Diag Invest*. 2011; 23:159-162.
15. Schmidt V, Marschang RE, Abbas MD, et al. Detection of pathogens in boidae and pythonidae with and without respiratory disease. *Vet Rec*. 2013; 172(9):236.

CASE III: G9428 (JPC 4085109).

Signalment: 28-year-old, female, Nilgiri langur, (*Trachypithecus johnii*).

History: An adult female captive born Nilgiri langur (*Trachypithecus johnii*) from a zoological garden in Central Europe developed an edematous swelling of the left thigh, which persisted for several months and was associated with periods of a decreased general condition, depression, and anorexia. Sonographic examination of the thorax and abdomen revealed cardiomegaly as well as poor demarcation and cloudy appearance of the liver. The animal was finally euthanized due to a poor general condition, anorexia, and therapeutic resistance.

Skeletal muscle, langur. The skeletal muscle of the left thigh (arrows) is separated and compressed by several encapsulated cysticerci containing numerous cross- ad tangential sections larval cestodes. (HE, 7X)

Gross Pathology: At necropsy, the animal was cachectic. The skeletal muscle of the left thigh was severely atrophic and replaced by fluctuant multilocular cysts containing numerous sand grain sized whitish structures. The left caudal lung lobe revealed a focal circumscribed area of atelectasis.

Laboratory results: PCR analysis of muscular metacestode tissue identified *Cysticercus longicollis*, the larval stage of *Taenia crassiceps*, as the etiologic agent.

Histopathologic Description: Within the skeletal muscle of the left thigh are multifocal extensive areas of fibrous connective tissue bearing multiple cystic structures with numerous larval cestodes (cysticerci). Cysts are surrounded by thick fibrous capsules that are multifocally infiltrated by plasma cells, lymphocytes, macrophages, and eosinophils. The inflammatory cells extend into the adjacent fibrous granulation tissue between muscle fibers that contains few multinucleated giant cells. Cysticerci are characterized by a 4 µm thick, eosinophilic tegument, a fibrillar, eosinophilic parenchyma, numerous 5 µm diameter, basophilic, calcareous corpuscles, and an invaginated scolex with muscular suckers and hooks.

Contributor's Morphologic Diagnoses: Skeletal muscle: Myositis, chronic, granulomatous and eosinophilic, multifocal, severe, with intralesional cysticerci, Nilgiri langur (*Trachypithecus johnii*), non-human primate.

Contributor's Comment: Non-human primates might act as aberrant hosts for a number of cestode species after oral infection and larval development in extra-intestinal locations.[2] *Taenia crassiceps* is a cestode parasite of the Northern hemisphere, whose life cycle includes canids as definitive hosts, most commonly the red fox (*Vulpes vulpes*) in Europe and the Artic fox (*Alopex lagopus*) as well as the red fox in North America.[6] Natural infection by *T. crassiceps* has also been reported in wolves (*Canis lupus*)[5] and coyotes (*Canis latrans*)[13] in North America as well as in wild cats (*Felis silvestris*)[12] and domestic dogs in Germany.[3] Several rodent species and rabbits serve as intermediate hosts for the metacestode larval stage of the parasite, *Cysticerus* (*C.*) *longicollis*. However, the

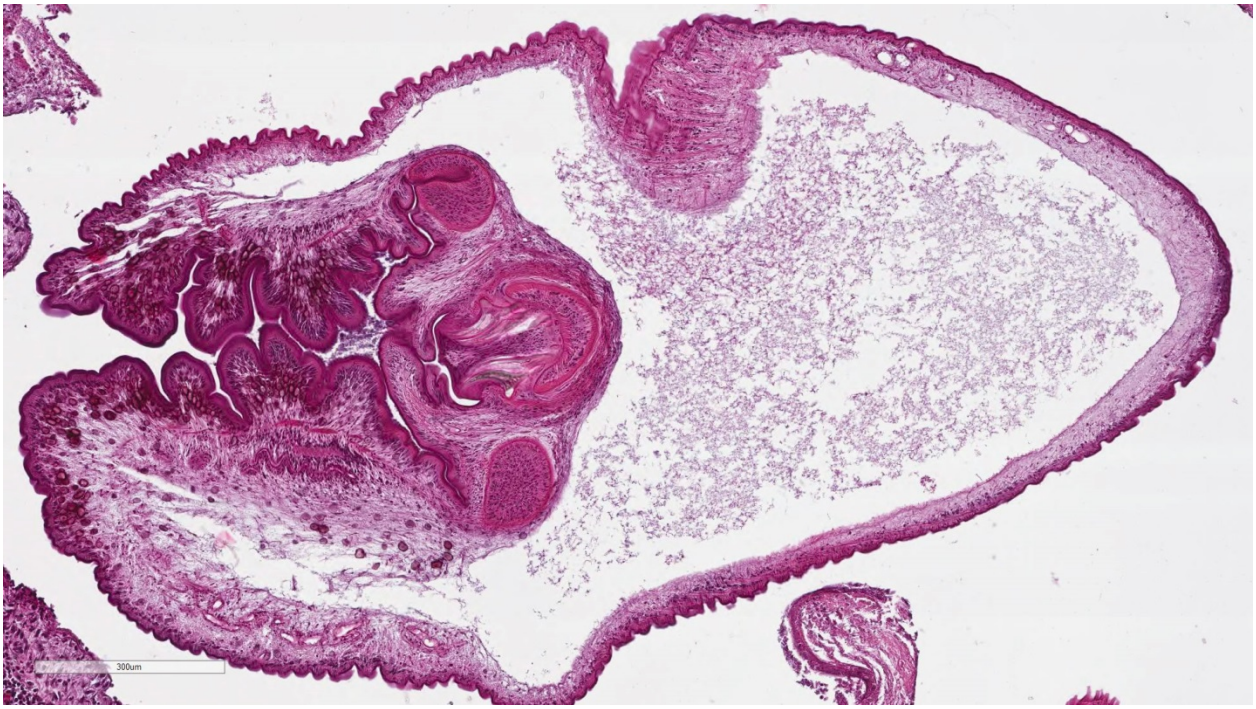

Skeletal muscle, langur. At low magnification, larval cestodes are characterized by a ridged tegument and an invaginated scolex. (HE, 69X)

common vole (*Microtus arvalis*) is the predominant intermediate host in Europe.[1] Sporadic cases of clinical cysticercosis caused by *T. crassiceps* have been reported in humans and domestic animals such as dogs and cats, many of them in immunocompromised individuals.[8,9,16] Infections by *T. crassiceps* may be particularly serious due to their proliferative nature. In contrast to cysticercosis associated with other *Taenia* species, *T. crassiceps* is able to proliferate by exogenous and endogenous budding. Exogenous budding may produce 1-6 daughter cysticerci at the abscolex pole of the maternal cyst. Daughter cysticerci may bud off or remain attached by a stalk, form a scolex of their own, and bud again. Endogenous budding occurs less commonly and is seen in larger, older cysticerci. Such reproductive capability may result in extensive infections, most frequently involving the subcutis and pleural and peritoneal cavities. In humans, there are occasional reports about intraocular manifestations of cysticercosis.[4]

In non-human primates, there are documented cases of *T. crassiceps* cysticercosis in a black lemur (*Eulemur macaco macaco*)[4] and in a ring-tailed lemur (*Lemur catta*)[10], both of them being prosimian species. *T. crassiceps* cysticercosis in an Old World monkey species like the Nilgiri langur has not been reported before. Interestingly, in the langur, metacestode tissue was not limited to the skeletal muscle, but could also be observed in the left caudal lung lobe, reflecting the proliferative and invasive nature of this parasite.

Other *Taenia* species causing cysticercosis in non-human primates include *Taenia solium*, *Taenia crocutae*, *Taenia hydatigena*, and *Taenia martis*.[2,14] However, infections with the larval cestodes mainly occur in Old

World monkeys and apes, while reports of taeniid cysticercosis in New World monkeys and prosimians are sparse.

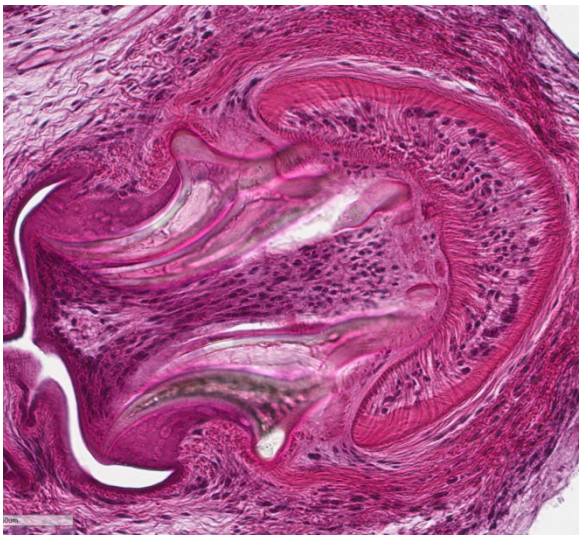

Skeletal muscle, langur: This cestode possesses an armed rostellum with birefingent hooklets. (HE, 400X).

Studies on the immune response elicited by *T. crassiceps* and its antigens in human and mice cells suggest a strong capacity of this parasite to induce a chronic Th2-type response that is primarily characterized by high levels of Th2 cytokines, a low proliferative response in lymphocytic cells, an immature and LPS-tolerogenic profile in dendritic cells, recruitment of myeloid-derived suppressor cells, and by activated macrophages.[11]

JPC Diagnosis: Skeletal muscle: Cysticerci, multiple, with mild chronic granulomatous inflammation, Nilgiri langur (*Trachypithecus johnii)*.

Conference Comment: The contributor provides a striking example of multiple intramuscular cysticerci containing cross sections of taeniid metacestodes, the larval form of cestode tapeworms. The class *Cestoda* has two orders of veterinary importance. The first is *Pseudophyllidea*, comprised of *Diphyllobothrium* sp. and *Spirometra* sp.[15] These parasites grow into extremely large adults, up to 15 meters in humans, lack suckers, and require two intermediate hosts, typically an aquatic copepod and fish. In contrast, the order *Cyclophyllidae*, which contains *Taeniidae*, *Mesocestoididae*, *Dipylidiidae*, *Anoplocephalidae*, and *Hymenolepididae*, require only one intermediate host, usually a land mammal or arthropod.[15] Adult cestodes are normally present in the intestine, hepatic ducts, and/or pancreas of the final definitive host while the larval forms are present within the tissue or body cavities of intermediate hosts. Adult cestodes are broken into segments, called proglottids, which contain both female and male reproductive organs. Cyclophyllidae have four anterior suckers present in both larval and adult cestodes and birefringent armed hooks, depending on the species. The four

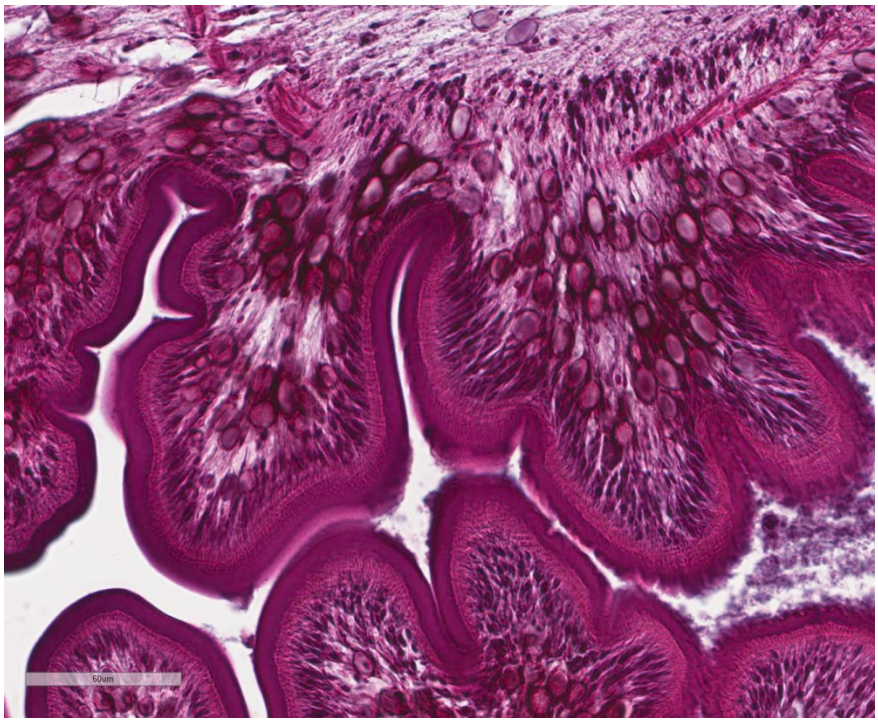

Skeletal muscle, langur. There are numerous oval calcareous corpuscles beneath the tegument and row of somatic cell nuclei. (HE, 400X)

anterior suckers may not all be visible histologically due to varying planes of section.[7,15]

While adult tapeworms are usually of minor significance in their carnivorous definitive hosts, the larval form can migrate into various tissue and cause significant pathology in intermediate or paratenic hosts. Conference participants discussed the four different forms of larval cestodes in tissue section. These include cysticercus, present in this case, strobilocercus, coenurus, and the hydatid cyst.[7,15] The cysticercus is thin walled, fluid filled, and contains a single larva with one inverted scolex and four suckers. The strobilocercus is later in development and contains an evaginated and elongated scolex and develops multiple segments, similar to the adult cestode. Coenurus is similar to cysticercus but contains more than one scolex, all of which can develop into an adult in the definitive host. Hydatid cysts, typical of the genus *Echinococcus* sp., have a bladder with large numbers of small protoscolicies grouped into clusters called brood capsules.[7,15]

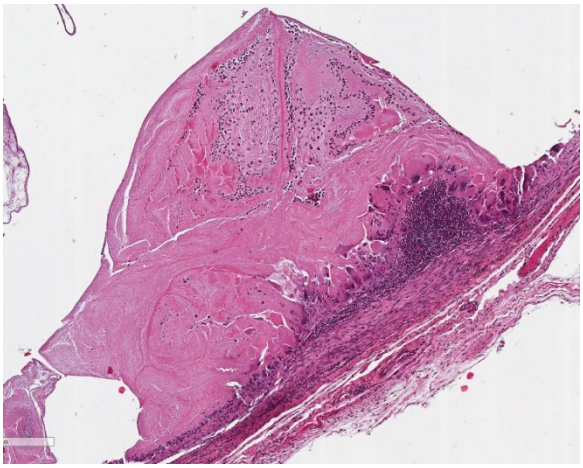

Skeletal muscle, langur. A degenerate cestode is adherent to the wall of one cyst, where it has stimulated an inflammatory response characterized by prominent foreign body macrophages overlying an aggregated of lymphocytes and plasma cells inside the fibrous capsule (HE,63X).

The inflammatory response in this case is mild and composed of a mixed population of histiocytes, multinucleated giant cell macrophages, lymphocytes, and plasma cells with mild atrophy of the adjacent skeletal muscle bundles. The glycoprotein-rich wall of the cysticerci provokes little to no host reaction when intact; however, rupture of the cysticerci results in a severe granulomatous inflammation, fibrosis, and mineralization.[15] Additionally, *Cysticercus longicollis*, the larval form of *Taenia crassiceps* present in this case, undergoes both endogenous and exogenous budding of the cysticerci leading to severe and disseminated infection.[4]

Contributing Institution:
German Primate Center
Kellnerweg 4, 37077
Göttingen, Germany
http://www.dpz.eu/

References:

1. Bröjer CM, Peregrine AS, Barker IK, et al. Cerebral cysticercosis in a woodchuck (*Marmota monax*). *J Wildl Dis*. 2002;38:621-624.
2. Brunet J, Pesson B, Chermette R, et al. First case of peritoneal cysticercosis in a non-human primate host (*Macaca tonkeana*) due to *Taenia martis*. *Parasit Vectors*. 2014;7:422.
3. Dyachenko V, Pantchev N, Gawlowska S, et al. *Echinococcus multilocularis* infections in domestic dogs and cats from Germany and other European countries. *Vet Parasitol*. 2008;157:244-253.
4. Dyer NW, Greve JH. Demar M, et al. Severe *Cysticercus longicollis* cysticercosis in a black lemur (*Eulemur macaco macaco*). *J Vet Diagn Invest*. 1998;10:362-364.

5. Freeman RS. Cestodes of wolves, coyotes and coyote-dog hybrids in Ontario. *Can J Zool*. 1961;39:527-532.
6. Freeman RS. Studies on the biology of *Taenia crassiceps* (Zeder, 1800) Rudolphi, 1810 (*Cestoda*). *Can J Zool*. 1962;40:969-990.
7. Gardiner CH and Poynton SL: Morphologic characteristics of cestodes in tissue section. In: *An atlas of metazoan parasites in animal tissues*: American Registry of Pathology, Washington, D.C. 1999, 50-55.
8. Hoberg EP, Ebinger W, Render JA. Fatal cysticercosis by *Taenia crassiceps* (*Cyclophyllidea: Taeniidae*) in a presumed immunocompromised canine host. *J Parasitol*. 1999;85:1174-1178.
9. Lescano AG, Zunt J. Other cestodes: sparganosis, coenurosis and *Taenia crassiceps* cysticercosis. *Handb Clin Neurol*. 2013;114:335-345.
10. Luzón M, de la Fuente-López C, Martínez-Nevado E, et al. *Taenia crassiceps* cysticercosis in a ring-tailed lemur (*Lemur catta*). *Zoo Wildl Med*. 2010;41:327-330.
11. Peón AN, Espinoza-Jiménez A, Terrazas LI. Immunoregulation by *Taenia crassiceps* and its antigens. *Biomed Res Internat*. 2013. doi: 10.1155/2013/498583.
12. Schuster R, Heidecke D, Schierhorn K. Contribution to the parasite fauna of local hosts. On the endoparasitic fauna of *Felis silvestris*. *Appl. Parasitol*. 1993;34:113-120.
13. Seesee FM, Sterner MC, Worley DE. Helminths of the coyote (*Canis latrans Say*) in Montana. J Wildl Dis. 1983;19:54-55.
14. Strait K, Else JG, Eberhard ML. Parasitic diseases of nonhuman primates. In: Abee CR, Mansfield K, Tardif S, Morris T, eds. 2nd ed. *Nonhuman primates in biomedical research: diseases*. San Diego, USA: Academic Press; 2012:197-298.
15. Uzal FA, Plattner BL, Hostetter JM. Alimentary system. In: Maxie MG ed. In: *Jubb Kennedy and Palmer's Pathology of Domestic Animals*. Vol 2. 6th ed. Philadelphia, PA: Elsevier Saunders; 2016:221-225.
16. Wüschmann A, Garlie V, Averbeck G, et al. Cerebral cysticercosis by *Taenia crassiceps* in a domestic cat. *J Vet Diagn Invest*. 2003;15:484-488.

CASE IV: 130055 (JPC 4083952).

Signalment: Adult male cynomolgus macaque (*Macaca fascicularis*).

History: This macaque was in a study to determine the efficacy of a novel therapeutic drug for treating Marburg virus (MARV) infection. All of the monkeys in this study were inoculated subcutaneously with MARV and then once daily intramuscular treatments with either saline (control group) or different doses of the therapeutic drug (experimental groups) began. This animal was in one of the experimental groups and it was found dead on Day 11 after viral challenge.

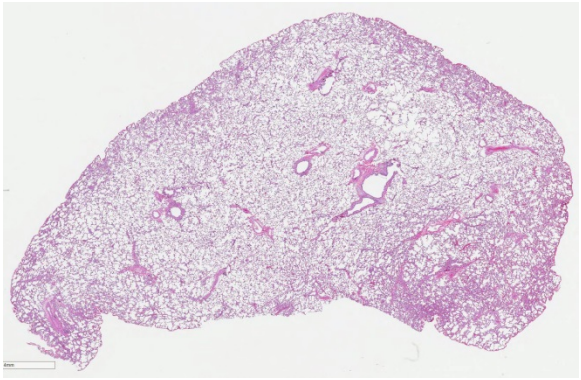

Lung, cynomolgus macaque. At low magnification, the submitted section of lung appears well-aerated with no gross lesion. (HE, 5x).

This monkey was part of a research project conducted under an IACUC approved protocol in compliance with the Animal Welfare Act, PHS Policy, and other federal statutes and regulations relating to animals and experiments involving animals. The facility where this research was conducted is accredited by the Association for Assessment and Accreditation of Laboratory Animal Care, International and adheres to principles stated in the 8th edition of the Guide for the Care and Use of Laboratory Animals, National Research Council, 2011.

Gross Pathology: The mucosa of the rectum and distal 20 cm of the colon was diffusely hemorrhagic. The liver was enlarged (~1.5 X), pale tan, and markedly friable. The spleen was also friable. Other organs were unremarkable.

Laboratory results: None

Histopathologic Description: Lung (right inferior lobe): Multifocally within alveoli and often attached to the alveolar septa, there are low numbers of multinucleated giant cells, measuring up to 100 µm in diameter, most of which contain intra-cytoplasmic aggregates of pale blue-gray amorphous to spicular refractile material. The interstitium also contains scattered aggregates of low numbers of histiocytes containing intracytoplasmic brown-black finely-granular material. Many blood vessels contain numerous intraluminal mononuclear leukocytes (monocytes).

Contributor's Morphologic Diagnoses:

1. Lung; intravascular leukocytosis (monocytic), moderate
2. Lung; multifocal histiocytic (multinucleated giant cell) alveolitis, mild, with intracytoplasmic crystalline foreign bodies
3. Lung; multifocal interstitial anthracosilicosis, minimal

Contributor's Comment: The timing of this monkey's death is within the usual interval (i.e. 7-11 days) that cynomolgus macaques die after experimental exposure to a lethal dose of MARV. There were histologic lesions in the liver, spleen, adrenal glands, tonsils, and lymph nodes of this monkey that were caused by MARV infection; these organs are considered "target organs" for the virus.[7] Immuno-histochemistry (IHC) revealed MARV antigen in every organ examined from this animal. The histologic findings and IHC

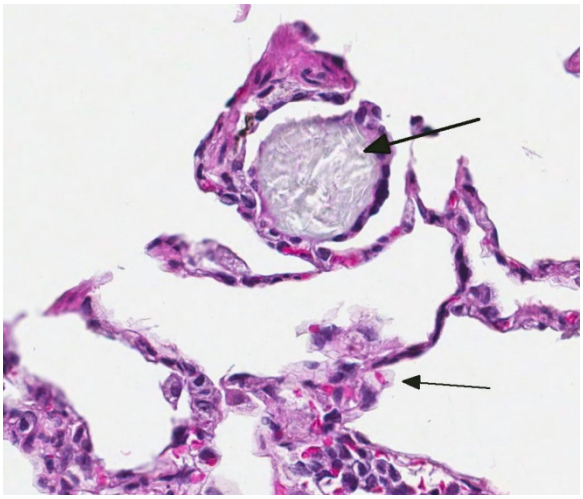

Lung, cynomolgus macaque. At high magnification, alveolar histiocytes and multinucleated giant cell macrophages contain vary amounts of a granular amphophilic crystalline protein within their cytoplasm. (HE, 400X)

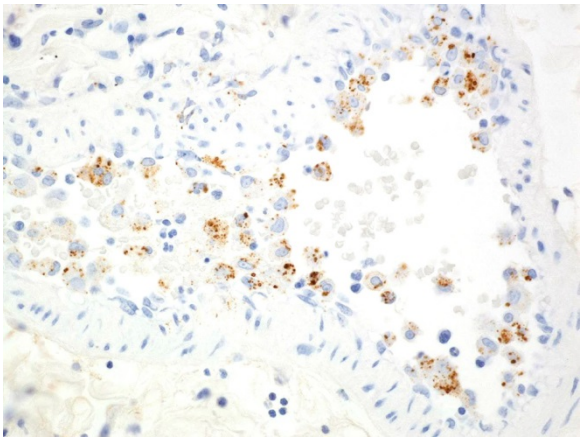

Lung, cynomolgus macaque. Immunohistochemistry demonstrates that many of the monocytes in the lumen of a pulmonary artery contain MARV antigen (brown stain) within their cytoplasm. Immunoperoxidase stain with hematoxylin counterstain. (anti-MARV, 400X) (Photo courtesy of: US Army Medical Research Institute of Infectious Diseases, Pathology Division, Fort Detrick, MD http://www.usamriid.army.mil/)

results confirmed that this macaque died from a disseminated MARV infection. Although the exact cause of the intestinal bleeding noted at necropsy was not determined, this was most likely associated with MARV-induced coagulopathy; disseminated intravascular coagulopathy (DIC) occurs commonly in primates (including humans) infected with viruses in the family *Filoviridae* (i.e. ebolaviruses and MARV).[6,7]

The monocytic leukocytosis noted within pulmonary blood vessels of this monkey is attributable to the viral infection. IHC revealed abundant MARV antigen in many of these monocytes. Cells of the monocyte-macrophage system are infected very early during the course of filovirus infection and are primarily responsible for disseminating the viruses throughout the body.[5,7]

The presence of multinucleated giant cells within alveoli and/or attached to alveolar septa of this monkey was an unexpected finding and was unrelated to the MARV infection. This lesion was seen in the right inferior lung lobe but not in the other lung lobes that were examined histologically. These giant cells were an inflammatory response to the presence of intra-alveolar crystalline foreign material; the foreign material was initially phagocytized by macrophages that then fused to form large multinucleated cells.[1] IHC revealed that some of the giant cells also contained intracytoplasmic MARV antigen.

The composition of the crystalline foreign material, which is anisotropic in polarized light, is unknown. However, a review of the medical records for this monkey revealed that approximately one month before the initiation of the MARV study, this animal had been administered an oral suspension of Pepcid® once a day for three consecutive days. It is possible that some of the suspension was aspirated into the right inferior lung lobe (which is a dependent lung lobe in a primate). The active ingredient in the Pepcid® suspension is

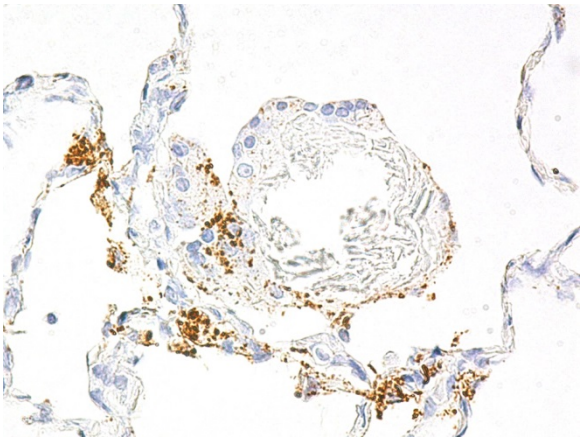

Lung, cynomolgus macaque. . Immunohistochemistry demonstrates MARV antigen within the cytoplasm of interstitial fibroblasts, alveolar macrophages, and a multinucleated giant cell that also contains crystalline material. Immunoperoxidase stain with hematoxylin counterstain. (anti-MARV, 600X) (Photo courtesy of: US Army Medical Research Institute of Infectious Diseases, Pathology Division, Fort Detrick, MD http://www.usamriid.army.mil/)

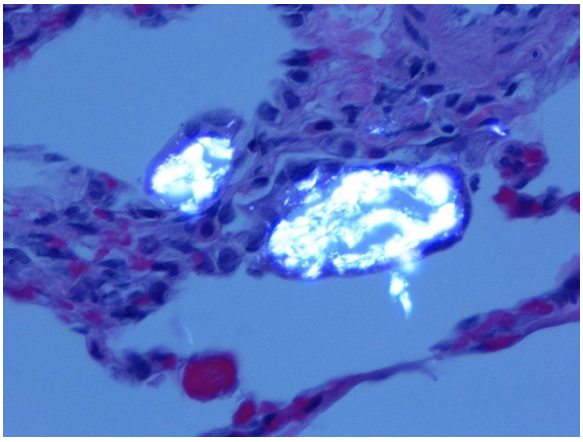

Under polarized light, the crystalline foreign material within alveolar giant cells is anisotropic Hematoxylin and eosin stain. (HE, 400X) (Photo courtesy of: US Army Medical Research Institute of Infectious Diseases, Pathology Division, Fort Detrick, MD http://www.usamriid.army.mil/)

famotidine, which is a crystalline compound, and inactive ingredients include microcrystalline cellulose.[2] Overall, the foreign-body alveolitis was a very mild and clinically insignificant lesion that did not affect the pathogenesis or outcome of the MARV challenge. Anthracosilicosis is a common finding in adult macaques and is usually an incidental lesion (as in this case).

Note: Opinions, interpretations, conclusions, and recommendations are those of the author and are not necessarily endorsed by the U.S. Army.

JPC Diagnosis: Lung: Alveolitis, histiocytic, multifocal, mild with low numbers of multinucleated giant cell macrophages and abundant intracytoplasmic crystalline protein, cynomolgus macaque, *Macaca fascicularis*.

Conference Comment: This interesting case was submitted by the conference moderator and presented participants with a diagnostic challenge to identify the origin of the amphophilic, anisotropic, and crystalline material within macrophages and multinucleated giant cells in this section of lung. Most favored the diagnosis of pneumoconiosis, which is a lung disease secondary to inhalation of inorganic particulate material, such as asbestos or silica.[4] Readers are encouraged to review Wednesday Slide Conference 2015 Conference 3 Case 4 for a review and fascinating discussion of silicate pneumoconiosis in a horse from California. Silica dusts typically generate a granulomatous inflammatory response with fibrosis, not seen in this case. Additionally, asbestos fibers in the lung are linear and beaded with globoid ends, also not a feature of this case.[4]

There have been sporadic reports of kaolin aspiration in nonhuman primates causing similar lesions to this case.[3,8,9] Kaolin is a common crystalline compound found in antidiarrheal medication as well as a variety of other products, such as toothpaste, ceramics, soap, and paint. Initially, the terminal bronchioles and alveoli of animals exposed to aspirated or inhaled kaolin are acutely inflamed, but by day seven post exposure, there is only mild mononuclear inflammation, type II pneumocyte hyperplasia, and aggregates of anisotropic dust-laden macrophages and multinucleated cells.[9] This is in contrast to silica inhalation, which induces a progressive granulomatous and fibrotic response.[4,9] The route of exposure of most reported cases in nonhuman primates is aspiration of oral antidiarrheal medication.[8] Kaolin can also cause granulomas containing numerous macrophages filled with birefringent crystals if delivered subcutaneously.[3]

To this author's knowledge, there have been no reported cases of famotidine aspiration causing aspiration alveolitis in humans or animals; although the pathogenesis posited by the contributor is plausible. Unfortunately, given strict regulations on

tissue handling of Marburg (MARV)-infected animals, a tissue block was unable to be submitted for further chemical analysis. Regardless of the origin of the crystalline proteinaceous material, conference participants agreed that this lesion is likely unrelated to MARV infection and is an incidental finding.

Contributing Institution:
US Army Medical Research Institute of Infectious Diseases
Pathology Division
Fort Detrick, MD
http://www.usamriid.army.mil/

References:

1. Ackermann MR. Inflammation and healing. In: Zachary JF and McGavin MD, ed. *Pathologic Basis of Veterinary Disease.* 5th ed. St Louis, Mo: Elsevier, 2012:89-146.
2. Anonymous. Pepcid oral suspension. Retrieved from: http://www.drugs.com/pro/pepcid-oral-suspension.html.
3. Baskin GB. *Pathology of nonhuman primates*. 1993. New Orleans: Tulane Regional Primate Research Center.
4. Caswell JL, Willims KJ. Respiratory system. In: Maxie MG ed. *Jubb, Kennedy, and Palmer's pathology of domestic animals.* Vol 2. 6th ed. St. Louis, Missouri: Elsevier; 2016:518.
5. Geisbert TW, Hensley LE, Larsen T, et al. Pathogenesis of ebola hemorrhagic fever in cynomologus macaques. Evidence that dendritic cells are early and sustained targets of infection. *Am J Path*. 2003; 163(6):2347-2370.
6. Geisbert TW, Young HA, Jahrling PB, et al. Pathogenesis of ebola hemorrhagic fever in primate models. Evidence that hemorrhage is not a direct effect of virus-induced cytolysis of endothelial cells. *Am J Path*. 2003; 163(6): 2371-2382.
7. Hensley LE, Alves DA, Geisbert JB, et al. Pathogenesis of Marburg hemorrhagic fever in cynomolgus macaques. *J Inf Dis*. 2011; 204 (Suppl 3): S1021-S1031.
8. Herman SJ, Olscamp GC, Weisbrod GL. Pulmonary kaolin granulomas. *J Can Assoc Radiol*. 1982; 33(4):279-280.
9. Vallyathan V, Schwegler D, et al. Comparative in vitro cytotoxicity and relative pathogenicity of mineral dusts. *Ann Occup Hyg*. 1988; 32:279-289

Self-Assessment - WSC 2016-2017 Conference 15

1. *Beuavaria bassiana* is a soil fungus that most often causes infections in?
    a. Fish
    b. Birds
    c. Reptiles
    d. Insects

2. Recent evidence has placed the causative agent of boid inclusion body disease in which of the following families?
    a. Herpesviridae
    b. Arenaviridae
    c. Papillomaviridae
    d. Polyomaviridae

3. Which of the following clinical signs is not seen with boid inclusion body disease in pythons?
    a. Opithotonus
    b. Regurgitation
    c. Head tremors
    d. Anisocoria

4. Which of the following is not true concerning *Taenia crassiceps*?
    a. Unlike other *Taenia* species, *T. crassiceps* is able to proliferate by exogenous and endogenous budding.
    b. The definitive host is a canid.
    c. The most severe lesions of this cestode are seen in the definitive host.
    d. The presence of this parasite elicits a chronic Th2-type response.

5. Which of the following, when inhaled, typically causes a progressive fibrotic response?
    a. Kaolin
    b. Famotidine
    c. Carbon
    d. Silica

Joint Pathology Center

Veterinary Pathology Services

WEDNESDAY SLIDE CONFERENCE 2016-2017

C o n f e r e n c e 16

25 January 2017

CASE I: AR-14-1021 (JPC 4066394).

Signalment: Eight-month-old, Dorset ewe, (*Ovis aries*).

History: This ewe was enrolled in a research study in which it underwent surgery and MRI the following day, both under general anesthesia. The ewe initially recovered normally, displaying brief weakness in the hindlimbs immediately after surgery. However, over the next two weeks, it gradually became dull and lethargic, dehydrated, inappetent, and weakened despite supportive care. The animal was found recumbent, hypothermic, tachycardic, and dyspneic 13 days after surgery and died before it was able to be euthanized.

Gross Pathology: The major gross lesion was in the lungs. The right cranial lung lobe was half normal size, mottled dark red to black, and firm on palpation. The cranial aspect of the right middle lung lobe appeared similarly. Dissection of the bronchial tree did not reveal the presence of foreign material. Additionally, several ulcers, up to 1 x 2 cm, were present in the trachea.

Gross Morphologic Diagnosis: Broncho-pneumonia, multifocal, subacute, severe, necrotizing.

Laboratory results: Bacterial culture of the lung yielded a pure culture of *Trueperella pyogenes.*

Histopathologic Description: The lung is markedly hypercellular, owing to filling of alveoli by degenerate inflammatory cells, amorphous and fibrillar eosinophilic material (edema and fibrin, respectively), basophilic streaming nuclear and eosinophilic cytoplasmic debris, and myriad gram-positive bacterial rods. In some regions, well-defined areas with architectural preservation without cellular

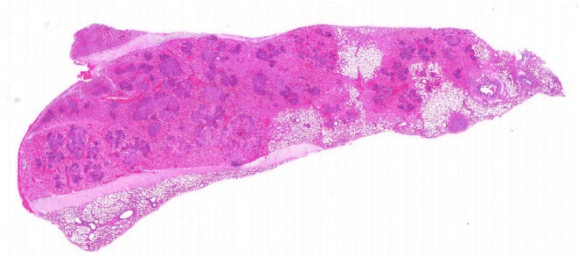

Lung, ewe. At subgross magnification – there is diffuse severe alveolar edema and hemorrhage, marked intraseptal edema, and numerous well-demarcated areas of cellular infiltrate and necrosis. (HE, 5X)

detail (coagulative necrosis) are present. Bronchi and bronchiole lumina frequently contain abundant bacteria and sloughed bronchial epithelium. Interlobular septa are thickened up to 2mm wide by fibrin and edema, and blood vessels were congested and contained bacteria. The pleura is expanded up to 3x normal with blood.

Contributor's Morphologic Diagnoses: Bronchopneumonia, diffuse, subacute, severe, necrotizing, with myriad gram-positive bacteria.

Contributor's Comment: All findings in this case were consistent with bronchopneumonia caused by *Trueperella pyogenes* (formerly *Arcanobacterium pyogenes),* a gram-positive non-motile, non-sporeforming, short, rod-shaped bacterium.[6] *Trueperella pyogenes* is one of the most common opportunistic pathogens in domestic livestock and is often commensal flora in the mammary gland, upper respiratory, urogenital, and gastrointestinal tracts.[6,10] Although *T. pyogenes* can act as a primary pulmonary pathogen, infection usually follows physical or microbial trauma which overcomes the pulmonary defense mechanisms, allowing for colonization of the lungs.[1,8] The pneumonia was initially suspected to be due to aspiration shortly after recovery from anesthesia, but foodstuff was not present in the respiratory tract. The reason for the infection was likely due to a combination of stressors, including what was interpreted as intubation-associated ulceration of the trachea.

Trueperella pyogenes produces and utilizes a variety of virulence factors to colonize, damage, and persist within a variety of tissues in the host. The most important factor is pyolysin (PLO), a cytolysin, which is able to bind to and create pores in the cell membranes of erythrocytes,

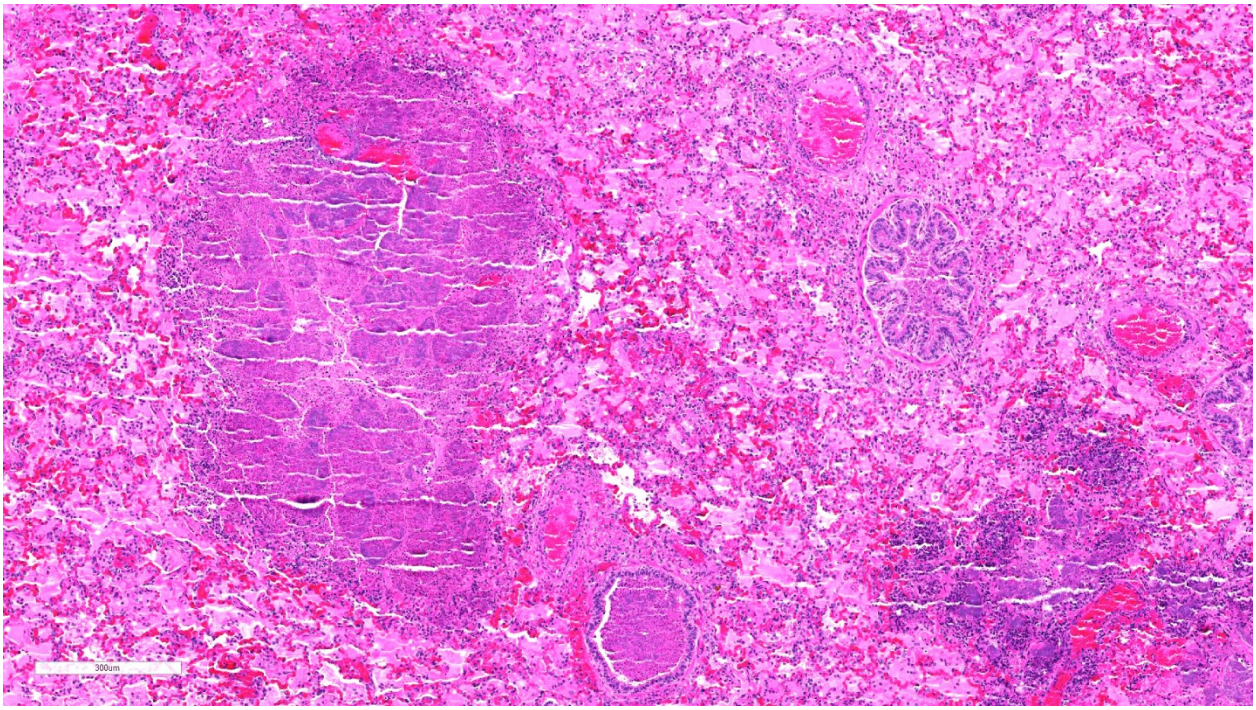

Lung, ewe. Multifocally airways and alveoli contain varying combinations and concentrations of necrotic debris, large colonies of bacilli, edema, and hemorrhage. (HE, 88X)

polymorphonuclear cells, and macrophages resulting in cell lysis.[6] *Trueperella pyogenes* mutants lacking the PLO gene were unable to cause an intraperitoneal infection in mice injected with 10^8 bacteria, whereas replacement of the PLO gene to the *T. pyogenes* mutants restored full virulence.[5] Additional virulence factors used by *T. pyogenes* include fimbriae[13], extracellular matrix binding proteins specific for collagen[4], fibrinogen, fibronectin[5], and exoenzymes including DNases[11], proteases[12], and neuraminidases[7] which degrade host nucleic acids, proteins, and sialic acid residues, respectively.

Note: Multiple different tissue sections of lung were used for the slides submission; therefore, not all the participants will receive similar serial microslide sections.

JPC Diagnosis: Lung: Bronchopneumonia, necrotizing and fibrinosuppurative, multifocal to coalescing, severe, with marked alveolar and septal edema and numerous large colonies of bacilli, Dorset sheep, *Ovis aries*.

Conference Comment: This case demonstrates the characteristic gross and histologic lesions associated with bacterial bronchopneumonia. Conference participants described the suppurative inflammation filling bronchi and bronchioles surrounded by multifocal to coalescing areas of necrosis, and readily identified numerous large colonies of bacilli within the areas of inflammation. Participants discussed the differential diagnosis for large colony forming bacteria in tissue section to include: *Yersinia* sp, *Actinomyces* sp., *Actinobacillus* sp., *Corynebacterium* sp, *Staphylococcus* sp., *Streptococcus* sp., and *T. pyogenes*. *Trueperella pyogenes* is one of the most common opportunistic pathogens present on the mucosal surfaces of domestic animals.[1,2,5,8] The bacterium induces suppurative inflammation within a wide

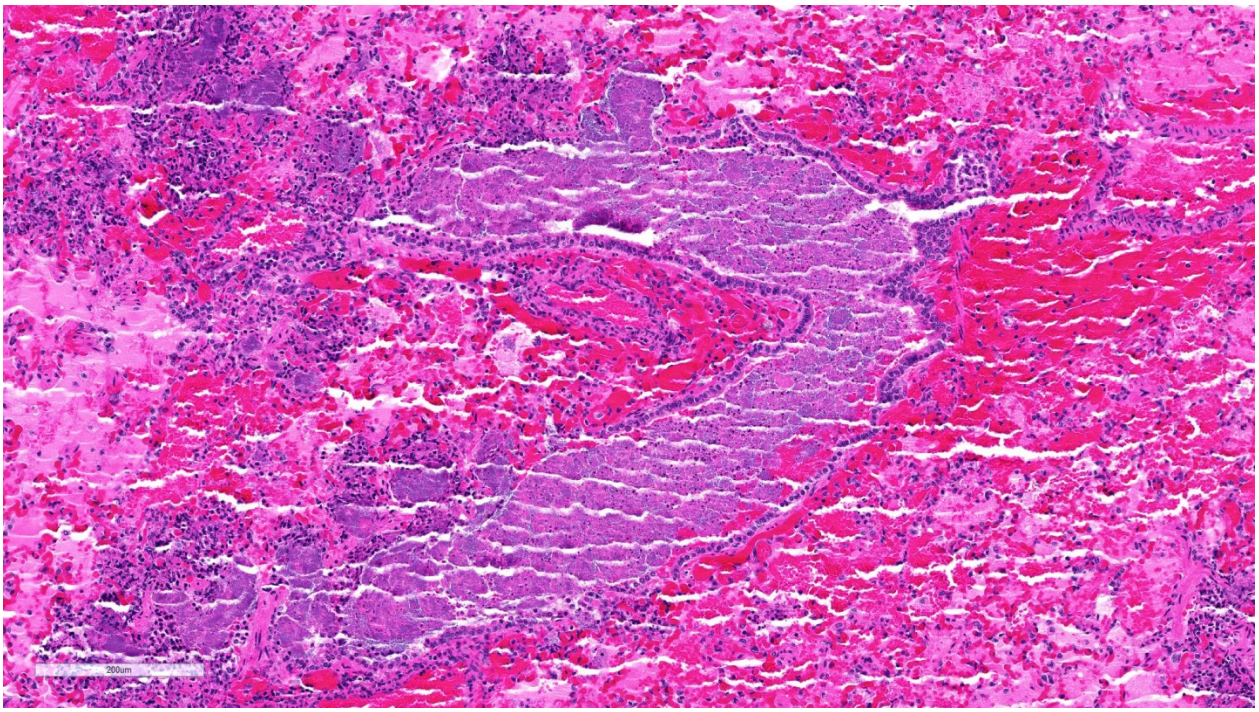

Lung, ewe. There is extensive involvement of airways and necrosis is primarily relegated to the adjacent alveoli, suggesting an aerogenous entry for the causative agent. (HE, 96X)

variety of organs and is an important cause of abortion, arthritis, endocarditis, mastitis, osteomyelitis, and pneumonia resulting in significant losses in production animals.[2,4] Additionally, *T. pyogenes* is widespread in the wild animal population and has been reported as an important cause of cerebral abscesses in young male white-tailed deer as a consequence of antler development and conspecific aggression between bucks. Mortality can reach up to 35% in affected free-ranging adult male deer.[3]

As mentioned by the contributor, while *T. pyogenes* can be a primary pathogen, it is usually associated with physiologic trauma to a mucosal membrane, concurrent primary infection, or immune suppression.[1,2,3,8] As postulated by the contributor in this case, there well may be an association with placement of the endotracheal tube. Other common commensal organisms of the ruminant upper respiratory tract that can cause opportunistic bronchopneumonia include *Mannheimia haemolyica*, *Pasteurella multocida*, and *Bibersteinia trehalosi*. Causes of primary infectious pneumonia in sheep include parainfluenza virus 3, respiratory syncytial virus, and *Bordetella parapertussis*, which can predispose sheep to secondary infection by the commensal bacteria mentioned above.[1,3,8] *Mycoplasma ovipneumoniae* is another important primary etiologic agent involved in chronic enzootic pneumonia; also known as chronic non-progressive pneumonia, it is a multi-factorial disease complex affecting lambs less than one-year-old. *Mycoplasma ovipneumoniae* usually causes a mild, subclinical infection that results in poor growth unless complicated by stressors such as over-crowding, inclement weather, or poor air quality.[1,2,3,8]

Another primary cause of pneumonia in sheep includes the maedi-visna virus, which

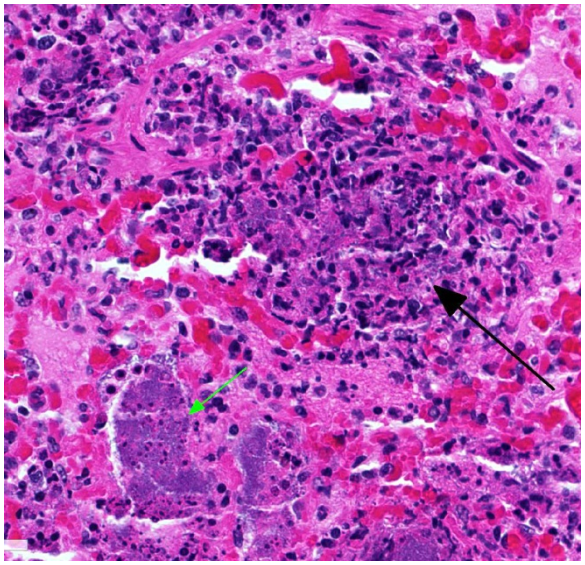

Lung, ewe. Alveoli are filled with a combination of degenerate epithelium and heterophils with streaming nuclear material (consistent with "oat cells") (black arrow) and large colonies of bacilli predominate in some alveoli (green arrow.)

results in lifelong persistent viral infection and leads to ovine progressive pneumonia (OPP), encephalitis, arthritis, and mastitis in sheep. This lentivirus is a member of the family *Retroviridae*, and is closely related to caprine arthritis-encephalitis virus. First reported in Iceland, the "maedi" (respiratory form) occurs in sheep older than three years, while the "visna" (neurologic form) occurs in younger sheep.[1,9] The respiratory form is characterized by interstitial pneumonia with prominent perivascular and peribronchial lymphoid nodules. This slowly progressive pneumonia is often complicated by secondary bacterial infection, especially *T. pyogenes*.[1] Peste des petits ruminants (PPRV), a morbillivirus, has also been reported to cause primary respiratory disease in small ruminants in Africa and parts of Asia. This virus primarily affects the cranioventral lung lobes and causes a bronchointerstitial pneumonia.[1,8,9]

Contributing Institution:
Wake Forest School of Medicine

Department of Pathology/Comparative Medicine
Medical Center Boulevard
Winston Salem, NC 27157-1040
http://www.wakehealth.edu/Comparative-Medicine/

References:

1. Caswell JL, Williams KJ. Respiratory system. In: Maxie MG, ed. *Jubb, Kennedy, and Palmers Pathology of Domestic Animals*. 6th ed. Vol. 2. Philadelphia, PA: Elsevier; 2016:557-560.
2. Cohen BS, Belser EH, et al. Isolation and genotypic characterization of *Trueperella* (*Arcanobacterium*) *pyogenes* recovered from active cranial abscess infections of male white-tailed deer (Odocoileus virginianus). *J Zoo Wildl Med*. 2015; 46(1):62-67.
3. Dassanayake RP, Shanthalingam S, Herndon CN, et al. *Mycoplasma ovipneumoniae* can predispose bighorn sheep to fatal *Mannheimia haemolytica*pneumonia. *Vet Microbiol*. 2010; 145:354-359.
4. Esmay PA, et al. The *Arcano-bacterium pyogenes* collagen-binding protein, CbpA, promotes adhesion to host cells. *Infect Immun*. 2003; 71(8):4368-74.
5. Jost BH, Billington SJ. *Arcano-bacterium pyogenes*: Molecular pathogenesis of an animal opportunist. *Antonie Van Leeuwenhoek*. 2005; 88(2):87-102.
6. Jost BH, Songer JG, Billington SJ. An *Arcanobacterium (Actinomyces) pyogenes* mutant deficient in production of the pore-forming cytolysin pyolysin has reduced virulence. *Infect Immun*. 1999; 67(4):1723-8.
7. Jost BH, Songer JG, Billington SJ. Cloning, expression, and characterization of a neuraminidase gene from *Arcanobacterium pyogenes*. *Infect Immun*. 2001; 69(7):4430-7.
8. Lopez A, Martinson SA. Respiratory system, mediastinum, and pleurae. In: *Pathologic Basis of Veterinary Disease*. Zachary JM ed. 6th ed. St. Louis: Elsevier; 2017:537-540.
9. MacLachlan NJ, Dubovi EJ, eds. *Fenners Veterinary Virology*. 4th ed. London, UK: Elsevier; 2011:267-268,308-323.
10. Queen C, Ward AC, Hunter DL. Bacteria isolated from nasal and tonsillar samples of clinically healthy Rocky Mountain bighorn and domestic sheep. *J Wildl Dis*. 1994; 30(1):1-7.
11. Ramos, CP, Foster G, Collins MD. Phylogenetic analysis of the genus Actinomyces based on 16S rRNA gene sequences: description of *Arcanobacterium phocae* sp. nov., *Arcanobacterium bernardiae* comb. nov., and *Arcanobacterium pyogenes* comb. nov. *Int J Syst Bacteriol*, 1997; 47(1):46-53.
12. Takeuchi S, Kaidoh T, Azuma R, Assay of proteases from *Actinomyces pyogenes* isolated from pigs and cows by zymography. *J Vet Med Sci*. 1995; 57(5):977-9.
13. Yanagawa R, Honda E Presence of pili in species of human and animal parasites and pathogens of the genus *Corynebacterium*. *Infect Immun*. 1976; 13(4):1293-5.

CASE II: Case 2 (JPC 4085015).

Signalment: Six-month-old, male, Tonkinese cat, (*Felis catus*).

History: The cat presented for further investigation of a vestibular ataxia, head tremors, inappetence, and lethargy. The cat was in poor body condition compared to its littermate and had previously been found to be pyrexic. Neurological examination findings were consistent with a central vestibular syndrome. MRI of the brain revealed marked dilatation of the third and fourth ventricles and mild dilatation of the lateral ventricles. There was marked contrast enhancement of the ependymal lining and meninges, consistent with feline infectious peritonitis and obstructive hydrocephalus. Cerebellar herniation was present with caudal displacement of the cerebellar vermis through the foramen magnum, consistent with elevated intracranial pressure. A provisional diagnosis of feline infectious peritonitis (FIP) was made. Due to a grave prognosis, the cat was euthanized and submitted for necropsy examination.

Gross Pathology: An increased volume of clear fluid drained from the cranium as the brain was removed and there appeared to be diffuse flattening of the cortical gyri. The brain was dissected following fixation and there was moderate dilation of the third, fourth and lateral ventricles.

Laboratory results: Feline coronavirus antibody titer was extremely high; CSF (post mortem) showed a marked, mixed pleocytosis with neutrophilic predominance and markedly increased protein concentration.

Histopathologic Description: Brain: Sections of forebrain, midbrain, cerebellum and brainstem are examined. Variably within the examined sections the meninges, choroid plexus and ependyma are multifocally and extensively expanded by dense infiltrates of lymphocytes, plasma cells, macrophages and rare viable and degenerate neutrophils. There is prominent perivascular cuffing, predominantly targeting veins, of periventricular and meningeal blood vessels by lymphocytes, macrophages, plasma cells and occasional viable and degenerate neutrophils. The inflammatory infiltrate extends into both vascular walls and beyond the Virchow-Robin spaces into the adjacent neuropil. There is a mild to moderate gliosis within the adjacent neuropil and periventricular white matter contains variably-sized extracellular clear spaces (edema). Ependymal cells lining the ventricles appear mildly elongate with disruption and increased spacing between cells.

Cat, fourth ventricle. There is marked hypercellularity surrounding the 4th ventricle and brainstem meninges (black arrow), as well as expansion of the choroid plexus (green arrow.) (HE, 5X)

Multifocally, there is necrosis of the ventricular lining with deposition of fibrin.

Immunohistochemistry:
Immunohistochemical labeling for feline coronavirus antigen identified scattered, large, foamy round cells (macrophages) which labeled positively for Coronavirus antigen within the lesions in the brain tissue.

Contributor's Morphologic Diagnoses: 1. Brain: multifocal, marked, pyo-granulomatous and lymphoplasmacytic meningoencephalitis with vasculitis and perivasculitis, ventriculitis, choroiditis and ependymitis
2. Brain: moderate acquired hydrocephalus

Contributor's Comment: Feline coronaviruses (FCoVs) are enveloped, single-stranded, positive-sense RNA viruses that belong to the *Coronaviridae* family, *Alphacoronavirus* genus and exist as two pathotypes, feline infectious peritonitis virus (FIPV) and feline enteric coronavirus (FECV).[1,3] Despite FCoVs being ubiquitous in the environment, with a prevalence of more than 90% of cats in multicat households, feline infectious peritonitis (FIP) is sporadic, with young, entire male, purebreed cats most commonly affected[1]. Feline enteric coronavirus is generally considered avirulent, however, can be associated with hemorrhagic enteritis and diarrhoea[3] and affected cats may become persistently infected and continue to shed virus. In contrast, FIPV results in severe, systemic disease and is a common cause of neurologic disorders in young cats.[2]

Feline coronavirus is generally transmitted via the fecal-oral route following which it infects enterocytes, eventually being restricted to the caecum and colon.[1] Analysis of FECVs and FIPVs suggests a

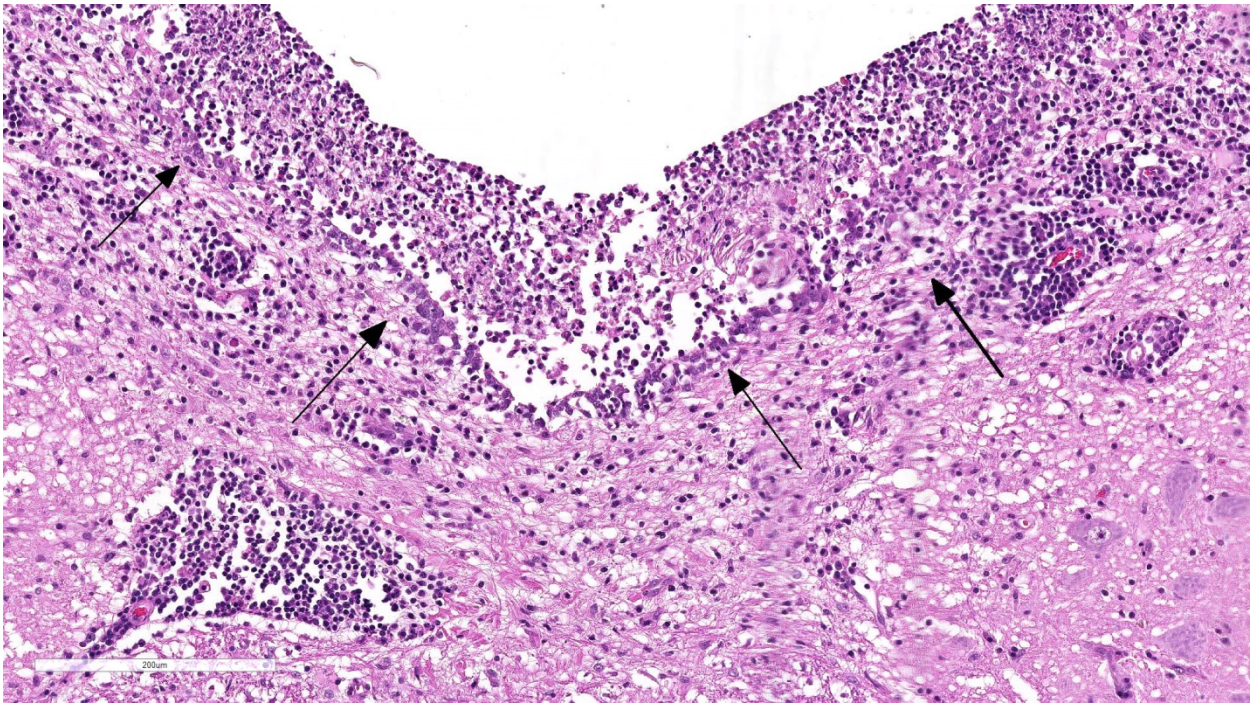

Cat, fourth ventricle and underlying brainstem. The lumen of the fourth ventricle contains numerous degenerate neutrophils and macrophages, admixed with polymerized fibrin and cellular debris. The ependyma (black arrows) is multifocally ulcerated. Brainstem vessels are surrounded by large numbers of lymphocytes and plasma cells. (HE, 196X)

complex scenario involving several gene mutations to result in increased virulence[1,3]. Feline infectious peritonitis viruses appear to have an increased ability to replicate in macrophages and monocytes and result in systemic disease.[1] Virus-infected macrophages localize to small and medium sized veins within the serosa and damage endothelial cells with the subsequent immune response resulting in a vasculitis. A strong cell-mediated response is protective against FIP, whereas a weak cell-mediated response results in the 'dry' form of the disease. The 'wet' form of disease results from a lack of cell-mediated immune response to the virus. Both type III and type IV hypersensitivity responses have been implicated in the pathogenesis of FIP.[5]

Feline infectious peritonitis is often distinguished by a 'wet' or effusive form and a 'dry' non-effusive form with a proportion of cases showing a combination of the two. Typical gross findings associated with the effusive form of FIP include a fibrinous and granulomatous peritonitis, protein rich effusions and visceral granulomatous inflammatory foci. In 60% of non-effusive cases of FIP there is involvement of the eyes and/or CNS with or without granulomatous lesions in the thoracic and abdominal viscera and frequently in the absence of a grossly apparent peritonitis[2]. Gross lesions in the brain are often unapparent, however may include thickening and opacity of the meninges, and an obstructive hydrocephalus, as seen in this case. Proteinaceous material within the ventricular system may be visible as grey-blue gelatinous material.[4] Clinical signs associated with FIP are often vague and include pyrexia, lethargy and inappetence with additional changes dependent on the distribution of tissues affected.[2]

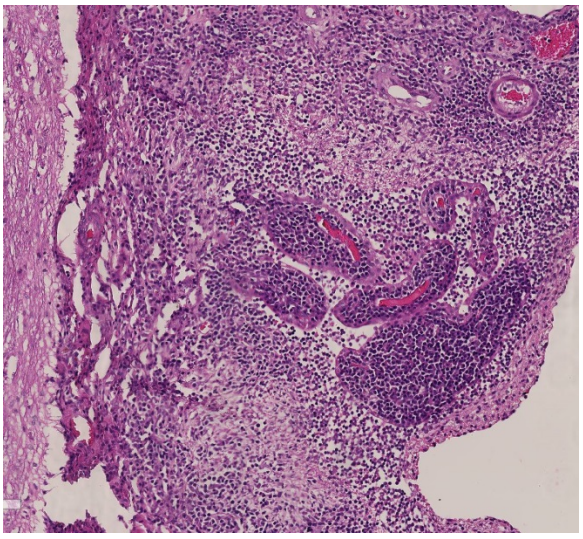

Cat, brainstem meninges: The meninges are expanded by large numbers of macrophages, lymphocytes and plasma cells. Lymphocytes and plasma cells have a marked perivascular distribution. (HE, 100X)

The characteristic microscopic findings associated with FIP include a vasculitis and perivasculitis, predominantly affecting small to medium sized venules.[3] A high proportion of macrophages alongside variable numbers of neutrophils, lymphocytes and plasma cells infiltrate and surround vessels. Vascular necrosis with thrombosis and infarction may also occur.[2] Feline infectious peritonitis may be suspected based on the signalment, compatible clinical signs, and identification of pathognomonic gross and histologic lesions. Identification of viral antigen in lesions using immunohistochemistry or real time RT-PCR is confirmatory for a diagnosis of FIP.[3]

JPC Diagnosis: Cerebrum, brainstem: Meningoencephalitis, lymphoplasmacytic and histiocytic, perivascular, diffuse, moderate to marked with lymphoplasmacytic and histiocytic choroiditis and phlebitis, Tonkinese cat, *Felis catus*.

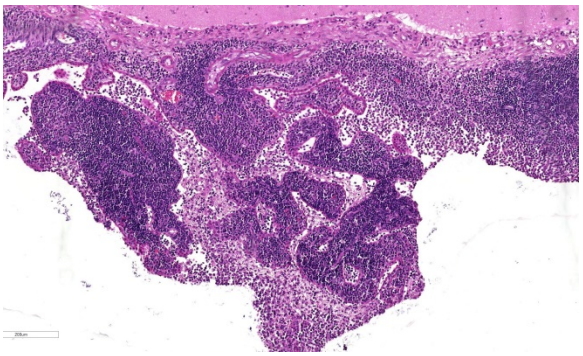

Cat, choroid plexus, fourth ventricle. The vascular bed of the choroid plexus is also markedly expanded by numerous lymphocytes and plasma cells. (HE, 100X)

Conference Comment: Although there is some moderate slide variability, we thank the contributor for providing an excellent example and review of feline infectious peritonitis (FIP), a disease that is caused by a mutated feline enteric coronavirus (mutated FCoV). Given the history provided by the contributor, this case is likely more consistent with the non-effusive form of FIP with lesions restricted to the central nervous system, although the distinction between the wet and dry form is somewhat arbitrary and the disease likely represents a continuum rather than two distinct clinical forms.[3] As mentioned by the contributor, neurologic signs due to encephalitis or meningitis are present in approximately 60% of all FIP cases.[4,5] Chronic ventriculitis, choroiditis, and ependymitis causes outflow obstruction of the cerebrospinal fluid from the ventricular system of the brain leading to marked dilation of the ventricles.[5] This dilation of the ventricles leads to a compression atrophy of the proximate neuroparenchyma because of the lack of expansibility within the skull. The resulting increased intracranial pressure then results in both hydrocephalus and caudal displacement and herniation of the cerebellum through the foramen magnum, present in this case. FIP remains as one of the most common causes of infectious death in cats with Bengals, Birmans, Himalayans, ragdolls, and Rexes significantly overrepresented for the development of the disease.[3]

A recent publication in *Veterinary Pathology* by Kiper and Meli[1] outlined three key features as prerequisites for the development of FIP: a) systemic infection with virulent mutated FCoV, b) effective viral replication in circulating monocytes, and c) activation of mutated FCoV-infected monocytes.[1] Although avirulent FCoV is readily transmitted via the fecal-oral route, most believe that the mutated virulent form is not transmitted horizontally, but is rather the result of spontaneous mutation within each cat that develops FIP. The hallmark lesion of FIP is granulomatous or lymphohistiocytic phlebitis, present in this case, which is mediated by activated

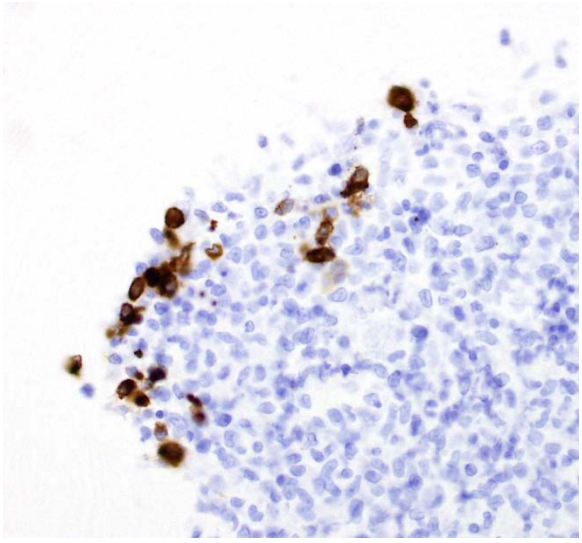

Cat, fourth ventricle: Macrophages within these areas multifocally exhibited strong cytoplasmic labeling for coronaviral antigen. (400X)

circulating monocytes during viremia. Activated monocytes upregulate adhesion molecules such as CD18, and produce pro-inflammatory cytokines such as TNF-α, IL-1b, GM-CSF, and IL-6, in addition to matrix metalloproteinases (MMP-9), and vascular endothelial growth factor (VEGF). Endothelial cells appear to be selectively responsive and activated by the cytokine

storm generated, which limits the distribution of lesions to veins within select organs. The trigger for the massive monocyte activation and selectivity of lesion location is not currently known.[1]

Conference participants discussed the nature of the immune response by the host as a determining factor for which form of the disease the animal will have. As mentioned by the contributor, mutated FCoV-infected circulating monocytes are likely responsible for viremia. The conference moderator instructed that cats with a strong cell-mediated immune (CMI) response do not develop FIP.[1,3,5] Alternative, a weak CMI and strong humoral response results in the effusive, or wet form of the disease. This form is characterized by vasculitis, peritonitis and profound thoracic and peritoneal effusion as a result of deposition of antigen-antibody complexes (type III hypersensitivity).[3,5] In addition, these cats are hypergammaglobulinemic due to the overproduction of ineffective antibodies. In contrast, the noneffusive dry form of the disease is associated with a moderate CMI response with pyogranulomatous inflammation (type IV hypersensitivity) and develop clinical signs based on the organs affected, such as the brain in this case. However, as noted above, the different forms represent a continuum and most cases are likely a mix of the two extreme forms of the disease.[1,3,5]

Contributing Institution:
Dept. of Pathology and Pathogen Biology
Royal Veterinary College, London, UK
http://www.rvc.ac.uk/pathology-and-diagnostic-laboratories

References:

1. Kipar A, Meli ML. Feline infectious peritonitis: still an enigma? *Vet Pathol*. 2014; 51(2)**:**505-526.
2. Pedersen NC: A review of feline infectious peritonitis virus infection: 1963-2008. *J Feline Med Surg*. 2009; 11(4)**:**225-258.
3. Uzal FA, Plattner BL, Hostetter JM. Alimentary System. In: Maxie MG, ed. *Jubb, Kennedy and Palmer's Pathology of Domestic Animals*. Vol 2. 6th ed. Missouri: Elsevier; 2016:253-254.
4. Vandevelde M, Higgins RJ, Oevermann A. *Veterinary Neuropathology: Essentials of Theory and Practice*. Oxford: Wiley-Blackwell; 2012.
5. Zachary J, McGavin M. Nervous system. In: *Pathologic Basis of Veterinary Disease*. 5th ed. Missouri: Elsevier; 2012:860-861.

CASE III: 15-008432 (JPC 409).

Signalment: Two-year-old, male, spayed female, beagle (*Canis familiaris*).

History: The dog presented for chylothorax after lobectomy at a referral surgical center several months before. After surgery, there was a persistent effusion that was managed with an indwelling Pleura-Port. The dog received a short course of cyclosporine for the effusion. On recheck, there was a significant decline in clinical condition (not really consistent with a cylothorax). Radiographs at that time showed the development of a diffuse milliary pattern not reported on original films or seen at rDVM a few weeks earlier. Based on the report, cyclosporine was discontinued and the dog was sent to the rDVM (owner's relative) to consider options. The plan was for the patient to return for lung biopsy in a few days but the dog continued to decline and after a night on oxygen with minimal

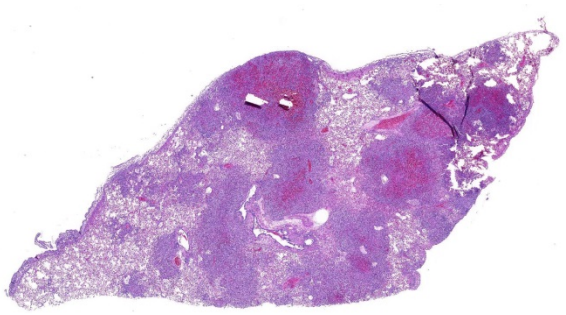

Lung, dog. The submitted sections contains numerous well-defined areas of hypercellularity which efface underlying parenchyma. (HE, 5X).

stabilization and much less improvement, euthanasia was performed. Only lung tissue was submitted by the clinician for histopathology.

Gross Pathology: Sections of formalin-fixed lung were mottled tan-red on cut section.

Laboratory results: N/A

Histopathologic Description: Lung: There are extensive multifocal to coalescing areas of tissue necrosis admixed with hemorrhage, fibrin, edema, karyorrhectic and occasionally mineralized debris; these areas are variably centered on partially or fully effaced bronchioles. Within these foci are florid infiltrates of viable and degenerate neutrophils, large foamy macrophages, and multinucleated macrophages, as well as myriad amoebic trophozoites and rare cysts. Trophozoites are 25-30-um in diameter, with flocculent pale eosinophilic cytoplasm and a 6-8-um karyosome with a prominent central basophilic endosome. Cysts measure 15-20-um and have a thick, bilayered wall (exocyst and endocyst). Within the nucleus of macrophages (including multinucleated macrophages phagocytizing trophozoites) adjacent to and within the most severely affected regions of the lung, there are one to multiple prominent brightly eosinophilic intranuclear inclusions that peripheralize the chromatin. In areas of the lung that are less severely affected, there is filling of alveolar spaces with edema, foamy macrophages, and low numbers of neutrophils, as well as scattered type II pneumocyte hyperplasia, hypertrophy of vascular endothelial cells, and expansion of residual septa by fibrin, similar inflammatory cells, and hyper-trophied fibroblasts. There is mild multifocal mesothelial hypertrophy.

Immunohistochemistry for canine distemper virus was negative. In-situ hybridization with a probe directed against canine herpesvirus was also negative. Indirect immunofluorescence at the CDC confirmed the amoebae to be *Acanthamoeba* spp.

Contributor's Morphologic Diagnoses: Lung: Pneumonia and bronchiolitis, necrosuppurative and hemorrhagic, multi-focal, chronic-active, severe, with free and intrahistiocytic *Acanthamoeba* spp. trophozoites and cysts.

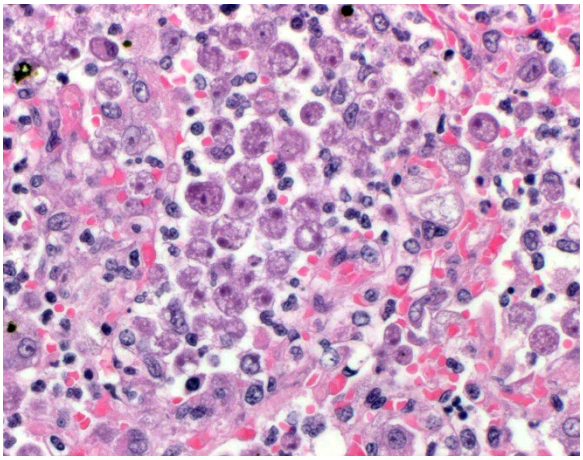

Lung, dog. Numerous Acanthamoeba trophozoites are present within the remnants of a bronchiole, as well as within the surrounding alveoli. (HE, 100X) (Photo courtesy of: Auburn University College of Veternary Medicine, Dept. of Pathobiology , 166 Greene Hall, College of Veterinary Medicine, Auburn University, Auburn, AL 36849).

Contributor's Comment: *Entamoeba histolytica, Sappinia diploidea, Acanthamoeba, Balamuthia* and *Naegleria* species are free-living amoebas that act as secondary decomposers and regulate bacterial population in the soil. However, they are also opportunistic pathogens and can cause severe disseminated disease or necrotizing granulomatous encephalitis in immunosuppressed animals and humans. In the present case, the patient had received a short course of cyclosporine to treat the pleural effusion, which was potentially responsible for the immune suppression and increased susceptibility to opportunistic pathogens. Due to the presence of both cysts and trophozoites in the lung tissues, infection with *Acanthamoeba spp.* or *Balamuthia mandrillaris* was suspected.[18] *Naegleria fowleri* is only present as trophozoites and does not form cysts in infected tissues.[18] However, a definitive diagnosis of *Acanthamoeba* infection was based on the positive results of indirect immunofluorescence.

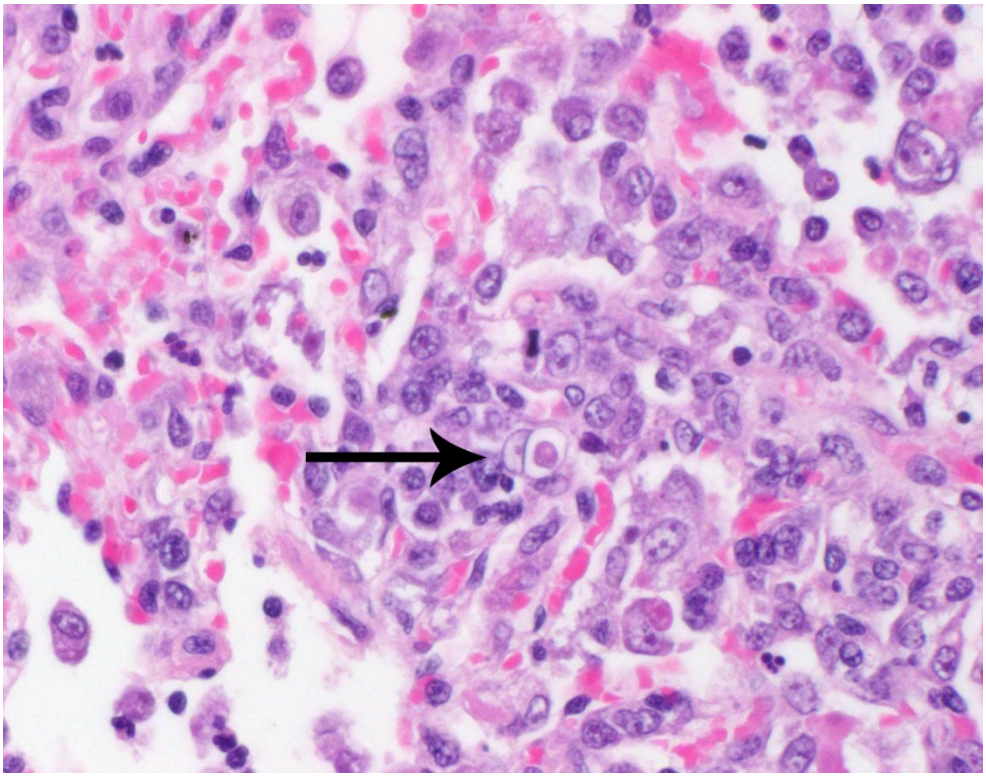

Lung, dog. Acanthamoeba cyst in the lung parenchyma that has a clear space between the exocyst and endocyst (arrow). (HE, 400X) (Photo courtesy of: Auburn University College of Veterinary Medicine, Dept. of Pathobiology, 166 Greene Hall, College of Veterinary Medicine, Auburn University, Auburn, AL 36849).

Acanthamoeba is ubiquitously present in the environment and has been isolated from diverse sources including sea water, beaches, pond water, soil, fresh water lakes, and even from the air. In human populations, anti-*Acanthamoeba* antibodies are present in up to 100% of people in healthy populations in New Zealand and in more than 85% of individuals of London who came from different countries.[3,5,18] In dogs, pulmonary infections usually result from inhalation or aspiration of the organisms from the water.

Acanthamoeba binds to host cells by a 130 kDa mannose-binding protein (MBP). *Other adhesions involved in this interaction include* laminin-binding protein with a predicted molecular mass of a 28.2 kDa, a 55 kDa laminin-binding protein and a > 207 kDa adhesion.[8,9,17] *Acanthamoeba* binding to the host cells results in its phagocytosis and release of toxins. Two superoxide dismutases, an iron superoxide dismutase and a copper-zinc superoxide dismutase

provide antioxidant defense. Toxins produced by *Acanthamoeba* cause activation of the phosphatidylinositol 3-kinase (PI3K) pathway, which further activates pro-apoptotic molecules, Bak and Bax, resulting in loss of mitochondrial membrane potential and apoptosis of host cells.[1,13,19] In host cells, toll-like receptor-4 (TLR4) is responsible for recognition of *Acanthamoeba*, which leads to activation of the Myd88 pathway and induces secretion of interleukin-8, tumor necrosis factor-alpha, and interferon-beta.[13,16] *Acanthamoeba* causes degradation of occludin and zonula occludens-1 tight junction proteins in human brain microvascular endothelial cells (HBMEC) in a Rho kinase-dependent manner, and thus leading to increased vascular permeability.[12]

Acanthamoeba causes cutaneous lesions, sinus infections, keratitis, and rare but fatal encephalitis, known as granulomatous amoebic encephalitis in humans. Similarly, *Acanthamoeba* causes encephalitis and disseminated disease in immunosuppressed animals. In addition, most isolates harbor endosymbionts including numerous viruses (vesicular stomatitis virus, adenovirus, and poliovirus), bacterias (*Burkholderia spp., Campylobacter jejuni, Coxiella burnetii, Francisella tularensis, Helicobacter pylori and Listeria monocytogenes*), and yeast organisms (*Cryptococcus neoformans, Blastomyces dermatitidis, Sporothrix schenckii, Histoplasma capsulatum*). However, the role of endosymbionts is not entirely clear. It is suspected that *Acanthamoeba* can transmit them to susceptible hosts or endosymbionts can increase the pathogenicity of *Acanthamoeba*.[11,18]

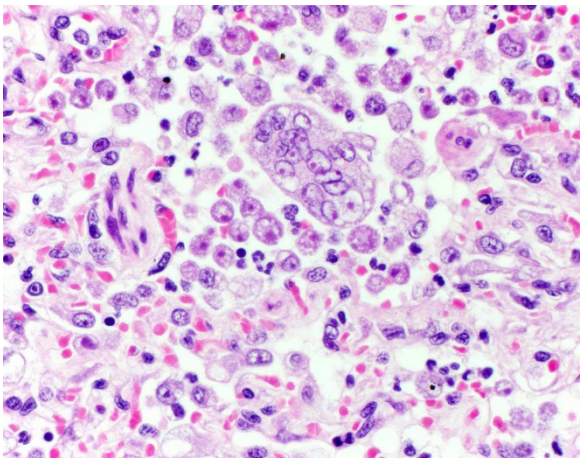

Lung, dog. Multifocally, alveolar spaces and discohesive lung parenchyma contained multinucleated giant cells with presumed intranuclear eosinophilic inclusion bodies. (HE, 400X) (Photo courtesy of: Auburn University College of Veterinary Medicine, Dept. of Pathobiology, 166 Greene Hall, College of Veterinary Medicine, Auburn University, Auburn, AL 36849).

The intrahistiocytic intranuclear inclusions present in this case are strongly suggestive of a co-infection with canine distemper virus. Unfortunately, the formalin-fixed tissue was held by the submitting clinician for several weeks prior to submission, so it is likely that this resulted in a loss of immunoreactivity due to antigen cross-linking.

JPC Diagnosis: Pneumonia, broncho-interstitial and necrotizing, multifocal to coalescing, marked, with free and intrahistiocytic trophozoites and rare cysts, beagle, *Canis familiaris*.

Conference Comment: We thank the contributor for providing an outstanding and challenging case that stimulated a great deal of discussion among the conference participants regarding whether *Acanthamoeba* is the primary cause of the significant pulmonary pathology in this case, or if it is secondary to concurrent infection with canine distemper virus (CDV). Like the contributor, many participants note numerous brightly eosinophilic intra-histiocytic nuclear inclusion bodies within multinucleated cells, which are interpreted as viral syncytial cells. However, others argue that the intranuclear structures may be

representative of prominent nucleoli in response to marked chronic inflammation and the multinucleated cells are reactive fused macrophages and megakaryocytes rather than viral syncytial cells. Participants also describe multinucleated cells that occasionally contain phagocytosed amoebic trophozoites.

bronchiolar epithelium do not contain prominent cytoplasmic inclusions typical of CDV. Unfortunately, as mentioned by the contributor, suboptimal tissue preservation techniques may have affected the immunoreactivity for canine morbillivirus immunohistochemistry (IHC). Additionally, formalin fixation dramatically reduces the

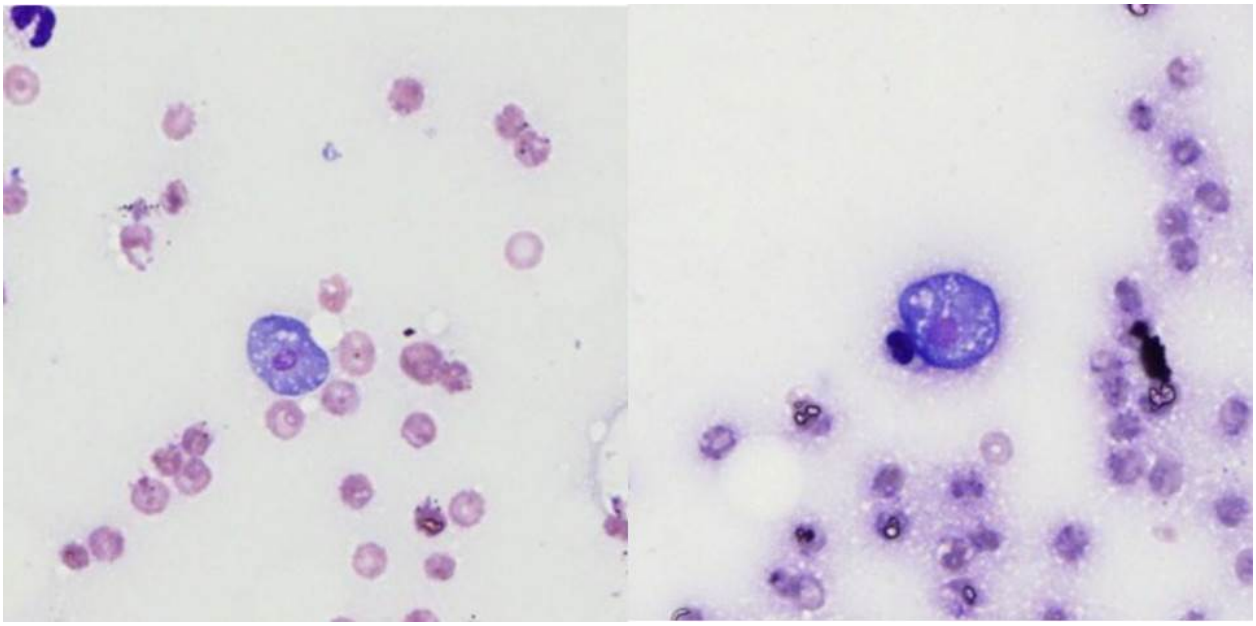

Lung, dog. Acanthamoeba trophozoites in lung aspirates stained with modified Wright's stain. (Wrights, 200X) (Photo courtesy of: Auburn University College of Veterinary Medicine, Dept. of Pathobiology, 166 Greene Hall, College of Veterinary Medicine, Auburn University, Auburn, AL 36849).

Ionized calcium binding adaptor molecule 1 (Iba1) immunohistochemical stain, provided by the contributor, demonstrated strong intracytoplasmic immunoreactivity for the multinucleated cells, confirming their macrophage lineage. The typical respiratory lesions associated with CDV include bronchointerstitial pneumonia with prominent cytoplasmic inclusion bodies in the bronchial and bronchiolar epithelium, type II pneumocyte hyperplasia with alveolar cytoplasmic inclusions, and alveolar epithelial syncytial cells.[4] Participants favoring primary *Acanthamoeba* infection note that bronchial and

ability to extract suitable DNA for PCR based diagnostic tests. These deleterious effects of formalin on DNA are time and concentration dependent.[14] The majority of participants agree with the contributor that there is likely primary concurrent infection with canine distemper virus in this case, despite negative IHC results.

Reports of pulmonary and systemic disease caused by free-living amoebae in dogs are uncommon and are usually associated with immune suppression with the majority of reported cases associated with underlying disease (such as co-infection with CDV) or long-term immunosuppressive doses of

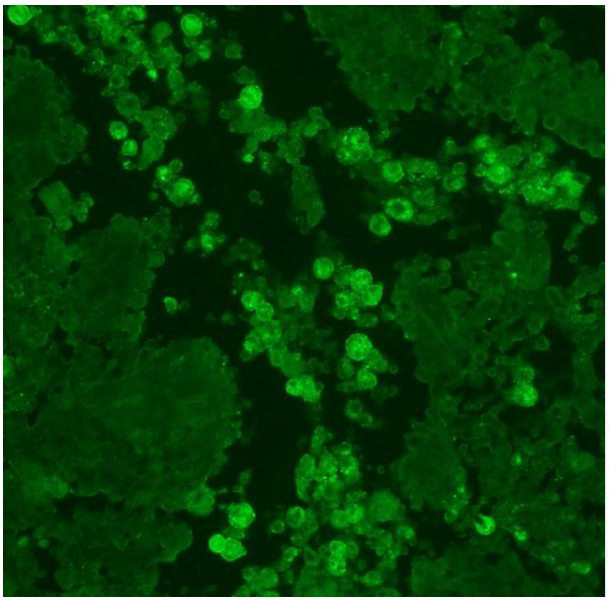
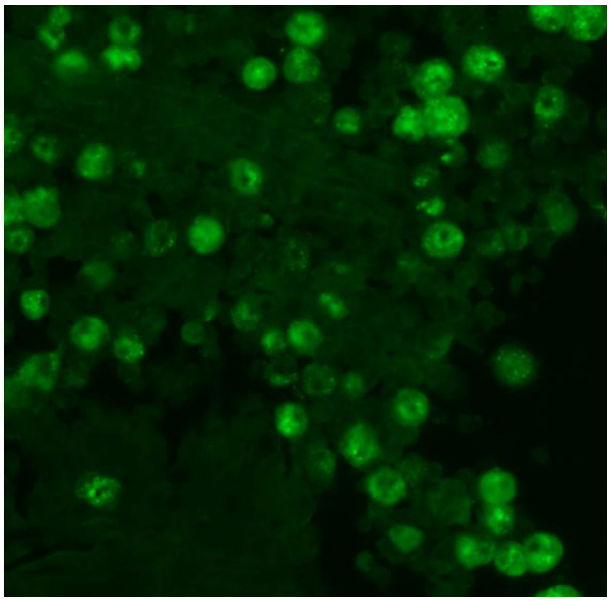

Lung, dog. Indirect immunofluorescence (IIF) assay on the lung tissue. In the IIF assay, 1:200 diluted rabbit anti-sera specific for Acanthamoeba species was used. Amoebae seen in the images ranged in size from 10-15 microns. (A) 200X magnification. (B) (Photo courtesy of: Auburn University College of Veterinary Medicine, Dept. of Pathobiology, 166 Greene Hall, College of Veterinary Medicine, Auburn University, Auburn, AL 36849).

corticosteroids[6,7,10,15]; however, there is a report of a greyhound naturally infected with *Acanthamoeba* sp. causing primary granulomatous pneumonia and encephalitis.[2] In this case, the dog was receiving cyclosporine to treat chylothorax after a lung lobectomy, which may offer an alternative explanation for immune suppression; however, the reported short course of treatment is inconsistent with the long course of immunosuppressive therapy reported in the literature.[6,7,1]

Contributing Institution:
Auburn University
College of Veterinary Medicine
Auburn, AL 36849
http://www.vetmed.auburn.edu/

References:

1. Alizadeh H, Pidherney MS, McCulley JP, Niederkorn JY. Apoptosis as a mechanism of cytolysis of tumor cells by a pathogenic free-living amoeba. *Infect Immun*. 1994; 62(4)**:**1298-1303.
2. Bauer R.W., Harrison L.R., Watson C.W., Styer E.L. & Chapman Jr W.L. 1993. Isolation of Acanthamoeba sp. from a greyhound with pneumonia and granulomatous amebic encephalitis. J. Vet. Diagn. Invest. 5:386-391.
3. Brindley N, Matin A, Khan NA. *Acanthamoeba castellanii*: High antibody prevalence in racially and ethnically diverse populations. *Exp Parasitol*. 2009; 121(3)**:**254-256.
4. Caswell JL, Williams KJ. Respiratory system. In: *Jubb Kennedy and Palmer's Pathology of Domestic Animals*. Vol 1. 6th ed. Philadelphia, PA: Elsevier Saunders; 2016:574-576.
5. Cursons RT, Brown TJ, Keys EA, Moriarty KM, Till D. Immunity to pathogenic free-living amoebae: Role of humoral antibody. *Infect Immun*. 1980; 29(2)**:**401-407.

6. Dubey JP, Benson JE, et al. Dissemninated *Acanthamoeba* sp. infection in a dog. *Vet Parasitol*. 2005; 125:183-187.
7. Foreman O, Sykes J, et al. Dissemniated infection with *Balamuthia mandrillaris* in a dog. *Vet Pathol*. 2004; 41:506-510.
8. Garate M, Cao Z, Bateman E, Panjwani N. Cloning and characterization of a novel mannose-binding protein of Acanthamoeba. *J Biol Chem*. 2004; 279(28)**:**29849-29856.
9. Hong YC, Lee WM, Kong HH, Jeong HJ, Chung DI. Molecular cloning and characterization of a cDNA encoding a laminin-binding protein (AhLBP) from Acanthamoeba healyi. *Exp Parasitol*. 2004; 106(3-4)**:**95-102.
10. Kent M, Platt S, et al. Multisystemic infection with Acanthamoeba sp in a dog. *J Am Vet Med Assoc*. 2011; 238:1476-1481.
11. Khan NA. Acanthamoeba: Biology and increasing importance in human health. *FEMS Microbiol Rev*. 2006; 30(4)**:**564-595.
12. Khan NA, Siddiqui R. Acanthamoeba affects the integrity of human brain microvascular endothelial cells and degrades the tight junction proteins. *Int J Parasitol*. 2009; 39(14)**:**1611-1616.
13. Mattana A, Cappai V, Alberti L, Serra C, Fiori PL, Cappuccinelli P. ADP and other metabolites released from *Acanthamoeba castellanii* lead to human monocytic cell death through apoptosis and stimulate the secretion of proinflammatory cytokines. *Infect Immun*. 2002; 70(8)**:**4424-4432.
14. Ramos F, Zurabian R, et al. The effect of formalin fixation on polymerase chain reaction characterization of *Entamoeba histolytica*. *Trans R Soc Trop Med Hyg*. 1999; 93:335-336.
15. Reed LT, Miller MA, Visvesvara GS, Gardiner CH, et al. Diagnostic exercise: Cerebral mass in a puppy with respiratory distress and progressive neurologic signs. *Vet Pathol*. 2010; 47(6):1116-1119.
16. Ren MY, Wu XY. Toll-like receptor 4 signalling pathway activation in a rat model of Acanthamoeba Keratitis. *Parasite Immunol*. 2011; 33(1)**:**25-33.
17. Rocha-Azevedo B, Jamerson M, Cabral GA, Marciano-Cabral F. *Acanthamoeba culbertsoni*: analysis of amoebic adhesion and invasion on extracellular matrix components collagen I and laminin-1. *Exp Parasitol*. 2010; 126(1)**:**79-84.
18. Siddiqui R, Khan NA. Biology and pathogenesis of Acanthamoeba. *Parasit Vectors*. 2012:5-6.
19. Sissons J, Kim KS, Stins M, Jayasekera S, Alsam S, Khan NA. *Acanthamoeba castellanii* induces host cell death via a phosphatidylinositol 3-kinase-dependent mechanism. *Infect Immun*. 2005; 73(5)**:**2704-2708.

CASE IV: 16-9986 (JPC 4084207).

Signalment: Seven-year-old quarter horse mare (*Equus ferus caballus*).

History: In June 2015, the horse presented to the referring veterinarian with bilateral conjunctivitis that progressed to severe anterior uveitis in the left eye. Foot abscesses, distal limb cellulitis, mandibular lymphadenopathy, nasal discharge, and hives developed subsequently. Treatments

Cerebellar meninges, horse. Meninges are diffusely and markedly hypercellular and expanded. (HE, 5X)

included ceftiofur, oxytetracycline, dexamethasone, nonsteroidal anti-inflammatory drugs, and a two-week course of doxycycline. Despite treatment, the horse remained hyperfibrinogenemic at 800-1300 mg/dL and developed narcolepsy a few months later. Due to health concerns and the poor prognosis, the horse was euthanized in January 2016 and submitted to Cornell Animal Health Diagnostic Center for necropsy and tissue collection.

Gross Pathology: There was approximately 200 mL of yellow tinged transparent fluid (serous effusion) within the peritoneal cavity. The capsular surface of the liver was diffusely thickened, mottled white to tan to purple to black. There were thousands of multifocal to coalescing, generalized, white, 1-3 mm, hard white nodules along the capsular surface with a few dozen similar nodules within the parenchyma. Similar nodules were present in the thymus and surrounding the mediastinal fat and in all lung lobes. These nodules were presumed to be parasitic granulomas, which were confirmed histologically. Evidence of chronic laminitis was present in both forelimbs. The brain was grossly normal.

Laboratory results: Bloodwork in early December 2015 revealed elevated gamma glutamyl transferase (GGT) at 61 U/L (normal range 9-24 U/L), rising globulins at 2.3 g/dL from a previous value of 1.6 g/dL (normal range 2.8-4.7 g/dL), and a lymphocyte count of 1,940 cell/uL, up from a previous count of 1,380 cells/uL (normal range 1,000-4,900 cells/uL; lymphopenia is <1,500 cells/uL).

B cell concentration was markedly decreased at 19 cells/uL of 1,940 total lymphocytes/uL (0.98% B cells), with 1.0% CD19 B cells (median, CI = 9.0%, 2.0%), 0.2% CD21 B cells (median, CI = 10.2%, 4.2%), and 0.9% IgM B cells (median, CI = 10.2%, 2.1%).
The CD4+ and CD8+ T-cell distributions were slightly increased, and the CD4/CD8 ratio was within the normal reference interval.

Serum IgG concentration was markedly decreased at 423 mg/dL (median, CI = 1,760 mg/dL, 603 mg/dL) and serum IgM concentration was within the normal reference interval at 63 mg/dL (median, CI = 100 mg/dL, 50 mg/dL; deficiency is < 25 mg/dL).

Lyme titers on multiplex PCR assay (OspA, OspC, OspF) decreased from 2013 when they ranged 100-300 to June 2015, August 2015, and January 2016 when antibody titers were in the single digits and teens.

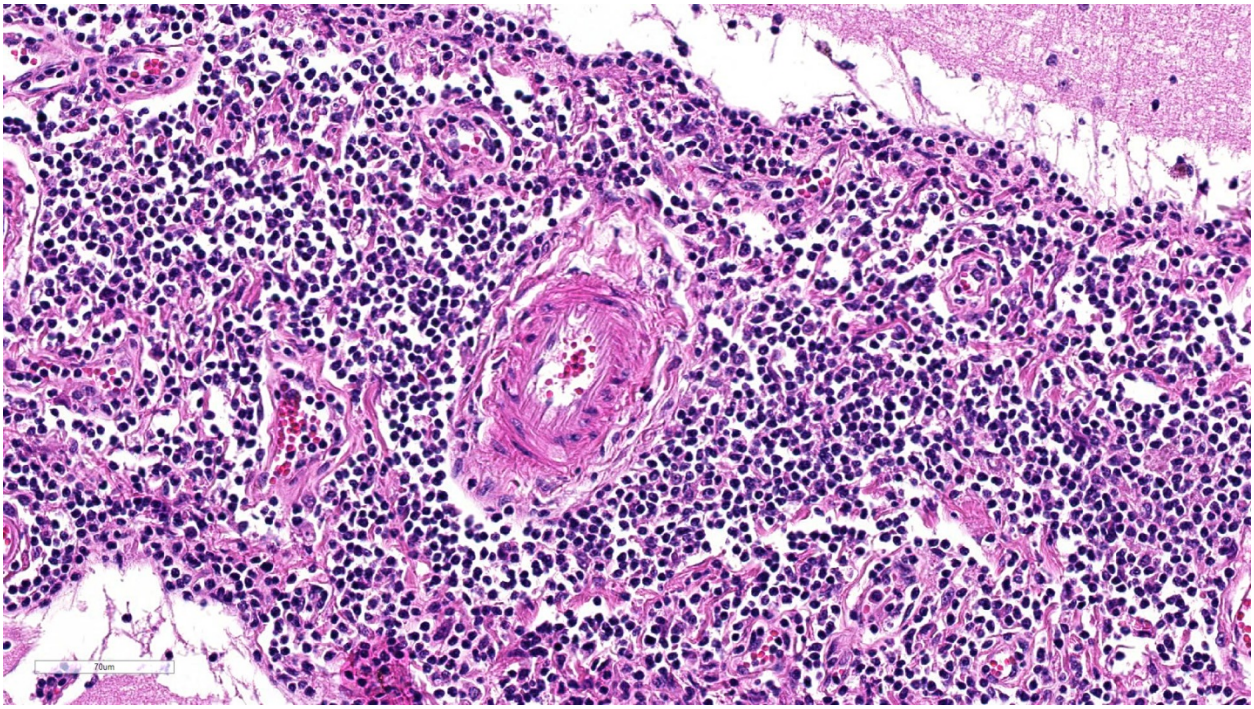

Cerebellar meninges, horse. Numerous lymphocytes and plasma cells with histiocytes and rare neutrophils expand the meninges. (HE, 164X)

Bacterial cultures and virus isolation of brain tissue were both negative. A quantitative PCR for *Borrelia burgdorferi* yielded a CT value of 32 (positive result).

Histopathologic Description: Brain, cerebrum, and cerebellum: Diffusely, meninges of the cerebellum and cerebrum are markedly expanded by a dense infiltrate of lymphocytes, macrophages, fewer neutrophils, and rare plasma cells interspersed with rare wispy spirochetal bacteria. Within the neuroparenchyma, the Virchow-Robin spaces of blood vessels are surrounded by a similar inflammatory infiltrate. Blood vessels are often prominent, characterized by endothelial hypertrophy and have variable branching. In the white and grey matters are increased numbers of enlarged glial cells with increased eosinophilic cytoplasm (astrocytes, presumptive). Multifocally within the choroid plexus are clusters of lymphocytes and histiocytes, along with few eosinophils.

Contributor's Morphologic Diagnoses: 1. Brain, cerebrum, and cerebellum: Severe, multifocal to coalescing, chronic lymphohistiocytic neutrophilic meningo-encephalitis with lymphohistiocytic eosinophilic choroid plexitis, branching blood vessels, astrocytosis, and rare intralesional spirochetal organisms

Other final morphologic diagnoses (slides not included):

2. Lymphohistoicytic meningo-myeloencephalitis and radiculoneuritis of the spinal cord and ganglia, respectively
3. Moderate, multifocal, chronic lymphocytic hypophysitis
4. Multifocal, chronic parasitic granulomas in the liver, lung, and thymus
5. Chronic lymphoplasmacytic portal hepatitis with capsular and bridging fibrosis
6. Multifocal laminitis and chronic foot abscess

7. Lymphoid depletion in spleen and thymus

Contributor's Comment: The histochemical stain of a section of brain with Modified Steiner silver stain and immunohistochemical (IHC) stain for *Borrelia burgdorferi* confirmed spiral organisms within areas of inflammation in the meninges of the cerebellum and cerebrum. IHC stains of section of cerebrum for eastern equine encephalitis virus, equine herpes virus-1, West Nile virus, and rabies virus yielded no immunoreactivity. Inflammatory cells were strongly immuno-reactive to CD3 and IBA1; however, rare CD20 and no Pax5 immunoreactivity were detected, confirming lack of plasma cells in areas of inflammation and consistent with common variable immunodeficiency (CVID).

CVID is a primary immunodeficiency disease of humans and horses that encompass a group of heterogenous disorders characterized by hypo-gammaglobulinemia. Generally, at least two isotypes of antibodies are affected, although IgG deficiency alone is recognized. Human CVID patients often present with recurrent respiratory infections and have a high frequency of autoimmune and lympho-proliferative disease.[1,8,9] It is one of the most common primary immuno-deficiencies reported in humans, with an incidence rate of 1 in 25,000 humans. In horses, CVID is a rare condition with relatively few cases reported,[1,2,3,10,14] though the Equine Immunology Laboratory at Cornell College of Veterinary Medicine has diagnosed this condition in over 50 horses since 2002 and has been actively investigating potential genetic and epigenetic mechanisms of disease.[12] Current research on equine CVID focuses on the disruption of B cell development in the bone marrow, and has identified decreased mRNA expression and incomplete demethylation of the *PAX5* gene, required for commitment and differentiation of B cells.[12,13]

Like human patients, horses clinically manifest with recurrent infections of the respiratory tract. In addition, persistent bacterial meningitis has been associated with infection by common skin contaminants such as *Staphylococcus* spp.,[3,10] while *Borrelia burgdorferi* has been highly suspected in other cases of meningitis. One case report of CNS and PNS inflammation in a CVID horse documented a positive Western blot analysis result with low to moderate *Borrelia burgdorferi* antibody response in serum and a positive PCR assay result from CSF using primers for the outer surface protein A (*ospA*) gene.[5] These tests confirm exposure to the bacterium; however, neither test demonstrates active *Borrelia burgdorferi* infection within areas of CNS inflammation. Lyme neuroborreliosis in horses, as with most species, is characterized by suppurative or non-suppurative, lymphoplasmacytic, histiocytic perivascular to diffuse inflammation most severely affecting the CNS, including the meninges, ganglia, and cranial and spinal nerve roots, with varying degrees of necrosis, fibrosis, and neuro-parenchymal invasion.[4]

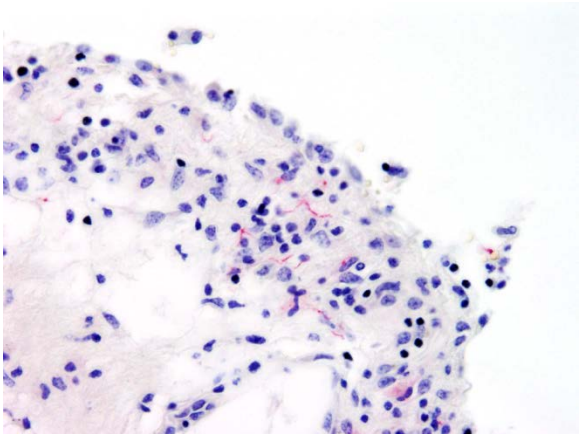

Cerebellar meninges, horse. Immunohistochemical stains demonstrate rare spirochetes perivascular areas within the meninges. (400X).

In the present case, the inflammation is predominately lymphocytic and histiocytic and the distribution includes the spinal cord and ganglia, meninges, choroid plexus, pituitary gland, and neuroparenchyma. By histochemistry and immunohistochemistry, rare spirochetal organisms were present within areas of perivascular inflammation, while a quantitative PCR confirmed the presence of *Borrelia burgdorferi* nucleic acid in the affected cerebrum. The history of uveitis and narcolepsy, the clinical data, histologic findings of severe meningo-myeloencephalitis, choroid plexitis, and hypophysitis, and ancillary testing are consistent with Lyme neuroborreliosis.[4,11] The severe inflammation, fibrosis and parasitic granulomas in the liver, lung, and thymus are attributed to massive parasitic migration; a finding consistent with CVID and a lack of antibody response to parasitic antigens.[2,14] The lack of humoral immunity, the primary host defense mechanism against *Borrelia burgdorferi*, likely contributed to chronic Lyme disease in this horse with CVID.

JPC Diagnosis: Cerebrum: Chorio-meningoencephalitis, lymphohistiocytic, multifocal to coalescing, marked, quarter horse, *Equus ferus caballus.*

Conference Comment: Lyme neuro-borreliosis is an uncommon manifestation of Lyme disease caused by *Borrelia burgdorferi sensu lato* infection in the nervous system, and is typically associated with immunosuppression in horses, humans, and experimental laboratory animal models.[4-6] The contributor provides an outstanding demonstration of that patho-genesis in this case of natural infection in a horse with common variable immuno-deficiency (CVID). As mentioned above, CVID is associated with a late-onset B cell lymphopenia and hypo-gammaglobulinemia with marked decrease in serum IgG. CVID typically manifests as opportunistic recurrent pneumonia, septicemia, and meningitis.[14]

White-footed mice are the principal reservoir host for *B. burgdorferi* in the endemic Northeastern United States, and the bacteria are transferred to susceptible host species by the *Ixodes* sp. tick vector. *B. burgdorferi* localizes in the digestive tract of ixodid ticks via its outer surface protein A (*OspA*) after feeding on an infected reservoir host.[7] When the vector attaches to a susceptible mammalian host and takes a blood meal, there is a subsequent increase in temperature within the tick digestive tract. This change in temperature represses *OspA* expression and induces *OspC* synthesis. This new conformation allows the spirochete to localize to the salivary glands of the tick. Interestingly, this change in conformation can take as long as 48 hours to complete, necessitating the prolonged attachment of the tick to the host. The spirochete then enters the host via the tick's salivary secretions during feeding.[7]

Previous reports of borreliosis in horses have documented arthritis, uveitis, encephalitis, and ataxia.[5] Uveitis, present in this case, is the most common reported extra-neural manifestation of *B. burgdorferi* infection in horses, but is rarely reported in other species.[6] The most common manifestation of disease in dogs is polyarthritis, with fewer cases of membranoproliferative glomerulonephritis.[4-6] Equine neuroborreliosis is challenging to diagnose clinically due to the wide variability in clinical presentation and current lack of reliable antemortem diagnostic tests; however, the conference moderator instructed that the index of suspicion for Lyme disease should be high in horses that present with neurologic deficits and concurrent uveitis.[4-6]

Few conference participants included Lyme disease as a differential diagnosis in this case. Most favored a viral encephalitis caused by an alphavirus (EEE, WEE, VEE), rabies, or West Nile virus due to the relatively non-specific lymphohistiocytic inflammation in this case. Others included equine protozoal myelitis caused by *Sarcocystis neurona*; however, one would expect to see necrotizing granulomatous and eosinophilic lesions, which are not a feature of this case.[6] In conjunction with the excellent images provided by the contributor, the Joint Pathology Center ran a Warthin-Starry silver stain, which highlights numerous argyrophilic spirochetes consistent with *B. burgdorferi* within the inflamed neuroparenchyma. This case demonstrates the importance of including Lyme disease as a differential diagnosis in horses with neurologic disease.

Contributing Institution:
Department of Biomedical Sciences
Section of Anatomic Pathology
College of Veterinary Medicine
Cornell University
Ithaca, NY 14853
http://www.vet.cornell.edu/biosci/pathology/

References:

1. Ardeniz O, Cunningham-Rundles C. Granulomatous disease in common variable immunodeficiency. *Clin Immunol*. 2009; 133:198-201.
2. Flaminio MJBF, LaCombe V, Kohn CW, et al. Common variable immunodeficiency in a horse. *J Am Vet Med Assoc.* 2002; 9:1296-1302.
3. Flaminio MJBF, Tallbridge RL, Salles-Gomes COM, et al. Common variable immunodeficiency in horses is characterized by B cell depletion in primary and secondary lymphoid tissues. *J Clin Immunol.* 2009; 9:107-116.
4. Imai DM, Barr BC, Daft B, et al. Lyme neuroborreliosis in 2 horses. *Vet Pathol*. 2011; 48:1151-1157.
5. James FM, Engiles JB, Beech J. Meningitis, cranial neuritis, and radiculoneuritis associated with *Borrelia burgdorferi* infection in a horse. *J Am Vet Med Assoc.* 2010; 37:1180-1185.
6. Johnstone LK, Engiles JB. Retrospective evaluation of horses diagnosed with neuroborreliosis on postmortem examination: 16 cases (2004-2015). *J Vet Intern Med*. 2016; 30:1305-1312.
7. Kurmaran D, Eswaramoorthy S, et al. Crystal structure of outer surface protein C (OspC) from the lyme disease spirochete, *Borrelia burgdorferi*. *EMBO J*. 2001; 20(5):971-978.
8. Maglione PJ. Autoimmune and lymphoproliferative complications of common variable immunodeficiency. *Curr Allergy Asthma Rep.* 2016; 16:19.
9. Pandit C, Hsu P, van Asperen P, et al. Respiratory manifestations and management in children with common

variable immunodeficiency. *Paediatric Resp Rev.* 2016; Epub ahead of print.
10. Pellegrini-Masini A, Bentz AI, Johns IC, et al. Common variable immunodeficiency in three horses with presumptive bacterial meningitis. *J Am Vet Med Assoc.* 2005; 227:114-122.
11. Priest HL, Irby NL, Schlafer DH, et al. Diagnosis of *Borrelia*-associated uveitis in two horses. *Vet Ophthalmol.* 2012; 15:398-405.
12. Tallmadge RL, Shen L, Tseng CT, et al. Bone marrow transcriptome and epigenome profiles of equine common variable immunodeficiency patients unveil block of B lymphocyte differentiation. *Clin Immunol.* 2015; 160:261-276.
13. Tallmadge RL, Such KA, Miller KC, et al. Expression of essential B cell development genes in horses with common variable immunodeficiency. *Mol Immunol.* 2012; 51:169-176.
14. Tennet-Brown BS, Navas de Solis C, Foreman JH, et al. Common variable immunodeficiency in a horse with chronic peritonitis. *Eq Vet Educ.* 2010; 22:383-399.

Self-Assessment - WSC 2016-2017 Conference 16

1. Trueperella pyogenes most commonly acts a primary pulmonary pathogen.
    a. True
    b. False

2. Which of the following is true about feline coronaviruses ?
    a. Feline infectious peritonitis virus is ubiquitous in the environment.
    b. Feline infectous peritonitis affecting young female purebred cats most commonly.
    c. The ability of feline infectious peritonitis virus to infect lymphocytes results in clinical disease.
    d. A weak cell-mediated immune response results in the “dry “ form of FIP.

3. Which of the following protect *Acanthamoeba* from host cell oxidative processes ?
    a. Mannose binding proteins
    b. Rho-kinase
    c. Toll-like receptor 4
    d. Iron superoxide dismutase

4. Common variable immunodeficiency in horses is characterized by all of the following except?
    a. Ocular disease
    b. Hypogammaglobulinemia
    c. Recurrent respiratory infections
    d. Persistent bacterial meningitis

5. Which has not been associated with borreliosis in horses?
    a. Arthritis
    b. Uveitis
    c. Encephalitis
    d. Myocarditis

Joint Pathology Center

Veterinary Pathology Services

WEDNESDAY SLIDE CONFERENCE 2016-2017

C o n f e r e n c e 17

1 February 2017

CASE I: 12A208 (JPC 4017925).

Signalment: Three-year-old, male, pigtail macaque, (*Macaca nemestrina*).

History: This animal was inoculated intravenously with SIVmac239, 177 days prior to humane sacrifice. It had a history of intermittent diarrhea, weight loss, mild dehydration, and upper respiratory signs (sneezing and nasal discharge). The day before sacrifice the animal began vocalizing and became progressively ataxic.

Gross Pathology: The animal was thin with atrophic thymus and peripheral nodes but enlarged mesenteric and internal iliac nodes. Distal esophageal mucosa was covered with a proliferative growth of *Candida sp*. The colon had a thickened mucosa and was dilated with fluid feces.

Laboratory results: *Moraxella sp*. and hemolytic staphylococcus were cultured from the nasal cavity. *Balantidium coli* and *Trichuris trichiura* were identified by fecal flotation. Cytomegalovirus was identified by PCR in paraffin sections of testis.

Histopathologic Description: The section of testis includes edematous rete testis with canaliculi, lobules made up of immature seminiferous tubules with multiple zones of necrosis, and thickened, inflamed, and partially fused tunica albuginea and vaginalis. Complete and partial lobules are destroyed by multifocal to coalescing coagulative necrosis involving seminiferous tubules and interstitium. Segments of small and medium-sized vessels are necrotic with hyalinized walls, fibrin thrombi and infiltration of neutrophils. Sertoli cells within the tubules, numerous Leydig cells, fibrocytes and myoid cells adjacent to the basal lamina of the tubules, and fibroblasts and endothelium lining interstitial vessels contain large round, oval, tear-drop and occasionally lobulated and multiple eosinophilic intranuclear inclusions usually surrounded by a clear halo. Some enlarged cells have additional amorphous granular eosinophilic aggregates within the cytoplasm. Interstitial stroma of the mediastinum, lobules, and both tunics is severely edematous with fibrin deposition, microhemorrhages, microthrombi, and predominantly neutrophilic infiltration, especially around small vessels. Neutrophils

are necrotic, fragmented and mixed with small numbers of eosinophils.

Contributor's Morphologic Diagnosis: Acute orchitis with multifocal to coalescing, coagulative and fibrinoid necrosis, intravascular fibrin thrombi and intranuclear inclusions, Cytomegalovirus, Testis

Contributor's Comment: Cytomegalovirus (CMV) is a betaherpesvirus comparable in sequence and pathogenesis to species-specific CMV of monkeys, humans, and other animals. CMV of Rhesus and Japanese macaques, African green monkeys (AGM), and chimps have distinct restriction fragment profiles.[1,6] Uncomplicated infections rarely cause disease, even in infants, usually become latent, and may reactivate later in life due to the immunosuppression of viral infection, cancer treatment, or organ transplantation. In breeding colonies, 50% of infants become seropositive by six months and nearly 100% by one year.[3] Transmission via breast milk,

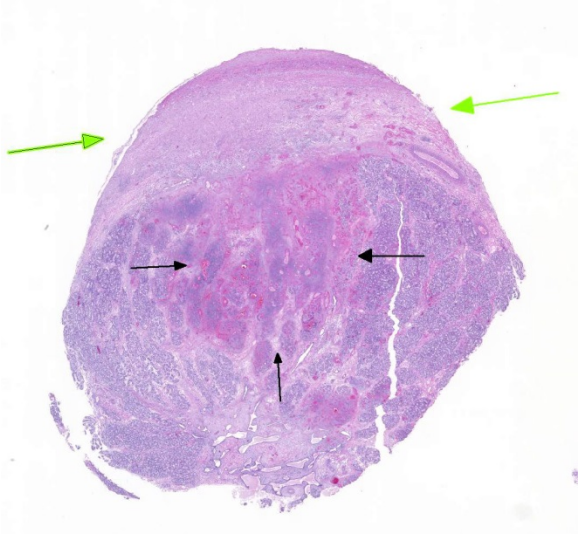

Testis, cynomolgus macaque. At low magnification, there is a large infarct at the edge of the testis (black arrows). The overlying tunics are fused. (HE, 5X)

saliva, and possibly urine[2] seem likely routes of transmission; transplacental infection is possible but rare[2]; transplantation of infected organs is a documented risk.[12]

The incidence of CMV disease in monkeys with SAIDS is variable but can be as high as 30-50% of seropositive animals.[12,15] Tissues displaying cytomegalic cells containing intranuclear inclusions include central and peripheral nervous system, lung, lymph nodes, liver, GI tract, testis, and arteries[4].

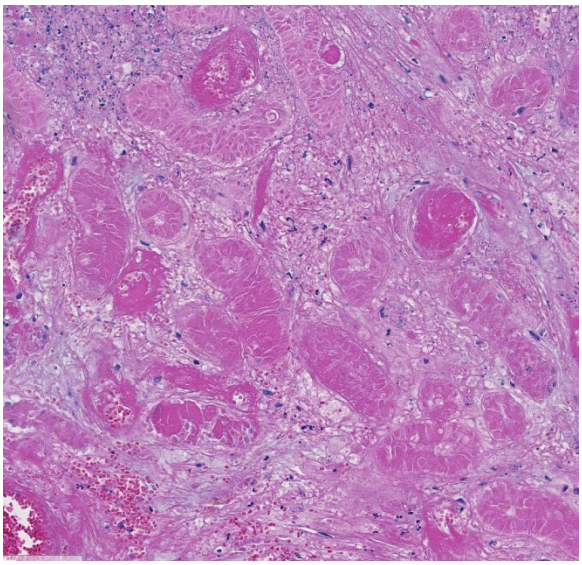

Testis, cynomolgus macaque. Higher magnification of the area of testicular infarction. (HE, 128X)

CMV disease in SIV-infected monkeys can be predicted by prolonged detection of CMV DNA in plasma and a decrease in anti-CMV titer and avidity[14]. Profound depletion of CD8 T cells (once thought linked[9]) is less important than the expanded target cell pool of activated CD4 cells.[4]

Genomes for rhesus and chimp CMV are sequenced and partial sequences for AGM and baboon CMV are reported.[6,7] There is a strong conservation of coding content between human and simian CMV, with even closer homologies among CMV of closely related primate hosts. While estimates of open reading frames in rhesus CMV vary

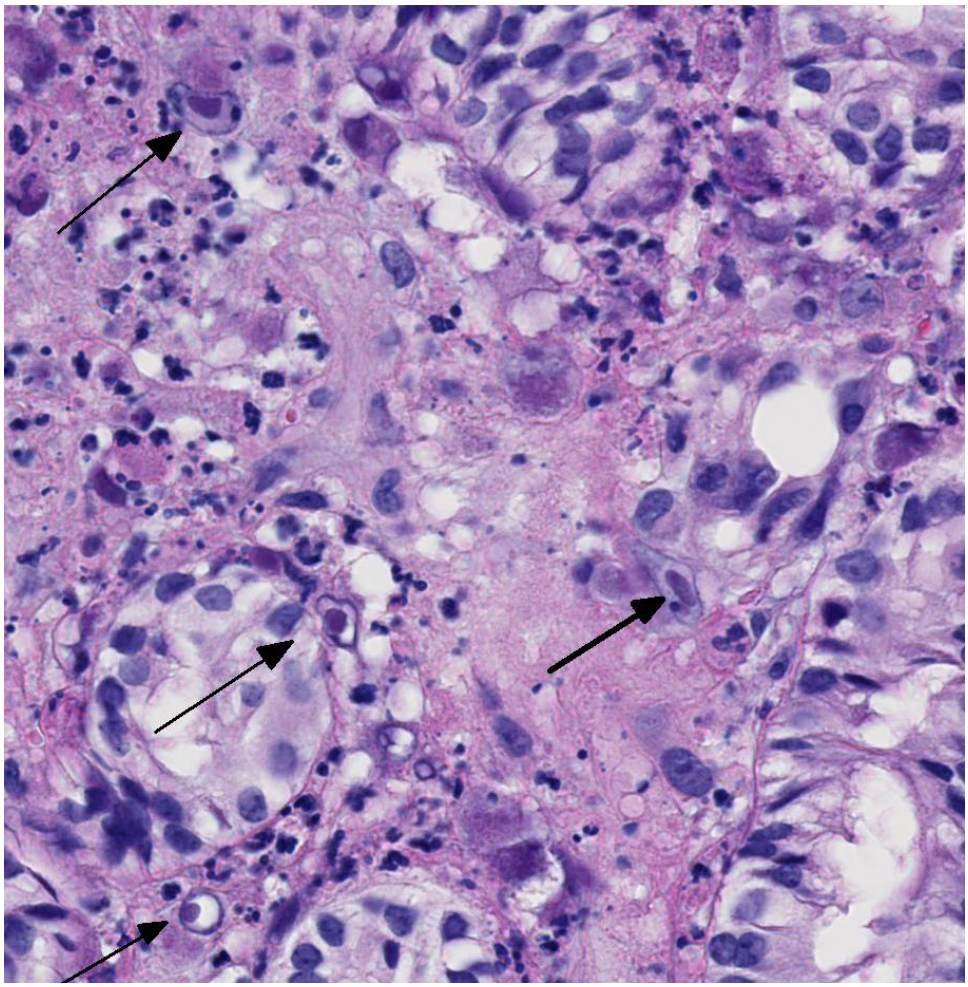

Testis, cynomolgus macaque. Necrotic seminiferous tubules often contain cytomegalic cells with a prominent karyomegalic inclusion (black arrows) characteristic of cytomegalovirus. (HE, 400X)

from 230-258 genes, it is clear that evolution has produced extra coding capacity in rhesus compared to human and chimp CMV.[3] Sequence homology demonstrates codes for proteins critical for neutrophil activation by CXC chemokines, TNF receptor, B-chemokine receptor, and IL-10 in rhesus CMV. In human fibroblasts, CMV can change levels of more than 250 cellular genes including cyclooxygenase 2 (COX-2)[17], which converts arachidonic acid (AA) to prostaglandin endoperoxide H. Rhesus CMV does not increase cellular COX-2 but produces a homologue protein[6] that could be used to modulate the host inflammatory process.

CMV establishes life-long infection in immunocompetent hosts in sites of latency and persistent infection. During latency, infected cells demonstrate limited viral gene expression, while in persistently infected cells; virions are continuously produced with minimal cytopathic effect. Endothelial cells, myeloid cells (particularly CD14+ monocytes) and possibly smooth muscle cells in large arteries are the likely sites of infection and latency.[9] CMV infection of endothelial cells increases expression of cell adhesion molecules (ICAM-1) which interacts with monocytes and could provide a means for distribution. Infected cells induce a vigorous immune response releasing pro-inflammatory cytokines (like gamma IFN and TNF-alpha) that play a role in reactivation[15]. Monocyte differentiation driven by con-A-stimulated T-cells has been shown to reactivate non-lytic infection in monocyte-derived macrophages as well as other myeloid precursors[7]. The precise combination of cells and mediators may vary depending on the system but inflammatory cytokines, chemokines, and even some anti-inflammatory cytokines like

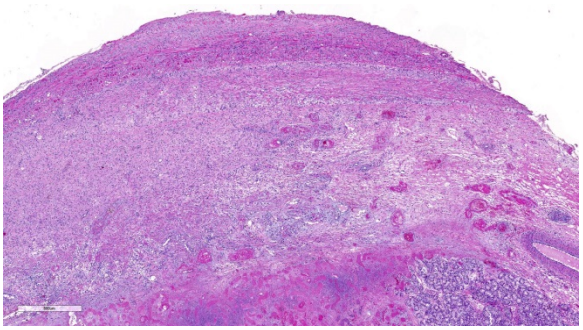

Testis, cynomolgus macaque. The overlying tunics are fused and expanded by abundant fibrous connective tissue. (HE, 20X)

IL-10 play a role in reactivation. The ability of CMV to bind to Fc-domains of neutralizing antibody and use it to infect naïve cells[13] enhances viral persistence. In one study all SIV-infected rhesus monkeys were latently infected with CMV, seven of eleven had productive infections demonstrated by immunohistochemistry in the gut, liver, lungs, and testicles, and two of these seven had typical inflammatory lesions.[11]

Our case demonstrates reactivation of CMV in the testis. Large numbers of classic "owls-eye" cells are noted in the endothelium and interstitial cells extending Baskin's earlier observations.[5] Evidence of vascular thrombosis could have contributed to the extensive necrosis observed in this tissue.

JPC Diagnosis: Testis: Coagulative necrosis (infarct), focally extensive, with vascular thrombosis, fibrinoid necrosis, chronic periorchitis with adhesions, and intranuclear viral inclusions, pigtail macaque, *Macaca nemestrina*.

Conference Comment: Rhesus cytomegalovirus (CMV), also known as macacine herpesvirus-3, is the most common opportunistic pathogen in SIV-infected rhesus macaques with a seroprevalence approaching 100% within the first year of life. Other nonhuman primates with host-adapted CMVs include chimpanzees, African green monkeys, sooty mangabeys, and owl monkeys.[2,3,4,6] These highly host-specific dsDNA viruses of the subfamily betaherpesvirinae have tropism for multiple organs producing interstitial pneumonia, gastroenteritis, poly-radiculoneuritis, encephalitis, and lymphadenitis, in addition to orchitis and periorchitis present in this case.[2] Lesions may also be in the liver, spleen, salivary gland, lymph node, and kidney. Both human and rhesus CMV are unique in that they encode a CXC chemokine, interleukin 8 (IL-8), which induces neutrophil chemotaxis, a prominent feature in this case.[2] This tissue section has marked karyomegaly and cytomegaly with prominent magenta intranuclear inclusions, typical for CMV. Necrotizing and proliferative vasculitis has also been reported in affected tissues.[2,3] In this case, there is fibrinoid vascular necrosis with thrombosis, which likely caused a focally extensive area of coagulative necrosis (infarct) in this testis.

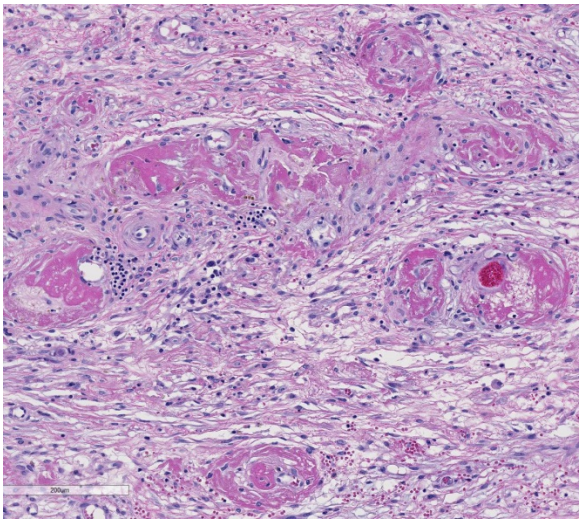

Testis, cynomolgus macaque. Blood vessels with in the fused tunics exhibit fibrinoid necrosis. (HE, 128X)

Additionally, a recent report in *Veterinary Pathology*[2] reported peripheral neuropathy in the facial nerve associated with systemic CMV infection in a group of SIV-positive rhesus macaques. Interestingly, the pathogenesis of the nerve damage is likely due to the bystander effect secondary to CMV-induced inflammation rather than direct viral infection of Schwann cells.[2] Readers are encouraged to review 2015 Wednesday Slide Conference 16 Case 1 for a great example of CMV-induced radiculitis within lumbar spinal roots of a rhesus macaque.

Conference participants discussed other cytomegaloviruses of veterinary importance. Guinea pig cytomegalovirus, also known as Cavid herpesvirus 1, is a common incidental finding in immunocompetent guinea pigs. Similar to CMV of other species, the salivary glands are the primary target tissue in the guinea pig.[15] Additionally, suid herpesvirus 2 is a CMV that affects pigs causing inclusion body rhinitis in suckling pigs and severe generalized disease in neonates (>3 weeks old).[18] Hamster, mice, and rats also have their own host adapted CMVs typically affecting the salivary and lacrimal glands.[15]

Contributing Institution:
Tulane National Primate Research Center
Department of Comparative Pathology
18703 Three Rivers Rd
Covington, LA 70433
http://www.tnprc.tulane.edu/

References:

1. Alcendor DJ, Barry PA, Pratt-Lowe E, Luciw PA. Analysis of the rhesus cytomegalovirus intermediate-early gene promoter. *Virology*. 1993;194:815-821.
2. Assaf BT, Knight HL, Miller AD. Rhesus cytomegalovirus (*Macacine herpesvirus-3*) associated facial neuritis in a simian immunodeficiency virus infected rhesus macaques. *Vet Pathol.* 2015; 52(1):217-223.
3. Barry PA and Chang WL. Primate betaherpesviruses. In: *Human Herpesviruses: Biology, Therapy, and Immunoprophylaxis*. Cambridge: Cambridge University Press; 2007.
4. Barry AP, Silvestri G, Safrit JT et al. Depletion of CD8+ cells in sooty mangabey monkeys naturally infected with simian immuno-deficiency virus reveals limited role for immune control of virus replicated in a natural host species. *J Immunol*. 2007; 178(12):8002-8012.
5. Baskin GB. Disseminated cyto-megalovirus infection in immuno-deficient rhesus monkeys. *Am J Path*. 1987; 29(2):345-352.
6. Davison AJ, Dolan A, Akter P et al. The human cytomegalovirus genome revisited: comparison with the chimpanzee cytomegalovirus genome. *J Gen Virol*. 2003; 84(1):17-28.
7. Hansen SG, Strelow LI, Franchi DC et al. complete sequence and genomic analysis of rhesus cytomegalovirus. *J Virol*. 2003; 77:6620-6636.
8. Ibanez CE, Schrier R, Ghazal P et al. A human cytomegalovirus productively infects primary differentiated macrophages. *J Virol*. 1991; 65:6581-6588.
9. Jarvis MA, Nelson JA. Molecular basis of persistence and latency. In: *Human Herpesvirus Biology, Therapy, and Immunoprophylaxis*. Cambridge University Press, 2007.
10. Kaur A, Daniel MD, Hempel D et al. Cytotoxic T-lymphocyte responses to cytomegalovirus in normal and

simian immunodeficiency virus-infected rhesus macaques. *J Virol*. 1996; 70(11):7725-7733.
11. Kuhn EM, Stolte N, Matz-Rensing K et al. Immunohistochemical studies of productive rhesus cyto-megalovirus infection in rhesus monkeys (*Macaca mulatta*) infected with simian immunodeficiency virus. *Vet Pathol*. 1999; 36(1):51-56.
12. Lee So, Razonable RR. Current concepts on cytomegalovirus infection after liver transplantation. *World J Hepatol*. 2010; 2(9):325-326.
13. Manley K, Anderson J, Yang F, et al. Human cytomegalovirus escapes a naturally occurring neutralizing antibody by incorporating it into assembling virions. *Cell Host Microbe*. 2011; 10:197-209.
14. Osborn KG, Prahalada S, Lowenstine LJ et al.The pathology of an epizootic of acquired immuno-deficiency in rhesus macaques. *Am J Pathol*. 1984; 114:94-103.
15. Percy DH, Barthold SW. *Pathology of Laboratory Rodents and Rabbits*, 4th ed. Ames, IA: Blackwell Publishing; 2016:15,122,175,219.
16. Sequar G, Britt WJ, Lakeman FD et al. Experimental coinfection of rhesus macaques with rhesus cytomegalovirus and simian immunodeficiency virus: Pathogenesis. *J Virol*. 2002; 76(15):7661-7671.
17. Waldman WJ, Knight DA, Cytokine-mediated induction of endothelial adhesion molecule and histo-compatibility leukocyte antigen expression by cytomegalovirus-activated T cells. *J Inf Dis*. 1995; 171:263-272.
18. Yoon KJ, Edington N. Porcine cytomegalovirus. In: Straw BE, et al, eds. *Diseases of Swine*. 9th ed. Ames, IA:Blackwell Publishing; 2006:323-329.
19. Zhu H, Cong JP, Mamtora G et al. Cellular gene expression altered by human cytomegalovirus: global monitoring with oligonucleotide arrays. *Proc Natl Acad Sci* 1998; 95(24):14470-14475.

CASE II: T1339/16 (JPC 4085507).

Signalment: Unknown age and gender, guinea pig, (*Cavia porcellus*).

History: The animal developed a skin tumor of 1 cm in diameter at the right flank. The mass was completely resected. Unfortunately, further clinical data were not available.

Gross Pathology: A 2 x 1 cm skin sample was submitted for histopathologic examination. Centrally there was a well-demarcated, 1 x 1 cm partially exophytic firm nodule. The cut surface was light brown.

Laboratory results: Immuno-histochemically the neoplastic cells were positive for Melan-A and PNL2.

Histopathologic Description: Haired skin: Elevating an ulcerated epidermis and infiltrating into the underlying dermis (in some slides, tumor overlies an intact epidermis) is densely cellular, well-demarcated, exophytic, partly infiltrative and ulcerated, unencapsulated neoplasm composed of sheets of pleomorphic round cells within a scant fibrovascular stroma. Neoplastic cells are round to polygonal, up to 40 um in diameter with variable distinct cell borders and moderate amounts of

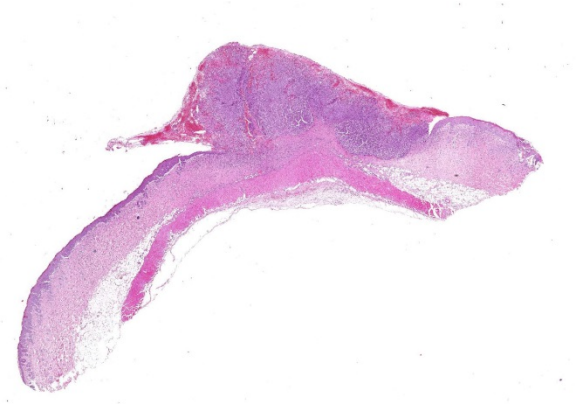

Haired skin, rabbit. Infiltrating the dermis, there is a 1cm, moderately cellular, exophytic neoplasm. (HE, 5X).

eosinophilic cytoplasm. Nuclei are round to oval, centrally located with finely stippled chromatin and up to four prominent magenta nucleoli. Mitoses average 2-3 per high power field (some bizarre) and cells show moderate anisocytosis and anisokaryosis. Occasionally, vascular invasion of tumor cells can be observed (not in all slides). There are multifocal hemorrhages within and around the tumor and hemorrhagic and serocellular crusts at the ulcerated surface. The adjacent skin is hyperplastic with a moderate perivascular infiltration with lymphocytes, plasma cells, and few heterophils.

Contributor's Morphologic Diagnosis: Haired skin: Amelanotic malignant melanoma, guinea pig, *Cavia porcellus*

Contributor's Comment: Melanomas are described in a variety of animal species including domestic animals and wildlife species. However, they are most common in dogs, horses and some breed of swine[10], only few reports of melanoma in birds, laboratory animals and more recently in reptiles exist.[6,16] The histologic diagnosis of melanoma is complicated due to variable degree of pigmentation and the high variability of cell shapes. With the help of immunohistochemistry, most amelanotic melanoma can be routinely diagnosed.[3,4,10]

With our case, we present a well-known neoplasm in an unusual species. Case reports of spontaneous melanoma in the guinea pig are extremely rare, but the guinea pig is a well-defined model of experimental melanoma using the potent carcinogen 7,12-dimethylbenz[*a*]anthracene (DMBA), a polycyclic aromatic hydrocarbon.[7] This substance is proven to transform cells in different oncogenic pathways.[2]

Mutations that affect cell cycle control (p16/INK4a, CDK4), pro-growth pathways (growth factor receptors, RAS, BRAF), and telomerase were identified in the patho-genesis of malignant melanoma. Furthermore, melanomas can be inherited, and UV light-induced DNA damage plays a role as do other factors.[8]

The most common naturally occurring skin tumors in guinea pigs are trichofolliculomas. They are a subtype of trichoepithelioma and occur as expansible, often centrally cystic neoplasia in the skin often of the lumbosacral region.[13,15,18] Other tumors, like fibrosarcoma, lipoma, sebaceous gland adenoma, and hemangioma were also reported in this species.

In this melanoma, there is abundant vascularity. As observed in other species[5,12] the amount of blood vessels may be a prognostic factor for this neoplasia in guinea pigs, and particularly mast cells may play a significant role in angiogenesis as the major source of VEGF.[1]

Unfortunately, further information regarding the clinical course of the presented case was not available.

JPC Diagnosis: Haired skin: Amelanotic melanoma, guinea pig, *Cavia porcellus*.

Conference Comment: Melanocytic neoplasms arise from melanocytes or melanoblasts which are derived from the neural crest ectoderm. As mentioned by the contributor, melanomas have been identified in most veterinary species and humans. The histologic diagnosis of melanomas is sometimes complicated due to the variability of pigmentation and arrangement of neoplastic cells into clear cells (balloon cell), spindle cell, epithelioid cell, and signet ring cell histomorphology.[10] Additionally, there are often multiple different tumor cell morphologies within a single neoplasm. For this reason, melanomas are sometimes referred to as one of the "great imitators" due to their common embryologic connection with both neural and epithelial origin.[10] This case nicely demonstrates this point, due to variation in round to polygonal cellular appearance across various regions of the neoplasm. Despite the rarity of melanocytic neoplasms in guinea pigs and the lack of melanin granularity in this case, most conference participants included amelanotic melanoma high within their differential diagnosis. Prior to the conference, the Joint Pathology Center ran the histochemical stain Fontana-Masson and immuno-histochemical stains melan-A and S100. The Fontana-Masson stain highlighted multifocal positive argentaffin granules and melanin within the cytoplasm of neoplastic cells. Additionally, neoplastic cells are immunopositive for S100 and melan-A red, confirming the diagnosis of an amelanotic melanoma, in this case.

As mentioned by the contributor, trichofolliculomas are the most common tumor in the skin of guinea pigs; although, spontaneous neoplasms in this species are rare in animals under three years old.[13]

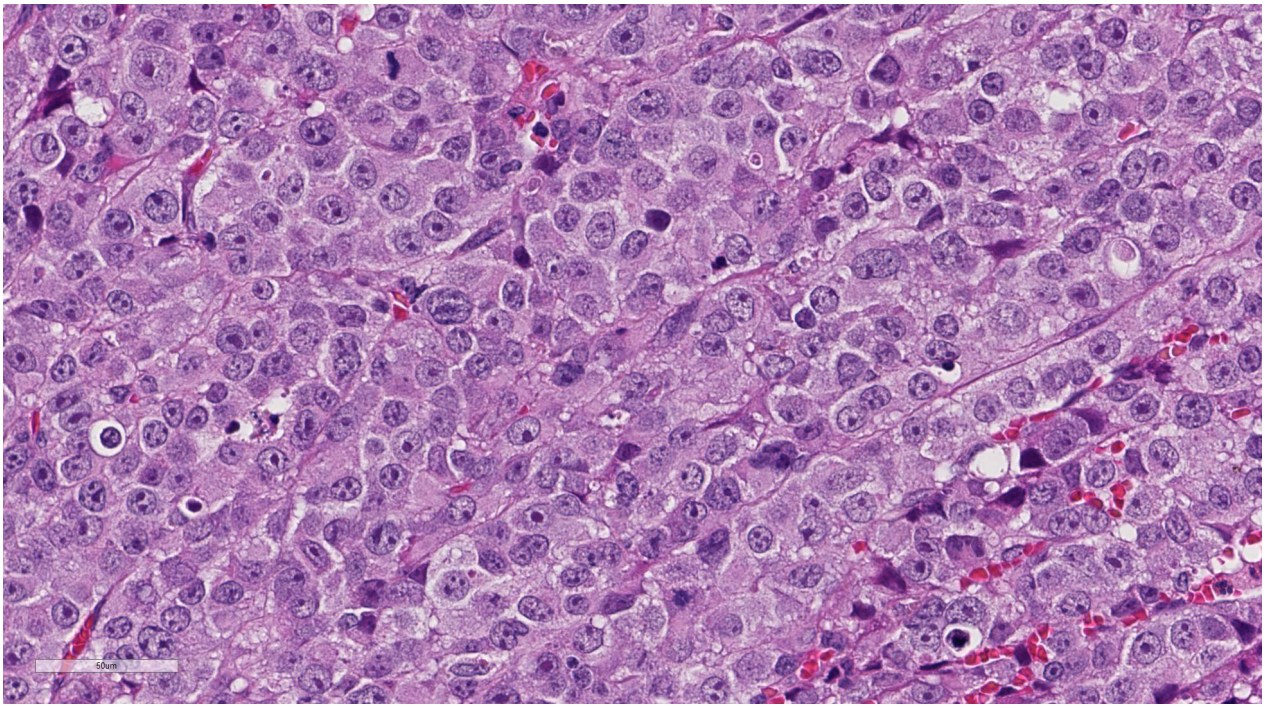

Haired skin, rabbit. Neoplastic cells are polygonal, arranged in nests and cords with abundant granular cytoplasm, and have large nuclei with prominent nucleoli. Mitotic figures are common.

These benign dome-shaped subcutaneous nodules, typically less than 2cm in diameter, most commonly occur along the dorsal lumbar region and may represent a hamartomatous rather than a neoplastic process.[10,13] Trichofolliculoma development is thought to occur secondary to inhibition of bone morphogenic protein (BMP), an important tumor suppressor gene.[13,14,18] Studies indicate that BMP plays a critical role in maintaining homeostasis of hair follicles and regulation of skin development.[14] In addition, BMP is an important growth factor for a variety of tissues throughout the body and its con-centration is tightly regulated in health. Interestingly, recent research in humans have shown that absence of BMP signaling leads to the progression of colorectal carcinoma; conversely, overexpression of BMP signaling induces epithelial-mesenchymal transition, tumor invasion, and metastasis in a variety of malignant neoplasms.[9,11,14]

Contributing Institution:
Institut fuer Veterinaer-Pathologie, Justus-Liebig-Universitaet Giessen
Frankfurter Str. 96, 35392
Giessen, Germany
http://www.uni-giessen.de/cms/fbz/fb10/institute_klinikum/institute/pathologie

References:

1. Ch'ng S, Wallis RA, Yuan L, Davis PF, Tan ST. Mast cells and cutaneous malignancies. *Mod Pathol*. 2006; 19(1):149-159.
2. Currier N, Solomon SE, Demicco EG, Chang DL, Farago M, Ying H, Dominguez I, Sonenshein GE, Cardiff RD, Xiao ZX, Sherr DH, Seldin DC. Oncogenic signaling pathways activated in DMBA-induced mouse mammary tumors. *Toxicol Pathol.* 2005;33(6):726-37.
3. Goldschmidt MH, Dunstan RW, Stannard AA, Tscharner CV, et al. *Histological classification of epithelial and melanocytic tumors of the skin of domestic animals*. Vol III. 2nd series. Washington D.C.: Armed Forces Institute of Pathology. 1998.
4. Goldschmidt MH, Hendrick MJ. Tumors of the skin and soft tissue. In: Meuten DJ, ed. *Tumors in Domestic Animals*. 4th Ed. Ames, IA, USA: Blackwell Publishing; 2002:45-117.
5. Gregório H, Raposo TP, Queiroga FL, Prada J, Pires I. Investigating associations of cyclooxygenase-2 expression with angiogenesis, proliferation, macrophage and T-lymphocyte infiltration in canine melanocytic tumours. *Melanoma Res*. 2016; 26(4):338-347.
6. Heckers KO, Schmidt V, Krastel D, Hildebrandt G, Kiefer I, Pees M. Malignant melanophoroma in a Hermann's tortoise (*Testudo hermanni*). A case report. *Tierarztl Prax* (K) 2011; 39:45-50.
7. Ingram AJ. Review of chemical and UV light-induced melanomas in experimental animals in relation to human melanoma incidence. *J Appl Toxicol*. 1992; 12(1):39-43.
8. Lazar AJF, Murphy GF. The skin. In: Kumar Abbas Aster Robbins and Cotran. *Pathologic basis of disease*. 9th Edition. Philadelphia, PA, Elsevier Saunders. 2015. 1147-1150.
9. Kan L, Liu Y, et al. Inhibition of BMP signaling in P-cadherin positive hair progenitor cells leads to tricho-folliculoma-like hair follicle neoplasms. *J Biomed Sci*. 2011; 14:92.
10. Mauldin EA, Peters-Kennedy J. Integumentary system. In: Maxie MG, ed. *Jubb, Kennedy and Palmers Pathology of Domestic Animals*. 6th ed.

Vol 1. Elsevier, St. Louis, Missouri; 2016:705,720-736.
11. Owens p, Pickup MW, et al. Inhibition of BMP signaling suppresses metastasis in mammary cancer. *Oncogene*. 2015; 34:2437-2449.
12. Pastushenko I, Vermeulen PB, Carapeto FJ, Van den Eynden G, Rutten A, Ara M, Dirix LY, Van Laere S. Blood microvessel density, lymphatic microvessel density and lymphatic invasion in predicting melanoma metastases: systematic review and meta-analysis. *Br J Dermatol*. 2014; 170(1):66-77.
13. Percy DH, Barthold SW. *Pathology of Laboratory Rodents and Rabbits*, 4th ed. Ames, IA: Blackwell Publishing; 2016:251.
14. Sharov AA, Mardaryev AN, Sharova TY, Grachtchouk M, Atoyan R, Byers HR, Seykora JT, Overbeek P, Dlugosz A, Botchkare VA. Bone morphogenetic protein antagonist noggin promotes skin tumorigenesis via stimulation of the Wnt and Shh signaling pathways. *Am J Path*. 2009; 175(3):1303-1314.
15. Sommerey CC, Köhler K, Reinacher M. Erkrankungen des Meerschweinchens aus Sicht der Pathologie. *Tierarztl Prax* (K) 2004; 32:377-383.
16. Thompson KA, Campbell M, Levens G, Agnew D. Bilaterally symmetrical oral amelanotic melanoma in a Boa constrictor (Boa constrictor constrictor). *J Zoo Wildl Med*. 2015; 46(3):629-32.
17. Voorneveld PW, Kodach LL, et al. Loss of SMAD4 alters BMP signaling to promote colorectal cancer cell metastasis via activation of Rho and ROCK. *Gastroenterology*. 2014; 147:196-208.
18. Williams BH. Non-infectious disease. III Guinea pigs. In: Suckow MA, Stevens KA, Wilson RP. *The laboratory rabbit, guinea pig, hamster and other rodents*. First Edition. London, Waltham, MA, San Diego, CA. Elsevier, Academic press, 2012, 685-704.

CASE III: 11A228 (JPC 4019364).

Signalment: Nine-year-old, female, rhesus macaque, (*Macaca mulatta*).

History: This adult female rhesus macaque was imported from China by a commercial vendor and completed international quarantine. It was acquired by this institution in December 2009 and completed domestic quarantine in January 2010. Multiple tests for tuberculosis were performed. The animal was housed individually in a room with 11 other adult rhesus macaques. Euthanasia and necropsy were performed when other animals housed in this room exhibited positive reactions to intradermal skin tests using mammalian old tuberculin (MOT).

Gross Pathology: A single 0.3cm firm nodule containing homogenous off-white

Tracheobronchial lymph nodes, rhesus macaque. These nodes are largely effaced by granulomas which bulge from the cut surface. (Photo courtesy of: Oregon National Primate Research Center, http://onprc.ohsu.edu).

material was present within the parenchyma of the right caudal lung lobe. There were several pale gray foci within the lung lobes measuring approximately 0.3 cm in diameter. All lung lobes exhibited diffuse, fine, gray-black stippling, consistent with anthracosilicosis. The tracheobronchial lymph nodes were moderately enlarged and distorted by multiple nodules. On sectioned surface the nodules contained cores of off-white material with a firm tan rim. The remaining lymph node parenchyma was dark gray.

Laboratory results:

Table 1: Eyelid scoring guide, intradermal tuberculin skin test (TST) with MOT:

Grade	Score	Description
0	Negative	No reaction
1	Negative	Bruise
2	Negative	Erythema, no swelling
3	Suspect	Erythema with minimal swelling OR slight swelling without erythema
4	Positive	Obvious swelling with eyelid droop and erythema
5	Positive	Swelling and/or necrosis with eyelid closed

Table 2: Tuberculosis testing

Date	Test	Result
12-14-09	TST MOT	Grade 0 (negative)
12-28-09	TST MOT	Grade 0 (negative)
01-05-10	Thoracic radiographs	unremarkable
01-11-10	TST MOT	Grade 0 (negative)
11-05-10	TST MOT	Grade 3 (suspect)
11-08-10	TST MOT	Grade 0 (negative)
11-08-10	PRIMAGAM®	Negative
11-08-10	PrimaTB STAT-PAK®	Negative
04-08-11	PrimaTB STAT-PAK®	Negative
04-14-11	PrimaTB STAT-PAK®	Negative

Histopathologic Description: The normal architecture of the lymph node is multifocally effaced and expanded by round to irregular granulomas (tubercles) characterized by variable central accumulations of homogeneous eosinophilic material and cellular and karyorrhectic debris admixed with neutrophils and surrounded by an inner rim of foamy, epithelioid macrophages, occasional multi-nucleated giant cells (Langhans type), fibroblasts, bands of eosinophilic material (collagen), and an outer rim of lymphocytes and fewer histiocytes. Numerous histiocytes in the medullary sinuses contain cytoplasmic granules that are black to brown and occasionally refractile (anthracosilicotic pigment). A Ziehl-Neelsen stain reveals rare acid-fast bacilli in epithelioid macrophages and multinucleated giant cells.

Contributor's Morphologic Diagnosis: Tracheobronchial lymph node: Lymphadenitis, necrogranulomatous, chronic, multifocal, moderate, with rare intracellular acid-fast bacilli, rhesus

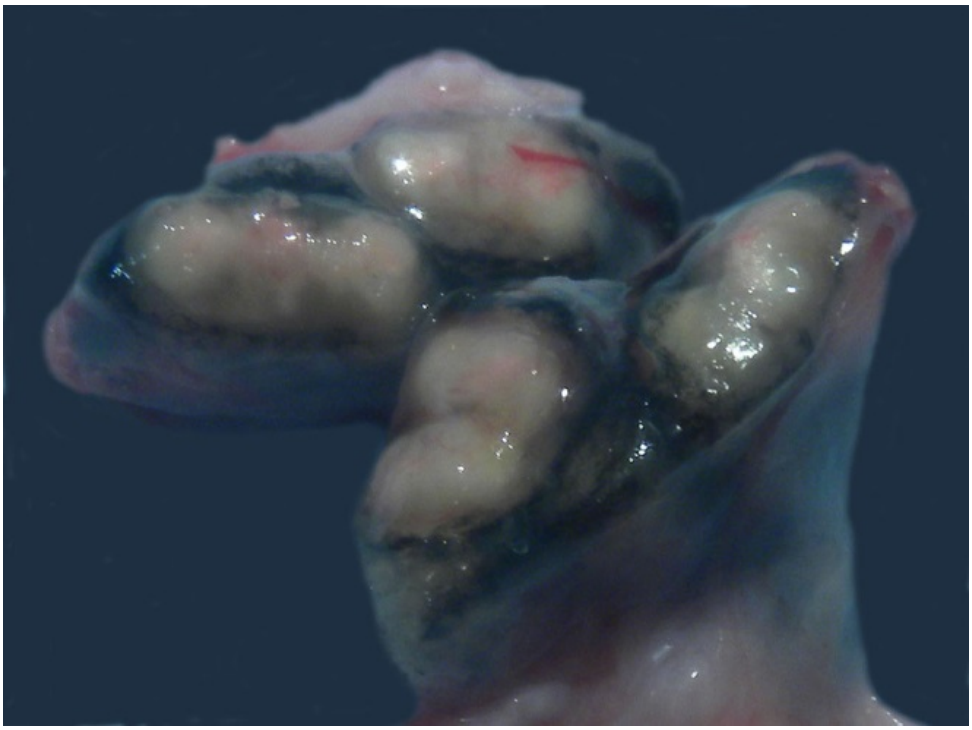

Lungs, rhesus macaque. Variably-sized granulomas are present within multiple lung lobes. (Photo courtesy of: Oregon National Primate Research Center, http://onprc.ohsu.edu).

macaque (*Macaca mulatta*), nonhuman primate.

Relevant microscopic findings of tissues not submitted: Similar focus of necro-granulomatous inflammation containing rare intracellular acid-fast bacilli in epithelioid macrophages and multi-nucleated giant cells was present in the lung.

Contributor's Comment: This was a case of spontaneous tuberculosis affecting a single room housing 12 rhesus macaques (*Macaca mulatta*). The primary gross and histologic findings are necrogranulomatous inflammation with rare intracellular acid-fast bacilli involving multiple tracheobronchial lymph nodes and the right caudal lung lobe. Characteristic tubercles were present in the lung and/or tracheobronchial lymph node of 10 of the 12 animals.

Mycobacterium tuberculosis (Mtb) was cultured from the tracheobronchial lymph node by the National Veterinary Services Laboratory (USDA, APHIS) in this case. Mtb was isolated from lung and/or tracheobronchial lymph node in 7 of 12 animals involved in the outbreak. Genotyping was performed and all isolates shared the same spoligotype and VNTR-11 profile, confirming a common source of infection. The results of tuberculosis testing on this animal from the time of acquisition to death appear in Table 2.

Mtb is an aerobic, nonmotile, nonsporulating, straight to slightly curved 1-4 micron rod-shaped bacillus from the order *Actinomycetales*. Mtb is a member of the *M. tuberculosis* complex, which includes other *Mycobacterium* species that induce tubercle formation including *M. bovis* and its variants *M. caprae* and *M. pinnipedi*, and less frequently identified species *M. africanum*, *M. canetti,* and *M. microti*.[10] The bacterium features a thick, waxy cell wall containing mycolic acids which impart unique characteristics including acid-fast staining positivity and, along with other cell wall components, resistance to environmental desiccation, antibiotics, and phagocyte destruction.

In macaques, infection occurs following inhalation of aerosolized bacteria into the lungs.[7] Ingestion is an infrequently encountered route of inoculation. Resident tissue macrophages phagocytize bacteria,

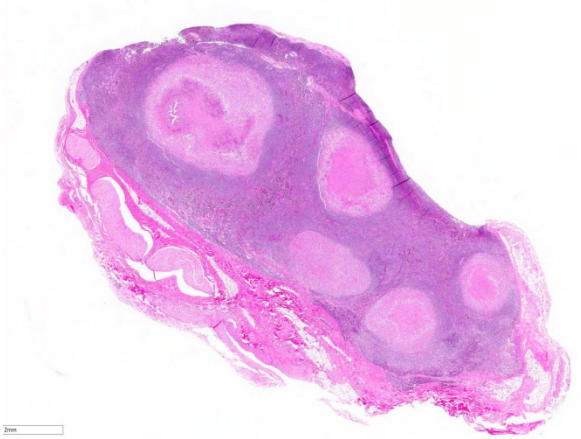

Tracheobronchial lymph node, rhesus macaque. Low magnification of a cross section of the lymph node demonstrates the granulomas seen in Figure 3-1. (HE, 5X)

and through multiple mechanisms, bacteria prevent lysosomal degradation and subsequently replicate within an intracytoplasmic phagosome.[10] Dendritic macrophages may then disseminate bacilli to draining lymph nodes and distant organs. Complex biochemical signaling and immune cell activation pathways, especially of CD4+ and CD8+ T cells, are required for control of primary infection.[2,4,7,9,10] The latent, non-infectious stage ensues when bacteria have been sequestered within granulomas characterized by a central accumulation of necrotic debris that is rarely mineralized surrounded by infected epithelioid macrophages and Langhans multinucleated giant cells, lymphocytes, and a fibrous capsule.[10] Bacteria persist within the tubercle and may reactivate, typically in association with immunosuppression.[5,9] Typical tubercles can be found in any organ and most commonly disseminate from the lungs and hilar lymph nodes to the liver, spleen, kidney, vertebra, and gastrointestinal tract.

Cases of spontaneous and experimental tuberculosis are reported in several primate species with variation in susceptibility to disease.[1,2,4,7,9] Macaques are known to be highly susceptible and present with a disease course of fulminate primary, active-chronic, or latent infection with or without reactivation. Active infection and bacterial shedding can occur over weeks to months, during which time clinical signs may be vague, weight loss and cough, or inapparent.[1,6,9] Intermittent bacterial shedding in latently infected macaques has been documented experimentally, evidenced by sporadic positive bacterial culture of gastric and bronchial alveolar lavage fluids.[9] This finding suggests that disease occurs on a continuum between active and latent infection. Cynomolgus macaques are thought to be relatively more resistant to clinical disease than rhesus macaques, and in experimental studies, 40-50% developed latency.[2,6,9] Spontaneous reactivation of latent infection in the absence of experimental immunosuppression is infrequent, reportedly less than 5% in cynomolgus macaques.[5]

Mtb is an important zoonotic pathogen with potentially devastating effects in captive macaque populations and routine measures have been adopted by US facilities for screening of imported and domestically-reared animals. The most commonly utilized screening test is the tuberculin skin test (TST).[8] MOT, a combination of *Mycobacterium* antigens from multiple species, is injected intradermally, typically into the upper eyelid.[8] The site is checked for reaction at 24, 48, and 72 hours post-injection (see Table 1 for grading).[8] In affected animals, a delayed-type hypersensitivity reaction to antigen produces swelling, erythema, and/or necrosis at the injection site. False negatives may occur in animals with anergy and disseminated disease, and in animals that are in the latent stage of infection.[8] The MOT antigen is not specific for *M. tuberculosis* and *M. bovis*, and false positives may occur in the face of

infection with a non-tubercular *Mycobacterium* species. The TST is the only approved screening test for internationally acquired animals undergoing US quarantine, and three negative tests two weeks apart are the standard requirement.[8] Typically, animals that have cleared international quarantine and domestically reared animals are tested on a semiannual basis.

Alternative commercial tests utilized during this outbreak included the whole-blood interferon gamma (INFγ) test PRIMAGAM® (Prionics USA Inc., La Vista, NE) and the lateral flow immunoassay PrimaTB STAT-PAK® (CHEMBIO).[8] In the PRIMAGAM® test, the concentration of INFγ is measured following incubation with purified protein derivative (PPD) of *M. bovis* (bPPD) and *M. avium* (aPPD).[8] Positive tests that yield a higher reaction to bPPD vs. aPPD indicate sensitization to antigens from either *M. tuberculosis* or *M. bovis*, while a higher aPPD suggests sensitization to *M. avium* and retesting after a 2-week period is recommended.[7] The PrimaTB STAT-PAK® test detects antibody response to three TB-specific antigens (ESTAT-6, CFP-10, MPB83).[8] Serum, whole blood, or plasma can be used.

During this outbreak, the first animal was initially detected by routine tuberculosis surveillance with a positive TST. Affected animals exhibited variable responses to TST, PRIMAGAM®, and PrimaTB STAT-PAK® testing performed during the outbreak. Five months prior to the outbreak this animal exhibited a grade 3 reaction with a TST. A follow-up TST on the contralateral eyelid and PRIMAGAM® and PrimaTB STAT-PAK® tests were all negative. Likewise, all three tests performed at the time of the outbreak were negative. The gold-standard for diagnosis of *M. tuberculosis* is culture,

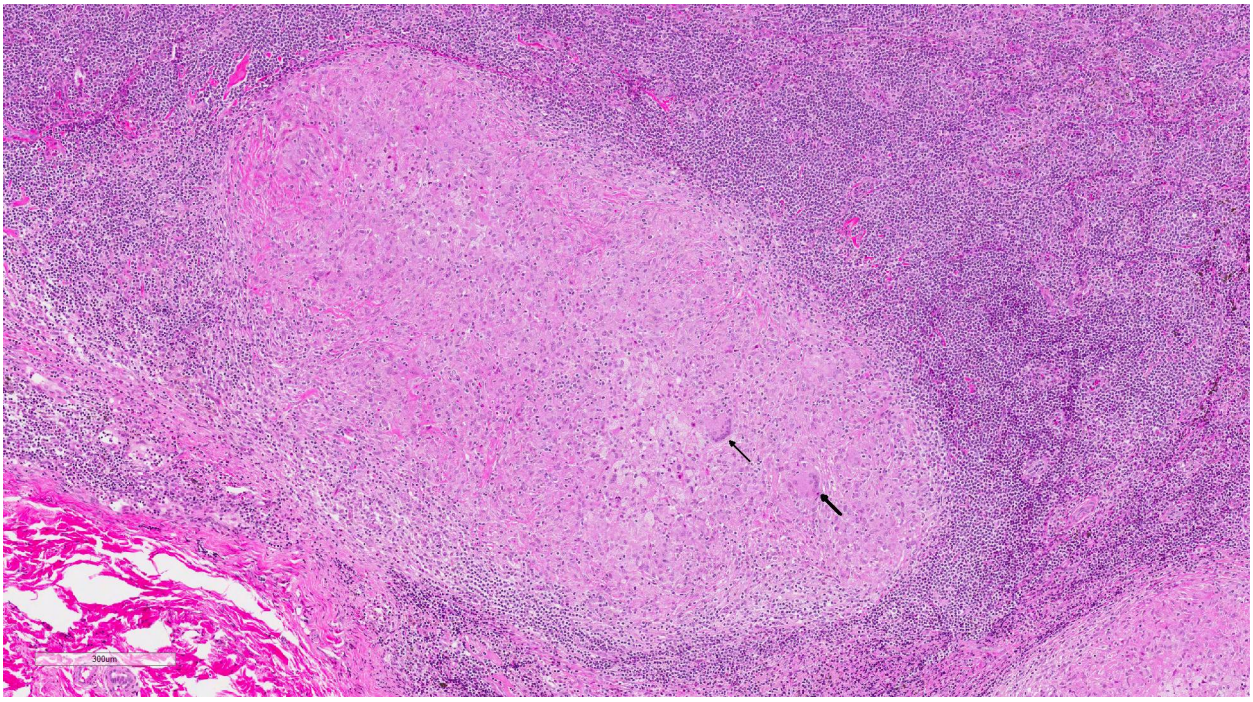

Tracheobronchial lymph node, rhesus macaque. Higher magnification of one of the granulomas. At 75X, several Langhans' giant cells are visible. (HE, 75X)

which was positive for this animal. This outbreak is thought to have occurred as a result of reactivation and shedding from a latently infected animal in the room. The source was not identified. This outbreak illustrates the challenges of antemortem diagnosis and underscores the importance of routine tuberculosis screening as clinical signs were not observed in any of the animals in this cohort.

JPC Diagnosis: Lymph node: Lymphadenitis, granulomatous, multifocal to coalescing, moderate, rhesus macaque, *Macaca mulatta*.

Conference Comment: The contributor provides a fantastic example of one of the classic manifestations of *Mycobacterium tuberculosis* (*Mtb*) in a nonhuman primate. Participants readily identified multifocal to coalescing well organized to nodular tuberculoid granulomas partially effacing the lymph node architecture. The classic tubercle forming bacilli are *Mtb*, primarily infecting humans and nonhuman primates, and *Mycobacterium bovis* affecting bovine species.[3]

Infection is typically via inhalation of aerosol droplets from an infected individual with pulmonary disease. Humans are the only known natural reservoir for *Mtb*. The bacilli then travel to the alveoli where they are phagocytized by alveolar macrophages. The ability of the organism to survive within macrophages is the key to its pathogenicity.[10] Once inside the macrophage, bacilli can survive and replicate by inhibiting the fusion of the phagolysosome, thus preventing oxygen radical formation and avoiding proteolytic enzymes produced by the host macrophage. Natural resistance-associated macrophage protein (NRAMP) is a membrane protein that is involved in innate immunity to

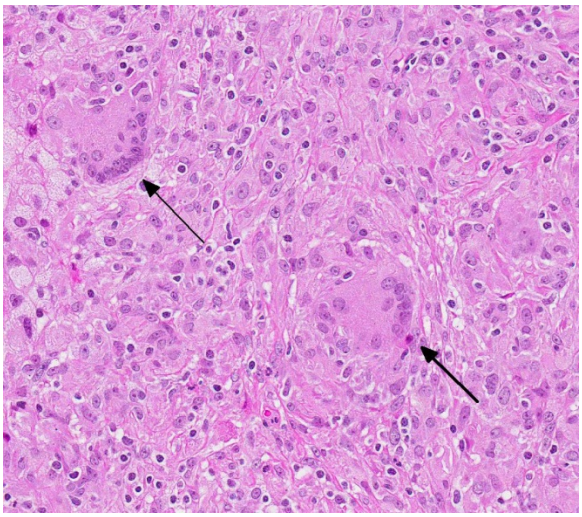

Tracheobronchial lymph node, rhesus macaque. Higher magnification of the Langhans' giant cells. Other multinucleated macrophages are present within this field. (HE, 316X)

infection by *M. bovis* in humans and mice.[1,3,10]

Once exposed to the bacteria, alveolar macrophages are stimulated by ligation of Toll-like receptor 2 (TLR2) and TLR4 to secrete pro-inflammatory cytokines such as tumor necrosis factor-alpha (TNF-alpha), interleukin-1 (IL-1) IL-6 and IL-12, in addition to a variety of C-C chemokines to recruit leukocytes to the site of infection. Alveolar macrophages also present phagocytized mycobacterial antigen to naïve T cells via major histocompatibility complex class II (MHC II).[3,10] This binding to the T-cell receptor and exposure to IL-12 secretion stimulates T cell differentiation to CD4+ T helper 1 (Th1) lymphocytes. These Th1 lymphocytes then secrete interferon gamma (IFN-gamma) and IL-2 stimulating the classical activation of macrophages, favoring a cell mediated immune response. TNF-alpha and IFN-gamma work synergistically to form tuberculoid granulomas in an effort to prevent the spread of the infection to other sites in the body and transmission of the infection to other animals.[3,10] This granuloma is maintained by

a type IV (delayed-type) hypersensitivity (DTH) reaction to persistent antigenic stimulation due to *Mtb*'s ability to survive within macrophages and extracellularly within the granuloma. Ongoing infection eventually leads to caseous necrosis within central area of the granulomas. Interestingly, bacilli can survive for years within the caseous centers and be reactivated by immunosuppression, malnutrition, or concurrent infection.[1,3,10]

Additionally, dendritic cells in the lung also phagocytize *Mtb* by binding receptor DC-SIGN via the bacterial cell wall virulence factors lipoarabinomannan mannose-capped (ManLAM), complement receptor 2 (CR3), and mannose receptor (MR) and then migrate to regional lymph nodes to present mycobacterial antigens to lymphocytes. Spread from the lungs to the tracheobronchial may lymph node may explain the location of the lesion within the tracheobronchial lymph node, in this case.[3,10]

Contributing Institution:

Pathology Services Unit
Department of Animal Resources
Oregon National Primate Research Center
Beaverton, OR 97006
http://onprc.ohsu.edu

References:

1. Bailey C, Mansfield K. Emerging and reemerging infectious diseases of nonhuman primates in the laboratory setting. *Vet Pathol*. 2010; 47(3):462-481.
2. Capuano III SV, Croix DA, Pawar S, et al. Experimental *Mycobacterium tuberculosis* infection of cynomolgus macaques closely resembles the various manifestations of human *M. tuberculosis* infection. *Infect Immunol*. 2003; 71(10):5831-5844.
3. Caswell JL, Willims KJ. Respiratory system. In: Maxie MG ed. *Jubb, Kennedy, and Palmer's pathology of domestic animals.* Vol 2. 6th ed. St. Louis, Missouri: Elsevier; 2016:547-551.
4. Chen CY, Huang D, Wang RC, et al. A critical role for CD8 T cells in a nonhuman primate model of tuberculosis. *PLoS Path*. 2009; Apr; 5(4):1-10.
5. Diedrich CR, Mattila JT, Klein E, et al. Reactivation of latent tuberculosis in cynomolgus macaques infected with SIV is associated with early peripheral T cell depletion and not virus load. *PLoS One*. 2010; 5(3):1-12.
6. Garcia MA, Bouley DM, Larson MJ, et al. Outbreak of Mycobacterium bovis in a conditioned colony of rhesus (Macaca mulatta) and cynomolgus (*Macaca fascicularis*) macaques. *Comp Med*. 2004; 54(5):578-584.
7. King Jr, NW. Tuberculosis. In Jones TC, Mohr U, Hunt RD, eds. *Nonhuman primates 1*. 1st ed. Germany: Springer-Verlage Berlin Heidelberg; 1993:141-148.
8. Lerche NW, Yee JL, Capuano SV, Flynn JL. New approaches to tuberculosis surveillance in nonhuman primates. *ILAR*. 2008; 49(2):170-178.
9. Lin PL, Rodgers M, Le'kneita S, et al. Quantitative comparison of active and latent tuberculosis in the cynomolgus macaque model. *Infect Immunol*. 2009 Oct; 77(10):4631-4642.
10. Sakamoto K. The pathology of *Mycobacterium tuberculosis* infection. *Vet Pathol*. 2012; 49(3):423-439.

CASE IV: 46519 (JPC 4089353).

Signalment: Two-year-old male Fisher 344 rat (*Rattus rattus*).

History: This male rat had been on test for 634 days as part of a 2-year carcinogenesis study; was found dead and reported as a natural death animal.

Gross Pathology: On gross examination, the abdomen was markedly distended with copious amounts of reddish-brown fluid (ascites). In addition, numerous, pale tan, firm, raised nodules were diffusely lining peritoneal viscera; the testes and epididymis were swollen and discolored containing multiple, discrete, pale tan nodules.

Laboratory results: N/A

Histopathologic Description: Testis and epididymis: An unencapsulated, exophytic neoplasm composed of arborizing papillary projections is diffusely infiltrating the vaginal tunic and lining the serosal surfaces of the testis and epididymis, often extending into the adjacent adipose tissue. The neoplasm is comprised of cuboidal epithelial cells, piling up to 4 cell-layers thick and supported by thick, fibrovascular stroma. Neoplastic cells have indistinct cell borders, with small amounts of finely granular, eosinophilic cytoplasm and a single, central, round to oval nucleus with 1-3 variably distinct nucleoli and finely stippled chromatin. Mitotic figures are rare. Anisocytosis and anisokaryosis are mild. Moderate numbers of mast cells with fewer hemosiderin-laden macrophages are scattered throughout the neoplasm. Small caliber vessels occasionally contain aggregates of neoplastic cells admixed with variable amounts of eosinophilic flocculent material (fibrin) and necrotic debris (vascular invasion). Multifocally within the adjacent adipose tissue, vascular lumina are partially occluded by adherent casts composed of fibrin and a mixture of inflammatory cells (vascular thrombosis). The epididymal ducts are devoid of spermatids (hypospermia) and contain numerous sloughed germ cells within their lumina, admixed with necrotic debris (germ cell exfoliation). Aggregates of basophilic, granular material are occasionally found within ducts or the vacuolated epithelial lining (mineralization and degeneration).

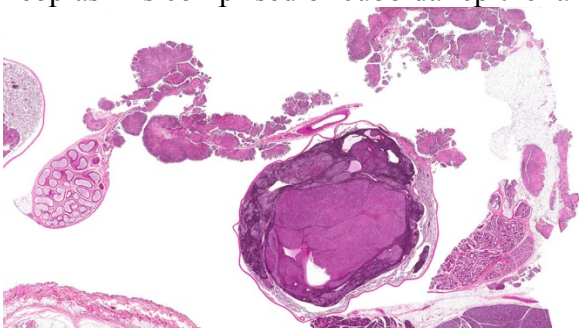

Testis, Fischer 344 rat. The vaginal tunics are expanded by an arborizing proliferative neoplasm (mesothelioma), and the testis is largely effaced by a multinodular neoplasm (interstitial cell tumor) which compresses the remaining seminiferous tubules. (HE, 6X) (Photo courtesy of: EPL, Inc., P.O. Box 12766, Research Triangle Park, NC 27709 http://epl-inc.com/)

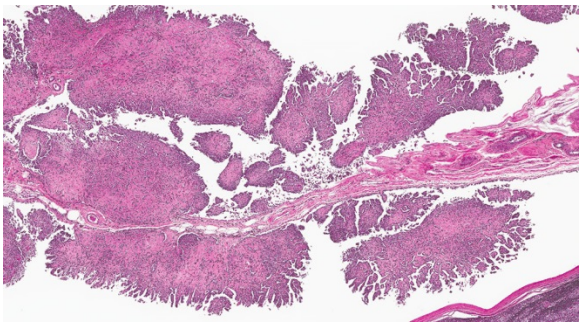

Testis, Fischer 344 rat. The mesothelioma diffusely infiltrates the vaginal tunics and lines the serosal surfaces of the testis and epididymis. (HE, 20X) (Photo courtesy of: EPL, Inc., P.O. Box 12766, Research Triangle Park, NC 27709 http://epl-inc.com

A second approximately 15 x 10mm, discrete, unencapsulated and expansile,

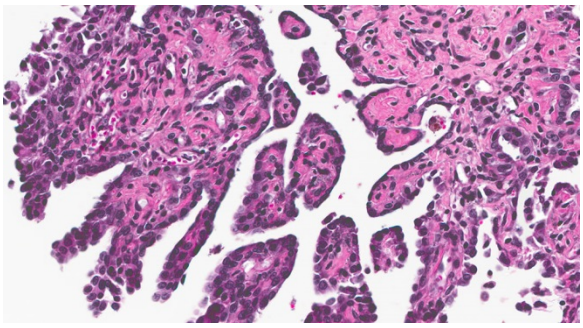

Testis, Fischer 344 rat. The mesothelioma is composed of cuboidal epithelial cells, piling up to 4 cell-layers thick and supported by abundant fibrous stroma. (HE, 400X) (Photo courtesy of: EPL, Inc., P.O. Box 12766, Research Triangle Park, NC 27709 http://epl-inc.com/)

multinodular neoplasm is diffusely effacing and replacing the testicular architecture. The neoplasm is composed of polygonal cells arranged in nests and cords supported by small amounts of fine, fibrovascular stroma. Neoplastic cells have variably distinct cell borders with abundant, finely granular, eosinophilic cytoplasm and a single, round to oval, eccentric to centrally located nucleus containing 1-2 distinct nucleoli and stippled chromatin. Mitotic figures are rare. Anisocytosis and anisokaryosis are mild. Large numbers of lymphocytes are surrounding and infiltrating the neoplasm. The majority of seminiferous tubules are lost; those remaining are shrunken and lined by vacuolated epithelial cells with pyknotic nuclei (tubular degeneration). There are multifocal areas of hemorrhage and mineralization throughout the testis. The contralateral testis is similar in appearance with two, discrete, neoplasms ranging from 2 x 2mm to 3 x 5mm and marked degeneration and atrophy of the seminiferous tubules.

Contributor's Morphologic Diagnoses:

1. Testis, tunica vaginalis: Malignant mesothelioma with vascular invasion and thrombosis.
2. Epididymis: 1) Malignant mesothelioma 2) Diffuse, subacute, severe hypospermia and degeneration with germ cell exfoliation and mineralization.
3. Testis, bilateral: 1) Interstitial cell adenoma, multiple 2) Diffuse, chronic, severe, tubular degeneration and atrophy with unilateral, marked lymphocytic infiltrate and multifocal mineralization.

Contributor's Comment: Spontaneous mesothelioma is a rare neoplasm in rats with an incidence of 0.2–5%, the highest frequencies of which are reported in the Fischer 344 rat strain. Rat mesotheliomas typically occur in aged male rats and originate from the tunica vaginalis with the potential to spread into the peritoneal cavity via transcoelomic extension or seeding.[1-9] To date, 17 studies from the National Toxicology Program have reported xenobiotic-induced mesotheliomas in F344 rats; the F344 rat is particularly sensitive to developing this tumor type and is the only rodent strain reported to develop mesothelioma following xenobiotic exposure by a route other than peritoneal injection.[6,7] Histologically, mesotheliomas may be difficult to distinguish from mesothelial hyperplasia as they can range from a single layer of hyperplastic mesothelial cells lining a thin fibrovascular stroma to papillary projections lined by multiple, irregular layers of cuboidal to polygonal cells that form a pavement or stratified pattern.[1-9] Rat mesotheliomas have a classification scheme similar to humans with sarcomatous, epitheliomatous or mixed types that stain positively with Wilm's tumor 1 (WT-1). Ultrastructural features of mesotheliomas include a distinct basal lamina, junctional complexes between mesothelial cells, microvilli, pinocytotic

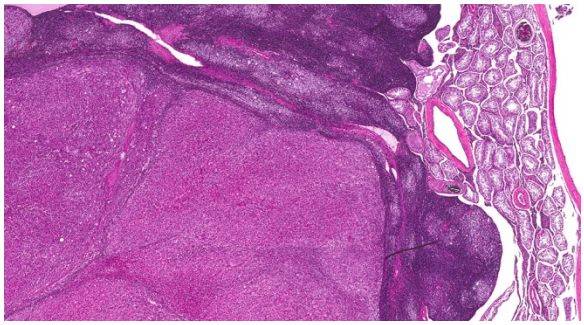

Testis, Fischer 344 rat. A 1.5x1.0cm multilobulated interstitial cell tumor replaces approximately 90% of the testicular parenchyma. (HE, 20X) (Photo courtesy of: EPL, Inc., P.O. Box 12766, Research Triangle Park, NC 27709 http://epl-inc.com/)

vesicles, abundant cytofilaments and dilated rough endoplasmic reticulum (RER).[5-7]

In the male rat, mesotheliomas of the testis, epididymis, and peritoneum are considered to have originated in the tunica vaginalis; all tunica vaginalis mesotheliomas (TVM) are deemed malignant, even those confined to the scrotal sac and lacking features of malignancy, such as local invasiveness, cytological atypia and pleomorphism. Proposed mechanisms of actions for both spontaneous and xenobiotic-induced mesotheliomas include endocrine disruption (leuteinizing hormone, prolactin and testosterone), mechanical stress (compression due to testicular tumors) or oxidative stress (asbestos-induced TVM).[4,6,7]

In the F344 rat, the most common proliferative disorders of the testes include interstitial cell (Leydig cell) hyperplasia and interstitial cell adenoma. Because interstitial cell adenoma is considered a continuum of interstitial cell hyperplasia, it is sometimes difficult to distinguish hyperplasia from adenoma based solely on differences in cellular morphology.[4,7] According to the International Harmonization of Nomenclature and Diagnostic Criteria for Lesions in Rats and Mice (INHAND), Leydig cell hyperplasia typically does not cause compression of the adjacent seminiferous tubules. However, in instances where there is no appreciable compression, proliferative lesions greater than 3 seminiferous tubules in diameter are generally regarded as adenoma.[3,4] Interstitial cell adenomas are common spontaneous and xenobiotic-induced neoplasms of rats and mice, particularly the F344 rat with an underlying pathogenesis that reflects endocrine disruption; a hormonal imbalance between the testicular levels of luteinizing hormone receptor and serum testosterone.

Five mechanisms by which hormone imbalance may contribute to Leydig cell tumor formation have been described and include: estrogen agonists (especially in mice), androgen receptor antagonists, gonadotropin releasing hormone (GnRH) and dopamine receptors, and 5α-reductase inhibitors. Leydig (interstitial) cell adenomas are usually benign, un-encapsulated, discrete neoplasms composed of sheets of uniform polyhedral cells with abundant, finely granular, eosinophilic cytoplasm and a single, centrally located nucleus; compression atrophy of the adjacent seminiferous tubules is common. Leydig cell adenomas are an age-related change, observed most frequently in F344

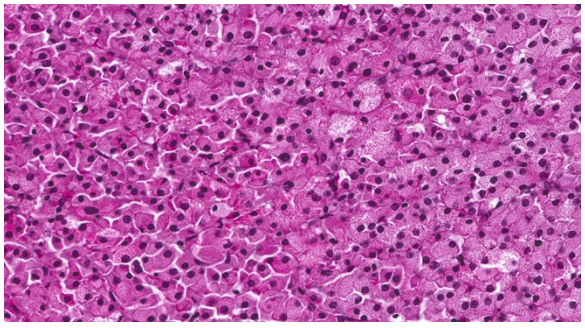

Testis, Fischer 344 rat. Neoplastic Leydig cells have distinct cell borders, vacuolated eosinophilic cytoplasm and mildly anisokaryotic eccentric hyperchromatic nuclei. Mitotic figures are rare. (HE, 200X) (Photo courtesy of: EPL, Inc., P.O. Box 12766 http://epl-inc.com/)

rats in their 2nd year of life, and appear to be inversely correlated with body weight, where increased body weights are associated with higher prolactin levels that reduce Leydig cell tumor incidence.[4,7]

JPC Diagnosis: 1. Testis: Interstitial cell tumor, Fischer 344 rat, *Rattus rattus*.
2. Testis, tunica vaginalis: Mesothelioma.

Conference Comment: The contributor provides an outstanding summary of the pathogenesis of spontaneous and xenobiotic-induced interstitial cell tumor (ICT) and mesothelioma in rats. ICTs (also known as Leydig cell tumor or interstitial adenona) are the most common spontaneous testicular tumor of rats with nearly 100% prevalence in 24-month-old Fisher 344 (F344) rats, as in this case.[8] Additionally, ICTs are commonly multicentric and can occur in one or both testes.[8] Leydig interstitial cells are normally found adjacent to the resident seminiferous tubules in the testis and produce testosterone under the stimulation of luteinizing hormone (LH). Hormonal imbalances as a result of disruption of the hypothalamic-pituitary-testicular axis can result in constitutive LH secretion, which is thought to be the main predisposing feature of ICT formation.[1] ICTs are composed to two cell types readily recognized by conference participants: polygonal cells with granular vacuolated cytoplasm present within the central part of the neoplasm, in this case, and smaller cells with dense hyperchromatic nuclei and scant cytoplasm at the periphery.[8] The conference moderator cautioned participants to not confuse the latter of these two cell types with lymphocytes. Ultrastructurally, interstitial cells contain lipid droplets, abundant smooth endoplasmic reticulum, and numerous mitochondria with tubulovesicular cristae, and desmosomes.[3,8] This neoplasm typically exhibits benign biologic behavior; however, it may be hormonally active and has been associated with hypercalcemia and elevated plasma inhibin levels.[1,3,8] It has a characteristic gross appearance of well-circumscribed yellow hemorrhagic nodules on the testes. Larger masses have areas of mineralization and necrosis.[8]

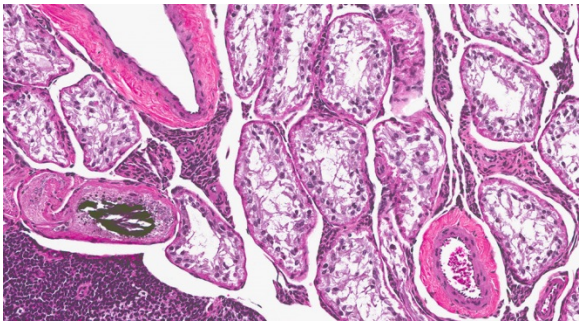

Testis, Fischer 344 rat. Seminiferous tubules at the periphery of the neoplasm are shrunken with a diffuse loss of spermatogonia and lined by a single layer of Sertoli cells in disarray. At bottom left, the periphery of the interstitial cell tumor is composed of numerous small Leydig cells with minimal cytoplasm. (HE, 200X) (Photo courtesy of: EPL, Inc., P.O. Box 12766, Research Triangle Park, NC 27709 http://epl-inc.com/)

Mesotheliomas are the third most common spontaneous testicular tumor of rats and are also particularly common in the F344 strain and they commonly occur concurrently with ICT, as in this case.[8] Mesothelial cells form a lining around the heart, pleural and peritoneal cavities, and the surface of most organs. In males, it extends into the scrotum and tunica vaginalis and wraps the testes and epididymis.[1,2,3,5,8] In male rats, the tunica vaginalis is the most common primary location, with subsequent spread to the rest of the mesothelial-lined surfaces.[8] Interestingly, mesothelalial cells have both an epithelial and mesenchymal component. Stains run by the Joint Pathology Center prior to the conference confirmed immuno-reactivity of neoplastic mesothelial cells to both pancytokeratin and vimentin. Other neoplasms of interest that typically express both vimentin and cytokeratin include: chordoma, synovial sarcoma, meningioma,

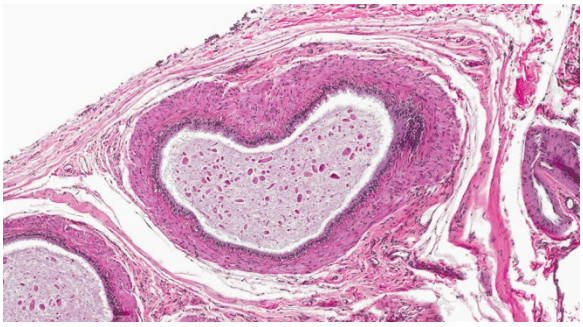

Testis, Fischer 344 rat. Epididymal ducts lack sperm and are filled with numerous sloughed germ cells admixed with cellular debris. (HE, 100X) (Photo courtesy of: EPL, Inc., P.O. Box 12766, Research Triangle Park, NC 27709 http://epl-inc.com/)

renal cell carcinoma, adrenal carcinoma, and endometrial sarcoma.[9] Grossly, mesotheliomas are multiple, well-circumscribed, firm sessile or pedunculated nodules, villous projections, or plaque-like with fibrous adhesions. Concurrent ascites and severe scrotal edema are not uncommon sequelae.[8] Ultrastructurally, mesothelial cells have a microvillous cell membrane, junctional complexes between cells, pinocytotic vesicles, and a distinct basal lamina.[3,5]

As mentioned by the contributor, several studies have attempted to establish a connection between the high incidences of concurrent ICT with mesothelioma in Fisher 344 rats. Some hypotheses include ICT causing direct mechanical stress on mesothelial cells of the tunica vaginalis leading to neoplastic transformation.[1,2] Another theory posits that LH and testosterone secretion by neoplastic ICT cells triggers local mesothelium proliferation. Others suggest that Fisher 344 strain-related sensitivity to chemical exposure causes the development of mesotheliomas and ICTs are an unrelated coincidental background lesion.[1,2] A definitive connection has not yet been established

Contributing Institution:
EPL, Inc.
P.O. Box 12766
Research Triangle Park, NC 27709
http://epl-inc.com/

References:

1. Blackshear PE, Pandiri AR, et al. Gene expression of mesothelioma in vindylidene chloride-exposed F344/N rats reveals immune dysfunction, tissue damage, and inflammatory pathways. *Toxicol Pathol*. 2014; 43:171-185.
2. Blackshear PE, Pandiri AR, et al. Spontaneous mesotheliomas in F344/N rats are characterized by dysregulation of cellular growth and immune function pathways. *Toxicol Pathol*. 2013; 42:863-876.
3. Boorman GA, Chapin BE, Mitsumori K. Testis and epididymis. In: Boorman GA, ed. *Pathology of the Fisher Rat*. San Diego, CA: Academic Press, Inc., 1990: 405-418.
4. Creasy D, Bube A, de Rijk E, Kandori H, Kuwahara M, Masson R, Nolte T, Reams R, Regan K, Rehm S, Rogerson P, Whitney K. Proliferative and nonproliferative lesions of the rat and mouse male reproductive system. *Toxicol Pathol*. 2012; 40: 40S-121S.
5. Hall W. Peritoneum, retroperitoneum, mesentery and abdominal cavity. In: Boorman GA, ed. *Pathology of the Fisher Rat*. San Diego, CA: Academic Press, Inc., 1990: 63-70.
6. Maronpot RR, Zeiger E, McConnell EE, Kolenda-Roberts H, Wall H, Friedman MA. Induction of tunica vaginalis mesotheliomas in rats by

xenobiotics. *Crit Rev Toxicol*. 2009; 39(6):512-537.
7. Maronpot RR, Abraham N, Foreman JE, Ramot Y. The legacy of the F344 rat as a cancer bioassay model (a retrospective summary of three common F344 rat neoplasms). *Crit Rev Toxicol*. 2016; 46(8):641-675.
8. Percy DH and Barthold SW. Rat: Neoplasms. In*:* Percy DH and Barthold SW, eds. *Pathology of Laboratory Rodents and Rabbits.* 4th ed. Ames, IA: Blackwell Publishing, 2016:169-170.
9. Takeshi Y, Tetsuo O, et al. Histochemical and immuno-histochemical characterization of chordoma in ferrets. *J Vet Med Sci.* 2015; 77(4):467-47

1. Which of the following are not considered a likely site for infection and latency by cytomegaloviruses?
    a. Smooth muscle cells
    b. Myeloid cells
    c. Arterial smooth muscle cells
    d. Macrophages

2. Which of the following is the most common skin tumor in the guinea pig?
    a. Trichoblastoma
    b. Trichofolliculoma
    c. Keratoacanthoma
    d. Melanoma

3. Which of the following bacteria do not form tubercles?
    a. Mycobacterium bovis
    b. Mycobacterium microti
    c. Mycobacterium caprae
    d. Mycobacterium leprae

4. Which of the following is the only known reservoir for Mycobacterium tuberculosis?
    a. Humans
    b. Rodents
    c. Non-human primates
    d. Insects

5. Which of the following is not true of proliferative Leydig cell lesions in rats?
    a. Leydig cell adenomas are an age-related change in rats.
    b. Leydig cell hyperplasia typically does not cause compression of the adjacent seminiferous tubules
    c. Leydig cell adenomas are usually benign unencapsulated discrete neoplasms.
    d. Disruption of the hypothalamic-pituitary-testicular axis, resulting in constitutive FSH secretion, is thought to be a main predisposing feature of ICT formation.

Joint Pathology Center

Veterinary Pathology Services

WEDNESDAY SLIDE CONFERENCE 2016-2017

C o n f e r e n c e 18

8 February 2017

Patricia Pesavento, DVM, PhD, Diplomate ACVP
Professor of Pathology, Microbiology & Immunology
UC Davis School of Veterinary Medicine
Davis, CA

CASE I: NF-15-1564 (JPC 4083683).

Signalment: Six-year-old female French Alpine goat, (*Capra aegagrus hircus*).

History: This goat was suspected to have aborted prior to necropsy, although no expelled fetus was found. This goat also aborted last year, but had successfully kidded in the past.

Gross Pathology: The uterine body contained two macerated fetuses with a crown to rump length of 16 cm and 10 cm. Within the uterus, all of the caruncles were enlarged (~4x2x1 cm), homogeneous, and pale tan.

Laboratory results: Bacterial culture and sensitivity (uterus):
Numerous *Escherichia coli*
Few *Enterococcus faecalis*
No growth of *Brucella species*
Chlamydophila sp, PCR (uterus): Negative
Coxiella burnetii, PCR (uterus): Negative

Histopathologic Description: The uterine caruncular labyrinth is diffusely expanded by abundant pale eosinophilic homogenous, extracellular material which is multifocally disrupted by areas of blue granular mineralization. The interdigitating cotyledonary villi are sparse, and the allantoic stroma is mildly expanded by edema. The aforementioned interstitial eosinophilic material within the caruncles

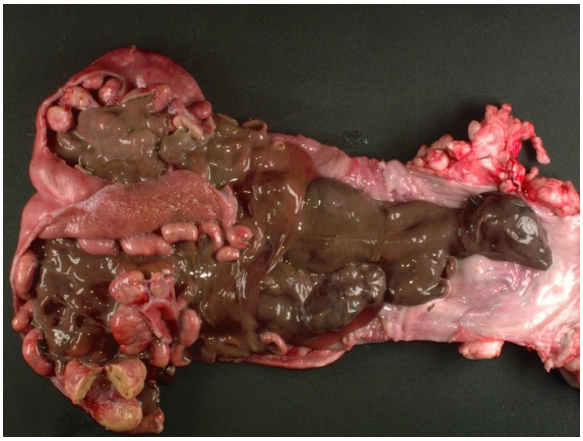

Uterus, goat. The uterus contained two macerated feti. Caruncles were enlarged and pale tan. (Photo courtesy of: Department of Pathobiology and Diagnostic Investigation, College of Veterinary Medicine, Michigan State University. www.pathobiology.msu.edu)

stains orange/pink with Congo red and exhibits apple green birefringence with polarized light, consistent with amyloid. The umbilicated surface of the placentome is multifocally ulcerated and replaced by large aggregates of neutrophils, lymphocytes, and histiocytes. Similar inflammatory cells extend into the subepithelial stroma of the caruncle, endometrium, and minimally throughout the labyrinth. The placental and endometrial stroma is expanded by moderate amounts of edema, few scattered inflammatory cells, and multifocal aggregates of mineral. There are also multifocal areas of mineralization throughout the tunica media of medium-sized vessels within the placenta and endometrium.

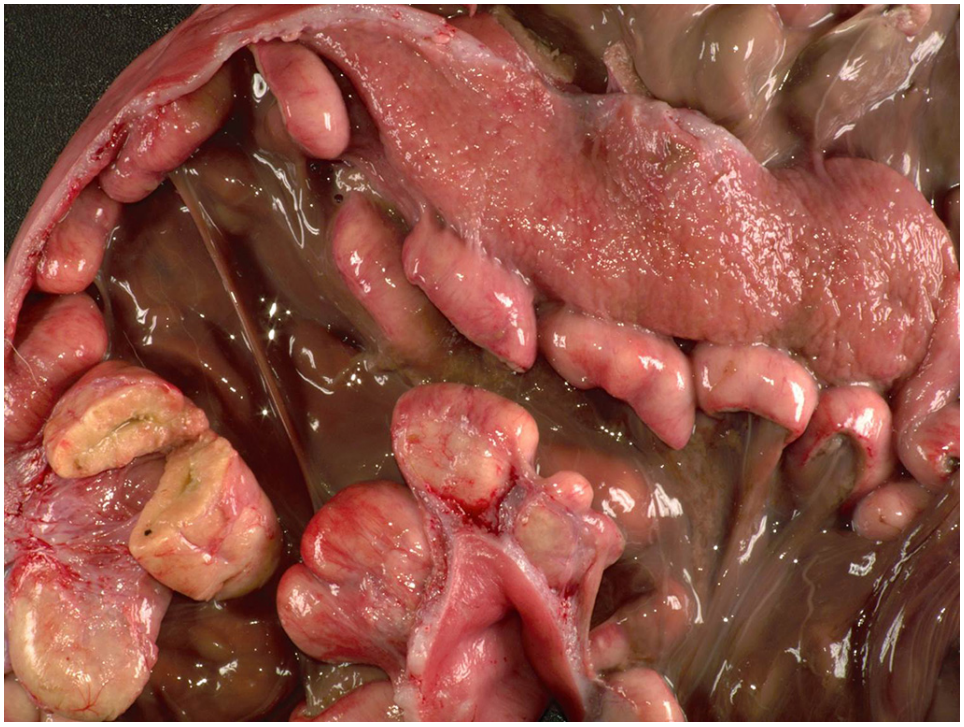

Uterus, goat. Closer view of caruncles, with one incised. (Photo courtesy of: Department of Pathobiology and Diagnostic Investigation, College of Veterinary Medicine, Michigan State University. www.pathobiology.msu.edu)

Contributor's Morphologic Diagnoses: 1. Uterus: Diffuse interstitial caruncular amyloid

2. Uterus and placenta: Chronic necrotizing placentitis and endometritis with mineralization

Contributor's Comment: Caruncular amyloidosis has been previously reported in a small number of goats in California. Clinical presentation of such goats included mid-to-late term abortion that often occurred repeatedly over multiple years which was attributed to impaired gas exchange at the site of fetal attachment.[2] Ages ranged from 3-8, and breeds included Toggenburg, La Mancha, and Saan. Similar to the California goats, this goat had no evidence of amyloid deposition in other organs nor was there evidence of a systemic or chronic disease process. Few bacteria were isolated from the inflamed region of the placentome but are considered to be secondary to the retained fetuses. Bacterial culture did not isolate *Brucella abortus*, and PCR was negative for *Chlamidophila species* and *Coxiella burnetti.*

In general, amyloid is composed of insoluble aggregates of misfolded proteins, and deposition of amyloid can occur in a wide variety of localized or systemic diseases.[8] Although the fibrillar component of amyloid is overall similar in composition, a diverse number of proteins with variation in sequence and structure are considered amyloidogenic.[7,8] Common amyloid precursors include: serum amyloid A (SAA),

Placentome, goat. At subgross magnification, the caruncle is diffusely pale and eosinophilic suggesting infarction (HE, 5X)

amyloid light chain (AL), islet amyloid polypeptide (IAPP), mutated forms of transthyretin, and beta protein amyloid.[7,8]

In particular, SAA proteins comprise a family of apolipoproteins that can be synthesized hepatically and/or extrahepatically. Hepatic derived SAA (SAA1 and SAA2) can dramatically increase in response to inflammation. In mice, rats, cows, and rabbits SAA3 appears to be the most common extrahepatic SAA in addition to being produced hepatically.[3] Increased production of SAA3 has also been described in bovine and human mammary gland epithelium in response to prolactin, and in uterine papillary cancer. In the goats in California increased levels of SAA3 were detected within the endometrium when compared to the liver, suggesting localized expression. The type and cause of the amyloid deposition in this case is currently unknown, but the localized caruncular involvement is similar to what has been previously described and may represent a new syndrome of goats.[2]

JPC Diagnosis: Placenta, caruncle: Amyloidosis, diffuse, marked, French Alpine goat, *Capra aegagrus hircus*.

Conference Comment: The contributor provides an informative summary of the pathogenesis of amyloidosis and review of previously reported cases of a unique syndrome of caruncular amyloidosis causing abortion in goats. This excellent case confounded conference participants on initial examination of the tissue section. Virtually every attendee interpreted the amorphous, smudgy, homogenous eosinophilic material that diffusely expands the uterine lattice as a geographic area of coagulative necrosis admixed with multifocal mineralization and mild inflammatory infiltrate in the subepithelial stroma of the caruncle and endometrium; collectively, the findings were attributed to normal post kidding involutional change, rather than caruncular amyloidosis. Similar to the findings reported by the contributor, Congo red histochemical staining of serial sections performed at the JPC demonstrates the eosinophilic proteinaceous material is diffusely congophilic and displays bright apple-green birefringence when viewed under polarized light.

Spirited discussion ensued among conference participants regarding the presence of concurrent diffuse necrosis, autolysis, or a combination of both admixed with the deposited amyloid in the tissue section. Most favored diffuse necrosis of

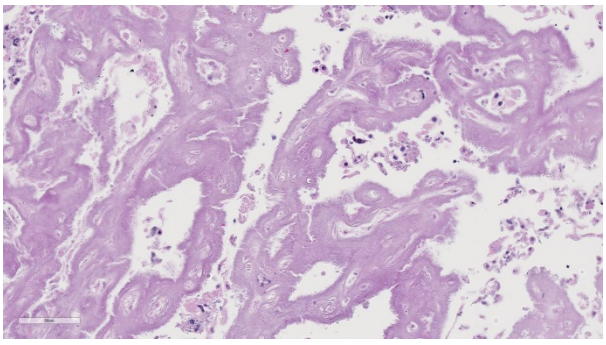

Placentome, goat. At high magnification, the caruncular labyrinth is diffusely eosinophilic and expanded with a loss of epithelium and there are small amounts of cellular debris in

both the epithelial and endothelial cells secondary to amyloid deposition, resulting in infarction of the placentome. Discord over the presence or absence of necrosis or autolysis nothwithstanding, this case nicely demonstrates a newly reported syndrome of reproductive failure in goats secondary to uterine amyloid deposition in the endometrium at the site of placental attachment.[2] Accumulation of amyloid within the carucle markedly compromises blood flow and both gas and nutrient exchange between the doe and the fetus; this leads to fetal hypoxia and eventually death.[2] Similar to previously reported cases of caruncular amyloidosis in goats[2], amyloid is not present within the intercaruncular endometrium, myometrium, endometrial glands, or vessels in this doe.

Before discussing this case, participants reviewed the normal placentation in small ruminants. All ruminants have similar cotyledonary placentation composed of the fetal cotyledon and the maternal caruncle. The placenta contains the maternal endometrium and the fetal chorioallantoic membranes (CAM).[1] Ruminant placentas are nondeciduate, indicating that the maternal endometrium and fetal CAM are in close contact, but they do not intimately fuse. In cotyledonary placentation, there are

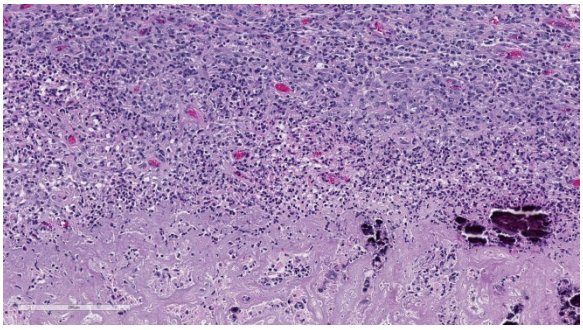

Placentome, goat. At the periphery of the placentome, there is an infiltrate of moderate numbers of viable and degenerate neutrophils as well as multifocal mineralization. (HE, 172X)

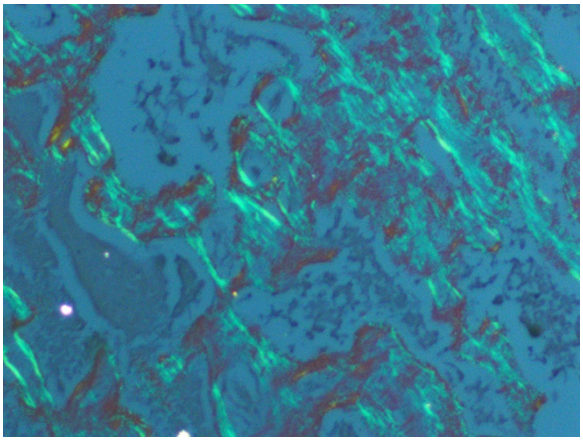

Placentome, goat. Caruncular amyloid demonstrates green birefringence when viewed with polarized light. (Congo Red, 400X) (Photo courtesy of: Department of Pathobiology and Diagnostic Investigation, College of Veterinary Medicine, Michigan State University. www.pathobiology.msu.edu)

numerous areas where the fetal cotyledon villar attachments interdigitate with the crypts of the caruncular epithelium. The combination of the fetal cotyledon and maternal caruncle make up the placentome.[1] In sheep and goats, the caruncles have a characteristic concave shape, nicely demonstrated in this case.[1] Bovine placentomes are similar in structure and function, but are convex rather than concave.

Conference participants discussed various causes of abortion in small ruminants, to include infectious agents such as *Chlamydophila abortus*, *Toxoplasma gondii*, *Brucella ovis*, *Campylobacter fetus*, *Coxiella burnetii*, and *Listeria monocytogenes*. Non-infectious causes include plant toxins, such as locoweed poisoning, and nutritional factors including dietary deficiencies of copper, magnesium, vitamin A, and selenium.[5,6] After reviewing this case, conference participants agreed that caruncular amyloidosis should be considered as an additional differential diagnosis of non-infectious abortion in the goat.

Contributing Institution:
Department of Pathobiology and Diagnostic Investigation
College of Veterinary Medicine
Michigan State University
http://www.pathobiology.msu.edu

References:

1. Bacha WJ, Bacha LM. *Color Atlas of Veterinary Histology*. 3rd ed. Baltimore, MD: Lippincott Williams & Wilkins; 2012:243-260.
2. Gaffney PM, Barr B, Rowe JD, Bett C, Drygiannakis I, Giannitti F, Trejo M, Ghassemian M, Martin P, Masliah E, Sigurdson C. Protein profiling of isolated uterine AA Amyloidosis causing fetal death in goats. *FASEB J*. 2015; 29:911-919.
3. Larson MA, Wei SH, Weber A, Weber AT, McDonald TL. Induction of human mammary associated serum amyloid A3 expression by prolactin or lipopolysaccharide. *Biochem Biophys Res Commun*. 2003; 301:1030–1037.
4. O'Brien TD, Butler PC, Westermark P, Johnson KH. Islet amyloid polypeptide: A review of its biology and potential roles in the pathogenesis of diabetes mellitus. *Vet Pathol*. 1993; 30: 317-332.
5. Sanad YM, Jung K, Kashoma I, et al. Insights into potential pathogenesis mechanisms associated with *Campylobacter jejuni*-induced abortions in ewes. *BMC Vet Res*. 2014; 10:274-287.
6. Schlafer DH and Foster RA. Diseases of the gravid uterus, placenta and fetus In: Maxie MG, ed. *Jubb Kennedy and Palmer's Pathology of Domestic Animals*. Vol 3. 6th ed. Philadelphia, PA: Elsevier Saunders; 2016:407-408.
7. Tani Y, Uchida S, Nakamura H, Nakayama N, Goto D. Amyloid deposits in the gastrointestinal tract of aging dogs. *Vet Pathol*. 1997; 34:415-420.
8. Teoh SL, Griffin MD, Howlett GJ. Apolipoprotein and amyloid fibril formation in atherosclerosis. *Protein Cell*. 2011; 2(2):116-127.

CASE II: 58716 (JPC 4084216).

Signalment: 16-year-old, male, bar-headed goose, (*Anser indicus*).

History: Between September 9 and September 17, 2015, three bar-headed geese housed in an open, outdoor enclosure near Village Lagoon died unexpectedly. The first two had been found dead on exhibit, while the third had been hospitalized shortly before death with clinical signs of labored breathing and lethargy. The hospitalized goose had a CBC within normal limits. At the same time, a fourth bar-headed goose was hospitalized with diarrhea.

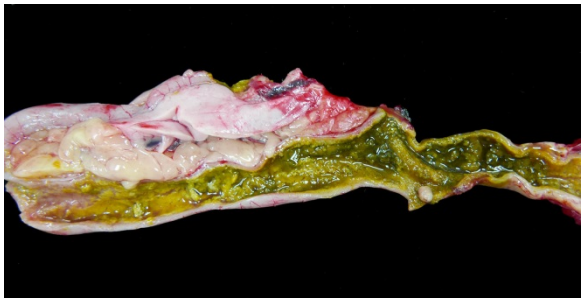

Intestine, bar-headed goose. The intestine is lined by a greenish yellow necrotic membrane. (Photo courtesy of: Wildlife Disease Laboratories, San Diego Zoo Institute for Conservation Research, San Diego Zoo Global (WSC 77) http:/institute.sandiegozoo.org/wildlife-disease-laboratories)

Gross Pathology: The spleen has a few ill-defined, pale tan foci of necrosis extending from the serosa into the parenchyma. The pancreas has 10 to 15 scattered, tan, well-circumscribed necrotic foci measuring up to 0.2 cm in diameter. The entire small and large intestine are filled with tan to green, fibrous, clumped soft material that coats the mucosa in some regions and sloughs away along other portions. Within the ceca, there is a small to moderate amount of tan-green watery fluid and tan fibrous strands that loosely adhere to the mucosal surface.

Laboratory results: PCR and virus isolation were performed by the California Animal Health and Food Safety diagnostic laboratory (CAHFS).

West Nile Virus (avian) PCR: Virus detected in brain

Virus isolation: West Nile Virus

Avian Influenza Matrix Gene qRT-PCR: Not detected in lung, duodenum, or spleen.

Avian Paramyxovirus-1 qRT-PCR: Not detected in lung, duodenum, or spleen.

Bacterial culture, colon contents (IDEXX): 3+ *Escherichia coli*, 1+ *Aeromonas species*,

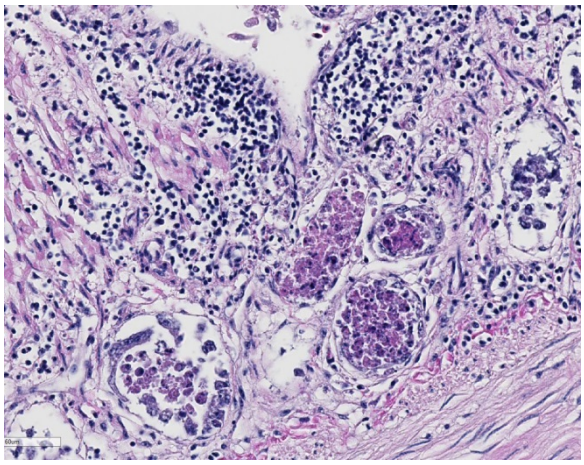

Intestine, bar-headed goose. There is marked necrosis of intestinal crypts. (HE, 324X).

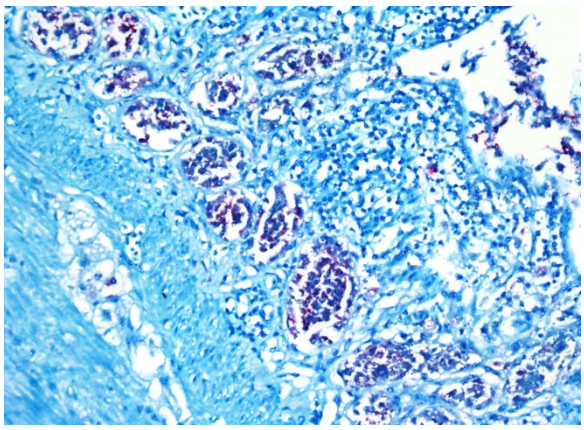

2+ Normal positive flora. No *Salmonella, Shigella, Pleisiomonas, Edwardseilla,*

Intestine, bar-headed goose. Intestinal epithelial cells within crypts exhibit strong cytoplasmic immunopositivity for West Nile virus. (Photo courtesy of: Wildlife Disease Laboratories, San Diego Zoo Institute for Conservation Research, San Diego Zoo Global (WSC 77) http:/institute.sandiegozoo.org/wildlife-disease-laboratories)

Aeromonas or *Yersinia* were isolated.

Histopathologic Description: Duodenum and pancreas: Sections are mildly autolyzed. In the duodenum, villi are markedly blunted and frequently fragmented. The majority of crypts are dilated with hypereosinophilic, karyorrhectic cellular debris (crypt abscesses), and glandular epithelial cells are frequently shrunken and hypereosinophilic with nuclear pyknosis (necrotic). The villous epithelium is sloughed and is regionally replaced by luminal bands of necrotic sloughed cells, degenerate heterophils, and large numbers of embedded bacteria (pseudomembrane). Moderate to large numbers of lymphocytes with fewer plasma cells populate the lamina propria. Throughout the exocrine pancreas, there are multiple, randomly distributed foci of necrosis, characterized by hypereosinophilia, loss of cellular detail and karyorrhexis, and small numbers of heterophils. Foci of necrosis are often surrounded by a band of acinar cells with

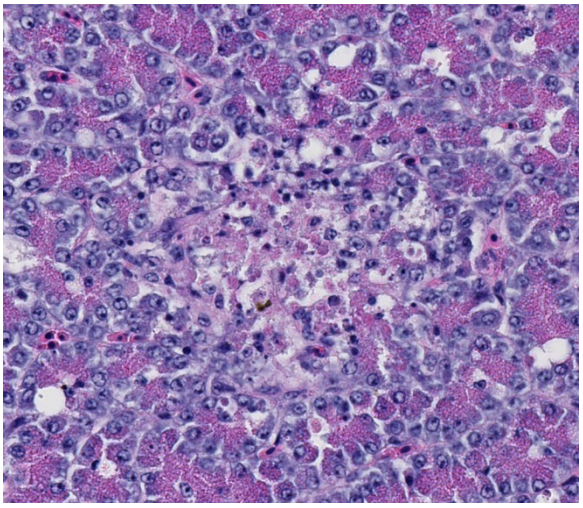

Pancreas, bar-headed goose. Foci of necrosis scattered randomly throughout the exocrine pancreas. (HE, 330X).

marked zymogen depletion. There are occasional ill-defined regions of exocrine pancreatic hyperplasia, with lobules of tightly packed, slightly haphazardly arranged acinar cells delineated by coarse fibrous septa.

Immunohistochemistry for West Nile Virus (performed in-house): Strong positive cytoplasmic immunoreactivity within intestinal epithelial cells or foci of crypt necrosis, pancreatic acinar cells, glial nodules in the brain, renal tubular epithelial cells, cardiomyocytes, hepatocytes, and in the spleen (macrophages).

Contributor's Morphologic Diagnoses: 1. Duodenum: Severe, diffuse, acute, necrotizing enteritis with segmental pseudo-membranes and mixed bacteria
2. Pancreas: Moderate, multifocal, acute necrosis

Contributor's Comment: Necropsy and histopathology findings on all three bar-headed geese (*Anser indicus*) were consistent with severe systemic viral infection, with acute necrosis most severely affecting the gastrointestinal tract, but also including pancreas, trachea, spleen, esophagus, feather follicle epithelium and brain. The three mortalities within a short time span, in conjunction with the spectrum of histologic lesions (widespread tissue necrosis), met internal criteria requiring notification of government regulatory officials (California Department of Food and Agriculture, CDFA) and testing to rule out highly-pathogenic avian influenza (HPAI). Immediate biosecurity measures were implemented. Suspicion of HPAI was heightened by the fact that bar-headed geese were the migratory waterfowl species predominantly affected in H5N1 HPAI virus epidemics in China in 2005 and 2006.[6,9] Within approximately 48 hours of notifying CDFA, we received negative test results for HPAI, and CDFA lifted the quarantine. Concurrently, West Nile virus (WNV) infection in all three geese was confirmed by in-house immunohistochemistry. These results were corroborated by PCR and virus isolation performed by the California Animal Health and Food Safety diagnostic laboratory (CAHFS). The presence of such striking, acute intestinal crypt necrosis was considered to be unusual for WNV in an avian species, especially with only minimal

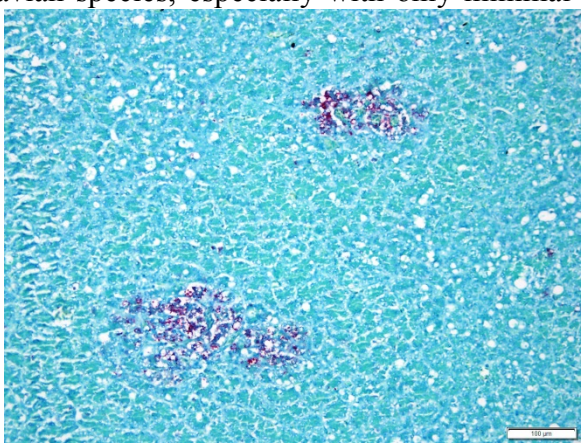

Pancreas, bar-headed goose. WNV antigen is present within foci of pancreatic necrosis. (Photo courtesy of: Wildlife Disease Laboratories, San Diego Zoo Institute for Conservation Research, San Diego Zoo Global (WSC 77) http:/institute.sandiegozoo.org/wildlife-disease-laboratories)

brain lesions and an absence of myocardial lesions.

West Nile Virus is in the genus *Flavivirus*, family *Flaviviridae*, and is serologically classified within the Japanese encephalitis antigenic group. The virus is distributed worldwide and has a wide potential host range, but is maintained primarily in a bird-mosquito cycle. Wild birds (especially corvids) act as amplifying hosts. *Culex spp* mosquitoes are the primary vector, although the virus is found in other vectors (other mosquito species, ticks) of undetermined significance in transmission.[3,5] Horizontal transmission[2] and transmission through prey or contaminated water have also been reported.[5] There are seven genetic lineages of WNV strains, with two major lineages, lineage 1 and lineage 2. WNV genetic lineage 1 is widespread geographically, including in North America. Lineage 2 WNV strains correspond primarily to enzootic areas in Africa, with recent detection in Europe. Lineage 1 strains have been considered more virulent, but both have been implicated in significant disease outbreaks in birds.[3,5] Mortality due to WNV has been documented in 24 orders of birds from North America, including anseriforms.[5]

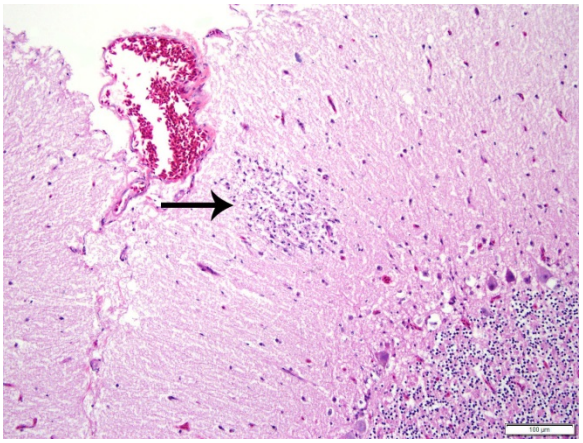

Cerebellum, bar-headed goose. Glial nodules are present throughout the brain. (Photo courtesy of: Wildlife Disease Laboratories, San Diego Zoo Institute for Conservation Research, San Diego Zoo Global (WSC 77) http:/institute.sandiegozoo.org/wildlife-disease-laboratories)

In mammals, after a bite by an infected mosquito, the virus replicates in keratinocytes, cutaneous dendritic cells, endothelial cells, and fibroblasts, followed by viremia and hematogenous spread.[3] In avian species, the mechanism and sites of replication are not completely understood. Experimentally in birds, virus has been detected in blood within 45 minutes of mosquito biting, suggesting that primary viremia can occur without local replication.[5] Clinical disease develops upon viral invasion of major organs and/or the CNS, usually by 5-6 days post-infection.[7] In most infected birds, virus is detectable first in the spleen, followed by spread to other visceral organs, and then to the CNS.[5] Lesions of WNV in birds are often more extensive in less susceptible species, such as chickens, with multi-organ failure, peracute death and few to no lesions in highly susceptible species like corvids. Chronic, persistent WNV infections have also been documented in some species of birds, including house finches (*Haemorhous mexicanus*) and Western scrub-jays (*Aphelocoma californica*).[7]

In most orders of birds, histologic lesions of WNV are primarily found in the CNS, heart, liver, kidney, and spleen. Typical lesions in the CNS include mononuclear meningo-encephalitis with perivascular cuffing, gliosis, and glial nodules. In other organs, lesions are characterized by lympho-plasmacytic and histiocytic inflammation, accompanied by cellular degeneration or necrosis. While the intestinal lesions seen in the present case, with striking enterocyte and crypt necrosis, have been described in

WNV-infected corvids and other passerines, they have not been described in Anseriformes.[1,2, 4,5, 8] Reports of naturally and experimentally infected geese of various species have emphasized pronounced myocardial lesions and moderate to severe mononuclear meningoencephalitis.[1,2, 4, 8]

JPC Diagnosis: 1. Small intestine: Enteritis, necrotizing, diffuse, severe with crypt abscesses, bar-headed goose, *Anser indicus*. 2. Pancreas: Pancreatitis, necrotizing, random, multifocal, mild.

Conference Comment: This excellent case demonstrates the widespread tissue tropism that West Nile virus (WNV) has in avian species. Most wild birds infected with WNV have a prolonged viremia allowing dissemination of the virus throughout the body, affecting nearly every organ. Typically, microscopic lesions associated with WNV viremia are lymphoplasmacytic and histiocytic inflammation with degeneration and necrosis within the central nervous system (CNS), heart, spleen, kidney, and liver. The virus is distributed throughout the world and outbreaks can cause acute death in a variety of different avian species. Highly susceptible birds include crows, jays, and magpies may die so acutely that there are little to no macroscopic lesions. Chronic disease, characterized by severe inflammatory lesions, emaciation, dehydration, hemorrhage, and congestion, occurs in avian species with lower susceptibility to WNV infection such as owls, hawks, and psittacine birds. Choroiditis, iridocyclitis, and retinal necrosis leading to progressive visual impairment and blindness are reported in naturally WNV infected red-tailed hawks and experimentally infected partridges and pheasants.

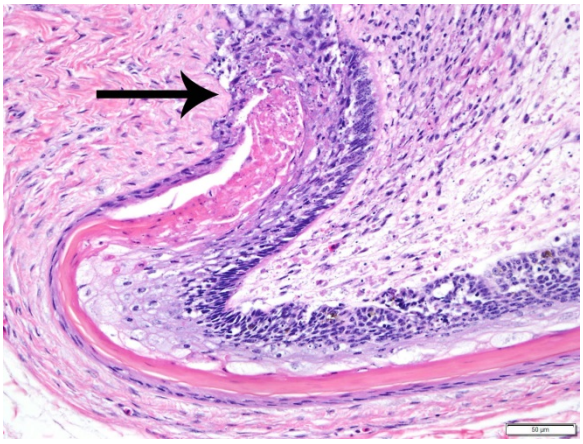

Feather follicle bar-headed goose. Necrosis of follicular epithelium was also seen in this individual. (Photo courtesy of: Wildlife Disease Laboratories, San Diego Zoo Institute for Conservation Research, San Diego Zoo Global (WSC 77) http:/institute.sandiegozoo.org/wildlife-disease-laboratories).

As mentioned by the contributor, the virus is transmitted predominantly by *Culex* sp. mosquitoes. Corvid birds, such as the American crow, are the main amplifying host and the virus is maintained in a bird-mosquito-bird lifecycle. Despite being dead end hosts, a variety of mammalian species can be infected, with humans and horses particularly susceptible to developing clinical disease. Transmission occurs during the late spring to early fall during favorable weather conditions for the mosquito vector. In contrast to avian species, lesions in horses are confined to the central nervous system, primarily within the grey matter of the brainstem and thoracolumbar spinal cord and less commonly in the cerebrum and cervical spinal cord. Histologic lesions are typically lymphoplasmacytic meningo-encephalomyelitis with glial nodules, lymphohistiocytic perivascular cuffing, ring hemorrhages, neuronal degeneration, and necrosis. The preferred modality for postmortem diagnosis of WNV infection in mammals includes histologic identification of the previously mentioned lesions, in addition to polymerase chain reaction (PCR) testing of the brainstem for WNV antigens.

Even in severe equine cases, viral antigen is typically scant within the central nervous system making immunohistochemistry (IHC) in-situ hybridization (ISH) less useful in horses.

Ruminants, dogs, cats, and pigs are susceptible to infection, but usually only have transient and subclinical disease; however, a recent report in *Veterinary Pathology* describes severe lympho-plasmacytic meningoencephalitis in six WNV infected sheep with neurological signs in California. In contrast to horses, a large amount of viral antigens accumulated in the CNS of sheep in this study. As a result, both PCR and IHC were useful testing modalities in these sheep. Viral antigens in avian species are widespread and the contributor provides excellent quality images of strong positive cytoplasmic immunoreactivity for WNV antigen within intestinal epithelial cells and crypts and pancreatic acinar cells.

After injection of the virus by the mosquito vector, the virus is deposited in the extracellular matrix where it can propagate in keratinocytes and infect Langerhans dendritic cells and tissue macrophages. The virus then spreads hematogenously via the leukocyte tracking system. Viral envelope proteins E2 and E1 are responsible for organ attachment and endocytosis respectively. Although not completely understood, entry of the virus into the CNS likely involves a combination of breakdown of the blood-brain barrier by proinflammatory cytokines and retrograde axonal transport from the peripheral nervous system.

Contributing Institution:
Wildlife Disease Laboratories
San Diego Zoo Institute for Conservation Research
San Diego Zoo Global
http://institute.sandiegozoo.org/wildlife-disease-laboratories

References:

1. Austin RJ, Whiting TL, Anderson RA, Drebot MA. An outbreak of West Nile virus-associated disease in domestic geese (*Anser anser domesticus*) upon initial introduction to a geographic region, with evidence of bird to bird transmission. *Can Vet J*. 2004; 45(2):11-23.
2. Banet-Noach C, Simanov L, Malkinson M. Direct (non-vector) transmission of West Nile virus in geese. *Avian Pathol*. 2003; 32(5):489-94.
1. Cantile C, Youssef S. Nervous system. In: Maxie MG, ed. *Jubb, Kennedy, and Palmer's Pathology of Domestic Animals*. Vol 1. 6th ed. St. Louis, MO: Elsevier; 2016:374-375.
3. Cox SL, Campbell GD, Nemeth NM. Outbreaks of West Nile virus in captive waterfowl in Ontario, Canada. *Avian Pathol*. 2015;44(2):135-41.
4. Gamino V, Höfle U. Pathology and tissue tropism of natural West Nile virus infection in birds: a review. *Vet Res*. 2013; 44:39.
5. Miller AD, Zachary JF. Nervous System. In: McGavin MD, Zachary JF, eds. *Pathologic Basis of Veterinary Disease*. 6th ed. St. Louis, MO: Elsevier Mosby; 2017:876-877.
6. Nemeth NM, Brown JD, Stallknecht DE, Howerth EW, Newman SH, Swayne DE. Experimental infection of bar-headed geese (*Anser indicus*) and ruddy shelducks (*Tadorna ferruginea*) with a clade 2.3.2 H5N1 highly pathogenic avian influenza virus. *Vet Pathol*. 2013; 50(6):961-70.

7. Pérez-Ramírez E, Llorente F, Jiménez-Clavero MÁ. Experimental infections of wild birds with West Nile virus. *Viruses*. 2014; 6(2):752-81.
8. Swayne DE, Beck JR, Smith CS, Shieh WJ, Zaki SR. Fatal encephalitis and myocarditis in young domestic geese (*Anser anser domesticus*) caused by West Nile virus. *Emerg Infect Dis*. 2001; 7(4):751-3.
9. Zachary JF. Mechanisms of microbial infection. In: Zachary JF ed. *Pathologic Basis of Veterinary Disease.* 6th ed. St. Louis, MO: Mosby Elsevier; 2017:223.
10. Zhou JY, Shen HG, Chen HX, Tong GZ, Liao M, Yang HC, Liu JX. Characterization of a highly pathogenic H5N1 influenza virus derived from bar-headed geese in China. *J Gen Virol*. 2006; 87:1823-33.

CASE III: 15N499 (JPC 4085377).

Signalment: 15-day-old, male, Angus x Nellore cross, ox (*Bos taurus*).

History: On September 2015, in a farm in Midwestern Brazil, eight out of 100, 15-day-old cross bred (Angus x Nelore) calves got sick. Affected calves were unable to follow their mothers and presented with lethargy and ataxia. They were unsuccessfully treated with florfenicol and sodium dipyrone. Five calves died on site; the remaining three sick calves were referred to the Veterinary Teaching Hospital of the Federal University of Mato Grosso do Sul, where they were clinically examined and given supportive therapy. Two of those calves died within 24 hours of the onset of clinical signs and were necropsied. The remaining calf was treated

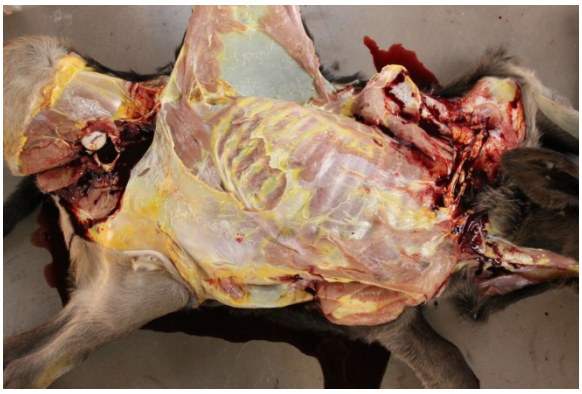

Cadaver, calf. There is moderate subcutaneous icterus. (Photo courtesy of: Laboratory of Anatomic Pathology, Universidade Federal de Mato Grosso do Sul, Campo Grande, MS, Brazil. https://www.ufms.br/)

for babesiosis and recovered. Clinical signs in the affected calves included fever, apathy, icterus, stiffness of the neck, and difficulty in keeping a standing position due to incoordination. This latter sign rapidly progressed to sternal decubitus, lateral decubitus, muscle tremors, paddling movements, nystagmus, tachycardia, and tachypnea. One calf had lost of menace reflex and another one had opisthotonus. All calves were parasitized by *Rhipicephalus* (*Boophilus*) *microplus* ticks.

Gross Pathology: In the two necropsied calves (one of each sex), the carcasses were moderated jaundiced, there was splenomegaly and the liver was swollen and had an orange-tan discoloration. The kidneys of one the calves were dark brown and the urine was faint red, although hemoglobinuria was not observed clinically. The grey telencephalic and cerebellar cortices and the basal nuclei had an intense cherry-pink discoloration which contrasted strongly with the white matter. One calf had omphalitis associated with myiasis (*Cochliomyia hominivorax*).

Laboratory results: Blood work: Erythrocytes 4.08 p/10^6µl (reference values 5.5-10.0 p/10^6µl); hemoglobin 6.2 g/dL (8-15 g/dL); mean corpuscular value 50

Spleen, calf. There is moderate splenomegaly. (Photo courtesy of: Laboratory of Anatomic Pathology, Universidade Federal de Mato Grosso do Sul, Campo Grande, MS, Brazil. https://www.ufms.br/)

reference values 40-60 fL); Fibrinogen: 1,000 mg/dL (reference values 300-700 mg/dL). Serum biochemistry: Aspartate aminotransferase (AST): 297.5 UI/L (reference values 20 a 34 UI/L); γglutamyl transferase (GGT) 37.4 UI/L (reference values 6.1-7.4 UI/L); glucose 5.8 mg/dL (reference values 45 a 75 mg/dL).
In Romanowsky-stained squashes from telencephalic cortex, capillaries appeared clogged with intraerythrocytic small (2 µm-diameter) paired or single spherical basophilic organisms (morphology compatible with *Babesia bovis*). Similar organisms were also observed within erythrocytes from blood smears.

Histopathologic Description: The most striking lesions are the diffuse and marked capillary engorgement with erythrocytes in the grey matter of the brain. Virtually every erythrocyte within these capillaries contained small paired or single faint basophilic spherical organisms. Perivascular and perineuronal edema are also observed in the grey matter. Mild to minimal mononuclear perivascular cuffings are observed in a few of the slides. There is marked intra-hepatocellular and canalicular cholestasis mainly in centrolobular areas associated with vacuolar hepatocellular degeneration and necrosis. Only minimal hemoglobinuric nephrosis is observed in the kidneys; focal mixed mononuclear cell reaction found in renal interstitium is considered incidental. Changes in the spleen are moderate diffuse congestion. There are no pathological changes in the lungs, heart and gastrointestinal tract.

Contributor's Morphologic Diagnosis: Cerebral cortical congestion, marked, acute, associated with intraerythrocytic organisms with morphology compatible with *Babesia bovis*.

Contributor's Comment: The diagnosis of bovine babesiosis caused by *Babesia bovis* was made based on the pathognomonic gross brain lesions, necropsy and microscopic lesions consistent with the hemolytic crisis, and visualization of the intraerythrocytic parasite in blood imprints, in the capillaries of brain cortical grey matter, in squashes of brain tissue, and HE stained slides.

Babesia was first described by Babés in Romania as a parasite of bovine erythrocytes. Although it is possible for a single *Babesia* species to infect more than one vertebrate host (e.g., *B. microti* affects

Kidney, calf. The renal cortex is discolored as a result of hemoglobinuria; the pelvis shows profound icterus. (Photo courtesy of: Laboratory of Anatomic Pathology, Universidade Federal de Mato Grosso do Sul, Campo Grande, MS, Brazil. https://www.ufms.br/)

rodent and humans; *B. divergens* and *B. bovis* affect cattle and humans), *Babesia* spp. are typically host specific.[2]

Bovine babesiosis (aka, piroplasmosis, Texas fever, redwater, and tick fever) is a febrile hemolytic condition caused by one of at least seven species the protozoan organisms *Babesia* spp. It is characterized by extensive intravascular hemolysis leading to depression, anemia, icterus, hemoglobinuria, and, in the case of *B. bovis* infections, neurological signs.[2]

In Brazil, bovine babesiosis is caused by *B. bovis* (formerly *B. argentina*) and/or *B. bigemina* and is transmitted to cattle by the tick *Rhipicephalus* (*Boophilus*) *microplus*.[8,10] The disease is frequently, but not always associated with icterus and hemoglobinuria and the animal may become extremely ill before severe anemia, parasitemia or hemoglobinuria are apparent.[5,15]

In general, the disease distribution follows that of the vector ticks producing three distinct epidemiological situations. The disease does not occur in areas without the tick vector. In areas of enzootic instability, there is an alternation of warm and cold seasons. The cold period prolongs the free-living stages of the tick, allowing cattle extended periods without vector contact, resulting in a significant drop in antibodies due to the absence of *Babesia* infection. When the warm period returns, the tick parasite load increases and outbreaks occur. In enzootic areas, weather condition allow the presence of tick on cattle all year round, which confers high level of lasting immunological protection.[1]

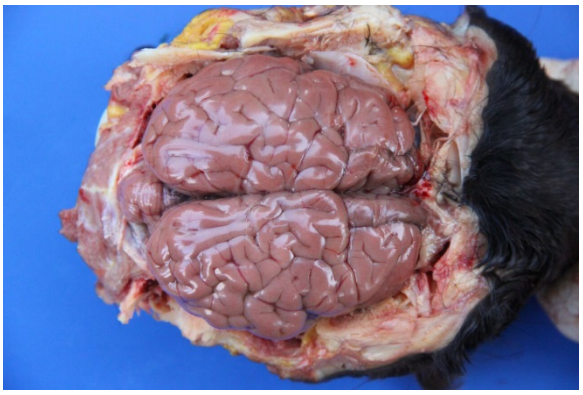

Cerebrum, calf. There is a diffuse pink discoloration of the brain as a result of marked cerebral congestion and sequestration of parasitized erythrocytes (Photo courtesy of: Laboratory of Anatomic Pathology, Universidade Federal de Mato Grosso do Sul, Campo Grande, MS, Brazil. https://www.ufms.br/)

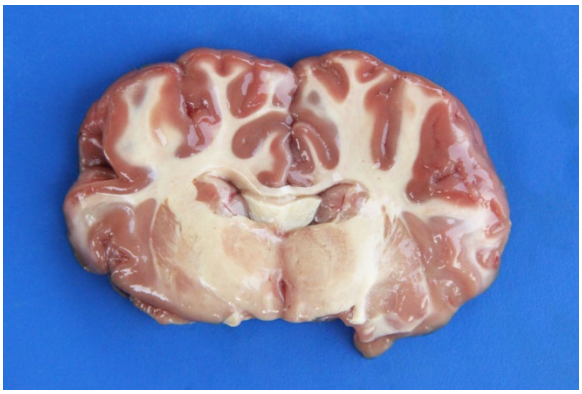

Cerebrum, calf. The grey telencephalic cortex and basal nuclei have an intense cherry-pink discoloration which contrast strongly with the subjacent white matter. (Photo courtesy of: Laboratory of Anatomic Pathology, Universidade Federal de Mato Grosso do Sul, Campo Grande, MS, Brazil. https://www.ufms.br/)

Factors influencing the occurrence of babesiosis outbreak include (1) over infestation by vector ticks resulting in a high inoculum of *Babesia*: (2) long periods without ticks with resultant loss of immunity, and (3) stress factor and nutritional deficiencies which can induce a drop in immunity and vulnerability to the disease.[2] Calves are typically more typically more resistant to infection by *Babesia* sp. than adult cattle.[15] Mortality is lower in enzootic areas due to resistance to infection.

B. bovis is small, pleomorphic apicomplexan parasite, and can occur as single or as paired pear-shaped bodies joined at an obtuse angle within the center of the mature erythrocyte. The round forms measure 1-1.5 µm, and the pear-shaped bodies 1.5 x 2.4 µm in size. Vacuolated signet ring forms are particularly common. Hosts are cattle, buffalo, and deer.[14]

The incubation period for bovine babesiosis is typically 2-3 weeks[1,15] for the natural disease. The natural infection caused by *B. bovis* tends to present a longer incubation time than that caused by *B. bigemina*. Cases of extremely short incubation periods (seven days) have been reported for B. bovis.[13,14]

Infection occurs after the tick vector feeds on the host. After the inoculation of the infectious sporozoites, the parasite penetrates the erythrocytes in the definitive host where they form a parasitophorous vacuole and change to the trophozoite form. Later these trophozoites undergo binary division, usually forming two merozoites. Ticks acquire *Babesia* infection during feeding on infected animals.[2]

Affected cattle develop depression, anorexia, paleness of mucous membranes, and fever (40 degrees/C-42 degrees C). Icterus and hemoglobinuria are also common clinical signs, but they can be minimal or absent in cases of peracute or acute disease. The elevation of serum activity of AST and GGT, observed in this case, may be due to the hepatic centrilobular hypoxic necrosis.[1] Additionally, this calf had omphalitis, which probably resulted in septicemia (high fibrinogen) which would explain the low blood sugar.[4]

B. bovis causes the most severe form of babesiosis in cattle in which peripheral circulatory disturbances with sequestration

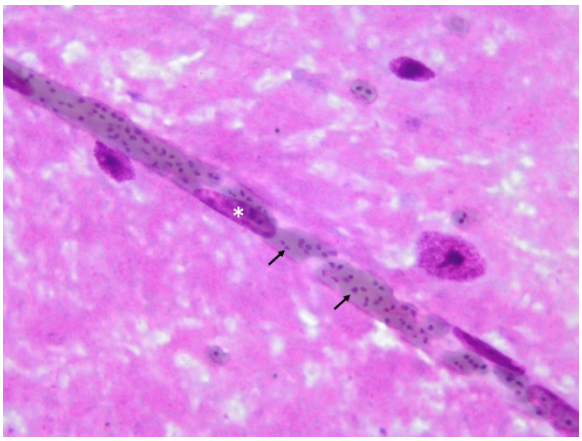

Cerebrum, calf. Squash preparation from the telencephalic cortex. An An isolated capillary distended by erythrocytes parasitized by Babesia bovis organisms (arrows). (Photo courtesy of: Laboratory of Anatomic Pathology, Universidade Federal de Mato Grosso do Sul, Campo Grande, MS, Brazil. https://www.ufms.br/)

of parasitized erythrocytes in the peripheral circulation are unique features.[3,11,12,16] In southern Brazil this form of disease is found in approximately two-thirds of the cases of babesiosis caused by *B. bovis* and is virtually always fatal.[11]

Necropsy findings include yellow discoloration (icterus) of mucosae, subcutaneous tissue, muscle fasciae and the intimal surface of arteries. In acute or peracute cases (which include the cases of cerebral babesiosis) icterus can be mild or absent. The serosal membranes of the abdominal viscera have hemoglobin imbibition. The liver is swollen, with rounded edges, and is yellow or tan discolored. The biliary vesicle is usually markedly distended by dark-green inspissated bile. Subepicardial and subendocardial hemorrhages (petechiae and ecchymosis) are virtually always observed. In cases where hemoglobinuria is a prominent sign, the kidneys are diffusely dark red-brown (hemoglobinuric nephrosis) and the urine is dark-red (red water disease). There is always some degree of splenomegaly. In severely enlarged spleens

the red pulp prolapses on the cut surface. In cerebral babesiosis, the grey matter of the telencephalic, and cerebellar cortex and that of the basal nuclei has a characteristic cherry pink color. Squashes made from cortical brain, stained with Wright-Giemsa reveal numerous capillaries engorged with parasitized erythrocytes.[3,5,6]

The encephalic lesion is characteristic of *B. bovis* infection and does not occur in any other *Babesia sp*. infection of cattle. However, it can be compared with the brain lesions seen in severe cases of malaria caused by *Plasmodium falciparum*. Microscopically the brain lesions are characterized by cortical capillaries diffusely engorged with red blood cells, and perivascular and perineuronal edema. In tissue sections of the brain, Giemsa and even HE stains demonstrate the parasites as small paired or single spherical faint basophilic bodies.[1,15] Parasitized erythrocytes may also be seen in vessels of virtually all tissues, such as the interstitial capillaries in the kidney, heart, and in skeletal muscle.[15] Other changes characteristic of hemolytic anemia are observed such hemoglobinuric nephrosis, centrilobular hepatic necrosis (due to hypoxia) and bile stasis.[15]

Ultrastructurally, capillaries in the brain are dilated and filled with densely packed parasitized erythrocytes. These erythrocytes have scalloped edges with fine strands apparently connecting adjacent red blood, as well as connecting erythrocytes and endothelial cells.[5,6] Masses of lysed red blood cells which have undergone lysis but still contain intact parasites are frequently seen in capillaries. Changes in the capillary endothelium of the affected parts in the brain range from swelling of the cytoplasm and nucleus to necrosis. Perivascular and perineuronal spaces are enlarged. In the kidneys, capillaries are not packed as tightly with red blood cells as in the brain, and the parasitemia does not exceed 50% of red blood cells. Other changes are similar to those seen in the brain. Capillaries in the lung are packed with red blood cells, but only a small proportion of the cells are parasitized.[5]

Although usually reported resistant to babesiosis, calves in enzootic areas can be parasitized by *R. microplus* on the first day of life.[8] Since the protection of neonates calves is conferred by passive immunity through colostral ingestion, a failure in the transfer of passive immunity from the dam can explain very young calves being affected by the disease. A lack of passive immunity caused by the failure of colostral ingestion in the calf of this report could be suspected since omphalitis was also present.

The pathogenesis of the disease caused by *B. bovis* in cattle is not completely understood, but some mechanisms are proposed.[5,15] Acute disease is characterized by a hypotensive shock syndrome with vascular stasis and accumulation of parasitized erythrocytes in the peripheral circulation. It is accompanied by activation of coagulation/complement cascades and the release of vasoactive compounds resulting in vasodilation and circulatory stasis as well as generalized organ damage due to anoxia and toxic products from both parasites and damaged host tissue.

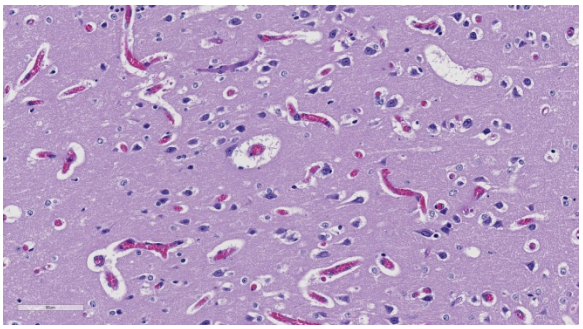

Cerebellum, calf: Capillaries are diffusely expanded and as a result are more visually prominent than expected within the submitted section. (HE, 224X).

Parasite proteases cause hydrolysis of fibrinogen which results in the accumulation of large quantities of soluble fibrin complexes which are not cross-linked, as well as in altered fibrinogen in the circulation. Thus, the coagulability and viscosity of blood increases but insoluble fibrin is not produced, suggesting that classic disseminated intravascular coagulopathy is not a feature of *B. bovis* infections.[5]

The cause of cytoadherence of in *B. bovis* organisms to endothelial cells is also uncertain,[5,15] but the *Babesia* organisms remodel the erythrocyte surface with their erythrocyte surface antigen proteins, which changes the membrane mechanical and adhesive properties.[15]

In the severe form of malaria caused by *Plasmodium falciparum*, a disease that in many aspects resemble cerebral babesiosis, the causative organism induce infected red cells to clump together and to stick to endothelial cells lining of small blood vessels (sequestration), which blocks blood flow. Several proteins, including *P. falciparum* erythrocyte membrane protein 1 (PfEMP1), associated and form knobs on the surface of erythrocytes. PfEMP1 binds to thrombospondin, VCAM-1, ICAM-1, CD36, and E-selectin on the endothelial cells. Erythrocytes sequestration decreases tissue perfusion and leads to ischemia, which is responsible for the manifestations of cerebral malaria, the major cause of death in children with malaria.[9] Mild to minimal mononuclear perivascular cuffing can be observed in a few of the slides of this case. This change is of no clinical significance encountered in one-third of symptomless cattle.[7]

JPC Diagnosis: Cerebrum, vessesls: Intraerythrocytic protozoal trophozoites, numerous, Angus x Nellore ox, *Bos taurus*.

Conference Comment: The contributor provides an exhaustive review of *Babesia bovis* infection in an ox in addition to excellent quality gross photographs of the striking and pathognomonic uniformly cherry-red cerebral grey matter, referred to colloquially as “cerebral flush” or “pink brain”. This disease is one of the leading causes of infectious mortality of cattle in Brazil.[2,15] As mentioned by the contributor, this pink discoloration of the brain is secondary to marked congestion of the cerebral microvasculature by infected erythrocytes. In this case, nearly every erythrocyte is infected with at least one round to pyriform trophozoite. Parasitized erythrocytes have a tropism for the cerebral grey matter, kidney, heart, and skeletal muscle, but infected erythrocytes can be found in any tissue. Interestingly, the parasite is only rarely found in about 5% of circulating red blood cells.[15]

The sequestration of infected erythrocytes within the microvasculature of the cerebrum and other visceral organs leads to occlusion of the vessels and subsequent hypoxic injury. *Babesia bovis* also releases vasoactive proteases that activate the hypotensive agent, kallikrein, which then activates another potent vasodilator, bradykinin.[15] The dilatory effect of these

vasoactive proteins shifts blood away from veins and further contributes to apparent anemia. Additionally, infected animals are typically markedly anemic secondary to both intravascular and extravascular hemolysis, described by the contributor.[15] The combination of vascular congestion, vasodilation, and hemolysis leads to both metabolic alkalosis and a hemodynamic crisis, often resulting in the death of the animal.

Most conference participants noted congestion and dilation of the cerebral microvasculature in this case; however, some attendees offered a dissenting opinion that the apparent congestion is a result of post-mortem pooling of blood within the brain rather than an antemortem change. The conference moderator agreed with the majority of the participants that the cerebral congestion is part of the pathogenesis of this disease and likely represents a real lesion, rather than an artifact. Participants also astutely noted that while vessels are congested in both the grey and white matter histologically, congestion is only apparent within the grey matter macroscopically.[15]

Contributing Institution:
Laboratory of Anatomic Pathology
Universidade Federal de Mato Grosso do Sul
Campo Grande, MS, Brazil.
https://www.ufms.br/

References:

1. Barros CSL, Driemeier D, Dutra IS, Lemos RAA. Babesiose cerebral [Cerebral babesiosis]. In: Barros CSL, Driemeier D, Dutra IS, Lemos RAA, eds. *Doenças do sistema nervoso de bovinos no Brasil* [Diseases of the central nervous system in cattle in tick Brazil]. São Paulo, SP: Coleção Vallée; 2006:87-95.
2. Barros CSL, Fighera RA. Babesiosis. In: *Foreign animal diseases*. Washington DC, United States: Animal Health Association, 2008:147-157.
3. Callow LL, McGavin MD. Cerebral babesiosis due to *Babesia argentina*. *Aust Vet J*. 1963; 39:15-21.
4. Carlson GP. Clinical chemistry tests. In: Smith BP, ed. *Large Animal Internal Medicine*. 4th ed. St. Louis: Mosby; 2009:393.
5. de Vos AJ, de Waal DT, Jackson LA. Bovine babesiosis. In: Coetzer JAW, Tustin RC, eds. *Infectious Diseases of Livestock*. 2nd ed., vol. 1. Cape Town: Oxford University; 2004:406-424.
6. Everitt JI, Shadduck JA, Steinkamp C, Claubaugh G. Experimental *Babesia bovis* infection in Holstein calves. *Vet Pathol*. 1986;23:556-562.
7. Gavier-Widen D, Wells GAH, Simmons MM, Wilesmith JWW, Ryan J. Histological observations on the brains of symptomless 7-year-old cattle. *J Comp Path*. 2001; 124:52-59.
8. Kessler RH, Madruga CR, Schenk MAM Ribeiro OC. Babesiose cerebral por *Babesia bovis* em bezerros no Estado de Mato Grosso do Sul [Cerebral babesiose by *Babesia bovis* in calves in Mato Grosso do Sul]. *Pesq Agropec Bras*. 1983;18:931-935.
9. McAdams AJ, Milner, Sharp AH. Parasitic infections. In: Kumar V, Abbas A, Aster J, eds. *Robbins & Cotran Pathologic Basis of Disease*. 9th ed. Philadelphia: Elsevier Saunders; 2014:389-402.
10. Patarroyo JH, Vargas M.L., Bicudo PL. Description of lesions in cattle in

a natural outbreak of *Babesia bovis* infection in Brazil. *Vet Parasitol*. 1982;11:301-308.
11. Rodrigues A, Rech RR, Barros RR, Fighera RA, Barros CSL. Babesiose cerebral em bovinos: 20 casos [Cerebral babesiosis in cattle: 20 cases]. *Ciência Rural*. 2005;35:121-125.
12. Rogers RJ. Observations on the pathology of *Babesia argentina* infections in cattle. *Aust Vet J*. 1971; 47:242-247.
13. Santarosa BP, Dantas GTN, Ferreira DOL, et al. Infecção neurológica por *Babesia bovis* em bovino neonato – relato de caso [*Babesia bovis* neurological infection in bovine neonates - case report]. *Vet. Zootec*. 2013; 20:9-14.
14. Taylor MA, Coop RL, Wall RL. *Veterinary parasitology*. 3rd ed. Oxford: Blackwell; 2007:105-107.
15. Valli VEO, Kiupel M, Bienzle D. Babesiosis. In: Maxie MD, ed. *Jubb, Kennedy & Palmer Pathology of Domestic Animals*. 6th ed. vol. 3. St. Louis, MO: Elsevier; 2016:118-120.
16. Zlotnic L. Cerebral piroplasmosis in cattle. *Vet Rec*. 1953; 40:642-643.

CASE IV: 14-9 (JPC 4087119).

Signalment: Five-year-old female ragdoll mix cat (*Felis catus*).

History: The cat was found dead at home in January 2014, after one day of anorexia, open-mouth breathing, and hiding. The cat had lived with two littermates and had no outdoor access. On the day before this cat's death, a littermate from the same home had developed severe respiratory distress and been euthanized but not necropsied. The third littermate never became ill and is still alive 2.5 years later at the time of submission.

Gross Pathology: At necropsy, both lungs were diffusely consolidated and edematous. Formalin-fixed slabs of lung had prominent, grossly visible, pale cuffs around bronchioles. There were no other gross abnormalities in any organ system.

Laboratory results: Samples of lung were submitted to a commercial diagnostic laboratory for a feline upper respiratory disease panel. This panel was negative by real-time PCR for all agents tested: feline calicivirus, *Chlamydophila felis*, feline herpesvirus 1, *Bordetella bronchiseptica, Mycoplasma felis* and H1N1 influenza virus.

Histopathologic Description: Lung: In most bronchioles, the lining epithelium is segmentally to completely sloughed or attenuated, with occasional attempts at regeneration. The lumens of affected bronchioles frequently contain adherent strands of fibrin and cellular debris

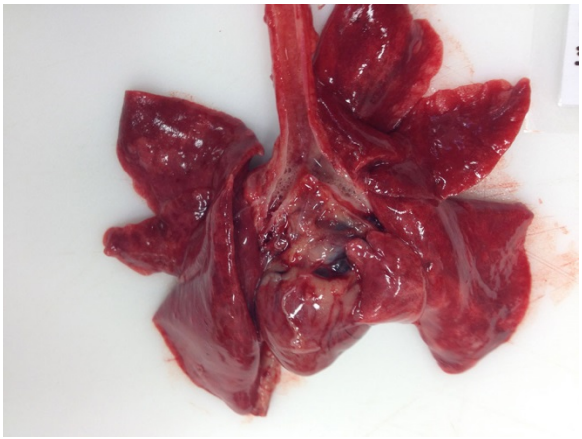

Lungs, cat. All lung fields are consolidated and edematous. (Photo courtesy of: Department of Veterinary Clinical and Diagnostic Sciences, Faculty of Veterinary Medicine, University of Calgary, 3280 Hospital Dr. NW, Calgary, Alberta T2N 4Z6, Canada, http://vet.ucalgary.ca/)

composed of macrophages, sloughed epithelial cells, and free red blood cells.

Diffusely, alveolar airspaces contain moderate numbers of cells, predominantly macrophages and lymphocytes, with fewer non-degenerate neutrophils and red blood cells. In addition, alveolar airspaces contain abundant eosinophilic beaded to fibrillar material (fibrin). Numerous peribronchiolar alveoli are lined by markedly hypertrophied cuboidal epithelial cells with large nuclei and prominent nucleoli (type II pneumocyte hyperplasia). Multinucleate pneumocytes are occasionally seen.

Around larger pulmonary vessels, connective tissue is moderately expanded by clear space (perivascular edema). Throughout all sections, muscular pulmonary arteries and arterioles have moderately thickened walls (smooth muscle hyperplasia).

Contributor's Morphologic Diagnosis: Lung: Severe, diffuse, acute to subacute, multifocal to coalescing, necrotizing bronchointerstitial pneumonia with alveolar edema and marked peribronchiolar type II pneumocyte hyperplasia.

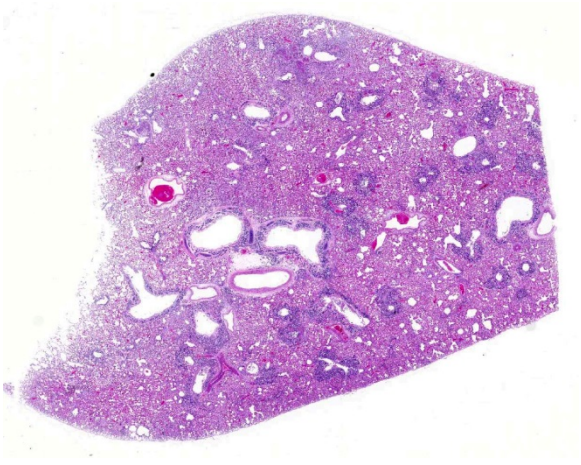

Lung, cat. There is marked hypercellularity surrounding airways. (HE, 5X)

Contributor's Comment: This cat died from severe bronchointerstitial pneumonia, which is most frequently caused by feline herpesvirus or feline calicivirus infection.[4] Lung samples were submitted to a commercial diagnostic laboratory and no viral or bacterial sequences were detected using real time PCR. However, because this cat's gross and histologic lesions were nearly identical to those described previously in two cats that died of influenza A(H1N1)pdm09 virus infection (so-called pandemic influenza),[8] we submitted samples to a provincial diagnostic laboratory, which detected this virus. This is, to our knowledge, the first confirmed case of influenza A(H1N1)pdm09 infection in a Canadian cat.

Influenza A viruses are RNA viruses in the family *Orthomyxoviridae* that can infect multiple species of mammals and birds, although different viral subtypes tend to be host-specific.[17] These viruses have caused multiple epidemics and pandemics in human populations,[11] as well as epizootics and panzootics in animal species.[12,16] Rapid mutation and gene reassortment of influenza A viruses lead to a high diversity of viral subtypes, and this genetic flexibility results in a propensity for between-species and cross-class transmission.[18] The so-called pandemic strain of the H1N1 influenza virus isolated in 2009 (influenza A(H1N1)pdm09) contained a novel combination of genetic segments from influenza viruses affecting humans, pigs, and birds.[6]

Cats are susceptible to infection by multiple influenza A virus subtypes;[1] however, reports of clinical disease in cats resulting from natural infection with A(H1N1)pdm09 are relatively scarce.[3,5,8,10,13] The source of this particular cat's infection could not be determined. The owner lived alone, had received a seasonal influenza vaccination in

October of 2013, and had never become sick. However, she had hosted two house guests for a three day period after Christmas 2013, approximately 10 days before the deaths of her two cats in early January, 2014. One guest had "flu-like" symptoms and remained indoors for the majority of the visit. Although the cause of this guest's illness was never known, the 2013–2014 influenza season was intensive in Alberta; there were 35% more lab-confirmed cases of human influenza infection than the previous year and the predominant circulating strain was influenza A(H1N1)pdm09.[14] Thus, the sick guest could not be ruled out as the source of this cat's, and/or her littermate's, infection.

The possibility of anthroponotic transmission of influenza A(H1N1)pdm09 to cats is supported by two earlier reports. The first describes an indoor-only cat that was infected with influenza A(H1N1)pdm09 after exposure to human family members with a non-diagnosed flu-like illness.[13] The second shows that pet cats are nearly three times more likely to be seropositive for influenza A(H1N1)pdm09 than free-roaming cats.[18] Cat-to-cat transmission of influenza A(H1N1)pdm09 has also been documented, both experimentally[15] and in an outbreak in cats with little human contact living in a cat colony in Italy.[5] Zoonotic transmission of influenza viruses from cats to humans may also occur, and the role that cats may play in the epidemiology of human influenza infections needs further investigation.[1]

The cat described here died from severe pneumonia caused by pandemic influenza A virus infection. This virus was not detected in samples sent to a commercial laboratory, but was detected in samples sent to a second laboratory. Therefore, if clinical signs, history (exposure to people or animals

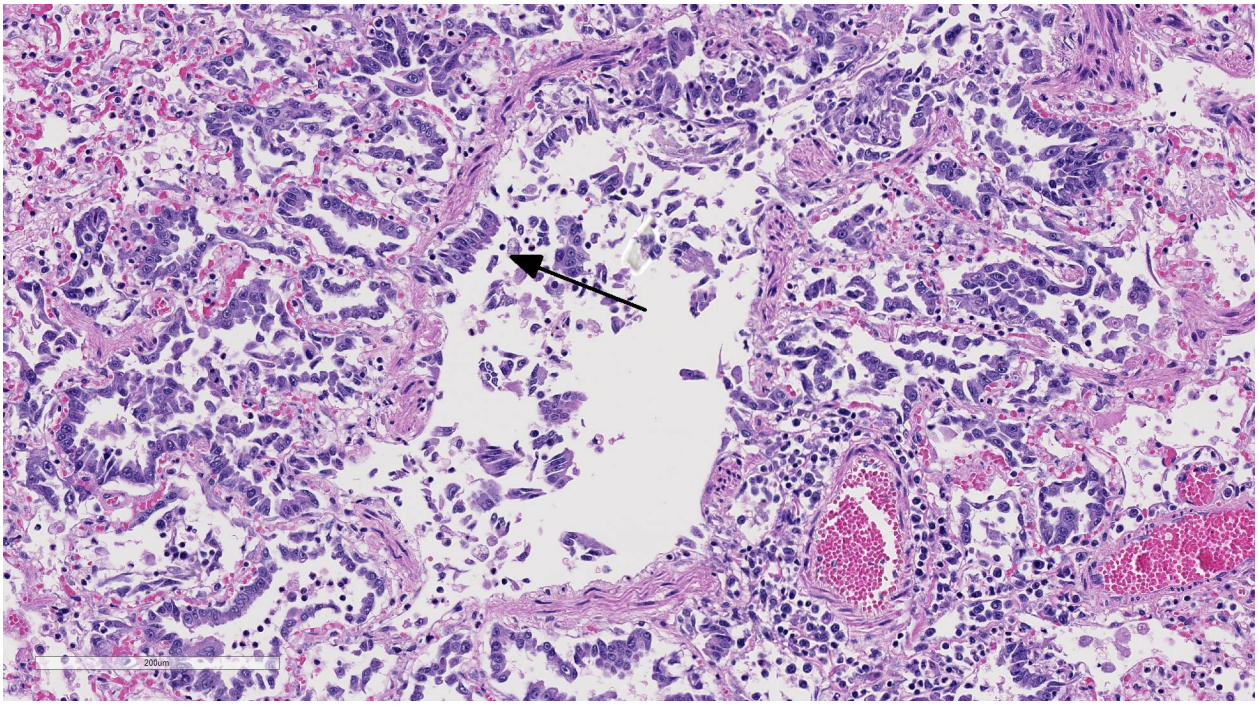

Lung, cat. Diffusely, airway epithelium is necrotic and almost totally sloughed. There is marked bronchiologenic type II pneumocyte hyperplasia. (HE, 104X)

infected with influenza virus), gross lesions, and histologic findings are suggestive of influenza virus infection, it is reasonable to test samples in a second laboratory should a first laboratory provide a negative result for influenza virus infection. This case highlights the importance of including influenza virus infection in the differential diagnosis for respiratory disease in cats. It also further demonstrates the importance of investigating any discrepancy between histologic findings and expected laboratory results.

JPC Diagnosis: Lung: Pneumonia, bronchointerstitial, necrotizing, multifocal to coalescing, severe with marked peri-bronchiolar type II pneumocyte hyperplasia, ragdoll mix cat, *Felis catus*.

Conference Comment: The diagnosis of bronchointerstitial pneumonia was the subject of much debate among conference participants. It is usually reserved for cases where there is microscopic evidence of viral targeting of both the bronchiolar and alveolar epithelium, which is the typical behavior of aerogenous viral infections or inhaled toxins.[4] Damage to the airway epithelium and alveolar septa causes epithelial necrosis and hyperplasia of type II pneumoncytes.[4] This case is an excellent example of bronchointerstitial pneumonia with profound multifocal bronchiolar-centric type II pneumocyte hyperplasia, nicely highlighted by pancytokeratin immuno-histochemical stain run by the Joint Pathology Center prior to the conference. Interestingly, marked type II pneumocyte hyperplasia can occur as early as two days after initial insult to the respiratory epithelium and alveolar septum, coinciding with the acute onset reported in the history of this case.[7,8] Conference participants discussed other differential diagnoses for bronchointerstitial pneumonia in cats, such

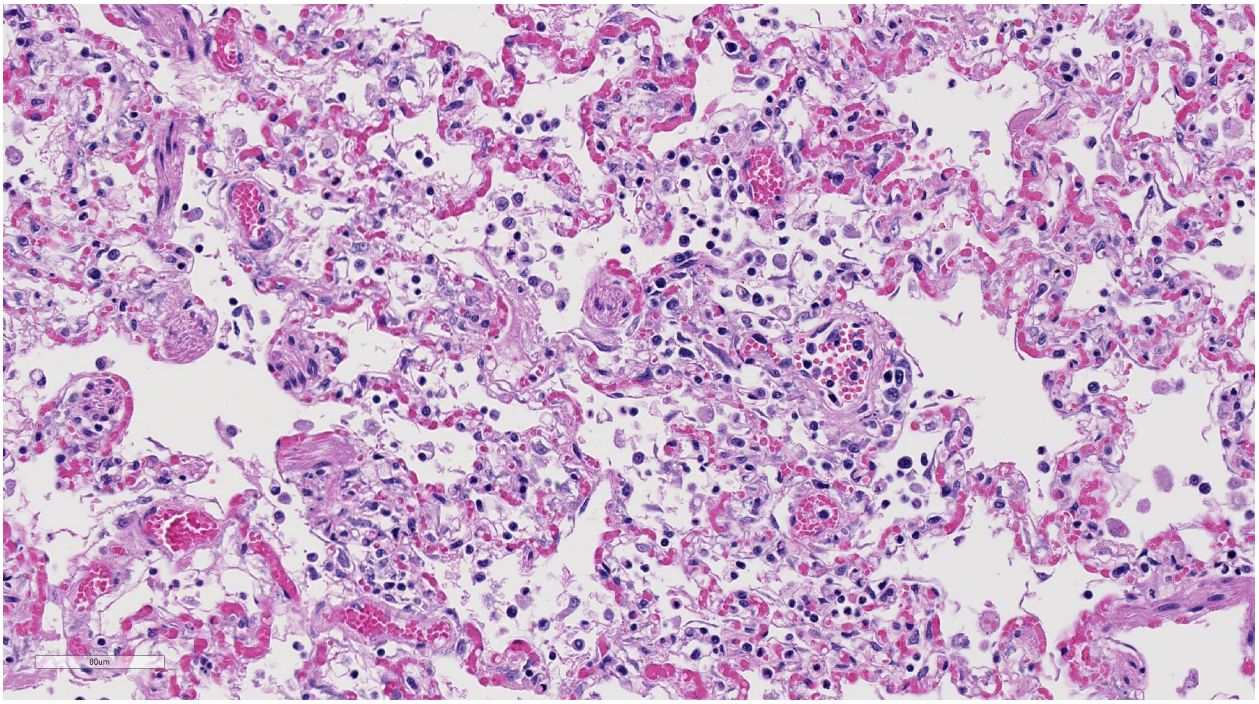

Lung, cat. Diffusely, alveoli are expanded by moderate amounts of fibrin, congestion, and edema. Alveolar spaces contain variable combinations and concentrations of inflammatory cells, polymerized fibrin and cellular debris. (HE, 228X)

as feline herpesvirus-1 and feline calicivirus.[4,7,8]

The conference moderator also noted that in this case the virus appears to exhibit a tropism for terminal airways with relative sparing of the larger bronchi. The specific anatomic location of lesions associated with influenza virus has been reported to correlate with the distribution of sialic acid molecules on the cell surface of the host.[8,9] In human pandemic H1N1 influenza A, these sialic acids are distributed in the trachea and larger airways, resulting in necrotizing tracheitis and bronchitis in severely affected human patients. In pathogenic avian influenza H5N1, the virus binds to sialic acids present mainly on terminal bronchioles and pneumocytes.[8,9] Interestingly, the distribution of lesions in this case differs from the typical presentation of human H1N1 influenza A, and resembles binding of avian influenza viral particles. This distribution pattern has been reported in other cases of H1N1 infection in cats.[8]

Influenza viruses are RNA viruses of the *Orthomyxovridiae* family, and are able to rapidly mutate through antigenic drift and genetic reassortment.[1,7,8,9] This leads to a high degree of viral diversity and genetic flexibility, thus allowing the virus to quickly adapt and infect multiple different species.[7,8] In addition to human origin H1N1, presented in this case, cats are also susceptible to highly pathogenic avian influenza H5N1 and H7N2 viruses.[4] Cats have been reported to be infected with H1N1 by interaction with infected humans, as is suspected in this case, and then transmit the disease horizontally to other felids. There are currently no reports of transmission from cat to human with H1N1 virus.[7,8] Infection with highly pathogenic avian influenza in cats is thought to be secondary to both inhalation of aerosolized virus and consumption of infected birds.[4]

In December 2016, there was an outbreak of H7N2 avian influenza in almost 400 shelter cats in New York City.[2] A shelter veterinarian who had prolonged and unprotected exposure to affected cats was also infected with the virus. This is the first documented case of cat to human transmission of influenza and only the third case of human H7N2 avian influenza infection in the United States.[2] Given their close relationship with humans and susceptibility to both human and avian influenza strains, cats have the potential to be important reservoirs for infection.[2,7,8] Feline co-infection with human and avian strains may allow genetic reassortment and antigenic shift creating a novel influenza A subtype and provide the basis for a new influenza pandemic.[7] As a result, influenza virus should be carefully considered as a differential diagnosis for respiratory disease in cats.

Contributing Institution:
Faculty of Veterinary Medicine
University of Calgary
3280 Hospital Dr. NW
Calgary, Alberta
Canada
http://vet.ucalgary.ca/

References:

1 Ali A, Daniels JB, Zhang Y, Rodriguez-Palacios A, Hayes-Ozello K, Mathes L, Lee C-W. Pandemic and seasonal human influenza virus infections in domestic cats: Prevalence, association with respiratory disease, and seasonality patterns. *J Clin Microbiol*. 2001; 49:4101-4105.

2 Avian influenza A (H7N2) in cats in animal shelters in NY; one human

infection. Centers for Disease Control and Prevention website. https://www.cdc.gov/flu/spotlights/avian-influenza-cats.htm. Updated January 4, 2017. Accessed February 16, 2017.

3 Campagnolo ER, Rankin JT, Daverio SA, Hunt EA, Lute JR, Tewari D, Acland HM, Ostrowski SR, Moll ME, Urdaneta VV, Ostroff SM. Fatal pandemic (H1N1) 2009 influenza A virus infection in a Pennsylvania domestic cat. *Zoonoses Public Health*. 2011; 58:500-507.

4 Caswell JL, Williams KJ. Respiratory system. In: Maxie MG ed. *Jubb, Kennedy and Palmer's Pathology of Domestic Animals*. Vol 2. 6th ed. St. Louis, MO: Elsevier; 2016:511,587-591.

5 Fiorentini L, Taddei R, Moreno A, Gelmetti D, Barbieri I, De Marco MA, Tosi G, Cordioli P, Massi P: Influenza A pandemic (H1N1) 2009 virus outbreak in a cat colony in Italy. *Zoonoses Public Health*. 2011; 58:573-581.

6 Garten RJ, Davis CT, Russell CA, Shu B, Lindstrom S, Balish A, Sessions WM, Xu XY, Skepner E, Deyde V, Okomo-Adhiambo M, Gubareva L, Barnes J, Smith CB, Emery SL, Hillman MJ, Rivailler P, Smagala J, de Graaf M, Burke DF, Fouchier RAM, Pappas C, Alpuche-Aranda CM, Lopez-Gatell H, Olivera H, Lopez I, Myers CA, Faix D, Blair PJ, Yu C, Keene KM, Dotson PD, Boxrud D, Sambol AR, Abid SH, George KS, Bannerman T, Moore AL, Stringer DJ, Blevins P, Demmler-Harrison GJ, Ginsberg M, Kriner P, Waterman S, Smole S, Guevara HF, Belongia EA, Clark PA, Beatrice ST, Donis R, Katz J, Finelli L, Bridges CB, Shaw M, Jernigan DB, Uyeki TM, Smith DJ, Klimov AI, Cox NJ. Antigenic and genetic characteristics of swine-origin 2009 A(H1N1) influenza viruses circulating in humans. *Science*. 2009; 325:197-201.

7 Knight CG, Davies JL, Joseph T, Ondrich S, Rosa BV. Pandemic H1N1 influenza virus infection in a Canadian cat. *Can Vet J*. 2016; 57(5):497-500.

8 Lohr CV, DeBess EE, Baker RJ, Hiett SL, Hoffman KA, Murdoch VJ, Fischer KA, Mulrooney DM, Selman RL, Hammill-Black WM. Pathology and viral antigen distribution of lethal pneumonia in domestic cats due to pandemic (H1N1) 2009 influenza A virus. *Vet Pathol*. 2010; 47:378-386.

9 Marschall J, Hartmann K. Avian influenza A H5N1 infections in cats. *J Fel Med Surg*. 2008; 10:359-365.

10 Pigott AM, Haak CE, Breshears MA, Linklater AKJ. Acute bronchointerstitial pneumonia in two indoor cats exposed to the H1N1 influenza virus. *J Vet Emerg Crit Care*. 2014; 24:715-723.

11 Pleschka S. Overview of influenza viruses. In: Richt JA, ed. *Current Topics in Microbiology and Immunology: Swine Influenza*. Webby RJ: Springer-Verlag, Berlin; 2013:1-20.

12 Schultz-Cherry S, Olsen CW, Easterday BC. History of swine influenza. In: Richt JA, ed. *Current Topics in Microbiology and Immunology: Swine Influenza*. Webby RJ: Springer-Verlag, Berlin; 2013:21-28

13 Sponseller BA, Strait E, Jergens A, Trujillo J, Harmon K, Koster L, Jenkins-Moore M, Killian M, Swenson S, Bender H, Waller K,

Miles K, Pearce T, Yoon KJ, Nara P. Influenza A pandemic (H1N1) 2009 virus infection in domestic cat. *Emerg Infect Dis*. 2010; 16:534-537.
14 Surveillance and Assessment Branch AH: Seasonal Influenza in Alberta – 2012/2013 Summary Report. http://www.health.alberta.ca/documents/Influenza-Summary-Report-2014.pdf. Edmonton, Alberta, 2014.
15 van den Brand JMA, Stittelaar KJ, van Amerongen G, van de Bildt MWG, Leijten LME, Kuiken T, Osterhaus A. Experimental Pandemic (H1N1) 2009 virus infection of cats. *Emerg Infect Dis*. 2010; 16:1745-1747.
16 Vijaykrishna D, Bahl J, Riley S, Duan L, Zhang JX, Chen HL, Peiris JSM, Smith GJD, Guan Y. Evolutionary dynamics and emergence of panzootic H5N1 influenza viruses. *PloS Path*. 2008; 4:10.
17 Webster RG, Bean WJ, Gorman OT, Chambers TM, Kawaoka Y. Evolution and ecology of influenza A viruses. *Microbiol Rev*. 1992; 56:152-179.
18 Zhao FR, Liu CG, Yin X, Zhou DH, Wei P, Chang HY. Serological report of pandemic (H1N1) 2009 infection among cats in Northeastern China in 2012-02 and 2013-03. *Virol J*. 2014; 11:4.

Self-Assessment - WSC 2016-2017 Conference 18

1. Which of the following is not true concerning caruncular amyloidosis in the goat??
    a. Affected reeds include Toggenburg and Saan.
    b. Affected goats had no other amyloid deposits .
    c. Amyloid in the caruncles exhibited apple-green birefringence when stained with Congo Red.
    d. Causative bacilli, including Chlamydophila among others, were isolated in affected placentas.

2. Which of the following is not true concerning West Nile Virus infection in birds ?
    a. *Aedes* mosquitoes are the intermediate host.
    b. Corvid species, like crows, are a major amplifying host.
    c. Histologic lesions are primarily found in the CNS, ,heart, liver, kidney, and spleen.
    d. In birds, primary viremia may occur without local replication.

3. True or false: Capillary engorgement, sequestration of parasitized erythrocytes, and a pink discoloration to the brain is seen only with *Babesia bovis* infection, but not with other *Babesia* species.
    a. True
    b. False

4. Which of the following is not true concerning *Babesia bovis* in cattle?
    a. Splenomegaly is a consistent finding
    b. Neonatal calves are protected by colostral ingestion
    c. Classical DIC is a terminal and usually fatal effect of infection.
    d. Icterus and hemoglobinuria may be minimal or absent in acute disease.

5. Which of the following influenza subtypes are cats not susceptible to?
    a. H1N1
    b. H5N1
    c. H5N2
    d. H7N2

Joint Pathology Center

Veterinary Pathology Services

WEDNESDAY SLIDE CONFERENCE 2016-2017

C o n f e r e n c e 19

15 February 2017

Karen Terio, DVM, PhD, Diplomate ACVP
Clinical Professor
Chief, Zoological Pathology Program
Chicago Zoological Society
Brookfield, IL

CASE I: 15-0609 (JPC 4067574).

Signalment: Adult, male, eastern gray squirrel, (*Sciurus carolinensis*).

History: Three recuperating eastern gray squirrels were housed in an outdoor cage at a wildlife rehabilitation facility. Shortly after being fed a whole pumpkin, one was found dead, and the other two were ataxic, disoriented, and pawing the air. The pupils were dilated. The attending veterinarian began treatment with fluids, a non-steroidal anti-inflammatory drug (meloxicam), and an anti-convulsant (gabapentin). The neurologic signs did not improve with treatment and time. The squirrels were humanly euthanized, and a necropsy was performed.

Gross Pathology: No gross lesions noted.

Laboratory results: No laboratory analysis performed.

Histopathologic Description: Cerebrum: Multifocally, there is necrosis of both gray and white matter characterized by disruption and loss of neural tissue with replacement by moderate numbers of macrophages with vacuolated cytoplasm (gitter cells), lymphocytes, few plasma cells, and rare eosinophils. Scattered throughout the neural tissue are cross and tangential sections of larval nematodes. The larvae are 50 µm in diameter, have a 5 µm thick cuticle with lateral chords and alae, coelomyarian-polymyarian musculature, a pseudocoelom, and an intestine lined by uninucleate columnar cells with a brush border. Some larvae are associated with areas of necrosis and inflammation and some have no

Diencephalon, squirrel. There are multifocal areas of cavitation within the hippocampus and thalamus (arrows). (HE, 5X)

surrounding inflammation but are associated with adjacent vague linear tracks of necrosis and inflammation. Multifocally, throughout the section, there are moderate numbers of lymphocytes with fewer plasma cells and eosinophils expanding perivascular spaces and the meninges. There are moderately increased numbers of glial cells (gliosis) along with spheroids and numerous reactive astrocytes in affected areas.

Contributor's Morphologic Diagnosis: Cerebrum: Meningoencephalitis, necrotizing and granulomatous, multifocal, marked, with perivascular cuffing, gliosis, astrocytosis, spheroids, and numerous larval nematodes.

Contributor's Comment: The initial clinical suspicion was that these squirrels were suffering from a toxin which was associated with the pumpkin. Examination of the enclosure revealed desiccated feces, which when evaluated by fecal floatation revealed the presence of ascarid eggs, consistent with *Baylisascaris procyonis*. Subsequently, histology of the brain provided the definitive diagnosis of neural larval migrans (NLM). *B. procyonis* is a member of the ascarid (roundworms) group of nematodes.[2] The raccoon (*Procyon lotor*) is the definitive host.[3] Dogs can also become infected with *B. procyonis* and shed eggs in feces.[1] Raccoons become infected by consuming *B. procyonis* eggs or intermediate hosts infected with larvae.[1,3] Larvae develop into adults in the raccoon intestine and produce large numbers of eggs which are shed in the feces.[3] Intermediate hosts ingest the eggs in environments contaminated with raccoon feces. In intermediate hosts, the larvae migrate

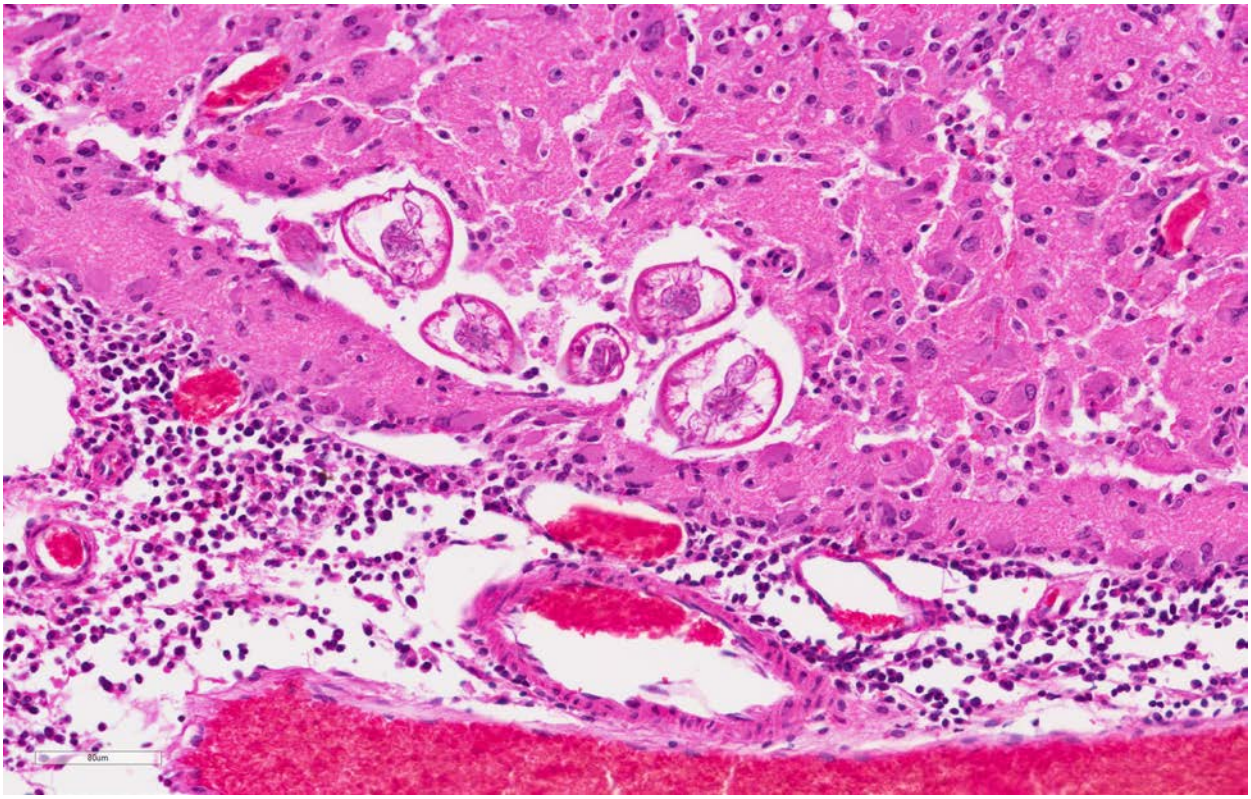

Diencephalon, squirrel. Areas of necrosis occasionally contain cross sections of larval ascarids with prominent lateral alae. Adjacent meninges are expanded by eosinophils and histiocytes. (HE, 228X)

through the body of the host. The third stage larvae of *B. procyonis* can be up to 2 mm in length.[1]

In most tissue, larvae are encapsulated in granulomas, however, in the brain encapsulation is slow to absent.[1] The large larvae migrate through neural tissue causing mechanical damage followed by an inflammatory response.[1,3] In this case, several larvae are present in neural tissue with no surrounding inflammation. Potentially, the pace of the migrating larva was faster than the immune response. Most inflammation present is associated with the migration tracks.

Eosinophils are a typical feature of parasite-induced inflammation, but were less apparent in this case. There may have been some modulation of the immune response in this squirrel due to treatment. In this case, several larvae were present in the brain. However, even low numbers of larvae can result in severe pathology due to their large size and aggressive migration.[1,3] A variety of mammals and birds have been reported as intermediate hosts of *B.* procyonis.[3] *B. procyonis* NLM is also recognized as an important zoonotic disease which predominantly affects children who engage in pica.[1] The eggs of *B. procyonis* can remain viable in the environment for years, even at below freezing temperatures.[3] The hardiness of the eggs and low infectious dose have even lead one investigator to speculate that *B. procyonis* could be utilized as a possible agent of bioterrorism.[5]

JPC Diagnosis: Cerebrum: Encephalitis, necrotizing, granulomatous and eosinophilic, multifocal, moderate with perivascular cuffing, gliosis, and numerous nematode larvae, eastern gray squirrel, *Sciurus carolinensis*.

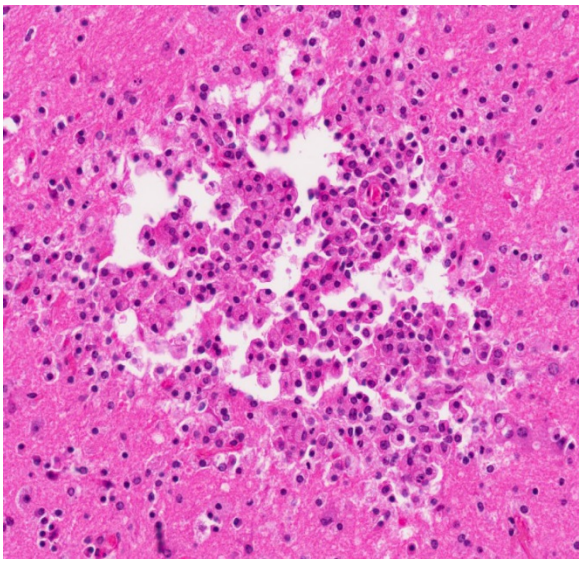

Diencephalon, squirrel. Foci of necrosis without larval parasites suggest parasite migration tracks. (HE, 300X)

Conference Comment: This case represents an excellent example of the characteristic eosinophilic and granulomatous inflammation with linear necrotic tracts present in neural larval migration of *Baylisascaris procyonis*, a common ascarid nematode parasite found predominantly in the Midwest, Northeast, and West Coastal United States.[7] As mentioned by the contributor, the raccoon is the definitive host and this roundworm parasite typically does not cause clinical disease in this species.[6] The adult nematodes are confined to the small intestine of the definitive host; however, *Baylisascaris procyonis* neural, somatic (visceral), and ocular larval migration are well documented in humans and over 100 wild and domestic animal species, including over 13 species of birds in North America.[1,3,6,7] In this case, the squirrel was likely exposed to raccoon feces from its enclosure and accidentally ingested infective eggs. In addition to raccoons, other species of have been reported to shed *Baylisascaris procyonis* eggs in their feces, including dogs, kinkajous, and skunks.[3,6,7]

Eggs are infective about two weeks after they are excreted by the raccoon host, and may persist in the environment for months to years. After the eggs are ingested by an intermediate host, the larvae hatch, penetrate the intestinal wall, and then enter the portal circulation. After passing into the arterial circulation, the larvae are distributed throughout the body.[5] A small number of larva enter the brain and aggressive larval migration in predominantly the white matter of the brain and spinal cord often leads to rapid debilitation, fulminant neurologic disease, and death of the intermediate host.[4,5] Humans, nonhuman primates, rodents, rabbits, and birds are reported to be the most susceptible to neural larval migrans.[3] Other *Baylisascaris* species include *B. melis* in badgers, *B. columnaris* in skunks, *B. laevis* in woodchucks, *B. schroederi* in pandas, *B. devosi* in the American pine marten, and *B. transfuga* in bears. Any of the above mentioned *Baylisacaris* sp. can cause similar larval migration lesions if infective fecal eggs are ingested by an intermediate or aberrant host.[5,6]

The conference moderator noted that while in this case numerous cross sections of larva are present and readily identified in the neuroparenchyma, most natural cases only have subtle evidence of larval neural migration tracts without identifiable larval cross sections. Additionally, the larva will continue to migrate after the death of the animal, and migration tracts may not always have associated inflammation and necrosis. There are currently no serologic tests commercially available to distinguish active infection from prior exposure.[7] Definitive diagnosis is based on identifying larva in histologic sections, although a presumptive diagnosis is usually made by a combination of history, clinical signs, and serologic testing.[7]

Contributing Institution:
Walter Reed Army Institute of Research
http://www.wrair.army.mil

References:

1. Bauer C. Baylisascariosis: Infections of animals and humans with 'unusual' roundworms. *Vet Parasitol*. 2013; 193:404-412.
2. Gardiner CH, Fayer R, Dubey J. An Atlas of Protozoan Parasites in Animal Tissues, 2nd ed. Armed Forces Institute of Pathology, Washington, DC, 1998: 19-21.
3. Gavin PJ, Kazacos KR, Shulman ST: Baylisascariasis. *Clin Microbiol Rev*. 2005; 18: 703-718.
4. Kazacos KR. *Baylisascaris procyonis* and related species. In: Samuel WM, Pybus MJ, Kocan AA, eds. *Parasitic Diseases of Wild Mammals*. 2nd ed. Ames IA: Iowa State University Press; 2001:301-335.
5. Okulewicz A, Bunkowska K. Baylisascariasis: A new dangerous zoonosis. *Wiad Parazytol*. 2009; 55:329-334.
6. Santiago SD, Uzal FA, Giannitti F, Shivaprasad HL. Cerebrospinal nematodiasis outbreak in an urban outdoor aviary of cockatiels (*Nymphicus hollandicus*) in southern California. *J Vet Diagn Invest*. 2012; 24(5):994-999.
7. Sircar AD, Abanyie F, et al. Raccoon roundworm infection associated with central nervous system disease and ocular disease-- six states, 2013-2015. *MMWR Morb Mortal Wkly Rep*. 2016; 65(35):930-933.

CASE II: WHL16188 (JPC 4084212).

Signalment: Female, Rocky Mountain elk calf (*Cervus elaphus nelsoni*).

History: Over a three week period, 11 free-ranging Rocky Mountain elk (mostly calves) were found dead at a Colorado ranch in late January.

Rumen, elk calf: The mucosa of the rumen was severely ulcerated, characterized by focal, irregularly round to linear, black, roughened depressions bordered by a hemorrhagic rim. (Photo courtesy of: Colorado State University, Microbiology, Immunology, and Pathology Department, College of Veterinary Medicine and Biomedical Sciences, http://csu-cvmbs.colostate.edu/academics/mip/Pages/default.aspx))

Gross Pathology: Postmortem examination was performed on a female elk calf in poor body condition with mild autolysis. The calf was very thin with minimal fat stores throughout and moderate serous atrophy of fat within the bone marrow (emaciation). Subcutaneous and intramuscular facial edema was prominent in the hind limbs. The abdomen contained scant serous fluid and large, extensive mats of fibrin along serosal surfaces (fibrinous peritonitis). Multifocally, the mucosa of the rumen was severely ulcerated, characterized by focal, irregularly round to linear, black, roughened depressions bordered by a hemorrhagic rim. Ulcerated areas were mural to nearly transmural without perforation. Rumen pillars were most severely affected, and rumen contents were dry. The epicardial surface had moderate multifocal petechial hemorrhages. The ventral margins of the cranioventral lung lobes were dark purple and consolidated.

Laboratory results: *Odocoileus* adenovirus PCR of lung: Positive
Bovine viral diarrhea I&II PCR of lymph node: Negative
Aerobic culture of lung: *Pasteurella multocida*, heavy growth

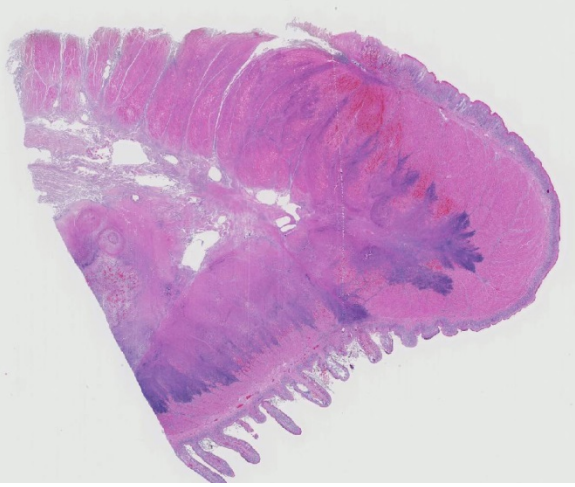

Esophogeoruminal junction:, elk calf: Large areas of infarction primarily involving the tunica muscularis and serosa are outlined by basophilic cellular debris and hemorrhage. (HE 5X)

Histopathologic Description: Rumen: Affecting approximately 50% of the section is a wedge-shaped region of the rumen obscured by transmural coagulative necrosis with preservation of tissue architecture but loss of cellular detail (infarction). The center of the lesion has regions of eosinophilic cellular and karyorrhectic debris, fibrin deposition, and multifocal mineralization. Necrotic regions are ulcerated and coated by myriad mixed bacteria. They are bordered by extensive hemorrhage, edema, fibrin, infiltration by high numbers of neutrophils, lymphocytes, and plasma cells and mild fibroblastic proliferation (fibroplasia). The walls of vessels throughout the tissue are frequently obscured, either segmentally or diffusely by finely fibrillar, brightly eosinophilic acellular material (fibrinoid necrosis) and moderate to high numbers of neutrophils and lymphocytes admixed with karyorrhectic debris and edema (leukocytoclastic vasculitis). Affected vessels often contain organizing fibrin aggregates and eosinophilic cellular and karyorrhectic debris (vascular thrombosis). Endothelial cells lining affected and unaffected vessels (predominately along the margin of the infarct) are hypertrophic and frequently contain basophilic, smudged, 8-10 μm inclusions that fill the nucleus. The adjacent mucosa and submucosa are infiltrated by moderate to high numbers of neutrophils and lymphocytes admixed with edema. Intact mucosal epithelium also has intracellular edema fluid, occasionally resulting in ballooning epithelial cells.

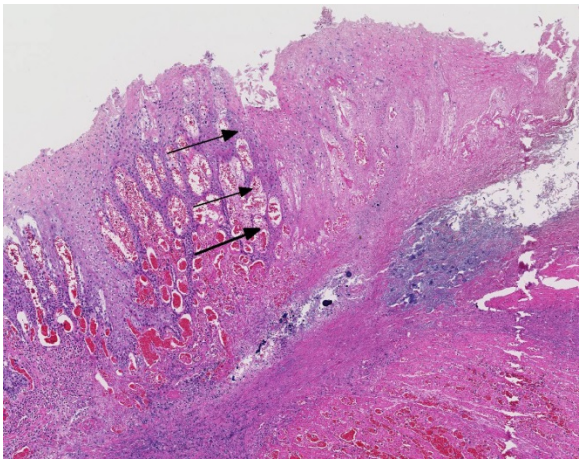

Esophageoruminal junction:, elk calf: At one edge of the section, the necrosis is transmural; necrotic mucosa is has a sharp line of demarcation from adjacent viable mucosa (arrows). (HE, 54X)

Microscopic diagnoses of tissues not submitted:

1. Lungs: Bronchopneumonia, suppurative and necrotizing, subacute, moderate, with mild lymphoid hyperplasia.
2. Lungs: Vasculitis, mild, subacute, multifocal (no viral inclusions detected).
3. Heart: Necrotizing myocarditis, multifocal, mild, acute (no viral inclusions detected).

Contributor's Morphologic Diagnosis: Rumen: Severe necrotizing vasculitis with thrombosis and infarction, subacute to chronic, multifocal, with ulcerative rumenitis and endothelial cell intranuclear viral inclusions consistent with *Odocoileus* adenovirus.

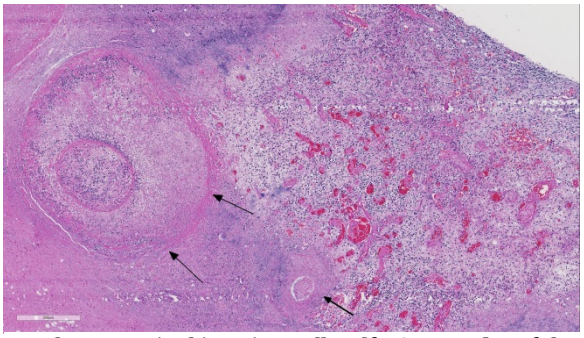

Esophageoruminal junction:, elk calf: At one edge of the section, multiple arterioles show evidence of mural destruction and thrombosis. (HE, 54X)

Contributor's Comment: Adenoviruses are non-enveloped icosahedral viruses that contain double-stranded DNA. A wide range of veterinary species are affected by this class of virus, often resulting in respiratory, gastrointestinal, or systemic disease.[4] In most species, clinical disease is mild, unless the animal is young or immunocompromised.[4] *Odocoileus* adenovirus (OdAdV) was first discovered in mule deer in Northern California in 1993 and was determined to be the causative agent of adenovirus hemorrhagic disease (AHD).[11,12] Since that time, the virus has been found to infect multiple species of deer,[11,13] moose,[8] and more recently, pronghorn and elk (unpublished data). Transmission has been documented via direct contact of cervids and is thought to occur through infected secretions or feces.[13] Studies have shown that OdAdV is most closely related to bovine adenovirus,[5] however, experimental infection studies of domestic cattle with OdAdV have not demonstrated viral replication or disease in this species.[15]

As is true with other adenovirus infections, young animals experience a significantly higher morbidity and mortality rate when compared to adults.[1,9,11] Death can occur as rapidly as five days post-infection, but chronic cases can also occur.[12,13] Acute cases usually have no symptoms or may exhibit ptyalism, diarrhea (with or without blood), weakness, lethargy, anorexia, and edema.[1,9,10] Chronic infections are usually associated with ulcers and abscesses of the mouth and throat, emaciation, and/or sepsis.[1,13]

Disease can be systemic or local.[11] Typical necropsy findings of systemic infections include severe pulmonary edema expanding the interlobular septa with ecchymotic hemorrhages of the lungs and pulmonary artery, and a hemorrhagic enteropathy characterized by hemorrhage within the lumen of the small and large intestine.[12,13] Additionally, multiple ulcerative lesions of the mouth, nasal cavity, mandible, maxilla, and forestomach can be present in systemic disease.[11] Local disease is restricted to the upper alimentary tract (stomatitis, pharyngitis, mandibular/maxillary osteomyelitis, and/or rumenitis).[13] In either form, secondary bacterial infections are common, primarily presenting as abscesses of the oral and nasal cavities.[12-15] Secondary bacterial agents include *Trueperella pyogenes*, *Prevotella* spp., *Fusobacterium necrophorum*, *Streptococcus* spp., *Pasteurella multocida*, and *Peptostreptococcus* spp.[12-15]

Histologic findings of OdAdV are predominately associated with vascular changes, including endothelial hypertrophy, fibrinoid vascular necrosis, leukocytoclastic vasculitis, and thrombosis, with resulting mucosal ulcerations, tissue infarctions, and extensive edema.[10,11] All types of vessels can be affected and endothelial cell inclusions can be seen in any tissue, with or without significant vascular changes.[12,13] Animals with infection localized to the upper alimentary tract, especially in more chronic infections, can lack endothelial intranuclear inclusions and viral detection methods may be ineffective.[1,11,13] Diagnosis of adenovirus infection in cervids can be

accomplished by histopathology with characteristic endothelial intranuclear inclusions,[11] immunohistochemistry of infected tissue,[12] enzyme-linked immunosorbent assay (ELISA),[6] serum neutralization,[13] virus isolation,[11] immunofluorescence,[11] and PCR (unpublished data).

Differential diagnoses for rumen ulceration include bluetongue (BT) and epizootic hemorrhagic disease of deer (EHD), which are both associated with widespread hemorrhage, edema, necrotizing vasculitis, thrombosis, and ulceration of the alimentary tract.[10] Unlike acute adenovirus infection, inclusions are not detected in tissues with either of these diseases, and additional diagnostic testing may be necessary for definitive diagnosis.[10] In this case, BT and EHD were considered unlikely based on the time of year, since the insect vector (*Culicoides*) is inactive during the winter in Colorado. However, in the warmer season and with chronic cases of OdAdV where inclusions may not be present, all three hemorrhagic diseases (BT, EHD, and AHD) should be considered. Additional differentials for rumen ulceration include mycotic rumenitis and rumen acidosis with Fusobacterium necrophorum infection (necrobacillosis).

In this case, the cause of death was likely multifactorial: malnutrition (emaciation), *Pasteurella multocida* infection, and OdAdV infection. Pasteurellosis is a known cause of mortality in elk calves and can result in rapid septicemia and death.[3] For this animal, it was unclear if the pulmonary vasculitis and necrotizing myocarditis were related to *P. multocida* infection and bacterial sepsis, OdAdV, or both. Unfortunately, the definitive role of adenovirus as a primary pathogen in elk and/or a predisposition for other infectious organisms requires further investigation.

JPC Diagnosis: Rumen: Vasculitis, fibrinonecrotic, multifocal to coalescing, subacute, severe with fibrin thrombi, infarction, ulcerative rumenitis, and endothelial intranuclear viral inclusion bodies, Rocky Mountain elk, *Cervus elaphus nelsoni*.

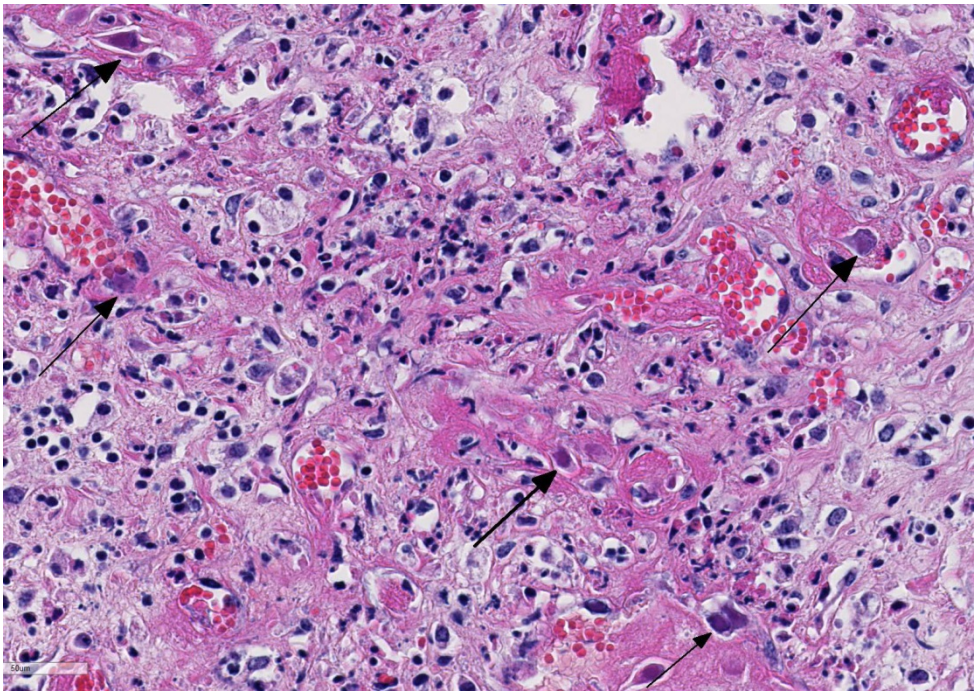

Esophogeoruminal junction:, elk calf: Endothelium lining necrotic and thrombosed vessels occasionally are swollen by large karyomegalic adenoviral inclusions. (HE, 400X)

Conference Comment: We thank the contributor for providing an outstanding example and superb overview of *Odocoileus*

adenovirus (OdAdV) causing adenovirus hemorrhagic disease (AHD) in the rumen of a Rocky Mountain elk. Participants readily identified necrotizing arteritis within the rumen wall with throm-bosis and large geographical areas of infarcted tissue. These infarcted areas correspond to the large ulcerated areas in the rumen seen grossly in the image provided by the contributor. This case nicely demonstrates frequent large basophilic intranuclear inclusion bodies within reactive and hypertrophic endothelial cells, characteristic for endotheliotropic adeno-virus infection.[2,10]

Conference participants discussed the top two differentials for necrotizing vasculitis causing severe hemorrhagic disease in elk and white-tailed deer. Bluetongue virus (BTV) and epizootic hemorrhagic disease virus (EHD) of the genus *Orbivirus* and family *Reoviridae*, mentioned by the contributor, are the top two differentials that must be considered in cases of widespread hemorrhage, necrotizing vasculitis, edema, thrombosis, and ulceration of the alimentary tract.[1,2,4,10,11-15] EHD and BTV are both spread by the salivary secretions of the biting *Culicoides* spp. vector. In North America, EHD is the mist significant viral disease in the highly susceptible white-tailed deer, and devastating epizootics have been reported in the United States. Elk are generally less severely affected by BTV and EHD infection. Both BTV and EHD circulate throughout North America and outbreaks often occur simultaneously.[10,11-15] Interestingly, both viruses can be concurrently isolated from the same individual *Culicoides* vector. Conference participants also noted that malignant catarrhal fever caused by ovine herpesvirus-2, a highly pathogenic gammaherpesvirus, can also produce intestinal hemorrhage, pulmonary congestion, edema, and petechiae of the spleen, intestines, heart, and liver with lymphocytic necrotizing vasculitis, and thrombosis in cervids and should also be considered as a potential differential in similar cases.[7]

The conference moderator mentioned that orbivirus infection will not produce the characteristic intranuclear viral inclusion bodies of adenovirus. To further differentiate these two diseases, orbiviral disease outbreaks are usually associated with acute onset of fulminant disease with high morbidity and mortality and viral tropism for the microvasculature endothelial cells. OdAdV typically results in a more chronic onset with targeting of the larger vessels and resulting in larger areas of coagulative necrosis.[1,2,4,5,10-15] Additionally, petechial and/or ecchymotic hemorrhages present at the base of the pulmonary artery has been reported to be highly characteristic and potentially pathognomonic for orbivirus infection in susceptible species. As mentioned by the contributor, diagnosis of adenovirus infection is done by a combination of testing modalities, including visualization of the characteristic endothelial intranuclear inclusions with histopathology, immunohistochemistry (IHC), virus isolation, and polymerase chain reaction (PCR).[11]

Contributing Institution:
Colorado State University
Microbiology, Immunology, and Pathology Department
College of Veterinary Medicine and Biomedical Sciences
http://csu-cvmbs.colostate.edu/academics/mip/Pages/default.aspx

References:

1. Boyce WM, Woods LW, Keel MK, MacLachlan NJ, Porter CO, Lehmkuhl HD. An Epizootic of

Adenovirus-Induced Hemorrhagic Disease in Captive Black-Tailed Deer (Odocoileus hemionus). *J Zoo Wildl Med*. 2000; 31:370-373.
2. Fox KA, Atwater L, Hoon-Hanks L, Miller M. A mortality event in elk (Cervus elaphus nelsoni) calves associated with malnutrition, pasteurellosis, and deer adenovirus in Colorado, USA. J Wildl Dis. 2017; 53(3): DOI: 10.7589/2016-07-167. [Epub ahead of print].
3. Franson, JC, Smith BL. Septicemic pasteurellosis in elk (*Cervus elaphus*) on the United States National Elk Refuge, Wyoming. *J Wildl Dis*. 1988;24:715–717.
4. Gelberg HB. Alimentary system and the peritoneum, omentum, mesentery, and peritoneal cavity. In: McGavin JF, Zachary MD, eds. *Pathologic Basis of Veterinary Disease*. 6th ed. St. Louis, MO: Elsevier Mosby; 2017:325-375.
5. Lapointe, JM, Hedges JF, Woods LW, Reubel GH, MacLachlan NJ. The adenovirus that causes hemorrhagic disease of black-tailed deer is closely related to bovine adenovirus-3. *Arch Virol.* 1999;144:393-396.
6. Lapointe, JM, Woods LW, Lehmkuhl HD, et al. Serologic detection of adenoviral hemorrhagic disease in black-tailed deer in California. *J Wildl Dis.* 2000;36:374-377
7. Palmer MV, Thacker TC, et al. Active and latent ovine herpesvirus-2 (OvHV-2) infection in a herd of captive white-tailed deer (Odocoileus virginianus). *J Comp Path*. 2013; 149:162-166.
8. Shilton CM, Smith DA, Woods LW, Crawshaw GJ, Lehmkuhl HD. Adenoviral infection in captive moose (Alces alces) in Canada. *J Zoo Wildl Med*. 2002;33:73-79.
9. Sorden SD, Woods LW, Lehmkuhl HD. Fatal pulmonary edema in white-tailed deer (*Odocoileus virginianus*) associated with adenovirus infection. *J Vet Diagn Invest*. 2000;12:378–380.
10. Uzal FA, Plattner BL, Hostetter JM. In: Maxie MG, ed. *Jubb, Kennedy, and Palmer's Pathology of Domestic Animals*. Vol 2. 6th ed. Philadelphia, PA: Elsevier; 2016:131-140.
11. Woods, LW, Swift PK, Barr BC, et al. Systemic adenovirus infection associated with high mortality in mule deer (Odocoileus hemionus) in California. *Vet Pathol*. 1996;33:125-132.
12. Woods, LW, Hanley RS, Chiu PH et al. Experimental adenovirus hemorrhagic disease in yearling black-tailed deer. *J Wildl Dis.* 1997;33:801-811.
13. Woods, LW, Hanley RS, Chiu PH, et al. Lesions and transmission of experimental adenovirus hemorrhagic disease in black-tailed deer fawns. *Vet Pathol.* 1999;36:100-110.
14. Woods LW, Lehmkuhl HD, Swift PK, et al. Experimental adenovirus hemorrhagic disease in White-tailed deer fawns. *J Wildl Dis.* 2001;37:153–158.
15. Woods LW, Lehmkuhl HD, Hobbs LA, Parker JC, Manzer M. Evaluation of the pathogenic potential of cervid adenovirus in calves. *J Vet Diagn Invest*. 2008;20:33–37.

CASE III: X-25548-15 (JPC 4085402).

Signalment: Two-year-old, hermaphrodite, veiled chameleon, (*Chamaeleo calyptratus*).

History: Initially the chameleon exhibited open mouth breathing and declining appetite, eventually requiring forced feeding. The patient returned to the clinic 4 weeks later with severe dehydration and obvious weight loss. The chameleon was euthanized at that time.

Gross Pathology: The chameleon was in good nutritional condition with normal muscle mass and moderate coelomic adipose stores. A small amount of clear red-tinged fluid was present in the coelom. Diffuse red discoloration was evident in the expanded lungs and the liver was mottled tan and red with slight rounding of the margins. Ovotestes were present bilaterally. Mucoid content was evident in the lumen of the stomach and the colon; the intestinal content was otherwise scant.

Laboratory results: Sections of lung were submitted for bacterial culture. Primary culture on a sheep blood agar plate after 48 hour aerobic incubation at 37^{o}C resulted in heavy growth of tiny smooth cream-colored colonies. Gram's stain revealed pleomorphic gram-positive bacilli. The bacteria were acid-fast with the Ziehl-Neelsen stain. The isolate was sent to the National Reference Centre for Mycobacteriology (Public Health Agency of Canada). Based on *16s* and *hsp65* gene sequencing, the isolate had 100% sequence identity to *Mycobacterium chelonae* chemovar *niacinogenes.*

Histopathologic Description: Lung: The faveolar septa are expanded with moderate to marked congestion of the vasculature and myriad slender bacilli are present within the lumina of blood vessels; bacteria are both free within the lumina and present within the cytoplasm of macrophages. Hemorrhage, intravascular fibrin thrombi and necrotic cellular debris often accompany the bacterial colonies and scattered small aggregates of epithelioid macrophages are present multifocally in the septa. In areas, there is necrosis of the faveolar epithelium and erythrocytes, proteinaceous fluid and cellular debris are noted with the faveolar spaces.

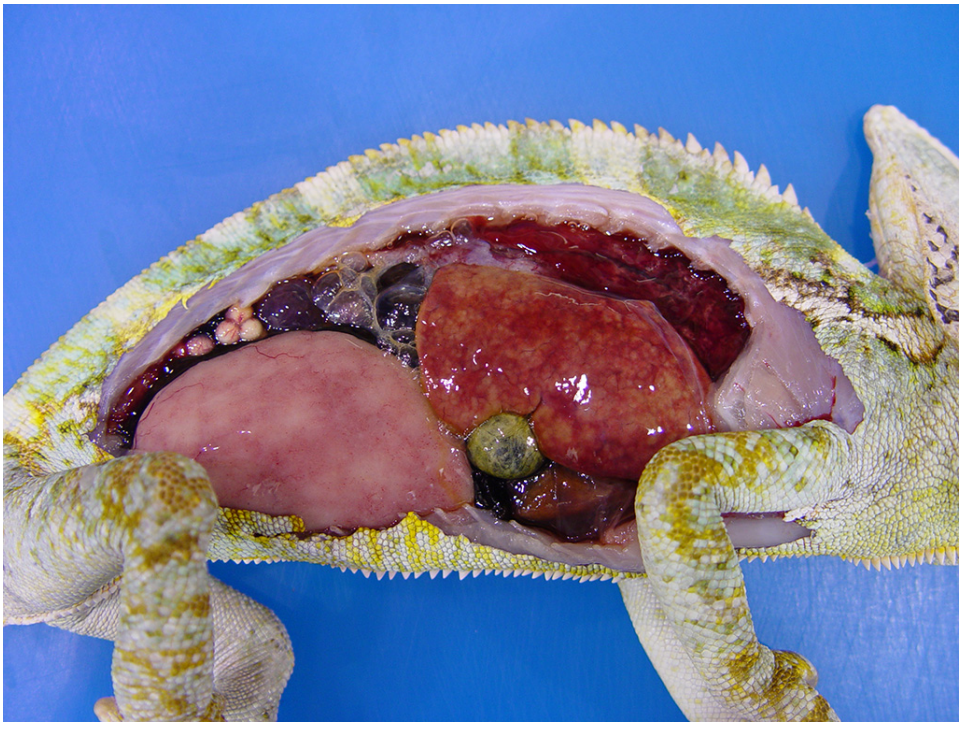

Lung, chameleon. The lungs are expanded and diffusely red. The liver is enlarged and a mottled tan-red. (Photo courtesy of: Dept of Path/Micro, Atlantic Veterinary College, UPEI, 550 University Avenue, Charlottetown, Prince Edward Island, C1A 4P3. http://www.upei.ca/avc/pathology-and-microbiology)

The bacteria are acid-fast with the Ziehl-Neelsen stain.

Similar intravascular bacteria and occasional small aggregates of macrophages containing bacteria are present in most organs (liver, pancreas, kidney, brain, spleen, skeletal muscle, adrenal glands, small intestine and ovotestes).

Contributor's Morphologic Diagnosis: Lung: Necrotizing and histiocytic interstitial pneumonia, diffuse, subacute, with myriad intravascular/intrahistiocytic acid-fast bacilli and intravascular fibrin thrombi

Contributor's Comment: Mycobacteria are ubiquitous in nature and can be isolated from the soil, dust, water and bioaerosols.[1] Reptiles are generally thought to acquire mycobacterial infections via ingestion or through defects / penetrating injury in the skin.[11] In this chameleon, there was a localized area of intestinal ulceration and granulomatous enteritis, suggesting that infection may have been acquired through the intestinal tract.

In reptiles, like most species, mycobacterial infections tend to be chronic with rare acute infections reported.[5] The typical gross lesions are grey-white nodules in multiple organs. Microscopically, early lesions are composed of organized collections of foamy macrophages that with time may become chronic granulomas composed of a mixture of epithelioid macrophages, lymphocytes, plasma cells, and multinucleated giant cells often surrounding a central region of necrosis and occasionally with a surrounding wall of fibrous connective tissue.[11] In this case, there were a few small early granulomas in multiple organs including the brain, lung, liver, kidneys and intestine. More striking, however, was the presence of myriad intravascular bacteria in

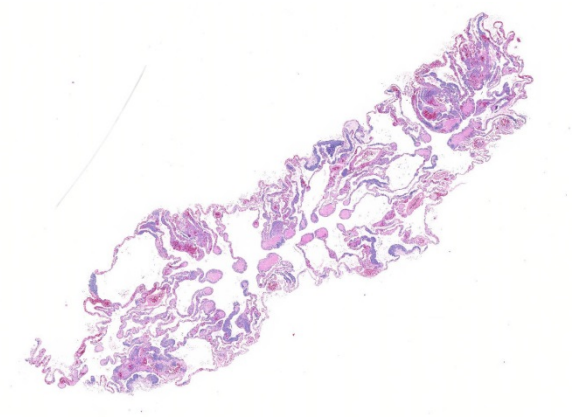

Lung, chameleon. Aggregates of gray macrophages multifocally distend the faveolar septa. (HE, 6X)

multiple organs and frequent intravascular fibrin thrombi. These changes are compatible with acute to subacute infection with acute bacteremia and disseminated intravascular coagulation.

Mycobacteria are broadly divided into two groups: *Mycobacterium tuberculosis* complex and non-tuberculous myco-bacteria.[2] While only non-tuberculous mycobacteria have been reported to cause infections in reptiles, several different species have been associated with these infections. These include *M. confluentis, M. chelonae, M. haemophilum, M. hiberniae, M. neoarum, M. confluentis, M. nonchromogenicum, M. marinum, and M. thamnopheos*.[2,5,11] The most common causes of mycobacteriosis in reptiles are reported to be *M. marinum, M. chelonae* and *M. thamnopheos*.[5] The isolate in this case was confirmed to be *M. chelonae* chemovar *niacinogenes.*

Non-tuberculous mycobacteria are classified into four Runyon groups according to growth rate and pigmentation.[5] Runyon group I mycobacteria are slow growing and form pigment in the light following growth in the dark. Runyon group II organisms are also slow growing bacteria; these bacteria

form pigment in the dark following growth in the light. Runyon group III bacteria are slow growing and do not form pigment in the dark or light. Fast growing non-pigmented mycobacteria are placed in Runyon group IV. These mycobacteria form mature colonies on solid agar within 7 days, while bacteria in Runyon groups I to III take longer periods of time for cultivation.[2] Most mycobacteria which infect reptiles fall into Runyon groups I and IV.[5] *Mycobacterium chelonae* is a rapidly growing mycobacteria belonging to Runyon group IV.[4] Rapidly growing mycobacteria are relatively resistant to standard disinfectants and antibiotic treatment and are increasingly recognized as opportunistic pathogens in humans.[1,2]

in a loggerhead sea turtle[8] and a veiled chameleon.[9] There is a single report of this bacterium causing acute fatal sepsis and disseminated intravascular coagulation in an eastern spiny softshell turtle[8] with lesions very similar to those described in this case. Because of poor response to treatment and the zoonotic potential, euthanasia is often recommended for reptiles with myco-bacterial infections.

JPC Diagnosis: Lung: Pneumonia, histiocytic and necrotizing, multifocal to coalescing, moderate, with numerous intrahistiocytic and intravascular bacilli, veiled chameleon, *Chamaeleo calyptratus*.

Conference Comment: The contributor provides an outstanding review of non-

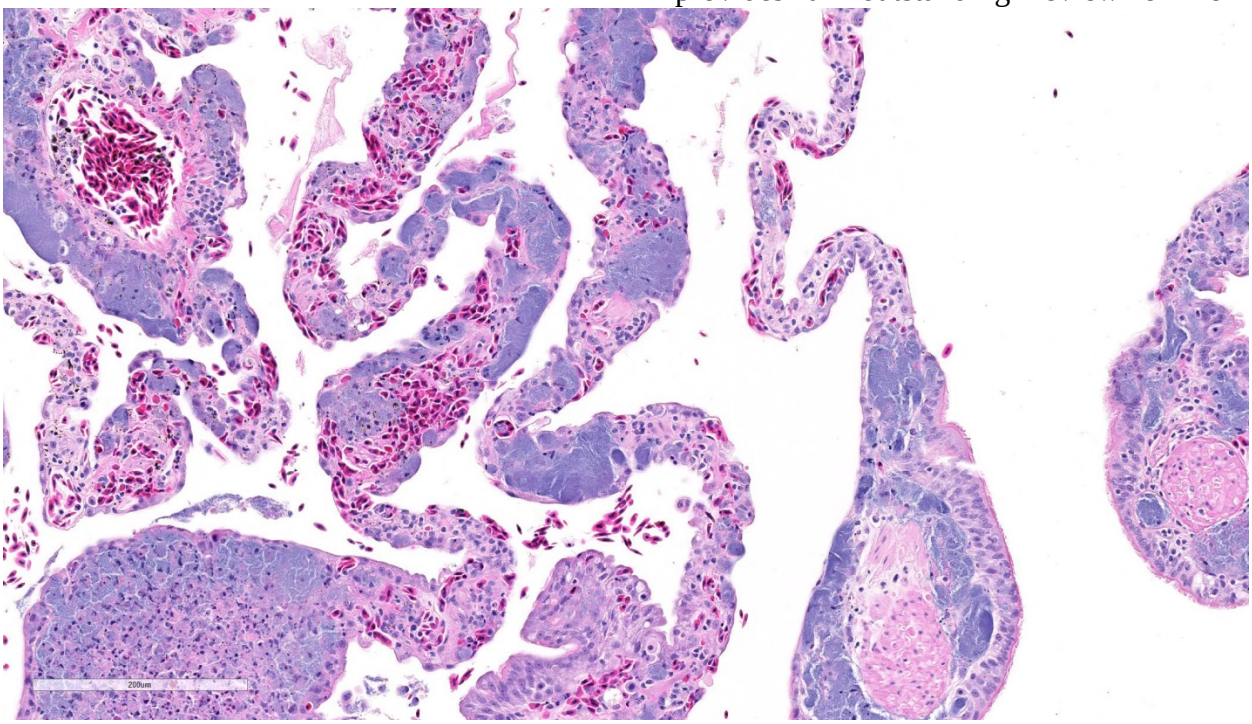

Lung, chameleon. Higher magnification of the faveolar septa. Intracytoplasmic bacilli appear filamentous within macrophage cytoplasm. (HE, 164X)

In reptiles, *M. chelonei* has been reported in association with osteoarthritis in a Kemp's Ridley sea turtle,[4] with stomatitis and subcutaneous granulomas in a boa constrictor,[6] and with disseminated infection

tuberculous *Mycobacteria* in reptiles. *Mycobacteria* spp. are a large genus comprised of over 100 species of obligate pathogenic, potentially pathogenic, and environmental saprophytic bacteria.[6] They

are all morphologically similar and are composed of aerobic, gram-positive, acid-fast, non-spore forming bacilli.[6] Conference participants were impressed by the large numbers of intrahistiocytic and intravascular thin filamentous bacilli that stain slightly basophilic on hematoxylin and eosin stained tissue section. These bacilli are intensely acid-fast positive with Fite-Faraco and Ziehl-Neelsen acid-fast stains, run by the Joint Pathology Center prior to the conference. *Mycobacterium chelonae* infection, confirmed by the contributor as the cause of rapid disseminated disease in this animal, is an opportunistic and potentially zoonotic pathogen that is characterized by rapid growth and high resistance to antibiotics.[1,2]

As mentioned by the contributor, spontaneous non-tuberculous *Mycobacteria* sp., including *M. avium*, *M. chelonae*, *M. szulagai*, *M. fortuitum*, *M. marinum*, *M. hemophilum*, *M. kansasii*, and *M. ulcerans* have been reported to be the classic etiologic agents that cause histiocytic granulomas snakes, turtles, lizards, and crocodiles and should top the list of differential diagnoses for lesions similar to this case.[2,5,10,11] The obligate intracellular bacteria, *Chlamydophila pneumoniae*, can also occasionally infect reptilian species and induce histiocytic granulomas and should be considered as a differential diagnosis. Additionally, relatively recently described "Chlamydia-like" bacteria *Parachlamydia acanthamoebae* and *Simikania negevensis*, have been sporadically reported to form histiocytic granulomas in reptiles as well.[11]

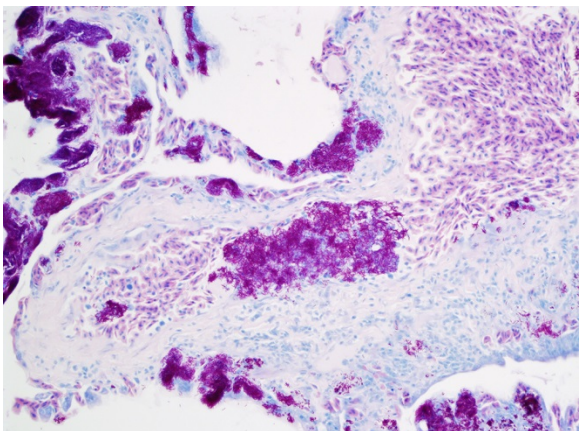

Lung, chameleon: Macrophages contain numerous intracytoplasmic acid-fast bacilli. (Ziehl-Nielson, 400X)

While histiocytic granulomas in reptiles are often induced by intracellular bacteria, such as in this case, heterophilic granulomas in reptiles are caused by extracellular pathogens, including most bacterial and fungal etiologies. Tissue injury can also induce heterophilic granulomas in reptiles.[5] Heterophilic granulomas are characterized by accumulation and degranulation of heterophils leading to a central area of necrosis, stimulating a strong macrophage foreign body-like response. Caseocalcareous nodules, lymphoid infiltration, and peripheral fibrosis, typical of mammalian granulomas, have not been observed in reptilian heterophilic granulomas.[5] Both histiocytic granulomas and heterophilic granulomas can progress to chronic granulomas, characterized by a fibrous connective tissue capsule, lymphocytes and plasma cell infiltration, and a central area of necrosis with a prominent lamellated appearance.[5]

Contributing Institution:

Dept of Path/Micro
Atlantic Veterinary College, UPEI
Charlottetown, Prince Edward Island
http://www.upei.ca/avc/pathology-and-microbiology

References:

1. De Groote MA, Huitt G. Infections due to rapidly growing *Mycobacteria*. *Clin Infect Dis.* 2006; 42:1756–63.

2. Ebani, VV, Fratini F, Bertelloni F, et al. Isolation and identification of *Mycobacteria* from captive reptiles. *Res Vet Sci*. 2012; 93:1136–1138.
3. Fremont-Rahl JJ, Ek C, et al. *Mycobacterium liflandii* outbreak in a research colony of Xenopus (Silurana) tropicalis frogs. *Vet Pathol*. 2011; 48(8):856-867.
4. Greer LL, Strandberg JD, Whitaker BR. *Mycobacterium chelonae* osteoarthritis in a Kemp's Ridley Sea Turtle (*Lepidochelys kempii*). *J Wildl Dis.* 2003; 39(3):736-741.
5. Jacobson, ER. Bacterial diseases of reptiles. In: Jacobson ER, ed. *Infectious Diseases and Pathology of Reptiles: Color Atlas and Text*. Boca Raton, Florida: CRC Press; 2007: 461–526.
6. Mauldin E, Peters-Kennedy J. Integumentary system. In: Maxie MG, ed. *Jubb, Kennedy, and Palmer's Pathology of Domestic Animals*. Vol 1. 6th ed. Philadelphia, PA:Elsevier; 2016:639-641.
7. Mitchell MA. Mycobacterial infections in reptiles. *Vet Clin Exot Anim.* 2012; 15(1):101–11.
8. Murray M, Waliszewski NT, Garner MM, et al. Sepsis and disseminated intravascular coagulation in an eastern spiny softshell turtle (*Apalone spinifera spinifera*) with acute mycobacteriosis. *J Zoo Wildl Med*. 2009; 40(3):572-575.
9. Nardini G, Florio D, DiGirolamo N, et al. Disseminated mycobacteriosis in a stranded Loggerhead Sea Turtle (*Caretta caretta*). *J Zoo Wildl Med.* 2014; 45(2): 357–360.
10. Reavill DR, Schmidt RE. Mycobacterial lesions in fish, amphibians, reptiles, rodents, lagomorphs, and ferrets with reference to animal models. *Vet Clin Exot Anim.* 2012; 15(1): 25–40.
11. Soldati G, Lu ZH, Vaughan L, et al. Detection of *Mycobacteria* and *Chlamydiae* in granulomatous inflammation of reptiles: A retrospective study. *Vet Pathol*. 2004; 41(4):388–397.

CASE IV: G13060-A786 (JPC 4085315).

Signalment: 25-year-old male California sea lion, (*Zalophus californianus*).

History: This sea lion was born in captivity in a zoo, where it stayed its entire life. Two weeks prior to euthanasia the animal lost 40kg of weight, suffered from ascites and a heart murmur was heard.

Gross Pathology: On post-mortem examination a yellow-white firm nodule was found near the trigone of the bladder, measuring 2 by 3 centimeters and 1 cm in thickness. Similar nodules were found extensively in the liver parenchyma and multifocally in the lung. The lung also

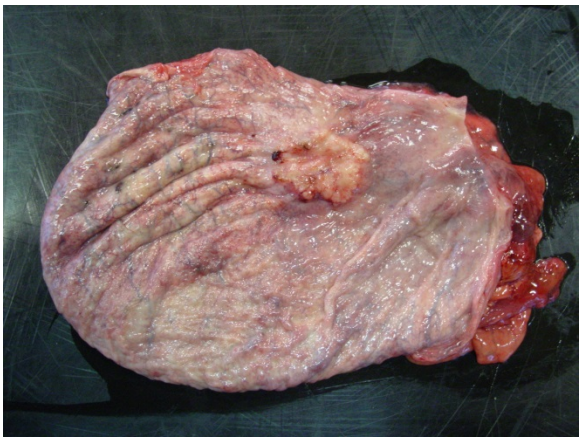

Sea lion, bladder. The bladder wall contains a single yellow-white 2x3cm nodule which is 1cm in thickness. (Photo courtesy of: Dept of Pathology, Bacteriology and Poultry diseases, Faculty of Veterinary Medicine – Ghent University, Salisburylaan 133, 9820 Merelbeke – Belgium, http://www.ugent.be/di/en/departments?ugentid=DI05).

contained large fibrotic interlobular septa. Several lymph nodes were severely enlarged, such as the mesenteric, pulmonary lymph nodes, and one lymph node close to the adrenal gland. The intestines were attached to one another and a large deposition of fibrin together with a large volume (700 ml) of serohemorrhagic fluid (fibrinoid exudative peritonitis).

Laboratory values:

Laboratory results:		Current Californian Sea Lion Reference[2]
IONS		
Sodium	148 meq/L	149-156 meq/L
Potassium	5.08 meq/L	3.7-5.0 meq/L
Phosphate	4.7 mg/dL	1.8-7.8 meq/L
KIDNEY		
Serum urea nitrogen (BUN)	109 mg/dL	14-38 mg/dL
Creatinine	1.47 mg/dL	1.1-2.6 mg/dL
LIVER- BILE DUCTS		
Bile acids	7 µmol/L	
AST (GOT)	41 U/L	12-66 U/L
ALT (GPT)	42 U/L	19-71 U/L
Gamma-GT	143 U/L	22-123 U/L
SERUM PROTEINS		
Total protein	7.2 g/dL	6.1-8.5 g/dL

Histopathologic Description: Urinary bladder: Originating from the bladder epithelium and infiltrating in the lamina propria and the muscular layer (*m. detrusor vesicae*), a well-demarcated, densely cellular, multilobular neoplasm is present. In between these lobules lays a dense cellular fibrovascular stroma with large infiltrates of lymphocytes. On some places in the epithelium, multiple groups of disorganized layers of dysplastic cells are visible, which do not breach the basal membrane (carcinoma *in situ*). The neoplastic cells are organized in closely packed smaller lobules and larger nests. The cells have a polygonal appearance, range from 20-40 µm in diameter, contain a moderate amount of light basophilic granular to foamy cytoplasm and have a round to oval, central nucleus with clumped chromatin along the nuclear envelope and 1-2 basophilic nucleoli. Only a few cells have large cytoplasmic vacuoles which pushes the nucleus to the cell periphery which gives the appearance of so-called 'signet cells'. Some cells are multinucleated and there is marked anisokaryosis, anisocytosis, as well as an augmented ratio of nucleus:cytoplasm. Two to five, sometimes bizarre, mitotic figures per HPF are seen. In many lobules of neoplastic cells, central necrosis is present, along with a moderate number of inflammatory cells. Within widened lymphatic vessels and blood vessels, large clumps of neoplastic cells are present showing central necrosis (tumor emboli). Using immunohistochemistry, these neoplastic cells stained positive for low molecular weight cytokeratin and uroplakin and negative for high molecular weight cytokeratin. A PAS-stain on the vacuoles within the 'signet cells' was negative.

Sea lion, bladder. Higher magnification of the neoplasm in the bladder trigone. (Photo courtesy of: Dept of Pathology, Bacteriology and Poultry diseases, Faculty of Veterinary Medicine – Ghent University, Salisburylaan 133, 9820 Merelbeke – Belgium, http://www.ugent.be/di/en/departments?ugentid=DI05)

Various metastases of this neoplasm were found in lymph nodes, liver, lung, adrenal gland, and eye. These metastases stained positive for uroplakin.

Contributor's Morphologic Diagnosis: Nonpapillary and infiltrating transitional cell carcinoma with multiple metastases to various lymph nodes, liver, lung, adrenal gland, and eye.

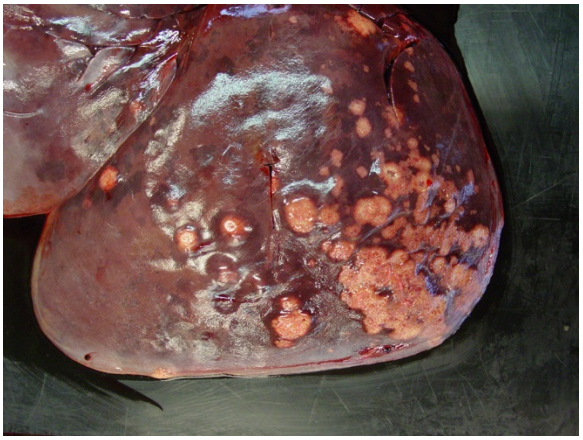

Sea lion, bladder. Foci of metastasis were present within the haptic parenchyma. (Photo courtesy of: Dept of Pathology, Bacteriology and Poultry diseases, Faculty of Veterinary Medicine – Ghent University, Salisburylaan 133, 9820 Merelbeke – Belgium, http://www.ugent.be/di/en/departments?ugentid=DI05)

Contributor's Comment: Transitional cell carcinoma (TCC) is the most common tumor of the urinary tract in domestic animals.[9] It is also a common neoplastic lesion in the urogenital tract of the Californian sea lion *(Zalophus Californianus).* In the Californian sea lion, it is a common cause of mortality.[5]

Most TCCs are found in the trigone of the bladder[8] and have a papillary, polypoid, or sessile morphology.[9] Various patterns of TCCs have been described, with the papillary and infiltrating TCC as the most common type and the nonpapillary, infiltrating type as the second most common.[9] Some TCCs may originate in the ureter or urethra and might be more difficult to diagnose.[5]

Histologically, nonpapillary infiltrating TCCs show a thickened bladder wall[9] due to neoplastic growth of the urinary epithelium. Neoplastic cells are organized in small nests and form a multilobular pattern.[5] Cyst-like structures may be visible, containing necrotic or keratinized debris may be seen.[5] Neoplastic cells may show cystic degeneration and contain large cytoplasmic vacuoles, pushing the nucleus to the periphery creating a characteristic 'signet ring morphology. The large polygonal to round cells have distinct cell borders[10], pale eosinophilic to amphophilic cytoplasm[5] and contain enlarged pleomorphic to polygonal and vesicular nuclei, with prominent nucleoli[9] and clumped to reticular chromatin.[3] Syncytial cells, atypical nuclei, mitotic figures are abundant.[9] There might be variable desmoplasia and various amount of lymphoid inflammation. Vascular and lymphatic vessel invasion is often seen.[9]

The cause of TCC remains undetermined[6], but is likely multifactorial.[3] Environmental contaminants, such as polycyclic aromatic hydrocarbons like benzopyrine have been suggested to play a role.[5] Lipscomb et al. found intranuclear inclusion bodies in genital carcinoma and isolated a herpes virus (rhadinovirus) and an Epstein-Barr virus using PCR.[6,7] Polychlorinated biphenyls could also contribute to the occurrence this neoplasm.[10]

TCCs metastasize in about 50% of the cases in domestic animals; first affecting regional lymph nodes before spreading to other organs.[9] Metastases of TCC in Californian sea lions is also common, as in the current case[3]. The nonpapillary infiltrating type is the most likely to metastasize.[9] Bilateral hydronephrosis due to obstruction by the

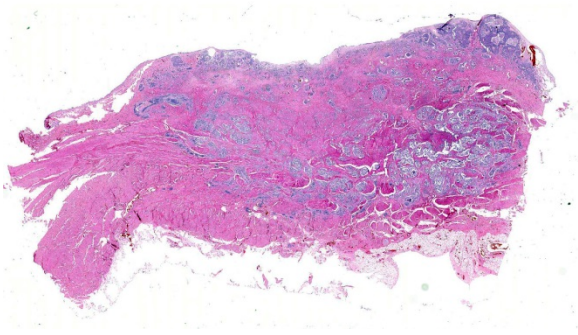

Sea lion, bladder. Nests of neoplastic cells extend downward from the ulcerated bladder mucosa through the full thickness of the urinary bladder. (HE, 5X)

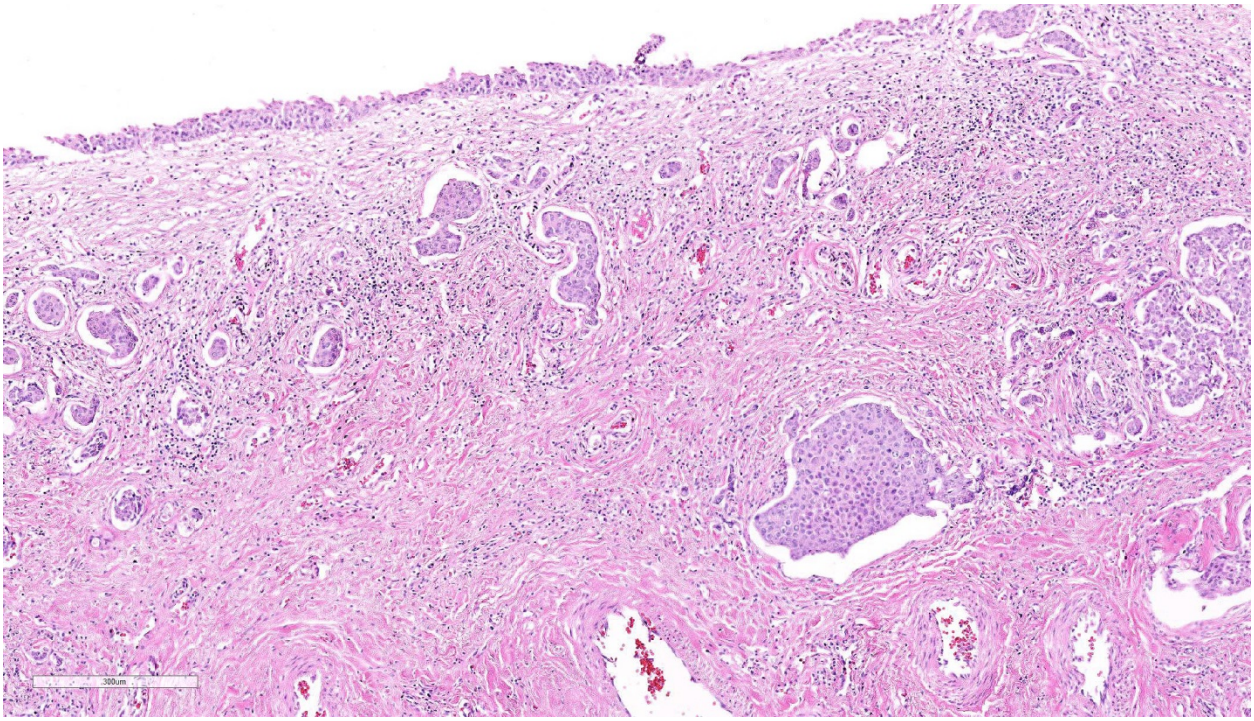

Nests of neoplastic cells are present within the submucosa. There is mild lymphocytic inflammation separating infiltrative nests. (HE, 140X)

neoplasm in either ureter or urethra is a possible associated lesion.[9]

JPC Diagnosis: Urinary bladder: Carcinoma, metastatic, California sea lion, *Zalophus californianus*.

Conference Comment: This case generated spirited discussion among conference participants regarding the tissue of origin of the numerous small islands and nests of neoplastic cells in the muscular layers of this section of urinary bladder. Most participants agreed with the contributor and favored the diagnosis of urothelial carcinoma (also known as transitional cell carcinoma); however, others preferred the diagnosis of metastatic carcinoma not otherwise specified, because the neoplastic cells generally do not associate with the overlying transitional epithelium, rather forming distinctive intra-epithelial neoplasms (IEN) and distinct islands within the muscular layers of the urinary bladder. IEN has been previously associated with genital carcinoma of California sea lions (CSL) described in similar lesions in the lower urinary tract (vagina, cervix, uterus, prepuce, penis, and urethra).[3,6,7] Interestingly, lesions of the urinary bladder had not been described in previous cases of genital carcinomas in CSL.[6,7] Unfortunately, in this case, most of the hematoxylin and eosin (HE) stained tissue sections provided to participants contained little to no overlying epithelium,

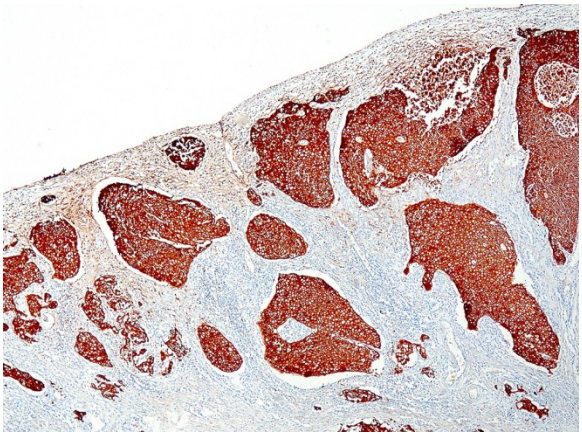

Sea lion, bladder. Neoplastic cells exhibit strong intracytoplasmic staining for cytokeratin. (anti-CK, 100X) (Photo courtesy of: Dept of Pathology, Bacteriology and Poultry diseases, Faculty of Veterinary Medicine – Ghent University, Salisburylaan 133, 9820 Merelbeke – Belgium, http://www.ugent.be/di/en/departments?ugentid=DI05)

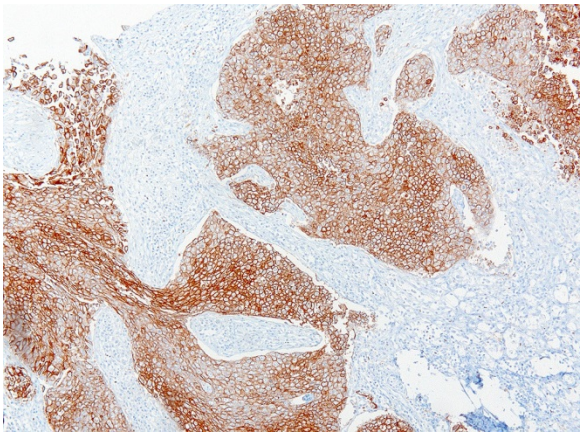

Sea lion, bladder. Neoplastic cells exhibit strong intracytoplasmic staining for uroplakin. (anti-uroplakin, 200X) (Photo courtesy of: Dept of Pathology, Bacteriology and Poultry diseases, Faculty of Veterinary Medicine – Ghent University, Salisburylaan 133, 9820 Merelbeke – Belgium, http://www.ugent.be/di/en/departments?ugentid=DI05)

so it was difficult to accurately assess the origin of the neoplasm. We thank the contributor for proving excellent quality images of strong and highly specific membranous immunoreactivity of the neoplastic cells for uroplakin-III in both the urinary bladder and eye metastasis.[11] Prior to the conference, the Joint Pathology Center also ran uroplakin-III and pancytokeratin and confirmed strong immunoreactivity of the neoplastic cells for both stains.

The mammalian urothelium is composed of 6–10 layers of cells that includes superficial, intermediate, and basal layers.[2,12] The superficial layer, commonly known as the umbrella cell layer, contains a specialized plasma membrane that forms rigid plaques covering the apical surface of the urothelium. Uroplakin is one of the major protein components of the umbrella cells in the superficial layer and is highly conserved through most, if not all, mammalian species. The immunohistochemical stain, uroplakin-III, is marker for urothelial cells of the renal pelvis, ureter, bladder and urethra and has been used to detect transitional cell neoplasms in humans, dogs, cattle, and laboratory rodents. Loss of uroplakin-III expression in bladder cancers has been associated with malignant, invasive and anaplastic urothelial carcinomas in humans and dogs.[2,12] Uroplakin-III is generally considered to be specific for urothelial carcinomas; however, positive immuno-reactivity for uroplakin-III has also been reported in prostatic carcinoma in humans and dogs.[2,12] Positive immunostaining for uroplakin-III provides strong evidence for urothelial origin of the neoplasm in this case; however, further study may be needed to determine the specificity of uroplakin-III in the genital and urinary tract in California sea lions.

Invasive and metastatic genital and urinary tract carcinomas are commonly diagnosed in stranded California sea lions. As mentioned by the contributor, these neoplasms have been associated with a number of predisposing causes, including otariine gamma herpesvirus[6,7] infection and exposure to polychlorinated biphenyl water

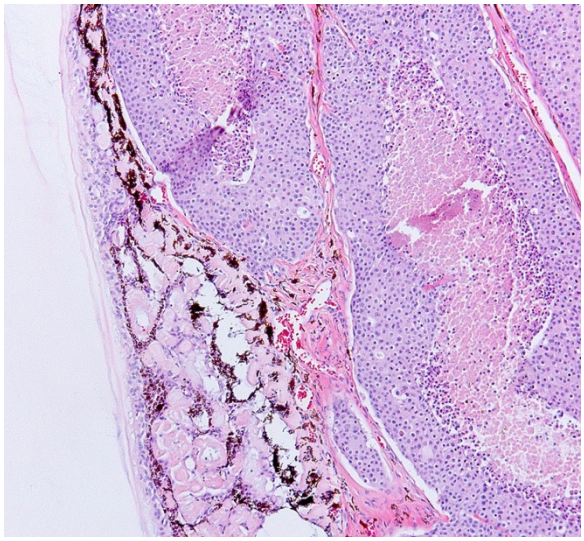

Sea lion, bladder. Metastasic cells are present within the ciiary body. (Photo courtesy of: Dept of Pathology, Bacteriology and Poultry diseases, Faculty of Veterinary Medicine – Ghent University, Salisburylaan 133, 9820 Merelbeke – Belgium, http://www.ugent.be/di/en/departments?ugentid=DI05)

pollutants.[3,10] Additionally, there is a reported association between development of urogenital carcinoma in sea lions with genetic homogenicity at the Pv11 microsatellite locus for the heparanase 2 gene (*HPSE2*).[1] Homogenicity at this site is also strongly correlated with decreased overall fitness within the stranded California sea lion population and may be secondary to inbreeding.[1] Conference participants did not note eosinophilic intranuclear inclusion bodies characteristic of herpesvirus infection in this tissue section.

Contributing Institution:

Faculty of Veterinary Medicine
Ghent University
Salisburylaan 133
9820 Merelbeke
Belgium
http://www.ugent.be/di/en/departments?ugentid=DI05

References:

1. Browning HM, Acevedo-Whitehouse K, et al. Evidence for a genetic basis of urogenital carcinoma in the wild California sea lion. *Proc Biol Sci*. 2014; 281(1796):20140240.
2. Charney VA, Miller MA, et al. Skeletal metastasis of canine urothelial carcinoma: Pathologic and computed tomographic features. *Vet Pathol*. 2016; pii:0300985816677152. [Epub ahead of print].
3. Colegrove KM, Gulland FMD, Naydan DK, et al. Tumor morphology and immuno-histochemical expression of estrogen receptor, progesterone receptor, p53, and Ki67 in urogenital carcinomas of California sea lions *(Zalophus Californianus). Vet Pathol*. 2009; 46:642-655.
4. Dierauf, L, Gulland FMD. *CRC Handbook of Marine Mammal Medicine: Health, Disease, and Rehabilitation*. CRC press; 2001.
5. Gulland, FMD, Trupkiewicz JG, Spraker TR, et al. Metastatic carcinoma of probable transitional cell origin in 66 free-living California sea lions (*Zalophus Californianus*), 1979 to 1994. *J Wildl Dis*.1996; 32:250–258.
6. Lipscomb TP, Scott DP, Schulman FY. Primary site of sea lion carcinomas. *Vet Pathol*. 2010; 47:185.
7. Lipscomb TP, Scott DP, Garber RL, et al. Common metastatic carcinoma of California sea lions (*Zalophus Californianus*): Evidence of genital origin and association with novel gammaherpesvirus. *Vet Pathol*. 2000; 37:609–17.
8. Martineau D, Lagace A, Masse R, et al. Transitional cell carcinoma of the urinary bladder in a beluga whale (*Delphinapterus Leucas*). *Can Vet J*. 1985; 26:297.
9. Meuten DJ, Everitt J, Inskeep W, et al. *Histological Classification of Tumors of the Urinary System of Domestic Animals*. 2nd ed. Vol. XI. Second Series. Washington; DC: World Health Organization and Armed Forces Institute of Pathology, 2004.
10. Newman SJ, Smith SA. Marine mammal neoplasia: A review. *Vet Pathol*. 2006; 43:865–880.
11. Van de Velde N, De Laender P, Chiers K. Transitional cell carcinoma metastasizing to different organs including the eye in a California sea lion (*Zaliophus californianus*). *J Comp Pathol*. 2017; 156(1):132.

12. Wilson CJ, Flake GP, et al. Immunohistochemical expression of cyclin D1, cytokeratin 20, and uroplakin III in proliferative urinary bladder lesions induced by o-nitroanisole in Fischer 344/N rats. *Vet Pathol*. 2016; 53(3):682-690.

Self-Assessment - WSC 2016-2017 Conference 19

1. Which of the following is not true concerning *Baylisascaris procyonis*i nfection?
    a. Neural damage is due to profound granulomatous inflammation in the brain.
    b. Adult nematodes are found only n the small intestine of the definitive host.
    c. Infection is also seen in avian species.
    d. Infective eggs can survive in the environment for years.

2. Localized infection with Odoicoleus adenovirus is seen in which organ system?
    a. Upper respiratory tract
    b. Reproductive tract
    c. Upper gastrointestinal tract
    d. Lower gastrointestinal tract

3. In which of the following cell types, will inclusions associated with Odocoileus adenovirus be found?
    a. Macrophages
    b. Fibroblasts
    c. Epithelial cells
    d. Endothelial cells

4. Which of the following is not a classical cause of histiocytic granulomas in reptiles?
    a. Mycobacterium fortuitum
    b. Mycobacterium microti
    c. Mycobacterium marinum
    d. Mycobacterium kansasii

5. The superficial layer of mammalian uroithelium contains specialized plasma membranes and is called the _____?
    a. Stratum rigidosa
    b. Umbrella layer
    c. “Roofed” urothelium
    d. Urotheial tiled layer

Joint Pathology Center

Veterinary Pathology Services

WEDNESDAY SLIDE CONFERENCE 2016-2017

C o n f e r e n c e 20

22 March 2017

Jey Koehler, DVM, PhD, Diplomate ACVP
Director, Histopathology Core Laboratory
Department of Pathobiology
Auburn University College of Veterinary Medicine

CASE I: W255-15 (JPC 4068726).

Signalment: Adult, thoroughbred gelding, (*Equus caballus*).

History: A mature, racehorse started to develop neurologic signs. When presented to the veterinarian, the horse showed severe ataxia and incoordination. The horse was also colliding with the box walls and displayed head pressing behavior. No significant changes were identified on hemogram or serum biochemistry. Blood collected for *Flavivirus* ELISA testing was negative. After unsuccessful treatment with dexamethasone and DMSO, the horse was humanely euthanized.

Gross Pathology: Gross examination of the brain on formalin-fixed cut sections revealed multifocal linear, beige discolorations within the thalamus and cerebellum (suspected areas of malacia). Within the brain stem, there was a focal loss of substance measuring. 0.8 x 0.6 x 0.6 cm.

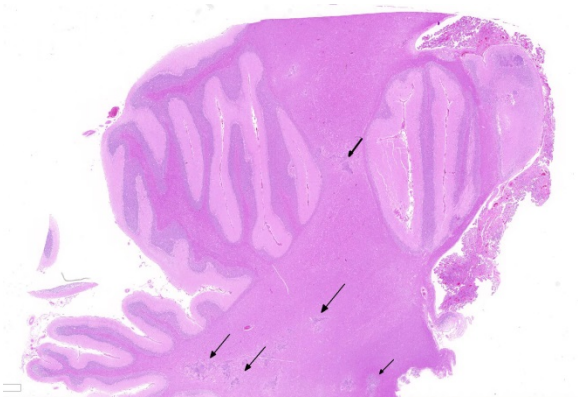

Cerebellum with choroid plexus, horse. There are multiple areas of necrosis and inflammation within the cerebellar white matters (arrows). (HE, 5X)

Laboratory results: No laboratory analysis performed.

Histopathologic Description: Expanding the cerebellar white matter and infiltrating the granular and molecular layers of the cerebellar cortex, there is a focally extensive inflammatory reaction. This inflammatory focus is composed of coalescing accumulations of numerous epithelioid macrophages and multinucleated giant cells (of Langerhans and foreign body types), centered around sections of nematodes eggs

(ca. 10-15 x 30 µm), as well as transverse and longitudinal sections of nematode larvae and adults. The larvae measured 10 x 20 to 30 µm and the adults 15-20 µm x 250-300 µm in diameter with a smooth cuticle, platymyarian-meromyarian musculature, a rhabditiform esophagus, occasionally displaying a distinct corpus, isthmus and terminal bulb, and numerous deeply basophilic 2-3 µm internal structures within the pseudocoelom. Large numbers of lymphocytes and plasma cells are also seen throughout the granulomatous reaction, surrounding vessels and infiltrating the vessel wall. Within the adjacent molecular layer there is marked vacuolation and clear tissue separation (edema), along with numerous nematode sections.

Within the cerebellar nuclei, there are multifocal, randomly distributed areas of necrosis, characterized by rarefaction of the neuropil, loss of architecture, and small amounts of eosinophilic cellular and karyorrhectic debris, admixed with several sections of nematodes and moderate numbers of gitter cells. Multifocally, perivascular infiltrates of macrophages, multinucleated giant cells, lymphocytes and plasma cells admixed with occasional nematodes expand the Virchow-Robin spaces and extend within the adjacent neuropil. Adjacent to the perivascular cuffs, there is marked vacuolation of the neuropil, dilated myelin sheaths and multiple round eosinophilic bodies (axonal spheroids). The meninges are multifocally infiltrated with low numbers of lymphocytes and macrophages.

Contributor's Morphologic Diagnosis: Brain: Granulomatous meningoencephalitis, marked, multifocal, with intralesional nematodes, horse (*Equus caballus*).

Contributor's Etiologic Diagnosis: Encephalitic nematodiasis.

Cause: Presumed *Halicephalobus gingivalis*.

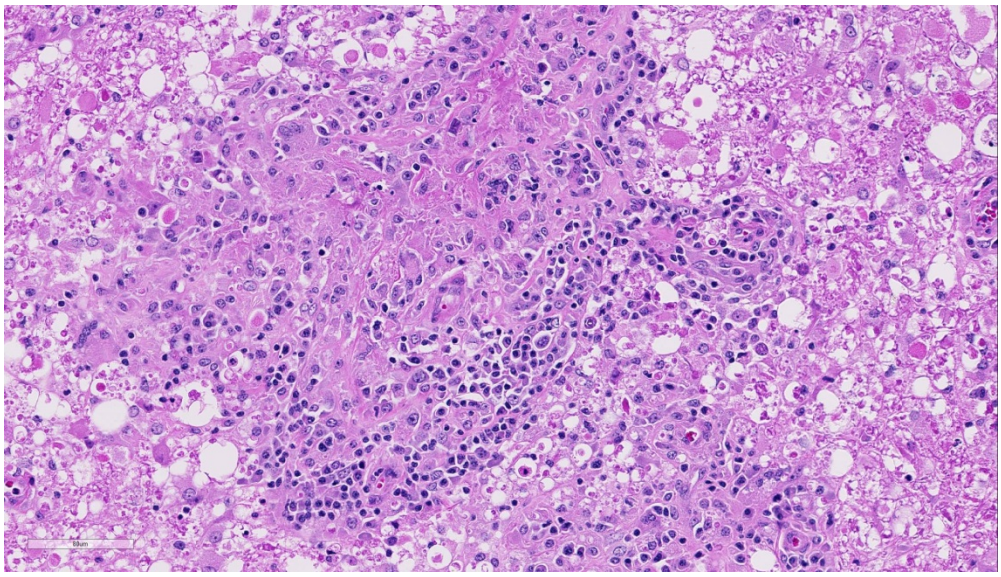

Cerebellum, horse. Foci of necrosis contain a range of inflammatory cells including numerous infiltrating macrophages, rare multinucleated giant cell macrophages, numerous lymphoyctes and plasma cells, but few if any neutrophils and eosinophilis. There is extensive edema at the periphera as well as dilated myelin sheaths and spheroids. (HE, 256X)

Contributor's Comment: Parasitic migratory encephalomyelitis is rare but represents an important cause of neurologic disease in horses and a number of parasites (protozoan and metazoan) have been described to be associated with central nervous system (CNS) disease.

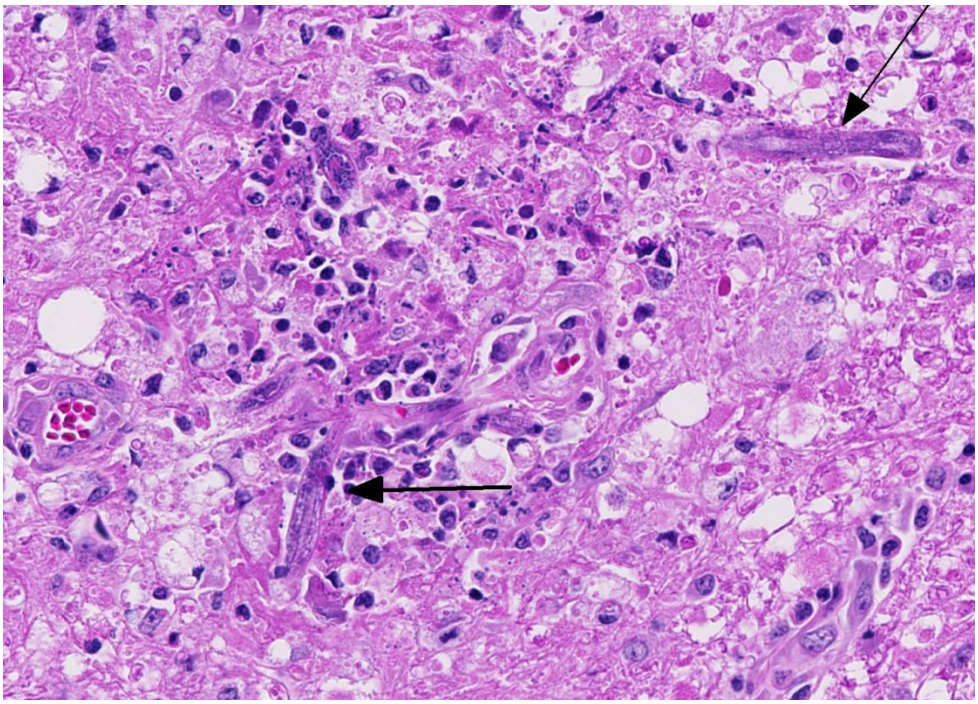

Cerebellum, horse. Several, but not all foci of necrosis contain cross sections of adult nematodes as well as abundant cellular debris, hypertrophic astrocytes, numerous spheroids, and vessels are surrounded by low to moderate numbers of lymphocytes and plasma cells. (HE, 400X)

A non-suppurative inflammation, similar to viral infections, is usually encountered in protozoal infections. Equine protozoal myeloencephalitis caused by *Sarcocystis neurona* (and much less commonly *S. hughesi*) occurs in North America in the geographical range of opposums (*Didelphis spp.*), as the latter represent the definitive host for *S. neurona*. The lesions with *Sarcocystis* infection more typically affect the cervical and thoracic spinal cord, but lesions in the brain stem can occur. *S neurona* schizonts are oval or irregularly round, have very thin walls and contain few basophilic ovoid merozoites.[4]

Horses are considered one of the less sensitive species to the pathogenic effect of *Toxoplasma gondii*, as a specific pathologic condition related to toxoplasmic infection has not been described under natural conditions or experimentally.[14]

Granulomatous amebic encephalitis, caused by *Balamuthia mandrillairs* infection, occurs worldwide, albeit rarely, and has been described in horses.[10] Amebae resemble large macrophages with foamy cytoplasm, large eccentric nucleus but can be distinguished by positive staining with PAS.

Trypanosoma evansi infection was reported to cause necrotizing encephalitis in Brazilian horses, with the most severe lesions occurring within the cerebral white matter.[12]

The larvae of tapeworms of the family Taeniidae, such as *Coenurus cerebralis* (larval stage of *Taenia multiceps*), although rarely affecting horses, can migrate and reach various organs, in particular the liver and the CNS, where they form cysts of varying size, which can be sometimes very large.

In acute helminth infections, the inflammatory pattern is typically suppurative in nature with variable numbers of eosinophils, while chronic lesions develop a granulomatous component. Rare cases of cerebrospinal nematodiasis in horse have been attributed to *Strongylus vulgaris*.[3] *Angiostrongylus cantonensis* has been reported to induce neurological disease in foals.[15] *Parelaphostrongylus tenuis*,

commonly called meningeal worm or brain worm, is a common neurotropic parasitic nematode of white-tailed deer in eastern North America; however a recent report revealed that horses are also susceptible to infection, and developed lesions mostly within the cerebellar parenchyma and associated meninges.[13] The lesions within the CNS result from aberrant nematode larval migration, inducing areas of malacia (mostly in the white matter) with swollen axons and hemorrhages. The migration tracks induce reactive changes including vascular proliferation, invasion of macrophages, and perivascular cuffing containing varying numbers of eosinophils.

Similar lesions, caused by larval wandering of the microfilaria *Setaria sp*. in the brain and spinal cord are described in horses (aberrant hosts) in Asia. *Setaria digitata* is normally found as an adult in the peritoneal cavity of cattle and buffalo.[8]

Intracranial invasion by the nematodes *Halicephalobus gingivalis* is reported in horses in Europe, North and South America. Depending on the area of the CNS affected, lesions are granulomatous and eosinophilic meningoencephalitis, myelitis, poly-radiculitis or even cauda equina neuritis-like lesions. Parasitic granulomas in the kidney and gingiva may accompany the cerebral invasion.[1] *Halicephalobus gingivalis* has a characteristic rhabditiform esophagus, composed of a corpus, isthmus and bulb. Little is known about the life cycle and method of transmission of this nematode; however oral ingestion or wound contamination followed by hematogenous distribution is suggested.[7]

Based on the granulomatous nature and the lack of hemorrhages, the verminous encephalitis encountered in our case reveals a chronic stage. The presence of nematodes with rhabditiform esophagus, in this case, suggests infection with the nematode *Halicephalobus gingivalis*. Attempts to definitively identify the organism with PCR were unsuccessful, and this could possibly be attributed to prolonged formalin fixation and processing procedures. Nevertheless, this case represents one of the rare equine verminous encephalitides reported in Australia.

JPC Diagnosis: Cerebellum: Encephalitis, necrotizing and granulomatous, multifocal, random, moderate, with numerous eggs, larvae, and adult rhabditid nematodes, thoroughbred, *Equus caballus*.

Conference Comment: The contributor provides a concise review of neurotropic parasite-induced disease in the equine central nervous system. *Halicephalobus gingivalis* (previously called *Micronema deletrix, Rhabditis gingivalis,* or *Tricephalobus gingivalis*) is a free-living and saprophytic rhabdditoid nematode that is a facultative (accidental) and opportunistic parasite primarily affecting horses.[3,16] There have been sporadic case reports of fatal disease in humans[11], rare reports in cattle[5], and a single case report in a zebra[9] with recurrent nematode-induced uveitis and disseminated granulomatous lesions.

Conference participants identified numerous tangential cross sections of larval and adult rhabditid nematodes ranging in size from 10-25 um in diameter within areas of granulomatous and necrotizing inflammation randomly scattered throughout the cerebellum. *H. gingivalis* has a thin smooth cuticle, platymyarian-meromyarian musculature, a pseudocoelom, and a highly characteristic rhabditiform esophagus composed of a corpus, isthmus and bulb.[2,3,6,16,] Additionally, the intestinal tract

is lined by uninucleate, low cuboidal cells and a single genital tract. Participants also recognized occasional 15-20 um ovoid embryonated eggs adjacent to adults and larvae.[3,6,16] Interestingly, only female adults, larvae, and eggs are identified within tissue sections. Free-living adult males have been found in the environment, but there are no reports of male *H. gingivalis* within host tissue. This likely indicates that *H. gingivalis* adults sexually reproduce in the environment and asexually within hosts.[2,3,6,16] The ability of the female parasite to reproduce parthenogenically within the host likely explains the massive numbers present within most affected tissue. Despite its small size, *H. gingivalis* can produce extensive tissue damage secondary to aggressive migratory behavior, typical of rhabditoid parasites.[2,6,16]

H. gingivalis usually causes severe perivascular granulomatous and eosinophilic inflammation. Organs other than the brain commonly infected by this parasite include the kidneys, lymph nodes, spinal cord, and adrenal glands. Additionally, tissue within the oral and nasal cavity also commonly contain granulomatous inflammatory lesions.[2,3,6,16] Lesions within the heart, liver, stomach, and bones are less common in horses. As mentioned by the contributor, little is known about the pathogenesis and life cycle of this parasite. Oral ingestion, inhalation or wound contaminations have all been proposed as portals of entry. There is also a single case report of probable transmission from a dam to a foal through the colostrum.[2,3,16] After entry, the nematode likely disseminates hematogenously throughout the body causing lesions in several organs. In this case, no additional lesions other than the brain are reported by the contributor. In horses, there are case reports with localized infection of the brain, without any other parasite associated lesions elsewhere in the body. It is thought that in those cases, the parasite is inhaled into the nasal cavity and enters the brain via penetration through the cribriform plate.[2,3,16]

Contributing Institution:
University of Melbourne
http://www.vet.unimelb.edu.au

References:

1. Brojer JT, et al. *Halicephalobus gingivalis* encephalomyelitis in a horse. *Can Vet J*. 2000; 41(7):559-61.
2. Bryant UK, Lyons ET, Bain FT, Hong CB. *Halicephalobus gingivalis*-associated meningoencephalitis in a Thoroughbred foal. *J Vet Diagn Invest*. 2006; 18(6):612-615.
3. Cantile C, Youssef S. Nervous system. In: Maxie MG, ed. *Jubb, Kennedy, and Palmer's Pathology of Domestic Animals*. Vol 1. 6th ed. Philadelphia, PA: Elsevier; 2016:390.
4. Dubey JP, et al. A review of *Sarcocystis neurona* and equine protozoal myeloencephalitis (EPM). *Vet Parasitol*. 2001; 95(2-4):89-131.
5. Enmark HL, Hansen MS, et al. An outbreak of bovine meningoencephalitis with identification of Halicephalobus gingivalis. *Vet Parisitol*. 2016; 218:82-86.
6. Gardiner CH, Poynton SL. *An Atlas of Metazoan Parasites in Animal Tissues*. Washington, DC: Armed Forces Institute of Pathology; 1999:14-16.
7. Henneke C, et al. The distribution pattern of *Halicephalobus gingivalis* in a horse is suggestive of a haematogenous spread of the nematode. *Acta Vet Scand*. 2014; 56:56.

8. Innes JR, Shoho C. Nematodes, nervous disease, and neurotropic virus infection; observations in animal pathology of probable significance in medical neurology. *Br Med J*. 1952; 2(4780):366-8.
9. Isaza R, Schiller CA, Stover J, Smith PJ, Greiner EC. *Halicephalobus gingivalis* (Nematoda) infection in a Grevy's zebra (*Equus grevyi*). *J Zoo Wildl Med.* 2000;31(1):77-81.
10. Kinde H, et al. Amebic meningoencephalitis caused by *Balamuthia mandrillaris* (leptomyxid ameba) in a horse. *J Vet Diagn Invest*. 1998; 10(4):378-81.
11. Lim CK, Crawford A, et al. First human case of fatal Halicephalobus gingivalis meningoencephalitis in Australia. *J Clin Microbiol*. 2015; 53:1768-1774.
12. Rodrigues A, et al. Neuropathology of naturally occurring *Trypanosoma evansi* infection of horses. *Vet Pathol*. 2009; 46(2):251-8.
13. Tanabe M, et al. Verminous encephalitis in a horse produced by nematodes in the family protostrongylidae. *Vet Pathol*. 2007; 44(1):119-22.
14. Tassi P. *Toxoplasma gondii* infection in horses: A review. *Parassitologia*. 2007; 49(12):7-15.
15. Wright JD, et al. Equine neural angiostrongylosis. *Aust Vet J*. 1991; 68(2):58-60.
16. Zachary JF. Nervous system. In: Zachary JF, eds. *Pathologic Basis of Veterinary Disease*. 6th ed. St. Louis, MO: Elsevier Mosby; 2017:846.

CASE II: 15842#185 (JPC 4086885).

Signalment: Nine-year-old female great Dane, (*Canis familiaris*).

History: The dog presented for clinical evaluation of progressive neurologic disease of two months duration and was diagnosed with canine cognitive dysfunction (CCD). Clinical signs include incoordination, weakness, lethargy, anorexia and locomotion difficulties. The animal was treated with antioxidants, tramadol, and propentophylin (vasodilator). Six months later, the dog's condition deteriorated with the onset of seizures and was euthanized.

Gross Pathology: The dog was in good body condition. There were no significant gross lesions of the thoracic, abdominal viscera, or eyes. In the left brain hemisphere, there was a 2x2.5 cm soft, grayish-tan, fixed mass with a velvet surface that protrudes from the fontal lobe. Following formalin fixation and sectioning, the mass extended 1cm into the gray matter of the brain parenchyma.

Laboratory results: No laboratory analysis performed.

Histopathologic Description: There is focally infiltration of the gray matter by a sharply demarcated but unencapsulated, multinodular, hypercellular mass compose by neoplastic cells arranged in concentric whorls separate into well-demarcated lobules by a delicate fibrous stroma. Neoplastic cells have variably distinct borders with varying amounts of eosinophilic microvacuolar cytoplasm, oval to spindle-shaped vesicular nuclei with finely stippled chromatin and predominantly one large open-faced nucleoli. Mitoses are rare with less than one mitotic figure per high power field. Occasionally necrotic foci

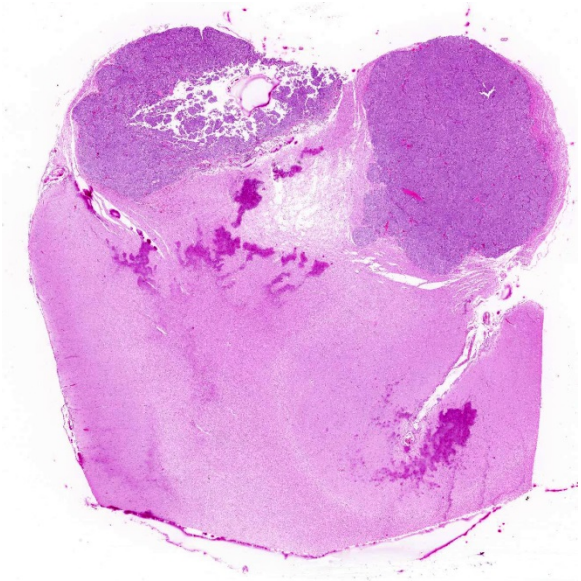

Cerebrum, dog: The meninges are expanded by a large, multilobular neoplasm which compresses the underlying cortex. (HE, 7X)

are present. There is no evidence of vascular invasion.

Brain tissue immediately adjacent to the mass is markedly compressed, and there are few lymphocytes and some pigment (hemosiderin) laden macrophages.

Contributor's Morphologic Diagnosis: Brain: Meningioma, transitional.

Contributor's Comment: The incidence of brain tumors in canine may approach 3.0%. It has been reported that meningiomas are the most common intracranial tumors in dogs, followed by glial tumors (astrocytoma and oligodendroglioma).[9] Meningioma is also the most common type of intracranial tumor in the cat. Meningiomas are rare in cattle and not recorded in horses.[10] Neoplastic cells arise from the cap cells covering the arachnoid, particularly at the point where they project into the venous sinuses[4] and pia mater of the nervous system.[3]

Older dogs may have a predisposition for primary brain tumors. Meningiomas occur in dolichocephalic breeds, especially German shepherds, golden retrievers and Labrador retrievers, with no consistent sex predisposition.[7,9]

Meningiomas may be present especially in the rostral cerebrum for a prolonged period before clinical signs of intracranial disease become obvious to the owner. Further, owners may attribute more subtle signs of forebrain disease (such as pacing or mentation change) to the normal aging process in a geriatric pet.[5] The majority of animals with brain tumors present with a variety of mild or ill-defined neurological signs.

Canine meningiomas clinically display variable behavior that currently makes outcome difficult to predict. The behavior of canine meningiomas varies widely from case to case. Individual cases receiving basic therapies (corticosteroids and supportive therapies, such as anticonvulsant drugs) can have a much better outcome than other individuals that undergo more aggressive therapeutic regimens, such as surgery and post-operative radiation.[1]

Meningiomas usually grow as well-demarcated, often lobulated, firm, granular masses that usually have a broad-based or pedunculated attachment to the overlying meninges. Less commonly they can form plaque-like masses over the meninges.[3,7] In some cases, canine meningioma shows a large cystic cavity or aggregation of severely vacuolated neoplastic cells as a consequence of ischemic events.[7] Meningiomas are gray, sometimes yellow on cut surface, firm, and may be gritty. These tumors grow either by compression or, less commonly, by infiltration of the adjacent brain. In dogs, meningiomas are found commonly in the

region of the olfactory bulb and frontal lobes, but can occur anywhere over the surface of the cerebral hemispheres. Supratentorial meningiomas are more common over the meninges of the convexities than in basilar sites.[3]

Due to the embryonic origin of the meninges, meningiomas exhibit highly variable morphological and immuno-phenotypic patterns.[7] A classification based mainly on the WHO classification of human histological subtype describes the following histological patterns: meningothelial, fibroblastic, transitional (mixed), psammo-matous, angiomatous, papillary, granular cell, myxoid, and anaplastic. All of these histological variants except anaplastic (malignant) meningiomas have similar biologic behavior. They are slow growing and cause clinical signs by compression of underlying nervous tissue.[5] Areas of chondroid, osseous, myxoid, and xanthomatous-like tissue can be found in the meningothelial and transitional forms.[3]

Most intracranial meningiomas are benign as indicated by low frequency of metastases and failure to invade the brain. By these criteria, ~ 2.5% are malignant and may metastasize. In contrast, extracranial meningiomas, which occur mainly in the paranasal region and orbit, are anaplastic and locally aggressive.[7,9,10]

In some cases, it can be difficult to distinguish meningiomas from other neoplasms, such as astrocytomas, oligo-dendrogliomas, metastatic carcinomas, germ cell tumors, and peripheral nerve sheath tumors. In these cases, a basic immuno-histochemical panel consisting of vimentin, CD34, and E-cadherin has been proposed for the characterisation of canine and feline meningiomas. [7] Meningiomas also stain sparse to moderate positively for cyto-keratin, NSE, and S-100 and negative for synaptophysin and GFAP.[10]

JPC Diagnosis: Brain, cerebrum: Meningioma, transitional, Great Dane, *Canis familiaris*.

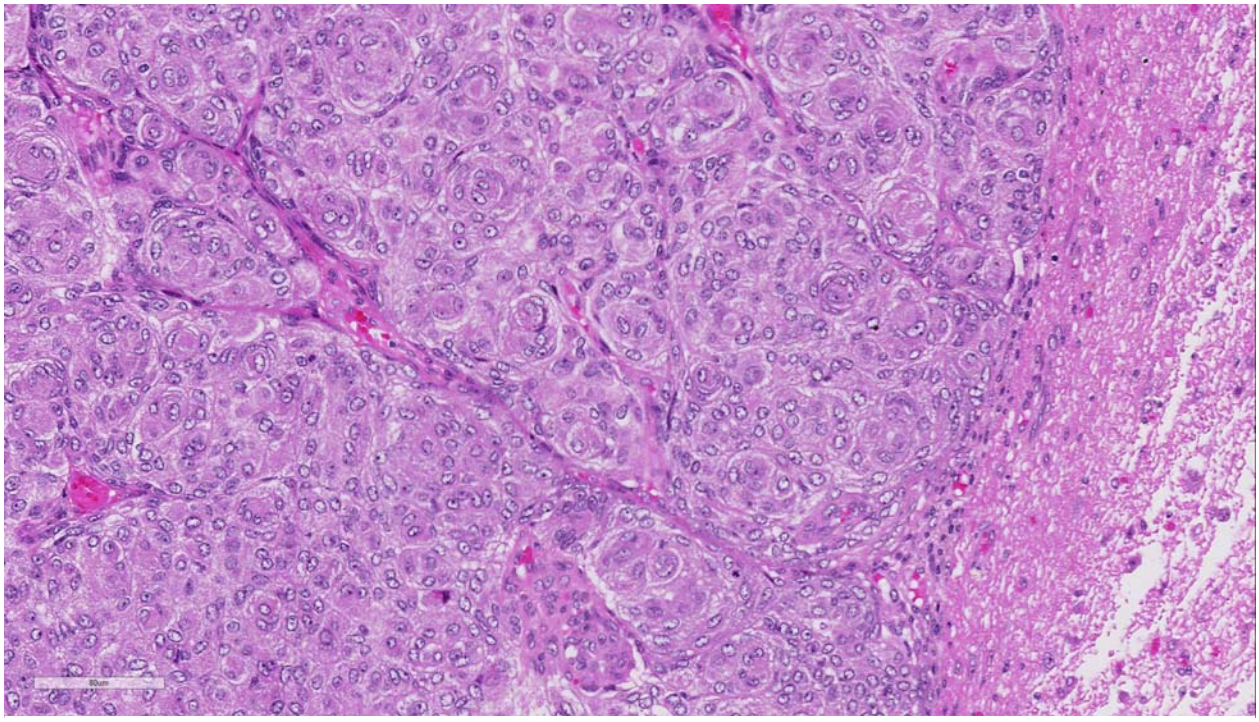

Cerebrum, dog: Neoplastic cells are arranged in lobules separated by fibrovascular septa. Neoplastic cells are arranged in nests and whorls. Compressed neuroparenchyma is at right. (HE, 288X)

Conference Comment: The contributor provides an excellent review of the biologic behavior, gross findings and, histopathologic patterns associated with the many different classifications of meningiomas in dogs and cats. Meningiomas arise from the meningothelial cells that line the arachnoid villi and cover the central nervous system.[2,3] As mentioned by the contributor, this is the most common type of intracranial tumor in dogs and constitutes between 30-50% of all primary intracranial tumors in this species.[2,3] Additionally, meningiomas account for approximately 60% of all primary intracranial neoplasms in cats. The vast majority of meningiomas occur either within the cranium (82%) or spinal cord (15%).[3] Most intracranial meningiomas occur within the olfactory bulb, but they have also been reported in the cerebral and cerebellar convexity, parasagittal and parasellar area, cerebellopontine angle, and foramen magnum.[2,3] Conversely, only about 2-3% occur in the retrobulbar or periorbital space.[2] Readers are encouraged to review 2015 Wednesday Slide Conference #20 Case 4 for an outstanding example of a periorbital meningioma in a dog.

With the exception of the less common invasive and atypical grade II and malignant and anaplastic grade III types, meningiomas rarely invade into the neuroparenchyma.[2,3] Instead, they will grow expansively within the cranium, as in this case, causing compression necrosis of the neuropil.[2,3,8] Canine meningiomas bear a striking similarity in both histomorphology and biologic behavior to human meningiomas. As a result, there has been widespread application of the World Health Organization (WHO) classification scheme for humans in scientific reports of canine meningiomas.[2-6,8] Conference participants discussed the nine histologic types of meningiomas, including: meningothelial, fibrous (fibroblastic), transitional (as in this case), psammomatous, angiomatous, papillary, granular cell, myxoid, and anaplastic. Other than the anaplastic type, all are slow growing and have a relatively benign biologic behavior.[4,5,8] However, regardless of the histomorphology, in meningiomas in domestic animals, malignancy is still based on mitotic rate, cellularity, growth pattern, and tumor invasion into the underlying nervous tissue.[2-5,8]

Atypical, choroid, and clear cell types are subcategories of grade II meningiomas. Grade II meningiomas require 4 mitoses/ 10 high powered fields and at least three of the following features: loss of architectural pattern replaced by sheets of cells, small cell formation with a high nuclear: cytoplasmic ratio, nuclear atypia or macronuclei, hypercellularity, and spontaneous necrosis.[2,3] The clear cell category is characterized by sheets of epithelial cells with abundant PAS positive cytoplasm, indicating glycogen accumulation. Grade III malignant meningiomas are comprised of papillary, anaplastic, and and rhomboid types and are characterized by extreme cellular anaplasia, >20 mitoses/10 high powered fields, necrosis, and neuroinvasion.[3]

Conference participants discussed doublecortin (DCX), Ki-67, E-cadherin, N-cadherin, and beta-catenin as potential immunohistochemical (IHC) stains that would help differentiate malignant from benign meningiomas. A relatively recent study in *Veterinary Pathology* used the previously mentioned IHC stains to predict the biologic behavior of meningiomas.[4] The authors found that doublecortin (DCX), which is important in neuroblast migration during development, is highly expressed in

invasive brain tumors, including malignant meningiomas. Additionally, Ki-67 staining, a standard marker of cell proliferation, is significantly higher in anaplastic meningiomas compared to benign varieties and is widely used to evaluate tumor grade and malignancy in humans.[4] The authors also found that there is positive correlation between DCX and N-cadherin expression and conversely a negative correlation between E-cadherin and N-cadherin expression. Additionally decreased E-cadherin expression is associated with increased nuclear beta-catenin expression suggesting that decreased E-cadherin, increased N-cadherin, DCX expression, and nuclear beta-catenin staining are all associated with malignant meningiomas.[4,8]

Contributing Institution:
Animal Pathology Department
Veterinary Oncology Service
Federal University of Pelotas
Pelotas, Brazil.
http://wp.ufpel.edu.br/sovet/

References:

1. Bentley RT. Small animal meningiomas: The information explosion tackles a challenging disease head on. *Vet J*. 2012;192:135–136.
2. Cantile C, Youssef S. Nervous system. In: Maxie, MG, ed. *Jubb, Kennedy, and Palmer's Pathology of Domestic Animals,* Vol I. 6th ed. Philadelphia, PA: Elsevier Ltd; 2016:396-398, 494.
3. Higgins RJ, Bollen AW, Dickinson PJ, Siso-Llonch S. Tumors of the nervous system. In: Meuten DJ, ed. *Tumors in Domestic Animal*, 5th Ed. Ames, IA: John Wiley and Sons Inc; 2017:864-869.
4. Ide T, Uchida K, et al. Expression of cell adhesion molecules and doublecortin in canine anaplastic meningiomas. *Vet Pathol*. 2011; 48(1):292-301.
5. Koestner A, Bilzer T, Fatzer R. Histological classification of tumors of the nervous system of domestic animals. In: Koestner, A., Bilzer, T., Fatzer, R. eds. *Histological Classification of Tumors of the Nervous System of Domestic Animals WHO International Classification of Tumors of Domestic Animals*, Vol. 5. Washington, DC: Armed Forces Institute of Pathology, 1999: 22.
6. Miller AD and Zachary JF: Nervous system. In: Zachary JF, ed. *Pathologic Basis of Veterinary Disease.* 6th ed. St. Louis, MO: Mosby, Inc.; 2017:874.
7. Motta L, Mandara MT, Skerritt GC. Canine and feline intracranial meningiomas: An updated review. *Vet J*. 2012; 192:153–165.
8. Ramos-Vara JA, Miller MA, Gilbreath E, Patterson JS. Immuno-histochemical detection of CD34, E-cadherin, claudin-1, glucose transporter 1, laminin, and protein gene product 9.5 in 28 canine and 8 feline meningiomas. *Vet Pathol*. 2010;47(4):725-737.
9. Snyder JM., Shofer FS, Van Winkle TJ, Massicotte C. Canine Intracranial Primary Neoplasia: 173 Cases (1986–2003). *J Vet Intern Med*. 2006; 20: 669–675.
10. Wilcock BP.Eye and ear. In: Maxie MG, ed. Jubb, *Kennedy and Palmers Pathology of Domestic Animals*. Vol 1. 5th ed. Philadelphia, PA: Elsevier; 2007:518.

CASE III: 16N74 (JPC 4085376).

Signalment: 15-month-old castrated male Nelore calf, (*Bos taurus indicus*).

History: This calf was part of a herd of 70 calves of about the same age that was shipped from another farm six months ago. The owner reported that the onset of neurological cases occurred one month after the calves' arrival on the farm. During a five-month period, three more calves (including the one of this report) died. The calf of this report presented for neurological disease with a 5-day fatal clinical course. Clinical signs observed were fever (41°C), apathy, blindness, drooling, grinding of the teeth, locked jaw, and flaccidity of the tongue.

Gross Pathology: Significant gross findings were restricted to the brain. In the cortex of the parietal and frontal lobes of the telencephalic hemispheres, there were bilaterally symmetrical depressed, red and soft areas and extensive areas of severe leptomeningeal hemorrhages (Fig.1). On cut section, the frontal cerebral cortex contained extensive, dark brown and granular areas of hemorrhage and malacia (Fig. 2).

Laboratory results: None available.

Histopathologic Description: Main lesions affected the frontal, temporal, and parietal cortex, the last of which is represented in the submitted slides. In these sites, there are intense leptomeningeal mononuclear infiltrates and multifocal areas with loss of neuropil and cavitation, with accumulation of large numbers of foamy macrophages (gitter cells). Segments of marked submeningeal hemorrhages are observed above these necrotic areas. In adjacent areas, the more acutely affected neuropil contained extensive areas of edema with astrogliosis and segmental areas of laminar neuronal necrosis where neurons exhibit hypereosinophilic and shrunken cytoplasm and pyknotic nuclei. Multifocally throughout the adjacent neuropil and neuroparenchyma, blood vessels have prominent endothelial cells, and perivascular spaces had cuffs (up to 5-cell thick) of lymphocytes and plasma cells that extend to the leptomeningeal vessels. The neuropil underlying the leptomeninges is partially collapsed and contain areas of fragmentation with accumulation of large numbers gitter cells. Large numbers of gitter cells are also seen in the perivascular space (interpreted that these cells are probably migrating from the necrotic areas into perivascular spaces to be reabsorbed then into the general circulation). Multifocal areas of edema eventually coalesce to dissect the cortical grey matter (spongiosis), sometimes in a laminar pattern. Occasional astrocytes contain large intranuclear amphophilic viral inclusions that pushed the chromatin peripherally. The neuropil within the necrotic areas is sprinkled with basophilic, granular chromatin-like material. Multifocal narrow ring hemorrhages are seen perivascularly

Cerebrum, calf. The parietal and frontal lobes are bilaterally depressed with extensive leptomeningeal hemorrhage. (Photo courtesy of: Laboratory of Anatomic Pathology, Universidade Federal de Mato Grosso do Sul, Campo Grande, MS, Brazil. https://www.ufms.br/)

and extend into the neuropil. The subcortical white matter is loose due to edema and also diffusely infiltrated by gitter cells. Similar perivascular cuffing is present in both gray and white matter. Perivascular cuffing is also present in the occipital cortex, mesencephalon, pons, medulla and cerebellum.

Contributor's Morphologic Diagnosis: Brain, necrotizing meningoencephalitis, focally extensive, acute to subacute, severe, with intranuclear inclusion bodies in astrocytes.

Contributor's Comment: The gross and microscopic findings reported in this calf are typical of those observed in cases of meningoencephalitis due to either bovine herpesvirus (BoHV) either by type 1 virus (BoHV-1) or type 5 (BoHV-5).[5,6,7] The history, clinical signs, and characteristic lesions in the brain of this calf warrant a presumptive diagnosis of necrotizing meningoencephalitis by BoHV-1 or BVH-5. This diagnosis was further supported by the finding of characteristic intranuclear inclusion bodies in astrocytes.[7] The occurrence of intranuclear astrocytic or neuronal viral inclusions may vary among cases, but when present they are important in the presumptive diagnosis of bovine herpes viral infection.[7]

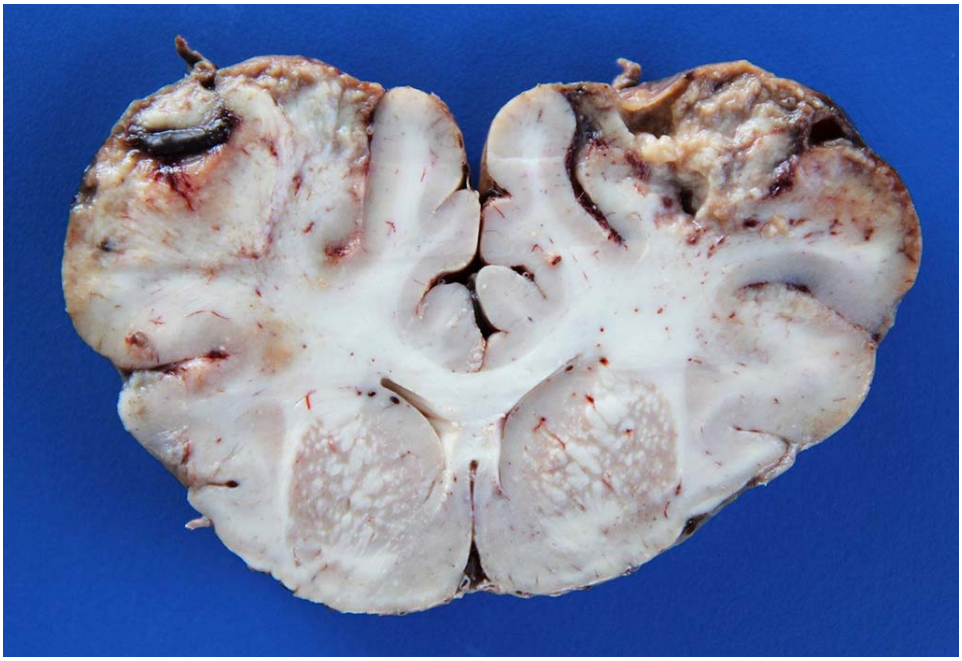

Cerebrum, calf. On cut surface, the frontal cerebral cortex contained extensive, dark brown and granular areas of hemorrhage and malacia. (Photo courtesy of: Laboratory of Anatomic Pathology, Universidade Federal de Mato Grosso do Sul, Campo Grande, MS, Brazil. https://www.ufms.br/)

Meningoencephalitis due to BoHV-1 or BoHV-5 shares many similarities regarding epidemiological and clinicopathological findings, and the diagnostic confirmation should be performed using FAT, viral isolation.[8,9] However, the differentiation between neurological infection caused specifically by BoHV-1 or BoHV-5 can only be achieved through the use of molecular ancillary tests such as the glycoprotein C–based PCR.[8,9] Results obtained from studies using this latter method of differentiation in south Brazil showed that BoHV-1 and BoHV-5 may be interchangeably involved in very similar clinicopathological conditions that were previously attributed to a single strain (either BoHV-1 or BoHV-5).[8,9] These tests are used only for research purposes in our diagnostic routine, and the confirmation of bovine herpesviral infection by either FAT or viral isolation is usually sufficient for confirmation of herpesviral

Cerebrum, calf. There is extensive cavitation and hypercellularity of the submeningeal cortex. (HE, 5X)

infection (but not viral typification) in the diagnostic routine service. In the present case, none of these ancillary tests were available.

The clinical course in cases of meningoencephalitis due to BoHV varies from 1 to 15 days, and affected cattle may develop a wide range of clinical signs such as severe depression, serous ocular and nasal discharge, grinding teeth, circling, blindness, incoordination, head pressing, nystagmus, recumbence, paddling, opisthotonus, and seizures.[5-8]

Based on the geographical location and gross findings in this calf, the main differential diagnoses at the time of necropsy included infection by bovine herpesvirus (BoHV-1 or BoHV-5) meningoencephalitis, polioencephalomalacia (PEM), and rabies.[7] Severe cases of PEM may rarely present with gross lesions that resemble those described for this calf. Gross findings in cases of bovine rabies are usually absent.[5-7]

Necrotizing meningoencephalitis due to BoHV affects mainly calves (as is the case on this report) and young adults submitted to environmental or management-related stressors, including weaning, high concentration of cattle, transportation, and introduction of new animals into the herd.[6-7] The stressors conditions precipitating the disease in the present case were not identified. However, the calf has been transported some months before the onset of clinical disease, which most likely provided close contact with other animals and might have facilitated infection or reactivation of a latent herpesviral infection.[3,4]

BoHV-1 and BoHV-5 are genetically and antigenically related viruses that belong to the family Herpesviridae, subfamily Alphaherpesvirinae, genus *Varicellovirus*.[2] BoHV-1 has been historically associated with abortion, respiratory, and genital disease, namely infectious bovine rhinotracheitis and infectious pustular vulvovaginitis or balanoposthitis. Although BoHV-5 has been classically associated with neurological disease in cattle, it is currently believed that both BoHV-1 and BoHV-5 cause identical neurological disease in endemic areas and cases of meningoencephalitis caused by BoHV-1 are not as uncommon as previously suspected.[7,9]

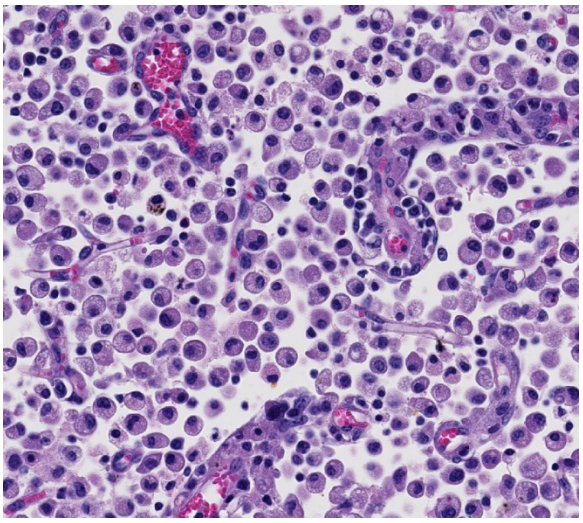

Cerebrum, calf. Areas of cavitation are populated by innumerable Gitter cells (transformed microglial which clean up myelin debris) (HE, 288X)

Necrotizing meningoencephalitis due to BoHV has been described worldwide, particularly in South America.[4,5,9] The reason for the lower incidence of meningoencephalitis due to BoHV in other parts of the world is unknown, but it has been proposed that widespread vaccination against BoHV in North America and Europe protects susceptible animals and prevents clinical disease in these areas.[10]

Viral transmission occurs via direct or indirect contact among susceptible individuals, with primary viral replication occurring in the ocular and oropharyngeal mucosal epithelium. Following primary replication, viral particles reach the rostral portions of the brain and sensory ganglia via axonal retrograde transportation and direct invasion through the olfactory bulb and trigeminal nerves.[2]

Viral invasion into the brain may result in secondary replication and neurological disease or subclinical infection and viral latency in the trigeminal ganglia and central nervous system.[3] Latently infected individuals will become an important source of virus to other susceptible cattle in the case of virus reactivation.[3,4] A hematogenous route of infection has been proposed, but it seems less likely due to the characteristic distribution of the lesions in the frontal areas of the brain, which support direct viral invasion through the olfactory bulb.[3,7]

The gross and microscopic findings reported in this calf are typical of those observed in cases of meningoencephalitis due to either BoHV-1 or BoHV-5. In addition, cases of neurological disease by BoHV with neither gross nor microscopic lesions despite the development of severe neurological disease have been observed.[7,8] These variations in the pathological

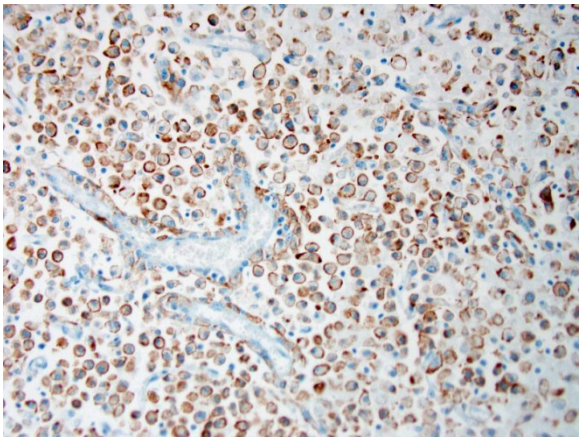

Cerebrum, calf. Gitter cells exhibit strong cytoplasmic reactivity for IBA-1 (a macrophage marker). The cytoplasm is diminished by the presence of numerous phagosomes containing myelin debris. (anti-IBA-1, 200X)

presentation of neurological disease due to BoHV are attributed to potential differences in the neurovirulence or to individual susceptibility of animals to viral infection.[1,8]

JPC Diagnosis: Cerebrum, telencephalon: Meningoencephalitis, necrotizing, multifocal to coalescing, severe, with marked gliosis, multifocal vasculitis and rare intraglial

intranuclear viral inclusion bodies, Nelore calf, *Bos taurus indicus*.

Conference Comment: We thank the contributor for the thorough review of the epidemiology, clinical presentation, gross and histologic lesions, and pathogenesis associated with neurotropic bovine herpesvirus (BoHV) infection in a calf. In addition, the excellent quality gross photographs provided by the contributor demonstrate the typical lesions of bilaterally symmetrical severe multifocal to coalescing encephalomalacia and hemorrhage affecting the rostral cerebrum. As mentioned above, both BoHV-1 and 5 are antigenically related members of the *Alphaherpesvirinae* subfamily and are part of genus *Varicellovirus*. Additionally, they both infect epithelial cells at the portal of entry and establish latent infection in the sensory trigeminal ganglia.[2,3,6,12,15] This is a relatively uncommon disease that primarily affects young and immunosuppressed cattle. Severe clinical illness is most frequently reported in South American, with a high prevalence in Brazil and Argentina.[2] Although conference participants were not given the country of origin of this animal before the conference (Brazil), most identified rare intranuclear inclusion bodies within degenerate neurons and astrocytes, highly characteristic of BoHV infection.[2]

Attendees also described numerous microglial phagocytic cells with an abundant amount of foamy eosinophilic cytoplasm (gitter cells) infiltrating into the necrotic areas. Gitter cells are microglial cells that transformed into phagocytic macrophages within the central nervous system and function to engulf cellular debris and degenerate myelin.[2] Microglial phagocytes also surround degenerate neurons (satellitosis) and phagocytose degenerate neuronal cell bodies (neuronophagia) during neurotropic viral infection. In severe lesions, as in this case, gitter cells can arise from peripheral blood monocytes as well as microglial cells.[2] These cells are nicely highlighted by intense membranous and

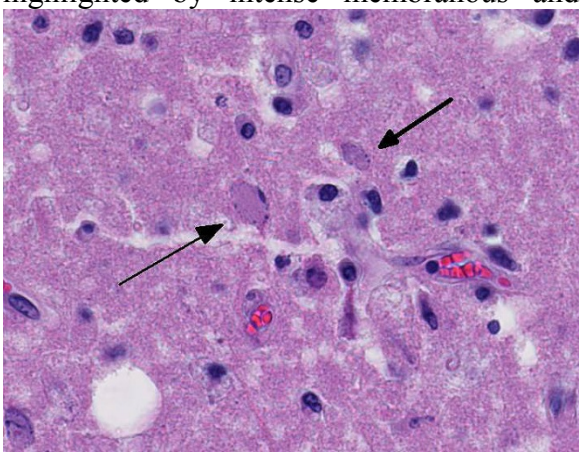

Cerebrum, calf. Astrocyte nuclei within the adjacent gray matter are expanded by amphophilic intranuclear viral inclusions.

cytoplasmic immunoreactivity for ionized calcium binding adapter molecule 1 (IBA-1), an immunohistochemical stain commonly used to identify microglial cells and macrophages run by the Joint Pathology Center prior to the conference.

Conference participants discussed differential diagnoses for laminar cortical necrosis and polioencephalomalacia in cattle. These include sulfur intoxication, sodium chloride intoxication/water deprivation, lead intoxication, and thiamine deficiency. Participants also discussed other infectious diseases that can cause neurologic disease in cattle, such as rabies virus, malignant catarrhal fever (MCF), listeriosis, and the neurotropic amoeba, *Naegleria fowleri*.[2,8,9,15]

The conference moderator noted that this case has excellent examples of ferruginated neurons. These are deeply basophilic dead neurons that become encrusted and replaced with finely beaded material interpreted as

mineral, rather than being removed by phagocytosis. The mineral is composed of both calcium and iron and affected neurons are highlighted by both von Kossa and *Perls' Prussian blue* staining techniques. These neurons are reported to occur in areas of ischemic and hypoxic damage in the central nervous system, particularly in juveniles and neonates.[5]

Contributing Institution:
Laboratory of Anatomic Pathology
Universidade Federal de Mato Grosso do Sul, Campo Grande, MS, Brazil.
https://www.ufms.br/

References:

1. Belknap EB, Collins JK, Ayers VK, et al. Experimental infection of neonatal calves with neurovirulent bovine herpesvirus type 1. *Vet Pathol*. 1994; 31:358–365.
2. Cantile C, Youssef S. Nervous system. In: Maxie MG, ed. *Jubb, Kennedy and Palmer's Pathology of Domestic Animals*. Vol 1. 6th ed. Philadelphia, PA: Elsevier Ltd; 2016:262-263, 381-382.
3. Del Medico Zajac MP, Ladelfa MF, et al. Boilogy of bovine herpesvirus 5. *Vet J*. 2010; 184:138-145.
4. Engels M, Ackermann M. Pathogenesis of ruminant herpesvirus infections. *Vet Microbiol*. 1996; 53:3-15.
5. Finnie JW. Forensic pathology of traumatic brain injury. *Vet Pathol*. 2016; 53(5):962-678.
6. Meyer G, Lemaire M, Ros C, et al. Comparative pathogenesis of acute and latent infections of calves with bovine herpesvirus types 1 and 5. *Arch Virol*. 2001; 146:633-652.
7. Perez SE, Bretschneider G, Leunda MR, et al. Primary infection, latency, and reactivation of bovine herpes-virus type 5 in bovine nervous system. *Vet Pathol*. 2002; 39:437-444.
8. Pimentel LA, Dantas AF, Uzal F, et al. Meningoencephalitis caused by *Naegleria fowleri* in cattler of northeast Brazil. *Res Vet Sci*. 2012; 93:811-812.
9. Rissi DR, Barros CSL. Necrotizing meningoencephalitis in a cow. *Vet Pathol*. 2013; 50:926-929.
10. Rissi DR, Oliveira FN, Rech RR et al. Epidemiologia, sinais clínicos e distribuição das lesões encefálicas em bovinos afetados por meningoencefalite por herpesvírus bovino-5 [Epidemiology, clinical signs and distribution of the encephalic lesions in cattle affected by meningoencephalitis caused by bovine herpesvirus-5]. *Pesq Vet Bras*. 2006;26:123-132.
11. Rissi DR, Pierezan F, Oliveira-Filho JC, et al. Abordagem diagnóstica das principais doenças do sistema nervoso de ruminantes e equinos no Brasil [Diagnostic approaches for the main neurological diseases of ruminants and horses in Brazil]. *Pesq Vet Bras*. 2010;30:958-967.
12. Rissi DR, Pierezan F, Sa e Silva M, et al. Neurological disease in cattle in southern Brazil associated with bovine herpesvirus infection. *J Vet Diagn Invest*. 2008; 20:346-349.
13. Silva MS, Brum MCS, Weiblen R, et al. Identificação e diferenciação do herpesvírus bovino tipos 1 e 5 isolados de amostras clínicas no Centro-Sul do Brasil, Argentina e Uruguai (1987–2006) [Identification and differentiation of herpesvirus types 1 and 5 isolated from clinical samples in central southern Brazil, Argentina and Uruguay (1987-

2006)]. *Pesq Vet Bras*. 2007; 27:403-408.
14. Thiry J, Keuser V, Muylkens B, et al. Ruminant alphaherpes-virus related to bovine herpesvirus. *J Vet Res*. 2006; 37:69-190.
15. Zachary JF. Mechanisms of microbial infection. In: Zachary JF eds. *Pathologic Basis of Veterinary Disease*. 6th ed. St. Louis, MO: Mosby Elsevier; 2017:224.

CASE IV: A00629 (JPC 4066658).

Signalment: Four-month-old male Labrador retriever, (*Canis familiaris*).

History: A 3-month-old Labrador retriever pup developed progressively worsening tetraparesis with a spastic swimming-puppy-like position of the thoracic limbs and a flattened chest. One month later mild vestibular signs and myoclonic jerks in the head and cervical region became obvious. General clinical examination was within normal limits. Neurological examination revealed absent patellar reflexes, weakness on the 4 limbs with an abnormal spasticity of the thoracic limbs and mild generalized muscle atrophy. During the second visit a vestibular strabismus in the right eye, a mild right-sided head tilt and regular myoclonic jerks at the head and thoracic limbs were noticed.

Electrophysiological examination was normal. RX of the thorax only confirmed the dorsoventral flattening of the thorax. Due to the worsening neurological signs further examinations were declined by the owner and the pup was euthanized at the age of 4.5 months.

Gross Pathology: Except for the dorso-ventral flattening of the thorax, no gross abnormalities were noted at necropsy.

Laboratory results: Blood examination and cerebrospinal fluid analysis were within normal limits.

Histopathologic Description: Cerebrum: Within the white and gray matter of the brain, some blood vessels are surrounded by numerous short, perpendicularly oriented, hypereosinophilic, amorphous intraastro-cytic accumulations, varying in diameter from 4 to 20 µm (Rosenthal fibers). These Rosenthal fibers are also found in the astrocytic endfeet in the subpial tissue and to a lesser extend throughout the parenchyma. Mainly in the white matter, there is proliferation of abnormal astrocytes with large nuclei, prominent nucleoli and glassy eosinophilic to pale cytoplasm. Occasionally, there are binucleated astrocytes.

GFAP-staining: All Rosenthal fibers are strongly immunopositive for GFAP.

Contributor's Morphologic Diagnosis: Cerebrum, gray and white matter, encephalopathy, multifocal, chronic,

Cerebrum, puppy. A section of cerebrum and ventricle is presented for examination. (HE, 5X)

moderate, perivascular and subpial accumulation of Rosenthal fibers, astrocytosis and astrocytic hypertrophy.

Contributor's Comment: In humans, Rosenthal fibers are found in Alexander disease (AxD), and, albeit in greatly reduced numbers in chronic reactive astrocytosis and low-grade astrocytomas.[4,5] They are seldom encountered in animal neuropathology. Alexander disease, or fibrinoid leukodystrophy, is a rare neurodegenerative disorder of astrocyte dysfunction in human. In veterinary medicine, Alexander disease is very rare and has been reported in a few dogs (two Labrador Retrievers, one Scottish Terrier dog, one Miniature Poodle, three Bernese Mountain dogs, one Bernese Mountain cross breed, one French bulldog, and one Chihuahua) and four sheep (one white Alpine sheep and three Merino sheep).[1-7]

There are no specific gross lesions of AxD. The classic histological lesions are Rosenthal fibers. These fibers are deeply eosinophilic, irregularly shaped, elongated, round to oval intra-astrocytic aggregates. Rosenthal fibers have been shown to be ubiquinated aggregates of GFAP, αβ-crystalin and HSP27.[3,4]

In humans AxD is classified based on the age of onset as infantile, juvenile and adult. Recently, Prust *et al.* proposed a reclassification in two age-dependent clinical subtypes: type I, characterized by an early age of onset, seizures, macrocephaly, encephalopathy, developmental delay, paroxysmal deterioration, failure to thrive and typical MRI features, and type II, characterized by a later age of onset, autonomic dysfunction, bulbar symptoms, ocular movement abnormalities and atypical MRI features.[5] The characteristic pathological feature of both types of AxD

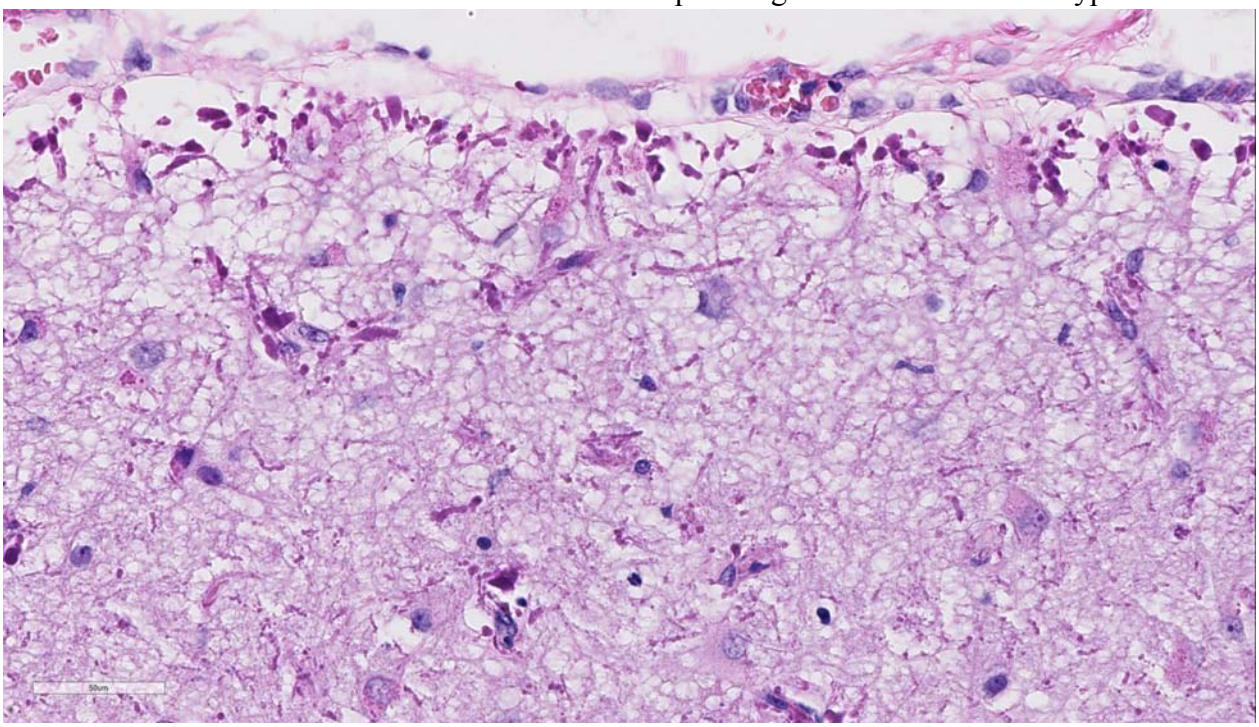

Cerebrum, puppy. Astrocytic endfeet within the subpial cortex and projecting onto superficial cortical vessels are swollen and brightly eosinophilic (Rosenthal fibers). Additionally, astrocytes are hypertrophic and often contain brightly eosinophilic granules within their cytoplasm. (HE, 400X)

are widespread and abundant Rosenthal fibers.

All known genetic causes of AxD are attributed to GFAP mutations (explaining more than 95% of the cases), mostly *de novo* dominant missense mutations with hotspots at R79 and R239, the latter one inducing the most aggressive form.[1]

JPC Diagnosis: Cerebrum: Astroglial dystrophy, diffuse, severe, with marked subpial, subependymal, and perivascular Rosenthal fiber formation, Labrador retriever, *Canis familiaris*.

Conference Comment: The contributor provides a concise review of Alexander disease (AxD), a rare neurodegenerative disorder previously reported in dogs, sheep, and humans.[1-7] Conference participants identified the large brightly eosinophilic and irregularly shaped Rosenthal fibers (RF) with astrocytes scattered throughout the white matter and aggregated in the subpial, subependymal, and perivascular spaces. This is the classic histologic lesion distribution associated with previously reported cases of AxD in all reported species.[1,7] As mentioned by the contributor, these accumulated fibers consist of large aggregates of glial fibrillary acidic protein (GFAP), αB-crystallin, heat shock protein (hsp-27) and ubiquitin, within markedly expanded astrocytic processes distributed throughout the central nervous system.[1,4,7] Prior to the conference, the Joint Pathology Center ran a GFAP immunohistochemical stain which demonstrated intense immuno-staining of the RF surrounding vessels and in the subpial and subependymal areas. RF have also been reported to be immuno-positive for ubiquitin. The presence of RF is not pathognomonic for AxD and has been reported in glial scars and multiple sclerosis in humans; however, the distribution of the RF in the subpial, subependymal, and perivascular areas in this and other reported cases is unique to AxD. In addition to Rs, other common histologic lesions of AxD include white matter demyelination and astrogliosis.[1,7]

As mentioned by the contributor, it is thought that a mutation in GFAP leads to glial intermediate filament disorganization, decreased solubility, and defective degradation of the protein.[1,3,7] This results in accumulation of the aberrant and misfolded protein, leading to cellular stress and the unfolded protein response (UPR) in the endoplasmic reticulum. Cellular stress and the resulting UPR are postulated to be the initiating factor for the production of ubiquitin and heat shock proteins (αB-crystallin, hsp-27) accumulating with GFAP and forming the RFs seen histologically.[1,4,7] Accumulation of these insoluble fibers is likely progressively toxic to astrocytes and degrades oligodendrocyte function, affecting myelin formation in the white matter. As a result, animals affected with AxD typically present as juveniles with rapidly progressive depression, ataxia, paresis, generalized tremors, decreased spinal reflexes, and seizures.[1]

Contributing Institution:
Dept. of Pathology, Bacteriology and Poultry Diseases
Faculty of Veterinary Medicine
Ghent University
Belgium
http://www.vetpbp.ugent.be/

References:

1. Aleman N, Marcaccini A, Espino L, et al. Rosenthal fiber encephalopathy in a dog resembling Alexander disease in humans. *Vet. Pathol.* 2006; 43: 1025-1028.

2. Gruber A, Pakodzy A, Leschnik M, et al. Morbus Alexander: 4 Fälle bei Hunden in Österreich. Wien. Tierärztl. Mschr. *Vet Med Austria*. 2010; 97:1-4.
3. Ito T, Uchida K, Nakamura M, et al. Fibrinoid leukodystrophy (Alexander's disease-like disorder) in a young adult French bulldog. *J Vet Med Sci*. 2010; 72:1387-1390.
4. Kessell A, Finnie J, Manavis J, et al. A Rosenthal fiber encephalomyelopathy resembling Alexander's disease in three sheep. *Vet Pathol*. 2012; 49: 248-254.
5. Prust M, Wang J, Morizono H, et al. GFAP mutations, age at onset, and clinical subtypes in Alexander disease. *Neurology*. 2011; 77: 1287-1294.
6. Richardson J, Tang K, Burns D. Myeloencephalopathy with Rosenthal fiber formation in a Miniature Poodle. *Vet Pathol*. 1991; 28: 536-538.
7. Wrzosek M, Giza E, Płonek M et al. Alexander disease in a dog: Case presentation of electrodiagnostic, magnetic resonance imaging and histopathologic findings with review of literature. *BMC Vet Res*. 2015; 11:115.

Self-Assessment - WSC 2016-2017 Conference 19

1. Which of the following organs are not commonly infected by *Helicephalobus gingivalis* ?
    a. Spinal cord
    b. Kidney
    c. Lymph nodes
    d. Spleen

2. Which of the following is not a good choice for a immunohistochemical panel to identify meningioma?
    a. CD34
    b. GFAP
    c. E-cadherin
    d. Vimentin

3. True or false? Encephalitis caused by BoHV-1 cannot be distinguished from cases caused by BoHV-5 without the use of ancillary tests like PCR.
    a. True
    b. False

4. Which of the following is not a cause of laminar cortical necrosis in cattle?
    a. Sulfur intoxication
    b. Lead intoxication
    c. Thiamine deficiency
    d. Naegleria fowleri

5. Which of the following immunohistochemical markers is most likely to be positive in chases of Alexander disease?
    a. GFAP
    b. Synaptophysin
    c. Neuron-specific enolase
    d. Doublecortin

Joint Pathology Center

Veterinary Pathology Services

WEDNESDAY SLIDE CONFERENCE 2016-2017

C o n f e r e n c e 21

31 March 2017

Linden Craig, DVM, PhD, Diplomate ACVP
Professor of Anatomic Pathology
University of Tennessee College of Veterinary Medicine

CASE I: 12B2212 (JPC 4050655).

Signalment: Nine-year-old castrated male Labrador retriever (*Canis familiaris*).

History: Right pelvic limb swelling noticed in July 2012. Treated with prednisone, diphenhydramine, cephalexin. Viscous fluid aspirate from limb 8/8/12. Presented to Internal Medicine 9/4/12 - chest x-rays unremarkable, right pelvic limb x-rays showed an aggressive lesion involving distal femur, with soft tissue swelling involving down to distal tibia. Aspiration cytology - probable sarcoma.

Abdominal ultrasound and pelvic CT scan showed a large cystic mass involving the right pelvic limb with bone invasion and presumed metastasis to the right inguinal and right medial iliac lymph node. Possible femoral vein thrombus. High coxofemoral disarticulation amputation performed. Clinical diagnosis: Sarcoma with lymph node metastasis.

Gross Pathology: A right pelvic limb from the femoral head and distally was submitted. The stifle joint and muscles of the thigh were expanded by palpably viscous, coalescing nodules. The popliteal lymph node was bi-lobed and measured approximately 2.6 x 1.4 x 1 cm. On cut surface, was mottled dull yellow, red to red-brown, slightly bulging and contained multifocal to coalescing round to oval, 0.2-0.5cm, soft to firm cystic structures filled alternatively with small amounts of clear, colorless fluid to opaque, firm, off-white material. On cut surface, the stifle joint was expanded by a 5x6x5cm, mottled dull yellow, red to red-brown, slightly bulging mass of multifocal to coalescing round to oval, soft to firm cyst-like structures that were filled alternatively with small amounts of clear, colorless fluid to opaque, firm, off-white material. Large amounts of mucoid, gelatinous, dull, yellow-red material expanded fascial planes, lymphatic vessels, and subcutaneous tissues from the mid-femur distally, and most severely, along the proximal and mid-tibia. The stifle joint was

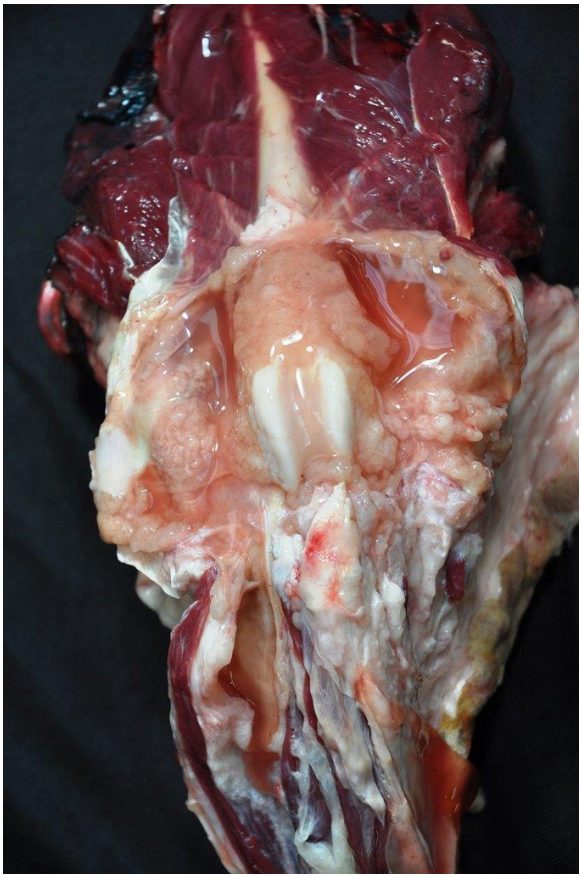

Stifle, dog. The joint is expanded by a 5x6x5cm, by a slightly bulging mass of composed of cyst-like structures that contain clear to slightly opaque material. (Photo courtesy of: University of California, Davis School of Veterinary Medicine, Veterinary Medical Teaching Hospital, Anatomic Pathology Department http://www.vetmed.ucdavis.edu/vmth/small_animal/anatomic_pathology/)

expanded by approximately 40 ml of the same material. The synovium of the stifle joint was diffusely thickened with papillary and ovoid projections and cavitations as previously described in the popliteal lymph node. The joint capsule as variably friable to firm. The entire limb was sagittally sectioned and on cut surface a firm to soft mass composed of thousands of small, firm, semi-transparent, off-white nodules emanated from the plantar aspect of the level of the stifle joint. The mass compressed the normal structures of the region. Approximately 3-5 small (0.8x0.5cm), ovoid, firm, semi-translucent, off-white masses tracked along and were adhered the femoral vasculature adventitia, including approximately 1.0cm from the surgical margin.

The inguinal lymph node was also submitted and measured 6 x 3.5 x 1.8 cm and on cut surface is expanded by multilobulated, multicavitated nodules that vary in size from 0.9 cm to 1.3 cm in diameter. They are round to oval and contain variable amounts of mucoid, tenacious, clear, colorless fluid.

Laboratory results: Radiographic findings: There is marked soft tissue swelling surrounding the tibia and loss of the normal fascial plane distinction. There are lobular soft tissue densities at the medial aspect of the right stifle joint. There is permeative lysis of the distal femur, resulting in a coarse trabecular pattern and sclerosis with an indistinct transition zone between normal and abnormal bone. Periarticular osteophytes are present on the apex of the patella, the fabellae, the proximal tibia, and the distal femur. There is marked increased soft tissue opacity associated with the stifle joint.

Stifle, dog. Sagittal section of the stifle joint showing extension of the neoplasm into adjacent skeletal muscle into adjacent muscle and subcutis. (Photo courtesy of: University of California, Davis School of Veterinary Medicine, Veterinary Medical Teaching Hospital, Anatomic Pathology Department http://www.vetmed.ucdavis.edu/vmth/small_animal/anatomic_pathology/)

Radiographic Impressions: Aggressive bone lesion affecting the distal right femur with adjacent lobular soft tissue opacities is concerning for a soft tissue neoplasm with extension to the bone such as a synovial cell sarcoma. Mild secondary joint disease. Marked edema of the right crus. An ultrasound examination of the right stifle is recommended if clinically indicated. Pulmonary osteomas. No radiographic evidence of pulmonary metastatic disease.

CT Scanning impressions: Large cystic right pelvic limb mass with associated sub-cutaneous edema and bone invasion. Filling defect of the right femoral vein may be secondary to tumor invasion or thrombus formation. Metastatic inguinal and sub-lumbar lymph nodes. The appearance of the right hypogastric and mesenteric lymph nodes may represent metastases or reactivity.

Cytology of stifle mass: Four moderately cellular coverslips are examined that have a medium pink stippled background and a mild amount of blood with erythrocytes frequently distributed in a prominent windrowing pattern. Nucleated cells are distributed individually and in variably sized loose aggregates. Thick pink fibrillar material is frequently seen associated with cell aggregates. Individual cells consist predominantly of macrophages / synoviocytes. Cells in clusters have a low to moderate amount of pale cytoplasm that frequently causes polar wisps giving the cells a spindloid shape. Nuclei are ovoid with coarsely stippled chromatin and small nucleoli. Low numbers of small mature lymphocytes are also noted.

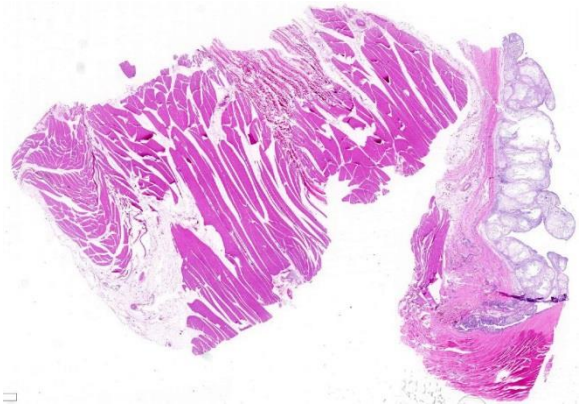

Stifle dog. Subgross view of submitted section with skeletal muscle at left, and mass arising to joint capsule at right. (HE, 4X)

Cytologic interpretation and comments: Probably sarcoma. The large aggregates of spindloid shape cells are consistent with a sarcoma, with considerations including spindle cell sarcoma, synovial sarcoma or even atypical chondrosarcoma, however, this is considered less likely.

Histopathologic Description: Examined are two cross sections of joint capsule which are markedly thickened up to 0.9 cm by a poorly cellular, abundantly myxoid, multinodular, unencapsulated, expansile neoplastic mass that primarily occupies the subintimal space. Individual variably-sized nodules are separated by thin bands of fibrous connective tissue. The neoplastic nodules often merge and are comprised of abundant amounts of lacy, gelatinous, pale, amphophilic to basophilic matrix and widely spaced stellate to spindloid cells. The cells are cytologically bland, have ill-defined borders and small amounts of a finely granular, eosinophilic cytoplasm. Nuclei are oval, with granular chromatin and variable numbers of ill-defined nucleoli. Aniso-cytosis and anisokaryosis are mild. No mitotic figures are observed. Multifocally along the most superficial aspects of the subintima, deep to synoviocytes, there are moderate to large numbers of lymphocytes and fewer plasma cells. Rarely, pigment-laden cells (macrophages) admix with the lymphocytes and plasma cells. The intimal

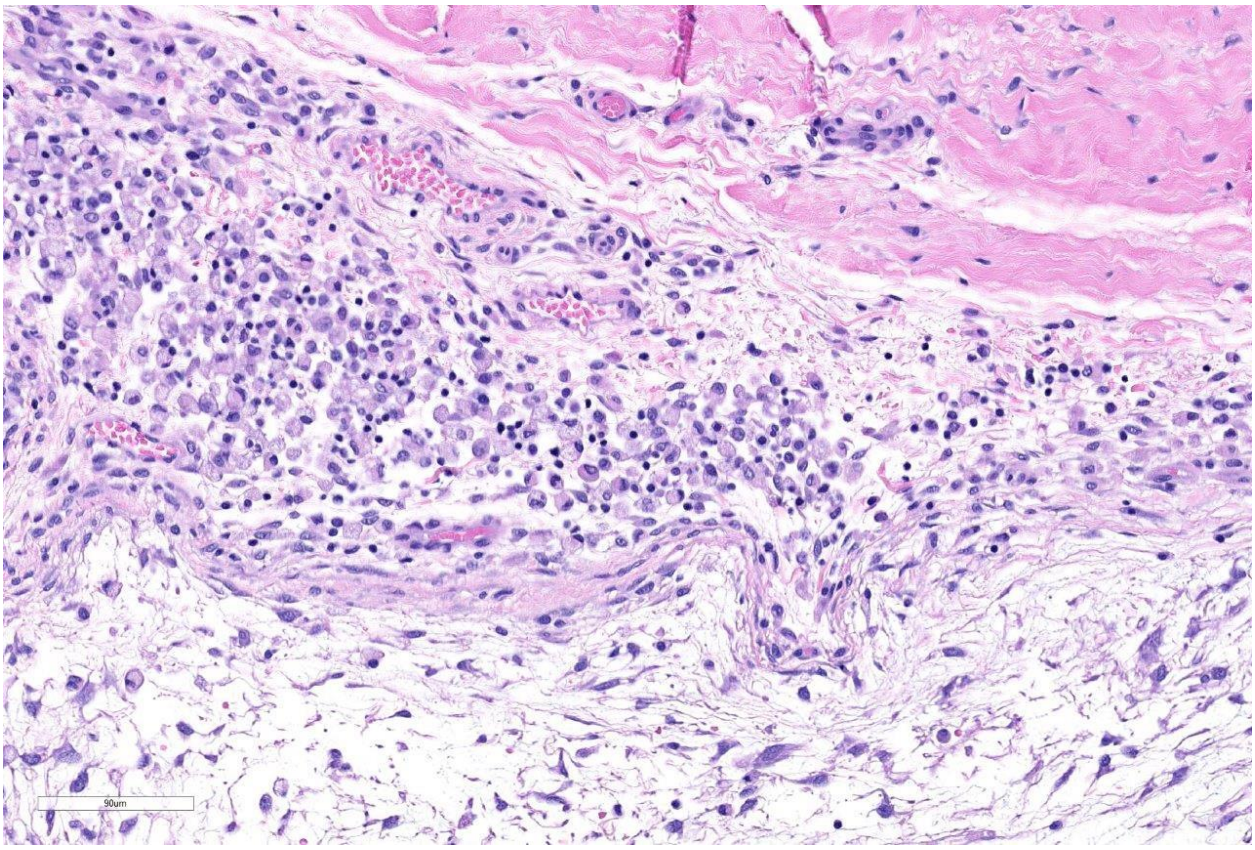

Stifle, dog. Higher magnification of the synovial neoplasm, demonstrated the multilobular nature, and myxomatous, occasionally cystic nature of the neoplasm. (HE, 16X)

layer is multifocally hyperplastic and jumbled up to 10 layers. The fibrous capsule is expanded by abundant fibrovascular tissue, adipose, and multifocal aggregates of plasma cells, lymphocytes, and fewer mast cells.

Contributor's Morphologic Diagnosis: Femorotibial (Stifle) Joint and associated skeletal muscle, Right Popliteal and Inguinal Lymph Nodes: Synovial myxoma with local invasion and multiple lymph node metastases

Contributor's Comment: Histiocytic sarcoma, synovial sarcoma, and synovial myxoma are three differentials for canine primary joint tumors.[2,3] All can cross joints and cause bony lysis and proliferation. Synovial myxoma occurs uncommonly in dogs and is widely considered to be a benign, but infiltrative, tumor of the joint. Numerous cases of lymph node metastases, however, have been observed (Contributing Institution experience). The stifle and digital joints are most commonly affected. The three types of cells in synovial membranes are Type A synoviocytes (macrophage/dendritic cell origin), type B (fibroblast-like), and type C ("transitional", hematopoietic, or stem cell-like). Although a joint tumor, the cell of origin of synovial myxomas is unknown; this is reflected in the non-specific immunohistochemistry (IHC). They are vimentin positive. Approximately 20-40% of synovial myxoma cells are CD18 immunoreactive and are morphologically indistinguishable from CD18 negative joint cells. Synovial myxomas are cadherin 11 and HSP25 immunoreactive, much like

synovial cell sarcomas and histiocytic sarcomas.[3] The most striking histologic feature of synovial myxomas is the sparse, stellate to spindle cells that elaborate abundant, coalescing nodules of myxomatous matrix.[2,3,5] Again, although cytomorphologic features are generally bland, synovial myxomas can metastasize to lymph nodes and be highly locally invasive.[2,3,5]

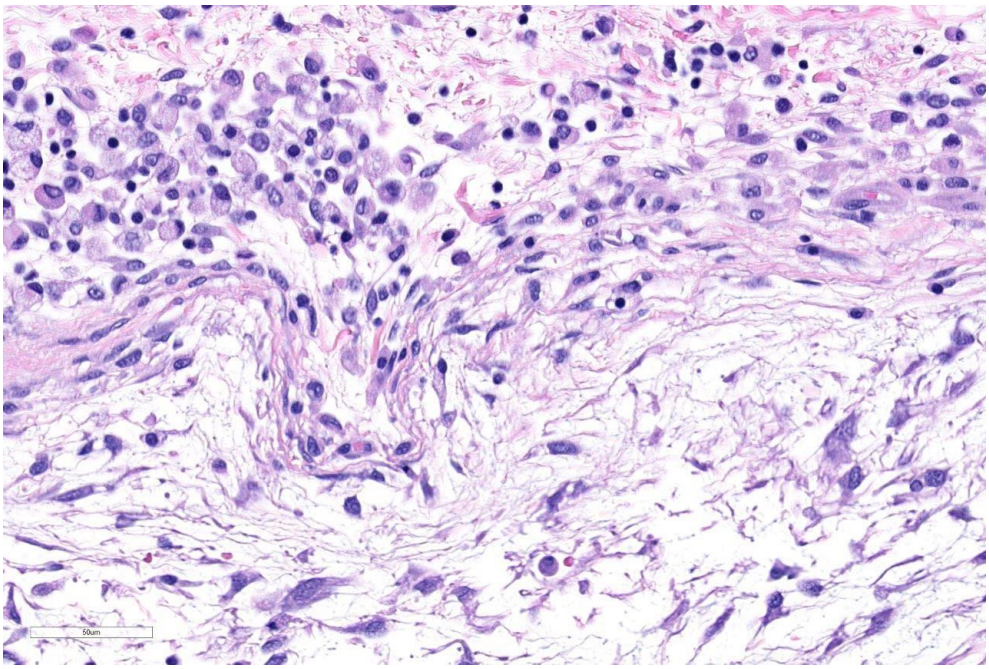

Stifle, dog. Neoplastic cells (at bottom) are spindled to stellate and separated by abundant myxomatous stroma. The periphery of the neoplasm contains numerous muciphages. (HE, 224X)

JPC Diagnosis: Joint, stifle (per contributor): Synovial myxoma, Labrador retriever, *Canis familiaris*.

Conference Comment: We thank the contributor for their institution's extensive work-up on this case and excellent quality gross images. Of the three differentials for canine joint neoplasms mentioned above, synovial myxoma is the second most common neoplasm occurring within the joints of dogs, behind histiocytic sarcoma and ahead of the rare synovial sarcoma (if such a tumor truly exists.) [1,3,4] This neoplasm most commonly affects middle-aged large breed dogs. Doberman pinschers and Labrador retrievers, as in this case, are most often affected. It has also been rarely reported in cats.[1,4] Synovial myxomas usually affect a single joint, with the stifle and digit the most commonly reported locations. These neoplasms are slow-growing and can persist for months to years and often present as chronic lameness with or without evidence of joint swelling.[1,3,4]

Although this is classified as a benign neoplasm, it can be locally infiltrative and cause lytic lesions in the bone with significant articular lesions and periarticular osteophyte formation. The conference moderator instructed that radiographically, synovial myxoma cannot be reliably differentiated from histiocytic sarcoma or synovial sarcoma.[3,4] Despite this locally invasive behavior, the prognosis is typically good after complete surgical excision. Bony lysis and infiltration usually necessitate amputation; however, cases that lack bone lysis and extension outside of the joint capsule can be treated with a simple synovectomy, which is curative in about 90% of reported cases. In contrast, histiocytic sarcomas are associated with a poor prognosis, with an average survival of just 5.3 months.[1,3,4] This significant

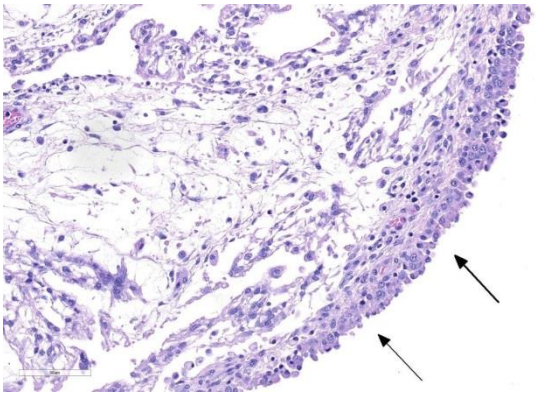

Stifle, dog. The surface of the neoplasm is covered by a layer of hyperplastic synovium up to 3 cell layers thick. (HE, 320X)

difference in biological behavior and prognosis highlights the importance of histopathology of the mass prior to treatment. Interestingly, the conference moderator and highly regarded veterinary pathologist with expertise in bone and joint pathology, Dr. Linden Craig, remarked that this is the first example of a synovial myxoma she has seen with metastasis. Given the observation by the contributor's intuition of multiple cases of lymph node metastasis for this neoplasm, Dr. Craig remarked that the biological behavior of this neoplasm may need further review.

Conference participants noted that once the tissue is identified as joint capsule with adjacent skeletal muscle, the diagnosis of synovial myxoma is relatively straight-forward. This neoplasm has a highly characteristic appearance of variably sized nodules of stellate to spindle cells with long cytoplasmic processes supported in a highly myxoid matrix and covered by a hyperplastic synovial lining.[1,3,4] The conference moderator noted that the cell of origin of synovial myxoma is not yet known; although, it is thought that given the abundant myxoid matrix, the cell type is likely type B (fibroblastic) synoviocytes. Type B synoviocytes normally produce hya-luronan, a large linear glycosaminoglycan and major component of synovial fluid.[1,3,4] Despite this uncertainty of cell origin, the diagnosis can usually be made without the aid of immuno-histochemical staining.

Contributing Institution:
University of California, Davis
School of Veterinary Medicine
Veterinary Medical Teaching Hospital
Anatomic Pathology Department
http://www.vetmed.ucdavis.edu/vmth/small_animal/anatomic_pathology/

References:

1. Craig LE, Ditmer KE, Thompson KG. Bones and joints. In Maxie, MG, ed. *Jubb, Kennedy, and Palmer's Pathology of Domestic Animals*, Vol I. 6th ed. Philadelphia, PA: Elsevier Ltd; 2016:159-162.
2. Craig LE, Julian ME, Ferracone JD. The diagnosis and prognosis of synovial tumors in dogs: 35 cases. *Vet Pathol*. 2002; 39(1):66-7.
3. Craig LE, Krimer PM, Cooley AJ. Canine synovial myxoma: 39 cases. *Vet Pathol*. 2010; 47(5):931-6.
4. Craig LE, Thompson KG. Tumors of joints. In: Meuten DJ ed. *Tumors in Domestic Animals*. 5th ed. Ames, IA: John Wiley and Sons Inc; 2017:337-350.
5. Izawa T, Tanaka M, Aoki M, Ohashi F, Yamate J, Kuwamura M. Incidental synovial myxoma with extensive intermuscular infiltration in a dog. *J Vet Med Sci*. 2012; 74(12):1631-3.

CASE II: JPC WSC-2 (JPC 4069828).

Signalment: Five-month-old Hereford-crossbred steer (*Bos taurus*).

History: Calves fed potatoes, 1 death in the herd. Calf showed neurological signs, focal seizures, blindness, head pressing. No response to thiamine or florfenicol.

Gross Pathology: The brain gyri were swollen and flattened. The rumen pH was 8, and the rumen contained two, small balls of plastic bags. The jejunum had several *Monezia expansa* cestodes. The costochondral junctions had a 7mm-thick, dense line of presumed cartilage core retention. Radiographs of thin sections have a dense white line.

Laboratory results: Blood lead concentration: 0.7 ppm (normal <0.3 ppm) Kidney lead concentration: 6.2ppm (Normal: 0.1-1.0 ppm) Hematocrit: 31%.

Histopathologic Description: A section of decalcified rib costochondral junction is examined. The zone of proliferating chondrocytes is longer than expected and proliferating chondrocytes can be seen in trabeculae far into the rib in retained, calcified cartilage. The invasion into chondrocytes is uneven, and while osteoblasts pile up in the hollow profiles of early-calcified chondrocytes, osteoclasts do not extend into these chondrocytes. The chambers of the initially invaded chondrocytes have erythrocytes, and a punctate, <2um basophilic "dusting" often fills these early chambers. The provisional calcified cartilage is retained far into the rib marrow space with only thin, apposed osteoid/bone. The provisional bone is thick and retained. Some osteoclasts are free in the marrow as opposed to being apposed to surfaces. Osteoclasts show more ani-socytosis with both size and shape variation and variable numbers of nuclei (osteoclastic dysplasia). Many dysplastic osteocytes have large, round and multiple inclusions. Bone marrow is otherwise hypocellular with serous degeneration of fat, and normal marrow constituents of the rib appear more distal from the costochondral junction than in a normal physis.

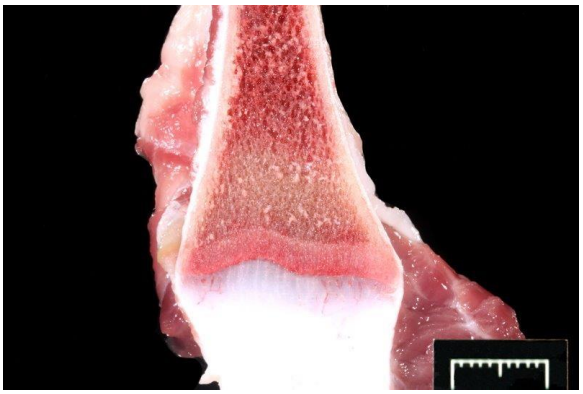

Rib, calf: The costochondral junctions had a 7mm-thick, dense line of presumed cartilage core retention (Photo courtesy of: Dept Vet Pathobiology, College Vet Med Biomed Sciences, Texas A&M University, http://vetmed.tamu.edu/vtpb)

Contributor's Morphologic Diagnosis: Rib, physis: chondrodystrophy with osteo-sclerosis, retained calcified cartilage**;** osteoclast dysplasia/hyperplasia.

Contributor's Comment: Costochondral line examination is part of a routine diagnostic necropsy examination. It demonstrates nutritional imbalances in any production mammal, or as in this case, mineralized cartilage retention usually due to osteoclast "problems" such as with BVDv persistently infected calves, canine distemper (Thompson 2007), and in our case, lead poisoning. Unfortunately, many people do not do it routinely.

The bone lesions of lead poisoning were well described in the early 1930's by several

Rib, calf: Radiographs of thin sections have a dense white line. (Photo courtesy of: Dept Vet Pathobiology, College Vet Med Biomed Sciences, Texas A&M University, http://vetmed.tamu.edu/vtpb)

authors studying poisoned children, and those descriptions remain valid. (Reviewed by Park 1933). The lead line in children will form once blood lead is 70-80 ug/dl. One month after treatment with chelating agents, the line separates from the zone of proliferating chondrocytes, and it will disappear in 4 years (Sachs 1981). Later descriptions added electron microscopic findings indicating that osteoclasts often lost their ruffled border and were less intimate with the surfaces (Eisenstein 1975). Nuclear and cytoplasmic inclusions were seen with EM. The cytoplasmic inclusions increased in size in osteoclasts more distant from the physis (inclusions fused?). Ultimately, morphologists concluded there is an inability for chondroclasts/osteoclasts to remove metaphyseal calcified cartilage cores presumably because they cannot degrade (or excrete) it. "They are thus constipated."(Eisenstein 1975) Interestingly, lead binds to osteocalcin to make a more compact molecule, and lead can cause a 40% increase of hydroxyapatite mineral over that bound with calcium (Dowd 2008). Might such modifications lead to "indigestion"- to continue the ANALogy (JFE)? The increase in osteoclasts is a compensatory hyperplasia. Lead poisoning-induced, osteoclast intra-nuclear inclusions are visible with electron microscopy (Hsu 1973). These inclusions of lead and protein aggregates are best-known in proximal renal tubules (where they make up 90% of the lead in kidneys), but are also in osteoclasts and less frequently in hepatocytes and glia (Goyer 1970, Moore 1974). Experimental and spontaneous studies demonstrate they may appear and regress in intoxicated individuals (Hzu 1973, Hamir 1983, Goyer 1970). EM shows them more frequently, and they are seen occasionally in light microscopy using Ziehl-Neelsen acid-fast stain. We could not see them reliably with acid-fast or PAS staining. In experimental lead poisoning of dogs (Zook 1972), metaphyseal sclerosis with retention of cartilage trabeculae having "more mineralized cartilage" with increased numbers of large osteoclasts distal from the physis were seen.

Obviously, the lines are seen in young animals' forming bones. Lead intoxication is more common in calves and thus are seen during calving season. Cattle usually have exposure to old lead base paints, discarded lead batteries, solder, linoleum, mining, smelting, and crankcase oil (ingested or used on skin as an insect repellant!) in pens or pastures (Blakley 1984, Burren 2010). Sometimes, recycling materials are incriminated (Payne 2008). Cases where pastures are previous shooting ranges have produced lead intoxications (Payne 2013). The decreased use of leaded gasolines has reduced risk of lead poisoning (Burren 2010). Blood, liver and kidney are favored samples to measure lead. When examining

blood, many animals having measurable blood lead will not show signs (diarrhea, seizures, bruxism, blindness, hemorrhages). The half-life of lead in exposed cattle is 135 days, std deviation 125 days (Bischoff 2012, Voigt 2010). Our calf was ill and had laminar cortical necrosis. Unfortunately, a specific lead source in this case was not found, and a farm visit was not allowed. The potatoes mentioned in the history were never provided and are considered a red herring.

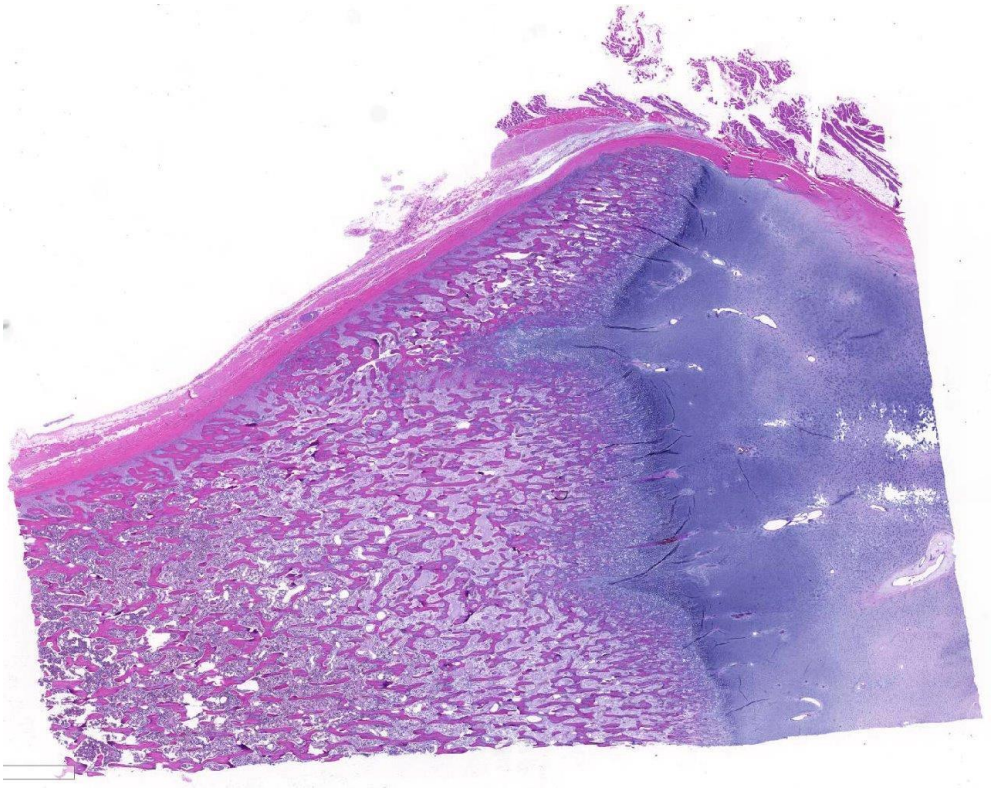

Rib, calf: Subgross magnification of the submitted tissue show a diffusely thickened epiphysis with two tongues of retained cartilage extending into the metaphysis. (HE, 5X)

JPC Diagnosis: Lone bone: Physeal dysplasia, with retention of cartilage cores, and focal necrosis, Hereford-crossbred steer, *Bos taurus*.

Conference Comment: We thank the contributor for his thorough and often satirical review of the skeletal lesions associated with lead toxicity in a young growing animal. The excellent quality gross image and radiographs provided by the contributor nicely demonstrate the thick band of sclerosis present in the metaphysis, known as the "lead line" mentioned above. Normally, growth of the bone at the metaphysis is the result of an orderly balance between osteoblastic deposition of bone and osteoclastic bone resorption at the zone of provisional calcification in the physeal zone of hypertrophy and primary spongiosa.[4,11] The majority of lead is stored within osseous tissues of the skeleton, and lead ions will preferentially deposit within the metaphysis and directly inhibit osteoclastic activity at this location.[16] As a result of this impairment of osteoclastic resorption of bone within the primary spongiosa, there is disruption of endochondral ossification and the formation of a growth retardation lattice.[4,11,16] This lattice is composed of elongated and vertically oriented trabecular bone with persistent cores of mineralized cartilage within the metaphysis. The sclerotic metaphysis is not radiopaque due to the lead itself; rather it is a result of calcium deposition and retention of mineralized cartilage trabeculae within the metaphysis.[4,11] As mentioned by the contributor, other diseases that cause growth retardation lattices include canine distemper virus (canine morbillivirus) and bovine

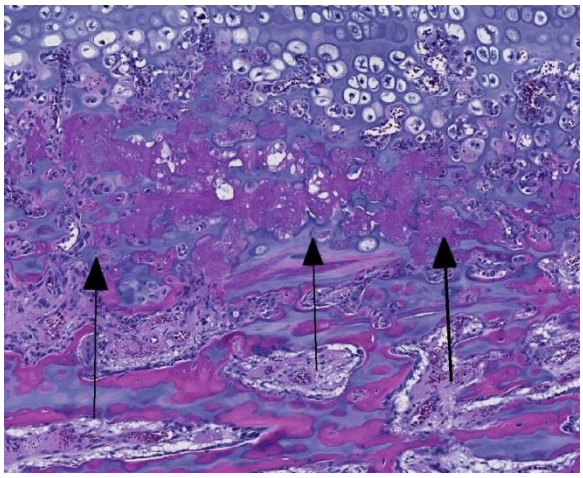

Rib, calf: Retained cartilage cores are lined by a necrotic coagulum (arrows). (HE, 88X)

pestivirus. Both viruses infect osteoclasts resulting in reduced bone resorption.[4,11]

This case generated spirited discussion among conference participants regarding whether the histologic lesions described in this case are consistent with lead intoxication. Conference participants described a diffusely thickened growth plate with multifocal tongues of cartilage cores extending into the metaphysis with a light blue to pink matrix and surrounded by a necrotic coagulum. Participants also noted few large vacuolated osteoclasts containing up to thirty nuclei within Howship's lacuna but were not able to identify intranuclear or intracytoplasmic inclusions noted by the contributor.

Prior to the conference, the moderator, Dr. Linden Craig, examined the long bones of several age-matched control calves without lead intoxication. The consensus opinion of the conference moderator and participants is that there is no significant difference between the amount of mineralized cartilage trabeculae in the calf from this case and an aged matched control animal. This represents a disconnect between the sclerotic metaphysis seen both grossly and radiographically in this case, and the histologic appearance which lacks the significant retention of mineralized cartilage trabeculae within the metaphysis when compared to the rib of age-matched control. Some participants posited that this may be an artifact of decalcification processing of this section. Without the aid of the gross, radiographic, and historical data, diagnosis of lead intoxication in this case is extremely difficult.

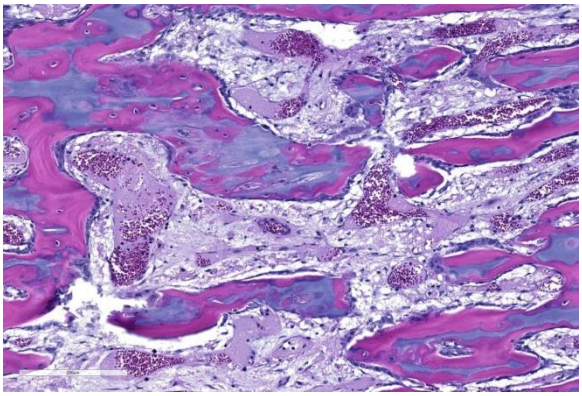

Rib, calf: Marrow spaces within the metaphysis are devoid of marrow elements. (HE, 152X)

Contributing Institution:
Department of Vet Pathobiology
College of Veterinary Medicine Biomed Sciences
Texas A&M University
http://vetmed.tamu.edu/vtpb

References:

1. Bischoff K, Thompson B, Erb HN, Higgins WP, Ebel JG, Hillebrandt JR. Declines in blood lead concentrations in clinically affected and unaffected cattle accidentally exposed to lead. *J Vet Dign Invest*. 2012; 24:182-7.
2. Blakley BR. A retrospective study of lead poisoning in cattle. *Vet Hum Toxicol*. 1984; 26: 505-7.

3. Burren BG, Reichmann KG, McKenzie RA. Reduced risk of acute poisoning in Australian cattle from used motor oils after introduction of lead-free petrol. *J Aust Vet Asso*. 2010; 88: 240-241.
4. Craig LE, Dittmer KE, ThompsonKG. Bones and joints. In: Maxie MG, ed. *Jubb, Kennedy and Palmer's Pathology of Domestic Animals*. Vol 1. 6th ed. Philadelphia, PA: Elsevier Ltd; 2016:16-87.
5. Dowd TL, Li L, Gundberg CM. The 1H NMR structure of bovine PB2-osteocalcin and implications for lead toxicity. *Biochim Biophys Acta*. 2008; 1784:1534-45.
6. Eisenstein R, Kawanoue S. The lead line in bon-A lesion apparently due to chondroclastic indigestion. *Am J Pathol*. 1975; 80: 309-16.
7. Goyer RA, May P, Cates M, Krigman MR. Lead and protein content of isolated intranuclear inclusion bodies from kidneys of lead-poisoned rats. Lab Invest. 1970; 22:245-251.
8. Hamir AN, Sullvan ND, Handson PD. Acid fast inclusions in tissues of dogs dosed with lead. J Comp Pathol. 1983; 93:307-17.
9. Hsu FS, Krook L, Shively JN, Duncan JR. Lead inclusion bodies in osteoclasts. *Science*. 1973; 181:447-8.
10. Moore JF, Goyer RA. Lead-induced inclusion bodies. Composition and probable role in lead metabolism. *Environ Health Perspec*. 1974; 7:121-7.
11. Olson EJ, Carlson CS. Bones, joints, tendons, and ligaments. McGavin MD,ed. *Pathologic basis of Veterinary Disease*. 6th ed. St. Louis, MO: Elsevier Mosby; 2017:964-965.
12. Park EA, Jackson D, Goodwin TC, Kajdi L. X-ray shadows in growing bones produced by lead; Their characteristics, cause, anatomical counterpart in the bone and differentiation. *J Pediatr*. 1933; 3: 265-300.
13. Payne JH, Holmes JP, Hogg RA, van der Burgt GM, Jewell NJ, Welchman G de B. Lead intoxication from clay pigeon shooting. *Vet Rec*. 2013; 173:552-4.
14. Payne J, Otter A, Cranwell M, Jones J, Wessells M, Whitaker K. Lead poisoning associated with recycled wood products. *Vet Rec*. 162: 191-2.
15. Sachs HK. The evolution of the radiographic lead line. *Radiol*. 1981; 139: 81-85.
16. Thompson K: Bones and joints. In: Maxie MG ed. *Jubb Kennedy and Palmer's Pathology of Domestic Animals*, 5th edition. Saunders Elsevier New York; 2007:53-54.
17. Voigt K, Benavides J, Rafferty A Howie F, Buxton D. Lead poisoning in calves with eosinophilic meningitis. *Vet Rec*. 2010; 167:791-2.
18. Zook BC. The pathologic anatomy of lead poisoning in dogs. Vet Pathol. 1972; 9, 310-327.

CASE III: 16N0558 (JPC 4084206).

Signalment: Nineteen-year-old quarter horse mare (*Equus ferus caballus*).

History: The horse presented to the teaching hospital for severe acute onset of right front limb lameness, from Middletown in Lake County, California. According to the owner,

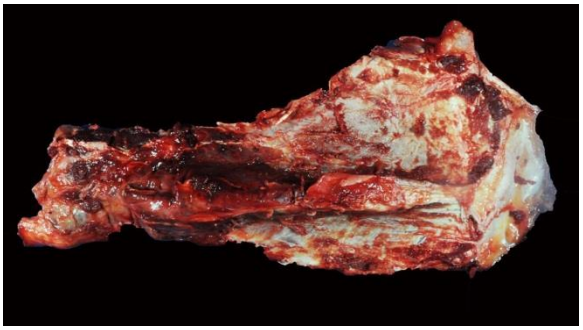

Scapula, horse: There is a transverse non-displaced fracture of the scapular neck and hemorrhage and edema within surrounding soft tissue (Photo courtesy of: University of California, Davis School of Veterinary Medicine, Veterinary Medical Teaching Hospital, Anatomic Pathology Department http://www.vetmed.ucdavis.edu/vmth/small_animal/anatomic_pathology/)

abnormal posturing began two weeks prior to presentation, and the horse was described as tucking its hind legs under itself. At that time, titers were negative for equine protozoal myeloencephalitis. Physical exam revealed toe dragging lameness of the right forelimb and asymmetric shoulder muscle atrophy, most pronounced on the right side. Radiographs of the proximal aspect of the right forelimb demonstrated a lytic bone lesion in the proximal scapula. In addition, multifocal heterogeneous mineral dense nodules were observed following the trachea from the thoracic inlet (cranial mediastinal lymph nodes), to the hilar region (tracheobronchial, caudal mediastinal lymph nodes). Ultrasound of the right scapula identified a severely irregular bone margin with mixed echogenicity, and soft tissue masses within the overlying skeletal muscle. A soft tissue sarcoma was suspected based on results from a fine needle aspirate of the masses.

Gross Pathology: Gross examination of the right scapula identified moderate hemorrhage and edema within the surrounding soft tissue as well as exuberant periosteal callus formation associated with a complete transverse, non-displaced fracture of the scapular neck. The skeletal muscle proximal to the fracture callus was diffusely atrophied, firm, pale, and intersected by bands of fibrosis. A second, more chronic complete fracture of the left supraglenoid tubercle was also identified. There were multifocal to coalescent regions of circumferential, porous cortical expansion of the ribs. Multiple, well-demarcated areas of bright red cortical discolouration were noted in the humeri. These lesions corresponded to regional osteolysis on clinical and post-mortem radiographs. The mineralized masses within the thorax were identified as enlarged, mineralized mediastinal and tracheobronchial lymph nodes

Laboratory results:

Biochemistry: (normal range)

Mild increase in creatinine kinase 348 IU/L (119-287)

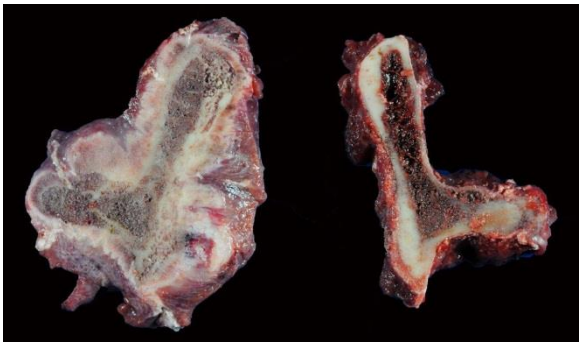

Scapula, horse: Sagittal section of the affected scapula (at left). (Photo courtesy of: University of California, Davis School of Veterinary Medicine, Veterinary Medical Teaching Hospital, Anatomic Pathology Department http://www.vetmed.ucdavis.edu/vmth/small_animal/anatomic_pathology/)

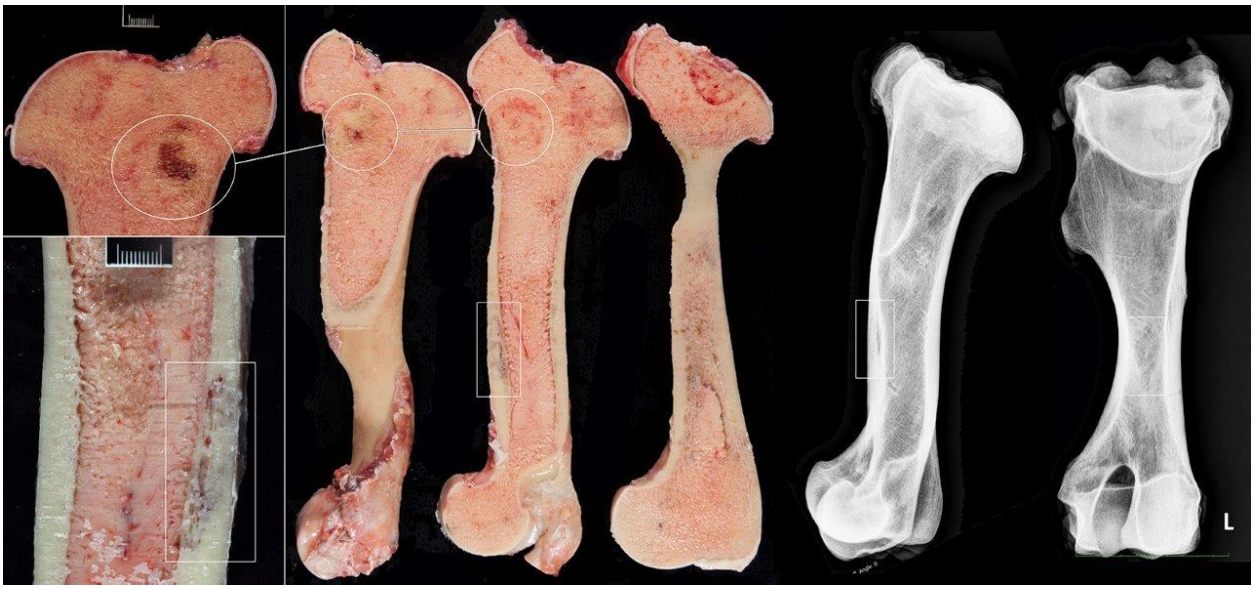

Scapula, horse: Multiple, well-demarcated areas of bright red cortical discoloration were noted in the humeri. (Photo courtesy of: University of California, Davis School of Veterinary Medicine, Veterinary Medical Teaching Hospital, Anatomic Pathology Department http://www.vetmed.ucdavis.edu/vmth/small_animal/anatomic_pathology/)

Histopathologic Description: Bone: The slide contains a single section of demineralized bone that lacks cortico-medullary distinction and consists of variably oriented and shaped, anastomosing osteochondral trabeculae. The section is embedded within and partially encased by a regionally necrotic and inflamed fibrovascular stroma. Dense fibrous and mildly congested tissue interdigitates with trabeculae at one section margin (presumed periosteal surface). Eighty percent of the bony trabeculae are composed of immature (woven) bone, and some contain cartilage. Lamellar bone is only preserved within larger trabeculae. Sharp edges, numerous, coalescing resorption bays (Howship's lacunae), and variation in trabecular shape and size is a result of resorption by large, hyperactive osteoclasts present in large numbers throughout the section. Osteoclasts contain up to 30 nuclei with often prominent eosinophilic nucleoli. Osteoclastic nuclei are occasionally arranged into circles resembling Langerhans giant cells. Osteoclasts are particularly abundant around the necrotic focus engulfing small shards of necrotic bone (presumed region of previous trauma) and some are noted within the surrounding stroma not adhered to the bone. Hyperactive osteoblasts accompany the osteoclasts and line most of the bone surfaces. A mosaic pattern of cement lines indicate ongoing dysregulated bone remodeling characterized by exuberant, seemingly random osteolysis and compensating osteoblastic activity. Inter-trabecular spaces are largely devoid of hematopoietic elements and filled by edematous, congested and mildly inflamed fibrous connective tissue. Inflammation consists of plasma cells, lymphocytes, and macrophages. Macrophages occasionally contain granular brown to golden cytoplasmic pigment (hemosiderin). Thin interlacing trabeculae of woven bone extend

There is extensive mineralization of the tracheobronchial lymph nodes. ((Photo courtesy of: University of California, Davis School of Veterinary Medicine, Veterinary Medical Teaching Hospital, Anatomic Pathology Department http://www.vetmed.ucdavis.edu/vmth/small_animal/anatomic_pathology/)

outwards from the presumed periosteal surface into the surrounding dense fibrous tissue (periosteal new bone formation vs callus).

Contributor's Morphologic Diagnosis: Bone, scapula: Severe, chronic, multifocal to coalescing osteolysis with atypical osteoclasts, aberrant bone remodeling, medullary fibrosis, and multifocal necrosis (consistent with silicate associated osteoporosis).

Contributor's Comment: Histologic examination of the tracheobronchial lymph nodes confirmed the presence of numerous fibrosing and mineralizing granulomas that contained moderate amounts of birefringent crystalline material. This finding, in conjunction with the osteoporotic skeletal lesions, and the geographic origin of the horse (from a location known to contain toxic soil silicate dioxide (cristobalite)) are consistent with a diagnosis of silicate associated osteoporosis (SAO). Without additional clinical information and knowledge of the bone sample skeletal site, differential diagnoses for this histological slide should broadly include a metabolic bone disease. For example, hyperactive osteoclasts and poor construction of new bone may be seen with fibrous osteodystrophy as a result of Ca++/P imbalance, variable nutritional deficiencies, vitamin D deficiency, and endocrinopathies.[4]

Pulmonary silicosis has been previously reported in both humans and horses, however, the associated osteoporotic syndrome appears unique to equids.[1] The underlying pathogenesis for this condition has yet to be elucidated.

Affected horses present with vague acute or chronic signs of lameness, often accompanied by weight loss, and variably by clinically evident pulmonary disease. Horses may appear to have bowing of one or both scapulae and accentuated lordosis. Acute lameness may be observed secondary to pathologic fractures often with ineffective attempts at repair as observed in this case. If

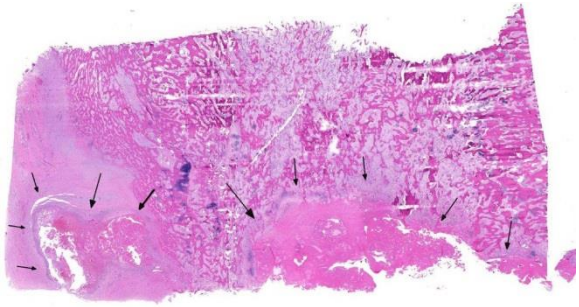

Scapula, horse: Subgross view of the submitted section of scapula. There is no evidence of cortical bone, and the section is composed of haphazardly arranged trabeculae of woven and lamellar bone, as well as extensive areas of necrotic bone. (HE, 6X)

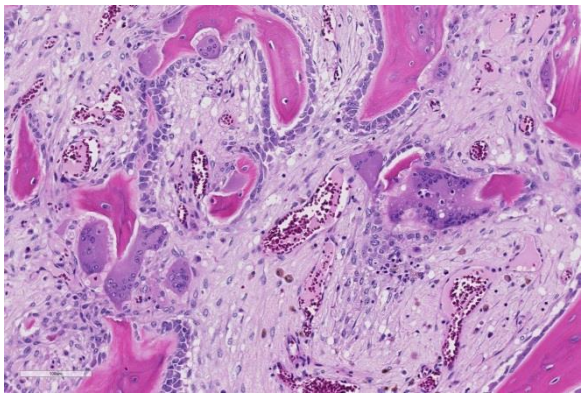

Scapula, horse: Osteoclasts are numerous, and in some cases, extremely large. (HE, 172X)

clinically silent, chronic fibrosing granulomas within the lung-draining lymph nodes and variably within the lungs are usually identified postmortem. Thoracic radiographs may detect an interstitial pattern of consolidated pulmonary nodules, but will often miss mineralized, lung-associated lymph nodes. Histologic examination of the granulomas reveals the typical pattern of central necrosis, marked fibrosis and mineralization surrounded by epithelioid macrophages and occasional giant cells. Small, angular, birefringent, intra- and extra-cellular crystals may be revealed under polarized light. The exorbitant reaction associated with such crystals is unique to the toxicity of cristobalite as compared to relatively innocuous accumulations associated with common anthracosilicotic nodules. Electron diffraction crystallography has been used to confirm the physical characteristics of crystals as cristobalite, (technique available in geology laboratories that analyze soil or stones).

Clinical and postmortem radiographs of the axilla and proximal appendicular skeleton are non-specific but may reveal poorly demarcated areas of osteoporosis and confirm bone deformity. Finding cervical facet joint osteoarthrosis is common in advanced cases of SAO. The radiographic appearance of bone lesions is variable but can be mistaken for neoplasia driven osteolysis as observed in this case.

Currently, the most sensitivity pre-mortem diagnostic test for this condition is bone nuclear scintigraphy.[4] The search for sensitive and specific clinical markers to detect early onset of the disease is ongoing.

Histologic examination of the affected bone reveals dysregulated resorption by morphologically atypical giant hyperactive osteoclasts.[1] Typical of SAO, the osteoclasts indiscriminately resorb pre-existing cortical and trabecular bone as well as newly formed woven bone. A mosaic pattern of cement lines is commonly observed in SAO bones; this microscopic feature is shared by human Paget disease of bone.[6] Multifocal areas of bony lysis, aberrantly increased regions of bone remodeling, pathologic fractures and aberrant giant osteoclasts are other similarities observed between these two disorders.[1] However, polyostotic Paget disease is restricted to specific age groups (elderly humans) and exhibits cessation of osteoclast activity over time. In contrast, SAO is observed in horses of all ages and shows progression of disease with time.[1,5] In addition, the skeletal distribution of SAO does not correspond with that observed in Paget disease.[1] The lesions of SAO have also been compared to fibrous osteodystrophy, however, skull lesions are uncommon in horses with SAO and only a

subset of affected horses exhibit elevations in parathyroid hormone.[1]

Unusual features of this case include the effacement of hematopoietic tissue within the medullary cavity and the identification of gross and radiographic lesions with the humeri.

JPC Diagnosis: Bone: Abnormal bone remodeling with myelofibrosis, proliferation of numerous large atypical osteoclasts, and focally extensive necrosis, quarter horse, *Equus ferus caballus*.

Conference Comment: This challenging case confounded even the most senior and experienced conference participants. Due to the lack of a recognizable corticomedullary junction or physiologic tissue border combined with severe distortion of the tissue by the disease process, attendees were unable to determine the type of bone this tissue section represented. Participants were impressed by the extensive and aberrant bone remodeling and resorption by atypically large and randomly located osteoclasts with vacuolated foamy cytoplasm and up to 30 supernumerary nuclei. These nuclei are sometimes arranged in circles resembling Langerhans giant cells in this section of bone. The constellation of lesions in this case combined with the historical data raise the index of suspicion for equine bone fragility syndrome (BFS), also known as silicate associated osteoporosis (SAO), although, as mentioned by the contributor, other metabolic bone diseases should also be considered as differential diagnoses.[1,2]

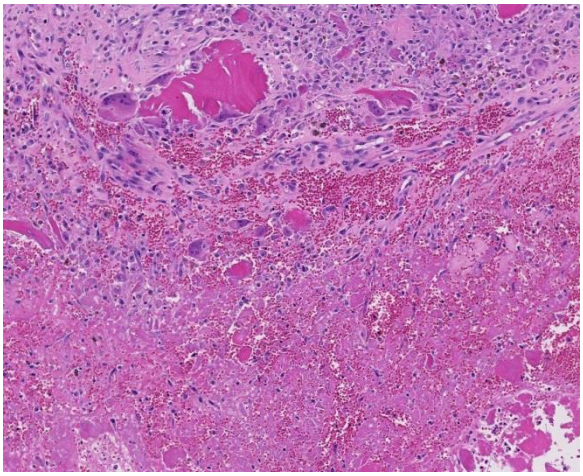

Scapula, horse: In the area of the fracture, there is abundant necrotic bone, granular debris, and hemorrhage, surrounded by a layer of granulation tissue. Bone fragments are being resorbed by multinucleated giant cell macrophages. (HE, 84X)

The pathogenesis and cause of bone fragility syndrome in horses is unknown. The vast majority of affected horses present concurrently with pulmonary silicosis and there is likely a causal relationship between the two conditions. As mentioned by the contributor, pulmonary silicosis, defined as silicate pneumoconiosis with accompanying pulmonary fibrosis, occurs secondary to inhalation of cytotoxic silica dioxide (SiO2) crystal polymorphs, including quartz, cristobalite, and tridymite.[1,2,3] Pulmonary silicosis with concurrent bone fragility syndrome has been reported with increased frequency in horses from areas with high levels of soil cristobalite, such as Monterey, Napa, and Sonoma regions of California; however, affected horses have also been seen in Oregon, Texas, Virginia, Illinois, and Kentucky.[1,2,3] The cytotoxic crystals associated with pulmonary silicosis are found worldwide, perhaps suggesting that this disease may be more widespread.[1,2] Readers are encouraged to review 2015

Wednesday Slide Conference #3 Case 4 for an excellent review of a suspected case of pulmonary silicosis in a horse from Monterey, California.

It is thought that the inhaled silicate stimulates the massive release of proinflammatory cytokines, IL-1, IL-6, and TNF-alpha, which stimulate inflammation and osteoclastogenesis via increased production of the RANKL and decrease in expression of the decoy receptor, osteo-protegerin.[1] Other proposed mechanisms of pathogenesis include hyperparathyroidism or an equine variant of Paget disease of bone in humans.[1,2]

Horses with bone fragility usually present with chronic lameness and skeletal deformities such as lateral bowing of the scapulae, lateral bowing of the rib cage, lordosis, and decreased range of motion in the cervical vertebrae.[1,2] Bones of both the axial and proximal portions of the appendicular skeleton, such as the scapula, in this case, are typically affected. Radio-graphically, there is severe osteopenia with multiple bony lucencies and exostoses at the articular facets as well as thickening of the rib consistent with extensive bone remodeling.[1,2] As a result of the severe osteoporosis associated with this disease entity, most animals die from a catastrophic pathologic fracture.[1,2] Conference participants noted that the large focally extensive area of necrosis in this tissue section may be the site of a pathologic fracture of the scapula.

Contributing Institution:

University of California, Davis
School of Veterinary Medicine
Veterinary Medical Teaching Hospital
Anatomic Pathology Department
http://www.vetmed.ucdavis.edu/vmth/small_animal/anatomic_pathology/

References:

1. Arens AM, Barr B, Puchalski SM, et al. Osteoporosis associated with pulmonary silicosis in an equine bone fragility syndrome. *Vet Pathol*. 2011; 48(3):593-615.
2. Arens AM, Puchalski SM, Whitcomb MB, et al. Comparison of the use of scapular ultrasonography, physical examination, and measurement of serum biomarkers of bone turnover versus scintigraphy for detection of bone fragility syndrome in horses. *J Am Vet Med Assoc*. 2013; 242(1):76-85.
3. Berry CF, OBrien TR, Madigan J, Hager DA. Thoracic radiographic features of silicosis in 19 horses. *J Vet Intern Med*. 1991; 5:248-256
4. Carlson CS, Weisbrode SE. Bones, joints, tendons, and ligaments. In: McGavin MD, Zachary JF, eds. *Pathologic Basis of Veterinary Disease*. 5th ed. St. Louis, MO, PA: Mosby Elsevier; 2012.
5. Symons JE, Entwistle RC, Arens AM, et al. Mechanical and morphological properties of trabecular bone samples obtained from third metacarpal bones of cadavers of horses with a bone fragility syndrome and horses unaffected by that syndrome. *Aust Vet J*. 2012; 73(11):1742-1751.
6. Seitz S, Priemel M, Zustin J, et al. Paget's disease of bone: histologic analysis of 754 patients. *J Bone Miner Res*. 2009; 24:62-69.

CASE IV: P3554.15 (JPC 4084557).

Signalment: 11-year-old castrated male domestic cat (*Felis catus*).

History: This cat presented with a history of chronic vomiting and weight loss. A firm and fixed intra-abdominal mass was palpated during physical examination. The mass consisted of a group of enlarged mesenteric lymph nodes and adjacent thickened intestinal wall at the ileocecocolic junction. The lymph nodes and a 20 cm-long intestinal segment were resected (limit between the normal and pathologic intestine not clear).

Gross Pathology: The mesenteric lymph nodes were moderately enlarged, irregular, white to pink, firm and gritty on cut section. The intestinal wall at the ileocecocolic junction was diffusely and severely thickened and focally expanded by a firm, multilobulated mass, 7 cm in diameter that partially occluded the lumen.

Laboratory results: N/A

Histopathologic Description: Mesenteric lymph node: The parenchyma is extensively effaced and replaced by thick branching and anastomosing, weakly cellular trabeculae of dense collagen separated by plump spindle-shaped cells (sclerosing fibroplasia) admixed with inflammatory cells, mainly eosinophils with fewer plasma cells, lymphocytes, mast cells and neutrophils. At the periphery of the sclerosing fibroplasia, spindle cells with fine branching collagen fibers dissect and efface the lymphoid tissue accompanied by a dense infiltrate of eosinophils. The remaining lymphoid tissue shows moderate follicular lymphoid hyperplasia. The branching collagen trabeculae were strongly positive for picrosirius red. Toluidine blue staining was performed to eliminate the possibility of a mast cell tumor.

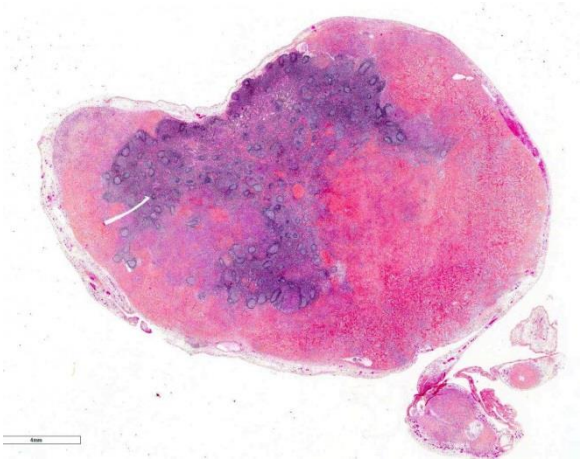

Mesenteric lymph node, cat. The periphery of the node is effaced by anastomosing trabeculae of fibrous connective tissue. The node is reactive as evidenced by prominent follicles. (HE, 6X)

Intestinal wall/mass (not submitted): Lesions similar to the mesenteric lymph nodes diffusely efface and replace the ileocecocolic submucosa and tunica muscularis, focally creating a mass effect. The mucosa has markedly increased numbers of eosinophils (lamina propria), and is multifocally and extensively ulcerated with granulation tissue. The lumen contains fibrinonecrotic debris admixed with numerous bacteria.

Contributor's Morphologic Diagnosis: Mesenteric lymph node: Eosinophilic lymphadenitis, marked, focally extensive, with sclerosing fibroplasia. Lesions are typical of feline gastrointestinal eosinophilic sclerosing fibroplasia (FGESF).

Contributor's Comment: Feline gastro-intestinal eosinophilic sclerosing fibroplasia (FGESF) is a recently described feline inflammatory condition affecting the gastrointestinal tract and associated lymph nodes.[1] FGESF is primarily a condition of

middle-aged cats although feline of almost any age can be affected. Male cats and the Ragdoll breed were overrepresented in a review of 13 cases.[5] Affected cats are usually presented with digestive signs, including vomiting, diarrhea, weight loss and inappetence. An abdominal mass is frequently detected, either by palpation or imaging and sometimes associated with regional lymphadenopathy. The mass most commonly occurs at the pyloroduodenal or ileocecocolic junction but can be found elsewhere along the intestines.[1,5] Bloodwork abnormalities that can be associated with this condition include hyperproteinemia associated with hyperglobulinemia, hypoalbuminemia, peripheral eosinophilia and mild neutrophilia.[5,8]

Histologically, FGESF lesions exhibit a characteristic pattern made of a network of coarse collagen trabeculae admixed with a large spindle cell population identified as myofibroblasts[1] mixed with inflammatory cells including numerous eosinophils.[1,5,7,8] The fibroplasia and inflammatory response extensively infiltrate the intestinal wall and, sometimes, regional lymph nodes. The intestinal mucosa is frequently ulcerated. Grossly and histologically, FGESF may resemble neoplasia, particularly, fibrosarcoma and extra-skeletal osteosarcoma; thus, FGESF must be included in the differential diagnosis of cats presented for abdominal mass and/or mesenteric lymphadenopathy.

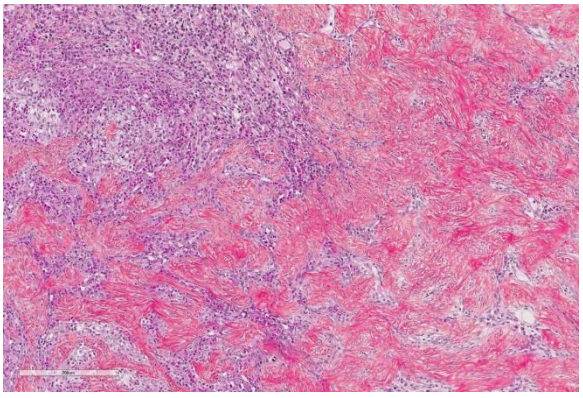

Mesenteric lymph node, cat. Higher magnification of the affected node, showing anastomosing collagenous trabeculae separated by a cellular infiltrate. (HE, 144X)

The etiopathogenesis of this condition is still not completely understood. The presence of bacteria, including gram-positive cocci as well as gram-positive and gram-negative rods have been associated with lesions in several studies,[1,5,8] but it is still unclear how bacteria contribute to the development and/or perpetuation of the condition. The location of lesions in close proximity or communicating with the normal bacterial flora makes it complicated to establish an association. In one study, IHC was performed and was negative for both FHV-1 and FCoV/FIP viral antigens.[5] It was also hypothesized that affected cats could suffer from immunologic dysregulation triggered by one or few factors, including parasitism, food allergy, dysbiosis or certain forms of IBD but again, no clear associations have been made. Nevertheless, eosinophilic inflammation seems to be a critical feature of this condition and is consistently predominant. Eosinophils produce a variety of mediators, including major basic protein (MBP), TGF-β, Il-1b, IL-6, that lead to tissue destruction and fibrosis.[1,5,7,8] A perpetuating inflammatory and fibrotic process is thought to be responsible for the proliferative nature of the pathology that gives rise to an intra-abdominal mass. Prognosis varies from good to guarded since infiltration is sometimes extensive and not surgically resectable (if located at the pyloroduodenal junction) but survival times can be good with a combination of appropriate surgical and medical treatments.[1,5,8]

JPC Diagnosis: Lymph node: Lymphadenitis, eosinophilic, diffuse, moderate with

marked anastomosing fibroplasia and moderate follicular and paracortical hyperplasia, domestic cat, *Felis catus*.

Conference Comment: Despite moderate slide variability, conference participants agree that this case is an excellent example of the characteristic microscopic features associated with feline gastrointestinal eosinophilic sclerosing fibroplasia (FGESF), which often includes effacement of mesenteric lymph nodes by haphazard branching and anastomosing trabeculae of dense collagen admixed with spindle cells and numerous eosinophils. These firm nodular lesions are typically identified at the pyloric sphincter or ileocecocolic junction in domestic cats, but can also be present in the duodenum, jejunum, colon, and mesenteric lymph nodes, as in this case.[1,3,5] As mentioned by the contributor, the prognosis following surgical removal depends on the location of the nodule and the surgeon's ability to completely excise the mass without causing functional impairment of the gastrointestinal (GI) tract. As a result, lesions in the distal intestinal tract (ileocecocolic junction and colon) are associated with a better surgical prognosis than lesions encompassing the pyloric sphincter.[1,2,8]

Prior to the initial description and publication of this unique lesion in the feline GI tract by Craig et al, the characteristic trabeculae of dense collagen were often misinterpreted as osteoid, leading to an erroneous diagnosis of extra-skeletal osteosarcoma.[1] Additionally, the marked eosinophilic component admixed with scattered, well-differentiated, perivascular mast cells resulted in the interpretation of some of these lesions as feline sclerosing mast cell tumors.[4] In this case, histochemical staining with Masson's trichrome produced intense blue staining of the anastomosing

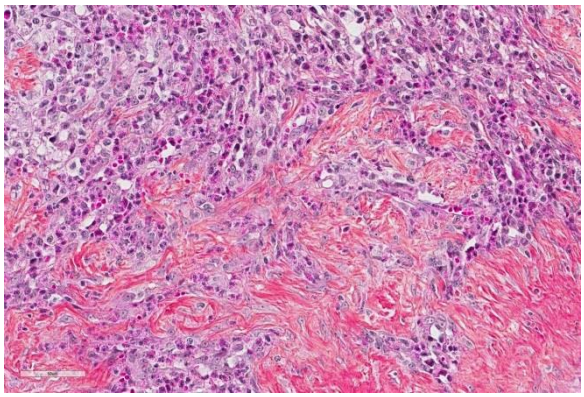

Mesenteric lymph node, cat. Higher magnification of the periphery of the mass, showing a dense, eosinophil rich inflammatory infiltrate enmeshed in fine fibrils of collagen. (HE, 400X)

trabeculae, confirming the presence of collagen.

Although the etiology and pathogenesis of this lesion is unknown, the conference moderator (Dr. Craig, referenced above) posits that it is likely an inflammatory process rather than neoplastic, similar to other feline eosinophilic inflammatory lesions, such as feline indolent ulcer, eosinophilic plaque, eosinophilic granuloma, and hypereosinophilic syndrome.[1,3] As mentioned by the contributor, the majority of previously reported cases are associated with bacterial infection, demonstrated by both gram-positive and gram-negative rods and cocci embedded within the sclerotic collagen;[1] however, there have been reports of FGESF associated with fungal infection, *Toxoplasma gondii* [1] and the alimentary nematode parasite (*Cylcoospirura* spp.) in a free-ranging puma. Additionally, there have also been reports of similar lesions present in the subcutis and abdomen of cats in Japan caused by methicillin-resistant *Staphylococcus* spp.[6]

Interestingly, in nearly half of reported cases by Craig, et al, no infectious etiology was detected.[1] In this case, a battery of histochemical stains run by the Joint

Pathology Center prior to the conference failed to reveal any infectious agents within dense bands of collagen. In cats that develop eosinophilic granulomatous disease, there may be an inherited genetic mutation leading to eosinophil dysregulation and inappropriate eosinophilic response to a variety of inflammatory stimuli.[1,3,7] This may contribute to the pathogenesis of this disease in certain predisposed individuals with or without evidence of an infectious agent.[1]

Contributing Institution:
Faculty of Veterinary Medicine
Université de Montréal
http://www.medvet.umontreal.ca/index.html

References:

1. Craig L, Hardam E, Hertzke D, et al. Feline gastrointestinal eosinophilic sclerosing fibroplasia. *Vet Pathol.* 2009; 46: 63–70.
2. Eckstrand CD, Barr BC, et al. Nematode-associated intramural alimentary nodules in pumas are histologically similar to gastro-intestinal eosinophilic sclerosing fibroplasia in domestic cats. *J Comp Pathol*. 2013; 148(4):405-409.
3. Grau-Roma L, Galindo-Cardiel I, et al. A case of feline gastro-intestinal eosinophilic sclerosing fibroplasia associated with phycomycetes. *J Comp Pathol*. 2014; 141:318-321.
4. Halsey CHC, Powers BE, Kamstock DA. Feline intestinal sclerosing mast cell tumour: 50 cases (1997-2008). *Vet Comp Oncol.* 2010; 8:72-79.
5. Linton M, Nimmo J S, Norris J M, et al. Feline gastrointestinal eosinophilic sclerosing fibroplasia: 13 cases and review of an emerging clinical entity. *J Feline Med Surg*. 2015; 17:392-404.
6. Ozaki K, Yamagami T, Nomura K, Haritani M, Tsutsumi Y, Narama I. Abscess-forming inflammatory granulation tissue with gram-positive cocci and prominent eosinophil infiltration in cats: Possible infection of methicillin-resistant *Staphylococcus*. *Vet Pathol*. 2003; 40:283–287.
7. Suzuki M, Onchi M and Ozaki M. A case of feline gastro-intestinal eosinophilic sclerosing fibroplasia. *J Toxicol Pathol*. 2013; 26:51-53.
8. Weissman A, Penninck D, Webster C, et al. Ultrasonographic and clinico-pathological features of feline gastrointestinal eosinophilic sclerosing fibroplasia in four cats. *J Feline Med Surg*. 2013; 15:148-154.

Self-Assessment - WSC 2016-2017 Conference 21

1. Which of following best describes synovial myxomas?
    a. Benign, expansile
    b. Benign, infiltrative
    c. Malignant, expansile
    d. Malignant, infiltrative

2. Which of the following is the likely cell of origin of synovial myxomas ?
    a. Type A synoviocytes
    b. Type B synoviocytes
    c. Type C synoviocytes
    d. Macrophages

3. Which of the following best describes a “lead line” ?
    a. Vertical streaks of woven bone extending downwards from the epiphysis.
    b. Horizontal bands of sclerotic bone in the metaphysis
    c. Radographic lucent lines in the metaphysis
    d. A line of cyanosis above the gums of affected cattle.

4. Which of the following is a histologic feature of silica-associated osteopetrosis?
    a. Multinucleated osteoblasts
    b. Granulomas containing bifringent cristobalite within marrow spaces
    c. Giant osteoclasts
    d. Well-ordered cement lines in remodeled bones

5. Which of the following breeds of cats is over-represented in studies of feline gastrointestinal eosinophilic sclerosing hyperplasia?
    a. Ragdoll
    b. Himalayan
    c. Burmese
    d. Havana Brown

Joint Pathology Center

Veterinary Pathology Services

WEDNESDAY SLIDE CONFERENCE 2016-2017

C o n f e r e n c e 22

5 April 2017

CASE I: 2671-16 (JPC 4081675).

Signalment: 10-days-preterm, male, cynomolgus macaque fetus (*Macaca fascicularis*).

History: A male cynomolgus macaque fetus was aborted from an 8-year-old female multiparous dam macaque of Vietnam origin. The female macaque had not undergone any experimental procedures or manipulations and was used as a control animal for pregnancy and infant developmental study. The dam was in good general health and was negative for Herpes B, SRV, SIV, STLV, tuberculosis, and parasites on routine health monitoring. The dam was mated to a breeding male cynomolgus macaque and pregnancy was confirmed by ultrasound diagnosis with the visualization of the gestational sac. At gestation day GD60, a large anechoic, abnormal round cystic space was observed in the abdominal region of the developing fetus. Abnormalities were not apparent on subsequent ultrasound scans at GD90 and GD120. The fetus had a viable heart beat up to the final ultrasound scan at GD120, before abortion occurred at GD146 (about ten days before estimated due date).

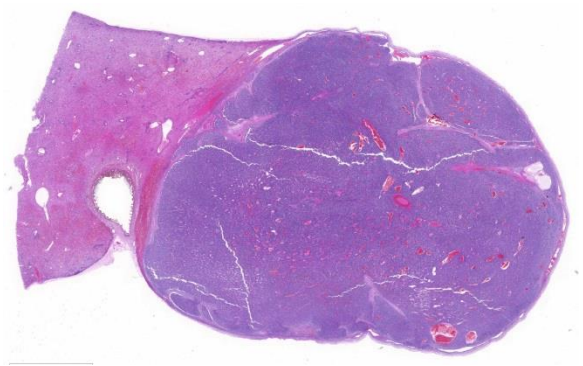

Liver, cynomolgus abortus: The liver is focally expanded by a nodular, moderately cellular neoplasm. (HE, 6X)

Gross Pathology: The fetus was presented dead with umbilical cord and placenta intact. On external examination, there was severe congestion of the head indicating dystocia at birth, likely caused by an enlarged fetal abdominal circumference resulting in difficult passage through pelvic canal. Meconium was present in the fetal fluid which indicated fetal stress at birth and confirmed that animal was alive during birth. Abdominal cavity contained a large amount of blood-tinged fluid. The fetus had

a large liver mass and a cystic structure attached to the left abdominal wall.
At necropsy and examination of visceral organs, expanding the right border of the right median liver lobe, compressing hepatic parenchyma and adjacent gallbladder was a 4cm x 1.7cm x 2.1cm, white to light brown nodular mass. Nodules of this neoplasm were surrounded by fibrovascular tissue, and the neoplasm was well-demarcated and encapsulated.

Laboratory results: None

Histopathologic Description: Histologically, neoplasm in the right median liver lobe was characterized by an expansile and fairly well-demarcated proliferation of neoplastic cells, arranged in sheets, cords and packets with primitive tubular and acinar formations, separated by fibrovascular stroma. Cells are polygonal, have well-defined cell borders, and often form pseudorosettes. Neoplastic cells are 10-15 µm in diameter, have high nuclear to cytoplasmic ratio, pale vesiculate eosinophilic to basophilic cytoplasm, central round to oval moderately stippled nuclei with 1-2 nucleoli. Large numbers of extramedullary hematopoietic cells are present between the cords and packets of neoplastic cells. The neoplastic cells have strong diffuse positive cytoplasmic immunolabelling for pancytokeratin (MNF116), cytokeratin 18 and alpha-fetoprotein, strong membrane and moderate to weak cytoplasmic beta-catenin immuno-labelling. The neoplastic cells are diffusely negative for vimentin, chromogranin-A, neuron specific enolase (NSE). Histopathology and immunohistochemistry results indicate a hepatoblastoma of embryonal subtype for this neoplasm.

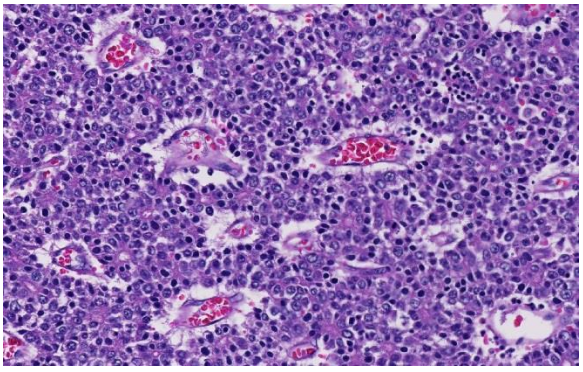

Liver, cynomolgus abortus: Neoplastic cells are polygonal to pyramidal and often palisade around blood vessels (pseudorosette formation.) (HE 240X)

Contributor's Morphologic Diagnosis: Macaque fetal liver: Hepatoblastoma (embryonal subtype).

Contributor's Comment: Hepatoblastoma (HBL) is a malignant tumor that arises from embryonic and fetal hepatocytes and is comprised of mixed epithelial, mesenchymal, undifferentiated components, and typically classified into two categories of epithelial or mixed epithelial-mesenchymal.[1,2] Epithelial HBL is subcategorized into fetal, mixed fetal-embryonal (most common), macrotrabecular and anaplastic small cell types, while the mixed type contains immature mesenchymal components. [5,6] These tumor subtypes, among other pediatric liver tumors, are well-illustrated in a fairly recent publication by Tanaka Y, 2013.[8] In humans, HBL is the most common pediatric liver malignancy and is usually diagnosed within the first three years of life. About two-thirds of liver masses are malignant in children and approximately 70% of these are hepatoblastomas or hepatocellular carcinomas.[2]

Hepatoblastoma is a rare tumor in domestic animals and have been reported in the dog, alpaca, horse, mouse, and cat. [6,8,9,10,11,12,13,14] While other induced and naturally occurring hepatic tumors have been reported in cynomolgus macaques, hepatoblastoma is a tumor that has not been reported in literature from this species.

Hepatoblastomas and their subtypes in humans can be further characterized by immunohistochemistry markers such as alpha fetoprotein (AFP), glypican 3 (GPC3), carbamoyl phosphate synthetase 1 (CSP1), vimentin, cytokeratin and beta-catenin. [2, 7] Classification of the hepatic tumor in this fetal macaque tumor was attempted based on the neoplastic cell morphology and immunohistochemistry results using the recently published classification for pediatric liver tumor by López-Terrada D.[2]

AFP is expressed in normal, non-neoplastic human fetal liver and is also seen in human liver tumors and some germ cell tumors. In this study, AFP was weakly expressed by hepatocytes of liver parenchyma adjacent to the hepatoblastoma, while strong positive AFP immunolabelling by neoplastic cells of the hepatoblastoma highlighted architecture of the neoplastic embryonal hepatocytes and supported diagnosis of embryonal subtype of hepatoblastoma for this fetus's liver tumor. As AFP is also a secreted protein, increased background and serum labeling of AFP could also be seen in immuno-histochemically labeled sections, [7] and was also noted in blood vessels of AFP labeled sections of this fetal macaque's tumor. While AFP is currently the most reliable and consistent marker in hepatoblastoma,[4] approximately 5-10% of human hepato-blastomas are negative for AFP and other markers such as Delta-like homolog (DLK1) are being investigated as potential serum markers for diagnosis of this tumor.[15]

Pancytokeratin expression in human hepatoblastomas can be variable while vimentin is negative on the epithelial components.[7] Cytokeratin 18 (CK18) is expressed in adult epithelial tissues such as liver, lung, kidney, pancreas, gastrointestinal tract, mammary glands and their associated tumors, and an increased CK18 expression in several cancer types of human patient is linked to poorer prognosis.[16] In this study, the strong positive pancytokeratin and CK18 expression by the fetal hepatic neoplasm are consistent with hepatocyte lineage of the neoplastic cells. The negative and much smaller tumor area of vimentin labeling on the mesenchymal components of the liver tumor, in this case, indicate a hepatoblastoma with predominant epithelial cell component.

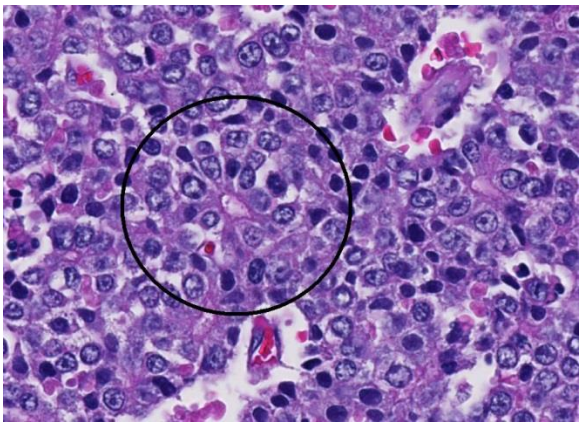

Liver, cynomolgus abortus: Neoplastic cells rarely form true rosettes (circled). (HE 400X)

Hepatoblastomas in both humans and mouse have high prevalence of deletion mutation in GSK-3β binding region of β-catenin gene of Wnt signalling pathway, with approximately 80-90% of hepatoblastomas in humans having mutations in beta-catenin (CTNNB1).[2, 7, 17] The nuclear and/or cytoplasmic pattern of expression of β-catenin could be used to distinguish between neoplastic hepatic and biliary hepatocytes. [2, 7] Specifically, non-neoplastic hepatocytes and biliary epithelium have only distinct membranous beta-catenin labeling, while cytoplasmic expression of beta-catenin indicates the epithelial cells of neoplastic nature.[2, 7]

Neoplastic cells of the liver, in this case, have cytoplasmic beta-catenin immunolabelling.
Based on histopathology findings and positive pancytokeratin (MNF116), cytokeratin 18, alpha-fetoprotein, as well as the cytoplasmic beta-catenin immunohistochemistry results, current findings are indicative of an embryonal subtype of hepatoblastoma in the liver of this macaque fetus.

JPC Diagnosis: Liver: Hepatoblastoma, cynomolgus macaque fetus, *Macaca fascicularis*.

Conference Comment: The contributor provides an outstanding review of the immunohistochemical staining characteristics of hepatoblastomas in a fetal cynomolgus macaque. Hepatoblastomas are thought to be derived from the pluripotential stem cell progenitor cells in the liver and usually occur in very young or fetal animals, as in this case; although there are rare reports in adults.[4,7] As in other embryonal neoplasms reported in animals, such as nephroblastomas, neuroblastomas, and medulloblastomas, hepatoblastomas are composed of primitive poorly differentiated blastic cells.[7,18] Participants noted the prominent arrangement of neoplastic cells into rosettes, pseudorosettes, sheets, and solid cords separated by variably sized vascular spaces.[3,4,7] Although not a prominent feature in this case, some reported hepatoblastomas can display squamous, chondrous, or osseus metaplasia, which reflect the ability the ability of this neoplasm to have widely divergent differentiation. In animals and humans, these neoplasms are classified in epithelial (fetal or embryonal), mesenchymal, and mixed patterns with combinations of neoplastic cell types occurring within a single neoplasm. The fetal form is composed of large polygonal cells with abundant vacuolated eosinophilic cytoplasm. The embryonal form is composed of smaller neoplastic polygonal cells arranged in ribbons and rosettes and is the predominant form featured in this case.[4] Human epithelial hepatoblastomas are further categorized into fetal, embryonal and mixed, macrotrabecular, or anaplastic small cell types.[4,7] The fetal macrotrabecular subtype can appear remarkably similar to hepatocellular carcinoma, with trabeculae of neoplastic cells piling up to ten layers thick. The Anaplastic small cell subtype is arranged in sheets and is difficult to distinguish from the other blastic neoplasms mentioned above. Mesenchymal subtypes are mainly comprised of undifferentiated spindle cells, cartilage, bone, or striated muscle.[4,7,18]

Conference participants noted that there is a marked increase in extramedullary hematopoiesis (EMH) as characterized by erythroid precursor cells and megakaryocytes within the solid portions of the mass when compared to the normal adjacent liver parenchyma. This is a commonly reported phenomenon of this neoplasm. Although EMH is not uncommon in the fetal liver, the marked increase within the neoplasm compared to the normal liver tissue stimulated some discussion among attendees. The molecular pathogenesis of EMH within hepatoblastomas is not yet known; however, it is thought that the primitive neoplastic cells may retain the CD34 positive multipotential nature of bone marrow origin cells and can differentiate into erythroid precursors and megakaryocytes under the influence of hematopoietic cytokines such as IL-6, G-CSF, and GM-CS.[15] The presence of EMH within the neoplasm can assist in differentiating hepatocellular carcinoma and macrotrabecular hepatoblastoma, which can have a similar morphology.[15]

Contributing Institution:
Advanced Molecular Pathology Laboratory
Institute of Molecular and Cell Biology
Proteos, Singapore

References:

1. Ano N, Ozaki K, Nomura K, Narama I. Hepatoblastoma in a cat. *Vet Pathol*. 2011; 48(5):1020-3.
2. De Vries C, Vanhaesebrouck E, Govaere J, Hoogewijs M, Bosseler L, Chiers K, Ducatelle R. Congenital ascites due to hepatoblastoma with extensive peritoneal implantation metastases in a premature equine fetus. *J Comp Pathol*. 2013 Feb;148(2-3):214-9.
3. Cullen JM. Tumors of the liver and gallbladder. In: Meuten DJ, ed. *Tumors in Domestic Animals*. 5th ed. Ames, IA: Wiley Blackwell; 2017:853-855.
4. Cullen JM, Stalker MJ. Liver and biliary system. In: Maxie MG, ed. *Jubb, Kennedy and Palmer's Pathology of Domestic Animals*. Vol 2. 6th ed. Philadelphia, PA: Elsevier Ltd; 2016:347-348.
5. Falix FA, Aronson DC, Lamers WH, Hiralall JK, Seppen J. DLK1, a serum marker for hepatoblastoma in young infants. *Pediatr Blood Cancer*. 2012 Oct;59(4):743-5.
6. Helmberger TK, Ros PR, Mergo PJ, Tomczak R, Reiser MF. Pediatric liver neoplasms: a radiologic-pathologic correlation. *Eur Radiol*. 1999;9(7):1339-47.
7. Kim Y, Sills RC, Houle CD. Overview of the molecular biology of hepatocellular neoplasms and hepatoblastomas of the mouse liver. *Toxicol Pathol*. 2005; 33(1):175-80.
8. López-Terrada D, Alaggio R, de Dávila MT, Czauderna P, Hiyama E, Katzenstein H, Leuschner I, Malogolowkin M, Meyers R, Ranganathan S, Tanaka Y, Tomlinson G, Fabrè M, Zimmermann A, Finegold MJ; Children's Oncology Group Liver Tumor Committee. Towards an international pediatric liver tumor consensus classification: proceedings of the Los Angeles COG liver tumors symposium. *Mod Pathol*. 2014 Mar;27(3):472-91.
9. Loynachan AT, Bolin DC, Hong CB, Poonacha KB. Three equine cases of mixed hepatoblastoma with teratoid features. *Vet Pathol*. 2007 Mar;44(2):211-4.
10. Neu SM. Hepatoblastoma in an equine fetus. *J Vet Diagn Invest*. 1993 Oct;5(4):634-7.
11. Nonoyama T, Fullerton F, Reznik G, Bucci TJ, Ward JM Nonoyama T, Fullerton F, Reznik G, Bucci TJ, Ward JM: Mouse hepatoblastomas: a histologic, ultrastructural, and immunohistochemical study. *Vet Pathol*. 25: 286–296, 1988
12. Nonoyama T, Reznik G, Bucci TJ, Fullerton F. Hepatoblastoma with squamous differentiation in a B6C3F1 mouse. *Vet Pathol*. 1986 Sep;23(5):619-22.
13. Shiga A, Shirota K, Shida T, Yamada T, Nomura Y. Hepatoblastoma in a dog. *J Vet Med Sci*. 1997 Dec;59(12):1167-70.
14. Tanaka Y, Inoue T, Horie H. International pediatric liver cancer pathological classification: current trend. *Int J Clin Oncol*. 2013 Dec;18(6):946-54.
15. Thambi R, Lekshmi D, et al. Extramedullary hematopoiesis as a clue to diagnosis of hepatoblastoma on fine needle aspiration cytology: A

report of two cases. *J Cytol*. 2013; 30(3):198-200.
16. Watt BC, Cooley AJ, Darien BJ. Congenital hepatoblastoma in a neonatal alpaca cria. *Can Vet J*. 2001 Nov;42(11):872-4.
17. Weng YR, Cui Y, Fang JY. Biological functions of cytokeratin 18 in cancer. *Mol Cancer Res*. 2012 Apr;10(4):485-93.
18. Wright JR Jr, Pinto-Rojas A, Trevenen CL, Yu W. Teratoid features in mixed hepatoblastoma. *Vet Pathol*. 2010 Sep;47(5):1003-4.

CASE II: MS1602402 (JPC 4087117).

Signalment: Four-month-old female arginase vasopressin receptor knock-out (V1aR KO) mouse (*Mus musculus*).

History: This breeder female mouse was found to have dystocia. It was treated with subcutaneous fluids and was subsequently euthanized.

Gross Pathology: A female 4-month-old black mouse was submitted following euthanasia. The subcutaneous tissues were mildly dry. The mouse was pregnant with two full term fetuses present within the left uterine horn and none present in the right uterine horn. The pubis was poorly dilated. The two fetuses within the left uterine horn appeared to be mild to moderately autolyzed, consistent with fetal death in utero. A placental disc was present associated with each fetus and five additional placental discs were present within the left uterine horn. The heart, lungs, liver, kidneys, spleen and GI tract appeared normal.

Laboratory results: A bacterial culture obtained from the uterus yielded *Pasteurella pneumotropica*, *Enterococcus faecalis* and *Enterococcus gallinarum*.

Histopathologic Description: Microscopic examination revealed a moderate acute suppurative placentitis with bacterial colonies of coccobacilli associated with the

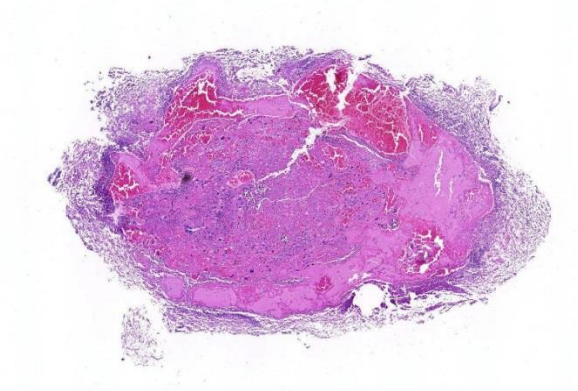

Placenta, mouse. Normal hemochorial placental architecture is effaced by large areas of hemorrhage and necrosis. The allantochorion is arrayed around the placenta as a result of placement in the cassette. (HE, 16X)

inflammation. Moderate numbers of degenerative neutrophils were present along the maternal and fetal margins of the placenta. Some sections had neutrophilic foci within the placenta. Mild multifocal mineralization was noted within the placental disc. Moderate diffuse mineralization of the placental labyrinth capillary walls was evident and confirmed by von Kossa stain. Some sections included placental membranes with a moderate necrosuppurative amniochorionitis evident, associated with coccobacilli. Coccobacilli are gram-negative on gram stains.

There was moderate to severe multifocal necrosuppurative endometritis with bacterial colonies present associated with the uterine inflammation. One of the two fetuses examined had moderate autolysis consistent with death in utero, with no evidence of inflammation or bacteria. No other significant lesions were noted.

Contributor's Morphologic Diagnosis: 1. Placenta, placentitis, acute, suppurative, moderate to severe, with gram-negative coccobacilli.
2. Placental labyrinth capillaries, mineralization, diffuse, moderate
3. Placental membranes, amniochorionitis, necrosuppurative, acute, moderate to severe

Contributor's Comment: Morbidity, in this case, was due to endometritis, placentitis, and fetal death in utero due to reproductive tract infection with *Pasteurella pneumotropica*. *Pasteurella pneumotropica* is a non-motile, gram-negative cocco-bacillus. Diagnosis is usually by bacterial culture or PCR analysis. It grows well on blood agar under aerobic conditions with 7-10% CO2 at 37 degrees Celsius.[12] It is non-hemolytic, oxidase, catalase, urease and indole positive and ferments glucose, sucrose, and maltose without gas production.[7] Two biotypes, Heyl and Jawetz, have been described and can be differentiated by PCR.[7,12]

Pasteurella pneumotropica is generally considered an opportunistic agent and some degree of immunodeficiency often plays a role in disease pathogenesis.[8] It has been isolated from the skin, conjunctiva, nasopharynx, trachea, lung, intestinal tract, vagina, uterus, urinary bladder, prepuce, preputial glands, bulbourethral glands and seminal vesicles in asymptomatic and clinically affected mice.[6,13] Infections have been reported in mice, rats, guinea pigs, hamsters, cotton rats, rabbits, dogs, cats and humans.[1] The agent can infect the vaginal tract and ascend to the uterus causing infertility associated with metritis, abortion and stillbirths.[1]

The primary route of infection is by direct contact with oropharyngeal or reproductive tract secretions.[12] Mice and rats with infected uteri are typically found in colonies known to have a positive incidence of *Pasteurella pneumotropica* in the upper respiratory tract.[3] Bacterial toxins PnxlA,llA and lllA have been identified on infected cell surfaces and are associated with adhesion to extracellular matrix and virulence. These toxins may also act as leukotoxins and disrupt actin cytoskeleton.[11]

Treatment in drinking water with enrofloxacin (Baytril) a broad spectrum, bactericidal, fluoroquinolone antibiotic has been used effectively to eliminate *Pasteurella pneumotropica* from infected mice.[12]

The finding of diffuse mineralization of placental labyrinth capillaries was interesting. This may be a manifestation of dystrophic calcification, and associated

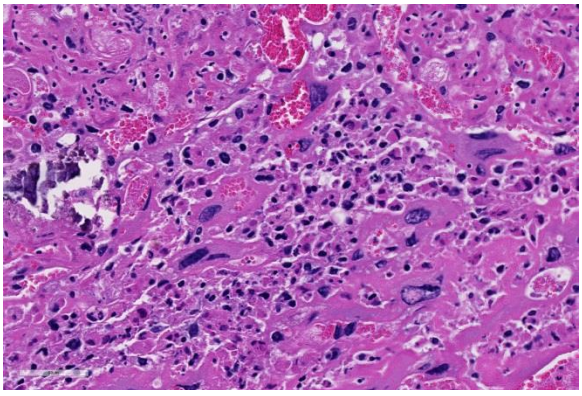

Placenta, mouse. Chorionic villi are separated by moderate amounts of degenerate neutrophils admixed with fibrin and cellular debris. There is crystalline mineral at left. (HE, 324X)

ineffective placental circulation may be a direct cause of fetal death in utero in this case.

JPC Diagnosis: Placenta and membranes: Placentitis and amniochorionitis, necrotizing, multifocal to coalescing, moderate, with colonies of coccobacilli, V1aR KO mouse, *Mus musculus*.

Conference Comment: Prior to discussing this case, the conference moderator led a

discussion on the normal placentation in mice. Both rats and mice have a hemochorial and discoid type of placenta.[2,4,9] In this type of placentation, maternal blood comes into direct contact with the fetal chorion, which does not occur in epitheliochorial placentation of ruminants and endotheliochorial placentation of dogs and cats.[2,4] Histologically, the mouse placenta is composed of the labyrinth and basal zones, the decidua, and the metrial glands. The labyrinth zone is composed of three layers of trophoblasts which separate maternal and fetal vasculature. The outer layer is composed of cyntrophoblasts, which directly contact maternal blood and has a microvillous surface. Beneath this layer are two layers of syncytiotrophoblasts.[4]

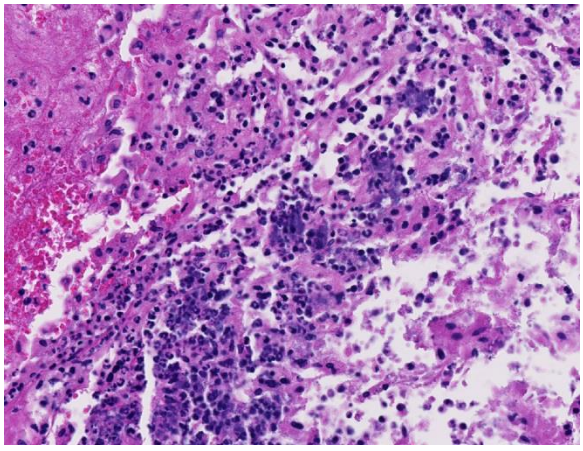

Placenta, mouse. Placental membranes are multifocally effaced by aggregates of degenerate neutrophils and colonies of bacilli. (HE, 324X)

Subjacent to the labyrinth zone is the basal zone which is composed of spongio-trophoblasts, trophoblastic giant cells, and glycogen cells. Spongiotrophoblasts are located at the maternal and fetal interface between the trophoblastic giant cell and inner labyrinth layer.[4] The trophoblastic giant cells are large pleomorphic cells that show extensive DNA replication and can have the equivalent of up to 1000 copies of the genome within a single cell.[4,6] These cells are vital for implantation and secretion of a wide array of hormones. Care should be taken to not interpret these cells as anaplastic tumor giant cells.[6] Glycogen cells have abundant intracytoplasmic glycogen and usually disappear prior to parturition. The origin and function of the glycogen cells is unknown. The decidua is composed of the maternal endometrial lining cells that are responsible for the exchange of nutrients, gas, and waste products between the fetus and the dam.[2,4,6] Finally, the metrial gland is present in the mesometrial triangle of the gravid mouse uterus and contains granulated endometrial gland cells (GMG), endometrial stromal cells, blood vessels, trophoblasts, and fibroblasts. Granulated mesometrial gland cells are bone marrow derived perforin-positive, natural killer cells that proliferate within the metrial gland upon pregnancy in mice. In health, GMG are mitotically active and often binucleated. The exact function of these cells has not yet been fully elucidated.[4,10]

Conference participants noted some moderate slide variation in this case, as some sections contain only the placental disk with no sections of the placental membrane or attached uterus. Additionally, the dystrophic mineralization of the capillaries within the placental labyrith, mentioned by the contributor, is not as prominent on every examined slide. Conference participants readily identified areas of lytic necrosis with moderate numbers of infiltrating neutrophils centered on small colonies of coccobacilli. *Pasteurella pneumotropica* is a common opportunistic pathogen in mice and infection often produces subclinical disease in immune competent mice.[9] The increased use of immunosuppressed strains of mice, however, has contributed to an increase in the incidence of clinical disease. Typically, it is implicated as a cause of severe pneumonia (hence its name), but has been

rarely reported as a cause of a wide variety of necrotizing and suppurative lesions, including those leading to infertility, reproductive failure and abortion, as in this case.[9] Most immunocompetent rats and mice with clinical respiratory disease are co-infected with Sendai virus, *Mycoplasma pulmonis*, cilia-associated respiratory (CAR) bacillus, *Streptococcus pneumoniae*, *Corynebacterium kutscheri*, *Bordetella bronchiseptica*, or *Klebsiella pneumonia*e as part of the chronic respiratory disease syndrome.[9]

Contributing Institution:
National Institutes of Health
Division of Veterinary Resources
Bethesda, Maryland, USA

References:

1. Ackerman JI, Fox JG. Isolation of *Pasteurella ureae* from reproductive tracts of congenic mice. *J Clin Microbiol*. 1981; 13(6):1049-53.
2. Bacha WJ, Bacha LM. *Color Atlas of Veterinary Histology*. 3rd ed. Baltimore, MD: Lippincott Williams & Wilkins; 2012:243-260.
3. Blackmore DK, Casillo S. Experimental investigation of uterine infections of mice due to *Pasteurella pneumotropica*. *J Comp Pathol*. 1972; 82(4):471-5.
4. Furukawa S, Kuroda Y, et al. A comparison of the histological structure of the placenta in experimental animals. *J Toxicol Pathol*. 2014; 27(1):11-18.
5. Hooper A, Sebesteny A. Variation in *Pasteurella pneumotropica*. *J Med Microbiol*. 1974; 7(1):137-40.
6. Hu D, Cross JC. Development and function of trophoblast giant cells in the rodent placenta. *Int J Dev Biol*. 2010; 54(3):341-354.
7. Kawamoto E, Sasaki H, Okiyama E, Kanai T, Ueshiba H, Ohnishi N, Sawada T, Hayashimoto N, Takakura A, Itoh T. Pathogenicity of *Pasteurella pneumotropica* in immunodeficient NOD/ShiJic-scid/Jcl and immunocompetent Crlj: CD1 (ICR) mice. *Exp Anim.* 2011;60(5):463-70.
8. Matsumiya LC, Lavoie C. An outbreak of *Pasteurella pneumotropica* in genetically modified mice: Treatment and elimination. *Contemp Top Lab Anim Sci*. 2003; 42(2):26-8.
9. Percy DH, Barthold SW. Mouse. In: *Pathology of Laboratory Rodents and Rabbits*, 4th ed. Ames, IA: Blackwell Publishing; 2016:66-67.
10. Picut CA, Swanson CL, et al. The metrial gland in the rat and its similarities to granular cell tumors. *Toxicol Pathol*. 2009; 37(4):474-480.
11. Sasaki H, Ishikawa H, Sato T, Sekiguchi S, Amao H, Kawamoto E, Matsumoto T, Shirama K. Molecular and virulence characteristics of an outer membrane-associated RTX exoprotein in *Pasteurella pneumotropica*. *BMC Microbiol*. 201; 11:55.
12. Towne JW, Wagner AM, Griffin KJ, Buntzman AS, Frelinger JA, Besselsen DG. Elimination of *Pasteurella pneumotropica* from a mouse barrier facility by using a modified enrofloxacin treatment regimen. *J Am Assoc Lab Anim Sci*. 2014; 53(5):517-22.
13. Ward GE, Moffatt R, Olfert E.J. Abortion in mice associated with

Pasteurella pneumotropica. *Clin Microbiol*. 1978; 8(2):177-80.

CASE III: EX54BF-1 or 2 (JPC 4035521).

Signalment: Eight-month-old female Balb/c mouse (*Mus musculus*).

History: The mouse is from another institute and was culled during routine surveillance.

Gross Pathology: There is an approximately 3cm diameter cystic subcutaneous mass in the ventral neck and cranial chest. The mass is composed of pale friable tissue and has a rich blood supply. When bisected, it contains a central cavity within which there is blood and viscous material. No other abnormalities were identified in the carcass.

Laboratory results: None

Histopathologic Description: (Participants will receive one of two slides: one sample is from the central region of the mass where it contains a large and partly collapsed central cavity. The second sample is smaller and more solid and was obtained from a lateral aspect of the mass).

There is a well-circumscribed multinodular and cystic subcutaneous mass composed of disorganized proliferation of plump spindle to polygonal cells arranged into interlacing fascicles, solid lobules and thick bands where the cells are often arranged in a palisade. The fibrovascular stroma is fine. The outline of the central cavity is irregular. It extends among lobules of neoplastic cells and contains a variable amount of necrotic debris and proteinaceous material. The neoplastic spindle cells have small to moderate amount of eosinophilic to amphophilic cytoplasm, indistinct cytoplasmic margins and oval finely granular nuclei with multiple small nucleoli. There is mild anisocytosis and anisokaryosis. In some areas, the cells are polygonal and have more abundant eosinophilic and often granular cytoplasm (some of these cells appear degenerate). The mitotic rate is approximately 0-2/HPF. The tumor compresses the surrounding tissue including the sublingual salivary gland and bundles of skeletal muscle. Mostly in the connective tissue around the tumor, there is moderate multifocal mononuclear infiltration and accumulation of some pigment-laden macrophages (hemosiderin, presumptive). In the outer region of the mass, there is multifocal fibrosis, which in some areas merges with a "compression capsule". At the periphery of the mass there is multifocal prolapse of neoplastic lobules into dilated veins (so-called "pseudoinvasion").

Contributor's Morphologic Diagnosis: Myoepithelioma

Ventral neck, Balb/c mouse: A 3cm cystic is present in the subcutis of the ventral neck which extends into the cranial aspect of the chest. Numerous cysts are visualized with bisected (bottom right). (Photo courtesy of: The Weizmann Institute of Science, Department of Veterinary Resources, http://www.weizmann.ac.il/vet/).

Contributor's Comment: Myoepithelial cells are ectoderm-derived modified epithelial cells found around acini and ducts of exocrine glands e.g. sweat glands, mammary glands, lacrimal glands and salivary glands.[2,5] They form a thin, basal layer between the basement membrane and the secretory cells of the luminal layer and are organized differently in ducts and alveoli.[2] In the former, they are arranged as a more or less continuous monolayer, whereas in the latter they are stellate shaped and their long branched cytoplasmic processes cradle the secretory unit like a loose basket.[2] Other than their involvement in mixed mammary tumors in dogs, primary tumors of myoepithelial cells are rare in domestic and laboratory animals.

In laboratory mice, myoepitheliomas are not uncommon but are usually limited to specific strains. The latest reference we found describing a relatively large group of these tumors in mice is Sundberg JP et al. *Vet Path* 28:313, 1991 which discusses myoepitheliomas diagnosed through routine surveillance of The Jackson Laboratory's production and research colonies. This is a study of 142 tumors in mice the majority of which were less than one-year-old. The following data is from this reference.

Myoepitheliomas occur spontaneously in strains A, Balb/c and their F1 hybrids. Most tumors were of salivary gland origin and the most common location was the ventral neck

(74%), as in the submitted case. Other locations included head (periorbital), perineum and ventral abdomen with origin from the salivary, Harderian, clitoral, preputial and mammary glands. The gender predisposition differed between the two strains. Balb/c females were predominantly affected whilst in A/J strain the reverse was true. In the Jackson study, the mean age at which tumors were detected was 234 days but other studies indicate that tumors arise predominantly in mice which are more than one-year-old. In the Jackson colony the frequency of malignancy, as determined by pulmonary metastases or invasion of underlying bone, was low (6%). A metastatic rate of >10% is reported in other studies of older mice, suggesting that the frequency of metastasis increases with age. Myoepitheliomas have been transplanted, but their etiology remains unknown. Virus particles were not identified in ultra-structural examination and molecular studies did not produce evidence implicating viral infection.[5]

The macroscopic and histologic appearance of myoepitheliomas appears to be fairly consistent and similar to the submitted case. [5] Grossly, the tumors were fluctuant, ranged in size from 0.5 - >4 cm in diameter and the single large central cavity contained opaque, odorless, pink to brown watery fluid. According to The International Classification of Rodent Tumors[1], the tumors are composed of pleomorphic cells that can resemble epithelial or mesenchymal cells. Adjacent to vessels, tumor cells tend to align themselves in an epithelial fashion. Multiple necrotic areas are present and mucoid material accumulates in pseudocysts as result of degeneration. The tumors can be invasive into surrounding tissue, and large tumors can metastasize to the lung.[2]

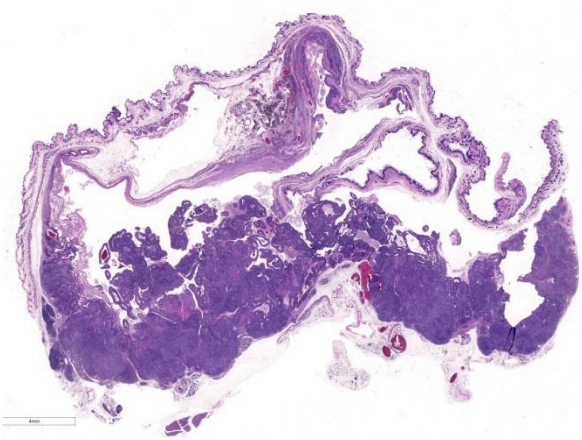

Ventral neck, Balb/c mouse: At subgross magnification, a densely cellular, cystic neoplasm is present within the subcutis. (HE 5X)

Immunohistochemical analysis showed that normal acinar and ductal myoepithelial cells and neoplastic cells were positive when stained with antibodies against cytokeratin, K5 and K14. Alpha-smooth muscle-1 antibody stained normal acinar myoepithelial cells but neither normal ductular myoepithelial cells nor neoplastic cells. This supports the notion that the tumors originate from ductular myo-epithelial cells.[5] Normal myoepithelial cells and neoplastic cells were negative for antisarcomeric actin, panmyosin, desmin, and S-100.[5]

JPC Diagnosis: Salivary gland: Myoepithelioma, Balb/c mouse, *Mus musculus*.

Conference Comment: Myoeptheliomas, also known as pleomorphic adenomas or benign mixed salivary gland tumors, are a relatively uncommon, spontaneously occurring salivary gland neoplasm in A strains and Balb/c mice, with a predilection for females.[4] Although typically considered to be benign, these neoplasms can grow tremendously and contain large cystic chambers containing necrotic cellular debris admixed with a mucinous secretory product. In humans, about 5% of myoepitheliomas undergo malignant transformation, but the

rate of malignancy in animal species is unknown. In mice, larger tumors can be aggressive with marked local invasion and metastasis to the lung.[3,4,5]

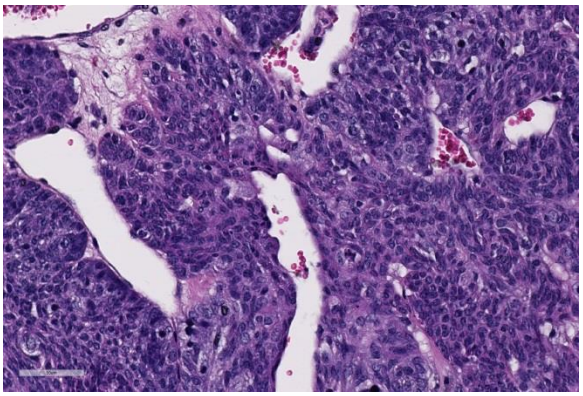

Ventral neck, Balb/c mouse: Neoplastic cells are spindled, and arrayed in small streams and bundles. Cells have a high N:C ratio. (HE 5X)

Myoepitheliomas can have a somewhat variable histomorphology but are typically composed of pleomorphic spindle cells that have features of both mesenchymal and epithelial cells.[4,5] As their name suggests, myoepithelial cells are contractile with both a smooth muscle and epithelial component, and myoepitheliomas are thought to be derived from the myoepithelial or ductal reserve cells of the salivary gland.[3,4,5] Normally, myoepithelial cells are located between the lumen and basal lamina of secretory structures, such as salivary glands, sweat glands, lacrimal glands, and mammary glands. The epithelial component of this neoplasm can form ducts or form nests of keratin-filled horn cysts, although that is not a striking feature in this case.[3,4,5] Myoepitheliomas have been reported infrequently in mammary glands in dogs, nonhuman primates, and humans. In mice, myoepitheliomas have been associated with salivary, mammary, preputial, and Harderian glands.[4] Conference participants agreed that the tumor is arising from the salivary gland based on the glandular or ductular profiles occasionally found in the neoplasm interpreted as preexisting salivary structures entrapped by neoplastic cells.

As noted by the contributor, there is significant slide variation in this case. This variability is due to the use of tissue from different parts of the neoplasm.

Contributing Institution:
The Weizmann Institute of Science
Department of Veterinary Resources
http://www.weizmann.ac.il/vet/

References:

1. Mohrs U, ed: *International Classification of Rodent Tumors: The Mouse*. Springer: Berlin; 2001:29.
2. Moumen M, Criche A, Cagnet S, Petit V Raymond K, Faraldo M, Dugnier MA, Glukohva MA. The mammary myoepithelial cell. *Int J Dev Biol*. 2011; 55:763-771.
3. Munday JS, Lohr CV, Kiupel M. Tumors of the alimentary tract. In: Meuten DJ, ed. *Tumors in Domestic Animals*. 5th ed. Ames, IA: Wiley Blackwell; 2017:853-855.
4. Percy DH, Barthold SW. Mouse. In: *Pathology of Laboratory Rodents and Rabbits*. 4th ed. Ames, IA: Blackwell Publishing; 2016:114-115.
5. Sundberg JP, Hanson CA, Roop DR, Brown KS, Bedigian HG. Myoepitheliomas in Inbred Laboratory Mice. *Vet Pathol*. 1991; 28:313-322.

CASE IV: AFIP 2013 (JPC 4039981).

Signalment: 19-year-old male rhesus macaque (*Macaca mulatta*).

History: This animal was part of a colony housed at the Texas Biomedical Research

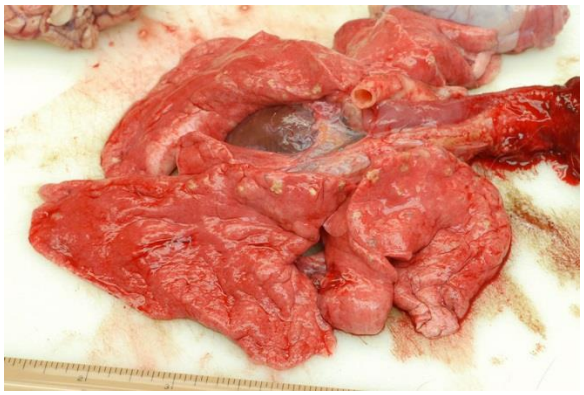

Lung, rhesus macaque. Numerous 2-5mm diameter tan nodules are present within all lung lobes. (Photo courtesy of: Covance Laboratories, Inc, Madison, Wisconsin, USA.
http://www.covance.com/products/nonclinical/toxicology/risk-assessment/index.php).

Institute. Clinical signs included chronic age-related arthritis in both knees and a general decline in condition associated with cachexia, diarrhea, and dehydration. The animal was euthanized due to poor condition.

Gross Pathology: External: The animal was dehydrated with low body fat but adequate muscle. Several teeth were missing. Both knees had reduced range of motion and periarticular thickening.

Internal: The liver was enlarged with pale tan edges on several lobes. The colon was distended with fluid feces. There was multifocal, 2-5 mm diameter, slightly raised tan nodules in all lung lobes.

Laboratory results: Simian retrovirus and herpesvirus serology were negative.

Histopathologic Description: Lung: Multifocally, bronchial and bronchiolar walls are irregularly thickened by large numbers of lymphocytes, plasma cells, macrophages, and eosinophils, with fewer neutrophils and multinucleated giant cells. Airway lumens are often enlarged and contain macrophages, granulocytes, and cross and tangential sections of arthropod parasites. Arthropods are approximately 300-500 um in width and characterized by a thin chitinized cuticle, jointed appendages, striated musculature, a body cavity, digestive tract, and reproductive organs. Many macrophages contain abundant intracytoplasmic golden-brown to black, finely granular, birefringent pigment (mite excrement). The inflammatory cell aggregates multifocally disrupt and/or obscure the bronchial and bronchiolar walls, form lymphoid follicles, variably compress or extend into adjacent alveolar tissue, and elevate the pleura (raised nodules noted grossly). Affected bronchi and bronchioles exhibit moderate smooth muscle hypertrophy and occasional peribronchiolar fibrosis. In less affected lung, terminal airways and alveoli are multifocally dilated with occasional loss of alveolar septa.

Lung, rhesus macaque. Numerous 2-5mm diameter tan nodules are present within all lung lobes. (Photo courtesy of: Covance Laboratories, Inc, Madison, Wisconsin, USA.
http://www.covance.com/products/nonclinical/toxicology/risk-assessment/index.php).

Contributor's Morphologic Diagnosis: Lung: Bronchitis/bronchiolitis, chronic and eosinophilic, multifocal, moderate, with bronchiolectasis, smooth muscle hypertrophy, and mites and mite pigment, etiology consistent with *Pneumonyssus sp*.

Other diagnoses in this animal included hepatic amyloidosis and chronic lympho-plasmacytic colitis.

Contributor's Comment: Although *Pneumonyssus simicola*, the lung mite of rhesus macaques, has become a less common parasite in most managed primate colonies; the incidence of pulmonary acariasis remains very high in feral and wild caught rhesus monkeys. Despite extensive microscopic findings in many affected animals, infection is typically subclinical. Sneezing, coughing, and dyspnea have been reported.[8] Antemortem diagnosis can be difficult. Radiographs are generally not helpful; however, tracheobronchiolar lavage has been a successful diagnostic tool, usually by identifying larva that migrates to the larynx. False negatives are possible.[1,4,5]

As demonstrated in the accompanying photographs, gross findings appear as multifocal and coalescing, discrete, irregularly round to ovoid, slightly raised, light brown foci several millimeters in size. In contrast to *M. tuberculosis*, the lesions of *Pneumonyssus simicola* are typically soft and cystic, or air-filled bullae.[1] Thin fibrous

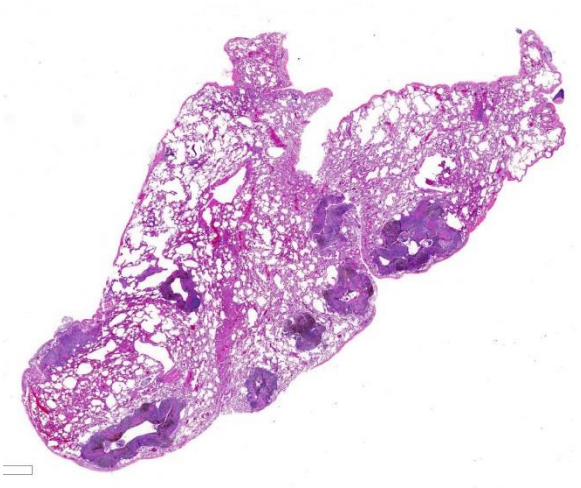

Lung, rhesus macaque. Bronchioles are ectatic and their walls are expanded by a dense cellular infiltrate. (HE, 5X)

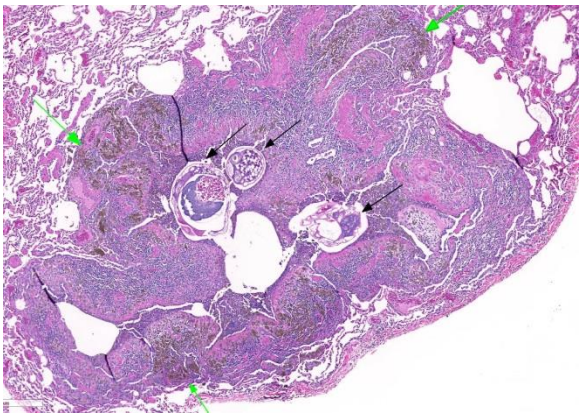

Lung, rhesus macaque. Walls of ectatic bronchioles are markedly expanded by lymphocytes and plasma cells, and aggregates of macrophages containing a dark brown pigment (green arrows). The lumen contains cross sections of numerous arthropod parasites (black arrows), surrounded by cellular debris. (HE, 57X)

adhesions within the pleural cavity are commonly observed.[9]

Microscopic lesions consist of multifocal chronic bronchiolitis and bronchiolectasis with hyperplasia of bronchiolar smooth muscle and prominent peribronchiolar lymphoid aggregates admixed with eosinophils and pigment-laden macrophages. Adult mites, most of which are females, are normally evident in sections of affected lung. Mites are identifiable by typical arthropod characteristics; a chitinized outer cuticle, body cavity, striated musculature, jointed appendages, and sometimes other structures including brain, gastrointestinal and reproductive tract, eggs and occasionally larvae. The presence of birefringent brown to black pigment in macrophages at the periphery of affected bronchioles is a hallmark of infection and considered diagnostic even in the absence of identifiable mites.[8]

JPC Diagnosis: Lung: Bronchiolitis and bronchitis, pyogranulomatous and eosino-philic, chronic, multifocal, moderate, with bronchiectasis and bronchiolar intraluminal

arthropods with mite pigment, rhesus macaque, *Macaca mulatta*.

Conference Comment: The contributor provides an outstanding example of pulmonary acariasis in a nonhuman primate, with numerous cross sections of well-preserved adults and eggs scattered throughout the larger conducting airways in this section of lung. *Pneumonyssus simicola* mites are ubiquitous in wild and wild-caught Old World primates with an incidence of nearly 100%.[2,3,9] As a result, mites and their associated lesions are considered a background incidental finding in these animals.[2,9] Previously reported pulmonary histologic lesions are generally similar to this case with eosinophilic to granulomatous bronchitis/bronchiolitis with variable amounts of brown to black mite pigment within bronchi and bronchioles and moderate to marked inflammation expanding the peribronchiolar interstitium.[2,9]

Other than the abundant mite pigment, conference participants agreed that the most striking histologic lesion is the profound bronchiectasis. Bronchiectasis is the permanent marked dilation of bronchi and is a consequence of chronic bronchial obstruction by the parasite.

As described by the contributor, adult mites have the typical arthropod characteristics of 300-500 um width, chitinous exoskeleton, mouth parts, jointed appendages, striated musculature, a body cavity, digestive tract, reproductive structures, yolk material in yolk glands, and developing eggs.[3] The highly characteristic birefringent golden brown to black crystalline mite pigment, thought to be a metabolite of digestion and excretion by the female mite, can be present in sections that lack mites and are diagnostic for the parasite.[2,3,9] This pigment does not contain melanin or carbon, but rather is composed predominantly of iron. This the

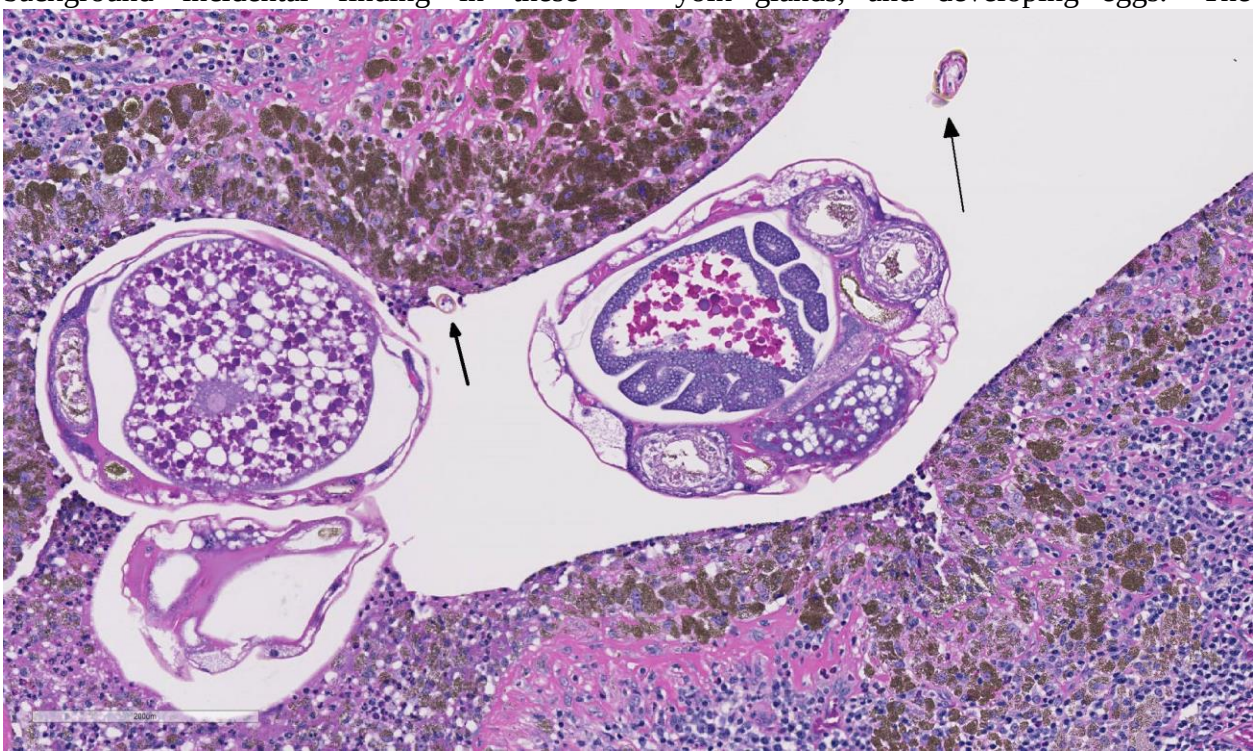

Lung, rhesus macaque. Higher magnification of lung mites (Pneumonyssus simicola) which demonstrates jointed appendages surrounded by a chitinous exoskeleton (black arrows), and digestive and reproductive tracts of the parasites. (HE, 125X)

result of the mite feeding on host erythrocytes with digestion and excretion of blood protein, hemoglobin.[9] Additionally, mite pigment is likely the cause of the majority of the inflammatory response within the lungs.[2] Widespread use of the anthelmintic medication, ivermectin, during quarantine of new animals and as a part of routine colony management has markedly reduced the incidence in laboratory nonhuman primates.[2,9]

Pulmonary acariasis and nasopharyngeal mites occur in many other animal species. Some of the most important nasal and pneumotropic arthropod parasites of veterinary importance include *Pneumo-nyssoides* sp. in the lungs of New-world primates; *Rhinophaga* sp. in the nasal cavity of Old-world primates; *Pneumo-nyssoides caninum*, the nasal mite in dogs; *Linguatula serrata* in the nasal cavity of dogs and cats; *Oestrus ovis*, the nasal botfly in sheep and goats; *Entonyssus* sp. and *Entophionyssus* sp. in the trachea and lung of snakes; *Cephenemyia* sp. in the nasal cavity of wild cervids; *Cytodites nudus* in the air sacs of poultry; and *Halarachne halichoeri* in the nasal passages of wild sea lions.[6]

Contributing Institution:
Covance Laboratories, Inc
Madison, Wisconsin, USA.
http://www.covance.com

References:

1. Andrade MCR, Marchevsky RS. Histopathologic findings of pulmonary acariasis in a rhesus monkeys breeding unit. *Revista Brasileira de Parasitologia Veterinária*. 2007; 16(4):229-234.
2. Cogswell F. Parasites of non-human primates. In: Baker DG, ed. *Flynn's Parasites of Laboratory Animals*. 2nd ed. Ames, Iowa: Blackwell Publishing; 2007:716-717.
3. Gardiner CH, Poyton SL. *An Atlas of Metazoan Parasites in Animal Tissues*. Washington, DC: Armed Forces Institute of Pathology; 1999:56-58.
4. Keeling M, Wolf R. Respiratory diseases. In: Bourne G, ed. *The Rhesus Monkey, Volume II: Management, Reproduction, and Pathology*. New York, NY: Academic Press; 1975:70-71.
5. Lowenstine LJ, Osborn KG. Respiratory system diseases of nonhuman primates. In: Abee C, Mansfield K, Tardif S, Morris T, eds. *Nonhuman Primates in Biomedical Research: Diseases*. London, UK: Academic Press; 2012:467-468.
6. *Pneumonyssus simicola*. Joint Pathology Center Systemic Pathology (updated Oct. 2014). Retrieved from: https://www.askjpc.org/vspo/show_page.php?id=595.
7. Purcell JE, Philipp MT. Parasitic diseases of nonhuman primates: In Wolfe-Coote S, ed. *The Laboratory Primate*. San Diego, CA: Elsevier; 2005:589-590.
8. Stookey J, Moe J. The respiratory system. In: Benirschke K, Garner F, Jones T, eds. *Pathology of Laboratory Animals*, Vol. 1. New York, NY: Springer-Verlag; 1978:106-107.
9. Strait K, Else JG, Eberhard ML. Parasitic diseases of nonhuman primates. In: Abee CR, Mansfield K, Tardiff S, Morris T, eds. *Nonhuman Primates in Biomedical Research: Diseases*. 2nd ed. Vol. 2. San Diego, CA: Academic Press;

Self-Assessment - WSC 2016-2017 Conference 22

1. Which of following is commonly seen in association with hepatoblastomas?
    a. Extramedullary hematopoiesis
    b. Emperipolesis
    c. Immature mesenchyme
    d. Liberation of insulin-like growth factors

2. Which form of placentation is common to rats and mice?
    a. Zonary
    b. Hemochorial
    c. Endotheliochorial
    d. Epitheliochorial

3. Which of the following is not true concerning myoepitheliomas in mice?
    a. Balb/c females and A/J males are predominantly affected.
    b. The ventral neck is the most common site.
    c. Tumors are often grossly and microscopically cystic.
    d. Metastasis occurs in 50% or more of cases.

4. Which of the following is a lung mite found in macaques?
    a. *Serrata linguatula*
    b. *Onithonyssus bacoti*
    c. *Pneumonyssus simicola*
    d. *Trombucula alfreddugesi*

5. What is the primary component of mite pigment?
    a. Carbon
    b. Chitin
    c. Iron
    d. Silica

Joint Pathology Center

Veterinary Pathology Services

WEDNESDAY SLIDE CONFERENCE 2016-2017

C o n f e r e n c e 23

19 April 2017

George A. Parker, DVM, PhD, DACVP, DABT, FIATP
Senior Scientific Director, Global Pathology
Charles River Laboratories

CASE I: TAMU-02 2013 (JPC 4033348).

Signalment: Four-month-old Hampshire ewe (*Ovis aries*).

History: One of a number of young meat sheep showing neurological signs and hyperthermia. This sheep progressed through phases of straight legs, muscle fasciculations, and recumbency. A neurological examination revealed cranial nerves normal, mentation normal, recumbency, good muscle tone, head turn to left, normal to increased muscle tone. Localized to cervical spinal cord. This sheep was treated with flunixin and antibiotics with no response by owner.

Gross Pathology: Bilaterally the superficial pectoralis muscle is green-black, dry, and firm with surrounding red tissue in an oval area measuring 8 x 5 x 1cm on the right and 7 x 6 x 1cm on the left (Figs1,2.: severe,

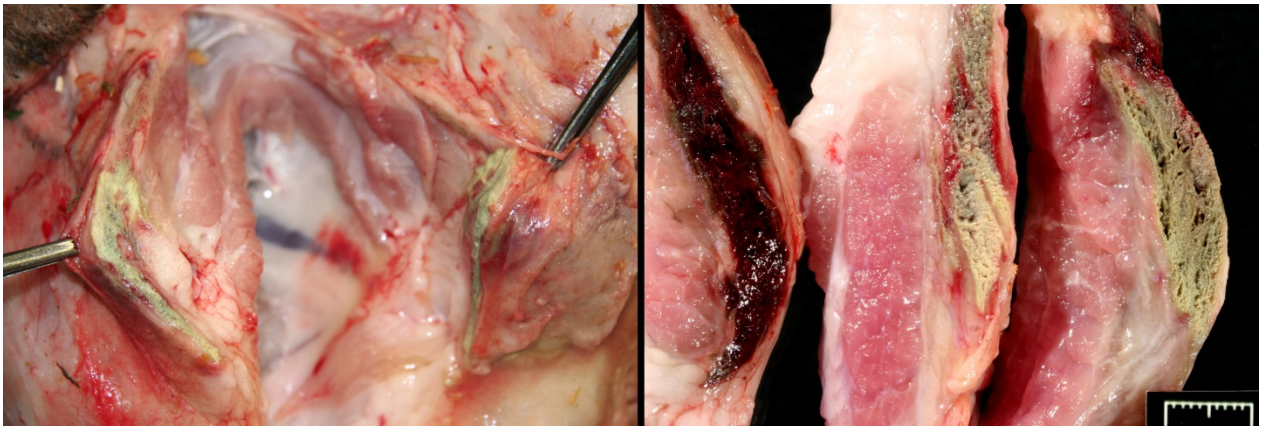

Skeletal muscle, sheep. The superficial pectoralis muscle bilaterally contains large areas of dry-greenish black necrotic muscle. (Photo courtesy of: Department of Veterinary Pathobiology, College of Veterinary Medicine, Texas A&M University, College Station, TX).

Skeletal muscle, sheep. The left quadriceps and the left lateral head of the triceps are irregularly pale pink to gray, evidence of myodegeneration and necrosis. (Photo courtesy of: Department of Veterinary Pathobiology, College of Veterinary Medicine, Texas A&M University, College Station, TX).

myonecrosis and hemorrhage). The left quadriceps and the left lateral head of the triceps are irregularly pale pink to gray (Fig3.: myodegeneration/myonecrosis).

Numerous *Hemonchus* and *Trichostrongyles* are in the abomasum.

Laboratory results: No monensin or lasalocid in rumen contents
Feed analysis: 3.4% lasalocid (this 10,000 times the legal limit of 30g/ton, 33mg/kg, 33ppm)

Histopathologic Description: Longitudinal and cross sections of triceps muscle are examined. On cross section, round, large sometimes hyalinized, hypereosinophilic or flocculant fibers are seen with central, large nuclei. Some fibers remain as aggregates of activated satellite cells in a shrunken endomysium. On longitudinal section, swollen, hyalinized, broken, flocculent fibers with myocyte nuclear loss and contraction bands are prominent. Satellite cells are activated and proliferating with a large vesiculate chromatin and blue-grey cytoplasm. Macrophages and small clusters of degenerate neutrophils enter pockets of broken fibers. Capillaries are lined by endothelial cells with hypertrophied nuclei.

Contributor's Morphologic Diagnosis: Subacute, monophasic myopathy with severe myofiber necrosis and satellite cell activation and early regeneration.

Contributor's Comment: The section shows a nice monophasic toxic myopathy. Ionophores are added to feeds for growth promotion and as a coccidiostat.[6,9] However, if toxic doses are achieved, they permit free cationic movement, especially calcium into myocytes and necrosis. Monogastrics such as the horse and dog are more susceptible.

This breeder had been having a chronic, sporadic, neurologic problem in the flock of show sheep. It affected sheep taken off pastured and "pushed" nutritionally for the show season. Upon opening this ewe, it was obvious that a myopathy was the problem, and given the history, we analyzed the rumen content (negative for ionophores additives), and then, the feed from the bag used to fed these ewes was tested (toxic levels of lasalocid). The levels of lasalocid the feed were extremely high, and it is presumed a pocket of unmixed, lasalocid

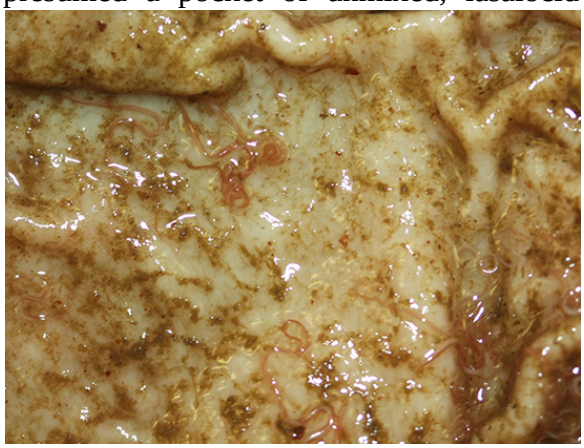

Abomasum, sheep: Numerous Haemonchus adults are attached to the mucosa. Photo courtesy of: Department of Veterinary Pathobiology, College of Veterinary Medicine, Texas A&M University, College Station, TX).

salt was included in the test sample. In some reports[2] and in this contributor's experience, once the ionophore is over a certain concentration, these additives are unpalatable, and animals refuse the feed rather than consume myotoxic levels. Unfortunately, toxicity studies are based on bolus feedings.[1,4]

In spontaneous, ionophore (usually monensin) intoxications of sheep[2,7,8,9,10] display an acute onset of signs of anorexia, dyspnea, muscle weakness, ataxia, a stiff gait and deaths follow feed changes. Firm or atrophic rear limb muscles are sometimes reported. A variety of autopsy lesions are reported including: cavitary effusions, pale-streaked hearts, diarrhea and pale-streaked skeletal muscles especially semimembranosus and semitendinosus. While some acute gastrointestinal lesions are reported, consistent macroscopic and/or histologic lesions are in cardiac and skeletal muscles. In ovine monensin toxicity studies[1,4], it was commented that acute myopathies were not visible in H&E-stained sections, but that lesions were demonstrable using electron microscopy. Early ultrastructure changes include mitochondrial swelling and myofibrillar disarray. Chronic histologic lesions include atrophy, fibrosis, and calcification. The severity of the present case is impressive, and the minimal cardiac lesion is unexplained. Is it possible that hypoxia from hemonchosis-exacerbated lesions?

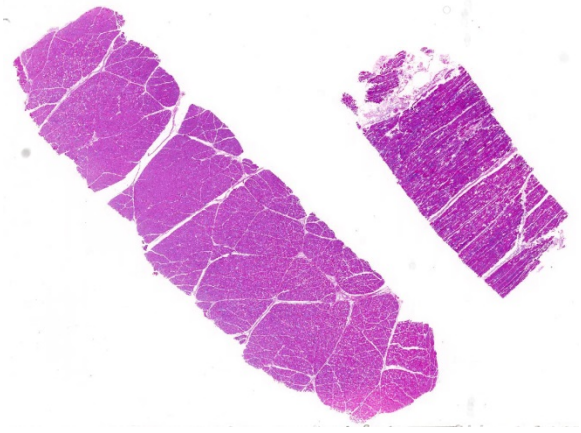

Skeletal muscle, sheep. Two sections of skeletal muscle from the triceps are submitted. The larger section on left shows muscle fibers in cross section; the smaller section on the right demonstrates fibers in longitudinal section. This is an excellent way to process muscle sections as many changes cannot be appreciated in cross section. (HE, 5X)

Finally, many ionophore intoxications present as CNS disease. Although in light of the muscle lesions, the signs could be explained as muscular pain and weakness, we should remember that an ionophore neuropathy is observed in some toxicity trials.[5] Our ewe had no lesions in the sciatic or femoral nerves, but some conduction problems may be occurring.

JPC Diagnosis: Skeletal muscle: Degeneration and necrosis, diffuse, severe, Hampshire ewe, *Aries ovis*.

Conference Comment: As mentioned by the contributor, this case is an excellent example of extensive monophasic skeletal muscle necrosis. Classification of muscle degeneration and necrosis is based on the distribution of the lesion and the duration of the insult. Characterization of the type of skeletal muscle necrosis gives insight on the potential cause and helps narrow down the list of differential diagnoses. As a result, a classification scheme breaks muscle necrosis into four broad categories, including focal monophasic, multifocal monophasic, focal polyphasic, and multifocal polyphasic. Focal monophasic is the result of a single mechanical injury, such as intramuscular injection or focal trauma. This case is representative of the multifocal monophasic pattern, which is caused by a single massive exposure of myotoxic drugs, such as ionophores (monensin and lasalocid), or metabolic disorder.[11] Exertional capture

myopathy also produces widespread monophasic skeletal muscle necrosis with a similar histologic appearance to this case. Polyphasic reactions are the result of repeated and ongoing skeletal muscle insult occurring over a prolonged period as a result of repeated trauma (focal) or nutritional deficiencies, inflammatory myopathies, or genetic disorders (multifocal). Skeletal muscle regeneration, mineralization, and deposition of fibrous connective tissue, all key features of polyphasic necrosis, are not prominent in this case.[3,11] Nice examples of multinucleated satellite cells are scattered throughout this tissue section and represent only the beginning stages of regeneration.

pressure, trauma, or ischemia can produce global myofiber necrosis. Necrosis is commonly triggered by increased intracellular calcium concentration, often released from high levels stored in the sarcoplasmic reticulum. Initially, segmental changes are represented by myofiber hyper-contraction, and cross sections appear large and dark with hyalinization and loss of cross striations. Further insult results in sarcoplasmic fragmentation that can lead to dystrophic myofiber mineralization, often seen in chronic myopathies.[3,11]

Skeletal myofibers are classified as permanent cells and are not capable of cell

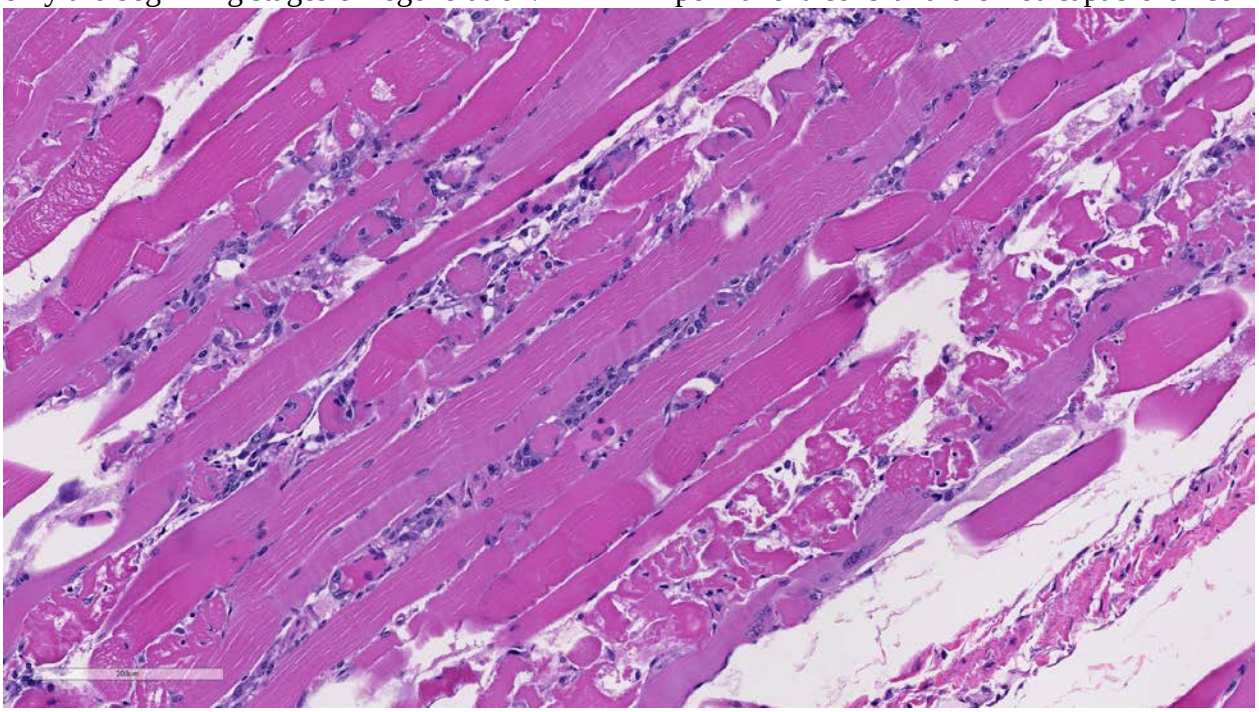

Skeletal muscle, sheep. Damaged myofibers exhibit a wide range of degenerative features: variation in fiber size myofiber swelling and hypereosinophilia; myofiber vacuolation (myofibrillolysis), an proliferation and hypertrophy of satellite nuclei. Necrotic changes contraction band formation, myofiber fragmentation and infiltration of the sarcolemma by macrophages. (HE, 200X).

Conference participants briefly reviewed the stages of skeletal muscle necrosis, re-generation, and repair. Myofibers are long and multinucleated and thus often undergo segmental necrosis rather than necrosis of the entire muscle fiber; however, extreme

division. As a result, skeletal muscle regeneration depends on the activation of satellite cells, normally resting between the sarcolemma and the basement membrane. These cells are highly resistant to injury and are activated by necrosis of adjacent myofibers.[3,11] Satellite cells begin

proliferation and differentiation into myoblasts in the early stages of skeletal muscle regeneration. Concurrently, macrophages migrate from the peripheral blood and phagocytose necrotic debris leaving a potential space within the damaged muscle. The initial infiltrating macrophages are of the M1 inflammatory phenotype but later switch to the M2 anti-inflammatory phenotype.[11] If the basement membrane is intact, the potential space is filled by a scaffold, called the sarcolemmal tube, which prevents the local migration of fibroblasts and instead acts as a guide for proliferating myoblasts. Within the sarcolemmal tubes, satellite cells, known as activated myoblasts at this stage, can be observed undergoing mitoses. Within hours, sarcolemmal tubes fuse end-to-end and form myotubes that eventually mature into skeletal myofibers over the course of a few days. Initial infiltrating M1 macrophages are tough to stimulate proliferation of the myoblasts, while M2 macrophages promote the formation of the myotubes.[3,11]

In contrast, if large enough numbers of satellite cells are killed and if the basement membrane is destroyed, the sarcolemmal tube is not formed, and there is no proliferation of myoblasts. This allows the influx of fibroblasts into the areas of necrosis resulting in healing by fibrosis rather than regeneration. Additionally, in cases where there is disruption of the basement membrane but satellite cells are still viable, regeneration is disorganized and ineffective due to disorganization of proliferating myotubes. This is typified by the presence of muscle giant cells (large, pleomorphic multinucleated giant myoblastic cells) and fibrous connective tissue.[3,11]

Contributing Institution:
Department of Veterinary Pathobiology
College of Veterinary Medicine
Texas A&M University
College Station, TX

References:

1. Anderson TD, Van Alstine WG, Ficken MD, Miskimins DW, Carson TL, Osweiler GD. Acute monensin toxocosis in sheep: Light and electronmicroscopic changes. *Am J Vet Res*. 1984; 45:1142-1147.
2. Bourque JG, Smart M, Wobeser G. Monensin toxicity in lambs. *Can Vet J*. 1986; 397-399.
3. Cooper BJ, Valentine BA. Muscle and tendon. In: Maxie MG ed. *Jubb, Kennedy, and Palmer's Pathology of Domestic Animals*. Vol 1. 6th ed. Philadelphia, PA: Elsevier; 2016:180-185.
4. Confer AW, Reavis DU, Panciera RJ. Light and electron microscopic changes in cardiac and skeletal muscle of sheep with experimental monensin toxicosis. *Vet Pathol*. 1983; 20:590-602.
5. Gregory DG, Vanhooser SL, Stair EL. Light and electron microscopic lesions of broiler cickens due to roxarsone and lasalocid toxicoses. *Avian Dis*. 1995; 39:408-416.
6. Horton GMJ, Stockdale PHG. Lasalocid and monensin in finishing diets for early weaned lambs with naturally occurring coccidiosis. *Am J Vet Res*. 1981; 42:433-436.
7. Jones A. Monensin toxicosis in 2 sheep flocks. *Can Vet J*. 2001; 42:135-136.
8. Mendes O, Mohamed F, Gull T, de la Concha Bermejello. Monensin poisoning in a sheep flock. *Sheep and Goat Res J*. 2003; 18: 109-113.
9. Novilla MN. The veterinary importance of the toxic syndrome induced by ionophores. *Vet and Hum*

Toxicol. 1992; 34: 66-70.
10. Nation PN, Crowe SP, Harries WN. Clinical signs and pathology of accidental monensin poisoning in sheep. Can Vet J. 1982; 23: 323-326.
11. Valentine BA. Skeletal muscle. In: McGavin MD,ed. *Pathologic basis of Veterinary Disease*. 6th ed. St. Louis, MO: Elsevier Mosby; 2017:922-926.

CASE II: 13A456 (JPC 4068000).

Signalment: 11-year-old male rhesus macaque (Macaca mulatta).

History: An 11-year intact male Indian origin rhesus macaque had an eight-year history of frequent intermittent vomiting. The animal was housed indoors. Over the course of eight years, this animal's therapeutic regime consisted of BSS 262-524mg/day, famotidine 3.5-5mg/day, and omeprazole 6mg/day. These medications were administered singularly or in combination. An underlying cause for the chronic emesis was not determined.

Gross Pathology: At necropsy, the animal weighed 10.3 kg and had a body condition score of 3.5/5. Significant gross findings included bilateral renal cortices that were uniformly dark green to black, with dark red medullas. The urinary bladder contained approximately 15 ml of clear, pale yellow urine. The remainder of the genitourinary system was unremarkable. Other gross findings included several diverticula in the transverse colon containing firm to inspissated black pigmented stool; the gastrointestinal tract was otherwise unremarkable.

Laboratory results: Toxic element screening, including bismuth levels, was performed on frozen kidney tissue at Michigan State University's Diagnostic Center for Population and Animal Health (Lansing, MI). Bismuth levels were 110.6 ppm. Lead levels were unremarkable at <0.50ppm.

Histopathologic Description: Light microscopy of H&E stained sections revealed numerous proximal renal tubular epithelial cells that contained a single, large, discrete, well-demarcated magenta to brown

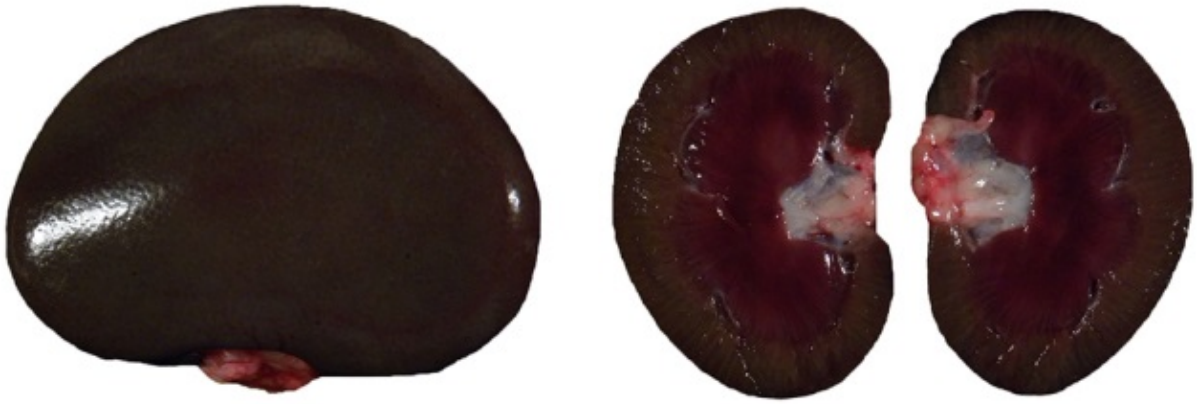

Kidney, rhesus macaque. Bilaterally, the renal cortex was uniformly dark green to black, with dark red medullas. (Photo courtesy of: Oregon National Primate Research Center, Division of Comparative Medicine and Pathology, 505 NW 185th Ave, Beaverton, OR 97006 http://www.ohsu.edu/xd/research/centers-institutes/onprc/).

intranuclear inclusion. A smaller number of tubular epithelial cells contained granular magenta to brown intracytoplasmic material. The remainder of the kidney was histologically unremarkable. The inclusions were negative when stained with Ziehl-Neelson acid fast, and appeared pale gray (negative) with Perl's Iron, blue to grey (negative) with Periodic Acid-Schiff (PAS), light brown (negative) with Alizarin red stain for calcium, and light grey (negative) with reticulin stain. In contrast, the inclusions stained black with Fontana Masson and Churukian- Schenk stains. With all these stains, the granular cytoplasmic material displayed the same staining characteristics as the intranuclear inclusions. Electron microscopy (EM) revealed numerous renal cortical tubular epithelial cells that contained a single, variably sized intranuclear inclusion. The inclusions are composed of densely grouped, co-aggregated, electron-dense crystalline material which appeared variably star or asterisk-shaped. The inclusions did not peripheralize or displace the nucleolus and the remaining nuclear structures appeared normal.

Contributor's Morphologic Diagnosis: Kidney, proximal convoluted tubules: Intranuclear pigmented inclusion bodies, marked, multifocal with mild, multifocal intracytoplasmic pigment deposition.

Contributor's Comment: Bismuth compounds are a rarely reported cause of both tissue pigmentation and intranuclear inclusions in man and laboratory animals. Historically, parenteral bismuth administration was used as a common treatment for syphilis. Histology of renal tissue from deceased patients routinely revealed intranuclear and intracytoplasmic bismuth deposition in epithelial cells of the convoluted tubules.[4,12] Oral bismuth

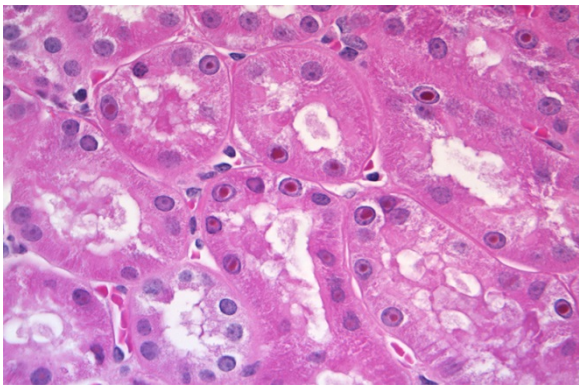

Kidney, rhesus macaque. Proximal renal tubular epithelial cells often contain a single large magenta intranuclear inclusion. (Photo courtesy of: Oregon National Primate Research Center, Division of Comparative Medicine and Pathology, 505 NW 185th Ave, Beaverton, OR 97006 http://www.ohsu.edu/xd/research/centers-institutes/onprc/). (HE, 400X)

preparations, a mainstay of treatment for diarrhea, can result in transient pigmentation of the tongue and fecal material within the colon through reaction of bismuth salts with hydrogen sulfide produced in the oral cavity or within the colon, creating an insoluble black salt.[2]

Bismuth subsalicylate (BSS) is the primary ingredient in Pepto-Bismol (Proctor & Gamble, USA). It is estimated that roughly 99% of bismuth ingested is excreted in the feces.[2] Bismuth levels in blood increase with chronic administration, but are not routinely associated with toxicity.[2] Despite the low levels of bismuth absorbed and the minimal risk of toxicity, the literature discourages prolonged administration.[2] The absorption of bismuth from the gastrointestinal tract may be increased under a variety of situations including patient variation, the formulation of the bismuth compound or salt, time of gastric emptying, alteration of gastric pH, and co-administration of bismuth with products or foodstuffs that contain thiol groups, cysteine, and/or fruit juice.[1-7, 11] Bismuth is deposited in multiple organs, but is preferentially retained longer in the

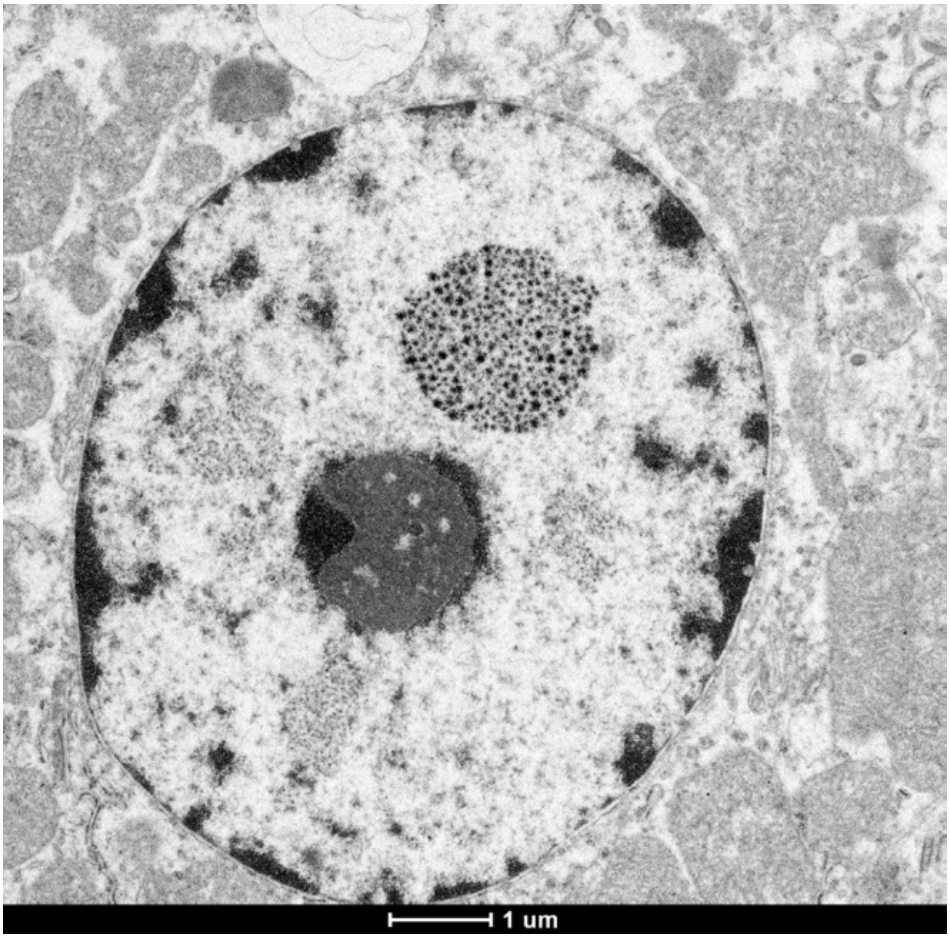

Kidney, rhesus macaque. Ultrastructurally, nuclei of proximal convoluted tubules contain one or multiple intranuclear inclusions which appear to be a composite of asterisk-shaped crystalline material. (Photo courtesy of: Oregon National Primate Research Center, Division of Comparative Medicine and Pathology, 505 NW 185th Ave, Beaverton, OR 97006 http://www.ohsu.edu/xd/research/centers-institutes/onprc/).

kidney when compared to other organs.[10] Renal bismuth inclusions have been identified 1-30 years after parenteral treatment.[10]

The diagnosis of gross renal bismuth pigmentation and intranuclear bismuth inclusions in this macaque was based on the combination of a history of chronic BSS administration, elemental screening, gross and histologic findings, histochemical stain results, and electron microscopy.

Toxic element screening confirmed not only the presence of bismuth (110.6ppm), but that the levels were measured at 500-1000 times higher than normal acceptable bismuth levels. Based on literature published in wild game birds normal levels of bismuth in liver and muscle are <0.1ppm.[5] Work performed in rats suggests that normal tissue levels for bismuth in kidneys are <0.2 ppm.[1] The heavy metal screening also revealed levels of lead considered within normal limits disproving lead as the source of the intra-nuclear inclusions.

The dark green to black renal cortical pigmentation is consistent with pigmented bismuth compound accumulation. As the kidney is the documented primary target organ for bismuth accumulation, this was the most likely organ to exhibit pigmentation.[10] There was no gross or histologic evidence of this pigment in any other organs. Other causes of grossly visible green black renal pigment such as hemozoin and melanin were disproved through microscopic appearance of intranuclear localization and patient history. The animal had lived in a non-endemic area for malaria-causing Plasmodium sp. throughout its lifetime and the animal had not received any blood or tissue transplants that could have resulted in iatrogenic transmission. Further, there was no histologic evidence of malaria, effectively ruling out hemozoin pigment.

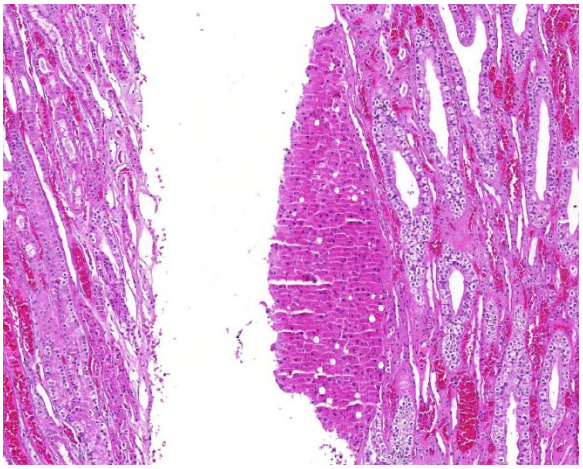

Kidney, rhesus monkey. A choristoma of hepatocytes is present within the renal medulla. (HE, 88)

A variety of histochemical stains were employed to help correlate the appearance of the intranuclear inclusions and intra-cytoplasmic granules observed in the renal tubular epithelium with the elemental screening results. Ziehl-Neelson acid fast stain is used primarily for the detection of acid-fast bacteria. However, lead inclusions are known to stain positive on paraffin embedded tissue, but less intensely when compared to fresh non-paraffin embedded samples.[12] Compared to bismuth inclusions that stain acid-fast positive with frozen tissue and negative with paraffin embedded tissues.[3] Perl's Iron stain used to detect ferric iron in tissue was negative, determining that iron and iron-containing compounds such as ferritin were not present. Alizarin Red stain for calcium was also negative. To demonstrate that the material was intrinsically pigmented, unstained tissues were examined revealing brown inclusions. When unstained tissue sections were treated with a 10 second application of 30% hydrogen peroxide, the inclusions were no longer visible. The presumptive mechanism for decolorization with hydrogen peroxide is that the hydrogen peroxide oxidizes the bismuth sulfide resulting in formation of colorless bismuth sulfate.[13] Melanin is resistant to decolorization with this short term hydrogen peroxide application.[13] Fontana Masson and Churukian-Schenk, silver based stains used for the non-specific demonstration of melanin and argyrophilic granules, stained the inclusions brown-black. As the hydrogen peroxide treatment suggested that the material was not actually melanin, it was presumed that the bismuth salt inclusions possessed the ability to bind silver from a silver solution and reduce it to visible metallic silver with and without a reducing agent thus exhibiting both argentaffin and argyrophilic properties.

Electron microscopy confirmed the presence of an electron dense material consistent with heavy metal or mineral within the nucleus of proximal renal tubule epithelial cells. The appearance of bismuth inclusions are dependent upon the method of fixation, sections fixed with glutaraldehyde exhibit a homogenous electron dense appearance.[4] However, inclusions in tissue fixed with osmium have a more granular and fibrillar appearance.[4] The latter is more consistent with the inclusions we identified in our osmium fixed samples.

Increased absorption of bismuth in this macaque is thought to be related to a variety of factors including chronic vomiting that likely altered the time of gastric emptying. Additionally, concomitant therapeutics, famotidine and omeprazole, were frequently administered with the primary therapeutic BSS for this animal's gastrointestinal disturbance. Famotidine is an H2 receptor antagonist. Work performed with other H2 receptor antagonists (ranitidine) has demonstrated an increased systemic absorption of tripotassium dicitrate bismuthate.[8] Omeprazole, a proton pump inhibitor has also been linked to increased

absorption of tripotassium dicitrate bismuthate.[11] Although this animal was administered BSS, not tripotassium dicitrate bismuthate, this still suggests an additional potential for increased absorption. Furthermore, this animal's diet of routine monkey chow contains normal dietary levels of cysteine, and as enrichment this animal routinely received whole fruits and fruit juices. Both cysteine because of its thiol group, and ascorbic acid derived from fruits and fruit juices have been linked to the formation of soluble bismuth in vivo and in vitro.[7,10] The prolonged administration of BSS by itself or in conjunction with drugs that alter gastric pH, and routine administration of foodstuffs that contain thiol group compounds and ascorbic acid could have singly or in combination been responsible for increased systemic absorption of bismuth and consequently this animal's gross and histologic findings.

JPC Diagnosis: Kidney, tubular epithelium: Intranuclear inclusions, multifocal, rhesus macaque, Macaca mulatta.

Conference Comment: We thank the contributor for their institutions' complete clinical workup and thorough review of bismuth subsalicylate (BSS) inclusions in a rhesus macaque with chronic intermittent vomiting. In this case, the inclusions are primarily localized to the proximal convoluted tubules, but they are also rarely present within the renal distal convoluted tubules and collecting ducts. No inclusions are observed within the glomeruli or vessels. While BSS has been reported to cause nephrotoxicity in other species, the inclusions within the renal tubules in this case are not associated with a lesion, indicating that these inclusions are likely incidental rather than contributing to this animal's clinical disease. As mentioned by the contributor, increased uptake of bismuth is thought to be secondary to a number of

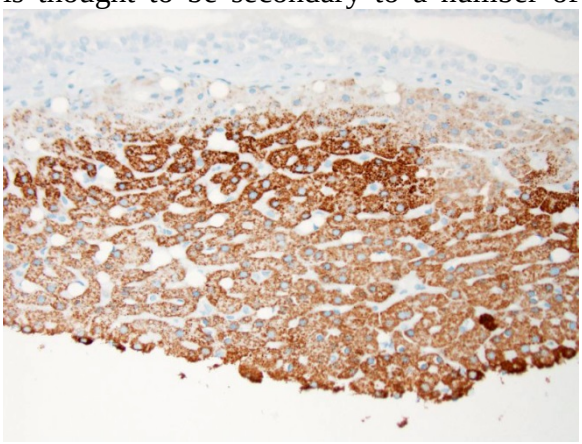

Kidney, rhesus monkey. Cells within the medullary choristoma stain strongly and intracytoplasmically positive for hepatocellular paraffin antibody 1. (anti-hepatocyte specific antigen, (110X)

factors, such as chronic vomiting altering gastric emptying time, and concurrent administration of famotidine and omeprazole, which all increase systemic absorption of orally administered BSS.[6,12] Conference participants briefly discussed other causes of intranuclear inclusion bodies, which included viral etiologies such as herpesviruses, adenovirus, and polyomavirus; other heavy metals, such as lead; and cytoplasmic invaginations. Likely due to the recent publication of this case in Veterinary Pathology, virtually every conference participant included BSS near the top of their list of differentials diagnoses for this lesion.[6]

In addition to the intranuclear inclusions predominantly within the renal proximal convoluted tubules, the more perceptive conference participants also identified what appeared to be a 3 x 2 mm section of liver attached to the kidney near the renal pelvis. This small section of tissue demonstrated intense and specific intracytoplasmic immunoreactivity for hepatocyte antigen run by the Joint Pathology Center after the conference. Conference participants could not reach a consensus on whether this

represented ectopic liver tissue (hepatic choristoma) or is simply a piece of liver that was dragged in during tissue processing. The tissue appears to be attached to the underlying renal parenchyma, but it is also present on a cut border, further adding to the disagreement. Hepatic choristomas have been typically reported as incidental findings in the kidney and various abdominal and extra-abdominal sites, with the gallbladder the most common location in humans. Other rare sites include the retroperitoneum and the adrenal gland. Ectopic liver has also been very rarely associated with the development of hepatocellular carcinoma.[8] If this case represents a true hepatic choristoma in the kidney, it is of academic interest, but likely of no clinical significance to this animal.

Contributing Institution:
Oregon National Primate Research Center
Division of Comparative Medicine
Beaverton, OR
http://www.ohsu.edu/xd/research/centers-institutes/onprc/

References:

1. Allain P, Krari N, Chaleil D, et al. Effects of some chelating agents on bismuth absorption in the rat. Fundam Clin Pharmacol. 1991;5(1):39-45.
2. Bierer DW. Bismuth subsalicylate: history, chemistry, and safety. Rev Infect Dis. 1990;12(Suppl 1):3-8.
3. Burr RE, Gotto AM, Beaver DL. Isolation and analysis of renal bismuth inclusions. Toxicol Appl Pharmacol. 1965;7(4):588-91.
4. Ghadially FN, Young NK. Ultrastructural and x-ray analytical studies on intranuclear bismuth inclusions. Virchows Arch B Cell Pathol. 1976;(1):45-55.
5. Jayasinghe R, Tsuji LJ, Gough WA, et al. Determining the background levels of bismuth in tissues of wild game birds: A first step in addressing the environmental consequences of using bismuth shotshells. Environ Pollut. 2004;132(1):13-20.
6. Johnson AL, Blaine ET, Lewis AD. Renal pigmentation due to chronic bismuth administration in a rhesus macaque (Macaca mulatta). Vet Path. 2015; 52(3):576-579.
7. Mahony DE, Woods A, Eelman MD, et al. Interaction of bismuth subsalicylate with fruit juices, ascorbic acid, and thiol-containing substrates to produce soluble bismuth products active against Clostridium difficile. Antimicrob Agents Chemother. 2005;49(1):431-3.
8. Merve A, Scheimberg I. Ectopic liver tissue in the kidney: Case report and literature review. Pediatr Dev Pathol. 2014; 17(5):382-385.
9. Nwokolo CU, Prewett EJ, Sawyerr AM, et al. The effect of histamine H2-receptor blockade on bismuth absorption from three ulcer-healing compounds. Gastroenterology. 1991;101(4):889-94.
10. Slikkerveer A, de Wolff FA. Pharmacokinetics and toxicity of bismuth compounds. Med Toxicol Adverse Drug Exp. 1989; 4(5):303-23.
11. Treiber G, Walker S, Klotz U. Omeprazole-induced increase in the absorption of bismuth from tripotassium dicitrato bismuthate. Clin Pharmacol Ther. 1994;55(5):486-91.
12. Wachstein M. Studies on inclusion bodies; acid-fastness of nuclear inclusion bodies that are induced by

ingestion of lead and bismuth. Am J Clin Pathol. 1949;19(7):608-14.
13. Wachstein M, Zak FG. Bismuth Pigmentation: Its Histochemical Identification. Am J Pathol. 1946 May;22(3):603-11.

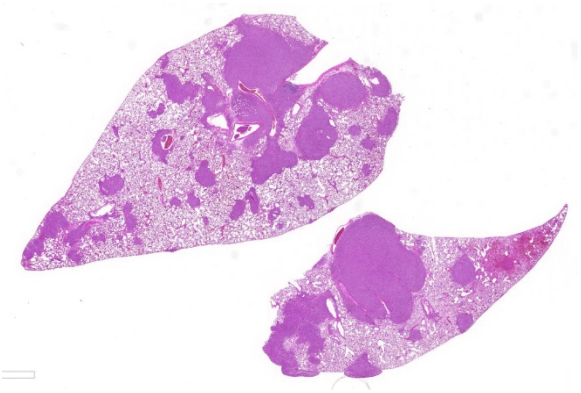

Lung, Sprague-Dawley rat: Numerous densely cellular neoplastic nodules surround vessels and occasionally elevate the pleura. (HE 5X)

CASE III: 1519 (JPC 4084474).

Signalment: >20-month-old male Sprague-Dawley rat (*Rattus norvegicus*).

History: The rat had 4ET telemetry device implantation surgery on 28 October 2014 & was exposed to test article on 8 December 2014. The rat had two routine battery exchange surgeries on 24 February 2015 and 22 July 2015. Post-op recovery was uneventful. In early September 2015, the rat developed fluid-filled distention on both flanks. Veterinary staff attempted to manually drain several times, but size remained the same. On 10 Sept 2015, a veterinarian performed a battery exchange. During the surgery, the surgeon removed fibrous/sac-like tissues (submitted for biopsy) from both sides while draining a copious amount of serosanguineous fluids (no purulent fluid noted). The rat was placed on enrofloxacin (1mg/kg) post-surgery. On 23 September 2015, chlorhexidine scrub & triple antibiotic ointment treatment was started because the area at the incision site appeared raw. The rat appeared bright, alert, and responsive during rounds on 25 Sept 2015, but was found dead in the cage on the morning of 27 September 2015.

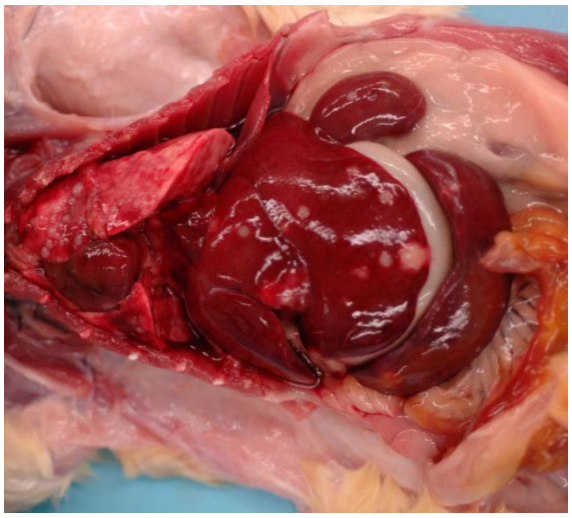

Viscera, Sprague-Dawley rat: White, firm, elevated nodules are present in the lungs, liver, spleen, and kidney.

Gross Pathology: This 689 g, male, CD rat is in optimum body condition with abundant SQ & visceral fat, 3/5 BCS, & moderate autolysis, especially the GI tract. The lungs are noncollapsed & pink with multifocal dark red areas & numerous 0.2-0.4 cm, pale, soft, smooth, round, well-demarcated masses affecting all lobes. The liver has numerous 0.2-0.6 cm, pale, soft, smooth, round, well-demarcated masses extending into the parenchyma & affecting all lobes. The spleen is 6.5 x 1.5 x 0.5 cm & has a focal, 0.4 x 0.4 x 0.2 cm, pale, soft, smooth, round, well-demarcated mass. The pancreas appears nodular & firm. The left kidney has a central, approximately 0.3 x 0.3 cm, slightly raised, pale area that is wedge-shaped extending into the cortex on cut surface. The right kidney has 2 similar areas on the caudal pole. The mediastinal & perirenal lymph nodes are greenish-yellow & enlarged. The urinary bladder is empty.

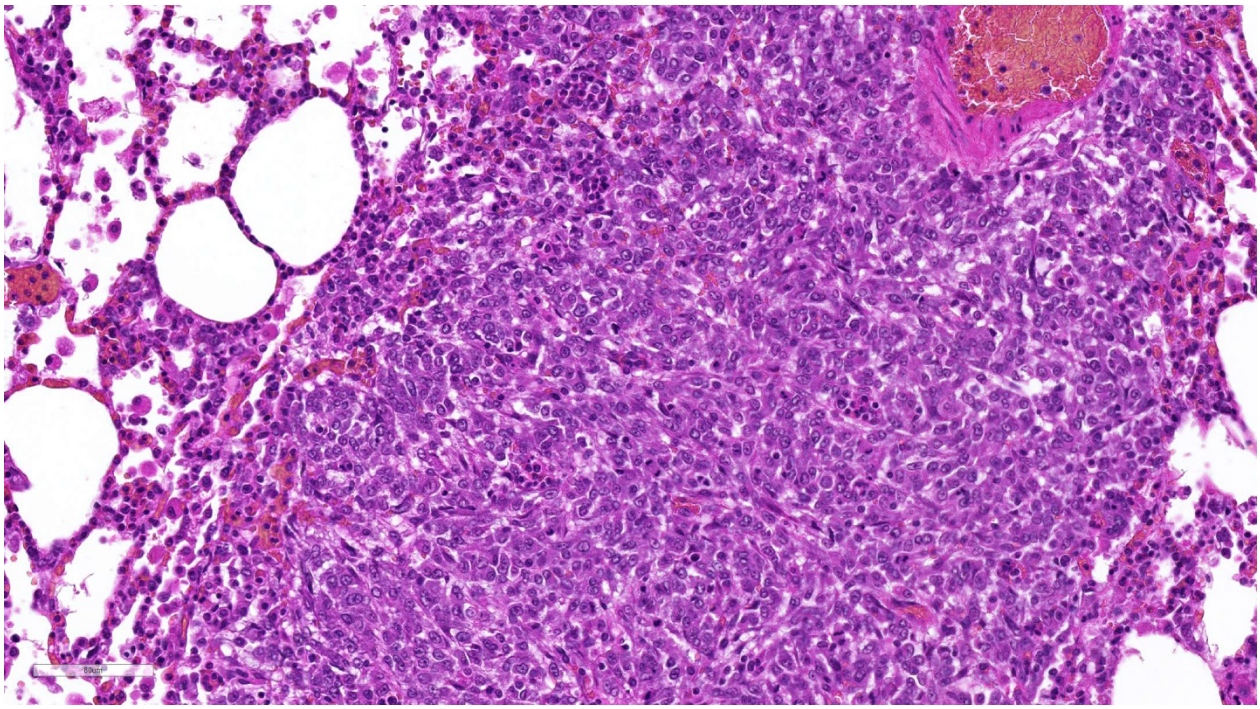

Lung, Sprague-Dawley rat: Neoplastic cells fill alveoli and efface alveolar architecture. They are spindled with indistinct cell borders and moderate amounts of a finely vacuolated cytoplasm. Aggregates of immature hematopoietic cells are scattered through the nodules. (HE 5X)

Laboratory results: None

Histopathologic Description: Lung: Multifocally invading and replacing alveoli, surrounding blood vessels and rarely filling and replacing bronchioles is an un-encapsulated, poorly demarcated, cellular neoplasm compose of either round cells arranged in sheets or less commonly palisading spindle cells all supported by a preexisting fibrovascular stroma. Neoplastic cells have indistinct cell borders, abundant pale, eosinophilic cytoplasm, round, oval or reniform nucleus with vesiculate chromatin and distinct nucleolus. Mitotic rate is 2 per HPF. Multifocally neoplastic cells are expanding pleura, filling or expanding alveolar septa and filling blood vessels. Within less affected areas, alveoli often contain fibrin, hemorrhage, cellular debris and small to moderate numbers of neutrophils, lymphocytes, and alveolar macrophages. Multifocally individual alveoli contain small clusters of neoplastic cells. Focally a large bronchiole is filled with fibrin/cellular debris/mucus admixed with few lymphocytes, macrophages and sloughed mucosal epithelial cells.

Contributor's Morphologic Diagnosis: Lung: Malignant neoplasm, favor histiocytic sarcoma.

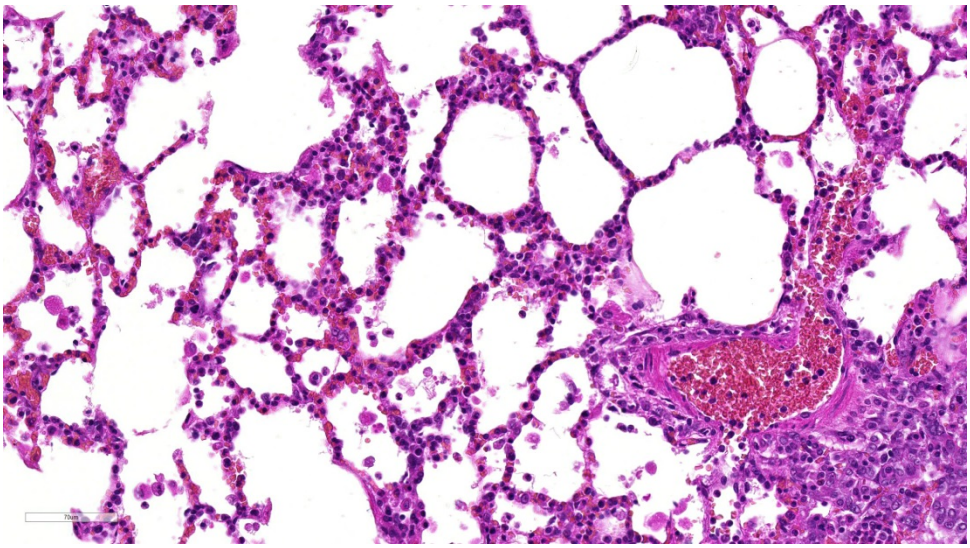

Lung, Sprague-Dawley rat. A diffuse interstitial pneumonia, characterized by thickened hypercellular alveolar septa, mild type II pneumocyte hyperplasia, and fibrin within alveoli is present. No previous manipulation of this animal was noted in the submitted history. (HE, 280X)

JPC Diagnosis: 1. Lung: Histiocytic sarcoma, Sprague-Dawley rat, *Rattus norvegicus*.
2. Lung: Pneumonia, interstitial, necrotizing, fibrinonecrotic and eosinophilic, multifocal, moderate with vascular necrosis.

Contributor's Comment: Histiocytic sarcoma in rats is the most common nonlymphoid hematopoietic neoplasm.[6] The incidence in Sprague-Dawleys has been reported to be as low as 1%[6] and as high as 4.7%[8] with no sex predilection. The occurrence of this neoplasm is seen in animals >12 months of age with one study showing over 50% of cases in animals in a 18-23 month age group.[7] At necropsy, sarcomas of this type may be present in the liver, lymph nodes, lung, spleen, mediastinum, retroperitoneum, or sub-cutaneous tissue.[1] The most common localizations of this tumor are different between rat strains and are as follows: the liver and lungs in Sprague-Dawley rats, liver, bone marrow, lymph nodes, spleen and lungs in Fischer and Donryu rats and subcutis in Wistar rats.[6] In our case, neoplastic cells were also seen in the kidney, pancreas, adipose tissue surrounding a number of the listed organs above as well as within vascular spaces.

Conference Comment: Histiocytic sarcoma (HS) is a relatively common neoplasm in aging Sprague-Dawley rats, but they have also been reported much less commonly in other strains (Wistar, Fischer 344, Osborne-Mendels).[1,6,7] Grossly, the neoplasm is typically pale white to tan, homogenous, and firm forming variably sized masses that infiltrate and efface normal tissue architecture. HS can develop at multiple locations, but primary sites are most often in the liver, lymph nodes, lungs, spleen, bone marrow, retroperitoneum, and the subcutis.[1,6,7,9] Metastatic sites can include any organ, but are most commonly present in the liver, kidneys, draining lymph node, and lungs.[9] Histologically, HS have a variable appearance of sheets of large pleomorphic and anaplastic cells with abundant vacuolated cytoplasm and Langhans-type multinucleated giant cells or interlacing bundles and streams of elongate palisading fusiform spindle cells, which is the predominant feature of this case.[1,9]

Although not mentioned by the contributor as a component of this case, conference participants discussed the frequent association of HS with hyaline droplet (HD) accumulation in the renal proximal convoluted tubules. In these cases, the hyaline droplets are immunopositive for lysozyme, a major protein secreted by macrophages and monocytes.[2-5] There is a direct qualitative correlation between a droplet accumulation in the kidney and increased tumor burden in rats. In cases where the HS is confined to a single location, there may be little to no hyaline droplet accumulation. The widespread metastatic disease and high tumor burden, described by the contributor, suggests that

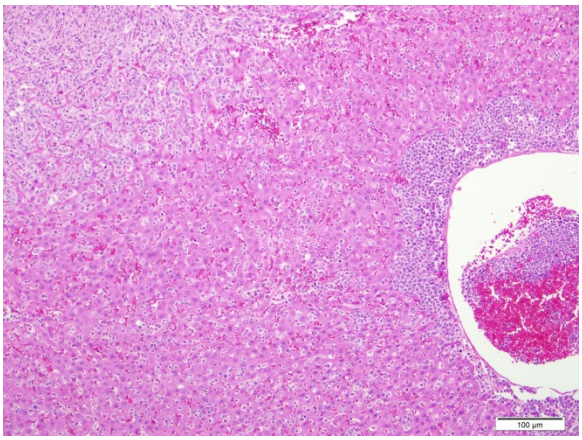

Liver, Sprague-Dawley rat. Neoplastic cells (upper left and adjacent to the vessel at right) are present within the liver. (HE, 100X)

there is renal tubule hyaline droplet in this case.[2-5] HD can also occur in response to a number of other pathologic conditions associated with accumulation of alpha-2u-globulin in the male rat. These droplets form in the P2 segment of the proximal tubule and represent secondary lysosomes containing alpha-2u-globulin bound to a variety of chemicals, including volatile hydrocarbons, d-limonene, unleaded gasoline, tetrachloroethylene, 1,3,5-trinitrobenzene, diethylacetylurea, and sodium barbital.[2-5] They have also been observed in chronic progressive nephropathy of rats associated with accumulation of albumin.[2,4] The HD seen in tumor-bearing rats are histologically indistinguishable from rats with alpha-2u-globulin nephropathy. As mentioned above, HD secondary to HS will be strongly immunopositive for lysozyme, but immunonegative for alpha-2u-globulin staining; the reverse is true for alpha-2u-globulin nephropathy.[2-5]

In addition to multifocal infiltration of HS within this section of lung, conference participants also noted a moderate infiltration of alveolar macrophages and eosinophils, predominantly infiltrating multifocal areas of alveolar septal thickening and necrosis. Accumulation of inflammatory cells is not uncommon in pulmonary neoplastic disease, especially HS[9]; however, conference participants could not explain the widespread presence of eosinophils within areas of inflammation and necrosis. It is possible that the inflammation present in this case may be related to the administration of the test article rather than the neoplasm; although, the nature of the test article is not specified by the contributor.

Contributing Institution:

References:

1. Barthold SW, Griffey SM, Percy DH. Rat. In: *Pathology of laboratory rodents and rabbits*. 4th ed. Ames, IA: John Wiley & Sons, Inc.; 2016:167.
2. De Rijk EPCT, Ravesloot WM, et al. A fast histochemical staining method to identify hyaline droplets in the rat kidney. *Toxicol Pathol*. 2003; 31:462-464.
3. Frith CH, Ward JM, and Chandra M. The morphology, immunohistochemistry, and incidence of hematopoietic

neoplasms in mice and rats. *Toxicol Pathol*. 193; 21:06–218. 1993.
4. Hard GC. Some aids to histological recognition of hyaline droplet nephropathy in ninety-day toxicity studies. *Toxicol Pathol*. 2008; 36:1014-1017.
5. Hard GC, Snowden RT. Hyaline droplet accumulation in rodent kidney proximal tubules: An association with histiocytic sarcoma. *Toxicol Pathol*. 1991; 19:88-99.
6. Kemmochi Y, Takahashi A, Miyajima K, Yasui Y, Tanoue G, Shoda T, Kakimoto K. Spontaneous histiocytic sarcoma of the popliteal lymph node in a young Sprague-Dawley rat. *J Toxicol Pathol*. 2010; 23:161-164.
7. Ogasawara H, Mitsumori K, Onodera H, Imazawa T, Shibutani M, and Takahashi M. Spontaneous histiocytic sarcoma with possible origin from the bone marrow and lymph node in Donryu and F-344 rats. *Toxicol Pathol*. 1993; 21:63–70.
8. Squire RA, Brinkhous KM, Peiper SC, Firminger HI, Mann RB, and Strandberg JD. Histiocytic sarcoma with a granuloma-like component occurring in a large colony of Sprague-Dawley rats. *Am J Pathol*. 1981; 105: 21–30.
9. Valli VEO, Kiupel M, Bienzle D. Hematopoeitic system. In Maxie MG, ed. *Jubb, Kennedy and Palmer's Pathology of Domestic Animals*. Vol 3. 6th ed. Philadelphia, PA: Elsevier Ltd; 2016:250-255.

CASE IV: 0601909 (JPC 4089360).

Signalment: Two-year-old male B6C3F1 mouse (*Mus musculus*).

History: This mouse was in the control group of a two-year study investigating the carcinogenicity of kava kava extract. It was sacrificed on Test Day 668, due to moribund condition. Clinical observations included ruffled fur, lethargy and thin body condition.

Gross Pathology: Gross lesions described at necropsy included: a single tan mass, approximately 27x17x12 mm, on the left lateral liver lobe; and several white nodules, up to 5 mm diameter, on the visceral pleura, lungs, and mediastinum.

Laboratory results: None

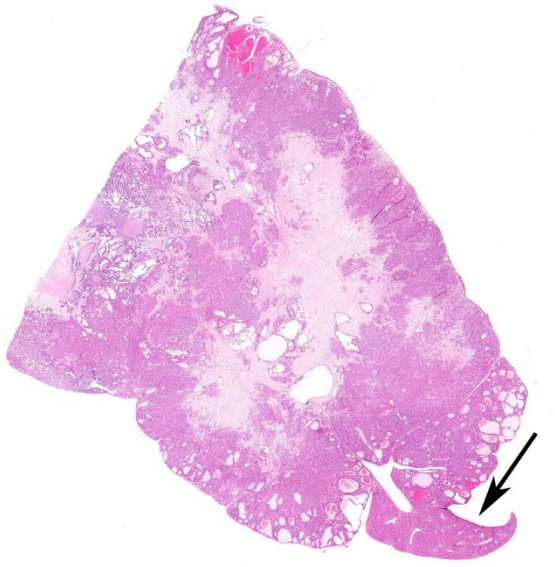

Liver, B6C3F1 mouse. 95% of the submitted section of liver is effaced by a multilobular, occasionally cystic neoplasm with large central areas of necrosis (normal liver at lower right.) (HE, 5X)

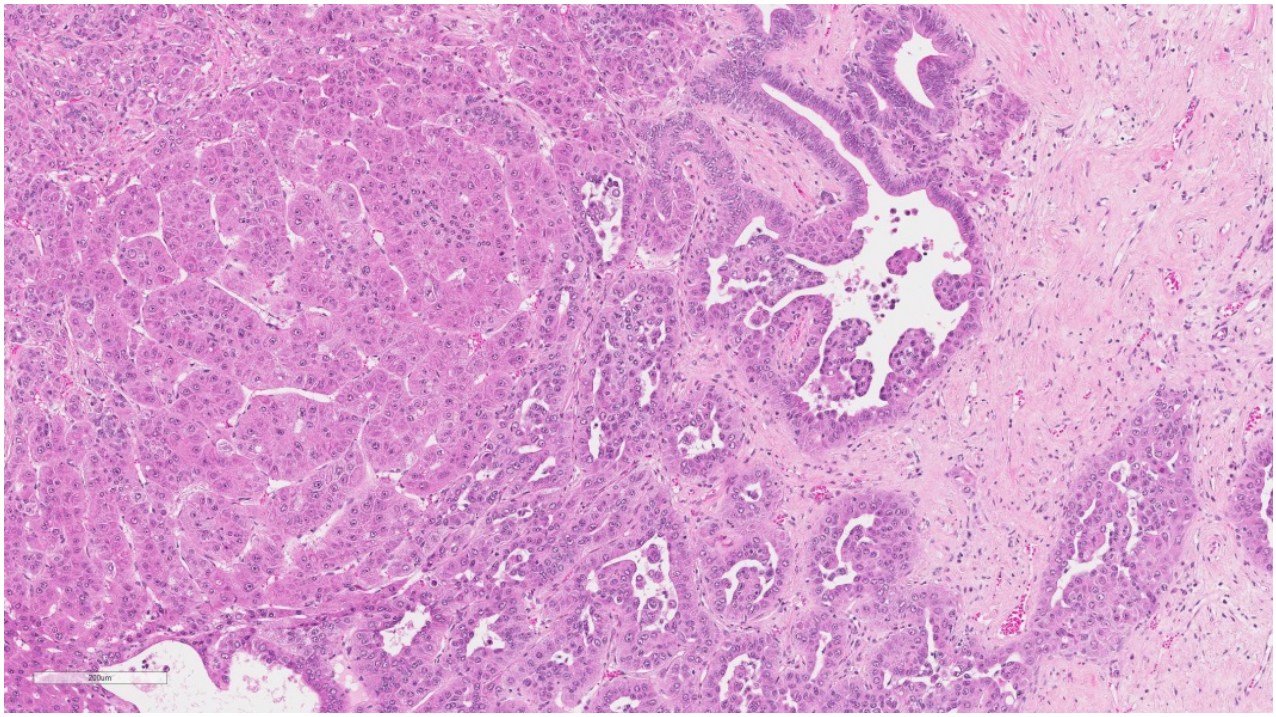

Liver, B6C3F1 mouse. Neoplastic cells differentiate along multiple phenotypic lines, with large plates of neoplastic cells resembling hepatocytes at left, and neoplastic cells recapitulating bile ducts with a single layer of columnar epithelium lining cystic spaces and forming micropapillary projections at right. (HE, 136X)

Histopathologic Description: Most of this section of liver lobe is replaced by a large mass extending to the capsular surface. The mass is composed of irregular acini and variably-sized cystic spaces interspersed with more densely cellular areas and areas of fibrosis or necrosis. Acini are lined by columnar epithelium with prominent hyperchromatic nuclei and scant cytoplasm. More densely cellular areas are comprised of hepatocytes with a central vesicular nucleus containing 1 or 2 prominent nucleoli, and abundant cytoplasm. These cells are arranged in packets, in trabeculae more than 3 cells thick, or around cystic spaces. The cystic spaces are lined by one or more layers of flattened to plump hepatocytes, with occasional papillary projections extending into the lumens; lumens often contain sloughed epithelial cells, lightly stained fibrillar eosinophilic material, and occasional extravasated erythrocytes. In other areas, densely-packed, small round to elongated cells with hyperchromatic nuclei form a sarcomatous pattern, often extending into areas of fibrosis. Occasional endothelial-lined spaces contain erythrocytes, small clusters of white blood cells (mainly neutrophils) and single or clusters of neoplastic cells.

Contributor's Morphologic Diagnosis:
Liver – Hepatocholangiocarcinoma
Tissue not included:
Lung – Hepatocholangiocarcinoma, metastatic
Lymph node, mediastinal – Hepatocholangiocarcinoma, metastatic
Thymus – Hepatocholangiocarcinoma, metastatic
Heart, pericardium – Hepatocholangiocarcinoma, metastatic

Contributor's Comment: This hepatocholangiocarcinoma (HCCC) typically contains both malignant hepatocellular and malignant biliary components, as well as foci of markedly undifferentiated sarcoma-

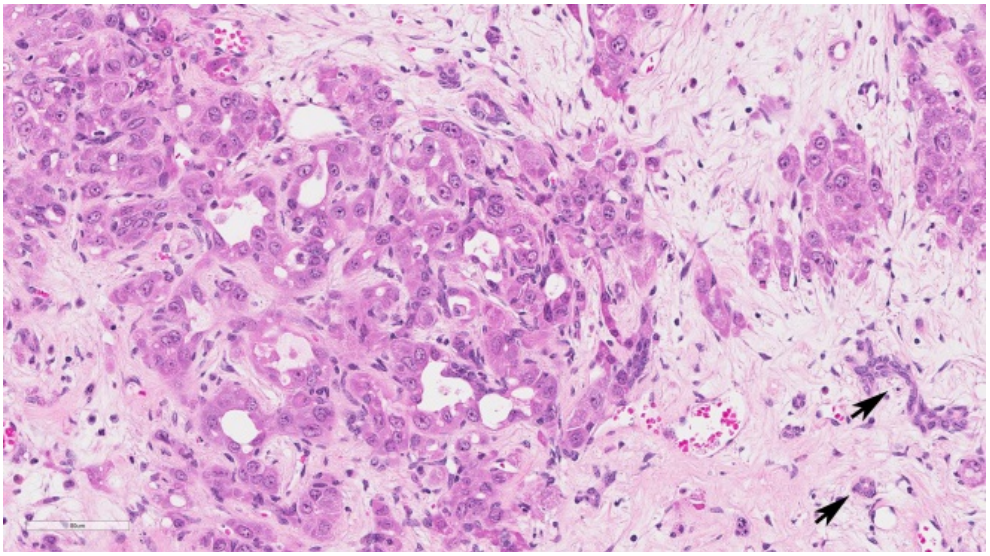

Liver, B6C3F1 mouse. Centrally, neoplastic cells formed well-differentiated neoplastic bile ducts on a dense fibrous stroma. A few pre-existent biliary ductules are present at lower right (arrows.) (HE, 168X)

like cells, as described in a poster presented by the National Institute of Environmental Health Sciences (NIEHS) and Experimental Pathology Laboratories, Inc. (EPL).[4] HCCC is rarely reported in mice and rats. However, it has been induced by some chemicals tested in the National Toxicology Program (NTP) studies.[2,4] It is an aggressive neoplasm that metastasizes readily.

JPC Diagnosis: Liver: Hepato-cholangiocarcinoma, B6C3F1 mouse, *Mus musculus*.

Conference Comment: Hepato-cholangiocarcinoma (HCCC) is a rare spontaneous neoplasm with an incidence of less than 0.5% in B6C3F1 mice, according to the National Toxicology Program (NTP) database.[4,6] HCCC is a primary liver neoplasm comprised of both neoplastic hepatocytes and neoplastic bile duct epithelial cells.[4,6] The biliary component forms tubules and acini or small nests, while the hepatocellular component forms trabeculae, glands, or solidly cellular areas of neoplastic cells. Both neoplastic hepatocytes and bile duct epithelial cells have many characteristics of malignancy, such as frequent mitoses, nuclear pleo-morphism, local invasion, and widespread metastasis.[4,6,7] HCCC often contains large cystic or necrotic areas within the central portions of the neoplasm, as demonstrated in this case. Additionally, there are occasional ducts within the neoplasm, lined by both hepatocytic and biliary epithelial cells, in conjunction with multifocal areas of poorly differentiated mesenchymal spindloid cells arranged in short interlacing streams and bundles. Proliferation of sarcomatous cells is a

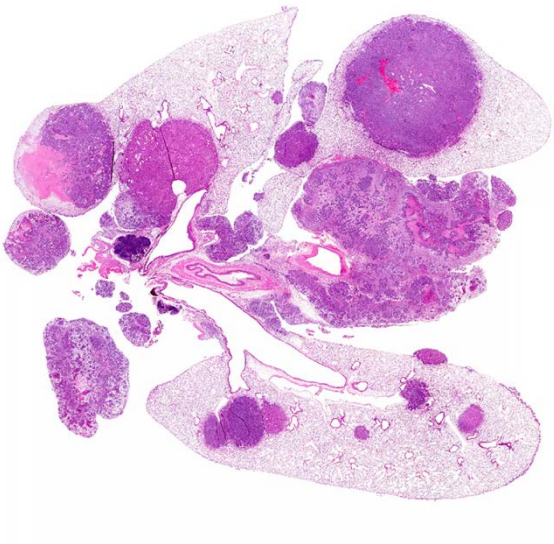

Lung, B6C3F1 mouse. All lung lobes contain metastatic nodules. (HE, 0.7X) (Photo courtesy of: Experimental Pathology Laboratories, Inc., P.O. Box 12766, RTP, NC 27709, www.epl-inc.com).

frequently reported feature of this malignant neoplasm.[6,7] In previously studies, 84% of mice with HCCC had metastasis to multiple tissues, similar to what is reported by the contributor here.[6] The histo-morphologic variability of this neoplasm and widespread metastasis may pose a diagnostic challenge in determining the site of origin. Metastatic lesions may contain only one of the three neoplastic populations mentioned above, further confounding the diagnosis.[6]

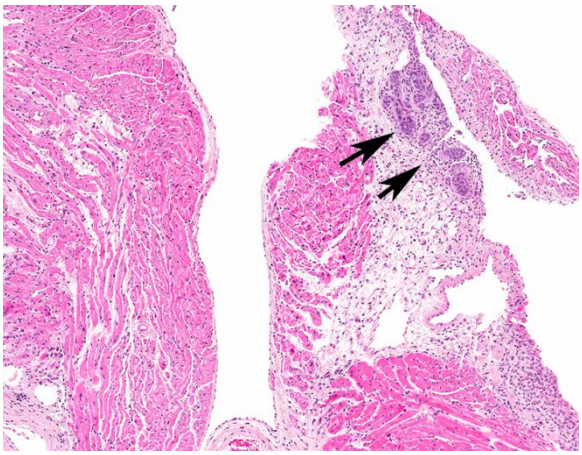

Mediastinum, B6C3F1 mouse. Neoplastic nodules are also present within the mediastinum at the heart base. (HE, 10X) (Photo courtesy of: Experimental Pathology Laboratories, Inc., P.O. Box 12766, RTP, NC 27709, www.epl-inc.com).

As mentioned previously, spontaneous occurrence of HCCC is exceedingly rare in mice; however, malignant transformation has been experimentally associated with chemical carcinogens, such as trimethylolpropane tricrylate, benzidine dihydrochloride, and N-2-acetylaminofluorene.[4] The B6C3F1mouse is a hybrid strain that is the result of a cross between a male C3H and a female C57BL/6 mouse. This relatively hardy mouse strain has been used by the NTP for decades as part of carcinogenesis, toxicity, and transplant studies.[2]

Contributing Institution:
Experimental Pathology Laboratories, Inc.
Research Triangle Park, NC
http://www.epl-inc.com

References:

1. Adams ET, Auerbach S, Blackshear PE et al. Proceeding of the 2010 National Toxicology Program satellite symposium. *Toxicol Pathol*. 2010; 39:240-246.
2. Gad SC, Clifford C, Goodman D. The mouse. In Gad SC ed. *Animal Models in Toxicology*. 3rd ed. Boca Raton, FL: CRC Press; 2016:76-78.
3. Hailey JR, Nold JB, Brown RH et al. Biliary proliferative lesions in the Sprague-Dawley rat: Adverse/non-adverse. *Toxicol Pathol*. 2014; 42:844-854.
4. Harada T, Enomoto A, Boorman GA, Maronpot RR. Liver and gallbladder. In: Maronpot RR, Boorman GA, Gaul BW eds. *Pathology of the Mouse*. Vienna, IL: Cache River Press; 1999:153.
5. Maronpot RR. Rodent Liver - Neoplastic. 2015. http://focusontoxpath.com/rodent-liver-lesions-neoplastic/
6. Moore R,Willson G, Miller R, Malarkey D, Kissling et al. Hepatocholangiocarcinomas in B6C3F1 Mice in National Toxicology Program (NTP) Studies.
7. Thoolen B, Maronpot RR, Harada T et al. Proliferative and nonproliferative lesions of the rat and mouse hepatobiliary system. *Toxicol Pathol*. 2011; 38:5S-81S.

Self-Assessment - WSC 2016-2017 Conference 23

1. Which of following is not a cause of monophasic muscle necrosis?
    a. Metabolic disorders
    b. Myotoxic drugs
    c. Exertional capture myopathy
    d. Nutritional deficiency

2. Which of the following is the most likely organ to exhibit pigmentation in cases of bismuth toxicity?
    a. Tongue
    b. Liver
    c. Kidney
    d. Skin

3. Subcutaneous histiocytic sarcomas are seen in which of the following strains of rats?
    a. Wistar
    b. Non-obese diabetic
    c. Sprague-Dawley
    d. Fischer 344

4. Which of the following has the highest incidence of histiocytic sarcoma?
    a. Sprague-Dawley
    b. Wistar
    c. Fischer 344
    d. Non-obese diabetic

5. One of the histologic characteristics of hepatocholangiocarcinoma is?
    a. Cystic areas of necrosis within the central parts of the neoplasm.
    b. Telangiectatic blood vessels and thrombosis
    c. Extensive mineralization of the stroma
    d. Extensive hemorrhage and siderosis

Joint Pathology Center

Veterinary Pathology Services

WEDNESDAY SLIDE CONFERENCE 2016-2017

C o n f e r e n c e 24

26 April 2017

R. Keith Harris, DVM, Diplomate ACVP
Office of the Dean
College of Veterinary Medicine
University of Georgia

Chris H. Gardiner, Ph.D.
Head, JCIDS Capability Document Cell
Capability Developments Integration Directorate U.S. Army Medical Department Center and School U.S. Army Health Readiness Center of Excellence
Fort Sam Houston, TX

CASE I: S354/10 or S370/10 (JPC 4002984).

Signalment: S354/10: Adult female barred parakeet (*Bolborhynchus lineola*).
S370/10: Adult male budgerigar (*Melopsittacus undulatus*).

History: In August 2010, sudden deaths of parakeets were noticed in an aviary close to Berlin,
Germany. Three barred parakeets (*Bolborhynchus lineola*) and two budgerigars (*Melopsittacus undulatus*) died within 2-5 days after a clinical history of reduced activity and food intake. Additionally, one barred parakeet and two juvenile budgerigars were clinically affected for about two weeks but finally recovered. During the past two years, new parakeets had not been introduced into the aviary.

Gross Pathology: At necropsy, multiple petechiae were present in the myocardium, the pectoral muscles and the gizzard walls of both animals. Liver and spleen were moderately enlarged.

Laboratory results: Nested PCR and subsequent DNA sequencing of the mitochondrial cytochrome *b* gene derived from protozoan megalomeronts was performed. Phylogenetic comparison of 479 bp of the cytochrome *b* gene with published sequences of avian hematozoa found 100% identity with avian malaria parasites (*Haemoproteus* spp.) of European songbirds. The sequence derived from the barred parakeet was identical to the lineage TURDUS2 of *Haemoproteus minutus*, a

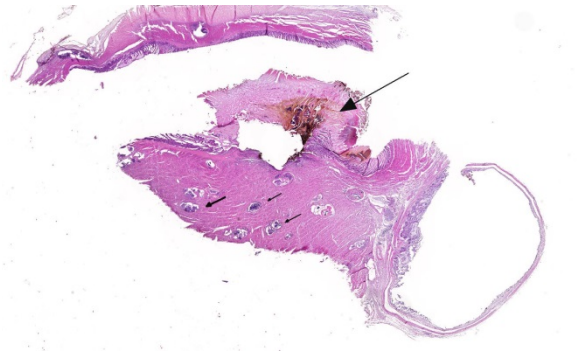

Ventriculus, parakeet. There are numerous protozoal megaloschizonts (small arrows) in the gizzard smooth muscle. There is focal hemosiderin pigment within the koilin layer, suggesting focal ulceration and hemorrhage. (HE, 5X).

parasite previously found in the blood of the common blackbird (*Turdus merula*) in Europe. The sequence from the budgerigar was identical with the lineage TUPHI1 of a so far unnamed *Haemoproteus* sp. previously found in the blood of a song thrush (*Turdus philomelos*) in Bulgaria. In blood smears of the three only clinically affected parakeets, no parasitic structures were detectable.

Histopathologic Description: Skeletal muscle (S 354/10), gizzard, smooth muscle (S 370/10, both tissues with some slide variation): Numerous large, often fusiform intact and partially ruptured cyst-like protozoan structures (size up to 800 µm in diameter) are present in the skeletal muscles and the smooth muscles of the gizzards of both parakeets. The cyst-like structures (megalomeronts) have a thick pale eosinophilic outer wall, are partly compartmented by internal septae, and filled with myriads of basophilic 1-2 µm, oval merozoites. Occasionally, adjoining muscle fibers are degenerate or necrotic and scattered are mild hemorrhages. Additionally, there are multifocal infiltrations by few lymphocytes, heterophils and macrophages, individually also forming multinucleate giant cells.

Contributor's Morphologic Diagnosis: Skeletal muscle (S354/10) / gizzard, smooth muscle (S370/10): Protozoan mega-lomeronts, numerous (variable: with myositis, minimal, lymphocytic and heterophilic and occasionally hemorrhage)

Contributor's Comment: Numerous outbreaks of fatal infections with strikingly similar parasitic structures have been reported in the past decades in European aviaries.[2,4,10,13] Psittacines from Australia, New Zealand and South America were predominantly affected. No cases of African parrots have been reported so far. Diagnosis in all reported cases was based on histopathologic detection of megalomeronts in the heart, skeletal and gizzard muscles and, to a lesser extent, in other organs such as the lung. Most often megalomeronts do only provoke minimal host response, as in the cases presented here. Previously, the parasites were described as *Leucocytozoon* spp. because of their morphologic features. Recent studies also suggest that these cases could have been infections of *Besnoitia* spp. (*Sarcocystidae*).[2]

Genetic analysis suggests *Haemoproteus* spp. from European songbirds as causative agents in both cases presented here.[9] In Europe, asymptomatic blood infections by *Haemoproteus* spp. have been regularly observed and are especially prevalent in songbirds.[12] In the German outbreak, psittacine species endemic to South Africa and Australia were infected with two different lineages of *Haemoproteus* spp. that are known to infect blackbirds and songthrushes (Turdidae), respectively. These results suggest that infection was the result of previously unknown cross-species transmission of *Haemoproteus* spp. between birds of only distantly related phylogenetic orders.[7,11] *Haemoproteus* spp. are closely

related to *Plasmodium* spp. causing avian malaria.[1] Whether the term avian malaria should be used for haemosporidian parasites other than *Plasmodium* spp. is still subject of discussion.[8,14] We propose to term the disease in parrots "Haemoproteosis" (G. Valkiunas, personal communication).[14]

The *Haemoproteus* spp. identified are highly prevalent in the native European songbird population but normally do not cause harm to their hosts. In contrast, the cases reported here suggest that the same parasites may cause overt disease in invading species such as exotic parrots. These parasites that have adapted to European songbirds may cause fatal outbreaks in native psittacines of Australia, New Zealand, and South America that are raised in captivity. Blood-sucking insects such as biting midges (*Culicoides*), the vectors for *Haemoproteus* spp. of passerine birds in Europe may transmit the parasite from songbirds to parrots.[8] Since no gametocytes in parrot blood have been found and no blood stages have ever been described in previous reports, a completely abortive development has to be assumed.

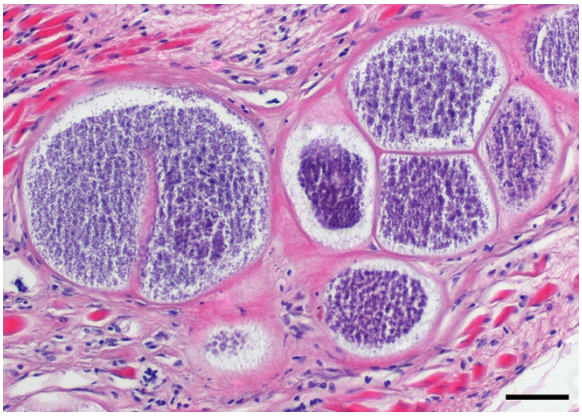

Ventriculus, parakeet. Haemoproteus minutus megaloschizonts with a thick eosinophilic cell wall, septation, and numerous zoites (HE, 100X). (Photo courtesy of: Department of Veterinary Pathology, Freie Universitaet Berlin, Germany (http://www.vetmed.fu-berlin.de/en/einrichtungen/institute/we12/index.html).

The pathogenesis in parrots is unknown. Presumably, tissue damage caused by megalomeronts in the conduction system of the heart may cause death in the affected birds.

Morphologically, the parasitic structures reported here were strikingly similar to the reported cases of numerous previous outbreaks in Europe. However, further retrospective, epidemiologic and experimental studies are needed to assess the full range of *Haemoproteus* spp. or other hematozoan parasites involved in this disease of parrots. Since blackbirds and songthrushes have been introduced to Australia and New Zealand in the 19th century, there is a concern that these parasites already have established in these areas and are potentially affecting the natural population of parrots.

JPC Diagnosis: 1. Skeletal muscle (S354/10)/Proventriculus, smooth muscle (S370/10): Protozoan megaloschizonts, multiple, barred parakeet, *Bolborhynchus lineola*/budgerigar, *Melopsittacus undulates*. 2. Proventriculus: Proventriculitis, ulcerative, focal, moderate with hemorrhage.

Conference Comment: There is significant slide variation in this case as a result of tissue submissions from two different psittacine birds from either the skeletal muscle or the proventriculus. Regardless of the tissue section received, conference participants readily identified numerous apicomplexan protozoal megaloschizonts undergoing various stages of degeneration within either the skeletal or smooth muscle. As mentioned by the contributor, *Haemoproteus* spp. are a large group of parasites that are found primarily in birds, but can also be seen in turtles and lizards.[5] All species of this parasite are transmitted via salivary secretions of hematophagic

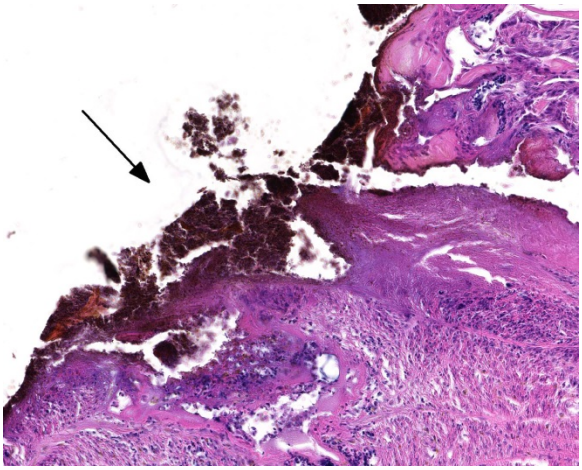

Ventriculus, parakeet: Base of the ulcer in the ventriculus, with necrosis, Heterophilic inflammation, and heme pigment in the overlying koilin layer. (HE, 288X)

biting midges, hippoboscids (louse flies), or tabanid flies containing infectious sporozoites.

Within the avian host, the sporozoites enter the vascular endothelial cells, most often within the lung, liver, bone marrow, and spleen where they undergo schizogony to form clusters of schizonts filled with merozoites. Sexual stages occur within the arthropod vector, while asexual reproduction occurs within the vertebrate host. Once the schizont ruptures, merozoites are released into the circulation, where they infect host red blood cells. Within erythrocytes, merozoites transform into macro or microgamonts. *Hemoproteus* infection is often subclinical in birds and clinical disease is associated with anemia due to parasitism of the host red blood cells. Additionally, clinically affected animals are usually concurrently immunocompromised. Severely affected animals can acutely die with no overt clinical signs.[3,5,10]

This case likely represents a manifestation of *Haemoproteus* infection associated with the pre-erythrocyte stage, characterized by large megaloschizonts within both the skeletal and smooth muscle. The conference moderator noted that in this stage, intra-erythrocytic gametocytes are not seen, consistent with the history provided by the contributor. Rather than anemia secondary to erythrocyte parasitism, lesions are associated with megaloschizonts within a variety of cell types, such as the muscular layers of the proventriculus and skeletal muscle, in this case.[3,5] The conference moderator also noted that similar to previously reported cases, the megaloschizonts in this case are large (200-500 um), have compartmentalized internal septae, and are often associated with hemorrhage.[5] Within mature megaloschizonts, there are numerous packeted merozoites within structures known as cytomeres. As they mature, megaloschizonts rupture and merozoites are released into the blood stream. These merozoites then infect erythrocytes and become gametocytes, ready to be ingested by biting flies to complete the life cycle of the parasite.[3,5,10] In previously reported cases, rupture of megaloschizonts and the release of merozites caused intense inflammation, hemorrhage, and necrosis[5]; however, in this case there is only very mild inflammation. It is unclear if the ulcerative proventriculitis with hemorrhage and hemosiderin laden macrophages in the koilin membrane is related to the parasite. Despite the relatively mild lesions present in these tissue sections, conference participants agreed with the contributor that there were likely megaloschizonts in the heart that interfered with signal conduction, ultimately leading to the death of these birds.

Contributing Institution:
Department of Veterinary Pathology
Freie Universitaet
Berlin, Germany
http://www.vetmed.fu-berlin.de/en/einrichtungen/institute/we12/index.html

References:

1. Atkinson CT, Van Riper CI. Pathogenicity and epizootiology of avian haematozoa: Plasmodium, Leucocytozoon, and Haemoproteus. In: Loye JE, Zuk M eds. *Bird–Parasite Interactions: Ecology, Evolution, and Behavior*. New York: Oxford University Press; 1999:19-48.
2. Bennett GF, Peirce MA, Ashford RW. Avian haematozoa: Mortality and pathogenicity. *J Nat Hist*.1993; 27:993-993.
3. Donovan TA, Schrenzel M, Tucker TA, Pessier AP, Stalis IH. Hepatic hemorrhage, hemocoelom, and sudden death due to *Haemoproteus* infection in passerine birds: Eleven cases. *J Vet Diagn Invest*. 2008; 20:304-313.
4. Frank W, Kaiser L. Infection with parasites of the genus *Leucocytozoon* (Protozoa, Sporozoa) in the breeding of parrots (Aves, Psittaciformes). Zeitschrift für Parasitenkunde (Berlin, Germany) 1967; 28:370-382.
5. Gardiner CH, Fayer R, Dubey JP. Apicomplexa. In: *An Atlas of Protozoan Parasites in Animal Tissues*. 2nd ed. Armed Forces Institute of Pathology, American Registry of Pathology, Washington DC; 1998:73-75.
6. Hellgren O, Waldenström J, Bensch S. A new PCR assay for simultaneous studies of *Leucocytozoon*, *Plasmodium*, and *Haemoproteus* from avian blood. *J Parasitol*. 2004; 90:797-802.
7. Krizanauskiene A, Hellgren O, Kosarev V, Sokolov L, Bensch S, Valkiunas G. Variation in host specificity between species of avian hemosporidian parasites: Evidence from parasite morphology and cytochrome B gene sequences. *J Parasitol*. 2006; 92:1319-1324.
8. Martinsen ES, Perkins SL, Schall JJ. A three-genome phylogeny of malaria parasites (*Plasmodium* and closely related genera): Evolution of life-history traits and host switches. *Mol Phylogenet Evol*. 2008; 47:261-273.
9. Olias P, Wegelin M, Zenker W, Freter S, Gruber AD, Klopfleisch R. Avian malaria deaths in parrots, Europe. *Emerg Infect Dis*. 2011; 17:950-952.
10. Pennycott T, Wood A, MacIntyre C, MacIntyre D, Patterson T. Deaths in aviary birds associated with protozoal megaloschizonts. *Vet Rec*. 2006; 159:499-500.
11. Ricklefs RE, Fallon SM. Diversification and host switching in avian malaria parasites. Proc Biol Sci. 2002; 269:885-892.
12. Scheuerlein A, Ricklefs RE. Prevalence of blood parasites in European passeriform birds. *Proceedings of the Royal Society of Biological Sciences*. 2004; 271:1363-1370.
13. Smith GA. Aberrant leucocytozoon infection in parakeets. *Vet Rec*. 1972; 91:106.
14. Valkiunas G, Anwar AM, Atkinson CT, Greiner EC, Paperna I, Peirce MA. What distinguishes malaria parasites from other pigmented haemosporidians? *Trends Parasitol*. 2005; 21:357-358.

CASE II: 3019-15 (JPC 4081674).

Signalment: 11-month-old intact male golden retriever, (*Canis familiaris*).

History: This 11-month-old Golden retriever dog was not eating for 5 days, did not defecate, vomited once over this period, and died suddenly. Necropsy was requested and performed.

Gross Pathology: The dog was in good nutritional status (body condition score 3/5), well-hydrated and had mild rigor mortis. There was generalized pallor of mucous membrane and non-haired dermis. Thoracic cavity contained approximately 1 liter of dark red, cloudy hemorrhagic fluid. Parietal pleural surfaces of the mediastinum, diaphragmatic surface as well as the dorsal aspect of the pleural cavity were diffusely thickened, friable, mottled red and white. Few fragments of friable dark red blood clot were present in the ventral thoracic cavity.

Immediately caudal to the heart base, 14 cm length of the descending aorta was adhered to 11 cm of the immediately adjacent esophagus and formed a fibrous, dark red to white, hemorrhagic mass. Affected segment of descending aorta wall was markedly thickened and had multifocal mural nodules and tunica intima ulceration. There was focal perforation of ventral aortic wall. Tissues and subpleural parenchyma around affected segment of aorta was thickened, hemorrhagic, soft, edematous and friable. The esophageal wall was multifocally thickened by coalescing round to oval nodules. Embedded within the aortic and esophageal nodules were 4-6cm long, 1mm diameter dark red nematodes (*Spirocera lupi*).

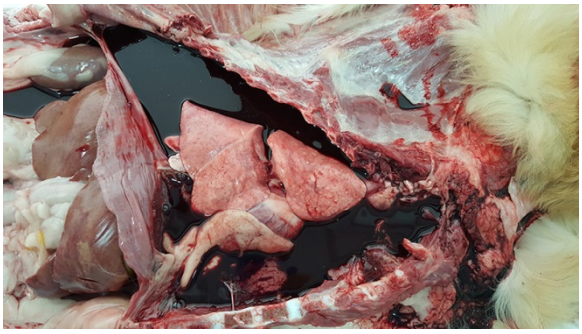

Thorax, dog. There was fatal hemothorax in this individual. (Photo courtesy of: Advanced Molecular Pathology Laboratory, Institute of Molecular and Cell Biology, 61 Biopolis Drive, Proteos, Singapore 138673).

Laboratory results: N/A

Histopathologic Description: Aorta: The aorta is characterized by variable loss of architecture with replacement by multifocal to coalescing necrosis, intense neutrophilic, eosinophilic, granulomatous and lympho-plasmacytic infiltrate that expands aorta wall. Abundant fibrin and multiple foci of dystrophic mineralization are present among the inflammatory cells. Embedded within tunica intima are cross and tangential sections of nematode organisms characterized by 0.6mm to 0.1mm diameter width, smooth cuticle, coelomyarian-polymyarian musculature, large lateral hypodermal chords, abundant amphophilic to basophilic fluid in the pseudocoelom and an intestine composed of individual cuboidal cells, each with a prominent brush border. The inflammation and necrosis are supported by dense fibrocollagenous stroma that extends into fibroadipose tissue around the aorta. Scattered within the inflammation and granulation tissue are small numbers of embryonated nematode eggs. Focally, the necrosis extends through entire aortic wall and there is continuity of aortic lumen to beyond tunica adventitia (focal rupture). The tunica adventitia is thickened by proliferation of mesothelial cells, granulation tissue and hemorrhagic exudate.

Esophagus: The grossly observed esophagal masses are characterized by expansion of the esophageal wall, mural architecture and replacement by marked necrosis, fibrin exudation and, intense mixed cell infiltrate. The inflammatory cells are intermixed with anisocytosis are both mild. Few scattered nematode eggs are present within the esophageal inflammation, necrosis and atypical mesenchymal cell proliferations.

Contributor's Morphologic Diagnoses:

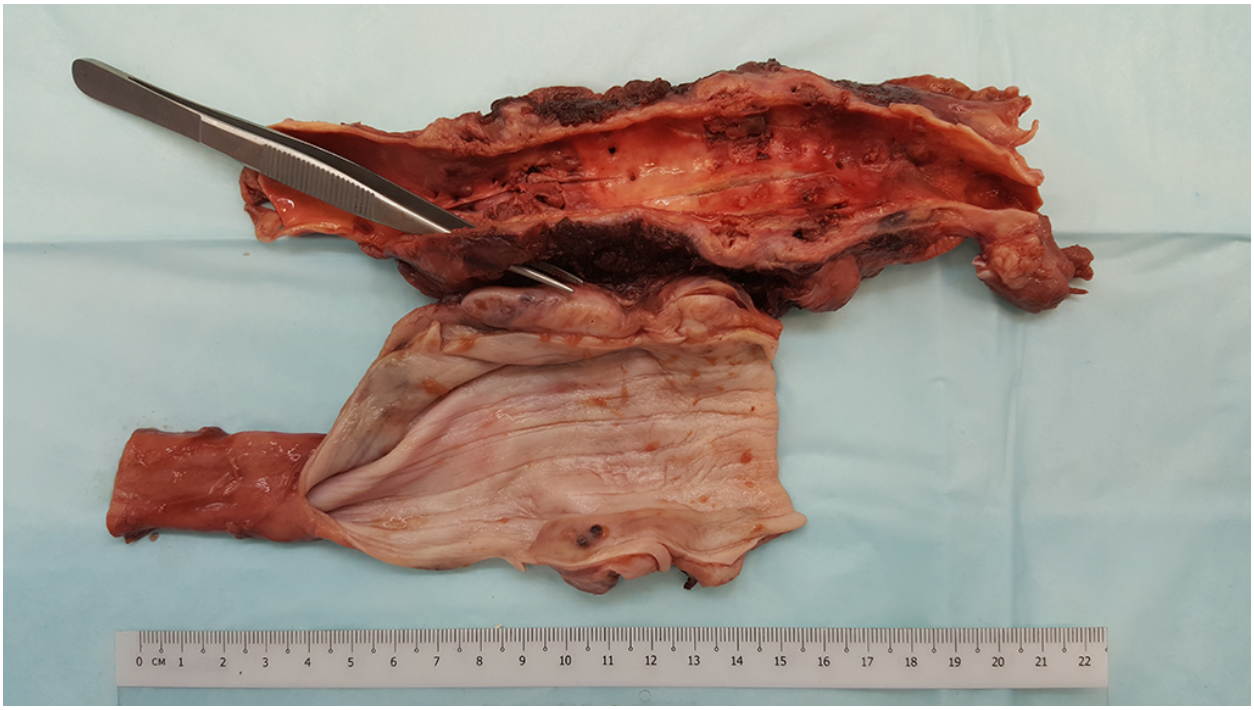

Aorta and esophagus, dog. There are multifocal thickenings of the ventral aortic wall and dorsal esophagus. A pair of forceps demonstrates the aortic perforation responsible for the hemothorax in this individual. Lung, penguin: Numerous small foci of necrosis, which are highlighted as they interrupt the diffuse congestion of the air capillary walls, are present throughout the section. (HE, 400X).

a large amount of fibrocollagenous stroma, which dissects and replaces tunica muscularis multifocally. Within the necrosis and inflammation, and embedded within esophagus wall are cross sections of 0.2 to 0.3mm diameter nematodes of similar morphology as that described above for the aorta. In a few nodules, among the inflammation and fibrocollagenous stroma are non-encapsulated lobules of atypical and dysplastic mesenchymal cells. Mesenchymal cells are spindle-shaped, arranged in streams, whorls, and bundles supported by loose fibrocollagenous to myxomatous stroma. Mitoses are present at 3 per 10 high power (400x) fields, and anisokaryosis and

Aorta:
1. Severe focally extensive, chronic active, necrotizing, pyogranulomatous, eosinophilic, lymphoplasmacytic arteritis with granulating fibrosis and spirurid nematodes (*Spirocerca lupi*) and ova
2. Focal perforation.

Esophagus:
1. Severe, focally extensive, fibrinonecrotizing, eosinophilic, pyogranulomatous, lymphoplasmacytic esophagitis with marked granulating fibrosis, and intralesional Spirurid nematodes (*Spirocerca lupi*) and ova

2. Multifocal, atypical, dysplastic mesenchymal cell proliferation (fibrosarcoma)

Contributor's Comment: Major findings in this dog include the hemothorax secondary to the ruptured aorta, as well as nematode-induced inflammation and fibrosis in the aorta and esophagus. There is also evidence of neoplastic change within some of the esophageal nodule. The cause of death in this dog is most associated with the hemothorax which would also explain the generalized pallor in this dog at presentation for necropsy. The morphological features of the nematodes indicate a spirurid, most consistent with *Spirocerca lupi* based on the location and lesion associated with this dog's pathology.

Spirocerca lupi is a spirurid nematode that parasitizes esophageal wall of dogs and some other carnivores and is mostly seen in warm climates where dung beetles act as intermediate hosts. The life cycle of the parasite involves passage of parasite eggs from the definitive host (canine) via feces followed by ingestion by coprophagous (dung-eating) beetle. The larva develops into infective third stage and encysts in the beetle's tissues. The beetle is then eaten by a definitive host or by a paratenic host (e.g. lizard, chicken or rodents) which in turn is eaten by the definitive host (dog). The ingested larvae penetrate gastric mucosa and migrate to the aorta via arteries, and embed in the intima aorta and form parasitic granulomas in aortic adventitia at the caudal thoracic area. After a few months, the nematodes migrate to the immediately underlying esophagus, develop to adulthood and form cystic granulomas in distal esophagus submucosa or gastric cardia. Esophageal lesions associated with *Spirocerca* are characterized by granulomatous inflammation with highly

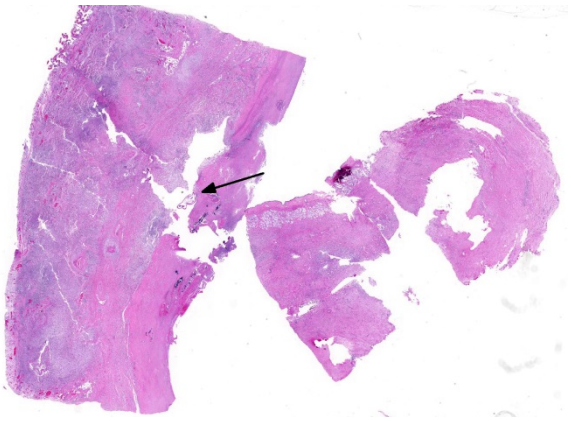

Aorta and esophagus, dog. Subgross examination of aorta (left) and esophagus (right) reveals thickening due to fibrosis and granulomatous inflammation, more severe in the aorta. A cross section of an adult nematode is present in the aortic wall (arrow). (HE, 5X)

reactive fibroblasts. These foci can develop into fibrosarcoma and osteosarcoma, with local tissue invasion and pulmonary metastasis. The parasites can extend from nodules through fistulas that lead into esophageal lumen, where female worms can oviposit into gastrointestinal tract. Aortic lesions are characterized by necrotizing, hemorrhagic, eosinophilic vasculitis, aneurysm and rare aortic rupture such as in this case. Advanced cases of *Spirocerca lupi* infection, such as in this case, are associated with guarded to poor prognosis. [2]

Aortic rupture due to vasculitis and vascular wall compromise secondary to *Spirocerca lupi* has been reported to cause a fatal hemothorax in older literature and likely occurred in this case.[7] Alternatively, perforation of the esophagus due to damaged esophageal wall from parasitic nodules and/or associated neoplasms can result in leakage of ingesta contents into thoracic cavity and a pyothorax.[8]

While the majority of the limited land in Singapore consists of built up urban environment, several species of dung beetles still do exist, typically in the remaining forested areas.[6,8] These insects, along with wild reptiles and rodents, are the suspected

intermediate hosts that infect dogs that come into contact with them in the outdoor environment.

JPC Diagnosis: 1. Esophagus: Esophagitis, granulomatous and eosinophilic, chronic, focal, severe, with adult spirurid nematodes and eggs, Golden retriever, *Canis familiars*.
2. Aorta: Arteritis, necrogranulomatous and eosinophilic, chronic, diffuse, severe with fibrin thrombi and marked mural fibrosis.

Conference Comment: There is significant slide variability in this case and not all conference participants received slides with nice cross sections of the adult nematode. However, all examined slides did, at minimum, contain variable numbers of small 20x40 um thick shelled oval embryonated eggs, highly characteristic of spirurids.[3] The conference moderator noted that the presence of spirurid eggs within proliferative and granulomatous lesions within the esophageal wall of a canine should point observers to the diagnosis of *Spirocera lupi*, even in the absence of adult nematode cross sections in the tissue. In sections that contained adult *Spirocerca lupi*, conference participants described nematodes as 600-800 um in diameter with an 8 um thick smooth cuticle, coelomyarian-polymyarian musculature, prominent lateral cords, a pseudocoelom containing a moderate amount of eosinophilic material, an intestine lined by uninucleate columnar epithelium with a prominent brush border, and male or female reproductive organs. Females have distended uteri containing numerous spirurid eggs.[1,3]

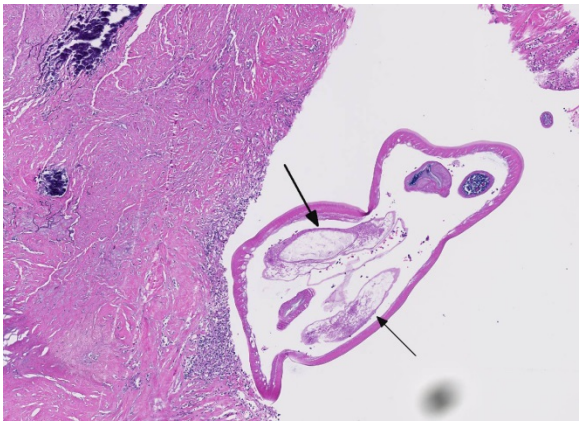

Aorta, dog. Within a large pseudocyst surrounded by a fibrotic and mineralized wall, there is a single tangential section of an adult nematode measuring approximately a millimeter in diameter with polymyarian-coelomyarian musculature, large lateral chords (arrows), and multiple cross-sections of a uterus. (HE, 66X)

Other esophageal parasites discussed by conference participants include *Gongylonema* sp. in ruminants, pigs, horses, primates, and rodents; *Gastophilus* sp. in horses; and *Hypoderma lineatum* in ruminants. With the exception of *Spirocerca lupi*, parasitic diseases of the esophagus are usually of little significance to the host.[2,4]

Conference participants were unable to reach a consensus regarding the multifocal nodular proliferation of atypical mesenchymal cells within the muscular layers of the esophagus. Some agreed with the contributor, that this likely represents an early neoplastic transformation of the tunica muscularis, while others favored a proliferation of highly activated fibroblasts secondary to chronic marked inflammation. Interestingly, *Spirocerca lupi* is known for the ability to induce malignant transformation within the wall of its associated esophageal granulomas. Mesenchymal neoplasms fibrosarcoma and osteosarcoma are the most common malignancies associated with the parasite.[2,4] Neoplasms that arise from areas of marked granulomatous inflammation are often highly infiltrative with frequent metastasis to the lungs. Additionally, *Spirocerca lupi* induced thoracic neoplasia has occasionally been associated with the development of hypertrophic osteopathy, a condition that results in the periosteal new bone

proliferation in the distal extremities. Other potential sequelae include dysphagia, aortic aneurysm, and aortic rupture leading to acute hemothorax, seen in this case.[2,4]

Attendees discussed other parasites that induce neoplastic transformation in veterinary species. Residents at the Joint Pathology Center use the acronym SOCCS-T as a mnemonic device to remember which parasites are associated with neoplastic transformation. *Spirocerca lupi* causes fibrosarcoma and osteosarcoma; *Opisthorchis felineus* causes cholangiocarcinoma in cats and humans; *Cysticercus fasciolaris* can induce hepatic sarcoma in rats; *Clonorchis sinensis* is associated with cholangiocarcinoma in cats and people; *Schistosoma haematobium* is a trematode that can induce transitional cell carcinoma of urinary bladder in people; and *Trichosomoides crassicauda* can cause papillomas of the urothelium in rats.[2-4]

Contributing Institution:
Advanced Molecular Pathology Laboratory
Institute of Molecular and Cell Biology
61 Biopolis Drive, Proteos
Singapore 138673

References:

1. Blume GR, Reis JL, Gardiner CH, et al. *Spirocerca lupi* granulomatous pneumonia in two free-ranging maned wolves (*Chrysocyon brachyurus*) from central Brazil. *J Vet Diagn Invest*. 2014; 26(6):815-817.
2. Uzal FA, Plattner BA, Hotetter JM. Alimentary system. In: Maxie MG, ed. *Jubb, Kennedy and Palmer's Pathology of Domestic Animals*. Vol 2. 6th ed. Philadelphia, PA: Elsevier Saunders; 2016:34-35.
3. Gardiner CH, Poynton SL. Spirurids. In: Gardiner CH, Poynton SL, eds. *An Atlas of Metazoan Parasites in Animal Tissues*. Washington, DC: Armed Forces Institute of Pathology; 1999:30-34.
4. Gelberg HB. Alimentary system and the peritoneum, omentum, mesentery, and peritoneal cavity. In: In: Zachary JF, ed. *Pathologic Basis of Veterinary Disease*. 6th ed. St. Louis, MO: Elsevier Mosby; 2017:356-357.
5. Klainbart S et al. Spirocercosis-associated pyothorax in dogs. *Vet J*. 2007; 173(1):209-214.
6. Lee JS, Lee IQW, Lim SL, et al. Changes in dung beetle communities along a gradient of tropical forest disturbance in South-East Asia. *J Tropic Ecol*. 2009; 25(6):677-680.
7. Rinas MA, Nesnek R, Kinsella JM, DeMatteo KE. Fatal aortic aneurysm and rupture in a neotropical bush dog (*Speothos venaticus*) caused by *Spirocerca lupi*. *Vet Parasitol*. 2009; 164(2-4):347-9.
8. Xin RO, Siew CC, Potts MD. Recent records of the dung beetle *Catharsius Molossus* (Coleoptera: *Scarabaeidae*) in Singapore. *Nature in Singapore*. 2013; 19(6): 1–6.

CASE III: 14-6189 (JPC 4084011).

Signalment: 27-year-old male African penguin, (*Spheniscus demersus*).

History: This captive bird was at the end of a molting period and had been depressed and lethargic for a couple of days before being found dead.

Gross Pathology: The lungs were described as congested by the submitting institution,

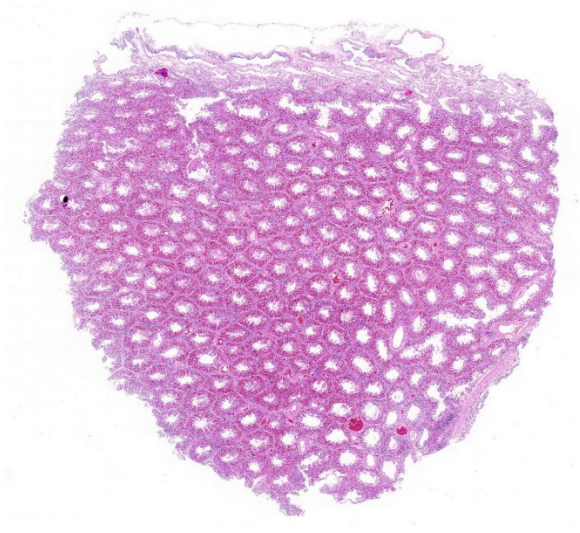

Lung, penguin: There is a moderate diffuse interstitial pneumonia, with prominent infiltration of the septa between air ostia with numeorus lymphocytes and fewer plasma cells and histiocytes. (HE, 256X)

which performed the necropsy. A complete set of formalin-fixed tissues was submitted for histopathologic examination.

Laboratory results:
Immunohistochemistry:
In house*:* *Toxoplasma gondii* (commercial rabbit polyclonal antibody) – weakly positive with some non-specific background staining

CAHFS Laboratory, Davis, CA
Sarcocystis sp. (rabbit polyclonal antibody) – strongly positive
Toxoplasma gondii (rabbit polyclonal antibody) – negative

PCR:
Wildlife Conservation Society, Bronx Zoo, NY
Two assays on formalin-fixed, paraffin-embedded lung: Apicomplexan 18S rRNA gene and Sarcocystis-specific ITS-1 18S rRNA gene – both positive – sequences of products match *Sarcocystis falcatula*

Histopathologic Description: Lung: Variably obscuring the parenchyma throughout the section are interstitial and luminal accumulations of inflammatory cells, eosinophilic fluid (edema), and sometimes necrotic cellular debris. Moderate numbers of macrophages and fewer heterophils are present in the lumens of parabronchi, atria and air capillaries mixed with amorphous to globular eosinophilic material and erythrocytes, and these air spaces are often lined by hypertrophied epithelial cells. Rarely, within disrupted air capillary walls, there are irregularly round to slightly elongated clusters of approximately 2-4 X 1 µm, fusiform, basophilic, protozoal zoites. There is prominent infiltration of septal and

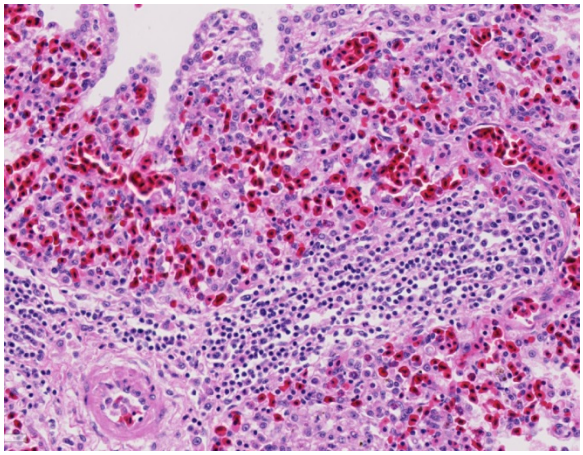

Lung, penguin: There is a moderate diffuse interstitial pneumonia, with prominent infiltration of the septa between air ostia with numeorus lymphocytes and fewer plasma cells and histiocytes. (HE, 256X)

perivascular interstitium by moderate to large numbers of lymphocytes, plasma cells, and fewer macrophages, along with numerous nodular aggregates of macrophages containing brown anisotropic pigment (anthracosis).

Contributor's Morphologic Diagnosis: Lung: severe diffuse necrotizing and lymphohistiocytic interstitial pneumonia

with epithelial hypertrophy, edema, hemorrhage and protozoal schizonts.

Contributor's Comment: Death of this penguin was due to a severe interstitial pneumonia caused by a protozoal infection. Occasional clusters of very small, elongated protozoal organisms present in air capillary walls throughout the lung were suggestive of apicomplexan schizonts, so differential diagnoses initially included *Sarcocystis* sp., *Toxoplasma gondii*, and *Plasmodium* sp. Both malaria and toxoplasmosis have previously been reported as causes of interstitial pneumonia in penguins,[6,13] whereas sarcocystosis is a common cause of pneumonia in various avian species but has not been described in penguins. The only relevant immunohistochemical stain available in house was a rabbit polyclonal antibody against *T. gondii* (BioGenex, San Ramon, CA). Organisms exhibited weak but positive reactivity with this immunostain. Because cross-reactivity between different cyst-forming apicomplexans has been reported with polyclonal antibodies, such as between *T. gondii* and *Neospora caninum*[1,11] and between *N. caninum* and *Sarcocystis* sp.,[12] more specific diagnostic methods were pursued. No fresh/frozen lung tissue was available, so formalin-fixed paraffin-embedded lung tissue was submitted to the Wildlife Conservation Society for apicomplexan and *Sarcocystis*-specific PCR assays. The DNA sequences obtained from both of these positive assays were 100% matches to *Sarcocystis falcatula*. The next closest match was *S. neurona* with a 98-99% identity. The pneumonia in this penguin is therefore attributed to *S. falcatula*. Subsequent additional immunohistochemical staining performed at the CAHFS laboratory in Davis, CA, confirmed strongly positive labelling of the protozoa with a *Sarcocystis* antibody. The *Toxoplasma gondii*

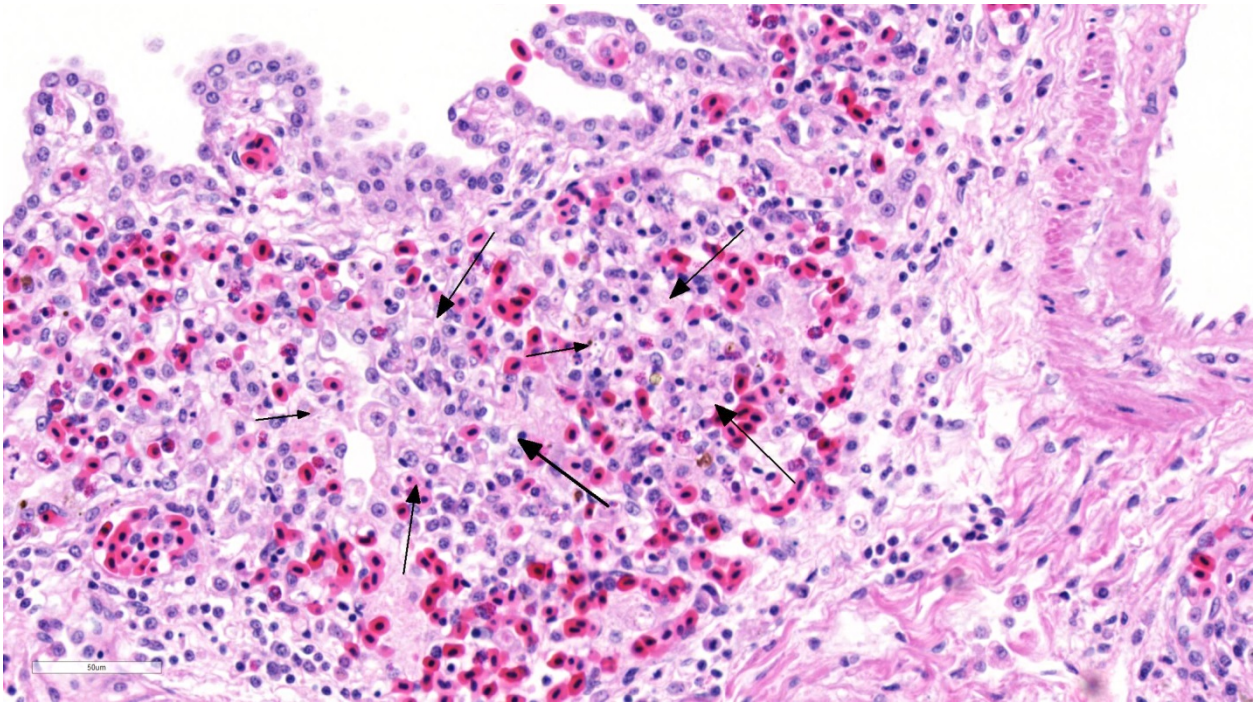

Lung, penguin: Numerous small foci of necrosis, which are highlighted as they interrupt the diffuse congestion of the air capillary walls, are present throughout the section. (HE, 400X)

immunohistochemical stain performed by this laboratory was negative.

In North America, the definitive host for *S. falcatula* and the closely related *S. neurona* is the Virginia opossum, *Didelphis virginiana*, which sheds infective sporocysts in feces.[9] Opossums had been seen on the premises of the aquarium institution where this penguin was housed. Infection of various bird species, most naturally grackles and cowbirds, as intermediate hosts is typically through ingestion of food contaminated with opossum feces, but insects such as cockroaches can serve as mechanical vectors.[2] In the intermediate host, asexual reproduction (merogony/schizogony) occurs in endothelial cells in various tissues but especially in the lung.[9,10] The merozoites produced eventually infect skeletal and cardiac muscle cells and form sarcocysts filled with bradyzoites, which are infective to the definitive host upon ingestion of the intermediate host tissue.[9] Replication in pulmonary endothelial cells can result in severe interstitial pneumonia, the most common form of fatal infection, although two other clinical forms of disease have been characterized: a neurologic form and a muscular form.[14] The neurologic form has been reported in psittacines and raptors.[14,15]

Fatal pulmonary infection with *S. falcatula* has been reported most often in psittacines,[2-5,14] and this is thought to be the first report in a penguin. The microscopic features of the pneumonia in this penguin were similar to what has been described in other avian species infected with *S. falcatula*, namely edema, fibrin deposition, congestion, hemorrhage, mononuclear inflammatory infiltrates, endothelial cell lysis, and pneumocyte hyperplasia.[7,10,14] The schizonts were rare in this case, occasionally exhibiting a "sunburst" or somewhat

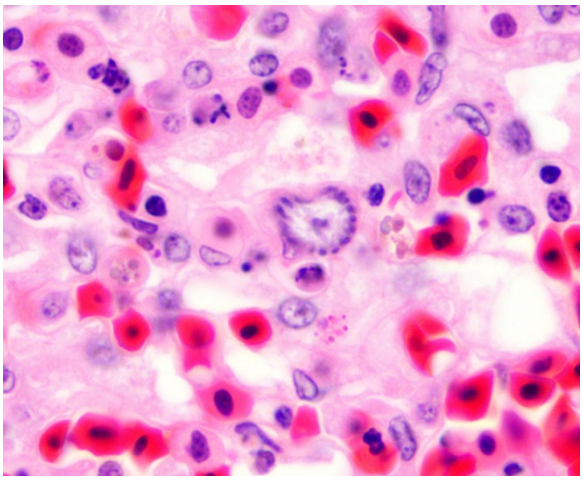

Lung, Sprague-Dawley rat. Lung, penguin: Schizonts of Sarcocystis falcatula are present within areas of necrosis in small numbers. This one exhibits a classic "sunburst" pattern. (Photo courtesy of: Department of Pathobiology and Veterinary Science, Connecticut Veterinary Medical Diagnostic Laboratory, College of Agriculture, Health and Natural Resources, University of Connecticut, 61 North Eagleville Rd, Unit 3089 Storrs, CT 06269-3089 (HE, 400X)

elongated arrangement, but characteristic serpentine forms that conform to pulmonary capillary lumens[2-5,7-10,14] were not seen in this penguin. Identification of the infected cells as endothelial cells was not possible in this case from microscopic examination alone. A complete set of tissues was examined histologically from this penguin, including brain, skeletal muscle and heart, but no extrapulmonary schizonts or sarcocysts were seen. There was, however, a mild lymphohistiocytic portal hepatitis in this bird, which can be seen with *S. falcatula* infection,[7,8] and for which no other etiology was identified.

JPC Diagnosis: Lung: Pneumonia, interstitial, necrotizing and lymphohistocytic, multifocal, moderate with intracellular apicomplexan zoites, African penguin, *Spheniscus demersus*.

Conference Comment: The contributor provides an outstanding summary of avian

sarcocystosis. The genus *Sarcocystis* is a large group of cyst-forming apicomplexan protozoal coccidian parasites that affect mammals, birds, and reptiles. They have also been rarely reported in amphibians and fish.[3,4,11,15] *Sarcocystis falcatula*, similar to all other members of this genus, utilizes a two-host life cycle based on the predator and prey dynamic. Carnivores and omnivores are the definitive hosts and become infected by preying upon intermediate hosts (usually herbivores) which contain mature sarcocysts in muscular or neural tissue. After digestion of the sarcocyst wall, bradyzoites are released and invade the intestinal epithelium of the carnivorous definitive host. These bradyzoites undergo sexual gametogony and develop into micro-(male), macro-(female) gamonts. Fertilization leads to the formation of infective oocysts, which sporulate in the intestinal lumen and are shed in the feces. Similar to other common apicomplexan coccidian parasites (*Besnoitia*, *Frenkelia*, *Isospora*, *Toxoplasma*), sporulated oocysts contain two sporocysts with four sporozoites each.[3,9]

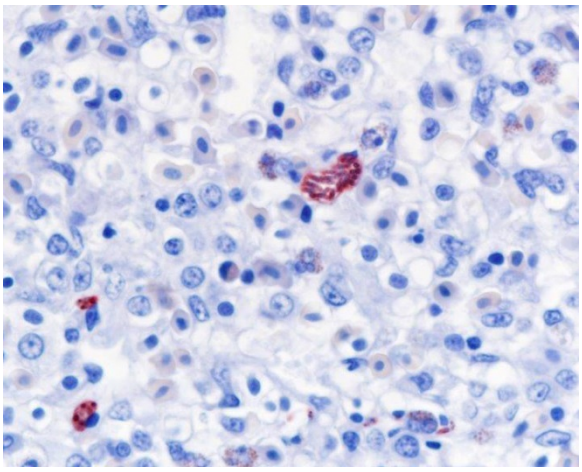

Lung, penguin: Schizonts stain strongly positive with a non-specific anti-Sarcocystis antibody. (Photo courtesy of: Department of Pathobiology and Veterinary Science, Connecticut Veterinary Medical Diagnostic Laboratory, College of Agriculture, Health and Natural Resources, University of Connecticut, 61 North Eagleville Rd, Unit 3089 Storrs, CT 06269-3089 (anti-Sarcocyst, 200X)

Sporulated oocysts are then ingested by susceptible intermediate hosts, such as herbivorous mammals or birds. After ingestion by the intermediate host, sporozoites excyst in the intestine and undergo two generations of asexual merogony (schizogony). Sporozoites are released and first migrate to endothelial cells where they undergo the first two generation of asexual reproduction, resulting in the development of meronts.[3,9,11,15] In birds, merogony is most pronounced in vascular endothelial cells within the lungs. Pulmonary capillary endothelial cells can become markedly swollen and inflamed, leading to lymphohistiocytic vasculitis, airway edema, interstitial pneumonia, and even vascular obstruction in birds with a heavy protozoan burden.[11,15] Merogony has also been reported in vessels of the liver, pancreas, spleen, adrenal glands and heart.[11]In animals that survive the maturation of the second generation of meronts, merozoites are liberated from meronts within capillaries and enter circulating mononuclear cells. Merozoites then undergo endodyogeny and enter muscle fibers to eventually form sarcocysts containing bradyzoites. They will remain encysted and viable in the muscular or nervous tissue until they are ingested by the definitive host to complete the lifecycle. There are over 90 *Sarcocystis* sp. known to infect mammals, birds, and reptiles. The vast majority of species are considered non-pathogenic; however, some species, such as *S. falcatula* in birds, are associated with severe clinical disease in the intermediate host.[3,4,11,15]

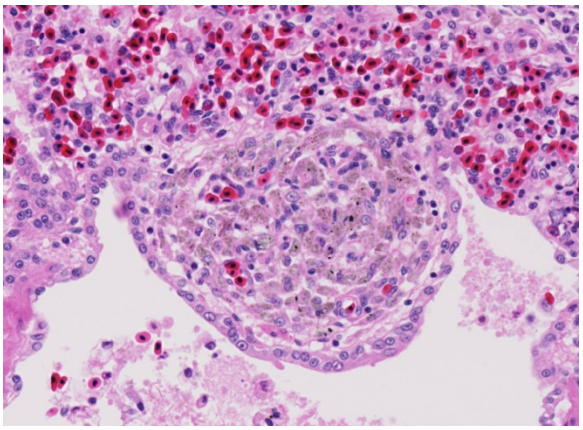

Lung, penguin. There are focal granulomas containing anthacosilicotic pigments adjacent to many air ostia. (HE, 286X)

As mentioned by the contributor, the only known definitive host for this protozoan in North America is the opossum (*Didelphis virginiana*). Most *Sarcocystis* sp. infect a specific intermediate host; however, *Sarcocystis falcatula* is unique in that it can infect a heterogeneous population of avian intermediate hosts from numerous avian species (Passeriformes, Psittaciformes, and Columbiformes).[4,9,11,15] Birds become infected by eating feed contaminated with opossum feces containing infective oocysts or sporocysts or ingestion of cockroaches, which is the main mechanical vector for the parasite.[2]

Contributing Institution:

Department of Pathobiology and Veterinary Science
Connecticut Veterinary Medical Diagnostic Laboratory
College of Agriculture, Health, and Natural Resources
University of Connecticut
http://www.pathobiology.uconn.edu/

References:

1. Barr BC, Conrad PA, Dubey JP, Anderson ML. *Neospora*-like encephalomyelitis in a calf: Pathology, ultrastructure and immunoreactivity. *J Vet Diagn Invest*. 1991;3:39-46.
2. Clubb SL, Frenkel JK. *Sarcocystis falcatula* of opossums: Transmission by cockroaches with fatal pulmonary disease in psittacine birds. *J Parasitol*. 1992; 78(1):116-124.
3. Gardiner CH, Fayer R, Dubey JP. Apicomplexa. In: *An Atlas of Protozoan Parasites in Animal Tissues*. 2nd ed. Armed Forces Institute of Pathology, American Registry of Pathology, Washington DC; 1998:20-42.
4. Godoy SN, De Paula CD, Cubas ZS, Matushima ER, Catão-Dias JL. Occurrence of *Sarcocystis falcatula* in captive psittacine birds in Brazil. *J Avian Med Surg*. 2009; 23(1):18-23.
5. Hillyer EV, Anderson MP, Greiner EC, Atkinson CT, Frenkel JK. An outbreak of *Sarcocystis* in a collection of psittacines. *J Zoo Wildlife Med*. 1991;22(4):434-445.
6. Ploeg M, Ultee T, Kik M. Disseminated toxoplasmosis in black-footed penguins (*Spheniscus demersus*). *Avian Dis*. 2011; 55:701-703.
7. Smith JH, Neill PJG, Dillard III EA, Box ED. Pathology of experimental *Sarcocystis falcatula* infections of canaries (*Serinus canarius*) and pigeons (*Columba livia*). *J Parasitol*. 1990; 76(1):59-68.
8. Smith JH, Neill PJG, Box ED. Pathogenesis of *Sarcocystis falcatula* (Apicomplexa: Sarcocystidae) in the budgerigar (*Melopsittacus undulates*). III. Pathologic and quantitative parasitologic analysis of extrapulmonary disease. *J Parasitol*. 1989; 75(2):270-287.
9. Smith JH, Meier JL, Neill PJG, Box ED. Pathogenesis of *Sarcocystis falcatula* in the budgerigar. I. Early pulmonary schizogony. *Lab Invest*. 1987; 56(1): 60-71.

10. Smith JH, Meier JL, Neill PJG, Box ED. Pathogenesis of *Sarcocystis falcatula* in the budgerigar. II. Pulmonary pathology. *Lab Invest*. 1987; 56(1):72-84.
11. Sundermann CA, Estridge BH, Branton MS, Bridgman CR, Lindsay DS. Immunohistochemical diagnosis of *Toxoplasma gondii*: potential for cross-reactivity with *Neospora caninum*. *J Parasitol*. 1997; 83(3):440-443.
12. Uzêda RS, Schares G, Ortega-Mora LM, et al. Combination of monoclonal antibodies improves immuno-histochemical diagnosis of *Neospora caninum*. *Vet Parasitol*. 2013; 197:477-486.
13. Vanstreels RET, da Silva-Filho RP, Kolesnikovas CKM, et al. Epidemiology and pathology of avian malaria in penguins undergoing rehabilitation in Brazil. Vet Res. 2015; 46:30.
14. Villar D, Kramer M, Howard L, Hammond E, Cray C, Latimer K. Clinical presentation and pathology of sarcocystosis in psittaciform birds: 11 cases. *Avian Dis*. 2008; 52:187-194.
15. Wünschmann A, Rejmanek D, Conrad PA, et al. Natural fatal *Sarcocystis falcatula* infections in free-ranging eagles in North America. *J Vet Diagn Invest*. 2010; 22:282-289.

CASE IV: E2889/15 (JPC 4084734).

Signalment: Six-year-old male castrated mixed-breed dog, (*Canis familiaris*).

History: The dog was presented to a local practitioner with suppurative conjunctivitis and permanent lacrimation. During examination a worm-like structure was found within the conjunctival sac. The worm measured about 2 cm long and 0.2 cm in diameter. The complete globe with adjacent thickened periorbital tissue was surgically removed, fixed in formalin and submitted for histological examination. Weeks later, clinical signs recurred at the other eye, again with evidence of worm-like structures within the conjunctival sac. No further clinical follow-up is available.

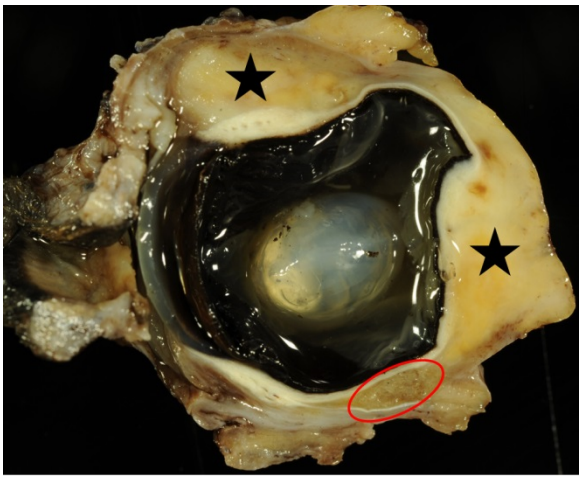

Eye, dog. Retrobulbar granuloma, eye, dog. Macroscopic overview of the enucleated eye in a cross section demonstrating several nematodes (circle) and the severely thickened periorbital tissue (asterisks). (Photo courtesy of: Department of Pathology, University of Veterinary Medicine, Hannover, Buenteweg 17, 30559 Hannover, Germany. (http://www.tiho-hannover.de/kliniken-institute/institute/institut-fuer-pathologie/).

Gross Pathology: Macroscopically, the retrobulbar tissue showed marked irregular thickening, firm consistency and a greyish-yellow appearance. In the periorbital tissue, multifocal nodular accumulations of curled, thin structures were evident.

Laboratory results: None.

Histopathologic Description: The cross-section of the globe reveals severe and irregular expansion of the periocular tissue by infiltration of numerous macrophages, fewer plasma cells, and rare lymphocytes. These infiltrates extend circumferentially into choroid, sclera, adipose tissue and periorbital musculature. Granulation tissue

composed of fibroblasts, collagen fibers, and newly formed blood vessels shows multifocal severe infiltration of neutrophilic granulocytes. Within the inflammatory infiltration, multiple cross and longitudinal sections of metazoan parasites, measuring approximately 200 – 300 µm in diameter are present. Parasites (nematodes) show a 4 – 5 µm thick, smooth, eosinophilic cuticle with cuticular ridges seen on longitudinal sections. Remnants of coelomyarian musculature are visible because the musculature is mainly atrophied and replaced by hypodermal tissue. Within the spacious body cavity, there is a faint intestine and larger genital organs with remnants of eggs present. Occasionally, nematode structures display a homogenous eosinophilic appearance with structural loss (necrosis of nematodes). Furthermore, the amount of periorbital fibrous tissue composed of collagen fibers and fibroblasts is moderately increased (fibrosis). The retinal pigment epithelium displays focally a mild hypertrophy with tombstone-like appearance. The retina is detached from the retinal pigment epithelium.

Eye, dog. Retrobulbar granuloma, eye, dog. Higher magnification of the granuloma with several coiled nematodes (circle). (Photo courtesy of: Department of Pathology, University of Veterinary Medicine, Hannover, Buenteweg 17, 30559 Hannover, Germany. (http://www.tiho-hannover.de/kliniken-institute/institute/institut-fuer-pathologie/).

Contributor's Morphologic Diagnosis: Globe and periorbital tissue: Scleritis, severe, multifocal to coalescing, chronic, granulomatous and pyogranulomatous with mild, multifocal, granulomatous choroiditis, myositis, steatitis and numerous nematodes.

Contributor's Comment: During the past decades, an increasing number of cases of ocular onchocerciasis have been reported in dogs from Europe and the United States.[12] In dogs, it is known to occur as an acute or chronic ocular disease with nodules located on the eyelids, conjunctiva, and sclera. Infections may remain undetected if verminous nodules are located within the retrobulbar areas,[10] as in the present case. In this case, *Onchocerca* sp. are suspected as the causative pathogen, because histologic criteria including atrophied coelomyarian musculature, a very small intestine, and cuticular annulations on female nematodes similar to those described in the literature.[4]

For a long time, ocular onchocercosis in dogs was thought to be an aberrant infection with *Onchocerca* (*O.*) *lienalis*, commonly found in cattle. The assumption that canine ocular onchocerciasis is associated with *O. lienalis* was only based on the microscopic morphology.[6] In contrast, a previously unrecognized species of *Onchocerca* was suspected to be spilling over from wild ungulates to canines, but it turned out that the nucleotide sequences of *Onchocerca* species found in canines are unique within the genus.[13] An analysis of the molecular genetic data suggested that the causative agent is rather *O. lupi* than *O. lienalis*.[6]

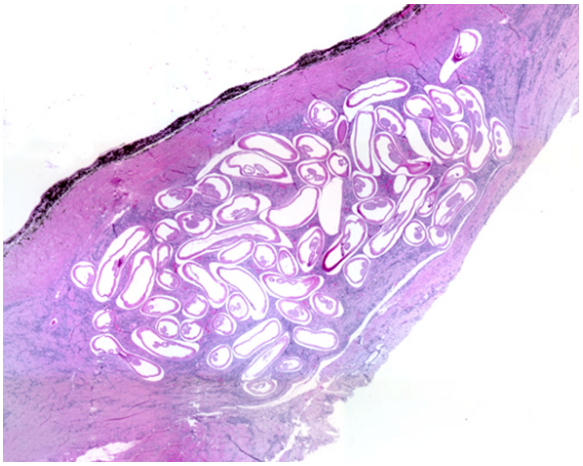

Eye, dog. Overview of the coiled female nematodes within the retrobulbar tissue. (Photo courtesy of: Department of Pathology, University of Veterinary Medicine, Hannover, Buenteweg 17, 30559 Hannover, Germany. (http://www.tiho-hannover.de/kliniken-institute/institute/institut-fuer-pathologie/).

A couple of nematodes are known to affect the eyes or the periorbital tissue. *Thelazia, Onchocerca, Ancylostoma, Dirofilaria, Angiostrongylus vasorum, Toxocara canis and Trichinella* sp. have been identified within ocular helminthic infections of dogs.[11] *O. lupi* is a vector borne nematode that was first described in 1967 in a Caucasian wolf (*Canis lupus*) from Russia.[5] The life cycle as well as the precise host range of canine *Onchocerca* is still not fully known, but it might be similar to those of other *Onchocerca* species. Within other *Ochocerca* species, blackflies and/or biting mites serve as intermediate hosts, for example *Simulium tribulatum,* was found to be a putative vector for *O. lupi* in Southern California.[12] All other *Onchocerca* sp. have a long prepatent period and patency of several months or even years within their hosts.[12]

In canine cases, gravid females, mature males, and microfilaria can be found within affected animals. Acute or chronic ocular disease with conjunctivitis, exophthalmos, periorbital swelling, photophobia, discomfort, lacrimation and discharge during the acute phase were reported as clinical signs.[8, 12] Chronic cases are characterized by granuloma formation in different parts of the eye and the periorbital tissue. The cuticle of females is a striking feature for the light microscopic identification of *Onchocerca* sp. It consists of two layers with an outer layer bearing ring-like ridges. In the anterior part of the nematode, these ridges are small and close together, becoming taller and more divergent in posterior direction. At the posterior part, they again get smaller with no visible ridges at the very end of the body.[12] The two distinct cuticular layers are hardly identifiable within the presented case most likely due to insufficient preservation. Histopathological examination of affected tissue may reveal coiled female nematodes within a mixture of fibrotic tissue admixed with mononuclear cells. Male nematodes as well as microfilariae may occasionally be present in the periocular tissue.[7]

Affected dogs are usually older than 1 year, which is most likely owed to the indirect life cycle of *Onchocerca* spp. as well as the slow development of these nematodes in their final hosts. Microfilariae can be isolated from skin samples, even if the animal has no clinical signs of onchocercosis. Microfilariae do not occur within the bloodstream, but larval concentration is high within the skin (50 - 3600 per g tissue), which might serve as a suitable screening method. Until today there is no serological test commercially available for the detection of *O. lupi.*[10,13]

O. lupi seems to be endemic in the United States. There have been also two proven cases of feline onchocercosis associated with *O. lupi*. Moreover, several cases of ocular onchocercosis have been reported in

humans worldwide.[5] *Onchocerca sp.* infect humans in tropical regions causing severe ocular inflammation known as "river blindness".[14] Nevertheless, *O. lupi* has been identified to act as the causative agent in two human ocular cases with similar clinical features compared to those in dogs.[8, 9]*Onchocerca* sp. represent a zoonotic pathogen and should be considered as differential diagnosis in canine ocular diseases.

JPC Diagnosis: Globe: Scleritis, granulomatous and eosinophilic, multifocal to coalescing, severe with lymphplasmocytic conjunctivitis, and adult filarid nematodes, mixed-breed dog, *Canis familiaris*.

Conference Comment: We thank the contributor for their excellent submission and thorough review of the epidemiology, pathogenesis, histologic lesions, diagnostic modalities, and zoonotic potential associated with ocular onchocerciasis. *Onchocerca lupi* is an emerging zoonotic disease affecting dogs, cats, and humans in the Southwestern United States, parts of Europe, and the Middle East.[4,5] Clinically, there are both acute and chronic forms of the disease. The acute form is characterized by conjunctivitis, chemosis, and periocular swelling. In chronic cases, such as in this dog, there are multiple adult filarid nematodes present within granulomatous nodules in the periocular tissue.[1,2] Exophthalmos, protrusion of the nictitating membrane, anterior uveitis, corneal edema, and corneal neovascularization may be seen in chronic cases.[2] Histologically, there are multifocal episcleral or conjunctival nodules with granulomatous and eosinophilic inflammation and fibrosis.[1,2] Conference participants also astutely noted that there is perilenticular proliferation of a fibroblastic epithelial membrane causing blockage of the filtration angle (pre-iridal fibrovascular membrane). This is a common finding in the eye secondary to chronic uveitis and may result in either eversion of the pupillary margin, known as ectropion uveae, or secondary glaucoma.[1,2] Grossly, proliferating periocular tissue containing adult nematodes can form pseudotumoral masses, resembling a neoplastic process.[2]

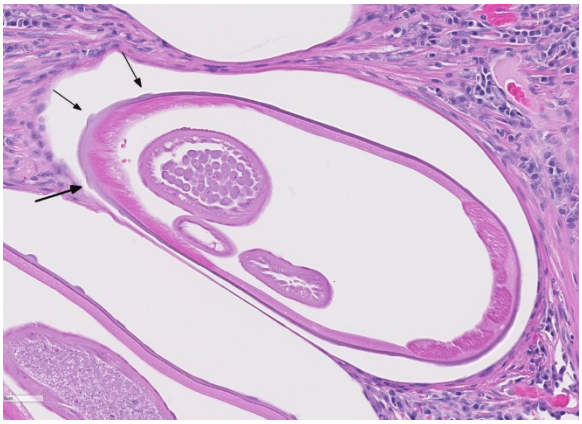

Eye, dog. Tangential section of a degenerate adult male nematode with external cuticular ridges (small arrows), atrophic polymyarian-coelomyarian musculature and a prominent hypodermis (large arrows) and a single testis. The nematodes are enmeshed in abundant fibrous connective tissue with numerous plasma cells. (HE, 260X).

Conference participants focused largely on the morphologic features distinguishing *Onchocerca* sp. in tissue section from other metazoan parasites. Filarid nematodes are small parasites that infect a number of different domestic animals. They are easily identified by their coelomyarian musculature, very small digestive tract, and larval microfilaria in the reproductive tract of gravid females.[3] In *Onchocerca* sp., the coelomyarian muscles atrophy and are replaced hypodermal tissue because adults reside within a fibrous capsule and are sedentary. The key diagnostic feature that differentiates *Onchocerca* sp. from other filarid nematodes is the presence of evenly spaced ring-like circumferential annular cuticular ridges seen on longitudinal

section.[2,3] This is the only nematode that has this cuticular manifestation. In contrast, *Dirofilaria immitis*, the canine heartworm, is a relatively common intraocular filarial nematode of dogs and has evenly spaced ridges that run longitudinally and can only be seen on cross section.[2,3] These characteristics also help differentiate *Onchocerca* sp. from *Thelazia* sp., a spirurid nematode parasite and another common ocular parasite in a wide range of mammalian hosts.[3]

Contributing Institution:
Department of Pathology
University of Veterinary Medicine
Hannover, Germany
http://www.tiho-hannover.de/kliniken-institute/institute/institut-fuer-pathologie/

References:

16. Cullen CL, Webb AA. Ocular manifestations of systemic disease. In: Gelatt KN, Gilger BC, Kern TJ, eds. *Veterinary Ophthalmology.* Vol 2. 5th ed. Ames, IA: Blackwell Publishing; 2013:1931.
17. Dubielzig RR, Ketring KL, McLellan GJ, Albert DM. *Veterinary Ocular Pathology: A comparative review.* St. Louis, MO: Saunders Elsevier; 2010:118-120..
18. Gardiner, *CH, Poynton, SL. An Atlas of Metazoan Parasites in Animal Tissues. Washington, D.C: Armed Forces Institute of Pathology, American Registry of Pathology*, 1999:35–38.
19. Hassan KH, Bolcen S, Kubofcik J, et al. Isolation of *Onchocerca lupi* in dogs and black flies, California, USA. *Emerg Infect Dis.* 2015; 21(5):789–796.
20. Labelle AL, Maddox CW, Daniels JB, et al. Canine ocular onchocercosis in the United States is associated with *Onchocerca lupi. Vet Parasitol.* 2013; 193(1-3):297–301.
21. Mutafchiev Y, Dantas-Torres F, Gianelli A., et al. Redescription of *Onchocerca lupi* (Spirurida: *Onchocercidae*) with histopathological observations. *Parasit Vectors*. 2013; 6:309–316.
22. Otranto D, Dantas-Torres F, Giannelli A, et al. Zoonotic *Onchocerca lupi* infection in dogs, Greece and Portugal, 2011–2012. *Emerg Infect Dis.* 2013; 19:2000–2003.
23. Otranto D, Giannelli A, Scotty Trumble N, et al. Clinical case presentation and a review of the literature of canine onchocercosis by *Onchocerca lupi* in the United States. *Parasit Vectors*. 2015; 8:89–96.
24. Otranto D, Giannelli A, Latrofa MS, et al. Canine infections with *Onchocerca lupi* nematodes, United States, 2011–2014. *Emerg Infect Dis.* 2015; 21:868–871.
25. Sreter T, Szell Z, Egyed Z, et al. Ocular onchocercosis in dogs: A review. *Vet Rec*. 2002; 151:176–180.
26. Sréter T, Széll Z. Onchocercosis: A newly recognized disease in dogs. *Vet Parasitol.* 2008; 151:1–13.
27. Széll Z, Sréter T, Erdélyi I., et al. Ocular onchocercosis in dogs: Aberrant infection in an accidental host or lupi onchocercosis? *Vet Parasitol.* 2001; 101:115–125.
28. Zimmermann PA, Dadzie KY, De Sole G, et al. *Onchocerca volvulus* DNA probe classification correlates with epidemiologic patterns of blindness. *J Infect Dis.* 1992; 165:946–968.

Self-Assessment - WSC 2016-2017 Conference 24

1. Fatal Hemoproteus infections in psittacine birds have their origin where ?
    a. European songbirds
    b. Pigeons
    c. Corvids such as crows and ravens
    d. Other psittacine species

2. Which of the following has not been seen in association with *Spirocerca lupi* infection in the dog?
    a. Metaphyseal osteopathy
    b. Esophageal malginancies
    c. Aortic aneurysm
    d. Aortic rupture

3. The definitive host of Sarcocystis falcatula is ?
    a. Dog
    b. Vole
    c. Cat
    d. Opossum

4. Bradyzoites of Sarcocystis falcatula are found in which cell type in affected birds?
    a. Macrophages
    b. Skeletal muscle cells
    c. Endothelial cells
    d. Astrocytes

5. Which of the following is not a key differentiating factor for identifying *Onchocerca* sp. in tissue section?
    a. Replacement of atrophied musculature with hypodermal tissue.
    b. Presence of larval microfilaria in the uterus
    c. A stichosome composed of large glandular cells around the esophagus
    d. Circumferential annual cuticular ridges

Joint Pathology Center

Veterinary Pathology Services

WEDNESDAY SLIDE CONFERENCE 2016-2017

C o n f e r e n c e 25

17 May 2017

Jeffrey C. Wolf, DVM, Diplomate ACVP
Chief Scientific Officer, Experimental Pathology Laboratories, Inc.
Sterling, VA

CASE I: WSC 1617 Conf 25 Case 1 (JPC 4065818).

Signalment: 13-month-old male zebrafish (*Danio rerio*).

History: This fish was from a breeding colony of zebrafish. Offspring produced from the breeding colony were either used in genomics research or were used to replace aged members of the breeding colony. Because the breeding colony had been maintained as a "closed colony" for several years, there was concern about inbreeding. Therefore, a group of adult zebrafish was purchased from a commercial vendor to be used to breed with the established colony and thus provide some genetic diversity.

After an uneventful 90-day quarantine period, one of the female fish from the recently-purchased group was bred with a male fish from the long-established colony. The resultant offspring were raised in several small groups up to the age of one month and then the groups were combined and maintained together in one large group in an 85-gal (~ 322 L) tank. At 13 months of age, eight fish from this group were selected at random for routine health assessment. These fish were euthanized by immersion in a solution of tricaine methanesulfonate (MS-222) and then the carcasses were fixed *in toto* in 10% neutral-buffered formalin. The fixed carcasses were then submitted for histopathologic examination.

The submitted slide contains whole-body transverse sections from one of the eight fish.

This fish was part of a research project conducted under an IACUC approved protocol in compliance with the Animal Welfare Act, PHS Policy, and other federal statutes and regulations relating to animals and experiments involving animals. The facility where this research was conducted is accredited by the Association for Assessment and Accreditation of Laboratory

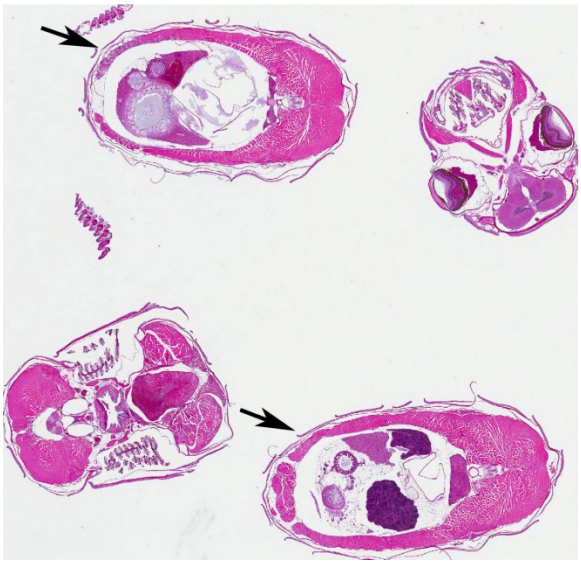

Skeletal muscle, zebrafish. Four transverse sections of a zebrafish are submitted for examination. At subgross inspection, there is mild hypercellularity of the musculature of the abdominal wall in multiple sections. (HE, 5X).

Animal Care, International and adheres to principles stated in the Guide for the Care and Use of Laboratory Animals, National Research Council, 2011.

Gross Pathology: NA

Laboratory results: NA

Histopathologic Description: There are four transverse sections of intact whole body at different levels on this slide. Within two of these sections, there are multifocal to coalescing degeneration and necrosis of skeletal muscle fibers accompanied by infiltrates of low to moderate numbers of macrophages and fewer lymphocytes. Numerous protozoa-like micro-organisms in various stages of development are present within the cytoplasm of affected myocytes. The different developmental stages of the organisms include: 1) 5-15 µm diameter round to oval basophilic uni-nucleate organisms with an eosinophilic refractile wall; 2) 15-30 µm round cyst-like structures with an eosinophilc refractile wall and containing multiple basophilic nuclei with poorly-defined borders; and 3) 25-40 µm cyst-like structures containing multiple approximately 3 X 5 µm oval refractile spores with basophilic to clear cytoplasm. One or more spores are also occasionally present with macrophages.

Other than autolysis, there are no significant changes in other organs.

Contributor's Morphologic Diagnosis: Skeletal muscle; multifocal to coalescing myodegeneration, moderate, with necrosis, lymphohistiocytic inflammation and numerous intracytoplasmic protozoa-like organisms at various stages of development (including spores).

Contributor's Comment: The lesions in the muscles of this fish were unexpected findings. These had not been seen previously in this fish colony and a review of the available literature at that time did not reveal descriptions of similar lesions in zebrafish.

Several special stains were done in an attempt to better characterize the organisms. These stains revealed that the spores often had annular bands and a PAS-positive polar granule (Figure 6). The more mature spores were Gram-positive but immature spores were Gram-variable (Gram-negative or did not stain with Gram's stain). These findings are characteristics of microsporidia.[2,3,6]

Further studies conducted by personnel at Oregon State University and the Zebrafish International Resource Center demonstrated that the species of microsporidia in this zebrafish is *Pleistophora hyphessobryconis*.[7] *P. hyphessobryconis* is a common pathogen of neon tetras (*Paracheirodon innesi*) and other species of ornamental tropical fish.[5,6] *P. hyphessobryconis* is so common in neon

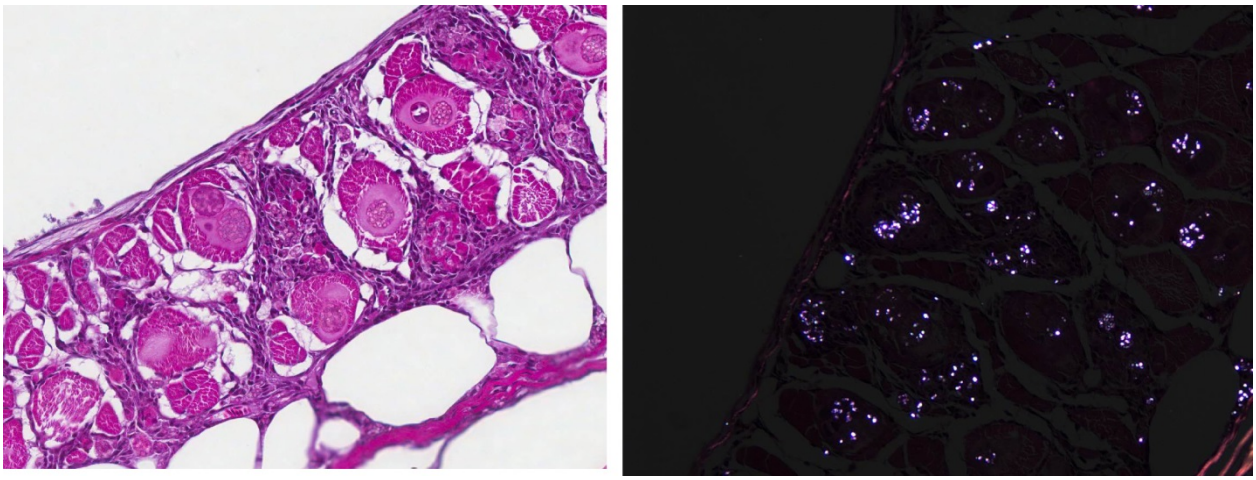

Skeletal muscle, zebrafish. Left: Higher magnification of affected skeletal muscle demonstrates the presence of uninucleate sporoblasts as well as larger sporonts containing numerous mature spores in affected myocytes. Degenerate myocytes are fragmented and infiltrated by numerous histiocytes, which also expanded the perimysium. Right: Mature microsporidian spores exhibit birefringence.(HE. 256X) (Photo courtesy of: US Army Medical Research Institute of Infectious Diseases, Fort Detrick, MD 21702-5011)

tetras that the disease it causes is simply called "neon tetra disease".[5,6] Although some older reports state that *P. hyphessobryconis* has been seen in zebrafish in the commercial pet trade, this case was the first time it was recognized in a laboratory research colony.[7] Subsequent to the discovery of this index case, other cases of *P. hyphessobryconis* infection in zebrafish have been seen in two other research colonies.[7]

For many years, microsporidia were taxonomically classified as protozoa. However, the results of more recent studies have caused them to be re-classified as fungi.[2,4] Microsporidial spores are the infectious stage and each spore contains a coiled structure called a polar filament or polar tube.[1] When a spore enters a suitable host (usually by ingestion of the spore), the polar filament uncoils, emerges from the spore, and penetrates a host cell. The sporoplasm is then injected through the polar filament into the host cell.[2] The parasite proliferates asexually inside the host cell, first through merogony and then sporogony.[3,6] The meronts of *Pleistophora* spp. (which at first are uninucleate and eventually become multinucleate) are surrounded by a membrane derived from the host cell and are said to reside within a parasitophorous vacuole.[2,5] The meronts of *Pleistophora* spp. mature into sporogonial plasomodia that undergo fission to produce sporoblasts which ultimately develop into spores; multiple spores are contained within each thick-walled sporophorous vesicle.[2,5]

Fish typically become infected by *P. hyphessobryconis* by ingesting spores released into the environment from necrotic muscle fibers of other infected fish or by scavenging dead, infected fish. It is not known how the fish of this report was exposed to *P. hyphessobryconis* spores. This animal had been raised in a laboratory setting without any exposure to neon tetras or other fish species. The water used to house this fish colony is a mixture of deep-well water and municipal water that has undergone reverse-osmosis filtration; thus, it is highly unlikely that this water was the source of infection. The food used to feed the fish is a commercial flake-food that contains ground fish meal. However, the

processing procedures used to produce this food should have inactivated any micro-sporidia spores that were accidentally present.

The mother of this fish had been purchased from a commercial vendor and thus may have been exposed to infected fish before her arrival at the research facility. Although the mother fish was clinically normal, it is possible that she was harboring a low-grade infection and thus may have shed spores into the water during breeding. However, the embryos produced from this breeding were treated with bleach before being transferred to fry-raising tanks, and this bleaching process should have inactivated any micro-sporidia spores present in the water. It is also worth noting that the affected fish was euthanized 13 months after conception and this would be a long time to harbor a subclinical infection.

When this infected fish was detected, all of the fish that had been purchased from the commercial vendor had been removed from the colony months previously. Thus, it was not possible to examine them to determine if they had been the source of infection.

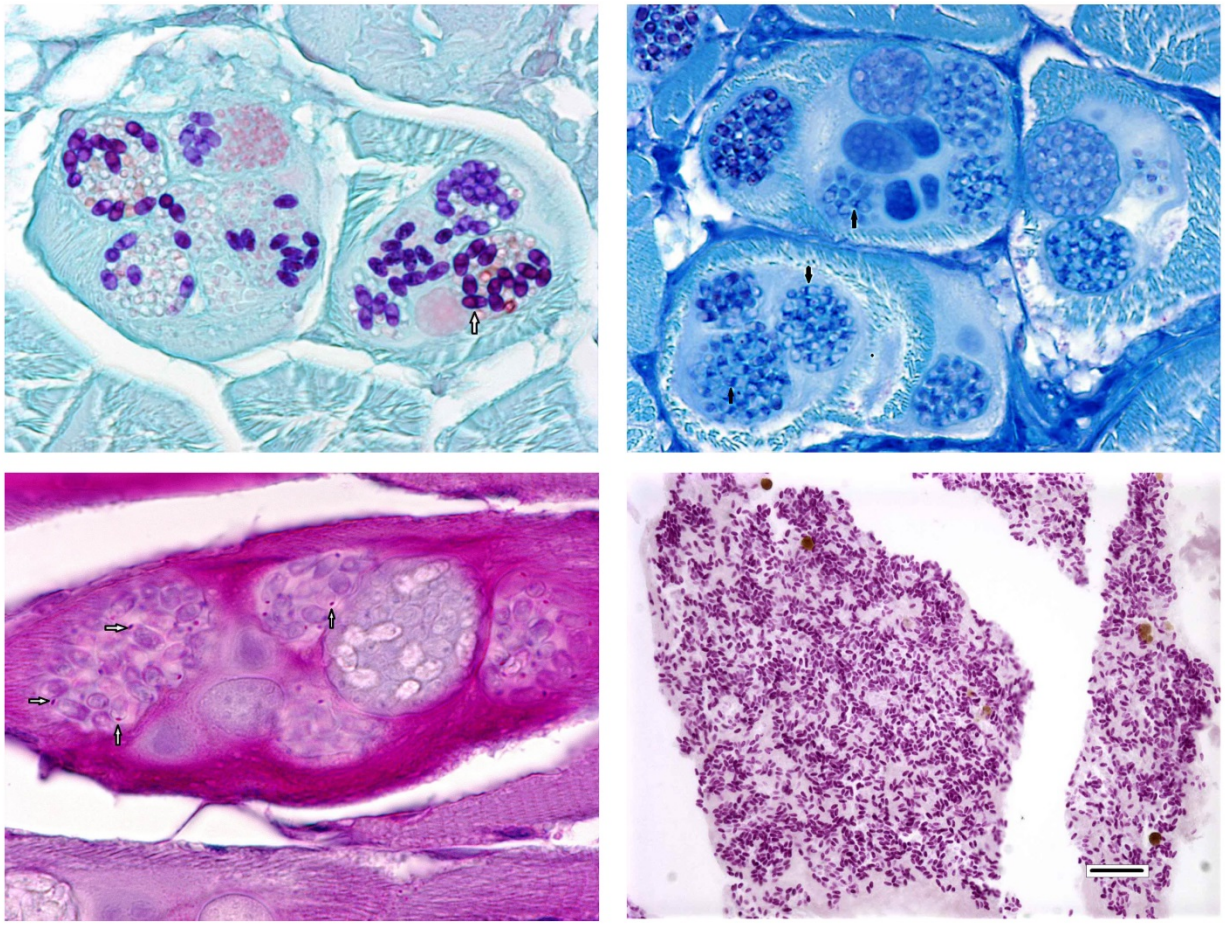

Skeletal muscle, zebrafish. Color plate showing various special stains. Top left: Spores stain strongly with Gram stains. (Lilly Twort, 400X). Top right: A Giemsa stain demonstrates annular bands (arrows). (Giemsa, 200X). Bottom left: A periodic Schiff stain demonstrates the polar granule. (PAS, 400X). Bottom right: A Luna mast cell stain is also an excellent choice for highlighting spores. (Luna, 100X) (Photo courtesy of: US Army Medical Research Institute of Infectious Diseases, Fort Detrick, MD 21702-5011)

After this fish was found to be infected, the remaining 135 fish in its sibling co-hort were euthanized and examined grossly (98 fish) and/or histologically (37); none of these were found to be infected and there have not been any other cases in this colony since then.

Note: Opinions, interpretations, conclusions, and recommendations are those of the author and are not necessarily endorsed by the U.S. Army.

JPC Diagnosis: Skeletal muscle: Myocyte deneneration and necrosis, multifocal, mild with numerous intrasarcoplasmic meronts, sporoblasts, and spores with histiocytic inflammation, zebrafish, *Danio rerio*.

Conference Comment: Zebrafish are of increasing importance as a research model for the study of infectious diseases, developmental biology, cancer, and toxicology. Their small size, ease of husbandry, and *ex-vivo* transparent embryonic development make them a highly sought after laboratory species with a burgeoning transgenic and specific pathogen free industry to support the increase in laboratory use.[8] This case represents infection by a microsporidian organism that may easily spread within a colony and could potentially confound experimental results; thus making this and other zebrafish diseases of particular concern for investigators and laboratory animal pathologists. Conference participants discussed the importance of proper animal acquisition, good husbandry, routine disease and pathogen monitoring, and a robust sentinel animal program as the cornerstones of laboratory animal disease prevention in any species.

The most commonly encountered infectious diseases of laboratory zebrafish include mycobacteriosis and microsporidiosis.[7,8] As mentioned by the contributor, based on phylogenetic analysis and the presence of chitin within the spore, microsporidia are classified as fungal-like organisms rather than protozoans, as previously thought. *Microsporidia* are a large group of obligate-intracellular eukaryotic parasites that infect a wide range of animal species.[1,3] Their relatively simple life cycle consists of two developmental stages: merogony and sporogony.[1,2,3,5,7,8] After infection, meronts multiply within the host cell, skeletal muscle in this case, eventually forming thick-shelled spores. Spores are released from the ruptured host cell and reach the environment through various bodily secretions. The infectious spores have a thick, chitinous shell and are resistant to environmental stress; thus allowing the infective spores to remain viable in the aquatic environment for a prolonged period of time. As mentioned by the contributor, infective spores can also be ingested through predation.[7,8]

The most commonly identified micro-sporidian parasite affecting zebrafish is *Pseudoloma neurophila*.[7,8] As is implied by the name, *P. neurophila* have tropism for the central and peripheral nervous system and is associated with encephalomyelitis and polyneuritis. Small groups and individual spores can be seen in a variety of extraneural organs, including smooth and skeletal muscle. Spores released from peripheral nerves and skeletal muscle typically cause severe inflammation.[7,8] In contrast, *Pleistophora hyphessobryconis* primarily develops within skeletal muscle with multiple developmental stages (meronts, sporoblasts, and spores) present within the sarcoplasm. The conference moderator noted that the two *Microsporidia* species can be easily distinguished histologically due to the presence of *P.hyphessobryconis'* intra-sarcoplasmic developmental stages and

thick-walled sporophorous vacuoles laden with spores.[7,8] Additionally, spores of *P. hyphessobryconis* are associated with only a mild inflammatory response, as seen in this case. In the areas of mild histiocytic inflammation in the skeletal muscle of the abdominal wall, birefringent spores are present within phagocytes. In photographs provided by the contributor, wet-mount preparations of skeletal muscle from infected fish show individual spores as well as sporophorous vacuoles containing spores with a prominent posterior vacuole and coiled polar filament, typical of *Microsporidia* spp.[1,7,8] Another microsporidium parasite of veterinary importance is *Encephalitozoon cuniculi*, which causes torticollis and phaecoclastic uveitis in the highly susceptible dwarf rabbit.[1] Readers are encouraged to review WSC 2015 Conference 12 Case 4 for an outstanding example of phaecoclastic uveitis caused by *E. cuniculi* in a double-maned lionhead rabbit.

Contributing Institution:
US Army Medical Research Institute of Infectious Diseases
Pathology Division
Fort Detrick, MD
http://www.usamriid.army.mil/

References:

1. Cantile C, Youssef S. Nervous System. In: Maxie MG, ed. *Jubb, Kennedy, and Palmer's Pathology of Domestic Animals.* 6th ed. Vol 1. St. Louis, MO: Elsevier; 2016:385.
2. Curry A. Microsporidiosis. In: Cox FEG, Wakelin D, Gillespie SH, Despommler DD, ed. *Topley & Wilson's Microbiology & Microbial Infections Parasitology.* 10th ed. London, UK: Hodder Arnold, 2005: 529-535.
3. Gardiner CH, Fayer R, Dubey JP. *An Atlas of Protozoan Parasites in Animal Tissues*. 2nd ed. Washington, DC: Armed Forces Institute of Pathology, 1998.
4. Lee SC, Corradi N, Byrnes EJ 3rd, et al. Microsporidia evolved from ancestral sexual fungi. *Curr Biol*. 2008;18(21):1675-9.
5. Li K, Chang O, Wang F, Liu C, Liang H, Wu S. Ultrastructure, development, and molecular phylogeny of *Pleistophora hyphessobryconis*, a broad host microsporidian parasite of *Puntius tetrazona*. *Parasitol Res.* 2012;111:1715–1724.
6. Post G. *Textbook of Fish Health*. 2nd ed. Neptune City, NJ: T.F.H Publications, Inc., 1987.
7. Sanders JL, Lawrence C, Nichols DK, et al. *Pleistophora hyphessobryconis* (Microsporidia) infecting zebrafish *Danio rerio* in research facilities. *Dis Aquat Org.* 2010;91:47-56.
8. Sanders JL, Watral V, Kent ML. Microsporidiosis in zebrafish research facilities. ILAR J. 2012; 53(2):106-113.

CASE II: 15-3213 (JPC 4084010).

Signalment: Adult female Northern puffer fish (*Sphoeroides maculatus*).

History: This fish was presented to the CVMDL for euthanasia and necropsy after a one-week history of anorexia and labored breathing. Reddish discoloration had been noted around multiple fins. Twelve individuals in two exhibits from this private aquatic education center exhibited the same clinical signs, and several fish from affected tanks had died over a one-month period. The

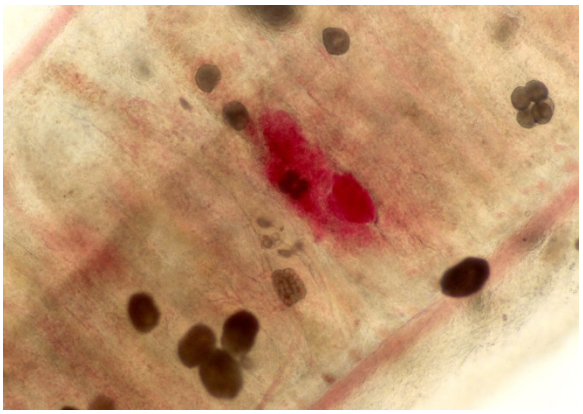

Gill, pufferfish. Wet mount of gill clip gill reveals tomonts and trophonts (presumptive trophonts of Amyloodinium ocellatum). (Photo courtesy of Department of Pathobiology and Veterinary Science, Connecticut Veterinary Medical Diagnostic Laboratory, Connecticut http://www.pathobiology.uconn.edu/

tank was treated with copper and metronidazole. Slight improvement was noted after the first treatment, but clinical signs then worsened with lethargy and lack of appetite. Additional treatment with increased iodine and copper had no effect. The submitted fish was euthanized with an overdose of MS-222 and necropsied immediately.

Gross Pathology: The fish was in poor body condition with scant coelomic adipose stores. External examination revealed slight reddening of the dorsal and pectoral fins that was more severe at the proximal aspect, and the pectoral fins had some indistinct, cloudy stippling. A skin scrape of the body was negative. The gills had disseminated, faint dark-red stippling. The liver was diffusely yellowish-tan and floated when placed in formalin. The gallbladder was moderately dilated with thin, green, watery bile. The gastrointestinal tract was empty except for a small amount of mucus.

Laboratory results: Cytology: Wet mount of the left pectoral fin and gill revealed few and numerous, respectively, round to ovoid, brown structures ranging in size from approximately 50 to 200 microns in diameter (presumptive trophonts of *Amyloodinium ocellatum*). Often smaller round forms were seen in organized aggregates of two to 16 organisms (dividing forms; tomonts).

Histopathologic Description: Gill: There is generalized mild to moderate hypertrophy and hyperplasia of lamellar epithelial cells that often results in fusion along the lengths of some lamellae or at the lamellar tips (synechiae). Pseudocystic spaces formed by synechiae frequently contain sloughed cellular debris, macrophages, numerous rod-shaped bacteria and occasional dinoflagellate organisms (consistent with *Amyloodinium* sp.) in varying stages of development. Present along the lamellar surfaces are dinoflagellate trophonts that are circular to ovoid, range in size from 25 to 100 microns in diameter, and have a single, round, deeply basophilic nucleus and wispy eosinophilic cytoplasm containing several 3-5 micron diameter, circular, brightly eosinophilic bodies and birefringent granules and spicules under polarized light. Tomonts are occasionally trapped in pseudocysts at varying stages of subdivision into 2-20 dinospores, which have a thin refractile and birefringent wall and are round and roughly 20-30 microns in diameter with granular eosinophilic cytoplasm and one to two irregularly shaped, stippled, deeply basophilic masses of chromatin. Lamellae are variably thickened by moderate to marked congestion, occasional hemorrhage and low to moderate numbers of inflammatory cells consisting predominantly of macrophages with fewer lymphocytes and rare granulocytes. There are a few, scattered areas of lamellar necrosis. The cytoplasm of a few lamellar epithelial cells is markedly expanded by an intracytoplasmic, discrete,

round, finely granular basophilic inclusion (bacterial inclusion of epitheliocystis).

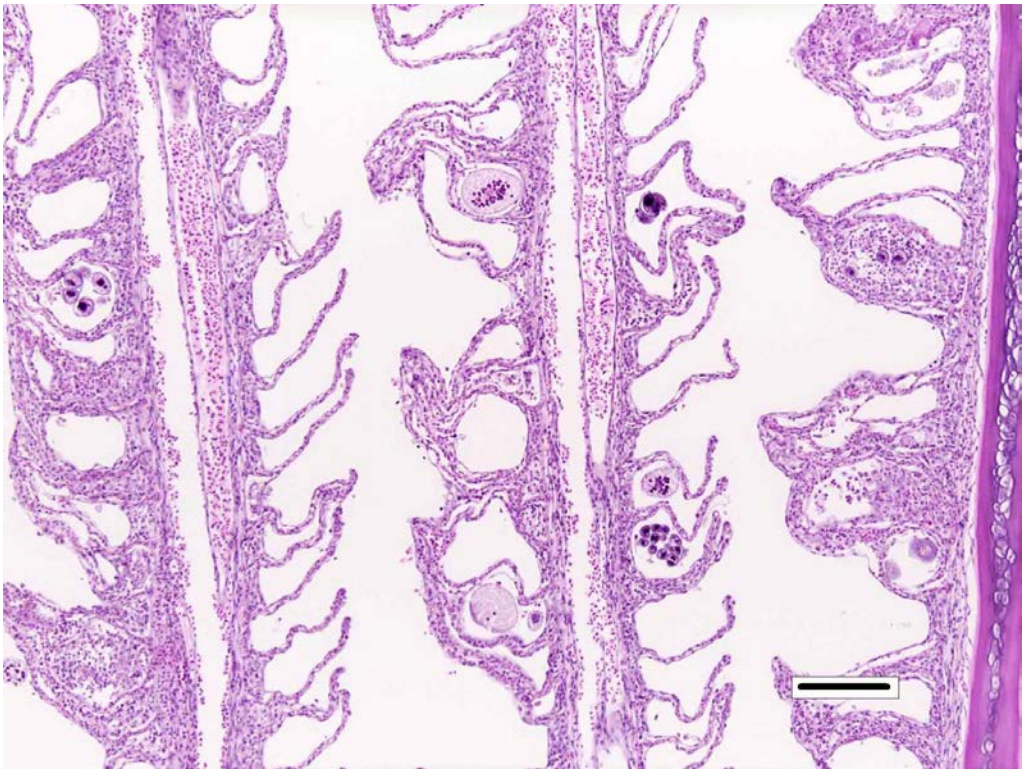

Gill, pufferfish. There are multifocal synechia of secondary lamellae with formation of pseudocysts, as well as secondary lamellae. Pseudocysts occasionally contain variable amounts of cellular debris and multiple trophonts and tomonts of Amyloodinium.

Contributor's Morphologic Diagnosis: Gill: severe diffuse, proliferative and histiocytic branchitis with lamellar fusion, synechiae, and intralesional dinoflagellate organisms, compatible with *Amyloodinium ocellatum*, gram-negative bacteria, and rare epitheliocystis inclusions.

Contributor's Comment: Although there were several etiologic agents seen microscopically in sections of gill that could have contributed to the extensive pro-liferative branchitis, the primary pathogen is believed to be a heavy infestation with the obligate ectoparasitic marine dinoflagellate, *Amyloodinium ocellatum*, the causative agent of marine velvet disease or oodiniosis.

This organism is considered an important parasite in aquarium fish and in tropical and subtropical brackish and marine fish culture, and it can infect both elasmobranch and teleost fish.[5] Natural epidemics have also been documented.[3] *Amyloodinium ocellatum* prefers warm water from 17 to 30 degrees Celsius (63-86 F) with potentially greater virulence in high temperatures.[2] Isolates vary in salinity tolerance with ranges from 3 to 45 ppt.[5] Certain species of fish are resistant to infection; these fishes typically produce a thick mucus, possibly preventing attachment of trophonts, or tolerate low oxygen levels.[5]

The life cycle of *A. ocellatum* is direct and triphasic. The parasitic, feeding stage, or trophont, attaches to the host's epithelium by a root-like structured called a rhizoid.[5] After a period of feeding on the host, the trophont detaches from the host, retracts its rhizoid and becomes the encysted, dividing tomont stage in the substrate.[5] The final stage is the free-swimming, infectious dinospore that is released from the dividing tomont (up to 256 dinospores can come from a single tomont) and has flagella to

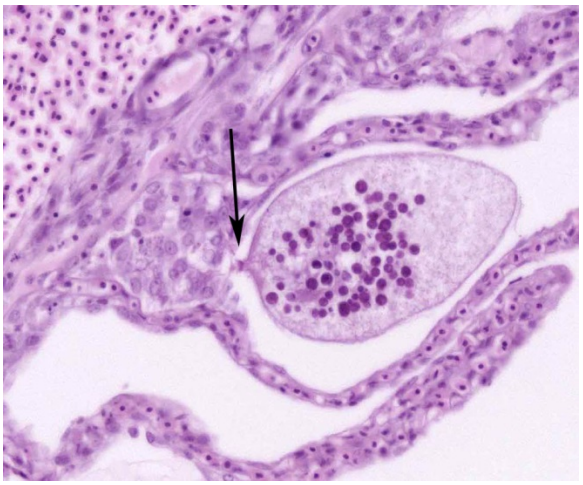

Gill, pufferfish. Amyloodinium trophont with stomatopode . (HE, 400X).

facilitate swimming to find a suitable host.[5] *Amyloodinium ocellatum* causes severe physical damage to the host cells through attachment of the trophont to epithelium, with the gill typically being the primary site of infestation.[5,6] In cases with heavy parasite burdens, the skin and eyes can also be infected, sometimes producing the dusty appearance of the skin that accounts for the name "velvet disease."[5] In some reports infestation of larval fish affected only the skin rather than the gill.[6] The gill was the tissue most severely affected in this puffer fish, although a few of the organisms were seen on a wet mount of the fin; cutaneous changes were mild in histologic sections. Trophonts may also be seen in the pseudobranch, branchial cavity, nasal passages, and gastrointestinal tract (if swallowed).[5]

Microscopic lesions of severely affected gill include epithelial hyperplasia, often with lamellar fusion and distortion, mild inflammatory infiltrates, hemorrhage and epithelial degeneration and necrosis,[3,5,6] as seen in this case. The feeding activity and the detachment of large numbers of organisms can damage epithelium, and potentially result in mortality as a consequence of hypoxia, osmoregulatory imbalance and secondary bacterial infections.[5] There are several modalities of treatment available, most of which only target the dinospore stage, which can make eradication of parasites difficult.[5]

Although not considered the primary disease in this case, epitheliocystis was also noted in this fish. Characterized histologically by large, granular, basophilic, intracytoplasmic, bacterial inclusions within enlarged branchial lamellar epithelial cells, this type of infection is caused by a group of obligate, intracellular, gram-negative, chlamydia-like organisms.[5] Recent advances in molecular techniques have identified various

Gill, pufferfish. Amyloodinium tomont with four divisions. There is a synechia between adjacent secondary lamellae. (HE, 400X).

epitheliocystis agents as belonging to the order Chlamydiales, the first of which was *Candidatus Piscichlamydia salmonis* in the Atlantic salmon.[1,7] Infections of gills, pseudobranch, and rarely the skin by these organisms have been described in many freshwater and marine species of fish.[7] Pathogenicity is dependent upon the host response and the chlamydiales bacterium, and microscopic lesions can range from none to severe epithelial hyperplasia with associated inflammation.[7]

JPC Diagnoses: 1. Gill: Branchitis, proliferative and necrotizing, multifocal, moderate with marked lamellar adhesions (synechiae) and fusion, and numerous dinoflagellate ectoparasites, Northern puffer fish, *Sphoeroides maculatus*.
2. Gill, lamellar epithelial cells: Chlamydial inclusions, multiple.

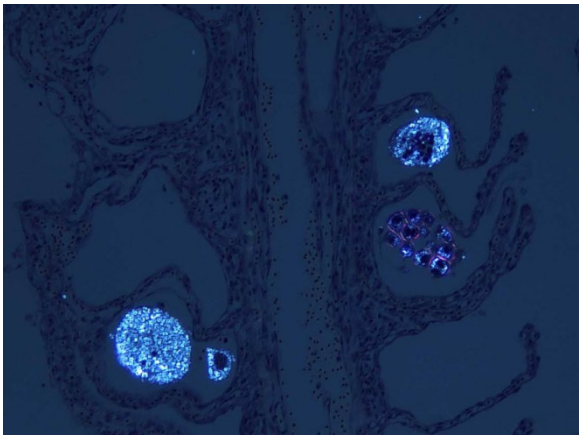

Gill, pufferfish. Bifringence of multiple life stages of Amyloodinium. (HE, 100X)

Conference Comment: *Amylodinuym ocellatum* is one of the most important pathogenic parasites of both marine and estuarine fish. It is one of the few organisms that can infect the gills and skin of both teleost fish (bony ray-finned fish) and elasmobranchs (cartilaginous fish, ex. sharks).[2,5] This dinoflagellate parasite has the capacity for rapid reproduction and severe infections, such as in this case, can cause devastating disease and high mortality in a wide range of fish species.[2] As nicely summarized by the contributor, the life cycle is simple and requires no intermediate hosts. The parasite has three different developmental stages. The trophont stage is the adult stage that feeds directly on the host and attaches via the rhizoid; the tomont stage is detached from the fish and divides to the third dinospore stage. Dinospores are the free swimming infectious flagellated phase.[2,5] The simple life cycle and free swimming infectious dinospore stage contribute to severe epizootics in both wild and cultured fish, especially when crowded. *A. ocellatum* is a major concern to the aquaculture industry because outbreaks have an acute onset, spread rapidly, and have a high mortality. There are many nice examples of all three life stages in this case, including several trophonts with prominent rhizoids.[2,5] This case is an excellent example of the gill as the primary site of infection for this parasite. Predominant antemortem clinical signs will most often be disturbances in the respiratory system, including increased respiratory rate (indicated by rapid movement of the gill opercula) and gathering at the surface or in other areas of increased oxygen concentration. The skin is also infected and fish can develop white or brown "velvety" appearance.[2] This case also contains excellent examples of epitheliocystis with large inclusions composed of colonies of *Chlamydia*-like organisms within the cytoplasm of lamellar epithelial cells. Epitheliocystis is often considered an incidental finding, and most conference participants agreed that its presence in this case is unrelated to the significant gill pathology caused by *Amylodinuym ocellatum*.[7]

Prior to the conference, the moderator briefly reviewed the normal anatomy and histology of the gill. The gill arch is a series of bony or cartilaginous curved structures that support double rows of paired filaments, also called the primary lamellae. Each filament is composed of numerous perpendicularly-arranged secondary lamellae.[4] The gill arch is covered by epidermis and at the origin of the primary lamellae the epidermis is thicker and contains many mucous cells and subjacent lymphoid tissue. The primary lamellae are covered by a mucoid epidermis which contains a pale-staining, eosinophilic, salt-

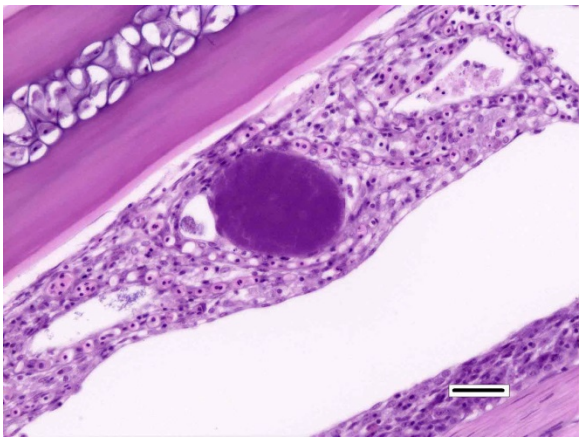

Gill, pufferfish. Occasional epithelial cells contain large bacterial inclusions characteristic of Epitheliocystis. (HE, 400X)

secreting chloride cells that function in ionic transport and detoxification. The surface of the secondary lamellae consists of a single layer of interdigitating squamous epithelial cells supported by pillar cells and lamellar blood channels.[4] The surface of the lamellar epithelium has numerous microvilli which serve as a substrate for cuticular mucus and aid in gas exchange and defense against infection and trauma. Thus, gills are important for gas exchange, ionic balance, and the excretion of the nitrogenous wastes. As a result, damage or infection of the gill often results in serious systemic consequences to the fish.[4]

Conference participants also discussed the difference between lamellar fusion and lamellar adhesion, both prominent features in this case. Lamellar fusion is most often associated with inflammation and is a consequence of marked epithelial proliferation. In contrast, lamellar adhesions (also known as lamellar clubbing or synechiae) occur when there is adherence of two or more secondary lamellae forming a pseudocyst, usually in the absence of epithelial proliferation or inflammation. Both lamellar fusion and lamellar adhesions are present in this case.

Multifocally, within the secondary lamellae of this case, there are dilated capillaries that contain organizing fibrin thrombi, interpreted by conference participants as examples of telangiectasia. The moderator noted that this vascular change can be a perimortem artifact secondary to capture of the fish or an antemortem change secondary to the disease process. Distinguishing between peri- and antemortem telangiectasis is often difficult, even for those experienced in gill histopathology; however, in this case, the presence of organizing fibrin thrombi is characteristic of antemortem telangiectasia rather than a perimortem capture artifact.

Contributing Institution:

Department of Pathobiology and Veterinary Science
Connecticut Veterinary Medical Diagnostic Laboratory
College of Agriculture, Health and Natural Resources
University of Connecticut
http://www.pathobiology.uconn.edu/

References:

1. Draghi A, Popov VL, Kahl MM, et al. Characterization of "*Candidatus Pischichlamydia* salmonis" (Order *Chlamydiales*), a Chlamydia-like bacterium associated with epitheliocystis in farmed Atlantic Salmon (*Salmo salar*). *J Clin Microbiol*. 2004; 42(11):5286-5297.
2. Francis-Floyd R, Floyd MR. Amyloodinium ocellatum, an important parasite of cultured marine fish. *SRAC*. 2011; 4705:1-12.
3. Kuperman, BI, Matey VE. Massive infestation by *Amyloodinium ocellatum* (Dinoflagellida) in a highly saline lake, Salton Sea, California, USA. *Dis Aquat Org*. 1999; 39:65-73.

4. Mumford S, Heidel J, Smith C, Morrison J, MacConnell B, Blazer V. *Fish Histology and Histopathology*. US Fish and Wildlife Service, National Conservation Training Center. http://nctc.fws.gov/resources/course-resources/fish-histology/index.html. Accessed May 25, 2017.
5. Noga EJ. Problem 27 Marine Velvet Disease (Amyloodiniosis, Marine Oodinium Disease, Oodiniosis). IN *Fish Disease: Diagnosis and Treatment*, 2nd ed, Ames, IA: Wiley-Blackwell; 2010:143-147.
6. Paperna I, Steinitz AH. *Amyloodinium ocellatum* (Brown, 1931) (Dinoflagellida) infestations in cultured marine fish at Eilat, Red Sea: epizootiology and pathology. *J Fish Dis*. 1980; 3:363-372.
7. Stride MC, Polkinghorne A, Nowak BF. Chlamydial infections of fish: Diverse pathogens and emerging causes of disease in aquaculture species. *Vet Microbiol*. 2014; 171:258–266.

CASE III: A15-25281 (JPC 4084652).

Signalment: Adult male long snout seahorse (*Hippocampus reidi*).

History: This animal was one of 20 seahorses that experienced an epizootic of ulcerative dermatitis shortly after arrival into quarantine facilities of a public aquarium. The 15.4 cm, snout to tail tip, the male became moribund and was euthanized 14 days after shipment.

Gross Pathology: Unlike other animals from the group, there was no evidence of dermatitis. The caudal third of the kidney was enlarged and pale, with an irregularly nodular surface that bulged into the coelomic cavity.

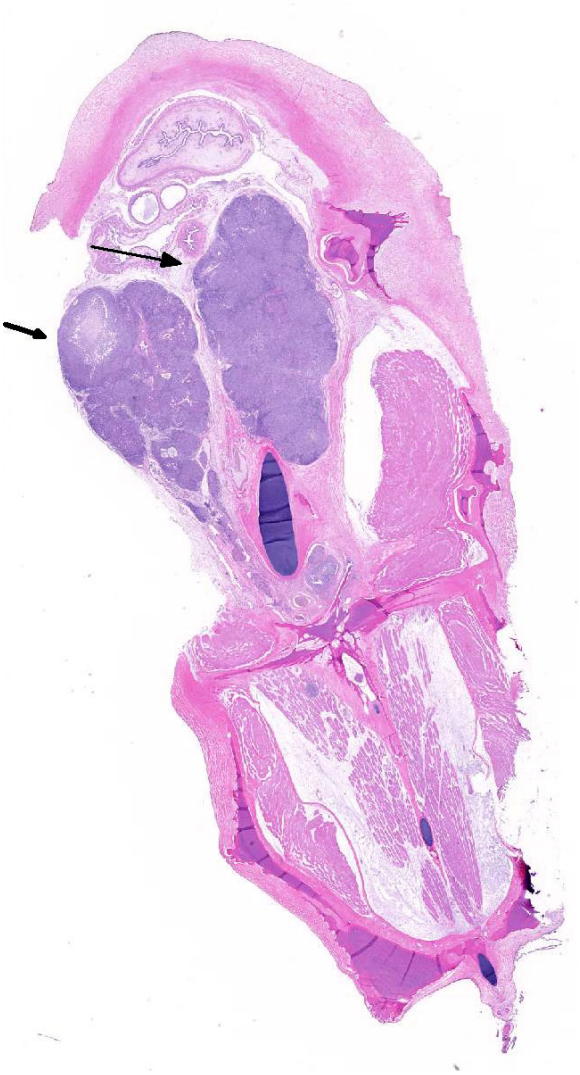

Kidney, seahorse: Renal parenchyma is expanded and architecture is diffusely effaced by granulomatous inflammation. (HE, 5X)

Laboratory results: Cultures of kidney and liver yielded a *Nocardia* sp. PCR amplification of the 16S rRNA gene produced a 524 bp sequence with 100% similarity to *Nocardia nova* (GenBank KP025810.1). Mycobacterial and fungal cultures were negative.

Histopathologic Description: Approximately 75% of the normal renal

parenchyma is severely altered by large numbers of variably-sized, multifocal to coalescing, haphazardly organized sheets and nodular collections of macrophages, with scattered lymphocytes and variable degrees of fibrous encapsulation. Similar streams of macrophages, fibrous tissue and scattered fibroblasts extensively displace and isolate normal hematopoietic tissue and groups of tubules. Discrete, well-organized granulomas are uncommon. Also present are multiple, often large, encapsulated foci with central areas of hemorrhage, necrotic cellular debris and individualized macrophages. On H&E and Ziehl-Neelsen stained sections, rod-shaped and filamentous bacteria can be poorly visualized, particularly in areas of necrosis. With Lillie-Twort stains, bacteria appeared as Gram-positive, coccobacillary forms and beaded filaments. Fite's stain reveals large numbers of elongate, slender, branching filaments.

Contributor's Morphologic Diagnosis: Kidney: Granulomatous nephritis, multifocal to coalescing, chronic, severe, with multiple granulomas, multiple foci of necrosis and modified acid-fast branching bacterial filaments.

Contributor's Comment: Microscopic findings are typical of piscine nocardiosis. Changes vary between groups of slides, particularly the extent of extrarenal involvement, which includes connective tissues, muscle, intestine and the coelomic cavity in some sections. Additional findings in some sections include renal calculi, intestinal nematodes, and parasitic granulomas. Smaller lesions were widely distributed in the gills, skeletal muscle, one ocular choroid, and dermal and hypodermal connective tissues. Similar bacteria were present in all lesions. Three additional animals from the group were examined microscopically, but none showed evidence of infection.

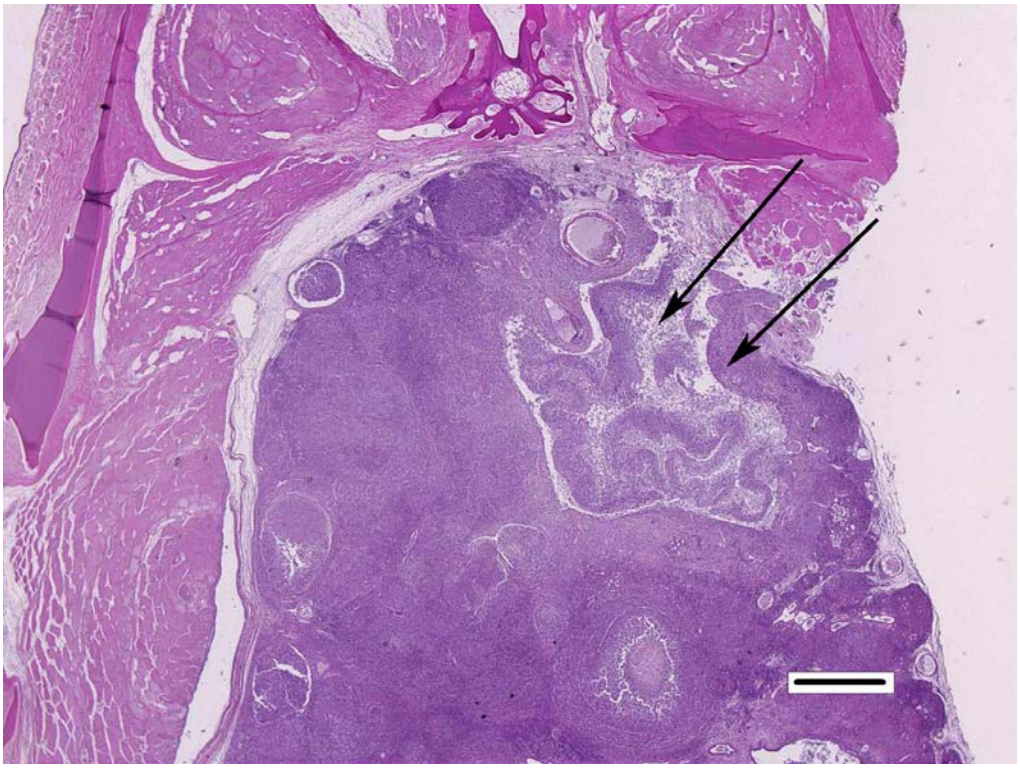

Kidney, seahorse: Higher magnification of the kidney, demonstrating poorly demarcated, coalescing granulomas with a necrotic core. (HE, 100X)

Nocardiosis in fish has been summarized in multiple sources.[3,7] *Nocardia asteroides* was first reported from neon tetra in 1962 and has

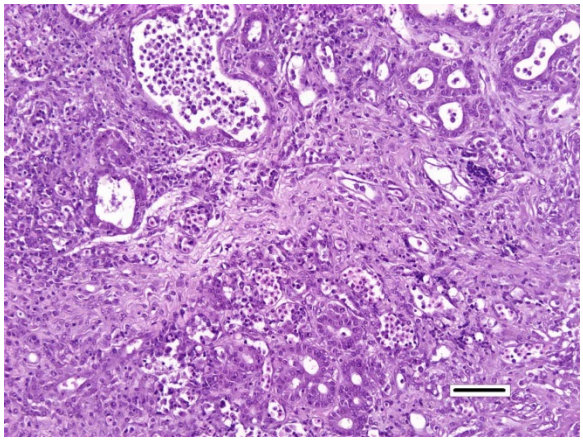

Kidney, seahorse: Higher magnification of affected kidney with marked loss of tubules. Remaining tubules are ectatic and contain numerous sloughed epithelial cells and cellular debris. (HE, 400X)

caused epizootics primarily in freshwater fish. *N. seriolae* is a major pathogen of marine fish worldwide, particularly in Asian mariculture.[2,9] *Nocardia salmonicida* has received little attention since its first isolation from sockeye salmon.[1] The systemic granulomatous disease is characterized by progressive lethargy and emaciation. Infections can be confused both clinically and grossly with those of mycobacteriosis, which is extremely common in captive seahorses. Gross lesions can include skin ulcers, muscle necrosis, and organomegaly, with small nodules in parenchymal organs and the gills. Microscopically, nodules are variously described as granulomas and abscesses, frequently with necrotic centers, peripheral macrophages, lymphocytes, possibly giant cells, and variable fibrous encapsulation.[7] The filamentous branching bacteria, stain weakly and irregularly gram-positive, poorly or not at all with the Ziehl-Neelsen acid-fast stain, and are best visualized with modified acid-fast stains, such as Fite's.

Although contaminated feed has been suggested as a source of infection, the pathogenesis of natural disease is poorly understood. Transmission has been demonstrated experimentally by injection, dermal abrasion, immersion, feeding and cohabitation.[6] Losses of 15-17% from *N. seriolae* have been reported in cultured sea bass and yellow croaker, respectively.[2,9] While microscopic lesions are frequently described, many reports only include bacterial identification to the genus level.[5] Identification of *Nocardia nova* in this case suggests greater species diversity of *Nocardia* could be involved in fish disease.[1]

JPC Diagnosis: Kidney: Nephritis, necro-granulomatous, diffuse, severe, with numerous extracellular filamentous bacilli, long snout seahorse, *Hippocampus reidi*.

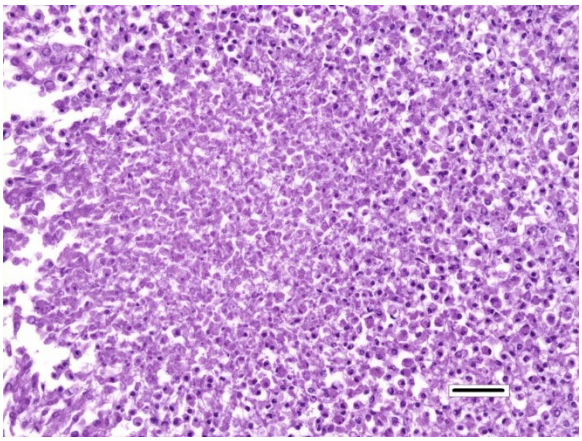

Kidney, seahorse: Necrotic core of one of the granulomas. (HE, 400X)

Conference Comment: *Nocardia* spp. are ubiquitous, saprophytic, gram-positive, higher order bacteria that are associated with both opportunistic and primary infections in a variety of terrestrial and aquatic species worldwide. Morphologically, the bacteria are long, thin, beaded filaments with frequent right-angle branching resembling Chinese letters.[8] They can be seen on standard H&E stained sections; however, they are best visualized by the histochemical stains Gomori methenamine silver (GMS), gram stains, and modified acid-fast stains, such as Fite-Faraco, as demonstrated by the

outstanding photographs provided by the contributor.[8]

Although generally thought to cause low mortality in fish, *Nocardia* spp. can induce severe chronic granulomatous systemic disease.[1,7] In this case, the normal renal architecture is almost completely effaced by multifocal to coalescing necrotizing and granulomatous inflammation. Although

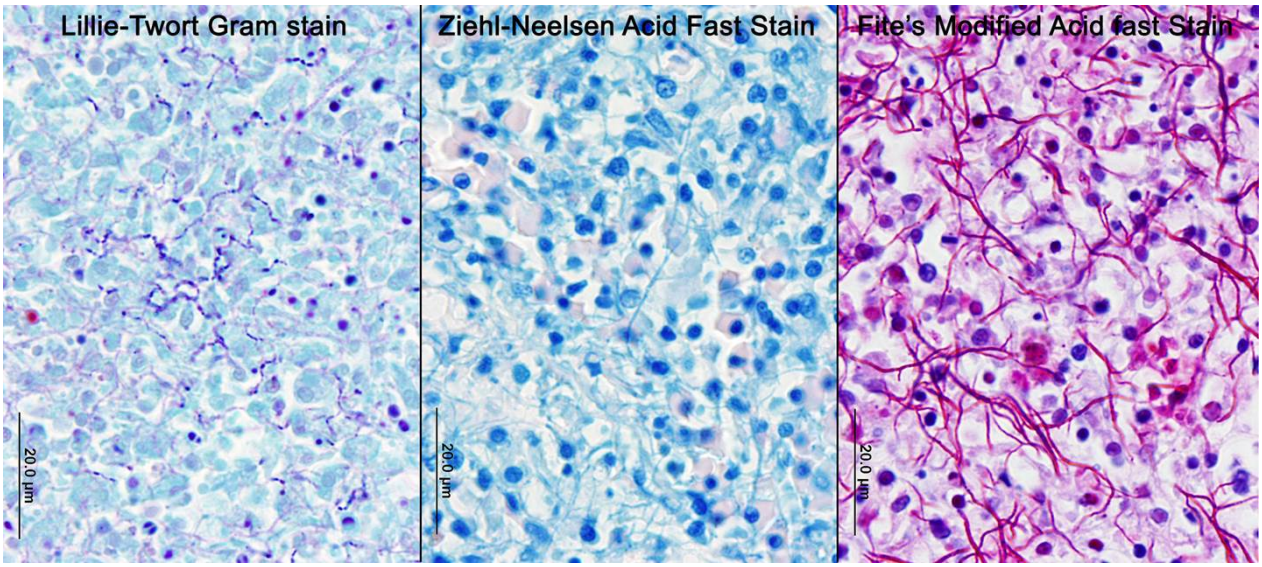

Lung, penguin: Special stain panel demonstrating numerous gram-positive and acid-fast bacilli within the necrotic cores of the granulomas. (Photo courtesy of: University of Georgia College of Veterinary Medicine, Department of Pathology, 501 DW Brooks Drive, Athens, GA 30602, http://www.vet.uga.edu/VPP)

there is some slide variability, in several examined tissue sections, inflammation extends into the adjacent coelomic cavity and skeletal muscle. As mentioned by the contributor, the primary differential diagnosis for piscine nocardiosis includes infection with the much more common *Mycobacteria* sp., which produces nearly identical gross and histological lesions in fish.[7] Gross lesions include cachexia, ascites, dermal ulceration, multifocal skeletal muscle necrosis, and small white well-circumscribed granulomas in the kidney, spleen, heart, and liver.[7] As a result, nocardiosis can be easily misdiagnosed as mycobacteriosis. Positive differentiation requires isolation and identification of the infectious organism and examination of histologic sections of infected organs. Histologically, *Mycobacteria* sp. are non-filamentous, non-branching, gram-positive, strongly acid-fast bacteria and are easily differentiated from *Nocardia* with the special histochemical stains previously mentioned.[1,7,8] Additionally, virulent *Mycobacteria* spp. are obligate intracellular pathogens that replicate within host macrophages. In contrast, pathogenic *Nocardia* spp. are facultative intracellular bacteria that have complex cell wall lipids that allow for resistance to phagocytosis by host macrophages.[7,8] In this case, the vast majority of bacteria are extracellular.

In a small number of tissue sections, conference participants noted a focal granuloma within the intestinal wall centered on a degenerate larval cestode characterized by a 2 um eosinophilic tegument, a lacy, fibrillar eosinophilic parenchymatous body cavity, scattered 5 um diameter, basophilic, calcareous corpuscles, and birefringent hooks in some sections.[4] The

pathologic significance of the parasitic granuloma in the intestinal wall, in this case, is unclear; however, it may indicate that this seahorse was immunocompromised, allowing for the proliferation of various concurrent opportunistic pathogens.

Contributing Institution:
University of Georgia
College of Veterinary Medicine
Department of Pathology
Athens, GA
http://www.vet.uga.edu/VPP

References:

1. Brown-Elliott BA, Brown JM, Conville PS, Wallace RJ. Clinical and laboratory features of the *Nocardia* spp. based on current molecular taxonomy. *Clin Microbiol Rev*. 2006; 19:259-282.
2. Chen SC, Lee JL, Lai JC, Gu YW, Wang CT, Chang HY, Tsai KH. Nocardiosis in sea bass, *Lateolabrax japonicus*, in Taiwan. *J Fish Dis*. 2000; 23:299-307.
3. Cornwell ER, Cinelli MJ, McIntosh DM, Blank GS, Wooster GA, Groocock GH, Getchell RG, Bowser PR. Epizootic *Nocardia* infection in cultured weakfish, *Cynoscion regalis* (Bloch and Schneider). *J Fish Dis*. 2011; 34:567–571.
4. Gardiner, *CH, Poynton, SL. An Atlas of Metazoan Parasites in Animal Tissues.* Washington, D.C: Armed Forces Institute of Pathology, American Registry of Pathology, 1999:35–38.
5. Elkesh A, Kantham KPL, Shinn AP, Crumlish M, Richards RH. Systemic nocardiosis in a Mediterranean population of cultured meagre, *Argyrosomas regius* Asso (Perciformes; *Sciaenidae*). *J Fish Dis*. 2013; 36:141-149.
6. Itano T, Kawakami H, Kono T, Sakai M. Experimental induction of nocardiosis in yellowtail, *Seriola quinqueradiata* Temminck & Schlegel by artificial challenge. *J Fish Dis.* 2006; 29:529–534.
7. Lewis S, Chinabut S. Mycobacteriosis and Nocardiosis. In: Woo PTK, Bruno DW eds, *Fish Diseases and Disorders, Volume 3: Viral, Bacterial and Fungal Infections* 2nd ed. CABI Publishing, Oxfordshire; 2011:397-423.
8. Mauldin E, Peters-Kennedy J. Integumentary system. In: Maxie MG, ed. *Jubb, Kennedy, and Palmer's Pathology of Domestic Animals*. Vol 1. 6th ed. Philadelphia, PA:Elsevier; 2016:637-638.
9. Wang G-L, Yuan S-P, Jin S. Nocardiosis in large yellow croaker, *Larimichthys crocea* (Richardson). *J Fish Dis*. 2008; 28:339-345.

CASE IV: R1 or R2 (JPC 4085971).

Signalment: Post-smolt, unknown gender, Atlantic salmon (*Salmo salar*).

History: This case was submitted as part of a sample of five fish from a seawater tank in which fish were presenting with loss of appetite and lethargy.

Gross Pathology: There was no digesta/ingesta in the gastrointestinal tract with small amounts of soft yellow material (fecal casts) in the distal intestine.

Laboratory results: Positive for salmonid alphavirus (SAV) by RT-PCR

Histopathologic Description: Pyloric caeca/pancreas: one section is examined consisting of multiple cross sections of

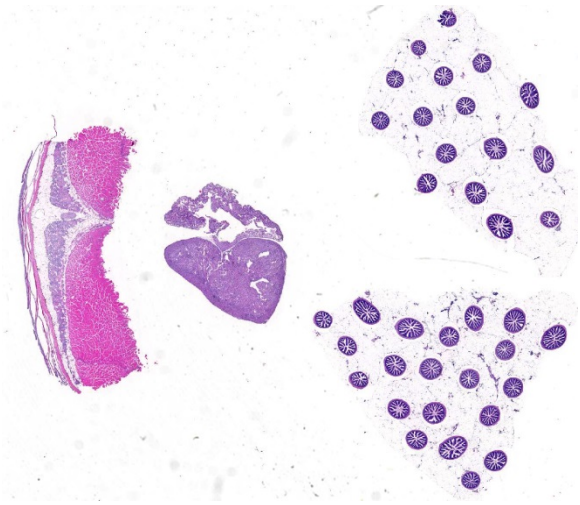

Viscera, Atlantic salmon. Left-right: Skeletal muscle, heart, and pyloric ceca and mesentery are presented for evaluation. (HE, 5X)

pyloric caeca and adjacent adipose tissue. There is extensive loss of exocrine pancreatic tissue. Multifocally, there are small to moderate numbers of mononuclear inflammatory cells (lymphocytes and macrophages). Remaining exocrine epithelial cells have reduced numbers of zymogen granules, and the islets of Langerhans remain intact.

Heart: There are degenerative changes of the cardiomyocytes in the spongy and compact layers of the ventricle, characterized by marked cytoplasmic hypereosinophilia, with variable vacuolation and occasional shrunken nuclei. In these areas, there are low to moderate numbers of lymphocytes and macrophages. Multifocally, there is increased cellularity, prominence and occasional karyomegaly of endocardial endothelium (hyperplasia). Multifocally, the epicardium is expanded by mild to moderate numbers of lymphocytes and macrophages.

Skeletal muscle: Multifocally, there is marked loss of myofibres in the red muscle. The majority of the remaining myofibres are shrunken with densely eosinophilic sarcoplasm, surrounded by moderate numbers of mononuclear inflammatory cells. In the white muscle, there are scattered necrotic and degenerating myofibres, with swollen fragmented, eosinophilic sarcoplasm, central migration of nuclei, and sarcoplasmic infiltration by macrophages. Affected myofibres are surrounded by low numbers of lymphocytes and macrophages.

Contributor's Morphologic Diagnoses: Exocrine pancreas: Severe, diffuse, pancreatic degeneration and loss

Heart, myocardium: Marked, multifocal to coalescing, cardiomyocyte degeneration and necrosis, with endocardial hyperplasia and hypertrophy, and mild to moderate, multifocal, lymphohistiocytic epicarditis

Skeletal muscle (red myofibres): Moderate to marked, chronic, multifocal to coalescing, necrotizing myositis

Skeletal muscle (white myofibres): Mild to moderate, chronic, multifocal, necrotizing myositis

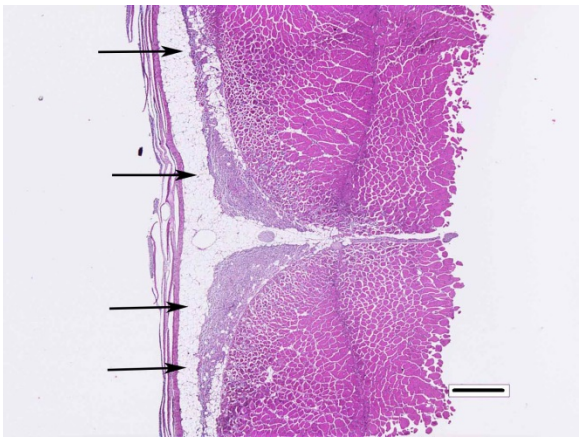

Skeletal muscle, lateral body wall, Atlantic salmon. There is marked degeneration of the overlying red muscle (arrows). There is milder degeneration and atrophy of the exterior portion of the underlying white muscle. (HE, 40X)

Contributor's Comment: The microscopic features of this case are consistent with previously published findings for pancreas disease (PD) in farmed Atlantic salmon, and the histopathological diagnosis was confirmed by RT-PCR. PD is caused by salmonid alphavirus (SAV), which was first described in farmed Atlantic salmon from Scotland in the mid-seventies.[16] It has subsequently been responsible for major economic losses to the Atlantic salmon farming industries in Scotland, Ireland, and Norway. At present, six closely related subtypes have been identified for SAV[4,5], which differ in host specificity, geographical location[7,10] and aquatic environments (Table 1). SAV-2 is the only subtype commonly detected in freshwater systems, causing sleeping disease in freshwater trout. Current research also suggests there may be differences between strains in the infection dynamics[7] as well as minor differences in prevalence and severity of the tissue damage[8]. Naturally occurring outbreaks of PD in farmed Atlantic salmon have only been reported in the seawater phase of production.[15] To date, there has been no evidence of vertical transmission of the disease[11] with horizontal transmission being by far the most important means of spreading the virus[1,19], with shedding of mucus and feces described as transmission routes for SAV.

Table 1. Summary of Salmonid alphavirus subtypes, their geographical distribution and species susceptibility

SAV Subtype	Species	Production Phase	Country
SAV-1	Atlantic salmon (*Salmo salar*)	Seawater	Ireland and Scotland
SAV-2	Rainbow trout (*Oncorhynchus mykiss*)	Freshwater	France, England, Scotland, Spain, Croatia and Germany
SAV-2 (Marine)	Atlantic salmon (*Salmo salar*)	Seawater	Scotland and Norway
SAV-3	Atlantic salmon (*Salmo salar*) Rainbow trout (*Oncorhynchus mykiss*)	Seawater	Norway
SAV-4	Atlantic salmon (*Salmo salar*)	Seawater	Ireland and Scotland
SAV-5	Atlantic salmon (*Salmo salar*)	Seawater	Scotland
SAV-6	Atlantic salmon (*Salmo salar*)	Seawater	Ireland

Gross findings at postmortem examination during the early stages of the disease may include the absence of food in the gut and the presence of fecal casts in the hindgut.[15] Occasionally, petechial hemorrhages can be detected over the surface of the pyloric caeca and surrounding visceral fat. During the chronic stages of the disease, non-feeding fish with low body condition and minimal internal body fat (runts) tend to be more common due to the failure of the pancreas to recover[20]; these fish are more susceptible to parasitic and secondary bacterial infections, which may present concurrently. Apparently healthy fish may also die suddenly due to cardiac and skeletal muscle damage and exhaustion; this manifestation of the disease appears to be more common when older grower fish are infected during their second year at sea.

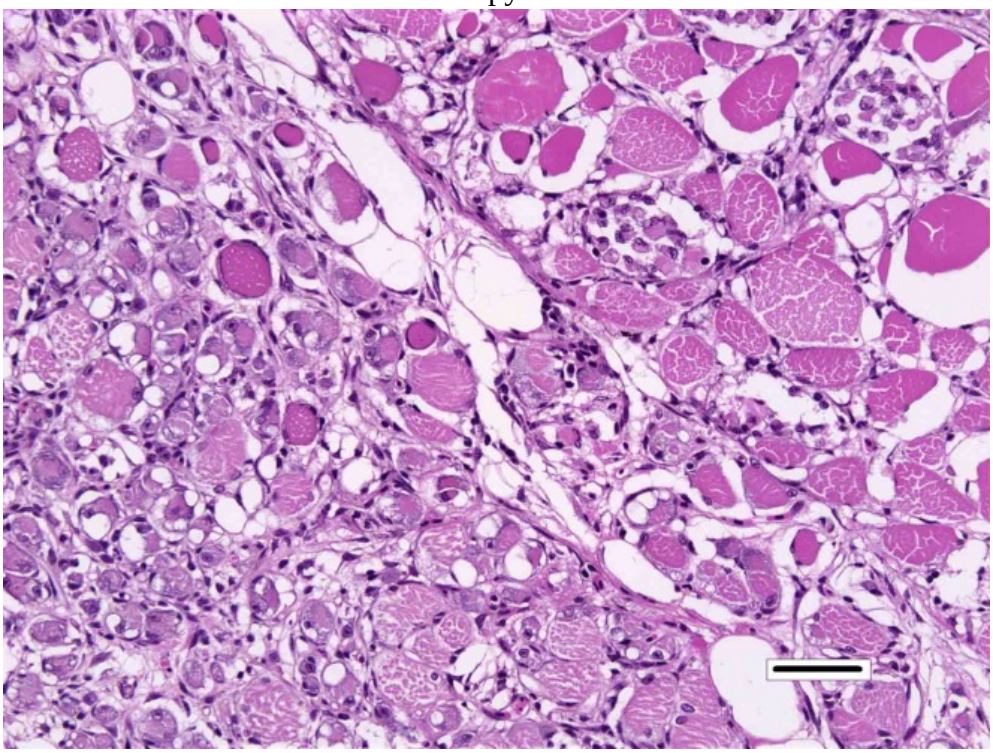

Skeletal muscle, lateral body wall, Atlantic salmon. Higher magnification of red (left) and white muscle(right.) There is marked muscle atrophy and numerous degenerate and necrotic fibers. There is prominent hypertrophy of satellite nuclei and expansion of the perimysium with histiocytes and lymphocytes. (HE, 100X)

The acute phase of the disease is relatively short-lived with rapid destruction of the exocrine pancreatic tissue and a variable inflammatory response ranging from no inflammation to moderate mononuclear cell infiltration and/or fibrosis of the periacinar tissue.[15] In recovering fish, regeneration of exocrine tissues can take place as early as four weeks post infection. Acute heart lesions can be observed concurrently or slightly lagging behind the acute pancreatic changes and includes multifocal cardio-myocyte necrosis with affected cells having a shrunken, deeply eosinophilic cytoplasm and pyknotic nuclei. Both the compact and spongy layer of the ventricular myocardium and the atrial myocardium can be affected to varying degrees, ranging from mild focal changes to involvement of the entire heart musculature.[15] Hypertrophy of myocardial nuclei, particularly at the junction of the spongy and compact ventricular myocardium can be evident in the recovery phase of the disease. Skeletal muscle pathology tends to first appear 3–4 weeks after the appearance of pancreatic and heart lesions, and fish sampled in late-phase disease may only have skeletal muscle lesions. The skeletal muscle lesions consist

of hyaline degeneration with swollen fragmented eosinophilic sarcoplasm, central migration of myocytic nuclei and subsequent invasion of the sarcoplasm by phagocytic macrophages.[15]

The differential diagnoses for these cardiac lesions should at least include the two following diseases:

Heart and skeletal muscle inflammation (HSMI) has been reported in farmed Atlantic salmon in Norway, Scotland, and Chile. It typically affects fish 5 to 9 months after sea-transfer. Mortality in affected cages may be negligible but in some cases can reach up to 20%. Histologically, HSMI mainly targets cardiomyocytes and myofibres of red skeletal muscle. Affected myocytes show signs of degeneration, including loss of striation, sarcoplasmic eosinophilia, vacuolation, centralized nuclei (in skeletal muscle), and karyorrhexis. In HSMI inflammation is more prominent than myocyte necrosis in most cases.[11,13,18] Recently piscine reovirus (PRV) has been suggested to be associated with HSMI infection[17,21].

Cardiomyopathy syndrome (CMS) affects harvest-sized Atlantic salmon, 12–18 months after sea-transfer, and mainly affects the heart without involvement of skeletal muscle. Histopathological changes include necrosis and inflammation of the spongy layer of ventricle and atrium, epicarditis, and infiltration of lymphocytes and macrophages, with rupture of atrium or sinus venosus visible macroscopically.[3,18] A *totivirus* (piscine myocarditis virus (PMCV)) is proposed as the causative agent for this syndrome[14,18,19,21]. Both HSMI and CMS are not typically associated with any pancreatic pathology.

Differential diagnosis for pancreatic necrosis should include infectious pancreatic necrosis (IPN), a viral disease that primarily targets the pancreatic tissue and is caused by an aquatic birnavirus (known as IPN virus). However, IPN does not typically cause cardiac and skeletal muscle pathology.

Table 2. Comparison of histopathological lesions in farmed Atlantic salmon with Pancreas disease (PD), Heart Skeletal Muscle Inflammation (HSMI), Cardiomyopathy Syndrome (CMS) and Infectious Pancreatic necrosis (IPN)

Lesions	PD				HSMI	CMS	IPN
	Acute	Sub-acute	Chronic	Recovery			
Myocardial necrosis	+	+	+	-	+	+	-
Endocardial proliferation	+	+	+	+	+	+	+/-
Cardiomyocyte hypertrophy	-	+/-	+	+	+	+	-
Epicarditis		+	+	+	+		-
Exocrine acinar necrosis	+	+	+	+/-	-	-	+
Myositis	-	-	+	+	+		-

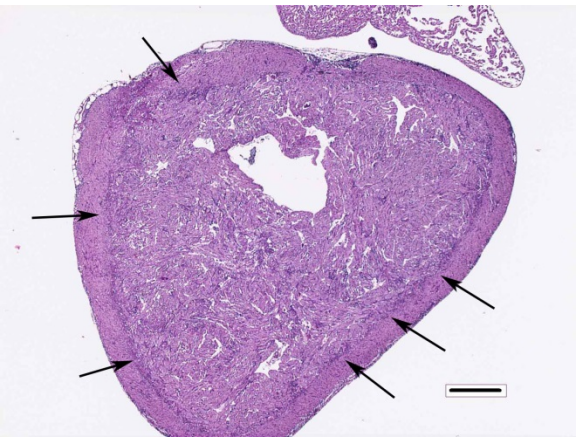

Heart, Atlantic salmon. At subgross magnification, there is a cellular infiltrate within the epicardium and at the junction between the compact and spongy layers of the ventricular myocardium (arrows). (HE, 20X).

JPC Diagnosis: 1. Pancreas: Loss, diffuse, severe with mild lymphocytic pancreatitis, Atlantic salmon, *Salmo salar*.
2. Heart, ventricle: Epicarditis and myocarditis, lymphocytic, diffuse, moderate with multifocal mild myocardiocyte necrosis.
3. Skeletal muscle, red: Degeneration and necrosis, multifocal to coalescing, severe with histiocytic myositis.
4. Skeletal muscle, white: Degeneration and necrosis, multifocal to coalescing, mild to moderate with histiocytic myositis.

Conference Comment: This excellent case demonstrates the prototypical constellation of lesions associated with chronic salmonid alphavirus (SAV) infection. Histological examination of infected fish typically reveals a near complete loss of exocrine pancreatic tissue, epicarditis and myocarditis centered on the ventricle, and skeletal muscle degeneration and necrosis of the white and red muscle.[9,15] Each subtype of SAV listed in Table 1 produces similar morphologic changes and are unable to be distinguished histologically. One of the most difficult tasks for the novice histopathologist is to recognize the complete absence of a normal structure in a tissue section, especially when there is little to no inflammation associated with that loss. Within the multiple cross sections of the pyloric cecae, in this case, conference participants astutely noted a near diffuse loss of exocrine pancreas with only small clusters of remaining exocrine pancreatic cells containing brightly eosinophilic zymogen granules surrounded by mild lymphocytic inflammation that extends into the peripancreatic fat. The islets of Langerhans are mostly unaffected. This diffuse loss of exocrine pancreas with relatively mild inflammation is typical for the chronic phase of this disease. As mentioned by the contributor, the acute phase is associated with a short-lived with rapid necrosis of the exocrine pancreatic tissue and an inflammatory response ranging from no inflammation to moderate mononuclear cell infiltration. The contributor provides an outstanding and thorough review to SAV and includes helpful tables to rule out potential differential diagnoses based on the lesions present in this case.

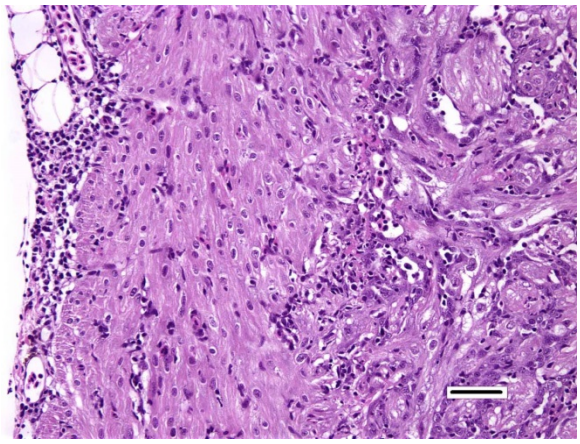

Heart, Atlantic Salmon. Higher magnification demonstrating the lymphocytic infiltrate in the epicardium (left) and within the myocardium (center). (HE, 200X)

Both pancreas disease (PD) of salmon, seen in this case, and sleeping disease (SD) of rainbow trout is caused by related SAV infection. This virus is in the genus *Alphavirus* and family *Togaviridae*, a group of important enveloped ssRNA viruses.[9,15] Other members of the *Togaviridae* family include eastern, western, and Venezuelan equine encephalitis viruses. Generally, this family of viruses is associated with transmission by insects, usually mosquitoes. An aquatic arthropod vector has not yet been identified for SAV; however, direct horizontal transmission has been well documented.[9,15] The virus can survive for extended periods of time in the water outside of the host with a marked increase in survival in sea water compared to fresh water. The virus can also survive for long periods within the fat of dead fish and leaked fat droplets floating on the surface may contribute to long distance spread of the virus. Vertical transmission has not been shown to be a significant route of infection.[9,15]

Contributing Institution:

The Royal (Dick) School of Veterinary Studies

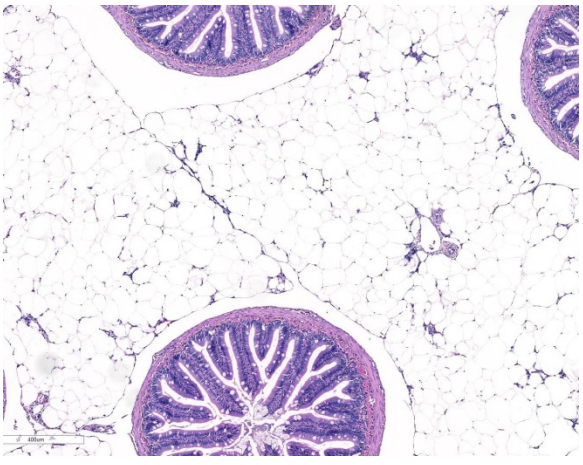

Mesentery and pyloric ceca, Atlantic salmon: The mesentery is devoid of pancreatic tissue. Few pancreatic islets remain. (HE, 30X)

University of Edinburgh
Easter Bush Campus
Midlothian
United Kingdom

References:

1. Bratland A, Nylund A. Studies on the possibility of vertical transmission of Norwegian salmonid alphavirus in production of Atlantic salmon in Norway. *J Aquat Anim Health.* 2009; 21:173–178.
2. Christie KE, Graham DA, McLoughlin MF, Villoing S, Todd D, Knappskog D. Experimental infection of Atlantic salmon Salmo salar pre-smolts by IP injection with new Irish and Norwegian salmonid alphavirus (SAV) isolates: a comparative study. *Dis Aquat Organ.* 2007; 75:13–22.
3. Ferguson HW, Poppe TT, and Speare DJ. Cardiomyopathy in farmed Norwegian salmon. *Dis Aquat Organ.* 1990; 8:225–231.
4. Fringuelli E, Rowley HM, Wilson JC, Hunter R, Rodger H, Graham DA. Phylogenetic analyses and molecular epidemiology of European salmonid alphaviruses (SAV) based on partial E2 and nsP3 gene nucleotide sequences. *J Fish Dis.* 2008; 31:811–23.
5. Graham DA, Fringuelli E, Wilson C, Rowley HM, Brown A, Rodger H, et al. Prospective longitudinal studies of salmonid alphavirus infections on two Atlantic salmon farms in Ireland; evidence for viral persistence. *J Fish Dis.* 2010; 33(2):123–35.
6. Graham DA, Fringuelli E, Rowley HM, Cockerill D, Cox DI, Turnbull T, et al. Geographical distribution of salmonid alphavirus subtypes in marine farmed Atlantic salmon,

Salmo salar L., in Scotland and Ireland. *J Fish Dis.* 2012; 35:755–65.
7. Graham DA, Frost P, McLaughlin K, Rowley HM, Gabestad I, Gordon A, et al. A comparative study of marine salmonid alphavirus subtypes 1–6 using an experimental cohabitation challenge model. *J Fish Dis.* 2011; 34:273–86.
8. Haugland Ø, Mikalsen AB, Nilsen P, et al. Cardiomyopathy syndrome of Atlantic salmon (Salmo salar L.) is caused by a double-stranded RNA virus of the Totiviridae family. *J Virol*. 2011; 85(11):5275–5286.
9. Herath TK, Ferguson HW, et al. Pathogenesis of experimental salmonid alphavirus infection in vivo: An ultrastructural insight. *Vet Res*. 2016; 47:7-18.
10. Jansen MD, Taksdal T, Wasmuth MA, Gjerset B, Brun E, Olsen AB, et al. Salmonid alphavirus (SAV) and pancreas disease (PD) in Atlantic salmon, Salmo salar L., in freshwater and seawater sites in Norway from 2006 to 2008. *J Fish Dis.* 2010; 33:391–402.
11. Kongtorp RT, Halse M, Taksdal T, and Falk K. Longitudinal study of a natural outbreak of heart and skeletal muscle inflammation in Atlantic salmon, Salmo salar L. *J Fish Dis.* 2006; 29(4):233–244.
12. Kongtorp RT, Sten A, Andreassen PA, Aspehaug V, Graham DA, Lyngstad TM, et al. Lack of evidence for vertical transmission of SAV 3 using gametes of Atlantic salmon, Salmo salar L., exposed by natural and experimental routes. *J Fish Dis.* 2010; 33:879–88.
13. Kongtorp RT, Taksdal T, and Lyngøy A. Pathology of heart and skeletal muscle inflammation (HSMI) in farmed Atlantic salmon Salmo salar. *Dis Aquat Organ.* 2004; 59(3):217–224.
14. Løvoll M, Wiik-Nielsen J, Grove S, et al. A novel totivirus and piscine reovirus (PRV) in Atlantic salmon (Salmo salar) with cardiomyopathy syndrome (CMS). *Virol J*. 2010; 7:309.
15. McLoughlin M, Graham D. Alphavirus infections in salmonids —a review. *J Fish Dis.* 2007; 30:511–31.
16. Munro ALS, Ellis EAE, McVicar AH, McLay HA, Needham EA. An exocrine pancreas disease of farmed Atlantic salmon in Scotland. *Helgol Meeresun.* 1984; 37:571–86.
17. Palacios G, Løvoll M, Tengs T, et al. Heart and skeletal muscle inflammation of farmed salmon is associated with infection with a novel reovirus. *PLoS One*. 2010; 5(7):e11487.
18. Poppe TT, and Ferguson HW. Cardiovascular system. In: Ferguson HW, ed. *Systemic Pathology of Fish: A Text and Atlas of Normal Tissue Responses in Teleosts, and Their Responses in Disease*. 2nd ed. London, UK: Scotian Press, 2006:141–167.
19. Rodger H, Mitchell S. Epidemiological observations of pancreas disease of farmed Atlantic salmon, Salmo salar L., in Ireland. *J Fish Dis.* 2007; 30:157–67.
20. Rodger HD, Murphy TM, Drinan EM, & Rice DA. Acute skeletal myopathy in farmed Atlantic salmon Salmo salar. *Dis Aquat Organ.* 1991; 12:17–23.
21. Wiik–Nielsen CR, Ski PMR, Aunsmo A, and Løvoll M. Prevalence of viral RNA from piscine reovirus and piscine myocarditis virus in Atlantic salmon,

Salmo salar L., broodfish and progeny. *J Fish Dis.* 2012; 35:169–171.

Self-Assessment - WSC 2016-2017 Conference 25

1. Pleisotophora hyphessobryconis is a common microsporidian parasite of what type of fish?
    a. Tilapia
    b. Catfish
    c. Goldfish
    d. Neon tetras

2. Tomonts of *Amylloodinium* divide into life stages known as what?
    a. Trophonts
    b. Dinospores
    c. Stomatopodes
    d. Sporocysts

3. The agent resulting in epitheliocystis is a?
    a. Bacteria
    b. Virus
    c. Apicomplexan
    d. Microsporidian

4. Which histochemical stain is best for demonstrating *Nocardia* in tissue?
    a. Giemsa
    b. Ziehl-Neelsen acid fast
    c. Fite's modified acid fast
    d. Gram

5. Which of the following histologic findings is not seen in alphavirus infection in salmon
    a. Skeletal muscle necrosis
    b. Necrosis of exocrine pancreas
    c. Necrosis of renal tubular epithelium
    d. Cardiomyocyte necrosis